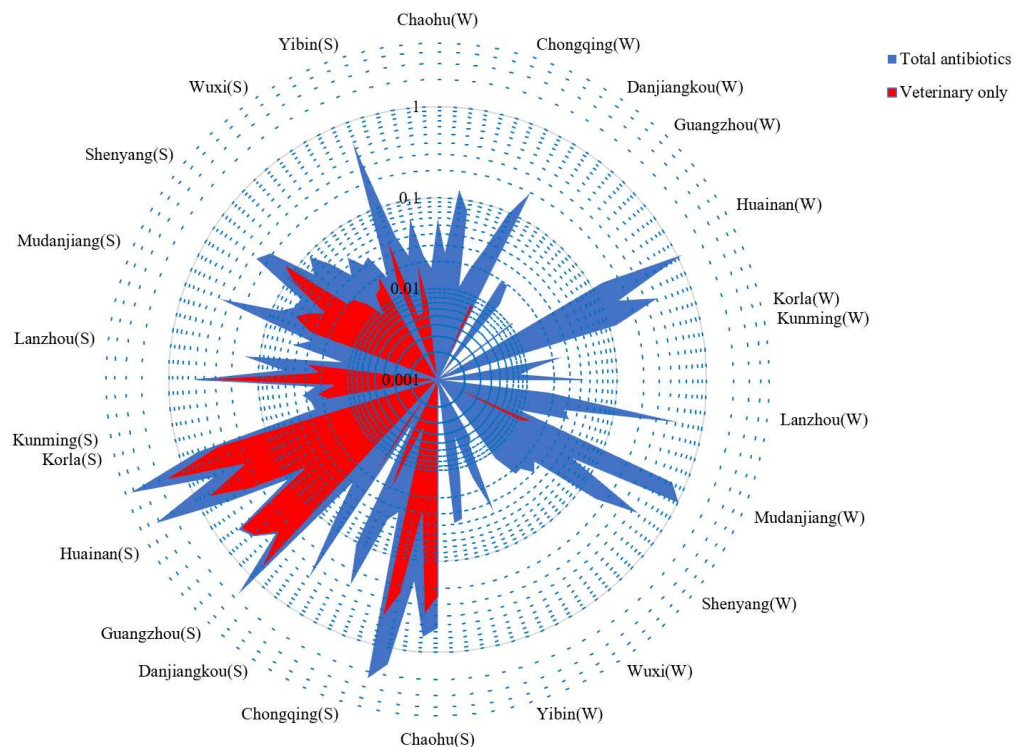


# Applied Ecology and Environmental Research

International Scientific Journal



VOLUME 19 \* NUMBER 1 \* 2021

Published: January 29, 2021  
<http://www.aloki.hu>  
ISSN 1589 1623 / ISSN 1785 0037  
DOI: <http://dx.doi.org/10.15666/aeer>

# CARBON DIOXIDE AND METHANE EMISSIONS BY URBAN TURFGRASSES UNDER DIFFERENT NITROGEN RATES: A COMPARISON BETWEEN TALL FESCUE (*FESTUCA ARUNDINACEA* SCHREB.) AND HYBRID BERMUDAGRASS (*CYNODON DACTYLON* [L.] PERS. VAR. *DACTYLON* X *CYNODON TRANSVAALENSIS* BURTT-DAVY)

BRANDANI, G.<sup>1</sup> – BALDI, A.<sup>1\*</sup> – CATUREGLI, L.<sup>2</sup> – GAETANI, M.<sup>2</sup> – GROSSI, N.<sup>2</sup> – MAGNI, S.<sup>2</sup> – PARDINI, A.<sup>1</sup> – VOLTERRANI, M.<sup>2</sup> – ORLANDINI, S.<sup>1</sup> – VERDI, L.<sup>1</sup>

<sup>1</sup>*Department of Agriculture, Food, Environment and Forestry, University of Florence  
Piazzale delle Cascine, 18, 50144 Firenze (FI), Italy  
(phone: +39-055-275-5700)*

<sup>2</sup>*Department of Agriculture, Food and Environment, University of Pisa  
Via del Borghetto, 80, 56124 Pisa (PI), Italy  
(phone: +39-050-221-6090)*

*\*Corresponding author  
e-mail: ada.baldi@unifi.it; phone: +39-055-275-5936*

(Received 15<sup>th</sup> Feb 2020; accepted 25<sup>th</sup> May 2020)

**Abstract.** Turfgrass is a major vegetation type in urban and peri-urban areas. Being high maintenance ecosystems, turfs can contribute substantially to urban climate change. The object of this study was to evaluate the contribution to GHG emissions by urban turfgrasses in Mediterranean conditions (Tuscany, central Italy). CO<sub>2</sub> and CH<sub>4</sub> emission fluxes from a mature stand of tall fescue and bermudagrass were evaluated, by static chambers method, for the assessment of C emission under different nitrogen fertilization rates (0 - 50 - 150 kg N ha<sup>-1</sup>). Both species showed a correlation between N fertilization rate and CO<sub>2</sub> emissions, whilst, no correlation was observed for CH<sub>4</sub>. In the case of tall fescue, cumulative CO<sub>2</sub> emissions were significantly higher with 150 kg N ha<sup>-1</sup> and no differences were observed between 0 and 50 kg N ha<sup>-1</sup>. As for bermudagrass differences were found between control and other treatments but no differences were observed on cumulative CO<sub>2</sub> emissions between 50 and 150 kg N ha<sup>-1</sup>. In both species, N fertilization did not affect CH<sub>4</sub> emissions. Results indicate that both N rate and turfgrass species influence C emissions, for this reason they should be considered in the management of green areas in the climatic transition zone.

**Keywords:** *greenhouse gasses, static chambers, fertilization, green areas, turf management*

## Introduction

Greenhouse gas emissions are now higher than ever, attracting broad interest because of their potential implications with climate change (Lal et al., 1995; Verdi et al., 2019). Given the high amount released into the atmosphere, carbon dioxide (CO<sub>2</sub>) can be considered the major contributor to the greenhouse effect (Forster et al., 2007). Since the mid-nineteenth century, almost 35% of CO<sub>2</sub> released by human activities has been associated with changes in land use (Houghton et al., 2001). The contribution of land use to global warming is difficult to be determined since greenhouse gases (GHGs) derive from diverse sources and complex systems (Foley et al., 2005).

Urbanization is one of the main causes of the change in land use (Patra et al., 2018) and urban and peri-urban areas are expected to sprawl rapidly in the next future (d'Amour et al., 2017; Ritchie and Roser, 2020). As the urban citizen density is destined to growth in

the coming decades (United Nations, 2014), urban land use and land cover has gained more attention because of the impact that anthropic activities have on ecosystems. Urbanization implies an increase in turf's environmental impacts due to the replacement of natural and agricultural lands with this type of green cover (Alig and Kline, 2004; Kaye et al., 2004; Caturegli et al., 2014; Magni et al., 2014). Thanks to its functional, environmental, recreational, social and aesthetic roles, nowadays turfgrass is the most important vegetation type in urban and peri-urban environment (Qian and Follet, 2012) covering more than 16 million ha in the United States of America (Milesi et al., 2005) and up to 70-75% of urban green spaces worldwide (Ignatieva et al., 2015).

Turfgrasses establishment and maintenance at high quality levels contribute substantially to carbon emissions in atmosphere. Van Delden et al. (2016) found that turfgrass establishment increases the global warming potential by another 30 kg CO<sub>2</sub>-e per ha in comparison with the native eucalypt forest in Brisbane (Australia), while Kong et al. (2014) state that turf maintenance contributes to carbon emissions at 0.17 to 0.63 kg CO<sub>2</sub>-e per month per year in Hong Kong. Furthermore, turfgrasses have the capacity to store carbon (C) (Jo and McPherson, 1995; Nowak and Crane, 2002; Jo, 2002). Due to the high variability observed on turfgrass capacity to store C, annual C storage rate varies among 0.9 tons C ha<sup>-1</sup>y<sup>-1</sup> to 5.4 tons C ha<sup>-1</sup>y<sup>-1</sup> (Selhorst and Lal, 2013). Furthermore, Selhorst and Lal (2013) found that the most managed is the lawn, the highest is its C storage rate depending on species, turf age, and management. On the contrary, turfgrasses may represent a detrimental factor due to their potential to affect the carbon cycle being CO<sub>2</sub> and methane (CH<sub>4</sub>) sources, increasing carbon emissions and carbon concentration in the atmosphere (Groffman and Pouyat, 2009). In these regards, within their experiments in Moscow city, Shchepeleva et al. (2007) estimated C balance of turfgrass comparing the annual C uptake in biomass with the CO<sub>2</sub> emission from soils and the results showed that C uptake did not compensate C emissions. Depending on N fertilization rate, Hamido et al. (2016) found a turfgrass emission range going from 292 to 394 kg CO<sub>2</sub> ha<sup>-1</sup>d<sup>-1</sup>. Allaire et al. (2008) state that turfgrass CO<sub>2</sub> emissions are neglected because of an underestimation of the contribution that urban land area could give since they are considered generally too small. On the contrary, according to Robbins and Birkenholtz (2003), turfgrasses occupy a substantial part of urban surfaces with an essential contribution to CO<sub>2</sub> emission. Groffman and Pouyat (2009) found that CH<sub>4</sub> uptake is almost completely absent in lawns, Selhorst and Lal (2013) found that CH<sub>4</sub> emissions depend on the decomposition of biomass. CO<sub>2</sub> and CH<sub>4</sub> emission rates from soil depend on many factors and soil characteristics such as microbial activity, root and heterotrophic respiration, soil texture, temperature, moisture, and pH (Ludwig et al., 2001; Rastogi et al., 2002; Groffman and Pouyat, 2009). Zhang et al. (2013) state that also the management is crucial because of the impact that it can bring to the soil-atmosphere gas exchange system. Urban and peri-urban areas are highly managed ecosystems (Zhang et al., 2013) requiring even daily irrigation, frequent mowing and fertilization treatments. However, they are not analyzed as deeply as forest and agricultural soils, thus quantifying their carbon emissions is a complex matter (Jo and McPherson, 1995; Pouyat et al., 2002, 2006; Townsend-Small and Czimczik, 2010).

The object of this study was to evaluate the effect of nitrogen fertilization on the contribution to GHG emissions by urban turfgrasses. For this purpose, CO<sub>2</sub> and CH<sub>4</sub> emission fluxes from a mature stand of tall fescue (*Festuca arundinacea* Schreb.) and hybrid bermudagrass (*Cynodon dactylon* [L.] Pers. var. *dactylon* x *Cynodon transvaalensis* Burt-Davy), two of the most commonly used turfgrass species, were evaluated for the assessment of C total amount emission at different nitrogen fertilization rates.

## Materials and methods

The experiment was carried out from May to September 2018 at the Centre for Research on Turfgrass for Environment and Sports (CeRTES) (Fig. 1), University of Pisa, located at San Piero a Grado, Pisa (43°40'N, 10°19'E, 6 m a.s.l.), Italy, on mature turfgrass stands of the cool-season (C<sub>3</sub>) 'Grande' tall fescue (*Festuca arundinacea* Schreb.) and the warm-season (C<sub>4</sub>) 'Patriot' hybrid bermudagrass (*Cynodon dactylon* [L.] Pers. var. *dactylon* x *Cynodon transvaalensis* Burt-Davy) (Caturegli et al., 2015).



**Figure 1.** Satellite image of experimental area (CeRTES) and the surrounding habitats (Source: Google Earth)

The trial was established on a calcareic fluvisol. The analyses of the main physical and chemical properties of soil (Table 1) were performed according to the Italian Ministry of Agriculture and Forestry procedures (MiPAF, 1994).

**Table 1.** Physical and chemical properties of the soil

Properties	Measure unit	Value
Sand	%	28
Silt	%	55
Clay	%	17
Organic matter	g kg <sup>-1</sup>	21
Total nitrogen	g kg <sup>-1</sup> d.m.	1
Available phosphorus	mg kg <sup>-1</sup>	12
Exchangeable potassium	mg kg <sup>-1</sup>	126
pH		7.7
Cation Exchange Capacity	meq 100 g <sup>-1</sup>	9.8
Electric conductivity	mS cm <sup>-1</sup>	0.2

Eighteen plots of 1 m x 1 m were organized with three fertilization treatments and three replicates per each species. Fertilization treatments were carried out once, at the beginning of the trial (7th May 2018) with a rotary spreader (ICL Specialty Fertilizers



AccuPro 2000, Ipswich, UK), applying ammonium sulfate at three different levels as 0 kg N ha<sup>-1</sup> (Control), 50 kg N ha<sup>-1</sup> (N1, minimum conventional rate for both tall fescue and bermudagrass) (Carey et al., 2012), and 150 kg N ha<sup>-1</sup> (N2, tripled minimum conventional rate). Weekly mowing at turf height of 2.0 cm was performed with a walk-behind lawnmower (John Deere 20SR7, Moline IL, USA) equipped with rear clippings bagger. In order to prevent drought stress, sprinkler irrigation was used when needed.

In this study, urban and peri-urban grasses were intended as a playing and ornamental surface for sport, relaxation and enjoyment and not as a pasture crops. For this reason, according to Kaye et al. (2004), Townsend-Small and Czimczik (2010), Kong et al. (2014), Van Delden et al. (2016), and Shchepeleva et al. (2017), carbon emissions were evaluated only through the quantification of fluxes without evaluating the dry matter production or the amount of carbon bound in the production. Eighteen static chambers (one per plot, nine per specie) were constructed as described by Parkin and Venterea (2010) and Verdi et al. (2018) for the monitoring of gas emissions (*Fig. 2*). Chambers were composed by an anchor system and the lid of the chamber. Anchor system was made by a PVC cylinder (20 cm diameter and 15 cm height). The anchor was inserted into the soil for approximately 10 cm as support for the lid. The lid of the chamber was made by a PVC cylinder (20 cm diameter and 25 cm height) and a PVC stopper sealed with a silicon glue. To reduce solar radiation disturbance of internal temperature of the chamber, a reflective Mylar tape was placed on the external surface of chamber's lid. To allow gas samplings, a hole of 13.2 mm diameter, was drilled on the top of the lid. A butyl rubber septum (20 mm diameter) was used to close the hole and allow gas samplings. Hermetic connection between anchor and the lid was ensured using a strip of tire tube of 7 cm that was sealed on the bottom of the lid with silicon glue. During measurements, the exceeding part of the strip from the lid (approximately 50% of the strip) was folded down on the anchor system.



**Figure 2.** Static chambers for the monitoring of CO<sub>2</sub> and CH<sub>4</sub> emissions by turfgrass

Gas samplings were performed by means of a portable gas analyzer Madur Sensonic X-CGM 400 (Zgierz, PL). X-CGM 400 uses non-dispersive infrared (NDIR) technology for CO<sub>2</sub> and CH<sub>4</sub> monitoring. X-CGM 400 was connected by chambers with a pipe system

equipped with a needle. Measurements were carried out by holding the needle inside the butyl rubber septum of the chamber for 1 min. Air flow was pumped inside the X-CGM 400 and released outside the analyser at the end of the analysis. Gas concentration data were obtained directly from the analyser (ppm). Measurement consisted in two gas samplings per chamber: the first one immediately after chamber closing and the second one after 1 h intervals (Parkin and Venterea, 2010; Verdi et al., 2018) of gas accumulation into the closed chamber. Difference between the two samplings represents gas concentration into the chamber. Gas fluxes calculation was performed using gas concentration, air temperature, chamber dimensions (area, 314 cm<sup>2</sup>, and volume, 9420 cm<sup>3</sup>) and the molar weight of each gas to convert data from ppm to Kg-C ha<sup>-1</sup>. Measurements were performed on mid-morning, from 9 am to 11 am, as it represents the time of the day that more closely corresponds to daily average temperature (Parkin and Venterea, 2010). CO<sub>2</sub> and CH<sub>4</sub> emissions monitoring were carried out on a period of 37 weeks from the day of the year (DOY) 127 (7th of May) to DOY 270 (17th September) in order to evaluate their trend and the total amount of C emissions. Measurements were carried out at 1, 3 and 5 days immediately after fertilization (DOY 127, 129 and 131, respectively), and once a week during the second and the third weeks. From the fourth week, measurements were performed once every two weeks, until the end of the experiment. Interpolation methodology was adopted to obtain missing data from the days when measurements were not performed.

Daily data of temperature (minimum, maximum and average) and precipitation were collected by a weather station of the Regional Hydrological Service of Tuscany located next to field trial in S. Piero a Grado (PI, Italy) (Fig. 3).

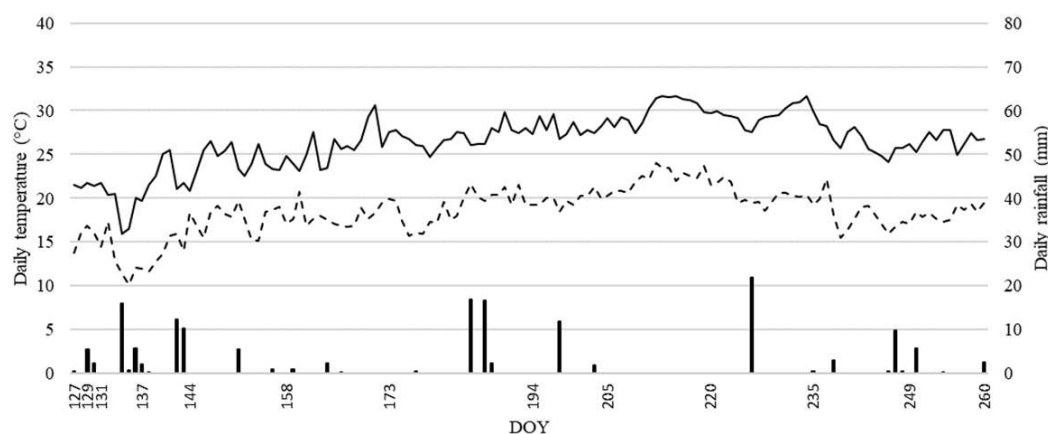


**Figure 3.** Maximum and minimum air temperatures trend and rainfall during monitoring period (DOY 127–DOY 260, 2018). Bars: precipitation (mm); solid line: maximum air temperature (°C); dashed line: minimum air temperature (°C). Numbers of DOY are in correspondence to GHG measurements

Statistical analysis was carried out according to CoStat software (Co Hort, Monterey, CA, USA). Carbon emission data of tall fescue and hybrid bermudagrass at the different N fertilization rates were analyzed using analysis of variance (ANOVA) followed by the Tukey's test to compare means at  $p \leq 0.05$  level of significance. The relationships among C emission and N fertilization rates for the species were studied using Pearson's correlation coefficient ( $r$ ).

## Results and discussion

### Carbon dioxide emissions

In tall fescue CO<sub>2</sub> emission flux didn't seem to be affected by the addition of N1, the conventional rate used in urban turfgrasses. In fact, no significant differences in total amount of C emissions between Control and N1 were observed (*Table 2*). Probably tall fescue uses organic matter in the soil more efficiently for its own development offsetting the lack of N in Control compared to N1. On the contrary significantly higher CO<sub>2</sub> emissions were recorded under N2 rate. This is in accordance with Hamido et al. (2016) which state that an intense increase of N rate can cause greater soil CO<sub>2</sub> emissions. A strong correlation ( $r=0.90$ ) between soil CO<sub>2</sub> emissions and N fertilization rates was observed (*Table 3*).

**Table 2.** Total amount of C emission (kg C ha<sup>-1</sup>) in terms of carbon dioxide (CO<sub>2</sub>) and methane (CH<sub>4</sub>) at the end of the monitoring period (DOY 260) for tall fescue and hybrid bermudagrass at 0 (control), 50 (N1), 150 (N2) kg ha<sup>-1</sup> of N

	Tall fescue kg CO <sub>2</sub> -C ha <sup>-1</sup>	Bermudagrass kg CO <sub>2</sub> -C ha <sup>-1</sup>	Tall fescue kg CH <sub>4</sub> -C ha <sup>-1</sup>	Bermudagrass kg CH <sub>4</sub> -C ha <sup>-1</sup>
0 (Control)	4472 b <sup>a</sup> (±1080) <sup>b</sup>	5245 b (±596)	18.64 a (±2.84)	15.69 a (±3.53)
N1	5223 b (±806)	7137 a (±649)	18.55 a (±1.33)	21.24 a (±5.44)
N2	7901 a (±599)	7576 a (±1149)	18.95 a (±1.95)	14.32 a (±1.56)

a Values on the same column followed by different letters are significantly different at  $p \leq 0.05$ ,

b Standard deviation

**Table 3.** Relationships among C emission and N fertilization rates for tall fescue and bermudagrass

	Tall fescue	Bermudagrass
Kg CO <sub>2</sub> -C	$y^a = 23.421x + 4304.6$ $r^b = 0.90^{**}$	$y = 13.994x + 5723.4$ $r = 0.71^*$
Kg CH <sub>4</sub> -C	$y = -0.0042x + 18.995$ $r = 0.15n.s.$	$y = 0.0033x + 17.301$ $r = 0.047n.s.$

a Regression equation,

b Pearson's correlation coefficient

In the short term, CO<sub>2</sub> emissions of tall fescue were stimulated by fertilization (*Fig. 4*). N2 had an immediate effect on C emission, N1 about two days later (DOY 129). However, it seems to be evident that soil bacteria need some days for fertilizers degradation since the respiration peak (75 kg CO<sub>2</sub>-C ha<sup>-1</sup> for N2 and 54 kg CO<sub>2</sub>-C ha<sup>-1</sup> for N1) occurred 10 days after fertilization (DOY 137) (*Fig. 4*). Thereafter, as observed by Alluvione et al. (2010) in their experiments, all treatments showed a reduction in CO<sub>2</sub> emissions. In particular, starting from 31 days (DOY 158) after fertilization until the end of the experiment, Control and N1 exhibited the same CO<sub>2</sub> emissions trend. Conversely, N2 maintained significantly higher CO<sub>2</sub> emissions than the other treatments until DOY 205 (*Fig. 4*). The average daily trends confirmed this result, showing significantly higher emissions in N2 (59.41 kg CO<sub>2</sub>-C ha<sup>-1</sup> d<sup>1</sup>) than in N1 and Control treatments (39.28 and 33.63 kg CO<sub>2</sub>-C ha<sup>-1</sup> d<sup>1</sup>, respectively).

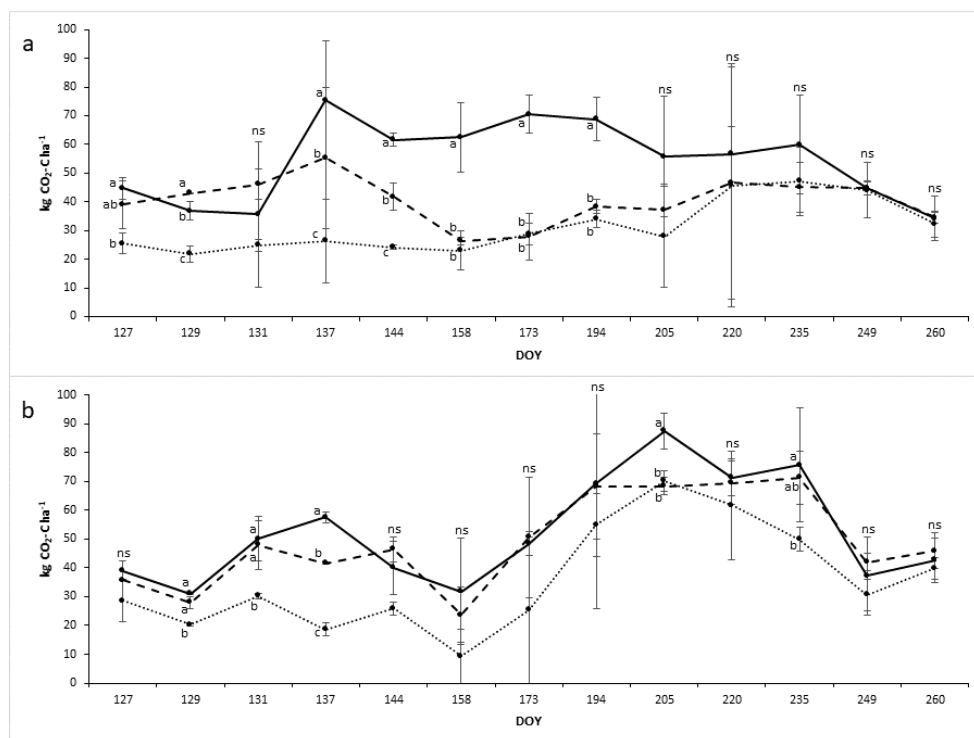


**Figure 4.** Carbon dioxide emissions ( $\text{kg CO}_2\text{-C ha}^{-1} \text{d}^{-1}$ ) trend during monitoring period (DOY 127 to DOY 260, 2018) from tall fescue (a) and hybrid bermudagrass (b) at 0 (control), 50 (N1), 150 (N2)  $\text{kg ha}^{-1}$  of N. Dotted line: control; dashed line: N1; solid line: N2. Vertical bars indicate standard deviation. Values with the same letter are not different according to Tukey test ( $P \leq 0.05$ ). Numbers of DOY are in correspondence to GHG measurements

Contrary to what observed in tall fescue, hybrid bermudagrass showed to be more reactive to N fertilization. In fact, soil microbial community and roots respiration was stimulated also at a low N input (Table 2). No significant differences on cumulative amounts of CO<sub>2</sub> emissions between N1 and N2 were observed. However, both N1 and N2 showed higher values compared to Control (Table 2). This is in accordance to the average daily emission trends that showed similar values between N1 and N2 (53.66 and 56.96  $\text{kg CO}_2\text{-C ha}^{-1} \text{d}^{-1}$ , respectively) but significantly higher in respect with the Control treatment (39.44  $\text{kg CO}_2\text{-C ha}^{-1} \text{d}^{-1}$ ). A weak correlation between soil CO<sub>2</sub> emissions and N fertilization rates was observed ( $r=0.71$ ) (Table 3). Immediately after fertilization, hybrid bermudagrass showed a reduction on soil CO<sub>2</sub> emissions for all treatments. Fertilization affected C emissions starting from DOY 129 until DOY 137; N1 and Control showed the same trend with significant differences, N2 gradually increased until DOY 137 with significant differences with respect to N1 only at DOY 137. This is in accordance with Alluvione et al. (2010) that observed a similar trend in CO<sub>2</sub> emissions from corn, also belonging to *Poaceae* family. From DOY 144, C emissions trend seems to be influenced more by temperatures than by fertilization (Fig. 3). In fact, significant differences between treatments were observed only in few cases (DOY 205 and 235).

Our results show that turfs represent an effective strategy to reduce soil CO<sub>2</sub> emissions fluxes when compared with other types of urban and peri-urban land use. As a matter of fact, we found a soil CO<sub>2</sub> average emissions accounts to 47.1  $\text{kg CO}_2\text{-C ha}^{-1} \text{d}^{-1}$  (considering both the species and the N rates used in our experiment) while research on

urban gardens reported daily CO<sub>2</sub> emissions of 68.8 kg CO<sub>2</sub>-C ha<sup>-1</sup> (Predotova et al., 2010), 73.97 kg CO<sub>2</sub>-C ha<sup>-1</sup> (Kaye et al., 2005), and 79.7 kg CO<sub>2</sub>-C ha<sup>-1</sup> (Lompo et al., 2012).

### Methane emissions

In this experiment, CH<sub>4</sub> emissions were not affected by N fertilization rate for both tall fescue and hybrid bermudagrass, as confirmed by the Person's correlation coefficients analysis reported in Table 3 ( $r=0.15$  and  $r=0.047$  for tall fescue and hybrid bermudagrass, respectively). This result is in accordance to Whalen (2005) and Oertel et al. (2016) who state that CH<sub>4</sub> is mainly produced in anaerobic conditions typical of wetlands. Due to the ornamental function of turfs, turf's soils are generally characterized by a high draining potential to avoid waterlogging, hindering anaerobic conditions and CH<sub>4</sub> emissions. In addition, the application of ammonium sulfate hampers CH<sub>4</sub> emission by inhibiting the methanogenesis in paddy lands (Schütz et al., 1989; Cai et al., 1997; Le Mer and Roger, 2001).

No significant differences in CH<sub>4</sub> emissions between treatments were observed in tall fescue (Table 2) confirming that dry climatic conditions (Fig. 3) as well as well-drained soil, hamper CH<sub>4</sub> emissions. CH<sub>4</sub> emissions showed an inconstant trend during the whole monitoring period. Differences were observed only at DOY 131 between Control and N2, and at DOY 144 when N2 resulted higher than the other treatments (Fig. 5).

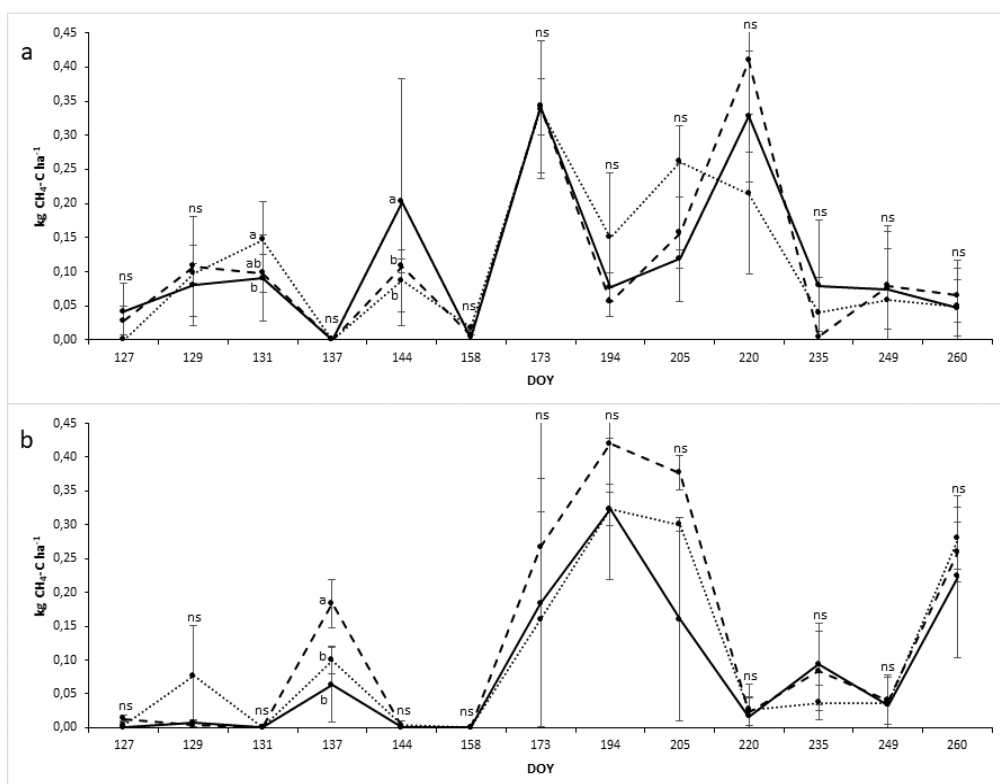


**Figure 5.** Methane emissions ( $\text{kg CH}_4\text{-C ha}^{-1} \text{d}^{-1}$ ) during monitoring period (DOY 127 to DOY 260, 2018) from tall fescue (a) and hybrid bermudagrass (b) at 0 (control), 50 (N1), 150 (N2)  $\text{kg ha}^{-1}$  of N. Dotted line: control; dashed line: N1; solid line: N2. Vertical bars indicate standard deviation. Values with the same letter are not different according to Tukey test ( $P \leq 0.05$ ). Numbers of DOY are in correspondence to GHG measurements

As observed in tall fescue, no significant results were obtained relatively to the effect of N fertilization rate on cumulative CH<sub>4</sub> emission fluxes of hybrid bermudagrass (Table 2). This is supported by the inconstancy in CH<sub>4</sub> emission fluxes during the monitoring period (Fig. 5). The main CH<sub>4</sub> production occurred between DOY 158 and DOY 220 in correspondence of the highest vegetative activity of the turf. Moreover, CH<sub>4</sub> emissions peaks mainly occurred some days after a period of cumulative precipitations of at least 10 mm of rain. In particular, at DOY 137, 194 and 235 the main CH<sub>4</sub> production were observed. If on one hand this is in accordance to Le Mer and Roger (2001) that observed a high correlation between soil water content and CH<sub>4</sub> emissions, from on the other hand tall fescue did not show the same results. This is probably due to the tendency of a mature hybrid bermudagrass stand to create a layer of partially decomposed plant material (thatch) at soil surface thus reducing soil aeration and CH<sub>4</sub> oxidation (Mc Carty and Miller, 2002).

To our knowledge, only few studies on CH<sub>4</sub> emissions by urban turfgrasses, measured with static-chambers, have been conducted yet (Kaye et al., 2004; Groffman and Pouyat, 2009), and no information is available on other type of urban vegetation. Nevertheless, on the contrary to what observed by Kaye et al. (2004) and Groffman and Pouyat (2009), which affirmed that urban lawns are a small net-sink for CH<sub>4</sub>, our results indicate that turf could be considered a small source (0.049 kg CH<sub>4</sub>C ha<sup>-1</sup> d<sup>-1</sup>).

## Conclusions

The massive presence of turfgrasses in urban areas makes it necessary to study the environmental impact of their design and management. Fertilization leads to CO<sub>2</sub> emissions from turfgrasses. In this study, nitrogen fertilization induced a low response in tall fescue with similar CO<sub>2</sub> emissions production between zero and low fertilization rates. On the contrary, hybrid bermudagrass was more sensitive to nitrogen fertilization and CO<sub>2</sub> emissions were stimulated both at low and high N fertilization rates. Nevertheless, similar production of CO<sub>2</sub> was observed between species at the same N rate. No substantial impacts were observed in CH<sub>4</sub> emissions.

Hence, our results highlight that N fertilization management and turf species affect CO<sub>2</sub> emissions. An accurate management of these two features may represent a key factor on C dynamics in green areas.

The authors suggest that further experiments should be focused on the estimation of the role of different turfgrass management practices and species on C storage capacity and GHG emissions. It might be interesting to evaluate the impact of N fertilizers type and time of application as well as the irrigation effect together with clipping management.

Accordingly, this study contributes to broadening the knowledge on a topic of international interest such as climate change and adds information about the management of two of the most used grass species in Mediterranean environment.

For this reason, the assessment of direct soil carbon emissions from different turf species may be considered exhaustive for the evaluation of urban environment.

## REFERENCES

- [1] Alig, R. J., Kline, J. D., Lichtenstein, M. (2004): Urbanization on the US landscape: looking ahead in the 21st century. – *Landscape and Urban Planning* 69(2-3): 219-234.



- [2] Allaire, S. E., Dufour-L'Arrivée, C., Lafond, J. A., Lalancette, R., Brodeur, J. (2008): Carbon dioxide emissions by urban turfgrass areas. – *Canadian Journal of Soil Science* 88(4): 529-532.
- [3] Alluvione, F., Bertora, C., Zavattaro, L., Grignani, C. (2010): Nitrous oxide and carbon dioxide emissions following green manure and compost fertilization in corn. – *Soil Science Society of American Journal* 74(2): 384-395.
- [4] Cai, Z., Xing, G., Yan, X., Xu, H., Tsuruta, H., Yagi, K., Minami, K. (1997): Methane and nitrous oxide emissions from rice paddy fields as affected by nitrogen fertilisers and water management. – *Plant and Soil* 196(1): 7-14.
- [5] Carey, R. O., Hochmuth, G. J., Martinez, C. J., Boyer, T. H., Nair, V. D., Dukes, M. D., Toor, G. S., Shober, A. L., Cisar, J. L., Threnholm, L. E., Sartain, J. B. (2012): A review of turfgrass fertilizer management practices: Implications for urban water quality. – *HortTechnology* 22(3): 280-291.
- [6] Caturegli, L., Lulli, F., Foschi, L., Guglielminetti, L., Bonari, E., Volterrani, M. (2014): Monitoring turfgrass species and cultivars by spectral reflectance. – *European Journal of Horticultural Science* 79(3): 97-107.
- [7] Caturegli, L., Lulli, F., Foschi, L., Guglielminetti, L., Bonari, E., Volterrani, M. (2015): Turfgrass spectral reflectance: simulating satellite monitoring of spectral signatures of main C<sub>3</sub> and C<sub>4</sub> species. – *Precision Agriculture* 16(3): 297-310.
- [8] d'Amour, C. B., Reitsma, F., Baiocchi, G., Barthel, S., Güneralp, B., Erb, K. H., Haberl, H., Creutzig, F., Seto, K. C. (2017): Future urban land expansion and implications for global croplands. – *Proceedings of the National Academy of Sciences* 114(34): 8939-8944.
- [9] Foley, J. A., Defries, R., Asner, G. P., Barford, C., Bonan, G., Carpenter, S. R., Chapin, F. S., Coe, M. T., Daily, G. C., Gibbs, H. K., Helkowsky, J. H., Holloway, T., Howard, E. A., Kucharik, C. J., Monfreda, C., Patz, J. A., Prentice, I. C., Ramankutty, N., Snyder, P. K. (2005): Global consequences of land use. – *Science* 309: 570-574.
- [10] Forster, P., Ramaswamy, V., Artaxo, P., Bernsten, T., Betts, R., Fahey, D. W., Haywood, J., Lean, J., Lowe, D. C., Myhre, G., Nganga, J., Prinn, R., Raga, G., Schulz, M., Van Dorland, R. (2007): Changes in atmospheric constituents and in radiative forcing. Chapter 2. – In: Solomon, S., Qin, D., Manning, M., Chen, Z., Marquis, M., Averyt, K. B., Tignor, M., Miller, H. L. (eds.) *Climate Change 2007. The Physical Science Basis. Contribution of Working Group I to the Fourth Assessment Report of the Intergovernmental Panel on Climate Change*. Cambridge University Press, Cambridge, United Kingdom and New York, NY, USA, pp. 129-234.
- [11] Groffman, P. M., Pouyat, R. V. (2009): Methane uptake in urban forests and lawns. – *Environmental Science & Technology* 43(14): 5229-5235.
- [12] Hamido, S. A., Wood, C. W., Guertal, E. A. (2016): Carbon dioxide flux from bermudagrass turf as affected by nitrogen rate. – *Agronomy Journal* 108(3): 1000-1006.
- [13] Houghton, R. A., Hackler, J. L., Cushman, R. M. (2001): Carbon flux to the atmosphere from land-use changes: 1850 to 1990. – Oak Ridge: Carbon Dioxide Information Center, Environmental Sciences Division, Oak Ridge National Laboratory.
- [14] Ignatieva, M., Ahrné, K., Wissman, J., Eriksson, T., Tidåker, P., Hedblom, M., Katterer, T., Marstorp, H., Berg, P., Eriksson, T., Bengtsson, J. (2015): Lawn as a cultural and ecological phenomenon: a conceptual framework for transdisciplinary research. – *Urban Forestry & Urban Greening* 14(2): 383-387.
- [15] Jo, H. K., McPherson, G. E. (1995): Carbon storage and flux in urban residential greenspace. – *Journal of Environmental Management* 45(2): 109-133.
- [16] Jo, H. K. (2002): Impacts of urban greenspace on offsetting carbon emissions for middle Korea. – *Journal of Environmental Management* 64(2): 115-126.
- [17] Kaye, J. P., Burke, I. C., Mosier, A. R., Guerscham, J. (2004): Methane and nitrous oxide fluxes from urban soils to the atmosphere. – *Ecological Applied* 14(4): 975-981.

- [18] Kaye, J. P., McCulley, R. L., Burke, I. C. (2005): Carbon fluxes, nitrogen cycling, and soil microbial communities in adjacent urban, native and agricultural ecosystems. – *Global Change Biology* 11(4): 575-587.
- [19] Kong, L., Shi, Z., Chu, L. M. (2014): Carbon emission and sequestration of urban turfgrass systems in Hong Kong. – *Science of the Total Environment* 473: 132-138.
- [20] Lal, R., Kimble, J., Stewart, B. A. (1995): World soils as a source or sink for radiatively-active gases. – In: Lal, R., Kimble, J., Levine, E. R., Stewart, B. A. (eds.) *Soil Management and Greenhouse Effect*. Lewis Publishing Inc., Boca Raton, pp.1-8.
- [21] Le Mer, J., Roger, P. (2001): Production, oxidation, emission and consumption of methane by soils: a review. – *European Journal of Soil Biology* 37(1): 25-50.
- [22] Lompo, D. J. P., Sangaré, S. A. K., Compaoré, E., Papoada Sedogo, M., Predotova, M., Schlecht, E., Buerkert, A. (2012): Gaseous emissions of nitrogen and carbon from urban vegetable gardens in Bobo-Dioulasso, Burkina Faso. – *Journal of Plant Nutrition and Soil Science* 175(6): 846-853.
- [23] Ludwig, J., Meixner, F. X., Vogel, B., Förstner, J. (2001): Soil-air exchange of nitric oxide: an overview of processes, environmental factors, and modeling studies. – *Biogeochemistry* 52: 225-257.
- [24] Magni, S., Gaetani, M., Grossi, N., Caturegli, L., La Bella, S., Leto, C., Virga, G., Tuttolomondo, T., Lulli, F., Volterrani, M. (2014): Bermudagrass adaptation in the Mediterranean climate: phenotypic traits of 44 accessions. – *Advances in Horticultural Science* 28(1): 29-34.
- [25] Mc Carty, L. B., Miller, G. (2002): *Managing Bermudagrass turf*. Seelection, construction, cultural practices, and pest management strategies. – John Wiley & Sons., Ann. Arbor. Press., Chelsea (MI).
- [26] Milesi, C., Running, S. W., Elvidge, C. D., Dietz, J. B., Tuttle, B. T., Nemani, R. R. (2005): Mapping and modeling the biogeochemical cycling of turf grasses in the United States. – *Environmental Management* 36(3): 426-438.
- [27] MiPAF (1994): *Metodi ufficiali di analisi chimica e fisica del suolo*. – MiPAF, Rome, Italy.
- [28] Nowak, D. J., Crane, D. E. (2002): Carbon storage and sequestration by urban trees in the USA. – *Environmental Pollution* 116(3): 381-389.
- [29] Oertel, C., Matschullat, J., Zurba, K., Zimmermann, F., Erasmi, S. (2016): Greenhouse gas emissions from soils - A review. – *Geochemistry* 76: 327-352.
- [30] Parkin, T. B., Venterea, R. T. (2010): USDA-ARS GRACEnet Project Protocols, Chapter 3. – In: Follett, R. F. (ed.) *Chamber-based Trace Gas Flux Measurements. Sampling Protocols*. Beltsville, MD, pp. 1-39.
- [31] Patra, S., Sahoo, S., Mishra, P., Chandra, S. C. (2018): Impacts of urbanization on land use/cover changes and its probable implications on local climate and groundwater level. – *Journal of Urban Management* 7(2): 70-84.
- [32] Pouyat, R., Groffman, P., Yesilonis, I., Hernandez, L. (2002): Soil carbon pools and fluxes in urban ecosystems. – *Environmental Pollution* 116: S107-S118.
- [33] Pouyat, R. V., Yesilonis, I. D., Nowak, D. J. (2006): Carbon storage by urban soils in the United States. – *Journal of Environmental Quality* 35(4): 1566-1575.
- [34] Predotova, M., Gebauer, J., Diogo, R. V., Schlecht, E., Buerkert, A. (2010): Emissions of ammonia, nitrous oxide and carbon dioxide from urban gardens in Niamey, Niger. – *Field Crops Research* 115(1): 1-8.
- [35] Qian, Y., Follett, R. (2012): Carbon dynamics and sequestration in urban turfgrass ecosystems. – In: Lal, R., Augustin, B. (eds.) *Carbon Sequestration in Urban Ecosystems*. Springer, Dordrecht, pp. 161-172.
- [36] Rastogi, M., Singh, S., Pathak, H. (2002): Emission of carbon dioxide from soil. – *Current Science* 82(5): 510-517.
- [37] Ritchie, N., Roser, M. (2020): *Urbanization*. – Published online at OurWorldInData.org. Retrieved from: <https://ourworldindata.org/urbanization>.

- [38] Robbins, P., Birkenholtz, T. (2003): Turfgrass revolution: measuring the expansion of the American lawn. – *Land Use Policy* 20(2): 181-194.
- [39] Schütz, H., Seiler, W., Conrad, R. (1989): Processes involved in formation and emission of methane in rice paddies. – *Biogeochemistry* 7(1): 33-53.
- [40] Selhorst, A., Lal, R. (2013): Net carbon sequestration potential and emissions in home lawn turfgrasses of the United States. – *Environmental Management* 51(1): 198-208.
- [41] Shchepeleva, A. S., Vasenev, V. I., Mazirov, I. M., Vasenev, I. I., Prokhorov, I. S., Gosse, D. D. (2017): Changes of soil organic carbon stocks and CO<sub>2</sub> emissions at the early stages of urban turf grasses' development. – *Urban Ecosystems* 20(2): 309-321.
- [42] Townsend-Small, A., Czimeczik, C. I. (2010): Carbon sequestration and greenhouse gas emissions in urban turf. – *Geophysical Research Letters* 37(2): L02707.
- [43] United Nations, Department of Economic and Social Affairs, Population Division (2014): *World Urbanization Prospects: The 2014 Revision. – Highlights (ST/ESA/SER.A/352)*.
- [44] van Delden, L., Larsen, E., Rowlings, D., Scheer, C., Grace, P. (2016): Establishing turf grass increases soil greenhouse gas emissions in peri-urban environments. – *Urban Ecosystems* 19(2): 749-762.
- [45] Verdi, L., Mancini, M., Ljubojevic, M., Orlandini, S., Dalla Marta, A. (2018): Greenhouse gas and ammonia emissions from soil: The effect of organic matter and fertilisation method. – *Italian Journal of Agronomy* 13(3): 260-266.
- [46] Verdi, L., Kuikman, P. J., Orlandini, S., Mancini, M., Napoli, M., Dalla Marta, A. (2019): Does the use of digestate to replace mineral fertilizers have less emissions of N<sub>2</sub>O and NH<sub>3</sub>? – *Agricultural and Forestry Meteorology* 269: 112-118.
- [47] Whalen, S. C. (2005): Biogeochemistry of methane exchange between natural wetlands and the atmosphere. – *Environmental Engineering Science* 22: 73-94.
- [48] Zhang, Y., Qian, Y., Bremer, D. J., Kaye, J. P. (2013): Simulation of nitrous oxide emissions and estimation of global warming potential in turfgrass systems using the DAYCENT Model. – *Journal of Environmental Quality* 42: 1100-1108.

## QUANTITATIVE ANALYSIS OF TOTAL PHENOLICS, FLAVONOIDS AND ANTIOXIDANT ACTIVITY OF OLIVE FRUITS (*OLEA FERRUGINEA*) BASED ON GEOGRAPHICAL REGION AND HARVESTING TIME IN ZHOB DISTRICT, PAKISTAN

MASOOD, A.<sup>1</sup> – MANZOOR, M.<sup>2</sup> – ANJUM, S.<sup>1</sup> – ACHAKZAI, A. K. K.<sup>1</sup> – SHAH, S. H.<sup>3</sup> –  
RIZWAN, S.<sup>4</sup> – TAREEN, R. B.<sup>1</sup> – ISMAIL, T.<sup>1,5\*</sup> – PONYA, Zs.<sup>5</sup> – MUSHTAQ, A.<sup>4</sup> – ULLAH, A.<sup>6</sup>

<sup>1</sup>*Department of Botany, University of Balochistan, Sariab Road, 87300 Quetta, Pakistan*

<sup>2</sup>*Department of Botany, Sardar Bahadur Khan, Women's University, Brewery Road, Quetta, Pakistan*

<sup>3</sup>*Department of Statistics University of Balochistan, Sariab Road, 87300 Quetta, Pakistan*

<sup>4</sup>*Department of Chemistry, Sardar Bahadur Khan, Women's University, Brewery Road, Quetta, Pakistan*

<sup>5</sup>*Department of Plant Protection and Production, Szent István University Kaposvár Campus, Hungary*

<sup>6</sup>*Centre of Advanced Studies in Vaccinology and Biotechnology (CASVAB), University of Balochistan, Pakistan*

\*Corresponding author  
e-mail: tariq.ismail@szie.hu

(Received 7<sup>th</sup> Mar 2020; accepted 11<sup>th</sup> Aug 2020)

**Abstract.** Present study aims to explore fluctuating levels of total phenolic content (TPC), total flavonoid content (TFC) and antioxidant activity (AA) in fruits of *Olea ferruginea* Royle with respect to changing altitude, slope direction and harvesting time in District Zhob, Pakistan. Sampling was performed from three altitudes with approximate difference of 183 meter (600 feet) between each point at north facing and south facing slopes. Fruits were collected from twenty trees around each point, thoroughly washed with running water, shade dried, grinded and extracted against four solvents *i.e.*, water, acetone, 80% ethanol and 80% methanol. Extracts were further analyzed for TPC, TFC and AA (as DPPH radical scavenging activity). Solvent efficiency appears as acetone > 80% methanol > 80% ethanol > water for maximum extraction of TPC, TFC and AA. Analysis of variance (ANOVA) and least significance difference (LSD) tests depicted that olives grown on south facing slopes have significantly higher TPC values as compared to north facing slopes whereas a reverse pattern was observed for TFC. Minimum TPC, TFC and AA was recorded in olives collected from middle altitude that increased with altitude. TPC, TFC and AA showed an increase when fruit fully matured while a drop was observed when green fruit turned purple.

**Keywords:** altitude, slope, ethanol, methanol, acetone

### Introduction

Zhob district, Balochistan is well recognized for its naturally occurring population of wild olive trees. It is located in an agro-ecological zone and occupies 126,719 hectares of agricultural land. It is significant for agriculture and well known for its naturally occurring wild olive forest population. Olive and its various components are valued for their

functional food components and bioactive nutrients that promote health (Ghanbari et al., 2012).

The fruits of *Olea ferruginea* are edible, pickled and utilized as appetizers, antidiabetics and has emmenagogue substances. Olives fruits oil is efficient in oleic acid, utilized for curing scabies, typhoid, eye burning, jaundice, biliousness, toothache and teeth caries (Zabihullah et al., 2006; Ahmad, 2007). Fresh fruit of *Olea ferruginea* Royle in summer season are collected, dried and recommended to diabetics in winter season for reducing blood glucose level in District Attok, Pakistan (Ahmad et al., 2009).

Fruit of *Olea ferruginea* is commercially overlooked and underutilized in Pakistan due to its smaller size apparently. Cultivated varieties of Olive hold important place commercially especially in pharmaceutical and food industry. Phytochemical composition varies in accordance with light availability in slopes, and altitudes (Måren et al., 2015) and on ripening stages. The microclimate has strong relationships with the direction of slope of the area as it influences the topography and the amount of solar radiation received by a specific slope (Sariyildiz et al., 2005). North facing slopes receive minimum amount of radiation and are therefore cool, moist and subject to slow changes in seasonal and daily microclimate. South facing slopes, however, receive maximum solar radiation so they are typically hot and dry and subject to rapid changes in seasonal and diurnal microclimate. Studies have proven that at different stages of development of the plant, the quality and the quantity of total phenols change (Amiot et al., 1986).

Cultivated varieties of Olive hold important place commercially especially in pharmaceutical and food industry. Few studies are available on phenolic contents and antioxidant activities of fruit of *Olea ferruginea* and no work is conducted on fluctuation in phenolics and antioxidant activities of olive fruit with changing slopes, altitudes and ripening stages. Present study deals with these issues. It can contribute to the identification of the best harvesting time, elevation and slope direction that can help to avail maximum phytochemical ingredients of fruit. The main objective of this study is to unveil the influence of geographical positioning and maturation stage on the level of TPC, TFC and AA of *Olea ferruginea* fruit in an area with forest ecosystem and huge climatic and geological variations.

## Materials and methods

Geographical representation of the area with the marked slopes and altitudes were taken. The area was first studied and discussed in the Department of Excellence in Mineralogy, University of Balochistan with the help of toposheets of district Zhob. Brunton® Compass and Global Positioning System (GPS) were used to select the sites for sample collection. The area map was prepared in Geological survey of Pakistan Quetta (*Fig. 1*). *Olea ferruginea* was identified with Flora of Pakistan (Grohmann, 1974) and was confirmed by Dr. Rasool Bakhsh Tareen (qualified plant Taxonomist, University of Balochistan Quetta).

On the basis of contrasting features of north facing and south facing slopes, these two type of slopes were chosen for sampling at different altitudes, at different growth stages of fruit.

The microclimate of area was evaluated with the help of monthly average data of rain fall, relative humidity and temperature for the year 2017 was obtained from Regional Metrological Centre, Pakistan Metrological Department. The 10<sup>th</sup> January was the coldest day of the year with -5°C while the 15<sup>th</sup> June was the hottest day of the year with 41°C. Maximum rainfall was observed on the 14<sup>th</sup> November (28 mm) (*Fig. 2*).

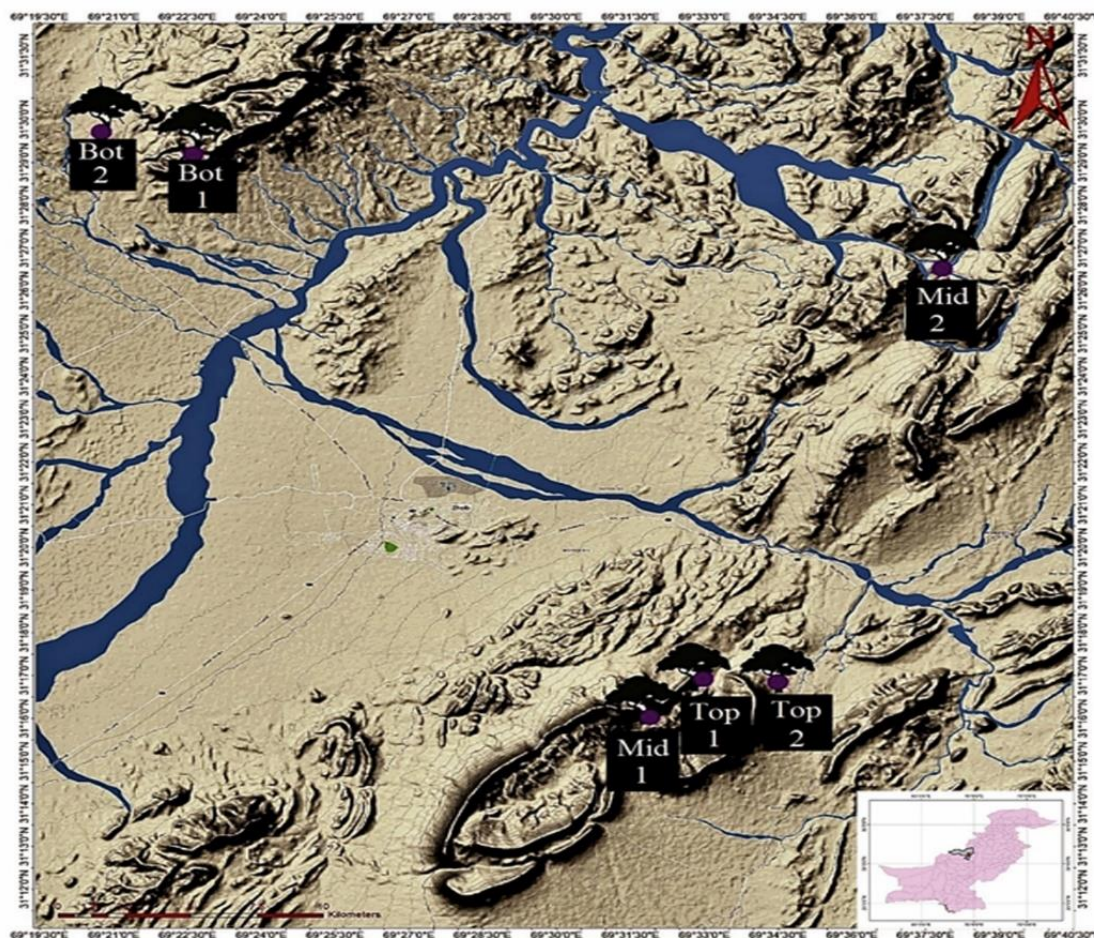


**Figure 1.** Sampling area map prepared on Terra incognita and Geographic Information System (GIS)

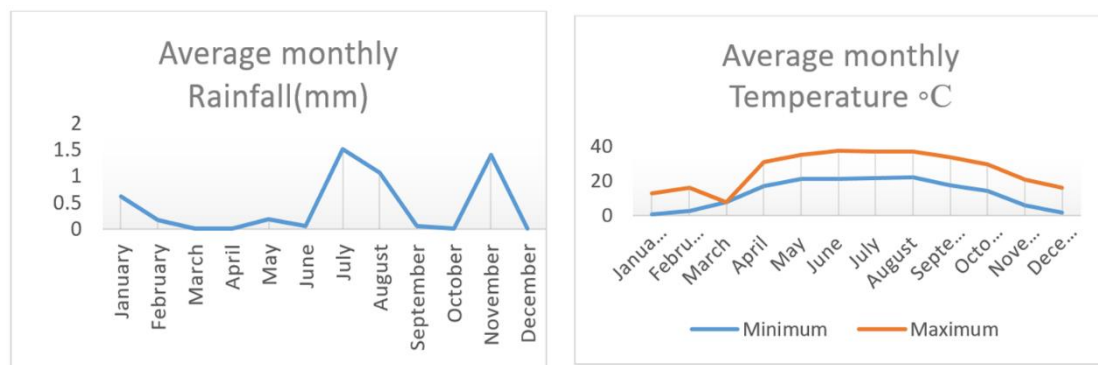


**Figure 2.** Metrological data of average monthly rainfall and average monthly temperature for the year 2017 obtained from Regional Metrological Centre, Metrological Department Pakistan

### Chemicals and reagents

The following chemicals and reagents were used: Methanol (for HPLC  $\geq 99.9\%$  Sigma-Aldrich), Acetone (Sigma-Aldrich), Ethanol (Sigma-Aldrich), Distilled water,



Folin-Ciocalteu's phenol reagent (purchased from BDH), Na<sub>2</sub>CO<sub>3</sub>, NaNO<sub>2</sub>, AlCl<sub>3</sub>, NaOH, Gallic acid, Catechin, diphenyl-picrylhydrazyl (DPPH), Butylated hydroxytoluene (BHT).

### *Fruit sampling*

Local community call Zhob olives "Shnaney", while in urdu olives are known as Zaitoon. Stratified randomized sampling was conducted thrice in a year during crop year 2017-18. North facing and south facing slopes with dense population of test species were further divided in three strata based on elevation difference of approximately 600 feet in between each point. Around each point sampling was performed in a fashion to maintain height and slope direction with the help of Global Positioning System and Brunton compass (*Table 1*). First fruit sampling was conducted on 26<sup>th</sup> June when green olives appeared on trees, second time purple, ripe olives were picked on 26<sup>th</sup> August while last sampling was conducted on 26<sup>th</sup> October when fruit color turned mature blackish purple. From each sampling site fruits were picked randomly from twenty trees and mixed in one zip lock bag to prepare a representative batch of specific site.

**Table 1.** Coordinates, elevation and slope direction of sampling sites recorded with Brunton® Compass and Global Positioning System (GPS)

S.No.	Sampling site code	Slope direction	Dip	Latitudes	Longitudes	Elevation (Meters)
1	TOP 1	North facing	45° N	31°16.637 N	069°32.033 E	1941m
2	MID 1	North facing	10°N	31°29 57.98 N	069°22 29.76 E	1758 m
3	BOTTOM 1	North facing	65°N	31°30 22.15 N	069°20 58.66 E	1576 m
4	TOP 2	South facing	20°S	31°17.0690 N	069°32.836 E	1944 m
5	MID 2	South facing	25°S	31°17.42 N	069°34 43.19 E	1758 m
6	BOTTOM 2	South facing	15°S	31°27 05.49 N	069°35 48.88 E	1576 m

### **Laboratory work**

#### *Processing*

After coming back from field, all fruits of one batch were washed thrice with running water and spread on clean white cloth sheet in a dark aerated room. Fruits were mixed daily and left like that for a month until hard dried fruits were obtained. Then dried fruits were grinded in an electrical grinder to obtain pasty powder.

#### *Extraction*

Powdered fruit was extracted in 80% methanol, 80% ethanol, acetone and water. Extraction was done as per method of Abideen et al. (2015). 50-gram plant material was mixed with 100 ml of each solvent and the mixture was kept in a shaking water bath (Memmert GmbH) for 3 hours maintaining the temperature at 40°C. After 3 hours the flasks were cooled to room temperature and then centrifuged at a speed of 4500 rpm for 15 minutes. Then the supernatant was collected in capped glass tubes and kept at 4°C and was used for further analysis.

### *Quantitative determination of Polyphenols*

#### *Total Phenolic Content (TPC)*

The total phenolic content in fruit extracts were determined by applying some modifications to the procedure described by Folin and Denis (1912). Briefly, 0.5 ml of extract was placed in a test tube, distilled water was added to make the final volume of 17 ml. To the solution, 1 ml of Folin-Ciocalteu reagent was added and then after 8 minutes 2 ml of 7% sodium carbonate solution was added. After 30 minutes of incubation in the dark, the absorbance was measured at 765 nm at Shimadzu UV-Visible Spectrophotometer (UV 160). Gallic acid was used to prepare a set of standards to build a calibration curve. The total phenolic content was expressed as mg of gallic acid equivalent (GAE) per gram of dried fruit.

#### *Total Flavonoid Content (TFC)*

The total flavonoid content of fruit extracts was determined by making a few changes to the method described by Dewanto et al. (2002). Briefly, 1.0 ml of fruit extract solution was placed in a volumetric flask, 5 ml of distilled water was added to it and then 0.3 ml of 5% NaNO<sub>2</sub> was poured into it. The solution was mixed and incubated for 5 minutes at room temperature. Afterwards, 0.6 ml of 10% AlCl<sub>3</sub> was added and the second incubation was performed for 5 minutes at room temperature. Finally, 2 ml of 1M NaOH solution was added and then a volume of 10 ml was achieved by adding distilled water. The absorbance was read at 510 nm using Shimadzu UV-Visible Spectrophotometer (UV 160). All the samples were analyzed in triplicate and the results were expressed as mg/g of Catechin.

#### *Antioxidant activity assay*

The antioxidant activity of fruit extracts were measured by applying the diphenyl-picrylhydrazyl (DPPH) radical degradation method (Queiroz, 2009) with slight modifications. Briefly, 0.5 ml of fruit extract was added in an equal volume of ethanolic solution of DPPH (0.1 mM). The solution was mixed and incubated for 30 min in the dark at room temperature. All the samples were prepared and analyzed in triplicate and the absorbance was noted at 517 nm by means of a Shimadzu UV-Visible Spectrophotometer (UV 160). BHT (Butylated hydroxytoluene) was used as standard control. Inhibition of free radical by DPPH was calculated with Eq. 1.

$$\text{Antioxidant activity (\%)} = \frac{A_{\text{blank}} - A_{\text{sampl}}}{A_{\text{blank}}} \times 100 \quad (\text{Eq.1})$$

where  $A_{\text{blank}}$  is the absorbance of the control reaction mixture without the sample and  $A_{\text{sample}}$  is the absorbance of the sample under investigation.

#### *Statistical analysis*

All the results obtained from chemical analysis were processed on MINITAB software to obtain interaction plots that could reveal any relations between the parameters under consideration *i.e.*, TPC, TFC and AA according to changing slopes, altitudes and plant development stages. STATISTIX software was used to perform analysis of variance (ANOVA) and Least Significance Difference (LSD): a statistically significant difference between groups was true if *p*-values were found less than 0.05.

## Results and discussions

The fruits of *Olea ferruginea* are edible, pickled and utilized as appetizers, antidiabetics, and an olive oil source efficient in oleic acid, utilized for curing scabies, typhoid, eye burning, jaundice, biliousness, toothache and teeth caries (Zabihullah et al., 2006; Ahmad, 2007). Fruit of *Olea ferruginea* is commercially overlooked and underutilized in Pakistan due to its smaller size apparently. Free radicals impair the proper functioning of the immune system leading to the various disease conditions. Flavonoids are naturally occurring phenolic compounds in plants which have antioxidant effect (Imaga et al., 2010).

### Slopes

South facing slopes were found to make TPC of olive fruits higher when compared with phenolics of olives collected from north facing slopes (Fig. 3a,b,c). Results showed a reverse pattern in olives extracted in 80% Methanol (Fig. 3d). TFC of olive fruits also show the same pattern of fluctuation as seen in TPC except for slopes *i.e.*, north facing slopes showed higher flavonoid content (Fig. 4a,c,d) whereas acetone extracts behaved oppositely (Fig. 4b).

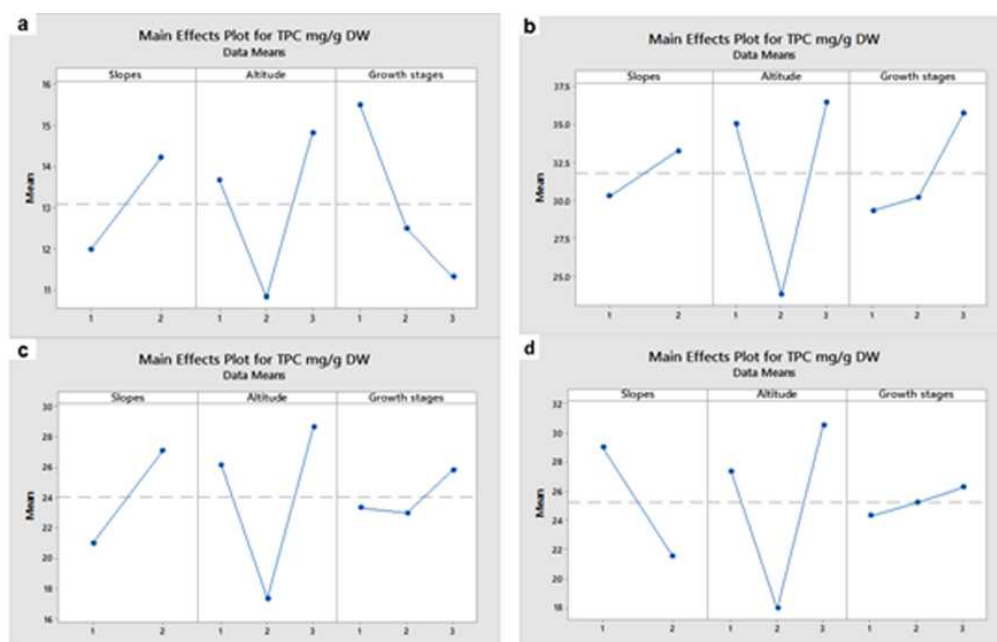


**Figure 3.** Main effect plot for total phenolic contents (TPC as mg/g) of *Olea ferruginea* Royle fruits with respect to slope, altitude, growth stages in four extraction solvents. Slopes: 1= North facing, 2= South facing; Altitude: 1= Top 2= Middle 3= Bottom; Growth stages: 1= Green fruits; 2= Purple ripened fruits; 3= Blackish mature fruits. Solvents: a= water, b= acetone, c= 80% ethanol, d= 80% methanol

### Altitude

Generally, there is an overall decline in TPC, TFC and DPPH radical scavenging activity from the highest to middle altitude while a sudden boost was noted again in fruits collected from bottom of hills *i.e.*, the lowest altitude. Pattern remained similar in all solvent extracts (Figs. 3,4,5).

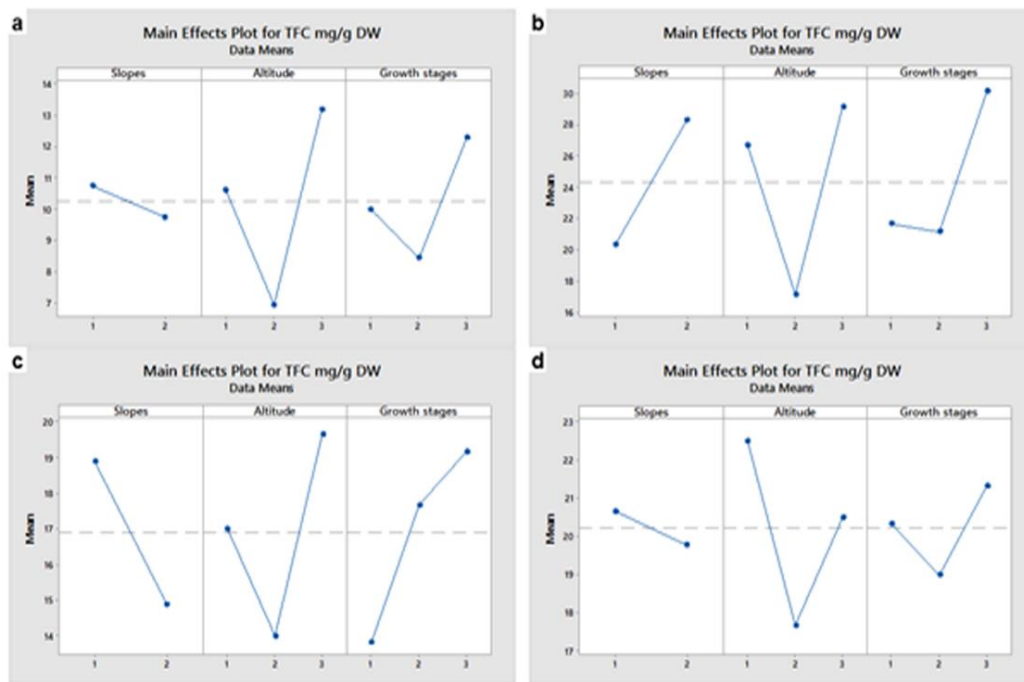


**Figure 4.** Main effect plot for total flavonoid contents (TFC as mg/g) of *Olea ferruginea* Royle fruits with respect to slope, altitude, growth stages in four extraction solvents. Slopes: 1= North facing, 2= South facing; Altitude: 1= Top 2= Middle 3= Bottom; Growth stages: 1= Green fruits; 2= Purple ripened fruits; 3= Blackish mature fruits. Solvents: a= water, b= acetone, c= 80% ethanol, d= 80% methanol

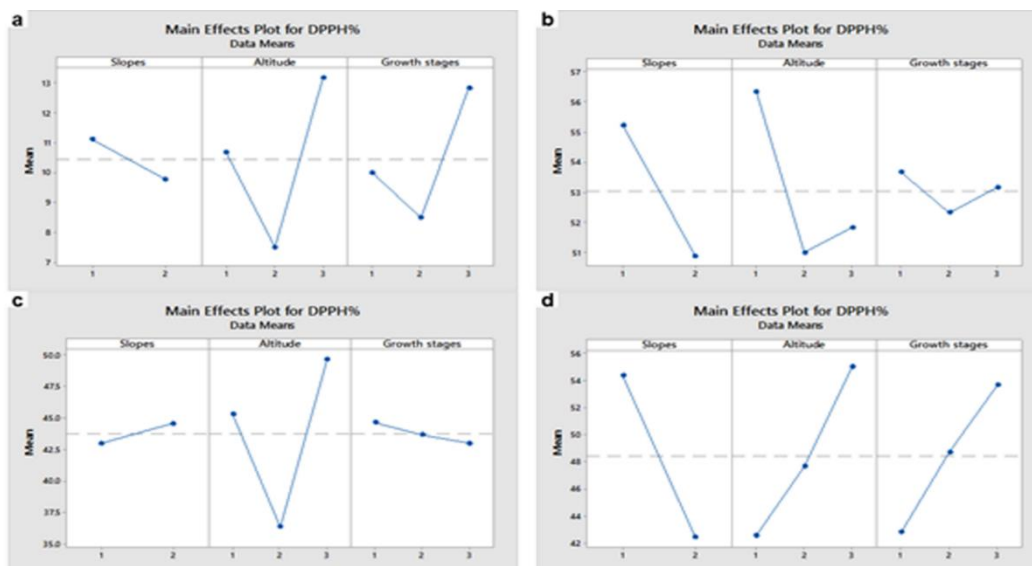


**Figure 5.** Main effect plot for Antioxidant activity (AA) as DPPH radical scavenging activity (%) of *Olea ferruginea* Royle fruits with respect to slope, altitude, growth stages in four extraction solvents. Slopes: 1= North facing, 2= South facing; Altitude: 1= Top 2= Middle 3= Bottom; Growth stages: 1= Green fruits; 2= Purple ripened fruits; 3= Blackish mature fruits. Solvents: a= water, b= acetone, c= 80% ethanol, d= 80% methanol

### Growth stages

Total phenolics of olive fruits increase with maturation and the highest levels were observed at the last maturation stage in the present study that supports the results of Bouaziz et al. (2004) in *Olea europea*. Present study is in agreement with Sharma et al. (2017) who concluded that ripened fruits of *Olea ferruginea* can serve as a good source of natural antioxidants. Peculiarly all phytochemical attributes evaluated (TPC, TFC and AA) in present study showed a steep drop at the second maturation stage of fruit while a maximum increase was observed in the last maturation stage when fruit turned blackish from purple (Figs. 3,4,5) except for TPC of olive fruits in aqueous extract, TFC and AA of 80% ethanol extracts of *Olea ferruginea* that came out differently (Figs. 3a, 4c, 5c).

Total phenolics increase with maturation and the highest levels were observed at the last maturation stage in *Olea europea*. A positive correlation between total phenolic content and antioxidant activity was also recorded. Antioxidant activity also increased with fruit maturation (Bouaziz et al., 2004).

### Extraction solvent

In the recovery process, the extraction solvent plays a fundamental role. In most experiments, either ethanol or methanol was used to extract plant material (Poudyal et al., 2010; Ahmad-Qasem et al., 2013; Kamran, 2016). In food products, ethanol is the predominant solvent but 80% of methanol is known to be the most active solvent in olive leaf biphenols (Malik and Bradford, 2008). Boiling water has also been used for the extraction of biphenols in some of the studies (Pereira et al., 2007; Malik and Bradford, 2008). Most of the phenolic compounds are thought to be present chiefly in free form and can be easily extracted by alcoholic solvents (Hung and Duy, 2012).

Result of analysis performed to examine level of TPC, TFC and AA of *Olea ferruginea* fruits showed significant differences when the fruit was harvested at different ripening stages and from two slopes and three altitudes (Table 2).

**Table 2.** LSD test of TPC, TFC and AA at different slopes, altitudes, growth stages in *Olea ferruginea* fruits extracted in four different solvents

Source	Variations	Total Phenolic Content (mg/g)				Total Flavonoid Content (mg/g)				DPPH (%)			
		Water	Acetone	Ethanol	Methanol	Water	Acetone	Ethanol	Methanol	Water	Acetone	Ethanol	Methanol
Slopes	North	12.00 <sup>b</sup>	30.29 <sup>b</sup>	21.00 <sup>b</sup>	29.00 <sup>a</sup>	10.74 <sup>a</sup>	20.33 <sup>b</sup>	18.89 <sup>a</sup>	20.67 <sup>a</sup>	11.11 <sup>a</sup>	50.89 <sup>b</sup>	43.00 <sup>b</sup>	54.37 <sup>a</sup>
	South	14.22 <sup>a</sup>	33.25 <sup>a</sup>	27.11 <sup>a</sup>	21.56 <sup>b</sup>	9.74 <sup>b</sup>	28.33 <sup>a</sup>	14.89 <sup>b</sup>	19.78 <sup>b</sup>	9.77 <sup>b</sup>	55.22 <sup>a</sup>	44.55 <sup>a</sup>	42.44 <sup>b</sup>
Altitude	Top	13.67 <sup>b</sup>	35.05 <sup>b</sup>	26.16 <sup>b</sup>	27.33 <sup>b</sup>	10.61 <sup>b</sup>	26.67 <sup>b</sup>	17.00 <sup>b</sup>	22.50 <sup>a</sup>	10.67 <sup>b</sup>	56.33 <sup>a</sup>	45.33 <sup>b</sup>	42.55 <sup>c</sup>
	Mid	10.83 <sup>c</sup>	23.83 <sup>c</sup>	17.33 <sup>c</sup>	17.94 <sup>c</sup>	6.94 <sup>c</sup>	17.16 <sup>c</sup>	14.00 <sup>c</sup>	17.67 <sup>c</sup>	7.50 <sup>c</sup>	51.00 <sup>b</sup>	36.33 <sup>c</sup>	47.67 <sup>b</sup>
	Bottom	14.83 <sup>a</sup>	36.44 <sup>a</sup>	28.67 <sup>a</sup>	30.56 <sup>a</sup>	13.16 <sup>a</sup>	29.16 <sup>a</sup>	19.67 <sup>a</sup>	20.50 <sup>b</sup>	13.16 <sup>a</sup>	51.83 <sup>b</sup>	49.67 <sup>a</sup>	55.00 <sup>a</sup>
Growth stages	Green	15.50 <sup>a</sup>	29.33 <sup>c</sup>	23.33 <sup>b</sup>	24.33 <sup>b</sup>	10.00 <sup>b</sup>	21.67 <sup>b</sup>	13.83 <sup>c</sup>	20.33 <sup>b</sup>	10.00 <sup>b</sup>	53.67 <sup>a</sup>	44.67 <sup>a</sup>	42.83 <sup>c</sup>
	Purple	12.50 <sup>b</sup>	30.22 <sup>b</sup>	23.00 <sup>b</sup>	25.22 <sup>b</sup>	8.44 <sup>c</sup>	21.16 <sup>b</sup>	17.67 <sup>b</sup>	19.00 <sup>c</sup>	8.50 <sup>c</sup>	52.33 <sup>b</sup>	43.67 <sup>b</sup>	48.72 <sup>b</sup>
	Black	11.33 <sup>c</sup>	35.77 <sup>a</sup>	25.83 <sup>a</sup>	26.27 <sup>a</sup>	12.27 <sup>a</sup>	30.16 <sup>a</sup>	19.16 <sup>a</sup>	21.33 <sup>a</sup>	12.83 <sup>a</sup>	53.16 <sup>ab</sup>	43.00 <sup>b</sup>	53.67 <sup>a</sup>

Different letters show significant difference between the groups (P < 0.05)

Analysis of variance study clearly shows significant differences between results of TPC, TFC and AA in response to different slope directions, altitudes and growth stages (Tables 3,4,5).

**Table 3.** Factorial analysis of variance for total Phenolic content on the basis of different slopes, altitudes, growth stages and extraction in different solvents

Sources	DF	Water		Acetone		80% Ethanol		80%Methanol	
		F	P	F	P	F	P	F	P
Replicate	2								
Slopes	1	37.99	0.00	79.71	0.00	519.44	0.00	360.53	0.00
Altitude	2	43.4	0.00	578.86	0.00	657.51	0.00	372.37	0.00
Growth	2	47.39	0.00	147.66	0.00	44.47	0.00	8.22	0.00
Slopes*Altitude	2	14.34	0.00	7.71	0.00	39.32	0.00	37.45	0.00
Slopes*Growth	2	0.66	0.52	196.13	0.00	58.90	0.00	107.01	0.00
Altitude*Growth	4	2.37	0.07	12.80	0.00	1.72	0.17	3.27	0.02
Slopes*Altitude*Growth	4	3.51	0.02	83.84	0.00	2.23	0.09	14.35	0.00

Significant at  $p < 0.05$

**Table 4.** Factorial analysis of variance for total Flavonoid content on the basis of different slopes, altitudes, growth stages and extraction in different solvents

Sources	DF	Water		Acetone		Ethanol		Methanol	
		F	P	F	P	F	P	F	P
Replicate	2								
Slopes	1	5.70	0.02	366.18	0.00	269.78	0.00	32.97	0.00
Altitude	2	74.35	0.00	305.79	0.00	180.69	0.00	328.15	0.00
Growth	2	28.25	0.00	195.17	0.00	170.07	0.00	76.24	0.00
Slopes*Altitude	2	8.54	0.00	6.57	0.00	52.46	0.00	219.97	0.00
Slopes*Growth	2	40.84	0.00	51.07	0.00	247.92	0.00	496.61	0.00
Altitude*Growth	4	6.62	0.00	13.99	0.00	14.57	0.00	113.33	0.00
Slopes*Altitude*Growth	4	9.13	0.00	16.95	0.00	47.46	0.00	122.61	0.00

Significant at  $p < 0.05$

**Table 5.** Factorial analysis of variance for total DPPH radical scavenging activity on the basis of different slopes, altitudes, growth stages and extraction in different solvents

Source	DF	Water		Acetone		Ethanol		Methanol	
		F	P	F	P	F	P	F	P
Replicate	2								
Slopes	1	48.32	0.00	164.00	0.00	31.14	0.00	4033.47	0.00
Altitude	2	292.24	0.00	95.85	0.00	793.76	0.00	1479.51	0.00
Growth	2	175.48	0.00	5.28	0.01	12.07	0.00	1112.24	0.00
Slopes*Altitude	2	19.13	0.00	18.44	0.00	31.14	0.00	406.29	0.00
Slopes*Growth	2	248.62	0.00	347.73	0.00	27.33	0.00	44.62	0.00
Altitude*Growth	4	25.00	0.00	110.25	0.00	3.26	0.02	143.99	0.00
Slopes*Altitude*Growth	4	27.68	0.00	17.31	0.00	18.03	0.00	65.80	0.00

Significant at  $p < 0.05$

Results of the present study showed that TPC of olive fruits showed the highest ranges (21-51 mg/g) when extracted in acetone *i.e.*, in opposition with the study of Kamran (2016) who stated that organic solvents are not applicable for the extraction of phenolic acids. These compounds are mainly bound by ester or glycosidic links to the cell wall (Ignat et al., 2011). Therefore, release of these compounds requires acid or base hydrolysis (Kamran, 2016).



After acetone, 80% methanol, 80% ethanol and water stood second, third and fourth for better recovery of TPC, TFC and AA as DPPH radical scavenging activity of olive fruit extracts (Fig. 6).

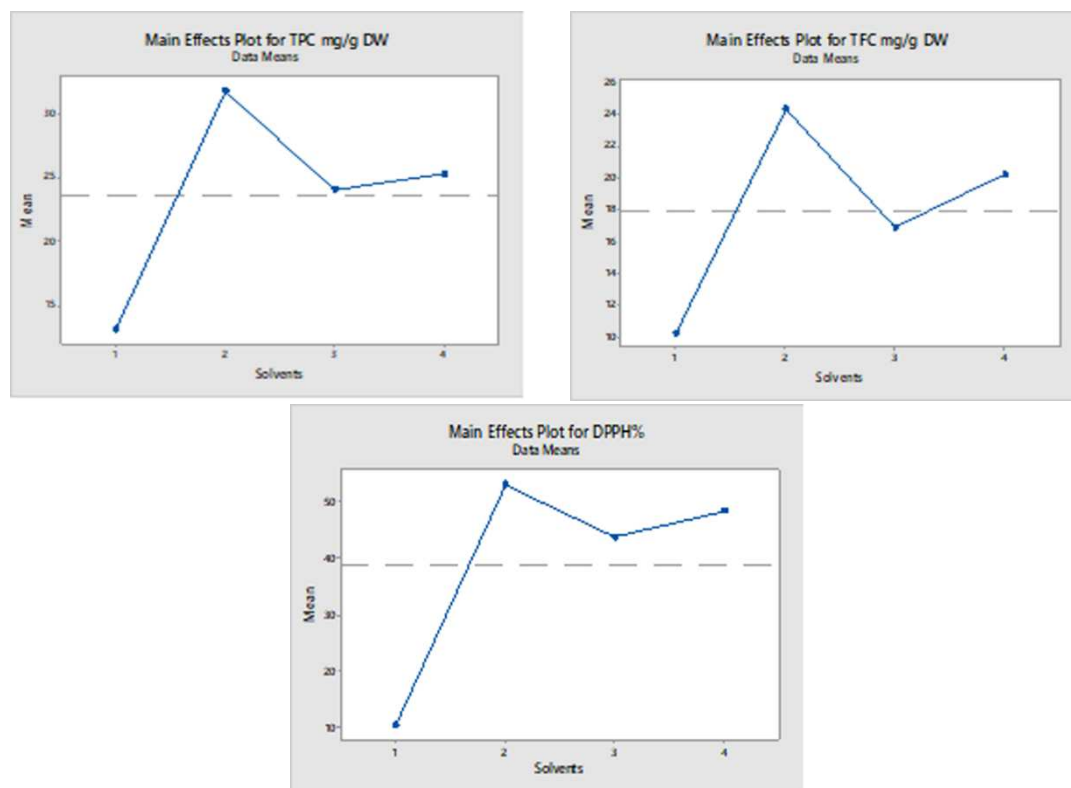


**Figure 6.** Main effect plot for total phenolic content, total flavonoid contents, and antioxidant activity of *Olea ferruginea* Royle fruits with respect to four extraction solvents. Solvents: 1= water, 2= acetone, 3= 80% ethanol, 4= 80% methanol

## Conclusion

*Olea ferruginea* Royale is a commercially underutilized species of naturally occurring olives of Zhob. As this species of olive has small sized fruit and recently oil is main demand from the *Olea sp.* commercially it is underutilized and a way it is a neglected species of olive. But this study revealed the importance of fruit extract to be used in pharmaceutical industry as the fruit is locally used in various ailments. Present work may contribute to finding of the best harvesting time, elevation and slope direction that can help to avail maximum TPC, TFC and AA in olive fruits. It can be concluded that all three studied factors have a strong impact on the quantity of secondary metabolites and radical scavenging capacity. Safely it can be stated according to recent findings that for maximum recovery of polyphenols and a good antioxidant activity, olives can be picked when fully matured. Considering altitudinal impact, it was found that good amount of phenolics can be extracted from olives collected from both extremes *i.e.*, the highest and the lowest altitudes among sampling sites according to the present study. The study also aimed to check the potency of profitable exploitation of olives coming from an underutilized widely distributed species of District Zhob that is non-commercial right now. This can help to boost local income and benefit consumers, industries, markets, and society.

**Acknowledgements.** Authors are very thankful to Professor Emeritus Dr. Akhtar Muhammad Kasi, Department of Geology, University of Balochistan Quetta and Professor Dr. Aimal Kasi, Centre of Excellence in Mineralogy, University of Balochistan Quetta for their technical support during field work and for providing scientific gadgets and maps. Authors are thankful to Nisar Ahmed, Assistant Director at Geological Survey of Pakistan Quetta for his help in preparing area map.

## REFERENCES

- [1] Ahmad, S. S. (2007): Medicinal wild plants from Lahore-Islamabad motorway (M-2). – Pakistan Journal of Botany 39: 355.
- [2] Ahmad, M., Qureshi, R., Arshad, M., Khan, M. A., Zafar, M. (2009): Traditional herbal remedies used for the treatment of diabetes from district Attock (Pakistan). – Pak J Bot 41: 2777-82.
- [3] Ahmad-Qasem, M. H., Barrajon-Catalan, E., Micol, V., Mulet, A., Garcia-Perez, J. V. (2013): Influence of freezing and dehydration of olive leaves (var. Serrana) on extract composition and antioxidant potential. – Food Research International 50(1): 189-196.
- [4] Amiot, M. J., Fleuriet, A., Macheix, J. J. (1986): Importance and evolution of phenolic compounds in olive during growth and maturation. – Journal of Agricultural and Food Chemistry 34: 823-826.
- [5] Bouaziz, M., Chamkha, M., Sayadi, S. (2004): Comparative study on phenolic content and antioxidant activity during maturation of the olive cultivar Chemlali from Tunisia. – Journal of Agricultural and Food Chemistry 52: 5476-5481.
- [6] Dewanto, V., Wu, X., Adom, K. K., Liu, R. H. (2002): Thermal processing enhances the nutritional value of tomatoes by increasing total antioxidant activity. – Journal of Agricultural and Food Chemistry 50: 3010-3014.
- [7] Folin, O., Denis, W. (1912): On phosphotungstic-phosphomolybdic compounds as color reagents. – Journal of Biological Chemistry 12: 239-243.
- [8] Ghanbari, R., Anwar, F., Alkharfy, K. M., Gilani, A.-H., Saari, N. (2012): Valuable nutrients and functional bioactives in different parts of olive (*Olea europaea* L.) - a review. – International Journal of Molecular Sciences 13: 3291-3340.
- [9] Grohmann, F. (1974): Flora of West Pakistan: Oleaceae. – University of Karachi.
- [10] Hung, P., Duy, T. (2012): Effects of drying methods on bioactive compounds of vegetables and correlation between bioactive compounds and their antioxidants. – International Food Research Journal 19: 327.
- [11] Ignat, I., Volf, I., Popa, V. I. (2011): A critical review of methods for characterisation of polyphenolic compounds in fruits and vegetables. – Food chemistry 126: 1821-1835.
- [12] Imaga, N. A., Gbenle, G. O., Okochi, V. I., Adenekan, S., Duro-Emmanuel, T., Oyeniya, B., Dokai, P. N., Oyenuga, M., Otumara, A., Ekeh, F. C. (2010): Phytochemical and antioxidant nutrient constituents of *Carica papaya* and *Parquetina nigrescens* extracts. – Scientific Research and Essays 5(16): 2201-2205.
- [13] Kamran, M. (2016): Olive (*Olea europaea* L.) leaf biophenols as nutraceuticals. – Master's Thesis, Charles Sturt University.
- [14] Malik, N. S., Bradford, J. M. (2008): Recovery and stability of oleuropein and other phenolic compounds during extraction and processing of olive (*Olea europaea* L.) leaves. – Journal of Food Agriculture and Environment 6: 8.
- [15] Måren, I. E., Karki, S., Prajapati, C., Yadav, R. K., Shrestha, B. B. (2015): Facing north or south: Does slope aspect impact forest stand characteristics and soil properties in a semiarid trans-Himalayan valley? – Journal of Arid Environments 121: 112-123.
- [16] Pereira, A., Ferreira, I., Marcelino, F., Valentão, P., Andrade, P., Seabra, R., Estevinho, L., Bento, A., Pereira, J. (2007): Phenolic compounds and antimicrobial activity of olive (*Olea europaea* L. Cv. Cobrançosa) leaves. – Molecules 12: 1153-1162.

- [17] Poudyal, H., Campbell, F., Brown, L. (2010): Olive leaf extract attenuates cardiac, hepatic, and metabolic changes in high carbohydrate-, high fat-fed rats. – The Journal of Nutrition 140: 946-953.
- [18] Queiroz, L. P. D. (2009): Leguminosas da caatinga. – Universidad Estadual de Feira de Santana.
- [19] Sariyildiz, T., Anderson, J., Kucuk, M. (2005): Effects of tree species and topography on soil chemistry, litter quality, and decomposition in Northeast Turkey. – Soil Biology and Biochemistry 37: 1695-1706.
- [20] Sharma, R., Kundra, R., Samant, S., Nandi, S. (2017): Antioxidant Properties of Methanol Extracts from *Olea ferruginea* Royle Seeds. – National Academy science letters 40: 379-382.
- [21] Zabihullah, Q., Rashid, A., Akhtar, N. (2006): Ethnobotanical survey in kot Manzaray Baba valley Malakand agency, Pakistan. – Pak J Plant Sci 12: 115-121.

## APPENDIX

**Table A1.** Total Phenolic Content (mg/g) in fruits of *Olea ferruginea* at different altitudes, slopes, growth stages and extracted in four solvents

Altitude	Growth stages	Northern slopes				Southern slopes			
		Acetone	Water	80% Ethanol	80% Methanol	Acetone	Water	80% Ethanol	80% Methanol
Top	Green fruit	32 ± 1	15 ± 3	22 ± 3	25 ± 1.7	37 ± 1	17 ± 2	28 ± 1	28 ± 1
	Purple fruit	21 ± 1	11 ± 2	12 ± 2	19 ± 1	21 ± 1	15 ± 0	22 ± 1	17 ± 1
	Black fruit	41 ± 4	18 ± 2	24 ± 2	28 ± 1.7	24 ± 2.5	17 ± 0	32 ± 1	29 ± 1
Mid	Green fruit	34 ± 1	10 ± 1.7	25 ± 1.7	32 ± 1	34 ± 2.6	15 ± 1	25 ± 1	22 ± 1
	Purple fruit	22 ± 2.6	8 ± 1	14 ± 1.7	21 ± 1.7	22 ± 1	12 ± 1	19 ± 1	15 ± 0
	Black fruit	43 ± 3	16 ± 1	27 ± 1	40 ± 1	37 ± 1	14 ± 0	28 ± 1	21 ± 1.5
Bottom	Green fruit	32 ± 2.6	12 ± 1	26 ± 1	32 ± 1	42 ± 1	13 ± 1	31 ± 2	25 ± 1
	Purple fruit	25 ± 3	7 ± 1	12 ± 2	22 ± 1	32 ± 1	12 ± 1	25 ± 1	17 ± 1
	Black fruit	33 ± 1.5	11 ± 1	27 ± 1	42 ± 1	51 ± 1	13 ± 1	34 ± 2	23 ± 1.7

Values presented as mean and ±Standard deviation

**Table A2.** Total Flavonoid Content (mg/g) in fruits of *Olea ferruginea* at different altitudes, slopes, growth stages and extracted in four solvents

Altitude	Growth stages	Northern slopes				Southern slopes			
		Acetone	Water	80% Ethanol	80% Methanol	Acetone	Water	80% Ethanol	80% Methanol
Top	Green fruit	22 ± 2.6	9 ± 1	15 ± 1	19 ± 1	22 ± 1	11 ± 1	15 ± 1	22 ± 1.0
	Purple fruit	12 ± 1	5 ± 0	9 ± 1	23 ± 1	19 ± 1	9 ± 1	11 ± 1	13 ± 0
	Black fruit	27 ± 2.6	11 ± 1	12 ± 1	25 ± 0	28 ± 7	15 ± 0	21 ± 1	20 ± 1.0
Mid	Green fruit	18 ± 2	11 ± 0	19 ± 1	27 ± 1	32 ± 1	9 ± 1.1	18 ± 2.6	21 ± 1.7
	Purple fruit	11 ± 1	6 ± 1	21 ± 1	22 ± 1	19 ± 1	6 ± 1	8 ± 0	11 ± 1.0
	Black fruit	22 ± 3	9 ± 1	25 ± 0	15 ± 1	25 ± 2	10 ± 1	15 ± 1	18 ± 1.7
Bottom	Green fruit	25 ± 2.6	15 ± 1	19 ± 1	21 ± 0	41 ± 2.6	9 ± 1	16 ± 1	25 ± 1.7
	Purple fruit	17 ± 1	11 ± 0	23 ± 2	16 ± 1	25 ± 1	8 ± 0	12 ± 1	21 ± 1.0
	Black fruit	29 ± 1	23 ± 1	27 ± 1	18 ± 1	44 ± 2	11 ± 2	18 ± 1.7	27 ± 1.0

Values presented as mean and ±Standard deviation

**Table A3.** Antioxidant activity as DPPH radical scavenging activity (%) in fruits of *Olea ferruginea* at different altitudes, slopes, growth stages and extracted in four solvents

Altitudes	Growth stages	Northern slopes				Southern slopes			
		Acetone	Water	80% Ethanol	80% Methanol	Acetone	Water	80% Ethanol	80% Methanol
Top	Green fruit	58 ± 2.6	35 ± 0	44 ± 1	26 ± 2.6	66 ± 2	42 ± 1	47 ± 1	36 ± 1.0
	Purple fruit	40 ± 1	48 ± 1	35 ± 2	45 ± 1	43 ± 2	32 ± 1	40 ± 1	23 ± 0
	Black fruit	52 ± 1	62 ± 1	50 ± 1	60 ± 1	53 ± 2.6	48 ± 1	52 ± 2	42 ± 1.0
Mid	Green fruit	60 ± 1	35 ± 0	42 ± 2	40 ± 2	52 ± 2	30 ± 0	48 ± 1	39 ± 1.0
	Purple fruit	54 ± 2.6	50 ± 1	38 ± 2	59 ± 2	32 ± 1	42 ± 0	35 ± 0	22 ± 1.0
	Black fruit	52 ± 3.6	64 ± 0	47 ± 1	65 ± 1	44 ± 0	58 ± 1	52 ± 1	50 ± 0
Bottom	Green fruit	57 ± 2.6	33 ± 2	44 ± 1.7	56 ± 2	45 ± 1	21 ± 1	47 ± 1	46 ± 1.7
	Purple fruit	51 ± 2	52 ± 0	38 ± 1	61 ± 1	32 ± 0	19 ± 1	32 ± 1	23 ± 1.0
	Black fruit	62 ± 2	63 ± 1	49 ± 1	65 ± 1	48 ± 1	25 ± 0	48 ± 1	48 ± 1.0

Values presented as mean and ±Standard deviation

# A REVIEW OF BIORETENTION TECHNOLOGY: NEW ISSUES, CURRENT RESEARCHES, AND LIMITATIONS OF NITROGEN REMOVAL PROCESSES UNDER MULTIPLE DRYING-REWETTING ALTERNATIONS

CHEN, Y.<sup>1\*</sup> – FENG, L. K.<sup>1</sup> – GAN, C. J.<sup>2</sup> – YUAN, S. C.<sup>1\*</sup>

<sup>1</sup>*Key Laboratory of Hydraulic and Waterway Engineering of the Ministry of Education, School of River and Ocean Engineering, Chongqing Jiaotong University, Chongqing 400074, China (phone: +86-23-6265-2714; fax: +86-23-6265-0204)*

<sup>2</sup>*Chongqing Municipal Research Institute of Design, Chongqing 400012, China*

*\*Corresponding authors*

*e-mail: chenyaoyao@cqjtu.edu.cn; yuansc@cqjtu.edu.cn*

(Received 18<sup>th</sup> Mar 2020; accepted 20<sup>th</sup> Aug 2020)

**Abstract.** Bioretention technology has become an optimal tool in restorative stormwater management. However, the performance of nitrogen removal lacks good stability in adapting to environmental changes and responding to natural disasters. More specifically, nitrogen leaching is an important problem to be solved under multiple drying-rewetting alternations. Focusing on processes of nitrogen removal in multi-media, the purpose of this manuscript is to summarize the new issues of bioretention system controlling nitrogen, and to elucidate the processes of nitrogen removal from three aspects, including influence of multiple drying-rewetting alternations, characterization of nitrogen process in different spatiotemporal scales and contribution of multi-media. We suggest that future studies of bioretention technology should focus on the explanation of nitrogen leaching mechanism. Wherein, the coupling response relationship between processes of the nitrogen removal is a key issue. To understand this relationship, the quantitative contribution of multi-media to fate and transport of nitrogen, community structure of functional microbes, and microbial metabolic characteristics to nitrogen under multiple drying-rewetting alternations should be studied.

**Keywords:** *stormwater, bioretention, multi-media, nitrogen, leaching, fate and transport, functional bacteria*

## Introduction

Urbanization leads to an increase in impervious surfaces (paved roadways, parking lots, sidewalks, and roof tops), thus decreasing the potential infiltration and evapotranspiration of precipitation, and reducing base flow. These results in accelerated and magnified surficial runoff from urban catchments, a higher intensity of flooding, increased stream bank erosion, and habitat fragmentation and loss (Olang and Fürst, 2011; Rhea et al., 2015). Meanwhile, stormwater runoff also transports pollutants and nutrients from corresponding urban landscapes. Furthermore, elevated levels of contaminants in urban runoff are adverse to the ecological health of urban streams and receiving waters (Qin et al., 2013), collectively referred to as the “urban stream syndrome” (Walsh et al.,

2005). With the continuous expansion of urban populations and urban land cover, these issues will continue to be so in the foreseeable future.

Over past decades, more and more hydraulically efficient drainage infrastructures, termed as the “drainage efficiency” approach, have been used in urban areas for flood mitigation. In practice, however, these approaches proved to be insufficient due to the limited capacity of drainage systems (Mitchell, 2006; Fletcher et al., 2014). Besides, many attempts to mitigate hydrological impacts of urbanization have been characterized by a focus on peak flows. Although stormwater management is essential to alleviate flooding, but above all, it should reduce in-stream erosion pressure, limit nutrient loads in estuaries, and improve stream benthic health. Full recognition of the negative impacts of such an approach to stormwater drainage on water quality and flow regimes reached a consensus (Fletcher et al., 2014), which leads to a more integrated approach to stormwater management, incorporating water quality treatment and mitigating hydrological changes. In a shift away from past peak flow-centric controls, many novel stormwater control measures (SCMs) (e.g. green roofs, permeable pavements, wetlands, ponds, and bioretention systems) are being emphasized and implemented with decentralized systems widely to mitigate the hydrologic impact of large tracts of impervious surface. These SCMs that base on the concept of low impact development (also known as sustainable urban drainage systems, green infrastructure or water sensitive urban design) aim to maintain a natural site water balance through hydrological landscapes, and reach a return to “predevelopment hydrology”. These decentralized measures have been recommended as an innovative solution for restorative stormwater management (Andoh and Declerck, 1997; Montalto et al., 2007; Palhegyi, 2010).

An effective SCM is bioretention, which is achieved by utilizing an engineered system containing a surface ponding layer, vegetation, a soil layer, a storage layer, overflow structures, and an optional underdrain system, depending on the surrounding soil characteristics (Liu et al., 2014). Bioretention (also called biofiltration systems, biofilters, or rain gardens) is increasingly used as a runoff management practice in urbanized areas. This technology has demonstrated excellent performance for reducing the concentrations and loads of pollutants in protection of waterways from polluted urban runoffs (Hatt et al., 2008; Hunt et al., 2008; Roy-Poirier et al., 2010; Debusk and Wynn Thompson, 2011; Liu et al., 2014; Lucke and Nichols, 2015). Furthermore, it can modulate peak flow through on-site retention of storm water with hydraulic capacity (Li et al., 2009; Roy-Poirier et al., 2010; Trowsdale and Simcock, 2011; Debusk and Wynn Thompson, 2011; Ahiablame et al., 2012; Davis et al., 2012; Liu et al., 2014). And bioretention may exist in many different forms, such as rain gardens, swales, or infiltration cells (Laurenson et al., 2013).

Similar as other stormwater treatment facilities, bioretention systems experience high levels of variability in the frequency and period of inundation and intervening dry period. While performance evaluation of bioretention system has mainly remained on actual rainfall events, with little consideration taken to their inter-event (dry weather) behavior.



Researchers using both field and laboratory scale studies have assessed the performance of bioretention systems highlighting the effect of drying-rewetting shifts on nitrogen removal processes. Alarmingly, some results showed that because of the frequency of drying-rewetting alternations bioretention systems not only fail to remove incoming nitrogen, but can leach additional nitrogen, such as nitrate-nitrogen (NO<sub>3</sub>-N) (Cho et al., 2011; Brown et al., 2013; Li and Davis, 2014; Mullane et al., 2015; Mangangka et al., 2015; Chahal et al., 2016; Manka et al., 2016; Wang et al., 2017, 2018; McPhillips et al., 2018; Shrestha et al., 2018), dissolved organic nitrogen (Blecken et al., 2010; Li and Davis, 2014; McPhillips et al., 2018; Shrestha et al., 2018), total Kjeldahl nitrogen (TKN) or total nitrogen (TN) (Blecken et al., 2010; Géhéniau et al., 2014; Mangangka et al., 2015; Mullane et al., 2015; Chahal et al., 2016; Wang et al., 2017; Poor et al., 2018; Shrestha et al., 2018). Thereby, the effluent nitrogen amounts were even elevated up to several orders of magnitude in the leachate compared to the stormwater itself (Payne et al., 2014c; Mangangka et al., 2015; Wang et al., 2017; Poor et al., 2018). Such a solubility and bioavailability of nitrogen flush in discharges could have significant ecological consequences, particularly for small waterways with limited buffering capacity. Unfortunately, to the best of our knowledge, the effect of variable rewetting/drying conditions on underlying nitrogen removal processes and the causes of nitrogen leaching in bioretention systems has been mostly unknown (LeFevre et al., 2014; Payne et al., 2014c). Restorative stormwater management requires the SCMs to adapt to changing climates and to protect the natural water ecologically sensitive areas to the utmost. Especially, it should achieve the protection (or remediation) of urban rivers, lakes and other aquatic ecosystems. Well, in which case, bioretention facilities located in urban areas should have good climate adaptability to control nitrogen in runoff effectively, and ultimately avoid the eutrophication in waters. More than 30 pilot cities in China are promoting the idea of the “sponge city” (Li et al., 2017). It has been found that bioretention technology is the choice for the preferential practices. Consequently, we can conclude that how to remove nitrogen efficiently and steadily is a fundamental issue for sponge city research in China. Meanwhile, the adapting ability of bioretention technology under changing conditions should also be urgently improved to achieve water quality standards in stormwater management. However, the existing theory, methods and measures related to bioretention technology cannot realize the climate adaptability of nitrogen process.

The main objective of this study is to develop a new knowledge relating to nitrogen multi-media process containing plant, soil and microorganism. Firstly, we discussed the unique issues faced in the nitrogen control of the bioretention system. Secondly, the limitation of nitrogen process was summarized and discussed from the following aspects: (1) the effects of multiple alternating wet and dry processes on the nitrogen process; (2) the characterization of nitrogen processes at different spatial and temporal scales; and (3) nitrogen partitioning and transport in multi-media. In this review, we aim to provide important insights and recommendations for future research on the processes of nitrogen

removal. The potential aim is to deepen understanding the mechanisms of the removal of nitrogen in biofiltration system, and assist in improving their design, and ultimately improve their ability to adapt to environmental changes and respond to natural disasters positively.

### **New issues of nitrogen control in bioretention technology**

Researches over the past decade have shown that for many pollutants, such as suspended solids, nutrients, hydrocarbons, and heavy metals, the load of bioretention effluent was low (LeFevre et al., 2014). Nonetheless, many design questions persist for this practice to achieve the permanency of pollutants removal, because removal performance of pollutants is highly variable and dependent on a range of factors including inflow pollution concentrations and environmental factors, especially for 10-years usage bioretention system (Lucke and Nichols, 2015). Few studies consider the long-term performance but focus on simple pollutant removal. In fact, when the removal of pollutants in stormwater is temporary retention, many processes within bioretention system may be better described as attenuation. And the pollutants will be at some point released, either in its original or transformed state. Nitrogen in stormwater is a critical pollutant, which can lead to the eutrophication of downstream waters. There are two pathways for nitrogen removal - temporary immobilization or permanent removal in gaseous form through transformation and cycling processes. Hence, the fate of nitrogen between temporary and permanent removal pathways is fundamental to long-time performance of nitrogen removal for bioretention. While nitrogen biogeochemical processes have been characterized across wide natural and engineered environments, they have not been explicitly quantified in bioretention system with the unique features including frequent alternating rewet and dry cycles, exposure in extreme weathers, and specific engineered structures different from other ecosystems. This knowledge gap of nitrogen permanent control for bioretention leaves the long-term efficiency of nitrogen removal open to question. Some issues of nitrogen processes for bioretention under uncertain rainfall conditions we must work out were proposed in the review, and these problems have constrained the potential for future design improvements in nitrogen removal.

### ***The intermittent wetting and drying conditions of bioretention system are multiplicity and randomness***

Depending on climate change, drought, flooding and human activities, bioretention system will undergo a frequent alternating rewet and dry process. Drying-rewetting cycle has an essential influence on the transfer and transformation of nitrogen (Tan et al., 2012; Payne et al., 2014c). Due to the uncertain feature of rainfall, the intensity and frequency of drying-rewetting alternation will vary. The cycle of wet and dry depends on precipitation intensity and patterns, and results in multiplicity (including drought

exposure, continuous flooding, constant wetting, or repeated rewetting-drying alternation) and high randomness for intermittent wetting and drying conditions. At present, the nitrogen removal characteristics of the bioretention system mainly focus on the simulation of a single rewetting-drying alternative condition. Results of these studies cannot adapt to the natural cycle of drying and rewetting caused by climate changes, and the bioretention facilities may not be able to meet the desired functional goals during operation in practice.

### ***Extreme weather changes the nitrogen process in the bioretention system***

In recent years, the frequently occurring extreme events (including frequent droughts, long-term continuous rainfall, etc.) also warn us that we need to explore and predict the possible changes in the process of nitrogen migration and transformation, to improve the adaptive ability of bioretention system to climate change (Hathaway et al., 2014; Wang et al., 2016). Great modified in the water cycle (e.g. evaporation and rainfall) will affect the intensity and frequency of rewetting and drying alternation cycles, thus affecting plant traits and soil microbial communities and its involved physiological and biochemical processes (Pesaro et al., 2004; Sheik et al., 2011; Evans and Wallenstein, 2012). This has led to some new changes in the role of multi-media (i.e. plant-soil-microbes) on nitrogen.

### ***Bioretention systems differ from other ecosystems characterized by drying-rewetting alternations***

Nitrogen leaching in bioretention systems has a commonality with other ecosystems, such as soils (including hydro-fluctuation belts) and wetlands characterized by alternating dryness and wetness (Gordon et al., 2008; Tan et al., 2012), but it has its individual specificity. Characteristics with rewetting and drying alternation of the lined bioretention facilities are utterly dependent on meteorological conditions and highly random. A lined bioretention system is different from the ecosystem connected to the water through hydrological processes. The path of nitrogen transport is not affected by the seasonal water level fluctuation but is only driven by surface runoff over a short term. As a stormwater treatment facility, plant selection, and its diversity are also different from wetland systems, resulting in a significant change in rhizosphere microbial community (Garbeva et al., 2008). Besides, the initial organic matter in bioretention facilities mainly dominates with engineering-grade sands, and its concentration is very low (Payne et al., 2015), which is different from a high carbon substance in sediments of other ecosystems. These particularities will significantly change the timing and location of nitrogen transfer and transformation in the bioretention system. Therefore, relevant research results and conclusions might not be wholly transferable to the systems.

## Current researches of nitrogen process in bioretention system

### *Influence of variable wetting and drying regimes on nitrogen process*

After the nitrogen in surficial runoff enters into the bioretention system, it undergoes a range of complex biogeochemical processes. The key pathways for nitrogen removal most likely to occur within biofilters are illustrated in *Figure 1*. Incoming nitrogen of the system primarily comprise inorganic and organic compounds. Immobilization (or uptake) by plants and microbes is the initial fate to incoming inorganic nitrogen through biotic processes. Following conversion to a range of organic compounds within the living biomass, nitrogen is released back to the soil through detritus release, exudation, or organism death. Dissolved organic nitrogen (input or released within system) may occur mineralization (or ammonification) to release simpler and more accessible nutrient forms (such as ammonium) through the microbial decomposition processes, and released ammonium may be rapidly re-uptake by plants and microbial biomass. Alternative fates of inorganic nitrogen within a bioretention system include a series of transformation processes.  $\text{NH}_4\text{-N}$  may be oxidized to  $\text{NO}_3\text{-N}$  via the process of nitrification under aerobic conditions, and then  $\text{NO}_3\text{-N}$  can be converted into gaseous nitrogen forms ( $\text{N}_2\text{O}$ ,  $\text{N}_2$ ) through the process of denitrification under submerged (anoxic) zone of biofilters. Other potential processes include the microbial conversion of  $\text{NO}_3\text{-N}$  to  $\text{NH}_4\text{-N}$  in the dissimilatory nitrate reduction to ammonium (DNRA) process (Silver et al., 2001), which acts to retain nitrogen within the system. Abiotic processes include the interaction of  $\text{NH}_4\text{-N}$  with mineral or organic particles through adsorption, chelation, and isomorphic substitution reactions. Therefore, the system can retain nitrogen via abiotic fixation and assimilation to temporary removal of nitrogen, and it also can export in gaseous forms through denitrification to achieve a permanent removal. But it is noteworthy that transformed nutrients can leach from system with effluent. During these processes, nitrogen gradually stores and attenuates, and biogeochemical process of nitrogen is driven by environmental factors (Payne et al., 2014c). The complex processes of nitrogen variation are related to multi-media involved plant, soil, water, and microbial. For example, soil moisture regulates the process of nitrogen transportation and transformation in multiple pathways, such as system connectivity, matrix migration, biological function, and adjusting chemical conditions. There is a remarkable difference between lined bioretention facility and other ecosystems. When bioretention is lined away from native soil, the uncertain multiple rewetting-drying alternations can directly influence multiple media on the process of nitrogen migration and transformation. The bioretention system changes the intrinsic nitrogen cycle mechanism and its corresponding output pathway of nitrogen to a certain extent, resulting in nitrogen leaching. Therein, drought exposure causes significant changes in soil moisture at different spatial and temporal scale, which can promote the coupling of nitrification and denitrification (Wilson and Baldwin, 2008; Minett et al., 2013). However, drought will affect the movement of rhizosphere microorganisms and the growth of plant roots if the dry period is too long. Prolonged

drought even promotes the occurrence of preferential flow in the subsequent rewetting process, resulting in a change of nitrogen migration pathway. At the same time, dry soils will also promote the release of nitrogen under re-humidification, and emission amount is almost logarithmic to antecedent drying days (Hatt et al., 2007; Payne et al., 2014c). In addition, the hydrodynamic processes formed in different wet/dry schemes during/after rainfall can be regarded as a selection pressure for the microbial community composition. It also drives the change of plant root system configuration to affect plant growth and its metabolic function. And in turn, plant activities alter soil oxygen-enrichment capacity and dry-wet cycles. Ultimately, plant, soil together with water drive the occurrence, distribution, and connectivity of nitrogen transformation (Hinsinger et al., 2009; Manka et al., 2016), and makes this process highly complex.

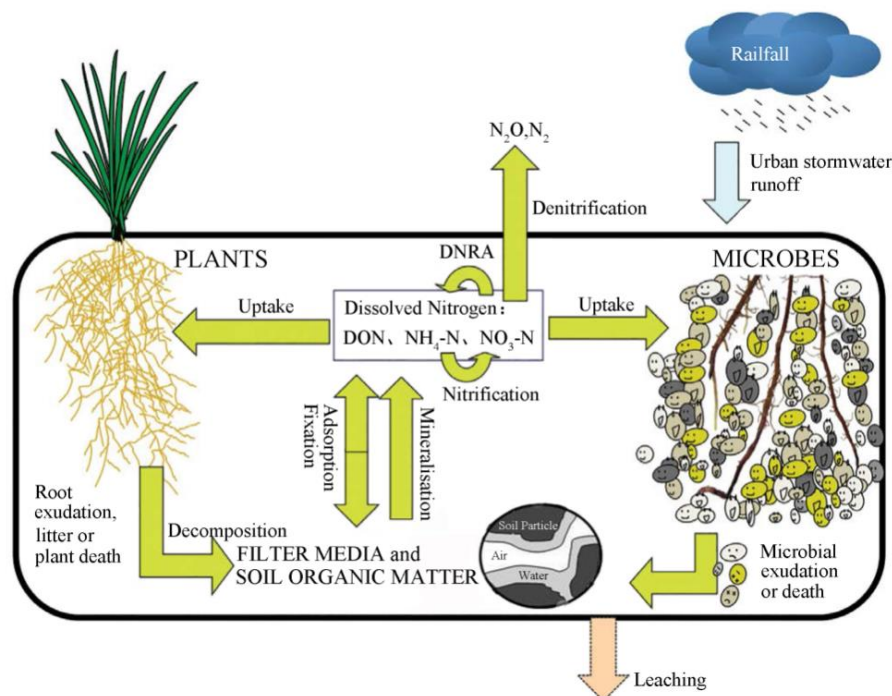


**Figure 1.** Nitrogen cycling in bioretention system. DNRA: Dissimilatory nitrate reduction to ammonium; DON: dissolved organic nitrogen (adapted from (Payne et al. 2014c, Payne et al. 2015), with permission)

### Characterization of nitrogen processes at different spatial and temporal scales

At present, scholars have conducted extensive and in-deep studies on the nitrogen removal characteristics of biofiltration systems from functional plant species screening (Read et al., 2008; Zinger et al., 2013; Payne et al., 2014b; Wang et al., 2017; Wu et al., 2017; Shrestha et al., 2018), filter media composition (Hsieh and Davis, 2005; Glaister et al., 2014; Wang et al., 2017; Shrestha et al., 2018), and optimization design (Davis et al., 2009; Zinger et al., 2013; Glaister et al., 2017; Wang et al., 2018), and have achieved a

series of significant research results. And these studies also promoted the development of bioretention technology. However, previous studies basically adopted a simple “black box” approach, which mainly focused on the cumulative mass reduction of nutrients or plant accumulation, and these static studies mostly last a short-term period. And in practice, the experiment is often simplified to an equivalent simulation of a single dry-wet alternation, in which adopted a single and constant dry-wet alternating frequency based on typical annual rainfall characteristics. These studies fail to fully reveal the nitrogen retention and transformation from the point of the intrinsic development and succession of the ecosystem driven by hydrology of multiple dry/wet schemes. Researchers have gradually regarded a variational hydrological characteristic caused by alternating wetting and drying as a significant influencing factor for nitrogen retention. However, studies mainly focused on the effects of intermittent wetting and drying conditions formed during different antecedent drying periods on nitrogen removal performance; and the results limited to the analysis of nitrogen forms during the wetting period. The previous results did not quantitatively reveal the evolution, migration, and transformation of nitrogen in biogeochemical processes, which was driven by multiple alternating wetting and drying alternations from different spatial and temporal scales (Hatt et al., 2007; Cho et al., 2011; Payne et al., 2014a; Manka et al., 2016; Subramaniam et al., 2016; Tang and Li, 2016). In order to improve the removal rate of  $\text{NO}_3\text{-N}$ , a submerged layer of internal water storage is often created using an upturned elbow in a lined bioretention facility to enhance denitrification (Zinger et al., 2013). Nonetheless, the equilibrium relationship between nitrification and denitrification rate also affects the concentration of  $\text{NH}_4\text{-N}$  and  $\text{NO}_3\text{-N}$  in the effluent (Randall and Bradford, 2013). Furthermore, a study found that even if the denitrification layer was optimized with an embedded carbon source, setting an appropriate height of submerged layer and other measures, it still cannot achieve a continuous and stable removal of  $\text{NO}_3\text{-N}$  (LeFevre et al., 2014). Barron et al. (2019) confirmed that the nitrogen removal performance of the best facility (*Cares appressa* as the dominant plant species) will also appear to a decrease of nitrogen removal rate and then result in leaching when a current best design practice has experienced an extended dry period, as shown in *Figure 2*. Authors’ subsequent research also found that switching water sources (stormwater or greywater) was still vulnerable to leaching again in the initial stage. For example, when the influent of bioretention facility switched from a stormwater source to a greywater source, the nitrogen removal rate decreased from 73% to 62%, and a significant nitrogen leaching phenomenon occurred. These results confirm that an optimal design study of biofilters conducted under controllable factors cannot achieve expected goals under uncertain meteorological conditions. Despite the fact that setting of the submerged layer in an optimal design can alleviate the adverse effect of water evaporation on plants and microorganisms during dry period. A study found that the bioretention system with submerged layer could reduce the soil moisture content to less than 5% after 5 weeks of drought, resulting in soil suffering the most disastrous drought, which severely affected

plant and microbial activity (Blecken et al., 2009). Consequently, the design of bioretention system for single rewetting and drying condition cannot adapt actual rainfall in practice.

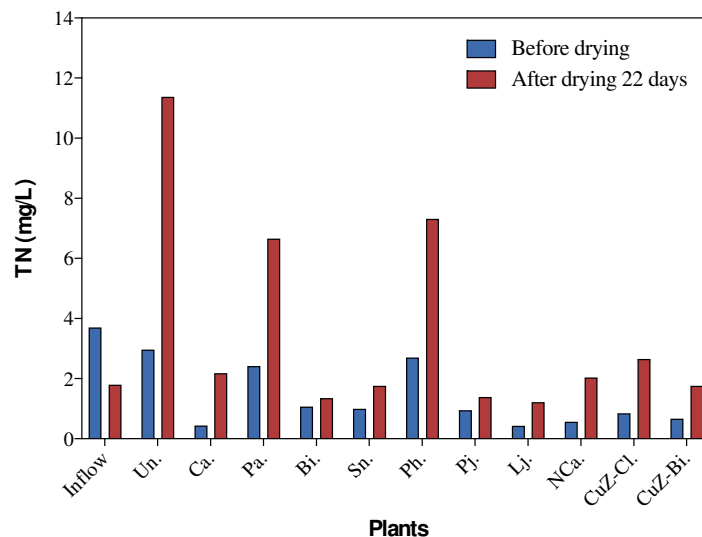


**Figure 2.** Nitrogen removal in dual-mode stormwater-greywater biofilters after long drying period. Species abbreviations: Un., Un-vegetated; Ca., *Cares appressa*; Pa., *Phragmites australis*; Bi., *Boston ivy*; Sn., *Strelitzia Nicolai*; Ph., *Phormiurn*; Pj., *Pandorea jasminoides*; Lj., *Lonicera japonica*; NCa., *Nil Carex appressa*; CuZ-Cl., *Canna lilies with anti-microbial CuZ in the topsoil*; CuZ-Bi., *Boston ivy with anti-microbial CuZ in the topsoil* (data from Barron et al., 2019)

In a bioretention system, which composed of different plants and soil matrix, the interaction process between nitrogen and environmental factors is complicated. Together with uncertain dry-wet alternating conditions, plant holding, microbial nitrification, denitrification, soil adsorption, and end products of nitrogen all have considerable uncertainty. While it is difficult to reflect the behavior and fate of nitrogen in bioretention system using a single research technique and oversimplified method, and exiting studies remain in a qualitative analysis of nitrogen conversion processes. Although a few studies have specialized in the behavior and fate of nitrogen in bioretention systems (Li and Davis, 2014; Payne et al., 2014b), they have not elucidated theoretically why did nitrogen leaching from systems, and lacked quantitative research on the microscopic conversion of nitrogen under variable wetting and drying regimes. The limitations of existing studies on bioretention technology have restricted the possibility of its future design improvements, and it also will affect the reliability of long-term performance, particularly its adaptability to extreme weather conditions.



### ***Nitrogen partitioning and transport in multi-media under different wetting and drying regimes***

Plant immobilization and microbial nitrification - denitrification are considered to be the two primary approaches for the fate of nitrogen in the hydro-fluctuation belt ecosystem up till now (Schade et al., 2002; Hefting et al., 2005), in which, the contribution of denitrification to  $\text{NO}_3\text{-N}$  can reach 30% to 100%. A study has confirmed that the contribution rate of denitrification in bioretention system was not more than 10% through isotopic tracer technology, while the contribution rate of the efficient functional plant to  $\text{NO}_3\text{-N}$  removal reached high than 90% (Payne et al., 2014a). This result is entirely different with the observed results in wetland simulation tests, which showed the relative contribution of nitrogen assimilated by plants was 1.9% to 71% (Koottatep and Polprasert, 1997; Hefting et al., 2005; Langergraber, 2005). It should be noted that wetlands are permanently wet systems, while biofiltration's dry weather treatment processes are crucial for their performance (Hatt et al., 2009). This makes their selection of plants very different (Read et al., 2008), and thus a significant difference in the nitrogen immobilization of plants between them. However, this study cannot fully trace out the fate and pathway of nitrogen because of the only two-month duration, nor did take the impact of environmental factors caused by uncertain dry/wet schemes into account. Plant fixation potential can change gradually and even disappear with the vegetation succession. Vegetation succession can regulate the contact of underground runoff with plant roots and soil particles, affect the metabolic intensity of nitrogen-functional microbes (Hefting et al., 2005), and then promote soil to keep a higher organic substance in a considerable time (Dosskey et al., 2010). Ultimately, organic matter rich in soil particle enhances metabolic activity and diversity of rhizosphere microbes (Zhang et al., 2010). The diversity of vegetation in bioretention system is relatively single and with landscape characteristics. Besides, plant traits are susceptible to seasonal and dry-wet alternations, and they are also different from the wetland plants. Therefore, whether the succession of plant traits in bioretention system under different dry-wet cycles will promote a formation of organic matter pools in low-carbon soils and then affect microbial community structure, to address this question, knowledge transfer needs to be done from other soil-water ecosystems such as hydro-fluctuation belts or wetlands.

Due to the limitations of single research techniques, instruments and methods, even in the widely studied ecosystems such as the riparian belts and wetlands, the researchers focusing on transformation and fate of nitrogen cannot fundamentally solve the quantitative characterization in nitrogen transformation (Groffman et al., 2002; de Vries, 2003; Zhao et al., 2015; Yang et al., 2016). In recent years, the  $^{15}\text{N}$  isotope tracer technology, stable isotope probe (SIP) technology, and gas quantification technology have been put forward to comparatively study the components and contents of nitrogen involved in plant uptake, metabolism, microbial assimilation, transformation (nitrification and denitrification), soil absorption, and other biochemical processes from

multi-level and multi-angle views (Ashkenas et al., 2004; Epstein et al., 2012; Charteris et al., 2016; Cui et al., 2017). And these techniques are widely accepted to be a practical approach for accurately quantifying the migration and transformation of nitrogen in the multi-media ecosystem under alternating wetting and drying environments (Morse and Bernhardt, 2013; Payne et al., 2014a; Oburger and Schmidt, 2016), which can provide a powerful technical tool for the quantitative contribution of multi-media to nitrogen process in bioretention system.

### **Limitations of nitrogen process research in bioretention systems**

The transformation process and fate of nitrogen in bioretention systems are more complex under climate change, and which are driven by many factors such as hydrological environment, climate, plant succession, soil properties, etc. Almost recent studies focused on the monitoring analysis of the difference between nitrogen speciation of inflow and outflow under different macroscopic habitats. It is not able to meet the studying needs on system design optimization, environmental driving mechanism of nitrogen behavior and dynamic mechanism model. Therefore, some critical scientific issues still lack of more explicit answers and await a further investigation. These issues include:

Firstly, the actual contribution of multi-media to fate and transport of nitrogen is still unclear, and its response to changes of environmental factors induced by soil hydrodynamic remains to be explored.

In recent studies on nitrogen fate of bioretention systems, the contribution of multi-media to exogenous imported nitrogen has been primary understood (Payne et al., 2014a), but coupling response studies have not been conducted with changes in environmental factors. A consensus has been basically reached in the academic community. It is widely accepted that hydrological regime caused by surficial runoff can significantly affect the soil water content and its dynamics in bioretention facilities, and then drive the succession of plant root system configuration characteristics. Meanwhile, it can change the oxygen dynamics in soil through root induction, resulting in a spatial heterogeneity with non-rhizosphere soils, and affect a spatial distribution of functional microbes in the rhizosphere. The rhizosphere environment determines the storage and migration processes of nutrients and water, thus regulating the nitrogen of plant uptake and immobilization (Hinsinger et al., 2009; Neuschütz and Greger, 2009). Consequently, these processes have an appreciable impact on nitrogen removal capacity of biofiltration system (Read et al., 2010). A rewetting process can also change soil structure by dissipating soil aggregates due to soil particles expansion and pressure generated by gas retention during wetting (Arias et al., 2005), ultimately resulting in a remarkable effect on plant and microbial functions (Payne et al., 2014c). However, these conclusions can only be used for the qualitative analysis of nitrogen behavior, and they are unclearly explained for the quantitative response relationship between multi-media contribution

and environmental factors change. In particular, it has remained unknown precisely what the source of nitrogen leaching in dry-wet cycles.

Secondly, the analysis of the coupling relationship between functional bacterial community structure and nitrogen process under soil water stress is absent, and the nitrogen metabolism characteristics of functional microbes under different wet-dry cycles are still unidentified.

The environmental behavior of nitrogen in bioretention systems involves many biochemical processes, but recent studies on the migration and transformation of nitrogen in bioretention systems mainly focus on quantitative determination of its input and output forms, qualitative analysis of transformation pathways, and overall effect on macroscopic habitats. Only a few researchers have focused on the spatial and temporal distribution characteristics of nitrogen functional microbial community in wet periods (Chen et al., 2013). There is still a lack of systematic research on the micro-ecological mechanism of nitrogen behavior in the bioretention system during dry-wet alternations. Studies have confirmed that nitrogen leaching from air-dried soils after rewetting mainly comes from the microbial hydrolysis in the drying period or the release of  $\text{NO}_3\text{-N}$  stored in the soil, while  $\text{NH}_4\text{-N}$  will accumulate during the drought and then participate in the subsequent rewetting processes. Consequently, it can safely conclude that nitrogen leaching is a comprehensive result of the synergistic metabolism of various nitrogen-metabolizing bacteria in the soil, and this process is closely related to microbial community structure and functional species. Above all, there is an interaction between nitrogen transport and transformation. If only the temporal and spatial distribution characteristics of the microbial population in the wet period are studied, it is evident that the microscopic mechanism of nitrogen transport and transformation in the multi-media cannot be indeed reflected. While the natural wet/dry alternations caused by meteorological changes positively will affect the ecological environment in biofiltration system, making the species and community structure of nitrogen metabolism bacteria more sophisticated.

## Conclusions

The current study on the contribution of multi-media to the transformation and fate of nitrogen in bioretention system has not been lucubrated, and there are still many problems need to be solved. The review of papers and reports suggest that the multiple rewetting and drying alternations in bioretention systems are the primary objective factors of nitrogen transport and fate without regard to the pulse of nutrient input, which affect or drive plant root system configuration, soil traits, and other habitat factors, and regulate the contribution of multi-media to nitrogen transport and fate, ultimately resulting in a nitrogen leaching.

Further fundamental studies focusing on nitrogen distribution characteristics and its source-sink, plant root architecture, soil properties, and microbial flora formation should be carried out, in order to: 1) clarify the contribution of multi-media to nitrogen transport

and fate under multiple rewetting and drying alternations, 2) reveal the coupling relationship between functional microbial communities and nitrogen conversion path and metabolic flux, 3) explain the nitrogen leaching mechanism in bioretention systems, and 4) assess nitrogen leaching potential. Continued research should lead to refinement of bioretention design and improved performance. In particular, understanding on nitrogen processes within bioretention system can provide a theoretical basis for design optimization of nitrogen removal characteristics, dynamic mechanism model of nitrogen processes and other subsequent studies.

**Acknowledgments.** The authors wish to acknowledge the financial from Natural Science Foundation of China (NSFC) (Grant No. 51709024), Basic Science and Frontier Technology Research Program of Chongqing Science and Technology Commission (Grant No. cstc2017jcyjAX0292), Chongqing Residual Innovation Program Funding Project (Grant No. cx2017065), Chongqing Research Innovation Project of Graduate Students (Grant No. CYS17200 and CYS18219), and Science and Technology Research Program of Chongqing Municipal Education Commission (Grant No. KJ1705140). And the authors would also like to thank three reviewers whose review greatly improved this manuscript.

## REFERENCES

- [1] Ahiablame, L. M., Engel, B. A., Chaubey, I. (2012): Effectiveness of low impact development practices: Literature review and suggestions for future research. – *Water, Air, & Soil Pollution* 223(7): 4253-4273.
- [2] Andoh, R. Y. G., Declerck, C. (1997): A cost effective approach to stormwater management? Source control and distributed storage. – *Water Science and Technology* 36(8-9): 307-311.
- [3] Arias, M., González-Pérez, J., González-Vila, F. J., Ball, A. (2005): Soil health - A new challenge for microbiologists and chemists. – *International Microbiology* 8(1): 13-21.
- [4] Ashkenas, L., Johnson, S., Gregory, S., Tank, J. L., Wollheim, W. M. (2004): A stable isotope tracer study of nitrogen uptake and transformation in an old-growth forest stream. – *Ecology* 85(6): 1725-1739.
- [5] Barron, N. J., Deletic, A., Jung, J., Fowdar, H., Chen, Y., Hatt, B. E. (2019): Dual-mode stormwater-greywater biofilters: The impact of alternating water sources on treatment performance. – *Water Research* 159: 521-537.
- [6] Blecken, G. T., Zinger, Y., Deletic, A., Fletcher, T. D., Viklander, M. (2009): Influence of intermittent wetting and drying conditions on heavy metal removal by stormwater biofilters. – *Water Research* 43(18): 4590-4598.
- [7] Blecken, G. T., Zinger, Y., Deletić, A., Fletcher, T. D., Hedström, A., Viklander, M. (2010): Laboratory study on stormwater biofiltration: Nutrient and sediment removal in cold temperatures. – *Journal of Hydrology* 394(3-4): 507-514.
- [8] Brown, R. A., Birgand, F., Hunt, W. F. (2013): Analysis of consecutive events for nutrient and sediment treatment in field-monitored bioretention cells. – *Water, Air, & Soil Pollution* 224(6): 1581.
- [9] Chahal, M. K., Shi, Z., Flury, M. (2016): Nutrient leaching and copper speciation in compost-amended bioretention systems. – *Science of the Total Environment* 556: 302-309.
- [10] Charteris, A. F., Knowles, T. D. J., Michaelides, K., Evershed, R. P. (2016): Compound-specific amino acid  $^{15}\text{N}$  stable isotope probing of nitrogen assimilation by the soil microbial biomass using gas chromatography/combustion/isotope ratio mass spectrometry. – *Rapid Communications in Mass Spectrometry* 30(16): 1846-1856.

- [11] Chen, X., Peltier, E., Sturm, B. S. M., Young, C. B. (2013): Nitrogen removal and nitrifying and denitrifying bacteria quantification in a stormwater bioretention system. – *Water Research* 47(4): 1691-1700.
- [12] Cho, K.-W., Yoon, M.-H., Song, K.-G., Ahn, K.-H. (2011): The effects of antecedent dry days on the nitrogen removal in layered soil infiltration systems for storm run-off control. – *Environmental Technology* 32(7-8): 747-755.
- [13] Cui, L., Kai, Y., Zhou, G., Huang, W., Zhu, Y. (2017): Surface-enhanced raman spectroscopy combined with stable isotope probing to monitor nitrogen assimilation at both bulk and single-cell level. – *Analytical Chemistry* 89(11): 5793-5800.
- [14] Davis, A. P., Hunt, W. F., Traver, R. G., Clar, M. (2009): Bioretention technology: Overview of current practice and future needs. – *Journal of Environmental Engineering* 135(3): 109-117.
- [15] Davis, A. P., Traver, R. G., Hunt, W. F., Lee, R., Brown, R. A., Olszewski, J. M. (2012): Hydrologic performance of bioretention storm-water control measures. – *Journal of Hydrologic Engineering* 17(5): 604-614.
- [16] de Vries, W. (2003): Uncertainties in the fate of nitrogen II: A quantitative assessment of the uncertainties in major nitrogen fluxes in the Netherlands. – *Nutrient Cycling in Agroecosystems* 66(1): 71-102.
- [17] Debusk, K. M., Wynn Thompson, T. (2011): Storm-water bioretention for runoff quality and quantity mitigation. – *Journal of Environmental Engineering* 137(9): 800-808.
- [18] Dosskey, M. G., Vidon, P., Gurwick, N. P., Allan, C. J., Duval, T. P., Lowrance, R. (2010): The role of riparian vegetation in protecting and improving chemical water quality in streams. – *Journal of the American Water Resources Association* 46(2): 261-277.
- [19] Epstein, D. M., Wurtsbaugh, W. A., Baker, M. A. (2012): Nitrogen partitioning and transport through a subalpine lake measured with an isotope tracer. – *Limnology and Oceanography* 57(5): 1503-1516.
- [20] Evans, S. E., Wallenstein, M. D. (2012): Soil microbial community response to drying and rewetting stress: Does historical precipitation regime matter? – *Biogeochemistry* 109(1): 101-116.
- [21] Fletcher, T., Vietz, G., Walsh, C. J. (2014): Protection of stream ecosystems from urban stormwater runoff : The multiple benefits of an ecohydrological approach. – *Progress in Physical Geography* 38(5): 543-555.
- [22] Garbeva, P., van Elsas, J. D., van Veen, J. A. (2008): Rhizosphere microbial community and its response to plant species and soil history. – *Plant and Soil* 302(1): 19-32.
- [23] Géhéniau, N., Fuamba, M., Mahaut, V., Gendron, M. R., Dugué, M. (2014): Monitoring of a rain garden in cold climate: case study of a parking lot near Montréal. – *Journal of Irrigation and Drainage Engineering* 141(6): 04014073.
- [24] Glaister, B. J., Fletcher, T. D., Cook, P. L., Hatt, B. E. (2014): Co-optimisation of phosphorus and nitrogen removal in stormwater biofilters: the role of filter media, vegetation and saturated zone. – *Water Science and Technology* 69(9): 1961-1969.
- [25] Glaister, B. J., Fletcher, T. D., Cook, P. L. M., Hatt, B. E. (2017): Interactions between design, plant growth and the treatment performance of stormwater biofilters. – *Ecological Engineering* 105: 21-31.
- [26] Gordon, H., Haygarth, P. M., Bardgett, R. D. (2008): Drying and rewetting effects on soil microbial community composition and nutrient leaching. – *Soil Biology and Biochemistry* 40(2): 302-311.
- [27] Groffman, P. M., Boulware, N. J., Zipperer, W. C., Pouyat, R. V., Band, L. E., Colosimo, M. F. (2002): Soil nitrogen cycle processes in urban riparian zones. – *Environmental Science & Technology* 36(21): 4547-4552.
- [28] Hathaway, J. M., Brown, R. A., Fu, J. S., Hunt, W. F. (2014): Bioretention function under climate change scenarios in North Carolina, USA. – *Journal of Hydrology* 519: 503-511.

- [29] Hatt, B. E., Fletcher, T. D., Deletic, A. (2007): Hydraulic and pollutant removal performance of stormwater filters under variable wetting and drying regimes. – *Water Science & Technology* 56(12): 11-19.
- [30] Hatt, B. E., Fletcher, T. D., Deletic, A. (2008): Hydraulic and pollutant removal performance of fine media stormwater filtration systems. – *Environmental Science & Technology* 42(7): 2535-2541.
- [31] Hatt, B. E., Fletcher, T. D., Deletic, A. (2009): Hydrologic and pollutant removal performance of stormwater biofiltration systems at the field scale. – *Journal of Hydrology* 365(3-4): 310-321.
- [32] Hefting, M. M., Clement, J.-C., Bienkowski, P., Dowrick, D., Guenat, C., Butturini, A., Topa, S., Pinay, G., Verhoeven, J. T. A. (2005): The role of vegetation and litter in the nitrogen dynamics of riparian buffer zones in Europe. – *Ecological Engineering* 24(5): 465-482.
- [33] Hinsinger, P., Bengough, A. G., Vetterlein, D., Young, I. M. (2009): Rhizosphere: Biophysics, biogeochemistry and ecological relevance. – *Plant and Soil* 321(1-2): 117-152.
- [34] Hsieh, C.-H., Davis, A. P. (2005): Evaluation and optimization of bioretention media for treatment of urban storm water runoff. – *Journal of Environmental Engineering* 131(11): 1521-1531.
- [35] Hunt, W. F., Smith, J. T., Jadlocki, S. J., Hathaway, J. M., Eubanks, P. R. (2008): Pollutant removal and peak flow mitigation by a bioretention cell in Urban Charlotte, N.C. – *Journal of Environmental Engineering* 134(5): 403-408.
- [36] Koottatep, T., Polprasert, C. (1997): Role of plant uptake on nitrogen removal in constructed wetlands located in the tropics. – *Water Science and Technology* 36: 1-8.
- [37] Langergraber, G. (2005): The role of plant uptake on the removal of organic matter and nutrients in subsurface flow constructed wetlands: A simulation study. – *Water Science and Technology* 51(9): 213-223.
- [38] Laurenson, G., Laurenson, S., Bolan, N., Beecham, S., Clark, I. (2013): The role of bioretention systems in the treatment of stormwater. – *Advances in Agronomy* 120: 223-274.
- [39] LeFevre, G., Paus, K., Natarajan, P., Gulliver, J., Novak, P., Hozalski, R. (2014): Review of dissolved pollutants in urban storm water and their removal and fate in bioretention cells. – *Journal of Environmental Engineering* 141(1): 1-23.
- [40] Li, H., Sharkey, L. J., Hunt, W. F., Davis, A. P. (2009): Mitigation of impervious surface hydrology using bioretention in North Carolina and Maryland. – *Journal of Hydrologic Engineering* 14(4): 407-415.
- [41] Li, L., Davis, A. P. (2014): Urban stormwater runoff nitrogen composition and fate in bioretention systems. – *Environmental Science & Technology* 48(6): 3403-3410.
- [42] Li, H., Ding, L., Ren, M., Li, C., Wang, H. (2017): Sponge city construction in China: A survey of the challenges and opportunities. – *Water* 9(9): 594.
- [43] Liu, J., Sample, D., Bell, C., Guan, Y. (2014): Review and research needs of bioretention used for the treatment of urban stormwater. – *Water* 6(4): 1069-1099.
- [44] Lucke, T., Nichols, P. W. B. (2015): The pollution removal and stormwater reduction performance of street-side bioretention basins after ten years in operation. – *Science of the Total Environment* 536: 784-792.
- [45] Mangangka, I. R., Liu, A., Egodawatta, P., Goonetilleke, A. (2015): Performance characterisation of a stormwater treatment bioretention basin. – *Journal of Environmental Management* 150: 173-178.
- [46] Manka, B. N., Hathaway, J. M., Tirpak, R. A., He, Q., Hunt, W. F. (2016): Driving forces of effluent nutrient variability in field scale bioretention. – *Ecological Engineering* 94: 622-628.

- [47] McPhillips, L., Goodale, C., Walter, M. T. (2018): Nutrient Leaching and Greenhouse Gas Emissions in Grassed Detention and Bioretention Stormwater Basins. – *Journal of Sustainable Water in the Built Environment* 4(1): 04017014.
- [48] Minett, D. A., Cook, P. L. M., Kessler, A. J., Cavagnaro, T. R. (2013): Root effects on the spatial and temporal dynamics of oxygen in sand-based laboratory-scale constructed biofilters. – *Ecological Engineering* 58: 414-422.
- [49] Mitchell, V. G. (2006): Applying integrated urban water management concepts: A review of Australian experience. – *Environmental Management* 37(5): 589-605.
- [50] Montalto, F., Behr, C., Alfredo, K., Wolf, M., Arye, M., Walsh, M. (2007): Rapid assessment of the cost-effectiveness of low impact development for CSO control. – *Landscape and Urban Planning* 82(3): 117-131.
- [51] Morse, J. L., Bernhardt, E. S. (2013): Using <sup>15</sup>N tracers to estimate N<sub>2</sub>O and N<sub>2</sub> emissions from nitrification and denitrification in coastal plain wetlands under contrasting land-uses. – *Soil Biology and Biochemistry* 57: 635-643.
- [52] Mullane, J. M., Flury, M., Iqbal, H., Freeze, P. M., Hinman, C., Cogger, C. G., Shi, Z. (2015): Intermittent rainstorms cause pulses of nitrogen, phosphorus, and copper in leachate from compost in bioretention systems. – *Science of the Total Environment* 537(10): 294-303.
- [53] Neuschütz, C., Greger, M. (2009): Ability of various plant species to prevent leakage of N, P, and metals from sewage sludge. – *International Journal of Phytoremediation* 12(1): 67-84.
- [54] Oburger, E., Schmidt, H. (2016): New methods to unravel rhizosphere processes. – *Trends in Plant Science* 21(3): 243-255.
- [55] Olang, L. O., Fürst, J. (2011): Effects of land cover change on flood peak discharges and runoff volumes: Model estimates for the Nyando River Basin, Kenya. – *Hydrological Processes* 25(1): 80-89.
- [56] Palhegyi, G. E. (2010): Designing storm-water controls to promote sustainable ecosystems: Science and application. – *Journal of Hydrologic Engineering* 15(6): 504-511.
- [57] Payne, E. G. I., Fletcher, T. D., Russell, D. G., Grace, M. R., Cavagnaro, T. R., Evrard, V., Deletic, A., Hatt, B. E., Cook, P. L. M. (2014a): Temporary storage or permanent removal? The division of nitrogen between biotic assimilation and denitrification in stormwater biofiltration systems. – *PLoS One* 9(3): e90890.
- [58] Payne, E. G. I., Pham, T., Cook, P. L. M., Fletcher, T. D., Hatt, B. E., Deletic, A. (2014b): Biofilter design for effective nitrogen removal from stormwater - Influence of plant species, inflow hydrology and use of a saturated zone. – *Water Science and Technology* 69(6): 1312-1319.
- [59] Payne, E. G. I., Fletcher, T. D., Cook, P. L. M., Deletic, A., Hatt, B. E. (2014c): Processes and Drivers of Nitrogen Removal in Stormwater Biofiltration. – *Critical Reviews in Environmental Science and Technology* 44(7): 796-846.
- [60] Payne, E. G. I., Hatt, B. E., Deletic, A., Dobbie, M. F., McCarthy, D. T., Chandrasena, G. I. (2015): Adoption Guidelines for Stormwater Biofiltration Systems. – Cooperative Research Centre for Water Sensitive Cities, Melbourne, Australia.
- [61] Pesaro, M., Nicollier, G., Zeyer, J., Widmer, F. (2004): Impact of soil drying-rewetting stress on microbial communities and activities and on degradation of two crop protection products. – *Applied and Environmental Microbiology* 70(5): 2577-2587.
- [62] Poor, C., Balmes, C., Freudenthaler, M., Martinez, A. (2018): Role of mycelium in bioretention systems: Evaluation of nutrient and metal retention in mycorrhizae-inoculated mesocosms. – *Journal of Environmental Engineering* 144(6): 04018034.
- [63] Qin, H. P., Li, Z. X., Fu, G. (2013): The effects of low impact development on urban flooding under different rainfall characteristics. – *Journal of Environmental Management* 129: 577-585.



- [64] Randall, M. T., Bradford, A. (2013): Bioretention gardens for improved nutrient removal. – *Water Quality Research Journal of Canada* 48(4): 372.
- [65] Read, J., Wevill, T., Fletcher, T., Deletic, A. (2008): Variation among plant species in pollutant removal from stormwater in biofiltration systems. – *Water Research* 42(4-5): 893-902.
- [66] Read, J., Fletcher, T. D., Wevill, T., Deletic, A. (2010): Plant traits that enhance pollutant removal from stormwater in biofiltration systems. – *International Journal of Phytoremediation* 12(1): 34-53.
- [67] Rhea, L., Jarnagin, T., Hogan, D., Loperfido, J. V., Shuster, W. (2015): Effects of urbanization and stormwater control measures on streamflows in the vicinity of Clarksburg, Maryland, USA. – *Hydrological Processes* 29(20): 4413-4426.
- [68] Roy-Poirier, A., Champagne, P., Filion, Y. (2010): Review of bioretention system research and design: Past, present, and future. – *Journal of Environmental Engineering* 136(9): 878-889.
- [69] Schade, J., Martí, E., Welter, J., Fisher, S., Grimm, N. (2002): Sources of nitrogen to the riparian zone of a desert stream: Implications for riparian vegetation and nitrogen retention. – *Ecosystems* 5: 68-79.
- [70] Sheik, C. S., Beasley, W. H., Elshahed, M. S., Zhou, X., Luo, Y., Krumholz, L. R. (2011): Effect of warming and drought on grassland microbial communities. – *The ISME Journal* 5(10): 1692-1700.
- [71] Shrestha, P., Hurley, S. E., Wemple, B. C. (2018): Effects of different soil media, vegetation, and hydrologic treatments on nutrient and sediment removal in roadside bioretention systems. – *Ecological Engineering* 112: 116-131.
- [72] Silver, W. J., Herman, D. J., Firestone, M. K. (2001): Dissimilatory nitrate reduction to ammonium in upland tropical forest soils. – *Ecology* 82(9): 2410-2416.
- [73] Subramaniam, D., Mather, P., Russell, S., Rajapakse, J. (2016): Dynamics of nitrate-nitrogen removal in experimental stormwater biofilters under intermittent wetting and drying. – *Journal of Environmental Engineering* 142(3): 04015090.
- [74] Tan, X., Shao, D., Liu, H., Yang, F., Xiao, C., Yang, H. (2012): Effects of alternate wetting and drying irrigation on percolation and nitrogen leaching in paddy fields. – *Paddy and Water Environment* 11(1-4): 381-395.
- [75] Tang, N. Y., Li, T. (2016): Nitrogen removal by three types of bioretention columns under wetting and drying regimes. – *Journal of Central South University* 23(2): 324-332.
- [76] Trowsdale, S. A., Simcock, R. (2011): Urban stormwater treatment using bioretention. – *Journal of Hydrology* 397(3-4): 167-174.
- [77] Walsh, C. J., Roy, A., Feminella, J. W., Cottingham, P., Groffman, P., Morgan II, R. P. (2005): The urban stream syndrome: Current knowledge and the search for a cure. – *Journal of the North American Benthological Society* 24(3): 706-723.
- [78] Wang, M., Zhang, D. Q., Adhityan, A., Ng, W. J., Dong, J. W., Tan, S. K. (2016): Assessing cost-effectiveness of bioretention on stormwater in response to climate change and urbanization for future scenarios. – *Journal of Hydrology* 543: 423-432.
- [79] Wang, S., Lin, X., Yu, H., Wang, Z., Xia, H., An, J., Fan, G. (2017): Nitrogen removal from urban stormwater runoff by stepped bioretention systems. – *Ecological Engineering* 106: 340-348.
- [80] Wang, C., Wang, F., Qin, H., Zeng, X., Li, X., Yu, S.-L. (2018): Effect of saturated zone on nitrogen removal processes in stormwater bioretention systems. – *Water* 10(2): 162.
- [81] Wilson, J., Baldwin, D. (2008): Exploring the 'Birch effect' in reservoir sediments: Influence of inundation history on aerobic nutrient release. – *Chemistry and Ecology* 24(6): 379-386.

- [82] Wu, J., Cao, X., Zhao, J., Dai, Y., Cui, N., Li, Z., Cheng, S. (2017): Performance of biofilter with a saturated zone for urban stormwater runoff pollution control: Influence of vegetation type and saturation time. – *Ecological Engineering* 105: 355-361.
- [83] Yang, D., Fan, D. Y., Xie, Z. Q., Zhang, A. Y., Xiong, G. M., Zhao, C. M., Xu, W. T. (2016): Research progress on the mechanisms and influence factors of nitrogen retention and transformation in riparian ecosystems. – *Chinese Journal of Applied Ecology* 27(3): 973-980. (in Chinese).
- [84] Zhang, X., Liu, X., Zhang, M., Dahlgren, R. A., Eitzel, M. (2010): A review of vegetated buffers and a meta-analysis of their mitigation efficacy in reducing nonpoint source pollution. – *Journal of Environmental Quality* 39(1): 76-84.
- [85] Zhao, S., Zhou, N., Liu, X. (2015): Occurrence and controls on transport and transformation of nitrogen in riparian zones of Dongting Lake, China. – *Environmental Science and Pollution Research International* 23(7): 6483-6496.
- [86] Zinger, Y., Blecken, G.-T., Fletcher, T. D., Viklander, M., Deletic, A. (2013): Optimising nitrogen removal in existing stormwater biofilters: Benefits and tradeoffs of a retrofitted saturated zone. – *Ecological Engineering* 51: 75-82.

# IDENTIFYING THE KEY ENVIRONMENTAL FACTORS AND BACTERIAL COMMUNITIES IN HUMIFICATION AND THEIR RELATIONSHIPS DURING GREEN WASTE COMPOSTING

LI, L.<sup>1</sup> – GUO, X. P.<sup>1\*</sup> – ZHAO, T. N.<sup>1</sup> – LIU, L.<sup>2</sup> – LI, T. Y.<sup>3</sup>

<sup>1</sup>*College of Soil and Water Conservation, Beijing Forestry University, No.35 Tsinghua East Road, Beijing 100083, PR China*

<sup>2</sup>*Xiong'an Institute of Eco-Environment, Hebei University, No. 180 Wusi East Road, Baoding, 071002 Hebei Province, PR China*

<sup>3</sup>*Tsinghua Tongheng Urban Planning & Design Institute, Qinghe Middle Street, Beijing 100085, PR China*

*\*Corresponding author  
e-mail: guoxp@bjfu.edu.cn*

(Received 23<sup>rd</sup> Mar 2020; accepted 6<sup>th</sup> Oct 2020)

**Abstract.** In this study, the key factors affecting the formation of humic substances (HS) during green waste composting (GWC) and their potential relationships were investigated by setting up different initial particle sizes (IPS) (2 and 5 mm) and C/N (23, 30, and 37) for composting, evaluating the dynamic of environmental factors and humification parameters during the composting, and performing high-throughput sequencing to detect the bacterial structure and diversity dynamics. The results showed that the 2 mm and C/N=23 treatment could promote the degradation of organic matter, increase the fermentation temperature and germination index (GI), and generate a high HS content and humification degree, indicating that the IPS and C/N ratio were the potential controlling factors for composting maturation. Taxonomic analysis showed that the bacterial community structure was significantly different at various stages of composting, while the bacterial community composition of the same composting stage for the different treatments was similar. In addition, a correlation analysis and redundancy analysis showed that the formation of HS was significantly affected by temperature, GI, polyphenols and polysaccharides. *Anaerolineales*, *Cytophagales* and *Blastocatellales* were the important microbial markers of the maturation process. The above results provide insights and potential methods for regulating HS formation during the composting process.

**Keywords:** *compost, humic substances, precursor, maturity, high-throughput sequencing, redundancy analysis*

## Introduction

With the development of ecological construction, the quantity of green waste (GW) could increase accordingly. Because GW is rich in organic matter and abundant nutrient elements, composting treatments represent an effective method of recycling GW. Composting is an aerobic process through which organic matter is decomposed into HS under a characteristic microbial succession. The composting environment and composition and succession of microbial communities all have an impact on the formation of HS (Guo et al., 2019); therefore, we investigated the multidirectional feedback relationship between HS, environmental parameters and microbial communities to determine the key factors that affect the formation of HS. This study provides insights into the regulation of HS formation to improve the quality of GWC.

HS is an important product of aerobic fermentation of organic wastes and an important evaluation standard for the quality of fermented products. During the

composting process, the formation of HS is extremely complex and affected by environmental factors, such as temperature, C/N ratio and particle size, and differences are observed in the influences of different composting processes. For example, studies have shown that composting could be effectively performed at low C/N (Huang et al., 2004; Zhu, 2007), while Silva et al. (2014) found that a low initial C/N could impede the stability of HS and affect the quality of composting. Both Zhang and Sun (2014) and Liu et al. (2018) believed that the appropriate IPS was a potential controlling factor for the physicochemical properties of composting and bacterial diversity, which could accelerate the composting process, although no unified standard was proposed. In addition, recent studies have demonstrated that the precursors of HS, such as polyphenols, proteins, and polysaccharides, have significant effects on the formation of HS (Wu et al., 2017); and Zhang et al. (2018) believed that the addition of exogenous precursors could also regulate the formation of HS. Considering the differences in the element composition and properties of different raw materials, the effect of environmental factors on the rate of HS synthesis and quality of HS varies greatly during the composting process (Wang et al., 2015). Therefore, the relationship between environmental factors and HS in GWC needs further investigation.

Microbial activities have a vital impact on the formation of HS (Song et al., 2014). Studies have shown that microbial diversity interacts with organic matter transformation and HS stability during the composting process (Xi et al., 2016; Zhang et al., 2016), during which bacteria have a strong and considerable influence due to their high quantity and good adaptability to adverse environmental conditions (López-González et al., 2015; Antunes et al., 2016). Bacteria have different activities during different composting stages, which may lead to different formation patterns of HS during the composting process. Therefore, it is important to study the community composition and dynamics of bacteria during the composting process to understand the overall mechanisms underlying the composting humification process. In addition, considering that complex composting environmental factors could influence the composition of microbial communities (Wang et al., 2015; Tortosa et al., 2017), the interactions between environmental factors, bacterial communities and HS must be clarified. Wu et al. (2017) studied the bacterial communities that affect HS using the traditional denaturing gradient gel electrophoresis (DGGE) technique to assess bacterial communities; however, this method is limited by the taxonomic resolution and cannot fully clarify the structure and diversity of composting communities. Therefore, detailed information on the bacterial community dynamics during humification is still lacking. In this study, the high-throughput sequencing method was used to comprehensively and accurately reflect the microbial community structure and objectively reflect the low-abundance but important functional microbes to provide thorough and accurate microbial information to explore the bacterial community succession pattern during the GWC process and its effect on HS.

Therefore, the objectives of this study are to 1) investigate the dynamic changes in environmental factors and the evolution of bacterial community diversity during GWC under different C/N ratios and IPS and 2) clarify the relationships among environmental factors, bacterial communities and HS during the GWC process. This study aimed to identify the key factors that affect HS formation during GWC and promote the formation of HS through the regulation of key influencing factors to provide new insights and technical references for improving the quality of GWC.

## Materials and methods

### Composting materials

GW is supplied by Shoufa Tianren Co. Ltd. in Beijing, China, and the degree of lignification is high. Based on studies by Hanc and Dreslova (2016) and Liu et al. (2018), the waste materials were crushed to two sizes of 2 mm and 5 mm for composting. Urea and sawdust were purchased from Kaiyin Horticulture Co., Ltd. and used to adjust the initial C/N of composting. Combining the results of previous studies (Huang et al., 2004; Silva et al., 2014) and preliminary experiments, three C/N ratios of 23, 30, and 37 were set to investigate the effect of the C/N ratio for GWC (*Table 1*). The microbial inoculum was purchased from Jingpuyuan Co., Ltd. to accelerate the initial composting (Zhang and Sun, 2014). *Table 2* lists basic properties of the green waste and initial composts.

**Table 1.** Set parameters of particle size and C/N

Treatment	Particle size (mm)	C/N
T1	2	23
T2	2	30
T3	2	37
T4	5	23
T5	5	30
T6	5	37

**Table 2.** Basic properties of green waste and initial composts

Treatment	TOC%	TN%	C/N ratio	pH value	EC (mS/cm)
GW	34.54±0.95	1.20±0.05	28.76±0.24	6.86±0.03	0.97±0.12
T1	33.31±1.62	1.39±0.06	23.90±0.17	7.25±0.07	1.19±0.08
T2	34.01±1.37	1.12±0.04	30.43±0.68	7.15±0.05	0.92±0.04
T3	37.22±0.65	1.02±0.04	36.50±0.77	7.05±0.05	0.86±0.00
T4	34.49±2.40	1.45±0.08	23.76±1.00	7.40±0.08	1.00±0.03
T5	35.01±0.48	1.14±0.08	30.71±0.38	7.00±0.03	0.82±0.06
T6	36.10±1.21	0.96±0.07	37.41±0.73	7.00±0.06	0.79±0.04

Notes: Data are reported as mean (n = 3). TOC: total organic carbon; TN: total nitrogen; EC: electrical conductivity

### Composting procedure and sampling

A total of 6 treatments were performed, with 3 replicates for each treatment (*Table 1*). The mixture was placed into plastic reactors (*Fig. 1*) with a diameter of 0.25 m, a height of 0.31 m and a volume of 10 L. A number of ventilation holes were left at the top, and a thermometer was fixed in the middle of the reactors to monitor the temperature change during the process. The reactor was placed in an incubator to compensate for the heat loss and simulate the self-heating process during the composting process. The temperature of the climate chamber was kept below the temperature of the fermenter by 3~5 °C (Li et al., 2013), and the composting process lasted 30 days. The water content in the compost was adjusted to 65% by the addition of

distilled water, and the water content was maintained at 55%-65% during the composting process. The reactors were manually flipped for 2 minutes every 2 days to ensure that sufficient oxygen was available. On the 0, 2, 5, 9, 15, 22 and 30 days, 150 g (wet weight) of the sample from each fermenter was collected, and it was divided into two parts: one part was air dried, the other part was stored at 4 °C. On the 2, 9, and 30 days, the samples were immediately subjected to microbiological examination. The samples used for the microbial analysis were labelled as T1D2-T6D2, T1D9-T6D9 and T1D30-T6D30, and they represented the composting heating phase, thermophilic phase and maturity phase.

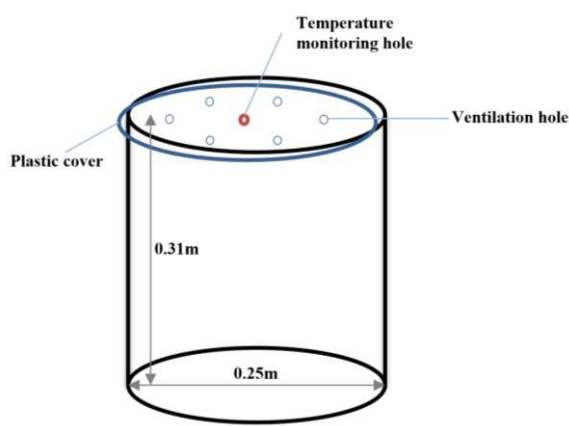


**Figure 1.** The illustration of the composting reactor

### **Chemical and physical analysis**

Air-dried samples were used to determine the total organic carbon (TOC), total nitrogen (TN), humic substance (HS), humic acids (HA), fulvic acid (FA), as described by Liu et al. (2018). Water content was measured with oven drying method (Zhang et al., 2020). The  $E_4/E_6$  ratio is the absorbance ratio at wavelengths 465 and 665 nm, which was measured using an ultraviolet spectrophotometer (TU-1810DS). The humification indexes were calculated as Wu et al. (2017) described. The pH, electrical conductivity (EC), germination index (GI) were measured using fresh samples in accordance with Li et al. (2012), GR (germination rate) and GI was calculated as follows (Zhang and Sun, 2019):

$$F_{GR} = \frac{S_T}{S_C} \times 100\% \quad (\text{Eq.1})$$

$$F_{GI} = \frac{S_T \cdot L_T}{S_C \cdot L_C} \times 100\% \quad (\text{Eq.2})$$

where  $F_{GR}$  – germination rate;  $S_T$  – seed germination of treatment;  $S_C$  – seed germination of control;  $F_{GI}$  – germination index;  $L_T$  – average root length of treatment (mm);  $L_C$  – average root length of control (mm).

The amino acid content was determined using a ninhydrin color liquid. The total polysaccharide and reducing sugar contents were determined using an anthrone reagent

and dinitrosalicylic acid (DNS) reagent. The calcium acetate method reported by Zhang et al. (2018) was used to determine the carboxyl group content. For detection of polyphenolic compounds contents, composting samples were extracted with 80% methanol, and the extraction was analysed by the Folin-Ciocalteu assay using an ultraviolet spectrophotometer (Li et al., 2015).

### ***Microbial analysis***

The DNA was extracted from fresh compost samples using the E.Z.N.A.® Bacterial DNA Kit (Omega Bio-tek, Norcross, GA, USA) following the manufacturer's protocol. Agarose gel electrophoresis (1%) and spectrophotometry were applied to detect the purity and quantity of the extracted DNA. Using universal primers forward 338F (5'-ACTCCTACGGGAGGCAGCAG-3') and the reverse 806R (5'-GACTACHVGGGTWTCTAAT-3') amplified the bacterial 16S rRNA gene (V3–V4 hypervariable region). Polymerase chain reaction (PCR) condition and the procedure were performed as Liu et al. (2018). Moreover, the PCR amplicons were extracted and purified using agarose gels (2%) and AxyPrep DNA Gel purification kit (AXYGEN Inc.). High-throughput sequencing and sequence read archive were on the Illumina MiSeq PE300 sequencing platform (Illumina Inc., CA, USA) by Beijing Allwegene Tech Ltd. (Beijing, China). The raw sequence data were processed and analyzed in the QIIME 1.8.0 to obtain high-quality sequences.

### ***Statistical analysis***

All analyses were repeated three times. Dynamics of environmental parameters were assessed by ANOVAs at significance  $p < 0.05$  level, when ANOVAs were significant, means were separated with an LSD test. For statistical analysis of data, Origin 2018 and SPSS version 23 were used. Besides, Canoco 5.0 was used to analyse the relationship among environmental factors, bacterial community composition, and humic substance by redundancy analysis.

## **Results and discussion**

### ***Dynamics of environmental factors during composting***

#### ***Temperature***

During the aerobic fermentation process, the oxidation reaction of microbes causes the self-heating effect of the compost, and the change in temperature reflects the severity of the decomposition activities of microorganisms (Dzulkurnain et al., 2017). As shown in the *Fig. 2a*, because of a suitable temperature and humidity create favorable conditions for fermentation, the temperature increased rapidly at the initial stage of composting, the average temperature at 5 mm (41.87°C) in the heating phase of the composting was higher than that of 2 mm (40.96°C), indicating that the 5 mm treatment had a stronger mineralization capacity, which might be due to the low initial oxygen content and lower microbial activity in the early stage caused by the small IPS. Afterwards, the proper compost turning treatment optimized the porosity of composting, the relatively high specific surface area of 2 mm IPS was more conducive to microbial growth and promoted heat accumulation. Thus, from heating phase to thermophilic phase, a larger average temperature increase was observed in the 2 mm treatments



(10.59°C) than that of 5 mm (8.61°C). During the whole composting process, the order of the average temperatures for the six treatments was T1>T2>T4>T3>T5>T6, the average temperature of the 2 mm IPS was higher than that of the 5 mm IPS and the average temperature decreased with increases in the C/N ratio.

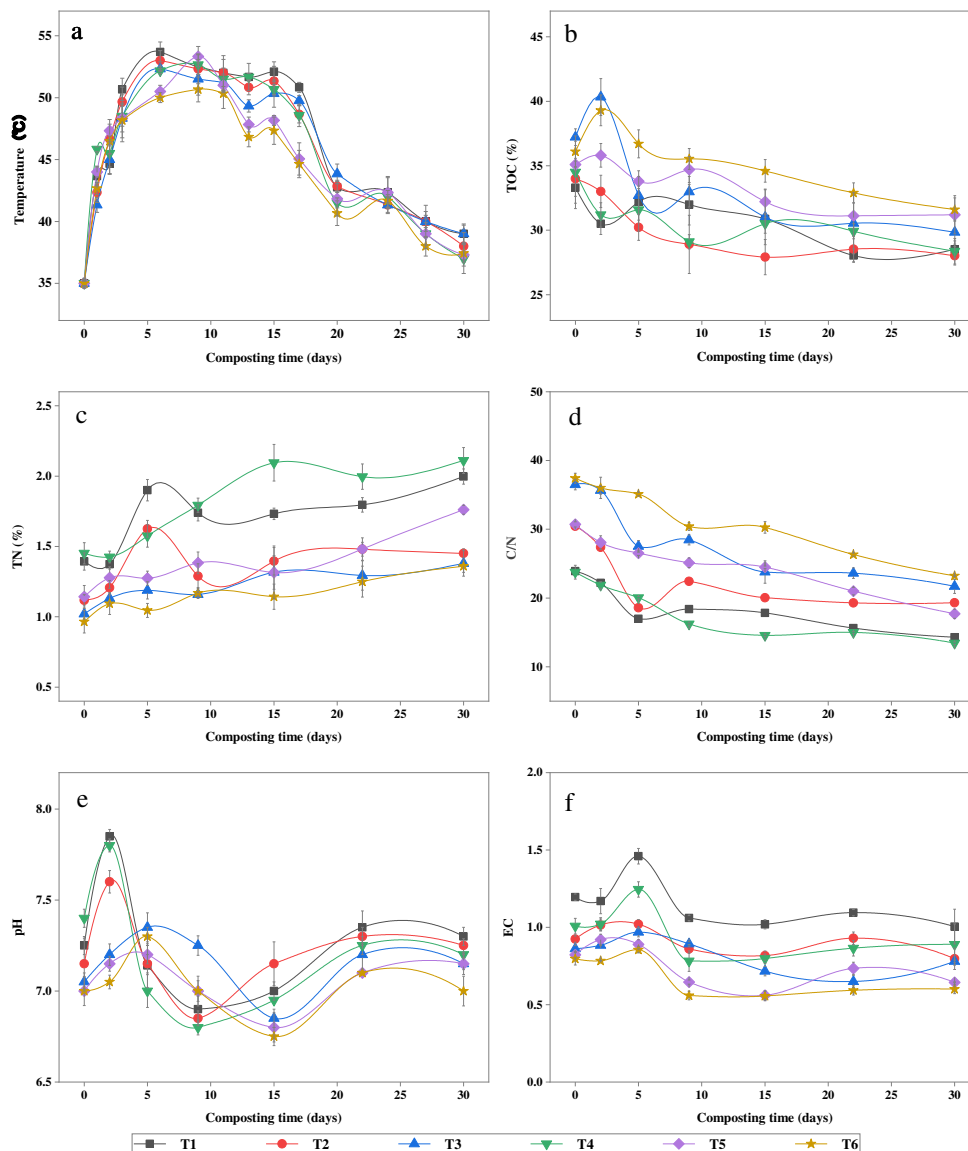


**Figure 2.** Dynamic of temperature (a), TOC(b), TN(c), C/N (d), pH (e) and EC (f) during composting [Error bars represent standard deviation (means  $\pm$  SD, n=3)]

### C/N ratio

As shown in Fig. 2b,c, compared with the initial composting, the organic carbon content of all composting products decreased and the TN content increased. The average reduction of organic carbon in the 2 mm treatment (6.04%) was greater than those of the 5 mm treatment (4.84%), indicating that the 2 mm IPS of GWC was more conducive to the decomposition activities of microorganisms.

The C/N ratio reflects the progress of mineralization in the composting process and is closely related to the maturity of the composting product (Khalil et al., 2008; Lobna et al., 2019). In this study, the organic carbon in the compost was catabolized faster than nitrogen under microbial action, all treatments C/N ratio showed a decreasing trend (Fig. 2d). Among them, the final C/N of T1 and T4 treatments is significantly lower than other treatments ( $p < 0.05$ ), which indicating that the low initial C/N ratio can accelerate the mineralization process of composting, thereby effectively promoting humification and improving the maturity of composting products.

#### *pH and EC*

pH plays an important role in the activity of composting microorganisms. Researchers in the composting field believe that the activity and reproductive capacity of common microorganisms are highest when the pH value is 6.5-7.5 (Zhang and Sun, 2018). In this study, the pH first increased, then decreased, and then fluctuated to a steady state (Fig. 2e). The pH in the 2 mm treatments started to increase faster than that in the 5 mm treatments. In the same IPS treatments, the lower the C/N ratio, the higher the pH value, which is because the increase in microbial activity at the initial stage could increase the decomposition of easily degradable organic nitrogen, thereby increasing the release of ammonia and resulting in a sharp increase in pH at the initial stage. The low-C/N ratio treatments can provide more nitrogen sources for the microorganisms so that the pH increases even faster. The decrease in pH value in the late stage might be due to the release of  $\text{NH}_3$  and  $\text{H}^+$  during the nitrification process (Wang et al., 2017).

EC reflects the total salt content in the compost (Awasthi et al., 2014) and thus can be used as an index for the decomposition and polymerization kinetics of organic matter. As shown as Fig. 2f, EC increased to a peak value in the early stage of decomposition and then decreased and stabilized with the binding and conversion of soluble products (such as organic acids and salts) into HS (Petric et al., 2012; Chen et al., 2017). The 2 mm IPS treatments had a high EC value, indicating that these treatments contained more salts and small molecules, which may be related to the high specific surface area of the small IPS treatments, thus increasing the ion exchange capacity.

#### *Precursors*

Polyphenols, carboxyl, amino acids, reducing sugars and polysaccharides are considered to be involved in the formation of HS through biochemical synthesis (Guo et al., 2019). The Fig. 3a-e showed changes in 5 HS precursor concentrations during composting. The contents of amino acids and reducing sugars showed a decreasing trend, the contents of phenolic and carboxyl groups first increased and then decreased, and the total polysaccharides showed an overall upward trend. The trends of different treatments were basically consistent, and the concentration changed more dramatically during the heating and thermophilic phases because of the many easily degradable substances and high activity of microorganisms in the early stage of composting. Under intense microbial degradation, lignin is partially degraded to produce small molecule polyphenols, and simultaneously, abundant enzymes are secreted to degrade fat and oxidize hydroxyl groups to form carboxyl groups; thus, polyphenols and carboxyl concentration are increased in the early stage. The produced amino acids and sugars, which are the main energy sources of microorganisms, are used in large quantities, and their concentrations decrease.

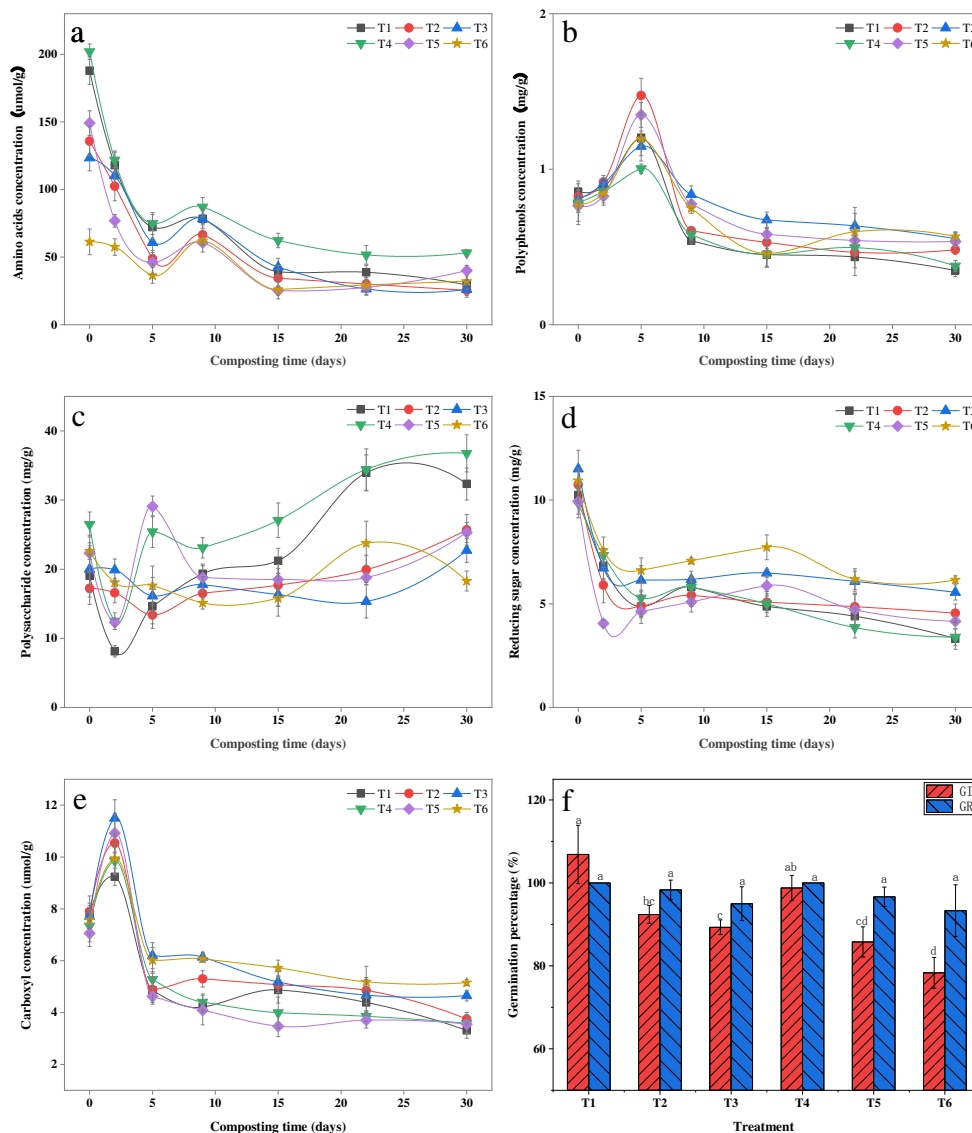


**Figure 3.** Changes in the precursors including (a) amino acids, (b) Polyphenols, (c) polysaccharides, (d) reducing sugars, (e) carboxyl; and (f) GI in different composting treatments [Error bars represent standard deviation (means  $\pm$  SD,  $n=3$ ); germination percentage with the same letter are not significantly different at  $p<0.05$ ]

### Phytotoxicity of the compost products

The germination index (GI) and germination rate (GR) can reflect the phytotoxicity and maturity of composting. High maturity can promote plant growth, whereas high levels of soluble salts, organic acids and pH can cause composting phytotoxicity (Wang et al., 2017). In this study, the GI gradually increased with composting time, and Fig. 3f showed the final GI (calculated as Eq.1) was ranked as  $T1>T4>T2>T5>T3>T6$ , GR (calculated as Eq.2) was ranked as  $T1=T4>T2>T5>T3>T6$ . The results of two-way ANOVA showed that C/N and IPS significantly affected GI ( $p<0.05$ ), but the interaction between them was not significant. The 2 mm IPS and C/N=23 treatment can significantly improve the GI value, indicating that this treatment was more conducive to the degradation of toxic substances. GI value  $>80\%$  indicates that composting is

completely decomposed (Zucconi et al., 1981), and based on this threshold, T1-T5 are all at a mature level.

### Dynamic changes in HS

During the composting process, HS forms via C and N cycles. HA and FA are important components of HS and play a decisive role in the quality of HS to a large extent. At the initial stage of composting, the concentrations of HS and its components decrease overall (Fig. 4a-c), thus reflecting the degradation of unstable compounds in the structure (Barje et al., 2012). Because of the presence of many acid functional groups and the low molecular weight in the early stage, the water solubility of FA is higher than that of HA; thus, the concentration of FA is relatively high in the initial composting stage. Subsequently, a series of polycondensation reactions of the decomposed phenols, carbohydrates, and nitrogen-containing compounds result in an increase in the concentrations of HS and HA (Zhou et al., 2014), and the gradual decrease in FA suggesting that the readily available carbon in composting is reduced and the stability of the composting is increased. Two-way ANOVA showed that C/N ratio had significant effect on HS ( $p < 0.05$ ), the treatments with low C/N ratio had higher HS content.

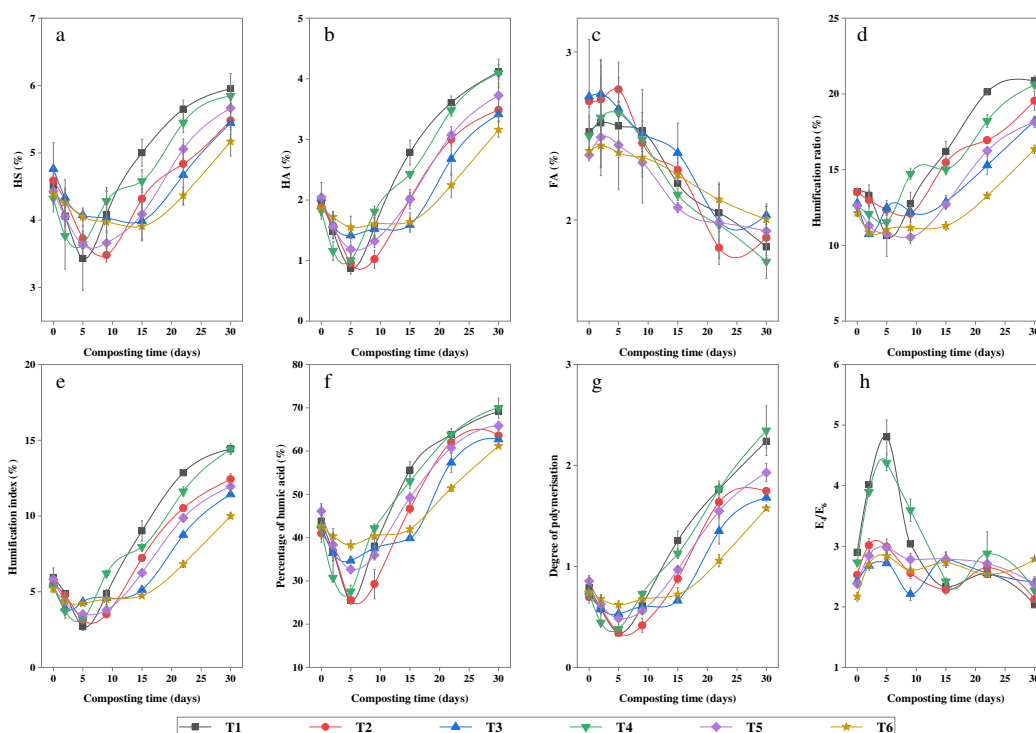


**Figure 4.** Variation in HS(a), HA(b), FA(c), HI(d), HR(e), PHA(f), DP(g) and  $E_4/E_6$  ratio(h) showing the humification process during the composting [Error bars represent standard deviation (means  $\pm$  SD,  $n=3$ )]

In addition to the changes in the HS concentration, the humification-related indices (DP, HI, HR and PHA) are considered to more accurately reflect the evolution of humification (Sánchez-Monedero et al., 1999; Kulikowska and Klimiuk, 2011). These indices generally showed an upward trend (Fig. 4d-g), and the increases in HI and HR

meant an increase in HS and a decrease in biodegradable organic matter, thus reflecting an increase in humification caused by composting. PHA and DP are the measurements of complex HA produced by FA, and an increase in these indices indicates an increase in the molecular weight of HS and structural complexity.  $E_4/E_6$  is the ratio of the absorbance at 465 nm and 665 nm, which can more intuitively describe the change in the polymerization degree of aromatic components in HS (Awasthi et al., 2014).  $E_4/E_6$  fluctuated constantly during the composting process (Fig. 4h), indicating that decomposition and aggregation occurred throughout the entire composting process, and  $E_4/E_6$  gradually decreased at the late stage, indicating the formation of more polycondensed HAs and a high degree of composting condensation.

### Dynamic changes in bacterial communities

16S rDNA high-throughput sequencing technology is an important method for the rapid, flexible, efficient, and accurate acquisition of microbial community composition and diversity. A total of 1169664 high-quality bacterial sequences were obtained from the 16S rRNA clone library of GWC samples collected during different composting stages, and they aggregated into 2208 bacterial operational taxonomic units (OTUs) with a 3% nucleotide difference. These 2208 OTUs belonged to 36 phyla. *Proteobacteria*, *Chloroflexi*, *Firmicutes*, *Actinobacteria*, *Bacteroidetes*, and *Acidobacteria* were the six most dominant phyla among the total treatments. The compost samples accounted for over 92% of the gene sequences. Previous studies also found these dominant bacteria in lignin waste composting and other types of composting (Awasthi, 2017a; Liu, 2018). The relative abundance of bacteria at the phylum level among all the treatments is shown in Fig. 5a.

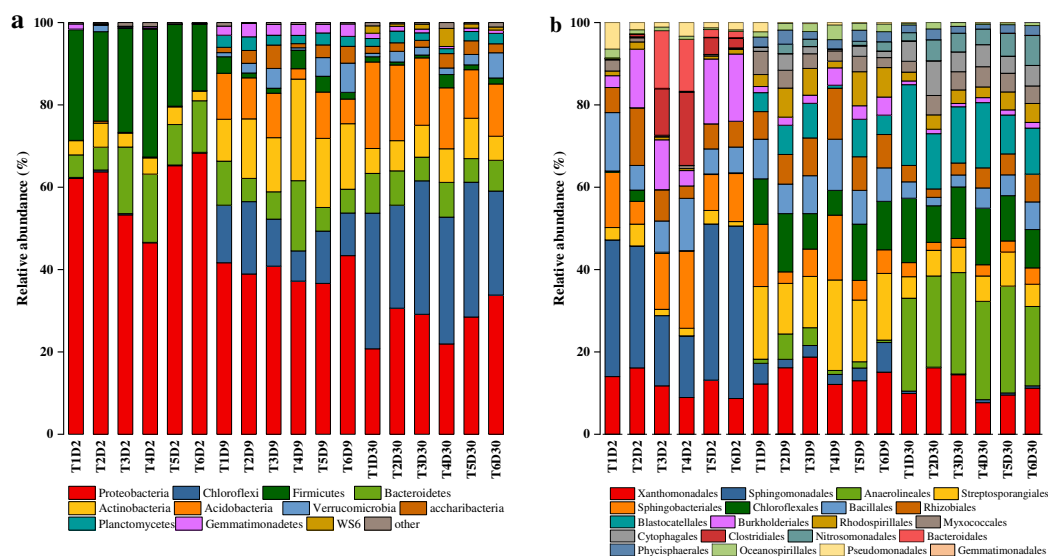


**Figure 5.** Relative abundance of the dominant bacteria in (a) phyla level and (b) order level by treatment

In the early stage of composting, which mainly focuses on the degradation of simple organic matter, *Proteobacteria* and *Firmicutes* are the most abundant and average abundances of 60% and 23%, respectively. The abundance of *Proteobacteria* at the

medium-C/N was the highest at 64.5%; the abundance of *Firmicutes* at the low-C/N was the highest at 1.4 and 1.5 times that of the other two C/N groups; and significant differences were not observed in the treatments with different particle sizes. The results suggested that the nutritional environment had a greater impact on bacterial activity at the initial stage of composting. *Proteobacteria* have been shown to play an important role in the degradation of small molecules (such as glucose, propionate, and butyrate) (Zhou et al., 2019). Because *Firmicutes* can effectively utilize carbohydrates, it is also the key for early composting (Ariesyady et al., 2007).

At the middle stage of composting, the mean abundance of *Proteobacteria* decreased to 40% and *Actinobacteria* increased from 3.9% to 15.9% to become the second major phylum, which was caused by *Actinobacteria*-induced microbial production of lignocellulosic enzymes. The lignocellulosic enzymes have an excellent effect on the degradation of lignocellulose (Taha et al., 2016), and their spores formed at high temperatures can resist the harsh environment during the composting process (growing at 50-60 °C) (Zhao et al., 2016; Wei, 2018). The abundance of *Actinobacteria* in the 5 mm treatments was 55% higher than that in the 2 mm treatments, and the average abundance of *Actinobacteria* with the low C/N ratio was 11-20% higher than that of the other treatments, indicating that the difference in porosity caused by particle size started to affect the composting process in the middle stage and became an important influencing factor.

In the maturity phase, *Chloroflexi* replaced *Proteobacteria* to become the dominant phylum, with the average abundance increasing from the initial 0.5% to 30%; *Acidobacteria* also continued to increase to 1.8 times that in the middle stage; and the abundances of other phyla decreased compared to those in the middle stage, which is because with the degradation of easily degraded organic matter in the early and middle stages and the stable increase in HS, the number of available nutrients decreased, which led to limited bacterial activity with simple organics as the energy source. The abundance of *Acidobacteria* for the 2 mm treatments was 41.8% higher than that for the 5 mm treatments, and the average abundance of the low-C/N treatments was 18% higher than that of the other treatments. The differences were not significant for *Chloroflexi*.

The top 20 orders of composting were characterized to complement and confirm the function of bacterial activity in the GWC (Fig. 5b). The choice of order level was based on the comprehensive classification hierarchy and identification rate to avoid a biased explanation (Shen et al., 2013). At the same time, LDA Effect Size analysis was used to analyze the bacterial community differences between groups to determine the specific major microbial population in groups. The results showed that the specific major bacteria species, which had significant effects (LDA>3) were consistent with the top 20 orders basically. Specifically, *Clostridiales*, *Bacillales*, *Sphingobacteriaceae*, *Sphingomonadales* and *Burkholderiales* had the most significant influence at the early stage. Studies have shown that *Clostridiales* and *Bacillales* widely occur during composting due to their good degradation ability. In particular, *Bacillus* is commonly found in lignocellulose composting systems and can rapidly colonize and decompose lignocellulolytic substrates (Tortosa et al., 2017). *Sphingobacteriaceae* is known for its ability to utilize a variety of C sources, and it is reduced by the decomposition of carbon resources (Anderson et al., 2011). Therefore, *Sphingobacteriaceae* also plays an important role in the initial stage of composting. *Streptosporangiales*, *Rhizobiales*, *Rhodospirillales* and *Phycisphaerales* have a significant impact in the middle stage, and they are all closely related to the C or N cycles (Anderson et al., 2011; Badhai et al.,

2015). *Rhodospirillales* can exhibit thermophilicity. With the decomposition of TOC and TN, the number of these bacteria gradually decreased. *Anaerolineales*, *Blastocatellales*, and *Chloroflexales* become the dominant orders in the late stage. These orders can promote the production of carboxymethyl cellulose, which is involved in the degradation of polysaccharides and lignocellulose compounds (Tortosa et al., 2017; Awasthi et al., 2017b). *Anaerolinaceae* was the major order in the final composting stage, with the average abundance rising from less than 0.1% to 18.5%. Studies have shown that these bacteria can digest carbohydrates and peptides and may promote the utilization of carbohydrates or amino acids in dead cells (Yamada et al., 2006), which promotes the polymerization of HS. These results provide insights into the complex microbial activities involved in the composting process, clarify the microbial species that have a significant impact on the composting process, and indicate potential methods that can be used future studies to improve composting quality via the inoculation and cultivation of key bacteria.

### ***Relationships among environmental factors, bacterial communities and HS***

According to Wu et al. (2017), environmental factors (including physicochemical parameters and precursors) and key bacteria are the main factors that affect the formation of HS. To further clarify the relationship among the three factors and determine the key factors affecting the formation of HS, we performed a correlation analysis on the environmental factors, bacterial communities and HS.

A Pearson correlation analysis was conducted between the environmental factors and humification parameters to study their possible role in the composting process (Fig. 6a) (Dias et al., 2010). The results showed that GI, temperature, polyphenols and polysaccharides had a strong correlation with humification parameters ( $r > 0.75$ ,  $p < 0.05$ ), thus indicating that these were key environmental factors affecting the formation of HS. Polyphenols and carboxyl were significantly negatively correlated with humification parameters, confirming that carboxyl groups and phenyl groups are the main substances that constitute the total acidity (deMelo et al., 2016), promote the formation of HS through structural integration and increase the aromaticity of HS. Polysaccharides were positively related with HS because these substances are formed via the degradation of lignin, cellulose and hemicellulose (Sánchez-Monedero et al., 1999) and can be used as the main carbon and energy sources of bacterial communities. We can infer that polysaccharides are the main energy source of the bacteria in the late stage and can promote the bacterial aggregation effect of small molecules, thus promoting the formation of HS. These results also support the idea that precursors play an important role in HS formation and aromatization. Previous studies also found that temperature and GI are related to bacteria composition. Temperature affects bacteria community succession and composition, and GI, as a maturity index, is associated with the phytotoxicity, which significantly affects bacterial activity. Therefore, temperature and GI can significantly affect the composting process by affecting bacterial communities.

As mentioned above, the top 20 orders were selected to analyze the relationship between the bacterial community and humification parameters and elaborate on the influence of bacterial communities on HS. As shown in the Fig. 6b, *Anaerolineales*, *Chloroflexales*, *Blastocatellales*, *Cytophagales*, *Myxococcales* and *Nitrosomonadales* were positively correlated with HS, HA, HI, HR, PHA and DP and negatively correlated with FA and E<sub>4</sub>/E<sub>6</sub>, which play positive roles in the composting process. According to the Pearson correlation analysis and previous reports (Tortosa et al., 2017), some genera



of the aforementioned orders could be used as biomarkers for the thermophilic phase and maturity phase in the composting. Among them, the OTUs of *Anaerolineales*, *Cytophagales* and *Blastocatellales* increased as composting progressed and were significantly correlated with all indices ( $r > 0.75$ ,  $p < 0.05$ ). Therefore, *Anaerolineales*, *Cytophagales* and *Blastocatellales* could be considered as important microorganisms affecting the maturity of GWC. Previous studies have confirmed that *Anaerolineales* and *Cytophagaceae* can digest proteins, cellulose and other macromolecules (Meng et al., 2018) to produce nitrogen and sugar, which may promote the formation of HS. However, more research is needed to confirm these results.

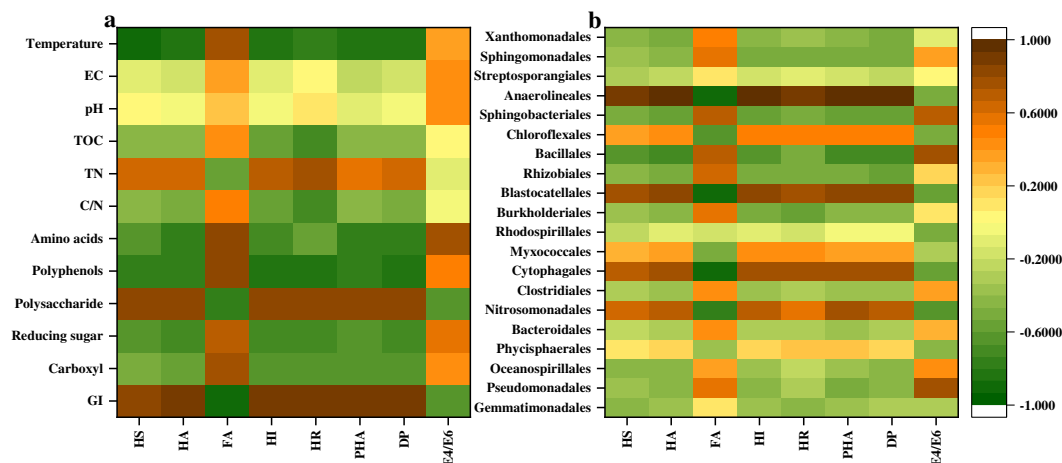


**Figure 6.** Pearson correlation heatmap of a) environmental factors and humification parameters and b) bacterial communities and humification parameters

According to Wang et al. (2015), environmental factors may be the most manageable factors affecting HS formation. Thus, exploring the influence of environmental factors on bacterial communities is of great important to regulate the production of HS more conveniently. However, the relationship between the two in the GWC remains unknown. Therefore, redundancy analysis (RDA) is performed based on environmental factor parameters and bacterial abundance (Fig. 7). Results of the Monte Carlo test showed that the first and all canonical axes were highly significant ( $p = 0.002$ ), moreover, eigenvalues showed that the total variation in the bacterial abundance statistically explained by these environmental factors accounting for 97.3%, indicating that these environmental factors may be significant in explaining bacterial community formation.

RDA indicated the relationship between environmental parameters and bacteria communities abundance at the order level. During the early stage of composting, the major bacteria (*Sphingobacteriales*, *Pseudomonadales*, *Burkholderiales*, and *Sphingomonadales*) were affected by more than one environmental factor, suggesting their growth in an intricate environment. Key bacterial and small molecule precursors (amino acids, reducing sugars, polyphenols and carboxyl) directly involved in the formation of HS were positively correlated. Therefore, the values of these indices could be increased in the initial stage to provide more nutrients and promote the composting process. Moreover, bacteria could also facilitate the generation and polymerization of these functional precursors by decomposing readily degradable cellulose and

hemicellulose, to produce more HS. As a key environmental factor, temperature had a certain impact on the major bacteria in the early and middle stages, and the positive correlation indicates that it can promote the composting process. However, temperature was negatively correlated with the formation of HS, indicating that the cooling stage after the thermophilic phase was more suitable for the formation of HS. *Anaerolineales*, *Cytophagales*, *Blastocatellales* and *Nitrosomonadales* were positively correlated with the composting samples in the late stage and the formation of HS, indicating that HS formation mainly occurred in the late stage and these bacteria may be related to the polymerization of substance.

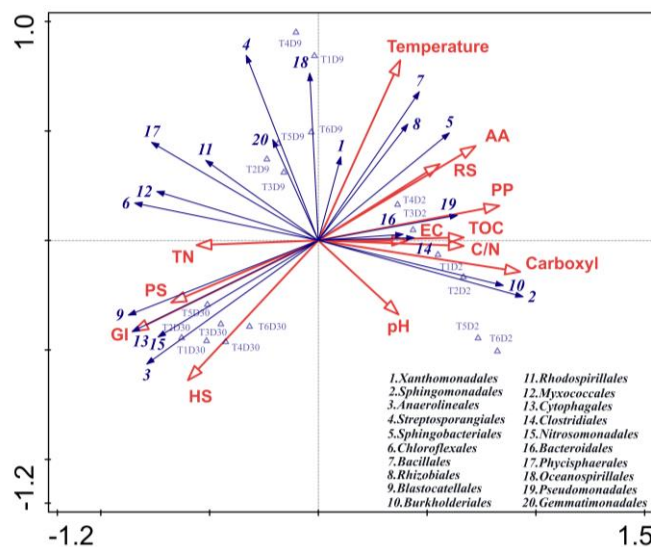


**Figure 7.** RDA of the correlation between environmental factors, bacterial community and compost samples (AA: amino acids, PP: polyphenols, PS: polysaccharides, RS: reducing sugars)

*Anaerolineales*, *Cytophagales*, and *Blatocatellales* are the key bacteria affecting HS, and they were positively correlated with GI, polysaccharides, and TN, indicating that the high lignin content of GW resulted in very low availability of nutrients in the late stage of composting and suggesting that polysaccharides and TN may be the main sources of energy for bacteria, which confirms our previous inference. The content and composition of nitrogen are considered to influence the bacterial community through the availability of essential elements that affect the bacterial survival (Chodak et al., 2013; Xi et al., 2016). We can increase the activity of key bacteria through the addition of various materials, such as bean dregs, fruit and vegetable waste, in the late stage to promote the formation of HS and effectively control the cost of composting. As an important biological indicator, GI is significantly related to quinone group, compost maturity and phytotoxicity (Tang et al., 2011). Increasing the abundance of these key bacteria could increase the content of terpenoids, thereby improving the phytotoxicity and maturity of composting.

Although we have provided some suggestions for increasing the HS of GWC, the complexity of the composting process necessitates further study of the aspects of operability, cost, and quantitative control so that more precise and effective regulations can be developed to improve the potential applicability of the suggested techniques.

## Conclusions

In this study, different IPS and C/N ratios were used, the dynamic changes in environmental factors and bacterial communities during the GWC were studied, and the correlations between these factors and the formation of HS were revealed. The results showed that the 2 mm and C/N=23 treatment could accelerate mineralization, increase fermentation temperature and GI, and generate a high HS content and humification degree. Temperature, GI, polyphenols, and polysaccharides are environmental factors that significantly affect the formation of HS; and *Analonineales*, *Cytophagales*, and *Blastocatellales* are important bacteria that affect the maturity process. In future studies, various spectroscopy techniques (e.g. Fourier transform infrared spectroscopy, nuclear magnetic resonance) can be used to explore the mechanism of HS formation in green waste composting from the perspective of material structure, so as to further improve the humification process and the quality of HS. Meanwhile, regulation methods suitable for different scales of composting should be proposed from the perspectives of cost and operability.

**Acknowledgement.** The authors are grateful for financial support from National Key R&D Program of China (2017YFC0504406). Thank American Journal Experts for their linguistic modification of this paper.

## REFERENCES

- [1] Anderson, C. R., Condon, L. M., Clough, T. J., Fiers, M., Stewart, A., Hill, R. A., Sherlock, R. R. (2011): Biochar induced soil microbial community change: Implications for biogeochemical cycling of carbon, nitrogen and phosphorus. – *Pedobiologia* 54: 309-320.
- [2] Antunes, L. P., Martins, L. F., Pereira, R. V., Thomas, A. M., Barbosa, D., Lemos, L. N. (2016): Microbial community structure and dynamics in thermophilic composting viewed through metagenomics and metatranscriptomics. – *Scientific Reports* 6(1): 38915.
- [3] Ariesyady, H. D., Ito, T., Okabe, S. (2007): Functional bacterial and archaeal community structures of major trophic groups in a full-scale anaerobic sludge digester. – *Water Research* 41(7): 1554-1568.
- [4] Awasthi, M. K., Pandey, A. K., Khan, J., Bundela, P. S., Wong, J. W. C., Selvam, A. (2014): Evaluation of thermophilic fungal consortium for organic municipal solid waste composting. – *Bioresource Technology* 168: 214-221.
- [5] Awasthi, M. K., Li, J., Kumar, S., Awasthi, S. K., Wang, Q., Chen, H. Y., Wang, M. J., Ren, X. N., Zhang, Z. Q. (2017a): Effects of biochar amendment on bacterial and fungal diversity for co-composting of gelatin industry sludge mixed with organic fraction of municipal solid waste. – *Bioresource Technology* 246: 214-223.
- [6] Awasthi, M. K., Zhang, Z., Wang, Q., Shen, F., Li, R. H., Li, D. S., Ren, X. N., Wang, M. J., Chen, H. Y., Zhao, J. C. (2017b): New insight with the effects of biochar amendment on bacterial diversity as indicators of biomarkers support the thermophilic phase during sewage sludge composting. – *Bioresource Technology* 238: 589-601.
- [7] Badhai, J., Ghosh, T. S., Das, S. K. (2015): Taxonomic and functional characteristics of microbial communities and their correlation with physicochemical properties of four geothermal springs in Odisha. – *Frontiers in Microbiology* 6: 1166.
- [8] Barje, F., El Fels, L., El Hajjouji, H., Amir, S., Winterton, P., Hafidi, M. (2012): Molecular behaviour of humic acid-like substances during co-composting of olive mill

- waste and the organic part of municipal solid waste. – *International Biodeterioration & Biodegradation* 74: 17-23.
- [9] Chen, W., Liao, X., Wu, Y., Liang, J. B., Mi, J., Huang, J., Zhang, H., Wu, Y., Qiao, Z., Li, X., Wang, Y. (2017): Effects of different types of biochar on methane and ammonia mitigation during layer manure composting. – *Waste Management* 61: 506-515.
- [10] Chodak, M., Golebiewski, M., Morawska-Ploskonka, J., Kuduk, K., Niklinska, M. (2013): Diversity of microorganisms from forest soils differently polluted with heavy metals. – *Applied Soil Ecology* 64: 7-14.
- [11] deMelo, B. A. G., Motta, F. L., Santana, M. H. (2016): Humicacids: Structural properties and multiple functionalities for novel technological developments. – *Materials Science and Engineering C* 62: 967-974.
- [12] Dias, B. O., Silva, C. A., Higashikawa, F. S., Roig, A., Sánchez-Monedero, M. A. (2010): Use of biochar as bulking agent for the composting of poultry manure: effect on organic matter degradation and humification. – *Bioresource Technology* 101: 1239-1246.
- [13] Dzulurnain, Z., Hassan, M. A., Zakaria, M. R., Wahab, P. E. M., Hasan, M. Y., Shirai, Y. (2017): Co-composting of municipal sewage sludge and landscaping waste: a pilot scale study. – *Waste and Biomass Valorization* 8: 1-11.
- [14] Guo, X. X., Liu, H. T., Wu, S. B. (2019): Humic substances developed during organic waste composting: Formation mechanisms, structural properties, and agronomic functions. – *Science of The Total Environment* 662: 501-510.
- [15] Hanc, A., Dreslova, M. (2016): Effect of composting and vermicomposting on properties of particle size fractions. – *Bioresource Technology* 217: 186-189.
- [16] Huang, G. F., Wong, J. W. C., Wu, Q. T., Nagar, B. B. (2004): Effect of C/N on composting of pig manure with sawdust. – *Waste Management* 24(8): 805-813.
- [17] Khalil, A., Domeizel, M., Prudent, P. (2008): Monitoring of green waste composting process based on redox potential. – *Bioresource Technology* 99(14): 6037-6045.
- [18] Kulikowska, D., Klimiuk, E. (2011): Organic matter transformations and kinetics during sewage sludge composting in a two-stage system. – *Bioresource Technology* 102(23): 10951-10958.
- [19] Li, R., Wang, J. J., Zhang, Z., Shen, F., Zhang, G., Qin, R., Li, X., Xiao, R. (2012): Nutrient transformations during composting of pig manure with bentonite. – *Bioresource Technology* 121: 362-368.
- [20] Li, Y., Li, W., Wu, C., Wang, K. (2013): New insights into the interactions between carbon dioxide and ammonia emissions during sewage sludge composting. – *Bioresource Technology* 136: 385-393.
- [21] Li, X., Hu, Q., Jiang, S., Li, F., Lin, J., Han, L., Hong, Y., Lu, W., Gao, Y., Chen, D. (2015): Flos *Chrysanthemi Indici* protects against hydroxyl-induced damages to DNA a MSCs via antioxidant mechanism. – *Journal of Saudi Chemical Society* 19(4): 454-460.
- [22] Liu, L., Wang, S., Guo, X., Zhao, T., Zhang, B. (2018): Succession and diversity of microorganisms and their association with physicochemical properties during green waste thermophilic composting. – *Waste Management* 73: 101-112.
- [23] Lobna, B., Guergueb, Z., Chaieb, M., Mekki, A. (2019): Co-composting of Olive Industry Wastes with Poultry Manure and Evaluation of the Obtained Compost Maturity. – *Waste and Biomass Valorization*. DOI: 10.1007/s12649-019-00901-9.
- [24] López-González, J. A., Suárez-Estrella, F., Vargas-García, M. C., López, M. J., Jurado, M. M., Moreno, J. (2015): Dynamics of bacterial microbiota during lignocellulosic waste composting: studies upon its structure, functionality and biodiversity. – *Bioresource Technology* 175: 406-416.
- [25] Meng, X., Liu, B., Xi, C., Luo, X., Yuan, X., Wang, X., Zhu, W., Wang, H., Cui, Z. (2018): Effect of pig manure on the chemical composition and microbial diversity during co-composting with spent mushroom substrate and rice husks. – *Bioresource Technology* 251: 22-30.

- [26] Petric, I., Helić, A., Avdić, E. A. (2012): Evolution of process parameters and determination of kinetics for co-composting of organic fraction of municipal solid waste with poultry manure. – *Bioresource Technology* 117: 107-116.
- [27] Sánchez-Monedero, M. A., Roig, A., Cegarra, J., Bernal, M. P. (1999): Relationships between water-soluble carbohydrate and phenol fractions and the humification indices of different organic wastes during composting. – *Bioresource Technology* 70: 193-201.
- [28] Shen, P., Zhang, J., Zhang, J., Jiang, C., Tang, X., Li, J., Zhang, M., Wu, B. (2013): Changes in microbial community structure in two anaerobic systems to treat bagasse spraying wastewater with and without addition of molasses alcohol wastewater. – *Bioresource Technology* 131: 333-340.
- [29] Silva, M. E. F., de Lemos, L. T., Nunes, O. C., Cunha-Queda, A. C. (2014): Influence of the composition of the initial mixtures on the chemical composition, physicochemical properties and humic-like substances content of composts. – *Waste Management* 34: 21-27.
- [30] Song, C., Li, M., Jia, X., Wei, Z., Zhao, Y., Xi, B., Zhu, C., Liu, D. (2014): Comparison of bacterial community structure and dynamics during the thermophilic composting of different types of solid wastes: anaerobic digestion residue, pig manure and chicken manure. – *Microbial Biotechnology* 7: 424-433.
- [31] Taha, M., Foda, M., Shahsavari, E., Aburto-Medina, A., Adetutu, E., Ball, A. (2016): Commercial feasibility of lignocellulose biodegradation: possibilities and challenges. – *Current Opinion in Biotechnology* 38: 190-197.
- [32] Tang, J. C., Wang, M., Zhou, Q. X., Nagata, S. (2011): Improved composting of *Undaria pinnatifida* seaweed by inoculation with *Halomonas* and *Gracilibacillus* sp. isolated from marine environments. – *Bioresource Technology* 102: 2925-2930.
- [33] Tortosa, G., Castellano-Hinojosa, A., Correa-Galeote, D., Bedmar, E. J. (2017): Evolution of bacterial diversity during two-phase olive mill waste (“alperujo”) composting by 16S rRNA gene pyrosequencing. – *Bioresource Technology* 224: 101-111.
- [34] Wang, X., Cui, H., Shi, J., Zhao, X., Zhao, Y., Wei, Z. (2015): Relationship between bacterial diversity and environmental parameters during composting of different raw materials. – *Bioresource Technology* 198: 395-402.
- [35] Wang, S. P., Zhong, X. Z., Wang, T. T., Sun, Z. Y., Tang, Y. Q., Kida, K. (2017): Aerobic composting of distilled grain waste eluted from a Chinese spiritmaking process: the effects of initial pH adjustment. – *Bioresource Technology* 245: 778-785.
- [36] Wei, H., Wang, L., Hassan, M., Xie, B. (2018): Succession of the functional microbial communities and the metabolic functions in maize straw composting process. – *Bioresource Technology* 256: 333-341.
- [37] Wu, J., Zhao, Y., Zhao, W., Yang, T., Zhang, X., Xie, X., Cui, H., Wei, Z. (2017): Effect of precursors combined with bacteria communities on the formation of humic substances during different materials composting. – *Bioresource Technology* 226: 191-199.
- [38] Xi, B. D., Zhao, X. Y., He, X. S., Huang, C. H., Tan, W. B., Gao, R. T., Zhang, H., Li, D. (2016): Successions and diversity of humic-reducing microorganisms and their association with physical-chemical parameters during composting. – *Bioresource Technology* 219: 204-211.
- [39] Yamada, T., Sekiguchi, Y., Hanada, S., Imachi, H., Ohashi, A., Harada, H., Kamagata, Y. (2006): *Anaerolinea thermolimosa* sp nov., *Levilinea saccharolytica* gen. nov., sp nov and *Leptolinea tardivitalis* gen. nov., so. nov., novel filamentous anaerobes, and description of the new classes *anaerolineae* classis nov and *Caldilineae* classis nov in the bacterial phylum Chloroflexi. – *International Journal of Systematic and Evolutionary Microbiology* 56: 1331-1340.
- [40] Zhang, L., Sun, X. Y. (2014): Effects of rhamnolipid and initial compost particle size on the two-stage composting of green waste. – *Bioresource Technology* 163: 112-122.

- [41] Zhang, L. L., Zhang, H. Q., Wang, Z. H., Chen, G. J., Wang, L. S. (2016): Dynamic changes of the dominant functioning microbial community in the compost of a 90-m<sup>3</sup> aerobic solid state fermentor revealed by integrated meta-omics. – *Bioresource Technology* 203: 1-10.
- [42] Zhang, L., Sun, X. Y. (2018): Effects of bean dregs and crab shell powder additives on the composting of green waste. – *Bioresource Technology* 260: 283-293.
- [43] Zhang, Z. C., Zhao, Y., Wang, R. X., Lu, Q., Wu, J. Q., Zhang, D. Y., Nie, Z. F., Wei, Z. M. (2018): Effect of the addition of exogenous precursors on humic substance formation during composting. – *Waste Management* 79: 462-471.
- [44] Zhang, L., Sun, X. Y. (2019): The use of coal fly ash and vinegar residue as additives in the two-stage composting of green waste. – *Environmental science and pollution research*. In Press.
- [45] Zhang, W. M., Yu, C. X., Wang, X. J., Hai, L. (2020): Increased abundance of nitrogen transforming bacteria by higher C/N ratio reduces the total losses of N and C in chicken manure and corn stover mix composting. – *Bioresource Technology* 297: 122410.
- [46] Zhao, X., He, X., Xi, B., Gao, R., Tan, W., Zhang, H., Li, D. (2016): The evolution of water extractable organic matter and its association with microbial community dynamics during municipal solid waste composting. – *Waste Management* 56: 79-87.
- [47] Zhou, Y., Selvam, A., Wong, J. W. C. (2014): Evaluation of humic substances during co-composting of food waste, sawdust and Chinese medicinal herbal residues. – *Bioresource Technology* 168: 229-234.
- [48] Zhou, G. X., Xu, X. F., Qiu, X. W., Zhang, J. B. (2019): Biochar influences the succession of microbial communities and the metabolic functions during rice straw composting with pig manure. – *Bioresource Technology* 272: 10-18.
- [49] Zhu, N. (2007): Effect of low initial C/N ratio on aerobic composting of swine manure with rice straw. – *Bioresource Technology* 98: 9-13.
- [50] Zucconi, F., Pera, A., Forte, M., De Bertoldi, M. (1981): Evaluating toxicity of immature compost. – *Biocycle* 22: 54-57.

# CORRELATION OF ION CONTENTS WITH ETHYLENE PRODUCTION DURING THE RIPENING PROCESS OF SUGARCANE (*SACCHARUM OFFICINARUM* L.) WITH THE APPLICATION OF CHEMICAL RIPENERS

TUFAIL, M. – HUSSAIN, K. \*

*Department of Botany, University of Gujrat (UOG), Gujrat, Pakistan*

*\*Corresponding author*

*e-mail: khalid.hussain@uog.edu.pk*

(Received 27<sup>th</sup> Apr 2020; accepted 11<sup>th</sup> Aug 2020)

**Abstract.** Chemical ripeners (Ethephon, Glyphosate and Sulfometuron-methyl) were used as foliar sprays on four sugarcane cultivars (HSF-242, NSG-311, HSF-240, NSG-555) to find their effects on quality, potassium (K<sup>+</sup>) and chloride (Cl<sup>-</sup>) contents and ethylene production. Chemical ripeners significantly increased the sucrose contents, juice purity, recovery % cane and sugar yield based on the mean data of two years. All the sugarcane cultivars sprayed with chemical ripeners responded well regarding early cane maturity and high production of sugar. Variations in antioxidant activities i.e. peroxidase (POD) and catalases (CAT) were also noted indicating the stimulating effects of various chemical ripeners. There was a negative correlation of K<sup>+</sup> and Cl<sup>-</sup> with ethylene production  $r = -0.8915, -0.7773$ , respectively. K<sup>+</sup> had a positive correlation with Cl<sup>-</sup> contents ( $r = 0.92205$ ). Sugar yielding attributes had positive correlations with ethylene while, K<sup>+</sup> and Cl<sup>-</sup> had negative correlations. Upon reaching maturity, ethylene production increased while, K<sup>+</sup> and Cl<sup>-</sup> contents in cane juice decreased resulting in high sucrose contents in sugarcane. It was concluded that chemical ripeners were useful reaching early cane maturity in sugarcane cultivars which were considered mid or late maturing. Chemical ripeners also increased the sucrose contents with high sugar yield by affecting various variables linked to cane maturity. These outcomes can be utilized by researchers and plant breeders to develop early cane maturity varieties during sugarcane variety development programs.

**Keywords:** *potassium, chloride, antioxidant activities, sucrose, sugar yield*

## Introduction

Sugarcane (*Saccharum officinarum* L.) is considered as an industrial crop for the production of sugar (Neliana et al., 2019). Sugarcane is cultivated on 1132 thousand hectares with a total production of 65,475 thousand tons (Manzoor et al., 2019). Sugarcane is rich in sucrose which is accumulated in stalk internodes and is used to manufacture many industrial goods such as furfural, alcohol, dextrans and some other natural pharmaceutical products (Ma et al., 2005).

Chemical ripeners (Ethephon, ethyl-trinexapac, glyphosate and sulfometuron methyl) are classified as growth retardants and growth inhibitors (Leite et al., 2010). Chemical ripening of sugarcane is profitable due to high sugar production throughout the world (Dalley and Richard, 2010). The key benefit of chemical ripeners is that they can suppress leaf and stalk growth more rapidly than natural mechanism (Van Heerden et al., 2015). Applications of Ethephon has accelerated the ripening process of sugarcane, its yield and it inhibited the flowering (Chong et al., 2010; De Almeida and Caputo, 2012).

The chemical ripener glyphosate is an amino acid synthesis inhibitor and it has been extensively used to increase sucrose contents in sugarcane (Solomon and Li, 2004). Glyphosate is a widely used herbicide throughout the world because it is an efficient killer of weeds, less toxic and available at low cost (Gosciny and Hanot, 2012). Leite et al. (2009) showed that the applications of ripeners used for early harvest sugarcane

resulted in an increase of quality, sugar yield which positively increased the profit per unit area. El-Hamd et al. (2013) noted that glyphosate applications helped to increase the total soluble solids in juice and other quality parameters and sucrose contents. Sulfometuron-methyl is a grass herbicide that was promising as a chemical ripener at low rates of application (Almodares et al., 2013). Many studies reported that sulfometuron-methyl has good potential of ripening in sugarcane varieties and it causes no damage in sugarcane production (Silva et al., 2007; Leite et al., 2010).

Chemical ripeners or herbicides can affect the production of ethylene that can induce early maturity. Lee and Dumas (1982) found the changes in ethylene production in Tobacco with the applications of Glyphosate. Glyphosate beneficially increased the sucrose contents in sugarcane (McDonald et al., 2001). Changes in ethylene level and its perception, directly or indirectly regulate the lifespan of plants. Ethylene is tightly correlated with the biosynthesis of volatile organic compounds (Iqbal et al., 2017). There are various nutrients that have a role in sugarcane maturity. Watanabe et al. (2016) showed that potassium ( $K^+$ ) and chloride ( $Cl^-$ ) contents show a relationship with sucrose contents. They have negative correlation with sucrose contents in sugarcane. The ripening of fruits is a unique coordination of various biochemical and developmental pathways regulated by ethylene, which affects color, texture, nutritional quality and aroma of fruits (Barry and Giovannoni, 2007).

Ethylene production and concentration of nutrients mainly potassium and chloride affect the sugar contents during maturity but so far, their relationship has not been established for selected sugarcane cultivars in Pakistan. This study was conducted to find the effect of chemical ripeners on sugar production and relationship between ethylene production with cation and anion contents in sugarcane.

## Materials and methods

Experiments were carried out at Shakarganj Sugar Research Institute (SSRI) Jhang and University of Gujrat, Pakistan during 2018-19. Planting of four sugarcane cultivars i.e. HSF-242, NSG-311, HSF-240 and NSG-555 was done in autumn 2018 and harvesting was carried out in autumn 2019. These cultivars were extensively cultivated in the country due to better growth, yield performance and good ratooning abilities with resistance against major diseases of sugarcane. These cultivars have not yet been evaluated to find the effect of chemical ripeners. Experimental design was RCBD (Plot size  $40 \times 40$  feet beds) with four replicates. Seed rate was 75000 double-bedded setts per hectares with 2.5 feet row spacing.

Each chemical ripener was used at cane formation and elongation phase that has not been studied so far in Pakistan and for selected cultivars. The following treatments were carried out calculated on hectare basis:

T0 = Water only (Control)

T1 = Sulfometuron-methyl ( $0.05 \text{ kg ha}^{-1}$ )

T2 = Glyphosate ( $0.05 \text{ L ha}^{-1}$ )

T3 = Ethephon ( $0.05 \text{ L ha}^{-1}$ )

T4 = Sulfometuron-methyl ( $0.05 \text{ kg ha}^{-1}$ ) + Glyphosate ( $0.05 \text{ L ha}^{-1}$ )

T5 = Sulfometuron-methyl ( $0.05 \text{ kg ha}^{-1}$ ) + Ethephon ( $0.05 \text{ L ha}^{-1}$ )

T6 = Glyphosate ( $0.05 \text{ L ha}^{-1}$ ) + Ethephon ( $0.05 \text{ L ha}^{-1}$ )

T7 = Sulfometuron-methyl ( $0.05 \text{ kg ha}^{-1}$ ) + Glyphosate ( $0.05 \text{ L ha}^{-1}$ ) + Ethephon ( $0.05 \text{ L ha}^{-1}$ )



Four cane samples were collected for the study of following the quality parameters, sugar yielding and antioxidant activities in autumn 2019:

1. Sucrose percentage (%)
2. Juice purity (%)
3. Sugar recovery % cane
4. Sugar yield ( $\text{t ha}^{-1}$ )
5. Antioxidant activities (POD and CAT)
6. Determination of  $\text{K}^+$  and  $\text{Cl}^-$  contents
7. Determination of ethylene production in leaf sheaths

Brix reading was measured using Brix hydrometer as a percentage of the total soluble solids in juice (w/w) by hand refractometer. Sucrose percentage was calculated from  $100 \text{ cm}^3$  of juice using the following equation described by Horwitz (1976):

$$\text{Sucrose percentage} = \text{direct reading of Saccharimeter} \times 1.04$$

Where 1.04 is a factor depending on the length of Saccharimeter's tube.

Juice Purity was calculated using the following equation:

$$\text{Purity percentage} = (\text{sucrose percentage} / \text{Brix reading}) \times 100$$

Theoretical sugar recovery was calculated according to the formula described by Legendre and Henderson (1972):

$$\text{Sugar recovery percentage} = [S - 0.4 (B - S)] \times 0.73$$

Where: B = Brix percentage, S = sucrose percentage, 0.4 and 0.73 constant factors.

$$5 - \text{Sugar yield (ton/fed)} = \text{net cane yield} \times \text{theoretical sugar recovery}$$

Total sugar yield was calculated for each treatment by using the following method:

$$\text{Total sugar (t ha}^{-1}\text{)} = \text{Sugar recovery} \times \text{Stripped-cane yield} / 100$$

Antioxidant activities i.e. Peroxidase (POD) and catalases (CAT) were determined by the procedure of Chance and Maehly (1955). Potassium ( $\text{K}^+$ ) contents in cane juice were determined with a flame photometer (model PFP7, Jenway Staffordshire, UK). Chloride ( $\text{Cl}^-$ ) contents in the juice of sugarcane were determined by a chloride meter. Leaf samples were collected and were immediately put into ethylene bottles and sealed.

Sugarcane leaves were kept in container for 5 h to measure ethylene production by portable Ethylene meter. These measurements were repeated five times and mean values were calculated for 2<sup>nd</sup> to 5<sup>th</sup> leaf.

Data were subjected to analysis of variance for three factor factorial in Minitab (Version: 19.2.0, Coventry, UK) and significant mean separation was done at  $P \leq 0.05$  using Tukey's test.

## Results

### Sucrose contents (%)

Effect of chemical ripeners was highly significant in sugarcane for sucrose contents (Table 1). The interaction of ripeners x cultivars was also significant. Higher sucrose contents (12.6%) were noted in cultivar NSG-555 with T<sub>2</sub> (Glyphosate (0.05 L ha<sup>-1</sup>)). Overall, Glyphosate and Sulfometuron-methyl (0.05 kg ha<sup>-1</sup>) + Ethephon (0.05 L ha<sup>-1</sup>) applications was best for the enhancement of sucrose contents (Fig. 1A). Chemical ripeners applied as separate treatments were more effective than combined applications (Table 2).

**Table 1.** Mean squares (MS) from the analysis of variance (ANOVA) of sugarcane cultivars for various attributes under the applications of chemical ripeners

Source Main effects	df	Sucrose contents	Juice purity (%)	Sugar recovery % cane	Total sugar yield	Peroxidase (POD) activities	Catalases (CAT) activities	K <sup>+</sup> in Juice	Cl <sup>-</sup> in juice
Replicates	3	24.345*	11.56**	0.342*	67.453**	0.003*	0.045*	0.023*	0.011*
Ripeners (Rip)	7	62.579**	52.524***	0.522**	479.487***	0.005**	0.076**	0.067**	0.043**
Cultivars (cv)	3	1379.752**	626.596**	6.256**	8236.089**	0.076**	0.150**	0.146**	0.231**
Interactions cv x Rip	21	17.396**	12.888***	0.121**	34.211**	8.823**	0.005*	0.098*	0.067*
Error	93	7.943	2.614	0.043	13.011	0.001	0.002	0.076	0.058
Total	127								

\*, \*\*, \*\*\* = significant at P < 0.05, 0.01, or 0.001, respectively

### Juice purity (%)

It was noted from the results that the effect of chemical ripeners was highly significant for juice purity % of sugarcane. Variations among cultivars as well as the interaction between ripeners x cultivar were also highly significant (Table 1). Higher juice purity % was calculated in NSG-555 and minimum juice purity was present in HSF-242 (Table 2). Sulfometuron-methyl (0.05 kg ha<sup>-1</sup>) + Ethephon (0.05 L ha<sup>-1</sup>) application increased juice purity up to 83.8% in HSF-240 (Fig. 1B).

### Sugar recovery % from cane

Sugar recovery % from cane significantly increased with the applications of chemical ripeners (Table 1). Ethephon (0.05 L ha<sup>-1</sup>) treatments were more effective as compared to other applications (Fig. 1C). Higher sugar recovery % from cane (12.12) was calculated in NSG-555 following Ethephon (0.05 L ha<sup>-1</sup>) treatment. All the chemical ripener treated plants showed higher sugar recovery % from cane as compared to control (Fig. 1C).

### Sugar yield (t ha<sup>-1</sup>)

Sugar yield was highly significantly affected by the applications of chemical ripeners in all the cultivars of sugarcane. Effect of chemical ripeners for cultivars and the effect of their interaction ripeners x cultivar were also highly significant (Table 1). Ethephon (0.05 L ha<sup>-1</sup>) treatments were the best for the enhancement of sugar yield (Fig. 1D). Higher sugar yield (116.85 t ha<sup>-1</sup>) was obtained from NSG-555 with Ethephon (0.05 L ha<sup>-1</sup>) treatments (Table 2).

**Table 2.** Means comparison for different variables of sugarcane using Tukey's test

Cultivar	Treatments	Sucrose contents (%)	Juice purity (%)	Sugar recovery % cane	Sugar yield (t ha <sup>-1</sup> )	Peroxidase (POD) activities	Catalases (CAT) activities	K <sup>+</sup> contents in juice	Cl <sup>-</sup> contents in juice
HSF-242	T0	9.7 B	71.82 B	9.12 E	74.32 BC	0.892 D	1.027 B	54.51 A	34.21 A
	T1	10.9 A	71.57 B	9.97 D	72.91 C	0.895 D	1.037 A	40.67 B	26.23 B
	T2	10.2 A	74.05 A	10.19 C	76.81 B	0.912 C	1.025 B	32.45 C	18.09 C
	T3	10.3 A	76.05 A	11.23 A	86.05 A	0.991 BC	1.042 A	37.56 C	19.02 C
	T4	9.9 B	71.97 B	10.21 BC	70.87 C	1.011 A	1.051 A	31.22 CD	21.43 C
	T5	10.1 A	72.82 B	10.39 B	75.98 B	1.002 B	1.062 A	37.01 C	23.34 B
	T6	9.8 B	78.55 A	10.51 B	83.63 A	1.012 A	1.034 B	28.34 D	18.17 C
	T7	9.7 B	70.55 B	10.06 C	78.83 B	1.061 A	1.067 A	31.21 CD	21.13 B
	T8	10 AB	73.31 A	10.25 B	84.48 A	1.037 A	1.064 A	32.45 C	19.15 C
NSG-311	T0	10.8 B	77.25 A	9.06 D	83.76 B	0.996 B	1.102 B	47.34 A	29.81 A
	T1	11.6 A	73.97 B	10.16 BC	86.81 A	0.967 BC	1.092 C	32.45 B	21.34 B
	T2	10.4 BC	74.77 B	10.30 B	91.15 A	1.011 A	1.107 B	24.67 C	17.34 C
	T3	11.1 A	75.55 A	11.40 A	92.29 A	1.015 A	1.121 A	21.56 C	15.23 C
	T4	10.7 A	74.21 B	10.24 B	80.28 B	0.895 D	1.102 B	23.62 C	18.19 C
	T5	11.0 A	77.12 A	10.36 B	82.56 B	1.010 A	1.107 B	20.71 D	17.16 C
	T6	10.9 B	80.02 A	10.40 B	89.69 A	1.027 A	1.134 A	19.34 E	12.31 D
	T7	11.2 A	72.82 B	10.16 BC	80.05 B	0.937 C	1.115 AB	21.71 C	16.15 C
	T8	11.1 A	74.11 B	10.32 B	82.17 B	1.012 A	1.117 AB	25.76 C	18.91 C
HSF-240	T0	10.2 BC	79.02 A	9.44 E	91.96 C	0.855 D	1.112 C	36.56 A	24.53 A
	T1	11.4 A	80.72 A	10.98 B	97.73 B	0.876 D	1.131 B	21.34 C	17.15 B
	T2	10.1 C	80.95 A	10.70 C	103.88 A	0.875 D	1.137 B	19.19 C	14.23 BC
	T3	11.0 A	82.95 A	11.67 A	107.36 A	0.935 B	1.132 B	20.93 C	18.31 B
	T4	10.8 B	81.05 A	10.34 D	94.84 B	0.941 B	1.151 A	26.54 B	19.18 B
	T5	11.6 A	81.75 A	10.48 D	103.45 A	0.952 B	1.135 B	24.51 B	14.25 BC
	T6	10.6 B	83.81 A	10.61 B	108.50 A	0.901 C	1.152 A	15.34 D	11.12 C
	T7	11.2 A	75.32 B	10.35 D	101.23 B	1.001 A	1.135 B	18.76 C	15.67 B
	T8	10.7 B	75.52 B	11.10 B	108.77 A	0.977 A	1.112 C	23.44 B	12.45 C
NSG-555	T0	10.9 C	77.50 B	10.01 D	100.26 C	0.796 E	1.123 B	37.45 A	34.56 A
	T1	12.6 A	81.25 A	11.45 B	106.97 B	0.806 DE	1.141 AB	25.67 B	20.91 B
	T2	11.7 B	81.91 A	11.13 BC	110.18 AB	0.812 D	1.132 B	24.21 B	23.56 B
	T3	12.0 AB	83.52 A	12.12 A	116.85 A	0.822 D	1.161 A	26.78 B	18.23 BC
	T4	11.4 B	82.72 A	11.66 B	104.74 B	0.841 C	1.132 B	22.34 BC	16.34 C
	T5	11.4 B	83.67 A	10.76 C	111.02 A	0.852 B	1.157 A	23.46 B	17.18 C
	T6	12.0 AB	83.05 A	11.44 B	113.95 A	0.912 A	1.152 A	19.45 C	19.18 BC
	T7	11.7 B	82.42 A	10.69 C	106.68 B	0.847 B	1.132 B	23.68 B	21.34 B
	T8	11.0 C	83.82 A	11.21 B	113.08 A	0.881 AB	1.123 B	21.39 BC	22.17 B

Capital alphabets show the significant variations among treatment means

### **Antioxidant activities**

Antioxidant activities i.e. peroxidase (POD) and catalases (CAT) were determined by evaluating the stimulatory effects of different chemical ripeners. Effect of chemical ripeners was highly significant on POD activities in sugarcane (*Table 1*). Higher POD activities were noted in cultivar HSF-242 and lower was present in HSF-240 (*Fig. 1E*). Higher POD value (1.06) was noted by the applications of Glyphosate (0.05 L ha<sup>-1</sup>) + Ethephon (0.05 L ha<sup>-1</sup>). Treatments in combinations had high POD values as compared to separate treatments. For CAT activities also a highly significant effect of chemical ripeners was observed (*Table 2*). Higher value of CAT (1.16) was noted in

NSG-555 with the applications of Ethephon ( $0.05 \text{ L ha}^{-1}$ ) and HSF-242 cultivar showed lower CAT activities (*Fig. 1F*).

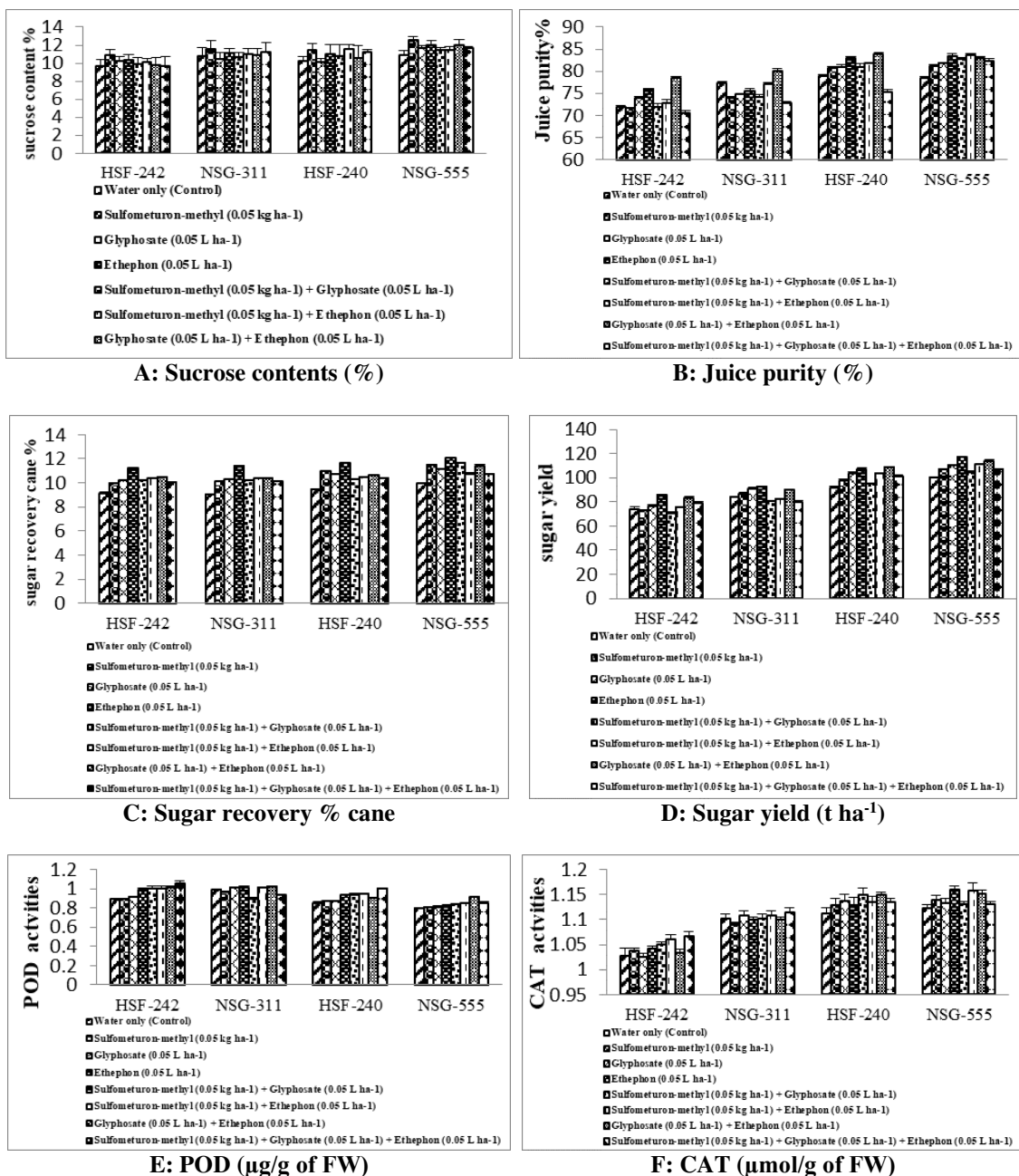


**Figure 1.** Effect of chemical ripeners on quality attributes and antioxidant activities of sugarcane

### Potassium ( $K^+$ ) contents

Means squares from ANOVA showed highly significant effects on  $K^+$  accumulation in the juice of sugarcane (*Table 1*). There were high contents of  $K^+$  in controls for the cultivars that reduced significantly with the applications of chemical cultivars (*Fig. 2A*). Sulfometuron-methyl ( $0.05 \text{ kg ha}^{-1}$ ) + Ethephon ( $0.05 \text{ L ha}^{-1}$ ) treatments showed

maximum reduction for  $K^+$  (Table 2). Higher  $K^+$  contents (15.34 mM) was noted in HSF-240 with the applications of Sulfometuron-methyl ( $0.05 \text{ kg ha}^{-1}$ ) + Ethephon ( $0.05 \text{ L ha}^{-1}$ ).

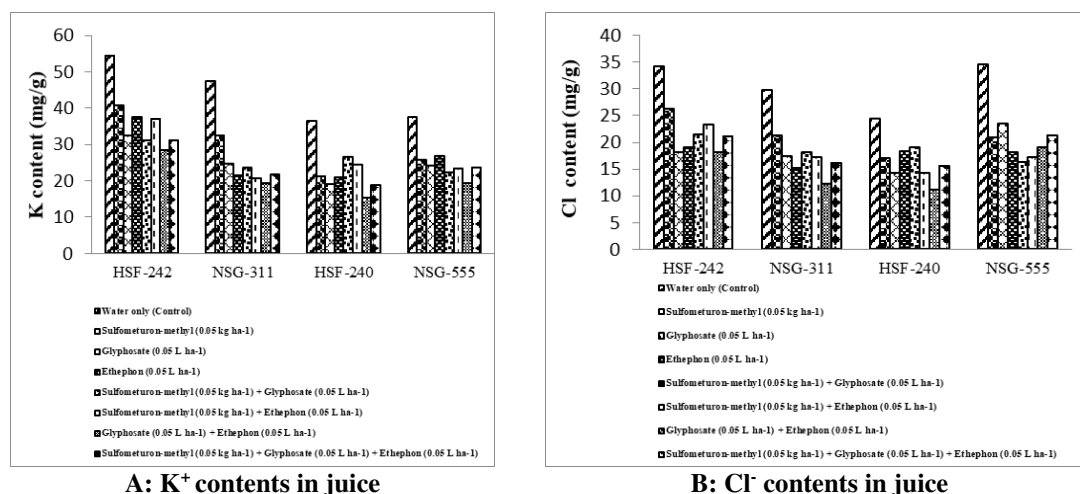


Figure 2. Effect of chemical ripeners on ionic concentrations of sugarcane

### Chloride ( $Cl^-$ ) contents

Chemical ripeners had highly significant effects on  $Cl^-$  accumulation in cane juice (Table 1). Pattern of  $Cl^-$  accumulation was similar as in the case of  $K^+$  contents in juice of sugarcane with the applications of chemical ripeners (Table 2). Sulfometuron-methyl ( $0.05 \text{ kg ha}^{-1}$ ) + Ethephon ( $0.05 \text{ L ha}^{-1}$ ) treatments showed maximum reduction in  $Cl^-$  in all the cultivars. Lower  $Cl^-$  contents (11.12 mM) were noted in HSF-240 with the applications of Sulfometuron-methyl ( $0.05 \text{ kg ha}^{-1}$ ) + Ethephon ( $0.05 \text{ L ha}^{-1}$ ). There were higher contents of  $Cl^-$  in controls that reduced significantly with the applications of chemical cultivars (Fig. 2B).

### Ethylene production in leaf sheath

Data related to ethylene production in leaf sheath is given in Table 3. Data of ethylene production was collected at the time of treatment and then at maturity. Ethylene production reduced significantly at maturity. Maximum reduction in ethylene production was noted in NSG-555. At maturity, there were much variations in ethylene production as compared to the data collected at the time of treatment. Low ethylene production resulted in the maturity of cane crop.

### Pearson correlation

Correlation was calculated for ethylene,  $K^+$  and  $Cl^-$  contents, sucrose contents and sugar yielding attributes under the influence of chemical ripeners. The correlations are shown in Table 4. There was a negative correlation of Ethylene with  $K^+$  and  $Cl^-$  and positive with sucrose, sugar recovery and sugar yield. Which showed that ethylene has direct relation with sugar yielding attributes, when the concentration of ethylene increased then sugarcane had maximum sugar production indicating its maturity.  $K^+$  contents positive relation with  $Cl^-$  showed cation and anion direct relationship.

**Table 3.** Determination of ethylene production in leaf sheaths (mean values from 2nd to 5th leaf) of sugarcane under the applications of chemical ripeners

Cultivar	Treatments	Production of ethylene ( $\text{nL}\cdot\text{g}^{-1}\cdot\text{h}^{-1} \times 10^{-4}$ )	
		At treatment time	At harvest stage
HSF-242	T0	21±1.12 AB	104±1.51 D
	T1	28±1.23 A	233±1.04 B
	T2	22±1.67 AB	227±2.10 B
	T3	27±1.75 A	231±1.12 B
	T4	29±2.10 A	216±2.11 C
	T5	29±1.11 A	254±2.34 A
	T6	21±1.76 AB	223±1.98 B
	T7	23±1.23 B	209±1.08 C
NSG-311	T0	23±1.01 A	98±1.19 E
	T1	22±1.43 B	207±2.01 C
	T2	20±1.22 B	231±1.08 B
	T3	26±1.83 A	186±2.11 D
	T4	26±1.56 A	257±1.23 A
	T5	23±1.09 A	204±1.56 C
	T6	21±1.12 B	214±1.23 BC
	T7	24±1.56 A	176±1.01 D
HSF-240	T0	29±1.45	78±1.04 D
	T1	27±2.31 C	186±1.11 BC
	T2	33±1.23 B	190±1.45 BC
	T3	23±1.54 CD	166±1.23 C
	T4	26±2.45 C	201±2.01 A
	T5	32±1.86 B	194±1.54 B
	T6	38±1.23 A	204±1.23 A
	T7	37±1.64 A	198±1.45 AB
NSG-555	T0	18±1.01 C	88±1.12 E
	T1	16±1.43 C	203±1.04 B
	T2	20±1.24 B	187±2.11 B
	T3	14±1.45 D	154±1.76 D
	T4	17±1.67 C	209±1.09 A
	T5	25±1.11 A	194±1.11 BC
	T6	22±1.03 A	201±1.23 B
	T7	21±1.34 B	219±1.43 A
	T8	19±1.14 B	183±2.11 B

Different alphabets show the significant variations

## Discussion

Results indicated that chemical ripeners had significant effect for the enhancement of sugar yield and early ripening of sugarcane. It might be due to the conversion of cane formation and elongation phase into ripening phase by Ethephon, Glyphosate and Sulfometuron-methyl. Similarly, Karmollachaab et al. (2016) noted a beneficial

increase in juice pole and brix value and comparatively high sugar yield can be achieved by applying Glyphosate and Ethephon. Different responses of sugarcane varieties were noted for different chemical ripeners like the effect of ethephon as a ripener was studied by many researchers (Silva et al., 2007). The reducing ability of ethephon on flowering reduces the cane stalk and increases the productivity of sugar. Ethephon anticipated harvesting stage with 21 days of applications and increased sugar yield (Caputo et al., 2008; Dalley and Richard, 2010).

**Table 4.** Pearson correlation coefficients (*r*) of sugarcane variables under the applications of chemical ripeners

	Ethylene	K Contents	Cl Contents	Sucrose contents	Sugar recovery % cane
K Contents	-0.891526812				
Cl Contents	-0.777345533	0.922058378			
Sucrose Contents	0.305346091	-0.078612401	-0.031781141		
Sugar recovery % cane	0.668635845	-0.571810994	-0.548581377	0.0267	
Sugar yield	0.857606233	-0.790316064	-0.79438101	0.22931	0.672011

r value >0 indicates positive correlation

Results demonstrated consistent improvement in sugarcane brix, pol with the applications of chemical ripeners. Sulfometuron-methyl can also result a reduction in pith process (50 to 60%) for cane maturity. An increase in pol (1.26%) and earlier ripening of 21 days and reduction in reducing sugar was observed by the application of sulfometuron-methyl (Caputo et al., 2008). Su et al. (1992) indicated that glyphosate brought about an expansion in sucrose content in the stalk only five days after application.

Different factors such as variety of sugarcane, time of application of ripeners, stage of plant life cycle, application rate of chemical, type or combination of ripener can affect sugarcane ripening by chemical ripeners. In different studies, the utilization of substance ripeners, for example, ethephon and glyphosate had been investigated with positive impacts in repining (Solomon and Li, 2004). Li et al. (2004) showed that compound ripener in sugarcane had an effect for high sugar accumulation in sugarcane. Watanabe et al. (2016) showed that K<sup>+</sup> and Cl<sup>-</sup> contents were the most abundant cation and anion present in sugarcane and both are negatively correlated with sucrose concentration. High K<sup>+</sup> and Cl<sup>-</sup> contents had significant effects on lowering sucrose concentration. Chemical ripeners can affect the ethylene production to enhance the maturity.

Plant hormone ethylene has a significant regulatory role in the ripening of many fruits with important contribution in nutritional and fiber contents. Molecular exploration of the role of ethylene in fruit ripening has led to the affirmation of mechanisms of ethylene perception (Barry and Giovannoni, 2007). Ethylene production changes when a fruit reaches maturity. The negative effects of ethylene on quality of fruit ripening are related to shifting or speeding up the natural processes of growth, maturity and deterioration with age, while the favorable outcomes of ethylene on quality center on generally the same features as the negative effects, but vary in both level and direction (Srividhya and Sujatha, 2017). Cunha et al. (2017) identified potential ethylene target genes and characterized the hormonal changes during ripening, providing insights into the action of ethylene at the site of sucrose accumulation. Changes in ethylene production level, its perception directly or indirectly regulate the lifespan of plants (Iqbal et al., 2017).

## Conclusion

It was concluded that chemical ripeners enhanced early cane maturity with high sugar production by increasing the ethylene production and reducing the K<sup>+</sup> and Cl<sup>-</sup> contents. Chemical ripeners can be used for early cane maturity for these sugarcane cultivars in Pakistan.

## Recommendation

It is suggested that chemical ripeners can be useful to induce early cane ripening for profitable productivity in sugarcane.

## REFERENCES

- [1] Almodares, A., Usufzadeh, M., Daneshvar, M. (2013): Effect of nitrogen and ethephon on growth parameters, carbohydrate contents and bioethanol production from sweet sorghum. – *Sugar Tech* 15(3): 300-304.
- [2] Barry, C. S., Giovannoni, J. J. (2007): Ethylene and fruit ripening. – *Journal of Plant Growth Regulation* 26: 143-159.
- [3] Caputo, M. M., Beauclair, E. G. F., Silva, M. D. A., Piedade, S. M. D. S. (2008): Response of sugarcane genotypes to the application of maturation inducers. – *Bragantia* 67(1): 15-23.
- [4] Chance, M., Maehly, A. C. (1955): Assay of catalases and peroxidases. – *Methods in Enzymology* 2: 764-817.
- [5] Chong, B. F., Mills, E., Bonnett, G. D., Gnanasambandam, A. (2010): Early exposure to ethylene modifies shoot development and increases sucrose accumulation rate in sugarcane. – *Journal of Plant Growth Regulation* 29(2): 149-163.
- [6] Cunha, C. P., Roberto, G. G., Vicentini, R., Lembke, C. G., Souza, G. M., Ribeiro, R. V., Machado, E. C., Lagoa, A. M. M. A., Menossi, M. (2017): Ethylene-induced transcriptional and hormonal responses at the onset of sugarcane ripening. – *Scientific Reports* 7: 43364.
- [7] Dalley, C. D., Richard, E. P. (2010): Herbicides as ripeners for sugarcane. – *Weed Science* 58(3): 329-333.
- [8] De Almeida, S. M., Caputo, M. M. (2012): Ripening and the Use of Ripeners for Better Sugarcane Management. – In: Marin, F. (ed.) *Crop Management - Cases and Tools for Higher Yield and Sustainability*. In Tech Europe, Rijeka. <https://doi.org/10.5772/28958>.
- [9] El-Hamd, A. S., Bekheet, M. A., Gadalla, A. F. I. (2013): Effect of chemical ripeners on juice quality, yield and yield components of some sugarcane varieties under the conditions of Sohag Governorate. – *American-Eurasian Journal of Agriculture and Environment Science* 13(11): 1458-1464.
- [10] Goscinny, S., Hanot, V. (2012): Glyphosate in pouch states. – *Scientific Institute of Public Health, Pesticides Unit Labinfo* 7: 12-16.
- [11] Horwitz, W. (1976): *Official Methods of Analysis of the Association of Official Analytical Chemists*. 12th Ed. – Association of Official Analytical Chemists, Washington, DC. <https://doi.org/10.1002/jps.2600650148>.
- [12] Iqbal, N., Khan, N. A., Ferrante, A., Trivellini, A., Francini, A., Khan, M. I. R. (2017): Ethylene role in plant growth, development and senescence: interaction with other phytohormones. – *Frontier in Plant Science* 8: 475.
- [13] Karmollachaab, A., Bakhshandeh, A., Telavat, M. M., Moradi, F., Shomeili, M. (2016): Sugarcane yield and technological ripening responses to chemical ripeners. – *Sugar Tech* 18(3): 285-291.



- [14] Legendre, B. L., Henderson, M. T. (1972): The history and development of sugarcane yield calculations. – Proceeding ASSCT 2: 10-18. <https://doi.org/10.1177/1032373211435501>.
- [15] Lee, T. T., Dumas, T. (1982): Effect of glyphosate on ethylene production in tobacco callus. – Plant Physiology 72: 855-857.
- [16] Leite, G. H. P., Crusciol, C. A. C., Silva, M. D. A., Venturini, F. (2009): Ripeness and technological quality of early harvest sugarcane variety RB855453. – Bragantia 68(3): 781-787.
- [17] Leite, G. H. P., Crusciol, C. A. C., Siqueira, G. F. D., Silva, M. D. A. (2010): Technological quality in different sections of the stalk and productivity of sugarcane under the effect of ripeners. – Bragantia 69(4): 861-870.
- [18] Li, Y. R., Zhu, Q. Z., Ye, Y. P., Wang, W. Z., Yang, L. T., Pan, L. Q., Xu, T. (2004): Sugarcane Ripening Trials with Glyphosate-Borate Complex in Commercial Plantation of Shansi County. – In: Li, Y. R., Solomon, S. (eds.) Proceedings of the International Symposium on Sustainable Sugarcane and Sugar Production Technology. Nanning, China. China Agriculture Press, Beijing. <https://doi.org/10.3133/b540o>.
- [19] Ma, J. K., Chikwamba, R., Sparrow, P., Fischer, R., Mahoney, R., Twyman, R. M. (2005): Plant-derived pharmaceuticals - the road forward. – Trends in Plant Sciences 10(12): 580-585.
- [20] Manzoor, R., Maken, A., Culas, R. (2019): Sustaining agricultural production in Pakistan: obstacles and prospects. – Current Political and Economics of Middle East 10(3): 331-356.
- [21] McDonald, M., Jackson, P. (2001): The effect of ripeners on the CCS of 47 sugarcane varieties in the burdekin. – Proceedings of the Australian Society of Sugar Cane Technology 23: 102-108.
- [22] Neliana, I. R., Sawitri, W. D., Ermawati, N., Handoyo, T., Sugiharto, B. (2019): Development of Allergenicity and Toxicity Assessment Methods for Evaluating Transgenic Sugarcane Overexpressing Sucrose-Phosphate Synthase. – Agronomy 9(1): 23.
- [23] Silva, M. D. A., Gava, G. J. D. C., Caputo, M. M., Pincelli, R. P., Jerônimo, E. M., Cruz, J. C. S. (2007): These cruise control regulators have the potential to be developed and manufactured separately. – Bragantia 66(4): 545-552.
- [24] Solomon, S., Li, Y. R. (2004): Chemical ripening of sugarcane: global progress and recent developments in China. – Sugar Tech 6(4): 241-249.
- [25] Srividhya, V., Sujatha, K. (2017): Role of ethylene in fruits ripening process. – 2017 International Conference on Energy, Communication, Data Analytics and Soft Computing (ICECDS). Chennai, India. [https://doi.org/10.1007/978-94-009-6178-4\\_45](https://doi.org/10.1007/978-94-009-6178-4_45).
- [26] Su, L. Y., Cruz, A. D., Moore, P. H., Maretzki, A. (1992): The relationship of glyphosate treatment to sugar metabolism in sugarcane: new physiological insights. – Journal of Plant Physiology 140(2): 168-173.
- [27] Van Heerden, P. D., Mbatha, T. P., Ngxaliwe, S. (2015): Chemical ripening of sugarcane with trinexapac-ethyl (Moddus®) Mode of action and comparative efficacy. – Field Crops Research 181: 69-75.
- [28] Watanabe, K., Nakabarua, M., Tairaa, E., Uenoa, M., Kawamitsua, Y. (2016): Relationships between nutrients and sucrose concentrations in sugarcane juice and use of juice analysis for nutrient diagnosis in Japan. – Plant Production Science 19(2): 215-222.

## EFFECTS OF SALINE-ALKALI MIXED STRESS ON THE GROWTH AND PHYSIOLOGICAL CHARACTERISTICS OF GIANT JUNCAO (*PENNISETUM GIGANTEUM* Z. X. LIN)

MA, Y. X.<sup>1</sup> – LI, G. T.<sup>1\*</sup> – WANG, G. H.<sup>1</sup> – LIANG, T. Y.<sup>2</sup> – YAN, J. Q. Z.<sup>1</sup> – LI, J. J.<sup>1</sup>

<sup>1</sup>College of Desert Control Science and Engineering, Inner Mongolia Agricultural University, Hohhot 010018, China

<sup>2</sup>School of Biological Science and Technology, Baotou Teachers' College, Baotou 014030, China

\*Corresponding author  
e-mail: 13848817183@163.com

(Received 21<sup>st</sup> May 2020; accepted 17<sup>th</sup> Sep 2020)

**Abstract.** In this paper, a pot experiment was conducted to simulate different degrees of saline-alkali stress to explore the response mechanism of *Pennisetum giganteum* Z. X. Lin to salt stress concerning its growth and physiological characteristics. The results showed that: (1) the growth of plant height decreased obviously with the increase of salt solution concentration; (2) with the increase of concentration, MDA content accumulated intermittently, *P. giganteum* reduced oxidative damage and maintained normal plant physiological metabolism through the complementary action of antioxidant enzymes SOD and CAT; (3) when the concentration of mixed salt solution was low, all osmotic regulatory substances accumulated slowly, and with the continuous increase of concentration, free proline content increased rapidly, which played a leading role in the process of plant osmotic regulation to ensure its physiological activities; (4) under mixed saline-alkali stress, the roots and stems of *P. giganteum* absorbed most of the Na<sup>+</sup>, and transported K<sup>+</sup> to the leaves at the same time.

**Keywords:** *Pennisetum giganteum* Z. X. Lin, saline-alkali stress, growth, antioxidant enzyme, osmotic adjustment, ion response

### Introduction

Soil salinization is a problem that concerns the whole world. It has great influence on agriculture, forestry and other aspects (Bless et al., 2018). In the world, salinization soil accounts for more than half of the land, and there are different types of salinization soil in various countries. The area of saline alkali land in China reaches up to  $1.0 \times 10^8$  hm<sup>2</sup> (Zhang et al., 2020). Soil salinization is not conducive to the absorption of nutrients by crops and seriously interferes with and restricts the growth of plants, which undoubtedly causes serious harm to the current resources and ecology. It is precisely because of the worsening of soil that the cultivated land keeps decreasing, so it is urgent to develop agriculture in saline alkali soil, and it is of great significance to improve the ecological environment for a long time (Singh, 2015; Liu, 2018). Most studies have found that plants can exhibit a variety of regulatory mechanisms under external stress, including detoxification effects, the absorption and balance of mineral elements, and the regulation of antioxidant systems (Ma et al., 2015; Zhu et al., 2020). The study of Song et al. (2017) show that the accumulation of proline, sugars and organic acids which make positive impacts in Alfalfa (*Medicago sativa* L.)'s regulation of cell osmotic pressure, pH balance and reactive oxygen species (ROS) removal under stress. Jia et al. (2017) reported Hall Crabapple (*Malus halliana* Koehne) responded to salt stress (SS), alkali stress (AS) and saline-alkali stress (MAS) by reducing leaf water content (WC), stomatal conductance (*G*<sub>s</sub>) and intercellular CO<sub>2</sub> concentration (*C*<sub>i</sub>), increasing water

use efficiency (WUE) and accumulating osmolytes, and in MAS, SS and AS had good synergistic effect.

Previous research has shown that the continuous expansion of saline alkali soil area and saline alkali stress will cause different degrees of harm to plant growth physiology, which has caused great trouble to the introduction and promotion of *Pennisetum giganteum* Z. X. Lin, a fine grass species (Hayat et al., 2020). However, at present, the researches on *P. giganteum* mainly focus on drought resistance and cold resistance, and there are few reports on the response of *P. giganteum* to saline-alkali stress. In this study, the mixed salt solution was applied to simulate the different degree of saline-alkali of the seedlings of *P. giganteum*, the growth physiological indexes of the seedlings were measured under various concentrations, and the response of the seedlings of *P. giganteum* to saline-alkali stress was studied, in order to reveal its physiological defense mechanism under saline-alkali stress, further master its physiological growth status in the adversity, and promote the development and promotion of *P. giganteum* in saline-alkali areas provide theoretical basis and reference.

## Experiments and methods

### Test materials

The test *P. giganteum* was introduced from Fujian Province of southeastern China and planted in the greenhouse of Inner Mongolia Agricultural University, Inner Mongolia Autonomous Region, China. The buds with the same growth were planted in the flowerpot to raise seedlings, and the seedlings with the same growth were selected for the test.

### Test method

Based on the main components of saline-alkali soil and the previous studies (Ashraf and Akram, 2009; Bui, 2013; Mambetale et al., 2017), the soil salinization types in the arid and semi-desert steppe salinization area of Inner Mongolia Plateau were artificially simulated. In this paper, NaCl, Na<sub>2</sub>SO<sub>4</sub>, NaHCO<sub>3</sub> and Na<sub>2</sub>CO<sub>3</sub> were mixed according to different molar ratio to simulate the salt damage of the saline-alkali mixed stress on the *P. giganteum*. According to the increasing mode of the alkali salt content, the ratio A, B, C, D, E was set in each of the five mixed treatment groups (Table 1), the tolerance threshold of single salt of *P. giganteum* was set with five gradients, namely 30 mmol·L<sup>-1</sup>, 60 mmol·L<sup>-1</sup>, 90 mmol·L<sup>-1</sup>, 120 mmol·L<sup>-1</sup> and 180 mmol·L<sup>-1</sup>.

**Table 1.** Salt composition of each treatment group

Treatment group	Proportion of salt and alkali in treatment group
A	NaCl : Na <sub>2</sub> SO <sub>4</sub> : NaHCO <sub>3</sub> : Na <sub>2</sub> CO <sub>3</sub> =1:1:0:0
B	NaCl : Na <sub>2</sub> SO <sub>4</sub> : NaHCO <sub>3</sub> : Na <sub>2</sub> CO <sub>3</sub> =1:2:1:0
C	NaCl : Na <sub>2</sub> SO <sub>4</sub> : NaHCO <sub>3</sub> : Na <sub>2</sub> CO <sub>3</sub> =1:9:9:1
D	NaCl : Na <sub>2</sub> SO <sub>4</sub> : NaHCO <sub>3</sub> : Na <sub>2</sub> CO <sub>3</sub> =1:1:1:1
E	NaCl : Na <sub>2</sub> SO <sub>4</sub> : NaHCO <sub>3</sub> : Na <sub>2</sub> CO <sub>3</sub> =9:1:1:9

### Simulated stress of mixed salt

When the seedlings grow to three pairs of leaves in the flowerpot, 80 seedlings with basically the same growth potential are selected and randomly allocated into 26 groups.

Three repetitions are set in each treatment group. One group is selected as CK and distilled water with pH of 6.8 is irrigated in the treatment project. The stress treatment was conducted from 8:00 to 9:00 in the morning. Each pot was irrigated with 200 ml of the corresponding mixed solution prepared in advance, which was stressed for 7 days, and the corresponding weight was recorded. The water content of potted soil was controlled by weighing method. From the second day of stress, each flowerpot was weighed at 9:00 a.m. every day, and compared with the previously recorded data, the water lost by evaporation in the flowerpot was supplemented in time. At the same time, in order to prevent the loss of mixed salt solution, a plastic tray is placed at the bottom of each flowerpot, and the solution in the tray is timely poured back into the flowerpot every day. After 7 days, the functional leaves of the same part in different treatment groups were taken back to the laboratory for physiological index determination under low temperature environment.

### ***Physiological indexes and measurement methods***

The growth of plant height was measured by the method of drying; the activity of malondialdehyde (MDA) and catalase (CAT) was measured as described by Liang et al. (2015) and Maia et al. (2010); superoxide dismutase (SOD) activity was determined by the nitroblue tetrazolium (NBT) method (Yang et al., 2013); soluble sugar content by anthrone colorimetry, free proline content by acid ninhydrin colorimetry, soluble protein content by coomassie brilliant blue G-250 (Zou, 2000).

### ***Determination of the Na<sup>+</sup> and K<sup>+</sup> in root, stem and leaf***

After 22 days of stress treatment, three seedlings were taken according to different proportions of mixed salt. After washing, the roots, stems and leaves were separated and killed in an oven at 105 °C for 10 minutes, then the temperature was adjusted to 80 °C to dry until constant weight. The dried root, stem and leaf samples were thoroughly crushed and passed through 1 mm sieve, 0.2 g was added to nitrifying solution (10 ml concentrated nitric acid, 2 ml 60% trichloroacetic acid, 1 ml concentrated sulfuric acid) and boiled water bath at 90 °C for 60 min. After cooling, the 1 ml mixture was taken and fixed in a 50 ml capacity flask, and the contents of the Na<sup>+</sup> and K<sup>+</sup> in roots, stems and leaves under different saline-alkali ratios and concentrations were determined by flame spectrophotometer (TAS-990, Purkinje General, Beijing, China).

### ***Data processing***

Data were analysed using least significant difference test (LSD<sub>0.05</sub>) by using IBM SPSS Statistics v20. Excel 2007 was used for mapping, and the data was represented by three times of repeated mean value and standard error (SE).

## **Results and analysis**

### ***Effects of mixed saline-alkali stress on growth indicators***

Saline-alkali stress has a certain effect on the apparent morphology of plant growth (Fig. 1). Figure 2 shows that in the treatment groups with different proportion of A, B, C, D and E, with the increase of salt concentration, the growth of plant height of *P. giganteum* shows a downward trend, but there are great differences between the various treatment groups. In the pure salt solution and the low alkali salt proportion of

A and B, the downward trend is relatively slow, among which, the trends of the two groups with concentration of  $30 \text{ mmol}\cdot\text{L}^{-1}$  and  $60 \text{ mmol}\cdot\text{L}^{-1}$  are basically the same. However, there was no significant difference between group B at  $30 \text{ mmol}\cdot\text{L}^{-1}$  and CK. In group B, when the concentration increased to  $180 \text{ mmol}\cdot\text{L}^{-1}$  the plant height growth decreased to the lowest value, 75.08% lower than CK. In the A, C, D, E treatment groups, the plant height growth of different concentrations of salt solution in various treatment groups were significantly lower than CK, and reached the minimum value at  $180 \text{ mmol}\cdot\text{L}^{-1}$ , which were 64.01%, 68.22%, 61.68% and 62.62% lower than CK, respectively. The above results showed that, in the process of stress, the overall trend of decline, in the pH value of 8.22, and the concentration of no more than  $30 \text{ mmol}\cdot\text{L}^{-1}$  B treatment group and CK no significant difference, more suitable for the growth of *P. giganteum*, and other treatments to varying degrees inhibited its growth.

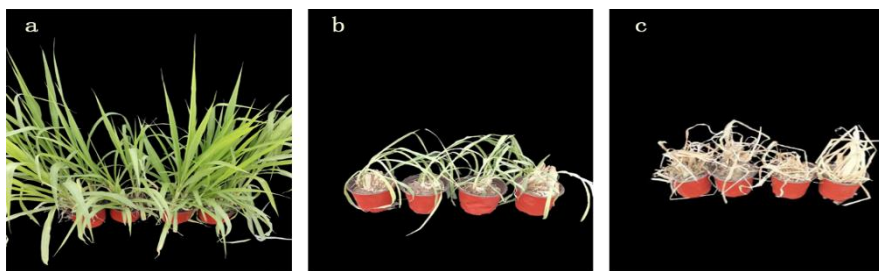


**Figure 1.** Influence of saline-alkali stress on the growth of *P. giganteum*: a) normal, b) Wilting under stress, and c) Death under stress

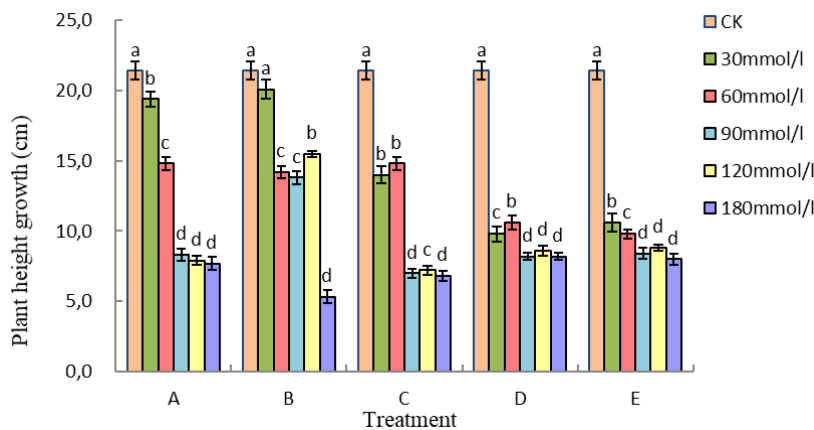
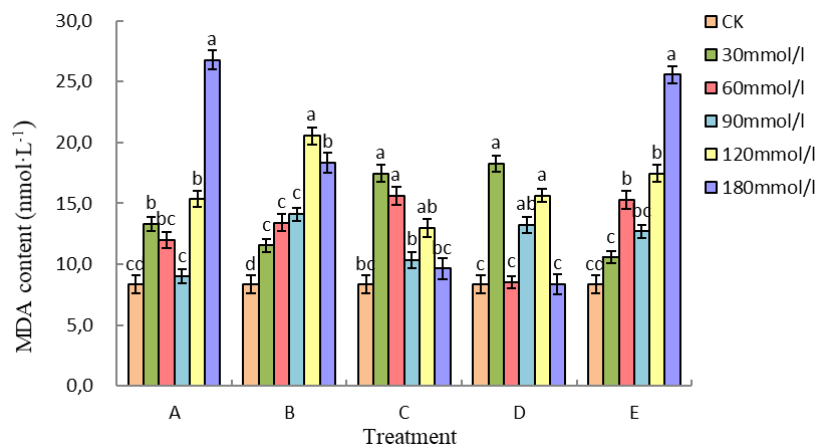


**Figure 2.** Changes in plant height growth in *P. giganteum* seedlings under saline-alkali stress. Different treatments: A)  $\text{NaCl} : \text{Na}_2\text{SO}_4 : \text{NaHCO}_3 : \text{Na}_2\text{CO}_3 = 1:1:0:0$ , B)  $\text{NaCl} : \text{Na}_2\text{SO}_4 : \text{NaHCO}_3 : \text{Na}_2\text{CO}_3 = 1:2:1:0$ , C)  $\text{NaCl} : \text{Na}_2\text{SO}_4 : \text{NaHCO}_3 : \text{Na}_2\text{CO}_3 = 1:9:9:1$ , D)  $\text{NaCl} : \text{Na}_2\text{SO}_4 : \text{NaHCO}_3 : \text{Na}_2\text{CO}_3 = 1:1:1:1$ , E)  $\text{NaCl} : \text{Na}_2\text{SO}_4 : \text{NaHCO}_3 : \text{Na}_2\text{CO}_3 = 9:1:1:9$ . Columns with different letters indicate significant difference ( $P \leq 0.05$ ) among various concentrations in the same treatment based on least significant difference test (LSD). The same as below

### Effects of mixed saline-alkali stress on physiological indexes

According to the data in Figure 3, the MDA content in the leaves of *P. giganteum* showed an increasing trend with the increase of salt concentration in each mixed salt

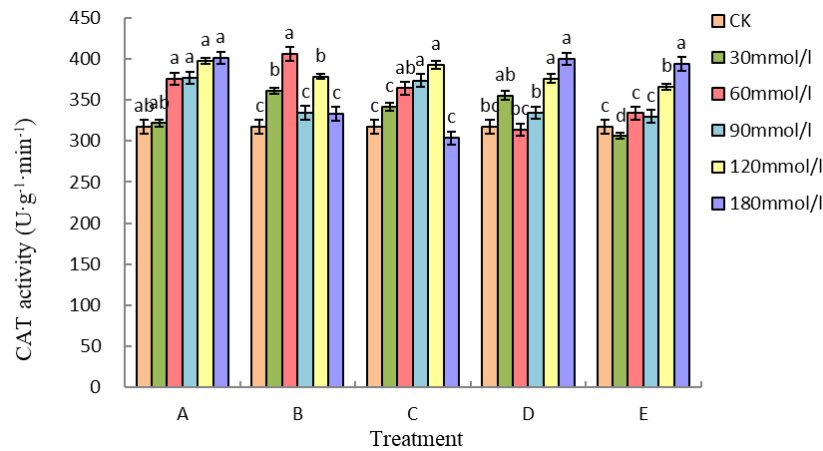
configuration group, and the MDA content in the leaves of *P. giganteum* under different proportions was higher than that of the control group, most of which were significantly higher than that of the control group. Both groups C and D reached the peak value of  $30 \text{ mmol}\cdot\text{L}^{-1}$ , 2.09 times and 2.19 times higher than the control, while groups A and E reached the peak value of  $180 \text{ mmol}\cdot\text{L}^{-1}$  and group B reached the peak value of  $120 \text{ mmol}\cdot\text{L}^{-1}$ , 3.10 times, 2.46 times and 3.07 times higher than the control. From the pH value, when the salt concentration reached the maximum, the MDA content in the leaves of *P. giganteum* group A, which was all neutral salt, and group E, which had A higher ratio of alkaline salt, suddenly increased to the peak, and was significantly higher than that of other treatment groups at the same concentration. The above results showed that under the treatment of high salt concentration and low pH (6.08) and high salt concentration and high pH (10.55), the peroxidation degree of the leaves of the *P. giganteum* increased, the growth and development of the plants were seriously damaged, and wilting and death appeared.



**Figure 3.** Changes in MDA content in *P. giganteum* seedlings under saline-alkali stress

It can be seen from *Figure 4*, compared with the control, catalase activity in the leaves of the *P. giganteum* in the five treatment groups A, B, C, D, and E all increased with the increase of the mixed salt concentration, but the difference was different. The proportion of the mixed salt is very different from the trend. Among them, in the treatment group A containing pure salt, the catalase activity of *P. giganteum* leaves increased numerically with the increase of the salt concentration, but there was no significant difference between the two groups, and the change was relatively gentle. The catalase activity in leaves of B and C treated groups with higher  $\text{Na}_2\text{SO}_4$  content showed a law of first increase and then decrease with the increase of the concentration of the mixed solution, which was significantly different from the control. The highest peak of peroxidase activity in the B treatment group appeared at  $60 \text{ mmol}\cdot\text{L}^{-1}$ , which was an increase of 1.28 times compared to the control; the maximum value of the peroxidase activity in the C treatment group appeared at  $120 \text{ mmol}\cdot\text{L}^{-1}$ , compared with the control increased by 1.24 times, and the catalase activity under the mixed salt concentration stress in the C treatment group was always maintained at a relatively stable level with a small change. The catalase activity of the leaves of *P. giganteum* and E treatment groups increased with the increase of the salt concentration. The catalase activity of the leaves of caterpillar fungus was relatively consistent. Both of them increased significantly with the increase of the salt concentration.

The highest peak appeared at 180 mmol·L<sup>-1</sup>, which increased by 1.26 times and 1.24 times compared with the control, respectively.



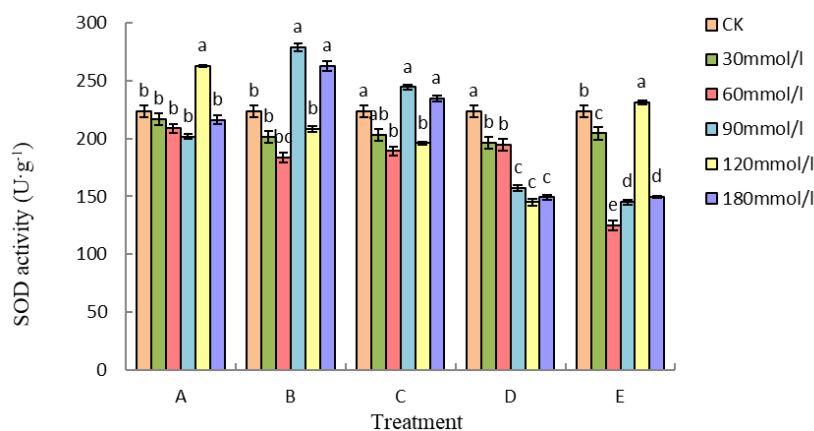
**Figure 4.** Changes in CAT activity in *P. giganteum* seedlings under saline-alkali stress

Figure 5 shows that the variation trend of superoxide dismutase activity in the leaves of *P. giganteum* with different saline-alkali ratio treatment groups is decreased in the context of gradually increasing mixed salt concentration. Among them, in the two extreme ratios of A and E, superoxide dismutase activity showed two extreme values, which first decreased, then increased and then decreased. At the same time, superoxide dismutase activity reached the maximum value when the mixture concentration was 120 mmol·L<sup>-1</sup>, 1.17 times and 1.03 times of the control, respectively. Treatment group A reached the minimum value at 90 mmol·L<sup>-1</sup>, which was 9.34% lower than the control group, while treatment group E reached the minimum value at 60 mmol·L<sup>-1</sup>, which was 44.08% lower than the control group B and C treatment group fluctuation is large, and the change process are complex, all showed down - up - then - rising change rule, and tendency in 90 mmol·L<sup>-1</sup> reach the peak of its active, comparison of 1.25 times and 1.09 times, respectively, but in A treatment is pure salt group, there was A significant difference compared with the peak, and join the alkali content of peak B treatment group compared with no significant difference. Superoxide dismutase activity in the environment of the D-treated group was in a downward trend, and there was no significant difference between the two groups. Moreover, the activity reached the minimum value at 120 mmol·L<sup>-1</sup>, which was 35.23% lower than that of the control group.

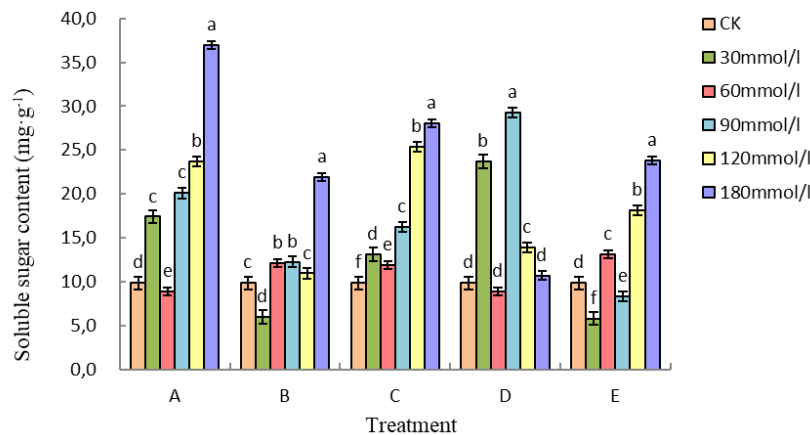
#### **Effects of mixed saline-alkali stress on osmotic regulators**

Figure 6 shows that the soluble sugar content increases intermittently in the context of increasing concentration in different ratio treatments. In the treatment group A, the soluble sugar content was significantly lower than that of the control only in the environment with A concentration of 60 mmol·L<sup>-1</sup>, while the other concentrations were significantly higher than that of the control, and reached the maximum value when the concentration reached 180 mmol·L<sup>-1</sup>, which was 2.75 times higher than that of the control. In the C treatment group, the soluble sugar content in the set concentration was significantly higher than that in the control group, and reached the maximum value when the concentration reached 180 mmol·L<sup>-1</sup>, an increase of 1.85 times compared with

the control group. Soluble sugar content in B and E in the context of two groups of treatment group were in the concentration of 30 mmol·L<sup>-1</sup> reaches the minimum value, fell 39.1% and 41.1% than control, respectively, which may be caused by plant metabolism and synthesis, the two groups of the soluble sugar content increased with the increase of concentration of accumulating, until the concentration reaches 180 mmol·L<sup>-1</sup>, its content is also maximum, significant differences compared with than control, respectively 2.23 times and 2.42 times of the control; in the D treatment group, the soluble sugar content fluctuated greatly, showing an M-type growth pattern in the intermittent accumulation, and reached the peak value at 30 mmol·L<sup>-1</sup> and 90 mmol·L<sup>-1</sup>, respectively, increasing by 140.5% and 196.9% compared with the control group. The soluble sugar content was significantly different from the control group when the concentration was 120 mmol·L<sup>-1</sup>, but there was no significant change in other groups.



**Figure 5.** Changes in SOD activity in *P. giganteum* seedlings under saline-alkali stress



**Figure 6.** Changes in soluble sugar content in *P. giganteum* seedlings under saline-alkali stress

It can be seen from *Figure 7* that the free proline in the 5 treatment groups will show a trend of different amplitude change, but the overall increase is with the increase of salt concentration. In treatment group A, D and E, the overall trend first increased to the peak value and then decreased slightly. In treatment group A and E, the peak value appeared at the concentration of 120 mmol·L<sup>-1</sup>, increased by 45.78 times and 44.70



times compared with the control, while in treatment group D, the peak value appeared at the concentration of  $120 \text{ mmol}\cdot\text{L}^{-1}$ , increased by 38.76 times compared with the control; in treatment group B and C, free proline content showed M-type growth. At the same time, it reached the peak at the concentration of  $90 \text{ mmol}\cdot\text{L}^{-1}$  and  $180 \text{ mmol}\cdot\text{L}^{-1}$ , and reached the maximum at the concentration of  $180 \text{ mmol}\cdot\text{L}^{-1}$ , which were 33.30 times and 51.92 times higher than the control.

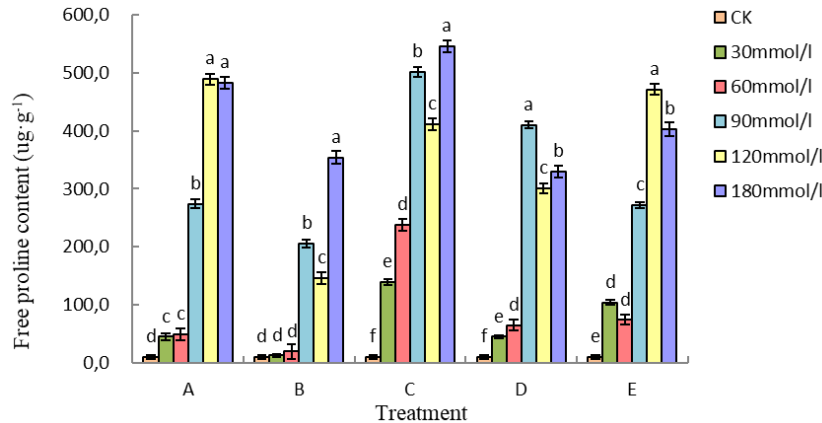


**Figure 7.** Changes in free proline content in *P. giganteum* seedlings under saline-alkali stress

Figure 8 shows that the soluble protein in the environment of increased concentration of each stress group shows the rule of gradual increase. Similarly, the soluble protein in the A and D stress group showed the rule of decreasing after increasing. In the treatment group, when the concentration of the stress environment was  $60 \text{ mmol}\cdot\text{L}^{-1}$ ,  $90 \text{ mmol}\cdot\text{L}^{-1}$  and  $120 \text{ mmol}\cdot\text{L}^{-1}$ , the content was significantly higher than that of the control group, and the peak value appeared at the concentration of  $90 \text{ mmol}\cdot\text{L}^{-1}$ . However, there was no significant difference in soluble protein content between the two groups. In the stress group D, except that the soluble protein content of  $30 \text{ mmol}\cdot\text{L}^{-1}$  was slightly lower than that of the control and there was no significant difference, the soluble protein content of other concentrations under stress appeared significant, and the peak value appeared at  $120 \text{ mmol}\cdot\text{L}^{-1}$ , increased by 8.9% compared with the control. For the treatment group B with low proportion of basic salt and the treatment group E with high proportion of basic salt, when the mixed salt concentration is lower ( $< 90 \text{ mmol}\cdot\text{L}^{-1}$ ), the soluble protein almost does not increase or the increase amount is very small, or even decreases. When the environmental concentration reaches  $\leq 120 \text{ mmol}\cdot\text{L}^{-1}$ , the soluble protein content in the treatment group E increases all the time, and there is significant difference until it reaches the peak value, compared with the control group, the concentration of soluble protein in treatment B increased by 8.94%. When the concentration of stress increased to  $180 \text{ mmol}\cdot\text{L}^{-1}$ , soluble protein content in treatment B reached the peak value, which was 1.05 times higher than that in the control group. In the C treatment group, under the increasing stress environment, the soluble protein will change in the form of W-type. When the mixed salt concentration is  $30 \text{ mmol}\cdot\text{L}^{-1}$  and  $120 \text{ mmol}\cdot\text{L}^{-1}$ , it reaches the minimum value of W-type accumulation mode. Although the content is reduced, it does not show significant. When the concentration was  $90 \text{ mmol}\cdot\text{L}^{-1}$  and  $120 \text{ mmol}\cdot\text{L}^{-1}$ , the peak value of this accumulation was 1.05 and 1.07 times of the control.

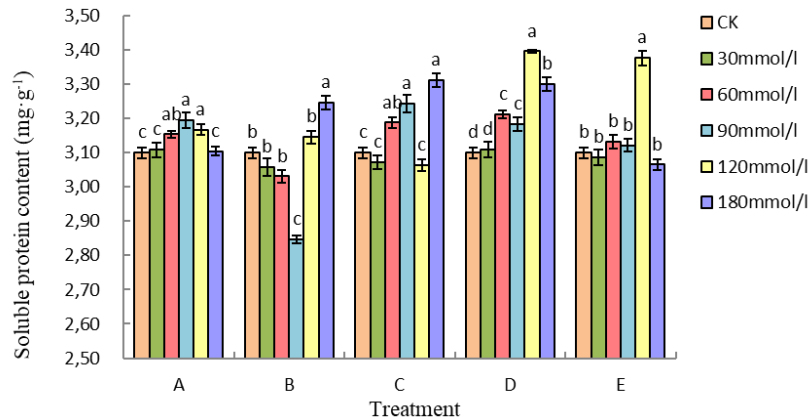


**Figure 8.** Changes in soluble protein content in *P. giganteum* seedlings under saline-alkali stress

### Effects of mixed saline-alkali stress on Na<sup>+</sup> content in various organs

The Na<sup>+</sup> content in the roots of each treatment group accumulated continuously with the increase of salt solution concentration, but the process of accumulation did not continue to increase (Fig. 9). In treatment group A, B, C and E, with the increase of mixed salt concentration, the Na<sup>+</sup> content in the root of *P. giganteum* increased at first, then decreased and then increased, and reached the maximum when the salt concentration was 180 mmol·L<sup>-1</sup>, which was significantly different from that of the control, which was 7.06, 7.40, 4.31, 7.96 times higher than that of the control, respectively. In group A, when the concentration was in the range of 30–90 mmol·L<sup>-1</sup>, the accumulation rate of the Na<sup>+</sup> in the root of *P. giganteum* became very slow or even decreased after reaching a certain amount, and when the concentration continued to increase, the content began to increase abruptly until it reached the maximum value. In group B and C, the Na<sup>+</sup> content decreased significantly when the concentration was in the range of 0–90 mmol·L<sup>-1</sup>. In the D treatment group, when the solution concentration was 30 mmol·L<sup>-1</sup> and 60 mmol·L<sup>-1</sup>, the Na<sup>+</sup> content continued to increase, and there was a significant difference between the control. With the increase of the concentration, the Na<sup>+</sup> content began to decrease significantly, and the Na<sup>+</sup> content began to increase at the concentration of 120 mmol·L<sup>-1</sup>, until it reached the maximum at 180 mmol·L<sup>-1</sup>.

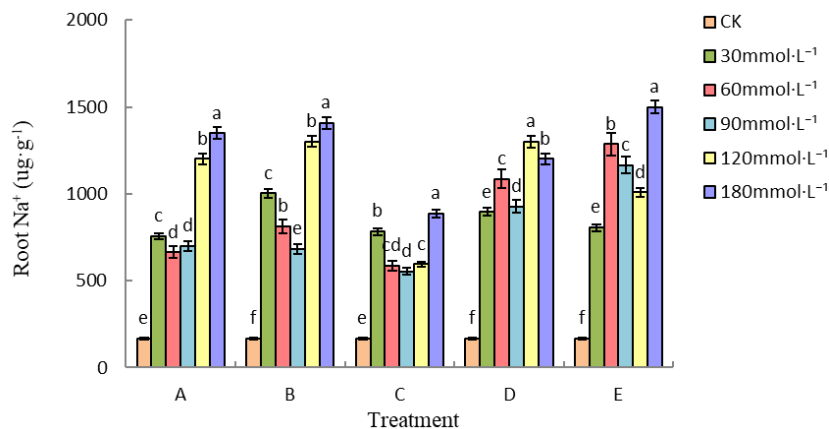


**Figure 9.** Change of the Na<sup>+</sup> content in root of *P. giganteum* seedlings under saline-alkali stress

In the A treatment group with pure salt ratio, the Na<sup>+</sup> content increased significantly with the increase of concentration, until the concentration changed to 180 mmol·L<sup>-1</sup>, the Na<sup>+</sup> content reached the maximum, which was 36.99 times higher than that of the control. In group B, C and D, the Na<sup>+</sup> content increased continuously with the increase of salt solution concentration and reached the maximum when the concentration was 180 mmol·L<sup>-1</sup> which was 33.6 times, 32.0 times and 42.9 times higher than that of the control, respectively. In the E treatment group, the Na<sup>+</sup> content in the stem increased at first, then decreased and then increased with the increase of concentration, and finally reached the maximum when the concentration was 180 mmol·L<sup>-1</sup>, which was 43.6 times higher than that of the control. On the whole, the accumulation of the Na<sup>+</sup> content in the stem of treatment group A, D and E was more than that of treatment group B and C, and the Na<sup>+</sup> content of treatment group E reached the maximum in the whole stress (Fig. 10).

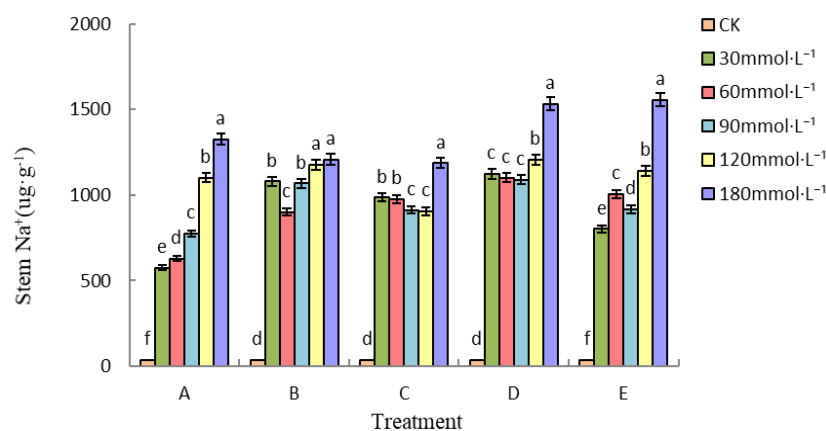


**Figure 10.** Change of the Na<sup>+</sup> content in stem of *P. giganteum* seedlings under saline-alkali stress

In group A, B and E, the Na<sup>+</sup> content in leaves reached the maximum when the concentration was 180 mmol·L<sup>-1</sup>, which was 21.62, 26.09, 25.11 times as much as that of the control, respectively. Treatment A showed a linear and significant increasing trend until the maximum value, and treatment B showed a law of accumulation that increased at first and then decreased and then increased. In group C, the Na<sup>+</sup> content in leaves increased at first and then decreased, and reached the peak at the concentration of 90 mmol·L<sup>-1</sup>, which was 18.35 times higher than that of the control, while in group D, the Na<sup>+</sup> content in leaves showed an M-type increasing trend, that is, increasing-decreasing-increasing-decreasing. The peak appeared when the concentration of the solution was 60 mmol·L<sup>-1</sup> and 120 mmol·L<sup>-1</sup>, and reached the maximum when the concentration was 120 mmol·L<sup>-1</sup>, which was 20.64 times higher than that of the control (Fig. 11).

#### **Effects of mixed saline-alkali stress on K<sup>+</sup> content in various organs**

For the root of *P. giganteum*, the K<sup>+</sup> content in groups A and B with low ratio of pure salt and alkaline salt was significantly lower than that of the control group, and the K<sup>+</sup> content in group A changed little when the solution concentration was ≥ 30 mmol·L<sup>-1</sup>, and the K<sup>+</sup> content remained at a stable level. In group B and C, the K<sup>+</sup> content showed a "W" pattern with the increase of concentration, that is, the trend of "decrease-increase-

decrease-increase". When the concentration was 90 mmol·L<sup>-1</sup>, the K<sup>+</sup> content in group C reached the maximum value of the whole treatment group, which was 1.04 times higher than that of the control, but it was not significant. In the D and E groups with relatively large alkaline salt, the root K<sup>+</sup> content increased and reached the maximum at the concentration of 30 mmol·L<sup>-1</sup>, which increased by 24.5% (significantly higher than the control) and 3.20% (no significant increase compared with the control), respectively, while the root K<sup>+</sup> content of the two groups was significantly lower than that of the control at other concentrations and reached the minimum at the concentrations of 180 mmol·L<sup>-1</sup> and 120 mmol·L<sup>-1</sup>, respectively (Fig. 12). Compared with the control, it decreased by 70.2% and 68.0%.

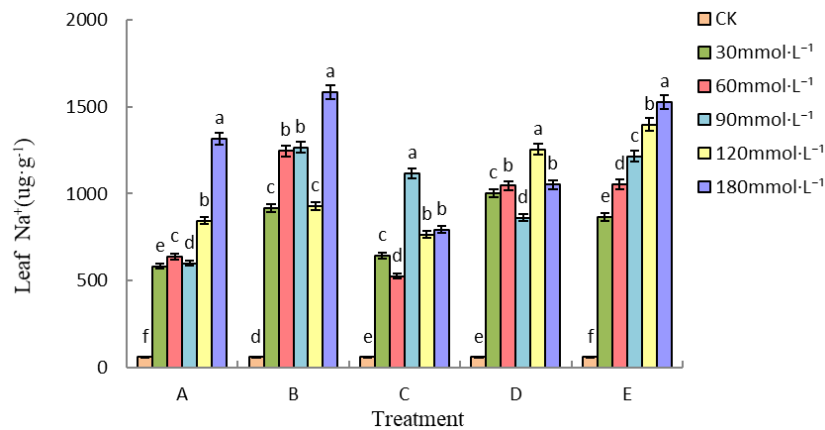


**Figure 11.** Change of the Na<sup>+</sup> content in leaf of *P. giganteum* seedlings under saline-alkali stress

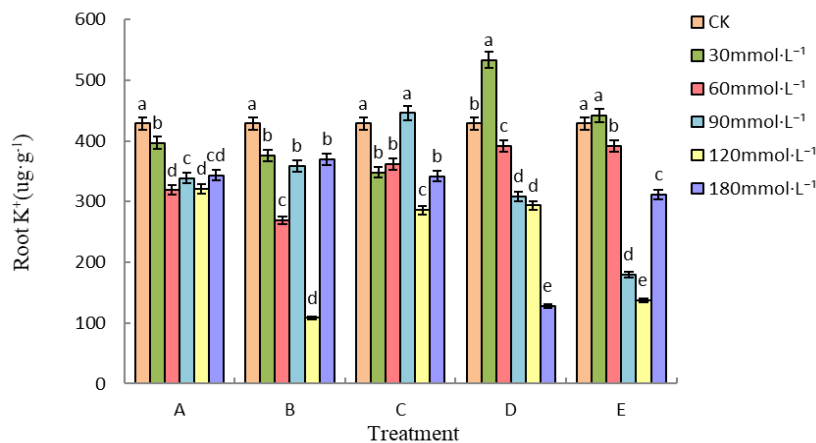


**Figure 12.** Change of the K<sup>+</sup> content in root of *P. giganteum* seedlings under saline-alkali stress

For stems, the K<sup>+</sup> content decreased significantly with the increase of mixed salt concentration in A, B, C and D groups, but the decreasing trend was different (Fig. 13). Among them, in the A and C treatment groups, the K<sup>+</sup> content decreased at first and then increased with the increase of the solution concentration, and the two groups reached the lowest value at the concentration of 90 mmol·L<sup>-1</sup> at the same time, which decreased by 34.2% and 33.7%, respectively compared with the control. In group B, the

$K^+$  content fluctuated and decreased with the increase of concentration. In the D treatment group, the  $K^+$  content decreased significantly with the increase of the mixed salt concentration, and when the concentration was  $180 \text{ mmol}\cdot\text{L}^{-1}$ , the  $K^+$  content of the stem decreased to the lowest value of the whole treatment group, which decreased by 89.2% compared with the control. In the E treatment group with high alkaline salt ratio, the  $K^+$  content increased significantly with the increase of mixed salt concentration, and reached the maximum when the concentration was  $180 \text{ mmol}\cdot\text{L}^{-1}$ , which was 1.58 times higher than that of the control.

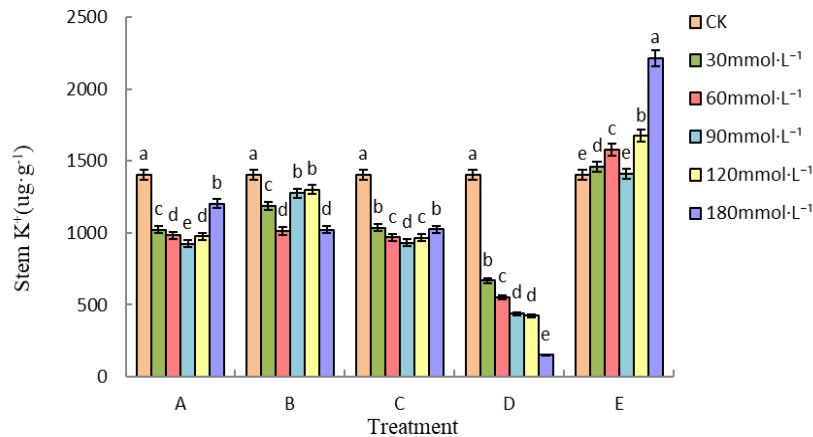


**Figure 13.** Change of the  $K^+$  content in stem of *P. giganteum* seedlings under saline-alkali stress

For leaves, in different treatment groups, the  $K^+$  content increased significantly with the increase of the concentration of mixed salt solution. In A, B, C and D treatment groups, the  $K^+$  content showed the law of fluctuation and accumulation, while the  $K^+$  content in E treatment group increased linearly. In the A treatment group with pure salt ratio and the E treatment group with high alkaline salt ratio, the  $K^+$  content in leaves reached the maximum when the concentration of mixed salt was  $180 \text{ mmol}\cdot\text{L}^{-1}$ , which was 4.51 times and 5.33 times higher than that of the control, respectively. In groups B, C and D with low alkaline salt, the  $K^+$  content in leaves reached the maximum when the concentration of mixed salt was  $30 \text{ mmol}\cdot\text{L}^{-1}$ , which was 3.12, 2.39 and 3.36 times higher than that of the control, respectively (Fig. 14). From the point of view of each treatment group, the  $K^+$  content in leaves of E treatment group with high alkaline salt ratio was significantly higher than that of other concentrations, thus it can be seen that under high alkali environment, it will promote the accumulation of the  $K^+$  content in *P. giganteum* leaves to balance the normal metabolic function of plants.

#### **Effects of mixed saline-alkali stress on the ratio of the $\text{Na}^+$ to $\text{K}^+$ in different organs**

As can be seen from Figure 15, the  $\text{K}^+/\text{Na}^+$  ratio of the roots, stems and leaves of *P. giganteum* seedlings in the treatment groups with different ratios had a small change range and was significantly lower than that of the control groups. In the three treatment groups of A, C and D, the  $\text{K}^+/\text{Na}^+$  ratio at the root decreased to the minimum when the concentration of mixed salt was  $180 \text{ mmol}\cdot\text{L}^{-1}$ , which decreased by 90.08%, 84.97% and 95.86%, respectively. In the two treatment groups of B and E, the ratio of the  $\text{K}^+/\text{Na}^+$  at the root decreased to the minimum when the concentration of mixed salt was

120 mmol·L<sup>-1</sup>, which decreased by 96.76% and 94.69%, respectively compared with the control group. In each treatment group, the ratio of the K<sup>+</sup>/Na<sup>+</sup> of stem in different mixed salt concentrations decreased little, with no significant difference, and the decrease was greater than 95%. In the D treatment group with a concentration of 180 mmol·L<sup>-1</sup>, the ratio of the K<sup>+</sup>/Na<sup>+</sup> of stem decreased the most, which was 99.13% lower than that of the control group. For the leaves, the decrease of the K<sup>+</sup>/Na<sup>+</sup> ratio in the two treatment groups A and E at different mixed salt concentrations was not significant. The K<sup>+</sup>/Na<sup>+</sup> ratio of B, C and D treatment group decreased significantly compared with the control group, and the decrease was significantly different under various mixed salt concentrations. Among them, the ratio of the K<sup>+</sup>/Na<sup>+</sup> in the middle lobe of the B and D treatment groups was reduced to the minimum when it was 180 mmol·L<sup>-1</sup>, which decreased by 90.87% and 87.34% respectively compared with the control group. However, the ratio of the K<sup>+</sup>/Na<sup>+</sup> in the middle lobe of the C treatment group was reduced to the minimum at 90 mmol·L<sup>-1</sup>, which was 84.55% lower than that of the control group.

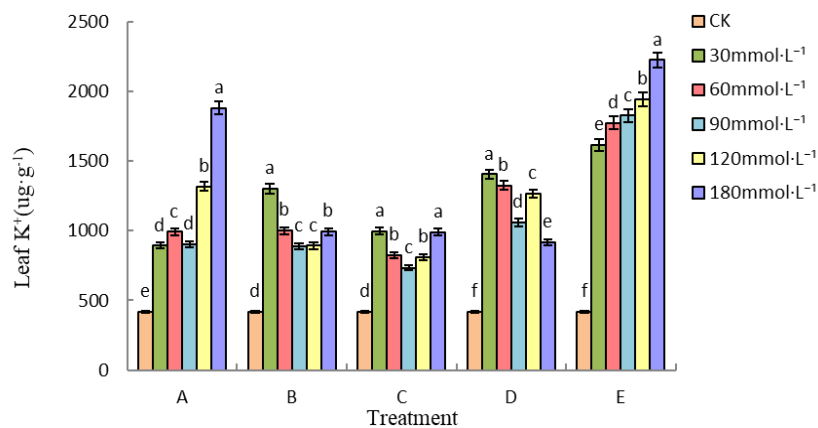


**Figure 14.** Change of the K<sup>+</sup> content in leaf of *P. giganteum* seedlings under saline-alkali stress

### ***Effects of mixed saline-alkali stress on selective transport capacity of mineral ions in individual organs***

Table 2 shows that there is a positive correlation between the selective transport of the K<sup>+</sup> and the selective coefficient of S<sub>K,Na</sub> under mixed saline-alkali stress, that is, the higher the selective coefficient of S<sub>K,Na</sub>, the stronger the selective transport of the K<sup>+</sup> by plants. In different treatment groups, with the increase of the concentration of saline-alkali mixed solution, the value of S<sub>K,Na</sub> transported from root to stem showed a downward trend, and the value of S<sub>K,Na</sub> was lower or significantly lower than that of the control, while in the same treatment group, with the increase of the concentration of saline-alkali mixed solution, the value of S<sub>K,Na</sub> transported from stem to leaf increased, and the value of S<sub>K,Na</sub> was significantly higher than that of the control. Thus it can be seen that in the process of mixed stress, the selective transport of stem inhibited the transport process of the Na<sup>+</sup> in varying degrees, hindered its entry into the leaves, and enhanced the transport capacity of the K<sup>+</sup> to a certain extent, making more K<sup>+</sup> into the leaves. On the other hand, the selective transport in the root is opposite to that in the stem, that is, it enhances the transport capacity of the Na<sup>+</sup>, but inhibits the transport process of the K<sup>+</sup> in varying degrees and weakens its absorption. However, in different

ratios of A, B, C and E treatment groups, the  $S_{K,Na}$  value transported from root to stem under various concentration stress was higher than that from stem to leaf at the corresponding concentration, while in D treatment group with higher alkaline salt ratio, the change rule of  $S_{K,Na}$  value was the opposite. The results showed that the ability of transporting  $K^+$  from stem to leaf was stronger than that of stem to leaf in A, B, C and E treatment groups, and wanted to intercept more  $Na^+$ , and keep it in the root to reduce the damage of saline-alkali mixed stress to aboveground parts, while in D treatment group, the ability of stem to transport  $K^+$  to leaf was stronger than that of root to stem, which balanced and ensured the normal physiological metabolism of leaves to some extent.

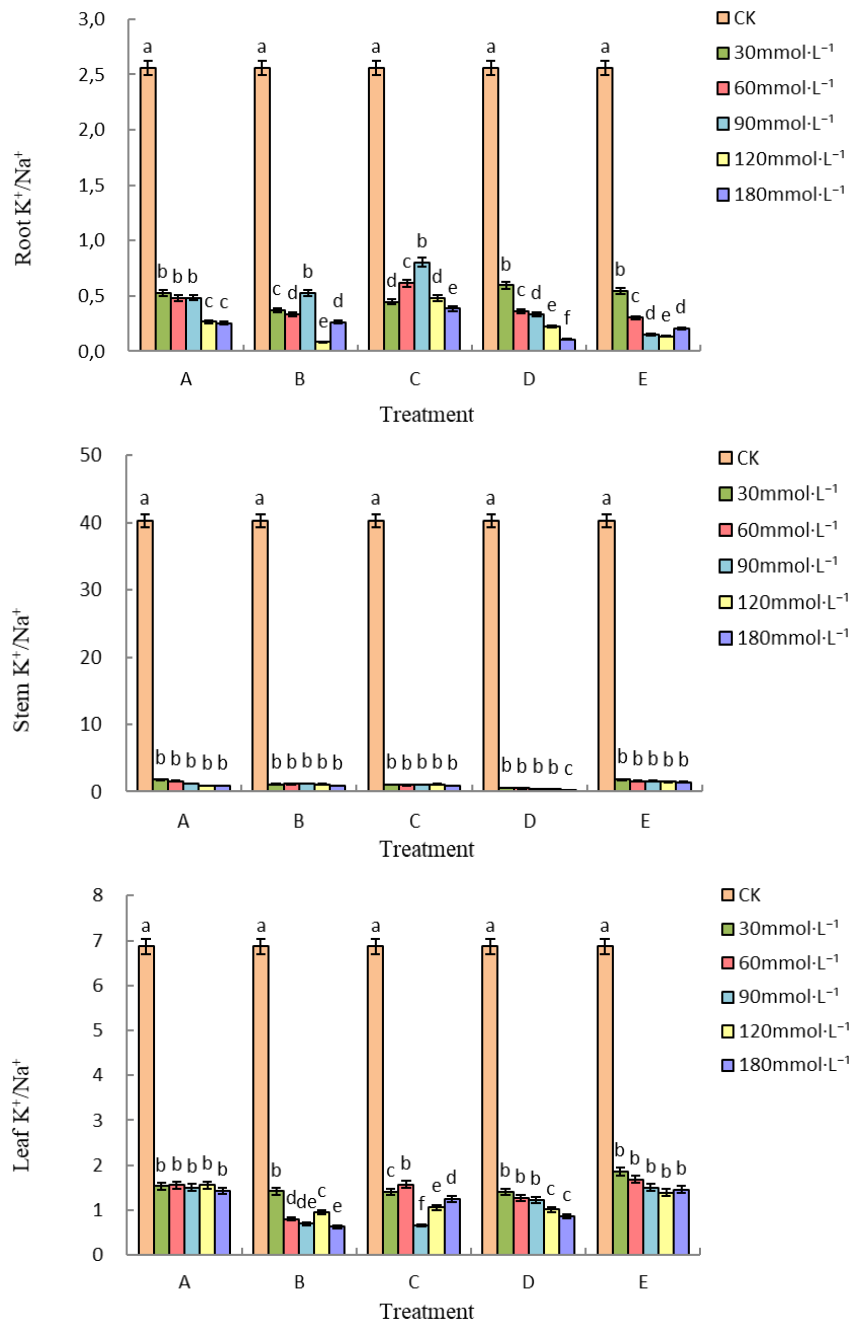


**Figure 15.** Change of the  $K^+/Na^+$  ratios in different organs of *P. giganteum* seedlings under saline-alkali stress



**Table 2.** Effect of saline-alkali stress on transporting selective ratios of the  $K^+$  to  $Na^+$  in *P. giganteum*

Saline-alkali mixture ratio and concentration (mmol·L <sup>-1</sup> )		S <sub>K,Na</sub>	
		Root - stem	Stem-leaf
A	CK	15.72±0.63a	0.17±0.01e
	30	3.39±0.02b	0.86±0.02d
	60	3.26±0.04bc	0.99±0.02c
	90	2.46±0.04c	1.26±0.03b
	120	3.31±0.00bc	1.76±0.01a
	180	3.57±0.02b	1.58±0.02a
B	CK	15.72±0.63a	0.17±0.01e
	30	2.93±0.03b	1.29±0.02a
	60	3.38±0.19b	0.71±0.02c
	90	2.28±0.06b	0.59±0.01d
	120	13.28±1.36a	0.87±0.00b
	180	3.22±0.11b	0.74±0.01c
C	CK	15.72±0.63a	0.17±0.01e
	30	2.36±0.01b	1.33±0.02b
	60	1.61±0.04cd	1.58±0.01a
	90	1.27±0.01d	0.64±0.02d
	120	2.22±0.02bc	0.99±0.01c
	180	2.24±0.01b	1.45±0.03b
D	CK	15.72±0.63a	0.17±0.01d
	30	0.99±0.04b	2.36±0.05c
	60	1.39±0.02b	2.52±0.12c
	90	1.21±0.02b	3.05±0.31b
	120	1.56±0.05b	2.86±0.42b
	180	0.93±0.00b	8.79±0.41a
E	CK	15.72±0.63a	0.17±0.01c
	30	3.31±0.02f	1.03±0.02ab
	60	5.16±0.01e	1.07±0.02a
	90	10.00±0.34c	1.02±0.01ab
	120	12.76±0.33b	0.95±0.04b
	180	6.86±0.28d	1.02±0.01ab

Different treatments: A) NaCl : Na<sub>2</sub>SO<sub>4</sub> : NaHCO<sub>3</sub> : Na<sub>2</sub>CO<sub>3</sub>=1:1:0:0, B) NaCl : Na<sub>2</sub>SO<sub>4</sub> : NaHCO<sub>3</sub> : Na<sub>2</sub>CO<sub>3</sub>=1:2:1:0, C) NaCl : Na<sub>2</sub>SO<sub>4</sub> : NaHCO<sub>3</sub> : Na<sub>2</sub>CO<sub>3</sub>=1:9:9:1, D) NaCl : Na<sub>2</sub>SO<sub>4</sub> : NaHCO<sub>3</sub> : Na<sub>2</sub>CO<sub>3</sub>=1:1:1:1, E) NaCl : Na<sub>2</sub>SO<sub>4</sub> : NaHCO<sub>3</sub> : Na<sub>2</sub>CO<sub>3</sub>=9:1:1:9. Different letters indicate significant difference ( $P \leq 0.05$ ) among various concentrations in the same treatment based on least significant difference test (LSD)

## Discussion

Saline-alkali stress is a particularly significant way to limit the normal growth and development of plants (Jia et al., 2020). When plants were subjected to saline-alkali stress, the growth of plants was inhibited in varying degrees with the increase of concentration (Zhao et al., 2017; Lou et al., 2018; Anam et al., 2019). Farooq et al. (2017) on chickpea (*Cicer arietinum* L.) and Rasouli and Kiani-Pouya (2015) on Rye (*Secale cereale* L.) showed that under saline-alkali stress, plants could not absorb enough water and mineral nutrients, resulting in a decrease in  $Pn$ , while consuming more organic matter to deal with osmotic stress and ion toxicity caused by saline-alkali stress, the most intuitive manifestation is the decrease of biomass. Many studies have shown that mixed saline-alkali compound stress is not a simple superposition of saline-alkali stress, but has a certain synergistic effect. Plants are not only subjected to osmotic injury and ion toxicity caused by salt stress, but also affected by high pH caused by alkali stress (Guo et al., 2017). The results showed that the growth of plant height of *P.*



*giganteum* was inversely proportional to the concentration of mixed salt, that is, the growth of plant height decreased gradually with the increase of salt concentration. In group A of pure salt solution and group B with lower proportion of alkaline salt, the growth of plant height decreased slowly when the solution concentration was lower 30 mmol·L<sup>-1</sup> and 60 mmol·L<sup>-1</sup>. However, in the latter three treatments with a large proportion of alkaline salt, the plant height growth decreased sharply with the increase of salt concentration, even in the mixed salt solution of low concentration of 30 mmol·L<sup>-1</sup>, the plant height growth was significantly lower than that of the control. This shows that the growth of *P. giganteum* is affected not only by salt concentration, but also by the synergistic effect of high pH. Similar effects of saline-alkali mixed stress have been found in sunflower (*Helianthus annuus* L.) and alfalfa (Shi and Sheng, 2005; Peng et al., 2008).

A large number of active oxygen free radicals (Reactive Oxygen Species, ROS) in plants are produced in the process of saline-alkali stress. In the first line of defense of plant antioxidant system, SOD first scavenges reactive oxygen free radicals, and then converts O<sub>2</sub><sup>-</sup> into H<sub>2</sub>O<sub>2</sub> and O<sub>2</sub> to achieve the purpose of antioxidation (Shafqat et al., 2019). The results showed that no matter what proportion of neutral salt and alkaline salt were mixed, the MDA content of *P. giganteum* was proportional to the salt concentration, and the MDA content increased continuously with the increase of salt concentration. This shows that mixed saline-alkali stress will lead to the accumulation of MDA in *P. giganteum*, and the degree of cell membrane peroxidation will increase continuously, whether in high-salt or high-alkali soil environment, it will lead to leaf peroxidation, thus affecting plant growth. Superoxide dismutase (SOD) is an important antioxidant enzyme, which can prevent the damage of reactive oxygen species to the cell membrane system (Zhang et al., 2019). During the whole stress process, the change range of CAT activity was less than that of SOD activity, which indicated that the antioxidant effect of CAT was relatively less than that of SOD under mixed salt stress. This is consistent with the results of the study of Amor in Sea rocket (*Cakile maritime*) (Amor et al., 2006).

Osmotic regulation is an important physiological mechanism for plants to resist adversity. Plants can regulate cell osmotic balance by synthesizing osmotic substances (proline, soluble sugars, organic acids, etc.) to increase their saline-alkali tolerance, so as to alleviate the damage caused by combined saline-alkali stress to plants (Capula-Rodríguez et al., 2016). Some studies have shown that the accumulation of proline is not only a signal of plant response to saline-alkali stress, but also a kind of defensive behavior. In this experiment, the proline content of *P. giganteum* increased slowly at low salt concentration, but accumulated at high salt concentration, which was similar to the results of Yang et al. (2007). It shows that proline is not the product of osmotic stress, but the product of stress degree. This may be that *P. giganteum* has a certain tolerance to saline-alkali compound stress, accumulate a large amount of proline when it exceeds the tolerance range, and alleviate the damage caused by saline-alkali compound stress, until it cannot bear the stress of high salt and high alkali. For soluble protein and soluble sugar, in the process of low concentration or slow increase, soluble protein and soluble sugar will increase periodically, when the concentration reaches a certain level, these two regulatory substances will also increase sharply to balance their own metabolism. It can be seen that *P. giganteum* can balance and regulate its own metabolism to a certain degree of stress, showing a certain ability to adapt.

Saline-alkali stress will produce ion toxicity to plants. Plant roots will maintain ion homeostasis inside and outside the cell or tissue by regulating the entry and exit of intracellular ions. Under compound saline-alkali stress, maintaining high  $K^+/Na^+$  ratio in leaves is an important index of plant saline-alkali tolerance (Shaheen et al., 2016). Ma et al. (2011) analyzed the ion contents of the  $K^+$ ,  $Na^+$  and  $Ca^{2+}$  in roots, underground stems and aboveground parts of Chinese leymus (*Leymus chinensis*) treated for 6 months under different degrees of alkali stress, and revealed the mechanism of *Leymus chinensis* maintaining ion balance under saline-alkali stress. The results showed that the  $Na^+$  content in roots was lower, but the selective absorption of the  $K^+$  and  $Ca^{2+}$  was stronger, which ensured a higher ratio of the  $K^+/Na^+$  and  $Ca^{2+}/Na^+$ . It is an important mechanism for *Leymus chinensis* to adapt to alkali stress.  $Na^+$  is one of the necessary elements for the growth and development of plants in saline-alkali soil, and its content can directly affect the salt tolerance of plants. The results of this experiment show that the accumulation of the  $Na^+$  in the upper part (stem and leaf) is larger than that in the underground part (root), which indicates that there is a strict regulation mechanism for the absorption and transport of the  $Na^+$ , and the regional distribution of the  $Na^+$ , this mechanism well avoids the excessive accumulation of ions in a certain organ of the plant, thus avoiding ion toxicity (Liu et al., 2015). As a necessary element for plant growth and a key ion for osmotic regulation,  $K^+$  participates in the activation of more than 50 enzymes needed for chlorophyll synthesis (Azarin et al., 2016). When the plant growth is not stressed, the cells contain more  $K^+$ , so as to maintain the normal growth of the plant. In this study, the  $K^+$  content in different organs decreased with the increase of salt solution concentration, which was opposite to that of the  $Na^+$ . This shows that there is a certain competition between  $Na^+$  and  $K^+$ , which is also a cation to maintain the normal function of cells, which is caused by the antagonism of ions, because they have similar physical and chemical properties, that is, the radius of ions is similar to the hydration energy of ions. At the same time, in this study, the ratio of the  $Na^+$  decreased significantly with the increase of mixed salt concentration in all organs, and the ratio of the  $K^+/Na^+$  in roots was significantly different at various concentrations, but there was no significant difference in the ratio of the  $K^+/Na^+$  in stems and leaves among multiple treatments. At the same time, the results of this experiment showed that the ratio of the  $K^+/Na^+$  in roots was less than 1, while that in stems and leaves was greater than 1, which indicated that *P. giganteum* mainly regulated ion osmosis under salt stress through roots, thus ensuring the ion balance of aboveground parts, indicating that *P. giganteum* had better physiological regulation mechanism and higher salt tolerance.

## Conclusion

(1) The response mechanism of the growth characteristics of *P. giganteum* to saline-alkali stress is: when the mixed salt concentration is small, the growth of *P. giganteum* plant and the relative water content of the leaves do not decrease significantly, but it decreases with the increase of the salt solution concentration. The trend is obvious, that is, high-concentration saline-alkali stress will inhibit the growth of *P. giganteum*.

(2) Under the saline-alkali mixed stress treatment, with the increase of concentration, MDA content accumulated intermittently, *P. giganteum* reduced oxidative damage and maintained normal plant physiological metabolism through the complementary action of antioxidant enzymes SOD and CAT.

(3) During the mixed saline-alkali stress, when the mixed salt solution concentration is low, the soluble sugar, soluble protein and free proline of *P. giganteum* slowly accumulate, and alternately complete the osmotic adjustment function. As the concentration continues to increase, the free proline content increases rapidly and plays a leading role in the process of osmotic regulation of plants to ensure their physiological activities.

(4) Under mixed saline-alkali stress, *P. giganteum* makes the root and stem absorb most of the Na<sup>+</sup>, to inhibit its entry into the leaves, and transport K<sup>+</sup> to the leaves at the same time to ensure its absorption of mineral elements and normal metabolic activities, which is one of the important mechanisms of resistance to mixed stress.

(5) In the future research, the next step will be to analyze the molecular response of *P. giganteum* to saline-alkali stress by new means such as biotechnology and genomics, which will help to provide novel insights into the saline-alkali stress tolerance mechanisms of plant.

**Acknowledgements.** The study was supported by the Transformation Project of Scientific and technological achievements in Inner Mongolia Autonomous region (CGZH2018137).

## REFERENCES

- [1] Amor, N. B., Jimenez, A., Megdiche, W., Lundqvist, M., Sevilla, F., Abdelly, C. (2006): Response of antioxidant systems to NaCl stress in the halophyte *Cakile maritima*. – *Physiologia Plantarum* 126(3): 446-457.
- [2] Anam, G. B., Reddy, M. S., Ahn, Y. (2019): Characterization of *Trichoderma asperellum* RM-28 for its sodic/saline-alkali tolerance and plant growth promoting activities to alleviate toxicity of red mud. – *The Science of the total environment* 662: 462-469.
- [3] Ashraf, M., Akram, N. A. (2009): Improving salinity tolerance of plants through conventional breeding and genetic engineering: An analytical comparison. – *Biotechnology Advances* 27(6): 744-752.
- [4] Azarin, K. V., Alabushev, A. V., Usatov, A. V., Kostylev, P. I., Kolokolova, N. S., Usatova, O. A. (2016): Effects of salt stress on ion balance at vegetative stage in rice (*Oryza sativa* L.). – *OnLine Journal of Biological Sciences* 16(1): 76-81.
- [5] Bless, A. E., Colin, F., Crabit, A., Devaux, N., Philippon, O., Follain, S. (2018): Landscape evolution and agricultural land salinization in coastal area: A conceptual model. – *The Science of the total environment* 625: 647-656.
- [6] Bui, E. N. (2013): Soil salinity: A neglected factor in plant ecology and biogeography. – *Journal of Arid Environments* 92: 14-25.
- [7] Capula-Rodríguez, R., Valdez-Aguilar, L. A., Cartmill, D. L., Cartmill, A. D., Alia-Tejacal, I. (2016): Supplementary calcium and potassium improve the response of tomato (*Solanum lycopersicum* L.) to simultaneous alkalinity, salinity, and boron stress. – *Communications in Soil Science and Plant Analysis* 47(4): 505-511.
- [8] Farooq, M., Gogoi, N., Hussain, M., Barthakur, S., Paul, S., Bharadwaj, N., Migdadi, H. M., Alghamdi, S. S., Siddique, K. H. M. (2017): Effects, tolerance mechanisms and management of salt stress in grain legumes. – *Plant Physiology and Biochemistry* 118: 199-217.
- [9] Guo, R., Shi, L. X., Yan, C. R., Zhong, X. L., Gu, F. X., Liu, Q., Xia, X., Li, H. R. (2017): Ionic and metabolic responses to neutral salt or alkaline salt stresses in maize (*Zea mays* L.) seedlings. – *Bmc Plant Biology* 17(1): 41.
- [10] Hayat, K., Zhou, Y. F., Menhas, S., Bundschuh, J., Hayat, S., Ullah, A., Wang, J. C., Chen, X. F., Zhang, D., Zhou, P. (2020): *Pennisetum giganteum*: An emerging salt

- accumulating/tolerant non-conventional crop for sustainable saline agriculture and simultaneous phytoremediation. – *Environmental pollution* 265(A): 114876.
- [11] Jia, X. M., Wang, H., Svetla, S., Zhu, Y. F., Hu, Y., Cheng, L., Zhao, T., Wang, Y. X. (2019): Comparative physiological responses and adaptive strategies of apple *Malus halliana* to salt, alkali and saline-alkali stress. – *Scientia Horticulturae* 245: 154-162.
- [12] Jia, X. M., Zhu, Y. F., Zhang, R., Zhu, Z. L., Zhao, T., Cheng, L., Gao, L. Y., Liu, B., Zhang, X. Y., Wang, Y. X. (2020): Iomic and metabolomic analyses reveal the resistance response mechanism to saline-alkali stress in *Malus halliana* seedlings. – *Plant Physiology and Biochemistry* 147: 77-90.
- [13] Liang, X. L., Fang, S. M., Ji, W. B., Zheng, D. F. (2015): The positive effects of silicon on rice seedlings under saline-alkali mixed stress. – *Communications in Soil Science and Plant Analysis* 46(17): 2127-2138.
- [14] Liu, B. S., Kang, C. L., Wang, X., Bao, G. Z. (2015): Physiological and morphological responses of *Leymus chinensis* to saline-alkali stress. – *Grassland Science* 61(4): 217-226.
- [15] Liu, Y. S. (2018): Introduction to land use and rural sustainability in China. – *Land Use Policy* 74: 1-4.
- [16] Lou, Y. H., Guan, R., Sun, M. J., Han, F., He, W., Wang, H., Song, F. P., Cui, X. M., Zhuge, Y. P. (2018): Spermidine application alleviates salinity damage to antioxidant enzyme activity and gene expression in alfalfa. – *Ecotoxicology* 27(10): 1323-1330.
- [17] Ma, H. Y., Liang, Z. W., Yang, H. Y., Huang, L. H., Zhao, M. L. (2011): Ion adaptive mechanisms of *Leymus chinensis* to saline-alkali stress. – *Journal of Food Agriculture and Environment* 9(3): 688-692.
- [18] Ma, Y. C., Wang, J. Y., Zhong, Y., Geng, F., Cramer, G. R., Cheng, Z. M. (2015): Subfunctionalization of cation/proton antiporter 1 genes in grapevine in response to salt stress in different organs. – *Horticulture Research* 2(1): 15031.
- [19] Maia, J. M., Costa De Macedo, C. E., Voigt, E. L., Freitas, J. B. S., Silveira, J. A. G. (2010): Antioxidative enzymatic protection in leaves of two contrasting cowpea cultivars under salinity. – *Biologia Plantarum* 54(1): 159-163. (in Chinese with English abstract).
- [20] Mambetale, A., Nurbulat, L., Gao, L. L., Zhang, J. S., Tian, L. W. (2017): Effect of salt stress on growth and physiological characteristics of sea island cotton and upland cotton cultivars. – *Chinese Bulletin of Botany* 52(4): 465-473.
- [21] Peng, Y. L., Gao, Z. W., Gao, Y., Liu, G. F., Sheng, L. X., Wang, D. L. (2008): Eco-physiological characteristics of alfalfa seedlings in response to various mixed salt-alkaline stresses. – *Journal of Integrative Plant Biology* 50(1): 29-39.
- [22] Rasouli, F., Kiani-Pouya, A. (2015): Photosynthesis capacity and enzymatic defense system as bioindicators of salt tolerance in triticale genotypes. – *Flora - Morphology, Distribution, Functional Ecology of Plants* 214: 34-43.
- [23] Shafqat, N., Ahmed, H., Shehzad, A., Chaudhry, S. K., Shah, S. H., Islam, M., Khan, W., Masood, R., Khan, U. (2019): Screening of wheat-*thinopyrum bessarabicum* addition and translocation lines for drought tolerance. – *Applied Ecology and Environmental Research* 17(5): 10445-10461.
- [24] Shaheen, H. L., Iqbal, M., Azeem, M., Shahbaz, M., Shehzadi, M. (2016): K-priming positively modulates growth and nutrient status of salt-stressed cotton (*Gossypium hirsutum*) seedlings. – *Archives of Agronomy and Soil Science* 62(6): 759-768.
- [25] Shi, D. C., Sheng, Y. M. (2005): Effect of various salt-alkaline mixed stress conditions on sunflower seedlings and analysis of their stress factors. – *Environmental and Experimental Botany* 54(1): 8-21.
- [26] Singh, A. (2015): Soil salinization and waterlogging: A threat to environment and agricultural sustainability. – *Ecological Indicators* 57: 128-130.
- [27] Song, T. T., Xu, H. H., Sun, N., Jiang, L., Tian, P., Yong, Y. Y., Yang, W. W., Cai, H., Cui, G. W. (2017): Metabolomic Analysis of Alfalfa (*Medicago sativa* L.) Root-Symbiotic Rhizobia Responses under Alkali Stress. – *Frontiers in Plant Science* 8: 1208-1222.

- [28] Yang, C. W., Chong, J. N., Li, C. Y., Kim, C. M., Shi, D. C., Wang, D. L. (2007): Osmotic adjustment and ion balance traits of an alkali resistant halophyte *Kochia sieversiana* during adaptation to salt and alkali conditions. – *Plant and Soil* 294(1-2): 263-276.
- [29] Yang, P. Z., Zhang, P., Li, B., Hu, T. M. (2013): Effect of nodules on dehydration response in alfalfa (*Medicago sativa* L.). – *Environmental and Experimental Botany* 86: 29-34.
- [30] Zhang, Y. Q., Yang, F., Ren, H. J., Liu, J. L., Mu, W. Y., Wang, Y. (2019): *Pseudomonas monteilii* PN<sub>1</sub>: A great potential *P*-nitrophenol degrader with plant growth promoting traits under drought and saline–alkali stresses. – *Biotechnology Letters* 41(6): 801-811.
- [31] Zhang, H. H., Li, X., Che, Y. H., Wang, Y., Li, M. B., Yang, R. Y., Xu, N., Sun, G. Y. (2020): A study on the effects of salinity and pH on PSII function in mulberry seedling leaves under saline–alkali mixed stress. – *Trees* 34(3): 693-706.
- [32] Zhao, X., Zhu, H. S., Dong, K. H., Li, D. Y. (2017): Plant community and succession in lowland grasslands under saline–alkali conditions with grazing exclusion. – *Agronomy Journal* 109(5): 2428-2437.
- [33] Zhu, Y. F., Jia, X. M., Wu, Y. X., Hu, Y., Cheng, L., Zhao, T., Huang, Z. C., Wang, Y. X. (2020): Quantitative proteomic analysis of *Malus halliana* exposed to salt-alkali mixed stress reveals alterations in energy metabolism and stress regulation. – *Plant Growth Regulation* 90(2): 205-222.
- [34] Zou, Q. (2000): *The guidance of plant physiology experiment*. – China Agricultural Press, Beijing.

## EFFECT OF DRY-WET ALTERNATION ON DISSOLVED OXYGEN CONCENTRATION IN CONSTRUCTED WETLAND

CHEN, X. Y.<sup>1,2,3\*</sup> – ZHU, J.<sup>1,2,3</sup> – TIAN, Z. F.<sup>1,2,3</sup> – LI, T.<sup>4</sup> – WU, Y. H.<sup>1,2,3</sup> – CHEN, J.<sup>5</sup>

<sup>1</sup>*School of Ecological and Environmental Sciences, East China Normal University, Shanghai 200062, China*

<sup>2</sup>*Hebei Provincial Academy of Ecological and Environmental Sciences, Shijiazhuang 050037, China*

<sup>3</sup>*Hebei Provincial Lab of water Environmental Sciences, Shijiazhuang 050037, China*

<sup>4</sup>*Hebei Provincial Shijiazhuang Qiaoxi Sewage Treatment, Shijiazhuang 050031, China*

<sup>5</sup>*Hebei Provincial Shijiazhuang City Drainage Monitoring Station, Shijiazhuang 050031, China*

*\*Corresponding author*

*e-mail: ecnuljj@163.com; phone: +86-1360-1903-991*

(Received 21<sup>st</sup> May 2020; accepted 17<sup>th</sup> Sep 2020)

**Abstract.** The effect mechanism of dry-wet alternation on dissolved oxygen (DO) concentration in constructed wetlands have not been fully studied. In this paper, the experimental device of constructed wetland in constant temperature box is taken as the research object, and the effect is analyzed at different temperature systematically, changes of DO concentration with different substrates and effects of different dry-wet ratios on DO concentration. The results showed that the dissolved oxygen (DO) concentration increased with the decrease of temperature at different dry-wet alternation times (DAWT) 4 h, 8 h and 12 h. At various temperatures (10°C, 20°C, 30°C), the DO concentration decreased with the increase of DAWT. At the same dry-wet alternation time, DO concentration in each substrate increased with the higher dry-wet ratios. At the same time, it was found that the concentration of DO in the Biochar substrate was lower than that in the Common substrate (Macadam, Zeolite, volcanic rock). Therefore, the dry-wet alternation can increase the dissolved oxygen content of constructed wetland significantly, that is, reducing the dry-wet alternation time (speeding up the frequency) and increasing the dry-wet time ratio are beneficial to the recovery of the reoxygenation ability in constructed wetland.

**Keywords:** *dry-wet ratio, biochar, substrate, dissolved oxygen, reoxygenation*

### Introduction

Dissolved oxygen (DO) concentration is the key factor affecting the purification effect of Constructed Wetland. The results show that the denitrification mechanism of wetland is mainly microbial nitrification, denitrification and anaerobic ammonia oxidation (Huang et al., 2014; Jiang et al., 2019). The amount of nitrogen removal by nitrification and denitrification can account for 60%~86% of the total amount of nitrogen removal (Liu et al., 2003; Faulwetter et al., 2009; Jiang et al., 2019), and the main reason is that wetlands create a good nitrification and denitrification environment for microorganisms. However, the concentration of dissolved oxygen in the wetland is low because of the limitation of Wetland structure, which greatly limits the purification capacity of the wetland, resulting in the unsatisfactory decontamination effect of the wetland (Van-Ostrom et al., 1994; Wu et al., 2001).

Generally speaking, there are great differences in the requirements for the dissolved oxygen content in the process of microbial denitrification in constructed wetland, because

nitrification is an aerobic process, denitrification and anaerobic ammonia oxidation are anaerobic processes, and all single oxygen environment is easy to cause the process of biological denitrification in wetland is not smooth. We know that the oxygen suitable for nitrification should be higher than 2 mg/L, otherwise DO will be the limiting factor of the reaction, and 0.2 mg/l is considered as the minimum do requirement for nitrification; in addition, DO of denitrification should be controlled below 0.5 mg/l, and denitrification above this value will be severely inhibited. Therefore, some new design processes that can improve the reoxygenation capacity of wetland have emerged, such as artificial aeration method (Li et al., 2001; Yan et al., 2007), tidal flow artificial wetland (Sun et al., 2005), wave type subsurface flow artificial wetland system design (He et al., 2004), indirect design water way design (Song et al., 2005; Wu et al., 2010; Zhang et al., 2015), pre aeration (Noorvee et al., 2007), ventilation pipe (Green et al., 1998; Lahav et al., 2001; Ouellet-Plamondon et al., 2006), blast aeration (Yan et al., 2007; Nivala et al., 2007), etc. Some results show that these reoxygenation measures can effectively improve the nitrification capacity of wetland, but the continuous oxygen increase will lead to a large increase in the concentration of nitrate nitrogen in the effluent of wetland, thus reducing the removal efficiency of total nitrogen (Jamieson et al., 2003). So, how to dynamically control and optimize the distribution of oxygen state in the wetland and promote the nitrification and denitrification is very important for the denitrification and decontamination effect of the wetland.

Alternation of drying and wetting is the most basic feature of wetland ecosystem. The alternation of soil / sediment / substrate water is closely related to the enrichment and removal of nutrients. Under the operation mode of dry and wet regulation, the change state of dry and wet alternation (water level fluctuation, anaerobic / aerobic environment alternation, etc.) can also occur in the constructed wetland. However, the mechanism of the effect of dry and wet alternation on the dissolved oxygen concentration in the constructed wetland has not been fully studied. In this paper, the experimental device of constructed wetland is taken as the research object, through the alternation of dry and wet regulation to improve the internal oxygen state of wetland, the change of dissolved oxygen concentration in different substrate types of constructed wetland under the alternation of dry and wet at different temperatures and the influence of different dry and wet ratio on the dissolved oxygen concentration are analyzed systematically, in order to provide theoretical reference for the optimal design of constructed wetland ecosystem Guide.

## Materials and methods

### *Experimental design*

The constructed wetland experimental device is mainly composed of raw water tank and substrate reactor, and the experimental device is placed in a constant temperature box for control, Water Environment Laboratory, Hebei Provincial Academy of Ecological and Environmental Sciences, China (*Figure 1*).

a) Device structure: the size of the experimental device is 100 mm×100 mm×500 mm, which is divided into six groups of devices, three in each group are parallel, which are respectively completed in three thermostatic boxes. The water is supplied by the raw water tank in a unified way, each device is separately discharged, and the water in and out is controlled by the control valve.

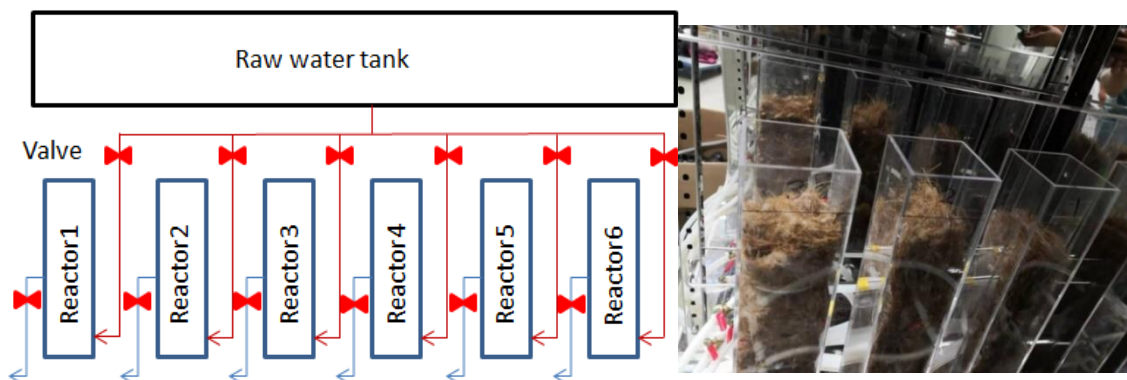


**Figure 1.** Experimental device diagram

b) Matrix: biocarbon matrix (reactor1-3, organic fiber material), size 100 mm×100 mm×50 mm; gravel (reactor4), particle size 10-20 mm; zeolite (reactor5), particle size 20-40 mm; volcanic rock (reactor6), particle size 20-30 mm.

c) Single structure: the biological carbon matrix adopts the "honeycomb" structure, i.e. the three-dimensional network structure, which is composed of straw and coconut fiber matrix, and is placed in unit 1-3 in three types respectively; gravel, zeolite and volcanic rock are placed in unit 4-6, respectively.

d) Water distribution mode: the raw water in the water tank enters the reactor from the bottom through the control of the inlet water level valve, and the outlet water level is controlled by the outlet valve.

e) Raw water: the raw water comes from the tail water of a sewage treatment plant in Shijiazhuang, Hebei Province, China. The tail water is regularly transported back to the laboratory through a transport vehicle in a bucket for standby.

f) Dry and wet alternation time (DAWT): 4 h, 8 h and 12 h, respectively.

### Operation

1) Table 1 shows the dry and wet alternative operation mode.

**Table 1.** Operation mode

No.	DAWT	Inlet/outlet mode	Control condition
1	4h	The dry/wet interval is 4h, i.e. the first hour is full of water, the fourth hour is 1/2V, the eighth hour is 1/2V, the 12th hour is 1/2V, the 16th hour is 1/2V,...	The samples were collected and analyzed at 10°C, 20°C, 30°C, and 20days after stable operation
2	8h	The dry/wet interval is 8h, i.e. the first hour is full of water, the eighth hour is 1/2V, the 16th hour is 1/2V, the 24th hour is 1/2V, the 32th hour is 1/2V,...	
3	12h	The dry/wet interval is 12h, i.e. the first hour is full of water, the 12th hour is 1/2V, the 24th hour is 1/2V, the 36th hour is 1/2V, the 48th hour is 1/2V,...	

2) Table 2 shows the Operation mode of different operation cycle (dry wet ratio).



**Table 2.** Dry wet ratio operation mode

No.	DAWT	inlet/outlet mode	Control condition
1	4h	The ratio of dry / wet time is 1h:3h, i.e. the control water volume is 1/2V from 0 to 1h, then the instantaneous water inflow is 1/2V, the instantaneous water outflow is 1/2V from full water level to 4h, the instantaneous water inflow is 1/2V from 1/2V to 5h, and the instantaneous water outflow is 1/2V from full water level to 8h,...	The samples were collected and analyzed at 10°C, 20°C, 30°C ,and 20days after stable operation
2	8h	The ratio of dry / wet time is 2h:6h, i.e. the control water volume is 1/2V from 0 to 2h, then the instantaneous water inflow is 1/2V, the instantaneous water outflow is 1/2V from full water level to 8h, the instantaneous water inflow is 1/2V from 1/2V to 10h, and the instantaneous water outflow is 1/2V from full water level to 16h,...	
3	12h	The ratio of dry / wet time is 4h:8h, i.e. the control water volume is 1/2V from 0 to 4h, then the instantaneous water inflow is 1/2V, the instantaneous water outflow is 1/2V from full water level to 12h, the instantaneous water inflow is 1/2V from 1/2V to 16h, and the instantaneous water outflow is 1/2V from full water level to 24h,...	

### **Analysis index and methods**

1) Do is determined by thermo Orion five star portable tester (Thermo Fisher Scientific Inc., American), NH<sub>3</sub>-N, NO<sub>3</sub>-N, NO<sub>2</sub>-N, TN and other chemical indexes are determined according to the national standard method (State Environmental Protection Agency).

2) Sampling time: The experiment was carried out in July-October 2019. The samples were collected at 10°C, 20°C and 30°C for 20 days, and three samples were collected for each time.

3) The results were statistically processed using one-way ANOVA, assuming the significance level of  $\alpha=0.05$ , with Origin version 8.0. The Spearman correlation analysis was carried out by using the SPSS 20.0.

4) Water quality sampling: Sampling ports were set at 40 cm in the lower layer of the reactor in the routine experiment; and at 10 cm in the upper layer, 15 cm in the middle layer and 40 cm in the lower layer of the reactor in the vertical experiment.

5) DO Sampling: The probe of portable detector was placed at 40 cm in the lower layer of the reactor in the conventional experiment; and, the probe was placed at 10 cm in the upper layer, 15 cm in the middle layer and 40 cm in the lower layer of the reactor in the vertical experiment.

## **Result**

### **DO concentration change**

#### *Change of dissolved oxygen with temperature at different dry / wet intervals*

It can be seen from *Figure 2* that in the constructed wetland experimental device, the DO concentration value in each substrate increases with the decrease of temperature (DO change value < 3 mg/L) at 4 h and 12 h of DAWT, while the DO concentration value in each substrate does not change significantly with the change of temperature at 8 h of DAWT. At the same time, the DO concentration in biochar matrix (1, 2, 3) is lower than that in common matrix (gravel, zeolite, volcanic rock) (DO change value < 3 mg/L). At

this time, under the dry and wet alternate condition, reducing the time of dry wet alternation (i.e. accelerating the frequency) is conducive to the improvement of wetland reoxygenation capacity (DO change value < 3 mg/L).

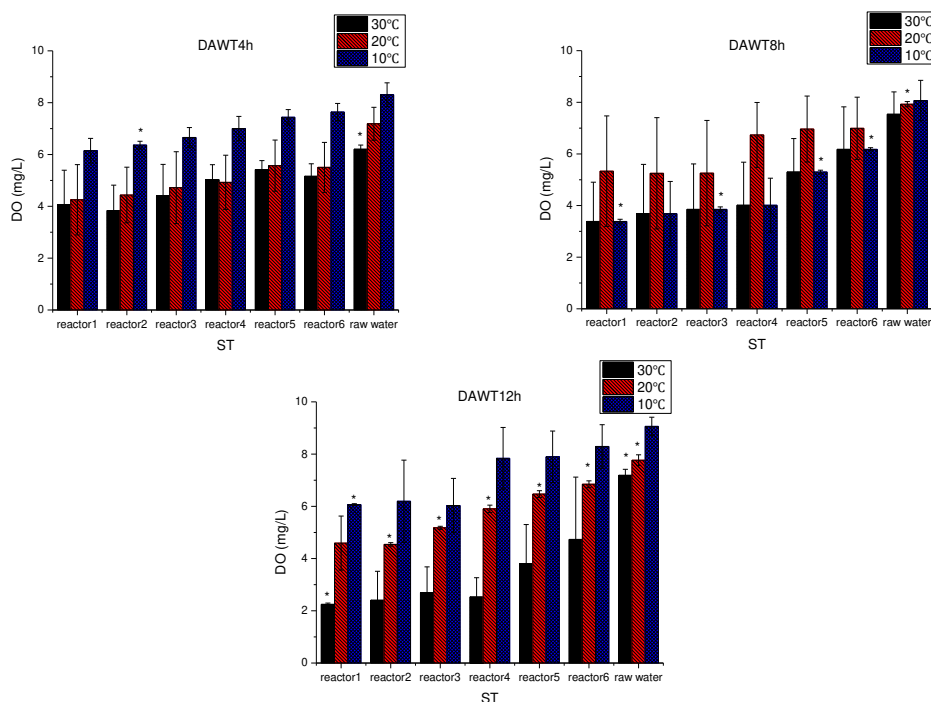


**Figure 2.** Change of dissolved oxygen with temperature (\*,  $\alpha=0.05$ ;  $n=9$ )

#### *Change of dissolved oxygen with dry/wet interval time at different temperatures*

It can be seen from *Figure 3* that at low temperature of 10°C, the concentration of DO in each matrix does not change significantly at 4 h and 12 h of DAWT, but decreases at 8 h of DAWT (DO change value < 3 mg/L); At 20°C, the concentration of DO in each matrix does not change significantly with the time of DAWT; At 30°C, the concentration of DO in each matrix does not change significantly. The concentration of oxygen (DO) decreased with the increase of DAWT time (DO change < 3 mg/L). At the same time, DO concentration in biochar matrix (1, 2, 3) is lower than that in common matrix (gravel, zeolite, volcanic rock). It is also found that reducing the dry wet alternate time (fast increase frequency) is conducive to the improvement of wetland reoxygenation capacity (DO change value < 3 mg/L) under low temperature.

#### *Change of dissolved oxygen in profile*

It can be seen from *Figure 4* that at low temperature of 10°C, the concentration of DO in the bottom of each matrix is less than the upper value, that is, DO decreases with the increase of depth (DO change value < 1.5 mg/L).

#### *Change of dissolved oxygen under different dry wet ratio*

In order to study and analyze the change of dissolved oxygen under different operation cycles (dry to wet ratio, D/W ratio), only biochar matrix is selected for comparative analysis.

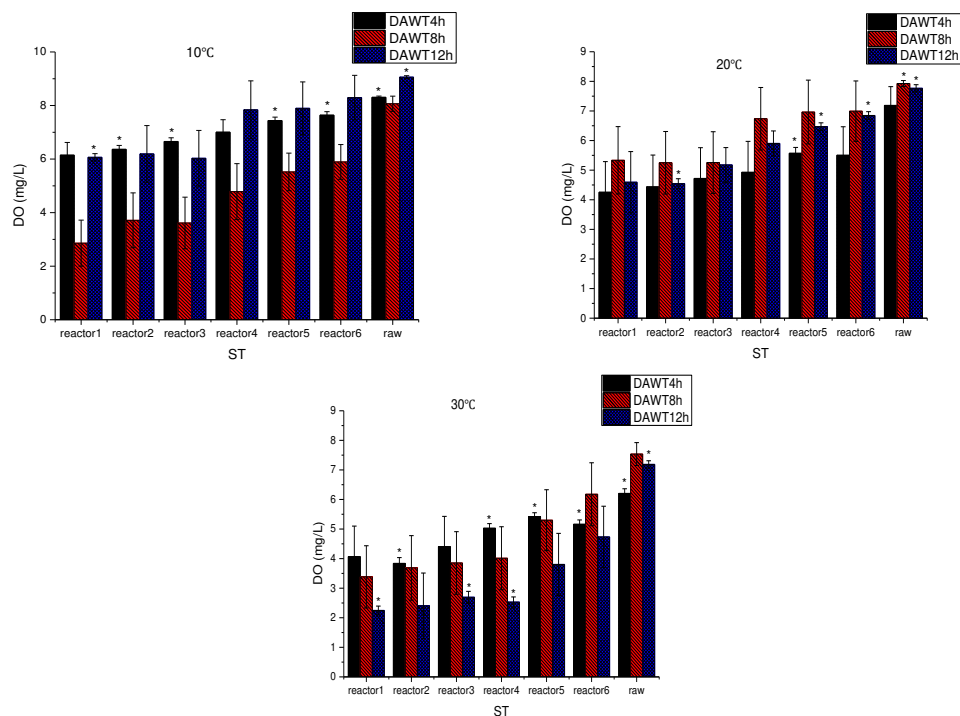


**Figure 3.** Change of dissolved oxygen with dry wet alternation time (\*,  $\alpha=0.05$ ;  $n=9$ )

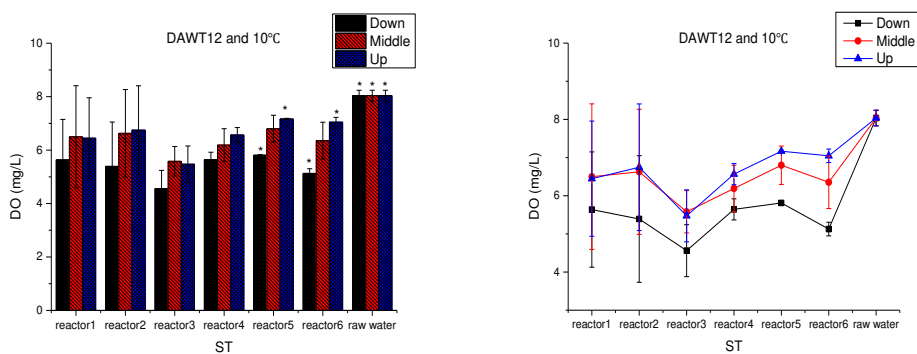


**Figure 4.** Change of dissolved oxygen in profile (\*,  $\alpha=0.05$ ;  $n=9$ )

It can be seen from *Figure 5* that the concentration value of DO in the substrate does not change significantly (DO change value is less than 1.5 mg/L) compared with the concentration value in the original water at the dry wet alternation (DAWT) 4 h (dry wet ratio 1 h:3 h, 2 h:2 h, 3 h:3 h), 8 h (dry wet ratio 2 h:6 h, 4 h:4 h, 6 h:2 h), 12 h (dry wet ratio 4 h:8 h, 4 h:6 h, 8 h:4 h).

When the temperature is 30°C, the DO concentration in the substrate decreases first and then increases with the time of DAWT; At 20°C, the DO concentration in the substrate increased first and then decreased with the time of DAWT; At the temperature of 10°C, the DO concentration in the substrate decreased with the increase of DAWT. At all of the temperature, the DO concentration in the substrate with the dry wet ratio of 3 h:1 h is higher than that in the other substrate. At the same time, it is found that the DO concentration in the biochar matrix increased with the increase of the ratio of dry to wet

(do change value < 1.5 mg/L). It is also found that under the low temperature condition, reducing the alternate time of dry to wet (fast increase frequency) and increasing the ratio of dry to wet time are beneficial to the improvement of the wetland's reoxygenation capacity (DO change value 1.5 mg/L).

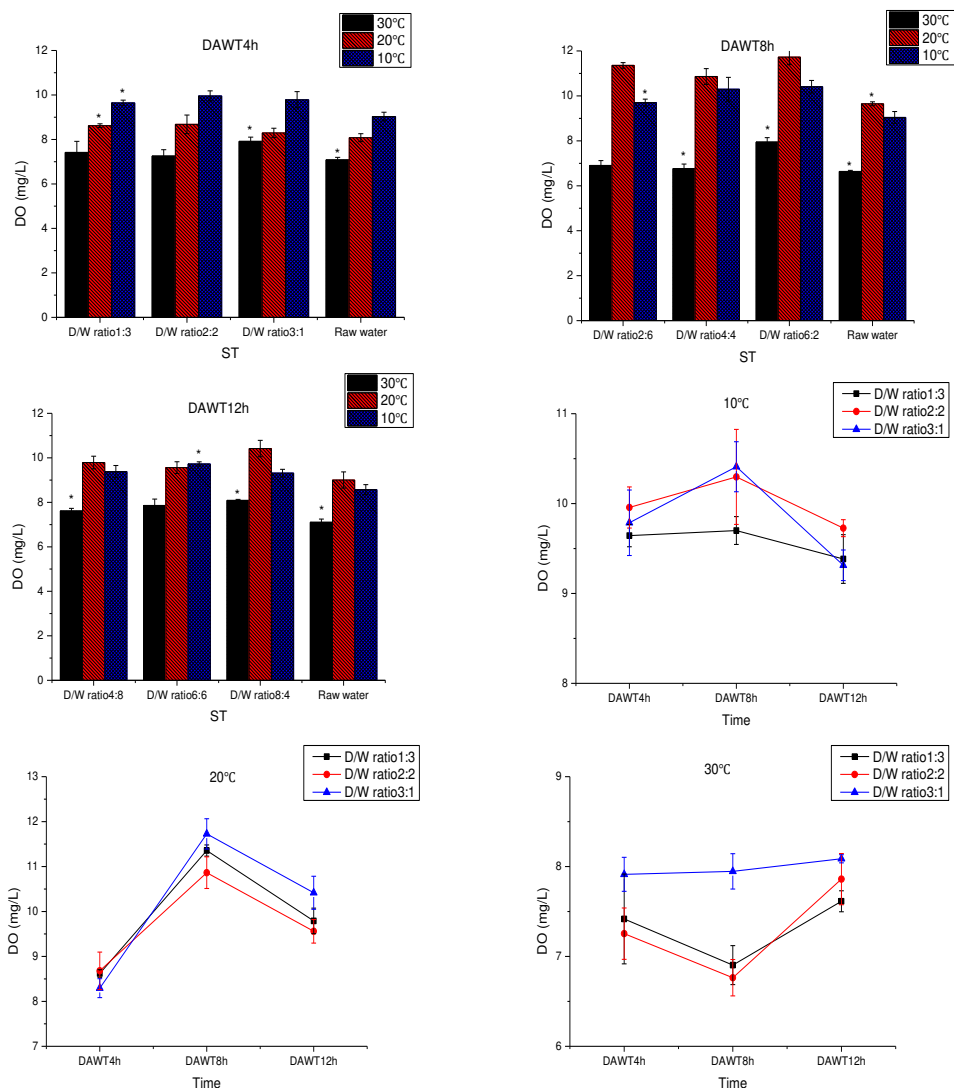


Figure 5. Change of dissolved oxygen under different dry wet ratio (\*,  $\alpha=0.05$ ;  $n=9$ )

### The relationship between dry wet alternation time and DO response

It can be seen from Table 3 that under the influence of alternation of dry and wet in constructed wetland, DO in each substrate is significantly correlated with the interval of dry and wet for 12 h (Pearson correlation,  $P < 0.01$ ), and DO in biocarbon matrix 2, gravel, zeolite and volcanic rock matrix is significantly correlated with the interval of dry and wet for 4 h (Pearson correlation,  $P < 0.05$ ), but not in other cases. And DO in crushed stone matrix is significantly correlated with temperature of 30°C (Pearson correlation,  $P < 0.05$ ), but not in other cases.

**Table 3.** The relationship between DAWT and DO response

Dry and wet conditions		Matrix type					
		Biochar1	Biochar2	Biochar3	Gravel	zeolite	volcanic rock
DAWT	4h	-0.578	-0.753*	-0.624	-0.667*	-0.741*	-0.794*
	8h	0.111	-0.006	0.054	-0.178	0.067	0.088
	12h	-0.908**	-0.794*	-0.814*	-0.923**	-0.760*	-0.701*
Temperature	30°C	-0.525	-0.381	-0.456	-0.677*	-0.479	-0.097
	20°C	0.085	0.029	0.126	0.326	0.331	0.486
	10°C	-0.020	-0.041	-0.164	0.213	0.150	0.223

Note: n = 9; \*, significant correlation at 0.05 level (bilateral); \*\*, significant correlation at 0.01 level (bilateral)

## Discussion

Generally, in natural wetlands, through the natural vegetation, substrate and water level fluctuations and other factors, can achieve the aerobic environment, anaerobic environment and facultative environment alternately, that is, it provides the conditions for the survival of aerobic and ANAEROBIC microflora in wetland, and is beneficial to the removal of pollutants (Faulwetter et al., 2009; Jiang et al., 2019). The dissolved oxygen (DO) content in constructed wetland can be changed by Water / Hydrology Regulation, which makes it appear dry-wet alternate (Anaerobic / Aerobic Environment Alternate). Therefore, wet-dry alternation is an effective method to realize aerobic and anaerobic environment in constructed wetland.

The concentration of dissolved oxygen in wetland is low, which greatly limits the purification space of wetland and leads to the unsatisfactory decontamination effect because of the limitation of wetland structure (Van-Oostrom and Russell, 1994; Wu and Franz, 2001). It has been studied that the reaeration efficiency and the wetland treatment effect can be improved when the dry-wet ratio is 1:2 (8 h:12 h) (Shi et al., 2015). We find that the dry-wet alternate operation mode adopted in this paper can effectively increase the dissolved oxygen (DO) content in the wetland, and the DO concentration in the substrate at the dry-wet ratio of 3:1 (3 h:1 h/6 h:2 h) is higher than that at other dry-wet ratios. The reason is that increasing the dry-wet time ratio, that is, increasing the time of the substrate exposed to the air, so that more oxygen in the air into the wetland substrate. Therefore, wet-dry alternation is an effective method to realize the reoxygenation of constructed wetland.

It was found that the dissolved oxygen content was the main factor affecting the removal rate of pollutants in constructed wetlands (Maltais-Landry et al., 2009), because oxygen content directly affected the biochemical pathways of pollutants in different reduction states (Liu et al., 2017). It is reported that the oxygen output of plants is only 1~8 g/(m<sup>2</sup>g), and the lack of oxygen supply becomes the speed-limiting step of pollutant removal (Zheng et al., 2011). The dry-wet alternate operation mode adopted in this paper is an important technology to effectively improve the removal efficiency of organic matter in constructed wetland (Ding et al., 2015). The results showed that the DO concentration decreased with the increase of dry-wet alternate time (DAWT), that is to say, reducing the dry-wet alternate time could increase the DO content in constructed wetland and promote the removal of pollutants (Zhao et al., 2011).

Through the significance analysis (*Table 3*), it is found that the alternation of dry and wet can significantly affect and improve the content of DO in the wetland matrix, and can realize the artificial aerobic, and create an aerobic environment for the wetland system microorganisms (Liu et al., 2017; Huang, 2018; Kang et al., 2019). In this study, it is found that temperature has no obvious effect on DO content.

## Conclusions

(1) It can be concluded from the study of the incubator constructed wetland experimental device that DO concentration in all substrates increases with the decrease of temperature in different DAWT at 4 h, 8 h and 12 h, and decreases with the increase of DAWT at 10°C, 20°C and 30°C in different temperature. The concentration of DO in biochar matrix (1, 2, 3) is lower than that in common matrix (gravel, zeolite, volcanic rock). At this time, under the dry and wet alternate condition, reducing the time of dry wet alternation (i.e. accelerating the frequency) is conducive to the improvement of wetland reoxygenation capacity.

(2) It was found that the concentration of DO in biomass matrix did not change significantly in 4 hours (1 h:3 h, 2 h:2 h, 3 h:3 h), 8 hours (2 h:6 h, 4 h:4 h, 6 h:2 h), 12 hours (4 h:8 h, 4 h:6 h, 8 h:4 h) of DAWT. At different temperatures of 30°C, 20°C and 10°C, the DO concentration in the matrix increased with the increase of the ratio of dry to wet time. In addition, the DO concentration in the substrate with the dry wet ratio of 3 h:1 h is higher than that in the other substrate. It is also concluded that reducing the frequency of dry wet alternation and increasing the ratio of dry wet time are conducive to the improvement of wetland reoxygenation capacity at dry and wet alternate condition (DO change value < 1.5 mg/L).

(3) In the study of constructed wetland profile at low temperature of 10°C, it was found that the concentration of DO in the bottom of each substrate was lower than that in the upper part, that is, the DO value decreased with the increase of depth.

(4) It is found that the alternation of dry and wet can significantly affect and improve the content of DO in the wetland matrix, and can realize the artificial aerobic, and create an aerobic environment for the wetland system microorganism. It is also found that temperature has no obvious effect on DO content.

(5) What is the dynamic change of dry-wet time ratio and DO concentration under the condition of dry-wet alternation? And how to optimize the design of pollutants removal effect? And other issues need to be further studied.

**Acknowledgements.** This work was supported by the Major Science and Technology Program for Water Pollution Control and Treatment [grant number 2018ZX07110-006].

## REFERENCES

- [1] Ding, Y., Wang, W., Wang, Y. H., Song, X. S. (2015): Research on the mechanism of nitrogen removal and its main influencing factors in horizontal subsurface flow constructed wetlands. – *Industrial Water Treatment* 5(6): 6-9.
- [2] Faulwetter, J. L., Gagnon, V., Sundberg, C., Chazarenc, F., Mark, D. B., Brisson, J., Anne, K. C., Otto, R. S. (2009): Microbial processes influencing performance of treatment wetlands: a review. – *Ecological Engineering* 35(6): 987-1004.

- [3] Green, M., Friedler, E., Safrai, I. (1998): Enhancing nitrification in vertical low constructed wetland utilizing a passive air pump. – *Water Research* 32(12): 3513-3520.
- [4] He, C. D., Tan, L., Ge, L. Y., Ji, J. J., Ye, Y. L., He, L., Wang, H. M. (2004): Application of Wavy Subsurface Constructed Wetland in Treating Domestic Sewage. – *Journal of Agro-Environment Science* 23(4): 766-769.
- [5] Huang, J., Yang, S. S., Li, R. Q., Fu, D. F. (2014): Nitrification intensity and ammonia-oxidizing microorganisms in wetland plant rhizosphere soil at low temperature. – *Research of Environmental Sciences* 27(8): 857-864.
- [6] Huang, J. (2018): Research on Transformation of Endogenous Nitrogen and Mechanism of Microorganism by Intermittent Aeration in Polluted River. – An Hui University.
- [7] Jamieson, T. S., Stratton, G. W., Gordon, R., Madani, A. (2003): The use of aeration to enhance ammonia nitrogen removal in constructed wetlands. – *Canadian Biosystems Engineering* 45: 109-114.
- [8] Jiang, X. Y., Ji, X. Y., Huang, D. Y., Zhang, J. B. (2019): Microbial community structure in the roots of three kinds of plants in integrated vertical flow constructed wetlands. – *Journal of Agro-Environment Science* 38(1): 176-183.
- [9] Kang, X. R., Liu, Y. L., Zhou, Y. X., Su, Y. (2019): Studies on Intermittent Aeration Enhancing Nitrogen Removal of Constructed Wetland at Low Temperature. – *Forest Engineering* 35(3): 74-78.
- [10] Lahav, O., Artzi, E., Tarre, S., Green, M. (2001): Ammonium removal using a novel unsaturated flow biological filter with passive aeration. – *Water Research* 35(2): 397-404.
- [11] Li, S., Wang, W. D., Qiang, Z. M., Zhang, M. X., Liang, X. Q., Wang, F. E., Chen, Y. X. (2001): Denitrification of rural domestic wastewater with self-aeration constructed wetland. – *Environmental Science & Technology* 34(3): 19-22.
- [12] Liu, C. X., Dong, C. H., Li, F. G., Hu, H. Y., Huang, X., Shi, H. C., Qian, Y. (2003): Study on Ability of Nitrification in a Subsurface Constructed Wetland System Treating Sewage. – *Environmental Sciences* 24(1): 80-83.
- [13] Liu, Y. J., Han, X., Liu, H., Wang, Z. (2017): Effects of Aeration Patterns on Nitrogen Removal in Constructed Wetlands. – *Shangdong Chemical Industry* 46(5): 152-155.
- [14] Maltais-Landry, G., Maranger, R., Brisson, J., Chazarenc, F. (2009): Nitrogen transformations and retention in planted and artificially aerated constructed wetlands. – *Water Research* 43(2): 535-545.
- [15] Nivala, J., Hoos, M. B., Cross, C., Wallace, S., Parkin, G. (2007): Treatment of landfill leachate using an aerated, horizontal subsurface-flow constructed wetland. – *Science of Total Environment* 380(1-3): 19-27.
- [16] Noorvee, A., Pöldvere, E., Ülo, M. (2007): The effect of pre-aeration on the purification processes in the long-term performance of a horizontal subsurface flow constructed wetland. – *Science of Total Environment* 380: 229-236.
- [17] Ouellet-Plamondon, C., Chazarenc, F., Comeau, Y., Brisson, J. (2006): Artificial aeration to increase pollutant removal efficiency of constructed wetlands in cold climate. – *Ecological Engineering* 27(3): 258-264.
- [18] Song, T. H., Yin, J., Cui, Y. B. (2005): Comparison and Analysis of the Different Inflows and Effluent Ways of Constructed Wetland for the Removal Rate of Wastewater. – *Safety and Environmental Engineering* 12: 46-49.
- [19] State Environmental Protection Agency (2002): Method for determination and analysis of water and wastewater (Fourth Edition). – Beijing: China Environmental Science Press, pp. 200-284.
- [20] Sun, G., Zhao, Y., Allen, S. (2005): Enhanced removal of organic matter and ammoniacal-nitrogen in a column experiment of tidal flow constructed wetland system. – *Journal of Biotechnology* 115(2): 189-97.
- [21] Van-Ostrom, A. J., Russell, J. M. (1994): Denitrification in constructed wastewater wetlands receiving high concentration of nitrate. – *Water Science Technology* 29: 7-14.

- [22] Wu, M. Y., Franz, E. H. (2001): Chen S. Oxygen fluxes and ammonia removal efficiencies in constructed treatment wetlands. – *Water Environmental Research* 73(6): 661-666.
- [23] Wu, S. B., Zhang, D. X., Liu, Q. Q., Zhai, X., Hu, J., Dong, R. J. (2010): Performance optimization of a lab-scale tidal flow constructed wetland for domestic wastewater treatment. – *Journal of China Agricultural University* 15(2): 106-113.
- [24] Yan, L., Wang, S. H., Zhong, Q. S., Huang, J., Liu, Y., Wang, F. (2007): Study on Running Characteristics of Aerating Subsurface Flow Wetlands. – *Environmental Sciences* 28(4): 736-741.
- [25] Zhang, Y. Q., Cui, L. J., Li, W., Li, K. (2015): Study on the Intensity of Matrix Nitrification and Denitrification in Tidal Flow Constructed Wetlands. – *Ecology and Environmental Sciences* 3: 480-486.
- [26] Zhao, Y., Li, F. G., Wang, H. Y., Li, Y., Zhang, M. Q., Wang, Z. Y. (2011): The relationship between microbial diversity and water purification capacity in aerobic/anaerobic subsurface flow constructed wetland. – *Acta Scientiae Circumstantiae* 31(11): 2421-2431.
- [27] Zheng, T. T., Ji, J. J., Ji, R. P., Chen, J. (2011): Progress of Nitrogen Removal in Constructed Wetlands. – *Environmental Science and Technology* 24(S1): 111-115.



## REGULATION OF IRRIGATION WATER QUALITY CAN FURTHER IMMOBILIZE CD IN CONTAMINATED SOILS

LI, P.<sup>1</sup> – ZHANG, Y.<sup>2</sup> – LIU, D.<sup>3</sup> – GUO, W.<sup>3</sup> – LI, K. Y.<sup>1</sup> – ZHANG, Z. L.<sup>4</sup> – QI, X. B.<sup>1,3\*</sup> – ZHAO, Z. J.<sup>1</sup>

<sup>1</sup>*Institution Laboratory of Quality and Safety Risk Assessment for Agro-Products on Water Environment Factors, Ministry of Agriculture and Rural Affairs, Xinxiang 453002, China*

<sup>2</sup>*Farmland Irrigation Research Institute, Chinese Academy of Agricultural Sciences, Xinxiang, Xinxiang 453002, China*

<sup>3</sup>*Agriculture Water and Soil Environmental Field Science Research Station, Chinese Academy of Agricultural Sciences, Xinxiang, Xinxiang 453002, China*

<sup>4</sup>*The James Hutton Institute, Craigiebuckler, Aberdeen AB15 8QH, United Kingdom*

*\*Corresponding author*

*e-mail: qxb6301@sina.cn; phone: +86-373-3393-402*

(Received 21<sup>st</sup> May 2020; accepted 17<sup>th</sup> Sep 2020)

**Abstract.** Combined use of surface water and groundwater is a common practice in agricultural activities, but how the immobilize cadmium and its decrease in grains induced with irrigation micro-polluted surface water and groundwater is still poorly understood. This paper presents field experimental results in attempts to reveal the effect of irrigation water quality on cadmium migration and accumulation in winter wheat/summer maize rotation systems in Huabei plain while the cadmium content in 0-10 cm topsoil is 3.8 times, permissible value for agricultural land in China. The results showed there was no obviously influence on cadmium accumulation in grains irrigated with micro-polluted surface water during emergence and seeding stage, but there was significantly increased Cd content and a higher bioaccumulation factor in grains with micro-polluted surface water irrigation during jointing and booting stage. It was found a significantly inhibition for grain weight and uniformity with groundwater irrigation during jointing and booting stage, and winter wheat yield was significantly decreased with micro-polluted surface water irrigation during jointing and booting stage. It could be concluded irrigation water type can further immobilize Cd in mild and moderate contaminated soils, thus micro-polluted surface water can be adopted in seeding stage, and groundwater irrigated in jointing and booting stage at heavy metal pollution arable farmland to minimize the risk of biological chain pollution and food safety.

**Keywords:** *cadmium, irrigation schedule, micro-polluted surface water, groundwater, bio-concentration factor, bio-accumulation factor*

### Introduction

Soil heavy metals are a common abiotic stress inhibiting crop growth. Heavy metals in the soil not only pose a serious threat to the quality of cultivated land and agricultural products, through the food chain they ultimately threat the health of human beings (Yang et al., 2018; Peng et al., 2019; Huang et al., 2019). Due to its estrogen-like activity, exposure levels of 30-50  $\mu\text{g}$  per day have been estimated for adults and these levels have been linked to increased risk of bone fracture, cancer, kidney dysfunction and hypertension (Satarug et al., 2003; Franz et al., 2008), yet according to a case-control study, cadmium might be related to a decreased risk of ER- and ER-/PR-breast tumors (Amadou et al., 2020). Especially, a very strong Cd contamination in fish organs (gills, posterior intestine, liver, kidneys and skeletal muscle) collected downstream from the metal source (Andres et al., 2000), moreover, the period of

ripening of sexual products led to an increase of condition index and to a decrease of Cd concentrations in the whole soft tissues of clams from both sites, hence reflecting the phenomenon of "biological dilution" (Smaoui-Damak et al., 2006). According to the results of the Ministry of Environmental Protection and the Ministry of Land and Resources' National Survey on Soil Pollution Status from China in 2014, the quality of cultivated soil in China is worrying. The total over-standard rate of soil in China is 16.1% and the pollution is mainly caused by inorganic heavy metals. The number of inorganic pollutants accounted for 82.8% of all over-standard points. At present, the over-standard rate of cultivated soil in China has reached 19.4%, among which the moderate to light pollution points account for 94.33% of the total pollution points, mainly including 8 pollutants such as Cd, Ni and Cu (Chen et al., 2017).

The Huabei Plain is an important grain production base and grain production accounts for 23.6% of China grain yield (Yin et al., 2016), which benefits from long-term high water and fertilizer input, agronomy technology and agricultural management since the 1980s (Chen et al., 2014; Wang et al., 2018a). Global climate change has resulted in more uncertainty in agricultural production systems, which cause potential risk to both food security and natural ecosystems (Hundecha and Bardossy, 2005; Wang et al., 2018b). Based on daily precipitation data from 63 national meteorological stations on the Huabei Plain from 1963 to 2012, the precipitation has since been in decline at a rate of 0.8 mm/per annum, the uncertainty of changes is more obvious due to the climate change (Li et al., 2015, 2018). That's to say, micro-polluted surface water needed to be used for food security, but the average Cd concentration in the micro-polluted surface water and groundwater is 21.6 and 0.5 µg/L respectively (Hu et al., 2016), and approximately 43 times of Cd enters the district via micro-polluted surface water irrigation compared with groundwater irrigation. Rotational irrigation management is therefore essential to block the migration of heavy metals to plant bodies (Li et al., 2014). As in most irrigation areas, groundwater pumped for agricultural irrigation is the main way to solve the shortage of agricultural water for food production in China (Kong et al., 2016; Yin et al., 2017), conjunctive use of micro-polluted surface water and groundwater in this area is to block Cd induced by irrigation with the micro-polluted surface water because the groundwater is relatively less Cd contamination and higher salt content to hinder soluble salts in soil moving into the plant bodies (Li et al., 2014; Arefin et al., 2016; Zhang et al., 2018). The key parameters for managing water usage in the area are bio-concentration factor (BCF) and bio-accumulation factor (BAF) (Safahieh, 2018), we will define BAF here ratio of Cd content in grain and the above-ground plants to the 0 to 40 cm soil layers.

Therefore, the overarching purposes of this paper are (1) to investigate cadmium accumulation in crop-soil system induced with micro-polluted surface water/groundwater irrigation; and (2) to reveal irrigation schedule with micro-polluted surface water/groundwater to ensure grain quality in typical rotation system of Huabei plain, China.

## Materials and Methods

### *The study area*

With Chinese economic fast development from 1980s, it has substantially increased water demand for this region which cannot be met from natural recharge to surface and subsurface watercourse as the average annual precipitation in the area was only 550 mm

since 1980s (Li et al., 2015). Currently, border irrigation with conjunctive use of micro-polluted surface water and groundwater is the dominant irrigation technology in the area. For food security in China, reclaimed water and sewage water from surface rivers participated in agricultural production, a clear increase in the quantity of annual wastewater recycled and reused was observed during the last decade, reaching 3.5 billion m<sup>3</sup> account for 1.60% of total agricultural water consumption in 2013 (Wang et al., 2017). The lasted research results of heavy metal contamination of cultivated soils in Huabei Plain showed exceedance percentages was 12.22% and the proportion of Cd, Ni, Cu, Zn, and Hg increased by 16.07%, 4.56%, 3.68%, 2.24%, and 1.96%, respectively (Shang et al., 2018).

The experiment was carried out in a typical winter wheat /summer maize rotation system area (latitude 35°23'45" N, longitude 113°59'31" E, and altitude 70 m) in Weihe irrigation district, Xinxiang city Henan Province, China from 2012 to 2013. The basic physical and chemical properties of the soil of the study area site are shown in *Table 1*. The winter wheat variety AiKang 58 was planted on October 8 and 2012, harvested on June 6, 2013, and the whole growth period was 241 days. According to the soil fertility status and target yield of the experimental site, urea (TN≥46.4%) 300 kg/hm<sup>2</sup> and compound fertilizer (N-P<sub>2</sub>O<sub>5</sub>-K<sub>2</sub>O=16%:22%:10%) 750 kg/hm<sup>2</sup> was applied as base fertilizer, and urea 225 kg/hm<sup>2</sup> was applied as topdressing at the jointing stage. The summer maize variety DanFu 6 was tested, planted on June 8, 2013, harvested on September 26, 2013, the whole growth period was 110 days, and the summer maize jointing stage was applied with urea 600 kg per hectare. The row spacing of winter wheat and summer maize is 20 cm, 60 cm, respectively, and the sowing rate for winter wheat and summer maize is 150 kg, 45 kg per hectare, respectively. The average annual precipitation in the region is 580 mm, of which 70% falls between June and September; the average annual evaporation measured from the 30 cm pan is 1860 mm. Irrigation is usually needed in the dry seasons including January, March, May and June at the withering, jointing and grain-filling stages of the winter wheat, with irrigation amount varying from 750 m<sup>3</sup>/hm<sup>2</sup> to 1000 m<sup>3</sup>/hm<sup>2</sup> depending on soil moisture and the potential demand of water for the crops. The precipitation occurred in the study period was shown in *Fig. 1*.

**Table 1.** Basic physical and chemical properties of the soil at the study area

Soil layer depth (cm)	Available Cd (mg·kg <sup>-1</sup> )	Total Cd (mg·kg <sup>-1</sup> )	pH	TN (g·kg <sup>-1</sup> )	TP (g kg <sup>-1</sup> )	OM (g·kg <sup>-1</sup> )	Soil texture	Bulk density (g·cm <sup>-3</sup> )
0-10	1.6505	2.2678	8.00	0.95	1.16	19.90	Silt clay	1.40
10-20	0.1915	0.3388	8.05	0.46	0.58	9.90	Silt clay	1.41
20-30	0.0345	0.1110	8.10	0.39	0.52	8.60	Silt clay	1.43
30-40	0.0083	0.0852	8.06	0.35	0.46	7.80	Silt clay	1.43

### Experimental design

According to local irrigation schedule and production habits, the winter wheat needs supplementary irrigation during emergence stage, jointing stage and booting stage, and the summer maize during seeding stage. Two irrigation water sources were available for the experiments, namely micro-polluted surface water and groundwater (W stands for micro-polluted surface water and T stands for groundwater). WTT represents micro-polluted surface water irrigation at the emergence stage, and groundwater irrigation at

the jointing and booting stage. CK represents groundwater irrigation at the emergence stage, jointing and booting stage. The field trial was a fully randomized design with three replicates of eight treatments using micro-polluted surface water and groundwater irrigation with border irrigation. Each experiment plot area is 100 square meters. Other management practices during the whole growth season were completely consistent.

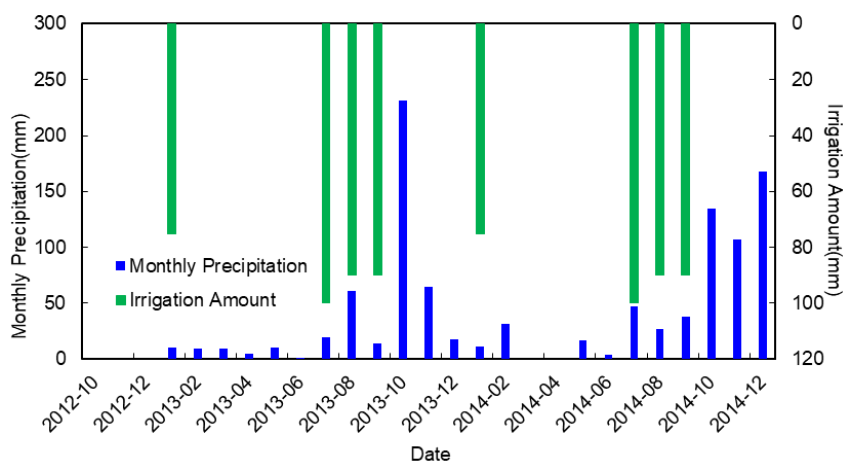


**Figure 1.** Change of monthly irrigation and precipitation within the experimental site

The experiment design was shown in Table 2. The ingredient of irrigation water sources was shown in Table 3.

**Table 2.** Experiment design in the study area

Growth stage	Emergence stage	Jointing stage	Booting stage	Seeding stage
Irrigation date	2012-10-18	2013-4-3	2013-5-2	2013-6-15
Days after sowing	7	174	203	8
Irrigation amount (m <sup>3</sup> .hm <sup>-2</sup> )	750	1000	900	900
WTT	MPSW	GW	GW	MPSW
TWT	GW	MPSW	GW	MPSW
TTW	GW	GW	MPSW	MPSW
WWT	MPSW	MPSW	GW	MPSW
WTW	MPSW	GW	MPSW	MPSW
TWW	GW	MPSW	MPSW	MPSW
CK	GW	GW	GW	MPSW
WWW	MPSW	MPSW	MPSW	MPSW

\*MPSW means micro-polluted surface water, GW means groundwater

**Table 3.** Composition of irrigation water used in the field experiment

Irrigation type	Cl <sup>-</sup> (mg·L <sup>-1</sup> )	K <sup>+</sup> (mg·L <sup>-1</sup> )	TN (mg·L <sup>-1</sup> )	Pb <sup>2+</sup> (mg·L <sup>-1</sup> )	Cu <sup>2+</sup> (mg·L <sup>-1</sup> )	Cd <sup>2+</sup> (μg·L <sup>-1</sup> )	Cr <sup>6+</sup> (μg·L <sup>-1</sup> )	COD <sub>Mn</sub> (mg·L <sup>-1</sup> )	pH	Salinity (g·L <sup>-1</sup> )
GW	321.27	18.67	17.16	0.0015	0.005	0.5	3.4	40.66	7.30	1.85
MPSW	291.42	13.26	23.17	0.0020	0.006	21.6	2.5	54.35	7.32	1.51
GB*	350	-	-	0.2	1	10	100	200	5.5-8.5	2

\*GB represent Standards for irrigation water quality (GB 5084-2005)

### ***Sampling and measurement***

Soil samples were collected before winter wheat planting, winter wheat harvesting, and summer maize harvesting, for detecting available cadmium content and total cadmium content. At each sample, there were further five sub-sampling points scattered uniformly over an area of 100 m<sup>2</sup>. At each sampling point, soil was cored using a 3.5 cm Ø soil auger at an interval of 10 cm down to the depth of 40 cm; approximately 100-200 g fresh soil was collected from each interval. The soils cored from the same depth from all the five sampling points at the same experimental plot were pooled and then stored in an aseptic bag before being shipped to the laboratory. The samples were then air dried at room temperature for one week and the electrical conductivity of each sample was measured based on the standard protocol from the 5:1 (w/v) water/soil extract (Rhoades et al., 1989). The pH was measured using a pH meter (PHSJ-5, Leici, Shanghai, China), the EC was measured using a conductivity meter (DDSJ-308A, Leici, Shanghai, China). The available Cd, Total Cd were measured using atomic absorption spectrometer (AA-7000, SHIMADZU, Kyoto, Japan).

Ten square meters was selected as the production area in each treatment, and the indexes of winter wheat yield, 1000-grain weight, dry matter weight and root weight were determined. 100 winter wheat plants were randomly selected to measure the Cd content in different parts (roots, stems, leaves and grain) of the plant. 20 summer maize were randomly selected for each treatment, and the yield, 100-grain weight, dry matter weight, root weight and Cd content in different parts (root, stem, leaves, package, grain) were determined. Dry matter weight was determined by oven drying method, with temperatures set at 105 °C for 0.25 h and 70 °C for 20 h. The determined method of Cd content in plants was similar to soil samples.

### ***Data processing and calculation***

Data were analyzed by Excel 2013 and DPS Statistical software package. Two-way analysis of variance (ANOVA) was performed with the general linear model procedure to calculate the effects of irrigation water type and irrigation period on the investigated parameters. When the F value was significant, a multiple means comparison was performed with Duncan's new multiple range test ( $p < 0.05$ ). The graphs were generated using Microsoft Excel 2013, and the standard error of the mean were calculated and presented in the tables.

Cd accumulation related indicators in soil and plant were calculated from:

$$Cd_g = C_g Y \quad (\text{Eq.1})$$

$$Cd_{sl} = C_{sl} Y_{sl} \quad (\text{Eq.2})$$

$$Cd_s = 4\rho C_s \quad (\text{Eq.3})$$

$$R_{r/s} = \frac{C_r}{C_s} \quad (\text{Eq.4})$$

$$BCF = \frac{C_{sl}}{C_s} \quad (\text{Eq.5})$$

$$BAF = \frac{(Cd_g + Cd_{sl})}{10^6 \times Cd_s} \quad (\text{Eq.6})$$

where  $Cd_g$ ,  $Cd_{sl}$ ,  $Cd_s$ ,  $C_g$ ,  $C_{sl}$ ,  $C_s$ ,  $C_r$ ,  $Y$ ,  $Y_{sl}$ ,  $R_{r/s}$ ,  $\rho$ ,  $BCF$ ,  $BAF$  is Cd accumulation in grain ( $\text{mg}/\text{hm}^2$ ), Cd accumulation in the above-ground plants ( $\text{mg}/\text{hm}^2$ ), Cd accumulation in the 0 to 40 cm layer ( $\text{mg}/\text{hm}^2$ ), content in grain ( $\text{mg}/\text{kg}$ ), content in the above-ground plants ( $\text{mg}/\text{kg}$ ), content in the 0 to 40 cm layer ( $\text{mg}/\text{kg}$ ), content in the root ( $\text{mg}/\text{kg}$ ), yield of summer maize ( $\text{kg}/\text{hm}^2$ ), biomass of the above-ground plants ( $\text{kg}/\text{hm}^2$ ), ratio of Cd content in root and 0 to 40 cm soil layer, soil density ( $\text{g}/\text{cm}^3$ ), bio-concentration factor (BCF) (Yadav et al., 2017) and bio-accumulation factor (BAF) (Safahieh, 2018) (%), respectively.

## Results and Discussion

### *The effect of different treatments on Cd content in winter wheat and summer maize*

The Cd content in roots, stems, leaves and grains of winter wheat under different treatments was shown in *Table 4*. The cumulative characteristics of Cd content in winter wheat plants indicated that the content of Cd in roots was the highest, accounting for 57.94% to 75.52% of the above-ground plants, followed by leaves, stems and grains, and the content of Cd in grains was the lowest, accounting for 1.55% to 4.09% of the above-ground plants.

**Table 4.** Cd content in winter wheat plants under different treatments

Treatment	root ( $\text{mg}\cdot\text{kg}^{-1}$ )	stem ( $\text{mg}\cdot\text{kg}^{-1}$ )	leaves ( $\text{mg}\cdot\text{kg}^{-1}$ )	grain ( $\text{mg}\cdot\text{kg}^{-1}$ )
TTW	4.070±0.909ab	0.299±0.084c	0.880±0.106c	0.141±0.028de
CK	2.036±0.104c	0.231±0.029c	0.659±0.052c	0.083±0.001f
WTT	4.300±0.436ab	0.283±0.045c	1.200±0.200b	0.091±0.003ef
TWT	4.200±1.000ab	0.490±0.095ab	1.200±0.100b	0.133±0.009def
TWW	3.453±0.162b	0.490±0.0240ab	1.773±0.214a	0.244±0.048ab
WWT	3.453±0.428b	0.537±0.045a	1.521±0.275ab	0.174±0.010cd
WTW	4.622±0.683a	0.417±0.027b	1.230±0.194b	0.203±0.047bc
WWW	4.808±0.297a	0.581±0.032a	1.230±0.112b	0.263±0.037a
Significance based on two-way analysis of variance (ANOVA) (F value)				
W (water type)	1.210*	5.861*	13.491**	35.886**
S (growth stage)	1.604*	0.574*	2.714	0.246
W×S	1.526*	3.716	2.933	6.204*

Note: Different letters after the same column data indicate the difference between the treatments at the 0.05 level (Duncan new complex range method), the same below. \*\*, \* Significance at the  $p < 0.01$ ,  $p < 0.05$ , respectively

The content of Cd in stems and grains treated by WTT was no significantly difference than that of CK treatment, but the content of Cd in roots and leaves treated by WTT was significantly higher than that of CK treatment, which increased by 2.11 and 1.82 times, respectively. The Cd content in grain treated by WTT was significantly

lower than TWW, WWT, WTW and WWW treatment. Furthermore, the Cd content in grain treated by WTT was lower than that of TTW and TWT, which decreased by 35.17%, 31.38%, respectively.

The Cd content in roots, stems, leaves, corn coating and grains of summer maize under different treatments was shown in *Table 5*. The cumulative characteristics of Cd content in summer maize plants indicated that the content of Cd in roots was the highest, accounting for 36.05% to 58.83% of the above-ground plants, followed by leaves, corn coating, stems and grains, and the content of Cd in grains was the lowest, accounting for 0.25% to 0.60% of the above-ground plants. The content of Cd in stems, leaves and grains treated by WTT was no significant difference from that in CK treatment, but the content of Cd in roots and corn coating treated by WTT was significantly higher than that in CK treatment, which increased by 1.90 and 1.59 times respectively. The Cd content in grain treated by WTT was significantly lower than TWT, TWW, WWT, WTW and WWW treatment. Furthermore, the Cd content in grain treated by WTT was lower than that in TTW, TWT, which decreased by 26.47%, 51.75%, respectively. It showed that the Cd content in grains was increased significantly by irrigation with micro-polluted surface water during jointing and booting stage, which may be due to the lower content of chloride ions and higher content of TN in micro-polluted surface water compared with groundwater (Jiang et al., 2019).

**Table 5.** Cd content in summer maize plants under different treatments

Treatment	root (mg·kg <sup>-1</sup> )	stem (mg·kg <sup>-1</sup> )	leaves (mg·kg <sup>-1</sup> )	corn coating (mg·kg <sup>-1</sup> )	grain (mg·kg <sup>-1</sup> )
TTW	1.870±0.110cd	0.176±0.011bc	0.898±0.151b	0.475±0.048de	0.013±0.002c
CK	1.123±0.119f	0.120±0.049c	0.689±0.187b	0.365±0.020e	0.009±0.001c
WTT	2.133±0.208bc	0.124±0.033c	0.780±0.060b	0.580±0.010cd	0.009±0.001c
TWT	2.400±0.200b	0.227±0.064abc	0.920±0.171b	0.637±0.015bcd	0.019±0.004b
TWW	2.753±0.208a	0.266±0.048ab	1.680±0.140a	0.880±0.092a	0.024±0.001ab
WWT	2.333±0.081b	0.252±0.012ab	1.520±0.139a	0.776±0.108ab	0.019±0.001b
WTW	1.528±0.233e	0.276±0.098ab	1.587±0.162a	0.705±0.122bc	0.024±0.006ab
WWW	1.677±0.112de	0.312±0.105a	1.720±0.302a	0.915±0.166a	0.028±0.005a
<b>Significance based on two-way analysis of variance (ANOVA) (F value)</b>					
W (water type)	1.462*	3.622*	20.328**	3.524*	13.432**
S (stage)	1.268*	0.665	2.641	0.632	0.123
W×S	1.328*	1.572*	12.347*	1.468*	3.204*

### *The effect of different treatments on Cd BAF and BCF of summer maize*

The Cd BAF and bio-concentration factor of summer maize under different treatments were shown in *Table 6*. There was no significant difference between Cd accumulation in grain of WTT and CK treatment, but the Cd accumulation in grain of WTT was significantly lower than TTW, TWT, TWW, WWT, WTW and WWW treatment, decreased by 21.89%, 50.15%, 57.86%, 47.39%, 58.34% and 61.85%, respectively. And the same rule appeared in above-ground Cd accumulation between treatments, the Cd accumulation in above-ground of WTT was significantly lower than TTW, TWT, TWW, WWT, WTW and WWW treatment, decreased by 26.08%, 44.95%, 49.47%, 48.15%, 52.51% and 56.44%, respectively. The content in the 0 to 40 cm soil layer of WTT treatment was significantly higher than CK, and the content of WTT treatment was obviously lower than TWW, WWT, WTW and WWW, decreased by

1.30%, 1.12%, 1.09% and 1.75%, respectively. And then ratio of Cd content in root and 0 to 40 cm soil layer of WTT treatment was significantly higher than TTW, CK, WTW and WWW, increased by 13.94%, 47.10%, 28.80% and 22.40%, respectively. Especially, BCF of WTT treatment was obviously lower than CK, TWT and TWW, decreased by 28.35%, 12.04% and 32.55%, respectively. But the BAF between WTT and CK treatment was no significant difference, and BAF of WTT was obviously lower than TTW, TWT, TWW, WWT, WTW and WWW, decreased by 26.27%, 44.46%, 49.78%, 47.70%, 50.83% and 54.75%, respectively.

**Table 6.** Cd BAF and BCF of summer maize under different treatments

Treatment	Cd <sub>g</sub> (mg·hm <sup>-2</sup> )	Cd <sub>st</sub> (mg·hm <sup>-2</sup> )	Cd <sub>s</sub> (kg·hm <sup>-2</sup> )	R <sub>r/s</sub>	BCF	BAF
TTW	98.697±10.86d	1530.245±75.25e	3.195±0.005c	3.279±0.160d	0.684±0.032d	0.051±0.002d
CK	77.093±7.71e	1132.695±139.76e	3.181±0.004d	1.977±0.097f	0.984±0.047a	0.038±0.002e
WTT	76.192±5.40e	1133.739±32.62e	3.192±0.004c	3.737±0.183c	0.705±0.032cd	0.038±0.002e
TWT	154.114±8.17c	2022.404±123.90d	3.194±0.003c	4.208±0.206b	0.802±0.037b	0.068±0.004c
TWW	182.968±10.76b	2246.042±69.52bc	3.223±0.003b	4.785±0.234a	1.045±0.048a	0.075±0.004b
WWT	146.902±7.71c	2181.490±103.88cd	3.217±0.006b	4.062±0.198b	0.763±0.035bc	0.072±0.003bc
WTW	183.717±9.40b	2302.374±48.92b	3.216±0.004b	2.661±0.130e	0.550±0.025e	0.077±0.002b
WWW	204.819±6.02a	2514.756±71.07a	3.237±0.004a	2.900±0.142e	0.725±0.033cd	0.084±0.004a
Significance based on two-way analysis of variance (ANOVA) (F value)						
W (water type)	51.168**	65.147**	3.416*	12.643**	21.214**	25.617**
S (stage)	12.402*	20.475*	0.714	1.246	0.604	1.574*
W×S	101.625*	123.622*	1.248	8.423*	12.639*	13.978**

### The effect of different treatments on yield and grain character of winter wheat and summer maize

The yield and grain character of winter wheat and summer maize under different treatments were shown in Table 7. CK treatment of winter wheat has the highest 1000-grains weight, reaching 42.34 g, followed by WTT, TTW, TWT, WWT, WTW, TWW and WWW treatment. Furthermore, CK treatment of winter wheat has the highest yield, reaching 8007.41 kg/hm<sup>2</sup>, followed by WTT, TTW, TWT, WTW, WWT, TWW and WWW treatment.

**Table 7.** Yield and grain character of winter wheat and summer maize under different treatments

Treatment	Winter Wheat		Summer Maize		
	10 <sup>3</sup> Grains weight (g)	Yield (kg·hm <sup>-2</sup> )	10 <sup>2</sup> Grains weight(g)	Cob Weight (g)	Yield (kg·hm <sup>-2</sup> )
TTW	40.29±0.43b	7824.07±59.92ab	26.94±0.17a	25.91±0.21a	7916.84 abc
CK	42.34±0.22a	8007.41±77.05a	26.96±0.19a	26.07±0.25a	8581.02 a
WTT	41.12±0.32ab	7964.81±59.92ab	26.17±0.14ab	25.17±0.28a	8311.87 ab
TWT	39.98±0.22bc	7751.85±103.99b	26.16±0.49ab	23.58±0.32b	8111.24 abc
TWW	38.84±0.95cd	6629.63±78.04de	25.69±0.18b	21.92±0.38c	7687.71 bc
WWT	39.88±0.51bc	6825.93±277.85d	26.21±1.26ab	22.55±0.37c	7869.73 abc
WTW	39.63±0.70bc	7248.15±120.74c	25.75±0.81b	21.89±0.77c	7583.58 bc
WWW	38.18±1.43d	6531.48±97.87e	25.64±0.54b	21.73±1.09c	7327.38 c
Significance based on two-way analysis of variance (ANOVA) (F value)					
W (water type)	6.127*	105.735**	1.915	2.684*	86.474**
S (stage)	1.423*	10.474*	0.682	0.547	6.457*
W×S	4.625*	123.612**	1.036	1.376	68.927*



CK treatment of summer maize has the highest 100-grains weight, reaching 26.96 g, followed by TTW, WWT, WTT, TWT, WTW, TWW and WWW treatment. And cob weight of summer maize in WTT treatment has no significantly difference with CK treatment. Furthermore, CK treatment of winter wheat has the highest yield, reaching 8581.02 kg/hm<sup>2</sup>, followed by WTT, TWT, TTW, WWT, TWW, WTW and WWW treatment.

The 1000-grains weight and yield of winter wheat between WTT and CK treatment had no obvious difference, but the values of WTT treatment were significantly higher than TWW, WWW treatment, furthermore, the standard deviation of 1000-grain weight for WTT and CK treatment was only 0.22, 0.32. It indicated that grain filling and yield formation of winter wheat had been slightly affected by the irrigated micro-polluted surface water in emergence stage and groundwater in jointing stage and booting stage, however, yield formation of winter wheat had been obviously affected by the irrigated micro-polluted surface water in jointing stage and booting stage (Gao et al., 2012).

The 100-grains weight and yield of summer maize between WTT, CK, TWT and WWT treatment had no obvious difference, but the values of WTT treatment were significantly higher than that of WTW, TWW and WWW. The results indicated that grain filling and yield formation of summer maize had been stressed from irrigated micro-polluted surface water in the winter wheat booting stage, which may be due to the limited root growth of winter wheat and summer maize under micro-polluted surface water irrigation (Rafiq et al., 2014; Yu et al., 2014).

### Correlation analysis between Cd content in summer maize grain and soil layers

The scatter plot and fit curve between Cd content in grain and available Cd, total Cd content in soil layers before summer maize planting were shown in Fig. 2. The determination coefficient of Cd content in grain and available Cd in 0-10 cm soil layer was the highest, reaching 0.9095, followed by 10-20, 20-30, 30-40 cm soil layers, and the determination coefficients were 0.8002, 0.2106, 0.0001, respectively. Furthermore, the determination coefficient of Cd content in grain and total Cd in 10-20 cm soil layer was the highest, reaching 0.8081, followed by 0-10, 20-30, 30-40 cm soil layers, and the determination coefficients were 0.7780, 0.4802 and 0.1463, respectively.

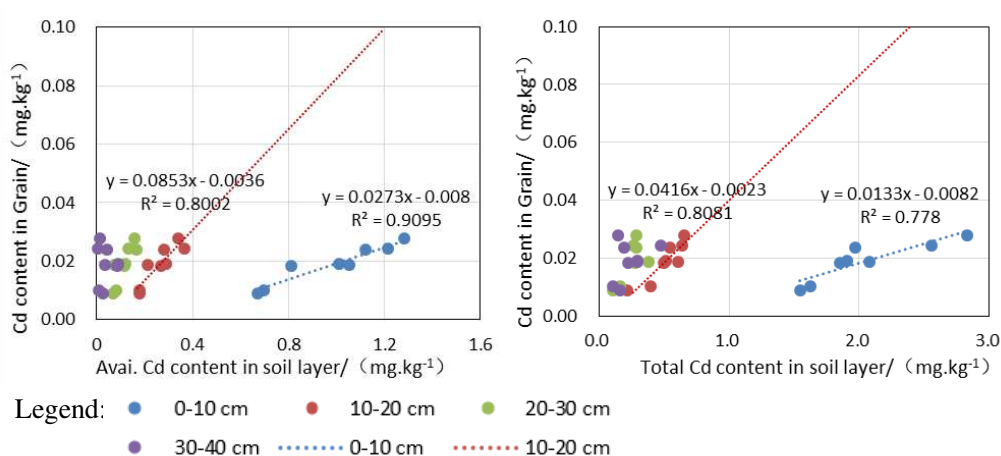


**Figure 2.** Correlation analysis between Cd content in grain and soil layers after summer maize harvest

The grains Cd limit value specified in National Food Safety Standards of China (GB 2762-2012) is 0.1 mg/kg. According to our prediction model for available Cd content between soil layers and grains, for ensuring the grain Cd content meets the Standards, the maximum value of available Cd content in 0 to 10, 10 to 20 cm soil layer was 3.95, 1.21 mg/kg, respectively. While we choose the prediction models for total cadmium between soil layers and grains, the maximum of total Cd content in 10-20 cm soil layer was a shocking 2.45 mg/kg, and the corresponding available Cd content in 10-20 cm soil layer was reached 1.24 mg/kg (Zhao et al., 2006; Li et al., 2016). Thus, in order to ensure food security, it is more suitable for us to choose the available cadmium content in 10 to 20 cm soil layer as the prediction index.

## Conclusions

Content of Cd in winter wheat and summer maize plants indicated, the value in root was highest, followed by leaves, stem, grain in winter wheat, while the value in root was highest, followed by leaves, corn coating, stem and grain in summer maize.

The Cd content in winter wheat and summer maize grain was lower than the National Standards when crops irrigated with micro-polluted surface water during the emergence stage, and groundwater was adopted during the jointing and booting stage in the study area.

Further work is needed, for example, soil types, fertilizers, precipitation and crop genotypes all affect the expressed model and the threshold range for the available Cd content in 10-20 cm soil layer, thus, it is necessary to study the effects of irrigation water quality on cadmium induced in winter wheat summer maize rotation system in different soil types and irrigation schedules. The threshold of soil environmental quality of producing areas should be set according to local conditions for ensuring the food safety.

**Acknowledgements.** This work was funded by Central Public-interest Scientific Institution Basal Research Fund (Grant No.: Y2020GH04), the National Key Research and Development Program of China (Grant No.: 2017YFD0800403) and the Agricultural Science and Technology Innovation Program of Chinese Academy of Agricultural Sciences (Grant No.: CAAS-ASTIP).

## REFERENCES

- [1] Amadou, A., Praud, D., Coudon, T., Danjou, A. M. N., Faure, E., Leffondre, K., Le Romancer, M., Severi, G., Salizzoni, P., Mancini, F. R., Fervers, B. (2020): Chronic long-term exposure to cadmium air pollution and breast cancer risk in the French E3N cohort. – *International Journal of Cancer* 146(2): 341-351.
- [2] Andres, S., Ribeyre, F., Tourencq, J. N., Boudou, A. (2000): Interspecific comparison of cadmium and zinc contamination in the organs of four fish species along a polymetallic pollution gradient (Lot River, France). – *Science of the Total Environment* 248(1): 11-25.
- [3] Arefin, M. T., Rahman, M. M., Wahid-U-Zaman, M., Eok, K. J. (2016): Heavy Metal Contamination in Surface Water Used for Irrigation: Functional Assessment of the Turag River in Bangladesh. – *Journal of Applied Biological Chemistry* 59(1): 83-90.
- [4] Chen, X., Cui, Z., Fan, M., Vitousek, P., Zhao, M., Ma, W., Wang, Z., Zhang, W., Yan, X., Yang, J., Deng, X., Gao, Q., Zhang, Q., Guo, S., Ren, J., Li, S., Ye, Y., Wang, Z., Huang, J., Tang, Q., Sun, Y., Peng, X., Zhang, J., He, M., Zhu, Y., Xue, J., Wang, G., Wu,

- L., An, N., Wu, L., Ma, L., Zhang, W., Zhang, F. (2014): Producing more grain with lower environmental costs. – *Nature* 514(7523): 486-489.
- [5] Chen, N., Zheng, Y., He, X., Li, X., Zhang, X. (2017): Analysis of the report on the national general survey of soil contamination. – *Journal of Agro-Environment Science* 36(9): 1689-1692.
- [6] Franz, E., Romkens, P., van Raamsdonk, L., Van der Fels-Klerx, I. (2008): A Chain Modeling Approach to Estimate the Impact of Soil Cadmium Pollution on Human Dietary Exposure. – *Journal of Food Protection* 71(12): 2504-2513.
- [7] Gao, X., Lukow, O. M., Grant, C. A. (2012): Grain concentrations of protein, iron and zinc and bread making quality in spring wheat as affected by seeding date and nitrogen fertilizer management. – *Journal of Geochemical Exploration* 121: 36-44.
- [8] Hu, Y., Li, P., Qi, X., Li, Z., Hu, C., Zhao, Z. (2016): Analysis of Winter Wheat Sensitive Period for Cd under Rotational Irrigation with Clean Water and Polluted Water. – *Journal of Irrigation and Drainage* 35(8): 21-24.
- [9] Huang, Y., Wang, L., Wang, W., Li, T., He, Z., Yang, X. (2019): Current status of agricultural soil pollution by heavy metals in China: A meta-analysis. – *Science of the Total Environment* 651: 3034-3042.
- [10] Hundecha, Y., Bardossy, A. (2005): Trends in daily precipitation and temperature extremes across western Germany in the second half of the 20th century. – *International Journal of Climatology* 25(9): 1189-1202.
- [11] Jiang, K., Long, J., Li, X., Dong, X., Wang, S., Liu, W., Hou, H., Peng, P., Liao, B. (2019): Effects of exogenous Cl<sup>-</sup> on Cd<sup>(2+)</sup> concentrations in soil solutions of different soil types. – *Acta Scientiae Circumstantiae* 39(2): 553-559.
- [12] Kong, X., Zhang, X., Lal, R., Zhang, F., Chen, X., Niu, Z., Han, L., Song, W. (2016): Groundwater Depletion by Agricultural Intensification in China's HHH Plains, Since 1980s. – *Advances in Agronomy* 135: 59-106.
- [13] Li, J., Li, F., Liu, Q., Song, S., Zhang, Y., Zhao, G. (2014): Impacts of Yellow River Irrigation Practices on Trace Metals in Surface Water: A Case Study of the Henan-Liaocheng Irrigation Area, China. – *Human and Ecological Risk Assessment* 20(4): 1042-1057.
- [14] Li, P., Qi, X., Magzum, N., Huang, Z., Liang, Z., Qiao, D. (2015): Response of precipitation to ratio of canal to wells and its environmental effects analysis in combined well-canal irrigation area. – *Transactions of the Chinese Society of Agricultural Engineering* 31(11): 123-128.
- [15] Li, F., Wen, D., Wang, F., Wang, X., Wan, K., Liu, X. (2016): Correlation Analysis of Cd Pollution between Soil and Brassica Leaf Vegetables and the Soil Cd Safety Threshold in Guangdong Region. – *Ecology and Environmental Sciences* 25(4): 705-710.
- [16] Li, Y., Xie, Z., Qin, Y., Zhou, S. (2018): Spatio-temporal variations in precipitation on the Huang-Huai-Hai Plain from 1963 to 2012. – *Journal of Earth System Science* 127(7): 101.
- [17] Peng, H., Chen, Y., Weng, L., Ma, J., Ma, Y., Li, Y., Islam, M. S. (2019): Comparisons of heavy metal input inventory in agricultural soils in North and South China: A review. – *Science of the Total Environment* 660: 776-786.
- [18] Rafiq, M. T., Aziz, R., Yang, X., Xiao, W., Rafiq, M. K., Ali, B., Li, T. (2014): Cadmium phytoavailability to rice (*Oryza sativa* L.) grown in representative Chinese soils. A model to improve soil environmental quality guidelines for food safety. – *Ecotoxicology and Environmental Safety* 103: 101-107.
- [19] Rhoades, J. D., Manteghi, N. A., Shouse, P. J., Alves, W. J. (1989): Soil electrical conductivity and soil salinity: new formulations and calibrations. – *Soil Science Society of America Journal* 53(2): 433-439.
- [20] Safahieh, A. (2018): Investigation on bio-concentration factor (BCF) and bio-accumulation factor (BAF) of aromatic compounds in the Ark clam. – *Journal of Natural Environment* 71(2): 227-236.

- [21] Satarug, S., Baker, J. R., Urbenjapol, S., Haswell-Elkins, M., Reilly, P. E. B., Williams, D. J., Moore, M. R. (2003): A global perspective on cadmium pollution and toxicity in non-occupationally exposed population. – *Toxicology Letters* 137(1-2): 65-83.
- [22] Shang, E., Xu, E., Zhang, H., Huang, C. (2018): Spatial-Temporal Trends and Pollution Source Analysis for Heavy Metal Contamination of Cultivated Soils in Five Major Grain Producing Regions of China. – *Environmental Science* 39(10): 4670-4683.
- [23] Smaoui-Damak, W., Rebai, T., Berthet, B., Hamza-Chaffai, A. (2006): Does cadmium pollution affect reproduction in the clam *Ruditapes decussatus*? A one-year case study. – *Comparative Biochemistry and Physiology C-Toxicology & Pharmacology* 143(2): 252-261.
- [24] Wang, Z., Li, J., Li, Y. (2017): Using Reclaimed Water for Agricultural and Landscape Irrigation in China: A Review. – *Irrigation and Drainage* 66(5): 672-686.
- [25] Wang, G., Luo, Z., Wang, E., Zhang, W. (2018a): Reducing greenhouse gas emissions while maintaining yield in the croplands of Huang-Huai-Hai Plain, China. – *Agricultural and Forest Meteorology* 260: 80-94.
- [26] Wang, G., Yan, D., He, X., Liu, S., Zhang, C., Xing, Z., Kan, G., Qin, T., Ren, M., Li, H. (2018b): Trends in extreme temperature indices in Huang-Huai-Hai River Basin of China during 1961-2014. – *Theoretical and Applied Climatology* 134(1-2): 51-65.
- [27] Yadav, P., Garg, V. K., Singh, B., Mor, S. (2017): Assessment of Bio-Concentration Factor of Heavy Metals in Indian Soil-Crop System. – *Journal of Scientific & Industrial Research* 76(6): 381-385.
- [28] Yang, Q., Li, Z., Lu, X., Duan, Q., Huang, L., Bi, J. (2018): A review of soil heavy metal pollution from industrial and agricultural regions in China: Pollution and risk assessment. – *Science of the Total Environment* 642: 690-700.
- [29] Yin, J., Yan, D., Yang, Z., Yuan, Z., Yuan, Y., Zhang, C. (2016): Projection of extreme precipitation in the context of climate change in Huang-Huai-Hai region, China. – *Journal of Earth System Science* 125(2): 417-429.
- [30] Yin, W., Hu, L., Jiao, J. (2017): Evaluation of groundwater storage variations in Northern China using GRACE data. – *Geofluids* 2017: 8254824.
- [31] Yu, L., Zhu, J., Huang, Q., Su, D., Jiang, R., Li, H. (2014): Application of a rotation system to oilseed rape and rice fields in Cd-contaminated agricultural land to ensure food safety. – *Ecotoxicology and Environmental Safety* 108: 287-293.
- [32] Zhang, P., Qin, C., Hong, X., Kang, G., Qin, M., Yang, D., Pang, B., Li, Y., He, J., Dick, R. P. (2018): Risk assessment and source analysis of soil heavy metal pollution from lower reaches of Yellow River irrigation in China. – *Science of the Total Environment* 633: 1136-1147.
- [33] Zhao, Y., Li, H., Sun, Z. (2006): Correlation analysis of Cd pollution in vegetables and soils and the soil pollution threshold. – *Transactions of the Chinese Society of Agricultural Engineering* 22(7): 149-153.

# QUANTIFYING THE CONTRIBUTIONS OF CLIMATE CHANGE AND HUMAN ACTIVITIES TO THE DRAMATIC REDUCTION IN RUNOFF IN THE TAIHANG MOUNTAIN REGION, CHINA

WANG, S.<sup>1</sup> – LI, Q.<sup>2\*</sup> – WANG, J.<sup>1</sup>

<sup>1</sup>*School of Geographical Science, Shanxi Normal University, Linfen 041004, Shanxi Province, P. R. China*

<sup>2</sup>*Institute of Geographical Sciences, Hebei Academy of Sciences, Hebei Engineering Research Center for Geographic Information Application, Shijiazhuang 050011, Hebei Province, P. R. China*

*\*Corresponding author  
e-mail: qingli2020@outlook.com*

(Received 21<sup>st</sup> May 2020; accepted 17<sup>th</sup> Sep 2020)

**Abstract.** The Taihang Mountain region, known as “the North China Water Tower”, is an important water source guarantee for the Jing-Jin-Ji Urban Agglomeration. Recently, a dramatic reduction of runoff has seriously threatened to the regional ecological security. Quantitative attribution of such remarkable reduction in runoff is important for designing sustainable watershed management strategies in the changing environment. This study selected three typical basins in the north, middle and south regions, the Zhangfang, Weishui and Guantai basins, to quantitatively attribute the reduction in runoff to climate change and human activities by using the physics-based Soil and Water Assessment Tools (SWAT). The results suggested that the annual runoff of three basins all decreased by over 60% since the change-point year of 1983, 1975 and 1973. Based on the SWAT model, the contribution rates of human activities are 54.19%, 60.16% and 68.39% for Zhangfang, Weishui and Guantai basins, respectively. Additionally, the contribution rates of climate change are 45.81%, 39.84% and 31.61%. The increased contribution rate of human activities from north to south indicates the gradually intensifying anthropogenic influence, which is reflected in water consumption.

**Keywords:** *rainfall-runoff variation, climate change, ecological security, water environment, SWAT*

## Introduction

The water cycle controls the process of natural and human development. It not only links “geosphere – biosphere – atmosphere” together, but also is the key issue of the three global change research themes of “carbon cycle, food fiber and water cycle” (Chen and Xia, 1999; Vörösmarty et al., 2000; Bekele et al., 2010). Climate change is a basic factor on regional water resources. IPCC AR5 indicated global climate had been warming continuously since the middle of 20th century. Problems caused by climate change include redistribution of precipitation, increasing frequency of extreme weather events, etc. (IPCC, 2014; Qin et al., 2014). The response of water cycle to climate change is characterized by “nonlinearity, regionalism and uncertainty”. Clarifying the unsteady driving and feedback mechanism of the hydrological regime has become a major challenge for hydrological science (Xia et al., 2007; Liu et al., 2014). On the other hand, intensive human activities, such as urbanization, industrial and agricultural water consumption, soil and water conservation measures and water conservancy projects, have resulted in dramatic changes of land surface conditions, which have threatened ecosystem stability (Milly et al., 2005; Zhao et al., 2014; Fu et al., 2017; Sun et al., 2020). Runoff variation, which has been impacted by climate change and human

activities, reflects the characteristics of hydrological evolution (Yao et al., 2016; Zhao et al., 2018; Yang et al., 2019). At present, understanding the hydrological process, studying on the law of river runoff change and its driving mechanism under changing environment have become the hotspot of hydrological science.

The Taihang Mountain region, known as “the North China Water Tower”, is a water guarantee and sand barrier for the Jing-Jin-Ji Urban Agglomeration. It provides 70% of the surface water resources to the North China Plain. In recent years, annual runoff of many rivers in this region, such as San-kan River, Hu-tuo River and Zhang River, showed significantly decreasing trend (Yang and Tian, 2009; Wang et al., 2013; Zhang et al., 2017). Water resource shortages and related environmental problems have seriously threatened local water resources security (Chu et al., 2010). Studies showed that climate change (temperature, precipitation, etc.) and human activities (groundwater exploitation, water conservancy project, and land use change, etc.) are the main driving factors (Chen and Xia, 1999; Liu and Xia, 2004). Based on the SWAT model, Zhang et al. (2017) presented the contribution rates of climate change and human activities for the runoff decrease in San-kan River Basin were 39.1% and 60.9%, respectively. Using three methods including hydrological model, hydrological sensitivity analysis and climate elasticity method, Wang et al. (2013) estimated that 70% of the runoff decrease was caused by climate change, while 30% was attributed to human activity in the Hu-tuo River Basin during 1957-2000. Meanwhile, the contribution rates of climate change and human activities in Zhang River Basin were 34% and 66%, respectively. A similar result was obtained by Bao et al. (2012) in Zhang River Basin by using the VIC hydrological model. The contribution rates of climate change and human activities were 26.1% and 73.9%, respectively.

In the Taihang Mountain region, studies on attribution of runoff change were often carried out in a single river basin, which ignored the comparison of spatial differences. Therefore, Zhangfang, Weishui and Guantai basins, located in the north, middle and south of Taihang Mountain are selected as study areas. Using the SWAT model, we analyzed the spatial and temporal variation of regional runoff, quantitatively distinguished the contribution of climate change and human activity to runoff variation. It not only offers scientific support for the sustainable utilization of water resource, but also has important values for regional socio-economic development.

## Materials and methods

### *Study area*

The Taihang Mountain region (35.15°N~40.46°N, 110.14°E~116.33°E) is an important geographical boundary of eastern China, which lies to the east of the Loess Plateau and the west of the North China Plain. This region is the headwater of many rivers, including Daqing River, Ziya River, Nanyun River and Qinhe River, with an area of approximately 134,900 km<sup>2</sup>. Among them the Daqing, Ziya and Nanyun rivers flow east to Haihe River, and Qinhe River enters the Yellow River. There is obvious difference in climate and landscape between east and west of the Taihang Mountain region. The eastern side is the North China Plain. Its climate is warm and humid, and the dominant landscape is deciduous broad-leaved forest. The west side belongs to the Loess Plateau, where located in semi-humid and semi-arid transition zone, and the dominant landscape are forest, grassland and steppe. Zhangfang, Weishui and Guantai basins belong to Daqing River, Ziya River, and Nanyun River systems, which are located in the northern,

central and southern parts of the Taihang Mountain region, respectively (*Fig. 1, Table 1*). Owing to the large span from north to south, analysis of typical basins in different regions can better reflect runoff variation rules of the Taihang Mountain region and the runoff response to human activities and climate change.

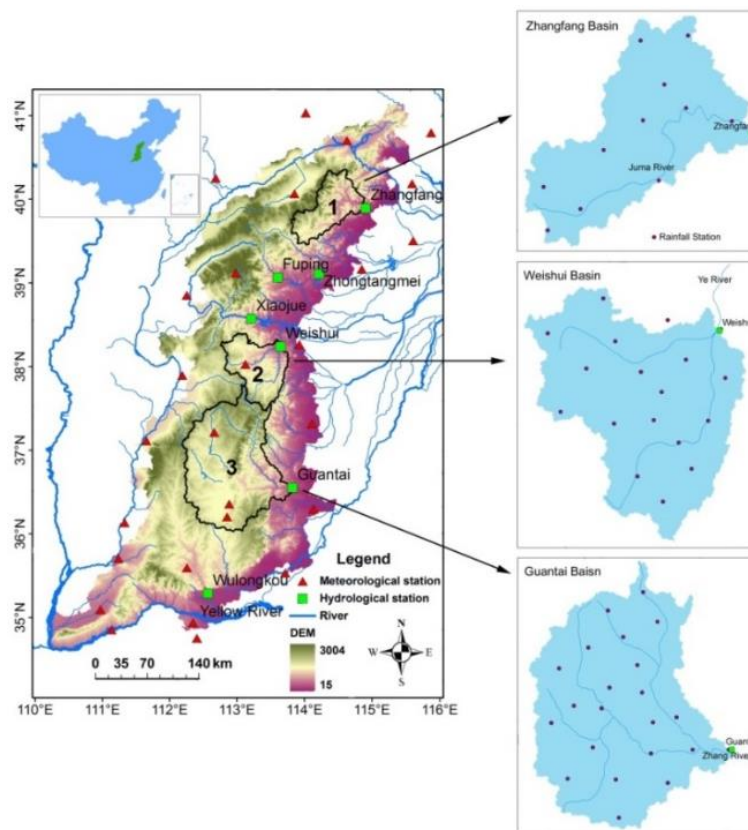


**Figure 1.** Location of the Taihang Mountain region and three selected basins

**Table 1.** The basic information of Zhangfang, Weishui and Guantai Basins

Basin	Area* (km <sup>2</sup> )	Precipitation** (mm)	Cultivated land coverage* (%)	Vegetation coverage* (%)	Total reservoir storage*** (10 <sup>8</sup> m <sup>3</sup> )
Zhangfang	4833	467	11.93	86.51	3.03
Weishui	5485	481	25.19	70.26	-
Guantai	17668	529	40.41	55.94	7.12

-: missing; \*: obtained by land use data in 2015; \*\*: average annual precipitation from 1955 to 2017; \*\*\*: total reservoir storage in 2012

### Data sources

The fundamental datasets used in this study include: meteorological, hydrological and remote sensing data. The meteorological data are derived from 20 meteorological stations and 51 rainfall stations around the Taihang Mountain region during 1951–2017, including air temperature, precipitation, wind speed and direction, relative humidity and sunshine duration. The hydrological data contain monthly runoff data from the Zhangfang, Weishui and Guantai hydrological stations during 1955–2017, which are

from the China Hydrological Yearbook-Haihe River Basin. Remote sensing data are consisted of land use, soil and Digital Elevation Model (DEM). Land use raster data (spatial resolution: 100 × 100 m) in 2000, 2005, 2010 and 2015 are provided by the Data Center for Resources and Environment Sciences Chinese Academy of Sciences (<http://www.resdc.cn/>). The soil type and property data are completed by the Institute of Soil Science, Chinese Academy of Science. DEM is from the Shuttle Radar Topography Mission, with a resolution of 90 m.

### ***Soil and Water Assessment Tool (SWAT)***

The Soil and Water Assessment Tool was used to quantitatively analyze the impact of climate change and human activities on hydrological processes. SWAT is a physically-based model developed by the U.S. Department of Agriculture (USDA) Agricultural Research Service (ARS). In the model, the Soil Conservation Service (SCS) curve number method was used for predicting surface runoff from daily rainfall (Neitsch et al., 2011; Arnold et al., 2012). Climate change and human activities are driving factors of runoff variation. According to the abrupt change year for the annual runoff, the research period is divided into natural and interferential phases. The natural phase is the period before abrupt change year, without significant variation in runoff, which shows that water recycling remains natural state without human activities. The interferential phase follows the abrupt change year and shows that hydrological process is significantly affected by both climate change and human activities.

Using the meteorological and hydrological data in natural phase, the parameters of SWAT model can be calibrated, and then a hydrological model suitable for the study area is built (Ficklin et al., 2009; Furey et al., 2012). The simulation in natural phase reflect the hydrological characteristics of a basin under natural conditions, while the simulation in interferential phase reflect the runoff change affected by both climate change and human activities. Thus, the difference between the simulated and observed runoff in the interferential phase presents the impact of human activities on runoff. The formula is as follows (Eqs. 1-4):

$$\Delta Q = Q_{obv} = \Delta Q_{climate} + \Delta Q_{human} \quad (\text{Eq.1})$$

$$\Delta Q_{human} = Q_{sim} - Q_{obv} \quad (\text{Eq.2})$$

$$\lambda_{climate} = \frac{\Delta Q_{climate}}{\Delta Q} \times 100\% \quad (\text{Eq.3})$$

$$\lambda_{human} = \frac{\Delta Q_{human}}{\Delta Q} \times 100\% \quad (\text{Eq.4})$$

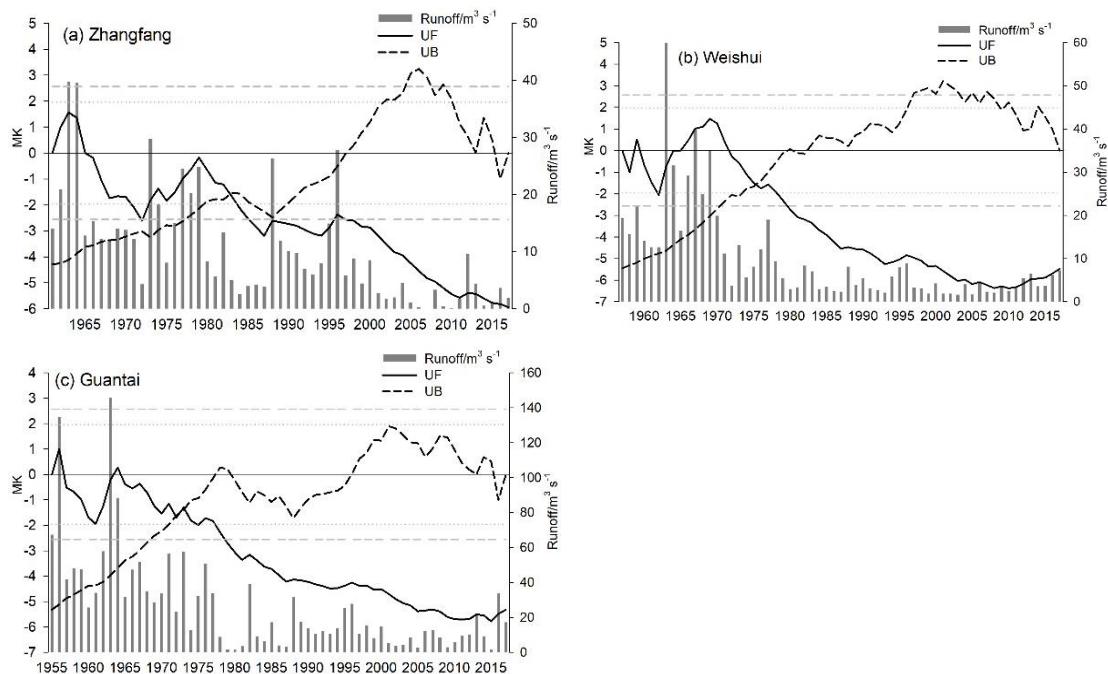
where  $\Delta Q$  (mm) is total runoff change;  $\Delta Q_{climate}$  (mm) is runoff change caused by climate change;  $\Delta Q_{human}$  (mm) is runoff change caused by human activities;  $Q_{sim}$  and  $Q_{obv}$  (mm) are simulated and observed runoff in the interferential phase, respectively;  $\lambda_{climate}$  (%) is contribution of climate change to runoff change;  $\lambda_{human}$  (%) is contribution of human activities to runoff change.



## Results

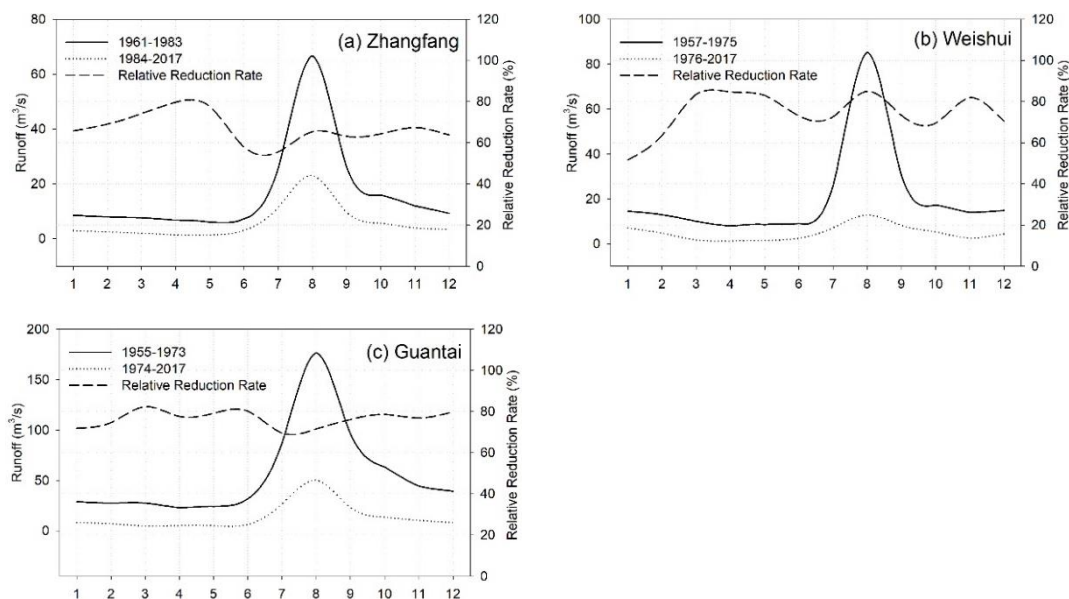
### Runoff change analysis

Fig. 2 illustrates the interannual variations and abrupt change testing results in runoff for Zhangfang, Weishui and Guantai basins during 1955–2017. The annual runoff of three basins all showed decreasing trend, at the rates of  $-0.116$ ,  $-0.122$  and  $-0.305 \times 10^8 \text{ m}^3 \text{ a}^{-1}$ , respectively. Mann–Kendall Method, a non-parametric statistical test method (Hirsch and Slack, 1984), was used to test the abrupt changes of annual runoff. The results showed the abrupt change was in 1983, 1975 and 1973 for Zhangfang, Weishui and Guantai basins, respectively. And the runoff continued to significantly decrease thereafter. Before and after abrupt change year, the annual average runoff in Zhangfang Basin decreased by  $3.38 \times 10^8 \text{ m}^3$  (63.9%), from  $5.29 \times 10^8 \text{ m}^3$  to only  $1.91 \times 10^8 \text{ m}^3$ . Meanwhile, the total loss in runoff for Weishui and Guantai basins were  $5.04 \times 10^8 \text{ m}^3$  (76.6%) and  $13.19 \times 10^8 \text{ m}^3$  (74.9%), respectively.



**Figure 2.** Interannual variations and Mann–Kendall's testing statistics values of runoff for Zhangfang, Weishui and Guantai basins during 1955–2017

The seasonal variations of runoff in three basins displayed similar characteristics before and after abrupt change year (Fig. 3). The monthly runoff appeared unimodal distribution, with flood and non-flood seasons. The average runoff of each month in the interferential phase was lower than that in the natural phase, and the maximum decrease occurred in August, with a reduced amount of  $43.57 \text{ m}^3/\text{s}$ ,  $72.56 \text{ m}^3/\text{s}$  and  $126.41 \text{ m}^3/\text{s}$ , respectively. The relative reduction rate all passed 55% in each month of Zhangfang Basin, with the maximum relative deduction rate in April. In Weishui Basin, the maximum relative deduction rate was in August, with 84.99%, while the minimum relative deduction rate occurred in winter. The Guantai Basin had a stable relative reduction rate throughout the year, passing 70%.



**Figure 3.** Monthly average runoff and relative reduction rate for three basins before and after abrupt change point

Runoff coefficient is a key index which reflects the capacity of water yield in a basin. In the natural and interferential phases, runoff coefficient decreased from 0.23 to 0.09 in Zhangfang Basin, from 0.24 to 0.05 in Weishui Basin, and from 0.18 to 0.05 in Guantai Basin. It indicated that the effect of recent climate change on runoff reduction was gradually weakened, and the impact of intense human activities gradually increased from north to south. The relationship between runoff and precipitation in the natural and interferential phases is shown in Fig. 4. Compared with the annual runoff depth in the natural phase, it decreased sharply in the interferential phases. The variation in annual runoff depth decreased from 36.1 mm to 18.0 mm for 100 mm decrease in precipitation for Zhangfang Basin in the two periods, with a reduction of 18.1 mm. Meanwhile, the reduction of annual runoff depth was 15.2 mm and 24.2 mm in Weishui and Guantai Basin. In the interferential phase, the correlation between runoff and precipitation decreased significantly in Zhangfang and Guantai Basin. The annual runoff depth was less than 100 mm in most years (97.5%) in three basins, especially in Weishui Basin, almost all less than 50 mm during 1976–2017.

### Runoff simulation based on the SWAT model

#### Model performance

Simulated and observed monthly runoff of the three basins is presented in Fig. 5. For Zhangfang basin, except the simulated runoff showed difference in the months with rainstorms and other hydrological events, the simulations were good in the whole period. The simulated runoff of Weishui basin were not good after August in the years 1960–1962 and 1971–1975. For Guantai basin, the peak values from June to September in the years 1958–1961 were overestimated, while the values in August were underestimated in most other years. Nevertheless, the model performance needs to be evaluated by the relative error,  $R^2$  (correlation coefficient) and  $E_{NS}$  (Nash-Suttcliffe simulated coefficient). In the calibrated phase, the relative error between the simulated and observed monthly runoff in Zhangfang,

Weishui and Guantai basins was 4.43%, 16.48% and 6.82%, respectively.  $R^2$  was 0.94, 0.96 and 0.79,  $E_{NS}$  was 0.84, 0.86 and 0.90, respectively. In the validated phase, the relative error between the simulated and observed monthly runoff of three basins was 12.48%, 17.68% and 11.50%, respectively;  $R^2$  was 0.73, 0.77 and 0.79, and  $E_{NS}$  was 0.65, 0.80 and 0.84, respectively. The relative error in the two phases is less than 15%,  $R^2 > 0.6$  and  $E_{NS} > 0.5$ , which means the simulated results meet the accuracy requirement, and the SWAT model can be well applied to the three basins.

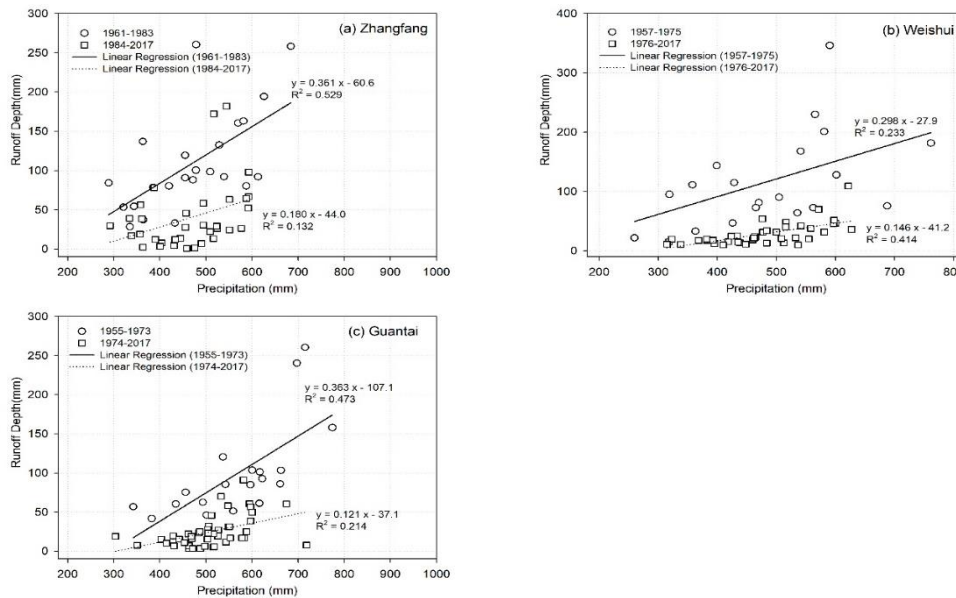


**Figure 4.** Relationship between annual precipitation and runoff during the two periods divided by abrupt change years

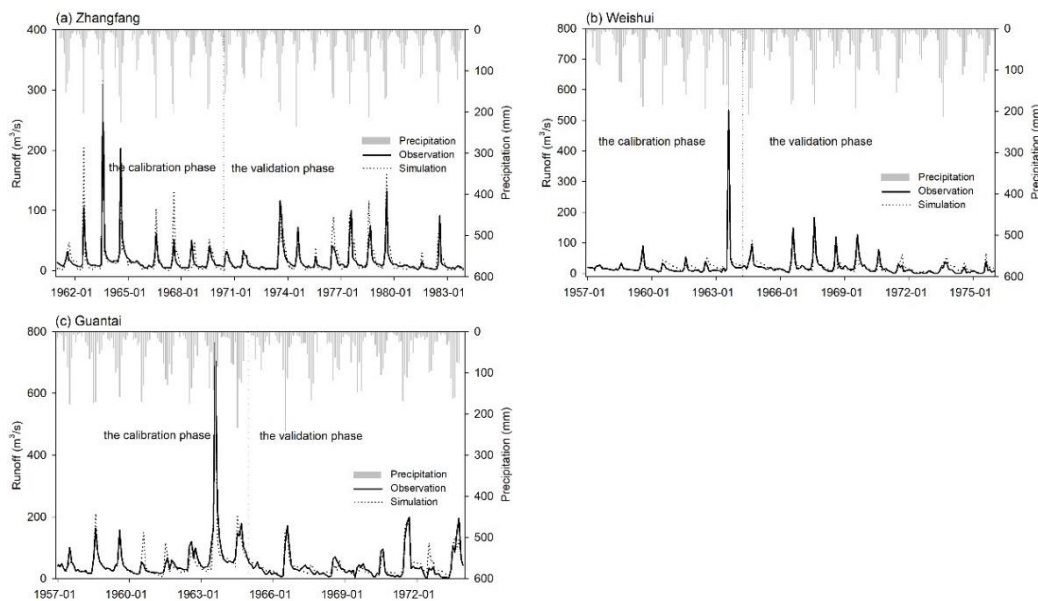


**Figure 5.** Comparison between observed and simulated monthly runoff for Zhangfang (1961–1983), Weishui (1957–1975) and Guantai (1957–1973) basin

Fig. 6 compares the observed and simulated annual runoff of the three basins in different periods based on the calibrated SWAT model. In the natural period,  $R^2$  for Zhangfang, Weishui and Guantai basins were 0.82, 0.97 and 0.86, respectively, and  $E_{NS}$  were 0.81, 0.85 and 0.82, respectively. The significant differences between the simulated and observed annual runoff started from 1983, 1975 and 1973, respectively, which is consistent with the runoff abrupt change year. This result shows that SWAT model can be used to analyze the response of runoff to climate change and human activities.

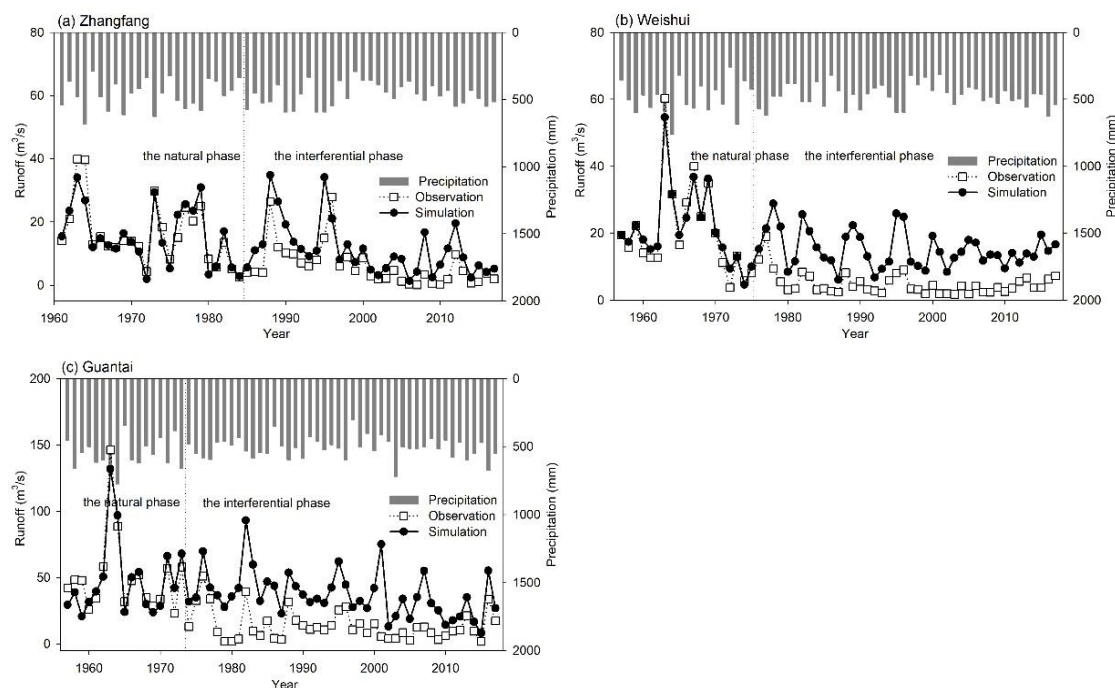


**Figure 6.** Simulated and observed annual runoff in the natural and the interferential phase for the three basins

### Contributions of climate change and human activities to runoff reduction

As shown in Table 2, for Zhangfang Basin, annual runoff reduced from 109.43 mm in the natural period (1961–1983) to 39.55 mm in the interferential period (1984–2017), with a 69.88 mm reduction. Meanwhile, the natural runoff in the two periods built by the SWAT model was 106.66 mm and 74.65 mm, with a 32.01 mm reduction. The average annual runoff observed in Weishui basin reduced to 28.08 mm in the interferential period (1976–2017) compared with 120.05 mm in the natural period (1957–1975), with 91.97 mm reduction. The natural runoff in the two periods built by the SWAT model was 123.76 mm and 87.13 mm, with a 36.64 mm reduction. The average annual runoff observed in Guantai basin reduced to 24.98 mm in the interferential period (1974–2017) from 90.05 mm in the natural period (1957–1973), with a 65.07 mm reduction. The natural runoff of the two periods built by the SWAT model was 86.67 mm and 66.10 mm, with a 20.57 mm reduction. Thus, the contribution rates of climate change to runoff reduction in Zhangfang, Weishui and Guantai basins, as calculated by formula in Eqs. 1-4, were 45.81%, 39.84% and 31.61%, respectively, while the contribution rates of human activities were 54.19%, 60.16% and 68.39%.

**Table 2.** Contributions of climate change and human activity for decreasing runoff based on SWAT model

Basin	Period	Observed runoff /mm	Simulated runoff /mm	Observed runoff change /mm	Simulated runoff change /mm	SWAT model	
						Contribution of Climate Change /%	Contribution of Human Activity /%
Zhangfang	1961-1983	109.43	106.65	69.88	32.01	45.81	54.19
	1984-2017	39.55	74.65				
Weishui	1957-1975	120.05	123.76	91.97	36.64	39.84	60.16
	1976-2017	28.08	87.13				
Guantai	1957-1973	90.05	86.67	65.07	20.57	31.61	68.39
	1974-2017	24.98	66.10				

The contribution of climate change and human activities to monthly runoff reduction can be calculated using the same method (Fig. 7) and the similar results were obtained. In Zhangfang basin, the highest contribution of climate change to runoff occurred in August, with a rate of 72.66%, and its contribution in other months fluctuated around 40%. In Weishui and Guantai basins, the highest contribution of climate change was 59.00% and 42.25%, respectively, likewise in August. The seasonal distribution patterns of contribution rates are similar in the two basins: the maximum climate change contribution occurred in summer, less in winter, and lowest in spring and autumn.

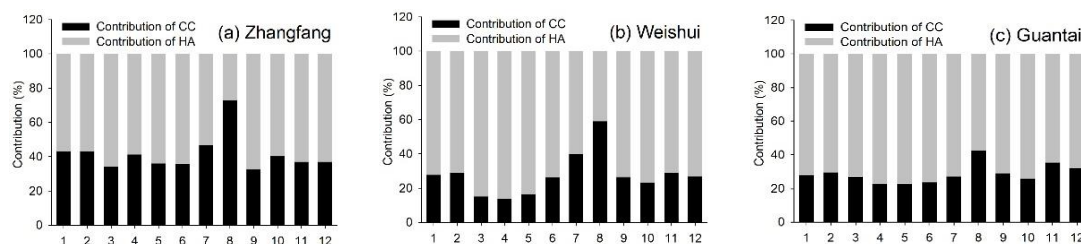


**Figure 7.** Contributions of climate change and human activity for decreasing monthly runoff in the three basins based on SWAT model (CC: Climate Change, HA: Human Activity)

## Discussion

Based on the SWAT method, the contribution rate of climate change on runoff in the three basins is lower than that of human activities, which implies human activities are the main impact factor for runoff decrease in the Taihang Mountain region. At the same time, the contribution rate of human activities in the three basins increases from north to south, which indicates that the influence of human activities from north to south is increasing.

The effect of human activities in the basin is reflected in water consumption, the variation in human water consumption directly reduced the water availability in rivers, and its effect was different in three basins. As shown in Fig. 8, both annual and per capita water consumption in the Zhangfang basin showed similar decreasing trends during 1991-2018, and the human water consumption reduced sharply after 2012. In addition, the surface water only supplied 23.5% of the human water consumption, with a utilization rate of 9.8%, thus the groundwater was a more important water source.



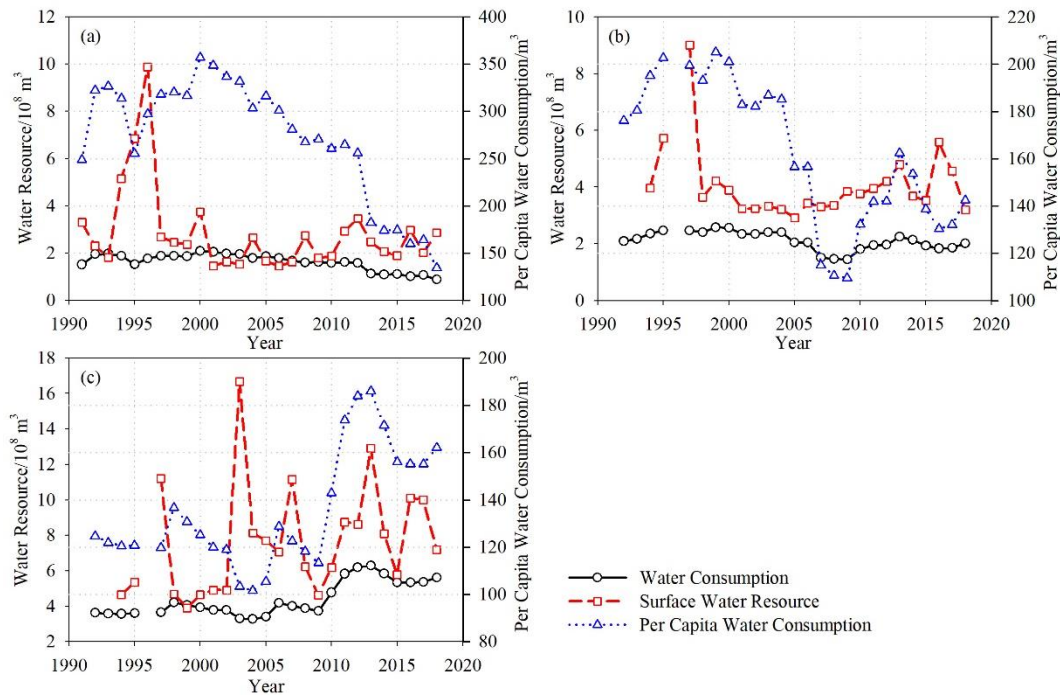


**Figure 8.** Per capita water consumption, total human water consumption, and surface water resource in the (a) Zhangfang, (b) Weishui and (c) Guantai basin

The series of annual and per capita water consumption in the Weishui basin presented the same abrupt point at 2004 by using the Mann-Kendall Method (Hirsch and Slack, 1984). Before and after abrupt year, both above series decreased firstly and then increased. The annual average water consumption reduced from  $2.38 \times 10^8 \text{ m}^3/\text{a}$  to  $1.91 \times 10^8 \text{ m}^3/\text{a}$  in two periods, and the per capita water consumption reduced by  $51.22 \text{ m}^3/\text{a}$ . The surface water supplied 64.9% of the human water consumption, with a utilization rate of 30.6%. In the basin, the farmland accounted for about 25% and was mainly dry farmland. The Jingxing and Xiyang County were known as the agricultural regions in the upstream. The effective irrigation area increased to  $3109 \text{ hm}^2$  in 2000 compared with  $1190 \text{ hm}^2$  in 1990. In addition, Yangquan City in the basin is an important energy and heavy industry base. The industrial, mining and residential land in 2000 increased by 8.3% compared with the 1980s. Human water consumption reached to the peak. Hereafter, the water consumption continued to fall until 2009 due to the effect of landscape engineering measures, while the increasing ecological and environmental water consumption led to the recent increase of total water usage (2010-2018).

Guantai basin is an area with intense human activities, farmland covers about 53.4%, and construction land covers 7.5%. There are three large reservoirs in the basin, with total reservoir storage  $7.12 \times 10^8 \text{ m}^3$  and covering about 29.81% of the basin. The annual water consumption showed a significant increasing trend during 1992-2018, with a rate of  $962.56 \times 10^4 \text{ m}^3/\text{a}$ . The series had an abrupt point at 2009, and the average water consumption increased from  $3.74 \times 10^8 \text{ m}^3/\text{a}$  to  $5.43 \times 10^8 \text{ m}^3/\text{a}$ . Meanwhile, the average per capita water consumption increased from  $119.96 \text{ m}^3/\text{a}$  to  $160.00 \text{ m}^3/\text{a}$  before and after abrupt point. The surface water supplied 46.1% of the human water consumption, with a utilization rate of 27.9%.

## Conclusions

Based on the analysis of trend and abrupt change for climate and hydrological factors in the Taihang Mountain region during 1955–2017, a SWAT hydrological model was built to simulate the hydrological process of the Zhangfang, Weishui and Guantai basins, and then the model was used to quantitatively estimate the contribution of climate change and human activity on runoff decrease. According to the above study, several facts were worth highlighting:

- The annual runoff of the Taihang Mountain region showed a decreasing trend during 1955–2017, and the abrupt change occurred at 1983, 1975 and 1973 for Zhangfang, Weishui and Guantai basins, respectively. The monthly runoff decreased by over 60% before and after abrupt change point.
- According to the comparison between observed and simulated runoff, the relative errors in the natural phase are less than 15%,  $R^2 > 0.6$  and  $E_{NS} > 0.5$ . The simulated results meet the accuracy requirement; thus the calibrated SWAT model can be well applied to the three basins.
- Through SWAT model, the contribution rates of human activity (climate change) in Zhangfang, Weishui and Guantai basins are 45.81% (54.19%), 39.84% (60.16%) and 31.61% (68.39%), respectively. Compared to climate change, human activity is a more important factor for runoff reduction in the Taihang Mountain region.

In the current study, we assume that the impacts of climate change and human activities on the water cycle at a river basin are independent, while the two factors have an interaction effect. Further, human activities include many factors, such as land use/cover change, water engineering measures, human water consumption, and government policies. In the future, an improved hydrological model, considering a variety of anthropogenic influence factors in detail, is needed to establish for simulating the water cycle process in the basins. Based on this model, a research on the future prediction of runoff changes will also be carried out. By setting different scenarios, the hydrologic regulation effects of the Grain-for-Green program, check-dams and terraces on runoff will be explored. The results can provide scientific basis and decision support for rational allocation of water resources and comprehensive management of ecological environment in the Taihang Mountain region.

**Acknowledgments.** This research was funded by the National Natural Science Foundation of China (No. 41801034), the Open Research Fund of Key Laboratory of Tibetan Environmental Changes and Land Surface Processes, Chinese Academy of Sciences (TEL201801), the National Basic Research Program of China (973 Program, No. 2015CB452705).

## REFERENCES

- [1] Arnold, J. G., Moriasi, D. N., Gassman, P. W., Abbaspour, K. C., White, M. J., Srinivasan, R., Santhi, C., Harmel, R. D., Griensven, A. V., Liew, M. W. V., Kannan, N., Jha, M. (2012): SWAT: Model use, calibration, and validation. – Transactions of the ASABE 55(4): 1345-1352.
- [2] Bao, Z., Zhang, J., Wang, G., Fu, G., He, R., Yan, X. (2012): Attribution for decreasing streamflow of the Haihe River Basin, Northern China: climate variability or human activities? – Journal of Hydrology 460-461: 117-129.

- [3] Bekele, E. G., Knapp, H. V. (2010): Watershed modeling to assessing impacts of potential climate change on water supply availability. – *Water Resources Management* 24(13): 3299-3320.
- [4] Chen, J. Q., Xia, J. (1999): Facing the challenge: barriers to sustainable water resources development in China. – *Hydrological Sciences Journal* 44(4): 507-516.
- [5] Chu, J. T., Xia, J., Xu, C. Y., Li, L., Wang, Z. G. (2010): Spatial and temporal variability of daily precipitation in Haihe River Basin, 1958–2007. – *Journal of Geographical Sciences* 20(2): 248-260.
- [6] Ficklin, D. L., Luo, Y. Z., Luedeling, E., Zhang, M. H. (2009): Climate change sensitivity assessment of a highly agricultural watershed using SWAT. – *Journal of Hydrology* 374(1-2): 16-29.
- [7] Fu, B. J., Wang, S., Liu, Y., Liu, J. B., Liang, W., Miao, C. Y. (2017): Hydrogeomorphic ecosystem responses to natural and anthropogenic changes in the Loess Plateau of China. – *Annual Review of Earth & Planetary Sciences* 45(1): 223-243.
- [8] Furey, P. R., Kampf, S. K., Lanini, J. S., Dozier, A. Q. (2012): A stochastic conceptual modeling approach for examining the effects of climate change on runoffs in mountain basins. – *Journal of Hydrometeorology* 13(3): 837-855.
- [9] Hirsch, R. M., Slack, J. R. (1984): A nonparametric trend test for seasonal data with serial dependence. – *Water Resources Research* 20(6): 727-732.
- [10] IPCC. (2014): *Climate Change 2014: Synthesis Report*. – In: Core Writing Team, Pachauri R. K., Meyer, L. A. (eds.) *Contribution of Working Groups I, II and III to the Fifth Assessment Report of the Intergovernmental Panel on Climate Change*. IPCC, Geneva, Switzerland.
- [11] Liu, C. M., Xia, J. (2004): Water problems and hydrological research in the Yellow River and the Huai and Hai River basins of China. – *Hydrological Processes* 18(12): 2197-2210.
- [12] Liu, C. Z., Zhan, C. S., Xia, J., Cao, J. T. (2014): Review on the influences of climate change and human activities on runoff. – *Journal of Hydraulic Engineering* 45(4): 379-385.
- [13] Milly, P. C. D., Dunne, K. A., Vecchia, A. V. (2005): Global pattern of trends in streamflow and water availability in a changing climate. – *Nature* 438: 347-350.
- [14] Neitsch, S. L., Arnold, J. G., Kiniry, J. R., Williams, J. R. (2011): *Soil and Water Assessment Tool: Theoretical documentation, version 2009*. – In: Texas Water Resources Institute Technical Report no. 406. Texas A&M University System, College Station, Texas.
- [15] Qin, D. H., Stocker, T., 259 Authors and TSU (Bern & Beijing) (2014): Highlights of the IPCC working group I fifth assessment report. – *Progressus Inquisitiones de Mutatione Climatis* 10(1): 1-6.
- [16] Sun, P. C., Wu, Y. P., Gao, J. E., Yao, Y. Y., Zhao, F. B., Lei, X. H., Qiu, L. J. (2020): Shifts of sediment transport regime caused by ecological restoration in the Middle Yellow River Basin. – *Science of the Total Environment* 698: 134261.
- [17] Vörösmarty, C. J., Green, P., Salisbury, J., Lammers, R. B. (2000): Global water resources: vulnerability from climate change and population growth. – *Science* 289(5477): 284-288.
- [18] Wang, W. G., Shao, Q. X., Yang, T., Peng, S. Z., Xing, W. Q., Sun, F. C., Luo, Y. F. (2013): Quantitative assessment of the impact of climate variability and human activities on runoff changes: a case study in four catchments of the Haihe River basin, China. – *Hydrological Processes* 27(8): 1158-1174.
- [19] Xia, J., Zhang, L., Liu, C. M., Yu, J. J. (2007): Towards better water security in North China. – *Water Resources Management* 21(1): 233-247.
- [20] Yang, Y. H., Tian, F. (2009): Abrupt change of runoff and its major driving factors in Haihe River Catchment, China. – *Journal of Hydrology* 374(3): 373-383.



- [21] Yang, X. N., Sun, W. Y., Li, P. F., Mu, X. M., Gao, P., Zhao, G. J. (2019): Integrating agricultural land, water yield and soil conservation trade-offs into spatial land use planning. – *Ecological Indicators* 104: 219-228.
- [22] Yao, W. Y., Xiao, P. Q., Shen, Z. Z., Wang, J. H., Jiao, P. (2016): Analysis of the contribution of multiple factors to the recent decrease in discharge and sediment yield in the Yellow River Basin, China. – *Journal of Geographical Sciences* 26(9): 1289-1304.
- [23] Zhang, L., Karthikeyan, R., Bai, Z. K., Srinivasan, R. (2017): Analysis of streamflow responses to climate variability and land use change in the Loess Plateau region of China. – *Catena* 154: 1-11.
- [24] Zhao, G. J., Tian, P., Mu, X. M., Jiao, J. Y., Wang, F., Gao, P. (2014): Quantifying the impact of climate variability and human activities on runoff in the middle reaches of the Yellow River basin, China. – *Journal of Hydrology* 519: 387-398.
- [25] Zhao, G. J., Mu, X. M., Jiao, J. Y., Gao, P., Sun, W. Y., Li, E., Wei, Y. H., Huang, J. C. (2018): Assessing response of sediment load variation to climate change and human activities with six different approaches. – *Science of the Total Environment* 639: 773-784.

## HABITAT SELECTION OF SMALL MAMMALS IN A MIXED FOREST IN TURKEY

BULUT, Ş.<sup>1\*</sup> – KARATAŞ, A.<sup>2</sup> – AYAŞ, Z.<sup>3</sup>

<sup>1</sup>*Hitit University, Faculty of Art and Science, Department of Molecular Biology and Genetics, Çorum, Turkey*

<sup>2</sup>*Niğde Ömer Halisdemir University, Department of Biology, Niğde, Turkey*

<sup>3</sup>*Hacettepe University, Faculty of Science, Department of Biology, Ankara, Turkey*

\*Corresponding author

e-mail: [safakbulut@hitit.edu.tr](mailto:safakbulut@hitit.edu.tr); phone: +90-364-227-7000

(Received 25<sup>th</sup> May 2020; accepted 19<sup>th</sup> Nov 2020)

**Abstract.** Small mammals is a non-taxonomic subgroup named on the basis of body size of individuals. This study was created from data obtained through the mark-recapture method of small terrestrial mammals in *Populus tremula*, thermophilic deciduous, steppes, conifer plantations and *Abies* sp. forest habitats in Turkey. Field studies were performed for a total of 14 months in 2014 and 2015. 758 individuals from seven species were captured in a total of 5250 days in trapping grid studies conducted in a total of 5 different types of habitat by a grid of 5 × 5 traps system. The average capture success in all was calculated as 14.44%. The species affected by temperature data were *M. glareolus* and *D. nitedula*. It was found that *M. subterraneus* showing increasing populations was negatively correlated with temperature. When considering the sex ratios, *M. glareolus* was under intense male pressure in steppe habitat. Indicator species were determined numerically and *M. glareolus*, *M. subterraneus* and *D. nitedula* were found to be decisive species for different habitats. The habitats showing most similarity to each other in terms of habitat preferences of small mammals the pine plantation and *Abies* forest, the most different habitat was steppe.

**Keywords:** *habitat preference, mark-recapture, populasyon dynamics, rodents*

### Introduction

Small mammals constitute a taxonomic group that can be used as an ideal model for studies in different fields (Barret, 1999). Distribution patterns of small mammals have important impacts on the biodiversity and the ecosystem (Aubry et al., 2003). Small mammal species can be classified into three trophic groups: those feeding on insects and other invertebrates (e.g. *Crocidura* spp.), those feeding on plant material or those that are omnivorous or graminivorous (e.g. *Apodemus* spp.), and those feeding on seeds (e.g. *Sciurus* spp.) (Kirkland Jr. et al., 1985). Consequently, the feeding behaviour of small mammals on seeds, fungi, plants, invertebrates, and bird eggs has strong effects on forest regeneration (Sullivan et al., 1993), biodiversity and the food cycle (McShea and Rappole, 2000). The effect of small mammals on forest regeneration is crucial for the entire ecosystem. Seeds dispersed by small mammals may promote this regeneration. Moreover, the mycorrhizal fungi, also dispersed by small mammals, are thought to be critical for tree growth (Luoma et al., 2003).

Species in the Rodentia order, which is represented by the highest number of species among all mammals, are one of the key components of ecosystems. This is especially true for forest ecosystems. The interactions of rodent species with other organisms and the physical environment are quite complex. These species feed on seeds and

vegetation, which may affect the regeneration patterns of forests (Sullivan et al., 1979; Christy and Mack, 1984). Seeds, mycorrhizal fungi and nitrogen-binding bacteria spread by these species may also affect plant diversity (Verts and Carraway, 1998; Luoma et al., 2003). Furthermore, rodent species are an essential part of the diet of many carnivorous species, and thus changes in their population size may have an impact on the dispersal and habitat use of carnivorous mammals, raptors and some reptiles (Carey et al., 1992). We may say that the demography and behaviour of these species are directly related to the distribution and density of their predators. For example, a decrease in rodent populations may cause owl species to end up with a limited reproduction rate or a lower number of eggs (Korpimäki et al., 1987; Hammer et al., 2001).

In recent years, small-scale ecological studies (i.e. fauna surveys in specific regions) were conducted on the small mammals in Turkey (Özkan, 1987; Karataş, 1996; Diker, 2007; Irmak, 2012; Tüzün, 2012). In addition to faunal inventory studies, reproductive and dietary behaviours were also studied in laboratory environments (Çolak et al., 1994; Yiğit et al., 1995, 1997; Buruldağ, 1999; Özkurt et al., 2001, 2005; Özkan et al., 2003).

Gür and Kart (2005) were the first to use the marking method in Turkey, for their study on the natural environment of Anatolian ground squirrels, in which they assessed the body mass, reproduction and annual hibernation activity of this species. Gür and Barlas (2006) surveyed the sex ratios of 235 Anatolian ground squirrel specimens. Yavuz (2007) calculated the estimated population size in closed populations based on 122 European water vole specimens she caught, by using mark-recapture technique. Şenol (2012) used the marking method in his study to determine the population size of rodents in a mixed deciduous forest habitat near Zonguldak. In this study, 130 live catch traps were placed in an area of one hectare at ten meter intervals according to the grid method. Parameters such as the estimated population size per hectare, sex ratios and home range were evaluated, and it became the first study to address these issues in Turkey.

Forest management is one of the most important factors causing a disturbance on the life and biodiversity of communities in the forests and in parts of them. Although biodiversity needs to be preserved and that the forest ecosystems require long-term sustainability, clear cutting has remained the major forest management technique in many places. While the forest management may have positive effects on some species or cause some species to remain completely unaffected, it does have negative effects on some species (Duguay et al., 2000; Payer and Harrison, 2000; De Bellefeuille et al., 2001). Small mammals are the potential indicators of forest management that looks out for the protection of forests. These species play a significant role in the forests; they are biologically important as being prey items for carnivorous animals, and they display typical responses when natural damage occurs due to intervention. In different types of forest, certain small mammals are known as indicator species. Small mammals have intensely changing population dynamics even without the existence of any disruption caused by forestry activities, so longer periods are needed to determine their response to the effects of such disruptions and alteration trends (Pearce and Venier, 2005). Small mammals are very suitable as habitat alteration indicators in temperate forests (full cutting of certain areas, emerging fragmentation, intentional reforestation, or spontaneous regrowth) (Carey and Harrington, 2001). Small mammal populations have a short transformation period, and their migration patterns can be tracked, and this is

why they are suitable for studying edge effects in ecotones between different habitat sections (Hansson, 1998; Manson et al., 1999; Nickel et al., 2003).

Small mammal populations either show a positive response or no response to the partial cutting practices in the forests (Medin and Booth, 1989; Steventon et al., 1998). Research results indicate a positive correlation between the abundance of small mammal populations and the leaf cover on the forest floor. For this reason, interventions reducing the amount of vegetation on the forest floor (i.e. herbicide application, machine correction of the land, tree plantations) also reduce the number of small mammals that feed on leaves until the subforest vegetation regrows (Lautenschlager, 1993). Small mammals also rely on the physical components of the forest, including tree stumps, overturned tree trunks, canopy openings, grass-layer vegetation, decayed trees, leaf remains and humus layer. Forest management may alter these factors significantly (Bowman et al., 2000; Carey and Harrington, 2001).

This study was compiled from the data obtained according to the “Capture-Mark-Recapture” model of terrestrial small mammals living on the floor of *Populus tremula* Forest, Thermophilic Deciduous Forest, Steppe (Mountain Steppe), Conifer Plantation, and *Abies* (Fir) Forest habitats in Soğuksu National Park in Central Anatolia Region. The subject of this study is to determine: recording qualitative and quantitative data regarding small mammals by sampling forest sections with different vegetation; evaluating qualitative data on small mammal species living on the forest floor; based on their relative ratios and changes in area usage in each sampling area; comparing the community components, structure, and species richness of small mammals according to different habitat types; assisting forest management practices (cutting, seeding, etc.) in their decisions on the type of trees to be planted, and their locations.

## Materials and Methods

### Study Area

Our studies were carried out in Soğuksu National Park, an important natural reserve in Kızılcahamam district, in the northernmost part of Ankara in Turkey. The National Park is located between 40°31'26"-40°34'13" S latitudes and 32°35'10"-32°39'31" E longitudes in the in the Upper Sakarya Section of Central Anatolia Region (*Figure 1*). The study area constitutes the Central Anatolia - Western Black Sea transition zone, and thus has a pivotal status in terms of biodiversity. As the study area is located between the geographic regions of Western Black Sea and Central Anatolia, its climate is influenced by both regions. Summers are dry and cool; winters are snowy and rainy. The area hosts Western Black Sea fir forests, Middle Black Sea pine forests, West Anatolian black pine forests, and Central Anatolian mountain steppe vegetation. The dominant forest vegetation in the area mainly consists of *Quercus pubescens*, *Pinus nigra ssp. pallasiana*, *Pinus sylvestris*, and *Abies nordmanniana ssp. bornmuelleriana* populations.

### Methodological Frame

In this study, we used the multi-faceted feature of Mark-Recapture data to investigate small mammal species and to look into the differences at the community level in five different habitat types [*Populus tremula* Forest (G1.9), Thermophilic Deciduous Forest (G1.7), Steppe (E1.2), Conifer Plantation (G3.F), and *Abies* (Fir) Forest (G3. 1)]

(Figure 1). Capturing stories collected from the sampling studies carried out with grid trapping systems were used for comparing the population densities of four small mammal species within and between mixed oak, young conifer plantation site, in-forest clearing, mixed coniferous and deciduous forest, and the coniferous forest habitats. The detection/nondetection data distributed to all habitat types was combined with co-variables at the trap level and used in logistic regression in order to reveal the preferences of living things at the microhabitat level. Species richness observed at the community level was compared between and within these five habitats. In addition, the abundance of caught species in each grid system enabled us to compare the structure and composition of small mammal community in all five explored habitats.

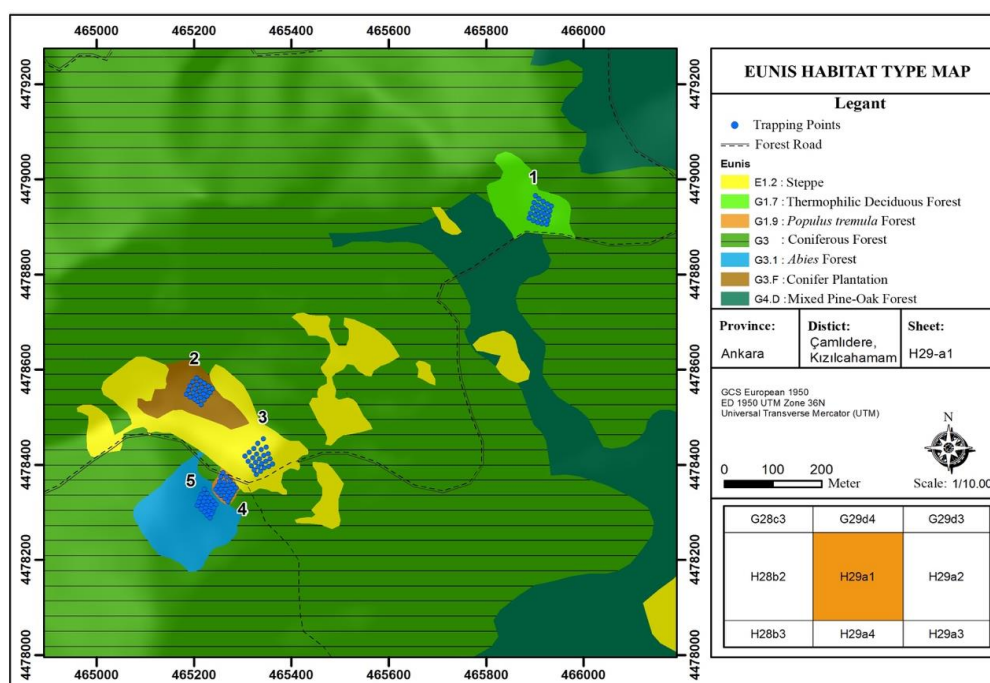


Figure 1. Study Area and EUNIS Habitat Classes Map

### Data Collection

In this study, we used a square grid containing 25 trapping stations of  $5 \times 5$ , depending on the frequency of ground cover and undercover vegetation of the habitat (Flowerdew et al., 2004). The distance between traps was determined as 10 m. Sherman-type live catch traps are  $23 \times 9 \times 7$  cm in size, and are among the most frequently used trap types in small mammal studies. We marked each determined trap location with numbered piles to avoid any possible confusion about trap locations. We used peanut butter and bread as bait, and marked all captured specimens with ear tags (National Band Tag Company, 1005-1). Sampling was carried out for three-day periods every month between May and November in 2014 and 2015. The number of trap days, which is calculated by multiplying the number of traps with the number of sampling days in each repetition was 525 for a one-year sampling period, 1,250 during the entire fieldwork, and 5,250 in total for selected five different habitats. The sampling was carried out with the permission of Hacettepe University, Experiment Animals Ethics Committee dated 03.26.2014, no. 52338575-41.

## **Statistical Analyses**

Since there were five habitats for each species (since  $n < 30$ ), we used the Kruskal-Wallis test to find out the differences between the capturing frequency of the species in all areas and the capturing rates according to months, and the Mann-Whitney U test to compare the differences in pairs ( $p < 0.05$  for all dual comparisons). The capturing numbers for species in individual habitat types were compared with the  $\chi^2$  test. All relationships between the vegetation structure, relative population density depending on temperature, and other quantitative small mammal data were tested by using regression analysis (Zar, 1996). Multiple regression analysis was used to test the relationship of quantitative small mammal data (mean number of captures, relative abundance value of common species) in terms of total and habitat-based effects of the selected five different habitat types.

The characteristic species of different habitats were determined by IndVal (Indicator Value) method, a relatively new statistical procedure (Dufrene and Legendre, 1997). We used IndVal 2.0 to determine the indicator values. IndVal also generates significance values for the calculated indicator values, based on random selection calculations. For the IndVal method, it is necessary to assign codes to the habitats based on the five forest habitats studied. The Bray-Curtis index was applied to calculate the similarities between habitats based on quantitative data of different species. Similarity structure was obtained using a hierarchical cluster analysis, and UPGMA was calculated to combine the data.

Diversity indices (Shannon-Weiner, Margalef species richness and Simpson indices) were used to obtain data about species richness and the distribution of individuals among species in habitats (grids). These indices were calculated using the Past 3.13 program.

## **Results**

### **Habitat Types**

**Thermophilic Deciduous Forest (G1.7):** These forests thrive on the andesite bedrock between 1,470 and 1,590 metres in Soğuksu National Park. They have 80-90% coverage, and a height of 6-7 metres. The dominant species are *Quercus petraea* ssp. *iberica*, *Sorbus torminalis*, *Crataegus tanacetifolia*, and *Carpinus betulus*. *Pinus nigra* was sparsely found in these forests.

**Conifer Plantation (G3.F):** Some parts of Soğuksu National Park are afforested, mainly with Scots pine (*Pinus sylvestris*). Species in the plantation are 15-20 years old, and are quite dense. Therefore, the floristic composition in this area developed rather poorly.

**Steppe (E1.2):** This is the most common habitat in the Central Anatolia Region. Usually found in the hills called steppes, it may also grow in forest openings. This habitat that develops in the forest openings in Soğuksu National Park is used as a pasture. The dominant species are herbaceous species such as *Astragalus microcephalus*, *Stipa holosericea*, *Dactylis glomerata*, and *Vicia caracca*. This habitat, composed of single-layer herbaceous species, has a cover of 100%, and a height between 10 and 150 cm.

**Populus tremula Forest (G1.9):** *Populus tremula* forests are distributed on andesite rocks at altitudes of 1,400-2,000 m in Soğuksu National Park, and are generally found

in the more humid areas on the northern slopes. These forests can be pure, or mixed with forests of *Pinus sylvestris* and *Abies nordmanniana* subsp. *bornmuelleriana*. The soil is rich in organic matter.

*Abies* Forest (G3.1): This habitat represents the pure *Abies nordmanniana* ssp. *bornmuelleriana* forests in Soğuksu National Park. Its floristic composition was observed to be weak. It may rarely include deciduous forest members such as *Pinus sylvestris* and *Sorbus torminalis*. These forests may have a cover of 100%, and a height of 10-15 metres. The soil is rich in organic matter.

### Trapping Ratios and Habitat Choices

In trapping studies carried out in 5 different habitat types according to the 5 × 5 square grid system, we caught 758 individuals from 7 different species in a total of 5,250 trap days. The mean capturing success in all habitat types was calculated as 14.44%. During the entire study, the most commonly captured species was *Mus macedonicus* (115 individuals) and the rarest was *Dryomys nitedula* (9). The habitat type represented by the highest number of individuals was *Populus tremula* forest (PtF), followed by Thermophilic Deciduous Forest (TDF), steppe (STP), conifer plantation (CP) and *Abies* (Fir) forest (AF) in order. Capturing rates according to habitats are given in Table 1.

**Table 1.** The number of individuals captured in habitats

Grid	<i>Apodemus</i> spp.	<i>M. macedonicus</i>	<i>M. glareolus</i>	<i>M. subterraneus</i>	<i>C. suaveolens</i>	<i>D. nitedula</i>	Total
PtF	139	24	57	19	7	2	248
TDF	154	6	13	9	6	7	195
STP	29	12	16	46	15	0	118
CP	53	34	9	11	4	0	111
AF	41	39	2	3	1	0	86
<b>Total</b>	<b>416</b>	<b>115</b>	<b>97</b>	<b>88</b>	<b>33</b>	<b>9</b>	<b>758</b>

PtF: *Populus tremula* Forest, TDF: Thermophilic Deciduous Forest, STP: Steppe, CP: Conifer Plantation, AF: *Abies* sp. Forest

Morphological distinction of *Apodemus flavicollis* and *A. witherbyi* can be quite difficult. Therefore, these two species were grouped as *Apodemus* spp. to avoid misidentification. According to this, the most preferred habitat types of species belonging to the genus *Apodemus*, which had the highest number of individuals in forest habitats, were TDF and PtF. Other preferred habitat types were AF and CP for *Mus macedonicus*, PtF for *Myodes glareolus*, and mountain steppe for *Microtus subterraneus*. A total of 33 *Crociodura suaveolens* specimens were captured, and this species generally does not use undercover fir forest floor. *Dryomys nitedula* individuals were seen as thermophilic deciduous forest animals. They were also observed in PtF, but not in other habitats (Figure 2).

In order to test whether there was a statistical difference between the capturing frequencies of species, capturing frequencies in the entire study area were analysed with the Kruskal-Wallis test since there were 5 different habitats for each species ( $n < 30$ ). The results showed a statistically significant difference between the capturing frequencies of species (KW-H (5; 30) = 18.2389;  $p = 0.0027$ ) (Figure 3).

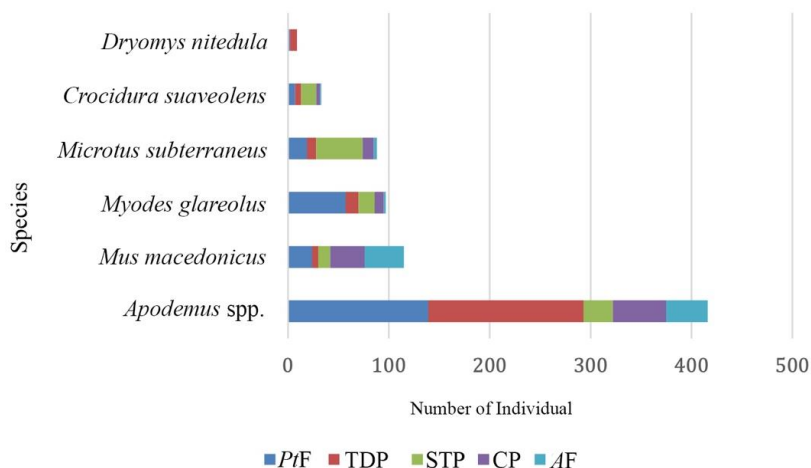


**Figure 2.** Habitat preferences of species (PtF: *Populus tremula* Forest, TDF: Thermophilic Deciduous Forest, STP: Steppe, CP: Conifer Plantation, AF: *Abies sp.* Forest)

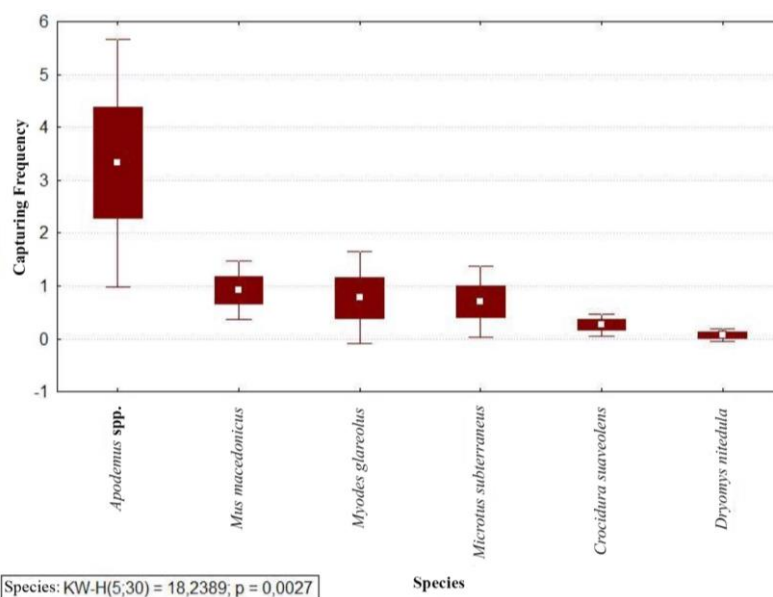


**Figure 3.** Distribution of capturing frequency according to species

The differences between the double capture rates of the species were compared with the Mann-Whitney U test ( $p < 0.05$  for all dual comparisons). Upon examining dual comparisons, we determined that the capturing rate of *Apodemus* spp. in the study area was different from those of *C. suaveolens* and *D. nitedula*, meaning *Apodemus* had a higher density. The capturing numbers of species in individual habitat types were compared with the  $\chi^2$  test. According to this, the difference was significant for *Apodemus* spp. ( $\chi^2 = 165.3462$ ;  $p = 0.000000$ ), *M. macedonicus* ( $\chi^2 = 34.26087$ ;  $p = 0.000001$ ), *M. glareolus* ( $\chi^2 = 96.76289$ ;  $p = 0.000000$ ), *M. subterraneus* ( $\chi^2 = 64.72727$ ;  $p = 0.000000$ ), and *C. suaveolens* ( $\chi^2 = 16.54545$ ;  $p = 0.002369$ ); but not for *D. nitedula* ( $\chi^2 = 0.4$ ;  $p = 0.982477$ ). When sex ratios were compared between habitats, the differences for all species in all five habitats are not significant ( $p < 0.05$  for all double comparisons).



### Indicator Values of Species

In order to evaluate the captured small mammals at the community level, their indicator values in different habitats were found. Results obtained by using a method that also includes multivariate statistical methods, can be seen related to the relationship between small mammals and the habitats or microhabitats they occupy. Indicator analysis was performed for spring, summer, autumn, and for combined seasonal data. We first created a table for indicator species with three separate periods, and determined the data for certain species and five sampling grids for each season. A maximum 0.46 IndVal was found for *Apodemus* spp., but this data was not significant ( $P = 1.178$ ). *Mus macedonicus* and *Crocidura suaveolens* also gave low IndVal values, and thus were not evaluated as indicator species for a particular habitat. *Myodes glareolus* generally preferring a specific habitat and also being seen in other habitats (although rare), *Microtus subterraneus* being the dominant species of the steppe, and *Dryomys nitedula* preferring thermophilic deciduous forest increased their indicator species values (Table 2, Figure 4).

**Table 2.** Maximum IndVal of species with hierarchical classification

Species	IndVal (%)	PtF	TDF	STP	CP	AF
<i>Apodemus</i> spp.	46.17	139/25	154/25	29/17	53/23	41/19
<i>Mus macedonicus</i>	29.60	24/13	6/4	12/7	34/16	39/21
<i>Myodes glareolus</i>	42.15*	57/22	13/6	16/5	9/4	2/2
<i>Microtus subterraneus</i>	63.84**	19/11	9/4	46/22	11/4	3/2
<i>Crocidura suaveolens</i>	17.11	7/4	6/3	15/8	4/3	1/1
<i>Dryomys nitedula</i>	69.21**	2/1	7/4	0/0	0/0	0/0
<b>Total</b>		248/76	195/46	118/59	111/50	86/45

The first number in each habitat is the number of individuals captured in that habitat, and the second value is the number of trap locations where species are captured in that habitat. \*\*:  $P < 0.01$ ; \*:  $P < 0.05$

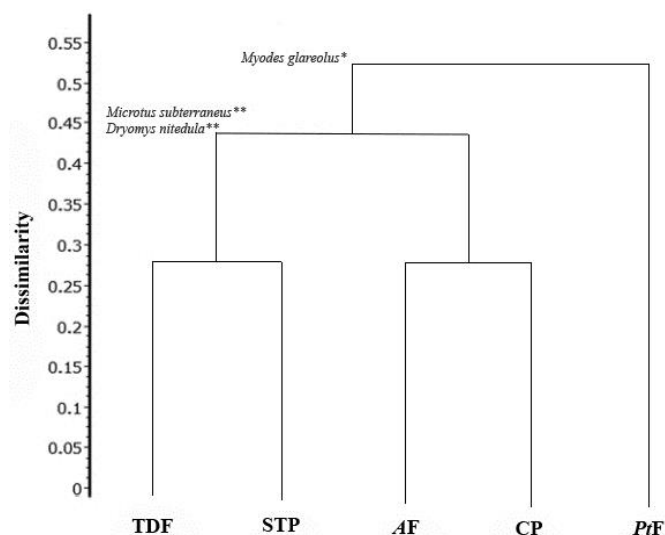


**Figure 4.** Dendrogram of the maximum indicator values on a certain hierarchical level, and the habitats analysed according to the significant IndVal values closest to the maximum value (Bray-Curtis index – UPGMA)

### **Habitat Diversity and Similarities**

According to the results for five different habitat types in Soğuksu National Park, some habitats have equal numbers of species, but have different characteristics as these species may be found in different proportions. To understand this difference numerically, we calculated the habitat similarities according to the Bray-Curtis similarity index. Habitats with the highest similarities were found between the coniferous plantation and *Abies* forest (82.2%), and between the *Populus tremula* forest and thermophilic deciduous forest (79%). Similarities of other habitats were low. We drew a dendrogram of habitat similarities according to the Bray-Curtis similarity index. *Populus tremula* forest, thermophilic deciduous forest, and the steppe habitat appear to be on a different branch than the coniferous plantation and *Abies* forest. The steppe habitat is also separated from the *Populus tremula* forest and thermophilic deciduous forest (Figure 5).

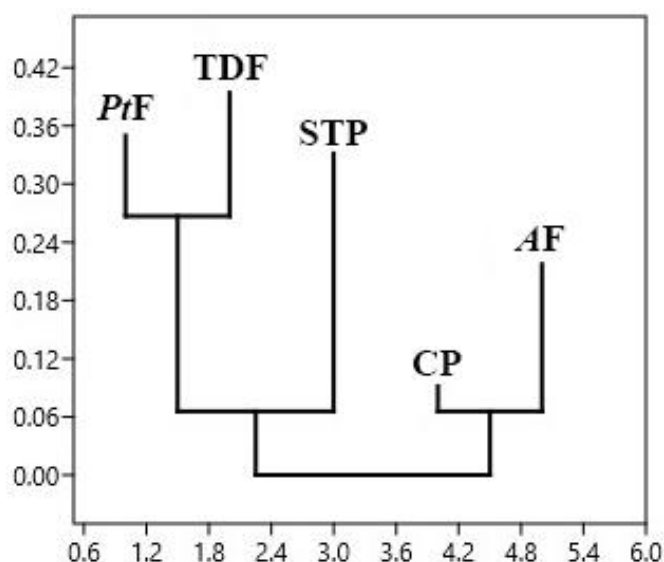


**Figure 5.** Dendrogram for habitat similarities according to the Bray-Curtis similarity index (Bray-Curtis index UPGMA)

Diversity indices of all five habitat types were calculated based on the number of small mammals captured in each of them during field studies (Table 3). The Simpson diversity index indicates the diversity of a habitat, with a value between 0 and 1. The diversity decreases as the  $D$  value approaches 1. According to this, the thermophilic deciduous forest was found to have the highest diversity ( $D = 0.3665$ ). The Shannon-Weiner index is used to numerically demonstrate the species diversity in an area, and the  $H$  value ranges from 0 to 5. Accordingly, the steppe habitat was found to be the richest in species diversity ( $H = 1.478$ ). Margalef index transforms the species richness of a habitat into a numerical value, and this value has no limit. The habitat with the highest value in the Margalef index has the highest species richness. Accordingly, the thermophilic deciduous forest was found to be have the highest species richness ( $M = 0.9482$ ). However, values from all habitats were close to each other.

**Table 3.** Diversity indices of habitats

	<b>PtF</b>	<b>TDF</b>	<b>STP</b>	<b>CP</b>	<b>AF</b>
<b>Number of Species</b>	6	6	5	5	5
<b>Number of Individuals</b>	248	195	118	111	86
Simpson_1-D	0.6169	0.3665	0.7427	0.6605	0.5652
Shannon_H	1.225	0.8426	1.478	1.268	0.9681
Margalef	0.9069	0.9482	0.8385	0.8493	0.898

## Discussion

Trapping studies in 5 different habitat types conducted with the 5 × 5 square grid system yielded 758 individuals from 7 different species in a total of 5250 trap days. The mean capturing success in all habitat types was calculated as 14.44%. Şenol (2012) captured 610 individuals in a mixed deciduous forest habitat on the Black Sea coast in 4680 trap days, with a trap success of 13.03%. The study continued during the winter months, and the capturing success was not affected by the winter as the study area was a coastal region. For example, Wells et al. (2007) captured 17 species in the rainforest during 17800 trap nights, achieving a trap success of 28.3%, while Nakagawa et al. (2006) achieved similar results by capturing 22 species in 6821 trap nights, with a trap success of 31%. Cusack (2011) captured 523 individuals from 22 different species for 995 times in 3420 trap night, achieving a trap success of 29.1%.

As a result, capturing rates of our study complies with the studies carried out in European forest habitats (Horváth and Kovačić, 2007). In this type of studies, trap success data in forest habitats show similarity when bait is not used. The capturing success varies in zoogeographic regions where species diversity, biomass, and abundance are high.

The most commonly captured species in this study were *Apodemus* spp. (54.9%), followed by *Mus macedonicus* (15.2%), *Myodes glareolus* (12.8%), *Microtus subterraneus* (11.6%), *Crocidura suaveolens* (4.3%) and *Dryomys nitedula* (1.2%), respectively. Kaynaş (2008), in her study comparing the successional phase of forests exposed to wildfires in different times, identified 75.7% of the individuals she captured as *Apodemus mystacinus* and 6.5% as *Apodemus flavicollis*, revealing 82.2% of all captured individuals belonged to *Apodemus* spp. Also captured in the same study, that investigated the red pine forest floor and scrub areas, were *Mus macedonicus* (8.6%), *Crocidura suaveoles* (7.7%), *Rattus rattus* (0.7%), and *Dryomys nitedula* (0.7%). The only similarity between our study and that of Kaynaş (2008) is that both sampling studies were conducted on the undergrowth of coniferous forests, and that *Apodemus* spp. were the dominant species.

In the study by Şenol (2012) conducted on a deciduous forest floor, the dominant species were *Apodemus* spp. (80.1%), followed by *Myodes glareolus* (12%), *Glis glis* (6.6%), and *Muscardinus avellanarius* (0.5%). The ratios are similar in studies from Central and Southern Europe. Horváth and Kovačić (2007) captured 430 individuals in their study in Croatia, 77.2% of which were *Apodemus* spp. and 22% were *Myodes glareolus*.

As a result, *Apodemus* spp. are the dominant small mammals in forest habitats, reaching a dominance value of 75% in mountain forests of medium altitudes. They were dominant in all kinds of forest floor in this study. They become a little rarer in

agricultural areas, making up only 6-7% of captured small mammals. Their optimum habitats in Central Europe are pure and mixed deciduous forests (Flowerdew et al., 1985). Based on the data from this study and other studies conducted in our country so far, they seem to be the dominant species in coniferous, mixed, and mixed deciduous forest habitats.

For some species, the number of captured individuals varied according to seasons. Although *Apodemus* spp. showed no big difference in any season, the highest number of captures were still made in September (93) and May (68). Şenol (2012) found the maximum population size for *Apodemus* spp. in June and March, the population density decreased after July, and increased again in November. It is known that population density generally increases in autumn (Horváth and Kovačić, 2007).

There was also no significant difference for *Myodes glareolus* and *Crocidura suaveolens*, but seasonal fluctuation is quite normal for *Dryomys nitedula*. Due to its hibernation behaviour and nutritional preferences, the species was found to be active in June, July, and August. The species showing the highest seasonal variation in relative population density in this study was *Microtus subterraneus*, whose population increased about 2-3 times in September, October, and November.

In the study area, we also recorded species of diurnal raptors and reptiles that can create hunting pressure on small mammals. We observed that the diurnal raptors used the area between May and September for feeding purposes, and the predator snakes (*Dolichophis caspius*, *Elaphe quatuorlineata*) were also active in the area between May and October.

An increase in the general population status in autumn may be due to the migration of diurnal raptors in September, and the hibernation of snake species in October, resulting in a decreased predator pressure particularly in open areas. The species that benefits the most from this decrease seems to be *Microtus subterraneus*. *M. subterraneus* individuals being the most common element in the diet of the tawny owl supports this view.

This study, covering all seasons except winter, showed the necessity for multiple study periods even for providing faunal data, and that the autumn period must be included in sampling as that is the season when small mammals reach peak densities.

Sex ratios of captured individuals showed no significant difference for *Apodemus* spp. ( $\chi^2 = 0.28571$ ;  $p = 0.5929$ ). In all habitats, 211 males and 205 females were captured, and the sex ratio was approximately 51:49. Sex ratios were also balanced for *Mus macedonicus* and *Myodes glareolus* considering all habitats and all study periods. However, a significant difference was in the mountain steppe habitat ( $\chi^2 = 5.6$ ;  $p = 0.01796$ ), which had a minimum distance of 50 m to the *Populus tremula* forest and was 140 m away from the conifer plantation. It is possible that male individuals, especially young males that survive the winter, increase their home range to find a partner.

To evaluate the captured small mammals at the community level, their indicator values were found for each habitat. The maximum 0.46 IndVal for *Apodemus* spp. was not significant ( $P = 1.178$ ). IndVal was also low for *Mus macedonicus* and *Crocidura suaveolens*, showing they are not indicator species for any particular habitat. *Myodes glareolus* was determined to be an indicator species for the *Populus tremula* forest as it generally preferred that habitat (IndVal = 42%) and was rarely seen in others. A study conducted in Croatia determined that *M. glareolus* was the indicator species by 29% among 4 species during summer months (Horváth et al., 2008). Horváth (2011) also

determined *M. glareolus* as an indicator species by 51.31% after *Micromys minutus*, *Apodemus sylvaticus*, and *Microtus arvalis* among 16 species.

In this study, *Microtus subterraneus* was the dominant species of the steppe, and *Dryomys nitedula* preferred thermophilic deciduous forest habitats, which increased their values as indicator species.

We calculated the habitat similarities according to the Bray-Curtis similarity index. Habitats with the highest similarity in this study were the coniferous plantation and *Abies* forest (82.2%). This is because the floor of both habitats have similar cover. They are usually occupied by opportunistic species (*Mus macedonicus* in this study) and have no diversity in terms of food (cone seeds, etc.). Therefore, these two habitats are not preferred by dominant species, and were found to be the two most similar habitats in terms of small mammal preference. *Populus tremula* forest and thermophilic deciduous forest were the other close habitats with a similarity of 79%. This is possibly due to similar species composition and cover percentages in both habitats. Other habitats had low similarities, but the mountain steppe was the most different type of habitat, likely because *Microtus subterraneus* was the dominant species, and it had a rich food variety, and was possibly used as a wintering area in times without predator pressure.

We collected qualitative and quantitative data on small mammals by sampling forest areas showing vegetation difference, and investigated how these different habitats affect small mammal abundance. We compared the composition, structure and species richness of small mammal communities in different habitat types, and found considerable differences in the densities and species compositions of the small mammal fauna elements, even when the habitat sections were adjacent. The richest habitats were those with more subforest cover and with soils rich in organic matter. Coniferous forests and plantation sites were poor in small mammal fauna.

**Acknowledgements.** I wish to thank Dr. Burak Akbaba for their help in the field studies. Also, thanks to Deniz Candaş for the help in translation and final editing of this paper. Legal permissions for this study were provided by The Turkish Ministry of Agriculture and Forestry, General Directorate of Nature Conservation and National Parks. This study was supported by the Research Fund of Hacettepe University (Nr. FBA-2015-5840) and it is part of the PhD thesis of Şafak Bulut.

## REFERENCES

- [1] Aubry, K. B., Hayes, J. P., Biswell, B. L., Marcot, B. G. (2003): The ecological role of tree-dwelling mammals in western coniferous forests. – In: Zabel, C. J., Anthony, R. G. (eds.) Mammals Community Dynamics. Management and Conservation in the Coniferous Forests of Western North America. Cambridge University Press, Cambridge, UK, pp. 405-443.
- [2] Barret, G. W., Peles, J. D. (1999): Small mammals ecology: A landscape perspective. – In: Barret, G. W., Peles, J. D. (eds.) Landscape Ecology of Small Mammals. Springer, New York, pp. 1-8.
- [3] Bowman, J., Sleep, D., Forbes, G., Edwards, M. (2000): The association of small mammals and coarse woody debris at log and stand scales. – Forest Ecology Management 124(2): 119-124.
- [4] Buruldağ, E. (1999): *Myomimus roachi* (Bate 1937) (Mammalia; Rodentia)'nın Üreme Biyolojisi ve Davranışları Üzerine Araştırmalar. – Yüksek Lisans Tezi, Trakya Üniversitesi Fen Bilimleri Enstitüsü, Biyoloji Anabilim Dalı, 55 sayfa (In Turkish).

- [5] Carey, A. B., Horton, S. P., Biswell, B. L. (1992): Northern Spotted Owls: influence of prey base and landscape character. – *Ecological Monographs* 62: 223-250.
- [6] Carey, A. B., Harrington, C. A. (2001): Small mammals in young forests: implications for management for sustainability. – *Forest Ecological Management* 154: 289-309.
- [7] Christy, J. E., Mack, R. N. (1984): Variation in demography of juvenile *Tsuga heterophylla* across the substratum mosaic. – *Journal of Ecology* 72: 75-91.
- [8] Çolak, E., Yiğit, N., Verimli, R. (1994): Periodic cycles in food intake and body weight of juvenile Dormice, *Glis glis orientalis* Nehring, 1903 (Rodentia: Gliridae) in northern Anatolia. – *Turkish Journal of Zoology* 18: 241-244.
- [9] Cusack, J. (2011): Characterising Small Mammal Responses to Tropical Forest Loss and Degradation in Northern Borneo Using Capture-Mark-Recapture Methods. – Master's thesis, Imperial College London.
- [10] De Bellefeuille, S., Bélanger, L., Pettorelli, J. H., Cimon, A. (2001): Clear-cutting and regeneration practices in Quebec boreal balsam forest: effects on snowshoe hare. – *Canadian Journal of Forest Research* 31(1): 41-51.
- [11] Diker, E. (2007): Uludağ'in böcekçil (Mammalia: Insectivora) ve kemirici (Mammalia: Rodentia) türleri. – Trakya Üniversitesi, Fen Bilimleri Enstitüsü (In Turkish).
- [12] Dufrene, M., Legendre, P. (1997): Species assemblages and indicator species: the need for a flexible asymmetrical approach. – *Ecological monographs* 67(3): 345-366.
- [13] Duguay, J. P., Wood, P. B., Miller, G. W. (2000): Effects of timber harvests on invertebrate biomass and avian nest success. – *Wildlife Society Bulletin* 28: 1123-1131.
- [14] Flowerdew, J. R., Gurnell, J., Gipps, J. H. W. (1985): The ecology of woodland rodents: bank voles and wood mice. – The proceedings of a symposium held at the Zoological Society of London on 23rd and 24th of November 1984. No. 55. Clarendon Press.
- [15] Flowerdew, J. R., Shore, R. F., Poulton, S. M. C., Sparks, T. H. (2004): Live trapping to monitor small mammals in Britain. – *Mammal review* 34(1-2): 31-50.
- [16] Gür, H., Gür, M. K. (2005): Annual cycle of activity, reproduction, and body mass of Anatolian ground squirrels (*Spermophilus xanthoprymnus*) in Turkey. – *Journal of Mammalogy (ISI, SCI)* 86: 7-14.
- [17] Gür, H., Barlas, N. (2006): Sex ratio of a population of Anatolian ground squirrels *Spermophilus xanthoprymnus* in Central Anatolia, Turkey. – *Acta Theriologica (ISI, SCI)* 51: 61-67. doi: 10.1007/BF03192656.
- [18] Hammer, O., Harper, D. A. T., Ryan, P. D. (2001): PAST: Paleontological Statistic software package for education and data analysis. – *Paleontologia Electronica* 4(1): 1-9.
- [19] Hansson, L. (1998): Local hot spots & their edge effects: small mammals in oak-hazel woodland. – *Oikos* 81: 55-62.
- [20] Horváth, Gy., Kovačić, D. (2007): Protokol za praćenje populacija i zajednica sitnih sisavaca na staništima duž Drave. [Protocol for the monitoring of small mammal populations and communities in habitats along the river Drava]. – In: Purger, J. J. (ed.) Priručnik za istraživanje bioraznolikosti duž rijeke Drave. [Manual for the investigation of biodiversity along the river Drava]. University of Pécs, pp. 219-234.
- [21] Horváth, Gy., Borsics, J., Purger, J. J. (2008): Habitat use of small mammals in disturbed patches of Haljevo forest in Croatia. – University of Pécs Publish.
- [22] Horváth, Gy., Herczeg, R., Tamási, K., Sali, N. (2011): Nestedness of small mammal assemblages and role of indicator species in isolated marshland habitats. – *Natura Somogyiensis* 19: 281-283.
- [23] Irmak, S. (2012): Zonguldak ili Erinaceomorpha, Soricomorpha ve Chiroptera (Chordata: Mammalia) türlerinin ve yayılışlarının belirlenmesi. – Bülent Ecevit Üniversitesi, Fen Bilimleri Enstitüsü (in Turkish).
- [24] Karataş, A. (1996): Yamanlar dağı (İzmir) Mammalia (Insectivora, Chiroptera, Rodentia) faunası. – Ege Üniversitesi, Fen Bilimleri Enstitüsü (in Turkish).

- [25] Kaynaş, B. Y. (2008): *Pinus brutia* orman ekosistemlerinde küçük memeli komünitesi üzerine yangının uzun dönem etkisi ve yangın sonrası komünite yapısının değişimi üzerine çalışmalar. – Hacettepe Üniversitesi, Fen Bilimleri Enstitüsü (in Turkish).
- [26] Kirkland Jr, G. L., Johnston Jr, T. R., Steblein, P. (1985): Small mammal exploitation of a forest-clearcut interface. – *Acta Theriologica* 30: 211-218.
- [27] Korpimäki, E., Lagerstrom, M., Saurola, P. (1987): Field evidence for nomadism in Tengmalm's Owl *Aegolius funereus*. – *Ornis Scandinavica* 18: 1-4.
- [28] Lautenschlager, R. A. (1993): Response of wildlife to forest herbicide applications in northern coniferous ecosystems. – *Canadian Journal of Forest Research* 23: 2286-2299.
- [29] Luoma, D. L., Trappe, J. M., Claridge, A. W., Jacobs, K., Cazares, E. (2003): Relationships among fungi and small mammals in forested ecosystems. – In: Zabel, C. J., Anthony, R. G. (eds.) *Mammal Community Dynamics. Management and Conservation in the Coniferous Forests of Western North America*. Cambridge University Press, Cambridge, UK, pp. 343-373.
- [30] Manson, H. R., Ostfeld, R. S., Canham, C. D. (1999): Responses of a small mammal community to heterogeneity along forest-old-field edges. – *Landscape Ecology* 14: 355-367.
- [31] McShea, W. J., Rappole, J. H. (2000): Managing the abundance and diversity of breeding bird populations through manipulation of deer populations. – *Conservation Biology* 14(4): 1161-1170.
- [32] Medin, D. E., Booth, G. D. (1989): Responses of Birds and Small Mammals to Single-Tree Selection Logging in Idaho. – US Department of Agriculture, Forest Service Intermountain Research Station, Ogden, Utah, Research Paper INT: 408.
- [33] Nakagawa, M., Miguchi, H., Nakashizuka, T. (2006): The effects of various forest uses on small mammal communities in Sarawak, Malaysia. – *Forest Ecology and Management* 231(1): 55-62.
- [34] Nickel, A. M., Danielson, B. J., Moloney, K. A. (2003): Wooded habitat edges as refugia from microtine herbivory in tallgrass prairies. – *Oikos* 100: 525-533.
- [35] Odum, E. P., Barrett, G. W. (2005): *Fundamentals of ecology*. – 5th edition Belmont, CA: Thomson Brooks/Cole.
- [36] Özkan, B., Yiğit, N., Çolak, E. (2003): Türkiye Trakyası'nda *Micromys minutus* Pallas, 1777 (Mammalia: Rodentia) üzerine bir çalışma. – *Turkish Journal of Zoology* 27: 55-60. (in Turkish).
- [37] Özkurt, Ş., Yiğit, N., Çolak, E., Sözen, M., Verimli, R. (2001): Observations on the reproduction biology of *Meriones meridianus* Pallas, 1773 (Mammalia: Rodentia) in Turkey. – *Zoology in the Middle East* 23: 23-29.
- [38] Özkurt, Ş., Yiğit, N., Çolak, E., Sözen, M., Gharkheloo, M. M. (2005): Observations on the Ecology, Reproduction and Behavior of *Spermophilus* Bennett, 1835 (Mammalia: Rodentia) in Turkey. – *Turkish Journal of Zoology* 29: 91-99.
- [39] Payer, D. C., Harrison, D. J. (2000): Structural differences between forests regenerating following spruce budworm defoliation and clear-cut harvesting: implications for marten. – *Canadian Journal of Forest Research* 30: 1965-1972.
- [40] Pearce, L., Venier, L. (2005): Small mammals as bioindicators of sustainable boreal forest management. – *Forest Ecology and Management* 208: 153-175.
- [41] Şenol, D. (2012): Zonguldak bölgesi karışık yaprak döken orman alanında yaşayan kemiricilerin (Mammalia: Rodentia) populasyon büyüklüklerinin markalama yöntemiyle belirlenmesi. – Bülent Ecevit Üniversitesi, Fen Bilimleri Enstitüsü.
- [42] Steventon, J. D., Mackenzie, K. L., Mahon, T. E. (1998): Responses of small mammals and birds to partial cutting and clearcutting in northwest British Columbia. – *The Forestry Chronicle* 74: 703-713.
- [43] Sullivan, J. L., Piereson, J. E., Marcus, G. E., Fledman, S. (1979): The More Things Change, The More They Stay the Same: The Stability of Mass Belief Systems. – *American Journal of Political Science* 23: 176-86.

- [44] Sullivan, W., Fogarty, P., Theurkauf, W. (1993): Mutations affecting the cytoskeletal organization of syncytial *Drosophila* embryos. – Development 118: 1245-1254.
- [45] Tüzün, T. E. (2012): Beytepe (Ankara) karasal küçük memeli faunasının belirlenmesi. – Hacettepe Üniversitesi, Fen Bilimleri Enstitüsü (in Turkish).
- [46] Verts, B. J., Carraway, L. N. (1998): Land Mammals of Oregon. – University of California Press, Berkeley. xvi + 668 pp. ISBN 0- 520-21199-5.
- [47] Wells, K., Kalko, E. K. V., Lakim, M. B., Pfeiffer, M. (2007): Effects of rain forest logging on species richness and assemblage composition of small mammals in Southeast Asia. – Journal of Biogeography 34(6): 1087-1099.
- [48] Yavuz, G. (2007): Ankara civarında yayılış gösteren su sıçanı *Arvicola terrestris* L., 1758 (Mammalia: Rodentia)'in ekolojisi üzerinde araştırmalar. – Ankara Üniversitesi, Fen Bilimleri Enstitüsü (in Turkish).
- [49] Yiğit, N., Çolak, E., Özkurt, Ş. (1995): Biology of *Meriones tristrami* Thomas, 1892 (Rodentia: Gerbillinae) in Turkey. – Turkish Journal of Zoology 19: 337-341.
- [50] Yiğit, N., Kıvanç, E., Çolak, E. (1997): Diagnostic characters and distribution of *Meriones Illiger*, 1811 (Mammalia: Rodentia) in Turkey. – Turkish Journal of Zoology 21: 361-374. (article in Turkish with an abstract in English).
- [51] Zar, J. H. (1996): Biostatistical analysis. – Prentice-Hall, New Jersey.



# THE EFFECT OF DIFFERENT PLANTING SYSTEMS ON THE GROWTH, YIELD AND FIBER QUALITY OF COTTON CULTIVARS

ALI, H. – HASSAN, W. – IRFAN, M.\*

*Department of Agronomy, Faculty of Agricultural Sciences and Technology, Bahauddin Zakariya University, Multan, Pakistan*

\*Corresponding author  
e-mail: [muhammad.irfan26@gmail.com](mailto:muhammad.irfan26@gmail.com)

(Received 24<sup>th</sup> Jun 2020; accepted 6<sup>th</sup> Oct 2020)

**Abstract.** Tillage system is a critical factor that limits plant growth and production all over the globe. The current study was to evaluate the performance of cotton cultivars and appropriate planting system for higher crop production in Punjab, Pakistan. Two factors; cultivars and planting system were examined under RCBD along four repeats. “CIM-602 cultivar” had the highest yield traits i.e. plant height, number of bolls/plant, boll weight, seed cotton yield, lint yield, biological yield and seed cotton harvest. The excellent increase was shown in yield and phenological attributes of cotton cultivars under bed sowing compared to all other studied planting systems. Regarding the cultivars, the higher fiber related attributes such as fiber fineness, fiber uniformity, fiber elongation, fiber strength and micronaire were measured in “CIM-602 cultivar” as compared to “CIM-678cultivar”. The bed sowing provides the best fiber quality as compared to other planting systems. Economic analysis confirmed that bed sowing is best planting system which provides higher output to farmers with little input. It has been concluded that from present study, “CIM-602” is good cultivar and provides higher production, while bed sowing is suitable planting system for cotton production.

**Keywords:** *fiber quality traits, economic analysis, growth related traits, physiological traits*

## Introduction

Cotton (*Gossypium hirsutum* L.) is famous as white gold and belongs to family *Malvaceae*. Three different species including *Gossypium hirsutum*, *Gossypium arboreum* as well as *Gossypium barbedense* are economically most important to fulfill fiber requirements worldwide (Zohaib et al., 2018). Among different countries, China is famous as one of the leading country for the cotton production worldwide because of its modern research and development (Pettigrew and Dowd, 2011). However, Pakistan ranks 4<sup>th</sup> after China, USA and India regarding the cotton production than other countries (Amouzou et al., 2018). Cotton had excellent role in economy of Pakistan. Cotton is major oil producing crop of Pakistan. Therefore, cotton is acknowledging as major cash as well as fiber crop in Pakistan (Shah et al., 2011).

In Pakistan cotton production is very poor because of different biotic and abiotic stresses as compared to other developed countries. Hence numerous other factors i.e. insect pest and disease attack, selection of genotypes, different planting system, inadequate fertilizer application, nutritional imbalance and improper agronomic practices resulted in poor yield of cotton. The performance of cultivars can vary from cultivar to other because of its different genetic background (Ahmad et al., 2019). Cultivation of those genotypes having unique genetic background suitable for higher production is major requirement with passage of time (Bellaloui et al., 2015). Therefore, huge efforts

were recommended for attaining higher yield regarding different low yielding aspects of cotton (Magare et al., 2018).

Though, massive efforts are requisite to improve crop growth which ultimately increase in cotton yield as well as improve cotton fiber quality. However, cotton cultivation is more in Pakistan than other agronomic crops but yield per hectare is found to be minimum because of different environmental constrains such as drought, salinity and many others (Zohaib et al., 2018). The shortage of water is big problem in Pakistan. Moreover, drought environments greatly reduced the plant growth and yield traits of many cotton cultivars. Therefore, numerous management practices such as cultivars development with superior traits, selection of higher yielding cultivars, cultivars potential against adverse environmental conditions, good fiber quality are needed for attaining higher production from (Pettigrew and Dowd, 2011).

Planting system is major constrain that is involved in production of different agronomic crops. Different yield reduction aspects were studied in previous work (Ali et al., 2010). However, examination of planting system is very negligible regarding cotton production. Suitable use of planting system is very important aspect for attaining higher production of cotton. Three different planting systems i.e. raised beds, flat beds and ridges are used for cotton cultivation (Nadeem et al., 2013). The most frequently used planting system is ridges cultivation since earlier times. However, many farmers more satisfied on ridges cultivation than other planting system. The excellent plant growth as well as production was recorded from ridges cultivation in numerous other crops (Anjum et al., 2019). In recent times, it has been identified that raised beds are greatly preferable than ridges under drought stress conditions because raised beds have excellent water holding potential than all other planting systems (Ali et al., 2015). Earlier research work indicated that planting system is successful involved in higher production of cotton. Huge research work is conducted on water stress conditions, while determination of suitable planting system under water stress conditions is novelty of the current work. Therefore, current study encourages the cultivation of drought resistant cultivars with suitable tillage system that will increase the cotton production.

## Materials and methods

Present study was accomplished at Central Cotton Research Institute (CCRI) Multan in 2017 & 2018. Current site lies at a latitude of 30°, and longitude of 71° and the altitude is 125 in the Punjab, Pakistan. Performance of two cultivars CIM-678 as well as CIM-602 was checked under three different planting systems such as flat, ridge and bed sowing. Experimental site was deeply ploughed and well prepared, become suitable for cotton cultivation. Experimental soil possessed organic matter (0.86%), nitrogen (0.09%) as well as phosphorous (12.5 ppm). The experimental plot size was nearly 6.1 m × 9.0 m with seed rate 110 g/plot. Crop was harvested from 07-11-2017 as well as 16-11-2018 with several pickings after 15 days interval.

Appropriate management practices i.e. timely irrigation, fertilizer application, weeds eradication and control of various insect pest and diseases were applied till crop harvesting. Urea fertilization was nearly 35 kg ha<sup>-1</sup>. Irrigation was applied after one week interval as when it required. Pendimethaline is famous herbicide successfully applied nearly 82.5 mL ha<sup>-1</sup> to suppress cotton weeds as applied by Ali et al. (2019). Different growth, yield as well as fiber traits were examined. Agro-climatic conditions of experimental site CCRI were presented (*Figure 1*).

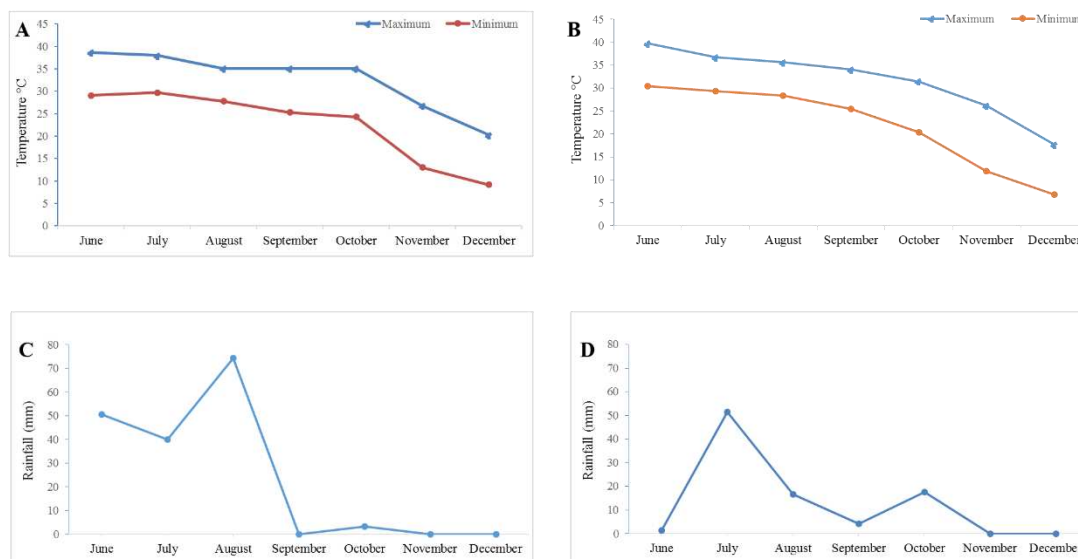


**Figure 1.** Eco-meteorological data of Multan, Punjab (Pakistan) during 2017 (A & C) and during 2018 (B & D)

### ***Yield related traits***

Plant height was determined through measuring scale. Average number of nodes and number of bolls/ plant were computed. Boll weight was measured through digital weighing balance. Lint yield, biological yield as well as harvest index were recorded as described (Apel and Hirt, 2004).

### ***Phenological related traits***

Leaf area index (LAI) = Area of leaf/ ground leaf area

Crop growth rate was determined by dividing leaf area on dried leaf samples at 70 °C (Fang and Xiong, 2015). Lead area duration (LAD) was determined by measuring leaf surface area against time (Farooq et al., 2008). Net assimilation rate (NAR) was calculated by dividing relative growth rate on ratio of leaf area as previously mentioned (Fahad et al., 2016).

### ***Fiber related traits***

Cotton bolls were dried at room temperature and then their fiber was collected using ginning machine manually. All samples were subjected to 65% humidity at 20 °C for determination of fiber finess, fiber uniformity, fiber length, fiber elongation and fiber strength and micronaire were calculated according earlier adopted methods (Apel and Hirt, 2004; Fang and Xiong, 2015).

### ***Data analysis***

RCBD design was used to test the significance level of collected data through software Statistix 8.1. Moreover, means were separated through LSD test at 5% probability level according to (Anjum et al., 2020). Economic analysis were performed by collecting input and output data, and benefit cost ration was determined by dividing net return on total cost as described (Ali et al., 2019).

## Results

### *Yield related traits*

The cultivars, planting system and their interaction was significantly affected the yield traits in the present study except biological yield (*Table 1*). Regarding the individual effect of cultivars, Cultivar CIM-602 had significantly longer plant height (163.56 cm), while the cultivar CIM-678 had significantly smaller plant height (157.67 cm). Regarding the effect of planting systems, bed sowing had the largest plant height (162.83 cm) than flat sowing (158.00 cm). The interaction of cultivars as well as planting systems indicated that significantly largest plant height was recorded in cultivar CIM-602 × bed sowing (165.33 cm). The highest number of bolls/ plant (34.67) as well as boll weight (1.90 g) were estimated from cultivar CIM-602 than other studied cultivar. The interactive effect of cultivars as well as different planting systems described that the larger number of boll/ plant (36.33) as well as weight of boll (2.11 g) were measured from CIM-602 × bed sowing. Significantly the maximum seed cotton yield (2246.6 Kg ha<sup>-1</sup>) and lint yield (38.56 Kg ha<sup>-1</sup>) were found in cultivar CIM-602, however significantly meager seed cotton yield (2071.4 Kg ha<sup>-1</sup>) and lint yield (32.56 Kg ha<sup>-1</sup>) were calculated in cultivar CIM-678. Significantly greater seed cotton yield (2278.2 Kg ha<sup>-1</sup>) and lint yield (37.67 Kg ha<sup>-1</sup>) were determined in bed sowing than other planting systems. The significantly higher biological yield (0.76 t ha<sup>-1</sup>) and seed cotton harvest (24.67%) were measured in cultivar CIM-602. Although, significantly meager biological yield (0.71 t ha<sup>-1</sup>) as well as seed cotton harvest (19.44%) were found in CIM-678. Higher biological yield (0.77 t ha<sup>-1</sup>) and seed cotton harvest (24.17%) were found on raised beds and lower biological yield (0.65 t ha<sup>-1</sup>) as well as seed cotton harvest (19.50%) were present in flat beds. The interaction of cultivars as well as planting systems were depicted that the higher biological yield (0.83 t ha<sup>-1</sup>) and seed cotton harvest (26.33%) were measured from CIM-602 × beds sowing (*Table 2*).

**Table 1.** Statistical analysis (LSD values) of different yield, physiological and fiber quality related traits of two cotton cultivars grown under different planting systems

Trait	Cultivars	Planting systems	Cultivars × Planting systems
Plant height (cm)	826.18**	189.12**	12.65**
Number of bolls/plant	240.00**	67.81**	8.44**
Boll weight (g)	0.23ns	77.46**	74.65**
Seed cotton yield (Kg ha <sup>-1</sup> )	108938**	78231.4**	3804.25**
Lint yield (Kg ha <sup>-1</sup> )	502.76**	104.14**	6.21*
Biological yield (t ha <sup>-1</sup> )	9.88*	28.11**	1.77ns
Seed cotton harvest (%)	251.02**	68.64**	7.27*
Leaf area index	130.39**	44.66**	8.97**
Leaf area duration (days)	2457.65**	1060.41**	2.19ns
Crop growth rate (g m <sup>-2</sup> day <sup>-1</sup> )	1920.76**	22.07**	5.24*
Net assimilation rate (g m <sup>-2</sup> day <sup>-1</sup> )	3082.92**	37.07**	7.76**
Fiber finess	3535.80**	40.10**	7.03**
Fiber uniformity	297.61**	32.17**	1.52ns
Fiber length (mm)	846.40**	69.10**	4.30*
Fiber elongation (mm)	1246.94**	60.63**	9.65**
Fiber strength (mm)	1209.14**	91.86**	6.14*
Micronaire (µg/inch)	1548.00**	26.67**	4.67*

ns = non-significant, \* = significant at p = 0.05, and \*\* = significant at p = 0.01

**Table 2.** Yield related traits of two cotton cultivars grown under different planting systems

Traits	Cultivars	Flat sowing	Ridge sowing	Bed sowing	Mean
Plant height (cm)	CIM-678	154.33 f	158.33 e	160.33 d	157.67 b
	CIM-602	161.67 c	163.67 b	165.33 a	163.56 a
	Mean	158.00 c	161.00 b	162.83 a	
Number of bolls/plant	CIM-678	25.67 e	30.33 d	32.00 c	29.33 b
	CIM-602	33.00 c	34.67 b	36.33 a	34.67 a
	Mean	29.33 c	32.50 b	34.16 a	
Boll weight (g)	CIM-678	1.31 d	1.70 bc	1.79 b	1.60 b
	CIM-602	1.59 c	1.99 a	2.11 a	1.90 a
	Mean	1.45 c	1.45 c	1.45 c	
Seed cotton yield (Kg ha <sup>-1</sup> )	CIM-678	1968.0 f	2072.3 e	2174.0 c	2071.4 b
	CIM-602	2077.7 d	2279.7 b	2382.3 a	2246.6 a
	Mean	2022.8 c	2176.0 b	2278.2 a	
Lint yield (Kg ha <sup>-1</sup> )	CIM-678	29.33 f	33.33 e	35.00 d	32.56 b
	CIM-602	36.67 c	38.67 b	40.33 a	38.56 a
	Mean	33.00 c	36.00 b	37.67 a	
Biological yield (t ha <sup>-1</sup> )	CIM-678	0.65 c	0.74 b	0.75 b	0.71 b
	CIM-602	0.66 c	0.80 ab	0.83 a	0.76 a
	Mean	0.65 b	0.77 a	0.79 a	
Seed cotton harvest (%)	CIM-678	16.00 e	20.33 d	22.00 c	19.44 b
	CIM-602	23.00 c	24.67 b	26.33 a	24.67 a
	Mean	19.50 c	22.50 b	24.17 a	

\* Mean values sharing similar letter(s) in a column are statistically non-significant at p = 0.05 (LSD test)

### **Phenological related traits**

The cultivars and planting system and their combined effect were significantly affected the *phenological* traits (Table 1). The significantly greater leaf area index (0.44) as well as leaf area duration (544.44 days) were calculated from cultivar CIM-602, while significantly lower leaf area index (0.38) as well as leaf area duration (427.78 days) were estimated from CIM-678. The maximum leaf area duration (536.83 days) and leaf area index (0.44) were calculated from beds sown cotton, while lower leaf area duration (411.00 days) and leaf area index (0.38) were calculated from flats sown plants. The interactive effects of two cultivars under three different planting systems showed that the much leaf area duration (592.00 days) and leaf area index (0.48 t ha<sup>-1</sup>) were measured in CIM-602 × beds than all other studied combinations. Significantly greater crop growth rate (5.07 g m<sup>-2</sup> day<sup>-1</sup>) and net assimilation rate (1.35 g m<sup>-2</sup> day<sup>-1</sup>) were calculated cultivar CIM-602, while significantly lower crop growth rate (4.79 g m<sup>-2</sup> day<sup>-1</sup>) and net assimilation (1.01 g m<sup>-2</sup> day<sup>-1</sup>) were calculated cultivar CIM-678. The maximum crop growth rate (4.95g m<sup>-2</sup> day<sup>-1</sup>) and net assimilation rate (1.21 g m<sup>-2</sup> day<sup>-1</sup>) were calculated from bed sowing, while lower crop growth rate (4.90 g m<sup>-2</sup> day<sup>-1</sup>) and net assimilation rate (1.14 g m<sup>-2</sup> day<sup>-1</sup>) were calculated from flat sowing. The interactive effects of cultivars under diverse planting systems showed that the higher crop growth rate

( $5.10 \text{ g m}^{-2} \text{ day}^{-1}$ ) and net assimilation rate ( $1.38 \text{ g m}^{-2} \text{ day}^{-1}$ ) were measured in CIM-602  $\times$  bed sowing than all other studied combinations (Table 3).

**Table 3.** Physiological related traits of two cotton cultivars grown under different planting systems

Traits	Cultivars	Flat sowing	Ridge sowing	Bed sowing	Mean
Leaf area index	CIM-678	0.36 d	0.39 c	0.40 c	0.38 b
	CIM-602	0.39 c	0.46 b	0.48 a	0.44 a
	Mean	0.38 c	0.42 b	0.44 a	
Leaf area duration (days)	CIM-678	352.33 f	449.33 e	481.67 c	427.78 b
	CIM-602	469.67 d	571.67 b	592.00 a	544.44 a
	Mean	411.00 c	510.50 b	536.83 a	
Crop growth rate ( $\text{g m}^{-2} \text{ day}^{-1}$ )	CIM-678	4.78 d	4.80 cd	4.81 c	4.79 b
	CIM-602	5.03 b	5.09 a	5.10 a	5.07 a
	Mean	4.90 b	4.94 a	4.95 a	
Net assimilation rate ( $\text{g m}^{-2} \text{ day}^{-1}$ )	CIM-678	0.99 e	1.02 d	1.03 d	1.01 b
	CIM-602	1.29 c	1.36 b	1.38 a	1.35 a
	Mean	1.14 c	1.19 b	1.21 a	

\* Mean values sharing similar letter(s) in a column are statistically non-significant at  $p = 0.05$  (LSD test)

### Fiber related traits

The cultivars and planting system and their combined effect were significantly affected the fiber quality related traits (Table 1). Cultivar CIM-602 had the highest fiber finess (3.44) and fiber uniformity (47.89), while cultivar CIM-602 had the lowest fiber finess (3.09) and fiber uniformity (39.67). Significantly greater fiber finess (3.29) and uniformity (46.00) were collected from beds sown plants, however significantly meager fiber finess (3.23) and uniformity (41.33) were recorded from flat sowing. The greater fiber length (33.67 mm) and elongation (30.21 mm) were recorded from cultivar CIM-602, while the lower fiber length (23.44 mm) and elongation (30.06 mm) were measured in CIM-678. The maximum fiber length (30.83 mm) and elongation (30.16 mm) were shown in bed plantings. The minimum fiber length (25.83 mm) and elongation (30.11 mm) were measured from flat plantings. The significantly higher fiber strength (25.56 mm) and micronaire (4.17  $\mu\text{g}/\text{inch}$ ) were recorded from CIM-602 cultivar, while the significantly lower fiber strength (15.33 mm) and micronaire (3.83  $\mu\text{g}/\text{inch}$ ) were measured in cultivar CIM-678. The greater fiber strength (22.67 mm) and micronaire (4.05  $\mu\text{g}/\text{inch}$ ) were assessed from beds sown plants, while the lower fiber strength (17.83 mm) as well as micronaire (3.99  $\mu\text{g}/\text{inch}$ ) were measured in those plants harvested from flat beds. The interactive effect of cultivars under planting systems mentioned that highest fiber strength ( $27.33 \text{ g m}^{-2} \text{ day}^{-1}$ ) as well as micronaire (4.21  $\mu\text{g}/\text{inch}$ ) were measured from CIM-602  $\times$  beds (Table 4).

Benefit cost ratio was higher on bed sowing and lower was recorded from flat sowing in both years study. The benefit ratio was higher on bed sowing cultivation. Detailed description of economic analysis was presented (Table 5).

**Table 4.** Fiber quality related traits of two cotton cultivars grown under different planting systems

Traits	Cultivars	Flat sowing	Ridge sowing	Bed sowing	Mean
Fiber finess	CIM-678	3.07 e	3.10 d	3.11 d	3.09 b
	CIM-602	3.39 c	3.46 b	3.48 a	3.44 a
	Mean	3.23 c	3.28 b	3.29 a	
Fiber uniformity	CIM-678	36.67 d	40.33 c	42.00 c	39.67 b
	CIM-602	46.00 b	47.67 b	50.00 a	47.89 a
	Mean	41.33 c	44.00 b	46.00 a	
Fiber length (mm)	CIM-678	20.00 f	24.33 e	26.00 d	23.44 b
	CIM-602	31.67 c	33.67 b	35.67 a	33.67 a
	Mean	25.83 c	29.00 b	30.83 a	
Fiber elongation (mm)	CIM-678	30.04 e	30.07 d	30.08 d	30.06 b
	CIM-602	30.17 c	30.22 b	30.24 a	30.21 a
	Mean	30.11 c	30.15 b	30.16 a	
Fiber strength (mm)	CIM-678	12.00 f	16.00 e	18.00 d	15.33 b
	CIM-602	23.67 c	25.67 b	27.33 a	25.56 a
	Mean	17.83 c	20.83 b	22.67 a	
Micronaire ( $\mu\text{g}/\text{inch}$ )	CIM-678	3.86 d	3.89 cd	3.90 c	3.88 b
	CIM-602	4.12 b	4.18 a	4.21 a	4.17 a
	Mean	3.99 b	4.03 a	4.05 a	

Mean values sharing similar letter(s) in a column are statistically non-significant at  $p = 0.05$  (LSD test)

**Table 5.** Role of planting systems on benefit cost ratio (BCR) of cotton

	Treatments	Yield ( $\text{kg ha}^{-1}$ )	Value ( $\text{\$ ha}^{-1}$ )	stick value ( $\text{\$ ha}^{-1}$ )	Gross value ( $\text{\$ ha}^{-1}$ )	Total cost ( $\text{\$ ha}^{-1}$ )	Net return ( $\text{\$ ha}^{-1}$ )	BCR
2017	Flat sowing	2500	1170.866	7.751938	1178.618	723.1912	455.4264	1.63
	Ridge sowing	2630	1231.751	7.751938	1239.503	733.2041	506.2984	1.69
	Bed sowing	2880	1348.837	7.751938	1356.589	715.4393	641.1499	1.90
2018	Flat sowing	2550	1194.283	7.751938	1202.035	723.4496	478.5853	1.66
	Ridge sowing	2680	1255.168	7.751938	1262.92	733.2687	529.6512	1.72
	Bed sowing	2930	1372.255	7.751938	1380.006	715.5685	664.438	1.93

Note: Cotton price = 16.15  $\text{\$/40 kg}$  (during 2017) and 18.73 $\text{\$/40 kg}$  (during 2018)

## Discussion

Regarding the mean performance of cultivars, cultivar CIM-602 showed the highest growth related traits i.e. plant height, number of bolls/ plant, boll weight, seed cotton yield, lint yield, biological yield and seed cotton harvest than other cultivar CIM-678. Regarding the effect of three different planting systems i.e. flats, ridges and beds, the excellent increase was exhibited in yield related traits of cotton cultivars from bed cultivation among other studied planting systems. Furthermore, interactive effect of cultivars as well as planting systems were potentially examined the involvement of planting systems in cotton production. The yield related traits were also increased under

interactive effect of cultivar CIM-602 and bed sowing. Current study is under conformity of earlier research who reported that bed sowing increased the yield of different agronomic crops especially cotton crop (Ali et al., 2016). Similarly, Duzy and Kornecki (2019) evaluated that suitable sowing method increased the cotton yield. In earlier decades, the ridge sowing is found to satisfactory for farmers as reported (Anjum et al., 2019). However, under water stress conditions, beds sowing is excellent and preferable planting system for best cotton productivity and ultimately higher yield can successfully be accomplished.

Regarding the physiological traits, the greater leaf area index, leaf area duration, crop growth rate and net assimilation rate were recorded in cultivar CIM-602 than other one cultivar CIM-678. Concerning the effect of planting systems, bed plantings of cotton cultivars showed the higher net assimilation rate, crop growth rate, leaf area duration and leaf area index than other two different planting methods. However, poor performance among physiological traits were measured from flat sowing. Furthermore, combined effect of cultivars like CIM-678 and CIM-602 and three planting methods such as flats, ridges and beds planting exhibited a greater involvement in improvement of cotton production. The net assimilation rate, crop growth rate, leaf area duration and leaf area index were increased from cultivar CIM-602 and bed plantings than other one cultivar CIM-678 and flat plantings. Current study indicated that appropriate use of tillage system had excellent capability to increase the production of agronomic crops especially cotton cultivars. In the current study, bed sowing is best tillage system for higher physiological related traits, because these physiological traits were involved in increase of growth and development of cotton crop (Nadeem et al., 2013). The highest physiological traits were attained from CIM-602 and bed sowing than other planting system. It has been assumed that water stress condition is very critical constrain that involved in reduction of plant growth and yield as in earlier work of Mahpara et al. (2019). Moreover, different suitable cultural practices, nutritional balance and selection of cultivars were played an imperative role in higher crop productivity of cotton crop with superior quality of cotton.

Fiber excellence related parameters such as fiber finess, uniformity, elongation, strength and micronaire were found to be effective for farmers and further for industrial purposes. Concerning the cultivars, the higher fiber related parameters like fiber finess, uniformity, elongation, strength as well as micronaire were measured from cultivar CIM-602 as compared to cultivar CIM-678. Regarding the tillage system, bed sowing provides the highest fiber finess, uniformity, elongation, strength as well as micronaire than other considered tillage methods. The highest moisture content was available to plants in beds plantings. Regarding the interactive consequence of cultivars as well as planting system, significantly greater fiber traits were found in cultivar CIM-602 as well as bed planting system. Hence, current study is more effective for attaining appropriate fiber traits. Current study indicated the benefits of beds sowing on fiber related traits (Zohaib et al., 2018). Several previous studies confirmed that bed sowing improved the fiber related attributes such as fiber finess, elongation, uniformity, strength and micronaire as recorded in current findings (Shah et al., 2011; Upadhyaya and Panda, 2019). Correspondingly, Ali et al. (2020) also determined that improvement fiber quality is more important for farmers and industry and use of appropriate cultivars is much imperative. Hence, current is helpful and encourages the use of suitable tillage system for cotton production with good quality fiber traits. The increase of net return and higher benefit cost ratio is found to be effective for increase of production and their earnings.



## Conclusion

Cotton is a major oil-producing crop, but the effects of the cultivation on the oil production had not been studied. It has been concluded that CIM-602 is important cultivar and performed better under water stress conditions than CIM-678. Regarding the tillage system, bed sowing is important for higher production than flat and ridge sowing. CIM-602 and ridge swing are favorable for farmers and required very low inputs. It has been recommended that the cultivation of CIM-602 on bed sowing increases the farmer's earnings and providing higher benefit cost ratio.

**Acknowledgements.** The authors are highly grateful to the Bahauddin Zakariya University, Multan for financial support to conduct the study.

## REFERENCES

- [1] Ahmad, R., Malik, W., Anjum, M. A. (2019): Genetic diversity and selection of suitable molecular markers for characterization of Indigenous *Zizyphus* germplasm. – *Erwerbs-Obstbau* 61(4): 345-353.
- [2] Ali, M., Ali, L., Sattar, M., Ali, M. A. (2010): Response of seed cotton yield to various plant populations and planting methods. – *J. Agric. Res.* 48(2): 163-169.
- [3] Ali, H., Tariq, N., Ahmad, S., Chattha, T. H., Hussain, A. (2012): Effect of irrigation at different growth stages and phosphorus application methods on agronomic traits of wheat (*Triticum aestivum* L.). – *J. Food Agric. Environ.* 10: 1371-1375.
- [4] Ali, F., Ali, A., Gul, H., Sharif, M., Sadiq, A., Ahmed, A., Ullah, A., Mahar, A., Kalhor, S. A. (2015): Effect of boron soil application on nutrients efficiency in tobacco leaf. – *Amer. J. Plant Sci.* 6(09): 1391.
- [5] Ali, M., Ali, L., Waqar, M. Q., Ali, M. A. (2016): Bed planting: a new crop establishment method for wheat (*Triticum aestivum* L.) in cotton-wheat cropping system of southern Punjab. – *Int. J. Agric. Appl. Sci.* 47: 777-780.
- [6] Ali, H., Ahmad, A., Hussain, S. (2019): The effect of exogenous phosphorous application on growth, yield, quality and net returns of Upland cotton (*Gossypium hirsutum* L.). – *Applied Ecology and Environmental Research* 18(1): 769-781.
- [7] Ali, H., Ahmad, A. and Hussain, S. (2020): The effect of exogenous phosphorous application on growth, yield, quality and net returns of upland cotton (*Gossypium hirsutum* L.). – *Appl. Ecol. Env. Res.* 18(1): 769-781.
- [8] Amouzou, K. A., Naab, J. B., Lamers, J. P., Borgemeister, C., Becker, M., Vlek, P. L. (2018): CROPGRO-Cotton model for determining climate change impacts on yield, water- and N-use efficiencies of cotton in the Dry Savanna of West Africa. – *Agric. Systems* 165: 85-96.
- [9] Anjum, M. A., Muhammad, H. M. D., Balal, R. M., Ahmad, R. (2019): Performance of two onion (*Allium cepa* L.) cultivars under two different planting systems in calcareous soil. – *J. Hortic. Sci. Technol.* 2(2): 54-59.
- [10] Anjum, M. A., Haram, A., Ahmad, R., Bashir, M. A. (2020): Physico-chemical attributes of fresh and dried Indian jujube (*Zizyphus mauritiana*) fruits. – *Pak. J. Agric. Sci.* 57(1): 165-176.
- [11] Apel, K., Hirt, H. (2004): Reactive oxygen species: metabolism, oxidative stress, and signal transduction. – *Ann. Review Plant Biol* 55: 373-399.
- [12] Bellaloui, N., Turley, R. B., Stetina, S. R. (2015): Water stress and foliar boron application altered cell wall boron and seed nutrition in near-isogenic cotton lines expressing fuzzy and fuzzless seed phenotypes. – *PloS one* 10(6): e0130759. 10.1371/journal.pone.0130759.

- [13] Duzy, L. M., Kornecki, T. S. (2019): Effects of cover crop termination and cotton planting methods on cotton production in conservation systems. – *Renew. Agric. Food Syst.* 34(5): 406-414.
- [14] Fahad, S., Hussain, S., Saud, S., Khan, F., Hassan, S., Nasim, W., Arif, M., Wang, F., Huang, J. (2016): Exogenously applied plant growth regulators affect heat-stressed rice pollens. – *J. Agron. Crop Sci.* 202(2): 139-150.
- [15] Fang, Y., Xiong, L. (2015): General mechanisms of drought response and their application in drought resistance improvement in plants. – *Cell. Mol. Life Sci.* 72: 673-689.
- [16] Farooq, M., Basra, S. M. A., Wahid, A., Cheema, Z. A., Cheema, M. A., Khaliq, A. (2008): Physiological role of exogenously applied glycinebetaine in improving drought tolerance of fine grain aromatic rice (*Oryza sativa* L.). – *J. Agron. Crop Sci.* 194: 325-333.
- [17] Magare, P. N., Jadhao, S. D., Farkade, B. K., Mali, D. V. (2018): Effect of levels of potassium on yield, nutrient uptake, fertility status and economics of cotton grown in Vertisol. – *Int. J. Curr. Microbiol. Appl. Sci.* 7(4): 1292-1300.
- [18] Mahpara, S., Shahnawaz, M., Rehman, K., Ahmad, R., Khan, F. U. (2019): Nitrogen fertilization induced drought tolerance in sunflower: a review. – *Pure App. Biol.* 8(2): 1675-1683.
- [19] Nadeem, M. A., Idrees, M., Ayub, M., Tanveer, A., Mubeen, K. (2013): Effect of different weed control practices and planting systems on weeds and yield of cotton. – *Pak. J. Bot.* 45(4): 1321-1328.
- [20] Pettigrew, W. T., Dowd, M. K. (2011): Varying planting dates or irrigation regimes alters cottonseed composition. – *Crop Sci.* 51(5): 2155-2164.
- [21] Rad, N. M. R., Kadir, M. A., Yusop, M. R. (2012): Genetic behaviour for plant capacity to produce chlorophyll in wheat (*Triticum aestivum*) under drought stress. – *Aust. J. Crop Sci.* 6(3): 415.
- [22] Shah, A. R., Khan, T. M., Sadaqat, H. A., Chatha, A. A. (2011): Alterations in leaf pigments in cotton (*Gossypium hirsutum*) genotypes subjected to drought stress conditions. – *Int. J. Agric. Biol.* 13(6): 902-908.
- [23] Upadhyaya, H., Panda, S. K. (2019): Drought stress responses and its management in rice. – In: *Advances in Rice Research for Abiotic Stress Tolerance*. Woodhead Publishing, pp. 177-200.
- [24] Zohaib, A., Jabbar, A., Ahmad, R., Basra, S. M. A. (2018): Comparative productivity and seed nutrition of cotton by plant growth regulation under deficient and adequate boron conditions. – *Planta Daninha* 36: 12-17.

## ALTERATION OF VOLATILE CHEMICAL COMPOSITION IN TOBACCO PLANTS DUE TO GREEN PEACH APHID (*MYZUS PERSICAE* SULZER) (HEMIPTERA: APHIDIDAE) FEEDING

SONG, Y. Z.<sup>1,2,3</sup> – GUO, Y. Q.<sup>1,2</sup> – CAI, P. M.<sup>2,3</sup> – CHEN, W. B.<sup>1,2</sup> – LIU, C. M.<sup>1,2\*</sup>

<sup>1</sup>*Biological Control Research Institute, College of Plant Protection, Fujian Agriculture and Forestry University, Fuzhou 350002, China*

*e-mail: 1023554932@qq.com (Song, Y. Z.); 1220576278@qq.com (Guo, Y. Q.); 447908983@qq.com (Chen, W. B.)*

<sup>2</sup>*State Key Laboratory of Ecological Pest Control for Fujian and Taiwan Crops, Fuzhou 350002, China*

*e-mail: caipumo@qq.com (Cai, P. M.)*

<sup>3</sup>*Department of Horticulture, College of Tea and Food Science, Wuyi University, Wuyishan 354300, China*

*\*Corresponding author*

*e-mail: cmliu@fjau.edu.cn; phone: +86-0591-8378-9420; fax: +86-0591-8378-9421*

(Received 10<sup>th</sup> Jul 2020; accepted 6<sup>th</sup> Oct 2020)

**Abstract.** In response to insect pest herbivory, plants can generate volatile components that may serve multiple roles as communication signals and defence agents in a multitrophic context. In the present study, the volatile profiles of tobacco plants *Nicotiana tabacum* L., with and without infestation by sap-sucking aphids *Myzus persicae* Sulzer, were measured by gas chromatography-mass spectrometry (GC-MS). The results revealed that a total of 10 compounds were identified from healthy tobacco plants, and a total of 14 and 16 compounds were isolated from aphid-infested tobacco plants at 24 and 48 hours after infestation, respectively. Compared to intact tobacco plants, tridecane, 1h-3a,7-methanoazulene, tetradecane, pentadecane, hentriacontane, nonane, 1,8-nonadien-3-ol, heneicosane, sulfurous acid, limonene, cedrene and dichloro acetaldehyde were newly produced in aphid-infested tobacco plants, followed by five special components that only emitted from tobacco plants at 48 hours after aphid-infestation, and were similar to aliphatic compounds. However, the abundance of aromatic compounds in infested tobacco plants was significantly reduced compared to intact plants. The science of HIPVs belongs to chemical ecology, which possess a powerful potential for exploiting effective and practical infochemical-based methods to regulate the population of natural enemies, and enhance the resistance of crops in an agricultural production system.

**Keywords:** *plant-insect interactions, aphid, Nicotiana tabacum, indirect defense, GC-MS*

### Introduction

Plants are constantly threatened by diverse abiotic and biotic stresses, in which biotic stress caused by herbivore damage is an important restriction in the yield and quality of crops of economic importance (Erb and Reymond, 2019). Nevertheless, plants have evolved direct and indirect defence mechanisms in response to herbivory via a series of morphological, biochemical and molecular alterations (Sharma et al., 2009; War et al., 2011). Direct defences against herbivorous insects could be physical or chemical, and contain morphological obstruction such as cell wall lignification, trichomes and silica deposition, and the production of toxic chemicals, including phenolics, alkaloids and terpenoids, which play as deterrents, repellents, anti-nutrients and digestion inhibitors (Kessler et al., 2001; Sharma et al., 2009; War et al., 2011; Aljbory and Chen, 2018).

Indirect defences, which are modulated by the emission of volatile components derived from attacked plants, are known as herbivore-induced plant volatiles (HIPVs) (Kessler et al., 2001; Arimura et al., 2009; Aljborg and Chen, 2018), and refers to the recruitment of natural enemies antagonistic to phytophagous insects. Furthermore, this also enhances the host-seeking ability of carnivores, thereby contributing to the better suppression of pests (Kessler et al., 2001; Cai et al., 2020).

Understanding the chemical ecology of the tritrophic interactions of natural enemies, pests and host plants plays an important role in the exploitation of effective and practical integrated pest management tactics, in which the distribution and abundance of natural enemies could be operated by infochemicals (Hilker and Fatouros, 2015). Herbivore-induced plant volatiles are the ‘words’ of a complex language that are not only used to communicate between attacked plants and natural enemies of infesting herbivores, but also informs neighbouring healthy plants of an impending attack, in addition to communicating between different parts of the same plant via intraplant signalling (Heil, 2008; Arimura et al., 2009; Karban, 2011; Aljborg and Chen, 2018; Erb and Reymond, 2019). HIPVs are released not only from the damaged parts of the plant, but also from intact parts, which amplifies the detectability of the chemical signal (Dicke et al., 2009). To date, approximate 2,000 volatile components emitted in response to herbivory have been identified from 900 plant families (War et al., 2011). A certain amount of volatile components is released by plants into the atmosphere from aboveground parts or into the soil from the roots. However, once damaged, the blend of these emitted volatiles would be altered (Kessler et al., 2001; Dicke et al., 2009; Aljborg and Chen, 2018). The plant protection implications for applying HIPVs, as an assistance within the framework of conservation biological control (CBC), are of significant importance (Turlings and Ton, 2006; Cai et al., 2020).

*Myzus persicae* Sulzer (Hemiptera: Aphididae), which is known as green peach aphid, is a cosmopolitan and highly polyphagous aphid species with high agronomical and ecological importance. This is mainly due to its ability of infesting plants distributed at 40 different families, which vector over 100 plant viral pathogens, and results in considerable quality and yield losses of crops (Martin et al., 1997; Blackman and Eastop, 2017; Hong et al., 2019). *Myzus persicae* has evolved its resistance to at least 70 synthetic components, and developed at least seven independent resistance mechanisms to several classes of insecticides, making it extremely difficult to suppress the population of this pest (Silva et al., 2012; Bass et al., 2014). To date, alternative strategies that can effectively control this aphid pest have been insufficient and highly sought after. Furthermore, numerous research groups have focused their attention on the substances of natural origins as pest control agents, which mainly concentrate on plant secondary metabolites that are considered as elementary compounds of natural plant resistance against insect pests (Wróblewska-Kurdyk et al., 2015; Philippi et al., 2015; Phuong et al., 2015; Jackowski et al., 2017).

Herbivory by phytophagous pests can elicit the indirect defence responses of plants, in which volatile components are released. These warn neighbouring plants and recruit natural enemies, such as parasitoids and predators (Hilker and Meiners, 2006; Aljborg and Chen, 2018). However, suppression can also occur (Peñaflor et al., 2011). Plants that can generate HIPVs in response to herbivory possess the metric of protecting themselves early, and before colonized pests can further attack the plant. As a plant with a short life cycle, tobacco *Nicotiana tabacum* L. (Tubiflorae: Solanaceae) would benefit from the indirect defence responses of plants induced by aphid infestation. However, the

qualitative and quantitative variation in the content of allelochemicals emitted from infested tobacco plants remain poorly known. Thus, the present study aims to determine the response of tobacco plants to herbivory by sap-sucking aphids, and specifically determine whether *M. persicae* feeding would induce tobacco plants to alter their headspace volatiles profile.

## Materials and Methods

### *Aphids rearing*

The research was conducted from August to November 2019 at the Institute of Biological Control, Fujian Agriculture and Forestry University (IBC, FAFU), Fuzhou, Fujian, China. The initial colony of *M. persicae* was collected from vegetable fields located at IBC, FAFU. Rearing was maintained on tobacco plants (cultivars K326), within 50-cm<sup>3</sup> mesh cage conditions of 25±1°C, 75±5% relative humidity (RH), and a L:D photoperiod of 14:10 hours. Emerging *M. persicae* adults were transferred to new cages with non-infested tobacco plants at the 4-6 leaf stage every two weeks.

### *Tobacco cultures*

The tobacco (cultivars K326) seeds were supplied by Nanping Tobacco Co. Ltd., Fujian, China, and planted following the protocols described by Wei et al. (2003). The tobacco plants were grown from seed in plastic trays (length × width × height: 30 × 25 × 10 cm) in a growth chamber with a natural lighting under the conditions of 25±1°C and 70±5% relative humidity (RH). The seedlings were individually transferred into a plastic bowl (upper diameter: 9 cm, bottom diameter: 6.5 cm, height: 7 cm) at the two-leaf stage, and deposited in 50-cm<sup>3</sup> insect-proof mesh cages. The tobacco plants were supplied with water, as needed, fertilized every two weeks at a dose of 0.05 g (N:P:K=20:20:20) per plant, and applied for the assays at the stage of four fully grown leaves.

### *Preparation of aphid-infested tobaccos*

At the four-leaf stage, the tobacco plants were infested with 400 third- or fourth-instar aphids at a density of 100 aphids/leaf, and were thereafter encased in individual insect-proof mesh cages after inoculation. Then, the aphids were removed from the tobacco plants at two hours after infestation, and the infested tobaccos were used for volatile collection at 24 and 48 hours after aphid-infestation, respectively. The control plants were similarly enclosed, but no aphids were introduced and maintained until these were used for volatile collection. Three plants were used for each treatment.

### *Volatiles collection*

The collection of feeding-induced volatiles by *M. persicae* on tobacco plants was conducted using the headspace absorption method in a static environment. The whole tobacco plant was deposited in a 30×50 cm<sup>2</sup> polyacetate bag for volatiles collection (Anfora et al., 2009). The charcoal-filtered air from the headspace of the bag was pushed at a rate of 200 mL/min through a sorbent column (50 mg Porapak Type Q, Sigma-Aldrich) connected to an air pump through Teflon tubing. The volatile collections for each treatment were replicated for three times, according to the same protocol. The collected volatiles were eluted from the sorbent column using 500 µL of

hexane (purity >99%, Sigma-Aldrich) as solvent desorption at room temperature. The collections were concentrated to 50  $\mu$ L by slow nitrogen stream, and 0.5  $\mu$ g of nonyl acetate (purity  $\geq$ 99%, Sigma-Aldrich) was added as the internal standard. The extracts were preserved in 2-mL brown vials at  $-20^{\circ}\text{C}$  until utilized for the GC-MS analysis.

### **Chemical analysis**

The specific headspace volatiles that blended within the tobacco plants were identified by gas chromatography-mass spectrometry, and analyzed in a 7890A GC equipped with a 5975C mass selective detector. The splitless mode comprised of the DB-5MS column (Agilent Technologies Inc., Folsom, CA, 60 m  $\times$  0.25 mm inner diameter, 0.25-mm film thickness) programmed to increase from  $50^{\circ}\text{C}$ , which was held for two minutes, up to  $80^{\circ}\text{C}$  at  $1^{\circ}\text{C}/\text{min}$  for one minute, up to  $90^{\circ}\text{C}$  at  $2^{\circ}\text{C}/\text{min}$ , up to  $110^{\circ}\text{C}$  at  $5^{\circ}\text{C}/\text{min}$ , up to  $130^{\circ}\text{C}$  at  $2^{\circ}\text{C}/\text{min}$ , and finally, up to  $200^{\circ}\text{C}$  at  $5^{\circ}\text{C}/\text{min}$  for two minutes, with helium (purity >99.99%) as the carrier gas at a flow rate of 1 mL/min. A 70-eV of electron impact energy was utilized for sample ionization. The putative identification of the volatile compounds was characterized by comparing with synthetic standards, taking into consideration the GC retention parameters, and comparing with the mass spectra through the Wiley 7N (John Wiley, NY) and NIST 11 (Gaithersburg, MD) mass spectral libraries. The quantification of the most abundant components in each extract was conducted by comparing the peak areas with that of the internal standard, according to the protocols mentioned by Faccoli et al. (2011).

### **Data analysis**

The data analysis was conducted using SPSS v.17.0 (SPSS, Inc., Chicago, IL, USA). The effects of the treatment on the percentage of each identified volatile compound was analyzed using Tukey's honestly significant differences (HSD) test for multiple mean comparisons after one-way ANOVA.

### **Results**

As shown in *Table 1*, 10 compounds were identified from healthy tobacco plants and 19 compounds were identified from tobacco plants that suffered from the infestation by *M. persicae*. A total of 14 and 16 compounds were isolated from the aphid-infested tobacco plants at 24 and 48 hours after herbivory, respectively. For 24 and 48 hours, benzene, nonadecane and tetracosane both vanished, when compared to the intact tobacco plants. Compared to the intact tobacco plants, tridecane, 1h-3a,7-methanoazulene, tetradecane, pentadecane, hentriacontane, nonane and 1,8-nonadien-3-ol were newly produced in aphid-infested tobacco plants with 24 hours after infestation. Otherwise, tridecane, 1h-3a,7-methanoazulene, tetradecane, 1,8-nonadien-3-ol, heneicosane, sulfurous acid, limonene, cedrene and dichloro acetaldehyde newly emerged in aphid-infested tobacco plants within 48 hours after infestation. Among these newly generated volatile components, pentadecane, hentriacontane and nonane were only isolated from tobacco plants with aphid infestation for 24 hours. Furthermore, heneicosane, sulfurous acid, limonene, cedrene and dichloro acetaldehyde were the special components only emitted from tobacco plants with the 48-hour aphid-infestation. Among all the identified compounds, the abundance of undecane and 1,8-nonadien-3-ol ascended as the aphid infestation time

increased, while the abundance of 1h-3a,7-methanoazulene peaked at tobacco plants within 24-hours of aphid-infestation, which was significantly higher than that of healthy tobacco plants. No significant differences in the content of other identified compounds were detected in the headspace composition profile between healthy plants and infested plants.

**Table 1.** Mean ( $\pm$  SE) percentage of main volatile components of tobacco plants after infection by *M. persicae* for various durations

ID	Compounds	Hours after infestation			F and P
		0	24	48	
1	(+)- $\alpha$ -Funebrene	4.68 $\pm$ 1.40	8.14 $\pm$ 1.86	5.64 $\pm$ 1.22NS	F <sub>2,6</sub> =1.38, P=0.32
2	Methylene chloride	3.65 $\pm$ 0.70	4.25 $\pm$ 0.79	3.55 $\pm$ 0.49NS	F <sub>2,6</sub> =0.32, P=0.74
3	trans-Decalin	1.54 $\pm$ 1.54	2.80 $\pm$ 1.40	2.08 $\pm$ 2.08NS	F <sub>2,6</sub> =0.14, P=0.87
4	Naphthalene	5.17 $\pm$ 2.74	2.62 $\pm$ 0.74	2.88 $\pm$ 1.72NS	F <sub>2,6</sub> =0.54, P=0.61
5	Undecane	5.23 $\pm$ 0.18b	5.69 $\pm$ 1.04b	10.54 $\pm$ 0.95a	F <sub>2,6</sub> =12.96, P=0.04
6	Dodecane	2.73 $\pm$ 1.16	5.23 $\pm$ 1.38	5.83 $\pm$ 1.15NS	F <sub>2,6</sub> =1.78, P=0.25
7	Octane	1.63 $\pm$ 0.82	2.21 $\pm$ 0.16	1.49 $\pm$ 0.81NS	F <sub>2,6</sub> =0.33, P=0.73
8	Benzene	4.47 $\pm$ 4.47 <sup>NS</sup>	-	-	F <sub>2,6</sub> =1.00, P=0.42
9	Nonadecane	0.35 $\pm$ 0.35 <sup>NS</sup>	-	-	F <sub>2,6</sub> =1.00, P=0.42
10	Tetracosane	0.51 $\pm$ 0.52 <sup>NS</sup>	-	-	F <sub>2,6</sub> =1.00, P=0.42
11	Tridecane	-	2.55 $\pm$ 0.76	3.96 $\pm$ 1.74 <sup>NS</sup>	F <sub>2,6</sub> =3.35, P=0.11
12	1H-3a,7-Methanoazulene	-	3.15 $\pm$ 0.76	1.37 $\pm$ 0.84 <sup>NS</sup>	F <sub>2,6</sub> =5.79, P=0.40
13	Tetradecane	-	1.24 $\pm$ 0.86	1.42 $\pm$ 0.38 <sup>NS</sup>	F <sub>2,6</sub> =2.05, P=0.21
14	1,8-Nonadien-3-ol	-	1.13 $\pm$ 0.32b	3.93 $\pm$ 0.26a	F <sub>2,6</sub> =71.43, P=0.00
15	Pentadecane	-	0.50 $\pm$ 0.50 <sup>NS</sup>	-	F <sub>2,6</sub> =1.00, P=0.42
16	Hentriacontane	-	1.61 $\pm$ 0.80 <sup>NS</sup>	-	F <sub>2,6</sub> =4.00, P=0.08
17	Nonane	-	1.31 $\pm$ 0.93 <sup>NS</sup>	-	F <sub>2,6</sub> =2.00, P=0.22
18	Heneicosane	-	-	0.52 $\pm$ 0.29 <sup>NS</sup>	F <sub>2,6</sub> =3.08, P=0.12
19	Sulfurous acid	-	-	0.71 $\pm$ 0.41 <sup>NS</sup>	F <sub>2,6</sub> =2.96, P=0.13
20	Limonene	-	-	1.20 $\pm$ 1.20 <sup>NS</sup>	F <sub>2,6</sub> =1.00, P=0.42
21	Cedrene	-	-	1.08 $\pm$ 1.08 <sup>NS</sup>	F <sub>2,6</sub> =1.00, P=0.42
22	Dichloro acetaldehyde	-	-	0.37 $\pm$ 0.37 <sup>NS</sup>	F <sub>2,6</sub> =1.00, P=0.42

Note: “-” refers to non-detectable. NS indicates that there is no significant difference between the three treatments. The different letters indicate the significant differences (Tukey’s HSD test after ANOVA, P<0.05)

As exhibited in *Figures 1 and 2*, the contents of emitted volatiles from tobacco plants were elevated as the aphid-infestation time increased, and the content of isolated volatile compounds from the 48-hour aphid infestation was significantly higher than that in intact tobacco plants ( $F_{2,6}=6.32$ ,  $P=0.03$ ) (*Fig. 1*). Similarly, the abundance of aliphatic compounds also exhibited the same upward trend, and a significant difference was also observed among tobacco plants with different aphid-infestation durations ( $F_{2,6}=11.58$ ,  $P=0.01$ ). Furthermore, the content of aromatic compounds emitted from infested tobacco plants significantly decreased, when compared to intact plants ( $F_{2,6}=10.97$ ,  $P=0.03$ ). This was the same for the content of terpenoids emitted from tobacco plants infested by *M. persicae* for 24 hours, when compared to healthy plants ( $F_{2,6}=11.12$ ,  $P=0.02$ ) (*Fig. 2*).

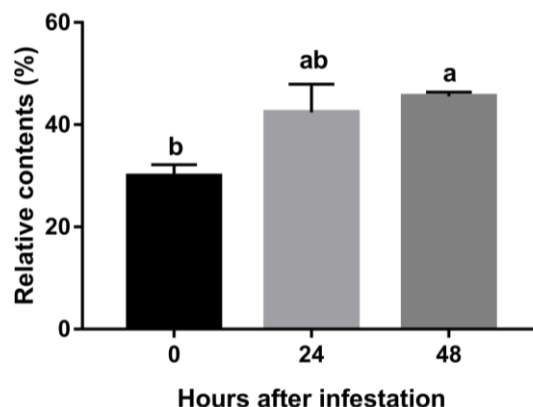


**Figure 1.** The total relative contents of released volatiles from tobacco after aphid-infestation for various durations. The different letters indicate the significant differences (Tukey's HSD test after ANOVA,  $P < 0.05$ )

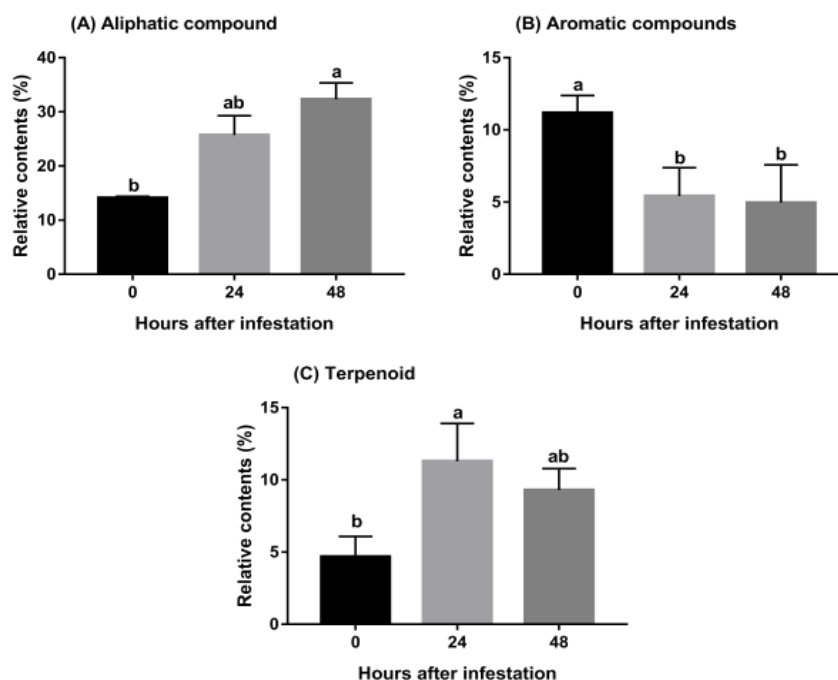


**Figure 2.** The relative contents of the different types of released volatiles from tobacco after aphid-infestation for various duration. The different letters indicate the significant differences (Tukey's HSD test after ANOVA,  $P < 0.05$ )

## Discussion

In the present study, the investigators indicated that tobacco plants bearing the attack by *M. persicae* are activated to generate HIPVs that may have multiple roles as communication signals and defence agents against herbivores. The headspace profiles of plant volatiles between tobacco plants with and without *M. persicae* infestation are qualitatively and quantitatively different, and these were highly consistent with the features of HIPVs that have the high variability and diversity (Lou and Cheng, 2000). It



has been widely accepted that the alterations of volatile release are one of the important and immediate responses of plants to insect herbivory (War et al., 2011; Aljbery and Chen, 2018; Erb and Reymond, 2019). The “chemical fingerprint” spectrum released by plants mediates the behaviors of insects, and the chemical volatile spectrum generally consists of numerous chemical components with different dosages (De Moraes et al., 1998; Runyon et al., 2020). For example, Takemoto and Takabayashi (2015) concluded that *Aphidius ervi* Haliday (Hymenoptera: Braconidae) are more attracted to the blend of plant volatiles induced by the host, when compared to each of the pure compounds. Thus, these distinct volatile compounds may play an important role in tobacco resistance against pests, and the natural enemies of attacking insects, or the surrounding of plants could perceive the qualitative and quantitative alterations of volatile compounds in aphid-infested plants in response to insect herbivore damage. Hence, the ecological function of the key components involved in these insect-plant interactions deserve further investigation.

Tobacco plants bear *M. persicae* feed with the newly produced 12 compounds, including tridecane, 1h-3a,7-methanoazulene, tetradecane, 1,8-nonadien-3-ol, pentadecane, hentriacontane, nonane, heneicosane, sulfurous acid, limonene, cedrene and dichloro acetaldehyde, and the later five volatile compounds were only isolated from tobacco plants at 48 hours after aphid infestation. Furthermore, the volatile compound found in both healthy tobacco plants and tobacco plants with *M. persicae* herbivory, such as the compound of undecane, was much more abundant in plant subjected to pests that have attacked for a long duration. A previous research demonstrated that *Aphidius gifuensis* Ashmead (Hymenoptera: Aphidiidae) is more attracted to the aphid/tobacco complex under Y-tube olfactometer determinations. Furthermore, the attractiveness was enhanced as the infestation levels increased, and this peaked at the aphid density of 400/plant (Yang et al., 2009). Additionally, Wu (2011) reported that 1/10 of the crude extracts of aphid-infested tobacco plants could significantly repel *M. persicae*, but crude extracts diluted to 1/10,000 could elicit a contrasting effect. Therefore, the investigators inferred that these specific chemical components may be more interesting due to the significant implications for plant protection in multitrophic contexts, which have been verified on some tobacco-pest-natural enemy systems, such as Tobacco, *Lasioderma serricornis* Fabricius (Coleoptera: Anobiidae) and *Lariophagus distinguendus* Foerster (Hymenoptera: Pteromalidae) (Lu et al., 2011).

Wu (2011) isolated undecane, dodecane, limonene and cedrene in headspace volatiles from both intact tobacco plants and plants with *M. persicae* infestation, while limonene and cedrene were detected only in tobacco plants with long durations of aphid-infestation, but not in the controls in the present study. Furthermore, undecane and dodecane were both released by infested or healthy tobacco plants. However, for the content of undecane, the delay emission in monoterpenes, such as limonene, have been demonstrated in other plants, such as lima bean leaves (Arimura et al., 2008). Increasing attention has been given to the newly emerged or significantly increased volatile components of plants induced by insect herbivory, which are considered as critical defence agents and communication signals, but are rarely noticed on vanished chemical components. The present study speculates that the neighbouring plants of attacked plants, and the natural enemies or companion of attacking pests may take action by perceiving the absence of a single volatile component or the blend of volatile components. Hence, it is interesting and warranted to research the ecological roles of

vanished volatile components due to insect attacks within the framework of the agricultural system.

In addition, the headspace profiles of tobacco plants with or without pest infestation were partly inconsistent with the previous research conducted by Wu (2011). Many factors, such as the varieties, developmental stage, cultivation methods and cultivation conditions of tobacco plants, volatile collection, GC-MS apparatus and program setting, may attribute to this difference. The headspace profile of tobacco plants is known to differ among varieties. For instance, Zhang et al. (2019) reported that the components and contents of tobacco volatiles from seven varieties were significantly different. Furthermore, a total of 43 volatiles were detected in the cultivars of K326, which were greater than that in the present research. In the research conducted by Wu (2011), the tobacco plants of cultivars Cuibi 2 were used as the research subject, and the water-cultivating method was applied to breed tobacco plants, which were different with that in the present study. Furthermore, the methods of volatile collection and GC-MS analysis, including the GC-MS instrument and the procedure setting in their study, were different from those in the present study. For example, Tenax-Ta was utilized as volatile sorbent in that research, while Porapak Q was used in the present research. A previous study compared the adsorption efficiency of five volatile sorbents toward maize (*Zea mays* L.) leaves, and it was found that different types of sorbents have different affinities for different substances, Porapak Q had better affinity to terpenes, when compared to Tenax-Ta (Zhao et al., 2011). Furthermore, the infestation level of tobacco by aphids in the research conducted by Wu was 50 aphids per tobacco plant, which was significantly lesser than that in the present research (400 aphids per tobacco). Many research studies have indicated that the infestation levels of pests would significantly affect the emission of attacked plants (Lou and Cheng, 2000; Aljbery and Chen, 2018). This may result in qualitative and quantitative differences in the volatile release of attacked plants with different infestation levels.

In the present study, it was also found that the total content of volatiles components emitted from aphid-infested tobacco plants were higher than those from intact plants, which highly agrees with various studies conducted on other plants (Kessler and Baldwin, 2001; Heil, 2008; Arimura et al., 2008, 2009; Dicke et al., 2009). The types of these released components were more abundant than those from intact plants, particularly aliphatic compounds and terpenoids. Wu (2011) reported that the content of aliphatic compounds in tobacco plants, such as olefins and alcohols, significantly increased after being damaged by aphids. Thus, it was speculated that these two kinds of substances are the key components that act as insect repellents or natural enemies of attraction. Combined with the results of the previous study, the investigators deduced that these aliphatic and terpenoid compounds may play an important role in evoking the indirect defence mechanisms of tobacco plants. However, further verifications are needed.

## Conclusion

The present study compared the headspace volatile profiles of tobacco plants, with or without aphid-infestation, at different time intervals by GC-MS. The total contents and types of tobacco volatiles increased after aphid infestation, and several specific components were newly emitted from aphid-infested tobacco plants. Understanding the ecological significance and roles of these specific HIPVs by combining biochemical and

molecular mechanisms would open up a novel channel for further research projects on primary signalling cascades to the ecological consequences in multifarious ecosystems. The identification and characterization of volatile compounds that regulate the olfaction-directed behavior of pests and the natural enemies are needed to set-up tactics for developing cultivars with induced and constitutive resistance to pests. Furthermore, this would also assist in enhancing the effectiveness of natural enemies for pest control via the manipulation of such volatiles, in order to recruit these biological control agents for crop pests.

**Acknowledgements.** We would like to express our deepest gratitude to Nanping Tobacco Co. Ltd., Nanping, Fujian, China for providing the tobacco seeds. We would also like to thank Pro. Weiyi He (Institute of Applied Ecology, College of Plant Protection, Fujian Agriculture and Forestry University) for the technical guidance, and for providing the GC-MS. This research was funded by the Education and Scientific Research Project for Young and Middle-aged Teachers in Fujian Province (JAT190805, JAT190801), the Advanced Talents Introduction Project of Wuyi University (YJ201910), and Science & Technology Innovation Platform Construction Project of Fujian Province (2018N2004).

**Conflict of interests.** The authors declare that they have no conflicts of interests. The funders had no role in the design of the study; in the collection, analyses, or interpretation of data; in the writing of the manuscript, or in the decision to publish the results.

## REFERENCES

- [1] Aljbory, Z., Chen, M. S. (2018): Indirect plant defense against insect herbivores: a review. – *Insect Science* 25(1): 2-23.
- [2] Anfora, G., Tasin, M., Anfora, G., Tasin, M., Cristofaro, A. D., Ioriatti, C., Lucchi, A. (2009): Synthetic grape volatiles attract mated *Lobesia botrana* females in laboratory and field bioassays. – *Journal of Chemical Ecology* 35: 1054-1062.
- [3] Arimura, G., Köpke, S., Kunert, M., Volpe, V., David, A., Brand, P., Dabrowska, P., Maffei, M. E., Boland, W. (2008): Effects of feeding *Spodoptera littoralis* Lima bean leaves: IV. Diurnal and nocturnal damage differentially initiate plant volatile emission. – *Plant Physiology* 146: 965-973.
- [4] Arimura, G., Matsui, K., Takabayashi, J. (2009): Chemical and molecular ecology of herbivore-induced plant volatiles: proximate factors and their ultimate functions. – *Plant and Cell Physiology* 50: 911-923.
- [5] Bass, C., Puinean, A. M., Zimmer, C. T., Denholm, I., Field, L. M., Foster, S. P., Gutbrod, O., Nauen, R., Slater, R., Williamson, M. S. (2014): The evolution of insecticide resistance in the peach potato aphid, *Myzus persicae*. – *Insect Biochemistry and Molecular Biology* 51: 41-51.
- [6] Blackman, R., Eastop, V. F. (2017): Taxonomic issues. – In: van Emden, H. F., Harrington, R. (eds.) *Aphids as Crop Pests*. Wallingford, England: CABI. pp. 1-36.
- [7] Cai, P. M., Song, Y. Z., Huo, D., Lin, J., Zhang, H. M., Zhang, Z. H., Huang, F. M., Xiao, C. M., Ji, Q. E. (2020): Chemical cues mediating behavioral and electrophysiological responses of *Fopius arisanus* (Hymenoptera: Braconidae): the role of herbivore-induced plant volatiles. – *Applied Ecology and Environmental Research* 18(4): 5475-5489.
- [8] De Moraes, C. M., Lewis, W. J., Paré, P. W., Alborn, H. T., Tumlinson, J. H. (1998): Herbivore-infested plants selectively attract parasitoids. – *Nature* 393(6685): 570-573.
- [9] Dicke, M., van Loon, J. J. A., Soler, R. (2009): Chemical complexity of volatiles from plants induced by multiple attack. – *Nature Chemical Biology* 5: 317-324.
- [10] Erb, M., Reymond, P. (2019): Molecular interactions between plants and insect herbivores. – *Annual Review of Plant Biology* 70: 527-557.

- [11] Faccoli, M., Anfora, G., Tasin, M. (2011): Stone pine volatiles and host selection by *Tomicus destruens* (Wollaston) (Coleoptera: Curculionidae, Scolytidae). – *Silva Lusitana* 19: 61-73.
- [12] Frost, C. J., Mescher, M. C., Carlson, J. E., De Moraes, C. M. (2008): Plant defense priming against herbivores: Getting ready for a different battle. – *Plant Physiology* 146: 818-824.
- [13] Gebreziher, H. G. (2018): The role of herbivore-induced plant volatiles (HIPVs) as indirect plant defense mechanism in a diverse plant and herbivore species: A review. – *International Journal of Agriculture and Food Science* 2: 139-147.
- [14] Heil, M. (2008): Indirect defence via tritrophic interactions. – *New Phytologist* 178: 41-61.
- [15] Hilker, M., Meiners, T. (2006): Early herbivore alert: insect eggs induce plant defense. – *Journal of Chemical Ecology* 32: 1379-1397.
- [16] Hilker, M., Fatouros, N. E. (2015): Plant responses to insect egg deposition. – *Annual Review of Entomology* 60(1): 493-515.
- [17] Hong, F., Han, H. L., Pu, P., Dong, W., Wang, J., Liu, Y. H. (2019): Effects of five host plant species on the life history and population growth parameters of *Myzus persicae* (Hemiptera: Aphididae). – *Journal of Insect Science* 19(5): 15.
- [18] Jackowski, J., Popłoński, J., Twardowska, K., Magiera-Dulewicz, J., Hurej, M., Huszcza E. (2017): Deterrent activity of hops flavonoids and their derivatives against stored product pests. – *Bulletin of Entomological Research* 107: 592-597.
- [19] Karban, R. (2011): The ecology and evolution of induced resistance against herbivores. – *Functional Ecology* 25: 339-347.
- [20] Kessler, A., Baldwin, I. T. (2001): Defensive function of herbivore-induced plant volatile emissions in nature. – *Science* 291: 2141-2144.
- [21] Lou, Y. G., Cheng, J. A. (2000): Herbivore-induced plant volatiles: primary characteristics, ecological functions and its release mechanism. – *Acta Ecologica Sinica* 20(6): 1097-1106.
- [22] Lu, Y. J., Wang, Z. Y., Liu, J., Li, Y. Y. (2011): Effects of semiochemicals on the tritrophic interactions among the stored tobacco, *Lasioderma serricornis* (Coleoptera: Anobiidae) and *Lariophagus distinguens* (Hymenoptera: Pteromalidae). – *Proceedings of 2011 International Symposium on Biomedicine and Engineering, Bali Island, Indonesia*, pp. 432-435.
- [23] Martin, B., Collar, L., Tjallingii, W. F., Fereres, A. (1997): Intracellular ingestion and salivation by aphids may cause the acquisition and inoculation of non-persistently transmitted plant viruses. – *Journal of General Virology* 78: 2701-2705.
- [24] Philippi, J., Schliephake, E., Jurgens, H. U., Jansen, G., Ordon, F. (2015): Feeding behavior of aphids on narrow-leafed lupin (*Lupinus angustifolius*) genotypes varying in the content of quinolizidine alkaloids. – *Entomologia Experimentalis et Applicata* 156: 37-51.
- [25] Phuong, T. T. H., Wróblewska-Kurdyk, A., Dancewicz, K., Gabryś, B. (2015): Selective acceptance of *Brassicaceous* plants by the peach potato aphid *Myzus persicae*: a case study of *Aurinia saxatilis*. – *Acta Biologica* 84(6): 51-62.
- [26] Runyon, J. B., Gray, C. A., Jenkins, M. J. (2020): Volatiles of high-elevation five-needle pines: Chemical signatures through ratios and insight into insect and pathogen resistance. – *Journal of Chemical Ecology* 46(3): 264-274.
- [27] Sharma, H. C., Sujana, G., Rao, D. M. (2009): Morphological and chemical components of resistance to pod borer, *Helicoverpa armigera* in wild relatives of pigeon pea. – *Arthropod-Plant Interaction* 3: 151-61.
- [28] Silva, A. X., Jander, G., Samaniego, H., Ramsey, J. S., Figueroa, C. C. (2012): Insecticide resistance mechanisms in the green peach aphid *Myzus persicae* (Hemiptera: Aphididae) I: a transcriptomic survey. – *PLoS One* 7: e36366.

- [29] Takemoto, H., Takabayashi, J. (2015): Parasitic wasps *Aphidius erviare* more attracted to a blend of host-induced plant volatiles than to the independent compounds. – Journal of Chemical Ecology 41: 801-807.
- [30] Turlings, T. C., Ton, J. (2006): Exploiting scents of distress: the prospect of manipulating herbivore-induced plant odours to enhance the control of agricultural pests. – Current Opinion in Plant Biology 9(4): 421-427.
- [31] War, A. R., Sharma, H. C., Paulraj, M. G., War, M. Y., Ignacimuthu, S. (2011): Herbivore induced plant volatiles: their role in plant defense for pest management. – Plant Signaling and Behavior 6(12): 1973-1978.
- [32] Wei, J. N., Li, T. F., Kuang, R. P., Wang, Y., Yin, T. S., Wu, X. F., Zou, L., Zhao, W. Y., Cao, J., Deng, J. H. (2003): Mass rearing of *Aphidius gifuensis* (Hymenoptera: Aphidiidae) for biological control of *Myzus persicae* (Homoptera: Aphidiidae). – Biocontrol Science and Technology 13: 87-97.
- [33] Wróblewska-Kurdyk, A., Nowak, L., Danciewicz, K., Szumny, A., Gabryś, B. (2015): In search of biopesticides: the effect of caraway *Carum carvi* essential oil and its major constituents on peach potato aphid *Myzus persicae* probing behavior. – Acta Biologica 22: 51-62.
- [34] Wu, P. (2011): Tobacco volatiles induced by *Myzus persicae* (Sulzer) infestation and their resistance to the aphid. – Master's thesis, Fujian Agriculture and Forestry University, Fuzhou, China.
- [35] Yang, S., Xu, R., Yang, S. Y., Kuang, R. P. (2009): Olfactory responses of *Aphidius gifuensis* to odors of host plants and aphid-plant complexes. – Insect Science 16(6): 503-510.
- [36] Zhang, S. Q., He, J., He, W. J., Zhang, J. H., Zhou, F., Duan, D. W., Yang, T. Z. (2019): Comparative analysis of volatiles in different types of tobacco leaves. – Chinese Agricultural Science Bulletin 35(33): 52-57.
- [37] Zhao, Z. J., Liu, T. X., Wang, X. P., Li, C. H. (2011): Adsorption efficiency of different adsorbents on volatiles of maize leaves. – Journal of Agricultural Science and Technology 13(2): 82-87.

## CHANGES IN FRESHWATER ECOSYSTEM SERVICES FROM 1960 TO 2017 UNDER CLIMATE CHANGE IN GUIZHOU, CHINA

HAN, H. Q.<sup>1\*</sup> – YANG, G. B.<sup>2</sup> – ZHANG, Y. J.<sup>1</sup>

<sup>1</sup>*School of Architecture and Urban Planning, Guizhou Institute of Technology, Guiyang 550003, PR China*  
(e-mail: cgp1963@126.com – Y. J. Zhang)

<sup>2</sup>*School of Geographical and Environmental Sciences, Guizhou Normal University, Guiyang 550025, PR China*  
(e-mail: 290857583@qq.com – G. B. Yang)

*\*Corresponding author*

*e-mail: hhuiqing2006@126.com; phone/fax: +86-137-6581-2715*

(Received 17<sup>th</sup> Jul 2020; accepted 7<sup>th</sup> Oct 2020)

**Abstract.** The supply capacity of freshwater ecosystem services (FES) is affected by climate change as a result of global temperature rising. However, previous studies have rarely focused on the interannual, seasonal, and periodic change characteristics of FES. We analyzed the effects of climate change on FES from 1960 to 2017 in the Guizhou Province in China. The water yield and soil retention in Guizhou at an annual scale exhibited a decreasing trend between 1960 and 2017, whereas the annual nutrient retention exhibited an increasing trend. The change trends of the three FES in spring and autumn were significantly different from the change trends in summer and winter. The change rate of the nutrient retention in all four seasons from 1960 to 2017 was opposite of that of the water yield and soil retention. The peak period of the water yield, soil retention, and nutrient retention at the annual scale occurred at 28a (i.e. 28 year), whereas differences were observed for the peak period of the three FES at the seasonal scale. The results of this study benefit the scientific management of the FES and contribute to reducing the negative effects of global climate warming.

**Keywords:** *ecosystem service change, climate impact, spatial pattern, change period, InVEST model, Guizhou*

### Introduction

Ecosystems are the basis for human survival and socioeconomic development and are critical support systems for all life on earth (Karp et al., 2015; Rau et al., 2018). Ecosystems provide humans with a variety of important services (e.g., biodiversity, carbon storage, soil retention, recreation, and grain production) that constitute the basis for the sustainable development of human society and economy (Costanza et al., 2014; Lee and Lautenbach, 2016). However, many ecosystem services have deteriorated in the past decades due to changes in the natural environment and increasing intensive human activities (Ma, 2005; Cerretelli et al., 2018). Therefore, research on ecosystem services is a topic of broad and current interest in many countries and regions (Dittrich et al., 2017; Dvarskas, 2018; Qiao et al., 2019).

Previous studies have indicated that natural environmental changes and human activities are important factors affecting ecosystem functions (Su and Fu, 2013; Wang et al., 2016; Mahmoud and Gan, 2018). As one of the key factors, climate change has affected ecosystem services by influencing the climate elements and climate-related factors (e.g., land use change) (Mooney et al., 2009; Gosling, 2013; Grimm et al., 2016). Research on the impacts of climate change on agriculture, freshwater, marine,

and forest ecosystem services has received considerable attention in many countries and regions (Costanza et al., 2011; Rocca et al., 2014; Maia et al., 2018; Huang et al., 2019). Lobell et al. (2011) found that the decline in food production in subtropical semi-arid regions was closely related to the reduction in precipitation. Future climate change will increase the occurrence and frequency of insect damage and thereby reduce the supply level of forest ecosystem services (Trumbore et al., 2015). Plant pollination will decline under the impacts of future climate change (Bartomeus et al., 2011). Furthermore, the loss of ecosystem service value is also a concern of many scholars. For example, Lam et al. (2016) observed that the global fishery income would decline by 35% by 2050 under a high CO<sub>2</sub> emission scenario. However, previous studies have focused more on the analysis of the impact of climate change on ecosystem services for two or more time periods (Lorencová et al., 2013; Fu et al., 2017) and less on the interannual, seasonal, and periodic characteristics of the changes in FES.

Guizhou Province in China is not only an ecologically fragile region but also an area sensitive to global climate change (Zhang et al., 2015). Key FES such as water yield, soil retention, and nutrient retention are provided by abundant natural vegetation in Guizhou (Han and Dong, 2017a; Han et al., 2016). FES are highly sensitive to climate change (Ma, 2005; Bangash et al., 2013; Hoyer and Chang, 2014). Climate change in Guizhou has strongly affected fragile ecosystems, thereby influencing the availability of FES (Han and Dong, 2017b). However, its complex influence on FES in this region remains unclear. Therefore, we analyzed the impacts of climate change on FES from 1960 to 2017 using Guizhou Province as an example. The results provide an understanding of the response mechanism of FES to climate change and scientific reference data for addressing the negative effects of climate change on ecosystem service management.

The following hypotheses are tested in this study: (1) there are differences in the impacts of climate change on different FES; (2) there are annual and seasonal characteristics of FES changes under the impact of climate change; (3) there is a periodicity in the changes in FES resulting from climate change.

## Methodology

### *Study area*

Guizhou Province is located in southwestern China (103°36'-109°35'E, 24°37'-29°13'N) and covers an area of 176 167 km<sup>2</sup> (Fig. 1). The climate is a subtropical humid monsoon climate. The annual average temperature in most parts of Guizhou is approximately 15 °C. The average temperature in January is 3-6 °C and the average temperature in July is 22-25 °C. The annual average precipitation is approximately 1100 mm (Han and Dong, 2017a). The temperature in Guizhou Province tends to show an increasing trend, while the amount of precipitation exhibits a decreasing trend over the past few decades (Ma et al., 2013). The topography is high in the west but low in the east. The main categories of landforms include plateau, mountain, hill and basin, with the mountainous areas accounting for 61.7% of the total across Guizhou Province (Han et al., 2020). The complex and diversified vegetation categories are attributed to the specific geographical conditions and the complications of topography (Han et al., 2019). An ecologically fragile Karst region consisting of carbonate rocks covers 13 × 10<sup>4</sup> km<sup>2</sup> and has the characteristics of low environmental capacity, instability, and low resilience (Zhang et al., 2002).

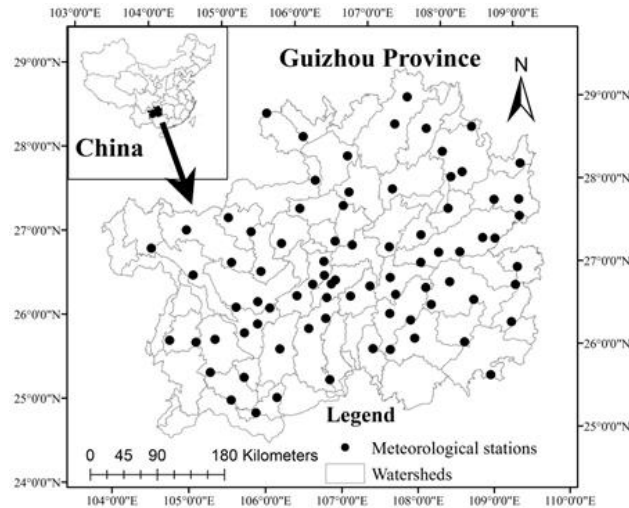


**Figure 1.** Location of study site

### Data source

The daily observation data of 84 meteorological stations from 1960 to 2017 in Guizhou was provided by the climate center of Guizhou. The land use data were obtained by interpreting Landsat ETM<sup>+</sup> remote sensing images from 2015. The soil data were provided by the soil database of China. The 30-m elevation data (ASTER GDEM) were downloaded from the Geospatial Data Cloud in China (<http://www.gscloud.cn>).

### Methods

#### Assessment of FES

We assessed the FES in Guizhou by using the InVEST model, which was developed by Stanford University, the World Wide Fund for Nature, and the Nature Conservancy (Sharp et al., 2014). The parameters we used in the InVEST model were based on the research results of Han and Dong (2017a) and Han et al. (2016). We assume the climate change with no land use change from 1960 to 2017.

#### (1) Water yield

The water yield assessment was based on the Budyko curve (Budyko and Miller, 1974) and precipitation data:

$$Y_{xj} = \left(1 - \frac{AET_{xj}}{P_x}\right) \bullet P_x \quad (\text{Eq.1})$$

$$\frac{AET_{xj}}{P_x} = \frac{1 + \omega_x R_{xj}}{1 + \omega_x R_{xj} + \frac{1}{R_{xj}}} \quad (\text{Eq.2})$$

$$\omega_x = Z \frac{AWC_x}{P_x} \quad (\text{Eq.3})$$



$$R_{xj} = \frac{k_{xj} \cdot ET_o}{P_x} \quad (\text{Eq.4})$$

where  $Y$  is the water yield,  $AET$  is the actual evapotranspiration,  $P$  is the precipitation,  $\omega$  is a non-physical parameter of climate and soil,  $R$  is the Budyko aridity index,  $Z$  is the coefficient used by Zhang,  $AWC$  is the available soil moisture,  $K$  is the vegetation evapotranspiration coefficient; the evapotranspiration was calculated using the FAO56 Penman–Monteith equation (Allen et al., 1998).

## (2) Soil retention

The soil retention was calculated using the Universal Soil Loss Equation (USLE):

$$W = RKLS \cdot USLE \quad (\text{Eq.5})$$

$$USLE = R \cdot K \cdot L \cdot S \cdot C \cdot P \quad (\text{Eq.6})$$

where  $W$  is the amount of soil retention,  $RKLS$  is the maximum soil erosion (assuming there is no vegetation on the ground),  $R$  is the rainfall erosivity, which is calculated using the method of Zhang and Fu (2003),  $K$  is the soil erodibility, which is calculated using the method of Zhou et al. (2005),  $L$  is the slope length,  $S$  is the slope,  $C$  represents the vegetation cover and management factors, and  $P$  is the engineering factor.

## (3) Nutrient retention

The retention of nitrogen and phosphorus represented the nutrient retention in this model (Redhead et al., 2018):

$$WP_i = 1 / ALV_i \quad (\text{Eq.7})$$

$$ALV_i = HSS_i \cdot pol_i \quad (\text{Eq.8})$$

$$HSS_i = \lambda_i / \lambda_w \quad (\text{Eq.9})$$

$$\lambda_i = \log\left(\sum_u Y_u\right) \quad (\text{Eq.10})$$

where  $WP$  is the nutrient retention value,  $ALV$  is the pollution load,  $pol$  is the output coefficient,  $HSS$  is the hydrological sensitivity,  $\lambda_i$  is the runoff coefficient,  $\lambda_w$  is the average runoff coefficient, and  $\sum_u Y_u$  is the water yield.

## Trend analysis

A linear regression analysis was used to determine the change trend of the FES; the slope of the equation represents the rate of change (Wei, 2007):

$$y = at + b \quad (\text{Eq.11})$$

where  $t$  is time,  $a$  is the slope of the regression equation, and  $b$  is the constant of the regression equation. A slope  $> 0$  represents an increasing trend in FES and a slope  $< 0$  represents a decreasing trend. The results are evaluated using the F-criterion.

### Periodicity analysis

A wavelet analysis was used in this study to determine the periodic characteristics of the changes in FES (Torrence and Compo, 1998). This method is a time-scale analysis that detects changes in the signal frequency over time; it has been widely applied for periodicity analyses of hydrological and meteorological change (e.g., precipitation change over time) (Charlier et al., 2015; Yi and Shu, 2012).

$$\psi(t) = e^{ict} e^{-t^2/2} \quad (\text{Eq.12})$$

$$Wf(a,b) = |a|^{-1/2} \int_{-\infty}^{+\infty} f(t)\psi^* \cdot \frac{(t-b)}{a} dt \quad (\text{Eq.13})$$

where  $c$  is a constant,  $i$  is the imaginary part,  $Wf(a,b)$  is the wavelet transform coefficient,  $f(t)$  is the signal analysis function,  $a$  is the amplification factor,  $b$  is the shift factor, and  $\psi^*$  is the conjugate function of the wavelet function.

## Results

### Water yield

The slope of the regression equation for the change in annual water yield change across Guizhou was -0.6242, which indicates a downward trend for annual water yield ( $P < 0.05$ ). The slope of the regression equation for the change to water yield in spring and autumn across the study area was -0.4406 and -0.7781, respectively, suggesting a declining trend of water yield in spring and autumn ( $P < 0.05$ ). The slope of the regression equation for the change to water yield in the summer and winter was 0.4525 and 0.1369, suggesting an increasing trend of water yield in summer and winter ( $P < 0.05$ ) (Fig. 2).

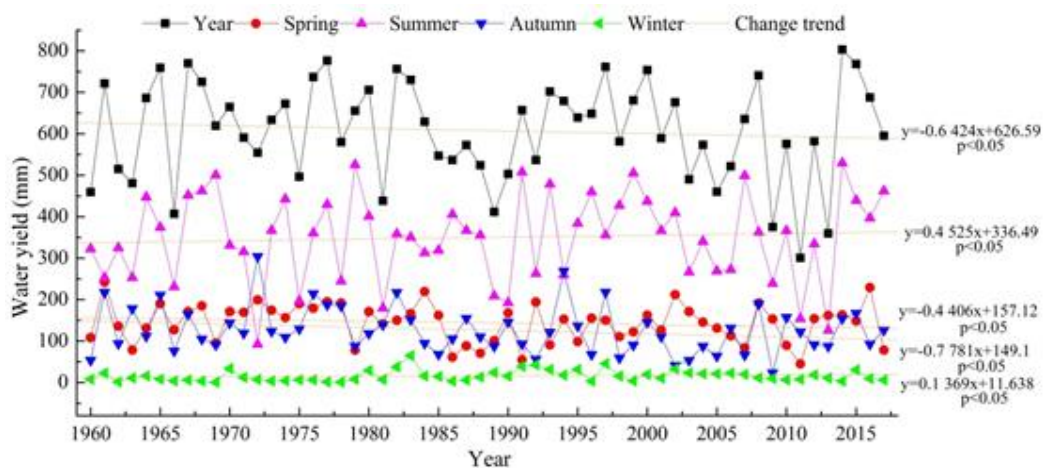
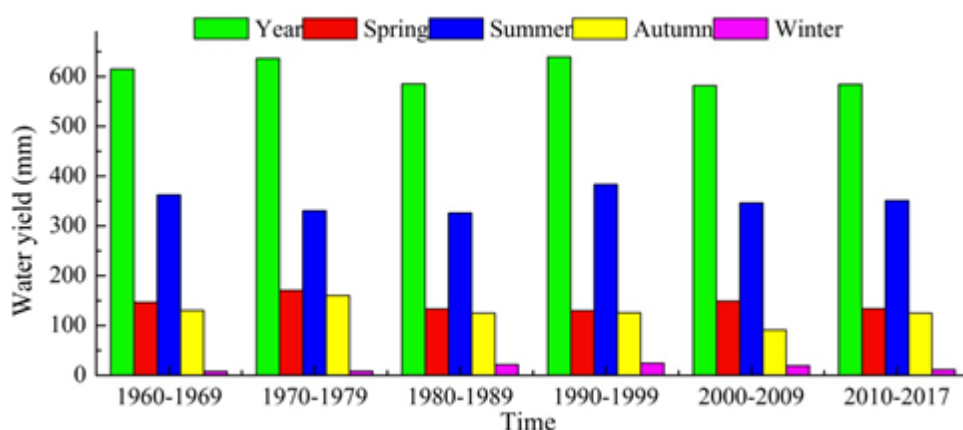


Figure 2. Inter-annual change in the water yield in Guizhou from 1960 to 2017

The amount of annual water yield during the periods of 1970-1979 and 1990-1999 was 636 mm and 639 mm, respectively, higher than in the periods 1980 and 1989, 2000 and 2009, as well as 2010 and 2017 (615 mm, 585 mm, 582 mm and 584 mm). The amount of water yield in spring and autumn (170 mm and 160 mm) during the period from 1970 to 1979 was higher than in other decades. While the amount of water yield in summer during the periods from 1960 to 1969 and from 1990 to 1999 (362 mm and 383 mm) was higher than in other decades. The amount of water yield in winter during such periods as 1980-1989, 1990-1999 and 2000-2009 was 22 mm, 25 mm and 19 mm, respectively, higher than in such periods between 1960 and 1969, 1970 and 1979, as well as 2010 and 2017 (Fig. 3).



**Figure 3.** Changes in the water yield in Guizhou for six decades

The annual water yield decreased in the central, western, and northern parts of Guizhou whereas it increased in the eastern and southeastern parts (Fig. 4e). The water yield in spring and autumn exhibited a decreasing trend in most areas of Guizhou, except for the southeastern part (Fig. 4a, b). The summer and winter water yield exhibited an increasing trend in most areas of Guizhou, except for some regions in the western part (Fig. 4c, d).

Two periodic oscillations were observed in the annual change in water yield in Guizhou from 1960 to 2017; 6a and 28a were the peak years and the highest peak occurred in 28a (Fig. 5e). There were five periodic oscillations in the change in water yield in the spring and 5a, 9a, 13a, 18a, and 29a were the peak years and the latter had the highest peak (Fig. 5a). There were four periodic oscillations in the summer and 4a, 8a, 15a, and 28a (highest peak) were the peak years (Fig. 5b). There were four periodic oscillations in the autumn and 5a, 8a, 17a, and 28a (highest peak) were the peak years (Fig. 5c). There were three periodic oscillations in the winter and 4a, 7a, and 17a (highest peak) were the peak years (Fig. 5d).

### Soil retention

The annual soil retention in Guizhou exhibited an increasing trend during 1960-2017 ( $P < 0.05$ ). The amount of soil retention decreased in spring and autumn and increased in summer and winter ( $P < 0.05$ ). The slope of the regression equation for the change to soil retention in summer (1.394) was higher than in spring, autumn and winter (-0.3683, -0.1828 and 0.1937) ( $P < 0.05$ ) (Fig. 6).

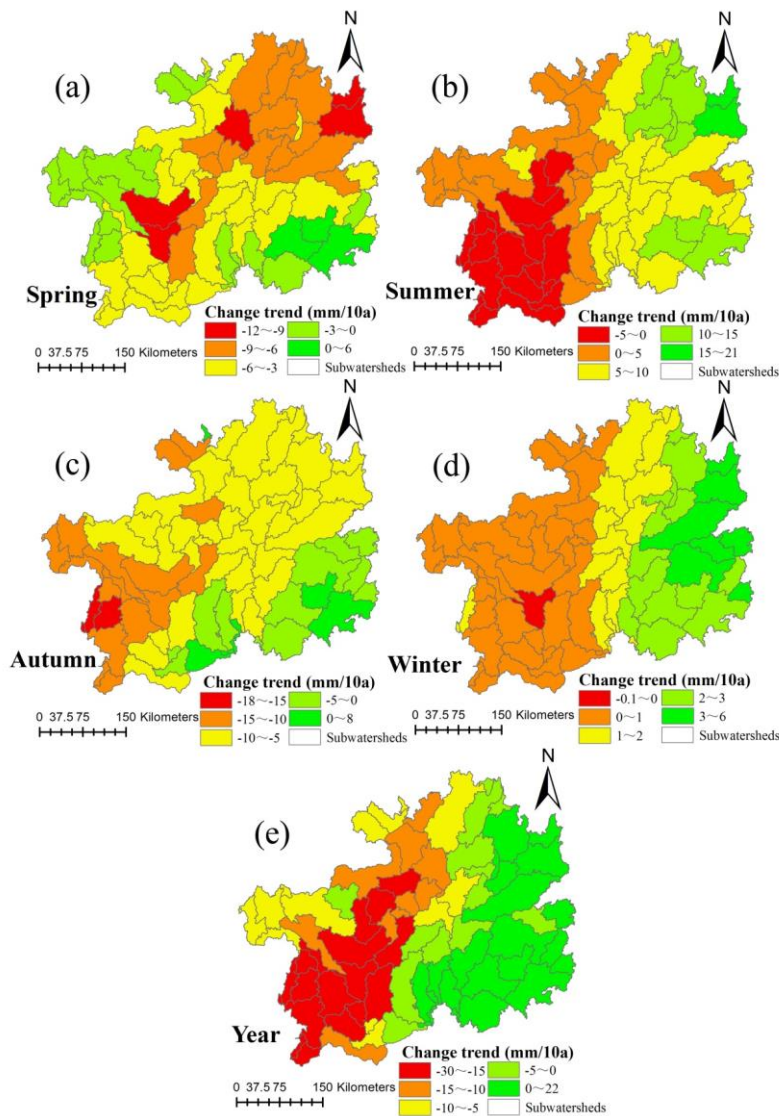


**Figure 4.** Spatial pattern of the changes in the water yield in Guizhou at annual and seasonal scales from 1960 to 2017

The decade of 1990-1999 showed the highest level of annual soil retention (1181 t/ha), while the low levels of soil retention observed during such periods as 1970-1979 and 1980-1989 (1041 t/ha and 1027 t/ha). The levels of soil retention in summer for six decades exceeded 550 t/ha, while those in spring, autumn, and winter for six decades fell below 300 t/ha (Fig. 7).

The annual soil retention exhibited an increasing trend from 1960 to 2017 in most parts of Guizhou, except for the northwestern and southwestern parts (Fig. 8e). Most areas in Guizhou showed decreases in the soil retention in spring and autumn. The areas of increasing soil retention in the spring were located in the northern part of Guizhou, whereas the areas of increasing soil retention in the autumn were located in the eastern and southern parts (Fig. 8a, c). The summer soil retention exhibited an increasing trend in most parts of Guizhou, except for some small regions of the southwestern and northwestern parts of Guizhou (Fig. 8b). The winter soil retention increased in all areas of Guizhou (Fig. 8d).

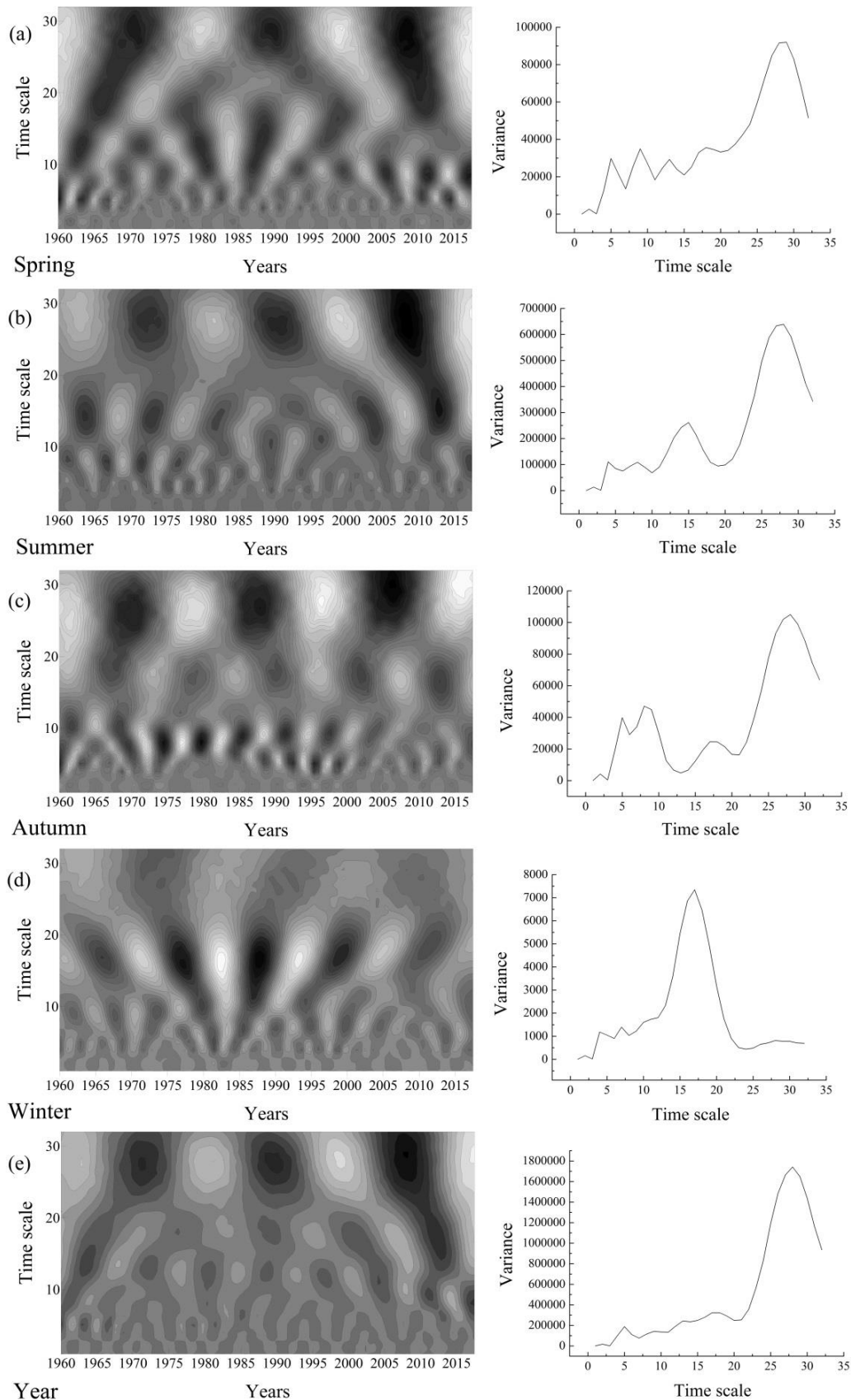


**Figure 5.** Periodicity of the water yield change in Guizhou at annual and seasonal scales from 1960 to 2017



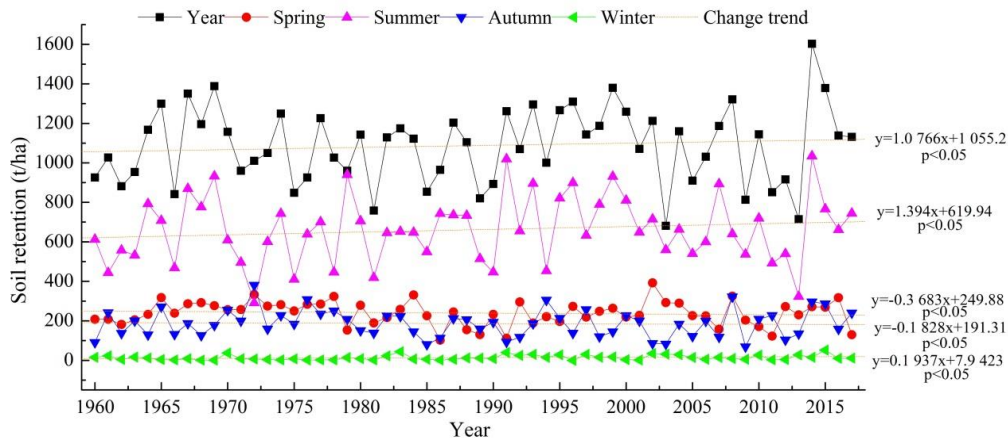


**Figure 6.** Inter-annual change in soil retention in Guizhou from 1960 to 2017

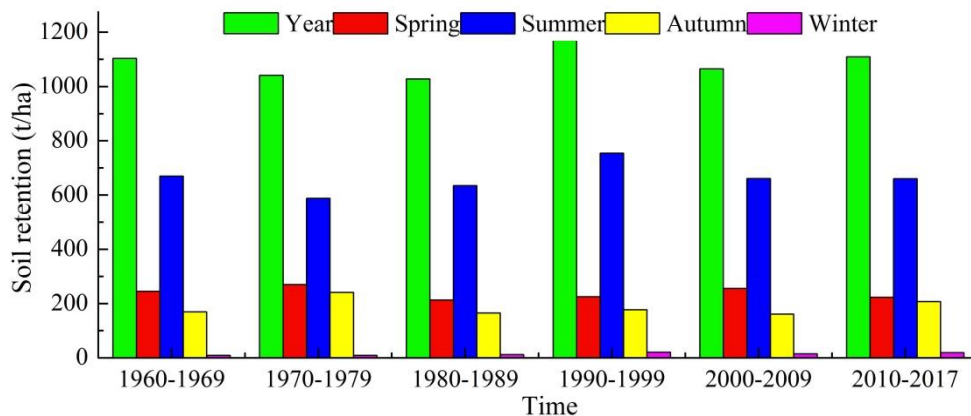


**Figure 7.** Changes in the soil retention in Guizhou for six decades

Three periodic oscillations were observed in the annual soil retention change in Guizhou between 1960 and 2017; the peak years included 7a, 15a, and 28a (highest peak) (Fig. 9e). Four periodic oscillations occurred for the spring soil retention change and the peak years included 4a, 9a, 13a, and 28a (highest peak) (Fig. 9a). Three periodic oscillations were observed for the summer soil retention change and the peak years included 7a, 15a, and 27a (highest peak) (Fig. 9b). There were four periodic oscillations in the autumn and the peak years included 5a, 9a, 17a, and 30a (highest peak) (Fig. 9c). Four periodic oscillations were observed for the winter and the peak years included 4a, 9a, 17a (highest peak), and 28a (Fig. 9d).

### Nutrient retention

The annual nutrient retention in Guizhou exhibited an increasing trend between 1960 and 2017 ( $P < 0.05$ ). The nutrient retention showed an increasing trend in spring and autumn, whereas a decreasing trend was observed for the summer and winter ( $P < 0.05$ ). The slope of the regression equation for the change in nutrient retention was higher in spring (0.0213) than in autumn (0.0042). In contrast, the slope of the regression equation for the change to nutrient retention was greater in summer (-0.0034) than in winter (-0.0018) ( $P < 0.05$ ) (Fig. 10).

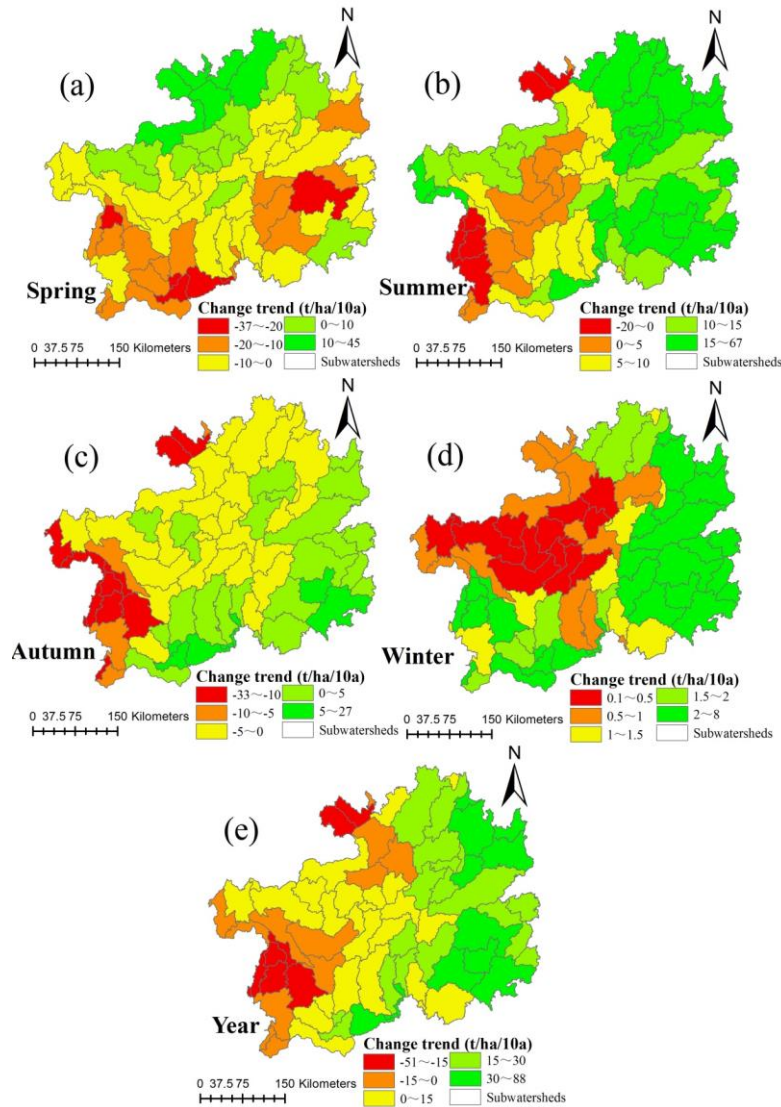


**Figure 8.** Spatial pattern of the changes in the soil retention in Guizhou at annual and seasonal scales from 1960 to 2017

The level of annual nutrient retention for six decades varied from 52.31 to 52.61 kg/km<sup>2</sup>, which is close to that of nutrient retention in summer (52.07-52.33 kg/km<sup>2</sup>), but lower than in spring (53.08-54.38 kg/km<sup>2</sup>) and autumn (52.77-53.57 kg/km<sup>2</sup>). Compared with other seasons, the level of nutrient retention in winter for six decades (42.83-45.85 kg/km<sup>2</sup>) was the lowest (Fig. 11).

Except for the southeastern and northeastern parts of Guizhou, the annual nutrient retention increased in most areas during 1960-2017 (Fig. 12e). An increasing trend in the spring nutrient retention was observed in most areas of Guizhou (Fig. 12a). The summer nutrient retention declined in most areas and only small areas in the northwestern, western, and southeastern parts exhibited an increasing trend (Fig. 12b). The autumn nutrient retention decreased in the western and southern parts, whereas it increased in the central, northern and southwestern parts (Fig. 12c). Except for the southwestern, central, and southeastern parts, the winter nutrient retention increased in most parts of Guizhou (Fig. 12d).

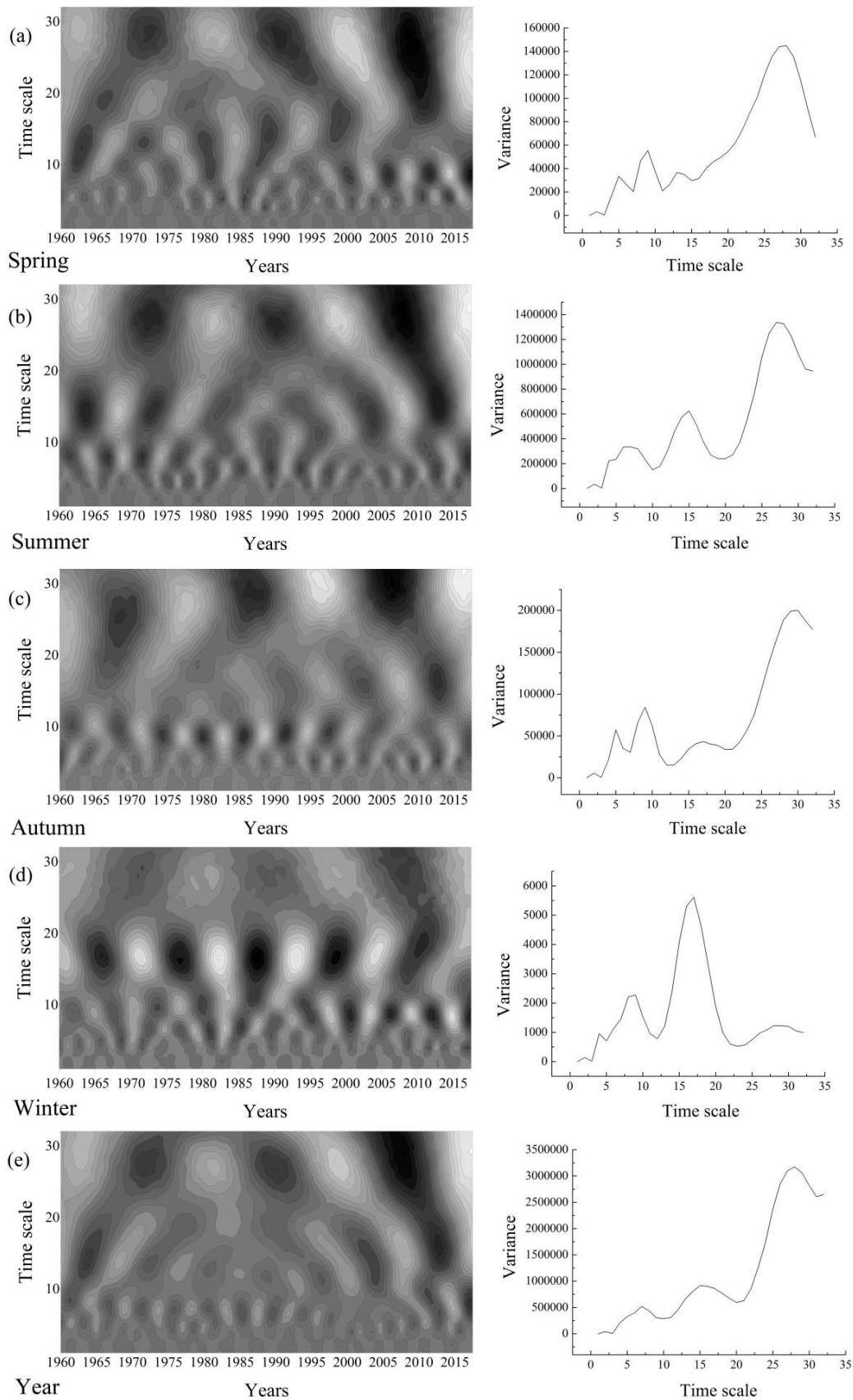


**Figure 9.** Periodicity of the soil retention change in Guizhou at annual and seasonal scales from 1960 to 2017



Only one periodic oscillation was observed in the spring, summer, autumn, and annual nutrient retention changes in Guizhou and the highest peak occurred in 28a (Fig. 13a, b, c, e). There were two periodic oscillations in the winter nutrient retention change in 10a and 28a (highest peak) (Fig. 13d).

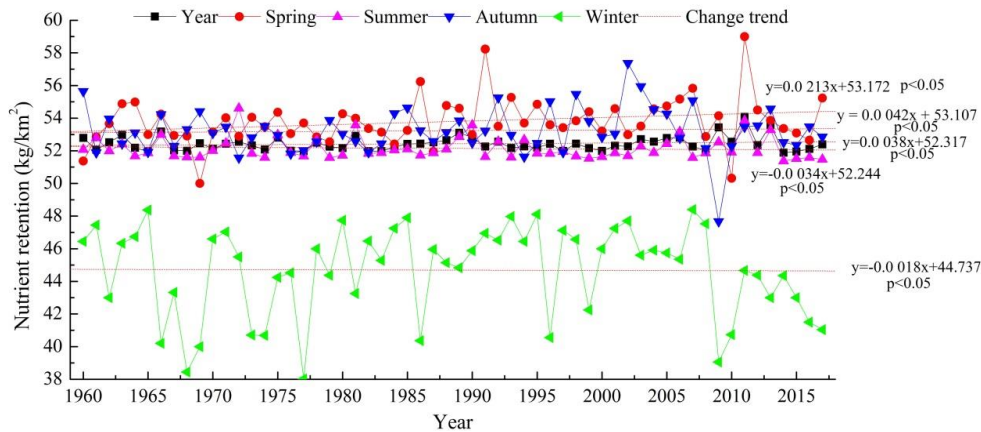


**Figure 10.** Inter-annual change in the nutrient retention in Guizhou from 1960 to 2017

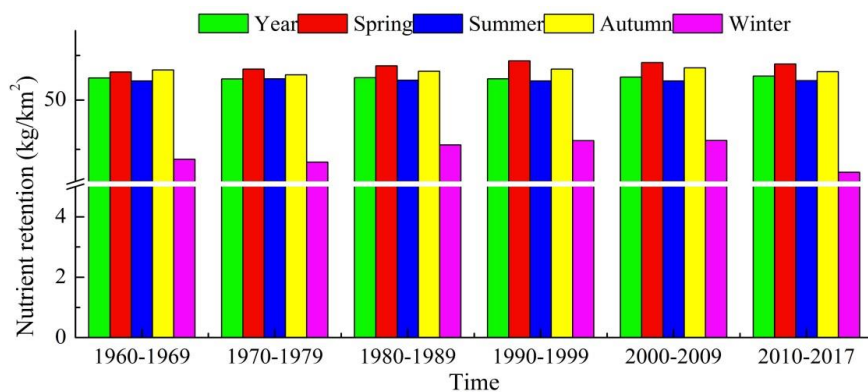


**Figure 11.** Changes in the nutrient retention in Guizhou for six decades

## Discussion

### Impacts of climate change on FES

The significant impact of climate change on FES in Guizhou is demonstrated in the study, as evidenced by the results of Bai et al. (2019) and Bucak et al. (2018). Nevertheless, there are some clear differences in the impact of climate change on different FES. Those similar results have been obtained in the research of Jorda-Capdevila et al. (2019) and Bai et al. (2019). Precipitation and evaporation are important climatic factors influencing changes in the water yield (Terrado et al., 2014; Fan et al., 2018). The decline in the annual, spring, and autumn precipitation in Guizhou was higher than the evaporation from 1960 to 2017, which led to a downward trend of the annual, spring, and autumn water yield. The increases in the winter and summer water yield were closely related to the increases in the winter and summer precipitation between 1960 and 2017 in this region (Table 1). The rainfall erosivity is an essential climatic factor affecting soil retention (Hoyer and Chang, 2014; Sánchez-Canales et al., 2015). The increases in the annual, summer, and winter rainfall erosivity

from 1960 to 2017 in Guizhou resulted in an increasing trend of the soil retention for the same periods. Similarly, the decline in the soil retention in spring and autumn were closely related to the decline in rainfall erosivity in spring and autumn (*Table 1*). In addition, precipitation and evaporation affected the amount of nutrient retention by influencing the surface runoff (Sharp et al., 2014). The increasing trend in the annual, spring, and autumn nutrient retention in Guizhou was related to the decrease in the water yield caused by the larger decrease in precipitation than evaporation from 1960 to 2017. Similarly, the declining trend in nutrient retention in summer and winter was closely related to the increase in the water yield resulting from an increase in precipitation (*Table 1*). In addition, the spatial pattern of FES change was closely associated with the distribution of changes in climatic factor. For example, the amount of precipitation showed decrease in the west but increase in the east over the last few decades in Guizhou (Zhao et al., 2018), which led to a declining trend in the west but an increasing trend in the east for the change to annual water yield. Similarly, the annual rainfall erosivity exhibited an upward trend in most parts of Guizhou except for west Guizhou (Liu et al., 2012), which contributed to spatial pattern of annual soil retention in this study.

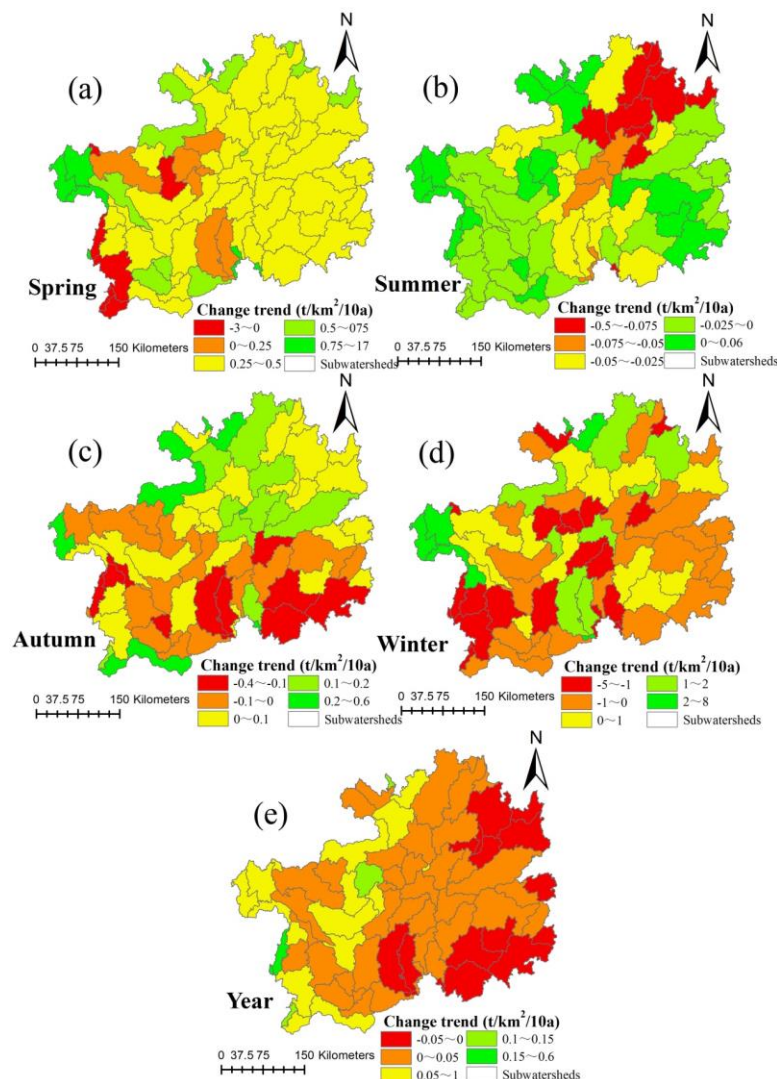


**Figure 12.** Spatial pattern of the changes in the nutrient retention in Guizhou at annual and seasonal scales from 1960 to 2017

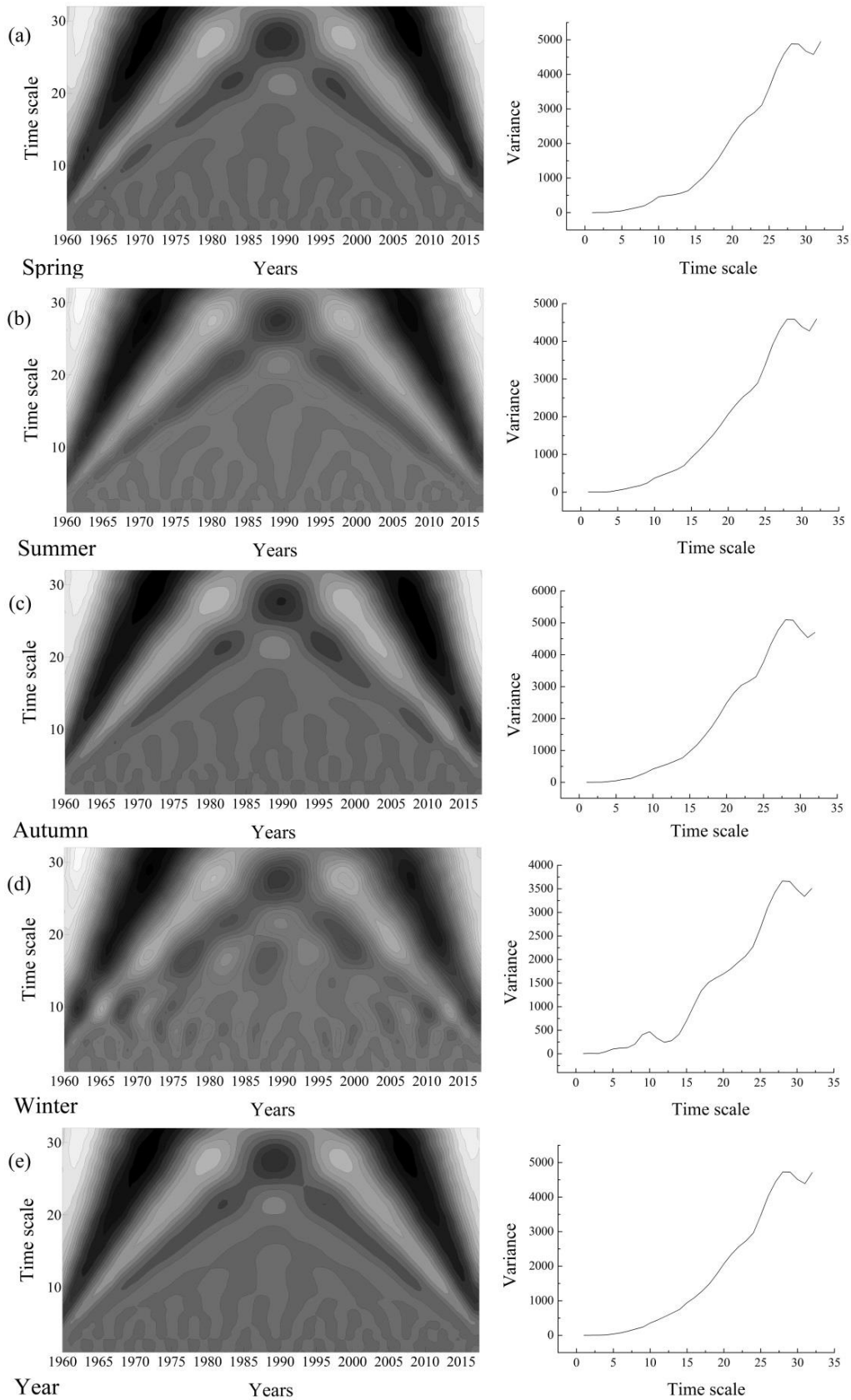


**Figure 13.** Periodicity of the nutrient retention change in Guizhou at annual and seasonal scales from 1960 to 2017

**Table 1.** Changes in climatic factors in Guizhou from 1960 to 2017

Climatic factors	Annual	Spring	Summer	Autumn	Winter
Precipitation (mm/10a)	-7.028	-4.899	2.125	-8.476	4.222
Evaporation (mm/10a)	-1.978	-0.211	-4.422	-0.427	3.102
Rainfall erosivity (MJ mm/ha/h/yr/10a)	61.827	-28.619	85.053	-5.115	11.187

### ***Ecosystem management under the influence of climate change***

The sustainable management of natural and human ecosystems is an important aspect when dealing with the negative impacts of climate change (Gutierrez et al., 2016; Anandhi, 2017). We should reduce the consumption of freshwater and improve the availability of freshwater for agricultural and industrial production, given the decreasing water yield in Guizhou. In addition, different types of water infrastructure should be established to minimize the negative influence of a decline in water yield. Although the annual precipitation in Guizhou exhibited a downward trend from 1960 to 2017, the annual rainfall erosivity exhibited an increasing trend. Thus, the natural vegetation cover (such as forest and grassland) should be improved in the study area to improve the soil retention capacity in the future. Furthermore, terraced fields are recommended for Guizhou because they are suitable for the mountainous area. Moreover, although the nutrient retention caused by the reduction in precipitation exhibited an increasing trend, it will result in decreasing water yield, which requires balancing the relationship between water yield and nutrient retention. The water yield should be increased to avoid a substantial decrease in nutrient retention in the future.

### **Conclusions**

Decreasing trends in the annual, spring, and autumn water yield and soil retention were observed, whereas increasing trends occurred for the water yield and soil retention in summer and winter from 1960 to 2017 in Guizhou. The nutrient retention increased annually and in the spring and autumn, whereas it decreased in summer and winter. The peak period in terms of annual changes in the water yield, soil retention, and nutrient retention in Guizhou occurred in 28a. There were apparent differences in the peak periods of the water yield and soil retention change in spring, summer, and autumn. The peak period of the nutrient retention change in the four seasons was 28a. There was significant spatial heterogeneity in terms of the changes in the water yield, soil retention, and nutrient retention at annual and seasonal scales in Guizhou. The changes to FES in different Karst landforms are supposed to be highlighted in the future research. In this sense, it is necessary for scholars to focus attention on the combined effects of land use and climate changes on the temporal FES changes in the future.

**Acknowledgements.** Project supported by the Joint Fund of the National Natural Science Foundation of China and the Karst Science Research Center of Guizhou province (Grant No. U1812401), the Science and Technology Foundation of Guizhou Province ([2020]1Y152), the Academic Cultivation and Exploration Innovation Project of Guizhou Institute of Technology (No. [2017]5789-23), and the Scientific Research Foundation of the Guizhou Institute of Technology (XJGC20190666). We thank Yue Liu and Siying Chen (Guizhou Institute of Technology) for part of the data analyses in the revised manuscript.

**Conflict of interests.** The authors declare no conflict of interests.

## REFERENCES

- [1] Allen, R. G., Pereira, L. S., Raes, D., Smith, M. (1998): Crop evapotranspiration: guidelines for computing crop water requirements. – FAO irrigation and drainage, Paper 56. Food and Agriculture Organization of the United Nations, Rome.
- [2] Anandhi, A. (2017): CISTA-A: conceptual model using indicators selected by systems thinking for adaptation strategies in a changing climate: case study in agro-ecosystems. – *Ecological Modelling* 345: 41-55.
- [3] Bai, Y., Ochuodho, T. O., Yang, J. (2019): Impact of land use and climate change on water-related ecosystem services in Kentucky, USA. – *Ecological Indicators* 102: 51-64.
- [4] Bangash, R. F., Passuello, A., Sanchez-Canales, M., Terrado, M., López, A., Elorza, F. J., Ziv, G., Acuña, V., Schuhmacher, M. (2013): Ecosystem services in Mediterranean river basin: climate change impact on water provisioning and erosion control. – *Science of the Total Environment* 458: 246-255.
- [5] Bartomeus, I., Ascher, J. S., Wagner, D., Danforth, B. N., Colla, S., Kornbluth, S., Winfree, R. (2011): Climate-associated phenological advances in bee pollinators and bee pollinated plants. – *Proceedings of the National Academy of Sciences of the United States of America* 108: 20645-20649.
- [6] Bucak, T., Trolle, D., Tavşanoğlu, Ü. N., Çakıroğlu, A. İ., Özen, A., Jeppesen, E., Beklioğlu, M. (2018): Modeling the effects of climatic and land use changes on phytoplankton and water quality of the largest Turkish freshwater lake: Lake Beyşehir. – *Science of the Total Environment* 621: 802-816.
- [7] Budyko, M. I., Miller, D. H. (1974): *Climate and life*. – Academic Press, New York.
- [8] Cerretelli, S., Poggio, L., Gimona, A., Takob, G., Boke, S., Habte, M., Coull, M., Peressotti, A., Black, H. (2018): Spatial assessment of land degradation through key ecosystem services: the role of globally available data. – *Science of the Total Environment* 628: 539-555.
- [9] Charlier, J. B., Ladouche, B., Maréchal, J. C. (2015): Identifying the impact of climate and anthropic pressures on karst aquifers using wavelet analysis. – *Journal of Hydrology* 523: 610-623.
- [10] Costanza, R., Bohensky, E., Butler, J. R. A., Bohnet, I., Delisle, A., Fabricius, K., Gooch, M., Kubiszewski, I., Lukacs, G., Pert, P., Wolanski, E. (2011): A scenario analysis of climate change and ecosystem services for the Great Barrier Reef. – *Treatise on Estuarine and Coastal Science* 12: 305-326.
- [11] Costanza, R., de Groot, R., Sutton, P., van der Ploeg, S., Anderson, S. J., Kubiszewski, I., Faerber, S., Turner, R. K. (2014): Changes in the global value of ecosystem services. – *Global Environmental Change* 26: 152-158.
- [12] Dittrich, A., von Wehrden, H., Abson, D. J., Bartkowski, B., Cord, A. F., Fust, P., Hoyer, C., Kambach, S., Meyer, M. A., Radzevičiūtė, R., Nieto-Romero, M., Seppelt, R., Beckmann, M. (2017): Mapping and analysing historical indicators of ecosystem services in Germany. – *Ecological Indicators* 75: 101-110.
- [13] Dvarskas, A. (2018): Mapping ecosystem services supply chains for coastal Long Island communities: implications for resilience planning. – *Ecosystem Services* 30: 14-26.
- [14] Fan, M., Shibata, H., Chen, L. (2018): Spatial conservation of water yield and sediment retention hydrological ecosystem services across Teshio watershed, northernmost of Japan. – *Ecological Complexity* 33: 1-10.
- [15] Fu, Q., Li, B., Hou, Y., Bi, X., Zhang, X. (2017): Effects of land use and climate change on ecosystem services in Central Asia's arid regions: a case study in Altay Prefecture, China. – *Science of the Total Environment* 607: 633-646.
- [16] Gosling, S. N. (2013): The likelihood and potential impact of future change in the large-scale climate-earth system on ecosystem services. – *Environmental Science & Policy* 27: S15-S31.

- [17] Grimm, N. B., Groffman, P., Staudinger, M., Tallis, H. (2016): Climate change impacts on ecosystems and ecosystem services in the United States: process and prospects for sustained assessment. – *Climatic Change* 135: 97-109.
- [18] Gutierrez, D., Akester, M., Naranjo, L. (2016): Productivity and sustainable management of the Humboldt current large marine ecosystem under climate change. – *Environmental Development* 17: 126-144.
- [19] Han, H., Luo, X., You, R., Luo, X., Chen, Y. (2016): Analysis of water purification function in the Pearl river basin in Guizhou province using InVEST model. – *Journal of Nanjing Forestry University (Natural Sciences Edition)* 40: 87-92 (in Chinese).
- [20] Han, H., Dong, Y. (2017a): Assessing and mapping of multiple ecosystem services in Guizhou Province, China. – *Tropical Ecology* 58: 331-346.
- [21] Han, H., Dong, Y. (2017b): Spatio-temporal variation of water supply in Guizhou Province, China. – *Water Policy* 19: 181-195.
- [22] Han, H., Gao, H., Huang, Y., Chen, X., Chen, M., Li, J. (2019): Effects of drought on freshwater ecosystem services in poverty-stricken mountain areas. – *Global Ecology and Conservation* 17: e00537.
- [23] Han, H., Liu, Y., Gao, H., Zhang, Y., Wang, Z., Chen, X. (2020): Tradeoffs and synergies between ecosystem services: a comparison of the karst and non-karst area. – *Journal of Mountain Science* 17: 1221-1234.
- [24] Hoyer, R., Chang, H. (2014): Assessment of freshwater ecosystem services in the Tualatin and Yamhill basins under climate change and urbanization. – *Applied Geography* 53: 402-416.
- [25] Huang, L., Liao, F., Lohse, K., Larson, D. M., Fragkias, M., Lybecker, D., Baxter, C. V. (2019): Land conservation can mitigate freshwater ecosystem services degradation due to climate change in a semi-arid catchment: the case of the Portneuf River catchment, Idaho, USA. – *Science of the Total Environment* 651: 1796-1809.
- [26] Jorda-Capdevila, D., Gampe, D., García, V. H., Ludwig, R., Sabater, S., Vergoñós, L., Acuña, V. (2019): Impact and mitigation of global change on freshwater-related ecosystem services in Southern Europe. – *Science of the Total Environment* 651: 895-908.
- [27] Karp, D. S., Tallis, H., Sachse, R., Halpern, B., Thonicke, K., Cramer, W., Mooney, H., Polasky, S., Tietjen, B., Waha, K., Walz, A., Wolny, S. (2015): National indicators for observing ecosystem service change. – *Global Environmental Change* 35: 12-21.
- [28] Lam, V. W. Y., Cheung, W. W. L., Reygondeau, G., Sumaila, R. (2016): Projected change in global fisheries revenues under climate change. – *Scientific Reports* 6: 32607.
- [29] Lee, H., Lautenbach, S. (2016): A quantitative review of relationships between ecosystem services. – *Ecological Indicators* 66: 340-351.
- [30] Liu, B., Tao, H., Song, C., Guo, B., Shi, Z. (2012): Temporal and spatial variations of rainfall erosivity in southwest China from 1960 to 2009. – *Advances in Earth Science* 27: 499-509 (in Chinese).
- [31] Lobell, D. B., Schlenker, W., Costa-Roberts, J. (2011): Climate trends and global crop production since 1980. – *Science* 333: 616-620.
- [32] Lorencová, E., Frélichová, J., Nelson, E., Vačkář, D. (2013): Past and future impacts of land use and climate change on agricultural ecosystem services in the Czech Republic. – *Land Use Policy* 33: 183-194.
- [33] Ma, Z., Liu, J., Zhang, S., Chen, W., Yang, S. (2013): Observed climate changes in southwest China during 1961-2010. – *Advances in Climate Change Research* 4: 30-40.
- [34] Mahmoud, S. H., Gan, T. Y. (2018): Impact of anthropogenic climate change and human activities on environment and ecosystem services in arid regions. – *Science of the Total Environment* 633: 1329-1344.
- [35] Maia, A. G., Miyamoto, B. C. B., Garcia, J. R. (2018): Climate change and agriculture: do environmental preservation and ecosystem services matter? – *Ecological Economics* 152: 27-39.

- [36] Millennium Ecosystem Assessment (MA) (2005): Ecosystems and human well-being: the assessment series (four volumes and summary). – Island Press, Washington, DC.
- [37] Mooney, H., Larigauderie, A., Cesario, M., Elmquist, T., Hoegh-Guldberg, O., Lavorel, S., Mace, G. M., Palmer, M., Scholes, R., Yahara, T. (2009): Biodiversity, climate change, and ecosystem services. – *Current Opinion in Environmental Sustainability* 1: 46-54.
- [38] Qiao, X., Gu, Y., Zou, C., Xu, D., Wang, L., Ye, X., Yang, Y., Huang, X. (2019): Temporal variation and spatial scale dependency of the trade-offs and synergies among multiple ecosystem services in the Taihu Lake Basin of China. – *Science of the Total Environment* 651: 218-229.
- [39] Rau, A. L., von Wehrden, H., Abson, D. J. (2018): Temporal dynamics of ecosystem services. – *Ecological Economics* 151: 122-130.
- [40] Redhead, J. W., May, L., Oliver, T. H., Hamel, P., Sharp, R., Bullock, J. M. (2018): National scale evaluation of the InVEST nutrient retention model in the United Kingdom. – *Science of the Total Environment* 610: 666-677.
- [41] Rocca, M. E., Brown, P. M., MacDonald, L. H., Carrico, C. M. (2014): Climate change impacts on fire regimes and key ecosystem services in Rocky Mountain forests. – *Forest Ecology and Management* 327: 290-305.
- [42] Sánchez-Canales, M., López-Benito, A., Acuña, V., Ziv, G., Hamel, P., Chaplin-Kramer, R., Elorza, F. J. (2015): Sensitivity analysis of a sediment dynamics model applied in a Mediterranean river basin: global change and management implications. – *Science of the Total Environment* 502: 602-610.
- [43] Sharp, R., Tallis, H. T., Ricketts, T., Guerry, A. D., Wood, S. A., Chaplin-Kramer, R., Nelson, E., Ennaanay, D., Wolny, S., Olwero, N., Vigerstol, K., Pennington, D., Mendoza, G., Aukema, J., Foster, J., Forrest, J., Cameron, D., Arkema, K., Lonsdorf, E., Kennedy, C., Verutes, G., Kim, C. K., Guannel, G., Papenfus, M., Toft, J., Marsik, M., Bernhardt, J., Griffin, R., Glowinski, K., Chaumont, N., Perelman, A., Lacayo, M., Mandle, L., Hamel, P., Vogl, A. L., Rogers, L., Bierbower, W., Denu, D., Douglass, J. (2014): InVEST User's Guide. – The Natural Capital Project, Stanford University, University of Minnesota, the Nature Conservancy, and World Wildlife Fund.
- [44] Su, C., Fu, B. (2013): Evolution of ecosystem services in the Chinese Loess Plateau under climatic and land use changes. – *Global and Planetary Change* 101: 119-128.
- [45] Terrado, M., Acuña, V., Ennaanay, D., Tallis, H., Sabater, S. (2014): Impact of climate extremes on hydrological ecosystem services in a heavily humanized Mediterranean basin. – *Ecological Indicators* 37: 199-209.
- [46] Torrence, C., Compo, G. P. (1998): A practical guide to wavelet analysis. – *Bulletin of the American Meteorological Society* 79: 61-78.
- [47] Trumbore, S., Brando, P., Hartmann, H. (2015): Forest health and global change. – *Science* 349: 814-818.
- [48] Wang, H., Zhou, S., Li, X., Liu, H., Chi, D., Xu, K. (2016): The influence of climate change and human activities on ecosystem service value. – *Ecological Engineering* 87: 224-239.
- [49] Wei, F. (2007): Modern climate statistics diagnosis and prediction. – China Meteorological Press, Beijing (in Chinese).
- [50] Yi, H., Shu, H. (2012): The improvement of the Morlet wavelet for multi-period analysis of climate data. – *Comptes Rendus Geoscience* 344: 483-497.
- [51] Zhang, W. B., Fu, J. S. (2003): Rain erosivity estimation under different rainfall amount. – *Recourses Science* 25: 35-41 (in Chinese).
- [52] Zhang, Y., Zhou, Z., Yan, L. (2015): On climate change characteristics of the typical ecologically vulnerable Karst area in the recent 25 years: a case study area of the central Guizhou Province. – *Journal of Anhui Normal University (Natural Science)* 38: 474-478 (in Chinese).

- [53] Zhao, Z., Luo, Y., Yu, J., Luo, X., Yang, Y. (2018): Analysis of precipitation variation characteristics and barycenter shift in Guizhou Plateau during 1960-2016. – Journal of Geo-information Science 20: 1432-1442 (in Chinese).
- [54] Zhou, W. Z., Liu, G. H., Pan, J. J., Feng, X. F. (2005): Distribution of available soil water capacity in China. – Journal of Geographical Sciences 15: 3-12.

## APPENDIX

### *Meteorological stations in Guizhou*

Meteorological stations	Meteorological stations	Meteorological stations	Meteorological stations	Meteorological stations	Meteorological stations
Hezhang	Yinjiang	Sansui	Tongzi	Zhenyuan	Tianzhu
Weining	Shiqian	Taijiang	Chishui	Yuping	Jinping
Shuicheng	Cenggong	Jianhe	Xishui	Tongren	Qinglong
Puan	Jiangkou	Leishan	Daozhen	Wanshan	Xingren
Panxian	Shibing	Liping	Zhengan	Nayong	Guanling
Wuchuan	Qianxi	Zhenfeng	Dafang	Zhenning	Ziyun
Yanhe	Zhijin	Wangmo	Renhuai	Xiuwen	Baiyun
Dejiang	Anshun	Xingyi	Zunyi	Qingzhen	Huishui
Songtao	Liuzhi	Anlong	Jinsha	Pingba	Longli
Bijie	Puding	Ceheng	Zunyixian	Guiyang	Huaxi
Xifeng	Changshun	Wudang	Meitan	Guiding	Dushan
Kaiyang	Fuquan	Luodian	Fenggang	Kaili	Sandu
Suiyang	Huangping	Pingtang	Wengan	Duyun	Libo
Yuqing	Majiang	Rongjiang	Sinan	Danzhai	Congjiang



## THE RELATIONSHIP BETWEEN THE PHOTOSYNTHETIC PIGMENTS, CAROTENOIDS AND YIELD OF BROOMCORN MILLET (*PANICUM MILIACEUM*; POACEAE)

LI, M.<sup>1</sup> – WANG, Z.<sup>1</sup> – CHEN, L. Q.<sup>1</sup> – WANG, J. J.<sup>1</sup> – LI, H. Y.<sup>1</sup> – HAN, Y. H.<sup>1,2,3</sup> – ZHANG, B.<sup>1,2,3\*</sup>

<sup>1</sup>College of Agricultural, Shanxi Agricultural University, Taigu, Shanxi 030801, People's Republic of China

<sup>2</sup>Institute of Agricultural Bioengineering, Shanxi Agricultural University, Taigu, Shanxi 030801, People's Republic of China

<sup>3</sup>Shanxi Key Laboratory of Resources and Genetic Improvement of Minor Crops, Taigu 030801, People's Republic of China

\*Corresponding author  
e-mail: Abingood@126.com

(Received 24<sup>th</sup> Jul 2020; accepted 22<sup>nd</sup> Oct 2020)

**Abstract.** With advantages, such as high efficiency of water use and drought-resistance, broomcorn millet (*Panicum miliaceum*; Poaceae) will be a potential crop to be developed in the future. Finding methods to achieve high yield and good quality for broomcorn millet is essential to relieve the pressure of growing population and deteriorating environment. Since photosynthetic pigments play important roles in photosynthesis and the blooming stage is a vital stage in determining yield, at this stage, we measured photosynthetic pigment contents of five varieties and analyzed the relationship between photosynthetic pigment contents, photosynthesis and yield. The results showed that photosynthetic pigment contents could influence the photosynthetic efficiency of broomcorn millet and there was a positive relationship between that and crop yield. But there was no direct relationship between that and crop yield, which could make it clear that photosynthetic pigment contents influence the yield by regulating photosynthesis. Besides, healthy and nutritious food has been sought by people. As a kind of healthy food, we analyzed the carotenoid contents in broomcorn millet and explored the relationship between yield and carotenoid contents. We found no significant correlation between qualities and yield, which provide a new idea that we can enhance yield and quality at the same time.

**Keywords:** broomcorn millet, photosynthetic pigment, photosynthesis, kernel traits, carotenoids, beige

### Introduction

Broomcorn millet is one of the oldest cultivated cereal, which has existed for 10000 years (Lu et al., 2009). As an extensively cultivated crop, it has the lowest requirements compared with many major cereals in water availability. Besides, it has other advantages, such as, high efficiency of water use (Diao, 2017; Hou et al., 2017), high drought-resistance, C4 photosynthetic pathway (Pinto et al., 2014; Xue et al., 2019) short growing season, heat resistance and superficial root system (Amadou et al., 2013; Habiyaremye et al., 2017). With the population growing rapidly and the environment deteriorating gradually, there is an augment in food demand (Challinor et al., 2014; Leipe et al., 2019). Confronted with the challenge in food security and environmental pollution, broomcorn millet may arise to be the greatest potential crop in the development of agriculture in the future. In addition, broomcorn millet is of great nutritious and its edible value (Habiyaremye et al., 2017; Azad et al., 2019), medicinal

value and energy value (Zhang et al., 2014; Dong et al., 2019) have also been gradually recognized and exploited.

The continuous decline of cultivated land, the increasing population and climate warming (Princiotta et al., 2014) have attracted people's attention to crop yield for a long time. The yield of crop is influenced by its internal factors and external factors, including genotype, agronomic characters, photosynthesis, water content, temperature and climate. Among those factors, photosynthetic efficiency is an important one, and it has a positive influence on the formation of yield. Then a unique C4 photosynthetic pathway has arisen to be a research hotspot in recent studies. Most studies have shown that C4 plants have a high photosynthetic rate, and the photosynthesis of C4 can improve the water use efficiency of plants. As a C4 plant, broomcorn millet is one of the favorite cereals because of its high drought resistance, high photosynthetic efficiency and high efficiency of water use. In addition, although most studies have been done to explore regulation enzymes in C4 photosynthetic pathway (Wang et al., 2014; Shi et al., 2020), almost no study has been made to explore the photosynthesis by analyzing physiological indices, such as the relationship between photosynthetic efficiency and photosynthetic pigment contents. It is well known that photosynthetic pigments, especially chlorophyll, plays a key role in the photosynthesis, and based on this idea, we intended to learn whether there is a direct relationship between them.

Besides, people have paid more and more attention to the nutrition and health of crops, and thus it is rather important to improve crop quality. Research shows that carotenoids are antioxidants and can prevent various eye and cardiovascular diseases. Broomcorn millet is rich in carotenoids. However, most tests showed that the yield of crop contradicts crop quality. So we intended to analyze whether high yield and high carotenoid contents can coexist in broomcorn millet, and provide a basis for further study of broomcorn millet yield and quality.

## Materials and methods

### *Plant material*

All broomcorn millet varieties, including Jinshu 2 (JS2), Jinshu 5 (JS5), Jinshu 7 (JS7), Nongjiazhong (NJZ) and Yidianhong (YDH), are from Shanxi Province, China. The varieties with good characters and qualities were selected in this study. All broomcorn millet varieties were sown on the 4<sup>th</sup> May, 2017 at the field research station in Shanxi Agricultural University. The area is located at 112°28'N, 37°12'E belonging to temperate continental climate, with an altitude of 803 m, annual rainfall of about 462.9 mm, average annual temperature of 9.9°C and frost-free period of about 176 d. Each variety is planted in a plot with an area of 50 m<sup>2</sup> (5×10). The sowing time of broomcorn millet in spring is generally in the middle and late May. The sowing depth of broomcorn millet is 3 ~ 5 cm. According to the soil moisture content, sowing can be done in advance or later, shallow sowing should be done when the soil moisture content is good, deep sowing should be done when the soil moisture content is poor, and moderate suppression should be done, and attention should be paid to taking advantage of the rain to rob the soil moisture for sowing. Water management: Irrigation was carried out twice in the whole growth period, once in the jointing stage (10th June) and once in the filling stage (20th July). Other cultivation measures are the same as those of general field production management. We made the following experimental design for five varieties of broomcorn millet (*Fig. 1*).

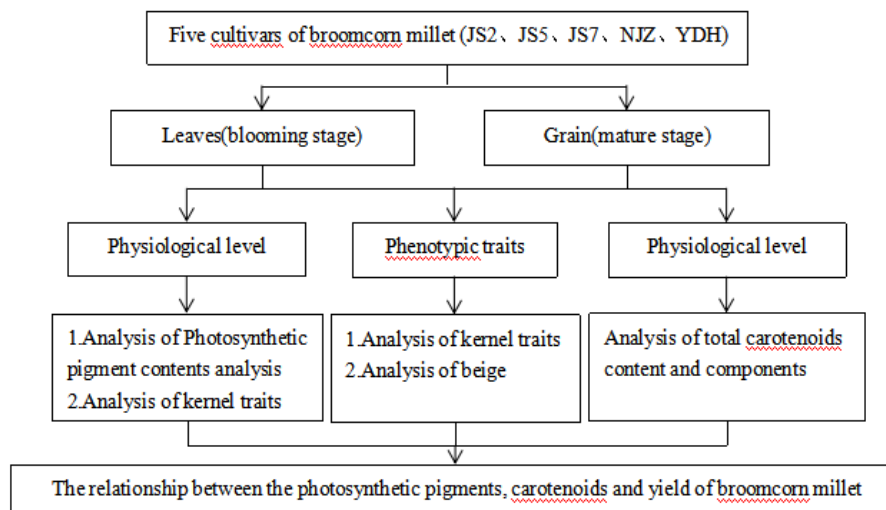


**Figure 1.** Experimental design for five varieties of broomcorn millet

### Photosynthetic pigment contents analysis

The photosynthetic pigment contents of five broomcorn millet varieties were measured at the blooming stage (30<sup>th</sup> July). The reciprocal first leaf of three healthy and consistent plants was selected for each variety, each of which was taken from the middle of the leaf to remove the midvein, and grind it with liquid nitrogen. Every sample (0.2 g for each of the three duplicates for each variety) was transferred to a new 10 mL centrifuge tube and mixed with 10 mL solution of 95% ethyl alcohol, then extracted in an oscillator for 24 h until the tissue faded. Centrifuged and measured. The content of photosynthetic pigments was determined at the wavelength of 470 nm, 665 nm and 649 nm with 95% ethanol as blank (Eqs. 1-4) (Rasool et al., 2020).

$$Chla = \frac{(13.95 \times A_{665} - 6.88 \times A_{649}) \times 0.01}{0.2} \quad (\text{Eq.1})$$

$$Chlb = \frac{(24.96 \times A_{649} - 7.32 \times A_{665}) \times 0.01}{0.2} \quad (\text{Eq.2})$$

$$Caro = \frac{(1000 \times A_{470} - 7.32 \times Chla - 104 \times Chlb) \times 0.01}{0.2 \times 229} \quad (\text{Eq.3})$$

$$Chl = Chla + Chlb \quad (\text{Eq.4})$$

### Analysis of photosynthetic indices

Three plants in the same growth were measured by using the LI-6400 portable photosynthesis analyzer in each variety. Photosynthetic indices and chlorophyll fluorescence kinetic parameters of reciprocal first leaf were analyzed at 8:30 on a sunny morning. Photosynthetic indices include Net Photosynthetic Rate (Photo), Transpiration Rate (Trmmol) and Stomatal Conductance (Cond) (Huang et al., 2016).

### ***Analysis of kernel traits***

Three kernel traits, including spike weight per plant (SWPP), grain weight per plant (GWP) and weight of 1000 grain (KGW), were analyzed with five varieties at the mature stage, and five plants were measured in every variety.

### ***Analysis of total carotenoids***

Millet (0.6 g for each of the three duplicates for each variety) was ground into powder, transferred to a 10 mL centrifuge tube, and mixed with 6 mL water-saturated n-butanol fully. After shaken about 3 h in room temperature, centrifuged at 8000 r/min for 10 min. 0.6 ml supernatant was transferred to a new centrifuge tube to have a high-performance liquid chromatography (HPLC) analysis. The surplus supernatant was to measure by ultraviolet-visible spectrophotometer (MAPADA UV-1200 type), and the extract was measured at 450 nm. The whole experiment was carried out under dark conditions due to the easy decomposition of carotenoids. Total carotenoid content (Eq.5) was calculated according to the formula, in which A represents the absorption value at 450 nm wavelength; V represents the extraction volume (mL); m represents the sample mass (g); and 0.250 represents the conversion coefficient (Dong et al., 2014).

$$\text{Total carotenoid content} = \frac{A}{0.25} \times \frac{V}{m} \quad (\text{Eq.5})$$

### ***Analysis of high-performance liquid chromatography (HPLC)***

By using the chromatographic instrument (Liu et al., 2016), carotenoids were separated by C30 column (250 mm × 4.6 mm, 5 μm, YMC Company, Japan); with mobile phase A, methanol : methyl tert-butyl ether (MTBE) : H<sub>2</sub>O (81:15:4, V/V/V) and mobile phase B, MTBE : methanol (90:10, V/V); with grads elution; at a flow rate of 1 mL/min; monitoring wavelength was 450 nm; injection volume was 20 μL; column temperature was 35 °C. Lutein and zeaxanthin were thoroughly separated with the average retention time of 9 min and 10 min, respectively. X represents the concentration of injection volume (μg/mL), Y represents peak area (mAU·min). The regression equation of lutein and zeaxanthin were obtained by analysis (Sigma company) (Eqs.6-7).

$$\text{Lutein} : Y = 2.2707 X (R^2 = 0.9991) \quad (\text{Eq.6})$$

$$\text{Zeaxanthin} : Y = 2.5785 X (R^2 = 0.99932) \quad (\text{Eq.7})$$

### ***Beige analysis***

After husking the broomcorn millet, the color of millets was determined with a non-contact colorimeter (X-Rite VS450 colorimeter). Through using CIE L\* a\* b\* colorimeter system, determination of index L\*, a\*, b\* and the orange index of CCI was calculated (Eq.8), where L\* denotes the brightness; a\* shows the level of red / green (red), and the positive numbers represent reddish and negative numbers represent greenish color, the greater the absolute is, the darker the color will be. b\* shows yellow / blue degree, and positive numbers express yellow, and negative bias blue, the greater the absolute value is, the darker of color will be. Positive CCI expresses red, a negative value indicates the blue

and green, and 0 presents the mixed color in red, yellow, blue and green (Zhou et al., 2010; Fu et al., 2012). Each species was set up with 3 biological repeats for beige determination.

$$CCI = \frac{1000 \times a^*}{L^* \times b^*} \quad (\text{Eq.8})$$

### Data analysis

All figures and tables were finished by using Excel 2003. One-way analysis of variance (ANOVA), the Duncan's multiple range tests and Pearson correlation tests were used to assess each of the parameters through SPSS statistics software (Version 19, SPSS, Chicago, IL, United States).

## Results

### Photosynthetic pigment contents analysis at the blooming stage

Photosynthetic pigment contents, including Chlorophyll A (Chla), Chlorophyll B (Chlb), Carotenoid (Caro) and total Chlorophyll contents (Total CHL), were analyzed during the blooming stage (30<sup>th</sup> July). Except for obvious aggrandizement in Chlb content in YDH (Fig. 2B), each variety had the same position in different photosynthetic pigment contents, and various photosynthetic pigment contents in JS7 were maximum and JS5 had minimum contents among all measured varieties. Then the analysis of photosynthetic pigment contents exhibited a slight difference in JS2 and NJZ, but no significant difference was found in two varieties (Fig. 2).

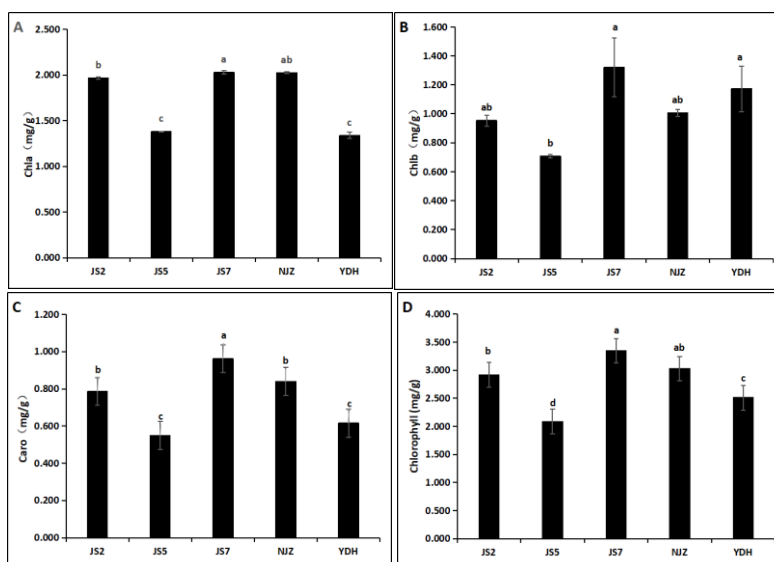


**Figure 2.** Photosynthetic pigment contents analysis with five varieties at the blooming stage. (A) Chlorophyll A (Chla) contents of five varieties. (B) Chlorophyll B (Chlb) contents of five varieties. (C) Carotenoid (Caro) contents of five varieties. (D) Chlorophyll contents of five varieties. Note: The error bars indicate standard error. Different lowercase letters indicate significant difference at  $P < 0.05$

### **Photosynthetic indices analysis of five varieties at the blooming stage**

Photosynthetic indices, including Net Photosynthetic Rate (Photo), Transpiration Rate (Trmmol), and Stomatal Conductance (Cond), were measured. Three plants with the same growth were measured by using the LI-6400 portable photosynthesis analyzer in each variety, respectively. Photosynthetic indices of reciprocal first leaf were analyzed at 8:30 on a sunny morning. The data revealed there were some distinctions in all varieties with three photosynthetic indices. Obviously, JS5 and YDH were different from other varieties, and JS7 had a maximum value in Photo (Fig. 3A-1). Then no marked difference was found between JS2 and YDH in Trmmol (Fig. 3A-3), and they significantly differed from other varieties in Trmmol and Cond (Fig. 3A-2, Fig. 3A-3). However, the data of Cond exhibited an obvious distinction between JS2 and YDH in Cond (Fig. 3A-2).

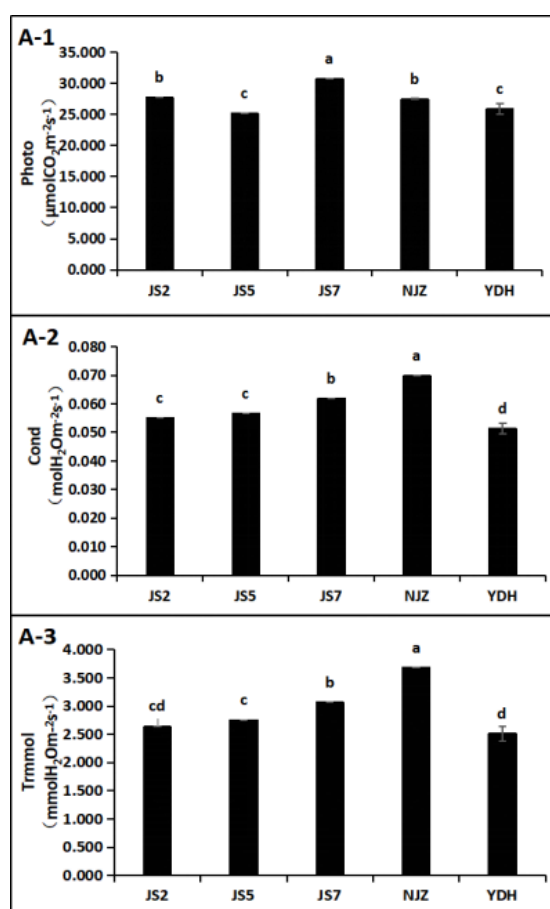


**Figure 3.** Photosynthetic indices analysis of five varieties in the blooming stage. (A-1) Net Photosynthetic Rate (Photo) of five varieties. (A-2) Stomatal Conductance (Cond) of five varieties. (A-3) Transpiration Rate (Trmmol) of five varieties. Note: The error bars indicate standard error. Different lowercase letters indicate significant difference at  $P < 0.05$

### **Correlation analysis between photosynthetic pigment contents and photosynthetic indices at the blooming stage**

Photosynthetic pigments occupied an important position in the photosynthesis of plants, and Chlorophyll played a main role in these pigments. To investigate whether

there was a correlation between photosynthetic pigment contents and photosynthetic indices, a correlation analysis was done (Table 1). Except for Chlb, a significant correlation was detected between photosynthetic pigment contents and Photo. Besides, an obvious correlation was revealed with each other in the photosynthetic pigment contents, but Chla was not markedly correlated with Chlb.

**Table 1.** Correlation analysis between photosynthetic pigment contents and Photo

Pearson	Chla	Chlb	Caro	Photo
Chla	1			
Chlb	0.266	1		
Caro	.881**	.652**	1	
Photo	.794**	0.466	.868**	1

“\*\*” means significant correlation at  $P < 0.01$

### Comparison of three kernel traits with five varieties at the mature stage

Most traits could influence the formation of yield and there was a direct correlation between kernel traits (spike weight per plant, grain weight per plant and weight of 1000 grain) and yield, so kernel traits were important to reflect the yield of crop. Five varieties were investigated in the mature stage and the result revealed that some distinctions were found in three kernel traits with five varieties. Then JS7 had a significantly higher yield than other varieties and YDH had a lower yield than others. Comparing GWP, the KGW of all varieties had a reduction, but YDH was different from them and it showed an obvious increase (Fig. 4).

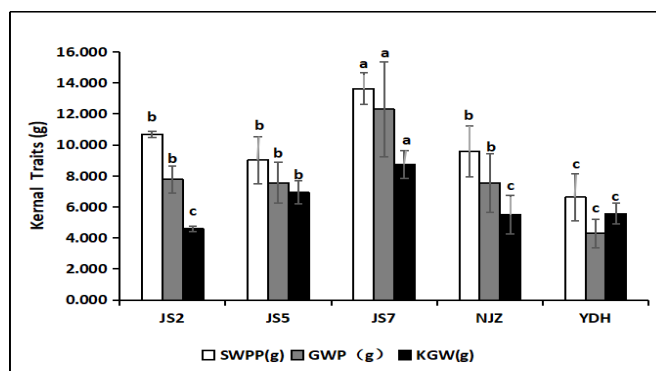


**Figure 4.** Three kernel traits comparison with five varieties in the mature stage. SWPP: spike weight per plant; GWP: grain weight per plant; KGW: weight of 1000 grain. Note: The error bars indicate standard error. Different lowercase letters indicate significant difference at  $P < 0.05$

### Correlation analysis between three kernel traits comparison and photosynthetic indices at the blooming stage

Photosynthesis has been reported to play a crucial role in the formation of yield, so the correlation was analyzed between three kernel traits and photosynthetic indices. The analysis showed there was a marked correlation between Photo and SWPP. Besides, a

very significant correlation was detected between GWP and SWPP, Cond and Trmmol, but no significant correlation was found between GWP and KGW, KGW and SWPP (Table 2).

**Table 2.** Correlation analysis between three kernel traits and photosynthetic indices

Pearson	Photo	Cond	Trmmol	SWPP	GWP	KGW
Photo	1					
Cond	0.416	1				
Trmmol	0.357	.989**	1			
SWPP	.887*	0.436	0.325	1		
GWP	0.843	0.469	0.358	.978**	1	
KGW	0.515	0.215	0.145	0.597	0.74	1

“\*\*” means significant correlation at  $P < 0.01$ ; “\*” means significant correlation at  $P < 0.05$ , the same as below

### **Correlation analysis between three kernel traits comparison and photosynthetic pigment contents in the blooming stage**

By this investigation, we found that photosynthetic pigment contents can directly influence the photosynthesis, and the photosynthesis played a crucial role in the formation of yield. To find out whether photosynthetic pigment directly affects crop yield analysis was done between photosynthetic pigment contents and three kernel traits (Table 3).

**Table 3.** Correlation analysis between three kernel traits comparison and photosynthetic pigment contents

	SWPP	GWP	KGW	Chla	Chlb	Caro
SWPP	1					
GWP	.978**	1				
KGW	0.597	0.74	1			
Chla	0.769	0.667	0.071	1		
Chlb	0.356	0.336	0.368	0.359	1	
CAR	0.821	0.757	0.33	.927*	0.654	1

“\*\*” means significant correlation at  $P < 0.01$ ; “\*” means significant correlation at  $P < 0.05$ , the same as below

### **Extract and analysis of carotenoid and beige in five variety seeds**

Carotenoids have a maximum absorption peak at 450 nm, so total carotenoid contents were measured at 450 nm, and the difference in every component of carotenoid was analyzed. On the whole, lutein and zeaxanthin were major components and the accumulation of lutein was greater than that of zeaxanthin. Some distinctions can be seen in every index among all varieties. JS5 had a maximum accumulation in lutein, zeaxanthin and carotenoid, while JS7 had a minimum accumulation in these components (Table 4).



**Table 4.** Carotenoid content analysis of five variety grains in the mature stage

	TCC (µg/g)	LC (µg/g)	ZC (µg/g)	(LC+ZC)/TCC (%)
JS2	11.720±0.040c	8.522±6.026b	2.552±1.804b	94.484
JS5	16.133±0.589a	12.371±8.747a	3.095±2.188a	95.860
JS7	11.720±0.069c	8.103±5.730b	2.207±1.560b	87.969
NJZ	15.440±0.101a	11.855±8.383a	2.924±2.068a	95.723
YDH	12.880±0.040b	9.339±6.603b	2.492±1.762b	91.850

TCC: Total Carotenoids; LC: Lutein; ZC: Zeaxanthin. Different lowercase letters in the same column indicate significant difference at  $P<0.05$

The color is a vital factor when people purchase crop, so colors of millets were determined with using the non-contact colorimeter (X-Rite VS450 colorimeter). Through analyzing the beige indices, the difference of millet color in all varieties could be seen. Compared with other varieties, the brightness of JS2 and JS7 had a remarkable difference. Then  $a^*$  and  $b^*$  of JS2 were the least bright and significantly differed in all varieties. Except for JS7, the result of CCI showed a slight but not significant distinction in all materials (Table 5).

**Table 5.** Beige of millet analysis of five variety seeds at the mature stage

	$L^*$	$a^*$	$b^*$	CCI
JS2	62.766±0.286b	6.546±0.083c	39.988±0.396d	2.609±0.035b
JS5	66.994±0.149a	7.444±0.148b	42.804±0.572bc	2.596±0.455b
JS7	63.174±0.254b	7.868±0.096a	43.504±0.383ab	2.864±0.043a
NJZ	67.550±0.249a	7.84±0.086a	44.122±0.237a	2.631±0.038b
YDH	67.242±0.303a	7.182±0.136b	42.156±0.452c	2.533±0.035b

Different lowercase letters in the same column indicate significant difference at  $P<0.05$

### Correlation analysis between carotenoid contents and kernel traits

The correlation between carotenoid contents and kernel traits was analyzed (Table 6). An obviously positive correlation could be seen in different carotenoid contents and a negative correlation was found between carotenoid contents and kernel traits, although the correlation was not significant.

**Table 6.** Correlation analysis between carotenoid contents and kernel traits

	SWPP	GWP	KGW	TCC	LC	ZC
SWPP	1					
GWP	.978**	1				
KGW	0.597	0.74	1			
TCC	-0.419	-0.293	-0.052	1		
LC	-0.437	-0.326	-0.124	.997**	1	
ZC	-0.466	-0.399	-0.319	.933*	.956*	1

“\*\*” means significant correlation at  $P<0.01$ ; “\*” means significant correlation at  $P<0.05$

## Discussion

### ***Relationship between photosynthetic pigment contents and photosynthetic indices***

Chlorophyll is a photosynthetic pigment to participate in the absorption, transfer and transformation of light energy (Soares et al., 2020). In addition, it is a significant deciding factor in the efficiency of photosynthesis (Kumar et al., 2020). Through this experiment, we intended to explore whether there was a relationship between photosynthetic indices and photosynthetic pigments. The analysis results about photosynthetic indices and photosynthetic pigment contents showed they were corresponding to each other in every variety and a significant correlation could be detected between photosynthetic indices and photosynthetic pigment contents. That can explain that photosynthetic efficiency will increase with the accumulation of photosynthetic pigment contents. Besides, our result was the same as Soares's result. Their experience showed that photosynthetic pigment contents directly influenced photosynthetic efficiency (Soares et al., 2020). Based on this result, we could enhance crop photosynthesis efficiency by postponing the degradation or wreck in photosynthetic pigments.

### ***Relationship between photosynthesis and yield***

Photosynthesis was one main process to accumulate dry matter, and dry matter served as the basis in the formation of yield (Buesa et al., 2020). So photosynthesis played an important role in the formation of yield. In order to further confirm that photosynthesis was connected with yield, we measured three kernel traits, and analyzed the correlation with each other. The result confirmed the correctness of our guess and that the rising rate of photosynthesis could enhance crop yield. Based on the result, we raised another guess: whether there was a direct relationship between photosynthetic pigment contents and yield. Unexpectedly, the correlation was lower and not remarkable between photosynthetic pigment and yield. The research explained that photosynthetic pigments did not have a direct influence on yield. However, our result was different with Gutierrez et al. (2010) and Hamblin et al. (2014), and they had a contrary conclusion. Gutierrez et al. (2010) found there was a positive relationship between chlorophyll contents with grain yield, while Hamblin et al. (2014) showed that decrease in chlorophyll contents could lead to high yields.

### ***Relationship between quality and yield of broomcorn millet***

In addition to yield, qualities and nutrition of crop have also been extensively concerned. Broomcorn millet has a long history as human food and is one of the important coarse cereals. As an important crop, it is rich in carotenoids, which are good for human health. Carotenoids mainly include zeaxanthin and lutein, and play a fundamental role in human nutrition. Carotenoids can prevent various eye and cardiovascular diseases. Most likely, it can be used as an antioxidant and to regulate the immune system which makes it effective against several types of age-related diseases (Tan and Norhaizan, 2019; Bernstein and Arunkumar, 2020). As important nutrition most studies have been done on maize (Owens et al., 2014; Chang et al., 2015). From previous experience, we found JS7 had a higher yield than other varieties, but it still remains unclear whether there is a positive relationship between yield and carotenoid contents. Millet color is an important factor for people to consume and it is affected by carotenoids. So we compared five varieties in carotenoid contents and the beige of

millet. The results showed that JS7, a high yield variety, had a middle level in the grain beige and had a maximum in CCI, but its zeaxanthin, lutein and total carotenoid content had a minimum value. Then, in order to further analyze the relationship between carotenoid contents and yield, the correlation was detected and the result showed that there was a negative correlation between them, but the negative correlation was not significant. Thus, there was no direct relationship between carotenoid contents and yield, and we may provide a new idea that the yield can be increased by keeping high carotenoid contents, or enhancing carotenoid contents but maintaining the crop high yield.

## Conclusions

In summary, we found photosynthetic pigment contents were related to photosynthetic efficiency, and they had a positive relationship, which could be used in agricultural production. Nevertheless, photosynthetic pigment contents do not directly influence the crop yield, and they may adjust yield via affecting photosynthetic efficiency. Then the analysis in carotenoid contents showed that there was no direct relationship between carotenoid contents and yield, so it was possible to enhance the carotenoid contents and yield at the same time, which provides a new idea, compared with the old thought that high yield is contradictory with good qualities in crop production. Carotenoids were also correlated with the accumulation of some important quality traits, such as starch, reducing sugar and crude protein (Xu et al., 2010), which further proves that it is possible to breed high-yield and high-quality varieties in the breeding practice of high carotene type varieties. Our results need to be further confirmed by molecular biology, crossbreeding, and other methods, which can provide scientific basis and parent materials for breeding of high quality, high yield and high carotene type varieties.

**Acknowledgements.** This work was financially supported by Creation of New Germplasm of Characteristic Crops and Demonstration of Organic Dry Farming Technology (KY202002002), the Scientific and Technological Innovation Breeding Programs of Shanxi Agriculture University (20132-23), and Technology Innovation Fund of Shanxi Agricultural University (2017GPY01).

## REFERENCES

- [1] Amadou, I., Gounga, M. E., Le, G. W. (2013): Millets: Nutritional composition, some health benefits and processing-A review. – Emir. J. Food Agric 25: 501-508.
- [2] Azad, M. O. K., Jeong, D. I., Adnan, M., Salitxay, T., Heo, J. W., Naznin, M. T., Lim, J. D., Cho, D. H., Park, B. J., Park, C. H. (2019): Effect of Different Processing Methods on the Accumulation of the Phenolic Compounds and Antioxidant Profile of Broomcorn Millet (*Panicum miliaceum* L.) Flour. – Foods 8: 230.
- [3] Bernstein, P. S., Arunkumar, R. (2020): The emerging roles of the macular pigment carotenoids throughout the lifespan and in prenatal supplementation. – Journal of lipid research. DOI: 10.1194/jlr.TR120000956.
- [4] Buesa, I., Miras-Avalos, J. M., Intrigliolo, D. S. (2020): Row orientation effects on potted-vines performance and water-use efficiency. – Agric. For. Meteorol. 294: 108148.
- [5] Challinor, A. J., Watson, J., Lobell, D. B., Howden, S. M., Smith, D. R., Chhetri, N. (2014): A meta-analysis of crop yield under climate change and adaptation. – Nat. Clim. Change 4: 287-291.

- [6] Chang, S., Berman, J., Sheng, Y. M., Wang, Y. D., Capell, T., Shi, L., Ni, X. Z., Sandmann, G., Christou, P., Zhu, C. F. (2015): Cloning and functional characterization of the maize (*Zea mays* L.) carotenoid epsilon hydroxylase gene. – PloS One 10: e0128758.
- [7] Diao, X. (2017): Production and genetic improvement of minor cereals in China. – The Crop Journal 5(2): 103-114.
- [8] Dong, Y. M., De, X. S., Yi, Z., Chen, Y. W., Yun, J. Z., Tian, C. G. (2014): Diversity of Antioxidant Content and Its Relationship to Grain Color and Morphological Characteristics in Winter Wheat Grains. – J. Integr. Agric. 13: 1258-1267.
- [9] Farre, G., Bai, C., Twyman, R. M., Capell, T., Christou, P., Zhu, C. F. (2011): Nutritious crops producing multiple carotenoids—a metabolic balancing act. – Trends Plant Sci 16: 532-540.
- [10] Fu, X., Kong, W., Peng, G., Zhou, J. Y., Azam, M., Xu, C. J., Grierson, D., Chen, K. S. (2012): Plastid structure and carotenogenic gene expression in red- and white-fleshed loquat (*Eriobotrya japonica*) fruits. – J. Ex.B 63: 341-354.
- [11] Gutierrez, M., Reynolds, M. P., Raun, W. R., Stone, M. L., Klatt, A. R. (2010): Spectral water indices for assessing yield in elite bread wheat genotypes under well-irrigated, water-stressed, and high-temperature conditions. – Crop Sci 50: 197-214.
- [12] Habiyaremye, C., Matanguihan, J. B., Guedes, J. D., Ganjyal, G. M., Whiteman, M. R., Kidwell, K. K., Murphy, K. M. (2017): Proso Millet (*Panicum miliaceum* L.) and Its Potential for Cultivation in the Pacific Northwest, U. S. - A Review. – Front. Plant Sci. 7: 1961.
- [13] Hamblin, J., Stefanova, K., Angessa, T. T. (2014): Variation in chlorophyll content per unit leaf area in spring wheat and implications for selection in segregating material. – PloS One 9: e92529.
- [14] Hou, S., Sun, Z., Li, Y., Wang, Y., Ling, H., Xing, G., Han, Y. H., Li, H. Y. (2017): Transcriptomic analysis, genic SSR development, and genetic diversity of proso millet (*Panicum miliaceum*; Poaceae). – Applications in Plant Sciences 5(7): 1600137.
- [15] Huang, M. X., Wang, J., Tang, J. Z., Yu, Q., Zhang, J., Xue, Q. Y., Chang, Q., Tan, M. X. (2016): Suitability of four stomatal conductance models in agro-pastoral ecotone in North China: A case study for potato and oil sunflower. – Ying Yong Sheng Tai Xue Bao J. Appl. Ecol. 27: 3585-3592.
- [16] Kumar, D., Singh, H., Raj, S., Soni, V. (2020): Chlorophyll a fluorescence kinetics of mung bean (*Vigna radiata* L.) grown under artificial continuous light. – Biochem. Biophys. Rep. 24: 100813-100813.
- [17] Leipe, C., Long, T., Sergusheva, E. A., Wagner, M., Tarasov, P. E. (2019): Discontinuous spread of millet agriculture in eastern Asia and prehistoric population dynamics. – Science Advances 5(9): eaax6225.
- [18] Liu, M., Zhang, Z., Ren, G., Zhang, Q., Wang, Y., Lu, P. (2016): Evaluation of selenium and carotenoid concentrations of 200 foxtail millet accessions from China and their correlations with agronomic performance. – J. Integr. Agric. 15: 1449-1457.
- [19] Lu, H., Zhang, J., Liu, K. B., Wu, N., Li, Q. (2009): Earliest domestication of common millet (*Panicum miliaceum*) in East Asia extended to 10,000 years ago. – P. Natl. Acad. Sci. USA 106: 7367-7372.
- [20] Owens, B. F., Lipka, A. E., Magallaneslundback, M., Tiede, T., Diepenbrock, C. H., Kandianis, C. B., Kim, E., Cepela, J., Mateos, M., Buell, C. R., Buckler, E. S., Penna, D. D., Gore, M. A., Rocheford, T. (2014): A foundation for provitamin A biofortification of maize: Genome-wide association and genomic prediction models of carotenoid levels. – Genetics 198: 699-716.
- [21] Pinto, H., Sharwood, R. E., Tissue, D. T., Ghannoum, O. (2014): Photosynthesis of C3, C3-C4, and C4 grasses at glacial CO2. – J. Exp. Bot 13: 3669-3681.
- [22] Princiotta, F. T., Loughlin, D. H. (2014): Global climate change: The quantifiable sustainability challenge. – J. Air Waste Manage 64: 979-994.

- [23] Rasool, A., Shah, W. H., Tahir, I., Alharby, H. F., Hakeem, K. R., Rehman, R. (2020): Exogenous application of selenium (Se) mitigates NaCl stress in proso and foxtail millets by improving their growth, physiology and biochemical parameters. – *Acta Physiol. Plant* 42: 116.
- [24] Shi, W., Yue, L., Guo, J. H., Wang, J., Yuan, X., Dong, S., Guo, J., Guo, P. Y. (2020): Identification and evolution of C-4 photosynthetic pathway genes in plants. – *Bmc Plant Biol* 20: 132.
- [25] Soares, C., Pereira, R., Martins, M., Tamagnini, P., Serodio, J., Moutinho-Pereira, J., Cunha, A., Fidalgo, F. (2020): Glyphosate-dependent effects on photosynthesis of *Solanum lycopersicum* L.-An ecophysiological, ultrastructural and molecular approach. – *J. Hazard. Mater* 398: 122871.
- [26] Tan, B. L., Norhaizan, M. E. (2019): Carotenoids: How Effective Are They to Prevent Age-Related Diseases? – *Molecules* 24: 1801.
- [27] Wang, Y., Long, S. P., Zhu, X. (2014): Elements required for an efficient NADP-malic enzyme type C4 photosynthesis. – *Plant Physiol* 164: 2231-2246.
- [28] Xu, J., Hu, Q., Wang, X., Luo, J., Liu, Y., Tian, C. (2010): Changes in the Main Nutrients, Phytochemicals, and Antioxidant Activity in Yellow Corn Grain during Maturation. – *Agric Food Chem* 58: 5751-5756.
- [29] Xue, L., Ma, J. J., Wu, J., Zhao, C., Liu, H., Liu, D., Ma, J. F. (2019): Comprehensive Evaluation on the Tolerance of Eight Crop Species to CO<sub>2</sub> Leakage from Geological Storage. – *Int. J. Agric. Biol.* 22: 561-568.
- [30] Zhang, L., Liu, R., Niu, W. (2014): Phytochemical and antiproliferative activity of proso millet. – *PloS One* 9: e104058.
- [31] Zhou, J. Y., Sun, C. D., Zhang, L. L., Dai, X., Xu, C. J., Chen, K. S. (2010): Preferential accumulation of orange-colored carotenoids in Ponkan (*Citrus reticulata*) fruit peel following postharvest application of ethylene or ethephon. – *Sci. Hortic-Amsterdam* 126: 229-235.

## EFFECTS OF PALM KERNEL BIOCHAR AND FOOD WASTE COMPOST ON THE GROWTH OF PALM LILY (*CORDYLIN FRUTICOSA*), COLEUS (*COLEUS* SP.), AND BOAT LILY (*RHOEO DISCOLOR*)

ABDULLAH, R.<sup>1,2\*</sup> – OSMAN, N.<sup>1</sup> – YUSOFF, S.<sup>3</sup> – MOHD YUSOF, H.<sup>1</sup> – ABDUL HALIM, N. S.<sup>1</sup> – MOHD ROSLI, N. S.<sup>1</sup>

<sup>1</sup>*Institute of Biological Sciences, Faculty of Science, University of Malaya, 50603 Kuala Lumpur, Malaysia*

<sup>2</sup>*Centre for Research in Biotechnology for Agriculture, University of Malaya, 50603 Kuala Lumpur, Malaysia*

<sup>3</sup>*Institute of Ocean and Earth Sciences, University of Malaya, 50603 Kuala Lumpur, Malaysia*

*\*Corresponding author*

*e-mail: rosazlin@um.edu.my; phone: +60-379-674-360; fax: +60-379-674-178*

(Received 24<sup>th</sup> Jul 2020; accepted 19<sup>th</sup> Nov 2020)

**Abstract.** In recent years, soil amendments have been widely used in agriculture to improve the soil quality, plant production and quality, and reduce the fertilizer usage. Thus, current study was carried out to investigate the effects of palm kernel biochar and food waste compost on soil properties, plant growth performance and physiological responses of *Cordyline fruticosa*, *Coleus* sp., and *Rhoeo discolor*. These plants were arranged in a randomized complete block design (RCBD) with eight treatments; control (T1), fertilizer (T2), food waste compost (T3), compost + < 20% of fertilizers (T4), biochar (T5), biochar + < 20% of fertilizers (T6), biochar + compost (T7), biochar + compost + < 20% of fertilizers (T8), with four replicates. The application of food waste compost and biochar in *Coleus* sp. showed the best performance concerning plant growth including the plant height (65.75 cm), the number of leaves (59), chlorophyll contents (29.70  $\mu\text{mol}/\text{m}^2$ ), photosynthetic rate (23.53  $\mu\text{mol CO}_2 \text{ s}^{-1}$ ), stomatal conductance (0.009  $\text{mmol m}^{-2} \text{ s}^{-1}$ ), transpiration rate (0.269  $\text{mmol m}^{-2} \text{ s}^{-1}$ ), water use efficiency (WUE) (88) and total biomass (62.50 g). It can be concluded that the addition of compost and biochar as a soil amendment can improve soil fertility and plant growth performance.

**Keywords:** *soil amendment, landscape plant, reduce, fertilizer, nursery*

### Introduction

Soil amendment is an addition of material to the soil which helps improve physical and chemical properties such as increasing soil aggregate stability, improve soil pH, nutrient content in soil and improve aeration and drainage in soil (Shainberg et al., 1990). In recent years, soil amendments have been widely used in agriculture development to improve the soil quality, increase crop yield and plant growth performance (Chan et al., 2008). The use of agricultural wastes as soil amendments also has received attention in recent years for agronomic application (McGeehan, 2012). Biochar and compost are organic agricultural waste that undergo a transformation that facilitates their use as soil amendments. These soil amendments provide benefits most people especially farmers where the application enable them to reduce the fertilizer usage which is harmful to the environment.

Biochar technology are a technology to boost agricultural production and at the same time helps to preserve the environment (Montanarella and Lugato, 2013). Biochar is a

charcoals that contain high carbon (C) which is more than 50% produced through pyrolysis process either with little or without oxygen (Nartey and Zhao, 2014), and it can last for a long period of time up to millions years. Biochar is similar to charcoal in terms of its shape and its black colour. Besides, biochar potentially reduces emissions compared to other biomass that will naturally lower the greenhouse gases and also have sufficient carbon absorption value (Woolf et al., 2010). The increase amount of biochar used in soil will raise the availability of major cation and phosphorus, total nitrogen and cation exchange capacity (CEC) (Lehmann et al., 2003) which ultimately will increase yield and plant growth performance. High nutrient availability for plants is a result of increased nutrition from biochar, increased nutrient retention, and changes in soil microbial dynamics (Ding et al., 2016) (Tian et al., 2016). Its long-term benefits to nutrient availability are associated with higher organic carbon stabilization along with slower nutrient release in biochar compared to commonly used organic materials (Sharma et al., 2017). The role of biochar on plant productivity improvement is influenced by the amount of biochar added as soil amendment.

In addition, compost is a nitrogen-rich organic fertilizer resulting from the decay of plant waste, food waste, and livestock faces. Matured compost can be used for soil treatment purposes, improving nutrient content in soil and planting on a small or large scale. The period of the materials to become compost is dependent on the materials used, the content of microorganisms and temperature. Food waste is widely used as a compost material because it contains high organic matter content and low heavy metals. Food waste has a wide ability for bioconversion to alternative fertilizers (Chang and Chen, 2010). This conversion requires the implementation of new technologies to recycle waste in the form of compost for use in agriculture. The addition of food waste compost to the soil has increased the bacteria in the rhizosphere and found that this compost is composed of high carbohydrates such as fruits and vegetables and it is easy to use as a carbon source and energy by microorganisms (Lee et al., 2004). Food waste compost helps increase the nutrient content in the soil to a more compact and easily absorbed by plant for healthy growth (Chang and Chen, 2010). Food waste compost also can even improve the chemical, biological and physical levels of soil resources and reduce density and soil compression to promote the beneficial bacteria growth to the soil (Senesi and Plaza, 2007). Moreover, it can improve the ventilation, water reservoir ability to prevent the disease from the soil and the ability of food waste compost to absorb carbon has reduced the occurrence of climate change.

The ornamental plants used in this study are *Cordyline fruticosa* (palm lily) *Coleus* sp. (coleus), and *Rhoeo discolor* (boat lily). These plants are fast growing plants which become the main landscape plants used by nursery in University of Malaya and always will be replanted for the purpose of landscaping and event in campus. Hence, the current study was conducted to measure the soil properties and physiological growth responses of palm lily, coleus and boat lily using various soil amendments such as food waste compost and biochar with fertilizer and reduction of fertilizer that can be suggested to nursery of the Department of Property Management and Maintenance (JPPHB), Universiti Malaya.

## Materials and methods

### *Experimental design*

The study was conducted at the nursery of the Department of Property Management and Maintenance (JPPHB), Universiti Malaya, Malaysia for about four months of

observation. The nursery receives a range of Photosynthetically Active Radiation (PAR) of 150-2000  $\mu\text{E m}^{-2} \text{s}^{-1}$ , relative humidity (RH), 60-90%, precipitation 5-9 mm/0.2 inches and temperature, 25-29 °C for 4 months starting from 29 October 2018 until 28 February 2019.

Palm lily, coleus and boat lily were grown by applying the treatments stated in *Table 1*. Each treatment was applied in the soil.

**Table 1.** List of treatments

Treatment	Types of treatment
Treatment	Without soil amendment (control)
Treatment 2	Fertilizer
Treatment 3	Food waste compost only
Treatment 4	Food Waste Compost + <20% of Fertilizers
Treatment 5	Biochar only
Treatment 6	Biochar + < 20% of Fertilizers
Treatment 7	Biochar + Food Waste Compost
Treatment 8	Biochar + Food Waste Compost + < 20% of Fertilizers

The experiment was arranged in a randomized complete block design (RCBD) with four replications. The amendments were mixed thoroughly into soil pots 15 days before transplanting.

### **Preparation of planting materials**

The species studied; *Cordyline fruticosa* (palm lily) *Coleus sp.* (coleus), and *Rhoeo discolor* (boat lily) (Lopez-Martinez Suguey, 2018) were chosen based on their prominent role as landscape plants which are fast growing and have aesthetic values such as attractive leaf color. After two weeks of sowing, the plants were transplanted into the pots (8 cm × 10 cm) size filled with soil according to the treatment. Each pot contained one plant. The ratio of the media that commonly used in the nursery is 3: 2: 1 which consists of topsoil, black soil organic, and sand. The topsoil refers to the top layer of about 5 cm to 30 cm from the surface of the earth. The topsoil is used to repair the soil structure by mixing or placing topsoil on the land area cultivated for agricultural purposes and supplying nutrients to the soil. The black organic soils in treatment 3, 4, 5, 6, 7 and 8 have been replaced by the biochar or compost or a mixture of both compost and biochar.

### **Biochar and food waste compost characteristic**

Biochar used in this study is obtained from Bangi, Malaysia which is produced with 500 °C pyrolysis process. Food waste compost is obtained from Zero Waste Campaign, University Malaya which is produced by the food waste from University Malaya campus. The characteristic of biochar and compost is listed in *Table 2*.

### **Data collection**

#### **Physiological parameters**

The relative chlorophyll content of the leaves was determined using a chlorophyll meter (SPAD-502 Plus, Minolta, Japan) (Aimee and Normaniza, 2014), providing a



rapid and non-destructive approach that enables in situ measurement. The observation was made starting at 15 days after transplanting (DAT) and continued fortnightly. The photosynthetic rate, transpiration rate, and stomatal conductance were measured using a portable photosynthesis system (Li6400XT, LI-COR, USA). These parameters were measured between 11.00 am and 2.00 pm where the plants receive optimum PAR throughout the experiment. The instantaneous water use efficiency (WUE) was determined as a ratio of photosynthetic rate (A) to transpiration rate (E) (Aimee and Normaniza, 2014).

**Table 2.** Chemical properties of amendment used

Biochar	pH	EC	Total OC	N	P	K	Ca	Mg	Cu
		(dS/m)	(%)						(ppm)
Oil palm kernel	8.61	3.67	43.41	0.5	0.15	0.74	2.27	0.25	17.85
Food waste compost	6.60	2.48	14.34	2.39	2.82	0.21	NA	0.36	21.49

NA = Not applicable

#### *Plant height, number of leaves and total biomass*

The plant height was measured using a measuring tape and the number of leaves was counted manually every fortnightly. The total biomass was recorded after oven-drying the sample at 40 °C for 72 h until the weight was constant using a mass balance (accuracy of 0.01 g). The dry weight of the plant was then regarded as the amount of biomass.

#### *Soil chemical analysis*

The soil pH in 1:2.5 (w:v) was determined after harvest by using a pH meter/mV with a resolution of 0.01 (HI211-01, Hanna ins., Italy). The total nitrogen (N) was determined by using the Kjeldahl method (Bremner, 1996). The sample was placed in the digestion tube with 10 ml concentrated H<sub>2</sub>SO<sub>4</sub> and a table of Kjeldahl catalyst. The sample was placed in the digestion block for 4 h at 330 °C or until the solution change into cloudish colour. The distillation method by collecting the distilled sample in 5 ml of 3% boric acid until change to green colour and titration method by titrating the solution with 0.01 N HCL until the colour change to purpled-brown colour was done for another steps to get the total nitrogen. The organic matter was determined using loss of ignition method (LOI) (Storer, 1984). The sample was placed in the crucible for heating in the oven 16 h at 110 °C and heating in the muffle furnace for 6 h at 600 °C.

#### *Data analysis*

A statistical analysis was performed using SPSS program (SPSS version 24.0). The two-way Analysis of Variance (ANOVA) was applied to determine the significant difference of eight treatment with four replication for all three different species. The post-hoc test was conducted using a Duncan's Multiple Range Test (DMRT). The correlations among the parameter studied (plant height, number of leaves, total biomass, photosynthetic rate, soil pH, total nitrogen, and organic matter) in all treatments were also determined using Pearson's correlation.

## Results

### *Effect of soil amendment on plant growth performance*

The application of soil amendments was positively affected the growth of palm lily, coleus and boat lily. The plant height showed significantly higher in the amendment-treated plants than those treatments without soil amendments (control and standard media + fertilizer). Amongst the plants, coleus showed the tallest in Treatment 8 with biochar + food waste compost + < 20% fertilizer (Table 3).

The application of soil amendments also positively affected the number of leaves among the plant species after the four-month observation. All the species exhibited significant increment in the number of leaves, showing coleus was the highest (Table 3). In addition, Treatment 4 (food waste compost + < 20% fertilizer) showed significantly the highest increment among the treatments.

**Table 3.** *Effect of soil amendments on the plant height and number of leaves of the species studied*

Treatment	Plant height (cm)			Number of leaves		
	<i>Cordyline sp.</i>	<i>Coleus sp.</i>	<i>Rhoeo discolor</i>	<i>Cordyline sp.</i>	<i>Coleus sp.</i>	<i>Rhoeo discolor</i>
1	24.75±2.06 <sup>e</sup>	26.75±4.11 <sup>c</sup>	19.00±4.25 <sup>e</sup>	14±2.99 <sup>d</sup>	34±2.45 <sup>d</sup>	21±1.71 <sup>d</sup>
2	27.50±3.11 <sup>c</sup>	47.25±5.12 <sup>c</sup>	24.00±11.14 <sup>c</sup>	16±2.65 <sup>cd</sup>	43±5.06 <sup>cd</sup>	27±5.68 <sup>cd</sup>
3	31.00±1.41 <sup>ab</sup>	64.75±9.11 <sup>ab</sup>	25.50±18.85 <sup>ab</sup>	21±2.99 <sup>ab</sup>	66±7.62 <sup>ab</sup>	40±10.21 <sup>ab</sup>
4	33.50±1.91 <sup>a</sup>	58.00±4.69 <sup>b</sup>	24.75±14.94 <sup>b</sup>	25±0.58 <sup>a</sup>	70±5.35 <sup>a</sup>	42±8.54 <sup>a</sup>
5	25.25±1.50 <sup>d</sup>	35.75±2.50 <sup>d</sup>	23.00±6.02 <sup>d</sup>	16±2.63 <sup>c</sup>	52±13.50 <sup>c</sup>	29±1.26 <sup>c</sup>
6	28.00±1.83 <sup>c</sup>	50.75±5.91 <sup>c</sup>	22.75±13.11 <sup>c</sup>	20±2.89 <sup>cd</sup>	40±3.86 <sup>cd</sup>	25±1.26 <sup>cd</sup>
7	31.50±1.29 <sup>ab</sup>	63.75±4.57 <sup>ab</sup>	23.50±18.34 <sup>ab</sup>	20±2.36 <sup>b</sup>	57±16.24 <sup>b</sup>	36±6.60 <sup>b</sup>
8	33.50±0.58 <sup>a</sup>	65.75±4.03 <sup>a</sup>	26.75±17.91 <sup>a</sup>	23±0.82 <sup>ab</sup>	59±10.08 <sup>ab</sup>	37±7.48 <sup>ab</sup>

T1 = control, T2 = standard media + fertilizer, T3 = food waste compost, T4 = food waste compost + < 20% fertilizer, T5 = biochar, T6 = biochar + < 20% fertilizers, T7 = biochar + food waste compost, T8 = biochar + food waste compost + < 20% fertilizer. Means followed by the same letter within a column are not significantly difference ( $p < 0.05$ ). Mean ± Standard deviation

All plants showed significant differences in total biomass after the four-month observation. The higher total biomass indicates a good plant growth performance because the plants received the optimum requirements of nutrients. The highest total biomass was found in Treatment 8 (biochar + food waste compost + < 20% fertilizer) (62.50 g), followed by Treatment 3 (food waste compost) (52.50 g) and Treatment 7 (biochar + food waste compost) (52.50 g), and Treatment 4 (food waste compost + < 20% fertilizer) (47.50 g). Coleus showed the highest reading in total biomass among the species (Table 4).

### *Effect of soil amendments on physiological response*

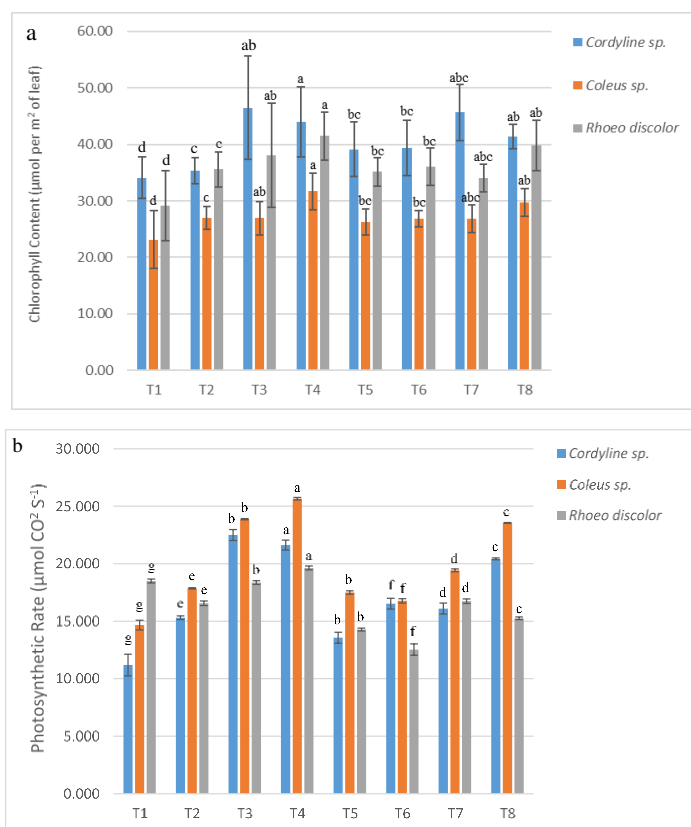
The chlorophyll content showed a positive increment after the four-month observation in all treatments. From the results, palm lily had the highest chlorophyll content between species and Treatment 3 (food waste compost) had the highest chlorophyll content among the treatment (Fig. 1a). Moreover, there was no significant interaction between species and treatment on the chlorophyll contents.

**Table 4.** Effect of soil amendments on the total biomass of *Cordyline sp.*, *Coleus sp.* and *Rhoeo discolor*

Treatment	Total biomass (g)		
	<i>Cordyline sp.</i>	<i>Coleus sp.</i>	<i>Rhoeo discolor</i>
1	11.25 ± 6.29 <sup>c</sup>	10.00 ± 0.00 <sup>c</sup>	13.75 ± 7.50 <sup>c</sup>
2	12.50 ± 5.00 <sup>b</sup>	30.00 ± 0.00 <sup>b</sup>	27.50 ± 15.00 <sup>b</sup>
3	26.25 ± 4.78 <sup>a</sup>	52.50 ± 17.08 <sup>a</sup>	48.75 ± 33.26 <sup>a</sup>
4	38.75 ± 13.15 <sup>a</sup>	47.50 ± 9.57 <sup>a</sup>	50.00 ± 14.14 <sup>a</sup>
5	10.00 ± 0.00 <sup>bc</sup>	15.00 ± 5.77 <sup>bc</sup>	18.75 ± 2.50 <sup>bc</sup>
6	13.75 ± 4.79 <sup>bc</sup>	30.00 ± 11.55 <sup>bc</sup>	17.50 ± 9.57 <sup>bc</sup>
7	23.75 ± 4.79 <sup>a</sup>	52.50 ± 12.58 <sup>a</sup>	37.50 ± 9.57 <sup>a</sup>
8	33.75 ± 6.29 <sup>a</sup>	62.50 ± 9.57 <sup>a</sup>	36.25 ± 18.87 <sup>a</sup>

T1 = control, T2 = standard media + fertilizer, T3 = food waste compost, T4 = food waste compost + < 20% fertilizer, T5 = biochar, T6 = biochar + < 20% fertilizers, T7 = biochar + food waste compost, T8 = biochar + food waste compost + < 20% fertilizer. Means followed by the same letter within a column are not significantly difference ( $p < 0.05$ ). Mean ± Standard deviation

The photosynthetic rate, stomatal conductance and transpiration rate of each plant species showed much affected by different treatments. The photosynthetic rate of each plant species showed a significant difference after the four-month observation where Treatment 4 (food waste compost + < 20% fertilizer) had a highest photosynthetic rate among treatments. Each species showed a significant interaction effect on photosynthetic rate where Treatment 4 (food waste compost + < 20% fertilizer) in coleus was the significant highest reading among the species.



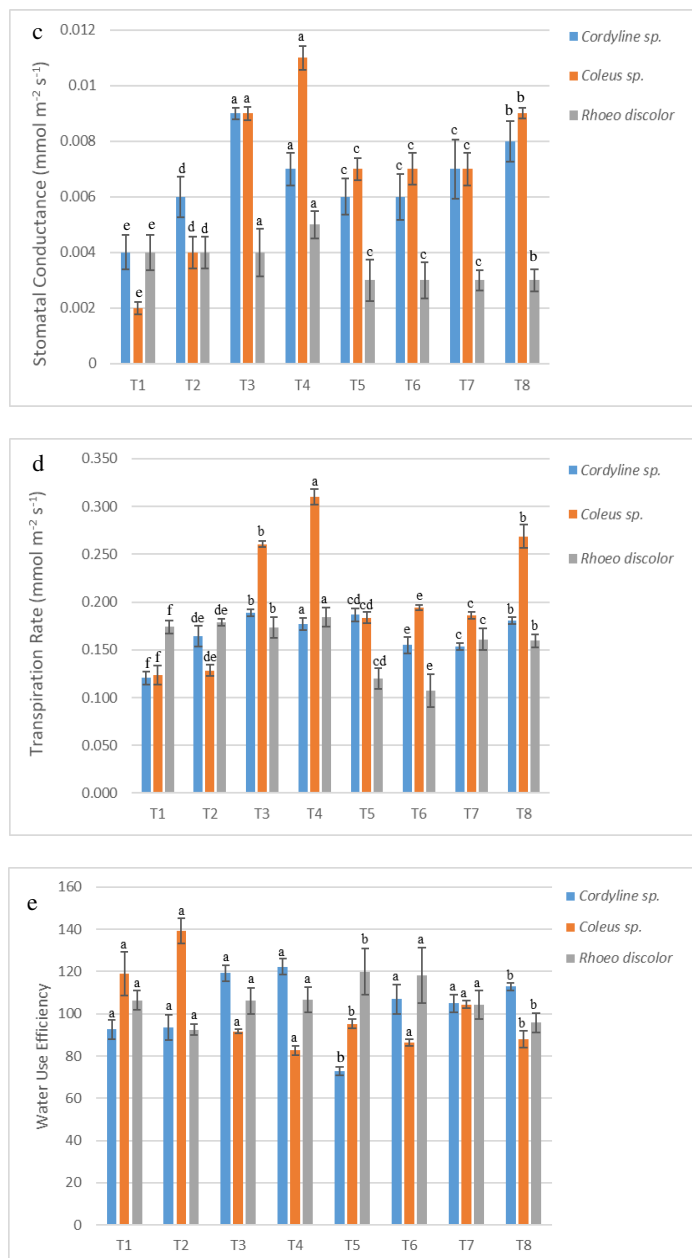


**Figure 1.** Effect of different treatments on (a) chlorophyll content (b) photosynthetic rate, (c) stomatal conductance, (d) transpiration rate and (e) water use efficiency after the four-month observation for each plant species. Each data item represents the mean of replicates and the vertical bar represents the standard deviation. T1 = control, T2 = standard media + fertilizer, T3 = food waste compost, T4 = food waste compost + < 20% fertilizer, T5 = biochar, T6 = biochar + < 20% fertilizers, T7 = biochar + food waste compost, T8 = biochar + food waste compost + < 20% fertilizer. Means followed by the same letter are not significantly difference ( $p < 0.05$ )

The increasing in stomatal conductance indicated the good and well plant characteristics meanwhile high transpiration rate indicated the excessive water discharge rates at plants. The results showed that there was a significant species and treatment effect on the stomatal conductance and also the transpiration rate. The results indicate that Treatment 4 (food waste compost + < 20% fertilizer) in coleus lost the

greatest amount of water through high transpiration and stomatal conductance, followed by Treatment 3 (food waste compost) and Treatment 8 (biochar + food waste compost + < 20% fertilizer) (Fig. 1 c, d). From the results, a significantly higher water use efficiency (WUE) was found in the Treatment 2 (fertilizer) in coleus while the lowest reading was recorded for the Treatment 5 (biochar) in palm lily (Fig. 1e). The WUE is a response between the photosynthetic and transpiration rates, where a high WUE was indicated by a high photosynthetic and low transpiration rate.

### ***Effect of soil amendment on soil ph, total nitrogen and organic matter for each plant species***

The overall plants species in all treatments have a significant increment in soil pH after the four-month observation. Treatment 5 (biochar) in both coleus and boat lily showed the highest reading (7.83) in soil pH respectively. The results also showed that there were significantly species and treatment effect on the soil pH. Based on the results, there were a significant species on the soil pH which are coleus was the significant highest among the species.

The application of soil amendment gives a significant increment reading in Total Nitrogen which lead by Treatment 4 (food waste compost + < 20% fertilizers) in palm lily meanwhile the least significant total nitrogen was in Treatment 5 (biochar) for coleus. The results in Table 5 also showed that there was no significant treatment and species effect on the total nitrogen.

**Table 5.** *Effect of soil amendments on the soil pH and total nitrogen for Cordyline sp., Coleus sp. and Rhoeo discolor*

Treatment	Soil pH			Total nitrogen (%)		
	<i>Cordyline sp.</i>	<i>Coleus sp.</i>	<i>Rhoeo discolor</i>	<i>Cordyline sp.</i>	<i>Coleus sp.</i>	<i>Rhoeo discolor</i>
1	7.56±0.09 <sup>bc</sup>	7.61±0.16 <sup>bc</sup>	7.61±0.16 <sup>bc</sup>	0.29±0.20 <sup>b</sup>	0.18±0.01 <sup>b</sup>	0.40±0.00 <sup>b</sup>
2	7.36±0.10 <sup>de</sup>	7.45±0.08 <sup>de</sup>	7.45±0.09 <sup>de</sup>	0.29±0.01 <sup>ab</sup>	0.29±0.05 <sup>ab</sup>	0.13±0.02 <sup>ab</sup>
3	7.21±0.13 <sup>e</sup>	7.32±0.10 <sup>e</sup>	7.32±0.10 <sup>e</sup>	0.50±0.21 <sup>a</sup>	0.20±0.07 <sup>a</sup>	0.33±0.18 <sup>a</sup>
4	7.30±0.25 <sup>cd</sup>	7.68±0.17 <sup>cd</sup>	7.68±0.17 <sup>cd</sup>	0.43±0.01 <sup>a</sup>	0.37±0.03 <sup>a</sup>	0.27±0.23 <sup>a</sup>
5	7.61±0.23 <sup>a</sup>	7.83±0.22 <sup>a</sup>	7.83±0.22 <sup>a</sup>	0.26±0.11 <sup>ab</sup>	0.11±0.04 <sup>ab</sup>	0.40±0.17 <sup>ab</sup>
6	7.54±0.27 <sup>cd</sup>	7.56±0.10 <sup>cd</sup>	7.56±0.10 <sup>cd</sup>	0.24±0.16 <sup>ab</sup>	0.30±0.02 <sup>ab</sup>	0.20±0.02 <sup>ab</sup>
7	7.62±0.23 <sup>ab</sup>	7.76±0.14 <sup>ab</sup>	7.76±0.14 <sup>ab</sup>	0.28±0.01 <sup>ab</sup>	0.26±0.09 <sup>ab</sup>	0.39±0.14 <sup>ab</sup>
8	7.37±0.12 <sup>d</sup>	7.49±0.15 <sup>d</sup>	7.45±0.24 <sup>d</sup>	0.37±0.13 <sup>ab</sup>	0.14±0.01 <sup>ab</sup>	0.33±0.03 <sup>ab</sup>

T1 = control, T2 = standard media + fertilizer, T3 = food waste compost, T4 = food waste compost + < 20% fertilizer, T5 = biochar, T6 = biochar + < 20% fertilizers, T7 = biochar + food waste compost, T8 = biochar + food waste compost + < 20% fertilizer. Means followed by the same letter within a column are not significantly difference (p < 0.05). Mean ± Standard deviation

In general, organic matter was affected by the soil amendments throughout the observation. Based on the result, the significant highest organic matter was found in Treatment 8 (biochar + food waste compost + < 20% fertilizers) in coleus (2.13%) and the least organic matter was in Treatment 1 (control) in boat lily (0.53%). The results also showed that there was a palm lily has the highest significant of organic matter

among the species (1.98%). Besides, there was no significant interaction between species and treatment effect on soil organic matter (Table 6).

**Table 6.** Effect of soil amendments on organic matter for *Cordyline sp.*, *Coleus sp.* and *Rhoeo discolor*

Treatment	Organic matter (%)		
	<i>Cordyline sp.</i>	<i>Coleus sp.</i>	<i>Rhoeo discolor</i>
1	0.99 ± 0.53 <sup>bc</sup>	0.71 ± 0.01 <sup>bc</sup>	0.53 ± 0.08 <sup>bc</sup>
2	0.62 ± 0.19 <sup>c</sup>	0.56 ± 0.33 <sup>c</sup>	0.58 ± 0.37 <sup>c</sup>
3	1.58 ± 0.22 <sup>ab</sup>	1.05 ± 0.02 <sup>ab</sup>	1.25 ± 0.50 <sup>ab</sup>
4	1.78 ± 0.47 <sup>a</sup>	1.67 ± 0.24 <sup>a</sup>	1.15 ± 0.50 <sup>a</sup>
5	1.78 ± 0.47 <sup>ab</sup>	1.07 ± 0.62 <sup>ab</sup>	0.67 ± 0.25 <sup>ab</sup>
6	1.30 ± 0.30 <sup>ab</sup>	1.52 ± 0.12 <sup>ab</sup>	0.91 ± 0.13 <sup>ab</sup>
7	1.98 ± 0.40 <sup>a</sup>	1.93 ± 0.45 <sup>a</sup>	1.00 ± 0.62 <sup>a</sup>
8	1.85 ± 0.64 <sup>a</sup>	2.13 ± 1.02 <sup>a</sup>	0.90 ± 0.60 <sup>a</sup>

T1 = control, T2 = standard media + fertilizer, T3 = food waste compost, T4 = food waste compost + < 20% fertilizer, T5 = biochar, T6 = biochar + < 20% fertilizers, T7 = biochar + food waste compost, T8 = biochar + food waste compost + < 20% fertilizer. Means followed by the same letter within a column are not significantly difference ( $p < 0.05$ ). Mean ± standard deviation

### Correlation between photosynthetic rate and plant height

The photosynthetic rate and plant height were significantly correlated ( $R = 0.5536$ ; Fig. 2), the higher the photosynthetic rate, the higher the plant heights.

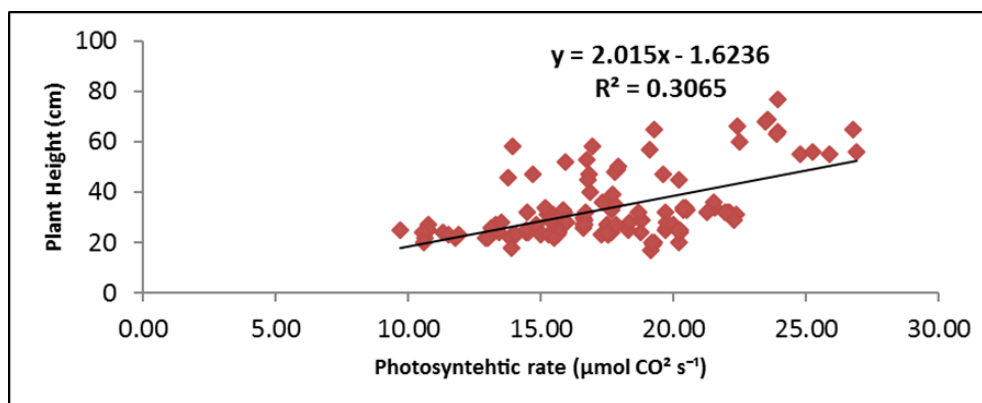


**Figure 2.** Correlation between photosynthetic rate and plant height

### Correlation between plant growth and soil properties

The correlation studies between plant growth and soil properties parameters showed that the plant height was significantly correlated with the number of leaves, total biomass and organic matter (Table 7). However, there was no correlation was observed between plant height with both soil pH and total nitrogen. In addition, the number of leaves is significantly correlated with total biomass and the number of leaves only meanwhile the total biomass only has a significant correlation with soil pH.

**Table 7.** Correlation analysis deduced between plant growth and soil properties using Pearson's correlation

Parameter	Plant height	Number of leaves	Total biomass	Soil pH	Total nitrogen	Organic matter
Plant height	-	0.834**	0.571**	- 0.024	- 0.019	0.255*
Number of leaves		-	0.615**	0.118	- 0.078	0.078
Total biomass			-	- 0.203*	0.111	0.128
Soil pH				-	- 0.174	-0.072
Total nitrogen					-	0.114
Organic matter						-

\*\*Significant at 0.01 level

\*Significant at 0.05 level

## Discussion

In general, the plant growth and soil properties were much affected by the soil amendments in a four-month observation. The best treatment was found to be combination of biochar and food waste compost and the best plant growth was exhibited by coleus.

In monitoring the growth performance of each plant species, several growth characteristics were observed such as plant height, number of leaves and total biomass. The growth performance showed that coleus. in Treatment 8 (biochar + food waste compost + < 20%) and Treatment 4 (food waste compost + < 20% of fertilizers) exhibited the highest reading in plant height and number of leaves. The compost effects have succeeded in increasing plant growth due to its higher cation-exchange capacity (CEC) and base saturation (BS) as well as providing Nitrogen (N) and Phosphorus (P) which useful for plant growth. In addition, cation and anion which contained in food waste compost treatments have an imbalance contents between  $\text{NH}_4^+$  and  $\text{NO}_3^-$  which may be a potential cause for increasing the plant growth (Schulz and Glaser, 2012).

Other than that, the total biomass of coleus in Treatment 8 (biochar + food waste compost + < 20% of fertilizers treatment) was the highest reading among the species. This was in line with (Schulz et al., 2013), in which the addition of composted biochar significantly increased the plant height and above-ground biomass. Biochar can act as a soil conditioner that increases the soil's nutrient deposition capacity (Miranda et al., 2017), enhances and maintains nutrients in the soil, hence will improve the plant growth. In addition, the potential of biochar as a source of nutrients can be depending on feedstock and temperature of pyrolysis where the lower pyrolysis temperatures may increase the availability of nitrogen (N) and phosphorus (P) (Yuan et al., 2019) besides reduces the  $\text{N}_2\text{O}$  emissions, while higher pyrolysis temperatures may increase potassium (K) availability (Ding et al., 2016). Furthermore, nutrients in compost contribute to increase in stem height, thus enhance the plant growth performance (Mensah and Frimpong, 2018). Despite a low reading of plant height in boat lily, it showed considerable increased in number of leaves especially in Treatment 3 (food waste compost) and Treatment 4 (food waste compost + less 20% of fertilizers) because of increase in nitrogen contents in these treatments.

The highest reading chlorophyll content was shown by coleus in Treatment 3 (food waste compost). Besides, the right combination of biochar, compost, and fertilizer significantly increased the total chlorophyll content of the species studied compared to the use of fertilizers alone. The use compost alone increased the chlorophyll content but by the combination of biochar, compost and fertilizer also increased the chlorophyll

content for each species. The organic amendment in soil increases the nutrients and water content in soil, thus restricting in increase of chlorophyll content and the plant age (Agegnehu et al., 2016).

The stomata play an important role in the process of photosynthesis and transpiration. Stomata is a small pore beneath the surface of the leaves which mostly allow air (CO<sub>2</sub>) to enter and allow water (H<sub>2</sub>O) and oxygen (O<sub>2</sub>) to come out. Photosynthesis is a process that plants produce food and energy. Based on the results in this study, the coleus has large pores which cause photosynthetic and transpiration to occur more efficiently. The midday stomatal closure occurs due to the effects of low atmospheric humidity as well as from water pressure and high temperature. Stomata tend to adjust regularly to maintain photosynthesis to transpiration ratio is and then increased the water use efficiency (WUE) (Noor and Harun, 2004).

In addition, the highest increment of photosynthetic rate and transpiration rate in coleus suggested that its roots absorb water and nutrients directly from the soil more efficiently as compared to other species. coleus has the highest reading water use efficiency (WUE) shows the ability of the species to store the water. The highest water use efficiency (WUE) in palm lily compared to coleus and boat lily may be caused by mesophyll ratio of surface cells to the surface of the leaves might increase the WUE by increasing photosynthesis more than an increased transpiration (Noor and Harun, 2004). Furthermore, plant mortality will result in the reduction of both rates of photosynthesis and transpiration. The old leaves have a low rate of photosynthesis and transpiration compared to the younger leaves (Mensah and Frimpong, 2018). Thus, the application of biochar and compost with fertilizer contributes to the higher chlorophyll content and number of leaves, consequently result in higher of photosynthetic rate (Hidayati and Anas, 2016).

This study found that the soil pH of all treatments and species mostly tends to be neutral around 7-7.5 after four months of observation. The application of soil amendments showed the decrement reading in soil pH, which may be due to the acidic materials produced from the oxidation and decomposition of organic matter in the soil (Senesi and Plaza, 2007; Dias et al., 2010). The formation of the acidic functional groups can neutralize alkalinity and eventually decrease soil pH (Xiang-Hong et al., 2012).

Accumulation of high Soil Organic Carbon (SOC) in biochar can increase total nitrogen and finally, resulting in increases of crop production. Moreover, both biochar and compost have significantly contributed higher total nitrogen after harvest compare to control (Schulz et al., 2013) but too much of total nitrogen also contributed in slowing the maturity of the plant. In addition, loss of the total nitrogen on the soil may be caused by several factors such as the use of the plant itself or microorganisms and also carried by rainwater (El-Sharkawi, 2012).

Soil organic matter is a major factor in determining the fertility of soil. It supplies energy for microbial biomass activity (Schnürer et al., 1985), provides nutrients for crops and improves the physical properties of the soil (Six et al., 2002). Organic matter in soil can be affected by treatments where higher values can be indicators of improving soil fertility. Biochar has the potential to affect microbial biomass and composition and the microbes are also able to change the properties of biochar (Lehmann et al., 2011). The porous nature of biochar because of its high surface area and its ability to adsorb soluble organic matter and inorganic nutrients, biochar provides a suitable habitat for



microbes (Lehmann et al., 2011). In addition, high amount of organic matter in compost increased organic carbon in the soil.

The photosynthetic rate and plant height has shown a positive correlation indicating that the increases of the carbon dioxide absorption and light trapping have contributed to the higher photosynthetic rate and then enhance the plant height. Chlorophyll green pigments in chloroplasts of the leaves of the plants are one of the photosynthetic pigments that play a key role in absorbing solar energy (Vasconcelos et al., 2017).

## Conclusions

The application of soil amendments can improve soil fertility and plant growth performance together with fertilizer. In this study, the application of food waste compost and biochar in coleus showed the best performance in the plant growth including the number of leaves, chlorophyll contents, photosynthetic rate, stomatal conductance, transpiration rate, water use efficiency (WUE) and total biomass.

Similarly, higher values of soil pH, amounts of total nitrogen, and organic matter content were observed in food waste compost and biochar treatment. It is evident that the combination effect of biochar and food waste compost either biochar alone or compost alone contributed the positive effect on plant growth performance as well as soil properties. Based on the overall result, the use of food waste compost and biochar have potential to be used to improve the quality of soil.

**Acknowledgements.** The authors thank the University of Malaya for financial support by UM Living Lab Grant Programme - SUS (Sustainability Science) (LL036-18SUS) and Knowledge Transfer Programme (KTP) grant (MRUN2019-2A).

## REFERENCES

- [1] Agegnehu, G., Nelson, P. N., Bird, M. I. (2016): The effects of biochar, compost and their mixture and nitrogen fertilizer on yield and nitrogen use efficiency of barley grown on a Nitisol in the highlands of Ethiopia. – *Science of the Total Environment* 569: 869-879.
- [2] Aimee, H., Normaniza, O. (2014): Physiological responses of *Melastoma malabathricum* at different slope orientations. – *J. Trop. Plant Physiol* 6: 10-22.
- [3] Bremner, J. M. (1996): Nitrogen-Total. – In: Sparks, D. L. et al. (eds.) *Methods of Soil Analysis: Part 3 Chemical Methods*. SSSA, Madison, WI, pp. 1085-1121.
- [4] Chan, K. Y., Van Zwieten, L., Meszaros, I., Downie, A., Joseph, S. (2008): Agronomic values of greenwaste biochar as a soil amendment. – *Soil Research* 45: 629-634.
- [5] Chang, J. I., Chen, Y. (2010): Effects of bulking agents on food waste composting. – *Bioresource Technology* 101: 5917-5924.
- [6] Dias, B. O., Silva, C. A., Higshikawa, F. S., Roig, A., Sanchez-Monedero, M. A. (2010): Use of biochar as bulking agent for the composting of poultry manure: effect on organic matter degradation and humification. – *Bioresource Technology* 101: 1239-1246.
- [7] Ding, Y., Liu, Y., Liu, S., Li, Z., Tan, X., Huang, X., Zeng, G., Zhou, L., Zheng, B. (2016): Biochar to improve soil fertility. A review. – *Agronomy for Sustainable Development* 36: 36.
- [8] El-Sharkawi, H. M. (2012): Effect of nitrogen sources on microbial biomass nitrogen under different soil types. – *ISRN Soil Science*. <https://doi.org/10.5402/2012/310727>.

- [9] Hidayati, N., Anas, I. (2016): Photosynthesis and transpiration rates of rice cultivated under the system of rice intensification and the effects on growth and yield. - HAYATI Journal of Biosciences 23: 67-72.
- [10] Lee, J.-J., Park, R.-D., Kim, Y.-W., Shim, J.-H., Chae, D.-H., Rim, Y.-S., Sohn, B.-K., Kim, T.-H., Kim, K.-Y. (2004): Effect of food waste compost on microbial population, soil enzyme activity and lettuce growth. – Bioresource Technology 93: 21-28.
- [11] Lehmann, J., Da Silva, J. P., Steiner, C., Nehls, T., Zech, W., Glaser, B. (2003): Nutrient availability and leaching in an archaeological Anthrosol and a Ferralsol of the Central Amazon basin: fertilizer, manure and charcoal amendments. – Plant and Soil 249: 343-357.
- [12] Lehmann, J., Rillig, M. C., Thies, J., Masiello, C. A., Hockaday, W. C., Crowley, D. (2011): Biochar effects on soil biota—a review. – Soil Biology and Biochemistry 43: 1812-1836.
- [13] Lopez-Martinez Sugay, G.-M. E. G., Lopez, Y. C. I., Lara Corona, V. H., Lagunas-Rivera, S. (2018): *Rhoeo discolor*: a medicinal plant with phytoremediation potential. – Int. J. Adv. Res. 6: 763-770.
- [14] McGeehan, S. L. (2012): Impact of waste materials and organic amendments on soil properties and vegetative performance. – Applied and Environmental Soil Science. <https://doi.org/10.1155/2012/907831>.
- [15] Mensah, A. K., Frimpong, K. A. (2018): Biochar and/or compost applications improve soil properties, growth, and yield of maize grown in acidic rainforest and coastal savannah soils in Ghana. – International Journal of Agronomy. <https://doi.org/10.1155/2018/6837404>.
- [16] Miranda, N. D. O., Pimenta, A. S., Silva, G. G. C. D., Oliveira, E., Mota, M., Carvalho, M. A. B. D. (2017): Biochar as soil conditioner in the succession of upland rice and cowpea fertilized with nitrogen. – Revista Caatinga 30: 313-323.
- [17] Montanarella, L., Lugato, E. (2013): The application of biochar in the EU: challenges and opportunities. – Agronomy 3: 462-473.
- [18] Nartey, O. D., Zhao, B. (2014): Biochar preparation, characterization, and adsorptive capacity and its effect on bioavailability of contaminants: an overview. – Advances in Materials Science and Engineering. <https://doi.org/10.1155/2014/715398>.
- [19] Noor, M. R. M., Harun, M. H. (2004): Importance of water use efficiency (WUE) in oil palm productivity. – Oil Palm Bulletin 2004: 24-30.
- [20] Schulz, H., Glaser, B. (2012): Effects of biochar compared to organic and inorganic fertilizers on soil quality and plant growth in a greenhouse experiment. – Journal of Plant Nutrition and Soil Science 175: 410-422.
- [21] Schulz, H., Dunst, G., Glaser, B. (2013): Positive effects of composted biochar on plant growth and soil fertility. – Agronomy for Sustainable Development 33: 817-827.
- [22] Schurer, J., Clarholm, M., Rosswall, T. (1985): Microbial biomass and activity in an agricultural soil with different organic matter contents. – Soil Biology and Biochemistry 17: 611-618.
- [23] Senesi, N., Plaza, C. (2007): Role of humification processes in recycling organic wastes of various nature and sources as soil amendments. – Clean; Soil, Air, Water 35: 26-41.
- [24] Shainberg, I., Warrington, D., Rengasamy, P. (1990): Water quality and PAM interactions in reducing surface sealing. – Soil Science 149: 301-307.
- [25] Sharma, A., Saha, T. N., Arora, A., Shah, R., Nain, L. (2017): Efficient Microorganism compost benefits plant growth and improves soil health in calendula and marigold. – Horticultural Plant Journal 3 67-72.
- [26] Six, J., Feller, C., Denef, K., Ogle, S., De Moraes Sa, J. C., Albrecht, A. (2002): Soil organic matter, biota and aggregation in temperate and tropical soils. - Effects of no-tillage. – Agronomie 22: 755-775
- [27] Storer, D. A. (1984): A simple high sample volume ashing procedure for determination of soil organic matter. – Communications in Soil Science and Plant Analysis 15: 759-772.

- [28] Tian, Q., He, H., Cheng, W., Bai, Z., Wang, Y., Zhang, X. (2016): Factors controlling soil organic carbon stability along a temperate forest altitudinal gradient. – *Scientific Reports* 6: 1-9.
- [29] Vasconcelos, A. C. F. D., Chaves, L. H. G., Gheyi, H. R., Fernandes, J. D., Tito, G. A. (2017): Crambe growth in a soil amended with biochar and under saline irrigation. – *Communications in Soil Science and Plant Analysis* 48: 1291-1300.
- [30] Woolf, D., Amonette, J. E., Street-Perrott, F. A., Lehmann, J., Joseph, S. (2010): Sustainable biochar to mitigate global climate change. – *Nature Communications* 1: 1-9.
- [31] Xiang-Hong, L., Feng-Peng, H., Xing-Chang, Z. (2012): Effect of biochar on soil aggregates in the Loess Plateau: results from incubation experiments. – *International Journal of Agriculture and Biology* 4(6): 975-979.
- [32] Yuan, P., Wang, J., Pan, Y., Shen, B., Wu, C. (2019): Review of biochar for the management of contaminated soil: preparation, application and prospect. – *Science of the Total Environment* 659: 473-490.

# RISK ASSESSMENT OF ANTIBIOTIC PREVALENCE IN DRINKING WATER AND ITS IMPACTS ON HUMAN HEALTH IN CHINA

LYU, J.<sup>1,2,3</sup> – YANG, L. S.<sup>2,3</sup> – CHEN, Y. Y.<sup>1</sup> – YE, B. X.<sup>1</sup> – ZHANG, L.<sup>1\*</sup> – WANG, L.<sup>2\*</sup>

<sup>1</sup>China CDC Key Laboratory of Environment and Population Health, National Institute of Environmental Health, Chinese Center for Disease Control and Prevention, No.29 Nanwei Road, Xicheng District, Beijing 100050, PR China  
(e-mail: lyjia@nieh.chinacdc.cn; phone: +86-10-5093-0228; fax: +86-10-5093-0228)

<sup>2</sup>Key Laboratory of Land Surface Pattern and Simulation, Institute of Geographical Sciences and Natural Resources Research, Chinese Academy of Sciences, 11A, Datun Road, Chaoyang District, Beijing 100101, PR China  
(e-mail: yangls@igsnr.ac.cn; phone: +86-10-6488-9276; fax: +86-10-6485-4230)

<sup>3</sup>University of Chinese Academy of Sciences, 19(A) Yuquan Road, Shijingshan District, Beijing 100049, PR China

\*Corresponding authors

e-mail/phone/fax: zhanglan@nieh.chinacdc.cn/+86-10-5093-0224/+86-10-5093-0228;  
wangli@igsnr.ac.cn/+86-10-6485-4841/+86-10-6485-4230

(Received 29<sup>th</sup> Jul 2020; accepted 19<sup>th</sup> Nov 2020)

**Abstract.** Drinking water is a known potential source of human exposure to antibiotics. However, risk of antibiotic exposure from drinking water has not been sufficiently quantified. We measured the levels of 23 antibiotics in drinking water from 12 cities of China during the summer and winter seasons, quantifying exposure doses and health risk quotients (HRQ) of antibiotic exposure via drinking water. High detection rates (above 70%) of macrolides (MLs), sulfonamides and fluoroquinolones were observed during summer season, with median concentrations of 0.26 ng/L, 0.59 ng/L and 0.36 ng/L, respectively, while only MLs were observed with a high detection rate in winter (median concentration 0.46 ng/L). Total antibiotic exposure via drinking water ranged from 0.0036 ng/kg/day to 4.36 ng/kg/day in summer and from 0.0046 ng/kg/day to 1.12 ng/kg/day in winter. High median antibiotic exposures were observed in Chaohu, Huainan and Guangzhou in summer and in Mudanjiang in winter. Of the 18 detected antibiotics, enrofloxacin, ciprofloxacin, sarafloxacin and roxithromycin had an HRQ  $\geq$  0.01. Drinking water is one of the principal pathways for human exposure to antibiotics. Accordingly, management of antibiotic exposure from drinking water should be a high public health priority, and the accompanying health risks merit greater attention from public health authorities.

**Keywords:** pollution, exposure, macrolides, sulfonamides, fluoroquinolones

**Abbreviations:** ADD: average daily potential dose, ADI: acceptable daily intake, DWTP: drinking water treatment plant, GP: glycopeptide, HLB: hydrophilic-lipophilic balance, HRQ: health risk quotient, LN: lincosamide, ML: macrolide, ND: not detected, QN: fluoroquinolone, RSC: relative source contribution, SA: sulfonamide, SPE: solid phase extraction, UPLC–MS/MS: ultra-performance liquid chromatography–tandem mass spectrometer,  $\beta$ L:  $\beta$ -lactam

## Introduction

Antibiotics include a range of powerful medication ingredients that can destroy or slow the growth of bacteria and are extensively used to treat human and animal diseases and to promote animal growth (Le Page et al., 2017). The rising rate of antibiotic use has led to the contamination of potable water sources from natural bodies of water

receiving effluents from municipal wastewater treatment plants (hospital and community, Aga et al., 2016), agricultural sources (aquaculture, husbandry, Kümmerer, 2009), and the pharmaceutical industry (de Jesus Gaffney et al., 2015). Incomplete removal of antibiotics by conventional technologies (e.g., flocculation, sedimentation and disinfection) in drinking water treatment plants (DWTPs) leaves antibiotic residues in tap water, which now constitutes continuous human exposure to antibiotics (Yang et al., 2011). It is imperative to evaluate the exposure and health risks of antibiotics in drinking water.

In recent years, the issue of human health risk due to overuse of antibiotics has attracted substantial attention from the general public worldwide (Knapp et al., 2010). Antibiotics are understood to pose human health risks, including hypersensitive reactions, abnormalities in digestive functioning (Bedford, 2000), development and spread of antibiotic-resistant bacteria (Gullberg et al., 2011), and protracted toxic effects due to long-term low-level exposure (Sarmah et al., 2006). The occurrence of antibiotics in aquatic environments and drinking water is well-documented in developed countries including the USA (Benotti et al., 2009) and in the European Union (Carmona et al., 2014). China is one of the world's largest producers and consumers of antibiotics (Zhang et al., 2015). Previous investigations on antibiotic residues in aquatic environment have provided evidence that China has problems of antibiotic pollution (Ma et al., 2015; Xu, 2018). Thus, concerns are rising about antibiotic exposure from drinking water. However, studies measuring exposure to antibiotics in drinking water and associated health risks in China are limited.

The objectives of this study were to: (1) quantify the levels of 23 antibiotics in drinking water from 12 cities in different water basins in China, including seasonal and spatial distributions; (2) assess human exposure to antibiotics in drinking water in China; and (3) estimate the potential risks of antibiotic exposure via drinking water in the Chinese population.

## **Materials and methods**

### ***Water sampling and analysis***

Tap water in China comes from the public water system and is treated at DWTPs for drinking and other household usages. Tap water samples were collected from 12 cities located in seven large river basins, three key lake basins and two key reservoir areas of China. Of the 12 cities sampled, 10 (Yibin, Lanzhou, Huainan, Shenyang, Mudanjiang, Guangzhou, Wuxi, Kunming, Chaohu and Chongqing) are prefecture-level cities with at least one million inhabitants and are located in the Yangtze River Basin, Yellow River Basin, Huaihe River Basin, Liaohe River Basin, Songhua River Basin, Pearl River Basin, Taihu Lake Basin, Dianchi Lake Basin, Chaohu Lake Basin, and Three Gorges Reservoir Area, respectively. Based on the population and number of DWTPs in each of these cities, five representative DWTPs were selected from each city for collection of tap water samples in corresponding water supply areas. The two remaining cities, Danjiangkou and Korla, are county-level cities with approximately one hundred thousand inhabitants and are located in the Danjiangkou Reservoir Area and Northwest River Basin, respectively. Based on the population and number of DWTPs in each of these cities, three DWTPs in Danjiangkou and one DWTP in Korla were selected for tap water sampling in corresponding water supply areas. This sampling plan yielded a total of 54 sampling points, from which tap water samples were collected in sunny or cloudy

weather in January and July 2017. The sampling locations are shown in *Figure 1*. Water samples were collected manually by qualified personnel in 2000 mL amber glass bottles with screw caps. The bottles were washed with water, methanol and ultrapure water and then dried prior to sample collection. A total of 30 mg of ascorbic acid was added for each liter of water as a pharmaceutical preservative (Lv et al., 2019). The water samples were maintained in dark conditions at 4 °C from the time of collection through reception and analysis at the laboratory.

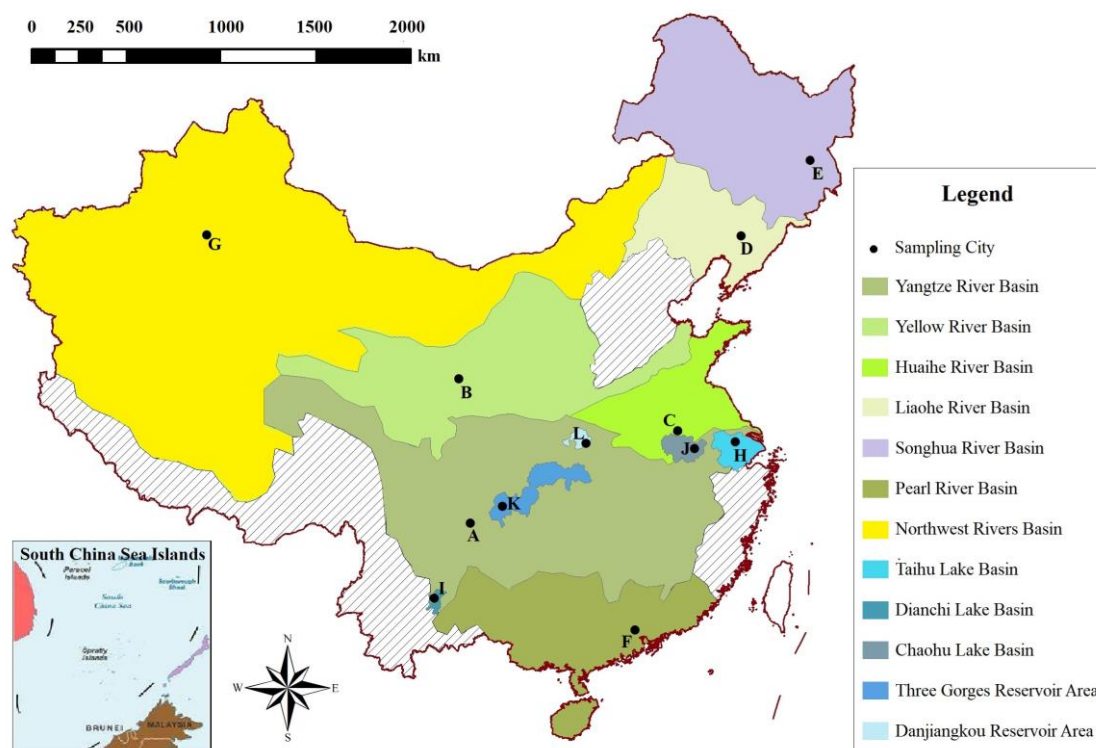


**Figure 1.** Sampling locations, including cities and river basins. A, Yibin; B, Lanzhou; C, Huainan; D, Shenyang; E, Mudanjiang; F, Guangzhou; G, Korla; H, Wuxi; I, Kunming; J, Chaohu; K, Chongqing; L, Danjiangkou

Twenty-three antibiotics of six different classes commonly used in China were analyzed, including four  $\beta$ -lactams ( $\beta$ LTs), three macrolides (MLs), eight sulfonamides (SAs), six fluoroquinolones (QNs), one lincosamide (LN) and one glycopeptide (GP). Information on standards for analytes is listed in *Table A1* in the *Appendix*. Target analytes were extracted from water samples using solid phase extraction and then analyzed by ultra-performance liquid chromatography–tandem mass spectrometer. Field blanks and method blanks were created to identify any contaminant from the sampling site and analysis process. Recovery and precision were used to validate the method performance. Analysis process and its quality assurance were described in detail in the *Appendix*.

### **Exposure assessment via drinking water consumption**

Drinking and dermal absorption are the main contaminant intake and uptake routes for human exposure to antibiotics through drinking water consumption. The average

daily potential dose (ADD) was used to evaluate antibiotic exposure through drinking and dermal absorption during water consumption, consumption of foods containing or cooked using water, and use of water for food washing and household activities including brushing teeth, bathing, and washing clothes.

ADD through intake water (ADD<sub>dw</sub>) was calculated using *Equation 1*:

$$ADD_{dw} = \frac{C_{dw} \times \text{IngR} \times \text{EF} \times \text{ED}}{\text{BW} \times \text{AT} \times 1000} \quad (\text{Eq.1})$$

where ADD<sub>dw</sub> is the ADD from intake of water (µg/kg/day), C<sub>dw</sub> is the concentration of antibiotics in drinking water (ng/L), IngR is the ingestion rate (L/day), including both direct and indirect ingestion, EF is the exposure frequency (days/year), ED is the exposure duration (years), BW is body weight (kg), and AT is averaging time (days). To reduce uncertainties in exposure variation between different geographical areas, across seasons, and between men and women, the IngR values corresponding to area, season and sex as well as the sex-specific BW value in China according to the *Exposure Factors Handbook of Chinese Population* (China EPA, 2009; area, season and sex-specific values are shown in *Table A2*) were used.

ADD through dermal absorption with water use (ADD<sub>dermal</sub>) was calculated using *Equation 2*:

$$ADD_{dermal} = \sum_{i=1}^9 \frac{DA_{\text{event}-i} \times SA_i \times \text{EF}_i \times \text{ED}_i}{\text{BW} \times \text{AT}_i} \quad (\text{Eq.2})$$

where ADD<sub>dermal</sub> is the ADD through dermal absorption (µg/kg/day). Dermal exposure was calculated from nine daily activities, including washing hands, face, hair, feet; washing vegetables, dishes, and clothes; bathing, and swimming. DA<sub>event-i</sub> refers to the absorbed dose from one event (µg/cm<sup>2</sup>/day), as calculated using *Equation 3*. SA<sub>i</sub> refers to the skin surface area available for contact (cm<sup>2</sup>), according to the *Exposure Factors Handbook of Chinese Population* (China EPA, 2009; values summarized in *Table A3*). EF<sub>i</sub> refers to the exposure frequency (days/year), ED<sub>i</sub> to the exposure duration (years), BW to body weight (kg), and AT<sub>i</sub> to averaging time (days). DA<sub>event-i</sub> was calculated as follows:

$$DA_{\text{event}-i} = K_p \times C \times T \times 10^{-6} \quad (\text{Eq.3})$$

where K<sub>p</sub> is the permeability coefficient (cm/hr), C is the chemical concentration in water that is in contact with the skin (ng/L), and T is the time of contact (hours/day), which was determined from references on water usage habits in northern and southern China (Duan et al., 2010; Huang et al., 2017), as summarized in *Table A4*.

It is difficult to obtain permeability coefficients of antibiotics directly from references. Accordingly, we used a model developed by ten Berge (2010) and recommended by Brown et al. (2016) in a study of eight models for calculating K<sub>p</sub> by *Equation 4*:

$$\log K_p = -2.80 + 0.66 \log K_{ow} - 0.0056 \text{MW} \quad (\text{Eq.4})$$

where  $K_{ow}$  is the octanol/water partition coefficient of the target antibiotic and MW is the molecular weight (g/mole).  $K_{ow}$  and MW of target antibiotics are summarized in *Table A5*.

The total exposure to each antibiotic through drinking water consumption (ADD) was defined as the sum of  $ADD_{dw}$  and  $ADD_{dermal}$ . The ADD for the population of one area in a given season was calculated as the sex ratio-weighted average ADD. Sex ratios for each city were taken from the *China Statistical Yearbook* (National Bureau of Statistics, 2018; sex ratio values summarized in *Table A6*).

### **Health risk assessment**

A health risk quotient (HRQ) is the ratio of a point estimate of exposure and a point estimate of health effects. HRQ for each antibiotic was calculated for each antibiotic by dividing its ADD by the acceptable daily intake (ADI) or risk-specific dose (RSD). HRQs were calculated using the most restrictive ADI or RSD for each antibiotic, which were adopted from provisional values established in the literature or derived using previously applied toxicological, microbiological or therapeutic approaches (Leung et al., 2013; Bengtsson-Palme and Larsson, 2016). The ADIs or RSDs used for HRQ calculation of each antibiotic are described in *Table A7*. The HRQ of each antibiotic in each city ( $HRQ_{ac}$ ) was defined as the maximum HRQ of the antibiotic among all sampling points in the city. The total HRQ in each city ( $HRQ_{tc}$ ) was the maximum value of the total HRQ for each sampling point ( $HRQ_{tp}$ ), where  $HRQ_{tp}$  was the sum of HRQs for each antibiotic from each sampling point.

## **Results**

### ***Distribution of antibiotics in drinking water***

Of 23 antibiotics quantified in this study, seventeen were detected in drinking water samples during the summer season, including three MLs, eight SAs, four QNs, one LN and one GP. Ten antibiotics were detected during the winter season, including one  $\beta$ L, two MLs, six SAs and one QN (*Fig. 2*). The detection rates and concentrations of antibiotics are summarized in *Table A8*. Detection rates in drinking water samples were above 70% during the summer for MLs, SAs and QNs, with median concentrations of 0.26 ng/L, 0.59 ng/L and 0.36 ng/L. During the winter, detection rates were above 70% only for MLs, with a median concentration of 0.46 ng/L.

The concentration levels of antibiotics in drinking water samples varied by city and season (*Fig. 3; Table A8*). In the summer, MLs were detected with a high median concentration of 10.12 ng/L in Guangzhou; the dominant ML was tylosin (range 6.82–15.04 ng/L). SAs and QNs were detected with high median concentrations of 2.73 ng/L and 3.41 ng/L respectively in Chaohu; the dominant antibiotics in these classes were sulfadiazine (0.81–5.20 ng/L), ciprofloxacin (1.17–1.94 ng/L), enrofloxacin (1.07–2.11 ng/L) and sarafloxacin (0.29–4.21 ng/L). SAs and QNs were also detected with high median concentrations of 1.73 ng/L and 6.40 ng/L, respectively, in Huainan; the dominant antibiotics in these classes were sulfamethoxazole (0.54–21.93 ng/L), sulfamethazine (0.11–7.63 ng/L), sulfadoxin (0.070–16.90 ng/L), ciprofloxacin (0.87–3.63 ng/L), enrofloxacin (1.97–4.47 ng/L) and sarafloxacin (0.82–1.64 ng/L). In the winter, SAs and MLs were detected with high median concentrations of 10.19 ng/L and 2.23 ng/L, respectively, in Mudanjiang; the dominant antibiotics in these classes were



sulfamethoxazole (1.27–6.82 ng/L), sulfadiazine (0.39–3.78 ng/L), trimethoprim (1.78–3.44 ng/L) and roxithromycin (0.39–17.28 ng/L). SAs were also detected in Lanzhou, Huainan and Chongqing with high median concentrations of 7.40 ng/L, 3.03 ng/L and 2.23 ng/L, respectively; the dominant SA in these cities was sulfamethoxazole (concentrations of 0.74–13.38 ng/L, 1.16–13.57 ng/L and 0.29–4.57 ng/L, respectively).

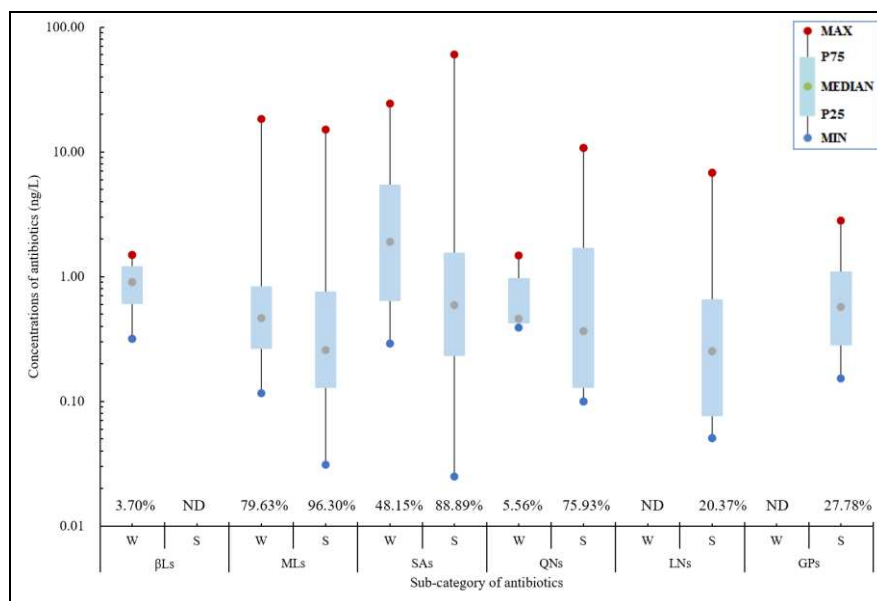


**Figure 2.** Concentrations of antibiotics in drinking water samples in China.  $\beta$ Ls,  $\beta$ -lactams; MLs, macrolides; SAs, sulfonamides; QNs, fluoroquinolones; LNs, lincosamides; GPs, glycopeptides; W, winter; S, summer; ND, not detected

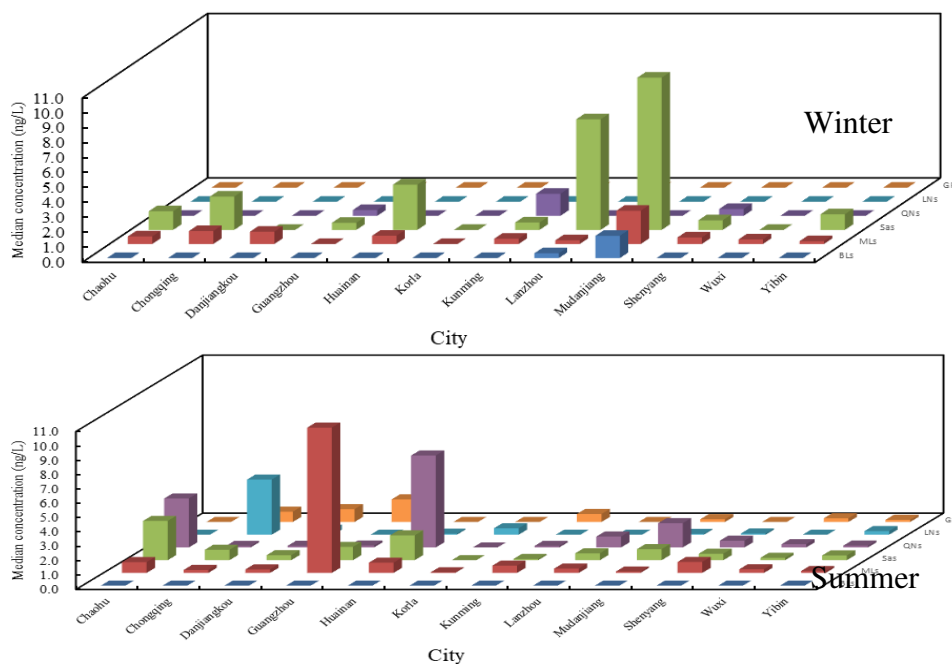


**Figure 3.** Spatiotemporal distribution of six sub-categories of antibiotics in drinking water by city.  $\beta$ Ls,  $\beta$ -lactams; MLs, macrolides; SAs, sulfonamides; QNs, fluoroquinolones; LNs, lincosamides; GPs, glycopeptides. Antibiotics were not detected in Korla in winter

### Human exposure to antibiotics contaminated drinking water consumption

Exposure to antibiotics from drinking water varied across cities (Fig. 4). The median exposure dose to total antibiotics from drinking water was 0.071 ng/kg/day during summer season and 0.029 ng/kg/day during winter season. During summer, the highest median antibiotic exposure was observed in Chaohu (0.68 ng/kg/day), where exposure mainly derived from exposure to SAs (24.61–98.07%) and QNs (1.16–73.16%). Relatively high antibiotic exposure levels were also observed in Huainan, with a median dose of 0.62 ng/kg/day, also derived mainly from exposure to SAs (12.62–84.68%) and QNs (7.93–77.79%). Finally, relatively high exposure levels were observed in Guangzhou (median dose 0.48 ng/kg/day), where exposure was mainly derived from MLs (3.42–90.57%). The highest exposure in winter was observed in Huainan (median dose 4.36 ng/kg/day). During winter, the highest median exposure level was observed in Mudanjiang (0.47 ng/kg/day), mainly derived from SAs (39.56–79.83%) and MLs (16.00–60.44%).

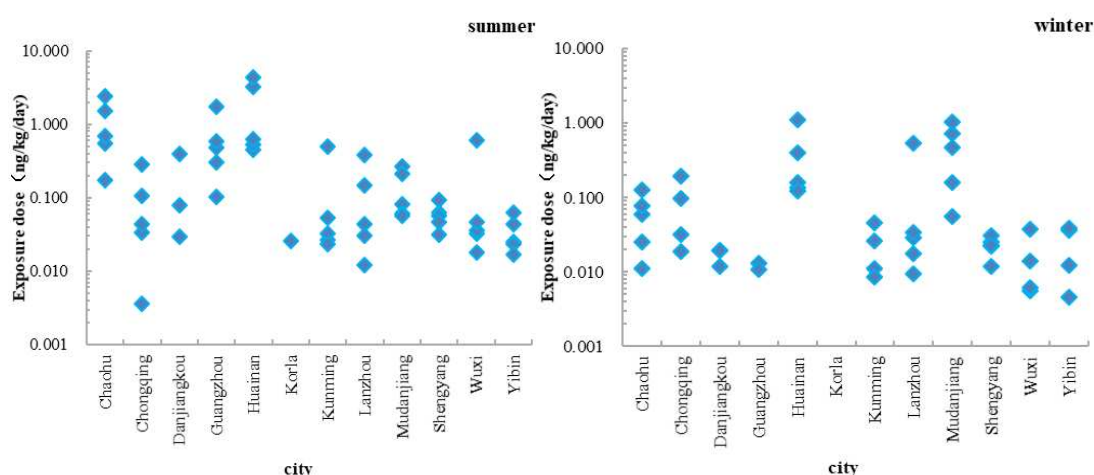


Figure 4. Total antibiotic exposure via drinking water by city, sampling point and season

Antibiotics were divided according to human or veterinary usage. Of 18 antibiotics detected in drinking water across summer and winter, 11 were used for both humans and animals, while 7 were used only for animals. Overall detection rates of veterinary antibiotics were 87.04% in the summer and 14.81% in the winter. Relatively high proportions of exposure to veterinary antibiotics were observed in Huainan, Guangzhou, Chaohu, Kunming and Mudanjiang during the summer, ranging from 22.71–58.44%, 44.73–97.64%, 16.14–57.41%, 40.51–97.30% and 30.91–69.31%, respectively (Fig. 5).

### Risk assessment of antibiotics in drinking water

Among the eighteen antibiotics detected in at least one sample, HRQs for each antibiotic at each sampling point ranged from  $1.8 \times 10^{-8}$  to 0.13 in the summer and from  $3.2 \times 10^{-7}$  to 0.020 in winter. The maximum HRQ of each antibiotic in each city by season and the  $HRQ_{tc}$  are shown in Figure 6. Antibiotics with  $HRQ \geq 0.01$  included three QNs (enrofloxacin, ciprofloxacin, sarafloxacin) and one ML (roxithromycin), with  $HRQ_{ac}$  ranging from  $4.4 \times 10^{-3}$  to 0.13,  $4.6 \times 10^{-3}$  to 0.11,  $2.2 \times 10^{-4}$  to  $1.5 \times 10^{-2}$  and  $5.8 \times 10^{-5}$  to  $1.8 \times 10^{-2}$ , respectively. Antibiotics with  $HRQ \geq 0.0001$  and  $< 0.01$

included one  $\beta$ L (cephalexin), two MLs (clarithromycin and tylosin), three SAs (trimethoprim, sulfamethoxazole and sulfamethazine), lincosycin and virginiamycin, with  $HRQ_{ac}$  ranging from  $9.3 \times 10^{-5}$  to  $3.9 \times 10^{-4}$ ,  $5.1 \times 10^{-4}$  to  $4.8 \times 10^{-3}$ ,  $2.1 \times 10^{-3}$  to  $4.5 \times 10^{-3}$ ,  $2.8 \times 10^{-4}$  to  $9.4 \times 10^{-3}$ ,  $1.2 \times 10^{-5}$  to  $2.7 \times 10^{-3}$ ,  $5.5 \times 10^{-6}$  to  $2.9 \times 10^{-4}$ ,  $3.3 \times 10^{-5}$  to  $3.5 \times 10^{-3}$  and  $9.5 \times 10^{-5}$  to  $1.7 \times 10^{-3}$ , respectively. High HRQs were observed in Huainan, Kunming and Mudanjiang in both summer and winter, whereas Chaohu, Shenyang and Lanzhou had high HRQs only in summer. Enrofloxacin was the main risk component in Kunming in both winter and summer, and in Huainan, Chaohu, Mudanjiang in the summer. Ciprofloxacin was the main risk component in Huainan, Chaohu, Mudanjiang in summer. Roxithromycin was the main risk component in Mudanjiang in winter and in Lanzhou in summer, and sarafloxacin was the main risk component in Chaohu during the summer.

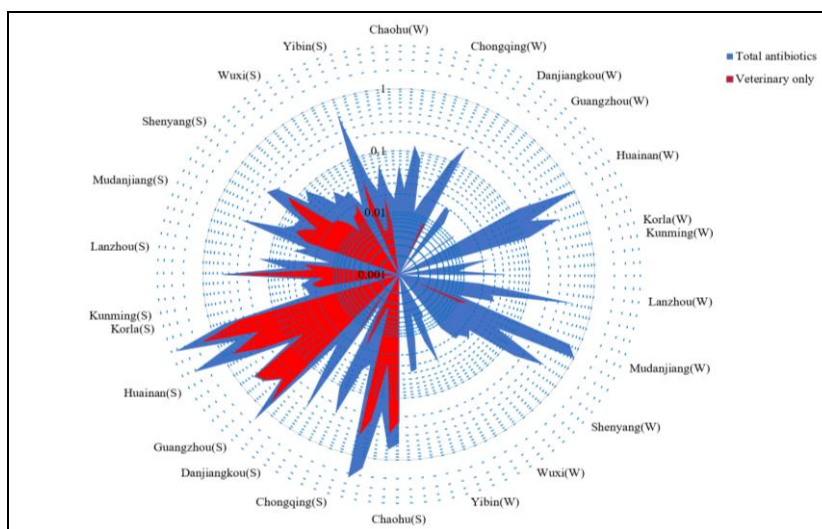


**Figure 5.** Contribution of exposure to veterinary antibiotics to total antibiotic exposure through drinking water by city and season. W, winter; S, summer

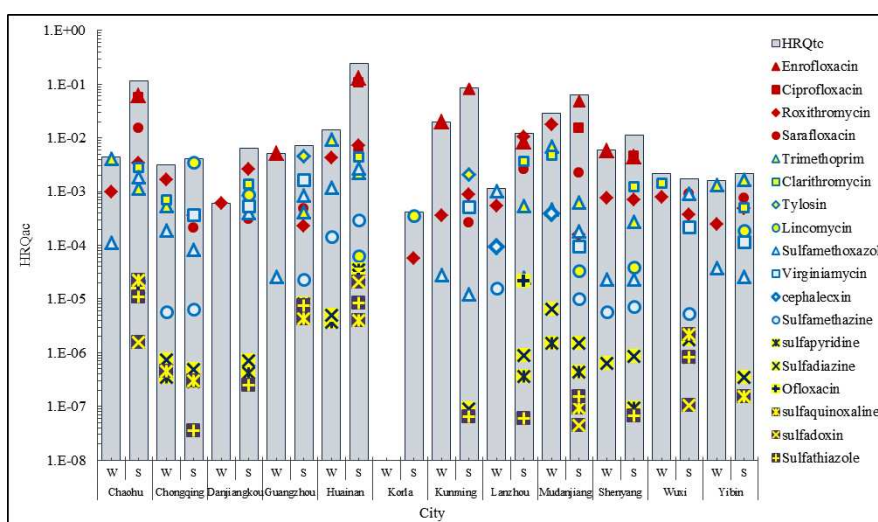


**Figure 6.**  $HRQ_{ac}$  and  $HRQ_{tc}$  profiles of detected antibiotics in drinking water by city and season.  $HRQ_{ac}$ , maximum health risk quotient of the antibiotic among all sampling points in the city;  $HRQ_{tc}$ , total  $HRQ$  in each city; W, winter; S, summer

## Discussion

In this study of antibiotic residues in drinking water from 12 cities in China, it was observed that large differences between regions and between summer and winter samples. Guangzhou, Chaohu and Huainan had the highest antibiotic levels in drinking water during the summer. Guangzhou is in the Pearl River Delta region located in South China and has among the highest antibiotic emission densities in China (Zhang et al., 2015). Chaohu and Huainan are in the Huaihe River watershed in eastern China and have the second highest antibiotic emission densities (Zhang et al., 2015). Exposure to antibiotics varied in summer and winter mainly because the dominant residues detected in drinking water. Among the dominant antibiotics detected during the summer months, tylosin, enrofloxacin and sarafloxacin are used only in veterinary medicine, indicating a significant contribution from increased usage of antibiotics in livestock, poultry breeding and aquaculture (Yang et al., 2011; He et al., 2016). The concentration of tylosin in drinking water in Guangzhou (6.82 ng/L to 15.04 ng/L) was higher than the residue level found in North Carolina, USA (4 ng/L, Ye et al., 2007). Although concentrations of SAs were relatively low in the summer compared to QNs and MLs, SAs did have high detection rates in both summer and winter, with high concentrations in Mudanjiang during winter. Sulfadiazine is widely used in veterinary medicine (Zheng et al., 2012). Sulfamethoxazole and sulfadiazine were grouped together, as sulfamethoxazole is used in veterinary medicine as well as in human medicine in China (Zhang et al., 2012).

The population of the 12 cities included in this study was generally exposed to antibiotics via water used for drinking and household purposes. Chaohu, Huainan and Guangzhou had summertime exposure doses that were more than five times the summertime exposures in other cities, whereas Mudanjiang had relatively high exposure doses in winter. Generally, human exposure to antibiotics comes from three sources: direct utilization, drinking water, and food (Wang et al., 2017). Urinary antibiotic levels were investigated in a general population study of adults aged 19 to 65 in Korea. Based on creatinine-adjusted urinary levels, the median daily intakes of sulfamethazine, trimethoprim, enrofloxacin and roxithromycin were estimated at 0.61 ng/kg/day, 0.054 ng/kg/day, 0.66 ng/kg/day, and 0.045 ng/kg/day, respectively, for men, and 0.73 ng/kg/day, 0.092 ng/kg/day, 0.71 ng/kg/day, 0.10 ng/kg/day, respectively, for women (Ji et al., 2010). The exposure contributions from drinking water to levels of these four antibiotics were 24%, 1.6%, 10%, and 46% for men and 11%, 1.5%, 9% and 26% for women. Sulfapyridine and sulfaquinoxaline, which are used only for animals, were not detected in meat, milk or aquatic products in Shanghai (Wang et al., 2017), indicating that the main exposure pathway for these two antibiotics is through drinking water, with particularly high exposures in winter. Some studies indicated that long-time boiling can break antibiotic residues in food (Tian et al., 2017). However, the effect of short-time boiling for antibiotic residues remove had not been well explored. In this study, drinking water boiling and indirect intake of water by food domestic cooking (such as rice and noodle) was not included. Additionally, this study evaluated the exposure in good weather in summer and winter, not considering the effect of rainy and snowy weather on water quality. Human exposure to antibiotics via medication use, food consumption and drinking water have not been well explored at the global level, and further investigation is required to improve understanding of the relative contribution of each of these pathways.

The HRQs of antibiotics varied across the different cities included in the study. Huainan, Chaohu, Kunming and Mudanjiang had relatively high HRQs in the summer, largely because the main antibiotic residues in these cities were enrofloxacin and ciprofloxacin, which had more restrictive ADIs for resistance selection pressure than other antibiotics. Among the four antibiotics with  $HRQ \geq 0.01$ , enrofloxacin and sarafloxacin are used only in veterinary medicine, whereas ciprofloxacin and roxithromycin are used in both human and veterinary medicine. The use of ciprofloxacin on animals in China is restricted, but in light of poor supervision, ciprofloxacin is still widely detected in water (including drinking water), soil, and food (Li et al., 2012; Xu et al., 2015; Wang et al., 2017). Based on the findings of our study, all the antibiotics detected posed a health risk less than 100%, though several posed significant risks. However, there are potential uncertainties in our analyses. Toxicities stemming from chronic exposure to trace amounts of antibiotic mixtures are not yet well understood (Rodriguez-Mozaz and Weinberg, 2010). Moreover, our assessment considered the relative source contribution (RSC) of ADIs from drinking water usage to be 100% based on a previous study (Leung et al., 2013). Based on a conservative estimate of RSC of 20%, the HRQs of antibiotics would increase five-fold, and these antibiotics would then pose potential health risks in Huainan during the summer ( $HRQ_{ct} > 1$ ).

## Conclusion

This study quantifies the seasonal and spatial distributions of 23 antibiotics in drinking water from 12 cities in different water basins in China. Exposure to antibiotics via drinking water and its potential risk are described. In light of the widespread detection of antibiotics in potable water, it appears that drinking water constitutes the main pathway for human exposure to antibiotics (especially veterinary antibiotics) in China. Among the antibiotics measured in our study, enrofloxacin, ciprofloxacin, roxithromycin and sarafloxacin were identified as posing the largest risk to human health. Moreover, there need further researches on adverse effects induced by exposure to antibiotics among sensitive groups such as children and pregnant women. The risk of antibiotic resistance by antibiotic exposure via drinking water also needs further studies for more precise evaluation.

## Recommendations

Of 23 antibiotics measured, more than eight were detected in all 12 cities investigated, with the exception of Korla during the summer, indicating widespread population exposure to antibiotics via drinking water. Upgrading current treatment technologies of DWTPs is a possible mitigation measure (Li et al., 2018). Further test and evaluation of advanced treatments like ozonation, GAC filtration, nanofiltration and reverse osmosis need to be conducted (Yang et al., 2017). Controlling antibiotic inputs to water source is also highly recommended. Insufficient sewage treatment is a dominant factor explaining contamination of Chinese water sources (Li et al., 2014). Improved waste water treatment and control of the treatment process have to be employed for removal of these contaminants, and more research is needed to evaluate their behavior and fate in aquatic environment.

Restriction of antibiotic usage at national level would like to be an effective measure to reduce the emission of antibiotics. In our study, enrofloxacin, ciprofloxacin, roxithromycin and sarafloxacin were identified as posing the largest risk to human health. Two of these antibiotics were used only in veterinary medicine, indicating a significant contribution from increased usage of antibiotics in livestock, poultry breeding and aquaculture. Restriction of veterinary antibiotic usage in agriculture and aquaculture would likely lead to reduced human exposure to antibiotics via drinking water, especially during the summer. Further study is needed to ascertain the causes of antibiotic usages and to make practical regulations for reducing the usage.

Improved supervision, surveillance and management plan should be implemented to limit the unnecessary use of antibiotics, especially in veterinary medicine. A comprehensive behavioral change communication strategy is central to the success of reduce risks of antibiotics exposure. Specific plans should be designed to restrict the use of antibiotic with high HRQ. Increased supervision is warranted to limit the usage of these antibiotics and to monitor their levels in drinking water.

**Acknowledgements.** This research is supported by the National Key R&D Program of China [2018YFC0407502, 2016YFD0801004]; the Science and Technology Project of Beautiful China Ecological Civilization Construction [XDA23100403]; and the Young Elite Scientist Sponsorship Program of Beijing Association for Science and Technology (2020-2022).

## REFERENCES

- [1] Aga, D. S., Lenczewski, M., Snow, D., Muurinen, J., Sallach, J. B., Wallace, J. S. (2016): Challenges in the measurement of antibiotics and in evaluating their impacts in agroecosystems: a critical review. – *Journal of Environment Quality* 45(2): 407-419. <https://doi.org/10.2134/jeq2015.07.0393>.
- [2] Bedford, M. (2000): Removal of antibiotic growth promoters from poultry diets: implications and strategies to minimise subsequent problems. – *World's Poultry Science Journal* 56(4): 347-365.
- [3] Bengtsson-Palme, J., Larsson, D. G. J. (2016): Concentrations of antibiotics predicted to select for resistant bacteria: proposed limits for environmental regulation. – *Environment International* 86: 140-149. <https://doi.org/10.1016/j.envint.2015.10.015>.
- [4] Benotti, M. J., Trenholm, R. A., Vanderford, B. J., Holady, J. C., Stanford, B. D., Snyder, S. A. (2009): Pharmaceuticals and endocrine disrupting compounds in U.S. drinking water. – *Environmental Science & Technology* 43(3): 597-603. <https://doi.org/10.1021/es801845a>.
- [5] Brown, T. N., Armitage, J. M., Egeghy, P., Kircanski, I., Arnot, J. A. (2016): Dermal permeation data and models for the prioritization and screening-level exposure assessment of organic chemicals. – *Environment International* 94: 424-435. <https://doi.org/10.1016/j.envint.2016.05.025>.
- [6] Carmona, E., Andreu, V., Picó, Y. (2014): Occurrence of acidic pharmaceuticals and personal care products in Turia River Basin: from waste to drinking water. – *Science of the Total Environment* 484: 53-63. <https://doi.org/10.1016/j.scitotenv.2014.02.085>.
- [7] China EPA. (2009): *Exposure Factors Handbook of Chinese Population*. – China Environmental Press, Beijing.
- [8] de Jesus Gaffney, V., Almeida, C. M. M., Rodrigues, A., Ferreira, E., Benoliel, M. J., Cardoso, V. V. (2015): Occurrence of pharmaceuticals in a water supply system and

- related human health risk assessment. – *Water Research* 72: 199-208. <https://doi.org/10.1016/j.watres.2014.10.027>.
- [9] Duan, X. L., Zhang, W. J., Wang, Z. S., Guo, Y. M., Zhang, Y. S., Zhang, J. L. (2010): Water related activity and dermal exposure factors of people in typical areas of Northern China. – *Research of Environmental Sciences* 23(1): 55-61. <https://doi.org/10.13198/j.res.2010.01.57.duanxl.009>.
- [10] Gullberg, E., Cao, S., Berg, O. G., Ilbäck, C., Sandegren, L., Hughes, D., Andersson, D. I. (2011): Selection of resistant bacteria at very low antibiotic concentrations. – *PLoS Pathogens* 7(7): e1002158. <https://doi.org/10.1371/journal.ppat.1002158>.
- [11] He, X., Deng, M., Wang, Q., Yang, Y., Yang, Y., Nie, X. (2016): Residues and health risk assessment of quinolones and sulfonamides in cultured fish from Pearl River Delta, China. – *Aquaculture (Amsterdam, Netherlands)* 458: 38-46. <https://doi.org/10.1016/j.aquaculture.2016.02.006>.
- [12] Huang, C., Ding, X., Zhang, L., Zhou, W. (2017): Analysis on drinking water exposure in Wuxi residents. – *Journal of Environmental Hygiene* 7(2): 95-101. <https://doi.org/10.13421/j.cnki.hjwsxzz.2017.02.003>.
- [13] Ji, K., Kho, Y., Park, C., Paek, D., Ryu, P., Paek, D., Kim, M., Kim, P., Choi, K. (2010): Influence of water and food consumption on inadvertent antibiotics intake among general population. – *Environmental Research* 110(7): 641-649. <https://doi.org/10.1016/j.envres.2010.06.008>.
- [14] Knapp, C. W., Dolfing, J., Ehlert, P. A. I., Graham, D. W. (2010): Evidence of increasing antibiotic resistance gene abundances in archived soils since 1940. – *Environmental Science & Technology* 44(2): 580-587. <https://doi.org/10.1021/es901221x>.
- [15] Kümmerer, K. (2009): Antibiotics in the aquatic environment—a review—part I. – *Chemosphere* 75(4): 417-434. <https://doi.org/10.1016/j.chemosphere.2008.11.086>.
- [16] Le Page, G., Gunnarsson, L., Snape, J., Tyler, C. R. (2017): Integrating human and environmental health in antibiotic risk assessment: a critical analysis of protection goals, species sensitivity and antimicrobial resistance. – *Environment International* 109: 155-169. <https://doi.org/10.1016/j.envint.2017.09.013>.
- [17] Leung, H. W., Jin, L., Wei, S., Tsui, M. M. P., Zhou, B., Jiao, L., Cheung, P. C., Chun, Y. K., Murphy, M. B., Lam, P. K. S. (2013): Pharmaceuticals in tap water: human health risk assessment and proposed monitoring framework in China. – *Environmental Health Perspectives* 121(7): 839-846. <https://doi.org/10.1289/ehp.1206244>.
- [18] Li, W., Shi, Y., Gao, L., Liu, J., Cai, Y. (2012): Occurrence of antibiotics in water, sediments, aquatic plants, and animals from Baiyangdian Lake in North China. – *Chemosphere* 89(11): 1307-1315. <https://doi.org/10.1016/j.chemosphere.2012.05.079>.
- [19] Li, X., Shi, H., Li, K., Zhang, L., Gan, Y. (2014): Occurrence and fate of antibiotics in advanced wastewater treatment facilities and receiving rivers in Beijing, China. – *Frontiers of Environmental Science & Engineering* 8(6): 888-894. <https://doi.org/10.1007/s11783-014-0735-0>.
- [20] Li, G., Yang, H., An, T., Lu, Y. (2018): Antibiotics elimination and risk reduction at two drinking water treatment plants by using different conventional treatment techniques. – *Ecotoxicology and Environmental Safety* 158: 154-161. <https://doi.org/10.1016/j.ecoenv.2018.04.019>.
- [21] Lv, J., Zhang, L., Chen, Y., Ye, B., Han, J., Jin, N. (2019): Occurrence and distribution of pharmaceuticals in raw, finished, and drinking water from seven large river basins in China. – *Journal of Water and Health* 17(3): 477-489. <https://dx.doi.org/10.2166/wh.2019.250>.
- [22] Ma, Y., Li, M., Wu, M., Li, Z., Liu, X. (2015): Occurrences and regional distributions of 20 antibiotics in water bodies during groundwater recharge. – *Science of the Total Environment* 518-519: 498-506. <https://doi.org/10.1016/j.scitotenv.2015.02.100>.



- [23] Rodriguez-Mozaz, S., Weinberg, H. S. (2010): Meeting report: pharmaceuticals in water—an interdisciplinary approach to a public health challenge. – *Environmental Health Perspectives* 118(7): 1016-1020. <https://doi.org/10.1289/ehp.0901532>.
- [24] Sarmah, A. K., Meyer, M. T., Boxall, A. B. A. (2006): A global perspective on the use, sales, exposure pathways, occurrence, fate and effects of veterinary antibiotics (VAs) in the environment. – *Chemosphere* 65(5): 725-759. <https://doi.org/10.1016/j.chemosphere.2006.03.026>.
- [25] ten Berge, W. (2010): QSARs for skin permeation of chemicals. – <https://home.wxs.nl/~wtberge/qsarperm.html>.
- [26] Tian, L., Khalil, S., Bayen, S. (2017): Effect of thermal treatments on the degradation of antibiotic residues in food. – *Critical Reviews in Food Science and Nutrition* 57(17): 3760. <https://doi.org/10.1080/10408398.2016.1164119>.
- [27] Wang, H., Ren, L., Yu, X., Hu, J., Chen, Y., He, G., Jiang, Q. (2017): Antibiotic residues in meat, milk and aquatic products in Shanghai and human exposure assessment. – *Food Control* 80: 217-225. <https://doi.org/10.1016/j.foodcont.2017.04.034>.
- [28] Xu, Y., Chen, T., Wang, Y., Tao, H., Liu, S., Shi, W. (2015): The occurrence and removal of selected fluoroquinolones in urban drinking water treatment plants. – *Environmental Monitoring and Assessment* 187(12): 729. <https://doi.org/10.1007/s10661-015-4963-y>.
- [29] Xu, Z., Li, T., Bi, J., Wang, C. (2018): Spatiotemporal heterogeneity of antibiotic pollution and ecological risk assessment in Taihu Lake Basin, China. – *Science of the Total Environment* 643: 12-20. <https://doi.org/10.1016/j.scitotenv.2018.06.175>.
- [30] Yang, J. F., Ying, G. G., Zhao, J. L., Tao, R., Su, H. C., Liu, Y. S. (2011): Spatial and seasonal distribution of selected antibiotics in surface waters of the Pearl Rivers, China. – *Journal of Environmental Science and Health, Part B* 46(3): 272-280. <https://doi.org/10.1080/03601234.2011.540540>.
- [31] Yang, Y., Sik Ok, Y., Kim, K. H., Kwon, E. E., Tsang, Y. F. (2017): Occurrences and removal of pharmaceuticals and personal care products (PPCPs) in drinking water and water/sewage treatment plants: a review. – *Science of the Total Environment* 596-597: 303-320. <http://dx.doi.org/10.1016/j.scitotenv.2017.04.102>.
- [32] Ye, Z., Weinberg, H. S., Meyer, M. T. (2007): Trace analysis of trimethoprim and sulfonamide, macrolide, quinolone, and tetracycline antibiotics in chlorinated drinking water using liquid chromatography electrospray tandem mass spectrometry. – *Analytical Chemistry* 79(3): 1135-1144. <https://doi.org/10.1021/ac060972a>.
- [33] Zhang, R., Zhang, G., Tang, J., Xu, W., Li, J., Liu, X., Zou, Y., Chen, X., Li, X. (2012): Levels, spatial distribution and sources of selected antibiotics in the East River (Dongjiang), South China. – *Aquatic Ecosystem Health & Management* 15(2): 210-218. <https://doi.org/10.1080/14634988.2012.689576>.
- [34] Zhang, Q. Q., Ying, G. G., Pan, C. G., Liu, Y. S., Zhao, J. L. (2015): Comprehensive evaluation of antibiotics emission and fate in the river basins of China: source analysis, multimedia modeling, and linkage to bacterial resistance. – *Environmental Science & Technology* 49(11): 6772-6782. <https://doi.org/10.1021/acs.est.5b00729>.
- [35] Zheng, Q., Zhang, R., Wang, Y., Pan, X., Tang, J., Zhang, G. (2012): Occurrence and distribution of antibiotics in the Beibu Gulf, China: impacts of river discharge and aquaculture activities. – *Marine Environmental Research* 78: 26-33. <https://doi.org/10.1016/j.marenvres.2012.03.007>.



## APPENDIX

### **Risk assessment of prevalence of antibiotics in drinking water and impacts on human health exposed to antibiotic contamination – China**

#### *Analysis method (Lv et al., 2019)*

##### *Sample extraction*

Target analytes were extracted from the water samples using SPE. One liter water samples were acidified to pH 2.0–2.5 with phosphoric acid and potassium phosphate monobasic. The samples were spiked with isotopically labeled standards, at a concentration of 20 ng, and 500 mg EDTA-2Na were added. Detailed information on internal standards is shown in *Table A1*.

The water samples were loaded on the automated SPE system at an approximate rate of 5 mL/min (Visiprep-DL 24-Ports SPE Vacuum Manifold, Supelco, USA). Oasis hydrophilic-lipophilic balance (HLB) cartridges (6 mL, 200 mg of sorbent, Waters, USA) were used for sample pretreatment. The cartridges were conditioned with 10 mL methanol and 10 mL ultrapure water prior to sample loading. After sample loading, the cartridges were rinsed with 10 mL ultrapure water, dried for 10 min under vacuum and eluted with 10 mL methanol. The eluates were concentrated to near dryness under a gentle stream of nitrogen in a 30 °C water bath and reconstituted in 1 mL of water/methanol (95/5; v/v). The concentrated extracts were then analyzed by UPLC–MS/MS.

##### *UPLC-MS/MS analysis*

A UPLC system (ACQUITY UPLC, Waters, USA) equipped with a Waters ACQUITY UPLC HSS T3 column (100 mm × 2.1 mm and 1.8 µm particle size) was used to separate the analytes. The column temperature was 40 °C, the injection volume was 10 µL, and the flow rate was 0.35 mL/min. The mobile phases consisted of water with 0.1% (v/v) formic acid (A) and methanol (B), and the following elution program was employed: 95% (A) to 80% (A) from 0 to 3 min, 80% to 70% (A) from 3 to 6 min, 70% to 60% (A) from 6 to 10 min, 60% to 30% (A) from 10 to 12 min, 30% to 5% (A) from 12 to 15 min, and then 95% (A) from 15 to 15.5 min. Finally, the column was re-equilibrated for 2.5 min before the next injection, for a total run time of 18 min.

A Waters TQ-S micro triple quadrupole mass spectrometer (Waters Technologies, USA) equipped with an electrospray ion source was used for the analysis of the pharmaceuticals. Multiple reaction monitoring (MRM) mode was used for quantitative analysis, and all pharmaceuticals were measured in positive ion mode. The source temperature was 120 °C, the desolvation temperature was 350 °C, the desolvation gas flow was 650 L/h, the collision gas flow was 50 L/h, and the capillary voltage was 2.0 kV.

##### *Method performance and quality assurance*

The determination of linearity, LOD and LOQ, recovery and precision were used to validate the method. Calibration curves were generated using mixtures of standards at concentrations from 0.05 to 100 µg/L and isotopically-labeled internal standards at a

concentration of 20 µg/L. Good linearity was observed, with correlation coefficients greater than 0.99.

The analytes were identified by their retention times, two characteristic ion transitions and specific ion ratios (deviation < 20% with respect to analytical standard ratios). Spiked ultrapure water with various concentrations were extracted and analyzed to determine the LOD and LOQ. The LOD and LOQ were defined as the lowest concentrations that gave signal-to-noise ratios greater than 3 and 10, respectively.

Field blanks and method blanks were created to identify any contaminant from the sampling site and analysis process. Recovery and precision were used to validate the method performance. Percent recovery and precision were determined using ultrapure water and spiked matrix samples (raw water and finished water) at three concentrations (5, 10, and 40 ng/L) and the IS solution (20 ng/L). Six replicates of each concentration were used to evaluate the analyte recovery during sample pretreatment and UPLC-MS/MS analysis. The recoveries as expressed as the average of six replicates. The recoveries and precision varied with the natures of the analytes, and an acceptable result was generated (U.S. EPA, 2007).

**Table A1.** Detailed information about target analytes standards and internal standards. *β*LS, *β*-lactams; MLs, macrolides; SAs, sulfonamides; QNs, fluoroquinolones; LN, lincosamide; GP, glycopeptide. IS, Internal standard

Antibiotics	CAS No.	Class of antibiotics	Molecular formula	Molecular weight
Penicillin G	61-33-6	βLS	C <sub>16</sub> H <sub>17</sub> N <sub>2</sub> O <sub>4</sub> S	334.39
Cloxacillin	61-72-3	βLS	C <sub>19</sub> H <sub>18</sub> ClN <sub>3</sub> O <sub>5</sub> S	435.88
Cephalexin	23325-78-2	βLS	C <sub>16</sub> H <sub>17</sub> N <sub>3</sub> O <sub>4</sub> S	365.4
Ceftiofur	80370-57-6	βLS	C <sub>19</sub> H <sub>17</sub> N <sub>5</sub> O <sub>7</sub> S <sub>3</sub>	523.56
Clarithromycin	81103-11-9	MLs	C <sub>38</sub> H <sub>69</sub> NO <sub>13</sub>	747.95
Roxithromycin	80214-83-1	MLs	C <sub>41</sub> H <sub>76</sub> N <sub>2</sub> O <sub>15</sub>	837.05
Tylosin	1401-69-0	MLs	C <sub>46</sub> H <sub>77</sub> NO <sub>17</sub>	916.1
Sulfapyridine	144-83-2	SAs	C <sub>11</sub> H <sub>11</sub> N <sub>3</sub> O <sub>2</sub> S	249.29
Sulfadiazine	68-35-9	SAs	C <sub>10</sub> H <sub>10</sub> N <sub>4</sub> O <sub>2</sub> S	250.28
Sulfamethoxazole	723-46-6	SAs	C <sub>10</sub> H <sub>11</sub> N <sub>3</sub> O <sub>3</sub> S	253.28
Sulfathiazole	72-14-0	SAs	C <sub>9</sub> H <sub>9</sub> N <sub>3</sub> O <sub>2</sub> S <sub>2</sub>	255.32
Sulfamethazine	57-68-1	SAs	C <sub>12</sub> H <sub>14</sub> N <sub>4</sub> O <sub>2</sub> S	278.33
Sulfaquinoxaline	59-40-5	SAs	C <sub>14</sub> H <sub>12</sub> N <sub>4</sub> O <sub>2</sub> S	300.34
Sulfadoxin	2447-57-6	SAs	C <sub>12</sub> H <sub>14</sub> N <sub>4</sub> O <sub>4</sub> S	310.33
Trimethoprim	738-70-5	SAs	C <sub>14</sub> H <sub>18</sub> N <sub>4</sub> O <sub>3</sub>	290.32
Norfloxacin	70458-96-7	QNs	C <sub>16</sub> H <sub>18</sub> FN <sub>3</sub> O <sub>3</sub>	319.33
Ciprofloxacin	85721-33-1	QNs	C <sub>17</sub> H <sub>18</sub> FN <sub>3</sub> O <sub>3</sub>	331.34
Enrofloxacin	93106-60-6	QNs	C <sub>19</sub> H <sub>22</sub> FN <sub>3</sub> O <sub>3</sub>	359.39
Ofloxacin	82419-36-1	QNs	C <sub>18</sub> H <sub>20</sub> FN <sub>3</sub> O <sub>4</sub>	361.37
Clinafloxacin	105956-97-6	QNs	C <sub>17</sub> H <sub>17</sub> ClFN <sub>3</sub> O <sub>3</sub>	365.79
Sarafloxacin	98105-99-8	QNs	C <sub>20</sub> H <sub>17</sub> F <sub>2</sub> N <sub>3</sub> O <sub>3</sub>	385.36
Lincomycin	154-21-2	LN	C <sub>18</sub> H <sub>34</sub> N <sub>2</sub> O <sub>6</sub> S	406.54
Virginiamycin	11006-76-1	GP	C <sub>28</sub> H <sub>35</sub> N <sub>3</sub> O <sub>7</sub>	525.59
D <sub>8</sub> -Ciprofloxacin	—	IS	C <sub>17</sub> H <sub>10</sub> D <sub>8</sub> FN <sub>3</sub> O <sub>3</sub>	339.39
<sup>13</sup> C <sub>6</sub> -Sulfamethazine	—	IS	C <sub>6</sub> <sup>13</sup> C <sub>6</sub> H <sub>14</sub> N <sub>4</sub> O <sub>2</sub> S	284.29
<sup>13</sup> C <sub>3</sub> -Trimethoprim	—	IS	C <sub>11</sub> <sup>13</sup> C <sub>3</sub> H <sub>18</sub> N <sub>4</sub> O <sub>3</sub>	293.3
<sup>13</sup> C-D <sub>3</sub> -Erythromycin	—	IS	C <sub>36</sub> <sup>13</sup> CH <sub>64</sub> D <sub>3</sub> NO <sub>13</sub>	737.94
D <sub>3</sub> -Lincomycin	—	IS	C <sub>18</sub> H <sub>31</sub> D <sub>3</sub> N <sub>2</sub> O <sub>6</sub> S	409.56
D <sub>5</sub> -cephalexin	—	IS	C <sub>16</sub> H <sub>14</sub> D <sub>5</sub> N <sub>3</sub> O <sub>4</sub> S	370.43
<sup>13</sup> C <sub>6</sub> -Sulfamethoxazole	—	IS	C <sub>4</sub> <sup>13</sup> C <sub>6</sub> H <sub>11</sub> N <sub>3</sub> O <sub>3</sub> S	259.21
D <sub>8</sub> -Sarafloxacin	—	IS	C <sub>20</sub> H <sub>9</sub> D <sub>8</sub> F <sub>2</sub> N <sub>3</sub> O <sub>3</sub>	393.4

**Table A2.** *IngR values corresponding to area, season and sex in China*

<b>Area</b>	<b>Season</b>	<b>Gender</b>	<b>IngR (L/day)</b>
Liaoning	winter	male	1742
Heilongjiang	winter	male	1881
Jiangsu	winter	male	2267
Anhui	winter	male	2944
Hubei	Winter	Male	1500
Guangdong	Winter	Male	1695
Chongqing	Winter	Male	1215
Sichuan	Winter	Male	1862
Yunnan	Winter	Male	1895
Gansu	Winter	Male	2587
Xinjiang	Winter	Male	2974
Liaoning	Summer	Male	2090
Heilongjiang	Summer	Male	2196
Jiangsu	Summer	Male	3204
Anhui	Summer	Male	4063
Hubei	Summer	Male	2570
Guangdong	Summer	Male	2411
Chongqing	Summer	Male	2053
Sichuan	Summer	Male	3184
Yunnan	Summer	Male	2719
Gansu	Summer	Male	3990
Xinjiang	Summer	Male	3716
Liaoning	Winter	Female	1425
Heilongjiang	Winter	Female	2180
Jiangsu	Winter	Female	1817
Anhui	Winter	Female	2432
Hubei	Winter	Female	1366
Guangdong	Winter	Female	1663
Chongqing	Winter	Female	1293
Sichuan	Winter	Female	1691
Yunnan	Winter	Female	1492
Gansu	Winter	Female	2050
Xinjiang	Winter	Female	2086
Liaoning	Summer	Female	1706
Heilongjiang	Summer	Female	1826
Jiangsu	Summer	Female	2558
Anhui	Summer	Female	3423
Hubei	Summer	Female	2376
Guangdong	Summer	Female	2347
Chongqing	Summer	Female	2164
Sichuan	Summer	Female	3062
Yunnan	Summer	Female	2203
Gansu	Summer	Female	3133
Xinjiang	Summer	Female	2703

**Table A3.** The skin surface area available for contact (cm<sup>2</sup>)

SA <sub>i</sub> (cm <sup>2</sup> )	Hand cleaning	Face and hair cleaning	Foot cleaning	Dish washing	Vegetable washing	Clothes washing	Bathing	Swimming
Male	800	1300	1100	800	800	800	17000	6300
Female	700	1200	1000	700	700	700	15000	5700

**Table A4.** The time of contact (T, hours/day) on water usage habits in northern and southern China

Time of contact (hours/day)	Hand cleaning	Face and hair cleaning	Foot cleaning	Dishes washing	Vegetable washing	Clothes washing	Bathing	Swimming
Male in South China	0.0500	0.0783	0.0167	0.0000	0.0000	0.0000	0.1750	0.086
Female in South China	0.0667	0.1117	0.0117	0.0850	0.0717	0.0467	0.2083	0.088
Male in North China	0.0627	0.1012	0.0146	0.0115	0.0091	0.0462	0.2553	0.086
Female in North China	0.0614	0.1168	0.0165	0.1606	0.1364	0.3050	0.2424	0.088

**Table A5.** Kow and MW of target antibiotics

Antibiotic	log Kow	MW (g/mol)
Penicillin G	1.83	334.38
Cloxacillin	2.44	435.88
Cephalexin	0.65	347.39
Ceftiofur	1.6	523.57
Clarithromycin	3.16	747.95
Roxithromycin	2.21	837.05
Tylosin	1.63	916.11
Sulfapyridine	0.35	249.29
Sulfadiazine	2.59	250.27
Sulfamethoxazole	0.89	253.28
Sulfathiazole	0.05	255.32
Sulfamethazine	0.14	278.33
Sulfaquinoxaline	1.68	300.34
Sulfadoxin	0.43	310.33
Norfloxacin	0.46	319.33
Ciprofloxacin	0.28	331.34
Enrofloxacin	0.64	359.4
Ofloxacin	-0.39	371.37
Sarafloxacin	0.57	385.36
Lincomycin	0.2	406.54
Trimethoprim	0.91	290.32

**Table A6.** Sex ratios for each city

City	Gender ratio (population of male/population of female)
Chaohu	0.5162
Chongqing	0.5127
Danjiangkou	0.5158
Guangzhou	0.5016
Huainan	0.525
Kuerle	0.5109
Kunming	0.5141
Lanzhou	0.5037
Mudanjiang	0.501
Shenyang	0.4941
Wuxi	0.5033
Yibin	0.5197

**Table A7.** The acceptable daily intake (ADI) or risk-specific dose (RSD) used for HRQ calculation of each antibiotic

Antibiotic	ADI or RSD (ug/kg/day)	Toxicity or effect endpoint
Cephalexin	0.13	Resistance selection
Clarithromycin	0.0083	Resistance selection
Roxithromycin	0.033	Resistance selection
Tylosin	0.13	Resistance selection
Sulfapyridine	10	Microbiological
Sulfadiazine	20	Reduced fetal bodyweight and C-R length at the next higher dose
Sulfamethoxazole	0.5	Resistance selection
Sulfathiazole	50	Changes in thyroid tissue. a NOEL of 5 mg/kg for the thyroid effects in animal studies
Sulfamethazine	1.6	Thyroid gland follicular adenoma in rats with tumor incidence data
Sulfaquinoxaline	10	Increased thyroid weights at the next higher dose
Sulfadoxin	50	Increased liver weights at the next higher dose
Norfloxacin	0.017	Resistance selection
Ciprofloxacin	0.0021	Resistance selection
Enrofloxacin	0.0021	Resistance selection
Ofloxacin	3.2	Microbiological
Sarafloxacin	0.017	Resistance selection
Lincomycin	0.067	Resistance selection
Virginiamycin	0.067	Resistance selection
Trimethoprim	0.017	Resistance selection

**Table A8.** The significance level of the antibiotic concentrations across cities and seasons

Class of antibiotics	Nonparametric tests	Significance level	
		Across seasons	Across cities
β-lactams	Mann Whitney U test	0.206	—
	Kolmogorov-Smirnov test	0.001*	—
	Wald Wolfwitz Runs	—	—
	Median test	—	0.0001*
	Kruskal-Wallis test	—	0.0001*
Macrolides	Mann Whitney U test	0.065	—
	Kolmogorov-Smirnov test	0.007*	—
	Wald Wolfwitz Runs	0.002*	—
	Median test	—	0.0001*
	Kruskal-Wallis test	—	0.0001*
Sulfonamides	Mann Whitney U test	0.0001*	—
	Kolmogorov-Smirnov test	0.0001*	—
	Wald Wolfwitz Runs	0.0001*	—
	Median test	—	0.0001*
	Kruskal-Wallis test	—	0.0001*
Fuoroquinolones	Mann Whitney U test	0.0001*	—
	Kolmogorov-Smirnov test	0.0001*	—
	Wald Wolfwitz Runs	0.0001*	—
	Median test	—	0.0001*
	Kruskal-Wallis test	—	0.015*
Lincosamide	Mann Whitney U test	0.0001*	—
	Kolmogorov-Smirnov test	0.187	—
	Wald Wolfwitz Runs	0.0001*	—
	Median test	—	0.0001*
	Kruskal-Wallis test	—	0.0001*
Glycopeptide	Mann Whitney U test	0.0001*	—
	Kolmogorov-Smirnov test	0.034*	—
	Wald Wolfwitz Runs	0.0001*	—
	Median test	—	0.0001*
	Kruskal-Wallis test	—	0.0001*

Mann Whitney U test, Kolmogorov-Smirnov test and Wald Wolfwitz Runs were conducted for the seasonal differences between winter and summer; Median test and Kruskal-Wallis test were conducted for the spatial differences across 12 cities. \*The significance level is 0.05

# ANALYSIS OF THE MICROCYSTIN-LR PRODUCTION ABILITY OF METAGENOMIC *MCY* GENES IN FRESHWATER AQUACULTURE PONDS FOCUSING ON THE ABUNDANCE OF METAGENOMIC *MCY* GENES AND SNP

DONG, S. J.<sup>1</sup> – BI, X. D.<sup>1\*</sup> – ZHANG, J. Y.<sup>2</sup> – DAI, W.<sup>1\*</sup> – ZHANG, P. P.<sup>3</sup> – ZHOU, K. R.<sup>3</sup> – WANG, X. Y.<sup>1</sup> – ZHANG, D. J.<sup>1</sup>

<sup>1</sup>Key Laboratory for Aqua-Ecology and Aquaculture of Tianjin, Department of Fisheries Science, Tianjin Agricultural University, Tianjin 300384, China

<sup>2</sup>Algae-Hub Big Data Center, MetaBio Science & Technology Co., Ltd., Wuxi 214135, China

<sup>3</sup>Jiangsu Wuxi Environmental Monitoring Centre, Wuxi 214023, China

\*Corresponding authors  
e-mail: yl801123@aliyun.com, daiweitj@126.com

(Received 29<sup>th</sup> Jul 2020; accepted 19<sup>th</sup> Nov 2020)

**Abstract.** MCs pollution have become a worldwide problem for freshwater aquaculture, and MC-LR has attracted considerable attention due to its potent hepatotoxicity. To analysis the MC-LR production ability of cyanobacteria in field, the relationship between the MC-LR production ability and MC-LR content, TN content, TP content, SNP of the metagenomic *mcy* genes were investigated in 5 freshwater fishponds during July 2018. The results showed that MC-LR content was significantly positively correlated with the abundance of metagenomic *mcy* gene A-J, while the MC-LR production ability of metagenomic *mcy* gene A-J was in indistinctive correlation with the abundance of metagenomic *mcy* gene, and MC-LR content, and the content of TN and TP in sufficient nitrogen and phosphate conditions. 18 SNPs significantly positively correlated with the MC-LR production ability and 388 SNPs significantly negatively correlated with the MC-LR production ability. The genotype of *mcy* C and *mcy* B in *Microcystis aeruginosa* NIES-843 was the most favorable for the MC-LR production in present study. There might be some mechanism to avoid substrate specific changes caused by genetic mutation of *mcy* C.

**Keywords:** harmful cyanobacteria, toxin, nutrient level, microcystin synthetase genes, correlation analysis

**Abbreviations:** MCs: microcystins; MC-LR: microcystins-LR; TN: total nitrogen; TP: total phosphate; SNP: the single nucleotide polymorphism; *mcy*: the microcystin synthetase; NRPS: nonribosomal peptide synthetase; PKS: polyketide synthase; HPLC: high performance liquid chromatography; Adda: 3- amino-9-methoxy-2, 6, 8-trimethyl-10-phenyldeca-4, 6-dienoic acid; MeAsp: methylaspartic acid; Mdha: methyldehydroalanine

## Introduction

In natural freshwater bodies, cyanobacteria genera, including *Anabaena*, *Aphanocapsa*, *Hapalosiphon*, *Nostoc*, *Oscillatoria*, *Pseudanabaena*, *Planktothrix* and *Microcystis*, often produce MCs (Falconer, 1999; Tillett et al., 2000; Carmichael, 2001; Codd et al., 2005). MCs are classified as possible human carcinogens (class B) by the International Agency for Research on Cancer (IARC) (Ngwa et al., 2014). MCs are a family of monocyclic heptapeptides hepatotoxins. They share a general structure of cyclic [-D-Ala1-L-X2-MeAsp3-L-Z4-Adda5-D-Glu6-N-Mdha7], in which X and Z represent two variable L-amino acids (Rastogi et al., 2014).

Microcystin-production cyanobacteria contain the *mcy* gene cluster. MCs cannot be produced when one or more of the required *mcy* genes are absent via gene deletion,

recombination, and transformation, or disrupted and inactivated by transposons or phages (Ngwa et al., 2014; Zuo et al., 2018). The *mcy* gene cluster spanning 55kb includes NRPS genes, PKS genes, fused NRPS-PKS genes and modifier genes (Noguchi et al., 2009). It is composed of 10 bidirectional transcribed open reading frames arranged in two putative operons (*mcy* A-C and *mcy* D-J) by a promoter region (Tillett et al., 2000; Zurawell et al., 2005). The *mcy* gene cluster cannot only be used as gene marker to quantify toxic genotypes, such as *mcy* A, *mcy* B, *mcy* D, *mcy* E and *mcy* J (Zuo et al., 2018), but can also provide a new tool for the investigation of microcystin variation, evolution and function (Mikalsen et al., 2003). For the reason that the *mcy* gene cluster does not well tolerate mutations with respect to toxin biosynthesis (Pearson et al., 2006), microcystin-production cyanobacteria often produce several isoforms of microcystin (Mikalsen et al., 2003; Pearson et al., 2006). In addition, variability is also probably influenced by environmental conditions (Davis, 2009). Among these variants, MC-LR (with leucine and arginine amino acids), a potent inhibitor of protein phosphatase and inducer of cytoskeleton alterations, is one of the most common and toxic variants of MCs (Oudra et al., 2002; Chen et al., 2016).

In natural freshwater suffering harmful cyanobacteria blooms, it is important to investigate content and variation of MCs for their widespread occurrence, acute toxicity and tumor-promoting property. Moreover, identifying the factors influencing the MCs production ability of toxic cyanobacteria is profitable for the control of MCs pollution in natural freshwater. As an important part of natural freshwater, aquaculture water experiences much less hydrologic changes and much more impacts of aquaculture activities compared to other freshwater bodies. Cyanobacteria blooms occur more frequently in aquaculture water (Hu et al., 2018). MCs produced in cyanobacteria blooms can be ingested and accumulated in the aquacultured animals, and eventually endanger human health via the food chain (Codd et al., 2005). In this paper, a field study in MC-LR content and the abundance of *mcy* genes was performed in five man-made freshwater fishponds suffering cyanobacteria blooms. Moreover, we respectively analyzed the relationship between the MC-LR production ability of toxic cyanobacteria and MC-LR content, TN content, TP content, SNP of the metagenomic *mcy* genes.

## Materials and Methods

### *Study sites and sampling*

5 freshwater fish ponds (warm water) with a surface area of 3500-7000 m<sup>2</sup> and mean water depth of 1.5 m were located in Xiqing district (XQ, site N38°57'20.74", E117°11'24.43"), Ninghe district (NH, site N39°26'30.81", E117°29'46.52"), Dagang district (DG, site N38°48'14.81", E117°28'59.48"), Jizhou district (JX, site N39°50'19.24", E117°20'46.21") and Beichen district (BC, site N39°17'0.24", E117°24'0.38") in Tianjin, China, respectively (*Fig. 1*).

Sampling was conducted during July 2018 and performed according the method of Bi et al. (2019). Briefly, to collecting mixed water sample from the surface to the bottom, a specially designed cylindrical organic glass sampler was used. Water samples were collected three times per sampling site. The mixed water sample using in the chemical analysis (2 L) was stored at 4 °C and transferred to the laboratory condition within 2 h. The mixed water sample using in DNA extraction (approximately 500 mL) was filtered through 0.22 µm millipore polycarbonate membrane, and then the membrane was immediately stored at -20 °C. The mixed water sample (1 L) was filtered through 0.45

$\mu\text{m}$  and  $0.22 \mu\text{m}$  cellulose acetate membranes sequentially, in which the filtered water sample and the seston retained on the membrane were using in MC-LR content analysis, respectively.

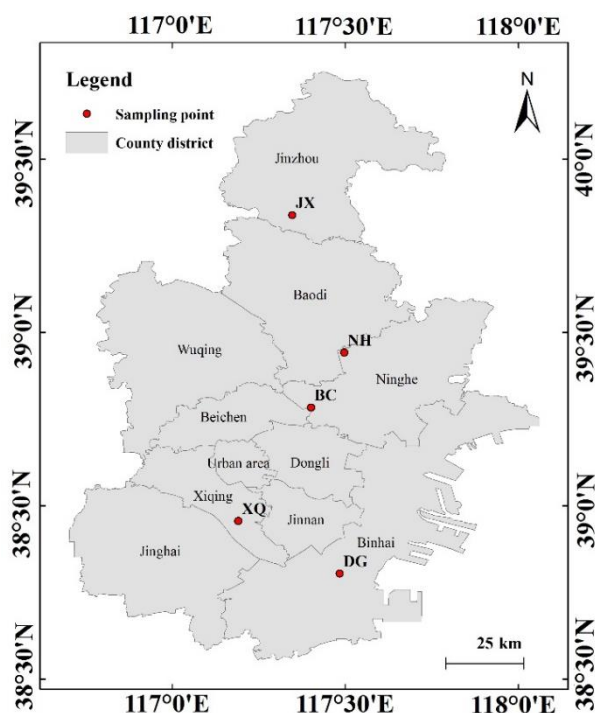


**Figure 1.** Map of sampling points in Tianjin, China

### **Total nitrogen and total phosphorus contents analysis**

TN and TP contents of the mixed water sample were detected via the alkaline potassium persulfate digestion method (China National Standard GB11894-89) and ammonium molybdate spectrophotometric method with or without potassium persulfate digestion (China National Standard GB11893-89), respectively.

### **MCs extraction and MC-LR determination**

Supelco SPE C<sub>18</sub> cartridge was preconditioned with 10 mL methanol and 10 mL Milli-Q (Millipore, UK) water and used to enrich MCs of the filtered water sample. MCs in cartridge was eluted with 20% aqueous methanol, and the elution was evaporated on a rotary evaporator to 0.5-1 mL and dried with nitrogen gas. The residue was redissolved in 1 mL of 50% methanol and filtered through a  $0.22 \mu\text{m}$  nylon membrane. After 4 freeze-thaw cycles, the seston was lyophilized at  $-40 \text{ }^{\circ}\text{C}$  under 8-11 mTorr and extracted three times with 20 mL of 90% aqueous methanol. The extraction liquid was centrifugated at 12000 g for 10 min. The mixed supernatant was evaporated to 0.5-1 mL, and then was added 6 mL Milli-Q to extract MCs using a SPE C<sub>18</sub> cartridge as described above.

Above concentrated MCs samples were analyzed via a HPLC system (SPD-M20A, Shimadzu, Japan) equipped with a Shim-Pack VP-ODS column (250 mm $\times$ 4.6 mm) and a DAD detector, using 60% aqueous methanol with 0.05% trifluoroacetic acid at a flow rate of 1 mL/min. MC-LR were identified by the retention time, and quantification was calculated based on the standard curve of certified MC-LR standards (Sigma, USA). The



sum of MC-LR contents dissolved in filtrate and retained in seston represents MC-LR content produced by the metagenomic *mcy* gene cluster of the water sample.

### ***DNA extraction and shotgun library preparation and sequencing***

Total genome DNA from samples was extracted using DNeasy PowerSoil (QIAGEN, U.S.) according to the manufacturer's instructions and eluted in 50  $\mu$ L of elution buffer. The harvested DNA was detected by the agarose gel electrophoresis and quantified by Qubit (Thermo Fisher, U.S.).

The metagenome DNA libraries were constructed with 1  $\mu$ g of DNA genomes, according to the Illumina TruSeq DNA Sample Prep v2 Guide (Illumina), with an average of 350 bp insert size. All qualified libraries were loaded to HiSeq X ten to perform pair-end sequencing. More than 10G raw reads were obtained for each sample.

### ***Bioinformatic analysis***

Illumina raw reads were filtered with the following constraints: (1) reads with more than 2 ambiguous N bases were removed; (2) reads with less than 80% of high-quality base (Phred score  $\geq 20$ ) were removed; (3) 3'-ends of reads were trimmed to the first high-quality base. Compared to reference of *M. aeruginosa* NIES-843, high-quality reads obtained through mapping metagenomic reads using BWA (<https://nchc.dl.sourceforge.net/project/bio-bwa/bwa-0.7.15.tar.bz2>) were assembled with multiple Kmer parameters using SOAPdenovo (version 2.04) (<http://soap.genomics.org.cn/>) to obtain the optimal assembled results. Local cavity filling and base correction were performed on the assembled results with GapCloser (version 1.12). The final assembled results are shown in *Table 1*. Assembled results were mapped to the *mcy* gene cluster of reference gene of *M. aeruginosa* NIES-843 using BWA, and bam files were obtained using samtools. The abundance of *mcy* gene A-J of samples were obtained using humann2 (<http://huttenhower.sph.harvard.edu/humann2>), and SNP identification of metagenomic *mcy* gene was using VarScan (<http://varscan.sourceforge.net/>). All sequences included in this paper were submitted to GenBank (Accession Number: SRP255704).

***Table 1.*** The assembly results were statistically analyzed

Sampling points	Jizhou (JX)	Ninghe (NH)	Xiqing (XQ)	Beichen (BC)	Dagang (DG)
No. of all contigs	35	1070	653	441	215
Bases in all contigs (bp)	60245	268446	226925	192314	112172
Average length (bp)	1721.3	250.9	347.5	436.1	521.7
No. of large contigs (>1000 bp)	20	4	13	19	19
Bases in large contigs	53295	5120	16395	24365	36064
Largest length (bp)	6500	1904	1598	1579	4757
Contig N50 (bp) (>1000 bp)	3302	1136	1275	1348	1915
Contig N90 (bp) (>1000bp)	1342	1026	1032	1049	1138
G+C content (%)	38.95	38.90	38.99	39.10	38.88

### ***Data analysis***

The correlation analyses were conducted using SPSS (version 17.0).

## Results

### *Relationship between the metagenomic mcy gene abundance and MC-LR content, TN and TP contents*

MC-LR content produced by toxic cyanobacteria and the abundance of metagenomic *mcy* genes in five fishponds were presented in *Table 2*. MC-LR content and the abundance of 10 metagenomic *mcy* genes varied with sample sites. Except for the metagenomic *mcy* H and I at sampling point NH, MC-LR content and the abundance of 10 metagenomic *mcy* genes increased in the order of JX, NH, XQ, BC, and DG. As shown in *Table 3*, there was positive correlation between MC-LR content and all metagenomic *mcy* gene abundance. MC-LR content had significant correlation with the metagenomic *mcy* A-C abundance ( $P < 0.05$ ) and extremely significant correlation with the metagenomic *mcy* E-J abundance ( $P < 0.01$ ). There was indistinctive correlation between the metagenomic *mcy* A-J abundance and contents of TN and TP ( $P > 0.05$ ).

**Table 2.** MC-LR content and the abundance of metagenomic *mcy* gene in five sampling sites

Sampling sites	MC-LR content (µg/L)	Gene abundance (Copies/L)									
		<i>mcy</i> C	<i>mcy</i> B	<i>mcy</i> A	<i>mcy</i> D	<i>mcy</i> E	<i>mcy</i> F	<i>mcy</i> G	<i>mcy</i> H	<i>mcy</i> I	<i>mcy</i> J
JX	12.56	189.44	236.6	231.28	501.2	343.05	29.46	321.63	114.15	45.39	32.76
NH	13.86	11135.14	18915.5	25456.45	10441.56	5743.14	526.67	9302.17	0	0	603.36
XQ	17.82	12458.23	21608.17	25892.17	40107.65	35942.4	2443.72	24634.97	6735.61	3614.12	3383.46
BC	20.55	16166.58	28035.62	33157.23	51039.3	44564.36	2708.76	31237.86	6893.65	4705.23	3858.43
DG	23.86	28337.19	48898.12	59991.29	88380.13	80683.54	6080.56	54817.68	14168.78	7906.41	7274.32

**Table 3.** Correlation between the abundance of metagenomic *mcy* A-J and MC-LR, TN and TP contents

	<i>mcy</i> C	<i>mcy</i> B	<i>mcy</i> A	<i>mcy</i> D	<i>mcy</i> E	<i>mcy</i> F	<i>mcy</i> G	<i>mcy</i> H	<i>mcy</i> I	<i>mcy</i> J
	r D.W	r D.W	r D.W	r D.W	r D.W	r D.W	r D.W	r D.W	r D.W	r D.W
MC-LR	0.93* 2.42	0.94* 2.43	0.91* 2.34	0.99** 2.68	0.99** 2.75	0.96** 2.33	0.99** 2.51	0.97** 2.96	0.99** 3.05	0.98** 2.85
TN	0.13 0.81	0.14 0.80	0.10 0.87	0.26 0.59	0.26 0.61	0.18 0.73	0.23 0.61	0.29 0.73	0.30 0.58	0.27 0.65
TP	0.81 1.79	0.81 1.76	0.81 1.93	0.80 1.33	0.81 1.34	0.87 1.37	0.81 1.34	0.83 1.38	0.77 1.38	0.82 1.31

\* Correlation is significant at  $P < 0.05$ , \*\* Correlation is significant at  $P < 0.01$ , 'r' is the correlation coefficient and 'D.W.' is the test value of Durbin-Watson

### *Relationship between the MC-LR production ability of all metagenomic mcy genes and MC-LR content, TN and TP contents*

As shown in *Table 4*, the natural log of the ratio of MC-LR content to the metagenomic *mcy* gene abundance ( $\ln \text{MC-LR}/mcy$ ) reflecting the MC-LR production ability of the metagenomic *mcy* genes was calculated. The MC-LR production ability of all metagenomic *mcy* genes at sampling point JX was the highest in 5 sampling points. As shown in *Table 5*, the MC-LR production ability of the metagenomic *mcy* gene A-J was in indistinctive correlation with the abundance of metagenomic *mcy* gene A-J and MC-LR content and TN and TP contents ( $P > 0.05$ ).

**Table 4.** The natural log of the ratio of MC-LR content to the metagenomic *mcy* gene abundance ( $\ln \text{MC-LR}/mcy$ )

Sampling points	$\ln \text{MC-LR}/mcy$									
	<i>mcy</i> C	<i>mcy</i> B	<i>mcy</i> A	<i>mcy</i> D	<i>mcy</i> E	<i>mcy</i> F	<i>mcy</i> G	<i>mcy</i> H	<i>mcy</i> I	<i>mcy</i> J
JX	-2.71	-2.94	-2.91	-3.69	-3.31	-0.85	-3.24	-2.21	-1.28	-0.96
NH	-6.89	-7.22	-7.52	-6.62	-6.03	-3.64	-6.51			-3.77
XQ	-6.55	-7.1	-7.28	-7.72	-7.61	-4.92	-7.23	-5.93	-5.31	-5.25
BC	-6.67	-7.22	-7.39	-7.82	-7.68	-4.88	-7.33	-5.82	-5.43	-5.24
DG	-7.08	-7.63	-7.83	-8.22	-8.13	-5.54	-7.74	-6.39	-5.8	-5.72

**Table 5.** The correlation between  $\ln \text{MC-LR}/mcy$  and the metagenomic *mcy* gene abundance and MC-LR, TN and TP contents

	$\ln \text{MC-LR}/mcy$ C		$\ln \text{MC-LR}/mcy$ B		$\ln \text{MC-LR}/mcy$ A		$\ln \text{MC-LR}/mcy$ D		$\ln \text{MC-LR}/mcy$ E	
	r	D.W	r	D.W	r	D.W	r	D.W	r	D.W
Gene abundance	-0.79	1.78	-0.80	1.71	-0.81	1.67	-0.81	1.67	-0.82	1.57
MC-LR content	-0.64	1.26	-0.67	1.30	-0.66	1.27	-0.83	1.39	-0.86	1.34
TN	-0.38	1.91	-0.41	1.83	-0.40	1.87	-0.54	1.25	-0.57	1.06
TP	-0.43	1.76	-0.45	1.67	-0.44	1.71	-0.52	1.23	-0.54	1.14

	$\ln \text{MC-LR}/mcy$ F		$\ln \text{MC-LR}/mcy$ G		$\ln \text{MC-LR}/mcy$ H		$\ln \text{MC-LR}/mcy$ I		$\ln \text{MC-LR}/mcy$ J	
	r	D.W	r	D.W	r	D.W	r	D.W	r	D.W
Gene abundance	-0.79	1.56	-0.79	1.74	-0.87	2.01	-0.88	2.04	-0.82	1.62
MC-LR content	-0.85	1.40	-0.79	1.40	-0.90	1.73	-0.90	1.65	-0.85	1.34
	-0.53	1.15	-0.50	1.43	-0.56	0.65	-0.56	0.61	-0.56	1.13
	-0.57	1.20	-0.51	1.35	-0.56	1.62	-0.52	1.59	-0.54	1.16

'r' is the correlation coefficient and 'D.W.' is the test value of Durbin-Watson

### Relationship between the MC-LR production ability of the metagenomic *mcy* genes and SNPs

As shown in Table 6 and Figure 2, at some single nucleotide sites in the metagenomic *mcy* gene A-J, SNPs presented significant ( $P < 0.05$ ) /extremely significant ( $P < 0.01$ ) correlation with the MC-LR production ability of the metagenomic *mcy* genes where 18 SNPs and 388 SNPs were strongly positively correlated and strongly negatively correlated with the MC-LR production ability of the metagenomic *mcy* genes, respectively. No significantly positive correlation between SNP and the MC-LR production ability in the metagenomic *mcy* B and C was observed. In the metagenomic *mcy* C, the number of SNPs significantly negatively correlated with the MC-LR production ability was 5, and the percentage of SNP significantly correlated with the MC-LR production ability/ the length of the metagenomic *mcy* gene was the lowest in NPRSs. Meanwhile, the percentage of SNPs significantly correlated with the MC-LR production ability for amino acid change / SNPs in the metagenomic *mcy* gene was the lowest in all metagenomic *mcy* genes. SNP for amino acid change in SNPs significantly correlated with the MC-LR production ability was not observed in *mcy* I and *mcy* J. The amino acid sites changed by SNPs significantly correlated with the MC-LR production ability in the metagenomic *mcy* A-J were shown in Table 7, respectively.

**Table 6.** Sites in the metagenomic *mcy* gene A-J that SNP was significantly/ extremely significantly correlated with the MC-LR production ability

Reference (NIES-843) Gene (length in base pair)	Correlation	The mutant single nucleotide site									
<i>mcy C</i> (3876)	Positive										
	Negative	S1213*	<b>S2204*</b>	<b>S3379**</b>	<b>S3566*</b>	S3604*					
<i>mcy B</i> (6381)	Positive										
	Negative	<b>S4309*</b>	S4938*	S4941*	<b>S4946*</b>	S5163**	S5184**	S5226**	<b>S5240**</b>	<b>S5246**</b>	
		<b>S5250**</b>	S5508**	S5664**	S5748*	S7482**	S7485**	<b>S7488**</b>	S7650*	S7668**	
	S7713*	S7716*	<b>S8062*</b>	<b>S8320*</b>	S8547*	<b>S9708*</b>	S9709*	<b>S9911**</b>			
<i>mcy A</i> (8364)	Positive	<b>S18576**</b>									
	Negative	S10317**	<b>S10553*</b>	<b>S11119**</b>	S11127**	S11319*	S11481*	<b>S11686**</b>	S12111*	S12141*	
		S12636*	S12711*	S13890**	S14274**	S14280**	<b>S14459**</b>	<b>S15559*</b>	<b>S15575*</b>	<b>S15676**</b>	
		S15834*	S16034*	S16293*	S16305**	S16404*	S16860*	S17247**	S17274*	<b>S17801**</b>	
	<b>S18019*</b>	<b>S18068*</b>	S18156*								
<i>mcy D</i> (11706)	Positive	S27665**	<b>S28915**</b>	S30725*	<b>S30934*</b>	S30938*	S30941*	<b>S31071**</b>			
	Negative	<b>S19655**</b>	S19673**	S19733**	<b>S19749**</b>	S19850**	S19928**	S20096**	S20108**	S20177**	
		S20183**	<b>S20415**</b>	S20438**	S20474**	S20504**	S20507**	<b>S20513*</b>	S20561**	<b>S20643**</b>	
		S20654**	S20666**	S20717**	S20783*	S21086*	S21101**	<b>S21160*</b>	<b>S21161*</b>	S21167*	
		<b>S21185*</b>	<b>S21261*</b>	<b>S21270*</b>	<b>S21285*</b>	<b>S21288*</b>	<b>S21294*</b>	<b>S21307*</b>	<b>S21322*</b>	<b>S21342**</b>	
		<b>S21348*</b>	<b>S21353*</b>	<b>S22011*</b>	<b>S22491*</b>	<b>S22518*</b>	<b>S22520*</b>	S22685*	S22697**	S22712**	
		<b>S22731*</b>	S22766*	S22772**	<b>S22773**</b>	S22787**	<b>S22882*</b>	S22886*	S22937*	<b>S22991**</b>	
		S23018**	<b>S23049*</b>	<b>S23101*</b>	S23123*	S23126*	S23144*	<b>S23145*</b>	<b>S23146*</b>	S23153**	
		<b>S23191**</b>	<b>S23328**</b>	<b>S23334*</b>	S23414**	S23438*	S23441*	<b>S23443*</b>	<b>S23465*</b>	S23528*	
		<b>S23571**</b>	<b>S23593**</b>	<b>S23598*</b>	S24137*	<b>S24141*</b>	S24144*	S24170**	<b>S24172**</b>	<b>S24173**</b>	
		<b>S24187*</b>	<b>S24279*</b>	<b>S24398*</b>	S24470*	<b>S24633*</b>	S24722*	S24794*	<b>S24769*</b>	S24849*	
		<b>S24906*</b>	<b>S24927*</b>	<b>S24972*</b>	<b>S24974*</b>	S24978*	<b>S25005*</b>	S25010*	<b>S25014*</b>	<b>S25071*</b>	
		S26042**	S26312**	S26384**	S26465**	S26630**	S26858**	S27356*	<b>S27396*</b>	S27929**	
		S27965*	S28034*	S28058*	S28106**	S28106**	<b>S28171*</b>	<b>S28209*</b>	S28292*	S28295*	
		S28301*	<b>S28500**</b>	<b>S28501**</b>	S28625**	S28688**	<b>S28777**</b>	S29153**	S29237*	<b>S29238*</b>	
		S29339*	S29703*	<b>S29819*</b>	<b>S29821*</b>	S29852*	<b>S29950*</b>	<b>S30052**</b>	S30119*	S30221**	
			S30335**	<b>S30401*</b>	S30491*	<b>S30709*</b>					
<i>mcy E</i> (10464)	Positive	S38712*									
	Negative	S31617**	S31692*	S31743**	S31854**	S31893**	S32013**	S32130**	S32502**	<b>S32515*</b>	
		S32568*	<b>S32628*</b>	S32748**	S32943**	<b>S33592*</b>	S33645**	S33903**	S34608**	S34770*	
		<b>S34878*</b>	S34932**	S35223**	S35232**	<b>S35234**</b>	S35253**	S35316*	S35328**	<b>S35594*</b>	
		<b>S35595*</b>	<b>S35596*</b>	<b>S35602*</b>	<b>S35604*</b>	<b>S35785*</b>	S35799*	<b>S35813*</b>	<b>S35814*</b>	S35889**	
		S36009**	S36063**	S36078**	S36438**	<b>S36439**</b>	S36454**	S36462*	<b>S36484**</b>	S36924**	
		S36945**	S37050**	S37089**	S37356*	S37386**	<b>S37457*</b>	<b>S37531*</b>	<b>S37570**</b>	<b>S37590**</b>	
		S37593**	<b>S37597**</b>	S37672**	S37686**	<b>S37717**</b>	S37734**	<b>S37950*</b>	S37953*	S38037*	
		S38139**	S38190**	S38280**	<b>S38467*</b>	<b>S38468*</b>	S38631*	S38715*	S38838*	S39303*	
		S39555*	S40786*	S40839*	<b>S40919*</b>	<b>S40961*</b>	S41010*	S41112*	<b>S41144*</b>	S41169*	
		S41319*	S41328**	<b>S41407*</b>	<b>S41473*</b>	S41535*	S41553*	<b>S41596*</b>	S41625**		

<i>mcy</i> F (756)	Positive	<b><i>S42113*</i></b>								
	Negative	S42196*	S42244*	<b><i>S42415*</i></b>	S42616*	<b><i>S42618*</i></b>	<b><i>S42621*</i></b>	S42637*	<b><i>S42645*</i></b>	
<i>mcy</i> G (7896)	Positive	S44772**	<b><i>S47707**</i></b>							
	Negative	S43053*	S43191*	<b><i>S43223*</i></b>	<b><i>S43316*</i></b>	S43350*	S43416*	S43464*	<b><i>S43519*</i></b>	S43536*
		S43563*	S43611*	S43647*	<b><i>S43664*</i></b>	S44730*	<b><i>S44732*</i></b>	<b><i>S44777*</i></b>	S44904*	S45048*
		S45066*	S45099**	<b><i>S45113*</i></b>	S45171*	S45321*	S45393*	S45408*	S45415*	S45459*
		S45480*	S45495*	<b><i>S45559*</i></b>	S45666*	S45669*	S46089**	S46197**	S46203**	<b><i>S46403**</i></b>
		S46452**	<b><i>S46530**</i></b>	S46560**	S46686*	S46695*	S46716*	S46734*	<b><i>S46769*</i></b>	<b><i>S46857*</i></b>
		S46866*	S46869*	S46872*	<b><i>S46934*</i></b>	S46962*	S46977*	S46992*	S47001*	S47028*
		S47631*	<b><i>S47656*</i></b>	S47706*	<b><i>S47719*</i></b>	S47725*	<b><i>S47731*</i></b>	<b><i>S47732*</i></b>	S47742*	<b><i>S47775*</i></b>
		<b><i>S47950*</i></b>	<b><i>S47953*</i></b>	S48312*	<b><i>S48886*</i></b>	S49410**	S49833*	<b><i>S49895*</i></b>	<b><i>S50017*</i></b>	<b><i>S50018*</i></b>
		<b><i>S50019*</i></b>	S50022*	S50070*	S50106*	S50139*	S50175*	S50187*	<b><i>S50322*</i></b>	<b><i>S50325*</i></b>
		<b><i>S50331*</i></b>	S50340**	<b><i>S50512**</i></b>						
<i>mcy</i> H (1758)	Positive	<b><i>S51149**</i></b>	<b><i>S51167**</i></b>	S51175**	S51181**	S51304**	S51353**			
	Negative	S51271**	<b><i>S51275**</i></b>	<b><i>S51371**</i></b>	<b><i>S51393**</i></b>	<b><i>S51611**</i></b>	<b><i>S51828*</i></b>	<b><i>S51831*</i></b>	<b><i>S51875**</i></b>	<b><i>S51881**</i></b>
<i>mcy</i> I (1014)	Positive									
	Negative	S53559**								
<i>mcy</i> J (936)	Positive									
	Negative	S54355**								

\* Correlation is significant at  $P < 0.05$ , \*\* Correlation is significant at  $P < 0.01$ , 'S' means the site of SNP in the metagenomic *mcy* gene cluster and the site of SNP in italics and bold means SNP for amino acid change

**Table 7.** The site of amino acid changed in the metagenomic *mcy* A-J by SNP significantly correlated with the MC-LR production ability

<i>Mcy</i> gene	The mutant site of amino acid									
<i>mcy</i> C	104	166	558							
<i>mcy</i> B	115	181	645	731	922	1668	1670	1672	1770	
<i>mcy</i> A	19	189	205	278	986	1020	1025	1392	2316	<b>2505</b>
<i>mcy</i> D	39	71	293	325	369	541	549	575	578	583
	586	590	595	602	604	605	825	985	994	1065
	1115	1151	1171	1188	1203	1218	1264	1266	1302	1309
	1351	1353	1535	1545	1550	1581	1620	1699	1744	1790
	1823	1826	1845	<b>2620</b>	2878	2891	2988	3080	3126	3234
<i>mcy</i> E	3428	3471	3605	3621	<b>3724</b>	3795	<b>3845</b>			
	369	406	728	1156	1275	1395	1396	1398	1459	1468
	1692	2016	2041	2054	2060	2063	2103	2180	2353	3184
<i>mcy</i> F	3245	3333	3355	3396						
	<b>70</b>	170	238	239	247					
<i>mcy</i> G	144	175	243	291	647	662	774	923	1204	1246
	1355	1381	1623	1640	1644	1647	1661	1720	1721	2032
	2409	2510	2511	2513	2574					
<i>mcy</i> H	<b>127</b>	<b>133</b>	169	201	208	281	353	354	369	

The amino sites in italics and bold were changed by SNPs positively correlated with the MC-LR production ability. The amino sites in normal font were changed by SNPs negatively correlated with the MC-LR production ability

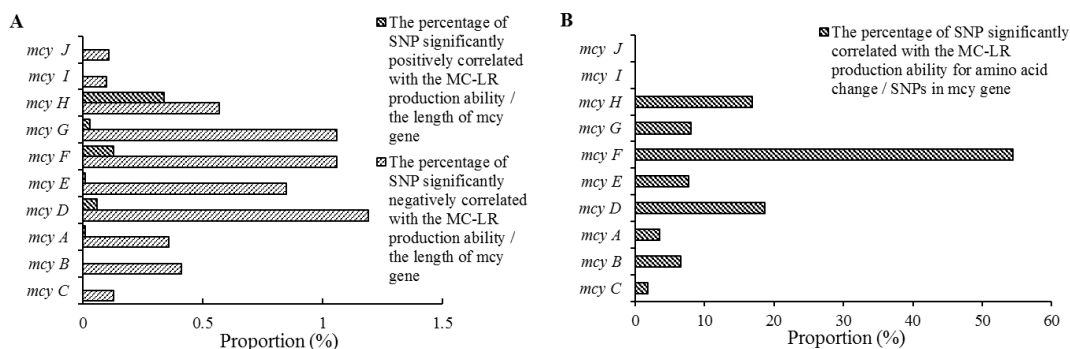


**Figure 2.** The proportion of SNP significantly correlated with the MC-LR production ability of *mcy* genes

## Discussion

Toxic cyanobacteria likely carried only one copy of the *mcy* gene cluster genetically structured similarly as the housekeeping genes and therefore the *mcy* gene cluster abundance was used to predict potential pollution of MCs in natural freshwater (Kyoung-Hee et al., 2012; Zuo et al., 2018), and most methods of detecting and identifying MCs producers were based on PCR using primers designed to recognize the *mcy* gene cluster (Rantala et al., 2006). In the present study, there was a strong positive correlation between MC-LR content and the abundance of metagenomic *mcy* gene A-J, while an indistinctive correlation between the MC-LR production ability of metagenomic *mcy* gene and abundance of metagenomic *mcy* gene and the MC-LR content was observed. It was suggested that we should take a closer look at the indicators predicting potential pollution of MCs in natural freshwater. Zuo et al. (2018) suggested that the ratio of toxic *Microcystis* determined by *mcy B* abundance was higher in both laboratory and field samples, which might result from sequence characteristics of *mcy B* amplicon. *mcy B* might be amplified more easily in a competitive PCR system. This characteristic of *mcy B* was not observed in the present study. *mcy H* are putatively involved in location and stabilizing the megasynthase (Tillett et al., 2000; Liu et al., 2019). *mcy I* may play a role in dehydration and stabilization of the microcystin synthase complex (Tillett et al., 2000; Liu et al., 2019). Notably, both *mcy H* and *I* abundance at site NH were 0, whereas MC-LR content was 13.86 µg/L. A similar result was also reported by Pearson et al. (2006), who found *Planktothrix agardhii* CYA126 without *mcy I* was capable of production MCs. The reason for this phenomenon might be that both *mcy H* and *mcy I* was not critical for the biosynthesis of MC-LR.

Cyanobacteria blooms in freshwater are broadly associated with eutrophic and poorly flushed water. As nutrients in freshwater bodies, especially phosphorus, become enriched, there is often a shift in the phytoplankton community towards dominance by cyanobacteria (Davis, 2009). The regulation factors as a whole governing MCs synthesis remain unknown (Kuniyoshi et al., 2013). Previous researches suggested the expression of the *mcy* gene cluster could be regulated by environmental factors and toxic cyanobacterial strains, which appear to have higher N and P requirements than nontoxic strains, possibly due to the extra energy and materials required for toxin synthesis (Zurawell et al., 2005; Davis, 2009). According to previous research, the correlation between MCs content and various P level was to be positive or negative (Davis, 2009), and it was hypothesized that the effects of nitrogen on toxin-production ability of

cyanobacteria depended on the limitation of phosphorus (Zurawell et al., 2005; Kuniyoshi et al., 2013). Under the P-limited condition, a negative correlation was shown between orthophosphate and TP, and MCs (Kuniyoshi et al., 2013). Content of total MCs, in particular the more toxic MC-LR variant, increased with increasing P limitation (Zurawell et al., 2005). Sevilla et al. (2010) suggested that both the transcription level of *mcy D* and MC-LR per cell had been shown to be independent of nitrate availability in sufficient P conditions. In the present study, there was higher level of both TP content (>0.10 mg/L) and TN content (>0.85 mg/L) at all 5 sampling sites, and both the abundance and the MC-LR production ability of all metagenomic genes were in indistinctive correlation with TP content, coinciding with the result of Sevilla et al. (2010). Davis (2009) suggested that toxic strains of *Microcystis* were able to outgrow non-toxic strains at high N levels. However, we found an indistinctive correlation between TN content and both the abundance and the MC-LR production ability of all metagenomic *mcy* genes.

In the *mcy* gene cluster, NRPSs including *mcy A-C, E* catalyzed the formation of peptides, and PKS including *mcy G, E* and *D* were involved in the formation of Adda, and *mcy F, H-J* encoded modifying genes involved in epimerization, localization, dehydration and O-methylation (Tillett et al., 2000; Zurawell et al., 2005). Attributed to the relaxed substrate specificity of the adenylation domain and genetic variation in the *mcy* gene cluster, toxic *Microcystis* strains often produce several isoforms of the cyclic hepatotoxin microcystin (Mikalsen et al., 2003). The main characteristic of MC-LR was L-leucine at the variable amino acid position X2 and especial L-arginine at the variable amino acid position Z4, in which the *mcy B1* module and the *mcy C* module were respectively involved in recognition of specific substrate of these amino acid position (Tanabe et al., 2009). In present study, no SNP significantly positively correlated with the MC-LR production ability was found in *mcy B* and *mcy C*. It was predicted that the genotype of *mcy C* and *mcy B* in *M. aeruginosa* NIES-843 was the most favorable for MC-LR production in present study. Some SNPs significantly positively correlated with MC-LR production ability of metagenomic *mcy* genes were observed in *mcy A* and *mcy D-H*, suggesting these sites just were critical to MCs production according to the role of the *mcy* genes including these sites in MCs synthesis. In the present study, *mcy C* had the lowest proportion of SNPs significantly correlated with MC-LR production ability in NRPSs and the lowest proportion of SNPs significantly correlated with MC-LR production ability for amino acid change in all metagenomic *mcy* genes. It was indicated that *mcy C* was more critical to the production of MC-LR and there might be some mechanism to avoid substrate specific changes due to genetic mutation. *mcy* genes belonging to PKS had higher mutation significantly negatively correlated with the MC-LR production ability of the metagenomic *mcy* genes, predicting that *mcy D, E* and *G* played important roles in MCs synthesis according to the role of PKS in MCs synthesis.

## Conclusion

In the present study, MC-LR content was positively correlated with the abundance of metagenomic *mcy* gene A-J. The MC-LR production ability of all metagenomic *mcy* genes was in indistinctive correlation with the metagenomic *mcy* gene abundance, and MC-LR content, and TN and TP content in sufficient N and P conditions. Both *mcy C* and *mcy B* of *M. aeruginosa* NIES-843 had the strongest MC-LR production ability in the metagenomic *mcy C* and *B* of five sampling sites. *mcy C* was the most critical to the production of MC-LR in all *mcy* genes and there might be some mechanism to avoid

substrate specific changes due to genetic mutation. It was necessary to take a closer look at the indicators predicting potential pollution of MCs in natural freshwater. Using genome-editing techniques to further identify critical SNPs correlated with the MC-LR production ability would offer novel insight into the correlation among SNP genotypes composition and toxin characteristic of microcystin-production cyanobacteria in aquaculture ponds.

**Acknowledgments.** This work was supported by the National Natural Science Foundation of China (grant no. 31772857), Natural Science Foundation Grant of Tianjin (grant nos. 18JCYBJC95900 and 20JCZDJC23600, 17JCYBJC29500), and Key Research and Development Projects of Tianjin (grant no. 19YFZCSN00070).

## REFERENCES

- [1] Bi, X. D., Dai, W., Wang, X. Y., Dong, S. J., Zhang, S. L., Zhang, D. J., Wu, M. (2019): Microcystins distribution, bioaccumulation, and *Microcystis* genotype succession in a fish culture pond. – *Science of the Total Environment* 688: 380-388.
- [2] Carmichael, W. W. (2001): Health effects of toxin-producing cyanobacteria: “the Cyano-HABs”. – *Human Ecological Risk Assessment* 7: 1393-1407.
- [3] Chen, L., Chen, J., Zhang, X. Z., Xie, P. (2016): A review of reproductive toxicity of microcystins. – *Journal of Hazardous Materials* 301: 381-399.
- [4] Codd, G. A., Morrison, L. F., Metcalf, J. (2005): Cyanobacterial toxins: risk management for health protection. – *Toxicology Applied Pharmacology* 203(3): 264-272.
- [5] Davis, T. (2009): Effects of nutrients, temperature, and zooplankton grazing on toxic and non-toxic strains of the harmful cyanobacterium *Microcystis* spp. – the Degree of Doctor of Philosophy, Stony Brook University.
- [6] Falconer, I. R. (1999): An overview of problems caused by toxic blue-green algae (cyanobacteria) in drinking and recreational water. – *Environmental Toxicology* 14: 5-12.
- [7] Hu, X. B., Zhang, R. F., Ye, J. Y., Wu, X., Zhang, Y. X., Wu, C. L. (2018): Monitoring and research of microcystins and environmental factors in a typical artificial freshwater aquaculture pond. – *Environmental Science and Pollution Research* 25: 5921-5933.
- [8] Kuniyoshi, T. M., Sevilla, E., Bes, M. T., Fillat, M. F., Peleato, M. L. (2013): Phosphate deficiency (N/P 40:1) induces *mcyD* transcription and microcystin synthesis in *Microcystis aeruginosa* PCC7806. – *Plant Physiology and Biochemistry* 65: 120-124.
- [9] Liu, T. Z., Mazmouz, R., Pearson, L. A., Neilan, B. A. (2019): Mutagenesis of the microcystin tailoring and transport proteins in a heterologous cyanotoxin expression system. – *Synthetic Biology* 8: 1187-1194.
- [10] Mikalsen, B., Boison, G., Skulberg, O. M., Fastner, J., Davies, W., Gabrielsen, T. M., Rudi, K., Jakobsen, K. S. (2003): Natural variation in the microcystin synthetase operon *mcyABC* and impact on microcystin production in *Microcystis* strains. – *Journal of Bacteriology* 185(9): 2774-2785.
- [11] Ngwa, F. F., Madramootoo, C. A., Jabaji, S. (2014): Comparison of cyanobacterial microcystin synthetase (*mcy*) E gene transcript levels, *mcy* E gene copies, and biomass as indicators of microcystin risk under laboratory and field conditions. – *MicrobiologyOpen* 3(4): 411-425.
- [12] Noguchi, T., Shinohara, A., Nishizawa, A., Asayama, M., Nakano, T., Hasegawa, M. (2009): Genetic analysis of the microcystin biosynthesis gene cluster in microcystis strains from four bodies of eutrophic water in Japan. – *Journal of General & Applied Microbiology* 55(2): 111-123.



- [13] Oh, K-H., Jeong, D-H., Cho, Y-C. (2012): Quantification of toxigenic *Microcystis* spp. In freshwaters by quantitative real-time PCR based on the microcystin synthetase A gene. – Journal of Microbiology 51(1): 18-24.
- [14] Oudra, B., Loudiki, M., Sbiyyaa, B., Sabour, B., Martins, R., Amorim, A., Vasconcelos, V. (2002): Detection and variation of microcystin contents of *Microcystis* blooms in eutrophic Lalla Takerkoust Lake, Morocco. – Lakes & Reservoirs: Research and Management 7: 35-44.
- [15] Pearson, L. A., Barrow, K. D., Neilan, B. A. (2006): Characterization of the 2-hydroxy-acid dehydrogenase *mcy* I, encoded within the microcystin biosynthesis gene cluster of *Microcystis aeruginosa* PCC7806. – The Journal of Biological Chemistry 282(7): 4681-4692.
- [16] Rantala, A., Rajaniemi-Wacklin, P., Lyra, C., Lepistö, L., Rintala, J., Mankiewicz-Boczek, J., Sivonen, K. (2006): Detection of microcystin-producing cyanobacteria in Finnish lakes with genus-specific microcystin synthetase gene E (*mcy E*) PCR and associations with environmental factors. – Applied and Environmental Microbiology 72(9): 6101-6110.
- [17] Rastogi, R. P., Sinha, R. P., Incharoensakdi, A. (2014): The cyanotoxin-microcystins: current overview. – Reviews in Environmental Science and Biotechnology 13: 215-249.
- [18] Sevilla, E., Martin-Luna, B., Vela, L., Bes, M. T., Peleato, M. L., Fillat, M. F. (2010): Microcystin-LR synthesis as response to nitrogen: transcriptional analysis of the *mcyD* gene in *Microcystis aeruginosa* PCC7806. – Ecotoxicology 19: 1167-1173.
- [19] Tanabe, Y., Sano, T., Kasai, F., Watanabe, M. M. (2009): Recombination, cryptic clades and neutral molecular divergence of the microcystin synthetase (*mcy*) genes of toxic cyanobacterium *Microcystis aeruginosa*. – BMC Evolutionary Biology 9: 115.
- [20] Tillett, D., Dittmann, E., Erhard, M., von Döhren, H., Börner, T., Neilan, B. A. (2000): Structural organization of microcystin biosynthesis in *Microcystis aeruginosa* PCC7806: an integrated peptide-polyketide synthetase system. – Chemistry & Biology 7: 753-764.
- [21] Zuo, J., Chen, L. T., Shan, K., Hu, L. L., Song, L. R., Gan, N. Q. (2018): Assessment of different *mcy* genes for detecting the toxic to non-toxic *Microcystis* ratio in the field by multiplex q PCR. – Journal of Oceanology and Limnology 36(4): 1132-1144.
- [22] Zurawell, R. W., Chen, H. R., Burke, J. M., Prepas, E. E. (2005): Hepatotoxic cyanobacteria: a review of the biological importance of microcystins in freshwater environments. – Journal of Toxicology and Environmental Health, Part B 8: 1-37.

## VARIATIONS OF N-P-K CONTENTS IN LIVESTOCK AND LIVESTOCK MANURE COMPOSTING

ZHEN, X. F.<sup>1\*</sup> – LUO, M.<sup>1</sup> – DONG, H. Y.<sup>1</sup> – LI, S. B.<sup>1</sup> – LI, M. C.<sup>1</sup> – KANG, J.<sup>2</sup>

<sup>1</sup>*School of New Energy and Power Engineering, Lanzhou Jiaotong University  
Lanzhou 730070, China*

<sup>2</sup>*School of Material Science and Engineering, Lanzhou University of Technology  
Lanzhou 730050, China  
(phone: +86-1391-930-2012)*

*\*Corresponding author  
e-mail: zxf283386515@163.com*

(Received 29<sup>th</sup> Jul 2020; accepted 19<sup>th</sup> Nov 2020)

**Abstract.** In this study, we used three kinds of fresh livestock manure as raw materials and 10% corn stalks as a leavening agent for aerobic static composting to investigate variations of total nitrogen (TN), ammonia nitrogen (AN), total phosphorus (TP), active phosphorus (AP), total potassium (TK), and active potassium (AK) during the three kinds of livestock and poultry manure composting in China. Results show that the percentage content of TN presented an increasing trend, and the fractions of AN in TN first rose and then declined as the composting proceeded in the compost heaps. The fraction of AN in TN for R1, R2, and R3 reached the peak of 7.38, 8.11, and 9.22%, respectively. The fraction of AP in TP for R1, R2, and R3 reached  $24.15 \pm 1.97$ ,  $29.33 \pm 3.34$ , and  $34.33 \pm 1.58\%$  with the increase of 31.89, 18.26, and 35.53%, respectively, at the end of composting. The fraction of AK in TK for R1, R2, and R3 reached  $49.44 \pm 2.74$ ,  $58.37 \pm 2.21$ , and  $64.25 \pm 3.56\%$  with the increase of 32.44, 35.05, and 45.32%, respectively, at the end of composting.

**Keywords:** *static composting, materials conversion, ammonia nitrogen content, active phosphorus content, compost fertility*

### Introduction

With the development of the livestock industry, waste generated by intensive livestock farming poses a lot of serious threats to the natural environment and can pollute water, air, and soil. Taking Lanzhou as an example, with the implementation of the poverty alleviation policy involving the breeding industry in Lanzhou in recent years, the development of the local livestock breeding has been accelerated, and the number and scale of farms have been greatly improved (Zhu et al., 2014; Meng, 2014). With the rapid development of the livestock industry, the pollution caused by livestock manure to the environment cannot be ignored. Recycling and harmless treatment of agricultural waste, such as livestock and poultry manure, will help reduce pollution caused by indiscriminate discharge of livestock manure. In recent years, with the development of livestock and poultry breeding and the implementation of national environmental protection policies, more and more scholars have invested in the research on recovery and reuse of livestock manure and turning waste into treasure (Zhang et al., 2015; Zhang, 2018; Menkem et al., 2018). In this study, considering many environmental problems in solid waste treatment and resource utilization in the livestock and poultry farming in Liaoning Province, we conducted experiments in a farm near Shenyang Aerospace University, Shenyang, Liaoning Province to study such problems. A 30-day static aerobic composting experiment with cow manure, pig manure, and chicken manure as composting raw

materials and straw as a leavening agent was conducted to analyze variations of total nitrogen (TN), ammonia nitrogen (AN), total phosphorus (TP), active phosphorus (AP), total potassium (TK), and active potassium (AK) in different livestock manure composting aiming at providing a data basis and theoretical basis for the recycling and reduction of livestock manure compost.

## Materials and methods

### *Experimental material*

Three kinds of fresh manure used in the composting experiments with livestock manures were procured from the breeding farm near Shenyang Aerospace University in Shenbei New District, Shenyang, Liaoning, China. Corn stalks were cut into pieces of 2-4 cm by the knife mill before use. The information of composting materials is shown in *Table 1*.

*Table 1. Parameters information of different compost materials*

Raw materials	Water content (%)	pH	Total carbon (%)	Total nitrogen (%)	Total potassium (K <sub>2</sub> O%)	Total phosphorus (P <sub>2</sub> O <sub>5</sub> %)	C/N
Cattle manure	68.9	7.64	38.32	1.78	1.48	1.45	21.53
Pig manure	73.4	7.35	39.41	1.80	1.58	1.78	21.89
Chicken manure	70.8	7.28	41.15	2.99	1.52	2.98	13.76
Corn stalk	21.5	7.19	54.82	1.04	0.98	0.46	52.71

### *Experimental apparatus*

The self-designed aerobic bioreactor was used in laboratory. The experiment photo and apparatus of the composting is shown in *Figure 1*.

### *Experimental scheme*

An aerobic static composting was conducted using the composting materials of three livestock manures, including cattle manure (R1), pig manure (R2) and chicken manure (R3). The 30 d composting reaction was conducted with 6 self-designed aerobic composting boxes among which 2 composting boxes were considered as a group to contain single type of livestock manure.

In the whole composting process, different parameters like temperature, oxygen concentration, carbon dioxide concentration, density, etc. were monitored. Besides, the stink gas produced during the composting process was treated using a bio-filter. The change in every parameter in the composting process was compared and the changing law of the pile nutrient (the content of C-N-P-K) in the composting process with different livestock manures, humus and free humus were mainly analyzed.

Temperature was measured by thermometer. Oxygen concentration was measured by gas analyzer.

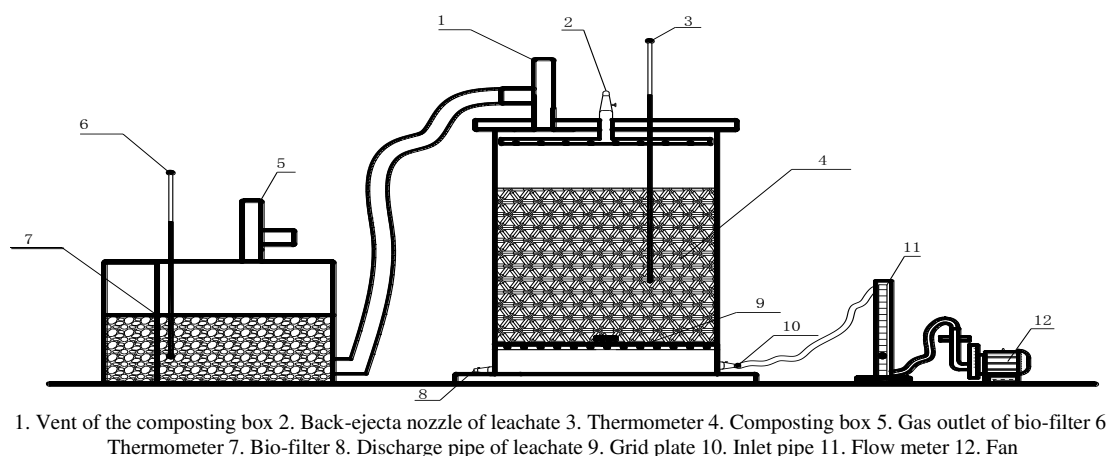


**Figure 1.** Experimental photo and apparatus used in the aerobic composting with livestock manures

### **Sample collection and preparation**

#### *The collection and conservation of the composting sample*

The sampling method was the mixing of multiple sites. The same amount of sample from the upper layer, the middle layer and the lower layer of the composting were extracted and mixed thoroughly. Fresh composting sample were determined directly or put into 4°C refrigerator for further determination of indexes such as the water content, pH, the conductivity (Petrie et al., 2015; Altenburger et al., 2015; Gou et al., 2018).

#### *The preparation of the composting water extracts*

Fresh sample which corresponded to 20 g dry sample was sampled and mixed with distilled water according to the weight ratio of 1:10 between sample and distilled water. Then it was oscillated for 32 h at the constant temperature of 26°C in the constant temperature oscillator and centrifuged for 20 min at 2000 rpm. The upper supernatant was preserved or determined (Wu et al., 2018).

#### *The preparation of air-dried composting sample*

A certain amount of the composting sample was put on the clean tray, dried for several days in the fume hood as well as grinded and filtered by 100 mesh (Liu et al., 2012).

## *Analytical methods*

### *Total nitrogen*

The TN content in the sample was measured with the Kjeldahl method:

Select a 100 mL Kjeldahl bottle, accurately weigh 0.1 g of dry sample with an electronic balance, and add about 2 g of mixed catalyst, and transfer 3 mL of concentrated sulfuric acid with a pipette gun to the reagent bottle under slow shaking in the same direction, and then seal. Place the Erlenmeyer flask under the receiving tube of the condenser and insert the nozzle into the boric acid solution. Add 40 mL of 10 mol·L<sup>-1</sup> sodium hydroxide solution to the distiller and close the distillation chamber for distillation. When the distillate reaches 30-40 mL, stop the distillation. Then titrate with 0.02 mol·L<sup>-1</sup> sulfuric acid standard solution until the solution is purple-red (Li et al., 2004; Cai et al., 2016).

### *Ammonia nitrogen*

The AN content was measured with the Nessler's reagent spectrophotometry method:

First, take 2 mL of the digestive fluid into a 100 mL measuring cylinder and dilute to 100 mL. Filter the diluted sample with a suction filter, and withdraw 50 mL of the clear solution and then place it in a 50 mL colorimetric tube. Then add in sequence 0.5 mL of analyzed sodium thiosulfate solution at a concentration of 3.5 g·L<sup>-1</sup>, 0.5 mL of analytically pure zinc sulfate solution at a concentration of 100 g·L<sup>-1</sup>, 4-5 drops of analytically pure NaOH solution at a concentration of 2.5 g·L<sup>-1</sup>, and 0.5 mL of analytically pure potassium sodium tartrate solution at a concentration of 500 g·L<sup>-1</sup> into the colorimetric tube. After adding NaOH, flocculation and precipitation obviously occur, so let stand it for 10 minutes and wait for complete flocculation and precipitation. Sodium thiosulfate addition removes residual chlorine to eliminate interference with Cl<sup>-</sup> and results in 0.25 mg removal of residual chlorine per 0.5 mL of the sodium thiosulfate solution. Take 10 mL of the sample from the lower part of the colorimetric tube with a pipette gun and place it into a 10 mL colorimetric tube. Wipe water stains on the surface of the colorimetric tube with lens cleaning paper, and put it into a multifunctional water quality detector. Measure the absorbance and AN concentration at a wavelength of 420 nm (Zhao, 2005).

### *Total phosphorus*

Take 0.1 g of air-dried sample and screen it with a 0.5 mm sieve, place it into a flask, and rinse the inner wall of the flask with deionized water to reduce the error caused by a sample loss. At the same time, add 1.5 mL of NaOH solution (30%) and 5.0 mL of H<sub>2</sub>SO<sub>4</sub> solution to the reagent bottle, shake the reagent bottle slowly for mixing and then let it stand for 8 hours after mixing well. Add 0.25 mL of distilled water after the bottle is cooled to room temperature, then heat it again to boiling. Pipette 10 mL of the sample solution into a 50 mL volumetric flask, add water to 30 mL, and check the color development. Make a color comparison and absorbance reading with a standard solution series under the same conditions. Select 7 volumetric flasks with suitable capacity and put 0, 1.0, 2.5, 5.0, 7.5, 10.0, 15.0 mL of phosphorus standard solution. Make up to 30 mL with distilled water, then add 2-3 drops of 2, 4-dinitrophenol solution to each volumetric flask with a pipette. Adjust with the NaOH solution and H<sub>2</sub>SO<sub>4</sub> solution, and add 10 mL of ammonium vanadium molybdate reagent when the color of the solution changes to

yellow, shake slowly and dilute to volume with distilled water. This solution is 1 mL containing phosphorus (Zhai, 2015; Wang et al., 2016).

#### *Active phosphorus*

The measurement of active phosphorus was done with the molybdenum-antimony anti-colorimetric method using  $0.5 \text{ mol} \cdot \text{L}^{-1}$  sodium bicarbonate leachate. In acid soil, acidic ammonium salt is used to extract the active phosphorus to produce  $(\text{NH}_4)_3\text{AlF}_6$  and  $(\text{NH}_4)_3\text{FeF}_6$  complexes, while calcium ions generate a calcium fluoride precipitate, and  $\text{PO}_4^{3-}$  ion is slowly released into the leaching solution (Wang, 2016).

#### *Data analysis*

Physicochemical parameters were determined in triplicate. Data were analyzed using One-way analysis of variance and multiple comparisons using the SPSS 18.0 software ( $p=0.05$ ). All data figures were drawn using Origin 8.0. Significant differences in physicochemical parameter values between treatments and between experimental procedures were determined using least significance difference ( $P<0.05$ ) (LSD).

### **Results and discussion**

#### *Variations of TN, AN in the experiments*

The organic nitrogen in the aerobic composting experiment goes through the processes of degradation, concentration, mineralization, and re-fixation, and the microbial flora converts mineral nitrogen into humus nitrogen through bioconcentration (Hall et al., 2015). Therefore, organic nitrogen is mainly distributed in different microbial flora and compost products of different humid levels during the composting process. This study focused on the changes in the TN and AN contents during the composting of the three kinds of livestock and poultry manures. *Figure 2* shows the changes in TN content during the composting of livestock and poultry manures. The experimental results showed that in the initial stage of composting of livestock and poultry manures, the TN content of the piles  $\text{R2} > \text{R3} > \text{R1}$  was  $1.57\% \pm 0.11\%$ ,  $1.41\% \pm 0.08\%$ , and  $1.28\% \pm 0.18\%$ , respectively. As the composting reaction progressed, the percentages of TN in the compost pile of livestock and poultry manures all showed an upward trend. When the experiments finished, the TN content in R2 was the highest at  $2.25\% \pm 0.18\%$  and that in R3 and R1 was  $2.14\% \pm 0.15\%$  and  $1.93\% \pm 0.18\%$ , respectively. The demand for organic carbon by microorganisms was higher than that for organic nitrogen, the general demand ratio being C:N=25:1. During the process of composting degradation, the degradation rate of organic carbon was higher than that of organic nitrogen, leading to a lower rate of organic nitrogen loss during composting compared with that of organic carbon. Therefore, the percentages of TN in livestock and poultry manures compost piles all showed an upward trend. After the composting process, the TN content of R1, R2, and R3 compost piles all increased by 50.78%, 43.33%, and 51.77%, respectively. Among them, R3 had the largest increase, while R2 had the smallest. After composting, the nitrogen element was mainly composed of organic nitrogen. Nitrogen assimilation and fixation effect were obvious when poultry manure containing more mineral nitrogen was used for high-temperature composting, which was conducive to nitrogen storage and fertility retention (Hua et al., 2012; Zhang, 2014).

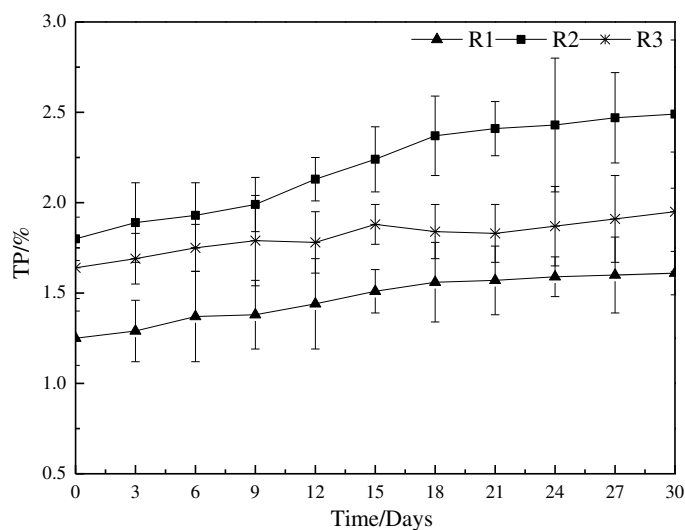


**Figure 2.** Changes in TN content during experiments

Figure 3 represents the change trend in the percentage of AN in TN during the composting process of livestock and poultry manures. The results showed that during the 30-day composting process, the percentage of AN in TN in the three types of livestock and poultry manure piles all increased first and then decreased. At the beginning of the composting reaction (0 days), the percentage of AN in the three manure compost piles of R1, R2, and R3 was 16.34, 15.28, and 15.97, respectively. After 3 days, AN accounted for the highest percentage in TN, which was 19.1, 20.08, and 21.14%, respectively. With the progress in composting, the percentage of AN in TN in the pile showed a downward trend. When the experiments finished, the percentage of AN in TN became the highest, being 7.38, 8.11, and 9.22, respectively. Therefore, the percentage of AN in TN in the three types of livestock and poultry manure piles increased first and then decreased, mainly because nitrogen in livestock and poultry manures was divided into inorganic and organic states. Among them, organic nitrogen accounted for a large percentage, but it could not be stably presented in the manures, and it was easily decomposed into ammonia. During the 0-3 days of the composting process, the livestock and poultry manures were rich in proteins, which was decomposed under the action of microorganisms to form amino acids or amide compounds or to finally form inorganic ammonium salts. Therefore, the AN content in TN in the three kinds of livestock and poultry manures increased during the composting process from 0 to 3 days. It showed a downward trend during the composting process from 4 to 30 days. This was because, as the temperature and the pH value increased, AN, mainly  $\text{NH}_3$  in the pile, was volatilized, reducing the AN content (Marhuenda-Egea et al., 2007; Awasthi et al., 2016). TN also dropped rapidly at this stage, but the decrease in AN was slightly greater than that in TN. Meanwhile, the high-temperature phase of the compost had passed, and the temperature of the pile had fallen. At this stage, humification was the primary factor, and mineralization was secondary. Most of the ammonium nitrogen was absorbed and utilized by the microorganisms and converted into humic acid nitrogen. On the contrary, with the enhancement of humification, the conversion of relatively simple acid-decomposed ammonium nitrogen into relatively complex other acid-decomposed nitrogen and non-acid-decomposed nitrogen resulted in a reduction in its quantity.

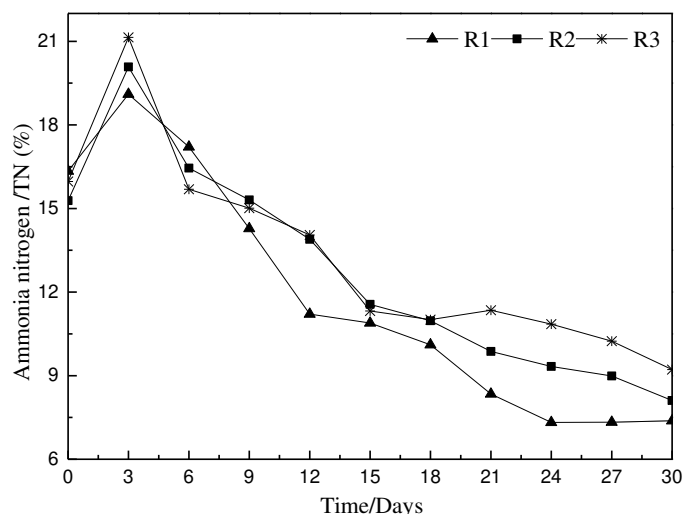


**Figure 3.** AN as a percentage of TN during experiments

The increase in humus retention of  $\text{NH}_4^+$  during humification was also one of the reasons for the decrease in AN/TN (Paradelo et al., 2013). Although the percentage of AN in TN of different livestock and poultry manures changed in the same way, at the end of composting, the percentage of AN in TN was different compared with that at the beginning, where R3 had the highest percentage, being 9.22. This was mainly because, compared with R1, R2, and R3, composting using R3 as raw material was conducive to the formation of ammonium nitrogen (Rajeshkumar et al., 2017).

#### **Variations of TP, AP in the composting of livestock manure**

Figure 4 shows the changes of TP content during the composting of different livestock and poultry manures. The experimental results show that the TP content in the compost heaps decreased from  $\text{R2} > \text{R3} > \text{R1}$  at the initial stage of composting of livestock and poultry manures to a value of  $1.80 \pm 0.12$ ,  $1.64 \pm 0.17$ , and  $1.25 \pm 0.15\%$ , respectively. As the composting reaction progressed, the percentage of TP in livestock manure compost heaps increased which was mainly due to organic carbon, organic nitrogen, and organic phosphorus absorption, assimilation, and decomposition by microorganisms in the process of livestock manure composting. Demand for organic carbon by microorganisms is higher than demand for organic nitrogen and also for organic phosphorus with a general demand ratio of  $\text{C:N:P}=100:5:1$  (Santos et al., 2009). After the composting, the TP content in all three livestock manure (R1, R2, and R3) composting products increased to a value of 25.61, 33.38, and 11.58%, respectively. During the experiments, 10% straw was selected as an additive to adjust the water content and void ratio. A reasonable material ratio promotes smooth progress of composting without a leachate and phosphorus loss in the whole process. Unlike nitrogen, which easily evaporates as a gas, phosphorus is stable which causes the smaller volatilization loss of the compost TP content (Villasenor et al., 2011; Singh et al., 2013). Besides, organic matter is decomposed and mineralized during the composting of livestock and poultry manure, and the dry matter content in the compost heaps reduces. So, the concentration of TP per unit mass of compost products from the three livestock manures increased.



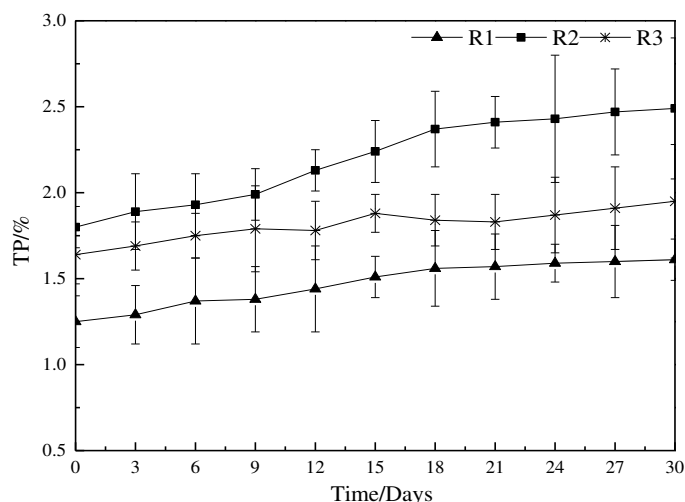


**Figure 4.** Changes of TP content during experiments

Figure 5 shows the changes of AP as a percentage of TP content during composting of livestock and poultry manures. The results show that the fractions of AP in TP in the three kinds of livestock manure compost heaps increased during the 30-day composting. At the beginning of the composting (0 d), the percentage of AP in the three compost heaps of R1, R2, and R3 was  $18.31 \pm 1.25$ ,  $24.8 \pm 1.15$ , and  $25.33 \pm 2.21\%$ , respectively. With the progress of composting, the percentage of AP in TP gradually increased, when the experiments finished, the percentage of AP in TP reached  $24.15 \pm 1.97$ ,  $29.33 \pm 3.34$ ,  $34.33 \pm 1.58\%$  and increased by 31.89, 18.26, and 35.53%, respectively.

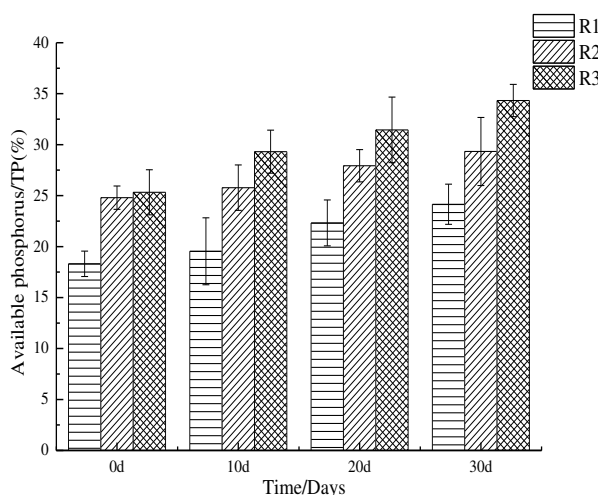
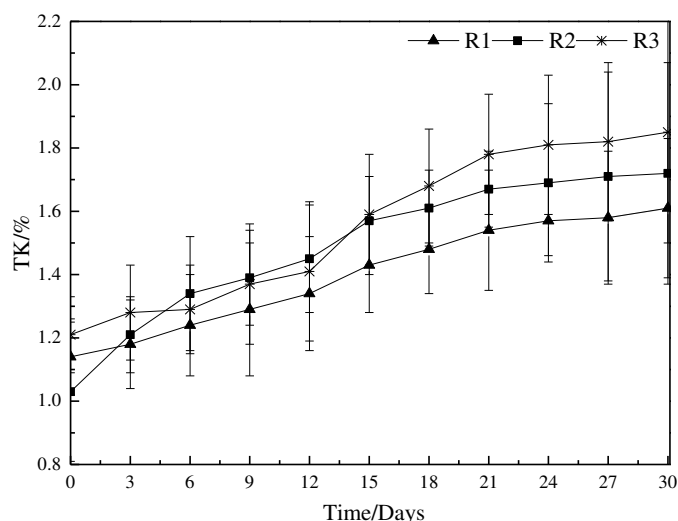


**Figure 5.** Changes of the percentage of AP in TP during experiments

### Variations of TK, AK in the composting of livestock manure

Figure 6 shows the changes of TK content during the composting of different livestock and poultry manures. The experimental results show that the TK content in the compost heaps decreased from  $R3 > R1 > R2$  at the initial stage of composting of livestock and poultry manures to a value of  $1.21 \pm 0.12$ ,  $1.14 \pm 0.12$ , and  $1.03 \pm 0.22\%$ , respectively.

As the composting reaction progressed, the percentage of TK in livestock manure compost heaps increased and reached  $1.61 \pm 0.22$ ,  $1.72 \pm 0.3$ , and  $1.85 \pm 0.35\%$ , respectively, when the experiments finished. These increasing trends are mainly due to assimilation and decomposition of organic carbon, organic nitrogen, and organic phosphorus by microorganisms during the composting of livestock and poultry manure with a lower utilization rate of potassium than that of organic carbon, nitrogen, and phosphorus by microorganisms and basically no loss of potassium during composting.



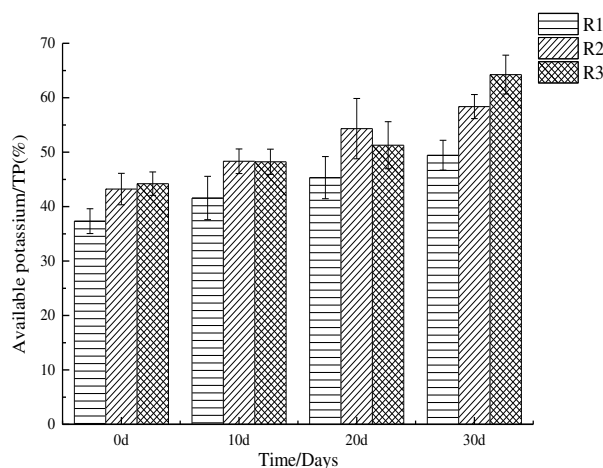
**Figure 6.** Changes of TK content during composting of livestock and poultry manure

Figure 7 shows the changes of fractions of AK in the TK content during composting of livestock and poultry manure. The results show that the fractions of AK in TK in the three kinds of livestock manure compost heaps increased during the 30-day composting. At the beginning of the composting (0 day), the percentage of AK in the three compost heaps of R1, R2, and R3 was  $37.33 \pm 2.28$ ,  $43.22 \pm 2.89$ , and  $44.21 \pm 2.15\%$ , respectively. With the progress of composting, the percentage of AP in TP gradually increased, and at the end of composting (30 days), the percentage of AP in TP reached  $24.15 \pm 1.97$ ,  $29.33 \pm 3.34$ ,  $34.33 \pm 1.58\%$  and increased by 31.89, 18.26, and 35.53%, respectively. As the composting progressed, the fractions of AK in TK gradually increased and reached  $49.44 \pm 2.74$ ,  $58.37 \pm 2.21$ , and  $64.25 \pm 3.56\%$  and increased by 31.89, 18.26, and 35.53%, respectively, at the end of composting.

### **Changes of total nutrients in the composting of livestock manure**

The total nutrient content in compost products is an important indicator of organic fertilizer quality (Santos et al., 2009) which is generally represented by the sum of N, P, and K elements where the element N is calculated as TN, the element P is calculated as the  $P_2O_5$  content, and the element K is calculated as the  $K_2O$  content. There are three transformation forms for the conventional element N in the process of composting. The first is that nitrogen is converted into  $NH_3$  and exits the heap as exhaust gas during the composting, resulting in the loss of nitrogen fertilizer (Wang et al., 2013). The second is that nitrogen is used by nitrifying bacteria or nitrosating bacteria for nitrification reactions to form  $NO_3^-$  or  $NO_2^-$  during the composting. The third is that nitrogen is absorbed by

microorganisms and converted into organic nitrogen (Wei et al., 2016). There are two transformation forms for the element P in the composting. One is that phosphorus is converted into  $\text{PH}_3$  and exits the heaps as exhaust gas during the composting, or a leachate is produced during the composting, resulting in the loss of phosphate fertilizer. But the loss rate is low compared to that of nitrogen (Zhang et al., 2017). The other is assimilation of phosphorus element by microorganisms into organic phosphorus which is also the main reason for enriched phosphorus in compost products. Transformation of K element is only microorganism absorption and utilization in the composting, and finally it exists in compost products. The total nutrients ( $\text{N} + \text{P}_2\text{O}_5 + \text{K}_2\text{O}$ ) content showed a rising trend in the composting of livestock and poultry manure due to the assimilation absorption and dissimilation decomposition of organic carbon, organic nitrogen, and organic phosphorus by microorganisms. Total experiments, the degradation rate of organic carbon is higher than that of organic nitrogen and organic phosphorus, and potassium is basically not lost. The loss of carbon and water causes a concentration effect (Wei et al., 2012) which increases the content of total nutrients (Liu et al., 2010). As shown in Table 2, pig manure compost had the highest total nutrient content of 6.33%, and cow manure compost had the lowest total nutrient content of 5.04% at the end of composting.



**Figure 7.** Changes of the percentage of AK in TK during composting of livestock and poultry manure

According to the Organic Fertilizer Industry Standard (NY525-2012) published in 2012, qualified products should meet conditions that the mass fraction of organic matter is  $\geq 45\%$ , the mass fraction of total nutrients ( $\text{N} + \text{P}_2\text{O}_5 + \text{K}_2\text{O}$ ) is  $\geq 5\%$ , the water mass fraction is  $\leq 30\%$ , and pH is in a range of 5.5-8.5. It can be seen from Table 2 that the nutrients of the three compost products reached the national standard (Zhou et al., 2014).

**Table 2.** Total nutrient content in livestock manure compost products

Compost products	TN/%	TP/%	TK/%	( $\text{N} + \text{P}_2\text{O}_5 + \text{K}_2\text{O}$ )/%
R1	1.93±0.18	1.57±0.19	1.54±0.19	5.04
R2	2.25±0.18	2.41±0.15	1.67±0.12	6.33
R3	2.14±0.15	1.83±0.16	1.78±0.19	5.75

## Conclusions

Based on the 30-day static aerobic composting experiment with cow manure, pig manure, and chicken manure, we observed the variations of TN, AN, TP, AP, TK, and AK. It was shown that at the initial stage of composting, the TN content in the heaps decreased from R2 > R3 > R1 to a value of  $1.57 \pm 0.11$ ,  $1.41 \pm 0.08$ , and  $1.28 \pm 0.18\%$ , respectively. As the composting reaction proceeded, TN increased and reached the peak with the highest value of  $2.25 \pm 0.18\%$  for R2. The fractions of AN in TN increased first and then declined. At the end of composting (30 days), the fraction of AN in TN for R1, R2, and R3 reached the highest percentage of 7.38, 8.11, and 9.22%, respectively. The TP content in all three manure compost heaps (R1, R2, R3) showed an upward trend, and the increase was 25.61, 33.38, and 11.58%, respectively. The fractions of AP in TP also showed increasing trends during the composting. At the end of composting (30 days), the fraction of AP in TP reached  $24.15 \pm 1.97$ ,  $29.33 \pm 3.34$ , and  $34.33 \pm 1.58\%$  with an increase of 31.89, 18.26, and 35.53%, respectively. The TK content in the compost heaps showed an increasing trend during the composting and reached  $1.61 \pm 0.22$ ,  $1.72 \pm 0.35$ , and  $1.85 \pm 0.35\%$ , respectively, when the experiments finished. The fraction of AK in TK for R1, R2, and R3 also showed increasing trends and reached the highest value of  $49.44 \pm 2.74$ ,  $58.37 \pm 2.21$ , and  $64.25 \pm 3.56\%$  with an increase of 32.44, 35.05, and 45.32%, respectively, at the end of composting (30 days).

**Acknowledgements.** This work was funded by the Yianyou Youth Talent Lift Program of Lanzhou Jiaotong University, Funds for Youth Science Foundation Project of Lanzhou Jiaotong University (2020018) and the National Natural Science Foundation of China (No.51606090, No.51866008).

## REFERENCES

- [1] Altenburger, R., Ait-Aissa, S., Antczak, P., Backhaus, T., Barceló, D., Seiler, T.-B., Brion, F., Busch, W., Chipman, K., López de Alda, M., de Aragao Umbuzeiro, G., Escher, B. I., Falciani, F., Faust, M., Focks, A., Hilscherova, K., Hollender, J., Hollert, H., Brack, W. (2015): Future water quality monitoring Adapting tools to deal with mixtures of pollutants in water resource management. – *Science of the Total Environment* 512-513: 540-551.
- [2] Awasthi, M. K., Wang, Q., Huang, H., Ren, X., Lahori, A. H., Mahar, A., Ali, A., Shen, F., Li, R., Zhang, Z. (2016): Influence of zeolite and lime as additives on greenhouse gas emissions and maturity evolution during sewage sludge composting. – *Bioresource Technology* 216: 172-181.
- [3] Cai, H. Z., Ning, X. C., Wang, Q. (2016): Effects of alkaline solids on the conditioning and composting of sludge and the potential of the products to improve the soil. – *Environmental Science* 37(12): 4848-4856.
- [4] Gou, M., Hu, H. W., Zhang, Y. J., Wang, J. T., Hayden, H., Tang, Y. Q., He, J. Z. (2018): Aerobic composting reduces antibiotic resistance genes in cattle manure and the resistome dissemination in agricultural soils. – *Science of the Total Environment* 612: 1300-1310.
- [5] Hall, D. J. M., Bell, R. W. (2015): Biochar and Compost Increase Crop Yields but the Effect is Short Term on Sandplain Soils of Western Australia. – *Pedosphere* 25(5): 720-728.
- [6] Hua, L., Chen, Y., Wu, W. (2012): Impacts upon soil quality and plant growth of bamboo charcoal addition to composted sludge. – *Environmental Technology* 33(1): 61-68.
- [7] Li, J. J., Hao, J. M., Zou, G. Y. (2004): Carbon and nitrogen circulation and humus characteristics of high-temperature composting. – *Ecology and Environment* 13(3): 332-334.

- [8] Liu, X. Y., Jin, J. Y., Ren, T. Z., He, P. (2010): Potential of organic manures nutrient resources and their environmental risk in China. – *Chinese Journal of Applied Ecology* 21(8): 2092-2098.
- [9] Liu, J., Li, J. N., Wen, K. J. (2012): Dynamic Transformation of Organic Carbon Under Different Communist Community Conditions. – *Northern Horticulture* 24: 174-178.
- [10] Marhuenda-Egea, F. C., Martínez-Sabater, E., Jordá, J., Moral, R., Bustamante, M. A., Paredes, C., Pérez-Murcia, M. D. (2007): Dissolved organic matter fractions formed during composting of winery and distillery residues: Evaluation of the process by fluorescence excitation–emission matrix. – *Chemosphere* 68(2): 301-309.
- [11] Meng, X. H. (2014): Study on Prevention Problem of China Livestock Environmental Pollution. – Huazhong Agricultural University.
- [12] Menkem, E. Z., Ngangom, B. L., Tamunjoh, S. S. A., Boyom, F. F. (2018): Antibiotic residues in food animals: Public health concern. – *Acta Ecologica Sinica*.
- [13] Paradelo, R., Moldes, A. B., Barral, M. T. (2013): Evolution of organic matter during the mesophilic composting of lignocellulosic winery wastes. – *Journal of Environmental Management* 116(Complete): 18-26.
- [14] Petrie, B., Barden, R., Kasprzyk-Hordern, B. (2015): A review on emerging contaminants in wastewaters and the environment: Current knowledge, understudied areas and recommendations for future monitoring. – *Water Research* 72: 3-27.
- [15] Rajeshkumar, S., Liu, Y., Zhang, X., Ravikumar, B., Bai, G., Li, X. (2017): Studies on seasonal pollution of heavy metals in water, sediment, fish and oyster from the Meiliang Bay of Taihu Lake in China. – *Chemosphere* 191(4): 626.
- [16] Santos, P. S. M., Duarte, R. M. B. O., Duarte, A. C. (2009): Absorption and fluorescence properties of rainwater during the cold season at a town in Western Portugal. – *Journal of Atmospheric Chemistry* 62(1): 45-57.
- [17] Singh, J., Kalamdhad, A. S. (2013): Assessment of bioavailability and leachability of heavy metals during rotary drum composting of green waste (Water hyacinth). – *Ecological Engineering* 52(2): 59-69.
- [18] Villasenor, J., Rodríguez, L., Fernández, F. J. (2011): Composting domestic sewage sludge with natural zeolites in a rotary drum reactor. – *Bioresource Technology* 102(2): 1447-1454.
- [19] Wang, L., Zhang, Y., Lian, J., Chao, J., Gao, Y., Yang, F., Zhang, L. (2013): Impact of fly ash and phosphatic rock on metal stabilization and bioavailability during sewage sludge vermicomposting. – *Bioresour Technol* 136(5): 281-287.
- [20] Wang, Y. F. (2016): Changes of Culturable Microorganisms, Humus Content and Enzyme Activities in Composting of Four Kinds of Livestock Dung. – Gansu Agricultural University.
- [21] Wang, Y. X., Gao, L. F., Ye, J., Li, Y., Weng, B. (2016): Change of carbon substance characteristics during composting of waste packing and fungus chaff. – *Transactions of the Chinese Society of Agricultural Engineering* 32(s2): 292-296.
- [22] Wei, Z., Zhao, X., Zhu, C., Xi, B., Zhao, Y., Yu, X. (2016): Assessment of humification degree of dissolved organic matter from different composts using fluorescence spectroscopy technology. – *Chemosphere* 95(1): 261-267.
- [23] Wu, W., Sheng, H., Gu, C., Song, Y., Willbold, S., Qiao, Y., Liu, G., Zhao, W., Wang, Y., Jiang, X., Wang, F. (2018): Extraneous dissolved organic matter enhanced adsorption of dibutyl phthalate in soils: Insights from kinetics and isotherms. – *Science of the Total Environment* 631: 1495-1503.
- [24] Zhai, Q. M. (2015): The Research about the Response of Farmland Animal Community to Pesticide and EM Compost Treatment. – Harbin Normal University.
- [25] Zhang, Z. (2014): Nutrient transformation during aerobic composting of pig manure with biochar prepared at different temperatures. – *Environmental Technology* 36(7): 1-28.
- [26] Zhang, Q. Q., Ying, G. G., Pan, C. G., Liu, Y. S., Zhao, J. L. (2015): Comprehensive evaluation of antibiotics emission and fate in the river basins of china: source analysis,

- multimedia modeling, and linkage to bacterial resistance. – *Environmental Science & Technology* 49(11): 6772-6782.
- [27] Zhang, C., Xu, Y., Zhao, M., Rong, H., Zhang, K. (2017): Influence of inoculating white-rot fungi on organic matter transformations and mobility of heavy metals in sewage sludge based composting. – *Journal of Hazardous Materials* 344: 163-168.
- [28] Zhang, B. B. (2018): Assessment of Raw Material Supply Capability and Energy Potential of Biomass Resource in China. – China Agricultural University.
- [29] Zhao, S. F. (2005): Study on the Phosphorus during the Aerobic Composting Process. – Zhejiang University.
- [30] Zhou, Y., Selvam, A., Wong, J. W. C. (2014): Evaluation of humic substances during co-composting of food waste, sawdust and Chinese medicinal herbal residues. – *Bioresource Technology* 168(3): 229-234.
- [31] Zhu, J. C., Zhang, Z. Q., Fan, Z. M., Li, R. H. (2014): Biogas Potential, Cropland Load and Total Amount Control of Animal Manure in China. – *Journal of Agro-Environment Science* 33(3): 435-445.

## RELATIONSHIPS BETWEEN BARK BEETLE DIVERSITY AND HABITAT CHARACTERISTICS IN PINE FORESTS OF SOUTH MARMARA, TURKEY

ACER, S.<sup>1</sup> – ARSLANGÜNDOĞDU, Z.<sup>1</sup> – HIZAL, E.<sup>1\*</sup> – KUMBAŞLI, M.<sup>2</sup>

<sup>1</sup>*Istanbul University – Cerrahpaşa, Faculty of Forestry, İstanbul, Turkey*

<sup>2</sup>*Bolu Abant İzzet Baysal University, Wildlife Research Center, Bolu, Turkey*

\*Corresponding author  
e-mail: hizal@istanbul.edu.tr

(Received 31<sup>st</sup> Jul 2020; accepted 19<sup>th</sup> Nov 2020)

**Abstract.** The bark beetles are of particular importance in the evolution and biodiversity of forest stands. To contribute to the knowledge on the biodiversity and ecology of bark beetles on pine species, we performed this research in South Marmara, Turkey. During 2014, Scolytinae species were obtained from baiting logs, which were 1.5 m long, and 0.2 m in diameter located at 8 sites in total in the research area. In total, 1100 individuals were collected representing 6 tribes, 11 genera, and 24 species. *Orthotomicus erosus* was the most abundant species and occurred in all areas. Our study demonstrated that black pine is associated with high diversity of beetles while brutian pine is correlated with high abundance of Scolytinae. In addition, stone pine has lowest diversity and abundance of bark beetles. *Pinus brutia*, which showed strong correlation with temperature, had relationship with *O. erosus* and *P. pennidens*. *Pinus nigra* showed a strong correlation with altitude, additionally it had relationship with *I. sexdentatus*. Our results indicate that these abiotic factors affect the composition and the number of bark beetles.

**Keywords:** *Pinus* spp., *Scolytinae* species, biodiversity, ecological relationships, dispersal

### Introduction

The bark beetles are of particular importance in the evolution and biodiversity of forest stands. During undisturbed forest succession, they commonly feed upon and kill the excess plants in the stand. The vast majority of bark beetles are saprophagous, strictly breeding in dead trees or tree parts. Tree-killing bark beetles, while relatively few in number, can have profound ecological effects, including impacts on species composition, age structure, density, woody debris inputs, and even global carbon balance (Bright and Stark, 1973; Kurz et al., 2008; Lindgren and Raffa, 2013). In addition to their ecological roles, some bark beetles compete with humans for valued plants and plant products, and so are significant forest and agricultural pests (Raffa et al., 2015). Like most insects, bark beetles have high reproductive potentials that provide the capability to undergo rapid, exponential population increase (Økland and Bjørnstad, 2006; Marini et al., 2013). At outbreak population levels, beetles can cause extensive tree mortality altering forest structure, reducing fiber production capacity, and diminishing stand aesthetics (Cole and McGregor, 1988; Fiddler et al., 1989; Cochran and Barrett, 1998). Increases in surface fuel loadings also follow bark beetle-caused mortality (Jenkins et al., 2008). In this case, these species cause substantial socioeconomic losses, and at times necessitate management responses (Klutsch et al., 2009; Raffa et al., 2015). In Europe, there are relatively few bark beetle species that are regarded as serious pests, the majority are secondary pests feeding and reproducing in dead and dying trees, and they rarely cause significant damage or losses, especially to

live trees (Grégoire and Evans, 2004; Sauvard, 2004). Secondary bark beetles have been observed attacking healthy trees far more frequently, presumably in response to changing climate patterns, particularly increased drought periods (Grégoire et al., 2001; Kuhnholz et al., 2001). However, coniferous monocultures are generally regarded as being poor structurally, lacking in biodiversity and highly susceptible to pest, pathogens and climate change (Koricheva et al., 2006; Jactel and Brockerhoff, 2007; Brockerhoff et al., 2008).

Environmental variables play a major role in shaping the bark beetles' diversity and dispersal. Temperature limits insect populations and regulates their distribution. Interactions between bark beetles and temperature are highly complex and include varying patterns of perpetuation, survival threshold, facultative diapause, and adaptation to harsh cold (Heliövaara and Peltonen, 1999). Air humidity acts on behalf of bark beetles such as host selection (Heliövaara and Peltonen, 1999), flight dispersal (Franklin and Grégoire, 1999), and overwintering (Košťál et al., 2011).

Dispersal by flight is obligatory for bark beetles in the subfamily Scolytinae. Adult bark beetles must leave the natal host and fly to seek new hosts for brood production (Jones et al., 2019). Wind speed and direction can have a large impact on the flight of small insects such as bark beetles. Bark beetles can be dispersed over quite a long distance by wind (Byers, 2000). Wind can influence the distance that bark beetles fly, the energy used during flight, and the direction in which beetles disperse. The average dispersal of most bark beetles is less than 5 km while long – distance dispersal can reach more than 100 km per day in flight aided by the wind (Jones et al., 2019).

In general, a greater diversity of insects is found at the lower or intermediate altitudes where conditions are less extreme and many species. Altitude has an effect limiting the diversity and distribution of bark beetles (Rubin-Aguirre et al., 2015).

The composition and richness of species assemblages also strongly influence ecosystem functioning and stability. The conservation of insect diversity is therefore a topic of global importance (Zou et al., 2011; Hlásny et al., 2019). While there were numerous studies in Europe (Jakus, 1998; Peltonen et al., 1998; Weslien and Schroeder, 1999; Kalapanida-Kantartzis et al., 2010; Foit, 2015), only a few researchers (Sarıkaya and Yıldırım, 2011; İbiş and Sarıkaya, 2012) investigated the composition and diversity of bark beetle communities under different environmental conditions in Turkey. It is necessary to research forest communities across the country and to observe which insects are present in a particular area. In this way, when a particular insect population begins to grow, researchers will be able to predict the extent of the damage and what control measures to use. In this study, the bark beetle species on pines were investigated at different stands in the South Marmara of Turkey. Brutian pine (*Pinus brutia* Ten.), black pine (*P. nigra* Arnold) and stone pine (*P. pinea* L.) are the main species of pine forests of the area. This section is the natural spreading boundary in the north for the brutian pine. In addition, it is an area where valuable black pine forests in Turkey. Stone pine in the area serves multi-functional purposes such as pine nut, timber, and landscape planning. If we want to perform holistic forest management in such an important area, it is necessary to better understand the biodiversity and ecology of bark beetles in relation to their habitat characteristics. The aim of this research is to contribute to the knowledge about biodiversity and ecology of bark beetles.



## Materials and Methods

Our research was carried out in Çanakkale and Balıkesir provinces in the south part of Marmara Region (*Fig. 1*). The area has coastal in the Marmara and Aegean Region of Turkey and hosts the Strait of Çanakkale that one of the two straits of Turkey. The climate in the region shows characteristic transition climate of the Mediterranean – the Black Sea (Doğukan et al., 2008). Average annual temperature is 14.8°C with the maximum summer temperature 30.6°C and minimum winter temperature 2.7°C. Average annual rainfall is approximately 615.4 mm (TSMS, 1998). The prevailing soil type is inceptisol soil according to American classification (Efe, 1999). Approximately 43% of the area is covered with forests while 74% of forest areas in the region are constituted by pine species (Anonymus, 2006; Karagöz and Demirci, 2015) (*Fig. 1*).

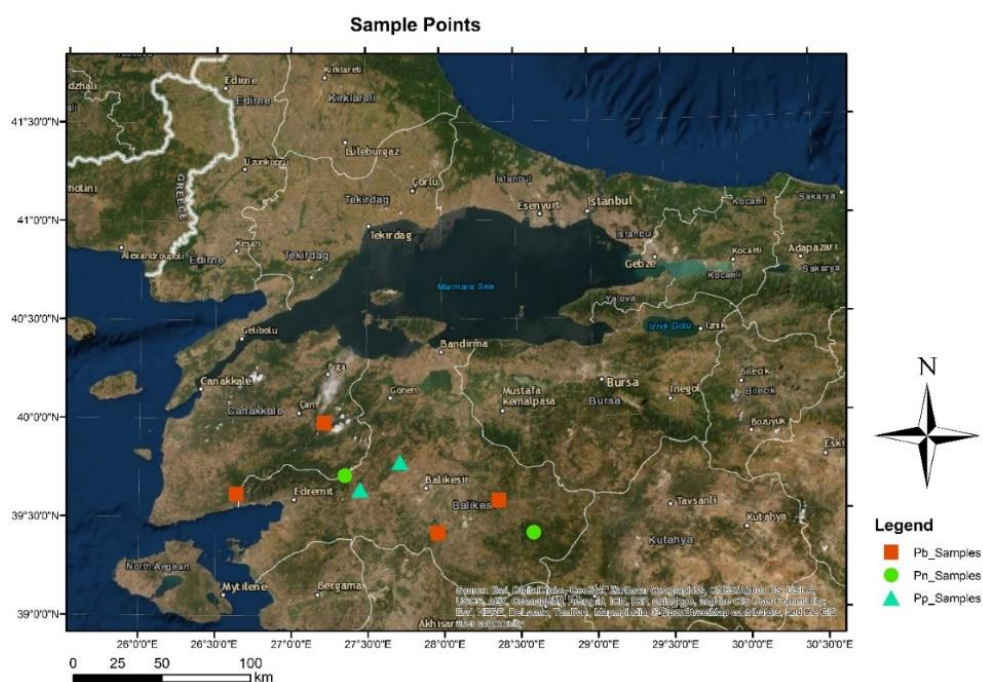


**Figure 1.** Sampling points in the field study conducted on pines in South Marmara in 2014

During 2014, Scolytinae species were collected from baiting logs in totally 8 sites in research area; 4 different pure stands of *P. brutia* (Pb-1 and 4 mature stands, Pb-2 and 3 young stands), 2 different pure mature stands of *P. nigra* (Pn-1 and 2) different pure young stands of *P. pinea* (Pp-1 and 2). Sampling points, altitudes, and geographical coordinates were also noted (*Table 1*) and pointed out on a map by ARCGIS 10.2 (*Fig. 1*) (ESRI, 2014). In February 2014, baiting logs, 1.5 m long and 0.2 m in diameter (bark thickness about 2 cm) were set in each stand, using the technique described by Tribe (1992). Traps were checked every twenty days and three logs at each site were inspected for the presence of beetle entrance holes. All beetles brought to the laboratory were morphologically identified with a LEICA S8APO stereomicroscope to determine with several taxonomic keys that provide taxonomic characteristics located in the pronotum, scutellum, elytra, metapisternum and antennal funiculum, etc. (Grüne, 1979; Wood, 1982; Selmi, 1998; Lompe, 2002; Benisch, 2007; Jordal and Knížek, 2007).

**Table 1. Sampling points characteristics**

Sampling Point	Geographical position	Altitude (m)	*Tree species / stand type	**Soil type	***Temperature (°C)	***Humidity (%)
<b>Pb-1</b>	39°34'46.6"N 28°21'42.1"E	508	<i>P. brutia</i> / c	Orthic luvisol	16,3	69,8
<b>Pb-2</b>	39°24'57.7"N 27°57'44.8"E	442	<i>P. brutia</i> / c	Eutric cambisol	18,1	69,3
<b>Pb-3</b>	39°37'02.6"N 26°38'19.3"E	557	<i>P. brutia</i> / c	Eutric cambisol	18,6	71,1
<b>Pb-4</b>	39°58'41.6"N 27°13'0.6"E	380	<i>P. brutia</i> / c	Orthic luvisol	17,1	76,3
<b>Pn-1</b>	39°24'47.9"N 28°35'18.6"E	1164	<i>P. nigra</i> / c	Orthic luvisol	16,3	69,8
<b>Pn-2</b>	39°42'34.9"N 27°21'09.3"E	730	<i>P. nigra</i> / c	Eutric cambisol	17,6	73,2
<b>Pp-1</b>	39°46'40.1"N 27°42'56.3"E	338	<i>P. pinea</i> / b	Eutric cambisol	15,9	80,9
<b>Pp-2</b>	39°38'23.7"N 27°27'04.7"E	280	<i>P. pinea</i> / b	Orthic luvisol	17,6	73,2

\*[“a” (0–8 cm), “b” (9–20 cm) and “c” (21–36 cm) mean diameter at breast height (DBH)], \*\*FAO Soil Map was used for soil classification (FAO, 2020), \*\*\* (TSMS, 1998)

Species accumulations by time and sample effort were assessed with rarefaction curves (Rodríguez et al., 2017). Species diversity was calculated by Shannon index ( $H'$ ) (Spellerberg and Fedor, 2003). Evenness was measured by Pielou index ( $J'$ ) (Pielou, 1969). For each area, the relative abundance of species was transformed to logarithm-10 ( $N + 1$ ) and the tabulated data from the most abundant species to the least abundant (Feinsinger, 2001). All analyzes were undertaken PAST 4.03 (Hammer et al., 2001). Species diversity results compared by overlapping of confidence intervals obtained in software ANAFAU (Moraes et al., 2003).

The air temperature, air humidity, and wind speed employed data represent the study period averages obtained from 7 automatic weather station (AWS) (18082, 18434, 17158, 18085, 17700, 18432, 18436) that are the nearest to each sampling point in the area (Fig. 2) (TSMS, 1998). Altitude data were taken from each sampling point using GPS.

To evaluate the effect of environmental variables on species composition and abundance in the 8 sampling area, Canonical Correspondence Analysis (CCA) was performed. Eigenvalues representing the contribution of each classification axis to the explanation of the change in data were used in CCA. There is one eigenvalue for each ordination axis, and the size for an axis is a direct indication of the importance of that axis in variation within the data set (Chung et al., 2001). The importance of individual variables for the CCA ordination model was assessed by the Monte Carlo test and forward selection. In this process, the explanatory environmental variables are added to a null model of a fully stochastic dataset according to their contribution to the explained variability. The significance of increase of the fit after adding a variable is tested by a Monte Carlo permutation test with 999 replicates.

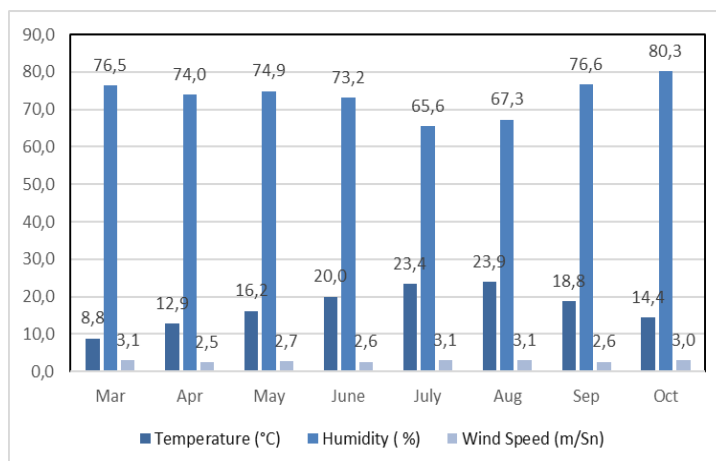


**Figure 2.** Air temperature, humidity and wind speed during the experiment in research area

Species with less than five individuals were excluded from the analysis and any remaining species or sample outliers were removed (due to their misleading effect on the analysis, and allowing species association patterns to be displayed more clearly), leaving a total of 16 species (98.7% of individuals) included in the analysis. Species abundance was studied by converting to logarithm-10 ( $N + 1$ ), (Hulcr et al., 2008; Mullen et al., 2008; Foit, 2015; Zhang et al., 2017). All analyzes were undertaken PAST 4.03 (Hammer et al., 2001).

## Results

In total, 1100 individuals were collected representing 6 tribes, 11 genera, and 24 species. The most abundant tribe was Ipini (78.18% - 9 species), followed by Tomicingi (12.73% - 5 species), Hylastini (5.18% - 3 species), Crypturgini (3.18% - 4 species), Polygraphini (0.55% - 1 species), and Xyleborini (0.18% - 2 species) (Table 2). Ipini had the highest abundance (860 individuals) and the greatest richness (9 species). The rarefaction curves for some sites have not approached an asymptote (Pb-2 and Pp-1) indicating efficiency in sampling species of Scolytinae beetles in this study (Fig. 3).

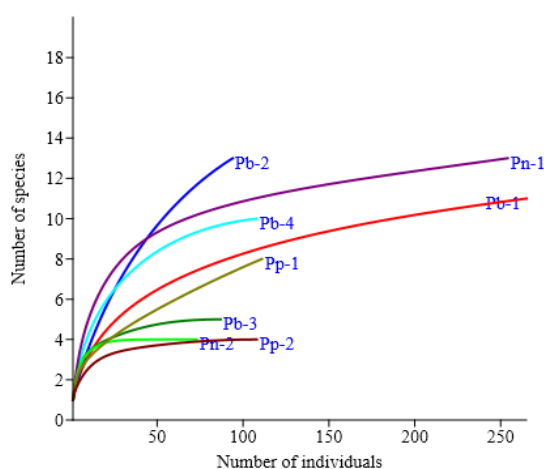


**Figure 3.** Individual based species accumulation curves

**Table 2.** Species of subfamily Scolytinae collected in eight sites at research area

	Pb 1	Pb 2	Pb 3	Pb 4	Pn-1	Pn-2	Pp-1	Pp-2	Total	%
<b>Tribe: Crypturgini</b>										
<i>Crypturgus cinereus</i>	1			5	14				20	1,82
<i>Crypturgus hispidulus</i>				2	1				3	0,27
<i>Crypturgus numidicus</i>	5			5					10	0,91
<i>Crypturgus pusillus</i>	1			1					2	0,18
<b>Tribe: Hylastini</b>										
<i>Hylastes angustatus</i>	3	1		15	4				23	2,09
<i>Hylastes linearis</i>		2							2	0,18
<i>Hylastes opacus</i>	14				11	7			32	2,91
<b>Tribe: Ipini</b>										
<i>Ips sexdentatus</i>	35	2	3		86	35			161	14,6
<i>Orthotomicus erosus</i>	187	67	42	58	70	23	41	83	571	51,9
<i>Orthotomicus longicollis</i>		2			16				18	1,64
<i>Pityogenes bidentatus</i>		1							1	0,09
<i>Pityogenes bistridentatus</i>					21				21	1,91
<i>Pityogenes calcaratus</i>							2		2	0,18
<i>Pityogenes calcographus</i>		1					8		9	0,82
<i>Pityogenes pennidens</i>	12		21	15	19	8			75	6,82
<i>Pityokteines spinidens</i>					1		1		2	0,18
<b>Tribe: Polygraphini</b>										
<i>Carphoborus henscheli</i>			2	2	1		1		6	0,55
<b>Tribe: Tomicini</b>										
<i>Hylurgus ligniperda</i>	4	6		2			1	11	24	2,18
<i>Hylurgus micklitzi</i>	2	2		3			1	2	10	0,91
<i>Tomicus destruens</i>		5	19						24	2,18
<i>Tomicus minor</i>		3			4				7	0,64
<i>Tomicus piniperda</i>		1			6		56	12	75	6,82
<b>Tribe: Xyleborini</b>										
<i>Xyleborus eurygraphus</i>		1							1	0,09
<i>Xyleborinus saxesenii</i>	1								1	0,09
<b>Numbers of individuals</b>	265	94	87	108	254	73	111	108	1100	
<b>Numbers of species</b>	11	13	5	10	13	4	8	4		
<b>Shannon Diversity Index (H')</b>	1,098	1,252	1,230	1,531	1,876	1,183	1,145	0,753		
<b>Equitability Index (J')</b>	0,475	0,488	0,764	0,665	0,731	0,853	0,550	0,543		

*Orthotomicus* Ferrari was the most abundant (53.55% of individuals) genus, represented by two species: *O. erosus* (Wollaston) and *O. longicollis* (Gyllenhal). *O. erosus* was the most abundant species in this study (571 individuals – 51.91%). *Ips* De Geer were the second highest in abundance (161 individuals – 14.64%) and represented by only one species is *I. sexdentatus* Börner. The third most abundant genus was *Pityogenes* Bedel (9.82% of 108 individuals -), represented by five species and most abundant species *P. pennidens* (Reitter) (75 individuals – 6.82%). This ranking was followed by *Tomicus* Latreille (106 individuals – 9.64%), *Hylastes* Erichson (57 individuals – 5.8%), *Crypturgus* Erichson (35 individuals – 3.8 %), *Hylurgus* Latreille (34 individuals – 3.09%), *Carphoborus* Eichhoff (6 individuals – 0.55 2%), *Pityokteines* (2 individuals – 0.18%), *Xyleborinus* Reitter (1 individual – 0.09%) and *Xyleborus* Eichhoff (1 individual – 0.09%) (Table 2).

Pb-1 presented the highest abundance with 265 individuals (23.1% of the sample) distributed in 11 species followed by Pn-1 (*P. nigra* stand) with 254 individuals (22.1% of the sample) of 13 species (Fig. 4). In this study, 21 species were determined in *P. brutia* stands, 13 in *P. nigra* and 8 in *P. pinea*.

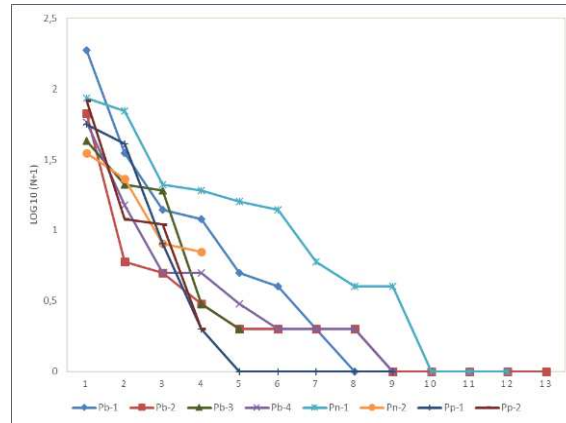


**Figure 4.** Distribution of abundance (LN) in logarithm base 10 ( $N + 1$ ) of the subfamily species Scolytinae collected in eight sites at research area. The numerical code corresponding to each species showed in Table 1

Pn-1 was the area representing the highest value for Shannon index ( $H' = 1.876$ ) differing statistically from other areas. Pb-2 showed the lowest values for this index (Table 2) (Fig. 5). Regarding evenness, Pn-2 presented the highest values ( $J' = 0.853$ ). *O. erosus* occurred in all areas. *O. erosus* was the most abundant species followed by *I. sexdentatus*, *P. pennidens* and *T. piniperda*. In addition, these species were the indicator species and together with *H. angustatus*, *C. henscheli*, *H. ligniperda* and *H. micklitzi* were constant species of the study. While *O. erosus* had the highest number of individuals in brutia pine stands, *I. sexdentatus* had the highest number of individuals on black pine and *T. piniperda* on stone pine.

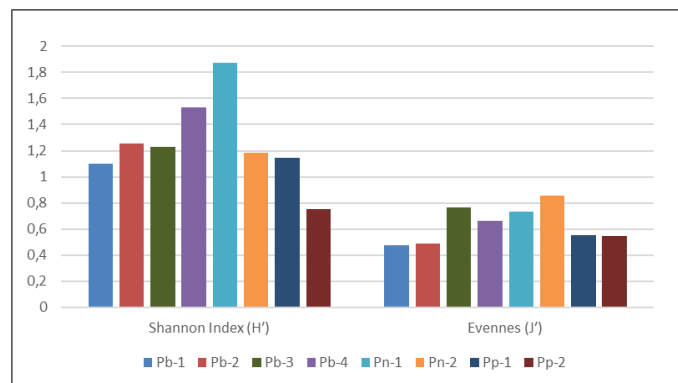


**Figure 5.** Bar diagrams of Shannon-Wiener Diversity Index ( $H'$ ) and Equitability ( $J'$ ) for eight sites, from the cumulative data of the traps in the study period

CCA was performed to determine the ecological relationship between 16 scolytinae species and 4 environmental variables (temperature, humidity, wind speed, altitude). In the ordination diagram, when the species and environmental arrows point in the same direction, species are predicted to have a large positive correlation with the environmental variable, whereas if the species and environmental arrows point in opposite directions, species are predicted to have a large negative correlation with the environmental variable. According to CCA, temperature, and humidity strongly

correlated with the first canonical axis that explains 67.2% of the variability in the species occurrence, whereas wind speed and altitude showed a strong correlation with the second axis that explains 23.2% of total variations (Table 3). Brutian pine sites (except Pb-4) and one stone pine site (Pp-2) distributed on the right side of the diagram and showed a stronger association with temperature and humidity. Black pine sites (Pn-1 and 2) and another stone pine site (Pp-1) were located on the left side of the diagram and indicated correlations with wind speed, and altitude. *O. erosus* and *P. pennidens* (among the most abundant species) located on the left side of the diagram and showed a positive correlation with temperature, while they were negatively related to humidity, wind speed and altitude. In addition, *T. destruens*, *T. minor*, *H. opacus*, and *H. ligniperda* had positive relation with temperature. Abundant species on the right side of the diagram, *I. sexdentatus* showed a positive correlation with altitude, whereas *T. piniperda* had a positively relationship to wind speed. In the same way, *C. cinereus*, *O. longicollis*, and *H. angustatus* had a positive correlation with altitude (Fig. 6).

**Table 3.** Canonical correspondence analysis results of environmental variables on bark beetle species

	Axis 1	Axis 2	Axis 3
<b>Eigenvalues</b>	0.038529	0.011768	0.0030908
<b>Environment-related variation of Species %</b>	72.2	22.0	5,8
<b>Temperature</b>	-0.672487	0.25891	0.328465
<b>Humidity</b>	0.582047	0.40004	-0.32935
<b>Wind speed</b>	0.330915	0.843203	0.123681
<b>Altitude</b>	0.508022	-0.582722	0.402564

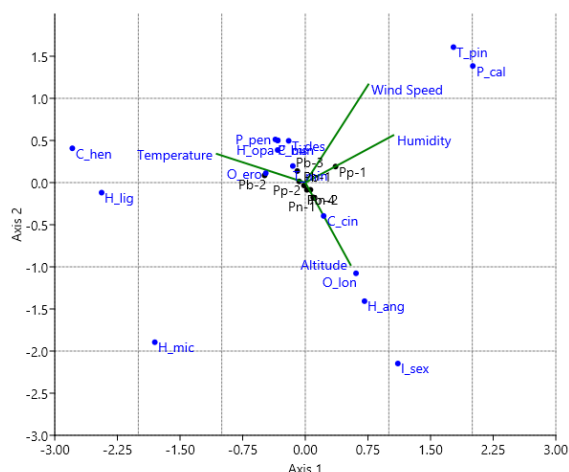


**Figure 6.** Canonical correspondence analysis (CCA) tri-plot showing the relation between scolytinae species (14) and environmental variables (4) in South Marmara Region, Turkey. Arrow length indicates relative importance (correlation strength) towards those parameters; arrow direction indicates a positive or negative (opposite) relationship with each variables and species or sites. (Species abbreviations used: *C\_cin*: *Crypturgus cinereus*, *C\_num*: *C. numidicus*, *H\_ang*: *Hylastes angustatus*, *H\_opa*: *H. opacus*, *I\_sex*: *Ips sexdentatus*, *O\_ero*: *Orthotomicus erosus*, *O\_lon*: *O. longicollis*, *P\_bis*: *Pityogenes bistridentatus*, *P\_cal*: *P. calcographus*, *P\_pen*: *P. pennidens*, *C\_hen*: *Carphobours henscheli*, *H\_lig*: *Hylurgus ligniperda*, *H\_mic*: *H. micklitzii*, *T\_des*: *Tomicus destruens*, *T\_min*: *T. minor*, *T\_pin*: *T. piniperda*)

## Discussion

Many studies have tended to concentrate on effective management practices have on the abundance of bark beetles and have not fully investigated the effect on diversity. This is mainly because these management practices, which usually amount to various thinning regimes, have been adopted as a means of preventing or attempting to control outbreaks of specific primary bark beetles hence maintaining or enhancing bark beetle diversity has not been an objective (Fettig et al., 2007; Williams et al., 2017). In areas where the severe impact of insects is not determined, the situation of not conducting studies on the subject is frequently encountered, especially in regions where there are no economically significant epidemics. Concerns about the impact of these organisms on the economy are often not taken seriously until significant outbreaks occur. Strategies such as saving the infested wood instead of controlling the epidemic are put forward (Ogden, 2008).

The current study demonstrated that black pine is associated with a high diversity of beetles while brutian pine is correlated high abundance of Scolytinae. In addition, stone pine has the lowest diversity and abundance of bark beetles. The Shannon-Weiner index ( $H'$ ) and Equitability Index ( $J$ ) showed in black pine sites, despite the lower number of individuals, demonstrated higher biodiversity ( $H' = 1.876$ ), and at the same time much more even distribution of individuals among species ( $J = 0.853$ ). On the other hand, in spite of the fact that in Turkish pine sites a slightly greater number of species (Totally 21 species) and the cumulative number of individuals was observed during the study period, diversity was lower and individuals were less evenly distributed among species. In general, despite the fact that the different species composition at each sampling point and the small difference in species richness, all display nearly identical “volume” of diversity when measured by the Shannon index. In the present study, 21 species in *P. brutia* stands, 13 species in *P. nigra* stands and 8 species in *P. pinea* stands were determined. The bark beetle species number identified in this research was higher than previous studies on each three-pine species in Turkey (Dönmez, 2006; Sarıkaya and Avcı, 2011; İbiş and Sarıkaya, 2012; Yıldız, 2012). We can say that this is an accurate reflection of the diversity in our research area.

*O. erosus* occurred in all areas and was the most abundant species. This was also in accordance with the literature (Kalapanida-Kantartzi et al., 2010; Sarıkaya and Avcı, 2011; İbiş and Sarıkaya, 2012). *I. sexdentatus* and *P. pennidens* were abundant species in this study and not detected in *P. pinea* sites. In previous studies *P. pennidens* was determined on *P. pinea*, while *I. sexdentatus* was not recorded (Selmi, 1998; Lieutier et al., 2016).

Our assessments of diversity have not reached an asymptote at two sampling points, indicating the need for further sampling to arrive at a reliable estimate of diversity. We can expect that with increased sampling, significantly more species would be found at each site. It cannot be predicted whether the increased sampling will lead to an increase or decrease in the similarity between the sites. That is because increased sampling may detect species that are both rare and localized (Rosenzweig, 1995), but equally probable is the discovery of more shared species (Hulcr et al., 2008).

In CCA analysis, the longer the arrow, the greater the confidence of the inferred correlation, either amongst environmental variables, or with the two principal ordination axes, and therefore, the greater the importance in explaining variation within the data. Species located near to or beyond the tip of the arrow are strongly positively correlated with that environmental variable (Mullen et al., 2008). In the current study, temperature



and humidity strongly correlated with the first canonical axis that explains 67.2% of the variability in the species occurrence. It is known that interactions between bark beetles and temperature are highly complex. Beetle development rates, and sometimes the number of generations per year, increases with temperature and are expected to increase in response to climate change (Hlásny et al., 2019). *O. erosus* and *P. pennidens* (among the most abundant species) showed a strong positive correlation with temperature, while they were negatively related to humidity, wind speed, and altitude. In previous studies, the geographical distribution of *O. erosus* suggests that it is suited to relatively high temperatures. Studies of the effect of temperature upon the development of *O. erosus* led to the conclusion that *O. erosus* can develop when temperatures are as high as 36 – 38°C (Mendel and Halperin, 1982; Mendel, 1983; Sarıkaya et al., 2013). Considering the different altitude, it was shown that the phenology of *O. erosus* changes inversely with the altitude (Özkazanç et al., 1985; Peltonen and Heliövaara, 1999; Sarıkaya et al., 2013). *P. pennidens* is also known from the eastern Mediterranean: Greece, Syria, Turkey, and the Caucasus region (Grüne, 1979; Wood and Bright, 1992; Selmi, 1998). According to our results, *P. brutia*, which showed a strong correlation with temperature, had a relationship with *O. erosus* and *P. pennidens*. Sarıkaya et al. (2013) recorded that *O. erosus* indicates that the increase in population density occurs when the average relative humidity is below 50%.

Abundant species on the right side of the diagram, *I. sexdentatus* showed a positive correlation with altitude and wind spread. Özcan et al. (2011) stated that the number of individuals was higher in higher altitudes for *I. sexdentatus* on oriental spruce. Jactel (1991) reported that wind speed was positively correlated with the flight of the *I. sexdentatus*. Likewise, *C. cinereus*, *O. longicollis* and *H. angustatus* showed a positive correlation with altitude. In accordance with our results, *P. nigra* showed a strong correlation with altitude, additionally, it had a relationship with *I. sexdentatus*. *T. piniperda*, which was the other abundant species, was on the right side of the diagram and related to the stone pine site on same side of the diagram. In addition, they had correlated with wind speed. Furthermore, *T. piniperda* had the highest individual number in stone pine sites. A study on the host preferences of *T. piniperda* and *T. destruens* in Portugal revealed that both insect species preferred stone pine in the south, and Aleppo pine in the north (Vasconcelos et al., 2003). This indicates that *T. piniperda* may also prefer stone pine depending on the geography.

## Conclusion

Insects are the most discussed species during ecosystem analyzes in terms of diversity and abundance because of their ability to complete their life cycle in a short time (usually 1 year) and to adapt quickly to environmental changes. Phytophagous insects are more used in these analyzes. On the other hand, it is known that plant groups also exhibit geographic and temporal changes. However, it takes longer to observe this change. In studies that have intensified in recent years, it has been revealed that global climate change is changing the species composition of the ecosystem faster. In this context, we have selected a transition zone for our coniferous forests and some abiotic factors that influence this transition such as temperature, humidity, altitude, and wind speed were discussed in our study. We have tried to understand the role of these abiotic factors in the diversity and abundance of bark beetles, which have destructive impacts on trees. The results presented in this study, demonstrate black pine is associated with a



high diversity of beetles while brutian pine is correlated high abundance of Scolytinae. These preliminary results suggest that the pine sites do not harbor the scolytine diversity expected for the native habitat. Temperature and humidity are strongly correlated with the species occurrence. In addition, *O. erosus* and *P. pennidens* showed a strong positive correlation with temperature whereas *I. sexdentatus* showed a positive correlation with altitude. Although it is difficult to isolate the effects of these factors in a transition zone, our data indicate that these abiotic factors affect the composition and the number of bark beetles. Additional studies outside the transition zones of coniferous forests will help us better understand the diversity and damage levels of these insects.

**Acknowledgements.** We would like to thank Balıkesir Regional Directorate of Forestry (Turkey) for support. We are also grateful to Mustafa Baydemir for his assistance in the fieldwork. This study was funded by Istanbul University - Cerrahpaşa, Scientific Research Project (project 40216).

## REFERENCES

- [1] Anonymus (2006): Our Forest Wealth. – T.C. Ministry of Environment and Forests, General Directorate of Forests, Ankara.
- [2] Benisch, C. (2007): Kerbtier.de: Beetle fauna of Germany. – <https://www.kerbtier.de/>.
- [3] Bright, D. E. J., Stark, R. W. (1973): The Bark and Ambrosia Beetles of California (Coleoptera: Scolytidae and Platypodidae). – University of California Press.
- [4] Brockerhoff, E. G., Jactel, H., Parrotta, J. A., Quine, C. P., Sayer, J. (2008): Plantation forests and biodiversity: oxymoron or opportunity? – *Biodiversity and Conservation* 17(5): 925-951. doi: 10.1007/s10531-008-9380-x.
- [5] Byers, J. A. (2000): Wind-aided dispersal of simulated bark beetles flying through forests. – *Ecological Modelling* 125: 241-243. doi: 10.1016/S0304-3800(99)00187-8.
- [6] Chung, A. Y. C., Chey, V. K., Eggleton, P., Hammond, P. M., Speight, M. R. (2001): Variation in beetle (Coleoptera) diversity at different heights of tree canopy in a native forest and forest plantation in Sabah, Malaysia. – *Journal of Tropical Forest Science* 13(2): 369-385.
- [7] Cochran, P. H., Barrett, J. W. (1998): Thirty-five-year Growth of Thinned and Unthinned Ponderosa Pine in the Methow Valley of Northern Washington. – Portland, OR.
- [8] Cole, D. M., McGregor, M. D. (1988): Stand Culture/Bark Beetle Relationships of Immature Tree Stands in the Inland Mountain West. – Ogden, UT.
- [9] Doğukan, H., Baran, Ş., Yorulmaz, H., Yenici, E. (2008): Province Environmental Situation Report. – T.C. Ministry of Environment and Urban, Provincial Directorate of Environment and Urban Planning Balıkesir, Çanakkale.
- [10] Dönmez, H. (2006): Scolytidae (Coleoptera) Species with Important Parasites and Predators to Determination Harmful on the Conifer Forest in Mersin Regional Forest Directorate. – Master of Science, Gazi University.
- [11] Efe, R. (1999): The Physical Factors Affecting Soil Formation and Properties of the Soils in the Western Part of the Southern Marmara Sub-region. – *Turkish Geographical Review* 34: 193-209.
- [12] ESRI. (2014): ArcGIS for Desktop, version 10.2.2. – Environmental Systems Research Institute. Redlands, CA, USA.
- [13] FAO. (2020): FAO Soils Portal. – <http://www.fao.org/soils-portal/en/>.
- [14] Feinsinger, P. (2001): Designing Field Studies for Biodiversity Conservation. – Island Press, Washington, USA.
- [15] Fettig, C. J., Klepzig, K. D., Billings, R. F., Munson, A. S., Nebeker, T. E., Negrón, J. F., Nowak, J. T. (2007): The effectiveness of vegetation management practices for

- prevention and control of bark beetle infestations in coniferous forests of the western and southern United States. – *Forest Ecology and Management* 238(1-3): 24-53.  
doi: 10.1016/j.foreco.2006.10.011.
- [16] Fiddler, G. O., Hart, D. R., Fiddler, T. A., McDonald, P. M. (1989): Thinning Decreases Mortality and Increases Growth of Ponderosa Pine in Northeastern California. – Pacific Southwest Forest and Range Experiment Station Berkeley, CA.
- [17] Foit, J. (2015): Bark- and wood-boring beetles on Scots pine logging residues from final felling: effects of felling date, deposition location and diameter of logging residues. – *Annals of Forest Research* 58(1). doi: 10.15287/afr.2015.302.
- [18] Franklin, A. J., Grégoire, J.-C. (1999): Flight behaviour of *Ips typographus* L. (Col., Scolytidae) in an environment without pheromones. – *Annals of Forest Science* 56(7): 591-598. doi: 10.1051/forest:19990706.
- [19] Grégoire, J.-C., Piel, F., De Proft, M., Gilbert, M. (2001): Spatial Distribution of Ambrosia-Beetle Catches: A Possibly Useful Knowledge to Improve Mass-Trapping. – *Integrated Pest Management Reviews* 6: 237-242. doi: 10.1023/A:1025723402355.
- [20] Grégoire, J.-C., Evans, H. F. (2004): Damage and Control of Bawbilt Organisms an Overview. – In: Lieutier, F., Day, K. R., Battisti, A., Grégoire, J.-C., Evans, H. F. (eds.) *Bark and Wood Boring Insects in Living Trees in Europe, a Synthesis*. Springer, The Netherlands.
- [21] Grüne, V. S. (1979): *Handbuch zur Bestimmung der europäischen Borkenkäfer - Brief Illustrated Key to European Bark Beetles*. – Verlag M. & H. Schaper Hannover, Deutschland.
- [22] Hammer, Ø., Harper, D. A. T., Ryan, P. D. (2001): PAST: Paleontological Statistics Software Package For Education And Data Analysis. – *Palaeontologia Electronica* 4(1): 9.
- [23] Heliövaara, K., Peltonen, M. (1999): Bark beetles in a changing environment. – *Ecological Bulletins* 47: 48-53.
- [24] Hlásny, T., Krokene, P., Liebhold, A., Montagné-Huck, C., Müller, J., Qin, H., Raffa, K., Schelhaas, M.-J., Seidl, R., Svoboda, M., Viiri, H. (2019): Living with bark beetles: impacts, outlook and management options. – European Forest Institute.
- [25] Hulcr, J., Beaver, R. A., Puranasakul, W., Dole, S. A., Sonthichai, S. (2008): A comparison of bark and ambrosia beetle communities in two forest types in northern Thailand (Coleoptera: Curculionidae: Scolytinae and Platypodinae). – *Environ Entomol* 37(6): 1461-1470. doi: 10.1603/0046-225x-37.6.1461.
- [26] İbiş, H. M., Sarıkaya, O. (2012): Bark Beetle Species Diversity in Brutian Pine (*Pinus brutia* Ten.) Forests of İzmir Province in Turkey. – In *Forestry science and practice for the purpose of sustainable development of forestry 20 years of the Faculty of forestry in Banja Luka 1st - 4th November 2012, Republic of Srpska*, pp. 533-543.
- [27] Jactel, H. (1991): Dispersal and flight behaviour of *Ips sexdentatus* (Coleoptera: Scolytidae) in pine forest. – *Annales des Sciences Forestières* 48(4): 417-428.  
doi: 10.1051/forest:19910405.
- [28] Jactel, H., Brockerhoff, E. G. (2007): Tree diversity reduces herbivory by forest insects. – *Ecology Letters* 10: 835-848.
- [29] Jakus, R. (1998): Patch level variation on bark beetle attack (Col., Scolytidae) on snapped and uprooted trees in Norway spruce primeval natural forest in endemic conditions: species distribution. – *Journal of Applied Entomology* 122(2-3): 65-76.  
doi: 10.1111/j.1439-0418.1998.tb01521.x.
- [30] Jenkins, M. J., Hebertson, E., Page, W., Jorgensen, C. A. (2008): Bark beetles, fuels, fires and implications for forest management in the Intermountain West. – *Forest Ecology and Management* 254(1): 16-34. doi: 10.1016/j.foreco.2007.09.045.
- [31] Jones, K. L., Shegelski, V. A., Marculis, N. G., Wijerathna, A. N., Evenden, M. L. (2019): Factors influencing dispersal by flight in bark beetles (Coleoptera: Curculionidae):

- Scolytinae): from genes to landscapes. – Canadian Journal of Forest Research 49: 1021-1041. doi: 10.1139/cjfr-2018-0304.
- [32] Jordal, B. H., Knížek, M. (2007): Resurrection of *Crypturgus subcribrosus* Eggers 1933 stat. n., and its close phylogenetic relationship to Nearctic *Crypturgus* (Coleoptera, Scolytinae). – Zootaxa 1606: 41-50. doi: 10.11646/zootaxa.1606.1.3.
- [33] Kalapanida-Kantartzi, M., Milonas, D. N., Buchelos, C. T., Avtsiz, D. N. (2010): How does pollution affect insect diversity. A study on bark beetle entomofauna of two pine forests in Greece. – Journal of Biological Research-Thessaloniki 13: 67-74.
- [34] Karagöz, G., Demirci, M. (2015): Forest Wealth of Turkey. – T.C. Ministry of Forest and Water, General Directorate of Forests, Ankara.
- [35] Klutsch, J. G., Negrón, J. F., Costello, S. L., Rhoades, C. C., West, D. R., Popp, J., Caissie, R. (2009): Stand characteristics and downed woody debris accumulations associated with a mountain pine beetle (*Dendroctonus ponderosae* Hopkins) outbreak in Colorado. – Forest Ecology and Management 258(5): 641-649. doi: 10.1016/j.foreco.2009.04.034.
- [36] Koricheva, J., Vehviläinen, H., Riihimäki, J., Ruohomäki, K., Kaitaniemi, P., Ranta, H. (2006): Diversification of tree stands as a means to manage pests and diseases in boreal forests: myth or reality? – Canadian Journal of Forest Research 36(2): 324-336. doi: 10.1139/x05-172.
- [37] Košťál, V., Doležal, P., Rozsypal, J., Moravcová, M., Zahradníčkov, H., Šimek, P. (2011): Physiological and biochemical analysis of overwintering and cold tolerance in two Central European populations of the spruce bark beetle, *Ips typographus*. – Journal of Insect Physiology 57: 1136-1146. doi: 10.1016/j.jinsphys.2011.03.011.
- [38] Kuhnholz, S., Borden, J. H., Uzunovic, A. (2001): Secondary ambrosia beetles in apparently healthy trees: Adaptations, potential causes and suggested research. – Integrated Pest Management Reviews 6: 209-219. doi: 10.1023/A:1025702930580.
- [39] Kurz, W. A., Dymond, C. C., Stinson, G., Rampley, G. J., Neilson, E. T., Carroll, A. L., Ebata, T., Safranyik, L. (2008): Mountain pine beetle and forest carbon feedback to climate change. – Nature 452(7190): 987-990. doi: 10.1038/nature06777.
- [40] Lieutier, F., Mendel, Z., Faccoli, M. (2016): Bark Beetles of Mediterranean Conifers. – In: Paine, T. D., Lieutier, F. (eds.) Insects and Diseases of Mediterranean Forest, Springer, Switzerland.
- [41] Lindgren, B. S., Raffa, K. F. (2013): Evolution of tree killing in bark beetles (Coleoptera: Curculionidae): trade-offs between the maddening crowds and a sticky situation. – The Canadian Entomologist 145(05): 471-495. doi: 10.4039/tce.2013.27.
- [42] Lompe, A. (2002): Käfer Europas. – <http://www.coleo-net.de/coleo/index.htm>.
- [43] Marini, L., Lindelöw, Å., Jönsson, A. M., Wulff, S., Schroeder, L. M. (2013): Population dynamics of the spruce bark beetle: a long-term study. – Oikos 122: 1768-1776. doi: 10.1111/j.1600-0706.2013.00431.x.
- [44] Mendel, Z., Halperin, J. (1982): The Biology and Behavior of *Orthotomicus erosus* in Israel. – Phytoparasitica 10(3): 169-181.
- [45] Mendel, Z. (1983): Seasonal history of *Orthotomicus erosus* (Coleoptera: Scolytidae) in Israel. – Phytoparasitica 11(1): 13-24.
- [46] Moraes, R. C. B., Haddad, M. L., Silveira Neto, S., Reyes, A. E. L. (2003): Software para análise faunística-ANAFU. – In: Pedro, S. (ed.) Simpósio de controle biológico 8: 195.
- [47] Mullen, K., O'Halloran, J., Breen, J., Giller, P., Pithon, J., Kelly, T. (2008): Distribution and composition of carabid beetle (Coleoptera, Carabidae) communities across the plantation forest cycle - Implications for management. – Forest Ecology and Management 256: 624-632. doi: 10.1016/j.foreco.2008.05.005.
- [48] Ogden, A. E. (2008): Forest management in a changing climate: building the environmental information base for southwest Yukon. – The Forestry Chronicle 83(6): 806-809. doi: 10.5558/tfc83806-6.

- [49] Økland, B., Bjørnstad, O. N. (2006): A Resource-Depletion Model of Forest Insect Outbreaks. – *Ecology* 87(2): 283-290. doi: 10.1890/05-0135.
- [50] Özcan, G. E., Eroğlu, M., Alkan-Akinci, H. (2011): Use of pheromone-baited traps for monitoring *Ips sexdentatus* (Boerner) (Coleoptera: Curculionidae) in oriental spruce stands. – *African Journal of Biotechnology* 10(72): 16351-16380.
- [51] Özkazanç, O., İktüeren, Ş. I., Yücel, M. (1985): Studies on Biology and Control of *Orthotomicus erosus* (Woll.) in Mediterranean and Aegean Regions. – Forestry Research Institute Publications, Technical Bulletin Series.
- [52] Peltonen, M., Heliövaara, K., Väisänen, R., Keronen, J. (1998): Bark beetle diversity at different spatial scales. – *Ecography* 21(5): 510-517. doi: 10.1111/j.1600-0587.1998.tb00442.x.
- [53] Peltonen, M., Heliövaara, K. (1999): Attack density and breeding success of bark beetles (Coleoptera, Scolytidae) at different distances from forest-clearcut edge. – *Agricultural and Forest Entomology* 1: 237-242. doi: 10.1046/j.1461-9563.1999.00033.x.
- [54] Pielou, E. C. (1969): An introduction to mathematical ecology. – Wiley Interscience, New York.
- [55] Raffa, K. F., Gregoire, J. C., Lindgren, B. S. (2015): Natural History and Ecology of Bark Beetles. – In: Vega, F. E., Hofstetter, R. W. (eds.) *Bark Beetles Biology and Ecology of Native and Invasive Species*. Elsevier, USA.
- [56] Rodrigez, S. C., Cognato, A. I., Righi, C. A. (2017): Bark and Ambrosia Beetle (Curculionidae: Scolytinae) Diversity Found in Agricultural and Fragmented Forests in Piracicaba-SP, Brazil. – *Environmental Entomology* 46(6): 1254-1263.
- [57] Rosenzweig, M. L. (1995): Species diversity in time and space. – Cambridge University Press, Cambridge, United Kingdom.
- [58] Rubin-Aguirre, A., Saenz-Romero, C., Lindig-Cisneros, R., del-Rio-Mora, A. A., Tena-Morelos, C. A., Campos-Bolaños, R., del-Val, E. (2015): Bark beetle pests in an altitudinal gradient of a Mexican managed forest. – *Forest Ecology and Management* 343: 73-79. doi: 10.1016/j.foreco.2015.01.028.
- [59] Sarıkaya, O., Avcı, M. (2011): Bark beetle fauna (Coleoptera: Scolytinae) of the coniferous forests in the Mediterranean region of Western Turkey, with a new record for Turkish fauna. – *Turkish Journal of Zoology* 35(1): 33-47. doi: 10.3906/zoo-0901-8.
- [60] Sarıkaya, O., Yıldırım, S. (2011): Scolytinae (Coleoptera: Curculionidae) Species of the Coniferous Forests in Isparta-Aksu Province. – *Journal of Bartın Faculty of Forestry* 13(20): 38-50.
- [61] Sarıkaya, O., İbiş, H. M., Toprak, Ö. (2013): The flight activity and population density of *Orthotomicus erosus* (Wollaston, 1857) in the Brutian pine (*Pinus brutia* Ten.) forests of İzmir Province, Turkey. – *International Journal of Sciences: Basic and Applied Research* 12(1): 208-219.
- [62] Sauvard, D. (2004): General Biology of Bark Beetles. – In: Lieutier, F., Day, K. R., Battisti, A., Gregoire, J. C., Evans, H. F. (eds.) *Bark and Wood Boring Insects in Living Trees in Europe, a Synthesis*. Springer, The Netherlands.
- [63] Selmi, E. (1998): Türkiye Kabuk Böcekleri ve Savaşı. – İstanbul University Press, İstanbul.
- [64] Spellerberg, I. F., Fedor, P. J. (2003): A tribute to Claude Shannon (1916–2001) and a plea for more rigorous use of species richness, species diversity and the ‘Shannon-Wiener’ Index. – *Global Ecology & Biogeography* 12: 177-179.
- [65] Tribe, G. D. (1992): Colonisation sites on *Pinus radiata* logs of the bark beetles, *Orthotomicus erosus*, *Hylastes angustatus* and *Hylurgus ligniperda* (Coleoptera: Scolytidae). – *Journal of the Entomological Society of Southern Africa* 55(1): 77-84.
- [66] TSMS. (1998): Turkish State Meteorological Service. – <https://www.mgm.gov.tr>.
- [67] Vasconcelos, T., Nazaré, N., Branco, M., Kerdelhue, C., Sauvard, D., Lieutier, F. (2003): Host Preference of *Tomicus piniperda* and *Tomicus destruens* for Three Pine Species. –

- In: Kamata, N., Liebhold, A. M., Quiring, D. T., Clancy, K. M. (eds.) *Forest Insect Population Dynamics and Host Influences*. IUFRO Kanazawa, Japan, pp. 19-21.
- [68] Weslien, J., Schroeder, L. M. (1999): Population levels of bark beetles and associated insects in managed and unmanaged spruce stands. – *Forest Ecology and Management* 115: 267-275. doi: 10.1016/S0378-1127(98)00405-8.
- [69] Williams, D. T., Straw, N., Fielding, N., Jukes, M., Price, J. (2017): The influence of forest management systems on the abundance and diversity of bark beetles (Coleoptera: Curculionidae: Scolytinae) in commercial plantations of Sitka spruce. – *Forest Ecology and Management* 398: 196-207. doi: 10.1016/j.foreco.2017.05.014.
- [70] Wood, S. L. (1982): *Great Basin Naturalist Memoirs the Bark and Ambrosia Beetles of North and Central America (Coleoptera: Scolytidae), a Taxonomic Monograph*. – Brigham Young University, Provo, Utah.
- [71] Wood, S. L., Bright, D. E. (1992): *A Catalog of Scolytidae and Platypodidae (Coleoptera), Part II: Taxonomic Index Volume A*. – Great Basin naturalist memoirs.
- [72] Yıldız, Y. (2012): *The Scolytidae Fauna of Bartın and Karabük Forest and Determination of Some Important Species Biology*. – Doctor of Philosophy, Bartın University.
- [73] Zhang, X., Zhao, G., Zhang, X., Li, X., Yu, Z., Liu, Y., Liang, H. (2017): Ground Beetle (Coleoptera: Carabidae) Diversity and Body-Size Variation in Four Land Use Types in a Mountainous Area Near Beijing, China. – *The Coleopterists Bulletin* 71(2). doi: 10.1649/0010-065x-71.2.402.
- [74] Zou, Y., Feng, J., Xue, D., Sang, W., Axmacher, J. (2011): Insect Diversity: Addressing an Important but Strongly Neglected Research Topic in China. – *Journal of Resources and Ecology* 2(4): 380-384. doi: 10.3969/j.issn.1674-764x.2011.04.013.

# FUNCTIONAL GROUPS OF BENTHIC MACROINVERTEBRATES IN RELATION TO PHYSICOCHEMICAL FACTORS IN KEQIN LAKE, ZHALONG NATIONAL NATURE RESERVE, NORTHEASTERN CHINA

LI, X. Y.<sup>1</sup> – LIU, M. H.<sup>1\*</sup> – SUN, X.<sup>1</sup> – LI, S.<sup>1</sup> – ZHAO, Y. X.<sup>1</sup> – LIU, D.<sup>1</sup> – CHAI, F. Y.<sup>2</sup> – YU, H. X.<sup>1\*</sup>

<sup>1</sup>*College of Wildlife and Protected Area, Northeast Forestry University, Harbin 150040, China*

<sup>2</sup>*School of Management, Heilongjiang University of Science and Technology, Harbin 150027, China*

*\*Corresponding authors*

*e-mail: manhong@nefu.edu.cn (M. H. Liu); china.yhx@163.com (H. X. Yu)*

(Received 31<sup>st</sup> Jul 2020; accepted 19<sup>th</sup> Nov 2020)

**Abstract.** Using functional traits to represent functional components and functional diversity help us better understand ecosystem and community functions. Species' functional traits are sensitive to environmental change, and can potentially indicate these changes through community and population succession. In order to grasp the spatial and temporal distribution pattern of functional characteristics and the influence of physicochemical factors on the functional diversity of benthic macroinvertebrates in Keqin Lake (in Zhalong National Nature Reserve of China), we investigated the benthic macroinvertebrates and physicochemical indexes in May, July and October 2019. Referring to the relevant literature, we selected the functional feeding groups and the locomotion groups for analysis. According to the research results, 21 taxa were identified; Palaemonidae, Viviparidae and Chironomidae accounted for the largest proportion, their relative abundances were 51.05%, 15.26%, and 13.68% respectively. OM (Omnivores) was the dominant group in the functional feeding groups, and CM (Climbers) was the dominant group among the locomotion groups. The One-way analysis of variance (ANOVA) and Honestly significant difference (HSD) tests showed significant differences in the following physicochemical factors: WT, SD, NTU, NH<sub>4</sub><sup>+</sup>-N, Cl and COD<sub>Mn</sub>. Redundancy analysis (RDA) results displayed that COD<sub>Mn</sub>, Cl and NTU were significant indexes that affected the functional feeding groups and the locomotion groups.

**Keywords:** *functional feeding groups, locomotion groups, lake, benthic macroinvertebrates, physicochemical factors*

## Introduction

Ecosystem function is a broad concept, including ecosystem processes (such as nutrient cycle), ecosystem services (such as providing fish, habitat, filtration, etc.), resilience and resistance to interference (Daily, 1997; Postel and Carpenter, 1997). Climate change leads to seasonal changes in the environmental characteristics of the whole lake area, including hydrological characteristics, physical and chemical factors, and lakeshore vegetation, and ultimately altering the community structure of benthic macroinvertebrates by affecting the growth, reproduction and species succession. The research of functional traits provides a new way to further understand this process (Zhang et al., 2016; Liu et al., 2019b; Alcocer et al., 2016).

At present a popular approach has been proposed in benthic macroinvertebrates functional groups to assess ecosystem health. These groups of species have more or less precisely defined demands via several different combinations of morphological and behavioral features. Compared with taxonomic methods, functional groups are more

accurate in assessing response to changes concerning the environment (Bremner et al., 2006; Gamito et al., 2009). As an example, variations have been observed in the functional feeding groups and the locomotion groups for benthic macroinvertebrates in a stressed environment subjected either to anthropogenic influence or to natural environmental stress. Thus, functional groups are useful as an assessment tool in ecosystem health (Usseglio-Polatera et al., 2000).

Benthic macroinvertebrates are typical biological groups in aquatic ecosystems, which have been regarded as model groups by some domestic scholars. The classification of species into functional groups according to the similar biological and ecological characteristics, and several domestic researchers have done researches on benthic macroinvertebrates functional groups in rivers and lakes ecosystems. Researchers believe that the specific characteristics of functional groups are more closely related to the environment. These characteristics can directly reflect the community structure and habitat adaptability of benthic macroinvertebrates, as well as the impact caused by human activities to aquatic ecosystem (Li et al., 2019; Liu et al., 2019a; Zhu et al., 2020).

Cummins (1973) was the first biologist to make clear use of the functional classification of aquatic organisms, and divide the functional groups of food intake by the priority feeding mode of macroinvertebrates. The functional feeding groups functional group are divided into six groups: Filter-feeders (FC), Omnivores (OM), Predators (PR), Scrapers (SC), Shredders (SH) and Collectors (GC). Morse et al. (1994), Usseglio-Polatera et al. (1994) and Poff et al. (2006) also proposed the classification of macroinvertebrates habits or modes of existence. He divided locomotion groups into eight groups: Burrowers (BU), Climbers (CM), Clingers (CN), Divers (DI), Sprawlers (SP), Skaters (SK), Planktonic (PL) and Swimmers (SW). In our research only mentioned four groups in functional feeding groups and five groups in locomotion groups (*Table 1*).

Zhalong National Nature Reserve (123°47'-124°37'E, 46°52'- 47°32'N, total area 2100 km<sup>2</sup>), located in western Heilongjiang Province, northeast China, was established in 1985. The reserve is mostly dominated by reed marsh, other common plants including Cattail (*Typha orientalis* Presl). The rapid development of industrialization and urbanization in the surrounding area of Zhalong National Nature Reserve (ZNNR) over the past decades to finally give the negative impacts on the water resources. The discharge of industrial wastewater, agricultural wastewater, and domestic sewage from the upper reaches (Wuyur River) of Keqin lake made water quality decline. However, in the ecosystem health assessment of Keqin Lake (the largest lake in ZNNR) vacancy benthic macroinvertebrates functional groups.

The purpose of this study was to assess the spatial and temporal variation of functional groups of benthic macroinvertebrates in the Keqin Lake, northeastern China, and how it is influenced by the seasonally varying physicochemical properties of the lake. Nine sites across the lake were sampled for benthic macroinvertebrates and physicochemical variables in spring, summer and autumn. benthic macroinvertebrates were categorized in functional feeding groups and locomotion groups and their relative abundance was evaluated in relation to major physicochemical factors. This is the first study that explores relationships between benthic macroinvertebrate functional groups and physicochemical factors in the Keqin Lake, and its results are expected to facilitate the development of ecological restoration strategies towards the sustainable management of the lake's biota.

**Table 1.** Division of functional groups of benthic macroinvertebrates

Functional group	Traits	Abbreviation	Modalities
Functional feeding groups	Filter-feeders	FC	Decomposing fine particulate organic matter (FPOM). Detritivores-filters or suspension feeders. Detritivores-gatherers or deposit (sediment) feeders (includes feeders on loose surface films).
	Omnivores	OM	Omnivores rely on the skin or gills to directly absorb the dissolved organics in water, and it can also eat the decayed leaves of plants, small bivalves and crustaceans.
	Predators	PR	Living animal tissue. Engulfers-carnivores, ingest whole animals or parts. Piercers- carnivores, pierce tissues and cells to suck fluids.
	Scrapers	SC	Periphyton-attached algae and associated material. Herbivores- grazing Scrapers of mineral and organic surfaces.
Locomotion groups	Burrowers	BU	Inhabiting the fine sediments of streams (pools) and lakes. Some construct discrete burrows that may have sand grain tubes extending above the surface of the substrate or the individuals may ingest their way through the sediments. Some burrow (tunnel) into plant stems, leaves, or roots (miners).
	Climbers	CM	Adapted for living on vascular hydrophytes or detrital debris (such as overhanging branches, roots and vegetation along streams, and submerged brush in lakes). With modifications for moving vertically on stem-type surfaces.
	Clingers	CN	Representatives have behavioral (such as fixed retreat construction) and morphological (such as long, curved tarsal claws, dorsoventral flattening, and ventral gills arranged as a sucker) adaptations for attachment to surfaces in stream riffles and wave-swept rocky littoral zones of lakes.
	Divers	DI	Adapted for swimming by “rowing” with the hind legs in lentic habitats and lotic pools. Representatives come to the surface to obtain oxygen, dive and swim when feeding or alarmed; may cling to, or crawl on, submerged objects such as vascular plants.
	Sprawlers	SP	Inhabiting the surface of floating leaves of vascular hydrophytes or fine sediments, usually with modification for staying on top of the substrate and maintaining the respiratory surfaces free of silt.

## Methods

### Study area

ZNNR is one of the most important wetland reserves in the world. Keqin lake is the largest inland lake in this region which is divided into two lakes, North Lake and South Lake, from 124°16'51" E to 124°19'9" E and from 47°17'7"N to 47°20'13"N, covering a total area of 27 km<sup>2</sup>, 3 m mean depth, and storage capacity is 34,500,000 m<sup>3</sup>. Keqin lake is adjacent to the eastern suburb of Qiqihar City (30 km away from Qiqihar city), located on the west bank of Wuyur River, the surrounding area is low-lying, with a large area of marsh wetland. The region where located the lake is influenced by the continental monsoon in the cold temperate with an annual average temperature of



1 °C~4.2 °C, and a range of -35.0 °C~36.6 °C. The lake area is dry and windy in the spring, hot and rainy in the summer, cool in the autumn, and long and cold in the winter. Water supply depends on the lake surface precipitation and the land runoff, and the main river entering the lake is Jiudaogou (a tributary of Wuyuer River). Meadow covers the lake beaches where mainly growing aquatic vascular plants are *Phragmites australis* and *Typha orientalis*. Keqin Lake is also a stocking lake which stocked fishes of the Cyprinidae (*Mylopharyngodon piceus*, *Ctenopharyngodon idellus*, *Hypophthalmichthys molitrix*, *Aristichthys nobilis*) and crab of the Eriocheir genus.

### Field sampling and laboratory analysis

According to the temperature conditions of the area where Keqin lake is located, benthic macroinvertebrates were collected in spring (May), summer (July) and autumn (October) of 2019 in Keqin lake, and 9 sampling sites were set according to the water conditions and surrounding environment characteristics of Keqin Lake (Fig. 1; Table 2). Sites S1, S2, S3 were near the bank, with luxuriant vegetation; Site S2 bottom was covered by sandy mud; Site S5 was inlet; Sites S4, S6, S7, S8, S9 were in the middle of the lake with white mud bottom.

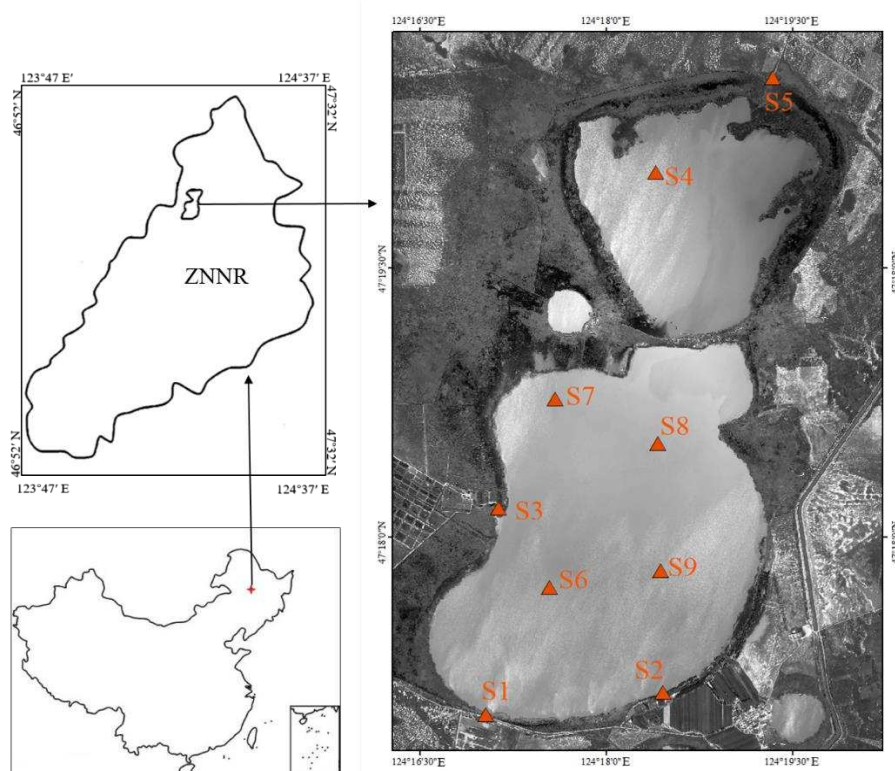


**Figure 1.** Location of the nine sites, sampled in spring, summer and autumn 2019, in the Keqin Lake, Northeastern China

D-frame aquatic net (30×30 cm frame, 500 μm mesh) was used to collect benthic macroinvertebrates; For the deep mud bottom, the Peterson dredger is used with a sampling area of 1/16 m<sup>2</sup>; Sampling area of the D-frame and the dredger were the same (1 m<sup>2</sup>). In three sampling periods, three duplicate samples were collected at each sampling

point and screened by 500  $\mu\text{m}$  mesh sieve. Macroinvertebrate populations are separated carefully by hand from matrix (sand and mud). All samples were stored in 95% ethanol for further analysis in the laboratory. The identification of benthic macroinvertebrates was carried out under anatomical microscope (Motic SMZ-168) and microscope (Motic BA400). Species identification used professional classification books (Thorpe and Covich, 1991; Morse et al., 1994; Merritt et al., 1996; Dudgeon, 1999; Duan et al., 2010), and most samples were identified to species, others to families and genera.

**Table 2.** Coordinates of sampling sites in Keqin Lake

Sampling sites	Latitude	Longitude
S1	N47.2834641272510	E124.283886360844
S2	N47.2855369101671	E124.307603087027
S3	N47.3026818647690	E124.285532823154
S4	N47.3338851781492	E124.306637783286
S5	N47.3426645628785	E124.322344250396
S6	N47.2953089333742	E124.292401182075
S7	N47.3128415296640	E124.293206284997
S8	N47.3086889661881	E124.306911649462
S9	N47.2968542838218	E124.307352675974

The physicochemical factors: WT (water temperature), EC (conductivity), DO (dissolved oxygen),  $\text{NH}_4^+\text{-N}$  (ammonium nitrogen),  $\text{NO}_3^-\text{-N}$  (nitrate nitrogen),  $\text{Cl}^-$  (chlorion), NTU (turbidity) and pH were measured by a portable multi-probe (YSI 6600) in the wild; Secchi disk was used to measure SD (Water transparency); The TN (total nitrogen), TP (total phosphorus) and  $\text{COD}_{\text{Mn}}$  (chemical oxygen demand) were measured in accordance with “water and wastewater monitoring and analysis method” for China (Wei et al., 2002).

### Data analysis

The significance of the differences in abiotic data between the three periods was tested using one-way ANOVA and a posteriori Tukey’s HSD tests. Data were analyzed using the SPSS 19.0 software.

Associations between the relative abundance of benthic macroinvertebrates functional groups and physicochemical parameters were measured by a redundancy analysis (RDA), by using the CANOCO 4.5 software. The RDA analysis was selected since the Detrended Correspondence Analysis (DCA) identified that biological data were linearly responding to environmental gradients (the largest lengths of gradient value of 4 axis was 2.691 (<3)). All continuous physicochemical factors and benthic macroinvertebrates abundance were  $\log_{10}(1 + x)$  transformed before DCA analysis.

## Results

### Variation of physicochemical factors in different seasons

The One-way ANOVA results showed in Table 3, we can find that most of these variables have significant differences between different sampling times, and they were

at a low significant level ( $p < 0.05$ ). HSD tests revealed that significant differences were found among three sampling periods.

WT was significantly higher in summer than in spring and autumn ( $p < 0.05$ ), while SD was remarkable lower in spring than in summer and autumn ( $p < 0.05$ ), NTU and  $\text{NH}_4^+\text{-N}$  were notable higher in spring than in summer and autumn ( $p < 0.05$ ,  $p < 0.05$ ), whereas Cl<sup>-</sup> and  $\text{COD}_{\text{Mn}}$  were significantly higher in autumn than in summer and spring ( $p < 0.05$ ,  $p < 0.05$ ).

**Table 3.** Variation of physicochemical factors in different seasons (mean  $\pm$  SE). SD: water transparency; WT: water temperature; EC: conductivity; Cl<sup>-</sup>: chlorion;  $\text{NH}_4^+\text{-N}$ : ammonium nitrogen,  $\text{NO}_3^-\text{-N}$ : nitrate nitrogen; NTU: turbidity; DO: dissolved oxygen; TN: total nitrogen; TP: total phosphorus;  $\text{COD}_{\text{Mn}}$ : chemical oxygen demand. P-value comes from One-way ANOVA and a, b, c measured by post-hoc test using Tukey HSD ANOVA, which mean differences between three seasons

	Spring	Summer	Autumn	P-value
SD (cm)	9.75 $\pm$ 0.12 <sup>a</sup>	24.89 $\pm$ 2.90 <sup>b</sup>	26.11 $\pm$ 2.61 <sup>b</sup>	0.000
WT (°C)	15.43 $\pm$ 0.09 <sup>a</sup>	21.39 $\pm$ 0.11 <sup>b</sup>	6.61 $\pm$ 0.29 <sup>c</sup>	0.000
EC (ms/cm)	0.39 $\pm$ 0.04 <sup>a</sup>	0.32 $\pm$ 0.04 <sup>a</sup>	0.35 $\pm$ 0.03 <sup>a</sup>	0.400
pH	9.50 $\pm$ 0.06 <sup>b</sup>	9.50 $\pm$ 0.04 <sup>b</sup>	9.72 $\pm$ 0.06 <sup>a</sup>	0.012
Cl <sup>-</sup> (mg/L)	23.11 $\pm$ 0.93 <sup>b</sup>	21.09 $\pm$ 1.41 <sup>b</sup>	53.06 $\pm$ 3.86 <sup>a</sup>	0.000
$\text{NH}_4^+\text{-N}$ (mg/L)	48.49 $\pm$ 4.73 <sup>a</sup>	21.24 $\pm$ 1.29 <sup>b</sup>	12.48 $\pm$ 1.66 <sup>b</sup>	0.000
$\text{NO}_3^-\text{-N}$ (mg/L)	15.58 $\pm$ 0.71 <sup>a</sup>	35.66 $\pm$ 2.41 <sup>b</sup>	24.28 $\pm$ 0.85 <sup>c</sup>	0.000
NTU	51.87 $\pm$ 1.04 <sup>a</sup>	26.30 $\pm$ 4.21 <sup>b</sup>	32.62 $\pm$ 4.58 <sup>b</sup>	0.000
DO (mg/L)	7.09 $\pm$ 0.41 <sup>b</sup>	9.29 $\pm$ 0.20 <sup>a</sup>	8.36 $\pm$ 0.23 <sup>a</sup>	0.000
TN (mg/L)	2.17 $\pm$ 0.28 <sup>a</sup>	1.41 $\pm$ 0.22 <sup>ab</sup>	2.33 $\pm$ 0.27 <sup>ac</sup>	0.042
TP (mg/L)	0.40 $\pm$ 0.02 <sup>a</sup>	0.58 $\pm$ 0.07 <sup>a</sup>	0.58 $\pm$ 0.15 <sup>a</sup>	0.322
$\text{COD}_{\text{Mn}}$ (mg/L)	21.56 $\pm$ 0.88 <sup>a</sup>	22.36 $\pm$ 0.39 <sup>a</sup>	40.09 $\pm$ 2.79 <sup>b</sup>	0.000

### ***The characteristics of benthic macroinvertebrates communities structures***

In the investigation, 21 taxa were identified in a total of 190 individuals (Table 4). Relative abundance is shown in Figure 2. The dominant taxonomic families identified were Palaemonidae, Viviparidae and Chironomidae, accounted for 51.05%, 15.26% and 13.68% relative abundance respectively. The *Palaemon paucidens* was the most abundant species accounting for 50.00% of the total abundance in spring, 39.13% in summer, 53.85% in autumn; Followed by *Bellamyia purificata* accounting for 8.00% of the total abundance in spring, 13.04% in summer, 18.80% in autumn. Additionally, it indicated from Figure 2 that the species diversity was higher in autumn than in spring and summer. Site S1 provides the highest relative abundance during the sampling period, and site S7 had the lowest relative abundance, as shown in Figure 3.

### ***Benthic macroinvertebrates functional groups in temporal variation***

It recorded 21 taxa of benthic macroinvertebrates belonging to 4 groups in functional feeding groups, and five groups in locomotion groups (Tables 1 and 4). In investigated period the dominant functional feeding groups functional group was OM mainly comprised by Decapoda (50.00%, 39.13%, 57.26% in spring, summer and winter respectively); Locomotion groups were dominated by CM, which also contributed by

Decapoda (50.00%, 39.13%, 57.26% in spring, summer and autumn respectively); DI, SP and PR were only appeared in autumn, and had the little relative abundance (Fig. 4). From Figure 5 we found that FC (in locomotion groups) and BU (in functional feeding groups) were dominant groups in S6, S7, S8 and S9.

**Table 4.** Diversity broad outline, functional groups, and relative abundance of benthic macroinvertebrates during three sampling periods collected in Keqin Lake

Order	Family	Species	Functional feeding groups	Locomotion groups	(%)
Decapoda	Palaemonidae	<i>Palaemon paucidens</i>	OM	CM	51.05
	Atyinae	<i>Neocaridina heteropoda</i>	OM	CM	2.11
Hemiptera	Belostomatidae	<i>Sphaerodema rusticca</i>	PR	DI	1.05
	Corixidae	<i>Corixinae</i> sp.	PR	DI	1.58
		<i>Agraptocorixa</i> sp.	PR	DI	0.53
Mesogastropoda	Viviparidae	<i>Bellamya purificata</i>	SC	CN	15.26
	Hydrobiidae	<i>Parafossarulus striatulus</i>	SC	CN	3.68
		<i>Bithynia fuchsiana</i>	SC	CN	0.53
Basommatophora	Valvatidae	<i>Vavata piseinatis</i>	SC	CN	0.53
	Planorbidae	<i>Polypylis hemisphaerula</i>	SC	CN	1.58
		<i>Radix ovata</i>	SC	CN	2.11
		<i>R. auricularia</i>	SC	CN	2.11
Eulamellibranchia	Sphaeriidae	<i>Sphaerium lacustre</i>	FC	CN	1.05
	Unionidae	<i>Cristaria plicata</i>	FC	CN	1.05
Odonata	Platycnemididae	<i>Platycnemididae</i> sp.	PR	SP	0.53
Diptera	Chironomidae	<i>Chironomus</i> sp.	FC	BU	5.77
		<i>Einfeldia</i> sp.	FC	BU	4.21
		<i>Glyptotendipes</i> sp.	FC	BU	2.11
		<i>Polypedilum</i> sp.	FC	BU	1.58
Pharyngobdellida	Erpobdellidae	<i>Erpobdella octoculata</i>	PR	CN	1.05
Rhynchobdellida	Glossiphoniidae	<i>Helobdella stagnalis</i>	PR	CN	0.53

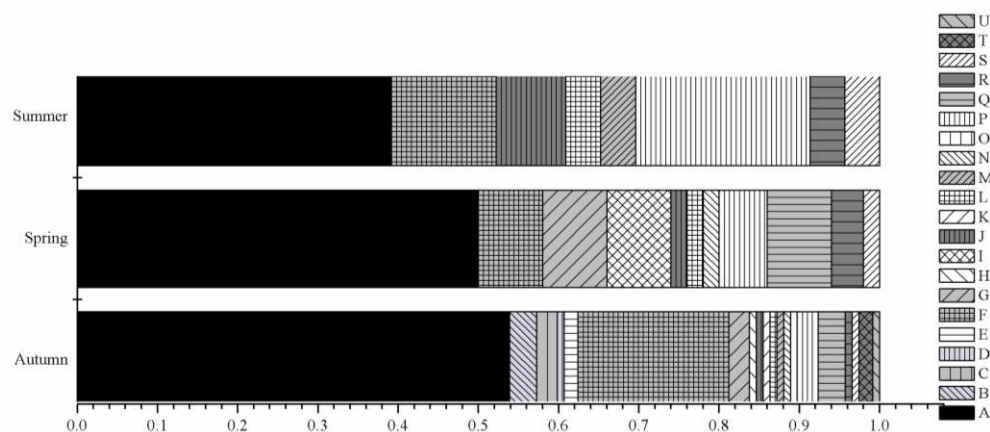


**Figure 2.** Relative abundance of 21 taxa according to identification. A: *Palaemon paucidens*, B: *Neocaridina heteropoda*, C: *Corixinae* sp., D: *Agraptocorixa* sp., E: *Sphaerodema rusticca*, F: *Bellamya purificata*, G: *Parafossarulus striatulus*, H: *Bithynia fuchsiana*, I: *Radix ovata*, J: *R. auricularia*, K: *Vavata piseinatis*, L: *Polypylis hemisphaerula*, M: *Sphaerium lacustre*, N: *Cristaria plicata*, O: *platycnemididae* sp., P: *Chironomus Meigen* sp., Q: *Einfeldia* sp., R: *Glyptotendipes* sp., S: *Polypedilum* sp., T: *Erpobdella octoculata* Linnaeus, U: *Helobdella stagnalis*

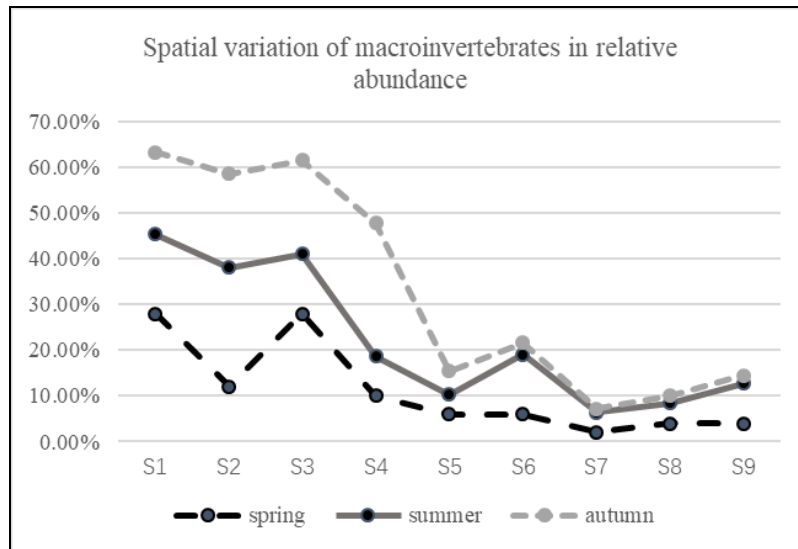


**Figure 3.** Relative abundance of benthic macroinvertebrates per site at each season (the sum of relative abundances of all sites is 100%)

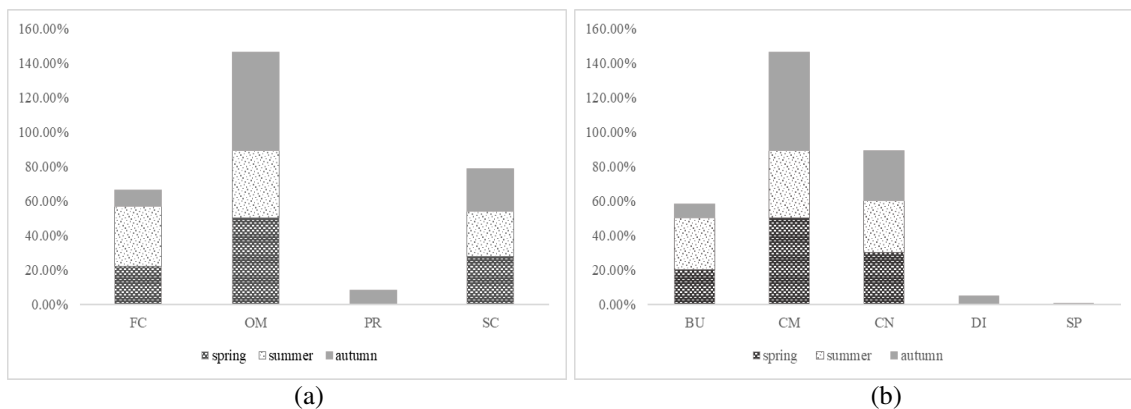


**Figure 4.** Relative abundance of benthic macroinvertebrates functional groups in three season. (a) Functional feeding groups; (b) locomotion groups. FC (Filter-feeders), OM (Omnivores), PR (Predators), SC (Scrapers), BU (Burrowers), CM (Climbers), CN (Clingers), DI (Divers), SP (Sprawlers)

### Relationships between benthic macroinvertebrates functional groups and physicochemical factors

The relationships between physicochemical factors and benthic macroinvertebrates functional groups were explained by RDA. The relationships between functional groups and physicochemical factors are described in the RDA ordination diagram (Figs. 6, 7). Different physicochemical indexes were significantly correlated with each functional groups.

The nine groups were categorized as follows: FC (Filter-feeders), OM (Omnivores), PR (Predators), SC (Scrapers), BU (Burrowers), CM (Climbers), CN (Clingers), DI (Divers), SP (Sprawlers). Among the variables included in the RDA,  $COD_{Mn}$ ,  $Cl^-$ ,  $NTU$  were crucial physicochemical factors which affected the functional feeding groups and locomotion groups significantly.

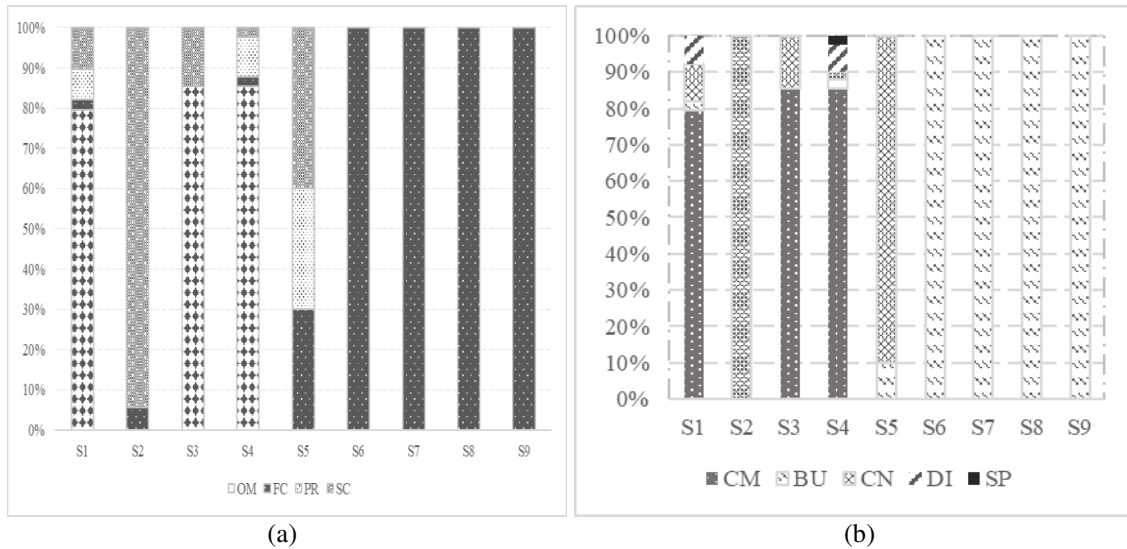


**Figure 5.** Relative abundance of benthic macroinvertebrates functional groups among sampling sites: (a) Functional feeding groups, (b) locomotion groups. FC (Filter-feeders), OM (Omnivores), PR (Predators), SC (Scrapers), BU (Burrowers), CM (Climbers), CN (Clingers), DI (Divers), SP (Sprawlers)

*The relationships between functional feeding groups and physicochemical factors*

The first two RDA axes respectively illustrated 0.796 and 0.609 of macroinvertebrate and environment correlation, with eigenvalues of 0.36 and 0.10.  $\text{COD}_{\text{Mn}}$  and  $\text{Cl}^-$  were positively associated with axis 1, NTU was negatively correlated with axis 1. OM, PR and SC were positively correlated with  $\text{COD}_{\text{Mn}}$  and  $\text{Cl}^-$ ; FC was positively correlated with NTU (Fig. 6).

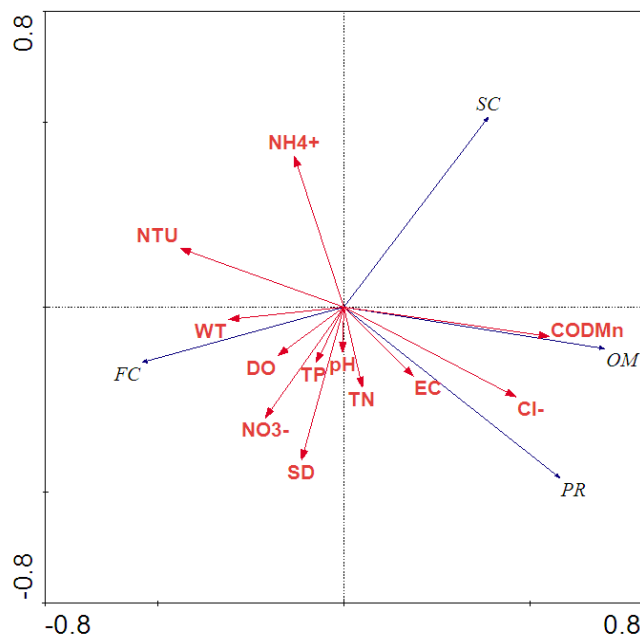


**Figure 6.** RDA ordination diagram of the functional feeding groups and physicochemical variables FC (Filter-feeders), OM (Omnivores), PR (Predators), SC (Scrapers)



### *The relationships between locomotion groups and physicochemical factors*

The functional groups and physicochemical correlations for axis 1 and axis 2 were 0.821 and 0.527, respectively. The eigenvalues were 0.36 in axis 1 and 0.10 in axis 2. COD<sub>Mn</sub> and Cl<sup>-</sup> were positively associated with axis 1, NTU was negatively correlated with axis 1. CN, CM, DI, SP were positively correlated with COD<sub>Mn</sub> and Cl<sup>-</sup>; BU was positively correlated with NTU (Fig. 7).

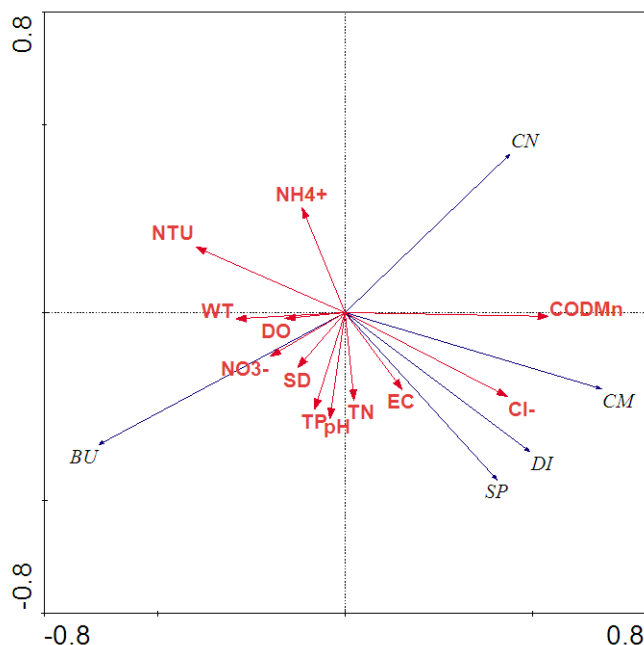


**Figure 7.** RDA ordination diagram of the locomotion groups and physicochemical variables BU (Burrowers), CM (Climbers), CN (Clingers), DI (Divers), SP (Sprawlers)

## Discussion

### *Benthic macroinvertebrates functional groups in Keqin Lake*

The functional feeding groups and locomotion groups show consistency in Keqin Lake, OM was dominant in functional feeding groups group, and CM was dominant in locomotion groups. OM and CM mainly composed of *Palaemon paucidens* (96.04% relative abundance in OM, 96.04% relative abundance in CM). *Palaemon paucidens* has the wide functional feeding groups, less influenced by seasonal changes, and the population number usually increases in autumn. SC (in functional feeding groups group) and CN (in locomotion groups) appeared in three seasons, and dominant by molluscs. Some studies demonstrated that molluscs played a crucial role in lake wetland ecosystem and had significant ecological functions (Ngor et al., 2018; Chea et al., 2016). The bottom of the west bank of Keqin Lake was covered by sandy mud, and relatively more molluscs were found here in three seasons, which indicating that the density distribution of molluscs were affected by the bottom material in lake (Zamorano et al., 2007). PR (in functional feeding groups), DI and SP (in locomotion groups) only appeared in autumn. One feasible reason is that the diversity of benthic macroinvertebrates in autumn is higher than other seasons in cold temperate region (Huo et al., 2013; Li, 2012).

The relative abundance was high in S1, S2 and S3 probably due to the habitat with lush aquatic vascular plant vegetation at edge of the macrophyte bed. The distribution of benthic macroinvertebrates is determined by vegetation types, especially the structure and growth form of the dominant aquatic vascular plants (Kaskela et al., 2017). Actions prioritizing the development of vegetation species-rich will be likely to benefit benthic macroinvertebrates biodiversity (Law et al., 2019). S6, S7, S8 and S9 were dominated by FC (in locomotion groups) and BU (in functional feeding groups), account for the location of sample sites and sediments of lake bottom. These sites locate in the middle of lake with fewer macrophyte but more white mud. Therefore, Chironomidae was dominated in S6, S7, S8 and S9.

### ***Physicochemical factors possessing the benthic macroinvertebrates functional groups***

The benthic macroinvertebrates play a significant role in ecosystem evolution, such as nutrient cycling, pollutant metabolism, and secondary production in lake sediments. The species composition and abundance of benthic macroinvertebrates varied with changes in water temperature (WT), dissolved oxygen (DO), sediment type, water velocity, and mud (or sand) content (Inagaki et al., 2012). The RDA ordination diagram described the relationships between functional groups and physicochemical factors: the different groups were significantly correlated with each physicochemical variables, illustrating that different groups were influenced by different physical and chemical factors, which were related to their ecological characteristics. Group OM was found to be the dominant group at the sampling period (Fig. 3), suggesting that OM was well adjusted to the habitat of Keqin Lake. In the current study, OM was significantly positively correlated with  $COD_{Mn}$  (Fig. 4). In our research, the groups OM which were contained by Decapoda mainly fed on plankton, containing phytoplankton and zooplankton. Zooplankton also feed on phytoplankton. This means that the group OM was basically commanded by phytoplankton. The growth and productivity of phytoplankton are affected by many factors. One of the most essential factors is the chemical oxygen demand ( $COD_{Mn}$ ) (Collins and Williner, 2003). Generally, phytoplankton reveals the maximum productivity in high  $COD_{Mn}$  (Petar et al., 2014; Wang et al., 2007). Consequently, it is no wonder that the groups OM is significantly positively correlated with  $COD_{Mn}$ .

It appears that the occurrence of these species in the Keqin Lake is not driven by a single environmental factor. BU and FC both were positively correlated with NTU, which could be interpreted by the biotope they stayed. FC is composed of Sphaeriidae, Unionidae and Chironomidae; BU is composed of Chironomidae. These three families generally settle in high polluted bottoms. But in the previous study, it has strong negative correlations between macroinvertebrate densities and turbidity (Anderson et al., 2006). According to Rosillon (1989), catastrophic and unpredictable fluctuation of abiotic factors will cause disturbance of stream invertebrate community, but the response to these events varies with species.

As it is indicated in RDA analysis, Chloride ( $Cl^-$ ) became the significant physicochemical factor, what probably due to industrial effluents from factories, and in some instances effluents form farmland nearby. The increasing chloride levels will lead to the death of benthic macroinvertebrates (Benbow and Merritt, 2004). Nevertheless, the higher chlorides improved stream conditions by flocculation of suspended solids and reducing turbidity (Darville and Harrel, 1980). Therefore, it is necessary to set valid pollution precaution plans to governance eutrophication in Keqin Lake.



## Conclusion

During the sampling periods in the Keqin Lake, 21 taxa of benthic macroinvertebrates were recorded belonging to four functional feeding groups and five locomotion groups. We found that *Palaemon paucidens* was the most species in the three seasons, autumn has the most significant number of species and individuals. In accordance with redundancy analysis (RDA), COD<sub>Mn</sub>, Cl<sup>-</sup> and NTU were significantly physicochemical factors correlated with functional groups. It was found that OM (Omnivores), PR (Predators), SC (Scrapers), CN (Clingers), CM (Climbers), DI (Divers), SP (Sprawlers) were positively correlated with COD<sub>Mn</sub> and Cl<sup>-</sup>; FC (Filter-feeders) and BU (Burrowers) were positively correlated with NTU.

If functional groups provide a valuable alternative for studying communities and lake ecosystems, this approach is highly dependent on the availability of biological and ecological information. But the lack of data forced us to omit potentially important variables such as, fecundity and dispersal potential. This fact emphasizes the importance to continue the basic researches on benthic macroinvertebrates species life history characteristics and ecological requirements which can improve our understanding of these biological and ecological information.

**Acknowledgements.** This work was supported by the National Key Research and Development Program of China (2016YFC0500406). We thank Zhalong Nature Reserve Administration for support during fieldwork.

**Conflict of interests.** None of the authors have any conflict of interests to declare.

## REFERENCES

- [1] Alcocer, J., Oseguera, L., Escobar, E., Reznickova, P. (2016): The littoral benthic macroinvertebrate community as a reflection of environmental heterogeneity. – *Hydrobiologica* 26(3): 403-418.
- [2] Anderson, B. S., Phillips, B. M., Hunt, J. W., Connor, V., Richard, N., Tjeerdema, R. S. (2006): Identifying primary stressors impacting macroinvertebrates in the Salinas River (California, USA): Relative effects of pesticides and suspended particles. – *Environmental Pollution* 141(3): 402-408.
- [3] Benbow, M. E., Merritt, R. W. (2004): Road-salt toxicity of select Michigan wetland macroinvertebrates under different testing conditions. – *Wetlands* 24(1): 68-76.
- [4] Bremner, J., Rogers, S. I., Frid, C. L. J. (2006): Methods for describing ecological functioning of marine benthic assemblages using biological traits analysis (BTA). – *Ecological Indicators* 6(3): 0-622.
- [5] Chea, R., Guo, C., Grenouillet, G., Lek, S. (2016): Toward an ecological understanding of a flood-pulse system lake in a tropical ecosystem: food web structure and ecosystem health. – *Ecological Modelling* 323: 1-11.
- [6] Collins, P. A., Williner, V. (2003): Feeding of *Acetes paraguayensis* (Nobili) (Decapoda: Sergestidae) from the Parana River, Argentina. – *Hydrobiologia* 493(1-3): 1-6.
- [7] Cummins, W. K. (1973): Trophic relations of aquatic insects. – *Annual Review of Entomology* 18(1): 183-206.
- [8] Daily, G. C. (1997): *Nature's Services* (Vol. 1997/1). – Island Press, Washington, DC.
- [9] Darville, R. G., Harrel, R. C. (1980): Macrobenthos of Pine Island Bayou in the Big Thicket National Preserve, Texas. – *Hydrobiologia* 69(3): 213-223.
- [10] Duan, X., Wang, Z., Xu, M. (2010): *Benthic Macroinvertebrates and Application in the Assessment of Stream Ecology*. – Tsinghua University Press, Beijing (in Chinese).

- [11] Dudgeon, D. (1999): *Tropical Asian Streams: Zoobenthos, Ecology and Conservation*. – Hong Kong University Press, Hong Kong.
- [12] Gamito, S., Furtado, R. (2009): Feeding diversity in macroinvertebrate communities: a contribution to estimate the ecological status in shallow waters. – *Ecological Indicators* 9(5): 1009-1019.
- [13] Huo, T., Li, Z., Jiang, Z., Ma, B., Yu, H. (2013): Macrozoobenthos community structure and water quality bioassessment in the mid-reaches of the Heilongjiang River. – *Journal of Fishery Sciences of China* 20(1): 177-188 (in Chinese).
- [14] Inagaki, Y., Takatsu, T., Ashida, Y., Takahashi, T. (2012): Annual changes in macrobenthos abundance in Funka Bay, Japan. – *Fisheries Science (Tokyo)* 78(3): 647-659.
- [15] Kaskela, A. M., Rousi, H., Ronkainen, M., Orlova, M., Zhamoida, V. (2017): Linkages between benthic assemblages and physical environmental factors: the role of geodiversity in eastern Gulf of Finland ecosystems. – *Continental Shelf Research* 142: 1-13.
- [16] Law, A., Baker, A., Sayer, C., Foster, G., Gunn, I. D., Taylor, P., Willby, N. J. (2019): The effectiveness of aquatic plants as surrogates for wider biodiversity in standing fresh waters. – *Freshwater Biology* 64(9): 1664-1675.
- [17] Li, J. J. (2012): *Study on the ecology of macrobenthos in Xiquanyan Reservoir*. – PhD thesis. University of Northeast Forestry, China (in Chinese).
- [18] Li, L. J., Chong, X. Y., Sheng, C. H., Yin, X. W., Xu, Z. X., Zhang, Y. (2019): Response of riparian land-use types to functional groups of benthic macroinvertebrates in Taizi River, Liaoning Province. – *Acta Ecologica Sinica* 39(22): 8667-8674 (in Chinese).
- [19] Liu, M. H., Meng, Y., Cui, J. J., Cao, X. B., Al, M. N. (2019a): Functional Traits of Macroinvertebrates in Naolihe Wetland. – *Journal of Northeast Forestry University* 47(1): 76-82 (in Chinese).
- [20] Liu, X., Li, K., Zhou, Y., Xu, Y., Ouyang, S. (2019b): Temporal and spatial changes in macrozoobenthos diversity in Poyang Lake Basin, China. – *Ecology and Evolution* 9(2).
- [21] Merritt, R. W., Cummins, K. W., Berg, M. B. (1996): *An Introduction to the Aquatic Insects of North America*. Third Ed. – Kendall/Hunt Publishing Company, Dubuque.
- [22] Morse, C. J., Yang, L., Tian, L. (1994): *Aquatic Insects of China Useful for Monitoring Water Quality*. – Hohai University Press, Nanjing, China.
- [23] Ngor, P. B., Sor, R., Prak, L. H., So, N., Hogan, Z. S., Lek, S. (2018): Mollusc fisheries and length–weight relationship in Tonle Sap flood pulse system, Cambodia. – *Annales de Limnologie - International Journal of Limnology* 54: 34.
- [24] Petar, Ž., Marija, G. U., Koraljka, K. B., Anđelka, P. M., Judit, P. (2014): Morpho-functional classifications of phytoplankton assemblages of two deep karstic lakes. – *Hydrobiologia* 740(1): 147-166.
- [25] Poff, N. L., Olden, J. D., Vieira, N. K., Finn, D. S., Simmons, M. P., Kondratieff, B. C. (2006): Functional trait niches of North American lotic insects: traits-based ecological applications in light of phylogenetic relationships. – *Journal of the North American Benthological Society* 25(4): 730-755.
- [26] Postel, S., Carpenter, S. (1997): *Freshwater Ecosystem Services*. – In: Daily, G. (ed.) *Nature's Services: Societal Dependence on Natural Ecosystems*. Island Press, Washington, DC, pp. 195-214.
- [27] Rosillon, D. (1989): The influence of abiotic factors and density-dependent mechanisms on between-year variations in a stream invertebrate community. – *Hydrobiologia* 179: 25-38.
- [28] Thorp, J. H., Covich, A. P. (1991): *Ecology and Classification of North American Freshwater Invertebrates*. – Academic Press, New York.
- [29] Usseglio-Polatera, P., Bournaud, M., Richoux, P., Tachet, H. (2000): Biological and ecological traits of benthic freshwater macroinvertebrates: relationships and definition of groups with similar traits. – *Freshwater Biology* 43(2): 175-205.

- [30] Wang, X. L., Lu, Y. L., He, G. Z., Han, J. Y., Wang, T. Y. (2007): Exploration of relationships between phytoplankton biomass and related environmental variables using multivariate statistic analysis in a eutrophic shallow lake: a 5-year study. – *Journal of Environmental Sciences* 19(8): 920-927.
- [31] Wei, F. S., Qi, W. Q., Sun, Z. G., Huang, Y. R., Shen, Y. W. (2002): *Water and Wastewater Monitoring and Analysis Method*. – China Environmental Science Press, China, pp. 211-284 (in Chinese).
- [32] Zamorano, P., Hendrickx, M. E., Toledano-Granados, A. (2007): Distribution and ecology of deep-water mollusks from the continental slope, southeastern Gulf of California, Mexico. – *Marine Biology* 150(5): 883-892.
- [33] Zhang, N., Xiao, X., Pei, M., Liu, X., Liang, Y. (2016): Discordant temporal turnovers of sediment bacterial and eukaryotic communities in response to dredging: non-resilience and functional changes. – *Applied and Environmental Microbiology* AEM 02526-16.
- [34] Zhu, C. X., Mo, K. L., Tang, L., Wu, Y., Li, T., Lin, Y. Q., Chen, Q. W. (2020): Spatial-temporal distribution and ecological effects of macroinvertebrate functional feeding groups in the Lijiang River. – *Acta Ecologica Sinica* 40(1): 60-69 (in Chinese).

## STOICHIOMETRIC CHARACTERISTICS OF THE ROOT, STEM, AND LEAF OF *SOPHORA ALOPECUROIDES* L. IN THE DIFFERENT HABITATS OF THE YILI VALLEY, XINJIANG, CHINA

LIU, S. Q.<sup>1,2</sup> – CUI, D.<sup>1,2\*</sup> – YAN, J. J.<sup>1,2</sup> – NIJAT, K.<sup>1,2</sup> – YANG, H. J.<sup>1,2,3</sup>

<sup>1</sup>*Institute of Resources and Ecology, Yili Normal University, Yining 835000, China*

<sup>2</sup>*College of Biology and Geography Sciences, Yili Normal University, Yining 835000, China*

<sup>3</sup>*Ministry of Education Key Laboratory of Vegetation Ecology, Institute of Grassland Science, Northeast Normal University, Changchun 130024, China*

\*Corresponding author  
e-mail: [cuidongw@126.com](mailto:cuidongw@126.com)

(Received 6<sup>th</sup> Aug 2020; accepted 19<sup>th</sup> Nov 2020)

**Abstract.** This study selected *Sophora alopecuroides* L. in the degraded grassland of the Yili Valley as the research target, the comparisons of the stoichiometric ratios of C:N, C:P, N:P before and after *Sophora alopecuroides* invasion in the soil were analyzed, and the eco-stoichiometry of the root, stem, and leaf of the plant in the different habitats (forest, roadside, farmland, desert) was discussed, as well as effects of habitats and organs on eco-stoichiometry of *Sophora alopecuroides*. The results showed that concentrations of C, N, P and their stoichiometric ratios in roots, stems and leaves changed with habitat, and only the concentrations of N and N:P ratios were in the order of leaves > stems > roots. The ratios of C:N and C:P were negatively correlated with the corresponding N and P concentrations. The N concentration was positively correlated with the P concentration, indicating a consistent demand of N and P during *Sophora alopecuroides* growth. According to the factorial analysis of the general linear model (GLM), we concluded that C:N ratio and the N concentration are mainly affected by the organs, while the P concentration and C:P ratio are mainly affected by the habitats.

**Keywords:** *plant, ecological stoichiometry, environment, organ, nutrient utilization*

### Introduction

Carbon, nitrogen and phosphorus are the basic chemical elements needed by plant growth. Carbon is the element with the highest dry matter concentration in plant corpus. Nitrogen and phosphorus are the important components of protein, enzyme and genetic material in cells and the basic elements of organisms (Wang and Yang, 2013; Ou et al., 2006). The ratio of N:P in plants can be used as an indicator to judge the adaptation of plant growth to nutrient supply (Wang et al., 2011). In the field of ecological research, chemometrics is usually applied to the study of the main elements of organisms (Aerts and Chapin, 2000). Ecological stoichiometry is a new discipline to explain the balance of various chemical elements in ecological interaction. In the field of ecological research, stoichiometric characteristics provide a new method to study the main element composition of organisms (Michaels, 2003; Elser et al., 2000; Zeng et al., 2013). Scholars at home and abroad have studied the relationship between plant nutrient elements and environment from different scales (Ashton et al., 2005; Yu et al., 2016). Li et al. (2014) and Luo et al. (2016) studied the stoichiometric characteristics of plants in different habitats, indicating that plants adjust nutrient utilization strategies to adapt to environmental changes, thus enabling them to have a strong ability to adapt to extreme environments.

*Sophora alopecuroides* L. is a member of the genus *Sophora* in the PEA (pea) family. It is a perennial herbaceous plant (Yang and Yu, 1998). It appeared in the desert regions of northwestern China (Ningxia, Xinjiang, Inner Mongolia, Gansu, Qinghai, Tibet, etc.) (Li et al., 2005), and grew mainly in sandy soil and various kinds of salt habitats. It has the characteristics of salt-resistance, drought resistance, and sand buried resistance. Because the seeds of *Sophora alopecuroides* can take root and germinate quickly in the wet sand, the underground rhizome can reproduce rapidly, the ability to spread is very strong (Liu et al., 2017). In the Yili region, a large area of the grassland was invaded and spread, forming single dominant community with simple structure and few companion species in degraded areas, leading to the decline of grassland quality and economic productivity, which has posed a threat to the farming and pastoral areas in the region, especially in the degraded grassland area (Lu et al., 2011). At present, there are many studies on the medicinal value (Shang et al., 2018; Shi et al., 2019) of *Sophora alopecuroides* and few studies on the ecological stoichiometry of each organ of *Sophora alopecuroides* in different habitats. This study analyzed the changes of C, N and P elements and their stoichiometric ratios in roots, stems, and leaves of *Sophora alopecuroides* based on the different habitats, aiming to understand the ecological mechanism of the growth environment of *Sophora alopecuroides* and the adaptation mechanism of *Sophora alopecuroides* in the various habitats, to provide theoretical basis for the restoration and protection of degraded grassland ecosystem vegetation.

## Materials and methods

### Experimental site

The study site is located in the Yili valley of Xinjiang, China (81°05'~91°09' E, 43°80'~43°84' N), which is a typical mountainous grassland area. The climate of this region is a temperate continental climate and belongs to the semi-arid region. The average annual temperature is 9-11.1 °C, the average annual precipitation is 250-551.7 mm and the average annual evaporation is 1621 mm. The altitude is 550-596.2 m. In the study area, as shown in *Figure 1*, we selected the forest (plot-I, at an altitude of 579.1-588.4 m), roadside (plot-II, 550-551.2 m), farmland (plot-III, 590-593.5 m) and desert (plot-IV, 596-596.3 m) invaded by *Sophora alopecuroides* (coverage up to 80%).

### Sample collection

The habitats invaded by *Sophora alopecuroides* layout for forest (plot-I), roadside (plot-II), farmland (plot-III) and desert (plot-IV). The soil difference analysis of the various habitats was shown in *Table 1*. The pH value of plot-IV was significantly higher than that of plot-II and III. The nitrate nitrogen of plot-I was higher than that of plot-II, III and IV. The concentrations of total nitrogen and total phosphorus in plot-II was the lowest compared with plot-I, III and IV. There was no significant difference in total carbon and organic matter concentration in the four habitats. There was no significant difference in organic matter concentration in the four habitats. Each habitat was randomly set three quadrats (5 m × 5 m). *Sophora alopecuroides* of uniform growth were randomly selected from the quadrat. The above-ground organs of *Sophora alopecuroides* were collected by the harvesting method and the root of *Sophora alopecuroides* were collected by the digging method. The root, stem, and leaf were cut into small pieces of 2-4 cm. They were marked and put in an envelope, while it was

taken to the laboratory to measure the concentration of the element in each organ. Soil samples were collected separately from habitats invaded by *Sophora alopecuroides*. Soil samples were collected at 10 cm intervals and 0-40 cm samples were collected. Each soil sample is about 500 g. At the same time, soil samples without invasion of *Sophora alopecuroides* around each habitat were collected. The above samples are used for the determination of soil physical and chemical properties.

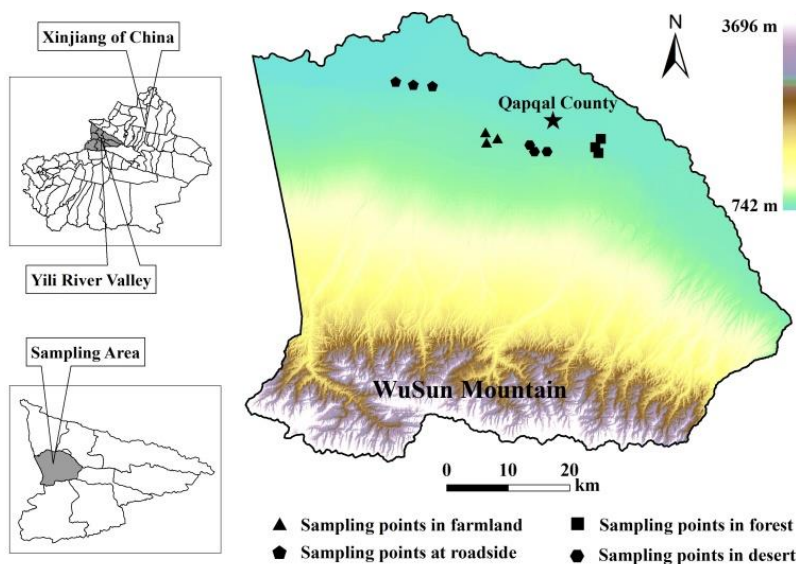


**Figure 1.** Sketch map of the study area

**Table 1.** Post-hoc test of soil physical and chemical properties in plot-I, II, III and IV

Plots	TN (g kg <sup>-1</sup> )	TP (g kg <sup>-1</sup> )	TC (g kg <sup>-1</sup> )	Organic matter (g kg <sup>-1</sup> )	pH	Nitrate nitrogen (mg kg <sup>-1</sup> )
I	1.06 ± 0.10ab	0.91 ± 0.03a	9.81 ± 1.19a	16.91 ± 2.05a	8.01 ± 0.03b	6.73 ± 1.07a
II	0.48 ± 0.02c	0.64 ± 0.05b	8.34 ± 1.10a	14.37 ± 1.90a	7.84 ± 0.02c	1.67 ± 0.22c
III	1.11 ± 0.09a	1.02 ± 0.50a	9.79 ± 0.64a	16.88 ± 1.11a	7.84 ± 0.03c	1.87 ± 0.05bc
IV	0.84 ± 0.08b	0.71 ± 0.20b	6.62 ± 1.51a	11.41 ± 2.01a	8.74 ± 0.05a	3.57 ± 0.48b

TN, TP, and TC represent total nitrogen, total phosphorus and total carbon; a, b, and c represent the significant characteristics of different organs in different habitats ( $P < 0.05$ )

### Experimental method

The root, stem, and leaf of *Sophora alopecuroides* were dried naturally, and all samples were dried to constant weight at 85 °C. Each organ of the sample was ground by a plant grinder, weighed and bagged for storage. The concentrations of total Carbon, total nitrogen and total phosphorus of *Sophora alopecuroides* were determined. The collected soil samples should be air-dried, and the roots and stones in the soil samples should be removed and bagged for testing. Total carbon, total nitrogen, total phosphorus, organic matter, pH and nitrate nitrogen of the soil were selected for the determination of soil physical and chemical properties.

Soil and plant TC (Total Carbon) were determined by the potassium dichromate volumetric method (external heating method) (Lu, 1999). TN (Total Nitrogen) is determined by the perchloric acid sulfuric acid digestion method and by the Fuchs 1035 automatic nitrogen determinator (Lu, 1999). TP (Total Phosphorus) was determined by acid-soluble molybdenum antimony anti colorimetry and Agilent Cary-60 UV spectrophotometer (Lu, 1999).

### ***Sample analysis and data processing***

The experimental data were processed using SPSS 24.0 and Excel 2010. The results were expressed by the mean and standard deviation (SD). One-way ANOVA was used to test the stoichiometric characteristics of C, N, and P in roots, stems, and leaves of *Sophora alopecuroides* and the differences of soil physical and chemical factors. Duncan's method was used for multiple comparisons, and the significance level was 0.05. The effects of different plots and organs on the C, N, and P concentrations were analyzed by GLM. The general linear model (GLM) was used to analyze the principal factor effects and interactions, and then the influence of each factor on the concentrations of C, N, P, and their stoichiometric characteristics.

## **Results**

### ***Comparison of the stoichiometric of C, N, and P in soil samples***

The distribution of  $R_{CN}$  (C:N Ratio),  $R_{CP}$  (C:P Ratio) and  $R_{NP}$  (N:P Ratio) in the soil profile in the invaded and uninvaded soil of *Sophora alopecuroides* were shown in *Figure 2*. In the profile of the invaded soil, the  $R_{CN}$  decreased obviously with the increase of depth, and the maximum of the  $R_{CN}$  appeared in the 0-10 cm soil layer (*Fig. 2A*). The maximum of  $R_{CP}$  was in the surface layer, the  $R_{CP}$  in the 20-30 cm soil layer was slightly higher than that in the 10-20 cm soil layer (*Fig. 2B*), and the minimum of  $R_{CN}$  and  $R_{CP}$  appeared in the 30-40 cm soil layer. The  $R_{NP}$  changed little, and the maximum of the  $R_{NP}$  was in the 20-30 cm soil layer (*Fig. 2C*). In the profile uninvaded soil of *Sophora alopecuroides*, the  $R_{CP}$  decreased with the increase of soil depth, the maximum of  $R_{CN}$  appeared in 10-20 cm soil layer, and the maximum of  $R_{CP}$  and  $R_{NP}$  appeared in 0-10 cm soil layer. The mean of  $R_{CN}$ ,  $R_{CP}$  and  $R_{NP}$  were 10.28, 10.73, 1.05 (invaded soil), 9.71, 10.05, 1.10 (the uninvaded soil).  $R_{CN}$  and  $R_{CP}$  in the invaded soil of *Sophora alopecuroides* were higher than those in the uninvaded soil, and the  $R_{NP}$  in the uninvaded soil was slightly higher than that in the invaded soil.

### ***Characteristics of C, N, P concentrations and their stoichiometric ratios in different organs of Sophora alopecuroides***

There are differences in the concentrations of C, N, and P in different organs of *Sophora alopecuroides* (*Fig. 3*). As shown in *Figure 3A*, the C concentrations showed an order of leaves > stems > roots in plot-I, II and III, while stem C concentration was slightly higher than that of leaf in plot-IV. There was no significant difference in C concentration among plot-I, II and III. There was a significant difference in the concentration of C between leaf and root in plot-IV. As shown in *Figure 3B*, there was no significant difference in the concentration of N between leaves and stems in the four plots, and there was a significant difference in root N concentration between plot-III and IV. As shown in *Figure 3C*, the leaf P concentration was significantly higher than the

stem and root P concentrations in plot-I. The leaf P concentration was significantly different from the stem P concentration between plot-III and IV. There was a significant difference in P concentration between leaf and root in plot-III. There was a significant difference in P concentration between stem and root in plot-III.

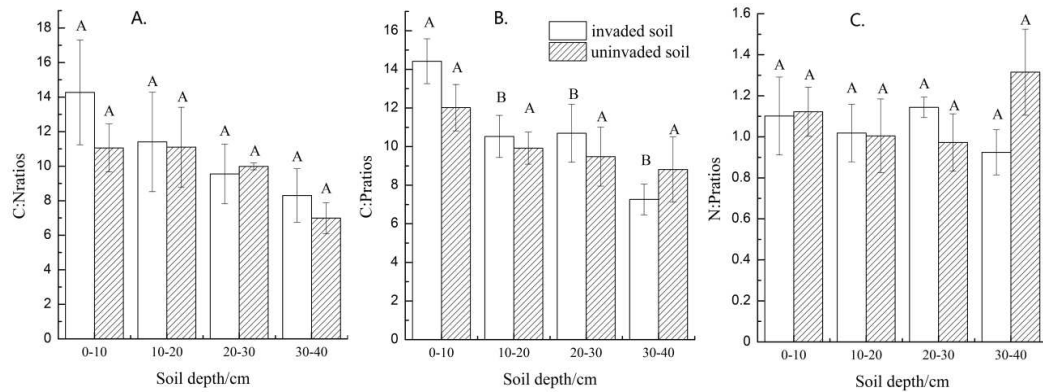


**Figure 2.** The distribution of  $R_{CN}$  (C:N),  $R_{CP}$  (C:P), and  $R_{NP}$  (N:P) in the soil profile in the invaded soil and in the uninvaded soil. A and B represent significant differences between the invaded soil and the uninvaded soil in the different depth ( $P < 0.05$ )

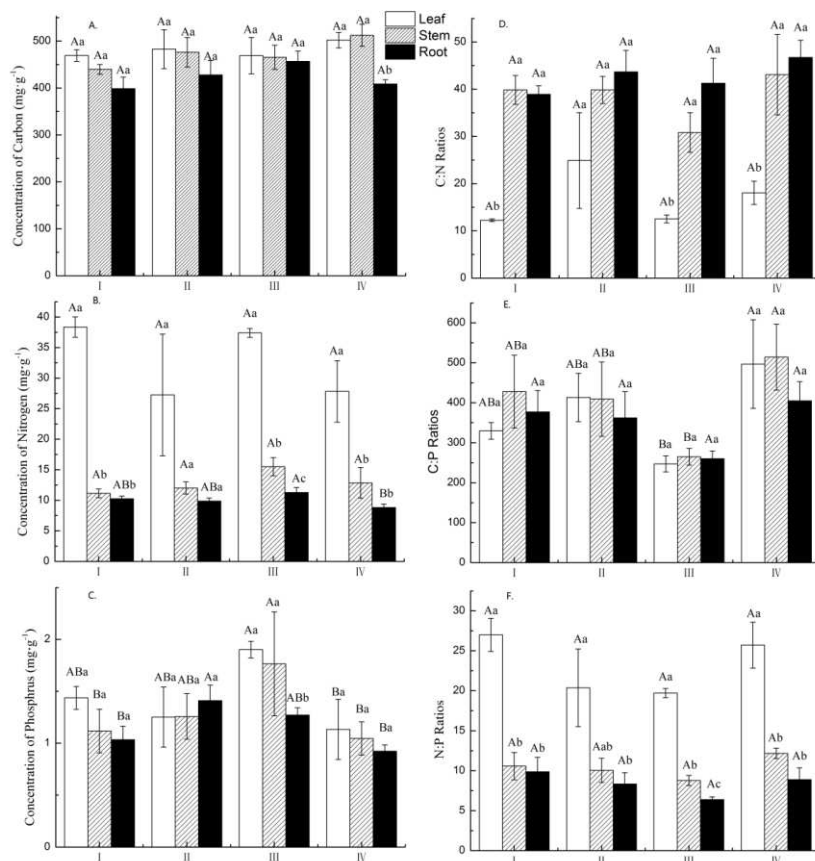


**Figure 3.** C, N, and P concentrations and their stoichiometry in the organs of *Sophora alopecuroides* in different habitats. A, B and C represent significant differences among organs in different habitats ( $P < 0.05$ ) and a, b and c represent significant differences among the different organs in the same habitat ( $P < 0.05$ )



The stoichiometric ratios of C:N, C:P, and N:P in different organs of *Sophora alopecuroides* showed the regular changes. As shown in *Figure 3D*, the stoichiometric ratio of C:N in plot-II, III, and IV showed the trend of roots > stems > leaves. There were significant differences in the C:N ratio between leaf and stem in plot-I, III and IV. There was no significant difference in C:N ratio among root, stem and leaf in plot-II. The ratio of the C:N did not differ among the four plots. As shown in *Figure 3E*, there were significant differences in the C:P ratio between the leaf and stem of plot-III and the leaf and stem of plot-I, II and IV. The ratio of the C:P did not differ among the roots, stems and leaves in the four plots. As shown in *Figure 3F*, the N:P ratio were in the order of leaf > stem > root. There was a significant difference in the N:P ratio among root, stem, and leaf in the plot-III, but the ratio of N:P did not differ among the four plots.

### ***Correlation between C, N, P concentrations and stoichiometric ratio of Sophora alopecuroides***

As shown in *Figure 4*, correlation analysis (*Fig. 4A, B, C, D*) showed that the correlation between C:N ratio and N concentration of *Sophora alopecuroides* was significantly negative ( $P < 0.01$ ). As shown in *Fig. 4E, F, G, I*, there was a significant negative correlation between C:P ratio and P concentration in plot-I, II, and IV ( $P < 0.05$ ). The correlation between C:P ratio and P concentration was not significant in plot-III ( $P > 0.05$ ). As a whole, the C:N and C:P ratios increase with the decrease of their corresponding N and P concentrations. The logarithmic equation in the figure can clearly show the above correlation. As shown in *Fig. 4I, J, K, L*, there was a significant positive correlation between N and P concentrations ( $P < 0.05$ ), There was a significant positive correlation between N and P concentrations in plot-III, but there was no significant difference between N and P concentrations in plot-II ( $P > 0.05$ ).

### ***Habitat and organ effect on C, N, P concentrations and their stoichiometric characteristics of Sophora alopecuroides***

The effects of organs and habitats on the C, N and P concentrations and their C:N, C:P, and N:P ratios of *Sophora alopecuroides* were quantified by GLM analysis. The C, N, and P concentrations and their C:N, C:P, and N:P ratios were affected differently by the single factor and the interaction of the two factors. As shown in *Table 2*, C:N ratio and the N concentration are mainly affected by the organs, while the P concentration and C:P ratio are mainly affected by the habitats. Organs and habitats had no significant effect on the concentration of C. The interaction between organs and habitats did not differ in C, N, and P concentrations and their stoichiometric ratios.

## **Discussion**

### ***Change of C, N, P concentrations and their stoichiometric ratio in organs of Sophora alopecuroides***

The concentrations of elements and stoichiometric ratios of roots, stems, and leaves of plants vary significantly due to their different functions and storage of nutrients, Leaves are the main aboveground components for plants to absorb and store nutrient elements. Because leaves are the most metabolic aboveground organs, the

concentrations of N and P in leaves are higher than that of roots and stems for storing nutrients (Luo and Gong, 2016). In this study, the concentrations of N and P in *Sophora alopecuroides* are consistent with the result. The concentration of P in leaf of *Sophora alopecuroides* in plot-II was slightly lower than that in stems and roots, and the concentration of P in soil physical and chemical factors was the lowest. It may be one of the reasons why the concentration of P in the leaves cannot be replenished. Leaves are the main photosynthetic organ of plants. Leaf C concentration increased during the peak growing season, and then it is transported to the stem and root. According to the research of Xiao et al., the nutrient content of the stem is generally smaller than that of leaves with the increase of plant biomass in most plants growth process (Xiao et al., 2014). The root is the main organ for the plant to absorb nutrients and transport nutrients. Because root grows underground, photosynthesis does not take place here and cell metabolism ability is not strong. The main function of the root is to transport nutrients and water from the soil, so the accumulation of C element by root is the least. Zhao et al. (2014) showed that the root N and P concentrations change because the elements flow to other organs. In the process of plant growth, the roots are growing. The root maintains its growth by absorbed nutrient elements, and output a lot of nutrients to assist the growth of other organs. The concentrations of N and P in roots are relatively lower.

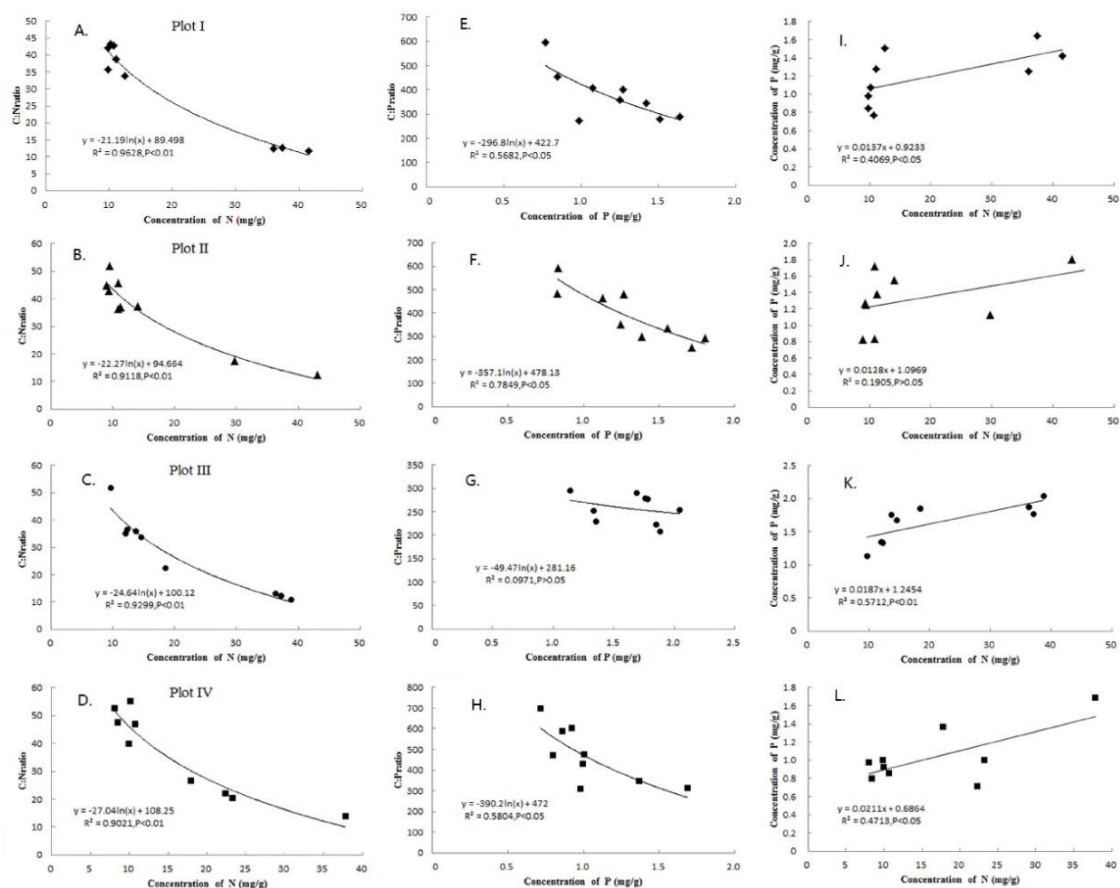


**Figure 4.** Relationship between the ratio of C:N and N concentration, between the ratio of C:P and P concentration, and between N and P concentration of *Sophora alopecuroides* in different habitats

**Table 2.** GLM analysis of habitat and organ effects on C, N, P concentrations and their stoichiometric characteristics

Independent variable	Dependent variable	Quadratic sum	DOF	Mean square	F	Significance
Organ	C	23779.651	2	11889.826	5.920	0.080
	N	3655.346	2	1827.673	52.586	0.000
	P	0.440	2	0.220	2.472	0.106
	C:N	4480.742	2	2240.371	31.678	0.000
	C:P	17117.127	2	8558.564	0.673	0.519
	N:P	1552.806	2	776.403	62.036	0.000
Plot	C	7221.278	3	2407.093	1.199	0.332
	N	169.318	3	56.439	1.624	0.210
	P	1.809	3	0.603	6.782	0.020
	C:N	452.333	3	150.778	2.132	0.123
	C:P	213173.795	3	71057.932	5.590	0.005
	N:P	113.479	3	37.826	3.022	0.049
Organ × Plot	C	8981.013	6	1496.835	0.745	0.619
	N	193.952	6	32.325	0.930	0.491
	P	0.602	6	0.100	1.129	0.376
	C:N	224.739	6	37.457	0.530	0.780
	C:P	23314.623	6	3885.770	0.306	0.928
	N:P	46.202	6	7.700	0.615	0.716

The ability of the plant to absorb nutrient and assimilate C can be expressed by C:N and C:P ratios of leaves, which reflect the productivity that can be achieved by unit nutrient supply and the utilization efficiency of the plant to absorb nutrition. The nutrient limitation of the environment on plants can be shown by the N:P ratio. In order to adapt to the changes of the environment, plants will adjust concentrations of the nutrient elements, namely the changes of stoichiometric ratios. The stoichiometric ratios form a certain feedback relationship between the environment and plants (Jiang et al., 2014; Xia et al., 2014; Carrie et al., 2015). Plant N:P ratio reflects the N and P nutrient conditions of its environment. It can judge the nutrient supply of the environment for plant growth and the growth rate of the plant (Li et al., 2012). In the extreme desert environment, the soil showed a severe N deficiency, and the concentrations of N and P and the ratio of N:P in leaves were significantly different (Tao et al., 2015). In this study, we can find that the N:P ratio of leaf was greater than that of other organs. Because of the sampling time in September, the roots and stems of plants are mature and the nitrogen and phosphorus nutrient elements are relatively stable, while the leaves of plants are in the rapid growth stage and the leaves belong to the nutritive organs. Leaves need to consume a lot of phosphorus-rich substances (DNA, ATP, etc.) to meet the needs of plant growth and reproduction process. Therefore, the ratio of N:P in leaves of the same plant is higher than that in roots and stems. The N:P ratio of leaves of herbaceous plants were much higher than that of roots (Wu et al., 2010), which was consistent with the results of this study.

### ***Stoichiometric ratio and correlation analysis of *Sophora alopecuroides* in different habitats***

The growth, development, and behavior of organisms are closely related to the concentrations of C, N, and P (Dong, 1996). The ratio of N:P in leaves can be used as an indicator to judge the nutrient supply of the environment for plant growth (Vitousek et al., 1982; Wassen et al., 1995). When leaf N:P ratio < 14, plant growth is mainly limited by N; when N:P ratio > 16, plant growth is mainly limited by P; when  $14 < \text{N:P ratio} < 16$ , plant growth is limited by N and P together (Venterink et al., 2003; Jiang et al., 2016). In this paper, N:P ratio > 16 in the leaves of *Sophora alopecuroides* in four habitats showed that the growth of *Sophora alopecuroides* was mainly limited by P, and there was no significant difference in the ratio of N:P in the leaves of *Sophora alopecuroides* in four habitats. To prevent the spread of *Sophora alopecuroides* in the pasture, it may be more effective to control the absorption of P. Correlation analysis showed that C:N and C:P ratios have negative correlation with corresponding N and P concentrations, and the logarithmic equation can reflect this changing relationship. The N and P concentrations have positive correlation and the linear equation showed this changing trend better (Fig. 4). The positive correlation between N and P reflected the relative consistency of the change of the two nutrient elements in the plant, which is a strong guarantee for the stable growth and development of the plant and also one of the most basic characteristics of the plant (Wu et al., 2010).

### ***Habitat and organ effects on C, N, P concentrations and their stoichiometric characteristics***

Stoichiometric characteristics reflect the synergistic and interactive effects of many factors. The changes of stoichiometric characteristics in plants can examine the relationship between plants and the environment and judge the structure, function and stability of the ecosystem in which plants are located (Tao et al., 2017; Gong et al., 2017). The distribution of chemical elements in plant organs is the common result of environment and phylogeny (Tang et al., 2016). In the growth stage, nutritional requirements for *Sophora alopecuroides* also increased with the improvement of the productivity level. *Sophora alopecuroides* mainly obtain C through photosynthesis of leaves, so organs have a relatively large impact on C concentration. N plays a very important role in the growth and development of plants. In this study area, the nitrogen is insufficient for the growth of *Sophora alopecuroides*, especially in the roadside habitat. Under this nutrient restriction, *Sophora alopecuroides* can gradually adapt to the change of N utilization strategy by adjusting the protein and its metabolite group in organs according to its own growth needs (Shao et al., 2013). Zheng et al. (2013) found that the adaptation mechanism of plants would change in the low-nutrient environment. This is part of survival strategy of *Sophora alopecuroides* in extreme environment. This is an important strategy of plant growth regulation and material distribution and a result of plant adaptation to the environment. In the process of natural growth, plants adapt to changes in the environment by adjusting the nutrient changes of different organs and their stoichiometric ratios (Ping et al., 2014). Therefore, organs have a greater influence on C and N concentrations and C:N and N:P ratios. The growth of *Sophora alopecuroides* requires much available P, but its transformation rate of P element is relatively lower and the external environment can provide sufficient P source for the growth of *Sophora alopecuroides*, which make its growth stable. The soil nutrients will

be reflected in plants and the external environment that affects the absorption of plant nutrients (Hu et al., 2014). Therefore, habitats have a greater influence on P concentration and C:P ratio of *Sophora alopecuroides*.

## Conclusions

The  $R_{CN}$  and  $R_{CP}$  in the profile of *Sophora alopecuroides* invasion soil changed obviously.  $R_{CN}$  showed a “ladder” decline. The maximum of  $R_{CN}$  and  $R_{CP}$  appeared in the 0-10 cm soil layer.  $R_{NP}$  did not change significantly and the maximum appeared in the 20-30 cm soil layer.  $R_{CN}$ ,  $R_{CP}$ , and  $R_{NP}$  in the profile of *Sophora alopecuroides* uninvaded soil are relatively gentle. The maximum of  $R_{CN}$  appears in the 10-20 cm soil layer. The maximum of  $R_{CP}$  appears in the 0-10 cm soil layer and the maximum of  $R_{NP}$  appears in the 30-40 cm soil layer. N:P ratios ( $R_{NP} = 1.05-1.10$ ) of the soil is far lower than the global average (13.1) (Cleveland and Liptzin, 2007) and the national average (5.2) (Tian et al., 2010). *Sophora alopecuroides* invaded and uninvaded soils were limited by N.

There are differences in the concentrations of C, N, P and their stoichiometric ratios in roots, stems and leaves differed with habitat. Only the concentration of N and ratio of N:P showed the order of leaves > stems > roots. There was a significant difference in the C concentration between root and leaf and there was a significant difference in the C concentration between root and stem in plot-IV. But there was no significant difference in other habitats. There were significant differences in the concentration of N between leaf and root and there were significant differences in the concentration of N between leaf and stem in plot-I and IV. There were significant differences in the concentration of N among the root, stem and leaf in plot-III. There was no significant difference in the concentration of N among the root, stem and leaf in plot-II. There was no significant difference in the P concentration among the root, stem and leaf in plot-IV. The C:N and N:P ratios of leaf and root were not significantly different among the four habitats. There were significant differences in the leaf and stem C:P ratios between plot-III and IV. The N:P ratio > 16 of leaves in different habitats indicated that the growth of *Sophora alopecuroides* was mainly limited by P.

Correlation analysis showed that C:N and C:P ratios of *Sophora alopecuroides* in different habitats were negatively correlated with the corresponding N and P concentrations, but there was no significant correlation between C:P ratio and P concentration in plot-III. There was a positive correlation between N and P concentration in the four plots. The results showed that the physiological activities of *Sophora alopecuroides* in different habitats were regulated by N and P.

The C, N, and P concentrations and their C:N, C:P, and N:P ratios *Sophora alopecuroides* were affected by habitat and organ. C:N ratio and N concentration are mainly affected by the organs, while the P concentration and C:P ratio are mainly affected by the habitat. This is the nutrient utilization strategy of *Sophora alopecuroides* in different habitats. *Sophora alopecuroides* adapted to the barren soil environment by N and P nutrient utilization strategy. At present, *Sophora alopecuroides* has become the dominant species of degraded pasture in the Yili valley, resulting in the decline of grassland quality and economic productivity. It is of great significance to study the changes of C, N, and P concentrations of organs in various habitats of *Sophora alopecuroides* for revealing the growth and spread process of *Sophora alopecuroides*.

**Acknowledgements.** This work was supported by the University scientific research program of Xinjiang Uygur Autonomous Region, P. R. China (XJEDU2018Y042).

## REFERENCES

- [1] Aerts, R., Chapin, S. (2000): The mineral nutrition of wild plants revisited: a re-evaluation of processes and patterns. – *Advances in Ecological Research* 30: 1-67.
- [2] Ashton, I. W., Hyatt, L. A., Howe, K. M., Gurevitch, J., Lerdau, M. T. (2005): Invasive species accelerate decomposition and litter nitrogen loss in a mixed deciduous forest. – *Ecological Applications* 15(4): 1263-1272.
- [3] Carrie, A., Deans, S. T., Behmer, A. K. (2015): The importance of dissolved N:P ratios on mayfly (*Baetis* spp.) growth in high-nutrient detritus-based streams. – *Hydrobiologia* 742: 15-26.
- [4] Cleveland, C. C., Liptzin, D. (2007): C:N:P stoichiometry in soil: is there a “Redfield ratio” for the microbial biomass? – *Biogeochemistry* 85(3): 235-252.
- [5] Dong, M. (1996): *Survey, Observation and Analysis of Terrestrial Biocommunities*. – Standards Press of China, Beijing.
- [6] Elser, J. J., Sterner, R. W., Gorokhova, E., Fagan, W. F., Markow, T. A., Cotner, J. B., Harrison, J. F., Hobbie, S. E., Odell, G. M., Weider, L. J. (2000): Biological stoichiometry from genes to ecosystems. – *Ecology Letters* 3(6): 540-550.
- [7] Gong, L., Li, H. L., Liu, Y. T., An, S. Q. (2017): Effect of nitrogen and phosphorus fertilizers on carbon, nitrogen, and phosphorus stoichiometry of oasis cotton in the upper reaches of Tarim River, Xinjiang, China. – *Acta Ecologica Sinica* 37(22): 7689-7697.
- [8] Hu, Q. W., Nie, L. Q., Zheng, Y. M., Wu, Q., Yao, B., Zheng, L. (2014): Effects of desertification intensity and stand age on leaf and soil carbon, nitrogen and phosphorus stoichiometry in *Pinus elliottii* plantation. – *Acta Ecologica Sinica* 34(9): 2246-2255.
- [9] Jiang, L. L., He, S., Wu, L. F., Yan, Y. F., Weng, S. F., Liu, J., Wang, W. Q., Zeng, C. C. (2014): Characteristics of stoichiometric homeostasis of three plant species in wetlands in Minjiang Estuary. – *Wetland Science* 12(3): 293-298.
- [10] Jiang, P. P., Cao, Y., Chen, Y. M., Wang, F. (2016): Variation of C, N, and P stoichiometry in plant tissue, litter, and soil during stand development in *Pinus tabulaeformis* plantation. – *Acta Ecologica Sinica* 36(19): 6188-6197.
- [11] Li, Y. Y., Feng, J. T., Zhang, X., Hu, L. F. (2005): Advance in research of chemical ingredients from *Sophora alopecuroides* L. and its bioactivities. – *Acta Agriculturae Boreali-occidentalis Sinica* 14(2): 133-136.
- [12] Li, Z., Han, L., Liu, Y. H., An, S. Q., Leng, X. (2012): C, N and P stoichiometric characteristics in leaves of *Suaeda salsa* during different growth phase in coastal wetlands of China. – *Chinese Journal of Plant Ecology* 36(10): 1054-1061.
- [13] Li, C. J., Xu, X. W., Sun, Y. Q., Qiu, Y. Z., Li, Y. S., Gao, P., Zhong, X. B., Yan, J., Wang, G. F. (2014): Stoichiometric characteristics of C, N, P for three desert plants leaf and soil at different habitats. – *Arid Land Geography* 37(5): 996-1004.
- [14] Liu, Y., Zhao, Y., Munir, Li, W. H. (2017): Canopy seed bank of *Sophora alopecuroides* L. in Ili River Valley. – *Chinese Journal of Ecology* 36(4): 910-915.
- [15] Lu, R. K. (1999): *Methods for Chemical Analysis of Soil Agriculture*. – China Agricultural Science and Technology Press, Beijing.
- [16] Lu, D. K., Ou, Y. Y., Deng, Y. X., Liu, B., Zhao, Y. (2011): Terrestrial biomass and reproductive allocation characteristics of *Sophora alopecuroides* L. in Ili River Valley. – *Xinjiang Agricultural Sciences* 48(7): 1333-1338.
- [17] Luo, Y., Gong, L. (2016): Stoichiometric characteristics in root, stem and leaf of *Phragmites australis* in different habitats in the southern marginal zone of Tarim Basin. – *Chinese Journal of Ecology* 35(3): 684-691.
- [18] Michaels, A. F. (2003): The ratios of life. – *Science* 300(5621): 906-907.

- [19] Ou, W. X., Yang, G., Gao, J. H. (2006): Retention effect of wetland for nitrogen and phosphorus nutrients in the coastal zone of Yancheng. – *Wetland Science* 4(3): 180-188.
- [20] Ping, C., Wang, C. K., Quan, X. K. (2014): Influence of environmental changes on stoichiometric traits of nitrogen and phosphorus for *Larix gmelinii* trees. – *Acta Ecologica Sinica* 34(8): 1966-1974.
- [21] Shang, B. Y., Yang, P., Chen, L., Gao, X. J., Yong, J. J., Zhang, X., Zhao, J. J., Wang, H. Q. (2018): Research on network pharmacology of alkaloids in *Sophora alopecuroides*. – *China Journal of Chinese Medicine* 43(1): 160-167.
- [22] Shao, X. X., Li, W. H., Wu, M., Yang, W. Y., Jiang, K. Y., Ye, X. Q. (2013): Dynamics of carbon, nitrogen and phosphorus storage of three dominant marsh plants in Hangzhou Bay coastal wetland. – *Environmental Science* 34(9): 3451-3457.
- [23] Shi, F. Y., Qiu, M. N., Li, G. Z., Zhang, G., Wu, C. C., Lu, H., Zhao, B. Y. (2019): Research progress on the resource status, chemical composition, toxicity, exploitation and utilization of *Sophora alopecuroides*. – *Heilongjiang Animal Science and Veterinary Medicine* 13: 34-38.
- [24] Tang, G. R., Zheng, G. W., Wang, X., Zhu, Y. Q. (2016): Effects of tourism disturbance on the ecological stoichiometry characteristics of C, N and P of the vegetation and soil in Kanas scenic area. – *Pratacultural Science* 36(8): 1476-1485.
- [25] Tao, Y., Zhang, Y. M. (2015): Leaf and soil stoichiometry of four herbs in the Gurbantunggut Desert, China. – *Chinese Journal of Applied Ecology* 26(3): 659-665.
- [26] Tao, W., Wu, J. W., Liu, C. F., Fang, L., Liu, Y., Yuan, J. H., Li, J. (2017): Response of stoichiometric homeostasis and allometric scaling in halophyte *Suaeda heteroptera* Kitag. to simulated nitrogen and phosphorus deposition. – *Journal of Hydroecology* 38(4): 18-26.
- [27] Tian, H. Q., Chen, G. S., Zhang, C., Melillo, J. M., Hall, C. A. S. (2010): Pattern and variation of C:N:P ratios in China's soils: a synthesis of observational data. – *Biogeochemistry* 98(1/3): 139-151.
- [28] Venterink, H. G. M. O., Wassen, M. J., Verkrout, A. W. M. (2003): Species richness-productivity patterns differ between N-, P-, K-limited wetlands. – *Ecology* 84(8): 2191-2199.
- [29] Vitousek, P. (1982): Nutrient cycling and nutrient use efficiency. – *The American Naturalist* 119: 553-572.
- [30] Wang, Z. N., Yang, H. M. (2013): Response of ecological stoichiometry of carbon, nitrogen and phosphorus in plants to abiotic environmental factors. – *Pratacultural Science* 30(6): 928-931.
- [31] Wang, W. Q., Xu, L. L., Zeng, C. S., Gong, C., Zhang, L. H. (2011): Carbon, nitrogen and phosphorus ecological stoichiometric ratios among live plant-litter-soil systems in estuarine wetland. – *Acta Ecologica Sinica* 31(23): 7119-7124.
- [32] Wassen, M. J., Olde Venterink, H. G. M., de Swart, E. O. A. M. (1995): Nutrient concentrations in mire vegetation as a measure of nutrient limitation in mire ecosystems. – *Journal of Vegetation Science* 6: 5-16.
- [33] Wu, T. G., Wu, M., Liu, L., Xiao, J. H. (2010): Seasonal variations of leaf nitrogen and phosphorus stoichiometry of three herbaceous species in Hangzhou Bay coastal wetlands, China. – *Chinese Journal of Plant Ecology* 34(1): 23-28.
- [34] Xia, C., Yu, D., Wang, Z., Xie, D. (2014): Stoichiometry patterns of leaf carbon, nitrogen and phosphorus in aquatic macrophytes in eastern China. – *Ecological Engineering* 70: 406-413.
- [35] Xiao, Y., Tao, Y., Zhang, Y. M. (2014): Biomass allocation and leaf stoichiometric characteristics in four desert herbaceous plants during different growth periods in the Gurbantunggüt Desert, China. – *Chinese Journal of Plant Ecology* 38(9): 920-940.
- [36] Yang, J. X., Yu, F. (1998): Advance on *Sophora alopecuroides*. – *Tian Jin Pharmacy* 10(1): 43-46.

- [37] Yu, H. L., Li, Y. Z., Fan, J. W., Zhong, H. P. (2016): Leaf N and P contents of different functional groups in relation to precipitation and temperature in China Grassland Transect. – Chinese Journal of Ecology 35(11): 2867-2874.
- [38] Zeng, D. P., Jiang, L. L., Zeng, C. C., Wang, W. Q., Wang, C. (2013): Reviews on the ecological stoichiometry characteristics and its applications. – Acta Ecologica Sinica 33(18): 5484-5492.
- [39] Zhao, Y. F., Xu, F. L., Wang, W. L., Wang, L. L., Wang, G. X., Sun, Y. P., Bai, X. F. (2014): Seasonal Variation in Contents of C, N and P and Stoichiometry Characteristics in Fine Roots, Stems and Needles of *Larix principis-rupprechtii*. – Chinese Bulletin of Botany 49(5): 560-568.
- [40] Zheng, Y. M., Yao, B., Wu, Q., Hu, B. H., Hu, Q. W. (2013): Dynamics of leaf carbon, nitrogen and phosphorus of two dominant species in a Poyang Lake wetland. – Acta Ecologica Sinica 33(20): 6488-6496.



## EFFECTS OF HUMIC ACID AND IRON APPLICATIONS ON THE YIELD, SOME PLANT CHARACTERISTICS AND OIL RATIO OF SAFFLOWER (*Carthamus tinctorius* L.)

BEYYAVAS, V. – HALILOGLU, H.\*

*Department of Field Crops, Faculty of Agriculture, Harran University, Osmanbey Campus, Sanliurfa 63050, Turkey*

\*Corresponding author

*e-mail: haliloglu@harran.edu.tr; phone: +90-530-205-0794*

(Received 10<sup>th</sup> Aug 2020; accepted 19<sup>th</sup> Nov 2020)

**Abstract.** This study was conducted to determine the effects of humic acid and iron applications on seed yield, some plant characteristics and oil ratio of Remzibey-05 safflower cultivar under Harran Plain conditions in the 2011-2012 and 2012-2013 growing seasons. The experiment was carried out in randomized complete block split plots design with three replications. The main plots were humic acid (HA) applications (0, 60 g ha<sup>-1</sup>, 120 g ha<sup>-1</sup>, 180 g ha<sup>-1</sup>), and the sub-plots were iron (Fe) applications (0, 12.5 kg ha<sup>-1</sup>, 25 kg ha<sup>-1</sup> and 37.5 kg ha<sup>-1</sup>). Humic acid was sprayed onto the leaves and iron was applied to the soil when the plants were leading the stage of 4-5 leaves. The highest seed yield, number of heads per plant and dry petal yield per plant were obtained from 120 g ha<sup>-1</sup> humic acid and 12.5 kg ha<sup>-1</sup> Fe applications. The highest number of seeds per head was obtained from 180 g ha<sup>-1</sup> HA and 12.5 kg ha<sup>-1</sup> Fe applications while biomass yield was from 60 g ha<sup>-1</sup> HA and 25 kg ha<sup>-1</sup> Fe applications. In conclusion; 120 g ha<sup>-1</sup> humic acid and 12.5 kg ha<sup>-1</sup> Fe should be applied to increase seed yield, number of heads per plant and dry petal yield per plant in safflower agriculture under semi-arid climate conditions.

**Keywords:** *semi-arid, carthamus, spiny, hoeing, dry petal*

### Introduction and literature review

Safflower is a multipurpose oil seed crop that can be used for cooking as vegetable oil, cut flower, forage crop for both forage and animal feeding, industrial crop for dye production and medicinal crop. Safflower is tolerant to drought, heat, cold and saline conditions (Emongor and Oagile, 2017). It is well adapted to dry regions and easy to cultivate. It is extremely effective in reaching moisture and nutrients that are difficult to obtain and are otherwise in limited supply due to the its taproot. This contributes to the improvement to the structure of soil, including the formation of organic matter and the improvement of soil structure and the promotion of water leakage. These features make safflower plant an excellent rotation crop in many regions (Anonymous, 2016).

Safflower is an annual herbaceous plant which is grown commercially to obtain vegetable oil. It was initially cultivated to get dye from its flowers. It was traditionally grown for its seeds and also used for dyeing of fabrics with some foodstuffs. Red and yellow dyes are obtained from safflower. Extracts of the plant are also used to make medicines. Oil has been commercially extracted from safflower seeds in recent years (Anonymous, 2019).

Dried petals are used to extract natural dyes from plants that are important nowadays due to their natural contents and fashion trends. The colored material in safflower is Carthamine that based on benzoquinone (Garcia, 2009). Flavonoid type dye exists in safflower plant. Cotton, wool and other hydrophilic fibers can be colored directly with safflower dye (Badiger et al., 2009). The water-soluble yellow dye (carthamidin) and

the insoluble red dye (carthamine) are used in the carpet-weaving industry in Eastern Europe and Indian subcontinent (Weiss, 1983).

Safflower plants have yellow, orange or red flowers, height between 30 and 210 cm and roots that can go down to 2-3 m (Emongor and Oagile, 2017). Each branch of the plant produces 1 to 5 heads and 15 to 20 seeds per head. Seed oil ratio is between 25-45 and 90% of this oil is oleic and linoleic acid (Baydar and Erbas, 2016). Safflower oils containing high percentage of linoleic acid are used in the production of paints, varnishes, printing inks, protective acrylic resins and soap industry with their excellent drying properties (Corleto et al., 1997).

The remaining cake after safflower oil was extracted is a good feed source in animal husbandry with a content of up to 25% crude protein (Weiss, 2000). In addition, safflower seeds are used as bird feed. The importance of safflower seed as oilseed product has increased in recent years especially with the increasing interest in biofuel production (Lakzayi and Sabbagh, 2015; Hussain et al., 2015). Safflower production in the world is about 718.161 tons. The countries producing the most safflower is Kazakhstan (174.900 tons), India (109.000 tons) and USA (95.360 tons). Turkey is an important country at the sixth rank with 45.000 tons (Anonymous, 2019). The growth and effectiveness of the safflower (*Carthamus tinctorius* L.) plant is affected by genotype, environment and agricultural practices (Koutroubas et al., 2009).

Growth, development and yield of the plant are under the influence of biotic and abiotic conditions that make up the environmental factors together with the genetic potential of the plant (Kaleem et al., 2010). Fertilization, which is one of the abiotic conditions, is one of the factors that have a significant effect on yield and yield components. For years, it has been tried to increase the yield in agricultural areas with inorganic fertilizer applications. However, it has long been overlooked that organic matter is needed in the soil for these fertilizers to be effective.

The most economical and rapid solutions to the organic matter problem is to apply humic or fulvic acid directly to soil or plant. As a plant biostimulants, humic and fulvic acids are produced mainly by biological degradation of plant organic matter containing lignin (Malan, 2015). The favorable effects of organic regulators or plant biostimulants based on humic substances are an alternative method for production and protection of soil fertility (Canellas et al., 2015).

Humic acids remain in the soil for a long time and decompose gradually over time. With the application of humic acid, the aeration of the soil and water retention, the development and proliferation of soil microorganisms are provided, the resistance of plants to stress conditions, diseases and pests are increased (Icel, 2005). Humic acid applications are effective on seed yield, oil and protein ratio along with plant characteristics; iron applications are effective on oil yield, seed quality and resistance to drought conditions; in humic x Fe form interaction, especially Fe-EDDHA with humic acid application was reported positive effects on plant development, microelements level and other properties (Korkmaz, 2000). It was reported that fulvic acid (1 kg ha<sup>-1</sup>) application on the leaves increased seed yield by 6.02% and oil yield by 85.67% (Moradi et al., 2017).

Iron by biosynthetic ways is required in a few steps. However, iron deficiency can restrain cell number and its size, cell cleavage, leaf growth, and contents of chlorophyll, protein, starch and sugar. Consequently, reduce the plant's fresh and dry weights (Marschner, 1995). Iron (Fe) is a cofactor for approximately 140 enzymes that catalyze

unique biochemical reactions (Brittenham, 1994). The stimulatory effect of zinc and/or iron was recorded by Pande et al. (2007) and Said-Al et al. (2009).

Safflower has a great potential for dry farmland of southeastern region of Turkey in dry years due to obtaining satisfy yield and high revenue of by-products. Especially the petals used as food color and spices have the potential to increase the income of farmers in arid agricultural areas (Esendal, 2001). However, depending on the climatic conditions and varieties, seed yields vary according to regions.

This study was conducted to determine the effects of humic acid and iron doses on seed yield and some plant characteristics of safflower plant and to help in future studies.

## Materials and methods

### Fields studies

This trial was carried out in a randomized complete split plots design with three replications at Eyyubiye campus experimental area, Agricultural Faculty, Harran University (37° 07'12" N 38° 49'14.91" E) (altitude = 510 m from sea level) during 2011-2012 and 2012-2013 growing seasons in the Sanliurfa, Turkey (Figures 1 and 2).



Figure 1. The political map of the Turkey



Figure 2. The map of the experimental area

Variety recommended for the region, Remzibey-05 (spiny) cultivar with yellow flower and head was used as plant material. Experimental area had been ploughed, herbicide (*Trifluarin* active ingredient) was applied by a sprayer before sowing. Then, disc-harrow was practiced for seedbed preparation. The seeds were sown by the experimental driller on 5<sup>th</sup> November, 2011 and 3<sup>th</sup> November, 2012. 2 m space was left between each plot.

Each plot consisted of 6 rows with 5 m long. Inter-row and intra-row spaces were 35 and 15 cm respectively. 100 kg ha<sup>-1</sup> of pure N and 80 kg ha<sup>-1</sup> of pure P<sub>2</sub>O<sub>5</sub> phosphorus fertilizer were applied. Half of the nitrogen (20.20.0) was applied as basal fertilizer and the remaining half (Ammonium Nitrate 33%) was applied as top fertilizer at the branching period.

Humic acid doses formed the main plots (HA<sub>0</sub>: Control, HA<sub>1</sub>: 60 g ha<sup>-1</sup>, HA<sub>2</sub>: 120 g ha<sup>-1</sup> and HA<sub>3</sub>: 180 g ha<sup>-1</sup>). Thinning was practiced in the stages of 3 or 4 leaves. In the period when the plants were 4-5 leaves, humic acid which is in the commercial name “Delta plus + 15”, whose active ingredient is 150 g/L humic acid + 30 g/L potassium oxide, was applied to the leaves at once. Iron doses formed the sub-plots (Fe<sub>0</sub>: Control, Fe<sub>1</sub>: 12.5 kg ha<sup>-1</sup>, Fe<sub>2</sub>: 25 kg ha<sup>-1</sup> and Fe<sub>3</sub>: 37.5 kg ha<sup>-1</sup>) and which is in the commercial name “Ferri Iron Sulphate (Fe<sub>2</sub> (SO<sub>4</sub>) 4H<sub>2</sub>O)” containing 23% iron was applied 5-6 cm next to the rows of the plant and 5-6 cm in depth by hand.

In the trial area shown in *Figure 3*, hoeing, weed and pest control were practised conventionally and harvests were done on 7 June in 2012, 8 June in 2013. 0.5 m of sides effect were discarded at the beginning and end of the 2 rows in the middle of each plot, and the seed and biomass yield (kg ha<sup>-1</sup>) were determined by hand over the remaining area (4 m x 0.7 m = 2.8 m<sup>2</sup>). Plant height (cm), number of heads per plant, number of seeds per head, 1000 seed weight (g) and dry petal yield (g plant<sup>-1</sup>) were determined on randomly selected and cutted 10 plants at the ground level (Esendal et al., 1992).



*Figure 3. Experimental area*

### ***Soil analysis***

The trial area possesses a low slope topography. The physical and chemical properties of the soil were specified before sowing. Trial area has good drainage, deep profile and stone-free. Clay ratio, salt content, pH degree and organic matter level were designated as 53%, 0.090%, 7.5, and 1.21%, respectively. In addition, the amount of pure N of 23 kg ha<sup>-1</sup>, P<sub>2</sub>O<sub>5</sub> of 31 kg ha<sup>-1</sup> and K<sub>2</sub>O of 1106 kg ha<sup>-1</sup> were determined (Anonymous, 2011).

### Oil ratio

For each application 10 g of seeds were grounded and dried in an oven at 70 °C for 72 hours. 5 g of each dried sample was taken and boiled for 6 hours using n-hexane in the Soxhlet device and oil ratios (%) were determined (Bilsborrow et al., 1993).

### Meteorological data

Meteorological datas were taken from the meteorology station, located approximately 3 km from the area where the research was established.

The amount of rainfall close to each other in both years. The average temperature was near to the average of long years (13.68 °C) in the 2011-2012 (13.76 °C), but the average temperature was observed higher than first year and long years in the 2012-2013 (15.31 °C) (Table 1). In the second year of the experiment, the average temperature and especially the higher amount of rainfall in May may have encouraged the plants to develop better.

**Table 1.** Meteorological data from trial seasons and average of long years

Months	2011-2012			2012-2013			1929-2013
	Average Monthly Temp. (°C)	Precipitation (kg m <sup>-2</sup> )	Average Relative Humidity (%)	Average Monthly Temp. (°C)	Precipitation (kg m <sup>-2</sup> )	Average Relative Humidity (%)	Average of Long-term (°C)
November	9.4	62.1	53.7	14.9	68.4	65.6	12.9
December	7.4	47.1	57.4	8.3	142.8	73.0	7.5
January	5.5	170.9	81.0	6.8	86.8	69.5	5.4
February	5.8	95.8	57.0	9.3	107.2	73.6	6.8
March	9.7	35.8	47.3	12.9	12.1	-	10.7
April	19.3	23.3	42.4	18.4	18.0	44.9	16.0
May	22.4	42.3	40.8	22.9	56.2	43.4	22.1
June	30.6	5.8	21.2	29.0	-	24.0	28.0
Average	13.76		50.1	15.31		49.25	13.68
Total		483.1			491.5		

Anonymous, 2013

### Statistical analysis

Data were analyzed in the statistical program of JMP 13.2.0 (SAS institute) according to randomized blocks design of humic acid and iron applications, and humic acid x iron interactions were analyzed according to randomized blocks split plots design. The means were grouped according to Tukey-HSD Multiple Comparison Test (P = 0.05). Relationship between each parameter was determined by Pearson correlation analysis.

### Results and discussion

As a result of the combined years analysis (ANOVA), there was a statistically significant difference between the years in terms of characteristics examined, and the data of each year were analyzed separately (Tables 2 and 3).

**Table 2.** Data of seed yield (kg ha<sup>-1</sup>), plant height (cm), number of heads per plant and number of seeds per head examined during the trial years

	Seed Yield (kg ha <sup>-1</sup> )		Plant Height (cm)		Number of heads per plant		Number of seeds per head	
	2011-12	2012-13	2011-12	2012-13	2011-12	2012-13	2011-12	2012-13
HA <sub>0</sub>	836.1 <sup>c†</sup>	1549.8 <sup>c†</sup>	131.90 <sup>ns</sup>	137.23 <sup>b†</sup>	10.50 <sup>b†</sup>	16.97 <sup>b†</sup>	12.41 <sup>b†</sup>	10.17 <sup>b†</sup>
HA <sub>1</sub>	1104.5 <sup>b</sup>	1334.1 <sup>d</sup>	127.83	140.63 <sup>a</sup>	13.10 <sup>a</sup>	14.97 <sup>c</sup>	14.67 <sup>a</sup>	5.92 <sup>d</sup>
HA <sub>2</sub>	1192.6 <sup>a</sup>	1946.7 <sup>a</sup>	128.70	139.23 <sup>ab</sup>	13.00 <sup>a</sup>	21.50 <sup>a</sup>	12.81 <sup>b</sup>	7.46 <sup>c</sup>
HA <sub>3</sub>	1062.6 <sup>b</sup>	1695.7 <sup>b</sup>	127.83	141.03 <sup>a</sup>	12.23 <sup>a</sup>	16.73 <sup>b</sup>	15.80 <sup>a</sup>	12.01 <sup>a</sup>
CV %	2.30	1.67	1.41	8.39	2.92	3.26	3.42	1.55
Fe <sub>0</sub>	836.1 <sup>d†</sup>	1549.8 <sup>b†</sup>	131.90 <sup>ns</sup>	137.23 <sup>c†</sup>	13.60 <sup>b†</sup>	16.97 <sup>b†</sup>	12.91 <sup>b†</sup>	10.17 <sup>c†</sup>
Fe <sub>1</sub>	1353.3 <sup>a</sup>	2040.7 <sup>a</sup>	131.83	140.43 <sup>ab</sup>	16.13 <sup>a</sup>	18.80 <sup>a</sup>	15.80 <sup>a</sup>	17.30 <sup>a</sup>
Fe <sub>2</sub>	1086.4 <sup>b</sup>	1534.4 <sup>b</sup>	129.87	139.90 <sup>bc</sup>	12.77 <sup>b</sup>	18.93 <sup>a</sup>	15.60 <sup>a</sup>	10.86 <sup>c</sup>
Fe <sub>3</sub>	919.1 <sup>c</sup>	1467.2 <sup>b</sup>	129.23	143.23 <sup>a</sup>	10.50 <sup>c</sup>	18.70 <sup>a</sup>	14.02 <sup>b</sup>	14.84 <sup>b</sup>
CV %	1.97	1.77	2.18	0.71	3.06	2.31	3.41	2.75
<b>Interactions</b>	<b>F Values</b>							
HA	119.03 <sup>**</sup>	268.08 <sup>**</sup>	3.39 <sup>ns</sup>	6.46 <sup>*</sup>	34.05 <sup>**</sup>	70.97 <sup>**</sup>	33.37 <sup>**</sup>	1172.78 <sup>**</sup>
Fe	366.57 <sup>**</sup>	243.84 <sup>**</sup>	0.69 <sup>ns</sup>	18.25 <sup>**</sup>	98.54 <sup>**</sup>	14.35 <sup>**</sup>	22.82 <sup>**</sup>	254.50 <sup>**</sup>
HA x Fe	78.90 <sup>**</sup>	77.63 <sup>**</sup>	5.87 <sup>**</sup>	9.59 <sup>**</sup>	78.26 <sup>**</sup>	62.53 <sup>**</sup>	18.05 <sup>**</sup>	38.05 <sup>**</sup>

Abbreviations used in the table: <sup>†</sup>Means that do not share a letter are significantly different, \*:(p≤0.05), \*\*: (p≤0.01), ns: non-significant, HA: Humic Acid, Fe: Iron, CV: Coefficient of variations

**Table 3.** Data of 1000 seed weight (g), oil ratio (%), dry petal yield per plant (g) and biomass yield kg ha<sup>-1</sup>) examined in the trial years

	1000 Seed Weight (g)		Oil Ratio (%)		Dry Petal Yield Per Plant (g)		Biomass Yield (kg ha <sup>-1</sup> )	
	2011-12	2012-13	2011-12	2012-13	2011-12	2012-13	2011-12	2012-13
HA <sub>0</sub>	28.03 <sup>ns</sup>	28.46 <sup>ns</sup>	30.07 <sup>ns</sup>	30.27 <sup>ns</sup>	0.81 <sup>c†</sup>	1.04 <sup>d†</sup>	5500.0 <sup>ab†</sup>	7686.7 <sup>b†</sup>
HA <sub>1</sub>	29.40	27.92	29.67	30.27	0.95 <sup>ab</sup>	1.25 <sup>c</sup>	5666.7 <sup>a</sup>	9333.3 <sup>a</sup>
HA <sub>2</sub>	28.47	28.62	30.20	30.80	1.05 <sup>a</sup>	1.73 <sup>a</sup>	5200.0 <sup>bc</sup>	7570.0 <sup>b</sup>
HA <sub>3</sub>	28.65	28.70	29.27	30.13	0.92 <sup>bc</sup>	1.46 <sup>b</sup>	5066.7 <sup>c</sup>	7980.0 <sup>b</sup>
CV %	1.96	2.66	1.64	1.80	4.51	1.46	2.04	4.40
Fe <sub>0</sub>	27.17 <sup>c†</sup>	28.46 <sup>ns</sup>	30.07 <sup>ns</sup>	30.27 <sup>ab†</sup>	0.81 <sup>b†</sup>	1.04 <sup>d†</sup>	5500.0 <sup>d†</sup>	7686.7 <sup>b†</sup>
Fe <sub>1</sub>	28.13 <sup>b</sup>	30.22	30.33	31.73 <sup>a</sup>	1.12 <sup>a</sup>	1.15 <sup>c</sup>	6033.3 <sup>c</sup>	9010.0 <sup>a</sup>
Fe <sub>2</sub>	29.87 <sup>a</sup>	30.76	30.54	30.60 <sup>ab</sup>	0.84 <sup>b</sup>	1.82 <sup>a</sup>	6933.3 <sup>a</sup>	8606.7 <sup>a</sup>
Fe <sub>3</sub>	28.03 <sup>b</sup>	31.05	29.73	29.80 <sup>b</sup>	0.82 <sup>b</sup>	1.43 <sup>b</sup>	6500.0 <sup>b</sup>	8966.7 <sup>a</sup>
CV %	0.82	3.25	1.57	1.77	3.77	1.74	2.09	2.83
<b>Interactions</b>	<b>F Values</b>							
HA	3.11 <sup>ns</sup>	0.64 <sup>ns</sup>	2.22 <sup>ns</sup>	0.88 <sup>ns</sup>	17.04 <sup>**</sup>	643.28 <sup>**</sup>	18.86 <sup>**</sup>	15.43 <sup>**</sup>
Fe	70.49 <sup>**</sup>	4.21 <sup>ns</sup>	1.63 <sup>ns</sup>	6.97 <sup>*</sup>	58.57 <sup>**</sup>	654.16 <sup>**</sup>	67.20 <sup>**</sup>	19.21 <sup>**</sup>
HA x Fe	13.57 <sup>**</sup>	3.32 <sup>**</sup>	3.84 <sup>**</sup>	3.17 <sup>*</sup>	8.50 <sup>**</sup>	658.56 <sup>**</sup>	33.18 <sup>**</sup>	4.88 <sup>**</sup>

Abbreviations used in the table: <sup>†</sup>Means that do not share a letter are significantly different, \*:(p≤0.05), \*\*: (p≤0.01), ns: non-significant, HA: Humic Acid, Fe: Iron, CV: Coefficient of variations

### ***Seed yield (kg ha<sup>-1</sup>)***

In both years of the experiment, H<sub>2</sub> (1192.6 kg ha<sup>-1</sup> and 1946.7 kg ha<sup>-1</sup>) application in terms of humic acid application, Fe<sub>1</sub> (1353.3 kg ha<sup>-1</sup> and 2040.7 kg ha<sup>-1</sup>) application in terms of iron application gave the highest seed yield. There were statistically significant ( $p \leq 0.01$ ) differences between humic acid, iron and HA x Fe interactions (*Table 2*). This showed that both humic acid and iron applications were important to increase seed yield of safflower.

Resulting that 120 g ha<sup>-1</sup> was recommended for humic acid applications and 12.5 kg ha<sup>-1</sup> for iron applications. Vaughan and Linehan (1976) postulated that the effect of humic acid on plant growth can be made directly by the use of iron exchanged, and indirect effects of these hormones by the end of increased of microbial activity while Lobartini et al. (1997) reported that soil humic substances increase the fertility of the soil by directly stimulating the metabolic and physiological events in plants and indirectly affecting the physical, chemical and biological properties of the soil.

Moreover, a reliable environment can be created by the use of humic acid that providing the structural development of soils regarding plant production and more environmentally efficient soil (Yilmaz and Alagoz, 2001). Fe element increases of plant photosynthesis and roots growth that lead to net photosynthesis and improved seed yield (Lewis and McFarlane, 1986). Similar results suggested by Movahhedy-Dehnavy et al. (2009), Moradi et al. (2017) and Ekin (2020) that humic acid applications increase seed yield of safflower.

The higher yield in the second year of the research may have been seen due to the amount of rainfall in different growth stages of the plants. When *Table 1* is examined, the plant growth was better and vegetatively more strong in the second year, as a result of the more rainfall in November and December compared to the first year, and more rainfall in May compared to the first year caused larger and round grains.

### ***Plant height (cm)***

Plant height varied from 127.83 to 143.03 cm in both experiment years. In the first year of the experiment, there was no statistically significant difference between humic acid and iron applications. In the second year of the experiment, there were statistically significant differences between humic acid ( $p \leq 0.05$ ) and iron doses ( $p \leq 0.01$ ), and there were significant differences between HAxFe interactions ( $p \leq 0.01$ ) in both years (*Table 2*).

However, in the second year HA<sub>1</sub> (140.63 cm) and HA<sub>3</sub> (141.03 cm) applications and Fe<sub>3</sub> (143.23 cm) applications resulted the highest plant height values as reported by Gursoy et al. (2017) and Sahan (2019).

### ***Number of heads per plant***

The most important selection criterion that determines seed yield for safflower plant is the number of heads per plant. In modern safflower varieties, well-developed 12-14 heads are sufficient (Weiss, 2000). Although it is highly affected by environmental conditions (especially sowing density), it is one of the defining characteristics of high yielding safflower varieties. Biological, physical and chemical properties of the soil are affected positively by humic acid application. Fe is a basic element for plant growth, chlorophyll production disorders can be seen in the deficient of Fe. First symptoms of



Fe chlorosis appear in young tissues due to its substitution within the plant body (Rashno et al., 2013).

Statistically significant differences were obtained between humic acid, iron and HAXFe interactions in terms of number of heads per plant during the experiment years. The highest number of heads per plant was obtained from HA<sub>2</sub> (13.00 and 25.00 per plant) and Fe<sub>1</sub> (16.13 and 18.80 per plant) applications in both years. According to the two-year results, 120 g ha<sup>-1</sup> humic acid and 12.5 kg ha<sup>-1</sup> Fe applications yielded the highest number of heads per plant.

This situation revealed that humic acid and iron applications had significant effects on the number of heads per plant. 120 g ha<sup>-1</sup> humic acid and 12.5 kg ha<sup>-1</sup> iron may be recommended for safflower farming to increase number of heads per plant. Karimi et al. (2016), Mehraban and Miri (2017) reported that the application of humic acid increases the number of heads. Rahimi et al. (2016) indicated that humic acid applications has positive effect on heads per plant therefore the seed number increased. In other word, using humic acid appropriate levels provide better nutrient and water uptake and plant photosynthesis through improving roots ~~expansion~~ development.

### ***Number of seeds per head***

Number of seeds per head is an important yield criterion as the number of heads per plant. The number of seeds per head is directly related to the size of the head. Although an average of approximately 100 flowers occur on the safflower head, 20% of these flowers form seeds on average (Baydar, 2000). In our study, statistically significant differences were found between humic acid, iron and HAXFe interactions in terms of number of seeds per head. HA<sub>1</sub> (14.67 per head) and HA<sub>3</sub> (15.80 per head) applications in the first year of the experiment, HA<sub>3</sub> (12.01 per head) applications in the second year, Fe<sub>1</sub> (15.80 and 17.30 per head) application in terms of Fe applications in both years gave the highest number of seeds per head. The fact that humic acid applications gave different results in both years might be affected from the different environmental and climatic factors during the experiment years.

Increasing of yield components might have been observed due to the positive effects of micronutrient applications on activation of photosynthetic enzymes, chlorophyll formation and plant growth and development (Movahhedy-Dehnavy et al., 2009).

Ekin (2020) indicated that the application of humic acid increases the number of seeds per head is consistent with our results.

### ***1000 seed weight (g)***

Another third important selection criterion that determines seed yield for safflower is 1000 seed weight. Humic acid applications on 1000 seed weight did not have any statistically significant effect in the two years of experiment and iron applications in the first year of experiment. However, statistically significant differences were observed between HAXFe interactions in both years. When evaluated as a whole, it can be said that humic acid and iron applications did not have any effect on 1000 seed weight when given separately but interaction was important when given together.

However, contrary to our findings, Karimi et al. (2016), Mehraban and Miri (2017), Moradi et al. (2017) and Ekin (2020) stated that humic acid applications positively affect 1000 seed weight. Differences between the studies may have resulted from the difference of cultivars and soil-environmental factors.



### ***Oil ratio (%)***

The most important quality criterion for safflower plant is the oil ratio of the seed. Oil ratio ranged from 29.67% to 31.73%. Humic acid applications did not have a statistically significant effect on oil ratio in the two years of the experiment and iron applications in the second year. Significant differences were observed between HAXFe interactions in both years.

In general, humic acid and iron applications did not have any effect on oil ratio when given separately, but interaction was important when given together (*Table 3*). Movahhedy-Dehnavy et al. (2009) stated that Fe applications increased the quality criteria of safflower, and Darinkaboud and Asl (2016), Karimi et al. (2016) stated that humic acid application increased the oil ratio that are incompatible with our results. This difference may be due to differences of experiment locations, variety used and environmental factors.

### ***Biomass yield (kg ha<sup>-1</sup>)***

Significant differences were found between humic acid, iron and humic acid x iron interactions in both years of the experiment. Among the humic acid applications, HA<sub>1</sub> application (5666.7 kg ha<sup>-1</sup> and 9333.3 kg ha<sup>-1</sup>) resulted the highest biomass yield for each year. In iron applications, Fe<sub>2</sub> application (6933.3 kg ha<sup>-1</sup> and 8606.7 kg ha<sup>-1</sup>) was in the first group statistically in both years of the experiment. Mustin (1987) reported that humic acid reduces the transpiration required for the production of unit dry matter by reducing plant water consumption, by changing the cell permeability of the root increase both selectivity and the absorption of minerals and water, and also reported that due to its effect on photosynthesis and carbohydrate metabolism the mineral substance consumption is lessened.

Biomass increased proportionally with fertilizer variant (Burzo et al., 1999; Haghghati, 2010). Micronutrients are critical for plants owing to increase leaf area index and correspondingly light absorption, dry matter accumulation and economic yield (Ravi et al., 2008). Galavi et al. (2012), informed that the application of foliar iron significantly increased the biological yield compared to the control is consistent with our study. Favorable effect of micronutrient elements on biological yield of safflower has been reported by Movahhedy-Dehnavy et al. (2009). Basalma (2015) stated that application of 60 and 120 g of seed humic acid per 100 kg have favorable effects on seedling growth and safflower seed germination when applied before sowing. Galavi et al. (2012) stated that foliar iron application increases biological yield by 80%.

### ***Dry petal yield per plant (g)***

Regarding dry petal yield per plant, significant differences were found between humic acid, iron and humic acid x iron interactions in both years of the experiment. Dry petal yields varied between 0.81 g and 1.182 g between applications. Among the humic acid applications, HA<sub>2</sub> application (1.05 g and 1.73 g) gave the best results in both years of the experiment. In iron applications, Fe<sub>1</sub> application (1.12 g) in the first year and Fe<sub>2</sub> application (1.82 g) in the second year formed the highest values.

Movahhedy-Dehnavy et al. (2009) indicated that Fe applications increased the quality criteria of safflower is consistent with our study.

### ***Correlation coefficients between characteristics examined***

When the correlation coefficients of humic acid and iron applications were analyzed according to the combined years analysis; significant and positive relationships were determined between seed yield and number of heads per plant (0.535 \*\*), 1000 seed weight (0.258 \*\*), oil ratio (0.289 \*\*), biomass yield (0.499 \*\*), dry petal yield per plant (0.700 \*\*); and between plant height and 1000 seed weight (0.336 \*\*); and between number of heads per plant and 1000 seed weight (0.269 \*\*), oil ratio (0.379 \*\*), biomass yield (0.700 \*\*), dry petal yield per plant (0.607 \*\*); and between 1000 seed weight and biomass yield (0.249 \*\*), dry petal yield per plant (0.254 \*\*); and between oil ratio and biomass yield (0.260 \*), dry petal yield per plant (0.333 \*\*); and between biomass yield and dry petal yield per plant (0.573 \*\*) (*Table 4*).

***Table 4. Correlation coefficients of examined properties***

	Seed Yield	Plant Height	Number of Heads Per Plant	Number of Seeds Per Plant	1000 Seed Weight	Oil Ratio	Biomass Yield	Dry Petal Yield Per Plant
<b>Seed Yield</b>	1.000							
<b>Plant Height</b>	0.116	1.000						
<b>Number of Head Per Plant</b>	0.535**	0.012	1.000					
<b>Number of Seed Per Plant</b>	-0.311**	-0.098	-0.881**	1.000				
<b>1000 Seed Weight</b>	0.258*	0.336**	0.269**	-0.250*	1.000			
<b>Oil Ratio</b>	0.289**	0.027	0.379**	-0.406**	0.196	1.000		
<b>Biomass</b>	0.499**	-0.055	0.700**	-0.606**	0.249*	0.260**	1.000	
<b>Dry Petal Yield Per Plant</b>	0.700**	0.144	0.607**	-0.533**	0.254*	0.333**	0.573**	1.000

Abbreviations used in the table: \*\*:  $p \leq 0.01$ , \*:  $p \leq 0.05$

Knowledge on the relationship between yield and plant characteristics for safflower plays a key role in the success of breeding studies.

The relationships between seed yield and number of head per plant, 1000 seed weight, oil ratio and dry petal yield per plant should be taken into consideration in the breeding studies, which to be carried out.

### **Conclusion**

Despite its versatility usage possibilities, safflower has not yet achieved the value it deserves. It is a very important product especially due to the high nutritional value of its dried flower and oil, and usage in pharmacological and medical, industrial, textile, food, animal feeding. For this reason, neglected and underused and high economic value of this plant deserves sufficient scientific studies and promotion should be done.

As a result of this study, the highest seed yield, number of heads, petal flower yield was obtained from H<sub>2</sub> (120 g ha<sup>-1</sup>) and Fe<sub>1</sub> (12.5 kg ha<sup>-1</sup>) applications, the number of seeds per head from H<sub>3</sub> (180 g ha<sup>-1</sup>) and Fe<sub>1</sub> (12.5 kg ha<sup>-1</sup>) applications, biomass yield from H<sub>1</sub> (60 g ha<sup>-1</sup>) and Fe<sub>2</sub> (25 kg ha<sup>-1</sup>) applications. Humic acid treatments had no significant effect on 1000 seed weight and oil ratio. The effect of iron applications varied according to years.

Generally, safflower producers apply little or no humic acid and iron outside of conventional fertilization programs.

Therefore, it was concluded that 120 g ha<sup>-1</sup> of humic acid and 12.5 kg ha<sup>-1</sup> of iron should be applied to increase seed yield, number of tables heads and petal flower yield in safflower cultivation to be carried out under semi-arid climate conditions.

**Acknowledgements.** This study was financially supported by the Harran University Scientific Research Board (HÜBAK Project No: 0984).

## REFERENCES

- [1] Anonymous (2011): GAP Agricultural Research Institute. – Sanliurfa, Turkey.
- [2] Anonymous (2013): Meteorological data obtained from Sanliurfa Meteorological Station. – Sanliurfa, Turkey.
- [3] Anonymous (2016): A crop profile for safflower production in California. – March 2016.
- [4] Anonymous (2019): Uses of Safflower. – <https://www.worldatlas.com/articles/world-s-top-safflower-producing-countries.html> (Date of access: 29.07.2019).
- [5] Badiger, P. K., Rudranaik, V., Parameshwarappa, K. G., Patil, M. S. (2009): Genotype x environmental interactions and stability analysis of non-spiny breeding lines in safflower. – Karnataka J. Agric. Sci. 22(5): 978-981.
- [6] Basalma, D. (2015): Effects of humic acid on the emergence and seedling growth of safflower varieties (*Carthamus tinctorius* L.). – Turkish Journal of Agricultural and Natural Sciences 2(2): 152-156.
- [7] Baydar, H. (2000): Effects of gibberellic acid on male sterility, seed yield and oil and fatty acid syntheses of safflower (*Carthamus tinctorius* L.). – Turkish Journal of Biology 24: 159-168.
- [8] Baydar, H., Erbas, S. (2016): Line development breeding for high yield, oil and oleic acid content in safflower (*Carthamus tinctorius* L.). – Journal of Field Crops Central Research Institute 25(2): 155-161.
- [9] Bilsborrow, P. E., Evans, E. J., Murray, F., Zhao, F. J. (1993): Glucosinolate changes in developing pods of single and double low varieties of autumn sown oilseed rape (*Brassica napus* L.). – Ann. App. Biol. 122: 135-143.
- [10] Brittenham, G. M. (1994): New advances in iron metabolism, iron deficiency and iron overload. – Current Opinion in Hematology 1: 549-556.
- [11] Burzo, I., Toma, S., Dobrescu, A., Ungurean, L., Stefan, V. (1999): Physiology of the growing plants, Volume II: Physiology of the field crops. – Entepreise for publishing Science Publishing House, pp. 180-207.
- [12] Canellas, L. P., Olivares, F. L., Aguiar, N. O., Jones, D. L., Nebbioso, A., Mazzei, P., Piccolo, A. (2015): Humic and fulvic acids as biostimulants in horticulture. – Scientia Horticulturæ 196: 15-27.
- [13] Corleto, A., Alba, E., Polignano, G. B., Vonghia, G. (1997): Safflower: A multipurpose species with unexploited potential and world adaptability. The Research in Italy. – IV<sup>th</sup> International Safflower Conference, (2-7 June), 23-31 Bari, Italy.
- [14] Darinkaboud, B. A., Asl, S. G. (2016): The oil and protein content of Isfahahn's safflower seed in different periods of irrigation, levels of humic acid and superabsorbent. – International Journal of Life Science Pharma Research 1 (Special Issue): 56-63.
- [15] Ekin, Z. (2020): Co-application of humic acid and *Bacillus* strains enhances seed and oil yields by mediating nutrient acquisition of safflower plants in semi-arid region. – Applied Ecology And Environmental Research 18(1): 1883-1900.
- [16] Emongor, V., Oagile, O. (2017): Safflower Production. – Published by: The Botswana University of Agriculture and Natural Resources Private Bag 0027 Gaborone, Botswana.

- [17] Esendal, E., Kevseroglu, K., Uslu, N., Aytac, S. (1992): The effect of spring and winter planting on yield and important characters of safflower. – University of Ondokuz Mayıs, Faculty of Agriculture, Years of Research, Project No: Z-044, pp. 119-121.
- [18] Esendal, E. (2001): Safflower production and research in Turkey. – V<sup>th</sup> International Safflower Conference, Williston, North Dakota, Sidney, Montana, USA, July 23-27, pp. 203-206.
- [19] Galavi, M., Ramroudi, M., Tavassoli, A. (2012): Effect of micronutrients foliar application on yield and seed oil content of safflower (*Carthamus tinctorius* L.). – African Journal of Agricultural Research 7(3): 482-486.
- [20] Garcia, A. (2009): Insulin production from transgenic safflower. <http://www.sembiosys.ca/>.
- [21] Gursoy, M., Kolsarici, O. (2017): The effects of different humic acid dose on the yield and yield components of summer rape (*Brassica napus* ssp. *oleifera* L.) under Ankara conditions. – KSU J. Nat. Sci. 20 (Special vol.): 186-191.
- [22] Haghghati, A. (2010): Study on the effects of nitrogen and phosphorus fertilizers on the yield and oil content of safflower lines in drylands. – Research Journal of Agronomy 4(3): 57-62.
- [23] Hussain, M. I., Dionyssia-Angeliki, L., Farooq, M., Nikoloudakis, N., Khalid, N. (2015): Salt and drought stresses in safflower: a review. – Agronomy for sustainable development 36: 1-31.
- [24] Icel, C. D. (2005): The effect of different application dates and doses of humic acids on yield, yield components and oil ratio of safflower (*Carthamus tinctorius* L.). – Ankara University Graduate School of Natural and Applied Sciences Department of Field Crops Master Thesis, 80p., Ankara, Turkey.
- [25] Kaleem, S., Hassan, F. U., Farooq, M., Rasheed, M., Munir, A. (2010): Physio-morphic traits as influenced by seasonal variation in sunflower; A Review. – Int. J. Agric. Biol. 12: 468-473.
- [26] Karimi, E., Tadayyon, A., Tadayyon, M. R. (2016): The effect of humic acid on some yield characteristics and leaf proline content of safflower under different irrigation regimes. – Journal of crops improvement (Journal of Agriculture) 18(3): 609-623.
- [27] Korkmaz, K. (2000): Effects of application of iron and humic acid the soybean growth and micro element content. – Gaziosmanpaşa University Graduate School of Natural and Applied Science Department of Soil Science Master Thesis, 69p., Tokat, Turkey.
- [28] Koutroubas, S. D., Papakosta, D. K., Doitsinis, A. (2009): Phenotypic variation in physiological determinants of yield in spring sown safflower under Mediterranean conditions. – Field Crops Research 112: 199-204.
- [29] Lakzayi, M., Sabbagh, I. (2015): Influence of foliar application and variety on some characteristics of Safflower. – Trends in Life Sciences 4(4): 585-588.
- [30] Lewis, D. C., McFarlane, J. D. (1986): Effect of foliar applied manganese on the growth of safflower (*Carthamus tinctorius* L.) and the diagnosis of manganese deficiency by plant tissue and seed analysis. – Aust. J. Agric. Res. 37: 567-572.
- [31] Lobartini, J. C., Orioli, G. A., Tan, K. H. (1997): Characteristics of soil humic acid fractions separated by ultrafiltration. – Com. Soil Sci. Plant Anal. 28: 787-796.
- [32] Malan, C. (2015): Review: humic and fulvic acids. A Practical Approach. – In: Sustainable Soil Management Symposium, Stellenbosch, 5-6 November 2015, Agrilibrum Publisher.
- [33] Marschner, H. (1995): Mineral nutrient of higher plants. – Second ed., Academic Press Limited, Harcourt Brace and Company, Publishers, London, pp. 347-364.
- [34] Mehraban, A., Miri, M. (2017): Influence of humic acid and mycorrhiza on some characteristics of safflower (*Carthamus tinctorius* L.). – Journal of Research in Ecology 5(1): 508-514.

- [35] Moradi, P., Pasari, B., Fayyaz, F. (2017): The effects of fulvic acid application on seed and oil yield of safflower cultivars. – Journal of Central European Agriculture 18(3): 584-597.
- [36] Movahhedy-Dehnavy, M., Modarres-Sanavy, S. A. M., Mokhtassi-Bidgoli, A. (2009): Foliar application of zinc and manganese improves seed yield and quality of safflower (*Carthamus tinctorius* L.) grown under water deficit stress. – Ind. Crops Prod. 30: 82-92.
- [37] Mustin, M. (1987): Le Compost: Gestion de LA Matiere organique. – Editions Francois Dubus C 35. Reu. Mathurin-Regnier 75015, Paris.
- [38] Pande, P., Anwar, M., Chand, S., Yadav, V. K., Patra, D. D. (2007): Optimal level of iron and zinc in relation to its influence on herb yield and production of essential oil in menthol mint. – Communications in Soil Science and Plant Analysis 38(5-6): 561-578.
- [39] Rahimi, A., Khoram, A., Biglarifard, A. (2016): Effect of using humic, foliar application of compost tea and wermiwash on yield and yield component of safflower (*Carthamus tinctorius* L.). – International Scientific Journal "Mechanization In Agriculture" 6: 22-24.
- [40] Rashno, M. H., Tahmasebi Sarvestani, Z. A., Heidari Sharifabad, H., Modarres Sanavi, S., Tavakkol Afshari, R. (2013): The effect of drought stress and iron spraying on yield and quality of two alfalfa cultivars. – Iranian Journal of Crop Plants Production 1: 125-148.
- [41] Ravi, S., Channal, H. T., Hebsur, N. S., Patil, B. N., Dharmatti, P. R. (2008): Effect of sulphur, zinc and iron nutrition on growth, yield, nutrient uptake and quality of safflower (*Carthamus tinctorius* L.). – Karnataka J. Agric. Sci. 21: 382-385.
- [42] Sahan, H. (2019): Effects of humic acid and potassium on quality and yield of safflower (*Carthamus tinctorius* L.). – Ordu University Institute of Science and Technology Field Crops Master Thesis, 43p., Ordu, Turkey.
- [43] Said-Al Ahl, H., Omer, E. A. (2009): Effect of spraying with zinc and/or iron on growth and chemical composition of coriander (*Coriandrum sativum* L.) harvested at three stages of development. – J. Medicinal Food Plants 1(2): 30-46.
- [44] Vaughan, D., Linehan, D. J. (1976): The growth of wheat plants in humic acid solutions under axenic conditions. – Plant Soil 44: 445-449.
- [45] Weiss, E. A. (1983): Oilseed crops: Safflower. – Longman Group Limited, Longman House, London, UK, pp. 216-281.
- [46] Weiss, E. A. (2000): Safflower. – In: Oilseed Crops, Blackwell Sci. Ltd., Victoria, Australia, pp. 93-129.
- [47] Yilmaz, E., Alagoz, Z. (2001): The effects of humic acid application on aggregate formation and stability in soils. – II. Ecological Agriculture Symposium, 16 November 2001, Antalya, Turkey, pp. 134-143.

# ASSESSMENT OF PHYSICOCHEMICAL AND MICROBIOLOGICAL WATER QUALITY AND BACTERIAL BIOFILM FORMATION IN THE COASTAL WATERS OF ÇANAKKALE, TURKEY

ONAT, B.<sup>1</sup> – DOĐRU HACIOĐLU, N.<sup>2\*</sup>

<sup>1</sup>Graduate School of Natural and Applied Sciences, Çanakkale Onsekiz Mart University, Çanakkale, Turkey

<sup>2</sup>Department of Biology, Faculty of Arts and Sciences, Çanakkale Onsekiz Mart University, Çanakkale, Turkey

\*Corresponding author

e-mail: nurcihan.n@gmail.com; phone: +90-286-218-001; fax: +90-286-218-05-33

(Received 11<sup>th</sup> Aug 2020; accepted 19<sup>th</sup> Nov 2020)

**Abstract.** This study, it was aimed to determine water quality based on the physicochemical and microbiological parameters, as well as microbial indicators (in addition to antibiotic-heavy metal resistance and biofilm formation) in Çanakkale Coastal waters, Turkey. The results showed that the stations were within acceptable limit values in terms of general sanitation values, however, the isolated bacteria showed high antibiotic and heavy metal resistance and biofilm formation capacity. A total of 68 Gram negative bacterial isolates were collected from the Çanakkale coastline, and were recorded as Aeromonadaceae, Burkholderiaceae, Enterobacteriaceae, Plesiomonadaceae, Pseudomonadaceae, Shewanellaceae and Vibrionaceae. The highest antibiotic resistances were detected against cephalothin, erythromycin, cefoxitin antibiotics from all bacterial isolates. Frequency of resistance of isolated bacteria against heavy metals (Cu<sup>2+</sup>, Cd<sup>2+</sup>, Cr<sup>3+</sup>, Pb<sup>2+</sup> and Mn<sup>2+</sup>) were detected as averages of 67.64%, 60.29%, 86.76%, 79.41% and 92.64%, respectively. Sixty bacterial isolates also exhibited strong biofilm formation. This study demonstrated that the coastal waters of Çanakkale represented a rich source of bacterial diversity and high incidence of antibiotic and heavy metal resistance and biofilm formation among isolated bacteria. It is expected that this study will lead to more comprehensive researches to investigate microbial quality in terms of public health in coastal waters and seafood in the region.

**Keywords:** coastline, monitoring, bacterial indicator, antibiotic - heavy metal resistance, biofilm

## Introduction

Pollution is a major problem that has negative effects on all of the planet's ecosystems, including the marine waters. In many parts of the globe, economic development has been most active in coastal zones, putting enormous pressures on coastal ecosystems. Coastal water pollution has increased throughout the world, mainly due to direct discharges from rivers, increased surface run-off and drainage from expanding port areas, oil spills and other contaminants from shipping, and domestic and industrial effluent. Most of the world's wastes- around 20 billion tons per year- end up in the sea, often without any preliminary processing (Krishnakumar and Asokan, 2017). The microbial quality of water is typically determined by monitoring microbial presence, especially faecal coliform bacteria and physicochemical parameters (EPA, 1999). Along with faecal bacteria, also potentially pathogenic bacteria such as *Aeromonas hydrophila*, *Campylobacter* spp., *Clostridium perfringens*, *Klebsiella pneumoniae*, *Neisseria* spp., *Pseudomonas aeruginosa*, *Salmonella* spp., *Shigella* spp., *Staphylococcus aureus* and *Vibrio cholera* whose normal habitat is not the marine

environment are introduced into the seawater. The accumulation of these and other pathogenic bacteria in the recreational seawater and the beach sand represents a hazard to bathers, i.e. leads to a potential disease (Zbigniew et al., 2014). In this case, microorganisms are the most appropriate objects for the studies, since they are distinguished by their unique capability of rapidly adjusting to the changing environment, can transform and utilize virtually all the organic substances existing in the environment, and feature high reproduction and growth rates (Buzoleva et al., 2008).

There is no report pertaining to exploration of periodically variation physicochemical and microbiological parameters in the Çanakkale (Turkey) coastal waters. The main aims of this study were to reveal (i) physicochemical and microbiological changes of 4 different stations representing the Çanakkale (Turkey) coastline (ii) identify important pathogen Gram negative bacteria and their virulence factors such as level of antibiotic-heavy metal resistance and biofilm formation.

## Materials and methods

### *Study area and sample collection*

Water samples were collected at four sites located at different places over the perimeter of the Çanakkale (Turkey) coastline; Station 1: Güzelyalı village (40°2'35" N, 26°20' 44" E); Station 2: Çınarlı village (40°08'18" N, 26°3'65" E); Station 3: Kepez waist (40°06'21" N, 26°22'41" E); and Station 4: Çanakkale center cord (40°9'0"N, 26°24'0"E) (Fig. 1).

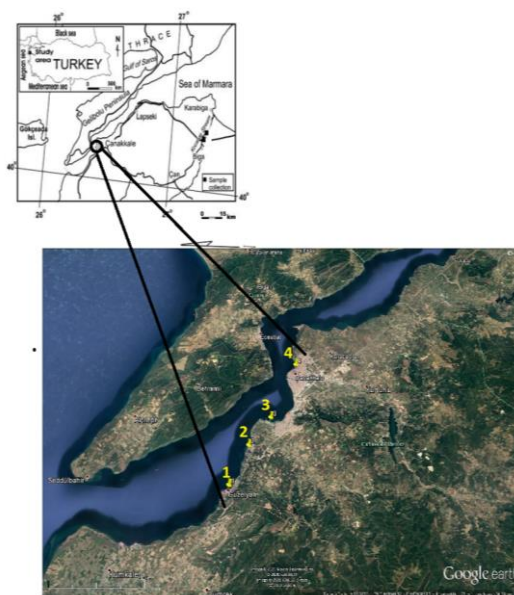


**Figure 1.** Location of coastal sampling sites

Sampling for water quality parameters were carried out in the four sites at seasonally intervals between December 2018 and September 2019 (1. sampling: December 2018; 2. sampling: March 2019; 3. sampling: June 2019; 4. Sampling: September 2019) covering dry and rainy seasons. Standard methods (APHA, 1998) were used during collection, preservation and estimation of different parameters. All samples were

collected in 2 litres sterile bottles, kept at 4 °C and analyzed within 3 h for microbiological and BOD<sub>5</sub> analysis. The collected water samples were analyzed for physicochemical parameters [temperature (T), dissolved oxygen (DO), biological oxygen demand (BOD), pH, electrical conductivity (EC), total suspended solid (TSS) and heavy metal rates] and microbiological parameters [total coliform (TC), faecal coliform (FC), faecal streptococci (FS)] by following the standard methods of American Health Association (APHA) (1998) in *Table 1*. The five heavy metal [Copper (Cu<sup>+2</sup>), Cadmium (Cd<sup>+2</sup>), Chromium (Cr<sup>+3</sup>), Lead (Pb<sup>+2</sup>), Manganese (Mn<sup>+2</sup>), in the water samples were analyzed by Perkin Elmer ICPOES Optime 8000 through procurement of services.

**Table 1.** Analytical method and standards of physicochemical parameters for analysis of Çanakkale coastline water quality

Parameters	Unit	Analytical Methods	Instruments	Standards* (Anonymous, 2004)
T	°C	Instrumental	Instrumental Hatche Lange pH meter	28-30
DO	mg/L	Instrumental	Instrumental Hatche Lange pH meter	>5
BOD	mg/L	Titrimetric (Winkler's)	Titration assembly and BOD incubator	20
pH	-	Instrumental	Instrumental Hatche Lange pH meter	6-9
EC	(µS/cm)	Instrumental	Instrumental Hatche Lange pH meter	n/a
TSS	g	Filtration technique	-	30 mg/L
Cu <sup>+2</sup>	mg/L	Instrumental	EPA 200.7 method	0.01
Cd <sup>+2</sup>	mg/L	Instrumental	EPA 200.7 method	0.01
Cr <sup>+3</sup>	mg/L	Instrumental	EPA 200.7 method	0.1
Pb <sup>+2</sup>	mg/L	Instrumental	EPA 200.7 method	0.1
Mn <sup>+2</sup>	mg/L	Instrumental	EPA 200.7 method	0.01
TC	MPN/100 mL	Multiple tube technique	-	1000
FC	MPN/100 mL	Multiple tube technique	-	200
FS	MPN/100 mL	Multiple tube technique	-	100

\*(Anonymous, 2004) State of Turkey, in Turkish Water Pollution Control Regulation, State of Turkey, 2004, Annexes, Table 4; n/a: not available; mg/L: miligram/Liter; MPN/100 mL: most probable number/100 mililiter; T: temperature; DO: dissolved oxygen; BOD: biological oxygen demand; EC: electrical conductivity; TSS: total suspended solid; Cu<sup>+2</sup>: Copper; Cd<sup>+2</sup>: cadmium; Cr<sup>+3</sup>: chromium; Pb<sup>+2</sup>: lead Mn<sup>+2</sup>: manganese; TC: total coliform; FC: faecal coliform; FS: faecal streptococci

### Bacterial isolation

Zobell Marine Agar (ZMA) and Mueller Hinton Agar (MHA) (Difco, USA) were used for the isolation of gram negative bacteria from water samples. Three to five colonies from each plate showing different colonial features were picked and inoculated to specific media (MacConkey agar (MAC); Eosin Methylene Agar (EMB); Thiosulfate citrate bile salts sucrose agar (TCBS), Glutamate starch phenol red agar (GSP), Ampicillin Aeromonas Agar, (AAA), Inositol brilliant green bile agar (IBG); Cetrimide Agar). All the plates were incubated at 25– 30 °C for 24–48 h. Biochemical tests (Murray et al., 1999) and Microgen ID-A Panel-Gram negative (MID-64) were performed to confirm the identity of obtained isolates.



### ***Antibiotic sensitivity testing***

Susceptibility testing was performed by an agar diffusion test, using MHA (Matyar et al., 2008) and 14 different of antibiotics: Trimethoprim (TR5 µg/mL), Tobramycin (TB10 µg/mL), Kanamycin (K30 µg/mL), Amoxycillin (AM10 µg/mL), Oxytetracycline (O30 µg/mL), Cephalothin (CH30 µg/mL), Cefmetazole (CMZ30 µg/mL), Gentamicin (G120 µg/mL), Furazolidone (FR50 µg/mL), Erythromycin (E15 µg/mL), Cefoxitin (CN30 µg/mL), Ampicillin (A10 µg/mL), Cefotaxime (CE30 µg/mL) and Chloramphenicol (C30 µg/mL).

### ***Determination of the minimal inhibitory concentration (MIC) of heavy metals***

MIC for each bacterial isolate for five heavy metals was determined by using MHA which is containing Cu<sup>2+</sup>, Cd<sup>2+</sup>, Cr<sup>3+</sup>, Pb<sup>2+</sup> and Mn<sup>2+</sup> at concentrations ranging from 100 to 12800 µg/mL. The metals were added as CuSO<sub>4</sub>.5H<sub>2</sub>O, CdCl<sub>2</sub>.2H<sub>2</sub>O, K<sub>2</sub>Cr<sub>2</sub>O<sub>7</sub>, Pb(NO<sub>3</sub>)<sub>2</sub> and MnCl<sub>2</sub>.2H<sub>2</sub>O. The isolates were considered resistant if the MIC values exceeded that of the *E. coli* K-12 strain which was used as the control (Matyar et al., 2008).

### ***Analysis of biofilm formation***

Bacterial biofilm formation activity of isolates was using the crystal violet technique adapted from (Julistiono et al., 2018) by using polystyrene 96-well microplate. Bacterial isolates were grown on seawater agar media for 48 h at 37 °C. Each colony was picked up by sterile tip needle and dipped into (inoculated) in three parallel wells of a 96 well microtiter plate containing 200 µl seawater media and incubated for 6 d at 37 °C. After the incubation period, the wells were rinsed with physiological saline and fixed with 2 µL of 99.99% ethanol for 10 min. The attached bacterial material was then stained by adding 2 µL of crystal violet (2%) for 20 min. The plate was rinsed with tap water gently and the attached biomass was measured using a microplate reader at 570 nm. The experiment was performed in triplicate and the mean of OD value is presented.

### ***Statistical analysis of data***

Mean and SE mean of physicochemical and microbiological analysis data were used to present seasonally values for these parameters. Statistical parameters of physicochemical and microbiological analyses data were used to present the values of these water quality characteristics. Pearson's correlation coefficient (r) was used to show correlation between the all parameters data using the MINITAB Statistical Software 13.20. The Student's t-test was used to determine the statistical significance. Probability was set at p < 0.05.

## **Results**

### ***Water quality***

The results of field measurements and laboratory analysis on the quality of Çanakkale coastline waters were presented in *Table 2*. Based on results of comparison of data with Anonymous (2004) (*Table 1*), it is seen that Çanakkale coastline waters in all station was acceptable limits for physicochemical parameters (T, DO, BOD, pH, EC, TSS and heavy metal contents) (*Table 2*).

**Table 2.** The physicochemical and microbiological parameters in coastal waters of Çanakkale, Turkey

Parameters	Stations				Average
	St.1	St.2	St.3	St.4	
<b>T</b>	12.6±1.83*	13.2±2.40	13.45± 0.35	11.2±1.97	12.61± 1.65
<b>DO</b>	10.525±0.40	10.035±0.07	9.335± 0.021	10.62±0.86	10.12±0.65
<b>BOD</b>	7.2±8.20	5.25±1.06	1.8±0.424	5.7±3.81	4.76±4.26
<b>pH</b>	7.95±0.148	7.98±0.084	7.93±0.035	8.07± 0.01	7.98±0.06
<b>EC</b>	51.8±0.84	52.6±0.14	35.7±0.28	45.5±0.28	46.4±7.80
<b>TSS</b>	0.032±0.012	0.0479±0.018	0.0326±0.022	0.041±0.014	0.038±0.007
<b>Cu<sup>+2</sup></b>	<0.01	<0.01	<0.01	<0.01	<0.01
<b>Cd<sup>+2</sup></b>	<0.01	<0.01	<0.01	<0.01	<0.01
<b>Cr<sup>+3</sup></b>	<0.1	<0.1	<0.1	<0.1	<0.1
<b>Pb<sup>+2</sup></b>	<0.01	<0.01	<0.01	<0.01	<0.01
<b>Mn<sup>+2</sup></b>	<0.01	<0.01	<0.01	<0.01	<0.01
<b>TC</b>	600±424.26	300±519.61	577500±120208.2	535±28.28	578260±449452.2
<b>FC</b>	685±162.34	610±0	1114000±766503.8	797.5±100.16	279023.12±365929.3
<b>FS</b>	462.5±0	11790±162.63	55325±714177.2	567.5±1032.37	17036.25±273377.7

\*: mean± std. deviation; St.1: station 1

In the coastline water, TC, FC, FS counts varied from 300±519.61 MPN/100 mL (St.2) to 577500±120208.2 MPN/100 mL (St.3); 610±0 MPN/100 mL (St.2) - 1114000±766503.8 MPN/100 mL (St.3); 462.5±0 MPN/100 mL (St.1) - 55325±714177.2 MPN/100 mL (St.3), respectively. St. 3 (Kepez waist) was recorded the highest densities for microbial quality indicator bacteria (Table 2). Table 3 provides the correlation matrix of the water quality parameters and also showed significant positive-negative correlation which is indicated by asterisk. There was a positive correlation between DO and EC ( $r = 0.577$ ), pH and TSS ( $r = 0.578$ ), TC and FC ( $r = 0.734$ ), TC and FS ( $r = 0.778$ ), FC and FS values ( $r = 0.997$ ). On the contrary, there was a negative correlation between T and pH ( $r = - 0.622$ ), T and TSS ( $r = - 0.914$ ), T and FC ( $r = - 0.502$ ), DO and TC ( $r = - 0.745$ ), DO and FS ( $r = - 0.527$ ), BOD and TC ( $r = - 0.560$ ) EC and TC ( $r = - 0.909$ ), EC and FC ( $r = - 0.617$ ), and EC and FS values ( $r = - 0.622$ ).

**Table 3.** Correlation coefficients between the parameters in coastal waters of Çanakkale

Parameters	T	DO	BOD	pH	EC	TSS	TC	FC	FS
<b>T</b>	1	-0.112	0.453	-0.622*	0.281	-0.914*	-0.193	-0.502*	-0.484
<b>DO</b>		1	0.452	0.219	0.577*	0.328	-0.745*	-0.489	-0.527*
<b>BOD</b>			1	0.312	0.487	-0.236	-0.560*	-0.398	-0.425
<b>pH</b>				1	0.146	0.578*	-0.341	-0.123	-0.146
<b>EC</b>					1	0.122	-0.909*	-0.617*	-0.662*
<b>TSS</b>						1	-0.153	0.310	0.272
<b>TC</b>							1	0.734*	0.778*
<b>FC</b>								1	0.997*
<b>FS</b>									1

\*Correlation is significant at the 0.05 level

### Bacterial diversity

During the study period, 7 bacterial families were recorded: Aeromonadaceae (8.82%), Burkholderiaceae (1.47%), Enterobacteriaceae (55.88%), Plesiomonodaceae (8.82%), Pseudomonadaceae (16.17%), Shewanellaceae (1.47%) and Vibrionaceae (7.35%). A total of 68 bacterial isolates were defined from Çanakkale coastline. The species belonging to Enterobacteriaceae family was the most common taxonomic group in the coastal areas of Çanakkale. Pseudomonadaceae family was the second most common group (Table 4).

**Table 4.** Diversity of Gram negative bacteria according to their isolated stations

Familia	Species	Stations			
		St.1 (n=17)	St.2 (n=15)	St.3 (n=16)	St.4 (n=20)
Aeromonadaceae	<i>Aeromonas hydrophila</i>	+	+	+	-
Burkholderiaceae	<i>Burkholderia pseudomallei</i>	-	+	-	-
Enterobacteriaceae	<i>Enterobacter aerogenes</i>	+	+	+	+
	<i>E. cloacae</i>	+	-	-	-
	<i>Escherichia coli</i>	+	+	+	+
	<i>Klebsiella oxytoca</i>	+	+	+	+
	<i>K. pneumoniae</i>	-	+	+	+
	<i>Pantoea agglomerans</i>	+	+	+	-
	<i>Proteus vulgaris</i>	-	+	-	-
	<i>Salmonella typhimurium</i>	-	-	-	+
Plesiomonodaceae	<i>Plesiomonas shigelloides</i>	+	+	-	+
Pseudomonadaceae	<i>Pseudomonas aeruginosa</i>	+	+	+	+
Shewanellaceae	<i>Shewanella putrefaciens</i>	+	-	-	-
Vibrionaceae	<i>Vibrio alginolyticus</i>	+	-	-	-
	<i>V. parahaemolyticus</i>	-	+	+	+

St.1: station 1; n: Isolate number

### Antibiotic susceptibility

The results of the antibiotic susceptibility test revealed 0% (TB10-C30) - 100% (E15-CN30), 6.66% (TB10) - 80% (CH30), 6.2% (TB10-G120) – 87.5% (CN30) and 15% (G120)- 95% (CH30) for the bacterial isolates of four sites, respectively (Fig. 2).

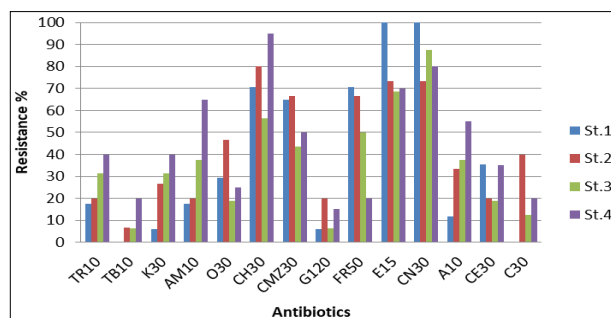


**Figure 2.** Antimicrobial resistant profile of isolated bacteria

### Heavy metal resistant

The results were shown as the frequency of resistance of these bacteria in Fig. 3. A hundred percent of all isolates were resistant to manganese. However, the higher frequencies of resistant bacteria were found in station 4, except copper. Frequency of resistance of  $\text{Cu}^{2+}$ ,  $\text{Cd}^{2+}$ ,  $\text{Cr}^{3+}$ ,  $\text{Pb}^{2+}$  and  $\text{Mn}^{2+}$  were detected as an average of 67.64%, 60.29%, 86.76%, 79.41% and 92.64%, respectively in a total of 68 bacteria isolated from Çanakkale coastline.

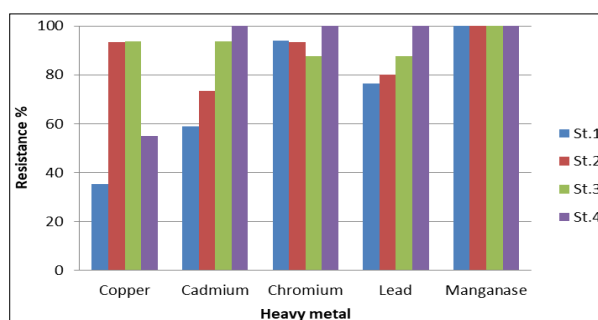


Figure 3. Heavy metal resistance isolated bacteria

### Results of biofilm formation

Out of eight, sixty bacterial isolates exhibited biofilm formation. Most of them formed moderate to strong biofilms.  $\text{OD}_{570} > 0.2$  indicated significant biofilm formation whereas that in the range of 0.1-0.2 indicated moderate biofilm formation. The results of biofilm formation in isolates were as tabulated (Table 5).

Table 5. Biofilm formation rates of isolated bacteria

Isolates (St.1)	Biofilm rates	Isolates (St.2)	Biofilm rates	Isolates (St.3)	Biofilm rates	Isolates (St.4)	Biofilm rates
A1	+++	B1	+	C1	+++	D1	+++
A2	+	B2	+++	C2	++	D2	+++
A3	+++	B3	+++	C3	++	D3	+
A4	+++	B4	-	C4	++	D4	+++
A5	+++	B5	+	C5	++	D5	+
A6	+++	B6	+++	C6	+++	D6	+++
A7	+	B7	-	C7	-	D7	+++
A8	+++	B8	+++	C8	+++	D8	+++
A9	++	B9	+++	C9	+++	D9	-
A10	++	B10	+++	C10	+++	D10	-
A11	+	B11	-	C11	+++	D11	+++
A12	+++	B12	-	C12	++	D12	+++
A13	+++	B13	+++	C13	-	D13	+++
A14	+++	B14	+++	C14	+++	D14	+
A15	+	B15	+	C15	+++	D15	+++
A16	+++			C16	+	D16	++
A17	+					D17	++
						D18	+++
						D19	+++
						D20	+++

St.1: station 1; A1: Number of isolated bacteria (A: St. 1, B: St. 2, C: St. 3, D: St. 4); (++++) = strong, (+++) = moderate, (++) = weak, (+) = Not detected

## Discussion

There is no study has been found that extensively investigates the water quality of the Çanakkale coastline in terms of physicochemical and microbiological parameters. For this reason, the present study was designed in which revealed these parameters and antibiotic-heavy metals resistance patterns and biofilm formation capacity of bacterial isolates.

Life of all marine organisms depends on water quality of the coastal environment. Water quality indices are the basic tools to sketch out the environmental or ecological condition of a water body and to simplify the presentation of results. Most considerable physical and chemical factors which greatly influence the aquatic environment are temperature, pH, carbon dioxide, dissolved oxygen and heavy metal concentration etc. (Zafar et al., 2018). In the present study these physicochemical parameters were found acceptable limits contrast to findings about different coastal waters (Türkođlu, 2010; Türkođlu and Oner, 2010; Sreenivasulu et al., 2015; Zafar et al., 2018; Tanjung et al., 2019).

In recent years, the increase of bacterial contamination in coastal waters has become a global problem that limits recreation functions and can create negative presentations for public health (Sreenivasulu et al., 2015). The use of TC, FC and FS, which is share the same environment with the pathogenic bacteria, is much routine analyses as the indicator of the presence of the pathogenic bacteria. In our study, especially FC and FS levels were above the limit values in all sites. This is a proof that the Çanakkale coastline is significantly pressured in terms of faecal pollution. In this sense, our findings have correlated with previous studies carried out on the Çanakkale coastline and other sea coasts (Çardak and Altuđ, 2010, 2014; Çardak et al., 2016; Çiftçi Türetken and Altuđ, 2016; Hulyar et al., 2020).

Coastlines are becoming the hotspots of some new emerging diseases. Many opportunistic pathogens, including *Aeromonas*, *Clostridium*, *Klebsiella*, *Legionella*, *Listeria*, *Pseudomonas*, and *Vibrio*, are naturally enterprising in sea waters. When present in coastal waters, these opportunistic pathogens can persist and infect humans through recreational exposures or consumption of contaminated sea-food (Mishra et al., 2018). Though there have been reports investigating the distribution of fecal, supplemental-indicator, human pathogenic bacteria in the Canakkale coastline (Çardak et al., 2016), no studies have been done so far which put forth antibiotic – heavy metal resistance and biofilm formation of these bacteria. In this regard, this investigation would be the first report to isolate biofilm-forming bacteria from Canakkale coastline and deduce their antibiotic-heavy metal susceptibility patterns.

The coastal sites of Çanakkale represented a rich source of bacterial diversity. High incidence of antibiotic and heavy metal resistance among isolated bacterial strains is captivating and might be a consequence of increased number of antibiotic and heavy metal resistance genes in the coastal area and their cross-generational transfer. Environment may be recognized as a giant repository of resistance agents and the propensity of environmental bacteria to form biofilms may be implicated as a selective advantage to survive in the natural environments and spawn infectious diseases.

## Conclusion

The correlation analysis on water quality parameters revealed that all parameters are more or less correlated with each other Person's Correlation matrix. It is observed that

some of the parameters do not have significant correlation between them indicating the different origin source of pollution. From correlation analysis, the positive relationship between TC, FC, and FS each other reveals the high organic pollution with anthropogenic activities on the Çanakkale coastline. Thus it can be concluded that the water of the Çanakkale coastline represents serious threat to the ecosystem due to anthropogenic pollution. Since Çanakkale coastline is lifeline for people of Çanakkale who use its water for swimming, fishing or recreation are at risk. The correlation study and correlation coefficient values can help in selecting a few parameters which could be frequently measured to determine the status of water quality regularly. This will help the regulatory bodies to issue a warning on deteriorating water quality and taking steps to implement control measures so that proper treatment of effluent could be done to minimize contaminants in Çanakkale coastline. However, the isolated bacteria showed high antibiotic and heavy metal resistance and biofilm formation capacity. Our study is the first report studying on marine biofilms isolated in the Çanakkale coastline and therefore it can serve as an elementary data to several future studies aspiring to understand the ecology and quality of marine habitats. This study also demonstrated that anthropogenic effects of people significantly affected water quality of the Çanakkale coastline. So, coastline should be followed and pollution sources must be taken under control. Hence, the main goals are to reduce the number of pollution incidents in watercourses, eliminate the sources of pollutants, and minimize the consequences of accidental discharges on marine ecosystem. In order to prevent the local marine pollution in the coastal cities drainage and treatment/discharge systems should be built.

**Acknowledgments.** This investigation is a part of Master thesis of Buket ONAT. This study was financially supported by the Çanakkale Onsekiz Mart University Scientific Research Projects Coordination Unit, Turkey (FYL-2019-2919).

## REFERENCES

- [1] Anonymous (2004): State of Turkey. – In: Turkish Water Pollution Control Regulation, Annexes, Table 4.
- [2] APHA (1998): American Public Health Association: Standard Methods for the Examination of Water and Wastewater. – 20<sup>th</sup> ed., American Public Health Association, Washington, D.C.
- [3] Buzoleva, L. S., Kalitina, E. G., Bezverbnaya, I. P., Krivosheeva, A. M. (2008): Microbial communities in the coastal surface waters of Zolotoi Rog Bay under the conditions of strong anthropogenic pollution. – *Marine Biology* 48(6): 882-888.
- [4] Çardak, M., Altuđ, G. (2010): Distribution of members of the family Enterobacteriaceae in the Istanbul strait. – *Journal of Black Sea/Mediterranean Environment* 16(3): 295-310.
- [5] Çardak, M., Altuđ, G. (2014): Species Distribution and Heavy Metal Resistance of Enterobacteriaceae Members Isolated from Istanbul Strait. – *Fresenius Environmental Bulletin* 23(10A): 2620-2626.
- [6] Çardak, M., Altuđ, G., May, M., Erol, Ö. (2016): Investigation of the Distribution of Antibiotic Resistance and the Presence of Vancomycin Resistance Genes (vanA and vanB) in Enterobacteriaceae Isolated from the Sea of Marmara, Canakkale Strait and Istanbul Strait, Turkey. – *Oceanological and Hydrobiological Studies* 1: 1-5.
- [7] Çiftçi Türetken, P. S., Altuđ, G. (2016): Bacterial pollution, activity and heterotrophic diversity of the northern part of the Aegean Sea, Turkey. – *Environmental Monitoring and Assessment* 188(2): 127.

- [8] EPA (1999): 25 Years of the Safe Drinking Water Act: History and Trends. – USA Environmental Protection Agency (816-R-99-007).
- [9] Hulyar, O., Altuğ, G. (2020): The Bacteriological Risk Transported to Seas by Rivers; the Example of Çırpıcı River, Istanbul, TR. – International Journal of Environment and Geoinformatics 7(1): 45-53.
- [10] Julistiono, H., Hidayati, Y., Yuslaini, N., Nditasari, A., Dinoto, A., Nuraini, L., Priyotomo, G., Gunawan, H. (2018): Identification of biofilm-forming bacteria from steel panels exposed in sea waters of Jakarta Bay and Madura Strait. – Inventing Prosperous Future through Biological Research and Tropical Biodiversity Management AIP Conf. Proc. 2002, 020029-1–020029-7.
- [11] Krishnakumar, P. K., Asokan, P. K. (2017): Environmental Impacts of Marine Pollution. – In: Mathrubhumi Year Book Plus, Chapter: Environmental Pollution. Publisher: Mathrubhumi, pp. 730-739.
- [12] Matyar, F., Kaya, A., Dinçer, S. (2008): Antibacterial agents and heavy metal resistance in Gram-negative bacteria isolated from seawater, shrimp and sediment in Iskenderun Bay, Turkey. – Sci Total Environ. 407(1): 279-285.
- [13] Mishra, S., Ali, S. K., Gautam, H. K. (2018): Biofilm forming ability and antibiotic susceptibility of bacterial strains isolated from Kavaratti Island, India. – Journal of Microbiology and Antimicrobial Agents 4(1): 3-10.
- [14] Murray, P. R., Baron, E. J., Pfaller, M. A., Tenover, F. C., Tenover, R. H. (1999): Manual of clinical microbiology. – 7<sup>th</sup> ed., Washington, D.C.: American Society for Microbiology.
- [15] Sreenivasulu, G., Jayaraju, N., Sundara, B. C., Reddy, R. T., Prasad, L. (2015): Physicochemical parameters of coastal water from Tupilipalem coast, Southeast coast of India. – Journal of Coastal Sciences 2(2): 34-39.
- [16] Tanjung, H. R., Hamuna, B., Alianto, R. (2019): Assessment of water quality and pollution index in coastal waters of Mimika, Indonesia. – Journal of Ecological Engineering 20(2): 87-94.
- [17] Türkoğlu, M. (2010): Temporal variations of surface phytoplankton, nutrients and chlorophyll a in the Dardanelles (Turkish Straits System): a coastal station sample in weekly time intervals. – Turkish Journal of Biology 34: 319-333.
- [18] Türkoğlu, M., Oner, C. (2010): Short time variations of winter phytoplankton, nutrient and chlorophyll a of Kepez harbor in the Dardanelles (Çanakkale Strait, Turkey). – Turkish Journal of Fisheries and Aquatic Sciences 10: 537-548.
- [19] Zafar, F. H. S., Ayub, Z., Karim, A., Zahid, M., Bat, L. (2018): Seasonal variations in physicochemical parameters of Buleji and Paradise Point rocky shores at Karachi coast. – International Journal of Environment and Geoinformatics 5(2): 154-168.
- [20] Zbigniew, J., Gackowska, J., Skórczewski, P., Perliński, P., Zdanowicz, M. (2014): Occurrence of potentially human pathogenic bacteria in the seawater and in the sand of the recreational coastal beach in the southern Baltic Sea. – Oceanological and Hydrobiological Studies 43(4): 366-373.

## AQUEOUS EXTRACT OF FALLEN INDIAN SOAPBERRY (*SAPINDUS MUKOROSI*) LEAVES DECREASED SEED GERMINATION BUT INCREASED SEEDLING GROWTH OF FOUR VEGETABLES

LI, Y.<sup>1,2</sup> – LI, X.<sup>3</sup> – LI, Q.<sup>1</sup> – YUE, M.<sup>1\*</sup>

<sup>1</sup>*Xi'an Botanical Garden of Shaanxi Province, Institute of Botany of Shaanxi Province, Xi'an 710061, China*

<sup>2</sup>*Shaanxi Engineering Research Centre for Conservation and Utilization of Botanical Resources, Xi'an 710061, China*

<sup>3</sup>*Shaanxi Institute of Technology, Xi'an 710300, China*

\*Corresponding author

*e-mail: yueming@nwu.edu.cn; phone: +86-29-8525-1800; fax: +86-29-8525-1800*

(Received 15<sup>th</sup> Aug 2020; accepted 28<sup>th</sup> Oct 2020)

**Abstract.** Utilization of fallen leaves is one challenge for modern sustainable agriculture. Allelopathy is selective, depending upon the concentrations of extracts and receptor species. Therefore, we conducted an experiment to confirm how the aqueous extract of fallen leaves of *Sapindus mukorossi*, an important virent tree species in south China, affected seed germination and seedling growth of four common vegetables, *Brassica rapa* var. *chinensis*, *B. oleracea* var. *capitata*, *Lactuca sativa* L., and *Chrysanthemum coronarium* L. Our results showed that the fallen leaf aqueous extracts inhibited the seed germination of the four vegetables. Moreover, the aqueous extracts stimulated seedlings growth of the four vegetables especially at appropriate concentration treatments. The effects of fallen leaf aqueous extracts on seedlings were related to phylogenetic characteristics and morphological characteristics of cultivated vegetables. According to our study, by and large, fallen leaf aqueous extracts of *S. mukorossi* decreased seed germination and increased seedling growth. Thus, we may take advantage of the negative allelopathic effects on germination via applying aqueous extracts after crop emergence to control weeds, and the positive allelopathic effects on seedling growth to stimulate crop yield in agriculture. Our results represent a step forward in the study of weed management and organic fertilizer by allelochemicals.

**Keywords:** *soapnuts, allelochemicals, biomass accumulation, morphological characteristics, life form*

### Introduction

Allelopathy is defined as the influence of chemical substances produced by plants and released into the surrounding environment affecting the growth, development, survival, and reproduction of neighboring plants (Rice, 1984). Allelochemicals are plant secondary metabolites such as saponins, tannins, flavonoids, terpenoids, and lactones (Caser et al., 2020), which are totally or partially water-soluble substances (Turk and Tawaha, 2003) that are released into environment through leaching, exudation, vaporization or decomposition (Fernandez et al., 2009). All plant organs could produce or store allelochemicals. Allelopathy has been found to widely exist in nature, and play important roles in ecosystem (Chou, 1999; Rout and Callaway, 2009; Zheng et al., 2014). Allelopathy has been suggested as an important mechanism contributing to the impressive success of invasive plants (Hierro and Callaway, 2003; Ooka and Owens, 2018), and can be one of the significant factors contributing to species distribution (Mallik, 2003). Furthermore, allelopathy has been theorized to play important roles in maintaining community stabilities by inhibiting



the invasion of newly introduced species (Callaway and Aschehoug, 2000; Mallik and Pellissier, 2000; Morgan and Overholt, 2005; Veen et al., 2019).

More and more studies have proved that allelochemicals released from plants not only play harmful effects on other plants, but also can benefit neighboring plants growth. The allelopathic effects are selective, depending upon the concentrations of extracts and receptor species (Turk and Tawaha, 2003; Cheema et al., 2013). For example, leaf aqueous extracts of *Castanea henryi* reduced seed germination, seedling growth of *Zea mays* and *Brassica pekinensis* at high concentrations in a recent study. However, extracts of low concentrations in this study promoted seed germination, shoot growth of *Z. mays*, but not for *B. pekinensis* (Ming et al., 2020). Nowadays, the potential selective impacts of allelopathy have been utilized in modern sustainable agriculture. In order to effective control of weeds, reduction of the input of chemical pesticides is feasible by utilizing negative allelopathic effects of crops on weeds (Anwar et al., 2018; Campos et al., 2019; Kong et al., 2019; Ojija et al., 2019). Furthermore, it is possible to promote crop yields by utilizing positive allelopathic effects (Iqbal et al., 2011). Reductions of the input of chemical pesticides and fertilizer permit the development of crops with low phytotoxic residue amounts in water and soil, thus facilitating environment safe (Cheng and Cheng, 2015).

The genus *Sapindus mukorossi*, better known as the soapnuts, has an extensive distribution spanning in tropical and sub-tropical of Asia (Singh et al., 2015). *S. mukorossi* is a traditional and important virescent tree species in the area south of Yangtze River of China (Diao et al., 2016; Ling et al., 2019). As a deciduous tree, *S. mukorossi* produce a large amount of fallen leaves every year, and such litter represents both a huge waste of resources and a potential pollutant. Therefore, it would be urgently to develop practical uses for the fallen leaves.

Although according to previous studies that leaf extracts of *S. mukorossi* contain different types of flavonoids such as quercetin, apigenin, kaempferol, and rutin (Singh et al., 2015), the allelopathic effects of leaf aqueous extracts is not clear. Thus, the aim of the present study was to investigate the allelopathic effects of fallen leaf aqueous extracts of *S. mukorossi* on the seed germination and seedling growth of four common vegetables in China, *Brassica rapa* var. *chinensis*, *Lactuca sativa* L., *Chrysanthemum coronarium* L., and *Brassica oleracea* var. *capitata*. Furthermore, in order to observe whether allelopathic effects of fallen leaf aqueous extracts of *S. mukorossi* on vegetables are depending on phylogeny, we took phylogenetic characteristics into account when we selected the four tested vegetables: *B. rapa* and *B. oleracea* are two Crucifer species, while *L. sativa* and *C. coronarium* are two Asteraceae species. Understanding allelopathic effects on other plants especially crops is meaningful for rational, sustainable, and economical utilization of resources of fallen leaves.

## Materials and Methods

### *Preparation of leaf aqueous extracts*

Fallen leaves of *Sapindus mukorossi* were collected in Xi'an Botanical Garden of Shaanxi Province (34° 21' N, 108° 96' E, alt. 413 m asl), China, in December 2019. Fallen leaves were air dried in shade for a week after collection. The dried leaves were ground using mortar then passed through 2 mm mesh sieve. 40 g, 20 g, 10 g, 5 g, 0 g (control) of the ground materials were soaked in 1000 ml sterilized distilled water. These gave the concentration of leaf aqueous extracts were 40 g/L, 20 g/L, 10 g/L, 5 g/L, and 0 g/L

(control). The mixtures were then shaken intermittently and allowed to stand for 24 hours in the laboratory at 25 °C. Thereafter, the suspensions were filtered by filter paper. All extracts were refrigerated at 4 °C.

### **Seed collection and germination**

Seeds of *B. rapa*, *L. sativa*, *C. coronarium*, and *B. oleracea* were selected in our study. The four vegetables seeds were obtained from suburban vegetable farm in Xi'an, China. The seeds were surface sterilized with 5% sodium hypochlorite. After 15 minutes, seeds were rinsed severally with distilled water to remove the excess of the chemical. Thereafter, seeds were primed in distilled water for 1 hour. 30 seeds of each vegetable were placed on filter paper in petri dishes (diameter: 9 cm, height: 2 cm). Each petri dish with clearly labeled was moistened with 2 ml leachate of one of five concentrations. Then seeds from each vegetable were subjected to 5 treatments (0 g/L, 5 g/L, 10 g/L, 20 g/L, and 40 g/L). There were 3 replications. All the petri dishes were placed in incubator at a constant temperature of 25 °C with 12 hours light. Numbers of germinated seed were recorded every 24 hours. Germination experiment was terminated after 15 days, and seedlings traits were measured. 5 seedlings were randomly harvested from each petri dish to determine seedlings traits (whole seedling length, shoot height, root length, fresh biomass). Root length indicated the length of the longest root. All seedlings were measured for seedling traits if there were less than 5 seedlings.

### **Index of germination and seedling growth**

*Germination percentage (GP)* was calculated by

$$GP(\%) = \frac{\sum n_i}{T} \cdot 100 \quad (\text{Eq.1})$$

*Germination index (GI)* is a time-weighted cumulative germination that measures the speed of germination and quantifies the seedling vigor. GI was calculated by

$$GI = \frac{\sum n_i}{t} \quad (\text{Eq.2})$$

*Mean germination time (MGT)* was used as an index to evaluate the phenomenon of germination speed. It is a measurement of the average length of time required for maximum germination of a seed lot (Ranal and Santana, 2006). MGT was calculated by

$$MGT = \frac{\sum_{i=1}^k n_1 t_i}{\sum_{i=1}^k n_1} \quad (\text{Eq.3})$$

*The synchronization index (SI)* can describe emergence patterns, with a higher index representing a more uniform germination (Ranal and Santana, 2006). SI was calculated by

$$SI = \frac{\sum C_{n_i,2}}{N} \quad (\text{Eq.4})$$
$$C_{n_i,2} = n_i(n_i - 1)/2$$
$$N = \sum n_i \left( \sum n_i - 1 \right) / 2$$

*Vigor index (VI)*, a comprehensive account for acorn germination and seedling growth, is a suitable index to evaluate seed vigor (Ranal and Santana, 2006). VI was calculated by

$$VI = GI \cdot S \quad (\text{Eq.5})$$

In these formulae above,  $n_i$  refers to the number of seeds germinated in time  $i$  (not the accumulated number, but the number corresponding to the  $i^{\text{th}}$   $C_{n_i,2}$  observation);  $T$  is the total number of tested seeds;  $S$  represents the average whole length on the 15<sup>th</sup> day;  $t_i$  refers to the time from the start of the experiment to the  $i^{\text{th}}$  observation (days); and  $k$  is the last germination time.

### **Data analysis**

Two-way ANOVAs were used to examine the effects of phylogenetic characteristic (P), concentration of fallen leaf aqueous extracts of *S. mukorossi* (C), and their interaction on seed germination traits (germination percentage, germination index, mean germination time, the synchronization index) and seedling traits (seedling whole length, shoot length, root length, vigor index, fresh biomass). One-way ANOVAs were used to examine the effects of leaf aqueous extracts of different concentrations on seed germination traits and seedling traits for one species. Tukey's test was used to compare the significance among treatments for one species. All the above statistical analyses were conducted with SAS software (SAS Institute Inc., Cary, NC, USA).

Structural equation models (SEMs) were used to investigate the direct and indirect effects of leaf aqueous extracts on seed biomass accumulation for the four test vegetables. Amos 17.0.2 (Amos Development Corporation, Chicago, IL, USA) was used to parameterize the SEM model.

## **Results**

### **Germination**

As a whole, phylogenetic characteristic (P) did not affect germination percentage (GP) ( $P > 0.05$ , *Table 1*). While GP significantly decreased with the concentration of fallen leaf aqueous extracts of *S. mukorossi* (C) increased as a whole ( $P < 0.05$ , *Table 1*). 20 g/L and 40 g/L extracts significantly reduced the whole GP by 50.28% and 65.28%, respectively. According to One-way ANOVAs, fallen leaf aqueous extracts of *S. mukorossi* significantly affected GPs of the four vegetables (all  $P < 0.05$ , *Table 2*). GPs of the four vegetables were all decreased as the concentration increased (*Fig. 1*). Compared with distilled water control treatment, 20 g/L and 40 g/L extracts significantly reduced GP of *B. rapa* by 58.89% and 84.44%, and reduced GP of *B. oleracea* by 90.00% and 100.00%, whereas 5 g/L and 10 g/L extracts had no significant effects (*Fig. 1*). For *C. coronarium*, aqueous extracts reduced GP by 27.78%, 32.22%, 44.45%, 61.11% with concentration increased, respectively (*Fig. 1*). For *L. sativa*, 40 g/L extract significantly reduced GP by 15.56%, whereas the other extracts had not significant effects compared with distilled water control treatment.

**Table 1.** Effects of phylogenetic characteristic (P), concentration of fallen leaf aqueous extracts of *S. mukorossi* (C), and their interaction on seed germination traits and seedling traits based on two-way ANOVAs

		Phylogenetic characteristic (P)		Concentration (C)		P*C	
		F-Value	P-Value	F-Value	P-Value	F-Value	P-Value
Seed	GR	1.34	0.25	22.70	<.001	6.26	<.001
	GI	17.55	<.001	56.09	<.001	12.78	<.001
	MGT	0.95	0.33	2.44	0.06	0.30	0.87
	SI	5.38	<.05	9.32	<.001	0.51	0.73
Seedling	Shoot length	4.73	<.05	9.13	<.001	2.70	<.05
	Root length	13.83	<.001	3.25	<.05	1.28	0.29
	Whole length	10.02	<.05	8.28	<.001	1.63	0.18
	S/R	16.13	<.001	0.82	0.52	2.13	0.09
	VI	13.45	<.001	10.91	<.001	4.39	<.05
	Biomass	24.97	<.001	1.90	0.13	1.71	0.16

GP: germination percentage; GI: germination index; MGT: mean germination time; SI: the synchronization index; S/R: the rate of shoot length to root length; VI: vigor index

**Table 2.** Results of one way ANOVAs on the effects of fallen leaf aqueous extracts of *S. mukorossi* on seed germination and seedling growth characters of the four vegetables. See Table 1 for abbreviations

		<i>B. rapa</i>		<i>L. sativa</i>		<i>C. coronarium</i>		<i>B. oleracea</i>	
		F-Value	P-Value	F-Value	P-Value	F-Value	P-Value	F-Value	P-Value
seed	GP	17.20	<.001	3.88	<.05	26.12	<.001	67.70	<.001
	GI	38.87	<.001	9.57	<.05	14.50	<.001	58.77	<.001
	MGT	202.31	<.001	13.70	<.001	0.88	0.51	36.43	<.001
	SI	4.10	<.05	7.70	<.05	25.54	<.001	14.89	<.001
seedling	Shoot length	19.52	<.001	5.03	<.05	29.96	<.001	4.24	<.05
	Root length	1.96	0.18	2.44	0.11	2.71	0.09	7.02	<.05
	Whole length	12.52	<.001	8.18	<.05	7.76	<.05	4.89	<.05
	S/R	0.16	0.95	0.72	0.60	13.50	<.001	26.61	<.001
	VI	14.38	<.001	4.36	<.05	5.39	<.05	2.96	0.07
	Biomass	4.57	<.05	3.11	0.06	1.07	0.42	4.95	<.05

As a whole, phylogenetic characteristic (P), concentration of fallen leaf aqueous extracts of *S. mukorossi* (C), and their interaction significantly influenced seed germination index (GI) (all  $P < 0.001$ , Table 1). With the concentration increased, the whole GI decreased by 21.00%, 26.86%, 70.17%, and 86.90%. In addition, GI of Crucifer species was 36.23% higher than that of Asteraceae species. According to One-way ANOVAs, GIs of the four vegetables significant decreased with the concentration increased (all  $P < 0.05$ , Table 2). Compared with distilled water treatment, 20 g/L and 40 g/L extracts significantly reduced GI of *B. rapa* aqueous by 71.99% and 95.48%, and reduced GI of *L. sativa* by 32.41% and 49.07%, whereas 5 g/L and 10 g/L extracts had no significant effects (Fig. 2). Aqueous extracts of different concentrations reduced GI of *C. coronarium* by 38.17%, 45.70%, 66.13%, and 91.40%, and reduced GI of *B. oleracea* by 22.22%, 35.96%, 94.44%, and 100.00% (Fig. 2).

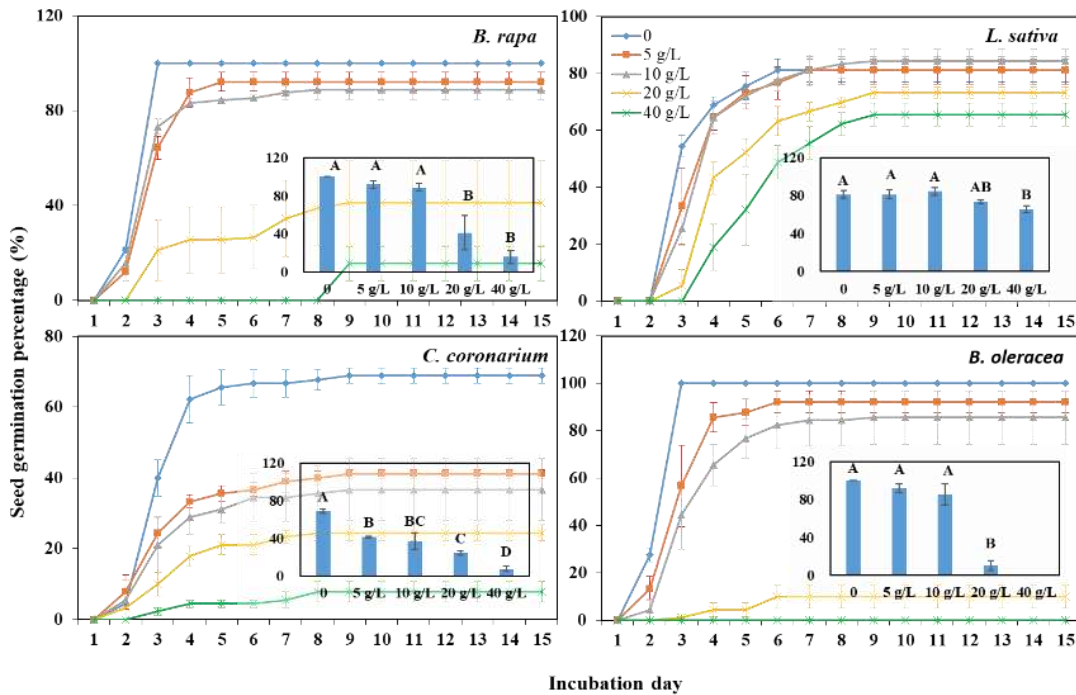


**Figure 1.** Effects of fallen leaf aqueous extracts of *S. mukorossi* on seed cumulative germination percentage (%) and final germination percentage (%; inserts, means  $\pm$  1 SE,  $n = 3$ ) of the four vegetables. Means with the same uppercase letter are not significantly different ( $P > 0.05$ )

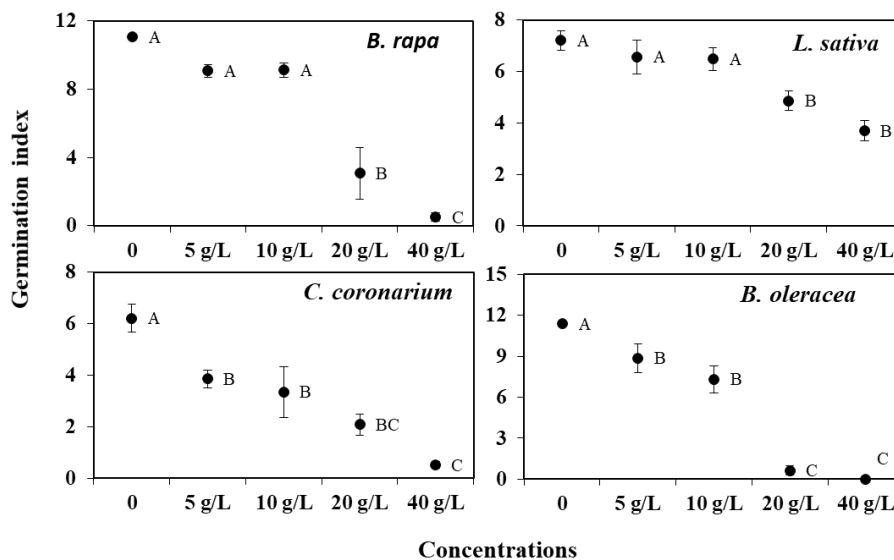


**Figure 2.** Effects of fallen leaf aqueous extracts of *S. mukorossi* on seed germination index (GI) of the four vegetables (means  $\pm$  1 SE,  $n = 3$ ). Means with the same uppercase letter are not significantly different ( $P > 0.05$ )

As a whole, phylogenetic characteristic (P), concentration of fallen leaf aqueous extracts of *S. mukorossi* (C), and their interaction all had no effects on mean germination time (MGT) (all  $P > 0.05$ , Table 1). According to One-way ANOVAs, except for

*C. coronarium*, MGTs of the other three vegetables significantly increased by aqueous extracts (all  $P < 0.001$ , Table 2). Aqueous extracts of different concentrations prolonged MGT of *B. rapa* by 15.38%, 12.64%, 80.40%, and 222.71%, prolonged MGT of *L. sativa* by 11.64%, 18.78%, 38.12%, and 60.28%, prolonged MGT of *B. oleracea* by 24.24%, 39.29%, 81.52%, and 100.00% (Fig. 3).

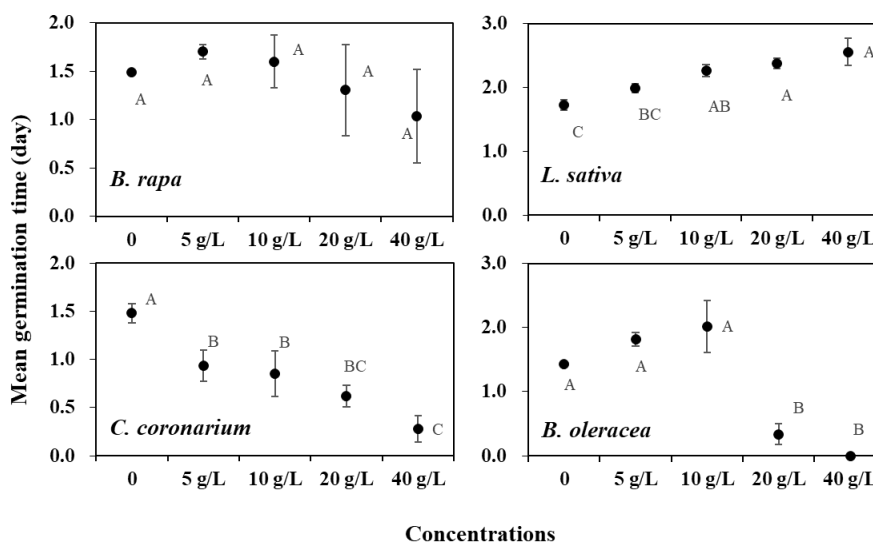


**Figure 3.** Effects of fallen leaf aqueous extracts of *S. mukorossi* on seed mean germination time (MGT) of the four vegetables (means  $\pm 1$  SE,  $n = 3$ ). Means with the same uppercase letter are not significantly different ( $P > 0.05$ )

As a whole, phylogenetic characteristic (P), and concentration of fallen leaf aqueous extracts of *S. mukorossi* (C) significantly influenced synchronization index (SI) (both  $P < 0.05$ , Table 1). With the concentration increased, the whole SI decreased by 25.22%, 25.23%, 52.05%, and 56.62%. In addition, SI of Crucifer species was 25.96% higher than that of Asteraceae species. According to One-way ANOVAs, fallen leaf aqueous extracts played significant roles on SIs of the four vegetables (all  $P < 0.05$ , Table 2). Aqueous extracts decreased SI of *B. rapa* by 30.81%, 19.66%, 54.93%, and 9.89%, decreased SI of *L. sativa* by 9.74%, 27.74%, 29.70%, and 36.76%, decreased SI of *C. coronarium* by 34.95%, 27.76%, 61.01% and 88.52% at 5 g/L, 10 g/L, 20 g/L, and 40 g/L concentrations, respectively (Fig. 4). Aqueous extracts decreased SI of *B. oleracea* by 61.48% at 20 g/L concentrations (Fig. 4).

### Seedling growth

As a whole, phylogenetic characteristic (P), and concentration of fallen leaf aqueous extracts of *S. mukorossi* (C) significantly influenced shoot length, root length, and whole length (all  $P < 0.05$ , Table 1). Phylogenetic characteristic (P) played a significant role on S/R as a whole ( $P < 0.05$ , Table 1). With the concentration increased, the shoot length increased by 160.00%, 248.89%, 206.67%, and 136.67%; the whole root length increased by 182.54%, 192.53%, 147.52%, and 92.53%; the whole length increased by 166.93%, 231.55%, 188.47%, and 123.09%. In addition, the shoot length, root length, and whole length of Crucifer species was 27.68%, 97.34%, and 84.75% higher than those of Asteraceae species, respectively.

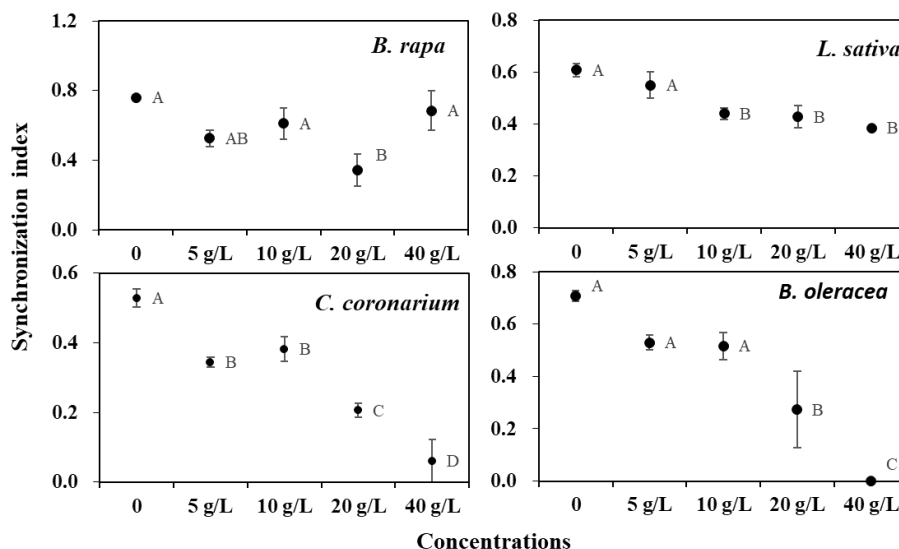


**Figure 4.** Effects of fallen leaf aqueous extracts of *S. mukorossi* on seed synchronization index (SI) of the four vegetables (means  $\pm$  1 SE,  $n = 3$ ). Means with the same uppercase letter are not significantly different ( $P > 0.05$ )

According to One-way ANOVAs, fallen leaf aqueous extracts of *S. mukorossi* significantly increased whole length of the four vegetable seedlings (all  $P < 0.05$ , Table 2, Fig. 5). Furthermore, aqueous extracts significantly stimulated shoot length of the four vegetables (all  $P < 0.05$ , Table 2, Fig. 5), whereas the extracts only significantly affected root length of *B. oleracea* ( $P < 0.05$ , Table 2, Fig. 5). However, aqueous extracts only significantly affected S/R of *C. coronarium* and *B. oleracea* (both  $P < 0.001$ , Table 2). Aqueous extracts significantly stimulated S/R of *C. coronarium* by 314.36% and 328.63% at 10 g/L and 40 g/L treatments. Aqueous extracts significantly increased S/R of *B. oleracea* by 112.90% at 20 g/L treatments and decreased it by 48.84% at 5 g/L treatments (Fig. 5). The 20 g/L extract stimulated shoot length and root length by 189.29% and 146.00%, resulting in 176.93% stimulation to whole length of *B. rapa* (Fig. 5). The 10 g/L extract stimulated shoot length and root length by 533.25% and 867.00%, resulting in 600.00% stimulation to whole length of *L. sativa* (Fig. 5). The 10 g/L extract stimulated shoot length and root length by 640.84% and 59.88%, resulting in 446.60% stimulation to whole length of *C. coronarium* (Fig. 5). The 10 g/L extract stimulated shoot length and root length by 103.88% and 146.91%, resulting in 118.75% stimulation to whole length of *B. oleracea* (Fig. 5).

As a whole, phylogenetic characteristic (P), concentration of fallen leaf aqueous extracts of *S. mukorossi* (C), and their interaction significantly influenced vigor index (VI) (all  $P < 0.05$ , Table 1). 5 g/L and 10 g/L aqueous extracts significantly stimulated the whole VI by 98.38% and 135.62%, respectively. In addition, VI of Crucifer species was 90.96% higher than that of Asteraceae species. According to One-way ANOVAs, fallen leaf aqueous extracts significantly affected VIs of *B. rapa*, *L. sativa*, and *C. coronarium* (all  $P < 0.05$ , Table 2). 5 g/L and 10 g/L aqueous extracts significantly stimulated VI of *B. rapa* by 101.90% and 125.00%, stimulated VI of *L. sativa* by 267.90% and 479.84%, and stimulated VI of *C. coronarium* by 139.81% and 308.32%, respectively (Fig. 6).

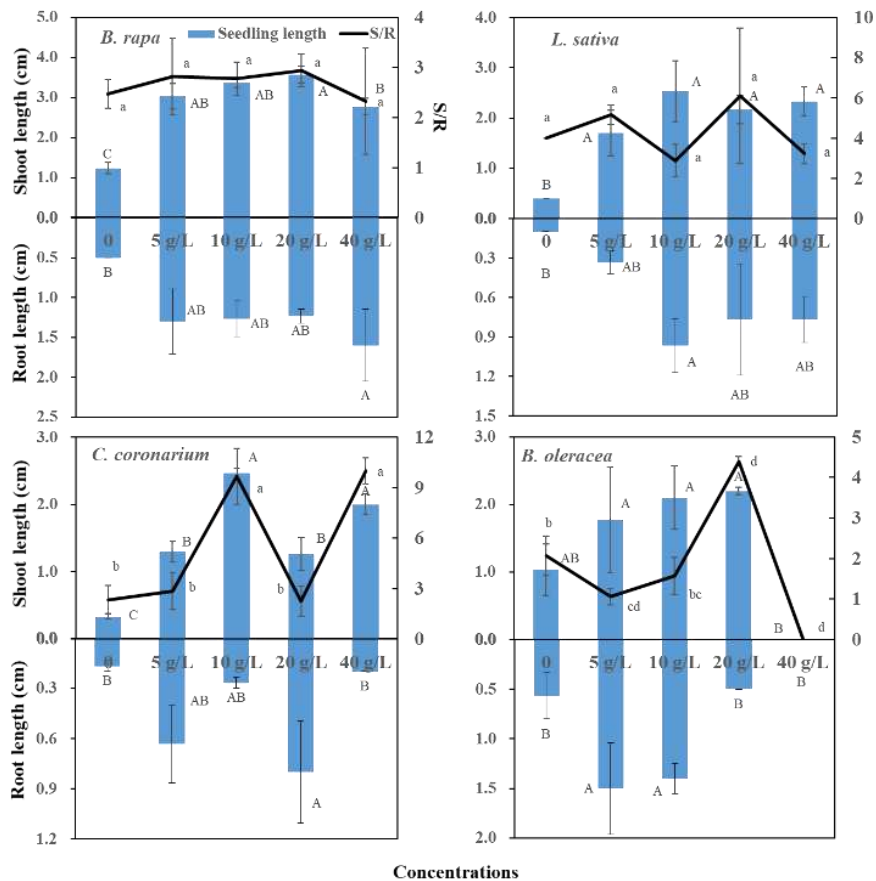


**Figure 5.** Effects of fallen leaf aqueous extracts of *S. mukorossi* on seedling length (Column) and S/R (Broken lines) of the four vegetables (means  $\pm$  1 SE,  $n = 3$ ). Means with the same uppercase letter are not significantly different in shoot length or root length ( $P > 0.05$ ). Means with the same lowercase letter are not significantly different in S/R ( $P > 0.05$ )

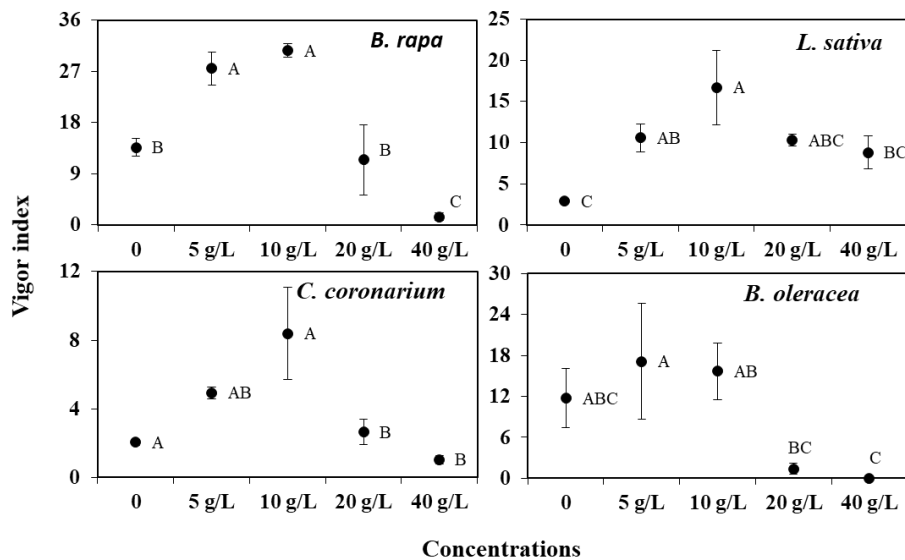


**Figure 6.** Effects of fallen leaf aqueous extracts of *S. mukorossi* on seedling vigor index (VI) of the four vegetables (means  $\pm$  1 SE,  $n = 3$ ). Means with the same uppercase letter are not significantly different ( $P > 0.05$ )



Phylogenetic characteristic (P) played significantly roles on biomass per plant ( $P < 0.05$ , Table 1). 10 g/L aqueous extracts significantly stimulated the whole biomass by 53.30%. In addition, biomass of Crucifer species was 84.84% higher than that of Asteraceae species. According to One-way ANOVAs, except for *C. coronarium*, fallen leaf aqueous extracts significantly affected biomass per plant of *B. rapa* and *B. oleracea* (both  $P < 0.05$ , Table 2), and marginally affected biomass of *L. sativa* ( $P = 0.06$ , Table 2). With the concentration increased, aqueous extracts increased biomass of *B. rapa* by 65.22% to 108.70%, while increased biomass of *L. sativa* by 86.51% to 124.71%. Fallen leaf aqueous extracts did not significantly affect biomass of *B. oleracea*, if 40 g/L extracts did not take into account, because that 40 g/L extracts totally inhibited germination of *B. oleracea* (Fig. 7).

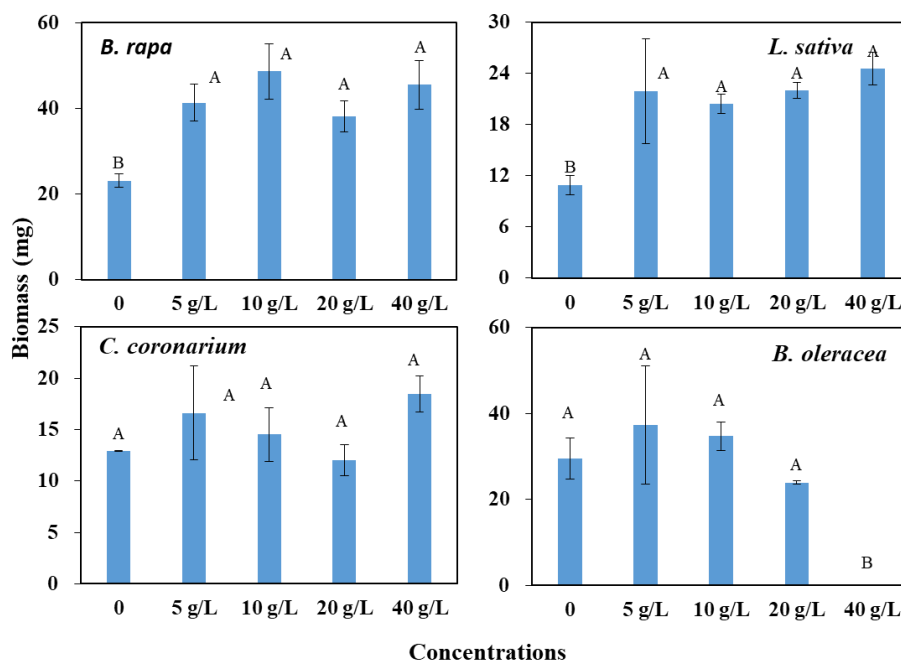


**Figure 7.** Effects of fallen leaf aqueous extracts of *S. mukorossi* on seedling biomass of the four vegetables (means  $\pm$  1 SE,  $n = 3$ ). Means with the same uppercase letter are not significantly different ( $P > 0.05$ )

The structural equation models (SEMs) showed that shoot length and root length can account for about 69.00%, 56.00%, and 85.00% variation for *B. rapa*, *L. sativa*, and *B. oleracea* in biomass accumulation resulting from fallen leaf aqueous extracts, respectively (Fig. 8). It also showed that leaf aqueous extracts can account for about 25.00% variation in root length of *B. rapa*, which resulting in 69.00% variation in biomass accumulation in combination with shoot length (Fig. 8a). SEMs showed that leaf aqueous extracts can account for about 26.00% variation in shoot length of *L. sativa*, which resulting in 56.00% variation in biomass accumulation in combination with root length (Fig. 8b). Although SEM showed that leaf aqueous extracts could affect biomass of *B. oleracea* by affecting root growth, it may mainly result by totally inhibition of germination by 40 g/L leaf aqueous extracts (Fig. 8d).

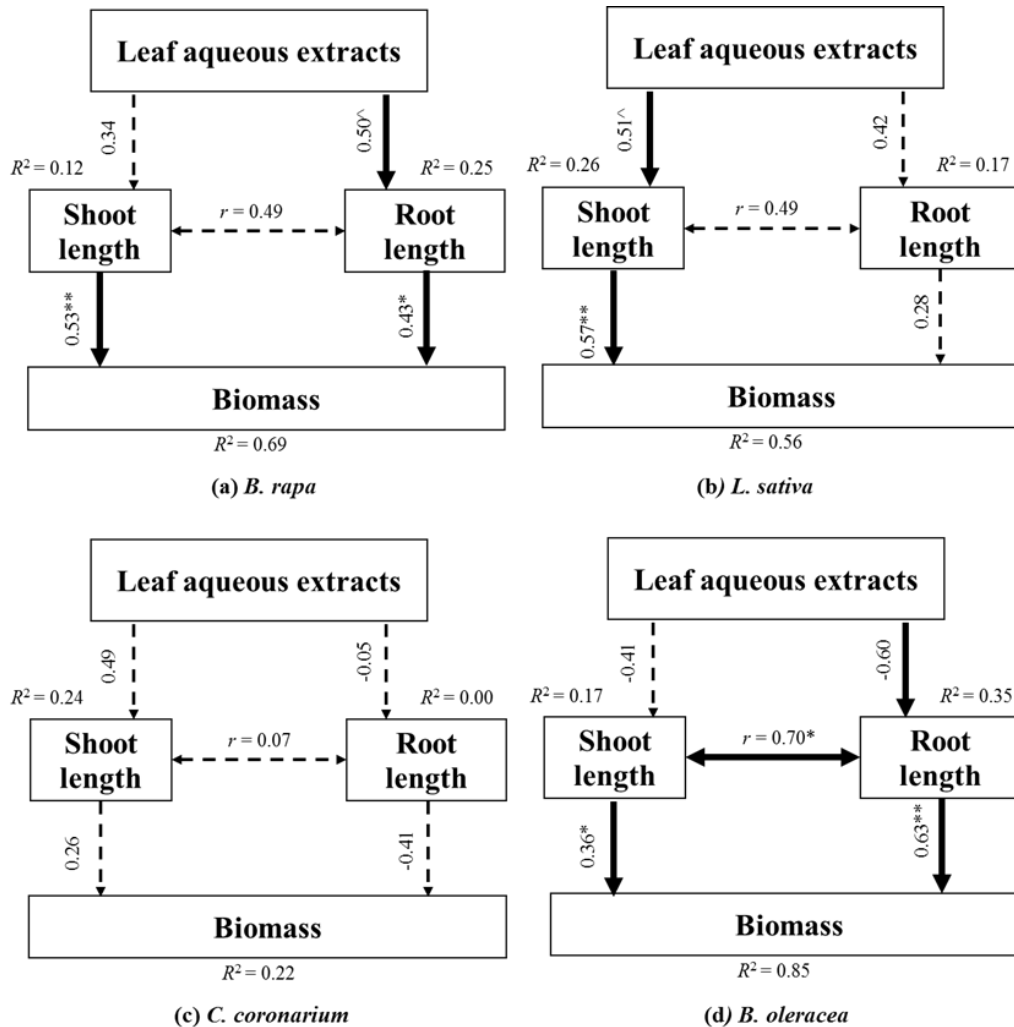


**Figure 8.** Structural equation models (SEMs) illustrating the direct and indirect effects of leaf aqueous extracts of *S. mukorossi* on seedling biomass. Boxes represent measured variables in the model. Values associated with single-headed arrows are the direct path coefficients. Values associated with double-headed arrows indicate the correlation coefficients. Solid arrows indicate significant relationships and dashed arrows indicate insignificant relationships in the model. The  $R^2$  values indicate the proportion of variance explained. \*\* indicates a significant difference at  $P < 0.001$ ; \* indicates a significant difference at  $P < 0.05$ ;  $^\wedge$  indicates a significant difference at  $P < 0.10$

## Discussion

### Impacts on seed germination

Our results demonstrated that fallen leaf aqueous extracts of high concentration of *S. mukorossi* significantly inhibited seed germination of all tested vegetables. Our results were accordance with previous studies demonstrated that plant extracts inhibit other plant seed germination (Ahn and Chung, 2000; Wang et al., 2009; Anwar et al., 2018; Ming et al., 2020), and the degree of inhibition increased with extract concentration increased (Chung and Miller, 1995; Ming et al., 2020). Aqueous extracts inhibited seed germination in three ways: decreased final germination percentage; decreased germination speed

(prolonged germination time); and decreased germination synchronization, especially at higher concentration treatments. Allelochemicals in extracts may prevent growth of embryo, or caused the death (Cheng and Cheng, 2015). According to previous studies, leaf extracts of *S. mukorossi* contain different types of flavonoids such as quercetin, apigenin, kaempferol, and rutin (Singh and Kumari, 2015). Flavonoid is one of important allelopathic substances (Caser et al., 2020). Flavonoids excreted from roots or eluted from fallen leaves released into the surrounding soil are usually considered to inhibit germination (Mierziak et al., 2014). For example, flavones excreted from barley significantly inhibited seed germination of neighboring weeds (Kong et al., 2004a; Kong et al., 2007); flavones released by rice seedlings were enough in the defense of rice against weeds (Kong et al., 2004b). Flavones may be a key type of allelochemicals that could interfere potently with other organisms in ecosystems (Kong et al., 2007). Thus, we can speculate that allelochemicals such as flavonoids in fallen leaf aqueous extracts of *S. mukorossi* in our study may be harmful to seed embryo and can cause decreased of seed germination percentage, germination rate, and synchronization.

Allelopathy of aqueous extracts has been gaining more and more attention in weed management due to their disruption on establishment and growth of plants (Anwar et al., 2018; Carrubba et al., 2020; Caser et al., 2020). Allelopathy pressure is not always delivered by weeds to crops, but also could be delivered by crops to weeds (Van Volkenburg et al., 2020). For example, residues of rice could release allelochemicals to inhibit seed germination of neighboring weed (Rimando et al., 2001). Further studies conclusively showed that secondary metabolites, such as flavonoids, terpenoids, alkaloids, and cyanogenic glycosides, which usually involved in aqueous extracts, could play important roles in plants and other organism interactions (Kong et al., 2019). Therefore, allelochemicals of aqueous extracts has become a new branch of herbicide development (Macías et al., 2007; Kong et al., 2019), because these compounds can be directly used (Duke et al., 2000). As bioherbicides, aqueous extracts are biodegradable and environmental friendly because they are not halogenated and are generally safer for non-target organisms (Scognamiglio et al., 2012; Cheng and Cheng, 2015). Therefore, it is important to take advantage of the negative allelopathic effects on heterospecific plant in weed management for modern eco-agriculture (Macías et al., 2008).

### ***Impacts on seedling growth***

Our results demonstrated that fallen leaf aqueous extracts of *S. mukorossi* could stimulate seed vigor, and increased seedling length and biomass accumulation consequently, especially on appropriate concentration treatments. In natural ecosystem, nutrients released from plant litter especially fallen leaf through eluting are accessible for plants uptake in a more available forms (Adams and Angradi, 1996), as fallen leaf can account for more than 70% of aboveground litter (Robertson and Paul, 1999). Thus, nutrients that could stimulate seedling growth may release from leaves to aqueous extracts during soaking in our study. Seedlings grew in aqueous extracts as they grew in fertilized environments. They utilized nutrients from aqueous extracts to increased growth and accumulated more biomass. Our results were in accordance with that litter is an important process of nutrient cycling in ecosystems (Barbe et al., 2017), and play an important role in productivity (Adams and Angradi, 1996; Field et al., 2006; Barbe et al., 2017). It is meaningful that fallen leaf aqueous extracts could stimulate seedling growth of crop in agriculture. In order to meet the needs of population growth, we have to apply more chemical fertilizer into soil to maintain productivity in agriculture (Ashour et al., 2020).

It makes soil degradation and environment pollution. Therefore, it is necessary to utilize all available sources of nutrients to maintain the productivity and fertility of soil (Cheng and Cheng, 2015). Aqueous extract of plant is one of the most important sources for supplying nutrients to crop and for improving soil health. More importantly, it is environment friendly. The applications of allelochemicals in crop production had been successful carried out (Iqbal et al., 2011). For example, the suitable application of allelochemicals could increase maize and canola yield (Cheema et al., 2013). Our results proved that aqueous extracts of plant could be applied in vegetable culture to stimulate yield.

Our results showed that the leaf aqueous extracts' effects were varied at different life-history stages for one species. According to our results, although leaf aqueous extracts of high concentrations inhibited seed germination of four vegetables, they did not decrease seedling growth of four vegetables. It meant that plants could need or tolerate different concentrations of nutrients at different life-history stage (Khan et al., 2009). Seed germination is rarely affected directly by nutrient in surrounding, because nutrients required for germination might mainly come from seed storage (Miransari and Smith, 2014; Peti et al., 2017). Furthermore, nutrient in extracts of high concentration in surrounding might play negative allelopathic effects or serve as an osmolyte to inhibit germination (Khan et al., 2009). Thus seeds germinated in leaf aqueous extracts exhibited germination inhibition in our study. However, after germination, seedling had to uptake nutrients from surrounding to stimulated growth, because storage in seed was not enough to provide nutrients for satisfying seedling growth requirements (Moles and Westoby, 2004). Therefore, the four vegetable seedlings could stimulate growth via absorbing nutrients from fallen leaf aqueous extracts in our study, as fallen leaf aqueous extracts may work as nutrients sources (Khan et al., 2009). It meant that we should apply aqueous extracts of different concentrations at different stages to stimulate plant growth.

### ***Impacts on different vegetables***

Our results showed that the responses to aqueous extracts could not only vary with phylogenetic characteristics, but also could vary with morphological characteristics of cultivated vegetables. Compared to Asteraceae species, Crucifer species exhibited better performances of seed germination and seedling growth according to two-way ANOVAs in our results. It proved that the effects of aqueous extracts were related to phylogenetic relationship. However, our results also demonstrated that the aqueous extracts influenced seedling biomass could through different pathways according to SEMs. For example, *B. rapa* and *B. oleracea*, two Crucifer species, exhibited different responses to aqueous extracts. Results from SEMs indicated that leaf aqueous extracts could account for shoot length and root length variance for *B. rapa*, resulting in biomass accumulation stimulation. Although shoot length and root length variance could significantly explain the biomass accumulation variance of *B. oleracea*, aqueous extracts could not stimulate biomass if the 40 g/L concentration was not being taken into account because no seed germinated under 40 g/L concentration. Similarly, *L. sativa* and *C. coronarium*, two Asteraceae species, also exhibited different responses to aqueous extracts. Aqueous extracts could account for root length variance for *L. sativa*, resulting in biomass accumulation stimulation. However, aqueous extracts could not affect biomass accumulation of *C. coronarium*. These results demonstrated that although Crucifer species exhibited better performances than Asteraceae species, morphological characteristic of each species maybe more important. It has been proved that domesticated

plants such as cultivated vegetables may differ widely in appearance from their wild progenitors, most of which are associated with seed germination and seedling growth (Abbo et al., 2014). During domestication, cultivated vegetables are produced by different modifications of leaf, shoot or root system, biomass allocation, and relatively growth rate consequently (Shannon and Grieve, 1998). Therefore, cultivated vegetables could response to environment changes depend on morphological characteristics. In our study, *B. rapa*, and *L. sativa* are common leaf vegetables, *B. oleracea* is one corm leaf vegetable, and the edible part of *C. coronarium* mainly is stem. The common leaf vegetable was selected for bigger leaf; the stem vegetable was selected for longer stem during cultivating. It was proved by our results which showed aqueous extracts significantly stimulated biomass, and/or shoot length of *B. rapa*, *L. sativa*, and *C. coronarium*. Whereas, the corm leaf vegetable, with shortened stem and form a compact, hard head, was not usually selected for longer aboveground component. Furthermore, empirical observations found that the common leaf vegetables used in our study took about 30-45 days from colonization to maturity, and *B. oleracea* took about 60 days. It meant that growth strategies of the common leaf or stem vegetable are taking advantage of environmental nutrients to stimulate aboveground component height and biomass as quickly as possible. However, as the corm leaf vegetable, *B. oleracea* had longer growth period to accumulate biomass (Paez-Garcia et al., 2015). Thus, we cannot investigate as significant difference as the other three vegetables exhibited on early growth stage for *B. oleracea*.

## Conclusions

Our results demonstrated that fallen leaf aqueous extracts of *S. mukorossi* could inhibit germination and stimulate seedling growth and biomass accumulation of *B. rapa*, *L. sativa*, *C. coronarium* and *B. oleracea*, especially at appropriate concentration treatments. Furthermore, the effects of fallen leaf aqueous extracts on seedlings were not only related to phylogenetic relationship, but also related to morphological characteristics of cultivated vegetables. According to our study, we could take advantage of the negative allelopathic effects of fallen leaf aqueous extracts of *S. mukorossi* on germination in weed management, and the positive allelopathic effects on seedling growth and biomass accumulation to stimulate crop yield in agriculture. The occurrence of significant effects of fallen leaf aqueous extracts on seed germination and seedling growth represents a step forward in the study of weed management and organic fertilizer through allelochemicals. Further laboratory study and field trial are both suggested in the future, involving to identify the active components of the fallen leaf aqueous extracts of *S. mukorossi*, and develop more comprehensive and evaluate the impacts on common weeds or crops.

**Acknowledgements.** This research was funded by Western Young Scholars Program of Chinese Academy of Science (XAB2019AW16), the Scientific Research Program of Shaanxi Province (2019JQ-436), and the Scientific Research Program of Xi'an City (2019112913CXSF007SF017). We thank Fangbing Ding, Shaoli Mao, Ying Zhang, Qian Wei, Guoqing Bai for their helps in collecting fallen leaves, making aqueous extracts, and providing vegetable seeds in the study.

## REFERENCES

- [1] Abbo, S., van-Oss, R. P., Gopher, A., Saranga, Y., Ofner, I., Peleg, Z. (2014): Plant domestication versus crop evolution: a conceptual framework for cereals and grain legumes. – *Trends Plant Sci.* 19: 351-360.
- [2] Adams, M. B., Angradi, T. R. (1996): Decomposition and nutrient dynamics of hardwood leaf litter in the Fernow Whole-Watershed Acidification Experiment. – *Forest Ecol. Manag.* 83: 61-69.
- [3] Ahn, J. K., Chung, I. M. (2000): Allelopathic potential of rice hulls on germination and seedling growth of barnyardgrass. – *Agric. J.* 92: 1162-1167.
- [4] Anwar, T., Ilyas, N., Qureshi, R., Munazir, M., Anwar, P., Rahim, B. Z., Ansari, K. A., Panni, M. K. (2018): Allelopathic potential of *lantana camara* against selected weeds of wheat crop. – *Appl. Ecol. Env. Res.* 15: 5405-5421.
- [5] Ashour, M., El-Shafei, A. A., Khairy, H. M., Abd-Elkader, D. Y., Mattar, M. A., Alataway, A., Hassan, S. M. (2020): Effect of *Pterocladia capillacea* seaweed extracts on growth parameters and biochemical constituents of Jew's Mallow. – *Agronomy* 10: 420.
- [6] Barbe, L., Jung, V., Prinzing, A., Bittebiere, A. K., Butenschoen, O., Mony, C. (2017): Functionally dissimilar neighbors accelerate litter decomposition in two grass species. – *New Phytol.* 214: 1092-1102.
- [7] Callaway, R. M., Aschehoug, E. T. (2000): Invasive plants versus their new and old neighbors: a mechanism for exotic invasion. – *Science* 290: 521-523.
- [8] Campos, J. A., Peco, J. D., García-Noguero, E. (2019): Antigerminative comparison between naturally occurring naphthoquinones and commercial pesticides. Soil dehydrogenase activity used as bioindicator to test soil toxicity. – *Sci. Total Environ.* 694: 133672.
- [9] Carrubba, A., Labruzzo, A., Comparato, A., Muccilli, S., Spina, A. (2020): Use of plant water extracts for weed control in durum wheat (*Triticum turgidum* L. Subsp. *durum* Desf.). – *Agronomy* 10: 364.
- [10] Caser, M., Demasi, S., Caldera, F., Dhakar, N. K., Trotta, F., Scariot, V. (2020): Activity of *Ailanthus altissima* (Mill.) swingle extract as a potential bioherbicide for sustainable weed management in Horticulture. – *Agronomy* 10: 965.
- [11] Cheema, Z., Farooq, M., Khaliq, A. (2013): Application of allelopathy in crop production: success story from Pakistan. – In: Cheema, Z. A., Farooq, M., Wahid, A. (eds.) *Allelopathy*. Springer-Verlag Press, Berlin Heidelberg.
- [12] Cheng, F., Cheng, Z. (2015): Research progress on the use of plant allelopathy in agriculture and the physiological and ecological mechanisms of allelopathy. – *Front. Plant Sci.* 6: 1020.
- [13] Chou, C. H. (1999): Roles of allelopathy in plant biodiversity and sustainable agriculture. – *Crit. Rev. Plant Sci* 18: 609-636.
- [14] Chung, I. M., Miller, D. A. (1995): Natural herbicide potential of alfalfa residues on selected weed species. – *Agron. J.* 87: 920-925.
- [15] Diao, S. F., Jiang, J. M., Yi, H., Yue, H. F., Dong, R. X., Sun, H. G., Shao, W. H. (2016): Flowering phenology of the multipurpose tree species *Sapindus mukorossi* Gaertn. in low mountain areas of Zhejiang Province. – *Acta Ecologica Sinica* 36: 6226-6234.
- [16] Duke, S. O., Dayan, F. E., Romagni, J. G., Rimando, A. M. (2000): Natural products as sources of herbicides: current status and future trends. – *Weed Res.* 40: 99-111.
- [17] Fernandez, C., Monnier, Y., Ormeño, E., Baldy, V., Greff, S., Pasqualini, V., Mévy, J. P., Bousquet-Mélou, A. (2009): Variations in allelochemical composition of leachates of different organs and maturity stages of *Pinus halepensis*. – *J. Chem. Ecol.* 35: 970-979.
- [18] Field, B., Jordan, F., Osbourn, A. (2006): First encounters-deployment of defence-related natural products by plants. – *New Phytol.* 172: 193-207.
- [19] Hierro, J. L., Callaway, R. M. (2003): Allelopathy and exotic plant invasion. – *Plant Soil* 256: 29-39.

- [20] Iqbal, M. F., Kahloon, M. H., Nawaz, M. R., Javaid, M. I. (2011): Effectiveness of some botanical extracts on wheat aphids. – *J. Anim. Plant Sci.* 21: 114-115.
- [21] Khan, W., Rayirath, U. P., Subramanian, S., Jithesh, M. N., Rayorath, P., Hodges, D. M., Critchley, A. T., Craigie, J. S., Norrie, J. (2009): Seaweed extracts as biostimulants of plant growth and development. – *J. Plant Growth Regul.* 28: 386-399.
- [22] Kong, C. H., Xu, X. H., Zhou, B., Hu, F., Zhang, C. X., Zhang, M. X. (2004a): Two compounds from allelopathic rice accession and their inhibitory activity on weeds and fungal pathogens. – *Phytochemistry* 65: 1123-1128.
- [23] Kong, C. H., Laing, W. J., Xu, X. H., Hu, F., Wang, P., Jiang, Y. (2004b): Release and activity of allelochemicals from allelopathic rice seedlings. – *J. Agric. Food Chem.* 52: 2861-2865.
- [24] Kong, C. H., Zhao, H., Xu, X. H., Wang, P., Gu, Y. (2007): Activity and allelopathy of soil of flavone O-Glycosides from rice. – *J. Agric. Food Chem.* 55: 6007-6012.
- [25] Kong, C. H., Xuan, T. D., Khanh, T. D., Tran, H. D., Trung, N. T. (2019): Allelochemicals and signaling chemicals in plants. – *Molecules* 24: 2737.
- [26] Ling, Y., Zhang, Q., Zhong, W., Chen, M., Gong, H., He, S., Liang, R., Lv, J., Song, L. (2019): Rapid identification and analysis of the major chemical constituents from the fruits of *Sapindus mukorossi* by HPLC-ESI-QTOF-MS/MS. – *Nat. Prod. Res.* 34: 2144-2150.
- [27] Macías, F. A., Molinillo, J. M. G., Varela, R. M., Galindo, J. C. G. (2007): Allelopathy-a natural alternative for weed control. – *Pest Manag. Sci.* 63: 327-348.
- [28] Macías, F. A., Oliveros-Bastida, A., Marin, D., Carrera, C., Chinchilla, N., Molinillo, J. M. G. (2008): Plant biocommunicators: their phytotoxicity, degradation studies and potential use as herbicide models. – *Phytochem. Rev.* 7: 179-194.
- [29] Mallik, A. U., Pellissier, F. (2000): Effects of *Vaccinium myrtillus* on Spruce regeneration: testing the notion of coevolutionary significance of allelopathy. – *J. Chem. Ecol.* 26: 2197-2209.
- [30] Mallik, A. U. (2003): Conifer regeneration problems in boreal and temperate forests with ericaceous understory: role of disturbance, seedbed limitation, and keystone species change. – *Crit. Rev. Plant Sci.* 22: 341-366.
- [31] Mierziak, J., Kostyn, K., Kulma, A. (2014): Flavonoids as important molecules of plant interactions with the environment. – *Molecules* 19: 16240-16265.
- [32] Ming, Y., Hu, G. X., Li, J., Zhu, Z. J., Fan, X. M., Yuan, D. Y. (2020): Allelopathic effects of *Castanea henryi* aqueous extracts on the growth and physiology of *Brassica pekinensis* and *Zea mays*. – *Chem. Biodivers.* e2000135.
- [33] Miransari, M., Smith, D. L. (2014): Plant hormones and seed germination. – *Environmen. Exp. Bot.* 99: 110-121.
- [34] Moles, A. T., Westoby, M. (2004): Seedling survival and seed size: a synthesis of the literature. – *J. Ecol.* 92: 372-383.
- [35] Morgan, E. C., Overholt, W. A. (2005): Potential allelopathic effects of Brazilian pepper (*Schinus terebinthifolius* Raddi, Anacardiaceae) aqueous extract on germination and growth of selected Florida native plants. – *J. Torrey Bot. Soc.* 132: 11-15.
- [36] Ojija, F., Arnold, S. E., Treydte, A. C. (2019): Bio-herbicide potential of naturalised *Desmodium uncinatum* crude leaf extract against the invasive plant species *Parthenium hysterophorus*. – *Biol. Invasions* 21: 3641-3653.
- [37] Ooka, J. K., Owens, D. K. (2018): Allelopathy in tropical and subtropical species. – *Phytochem Rev.* 17: 1225-1237.
- [38] Paez-Garcia, A., Motes, C. M., Scheible, W., Chen, R., Blancaflor, E. B., Monteros, M. J. (2015): Root Traits and phenotyping strategies for plant improvement. – *Plants* 4: 334-355.
- [39] Peti, E., Schellenberger, J., Németh, G., Málnási Csizmadia, G., Oláh, I., Török, K., Czóbel, S. Z., Baktay, B. (2017): Presentation of the HUSEED<sup>wild</sup> – a seed weight and germination database of the Pannonian flora – through analysing life forms and social behaviour types. – *Appl. Ecol. Env. Res.* 15: 225-244.

- [40] Ranal, M. A., Santana, D. G. D. (2006): How and why to measure the germination process? – Braz. J. Bot 29: 1-11.
- [41] Rice, E. L. (1984): Allelopathy, 2nd edition. – Academic Press: New York.
- [42] Rimando, A. M., Olofsson, M., Dayan, F. E., Duke, S. O. (2001): Searching for rice allelochemicals. – Agronomy J. 93: 16-20.
- [43] Robertson, G. P., Paul, E. A. (1999): Decomposition and soil organic matter dynamics. – In: Sala, O. E., Jackson, R. B., Mooney, H. A., Howarth, R. W. (eds.) Methods of ecosystem science. Springer Press, New York.
- [44] Rout, M. E., Callaway, R. M. (2009): An invasive plant paradox. – Science 324: 724-725.
- [45] Scognamiglio, M., Esposito, A., D'Abrosca, B., Pacifico, S., Fiumano, V., Tsafantakis, N., Monaco, P., Fiorentino, A. (2012): Isolation, distribution and allelopathic effect of caffeic acid derivatives from *Bellis perennis* L. – Biochem. Syst. Ecol. 43: 108-113.
- [46] Shannon, M. C., Grieve, C. M. (1998): Tolerance of vegetable crops to salinity. – Sci. Hortic-Amsterdam 78: 5-38.
- [47] Singh, R., Kumari, N. (2015): Comparative determination of phytochemicals and antioxidant activity from leaf and fruit of *Sapindus mukorossi* Gaertn. - a valuable medicinal tree. – Ind. Crop. Prod. 73: 1-8.
- [48] Turk, M. A., Tawaha, A. M. (2003): Allelopathic effect of black mustard (*Brassica nigra* L.) on germination and growth of wild oat (*Avena fatua* L.). – Crop Prot. 22: 673-677.
- [49] Van Volkenburg, H., Guinel, F. C., Vasseur, L. (2020): Impacts of smooth pigweed (*Amaranthus hybridus*) on cover crops in Southern Ontario. – Agronomy 10: 529.
- [50] Veen, G. F., Fry, E. L., ten Hooven, F. C., Kardol, P., Morriën, E., De Long, J. R. (2019): The role of plant litter in driving plant-soil feedbacks. – Front. Environ. Sci. 7: 168.
- [51] Wang, X. F., Xing, W., Wu, S. H. (2009): Allelopathic effects of seed extracts of four wetland species on seed germination and seedling growth of *Brassica rapa* spp. *pekinensis*, *Oryza rufipogon* and *Monochoria korsakowii*. – Fresen. Environ. Bull. 18: 1832-1838.
- [52] Zheng, Y. L., Feng, Y. L., Zhang, L. K., Callaway, R. M., Valiente-Banuet, A., Luo, D. Q., Liao, Z. Y., Lei, Y. B., Barclay, G. F., Silva-Pereyra, C. (2014): Integrating novel chemical weapons and evolutionarily increased competitive ability in success of a tropical invader. – New Phytol. 205: 1350-1359.



# RICE-DERIVED BIOCHARS ENHANCE THE YIELD OF SPRING ONION (*ALLIUM CEPA* L. VAR. *AGGREGATUM*), WHILE REDUCING PESTICIDE CONTAMINATION IN SOIL AND PLANT

HEMOWNG, S.<sup>1\*</sup> – SANGRIT, C.<sup>1</sup> – PHUNTHUPAN, P.<sup>1</sup> – BUTNAN, S.<sup>2</sup> – VITYAKON, P.<sup>3</sup>

<sup>1</sup>*Program of Plant Science, Faculty of Agriculture and Technology, Nakhon Phanom University, Nakhon Phanom 48000, Thailand*

<sup>2</sup>*Program of Plant Science, Faculty of Agricultural Technology, Sakon Nakhon Rajabhat University, Sakon Nakorn 47000, Thailand*

<sup>3</sup>*Department of Soil Science and Environment, Faculty of Agriculture, Khon Kaen University, Khon Kaen 40002, Thailand*

\*Corresponding author

e-mail: saowakon@hotmail.com; phone: +66-88-572-1525

(Received 25<sup>th</sup> Aug 2020; accepted 19<sup>th</sup> Nov 2020)

**Abstract.** The increasing demand for crop production has resulted in the excessive use of chemical fertilizers and pesticides, which is a problem due to toxic residuals. However, the application of biochar has been used to absorb pesticides to reduce contaminants in soil and increase soil fertility and spring onion growth. The objective of this experiment was to investigate the effects of biochar on chemical residual adsorption in the soil, as well as the yield and growth of spring onions. The experimental field was located at a farm in Nakhon Phanom Province, Thailand. Three treatments were implemented in a randomized complete block design (RCBD) with 4 replications: 1) raw rice husk (RH), 2) rice husk biochar (RHB) and 3) rice straw biochar (RSB). The results showed that the growth of spring onions under RSB and RH was greater than under RHB. The highest fresh yields were obtained when RSB (18 t/ha) was applied, which caused significant improvements in soil fertility, especially due to the high CEC and porosity of RSB. In addition, under biochar amendment, the adsorbed amounts of carbamate (9.18-9.31 mg/kg) and organophosphate (0.20-0.29 mg/kg) pesticides in spring onions decreased compared with those in spring onions in the RH amendment, and the soil concentrations also decreased (<10 mg/kg for both carbamate and organophosphate pesticides). The results suggested that biochar has the potential to reduce the residual chemicals in spring onions and soil more than raw rice husk, which is the current agricultural practice.

**Keywords:** *adsorption, crop production, residual chemical*

## Introduction

Vegetable production in many parts of the world faces problems from the extensive use of chemical pesticides that are harmful to human health and the environment (Shormar et al., 2014). Thailand has problems with low soil fertility and the extensive use of chemical pesticides, especially in spring onion cultivation. From the statistics on the quantity and value of the import of hazardous agricultural substances during years 2011 - 2017, it was found that the number of herbicides, insecticides, and plant disease prevention substances increased annually (Office of Agricultural Economics, 2018). Moreover, the addition of organic materials in the soil has also been found to counteract soil contamination (Khorram et al., 2016).

Biochar is an organic material that is burned under conditions of low oxygen content or no oxygen and high temperature of 300 - 600 °C, which is called pyrolysis (Bruun, 2011). Biochar is one of the most suitable materials used in agriculture for improving

physical, chemical, and biological properties of soil (Prendergast-Miller et al., 2014). Biochar is reported to have a positive effect on nutrient and water retention capacity and crop yields such as those of rice (*Oryza sativa*), maize (*Zea mays*), and Chinese chives (*Allium tuberosum*) (Yang et al., 2010; Zimmerman et al., 2011; Kamara et al., 2015; Naeem et al., 2016). It has been recognized that biochar amendment can reduce the bioavailability of pesticides (Ahmad et al., 2014) and enhance the sorption of different pesticides (Kookana, 2010; Chang et al., 2011). Moreover, biochar can reduce pesticide contamination in the soil up to 86 - 88% and lower residue levels of pesticide uptake by spring onions (*Allium cepa* L.) in biochar amended soil (Yu et al., 2009; Khorram et al., 2016) due to the adsorption capability of biochar (Khorram et al., 2016). The adsorption capacity of biochar for pesticides depends on its physicochemical properties, such as the organic carbon content, specific surface area and porous structure (Yu et al., 2009; Dechene et al., 2014). Despite increasing interest in biochar application in soil to improve soil fertility and carbon sequestration, there has not been sufficient knowledge about the effect of different biochar types on the growth and yield of vegetable crops and its efficiency for reducing soil contamination and plant uptake of pesticide residues. The objective of this study was to investigate the effects of biochar increasing the yield of spring onions and its effectiveness in reducing the contamination of pesticides in soil and plant uptake.

## Materials and Methods

### Biochar production

There were two types of biochar used in this study. Rice husk biochar (RHB) was produced by farmer-traditional kilns at a maximum temperature of 380 °C, while stove pyrolyzed rice straw biochar (RSB) was produced at an approximate temperature of 550 °C (Fig. 1). Microscopic images of both biochars were obtained using scanning electron microscopy (SEM) (JSM 5410LV, JEOL, Japan). The chemical properties of the biochar are presented in Table 1.



**Figure 1.** Biochar production used in this experiment: (A) rice husk biochar produced by farmer-traditional kilns and (B) rice straw biochar produced by biochar stoves

**Table 1.** Chemical properties of the rice husk biochar (RHB) and rice straw biochar (RSB) used in the experiment

Biochar type	pH (1:5 H <sub>2</sub> O)	EC (μS/cm)	Total C (%)	Total N (%)	C/N ratio	CEC (cmolc/kg)
RHB	7.8	0.36	33.68	1.14	29	11.45
RSB	8.7	0.96	42.92	1.42	30	15.76

### Experimental site

The experiment was conducted from January 12, 2018, to March 7, 2018, on silt loam soil (Isohyperthermic Oxyaquic (Ultic) Haplustalfs; That Phanom series) at a farmer field in Bueng Lom village, Dong Khwang Subdistrict, Mueang District, Nakhon Phanom Province, Thailand (17°11'09.8''N, 104°47'35.9''E) (Fig. 2). The soil characteristics were (0-10 cm): pH (H<sub>2</sub>O 1:5), 5.60; organic carbon content, 1.10%; cation exchange capacity (CEC), 2.20 cmolc/kg; and available P and exchangeable K, 4.80 mg/kg and 67 mg/kg, respectively. Weather conditions during the experimental period are presented in Fig. 3.



Figure 2. The experimental site at the farmer field

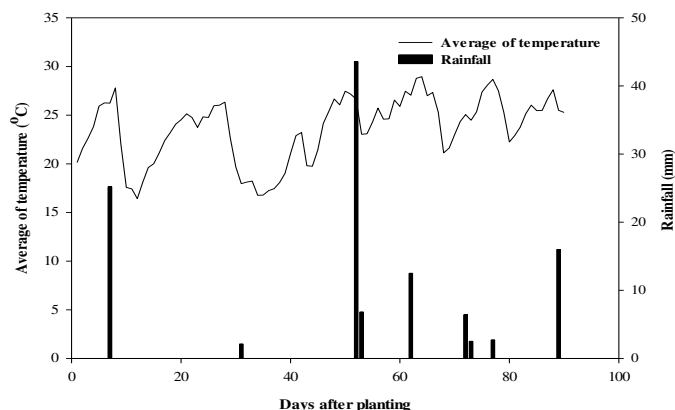


Figure 3. Daily rainfall (mm) and average temperature (°C) at the experimental site during the experimental period

The experimental plots were arranged in a randomized complete block design (RCBD) with three types of organic materials applied 1) raw rice husk (RH; farmer practice), 2) RHB and 3) RSB in 4 replications. One seedling per hill of the “Luplae” variety of spring onion (*Allium cepa* L. var. *aggregatum*) was planted at a spacing of 0.15 m x 0.15 m in the experimental plots of 1 × 2 m then covered uniformly on the soil surface with RH, RHB or RSB for each treatment at a rate of 0.60 kg/plot (3 t/ha). An NPK fertilizer combination of N, P<sub>2</sub>O<sub>5</sub> and K<sub>2</sub>O (15-15-15) was applied at 0.048 g N/plot, 0.048 g P<sub>2</sub>O<sub>5</sub>/plot and 0.048 g K<sub>2</sub>O/plot to spring onions at 7 days after planting.

The pesticides used in this experiment were carbaryl (a carbamate pesticide) and chlorpyrifos (an organophosphate pesticide) and were applied to each treatment. The

pesticide solution was a mixture of 20 ml of carbaryl and 30 grams of chlorpyrifos in 20 liters of water and was directly applied to the soil in each plot at a volume of 1000 ml. The pesticide solution was applied to plants at 14, 28, and 42 days after planting.

### **Data collections**

Ten holes of the spring onion plants per plot were sampled at 12 and 20 days after planting to assess growth (height, plant number per hole, fresh weight, and dry weight). At final harvest (54 days after planting), five holes per plot were uprooted, and the number of plants was carefully counted before plants were thoroughly washed with tap water to remove soil particles, air-dried at room temperature for 3 hours and weighed to obtain the fresh weight after oven drying at 70 °C for 48 hours. The economic return was calculated on a fresh weight basis (t/ha) multiplied by the market price of spring onions (one ton of spring onions = 1,161 USD in January 2018 at the Si Mum Mueang Market, Bangkok, Thailand) and minus biochar production and material costs (400 USD/ha for RH, 504 USD/ha for RHC and 600 USD/ha for RSH).

Fresh spring onion and soil samples (at 0-10 cm soil depth at 10 random locations per plot) were weighed as 1 kg samples in four replications of each treatment and kept in plastic containers at 10 °C until residual pesticide analysis. Analyses of carbamate and organophosphate pesticides in soil and plant samples were performed using the method according to Steinwandter (1985) Fresenius Z. Anal.Chem no. 1155 and no. 322, respectively.

### **Statistical analysis**

Analysis of variance (ANOVA) was performed to determine treatment effects on various measured parameters. A mean comparison was performed by the least significant difference (LSD) test. The significant level was set as  $P \leq 0.05$ . The Statistix 8 program (Analytical Software, 2008) was used.

## **Results**

### **Physical and chemical characteristics of the biochar**

The biochar scanning electron microscopy images clearly showed differences in the porous structures of the two biochars (*Fig. 4*), which was strongly influenced by pyrolysis temperature. A greater number of pores and larger macro-pores appeared in RHB than in RSB. Proximate analysis of the biochar showed that RSB had a higher pH (8.7), EC (0.96  $\mu\text{s}/\text{cm}$ ) and CEC (15.76  $\text{cmolc}/\text{kg}$ ) values than those of RHB (*Table 1*). The total carbon and nitrogen contents of RSB (42.92% and 1.42%, respectively) were higher than those of RHB (33.68% and 1.14%, respectively).

### **Growth and yield of spring onions**

Twelve days after planting, plant height and plant number per hole of the RSB treatment (23 cm and 7 plants/hole) were significantly ( $P < 0.05$ ) higher than those of the RHB treatment (20 cm and 5 plants/hole) but were similar to the RH treatment (22 cm and 6 plants/hole) (*Table 2*). Twenty days after planting, the RSB and RH treatments had a similarly significant effects ( $P < 0.05$ ) on spring onion height. However, the RSB treated spring onions had a lower fresh weight than those treated with RHB and RH

(Table 3). At the final harvest, the fresh weight of the RSB (18 t/ha) and RHB (16 t/ha) onions was significantly higher ( $P<0.05$ ) than that of RH-treated onions (Table 4). Similarly, the economic value of spring onions under RSB (19,828 USD/ha) and RHB (17,834 USD/ha) amendments was significantly greater than that of RH treatment (14,699 USD/ha).

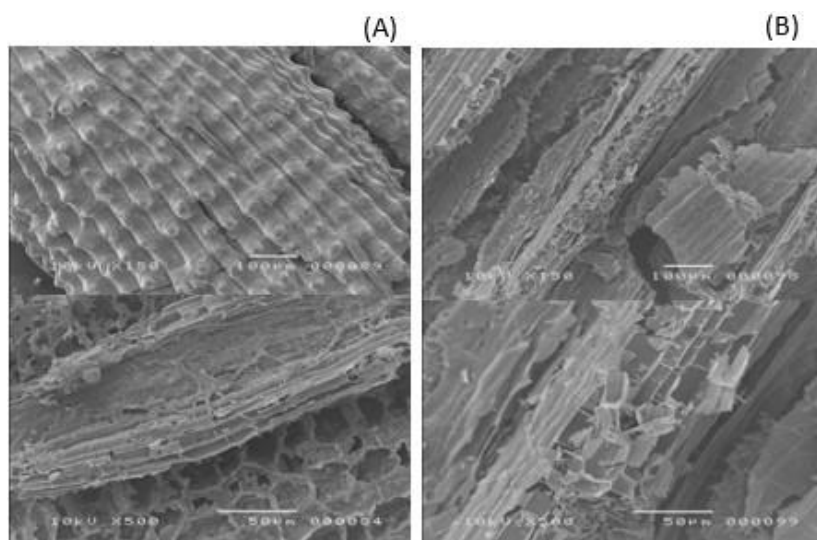


**Figure 4.** Scanning electron microscopy (SEM) images of (A) rice husk biochar (RHB) and (B) rice straw biochar (RSB) used in the experiment

**Table 2.** Growth of spring onions at 12 days after planting<sup>†</sup>

Treatment	Height (cm)	Plant number per hole	Fresh weight	Dry weight
			(g/plant)	
RH	22 ab	6 ab	2.83 a	0.28 a
RHB	20 b	5 b	2.39 a	0.25 a
RSB	23 a	7 a	2.34 a	0.22 a
LSD <sub>.05</sub>	2.37*	1.38*	0.84 <sup>ns</sup>	0.84 <sup>ns</sup>
C.V.(%)	6.34	14.32	19.16	19.39

<sup>ns</sup> = significantly different at  $P>0.05$  and \* = significantly different at  $P<0.05$ , <sup>†</sup>a and b represent significant differences between treatments ( $P<0.05$ )

**Table 3.** Growth of spring onions at 20 days after planting<sup>†</sup>

Treatment	Height (cm)	Plant number per hole	Fresh weight	Dry weight
			(g/plant)	
RH	25 a	7 ab	5.51 a	0.73 a
RHB	23 b	8 a	3.92 b	0.63 a
RSB	24 ab	6 b	5.13 ab	0.76 a
LSD <sub>.05</sub>	2.14*	1.38*	1.54*	0.23 <sup>ns</sup>
C.V.(%)	5.13	14.32	18.32	0.23

<sup>ns</sup> = significantly different at  $P>0.05$  and \* = significantly different at  $P<0.05$ , <sup>†</sup>a and b represent significant differences between treatments ( $P<0.05$ )

**Table 4.** Yield and economic return of spring onions at final harvest<sup>† ‡</sup>

Treatment	Plant number/hole	Fresh weight		Economic value <sup>†</sup> (USD/ha)
		g/plant	t/ha	
RH	7 a	29.25 b	13 b	14,699 b
RHB	7 a	35.53 ab	16 ab	17,834 ab
RSB	6 a	39.58 a	18 a	19,828 a
LSD <sub>.05</sub>	2.43 <sup>ns</sup>	6.36*	2.83*	3,281*
C.V.(%)	21.07	15.56	10.56	10.87

<sup>ns</sup> = significantly different at  $P>0.05$  and \* = significantly different at  $P<0.05$ , <sup>†</sup> Economic value (USD/ha) = (fresh weight (t/ha) × 1,161 USD/t) – biochar production cost, <sup>‡</sup>a and b represent significant differences between treatments ( $P<0.05$ )

### **Pesticide uptake in spring onions and soil contamination**

The fresh spring onions (including above- and below-ground parts) in the RSB and RHB amended treatments had lower concentrations of carbamate (9.18 and 9.31 mg/kg, respectively) than those in the RH treatments (9.65 mg/kg) (Table 5). In addition, plant uptake of organophosphate in RHB and RSB amended soil (0.20 mg/kg and 0.29 mg/kg, respectively) was lower than that in RH amended soil (0.44 mg/kg). Similarly, soil contamination of both carbamate and organophosphate was higher in RH amended soil (0.10 and 0.55 mg/kg, respectively) than in the biochar amended treatments (<0.10 mg/kg for both carbamate and organophosphate).

**Table 5.** The concentration of carbamate and organophosphate contamination in soil and spring onions<sup>†</sup>

Treatment	Carbamate		Organophosphate	
	(mg/kg)			
	soil	spring onion	soil	spring onion
RH	0.10 a	9.65 a	0.55 a	0.44 a
RHB	0.04 b	9.31 b	0.08 b	0.20 b
RSB	0.05 b	9.18 b	0.07 b	0.29 b
LSD <sub>.05</sub>	0.04*	0.14**	0.17**	0.11*
C.V.(%)	19.86	0.45	23.41	11.49

\* = significantly different at  $P<0.05$  and \*\* = significantly different at  $P<0.01$ , <sup>†</sup>a and b represent significant differences between treatments ( $P<0.05$ )

## **Discussion**

### **Biochar quality under different types and conditions**

RHB contains pores that are not connected, which may be attributed to insufficient carbonization at low temperatures compared with RSB. On the other hand, RSB produced at a relatively high temperature showed increased cracks and pores compared to those of RHB, which was also observed by Bai et al. (2017) and Peng et al. (2011). Proximate analysis revealed a high ash content in RSB, as indicated by its high EC content (Wu et al., 2012). Deka et al. (2018) also reported that rice straw-derived biochar was highly alkaline relative to its rice husk-derived counterpart. However, the

EC and CEC properties of biochar are largely determined by its total base content, which varies according to the feedstock type and pyrolysis temperature. The high pyrolysis temperature of 550 °C for RSB led to a higher base content than that of RHB (380 °C) as shown by their EC values. The results of Prima et al. (2015) and Wu et al. (2012) corroborated our results.

### ***Effects of biochar on the growth and yield of spring onions***

The increase in the growth and yield of spring onions under the biochar amendments (RSB and RHB) resulted from increased soil fertility and nutrient retention. Shackley et al. (2012) and Zheng et al. (2010) reported that the addition of RHB at application rates of 10 t/ha, 40 t/ha, and 41.5 t/ha increased rice grain yield and biological yield by 12%, 14%, and 33%, respectively, compared to that of the control. The results of this study showed that RHB and RSB application increased in spring onion yields by 22% and 35%, respectively, compared with that of RH amendment (current farmer practice).

The high total carbon and nitrogen contents of RSB (42.92% and 1.42%, respectively) followed by RHB (33.68% and 1.14%, respectively) may be due to an increase in the temperature of thermal degradation. The increase in nutrient content with thermal degradation by the loss of volatile compounds (C, H, and O) can be explained by Chan and Xu (2009). Naeem et al. (2016) showed that the concentrations of nutrients were greater in the biochar produced at 500 °C than biochar produced at lower temperatures, except for N, the content of which decreased as the temperature increased. However, nitrogen is removed through the loss of the ammonium and nitrate fractions as well as the loss of volatile matter containing N groups at a temperature of 200 °C, but with increased temperatures (>600 °C), N is gradually transformed into a pyridine-like structure (Bagreev et al., 2001). This is related to our result that RSB had a high N content, which was produced with a high pyrolysis temperature (550 °C). The influence of biochar on soil physicochemical and biological properties such as its porous structure and high surface area were conducive to the adsorption of water and nutrients (Mishra et al., 2017), which is shown graphically in *Fig. 4*, and the high CEC value of RSB was noted (*Table 1*). However, recent studies indicated that the influence of biochar depends on the feedstock composition (Jindo et al., 2014; Bai et al., 2017; Mishra et al., 2017), pyrolysis process conditions (Pituello et al., 2015; Butnan et al., 2015), biochar particle size and soil environmental conditions (Butnan et al., 2015). High-temperature biochars are expected to have a greater reactivity in soils than low temperature biochars and better contribution to soil fertility due to low volatile matter and high ash contents and a fixed C content (Butnan et al., 2015).

### ***Effect of biochar on pesticide uptake by plants and contamination in soil***

Biochar amendments increased the adsorption of pesticides in soil with a subsequent decrease in the plant uptake of carbamate and organophosphate pesticides by 3.52 - 4.87 and 34.09 - 54.50%, respectively, relative to that of spring onions grown in raw rice husk-amended soil. According to Yu et al. (2009), significantly lower residue levels of chlorpyrifos and carbofuran in spring onions were found under red gum wood chip biochar amendment compared with that observed under cultivation in unamended soil. Similarly, Khorram et al. (2015) reported that rice husk biochar amendments resulted in significantly enhanced fomesafen adsorption. Additionally, the pesticide adsorption capacity of biochar depends on its physicochemical properties such as pH (Yao et al., 2012), cation exchange capacity (Cheng et al., 2008), carbon content, and porous

structure (Dechene et al., 2014). Moreover, our rice straw biochar amendment stimulated plant growth and reduced pesticide contamination in plants and soil by adsorption due to its higher CEC and porosity than those of rice husk biochar and raw rice husk. Numerous studies have reported that biochar amendments decrease pesticide desorption, degradation and plant uptake because of their remarkably high pesticide adsorption capacities (Spokas et al., 2009; Yu et al., 2010; Khorram et al., 2015), which depend on decreased pesticide desorption, pyrolysis conditions and feedstocks (Ding et al., 2016).

## Conclusions

This study demonstrated the beneficial effects of biochar amendment on increasing plant production. Thus, the results suggested that replacing raw rice husk and/or rice straw with biochar in soil amendment practices led to altered nutrient cycling in soils, increased retention of pesticides in soil and reduced contents of pesticide residues in agricultural produce. Future research to fill pertinent knowledge gaps may allow to determine the optimum amount of biochar required to reduce pesticide residues.

**Acknowledgements.** The research was funded by Thailand Science Research and Innovation (TSRI) and cooperated with Nakhon Phanom University, Thailand.

## REFERENCES

- [1] Ahmad, M., Rajapaksha, A. U., Lim, J. E., Zhang, M., Bolan, N., Mohan, D., Ok, Y. S. (2014): Biochar as a sorbent for contaminant management in soil and water: a review. – *Chemosphere* 99: 19-33.
- [2] Analytical Software. (2008): User's Manual. – Analytical Software, Tallahassee, FL.
- [3] Bagreev, A., Bandosz, T. J., Lock, D. C. (2001): Pore structure and surface chemistry of adsorbent obtained by pyrolysis of sewage derived fertilizer. – *Carbon* 39: 1971-1979.
- [4] Bai, X. F., Zhou, X. Q., Li, Z. F., Ni, J. W., Bai, X. (2017): Properties and applications of biochars derived from different biomass feedstock sources. – *International Journal of Agricultural and Biological Engineering* 10(2): 242-250.
- [5] Bruun, E. W. (2011): Application of fast pyrolysis biochar to a loamy soil-effects on carbon and nitrogen and potential for carbon sequestration. – Ph.D. thesis, Risø National Laboratory of Renewable Energy, Technical University of Denmark.
- [6] Butnan, S., Deenik, J. L., Toomsan, B., Antal, M. J., Vityakon, P. (2015): Biochar characteristics and application rates affecting corn growth and properties of soils contrasting in texture and mineralogy. – *Geoderma* 237-238: 105-116.
- [7] Chan, K. Y., Xu, Z. (2009): Biochar: Nutrient properties and their enhancement. – In: Lehmann, J., Joseph, S. (eds.) *Biochar for environment: Science and technology*. London, Earthscan.
- [8] Chang, K. L., Lin, J. H., Chen, S. T. (2011): Adsorption studies on the removal of pesticides (carbofuran) using activated carbon from rice straw agricultural waste. – *International Scholarly and Scientific Research and Innovation* 5(4): 210-213.
- [9] Cheng, C-H., Lehmann, J., Engelhard, M. H. (2008): Natural oxidation of black carbon in soils: changes in molecular form and surface charge along a climosequence. – *Geochimica et Cosmochimica Acta* 72: 1598-1610.
- [10] Dechene, A., Rosendahl, I., Laabs, V., Amelung, W. (2014): Sorption of polar herbicides and herbicide metabolites by biochar-amended soil. – *Chemosphere* 109: 180-186.



- [11] Deka, K., Medhi, B. K., Kandali, G. G., Das, R., Pathak, K., Sarkar, L., Nath, K. D. (2018): Evaluation of physico-chemical properties of rice straw and rice husk-derived biochar. – *Ecology, Environment and Conservation* 24(2): 768-772.
- [12] Ding, Y., Liu, Y., Liu, S., Li, Z., Tan, X., Huang, X., Zeng, G., Zhou, L., Zheng, B. (2016): Biochar to improve soil fertility: A review. – *Agronomy for Sustainable Development* 36(2): 1-18.
- [13] Jindo, K., Mizumoto, H., Sawada, Y., Sanchez-Monedero, M. A., Sonoki, T. (2014): Physical and chemical characterization of biochars derived from different agricultural residues. – *Biogeosciences* 11: 6613-6621.
- [14] Kamara, A., Kamara, H. S., Kamara, M. S. (2015): Effect of rice straw biochar on soil quality and the early growth and biomass yield of two rice varieties. – *Agricultural Science* 6: 798-806.
- [15] Khorram, M. S., Wang, Y., Jin, X., Fang, H., Yu, Y. (2015): Reduced mobility of fomesafen through enhanced adsorption in biochar-amended soil. – *Environmental Toxicology and Chemistry* 34(6): 1258-1266.
- [16] Khorram, M. S., Zhang, Q., Lin, D., Zheng, Y., Fang, H., Yu, Y. (2016): Biochar: A review of its impact on pesticide behavior in soil environments and its potential applications. – *Journal of Environmental Science* 44: 269-279.
- [17] Kookana, R. S. (2010): The role of biochar in modifying the environmental fate, bioavailability, and efficacy of pesticides in soils: a review. – *Australian Journal of Soil Research* 48: 627-637.
- [18] Mishra, A., Taking, K., Hall, M. W., Shinogi, Y. (2017): Effects of rice husk and rice charcoal on soil physicochemical properties, rice growth and yield. – *Agricultural Sciences* 8: 1024-1032.
- [19] Naeem, M. A., Khalid, M., Ahmad, Z., Naveed, M. (2016): Low pyrolysis temperature biochar improves growth and nutrient availability of maize on Typic Calcic Argid. – *Communications in Soil Science Plant Analysis* 47(1): 41-51.
- [20] Office of Agricultural Economics (2018): Value of Agricultural Chemicals Imports in Thailand from 2011 to 2017. – Office of Agricultural Economics. Bangkok, Thailand.
- [21] Peng, X., Ye, L. L., Wang, C. H., Zhou, H., Sun, B. (2011): Temperature- and duration-dependent rice straw-derived biochar: Characteristics and its effects on soil properties of an Ultisol in southern China. – *Soil and Tillage Research* 112(2): 159-166.
- [22] Pituello, C., Francioso, O., Simonetti, G., Pisi, A., Torreggiani, A., Berti, A., Morari, F. (2015): Characterization of chemical-physical, structural and morphological properties of biochars from biowastes produced at different temperatures. – *Journal Soils and Sediments* 15(4): 202-214.
- [23] Prendergast-Miller, M. T., Duvall, M., Sohi, S. P. (2014): Biochar–root interactions are mediated by biochar nutrient content and impacts on soil nutrient availability. – *European Journal of Soil Science* 65: 173-185.
- [24] Prima, E., Ari Pratiwi, A., Shinogi, Y. (2015): Rice husk biochar application to paddy soil and its effects on soil physical properties, plant growth, and methane emission. – *Paddy and Water Environment* 14(4): 521-532.
- [25] Shackley, S., Carter, S., Knowles, T., Middelink, E., Haefele, S., Sohi, S., Cross, A., Haszeldine, S. (2012): Sustainable gasification-biochar systems? A case-study of rice-husk gasification in Cambodia, Part I: Context, chemical properties, environmental and health and safety issues. – *Energy Policy* 42: 49-58.
- [26] Shormar, B., Al-Saad, K., Nriagu, J. (2014): Mishandling and exposure of farm workers in Qatar to organophosphate pesticides. – *Environmental Research* 133: 312-320.
- [27] Spokas, K., Koskinen, W. C., Baker, J. M., Reicosky, D. C. (2009): Impacts of woodchip biochar additions on greenhouse gas production and sorption/ degradation of two herbicides in a Minnesota soil. – *Chemosphere* 77: 574-581.

- [28] Steinwandter, H. (1985): Universal 5-min on-line method for extracting and isolating pesticide residues and industrial chemicals. – Fresenius' Zeitschrift für analytische Chemie 322: 752-754.
- [29] Wu, W., Yang, M., Feng, Q., Mcgrouter, K., Wang, H., Lu, H., Chen, Y. (2012): Chemical characterization of rice-straw-derived biochar for soil amendment. – Biomass Bioenergy 42: 268-276.
- [30] Yang, X. B., Ying, G. G., Peng, P. A., Wang, I. (2010): Influence of biochars on plant uptake and dissipation of two pesticides in an agricultural soil. – Journal of Agricultural and Food Chemistry 58(13): 7915-7921.
- [31] Yao, Y., Gao, B., Zhang, M., Inyang, M., Zimmerman, A. R. (2012): Effect of biochar amendment on sorption and leaching of nitrate, ammonium, and phosphate in a sandy soil. – Chemosphere 89: 1467-1471.
- [32] Yu, X. Y., Ying, G. G., Kookana, R. S. (2009): Reduced plant uptake of pesticides with biochar additions to soil. – Chemosphere 76(5): 665-671.
- [33] Yu, X. Y., Pan, L. G., Ying, G. G., Kookana, R. S. (2010): Enhanced and irreversible sorption of pesticide pyrimethanil by soil amended with biochars. – Journal of Environment Sciences 22(4): 615-620.
- [34] Zheng, W., Guo, M. X., Chow, T., Bennett, D. N., Rajagopalan, N. (2010): Sorption properties of greenwaste biochar for two triazine pesticides. – Journal of Hazardous Materials 181(1-3): 121-126.
- [35] Zimmerman, A. R., Gao, B., Ahn, M. Y. (2011): Positive and negative carbon mineralization priming effects among a variety of biochar-amended soils. – Soil Biology and Biochemistry 43: 1169-1179.

# BIOMASS ESTIMATION BASED ON MULTILINEAR REGRESSION AND MACHINE LEARNING ALGORITHMS IN THE MAYOMBE TROPICAL FOREST, IN THE DEMOCRATIC REPUBLIC OF CONGO

OPELELE, O. M.<sup>1,2,3</sup> – YU, Y.<sup>1,2\*</sup> – FAN, W.<sup>1,2\*</sup> – CHEN, C.<sup>1,2</sup> – KACHAKA, S. K.<sup>3</sup>

<sup>1</sup>*School of Forestry, Northeast Forestry University, Harbin 150040, Heilongjiang, PR China*

<sup>2</sup>*Key Laboratory of Sustainable Forest Ecosystem Management – Ministry of Education, School of Forestry, Northeast Forestry University, Harbin 150040, Heilongjiang, PR China*

<sup>3</sup>*Department of Natural Resources Management, Faculty of Agricultural Sciences, University of Kinshasa, 117 Kinshasa XI, Mont-Amba/Lemba, Democratic Republic of Congo*

*\*Corresponding authors*

*e-mail: fanwy@163.com, yuying4458@163.com; phone: +86-139-4605-5384*

(Received 28<sup>th</sup> Aug 2020; accepted 19<sup>th</sup> Nov 2020)

**Abstract.** Accurate forest aboveground biomass estimations have always been of crucial importance for sustainable forest management. However, a choice of the suitable statistical modelling method and predictor variables from remotely sensed data remains the keystone for providing accurate aboveground biomass estimates. The present study intended to compare the potential of four modelling techniques, including RandomForest, Support vector machine, multilinear regression, and K-nearest neighbour for estimating aboveground biomass using vegetation indices, spectral information, and both vegetation indices and spectral bands. The results have revealed that machine learning algorithms provide better results than the multilinear regression method. Indeed, the multilinear regression method produced the lowest  $R^2$  and the greatest RMSE. Besides, the RandomForest performed better by providing accurate results compared to other machine learning algorithms. However, comparing the three sets of predictors, the vegetation indices have yielded accurate results of aboveground biomass and the strongest modelling power. Our results have also revealed that the RF is the best choice for predicting aboveground biomass for the purpose of reducing over- or under-estimation problems. This study has demonstrated the potential of the machine learning algorithms in predicting aboveground biomass in the tropical forest, using freely remotely sensed data derived from sensors with medium spatial resolution.

**Keywords:** *aboveground biomass, Landsat 8 Operational Land Imager, Mayombe, machine learning*

## Introduction

Forest ecosystems store up to 80% and 40% of aboveground and underground carbon, respectively (Mohammadi et al., 2017) and can strongly contribute to mitigating effects of climate change (Moroni, 2013; Caputo, 2009; Brown et al., 1996; Zhang et al., 2014). Numerous studies have shown that biomass is an essential parameter for the carbon sequestration description. However, forest programs based on reducing carbon emissions require the accurate estimation of forest biomass.

In general, the biomass comprises of aboveground biomass (AGB) and belowground biomass (BGB) (Lu, 2006). Therefore, due to the difficult works related to the acquisition and calculation of the BGB, several studies are focused principally on AGB.

Forest biomass has already been measured using several allometric methods based on numerous tree measurements (Manyanda et al., 2019; Mohammadi et al., 2017; Vashum and Jayakumar, 2012). Therefore, forest biomass estimation relying on field inventory

is more expensive, arduous, and unrealizable in unreachable areas, thereby making it practicable only in relatively small and accessible areas. Currently, it is possible to optimize this inventory work and reduce the field measurement costs using techniques combining remote sensing technology and field inventories. Indeed, the remote sensing technology, with its capabilities of providing updated information on large areas, has been successfully used for spatial distribution and temporal variation of forest biomass. Several studies have reported that remote sensing variables are useful predictors of biomass because of a strong correlation between biomass and reflectance at different wavelengths (Phua and Saito, 2003; Lu et al., 2004; Zheng et al., 2004). Also, McRoberts et al. (2013) have stated that biomass models using remotely sensed data produce more accurate results than other traditional models. Previously, much research has been completed to estimate AGB in forest ecosystems (Zhang et al., 2014; Dixon et al., 1994; Saatchi et al., 2009; Pflugmacher et al., 2014; López-Serrano et al., 2016; Zhu and Liu, 2015; Glenn et al., 2016). In this research, different remote sensing data (spectral bands and variables derived from spectral bands) and various modelling techniques have been used. However, the remote sensing technology for modelling aboveground biomass implies several main issues. Some of them are related to the remotely sensed derived spectral information that is used as predictor variables (Wang et al., 2013; Lu et al., 2016; Frazier et al., 2014), while others are related to the suitable statistical modelling approach (Shao et al., 2016; Alrababah et al., 2011). According to Lu et al. (2006), two categories of techniques have been used for modelling forest biomass, including parametric and nonparametric methods.

The parametric methods are related to statistical regression, such as linear regression (Lu et al., 2016). In fact, multilinear models are frequently applied to estimate aboveground biomass. However, the relationships between aboveground biomass and predictor variables derived from remotely sensed data might not be linear; consequently, it can lead to overestimation or underestimation problems for small or high aboveground biomass values (Zhao et al., 2016). Therefore, much research has been conducted to examine the use or the potential of nonparametric algorithms, including support vector regression, K-nearest neighbour, and random forest (Li et al., 2014; Vauhkonen et al., 2010; Lu et al., 2016; Gleason and Im, 2012). However, Kumar and Mutanga (2017) have mentioned that among various AGB modelling methods based on different remotely sensed and field data, it is difficult to state or declare that there is one more suitable model than others without assessing their performance separately. In fact, in the field of aboveground biomass estimation using remote sensing technology, the result accuracy depends on different factors, including forest types, remote sensing sensors, and topographical features. Similarly, Feng et al. (2017) have reported that no single modelling method has been determined to be the best for predicting aboveground biomass. Also, Fassnacht et al. (2014) have demonstrated that in the frame of modelling forest biomass based on remote sensing technique, the modelling approach is as important as the data type in deriving accurate AGB estimates.

However, among all previous studies that have tackled the main methods for modelling aboveground biomass, it is unclearly known how data types, forest types, and modelling methods affect aboveground biomass prediction results, especially in the Mayombe tropical forest of the Democratic Republic of Congo, where less research has been carried out for aboveground biomass estimation.

In this research, the main objective was to compare different statistical modelling methods for generating estimates of AGB in the Mayombe forest. The machine learning

algorithms and multilinear regression method were then used to estimate the aboveground forest biomass based on remotely sensed data and field biomass measurement. After comparing the performance of the four different models, the suitable model was used to produce a forest biomass map of our study area.

## Materials and methods

### Study area

The study area is located in the central zone of the Biosphere Reserve of Luki (Fig. 1), in the Southwestern part of the Democratic Republic of Congo. It is located between 5.5-5.6°S in latitude and 13.08-13.24°E in longitude. Its total land area is estimated at 8347 ha, entirely located in the Congolese Mayombe tropical forest. The region is dominated by tropical forest and humid tropical climate (Aw5, according to Köppen's classification). This climate is characterized by two seasons notably a rainy season of seven months (mid-October to mid-May) and a dry season of five months (mid-May to mid-October). The annual average temperature and the annual average precipitation are 28.8 °C and 1032.72 mm, respectively. The vegetation is dominated by the primary forest.

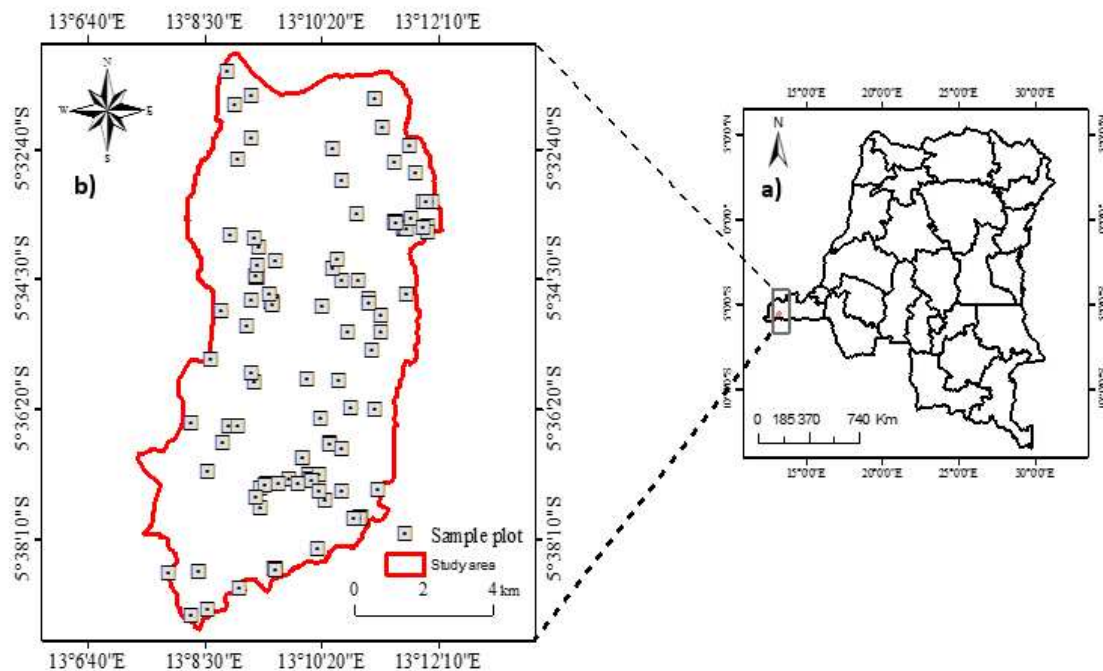


**Figure 1.** Study area location and forest sample plot. (a) The Democratic Republic of Congo, (b) the study area

### Data collection from the field and aboveground biomass estimation

One hundred fourteen square plots with size 30 × 30 m (corresponding to a Landsat pixel) were installed in the forest from June to July of the year 2019. We recorded the plot centre geographic coordinates using GPS (global positioning system) receivers. For the purpose of reducing the GPS horizontal locational error (~5 to 10 m), we considered

final plot positions based on the criterion that the forest structure and composition in a 10-m buffer around the plot are the same as within the plot. The tree height (m) and tree diameter at breast height (cm) were measured on each tree inside of each sample plot. Also, the name of each tree with diameter at breast height (DBH) greater than 10 cm was reported. To compute the aboveground biomass of individual trees using diameter and tree height, allometric models were used. Several allometric models have been developed for the tropical forest. However, due to the literature review, no allometric model for estimating aboveground biomass is available locally for the Mayombe tropical forest of the Democratic Republic of Congo. Therefore, the allometric equation of Fayolle et al. (2013) was adapted to convert field data to AGB per tree. The predicted tree aboveground forest biomass within each plot was summed to represent plot biomass (expressed in Mg/900 m<sup>2</sup>). After that, the expansion factor was used to calculate the AGB per hectare for each plot.

### **Remote sensing dataset and preprocessing**

Surface reflectance Landsat image of 2019 (the 18th of June), with 30 m resolution (path 183 and row 64), was acquired through the USGS Earth Explorer (earthexplorer.usgs.gov). The image was cloud-free and was corrected for atmospheric and topography conditions by the provider. Using the spectral bands (red, blue, and near-infrared bands), we calculated various vegetation indices (*Table 1*), which were used to estimate the aboveground biomass of the area under study. In this paper, based on the correlation between different spectral variables and biomass, numerous machine learning algorithms and a multilinear regression model were performed to predict aboveground biomass. Based on the geographic coordinates of the centre of each sample plot, the spectral variable values, were calculated within the area of each plot using R software; then, we established a database of predictors (vegetation indices and spectral bands) versus biomass values.

**Table 1.** Information on remote sensing variables

<b>Image spectral information</b>	<b>Band 2 (Blue), Band 3 (Green), Band 4 (Red), Band 5 (NIR), Band 6 (SWIR1), Band 7 (SWIR2)</b>
<b>Vegetation indices</b>	<b>Equation</b>
Soil adjusted vegetation index (SAVI)	$((\text{NIR} - \text{R}) / (\text{NIR} + \text{R} + \text{L})) \times (1 + \text{L})$ (Eq.1)
Normalized difference vegetation index (NDVI)	$\text{NIR} - \text{R} / \text{NIR} + \text{R}$ (Eq.2)
Ratio vegetation index (RDVI)	$(\text{NDVI} \times \text{DVI})^{0.5}$ (Eq.3)
Optimized soil-adjusted vegetation index (OSAVI)	$(\text{NIR} - \text{R} / \text{NIR} + \text{R} + \text{L}) \times (1 + \text{L})$ (Eq.4) where <i>L</i> is the soil brightness correction factor; <i>L</i> = 0.5 works well in most situations and is the default value
Simple ratio (SR)	$\text{NIR} / \text{R}$ (Eq.5)
Modified soil adjusted vegetation index (MSAVI)	$(2 * \text{NIR} + 1 - \text{sqrt}((2 * \text{NIR} + 1)^2 - 8 * (\text{NIR} - \text{R}))) / 2$ (Eq.6)
Difference vegetation index (DVI)	$\text{NIR} - \text{R}$ (Eq.7)
Enhanced vegetation index (EVI)	$5 \times (\text{NIR} - \text{R}) / (\text{NIR} + 6 \text{R} - 7.5 \text{Blue} + 1)$ (Eq.8)

NIR: near-infrared; R: red band

Among the four models under study, we selected the best model based on the performance of each of them in terms of predictive power and the accuracy in AGB estimates. Then, we performed the selection of the most important variables using the best model. Finally, the best model was used to produce the map of the AGB spatial distribution in the study area.

### ***Modelling methods***

In this study, four different modelling methods were tested to estimate forest AGB including RandomForest (RF), Support vector regression (SVR), multilinear regression (MLR), and K-nearest neighbour (KNN).

MLR is one among parametric prediction methods commonly used to predict forest AGB using remotely sensed data (Zhu and Liu, 2015; Fassnacht et al., 2014; Lu et al., 2016; Zhao et al., 2016). For this study, we used the ordinary least squares regression method to predict forest aboveground biomass values. However, compared to the machine learning algorithm, the linear regression approach depends on certain assumptions, including the linearity in the relationship between explained and explanatory variables, independence, and normal distribution of errors with a mean value of zero and constant variance. Therefore, the non-respect of these assumptions leads to their violation. Thus, the method is less flexible when facing nonlinear problems (Li et al., 2017), and cannot adequately handle the multicollinearity problem (Ju et al., 2008).

The RF algorithm has been widely used to predict aboveground biomass (Avitabile et al., 2012; Chen, 2015; Pflugmacher et al., 2014; Vauhkonen et al., 2010; Hudak et al., 2012; Tanase et al., 2014). A random forest (RF) algorithm is a tree-based modelling method using a set of rule-based decisions to assess the relationships between a response variable and its predictor variables (Gleason and Im, 2012). This method can generate a large number of small trees built through a different randomly permuted sample from the input dataset (Breiman, 2001). The target data are categorized through two offspring at each node split to maximize homogeneity, and the best split is selected. Finally, the target data for each tree are achieved using bootstrap resampling (Were et al., 2015). Applying unique tree bagging and selection of a random subset of covariates results in minimization of within-group variance and overcoming the over-fitting problem (Park et al., 2016).

The nearest neighbour approach is one of the nonparametric methods used in remote sensing technology (Shataee, 2013), to predict the values of variables using the information of its neighbours (Cover and Hart, 1967). With these techniques, predictions are computed as linear combinations of observations for population units in a sample that are similar or nearest in the space of auxiliary variables to population units requiring predictions (Chirici et al., 2016). The performance of this algorithm depends on the number of neighbours retained by the model (López-Serrano et al., 2016).

The support vector machine (SVM) algorithm states that each ensemble of predictor variables has a unique relationship to the response variable, and sets of explanatory variables can be used to identify the rules to predict a response variable from a set of predictor variables (Mountrakis et al., 2011). It changes the input dataset into a multidimensional hyperplane space by using a kernel function to separate groups of input data with similar response variables to predict a response variable (Were et al., 2015). Indeed, hyperplanes are multidimensional space. In consequence, each explanatory variable is represented by axes from which hyperplanes are built. In that space, the explained variables are placed by projecting it following its explanatory

variable values. The SVM applies support vectors to assign each target to a well-fragmented space (Görgens et al., 2015). The main idea behind SVM is to minimize structural risk and moderate the overfitting problem (Latifi et al., 2015).

### ***Model development and verification of estimation models***

In the field of biomass estimation, the assessment of the model's performance and accuracy are of crucial importance in terms of selecting a suitable model (Mayer and Butler, 1993). Thus, the k-fold cross-validation approach was considered to examine the performance of the different models. In this research, the 10-fold cross-validation approach was mainly applied as it involves the random partitioning of the original dataset into k subsets (10) with equal size. Among k subsets, every single subset should be held out and used as testing data, while the others k subsets are using as training data. The procedure has a k-times number of repetitions. Also, every k subset is used one time for testing the model. Then, the results are averaged depending on the k number, to provide an overall accuracy. This technique provides many advantages, of which, all instances can be used for validating and training the model. In addition to the cross-validation method, number of validation measures (Eqs. 9-11), including the root mean square percentage error (RMSPE), root mean squared error (RMSE), R<sup>2</sup>, were calculated to evaluate the model's performance and assess the accuracy of the model using the testing dataset (25%). All statistical analyses were carried out using R software.

Root mean square error (RMSE):

$$RMSE = \sqrt{\frac{1}{n} \sum_{i=1}^n (y_i - \hat{y}_i)^2} \quad (\text{Eq.9})$$

Root mean square percentage error (RMSPE):

$$RMSPE = \sqrt{\frac{1}{n} \sum_{i=1}^n \left( \frac{y_i - \hat{y}_i}{y_i} \right)^2} \times 100 \quad (\text{Eq.10})$$

Coefficient of determination:

$$R^2 = 1 - \sqrt{\frac{\sum_{i=1}^n (y_i - \hat{y}_i)^2}{\sum_{i=1}^n (y_i - \bar{y})^2}} \quad (\text{Eq.11})$$

where  $y_i$  is the observed AGB,  $\hat{y}_i$  is the predicted AGB, n is the number of plots, and  $\bar{y}$  is the mean observed AGB.

## **Results**

### ***Analysis of correlation between AGB and predictors subsection***

Table 2 presents the Pearson's correlation coefficient between all the explanatory variables and the forest AGB. Among all the vegetation indices, the forest AGB was significantly correlated with the NDVI, SR, and RDVI, respectively. For the spectral information, the forest AGB was significantly correlated with the Band4, Band3,



Band2, Band7, and Band6, respectively. However, it has been noted that the NDVI, SR, and RDVI had the highest positive correlation coefficient values among all the predictor variables retained for the present study. At the same time, all spectral bands were negatively correlated with AGB.

**Table 2.** Pearson's correlation coefficients between independent variables and AGB

Statistical parameters							
Variables	r	Variables	r	Variables	r	Variables	r
DVI	-0.069	MSAVI	0.0005	Band2	-0.42***	Band6	-0.29**
SAVI	0.021	OSAVI	0.13	Band3	-0.47***	Band7	-0.35**
EVI	-0.020	SR	0.53***	Band4	-0.52***		
NDVI	0.81***	RDVI	0.42***	Band5	-0.12		

Level of significance, \*\*\* < 0.001; \*\* < 0.01; r, correlation coefficient

### Field-based AGB estimates and predicted AGB estimates

Table 3 presents the descriptive statistics of the field-level forest aboveground biomass and predicted aboveground biomass. Table 3 indicates that the observed AGB biomass ranged between 192.22 to 301.11 t ha<sup>-1</sup>, with a mean value of 250.34 t ha<sup>-1</sup>, and a standard deviation of 29.39 t ha<sup>-1</sup>. For the predicted biomass, it has been found some slight differences among different models and data sources. Also, the predicted biomass was slightly greater or smaller than observed biomass, implying the overall underestimation or overestimation problems.

**Table 3.** Plot-level aboveground and predicted biomass statistics of 114 plots

Data	Model	Min (t/ha)	Max (t/ha)	Mean (t/ha)	SD (t/ha)
Vegetation indices	MLR	187.77	286.91	251.26	26.29
	SVM	204.10	290.53	251.41	25.61
	RF	199.32	290.92	250.39	28.15
	KNN	206.00	287.11	250.23	26.21
Spectral information	MLR	193.98	279.44	250.03	18.79
	SVM	204.90	284.33	248.61	21.53
	RF	209.90	282.19	251.03	20.92
	KNN	210.89	278.00	250.42	20.27
Combination VI and SI	MLR	32.19	291.76	242.23	54.12
	SVM	204.11	289.59	251.44	25.04
	RF	200.74	291.75	250.62	27.91
	KNN	212.04	279.01	251.08	22.80
Field data		192.22	301.11	250.34	29.39

SD, Min, and Max represent standard deviation, minimum, and maximum

### AGB estimates based on the machine learning and multilinear regression models

The performance assessment results of the different machine learning algorithms and multilinear regression based on different datasets, including vegetation indices, spectral

information, and combination of both vegetation indices and spectral information, are presented in *Table 4*. Overall, the machine learning algorithms provide the best prediction performance of aboveground biomass compared to the multilinear regression method, but each algorithm has its performance in predicting aboveground biomass using different data sources. For example, for the support vector machine method, the vegetation indices-based predictors and the combination of both vegetation indices and spectral information produced the highest  $R^2$  values and smallest RMSE and RMSEPE value; spectral information-based variables. For the K- nearest neighbours and RF algorithm, the conclusion is similar to the support vector machine, but for the RF, the  $R^2$  value between vegetation indices-based variables and combination of both vegetation indices and spectral information-based variables were similar. For multilinear regression method, the highest  $R^2$  was reached with vegetation indices-based variables. However, spectral information-based variables provide the greatest RMSE and RMSPE values compared with vegetation indices-based variables and a combination of both vegetation indices and spectral information, except for multilinear regression that has the greatest value with the combination of all predictors. Thus, in general, the vegetation indices-based predictors produced the most accurate results of AGB estimation regardless of which models were used, while the spectral information-based predictors yielded poor performance. The combination of both vegetation indices and spectral information could not improve the modelling performance. According to these results, the RandomForest algorithm provides the most accurate results in predicting biomass, but the accuracy decreases when using spectral information-based predictors. Besides, the Support vector machine yielded the best estimation of the aboveground biomass with spectral information-based predictors. Using the RF algorithm, the most important variables selected were NDVI, Band4, RDVI, SR, Band2, Band6, Band7, Band3, and SAVI, in decreasing order of importance (*Fig. 2*).

### ***Underestimation and overestimation measure based on the machine learning and multilinear regression models***

The goodness of fit can be visualized with the scatterplots showing the linear relationships between the predicted AGB and observed AGB from the sample plots (*Fig. 3*).

After computing the overestimation and underestimation mean values with regard to the mean observed values of aboveground biomass (*Table 5*), it was found that spectral data have much more significant overestimation and underestimation mean values than vegetation indices data and combination of both spectral information and vegetation indices data. The vegetation indices data have the smallest overestimation and underestimation mean values. The fact of combining both spectral information data and vegetation indices data improves the overestimation and underestimation problems regardless of which modelling approaches were used, compared to when the models use only spectral information. In view of the modelling algorithms based on the three datasets, in general, the machine learning algorithms have much smaller overestimation and underestimation problem than multilinear regression regardless of which data sources were used. Comparing the performance of machine learning algorithm in dealing with this issue, it was found that the RF and SVM have much smaller overestimation and underestimation problems than the KNN algorithm. However, the RF algorithm has produced the best performance with the lowest overestimation and underestimation problems.

**Table 4.** Comparison of AGB prediction performance

Data	Model	RMSE (t/ha)	RMSE-CV (t/ha)	RMSPE (t/ha)	R <sup>2</sup>
Vegetation indices	MLR	17.48	2.12	0.06	0.60
	SVM	16.38	1.32	0.06	0.65
	RF	10.22	1.08	0.04	0.86
	KNN	14.75	2.05	0.06	0.72
Spectral information	MLR	27.89	2.25	0.07	0.15
	SVM	24.72	2.04	0.10	0.20
	RF	26.55	2.13	0.11	0.08
	KNN	27.44	2.13	0.11	0.01
Vegetation indices and spectral information	MLR	89.13	1.51	1.58	0.25
	SVM	16.95	1.42	0.07	0.62
	RF	10.44	1.06	0.04	0.86
	KNN	18.47	1.46	0.07	0.55

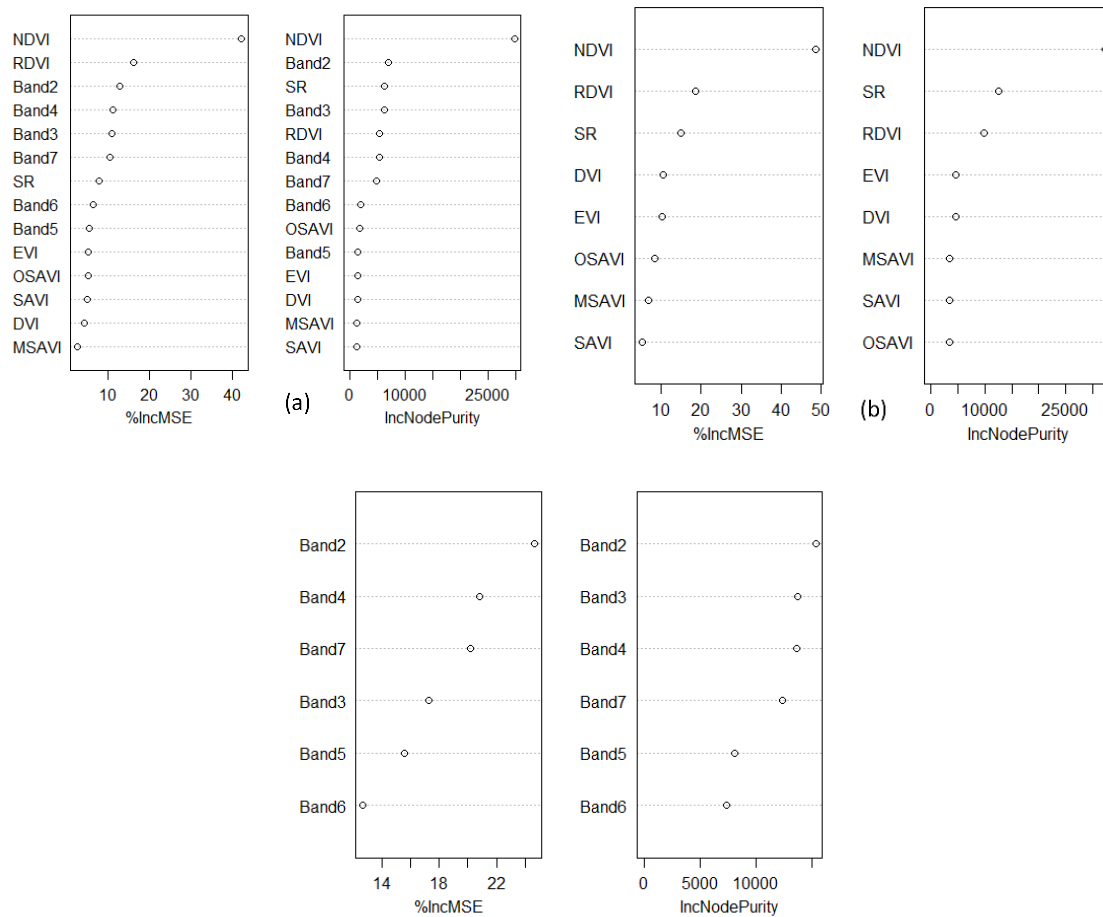


**Figure 2.** Important variable ranking by Random forest algorithm. (a) RandomForest with a combination of both vegetation indices and spectral information; (b) RandomForest with vegetation indices; (c) RandomForest with spectral information

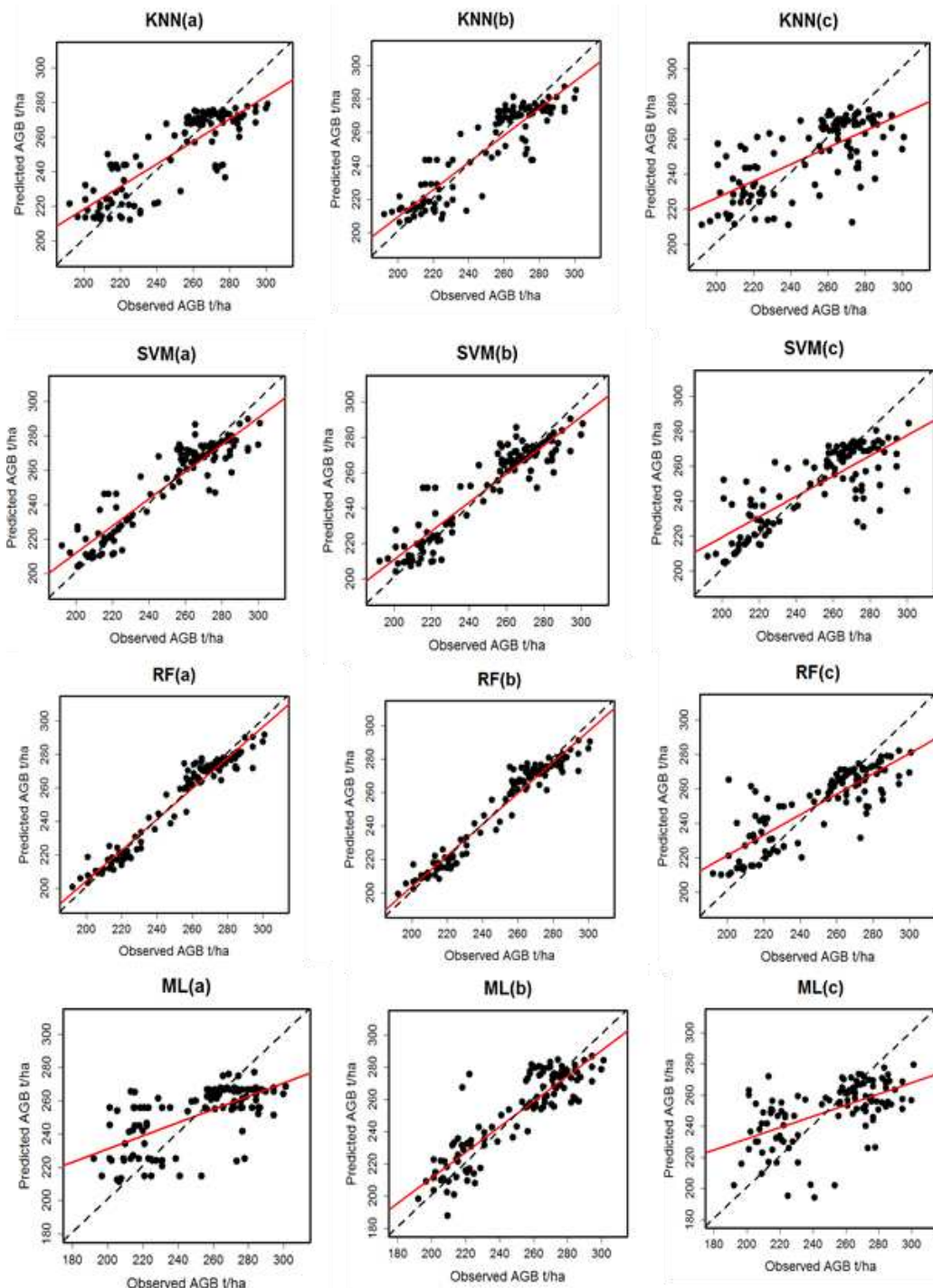


**Figure 3.** Observed AGB versus predicted AGB by KNN, SVM, RF and ML. The solid line indicates the optimal regression of observed versus predicted AGB and the dashed line indicates the 1:1 line of perfect agreement. (Note: (a) represents VI and SI, (b) represents VI and (c) represent SI

### AGB mapping using RF algorithm

Based on the RF algorithm, the suitable algorithm in this study concerning its best performance, as shown in Table 4 ( $R^2 = 0.86$  and  $RMSE = 10.22 \text{ t ha}^{-1}$ ), the map of the

forest AGB was generated. *Figure 4* presents the spatial distribution of the forest AGB within our study area. The prediction results produced different statistics, notably 190.32 t ha<sup>-1</sup>, 274.02 t ha<sup>-1</sup>, 302.8 t ha<sup>-1</sup>, respectively minimum, mean, and maximum predicted biomass value.

**Table 5.** A comparison of mean values of overestimation or underestimation from different data and algorithms

Data	Model	Overestimation	Underestimation
Vegetation indices	MLR	11.88	9.65
	SVM	8.74	7.45
	RF	5.17	5.62
	KNN	8.67	11.35
Spectral information	MLR	18.96	18.92
	SVM	10.62	14.08
	RF	11.79	12.55
	KNN	15.15	17.88
Combination VI and SI	MLR	9.81	23.13
	SVM	8.52	8.05
	RF	5.15	5.34
	KNN	11.94	14.11

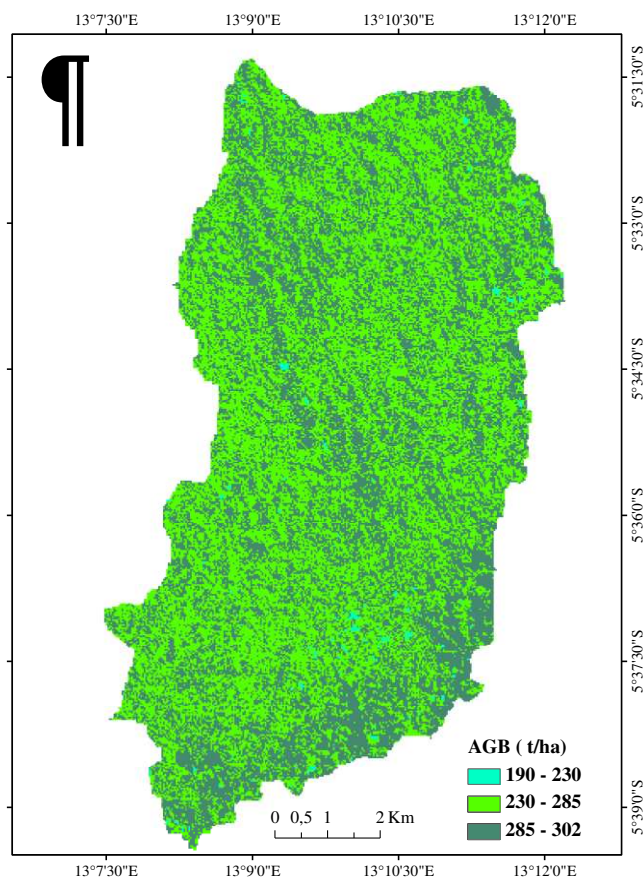


**Figure 4.** Aboveground biomass of the study area using the RF algorithm

## Discussion

Satellite images with medium resolution represent an alternative method to estimate aboveground biomass, especially where the acquisition of hyperspectral images still has serious problems. In fact, up to now, the acquisition of hyperspectral images constitutes a severe problem due to their high costs, limited accessibility or availability, and their manoeuvrability. However, Forest aboveground biomass estimation using remote sensing approaches remains a significant challenge requiring numerous studies to find related solutions concerning different modelling approaches and remote sensing data. According to GAO et al. (2018), the AGB model performance depends on remote sensing data, modelling algorithms, and forest type. Lu (2006) has stated that in the field of the aboveground biomass estimation based remote sensing technique, researchers should take great attention regarding many parameters, among others, the remote sensing variables and the modelling technique or algorithms. In this study, we compared the potential of four methods, including RandomForest, K-nearest neighbour, support vector machine, and multilinear regression, to predict the aboveground biomass of tropical forest using the Landsat 8 multispectral OLI.

In general, the machine learning algorithms have demonstrated the higher ability to predict aboveground biomass in comparison with the multilinear regression method, regardless of data sources that were used (vegetation indices, spectral bands, and combination of both). Indeed, the multilinear regression method yielded the lowest  $R^2$  and the greatest RMSE compared to all other models. Our results are in line with those found by Sadeghi et al. (2018) and Pandit and Dube (2018). Indeed, comparing the performance of the RF machine learning algorithm and the multilinear regression, the authors have reported that the RF algorithm provides high accuracy than multiple linear regression for mapping aboveground biomass. Another study conducted by Feng et al. (2017) has demonstrated the strong ability of RF and SVR to yield better aboveground biomass estimation than multilinear regression. Thus, many reasons were developed to explain the low accuracy of multilinear regression compared to the machine learning algorithm. Numerous studies have pointed out that the weaker performance of the linear regression method is based on the fact of the complexity and non-linearity between remote sensing-based variables and aboveground biomass (Baccini et al., 2004; Foody et al., 2003; Muukkonen and Heiskanen, 2005). Gao et al. (2018) stated that the multiple linear regression method was an essential tool of modelling aboveground biomass, especially for the biomass range of 40–120 Mg/ha. Another reason is that the linear regression method is less flexible when facing nonlinear problems (Li et al., 2017), and cannot adequately handle the multicollinearity problem (Ju et al., 2005). Still, according to Safari et al. (2018), when the biomass value is lower than saturation values, such as 150-ton/ha, as stated by Feng et al. (2017) and Gizachew et al. (2016), and when the relationship between Landsat-derived predictors and observed aboveground biomass is expected linear, the linear regression approach can be more efficient. In our study, the biomass range is 192.22–301.11 t/ha, greater than 40–120 Mg/ha. This can explain why the linear regression performed poorly than the machine learning algorithm.

However, it is essential to point out that the RF algorithm improves the forest aboveground biomass estimation. Indeed, the RF algorithm provided better results in AGB estimation regardless of the data source that was used. Indeed, recently, numerous studies have successfully revealed the effectiveness of the RandomForest algorithm to estimate aboveground biomass, and their results are similar to ours. Supporting our

results, Liu et al. (2017) reported a significant improvement of the RandomForest algorithm compared with the multilinear regression and support vector machine. In this study, the RandomForest algorithm has produced better performance in terms of accuracy and predictive power of the model ( $R^2 = 0.95$  RMSE = 17.73 Mg/ha). Another study carried out by Latifi et al. (2010), comparing the effectiveness of the K- nearest neighbour methods and the RandomForest algorithm to predict volume and biomass, have found accurate biomass estimation with the RandomForest algorithm, compared to all other nonparametric methods. Similarly, Sadeghi et al. (2018) also revealed that the RF algorithm could produce the accurate results in mapping aboveground biomass at the level of boreal forest stands ( $R^2 = 0.62$ , RMSE = 26 Mg ha<sup>-1</sup>).

In this research, we also analysed the power of the RandomForest algorithm using the important variable selection method, completed using the parameter tuning procedure. The present study has demonstrated the advantage of parameter tuning in predicting AGB employing the RF model. For instance, using the vegetation indices-based variables, the  $R^2$  value augmented from 0.86 to 0.91, while the RMSE value declined from 10.22 to 9.12 t ha<sup>-1</sup>. According to Kuhn et al. (2008), removing the less important variables from the model has no impact on its performance. However, the results obtained in this study proved the opposite. Hence, Biau and Scornet (2016) have mentioned that due to its complexity, it is difficult to understand the computation of the Random Forest's parameters.

Nevertheless, the RandomForest model provides the minimum number of subgroup input predictors that will improve the effectiveness of the model using the OOB method. Based on OOB data, the RandomForest algorithm produces an estimation error without bias for the testing data. Moreover, several parameters such as tree numbers (Oshiro et al., 2012), splitting at each node of each tree (Grömping, 2009), determine the performance of the algorithm. The sample numbers in each cell, below which the cell is not divided (Kuhn, 2008), but equals the default value of the node size (Tyrallis and Papacharalampous, 2017). However, the present study used the default value, as suggested by the literature. The RandomForest algorithm variables have many limit factors, one of which is that the ideal number of predictors with the smallest error is not selected automatically (Adam et al., 2012). According to Grömping (2009), numerous parameters can affect variable importance in RandomForest, one of which is based on the choice of mtry.

Additionally, the author confirmed that it should be better to avoid redundancy to achieve a suitable model in finding a minimum number of variables for a good prediction. Thus, the model does not necessarily need to contain all the appropriate predictors, as long as the results are accurate. In line with Oshiro (2012), in the present study, the RandomForest algorithm identified 15 input predictors as the minimum subgroup with acceptable prediction power.

The percentIncMSE and IncNodePurity were used in ranking predictors concerning their performance to estimate forest AGB provided an improvement in the accuracy of the model. Though the present study accomplished a satisfactory result, it is essential to point out that several parameters influence the effectiveness of the model, including the number of trees (Genuer et al., 2010) and the split numbers. Kuhn and Johnson (2013) recommended considering a minimum number of trees at 1000 for optimizing the parameterization of the model. Likewise, as recommended by Verikas et al. (2011), optimizing variable numbers to divide a node, rather than default values, leads to numerous predictor rankings.



However, the performance of each machine learning algorithm varied depending on data sources. Indeed, vegetation indices were better related to aboveground biomass than spectral information-based variables. The use of spectral information-based predictors did severely increase the performance of the model. Our findings support those discovered by Pandit et al. (2018) and Lu (2006). In their studies, the authors found that the vegetation indices-based variables were better correlated to AGB than spectral bands. Indeed, some researchers have revealed the strong relationship between vegetation indices-based predictors and biomass (Pearson et al., 1976; Bedard and LaPointe, 1987; Hardisky et al., 1984; Deering and Haas, 1980). For example, Piao et al. (2007) have reported that vegetation indices computed from spectral information reflect the photosynthetic activity of the vegetation and are consequently used for biomass monitoring.

Nevertheless, the fact of combining both vegetation indices-based predictors and spectral bands-based predictors could not improve the modelling performance. Hence, using RandomForest and, according to the increasing order of importance as shown in *Figure 2*, the most crucial vegetation indices-based variables are NDVI, RDVI, SR, DVI, EVI, OSAVI, MSAVI, and SAVI. Our results are in line with those found by Shao and Zhang (2016) and Pandit et al. (2018). The authors have found similar variables for estimating forest biomass by using Landsat 8 OLI sensor.

Finally, the present study found that the biomass was more linked to the vegetation indices than the spectral bands. Indeed, the best models have been found through the use of vegetation indices-based predictors. However, the results based on the linear model were less precise compared to those found using machine learning algorithms. This may be due to the complex structure of tropical forests that sometimes makes linear models ineffective in estimating biomass under these conditions. It should be emphasized that, of all the different existing AGB modelling methods, using various sensors and field data, the choice of the best model should be preceded by a parsimonious evaluation considering the number of parameters of which the sensor type, the forest types, and other environmental conditions. However, as Kumar and Mutanga (2017) reported, several factors influencing uncertainties in the aboveground biomass estimation methods, including vegetation types, landscape types, seasons, and data availability.

Seeing that our study area is located in relatively steep terrain with almost homogeneity in the structure of the canopy, and containing high aboveground biomass, we suggest for further research to investigate the potential of these four methods for predicting forest biomass in various forest conditions, to fill the gap existing in the lack of aboveground forest biomass data.

## Conclusions

The present study compared the potential of different machine learning algorithms (RF, KNN, and SVM) and the linear regression method for AGB estimation in the tropical forest using Landsat images and field data. Our study demonstrated that the machine learning algorithm has the potential to estimate AGB with high precision compared to the linear regression method. Comparing the three sets of predictors, the vegetation indices have yielded accurate results and the strongest modelling power in the present study. Our findings show that the RF algorithm is the best alternative for biomass estimation given its best accuracy and high modelling power, regardless of the



data source that was used. This study revealed as others the potential of machine learning algorithms based on Landsat images in predicting AGB in the tropical forest, using freely remotely sensed data, allied to field measurement data. This research confirms that machine learning algorithms, especially the RF and SVM, are powerful tools for aboveground biomass using variables derived from sensors with medium spatial resolution. However, we suggest for further research to examine the potential of these machine learning algorithms for predicting forest aboveground biomass in various forest conditions.

**Funding.** This study was supported by The Fundamental Research Funds for the Central Universities (2572019CP12).

## REFERENCES

- [1] Adam, E. M., Mutanga, O., Rugege, D., Ismail, R. (2012): Discriminating the papyrus vegetation (*Cyperus papyrus* L.) and its co-existent species using random forest and hyperspectral data resampled to HYMAP. – *Int. J. Remote Sens.* 33: 552-569.
- [2] Alrababah, M. A., Alhamad, M. N., Bataineh, A. L., Bataineh, M. M., Suwaileh, A. F. (2011): Estimating east Mediterranean forest parameters using Landsat ETM. – *International Journal of Remote Sensing* 32(6): 1561-1574.
- [3] Avitabile, V., Baccini, A., Friedl, M. A., Schmullius, C. (2012): Capabilities and limitations of landsat and land cover data for aboveground woody biomass estimation of Uganda. – *Remote Sensing of Environment* 117: 366-380.
- [4] Baccini, A., Friedl, M. A., Woodcock, C. E., Warbington, R. (2004): Forest biomass estimation over regional scales using multisource data. – *Geophysical Research Letters* 31: 1-4.
- [5] Bedard, J., LaPointe, G. (1987): The estimation of dry green biomass in hayfields from canopy spectroreflectance measurements. – *Grass Forage Sci.* 42: 73-78.
- [6] Biau, G., Scornet, E. (2016): A random forest guided tour. – *Test* 25: 197-227.
- [7] Breiman, L. (2001): Random forests. – *Mach. Learn.* 45(1): 5-32.
- [8] Brown, S., Sathaye, J., Cannell, M., Cannell, M., Kauppi, P. E. (1996): Mitigation of carbon emissions to the atmosphere by forest management. – *Commonw. For. Rev.* 75: 80-91.
- [9] Caputo, J. (2009): Sustainable Forest Biomass: Promoting Renewable Energy and Forest Stewardship. – Policy paper, Environmental and Energy Study Institute, Washington, DC.
- [10] Chen, Q. (2015): Modeling aboveground tree woody biomass using national-scale allometric methods and airborne LiDAR. – *ISPRS Journal of Photogrammetry and Remote Sensing* 106: 95-106.
- [11] Chirici, G., Mura, M., McInerney, D., Py, N., Tomppo, E. O., Waser, L. T., Travaglini, D., McRoberts, R. E. (2016): A meta-analysis and review of the literature on the k-Nearest Neighbors technique for forestry applications that use remotely sensed data. – *Remote Sensing of Environment* 176: 282-294.
- [12] Cover, T., Hart, P. (1967): Nearest neighbor pattern classification. – *IEEE Transactions on Information Theory* 13(1): 21-27.
- [13] Deering, D. W., Haas, R. H. (1980): Using Landsat digital data for estimating green biomass. – NASA Technical Memorandum #80727, Greenbelt, MD.
- [14] Dixon, R. K., Brown, S., Houghton, R. E. A., Solomon, A. M., Trexler, M. C., Wisniewski, J. (1994): Carbon pools and flux of global forest ecosystems. – *Science* 263: 185-190.

- [15] Fassnacht, F. E., Hartig, F., Latifi, H., Berger, C., Hernández, J., Corvalán, P., Koch, B. (2014): Importance of sample size, data type and prediction method for remote sensing-based estimations of aboveground forest biomass. – *Remote Sens. Environ.* 154: 102-114.
- [16] Fayolle, A., Doucet, J-L., Gillet, J-F., Lejeune, P. (2013): Tree allometry in Central Africa: testing the validity of pantropical multi-species allometric equations for estimating biomass and carbon stocks. – *Forest Ecology and Management* 305: 29-37.
- [17] Feng, Y., Lu, D., Chen, Q., Keller, M., Moran, E., dos-Santos, M. N., Bolfe, E. L., Batistella, M. (2017): Examining effective use of data sources and modeling algorithms for improving biomass estimation in a moist tropical forest of the Brazilian Amazon. – *International Journal of Digital Earth* 10(10): 996-1016.
- [18] Foody, G. M., Boyd, D. S., Cutler, M. E. (2003): Predictive relations of tropical forest biomass from Landsat TM data and their transferability between regions. – *Remote Sensing of Environment* 85: 463-474.
- [19] Frazier, R. J., Coops, N. C., Wulder, M. A., Kennedy, R. (2014): Characterization of aboveground biomass in an unmanaged boreal forest using Landsat temporal segmentation metrics. – *ISPRS Journal of Photogrammetry and Remote Sensing* 92: 137-146.
- [20] Gao, Y., Lu, D., Li, G., Wang, G., Chen, Q., Liu, L., Li, D. (2018): Comparative analysis of modeling algorithms for forest aboveground biomass estimation in a subtropical region. – *Remote Sensing* 10(4).
- [21] Genuer, R., Poggi, J. M., Tuleau-Malot, C. (2010): Variable selection using random forests. *Pattern Recognit.* – *Lett.* 31: 2225-2236.
- [22] Gizachew, B., Solberg, S., Næsset, E., Gobakken, T., Bollandsås, O. M., Breidenbach, J., Zhabu, E., Mauya, E. W. (2016): Mapping and estimating the total living biomass and carbon in low-biomass woodlands using Landsat 8 CDR data. – *Carbon Balance and Management* 11(1).
- [23] Gleason, C. J., Im, J. (2012): Forest biomass estimation from airborne LiDAR data using machine learning approaches. – *Remote Sens. Environ* 125: 80-91.
- [24] Glenn, N. F., Neuenschwander, A., Vierling, L. A., Spaete, L., Li, A., Shinneman, D. J., Philiod, D., Arkle, R., McIlroy, S. K. (2016): Landsat 8 and ICESat-2: Performance and potential synergies for quantifying dryland ecosystem vegetation cover and biomass. – *Remote Sensing of Environment* 185: 233-242.
- [25] Görgens, E. B., Montagni, A., Rodriguez, L. C. E. (2015): A performance comparison of machine learning methods to estimate the fast-growing forest plantation yield based on laser scanning metrics. – *Comput. Electron. Agric.* 116: 221-227.
- [26] Grömping, U. (2009): Variable importance assessment in regression: linear regression versus random forest. – *Am. Stat.* 63: 308-319.
- [27] Haboudane, D., Miller, J. R., Tremblay, N., Zarco-Tejada, P. J., Dextraze, L. (2002): Integrated narrow-band vegetation indices for prediction of crop chlorophyll content for application to precision agriculture. – *Remote Sensing of Environment* 81: 416-426.
- [28] Hardisky, M. A., Daiber, F. C., Roman, C. T., Klemas, V. (1984): Remote sensing of biomass and annual net aerial primary productivity of a salt marsh. – *Remote Sens. Environ.* 16: 91-106.
- [29] Hudak, A. T., Strand, E. K., Vierling, L. A., Byrne, J. C., Eitel, J. U. H., Martinuzzi, S., Falkowski, M. J. (2012): Quantifying aboveground forest carbon pools and fluxes from repeat LiDAR surveys. – *Remote Sensing of Environment* 123: 25-40.
- [30] Ju, C., Cai, T., Yang, X. (2008): Topography-based modeling to estimate percent vegetation cover in semi-arid Mu Us sandy land, China. – *Computers and Electronics in Agriculture* 64: 133-139.
- [31] Kuhn, M. (2008): Building Predictive Models in R Using the caret Package. – *J. Stat. Softw.* 28: 1-26.
- [32] Kuhn, M., Johnson, K. (2013): Applied Predictive Modeling. – Springer, New York.

- [33] Kumar, L., Mutanga, O. (2017): Remote sensing of above-ground biomass. – *Remote Sens.* 9: 935.
- [34] Latifi, H., Nothdurft, A., Koch, B. (2010): Non-parametric prediction and mapping of standing timber volume and biomass in a temperate forest: application of multiple optical/LiDAR-derived predictors. – *Forestry* 83: 395-407.
- [35] Latifi, H., Fassnacht, F. E., Hartig, F., Berger, C., Hernández, J., Corvalán, P., Koch, B. (2015): Stratified aboveground forest biomass estimation by remote sensing data. – *International Journal of Applied Earth Observation and Geoinformation* 38: 229-241.
- [36] Li, M., Im, J., Quackenbush, L. J., Liu, T. (2014): Forest biomass and carbon stock quantification using airborne LiDAR data: a case study over huntington wildlife forest in the Adirondack park. – *IEEE Journal of Selected Topics in Applied Earth Observations and Remote Sensing* 7(7): 3143-3156.
- [37] Li, Y., Zhou, L. W., Wang, R. Z. (2017): Urban biomass and methods of estimating municipal biomass resources. – *Renewable and Sustainable Energy Reviews* 80: 1017-1030.
- [38] Liu, K., Wang, J., Zeng, W., Song, J. (2017): Comparison and evaluation of three methods for estimating forest above ground biomass using TM and GLAS data. – *Remote Sensing* 9(4).
- [39] López-Serrano, P. M., López-Sánchez, C. A., Álvarez-González, J. G., García-Gutiérrez, J. A. (2016): Comparison of machine learning techniques applied to Landsat-5 TM spectral data for biomass estimation. – *Canadian Journal of Remote Sensing* 42(6): 690-705.
- [40] Lu, D. (2006): The potential and challenge of remote sensing-based biomass estimation. – *International Journal of Remote Sensing* 27: 1297-1328.
- [41] Lu, D., Mausel, P., Brondizio, E., Moran, E. (2004): Relationships between forest stand parameters and Landsat TM spectral responses in the Brazilian Amazon Basin. *For. – Ecol. Manag.* 198: 149-167.
- [42] Lu, D., Chen, Q., Wang, G., Liu, L., Li, G., Moran, E. (2016): A survey of remote sensing-based aboveground biomass estimation methods in forest ecosystems. – *Int. J. Digital Earth* 9(1): 63-105.
- [43] Manyanda, B. J., Mugasha, W. A., Nzunda, E. F., Malimbwi, R. E. (2019): Biomass and volume models based on stump diameter for assessing degradation of miombo woodlands in Tanzania. – *International Journal of Forestry Research* 2019: 1-15.
- [44] Mayer, D. G., Butler, D. G. (1993): Statistical validation. – *Ecological Modelling* 68: 21-32.
- [45] McRoberts, R. E., Næsset, E., Gobakken, T. (2013): Inference for LiDAR-assisted estimation of forest growing stock volume. – *Remote Sens. Environ.* 128: 268-275.
- [46] Mohammadi, Z., Limaie, S. M., Lohmander, P., Olsson, L. (2017): Estimating the aboveground carbon sequestration and its economic value (case study: Iranian Caspian forests). – *Journal of Forest Science* 63(11): 511-518.
- [47] Moroni, M. T. (2013): Simple models of the role of forests and wood products in greenhouse gas mitigation. – *Australian Forestry* 76: 50-57.
- [48] Mountrakis, G., Im, J., Ogole, C. (2011): Support vector machines in remote sensing: a review. – *ISPRS J. Photogramm. Remote Sens.* 66(3): 247-259.
- [49] Muukkonen, P., Heiskanen, J. (2005): Estimating biomass for boreal forests using ASTER satellite data combined with standwise forest inventory data. – *Remote Sensing of Environment* 99: 434-447.
- [50] Oshiro, T. M., Perez, P. S., Baranauskas, J. A. (2012): How Many Trees in a Random Forest. – In: Perner, P. (ed.) *International Workshop on Machine Learning and Data Mining in Pattern Recognition*. Springer, Berlin.
- [51] Pandit, S., Tsuyuki, S., Dube, T. (2018): Landscape-scale aboveground biomass estimation in buffer zone community forests of Central Nepal: coupling in situ measurements with Landsat 8 Satellite Data. – *Remote Sensing* 10(11).

- [52] Park, S., Im, J., Jang, E., Rhee, J. (2016): Drought assessment and monitoring through blending of multi-sensor indices using machine learning approaches for different climate regions. – *Agricultural and Forest Meteorology* 216: 157-169.
- [53] Pearson, R. L., Miller, L. D., Tucker, C. J. (1976): Hand-held spectral radiometer to estimate gramineous biomass. – *Appl. Opt.* 15(2): 416-418.
- [54] Pflugmacher, D., Cohen, W. B., Kennedy, R. E., Yang, Z. (2014): Using Landsat-derived disturbance and recovery history and LiDAR to map forest biomass dynamics. – *Remote Sensing of Environment* 151: 124-137.
- [55] Phua, M.-H., Saito, H. (2003): Estimation of biomass of a mountainous tropical forest using Landsat TM data. – *Canadian Journal of Remote Sensing* 29: 429-440.
- [56] Piao, S. L., Fang, J. Y., Zhou, L. M., Tan, K., Tao, S. (2007): Changes in biomass carbon stocks in China's grasslands between 1982 and 1999. – *Glob. Biogeochem. Cycles* 21. DOI: 10.1029/2005GB002634.
- [57] R Core Team (2019): R: A Language and Environment for Statistical Computing. – R Foundation for Statistical Computing, Vienna. <https://www.R-project.org/>.
- [58] Saatchi, S., Malhi, Y., Zutta, B., Buermann, W., Anderson, L. O., Araujo, A. M., Phillips, O. L., Peacock, J., Steege, H. T., Gonzalez, G. L. (2009): Mapping landscape scale variations of forest structure, biomass, and productivity in Amazonia. – *Biogeosci. Discuss.* 6(3): 5461-5505.
- [59] Sadeghi, Y., St-Onge, B., Leblon, B., Prieur, J. F., Simard, M. (2018): Mapping boreal forest biomass from a SRTM and TanDEM-X based on canopy height model and Landsat spectral indices. – *Int. J. Appl. Earth Obs. Geoinf.* 68: 202-213.
- [60] Safari, A., Sohrabi, H., Powell, S. (2018): Comparison of satellite-based estimates of aboveground biomass in coppice oak forests using parametric, semiparametric, and nonparametric modeling methods. – *Journal of Applied Remote Sensing* 12(04).
- [61] Shao, Z., Zhang, L. (2016): Estimating forest aboveground biomass by combining optical and SAR data: a case study in Genhe, Inner Mongolia, China. – *Sensors* 16: 834.
- [62] Shataee, S. (2013): Forest attributes estimation using aerial laser scanner and TM data. – *Forest Systems* 22(3): 484-496.
- [63] Tanase, M. A., Panciera, R., Lowell, K., Tian, S., Hacker, J. M., Walker, J. P. (2014): Airborne multi-temporal L-band polarimetric sar data for biomass estimation in semi-arid forests. – *Remote Sensing of Environment* 145: 93-104.
- [64] Tyralis, H., Papacharalampous, G. (2017): Variable selection in time series forecasting using random forests. – *Algorithms* 10: 114.
- [65] Vashum, K. T., Jayakumar, S. (2012): Methods to estimate above-ground biomass and carbon stock in natural forests - a review. – *J Ecosyst Ecogr* 2: 116.
- [66] Vauhkonen, J., Korpela, I., Maltamo, M., Tokola, T. (2010): Imputation of single-tree attributes using airborne laser scanning-based height, intensity, and alpha shape metrics. – *Remote Sensing of Environment* 114: 1263-1276.
- [67] Verikas, A., Gelzinis, A., Bacauskiene, M. (2011): Mining data with random forests: a survey and results of new tests. – *Pattern Recognit.* 44: 330-349.
- [68] Wang, X., Shao, G., Chen, H., Lewis, B. J., Qi, G., Yu, D., Zhou, L., Dai, L., Dai, L. (2013): An application of remote sensing data in mapping landscape-level forest biomass for monitoring the effectiveness of forest policies in northeastern china. – *Environmental Management* 52(3): 612-620.
- [69] Were, K., Bui, D. T., Dick, Ø. B., Singh, B. R. (2015): A comparative assessment of support vector regression, artificial neural networks, and random forests for predicting and mapping soil organic carbon stocks across an Afromontane landscape. – *Ecological Indicators* 52: 394-403.
- [70] Zhang, Y., Liang, S., Sun, G. (2014): Forest biomass mapping of northeastern China using GLAS and MODIS data. – *IEEE J. Sel. Top. In Appl. Earth Obs. And Remote Sens.* 7(1): 140-152.

- [71] Zhao, P., Lu, D., Wang, G., Liu, L., Li, D., Zhu, J., Yu, S. (2016): Forest aboveground biomass estimation in Zhejiang Province using the integration of Landsat TM and ALOS PALSAR data. – *International Journal of Applied Earth Observation and Geoinformation* 53: 1-15.
- [72] Zheng, D., Rademacher, J., Chen, J., Crow, T., Bresee, M., Le Moine, J., Ryu, S. R. (2004): Estimating aboveground biomass using Landsat 7 ETM+ data across a managed landscape in northern Wisconsin, USA. – *Remote Sensing of Environment* 93: 402-411.
- [73] Zhu, X., Liu, D. (2015): Improving forest aboveground biomass estimation using seasonal Landsat NDVI time-series. – *ISPRS J. Photogramm. Remote Sens.* 102: 222-231.

# VERBENONE PROTECTS CHINESE WHITE PINE (*PINUS ARMANDII*) (PINALES: PINACEAE: PINOIDEAE) AGAINST CHINESE WHITE PINE BEETLE (*DENDROCTONUS ARMANDII*) (COLEOPTERA: CURCULIONIDAE: SCOLYTINAE) ATTACKS

ZHAO, M.<sup>1</sup> – LIU, B.<sup>2</sup> – ZHENG, J.<sup>2</sup> – KANG, X.<sup>2</sup> – CHEN, H.<sup>1\*</sup>

<sup>1</sup>State Key Laboratory for Conservation and Utilization of Subtropical Agro-Bioresources (South China Agricultural University), Guangdong Key Laboratory for Innovative Development and Utilization of Forest Plant Germplasm, College of Forestry and Landscape Architecture, South China Agricultural University, Guangzhou 510642, China

<sup>2</sup>College of Forestry, Northwest A & F University, Yangling, Shaanxi 712100, China

\*Corresponding author

e-mail: chenhuiyl@163.com; phone/fax: +86-020-8528-0256

(Received 29<sup>th</sup> Aug 2020; accepted 19<sup>th</sup> Nov 2020)

**Abstract.** Bark beetle anti-aggregation is important for tree protection due to its high efficiency and fewer potential negative environmental impacts. Densitometric variables of *Pinus armandii* were investigated in the case of healthy and attacked trees. The range of the ecological niche and attack density of *Dendroctonus armandii* in infested *P. armandii* trunk section were surveyed to provide a reference for positioning the anti-aggregation pheromone verbenone on healthy *P. armandii* trees. 2, 4, 6, and 8 weeks after the application of verbenone, the mean attack density was significantly lower in the treatment group than in the control group ( $P < 0.01$ ). At twelve months after anti-aggregation pheromone application, the mortality rate was evaluated. There was a significant difference between the control and treatment groups (chi-square test,  $P < 0.05$ ). These results provide insight into the characteristics of infected *P. armandii* and demonstrate that anti-aggregation treatment of *D. armandii* can improve the protection of healthy *P. armandii*.

**Keywords:** *Dendroctonus armandii*, *Pinus armandii*, anti-aggregation, ecological niche, tree protection

## Introduction

The Chinese white pine beetle (*Dendroctonus armandii* Tsai and Li) is a primary native pest of Chinese white pines (*Pinus armandii* Franch) in the Qinling Mountains of China and can be fatal to *P. armandii* individuals that are more than 30 years of age (Chen et al., 2010; Hu et al., 2016). Attack by *D. armandii* can result in the gradual weakening of *P. armandii* resistance, allowing the infestation of many species of bark beetles, such as *Ips acuminatus*, *Ips sexdentatus*, *Hylurgops longipilis*, *Tomicus piniperda*, and *Trypodendron lineatum* (Chen and Tang, 2007). Since 1970, more than  $3 \times 10^8$  m<sup>3</sup> of *P. armandii* trees (more than 30 years of age) have been harmed by *D. armandii* (Xie and Lv, 2012), and younger *P. armandii* individuals were also found to have been attacked by *D. armandii* in a recent study (Chen et al., 2015). In a time series, *D. armandii*, as a dominant species infecting Chinese white pines in the Qinling forest ecosystem, which attacked healthy trees and then cooperated with blue stain fungus, which resulted in an abrupt decline in resistance and triggered additional bark beetle species to secondarily attack the infected or withered host trees (Hu et al., 2016; Chen and Tang, 2007). There are significant differences between *D. armandii* and other *Dendroctonus* spp. in terms of their attack, similar to those between

*Dendroctonus valens* and *Dendroctonus ponderosae*. *D. valens* is a secondary bark beetle and mainly invades weak, dying trees and stumps. *D. ponderosae* is a primary pest and mainly invades weak pines, but it has been found to invade pines during every state of an outbreak. *D. armandii* is not only a primary bark beetle but also affects the health of *P. armandii*. The infestation dynamics of *D. armandii* define it as a primary damaging bark beetle (Sun et al., 2013; Krause et al., 2018). Overall, *D. armandii* attack has caused great harm to the sustainable development of the Qinling ecosystem and has resulted in extensive economic losses (Hu et al., 2013; Pham et al., 2014).

Management measures for bark beetles in recent years have included forest management practices, chemical control and semiochemical-based trapping (Pureswaran et al., 2008; Perkins et al., 2015; Gillette et al., 2009). When *D. armandii* leaves its host, females first invade new individuals based on their volatiles and then release pheromones to attract more females and males (Zhao et al., 2017a), which is similar to what occurs in *D. valens*. Semiochemical communication among bark beetles “enables host and mate location, aggregation and resource partitioning” (Liu et al., 2013). Aggregation pheromones are considered key factors in the success of insect invasion and colonization (Faccoli and Stergulc, 2008; Blazenec and Jakus, 2009). Frontalin +  $\alpha$ -pinene is an aggregation pheromone released by virgin female and mated male *D. armandii* (Zhao et al., 2017a), and myrtenal might represent an aggregation pheromone produced by female *D. armandii* that induces aggregation effects in other females (Zhao et al., 2019). The addition of aggregation pheromones in field trapping can increase the number of trapped individuals and reduce the population density of beetles (Stephen et al., 2001; Cale et al., 2015; Shepherd and Sullivan, 2019). The anti-aggregation pheromones of bark beetles, such as verbenone in *D. ponderosae* and *D. valens*, and repellent terpene components from their hosts have been used to protect pine species from bark beetles (Gillette et al., 2006). Verbenone [(1S,5S)-4,6,6-trimethylbicyclo[3.1.1]hept-3-en-2-one], a beetle-produced anti-aggregation pheromone also found in pines (Kainulainen and Holopainen, 2002) and a wide variety of angiosperms (Molyneux et al., 1980; Buttery et al., 2000; Robles et al., 2003), can be effective in limiting damage to pines by *Dendroctonus* spp. bark beetles (Payne and Billings, 1989; Cale et al., 2019). Verbenone has been detected using gas chromatographic and mass spectral (GC-MS) analyses of the hindguts of female beetles and the fumes emanating from *P. armandii* logs naturally attacked by *D. armandii* (Xie and Lv, 2012; Chen et al., 2015). In our previous study, verbenone was verified as an anti-aggregation pheromone based on electrophysiological (EAG) and Y-tube laboratory assays. In addition, field trials indicated that the addition of verbenone to the bait used to trap *D. armandii* markedly decreased the efficiency of field trapping (Zhao et al., 2017b). However, the anti-aggregation release dose, release device, release position and effect for *P. armandii* tree protection still need to be considered.

To date, comprehensive management research on *D. armandii* has focused on the identification of volatiles associated with *P. armandii* and *D. armandii* during different periods and at different locations, and field trapping of volatiles and pheromones has been carried out (Xie and Lv, 2012; Chen et al., 2015; Zhao et al., 2017a, b). On the one hand, studies on how to protect *P. armandii* by allowing it to resist attack by *D. armandii* are still lacking, and further research is needed to determine whether verbenone is responsible for the improved efficacy observed in tree

protection studies. On the other hand, verbenone was identified as pheromone in a part of *Dendroctonus* spp. Even verbenone was as anti-aggregation pheromone in *D. valens*, verbenone functions as a multipurpose pheromone, attractive at very low concentrations but repellent at high concentrations (Sun et al., 2013). Thus, research on verbenone in *D. armandii* is necessary. The purpose of the study was to identify the characteristics of infested *P. armandii* and the regularities of the distribution of *D. armandii* infecting *P. armandii*. This information can provide a standard and requirements for selecting healthy experimental trees and determining the best position at which to hang anti-aggregation devices. Verbenone was further studied as an anti-aggregate in a field trial of its ability to protect trees. The results of this study could provide a basis for future studies and could be used in the biocontrol of these beetles and tree protection.

## Materials and methods

### Study location

The study sites were located on the southern slope of the middle Qinling Mountains, Ningshan County, Shaanxi, China, mainly in Huangguan Forest Farm (33°42'23"-33°43'25"N, 108°25'18"-108°25'46"E; the experimental area was approximately 133 ha) and Pingheliang Forest Farm (33°22'00"-33°34'00"N, 108°24'00"-108°36'10"E; the experimental area was approximately 159 ha) (Figs. 1, 2). The survey of infected *P. armandii* and the application of the anti-aggregation pheromone were conducted in the two forest farms. The *P. armandii* trees under investigation were located from 1500 to 1800 m above sea level. The two forest farms were chosen because they were severely affected by *D. armandii*. The investigated *P. armandii* trees were distributed widely within the two areas.



**Figure 1.** Study site (red circle) on a map of China. The map was downloaded from National Geomatics Center of China





**Figure 2.** Some affected areas of the study sites

### ***Survey of infested Pinus armandii***

Data regarding infested *P. armandii* were collected in May 2018. At this time, the *D. armandii* individuals present were in the larval stage and constituted the offspring of *D. armandii* invading from September to October of the previous year. During the almost eight months from September 2017 to May 2018, some resinous pitch tubes fell off, and the entry holes were difficult to distinguish accurately. Therefore, second-generation larvae were used as the statistical reference for attack density. Twenty infested *P. armandii* trees were randomly selected, and the trees were separated by at least 50 m. Diameter at breast height (DBH) (cm), tree height (m), basal area (m<sup>2</sup>/ha) and ecological niche (m) were measured. The ecological niche in the article refer to the vertical distribution range of *D. armandii* in infested *P. armandii* trunk section. The measurement of the ecological niche and count of the attack density of *D. armandii* were performed by hewing down the infested *P. armandii* trees (adhering to the silviculture and cutting policies of the Forestry Bureau in 2018). Every infested *P. armandii* individual was equally divided into five parts in the ecological niche. For convenience, five tree sections were considered from base to crown, they were named as the bottom, lower middle, middle, upper middle and top. Each of the five parts of every tree was sampled in three locations. Ten centimeters of bark was removed by band girdling at each location, *D. armandii* larvae were counted, and the area of sampled bark was calculated. Samplings were done in May when beetles were in the larval stage, laying the foundation for accurate statistical analysis during the investigation period. The attack density of *D. armandii* from bottom to top was calculated based on the density of *D. armandii* larvae.

### ***Screening of vulnerable, healthy Pinus armandii***

The choice of vulnerable healthy *P. armandii* was dependent on the data for infested *P. armandii*, especially the DBH (cm), tree height (m) and basal area (m<sup>2</sup>/ha) data.

Vulnerable healthy *P. armandii* were defined as healthy individuals with DBH, tree height, and basal area values that were within the ranges of values of the measured infected *P. armandii*. Forty vulnerable healthy *P. armandii* were randomly chosen for the study in June 2018. Twenty of the 40 healthy *P. armandii* were randomly allocated to the experimental group, and the others represented the control group. Additionally, the live crown ratio of the 40 trees was calculated and used to evaluate the difference between the experimental and control groups. The live crown ratio was the live crown percentage of total tree length, whereby a value near 0 indicated very little foliage and a value near 1 indicated foliage along most of the bole (Randolph, 2010; Bechtold, 2004). The distance between the vulnerable healthy *P. armandii* trees was more than 50 m.

### ***Chemicals, pheromone formulation and attraction of Dendroctonus armandii***

The chemicals used in the field trials were (R)-(+)- $\alpha$ -pinene (98% chemical purity (c.p.)), (-)- $\beta$ -pinene (99% c.p.), (+)-3-carene (> 98% c.p.), myrtenal (98% c.p.), verbenone (> 93% c.p.) and liquid paraffin (high-performance liquid chromatography (HPLC) certified) obtained from Sigma-Aldrich Co., Shanghai, China, and *exo*-brevicommin (> 95% c.p.) and frontalin (> 95% c.p.) obtained from Contech Enterprises Inc., Delta, BC, Canada. Multiple funnel traps were used in the *D. armandii* attraction experiment. The traps were obtained from Sino-Czech Trading Co. Ltd., Beijing, China. (R)-(+)- $\alpha$ -pinene, (-)- $\beta$ -pinene, (+)-3-carene, frontalin, *exo*-brevicommin and myrtenal were chosen as the attractants at a ratio of 300:300:300:1:1:1. Frontalin, *exo*-brevicommin and myrtenal were authenticated as pheromones of *D. armandii* and used as the main attractant components. The host volatiles (R)-(+)- $\alpha$ -pinene, (-)- $\beta$ -pinene, and (+)-3-carene were added as solvents. The attractant mixture was added to a 15 mL slow-release plastic vial with a release speed of 200 mg/day. The mixed reagent evaporated continuously for 8 weeks until the end of the field trial (from June 25, 2018, to August 21, 2018). As these lures were used to aggregate but not trap *D. armandii*, the insect collection box at the base of the traps was removed. Forty lures were paired with 40 vulnerable healthy *P. armandii* and placed near the trees. The distance between each lure and the vulnerable healthy *P. armandii* individual was 10 m. Multiple-funnel chemical attraction was applied beginning on June 25, 2018, and was used for 8 weeks.

### ***Application of the anti-aggregation pheromone verbenone***

According to the range of tree sections colonized by *D. armandii* on infested *P. armandii* trees and operational convenience, breast height was chosen as the release position for anti-aggregation pheromone. Mating disruption dispensers (tubular sustained release devices) obtained from Sino-Czech Trading Co. Ltd., Beijing, China, were used as carriers of the anti-aggregation compound and were constructed of polyvinyl chloride; the tubes were 150 cm long (1.7 mm inner diameter, 2.5 mm outside diameter). Verbenone and liquid paraffin were mixed together at a ratio of 1:1. Four milliliters of the mixed reagent was injected into the mating disruption dispensers, and both ends were immediately sealed. The release speed of verbenone was approximately 100 mg/day for the duration of the test (implantation dose divided by volatilization days). The mating disruption dispensers were refreshed every 20 days. The mating disruption dispensers with verbenone were bundled around the vulnerable healthy *P. armandii* at breast height on June 25, 2018, with verbenone released continuously for eight weeks. This release time was chosen to cover the outbreak period (July and

August) of *D. armandii*. The number of resinous pitch tubes attacked by *D. armandii* in a band from breast height to 50 cm above breast height was counted every two weeks. The numerical distribution of trees in different states (alive and dead) was determined twelve months after the fourth count. Individuals of *P. armandii* with dry frass instead of resinous pitch tubes, yellowing of needle-like leaves, and hollowed-out phloem at breast height were considered dead. When there were fewer than ten resinous pitch tubes and the needle-like leaves were green, the trees were considered healthy.

### ***Experimental design, sampling and statistical analysis***

DBH, tree height, basal area and live crown ratio were considered key factors in the process of host invasion by beetles (Gillette et al., 2006). Twenty infected *P. armandii* trees were randomly chosen as standards. The DBH, tree height and basal area of infected *P. armandii* were assessed to identify healthy *P. armandii* similar in condition to vulnerable healthy *P. armandii*. Forty vulnerable healthy *P. armandii* trees were randomly divided into two groups to represent the experimental and control groups. Chi-square tests were performed to ensure that there were no significant differences in DBH, tree height or basal area among the infected *P. armandii*, experimental and control groups (Fig. 3A, B, C). Considering the severe shedding of needles by infected *P. armandii*, the live crown ratio was not evaluated for these trees, but the live crown ratio of the selected vulnerable healthy *P. armandii* was calculated, and a chi-square test was performed to ensure that there was no significant difference in the live crown ratio between the experimental and control groups (Fig. 3D). All of the surveyed *P. armandii* in the experiment were more than 50 m apart. The ecological niche and change in attack density across the range of the ecological niche were also surveyed (Figs. 4, 5). This information can provide a basis for the application of and position at which to suspend verbenone on vulnerable healthy *P. armandii*.

SPSS (1999) was used for data processing, and SigmaPlot 12.0 was used to perform image processing. Mann-Whitney tests were performed to determine the significance of the differences in DBH, tree height and basal area between the infected, control and experimental groups and to determine the significance of the differences in the live crown ratio between the control group and experimental group. The differences in attack density by *D. armandii* 2, 4, 6 and 8 weeks after treatment were tested with Mann-Whitney tests for the treatment and control groups. A chi-square test was performed to test the difference between the control and treatment groups in terms of the mortality rate.

## **Results**

The DBH, tree height and basal area were assessed for the infected, control and experimental groups. The live crown ratio was evaluated only for the control and experimental groups. The results of the statistical analysis showed that the mean DBH, tree height and basal area did not significantly differ between the different groups ( $P < 0.05$ ) (Fig. 3A, B, C), and the mean live crown ratio also did not significantly differ between the control and experimental groups ( $P < 0.05$ ) (Fig. 3D).

The mean height (+standard error (SE)) of the infested *P. armandii* trees was  $16.89 + 0.78$  m. The range of the ecological niche (+SE) of *D. armandii* was  $0.36 + 0.05$  to  $12.59 + 0.83$  m (Fig. 4). The attack density of *D. armandii* from bottom to top in the range of the ecological niche did not significantly differ between the groups

( $P < 0.05$ , least significant difference (LSD) test in SPSS), being highest in the lower middle of the tree and gradually decreasing towards the two ends (Fig. 5).

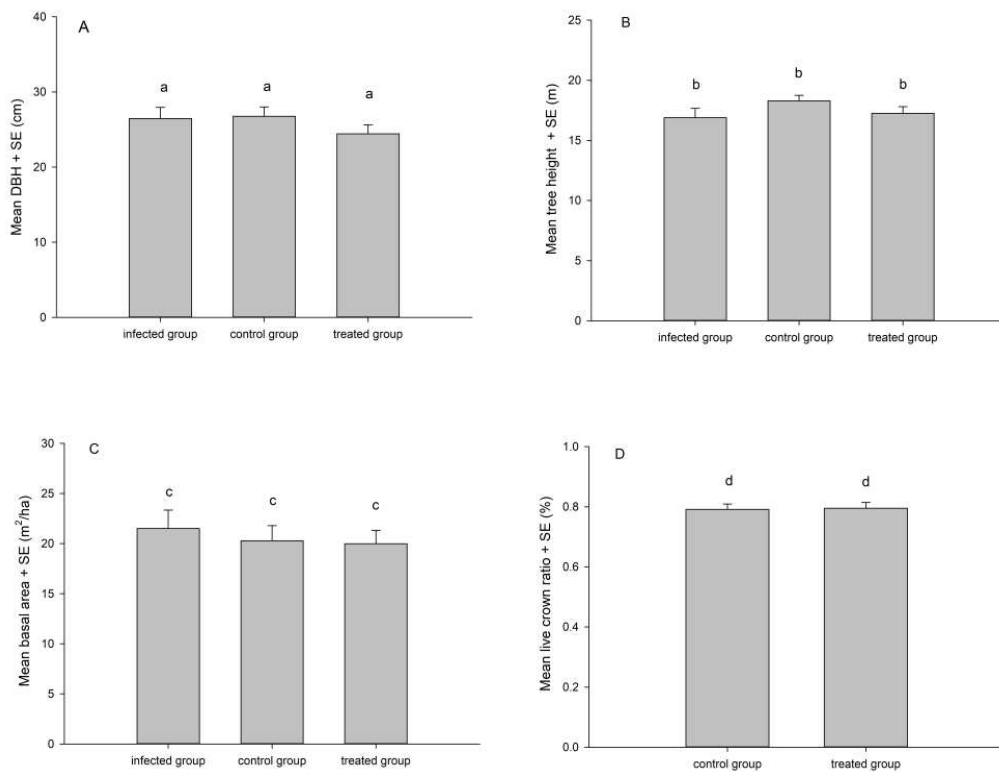


**Figure 3.** Mean + standard error (SE) of diameter at breast height (DBH) (cm) (A), mean tree height + SE (m) (B), and mean basal area + SE ( $m^2/ha$ ) (C) of the infected, control and treated groups and mean live crown ratio + SE (%) (D) of the control and treated groups. The same letters indicate no significant difference ( $P < 0.05$ )

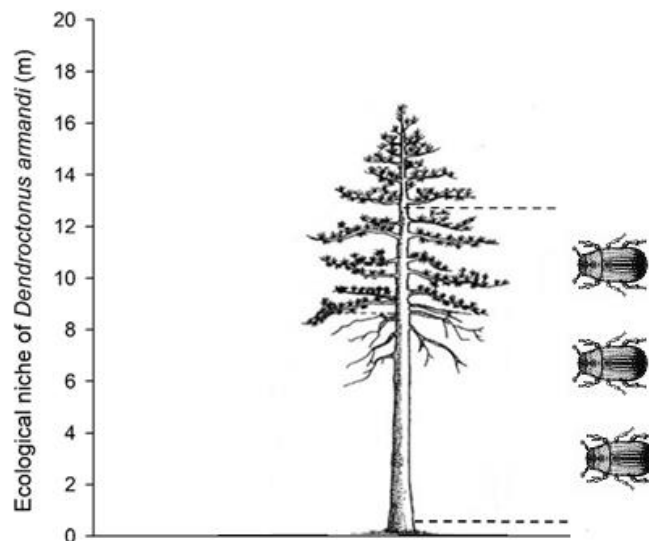


**Figure 4.** Ecological niche of *D. armandii* in an infested *P. armandii* trunk section (m). The three beetles indicate invading *D. armandii*, and the two dashed lines indicate the invasion scope of *D. armandii* in a *P. armandii* trunk section (m)

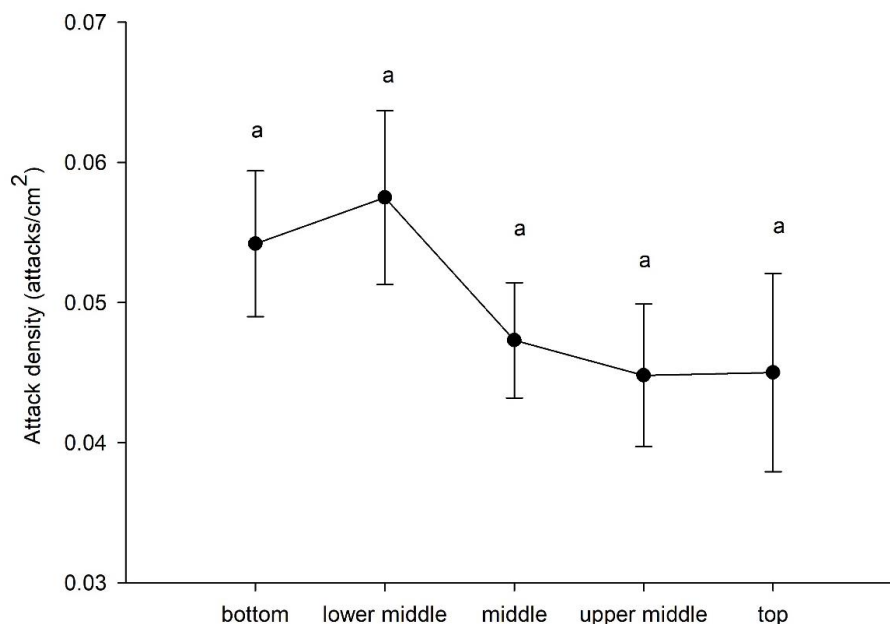


**Figure 5.** Attack density of *D. armandii* from bottom to top in infested trunk section. The same letters indicate no significant difference ( $P < 0.05$ )

The attack density of the control group reached a high value after 2 weeks and reached saturation after 4, 6 and 8 weeks. The attack density of the treatment group gradually increased but remained consistently lower than that in the control group during the experiment (Fig. 6). The treatment group showed a significant difference from the control group in terms of the mean attack density 2, 4, 6, and 8 weeks after the application of verbenone, with the treatment group showing a significantly lower attack density ( $P < 0.01$ ) (Fig. 6). The experimental results regarding the mortality rate showed that 50% of the treated trees were alive, 50% of the treated trees were dead, 20% of the control trees were alive, and 80% of the control trees were dead. There was a statistically significant difference between the control and treatment groups with respect to the mortality rate (chi-square test,  $P < 0.05$ ), with the mortality rate in the treatment group being 37.5% lower than that in the control group (Fig. 7).

## Discussion

The mean DBH + SE (cm) (Fig. 3A), mean tree height + SE (m) (Fig. 3B), and mean basal area + SE (m<sup>2</sup>/ha) (Fig. 3C) of the infected group reflected the common features of infected *P. armandii* in the Qinling Mountains. Both the DBH and live crown ratio are thought to be correlated with tree susceptibility to bark beetle attack, and the basal area of the tree surface per hectare is also thought to contribute to susceptibility to bark beetle attack (Gillette et al., 2006). The attack success rate of *D. armandii* was found to be positively correlated with stand density, tree height, tree age and DBH (Wang et al., 2010). *D. armandii* mainly attacks healthy *P. armandii* trees that are more than 30 years old (Chen and Tang, 2007). Although the survey of infected *P. armandii* (Fig. 3) and attack by *D. armandii* focused on adult trees, younger *P. armandii*, with a DBH of less than 6 cm, were also found to be attacked by *D. armandii* in the Pingheliang Forest Farm of the Qinling Mountains in September 2018 (a personal observation).

The attacks by *D. armandii* occur along the tree trunk from about 0.4 m till 14 m. This distribution in the tree distinguishes by other bark beetles species, such as *H. longipilis* that tend to occur on the lower parts of the tree trunk, as well as *Cryphalus lipingensis* and *Cryphalus chinlingensis* which are mainly found in the upper trunk and branches. Other species, as *I. acuminatus*, *Polygraphus sinensis*, and *Pityogenes japonicus* are primarily distributed in the middle of the tree trunks (Chen and Tang, 2007). *D. armandii* is a trunk-borer bark beetle, and a certain phloem thickness is required for its overwintering and feeding (Chen and Tang, 2007). With an increase in tree height, phloem thickness gradually decreases. Therefore, the choice of the lower parts of the tree trunk is consistent with the habits of *D. armandii*. The study of the ecological niche of *D. armandii* revealed the range of activity of *D. armandii* in *P. armandii*, providing a more effective operating range for the control of *D. armandii* in infected *P. armandii*. The attack density of *D. armandii* did not differ from the bottom to the top of the tree in the range of its ecological niche; therefore, for operational convenience, the middle of the bottom of the trees (at approximately breast height) was uniformly selected for the placement of the anti-aggregation pheromone. The anti-aggregation results significantly differed between the experimental and control groups 2, 4, 6, and 8 weeks after application.

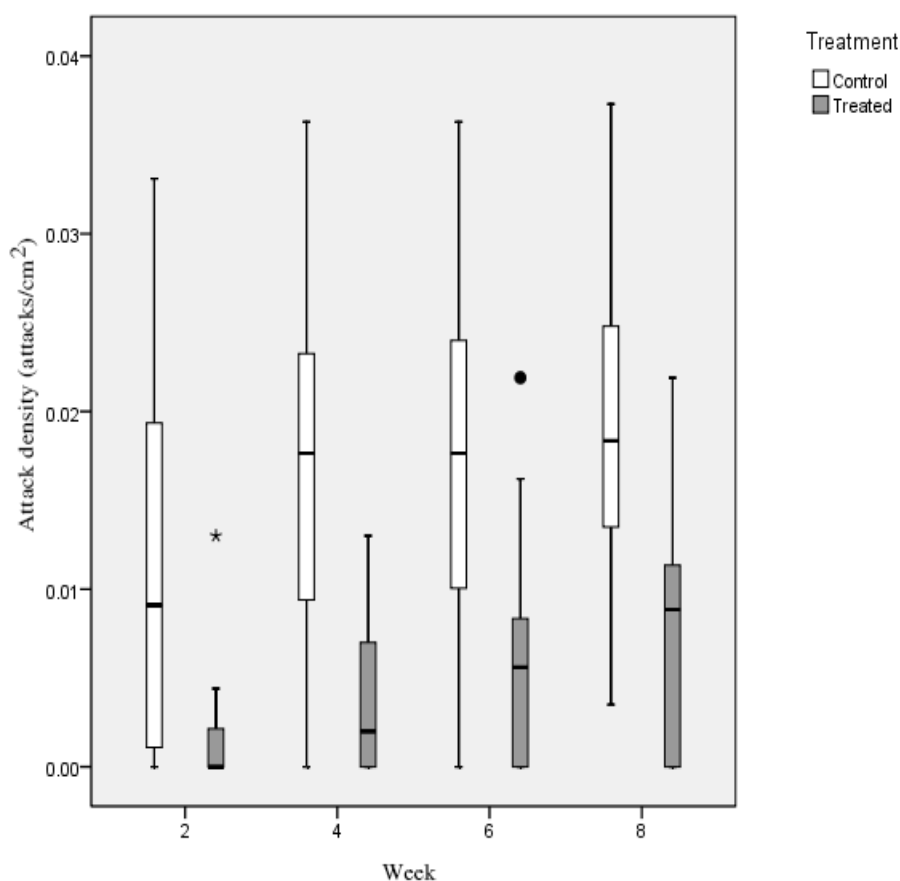


**Figure 6.** Mean density of attack by *D. armandii* 2, 4, 6 and 8 weeks after treatment. White boxes represent the interquartile range; whiskers represent the range of normal values; asterisks represent extreme values; and circles represent abnormal values. There were significant differences ( $P < 0.01$ ) between the treatment and control groups in every case (*U* test)



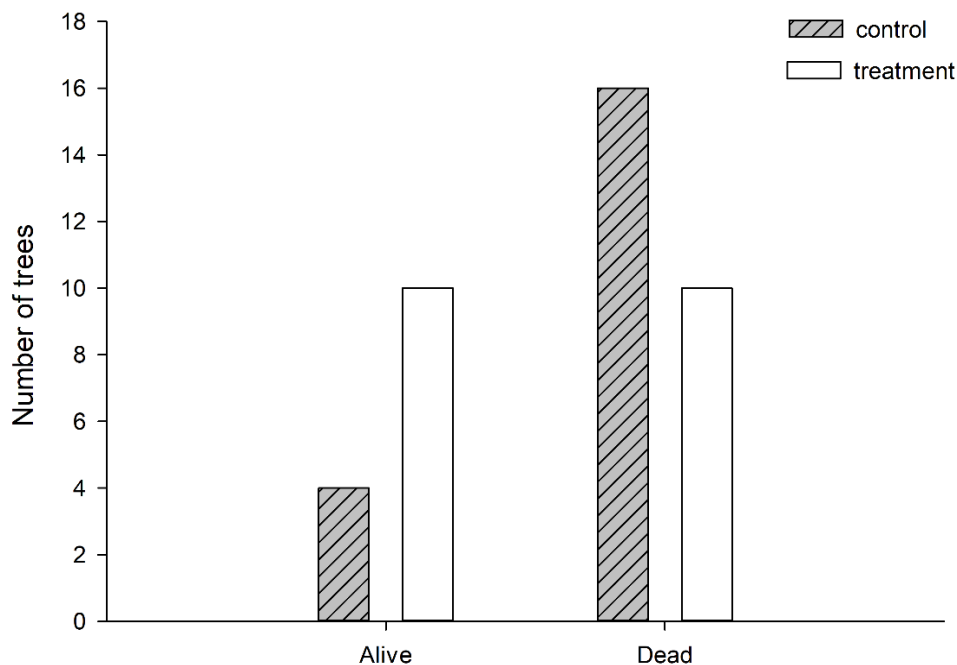


**Figure 7.** The numerical distribution of trees in different states (alive and dead). There was a significant difference between the control and treatment groups with regard to the mortality rate (chi-square test,  $P < 0.05$ )

*D. armandii* infestations appear to be increasing throughout the Qinling Mountains, and it is often difficult to use physicochemical methods and semiochemical traps to protect healthy Chinese white pines against attack by this beetle (Xie and Lv, 2012; Chen et al., 2015). It might be possible to use the anti-aggregation pheromone verbenone to reduce the mortality of Chinese white pines and thereby protect healthy pines. Bark beetle pheromone components can be derived from host tree precursors, often with simple hydroxylation producing the pheromone. The pheromone verbenone is produced from dietary  $\alpha$ -pinene in the fat bodies of some *Dendroctonus* spp. (Blomquist et al., 2010). Verbenone is thought to be an auto-oxidation product of verbenol and may work as an anti-aggregation signal along with frontalin (Lindgren and Miller, 2002; Cao et al., 2018). Field trapping and tree protection studies have been conducted to address the effects of verbenone on *Dendroctonus brevicomis*, *D. ponderosae* and *D. valens* (Gillette et al., 2006, 2012; Fettig et al., 2009b; Progar, 2003). The efficiency of verbenone pouch release devices is especially high when some *Dendroctonus* spp. beetles are abundant (Progar, 2005; Borden et al., 2006; Bertram and Paine, 1994). Although the production of verbenone by *D. armandii* has not been verified, verbenone was confirmed to act as an anti-aggregation pheromone in this species (Zhao et al., 2017b). In our previous study, verbenone significantly reduced the number of *D. armandii* trapped by approximately 30% in comparison to the control at two sites (Zhao et al., 2017b). Mating disruption dispensers containing insect pheromones have been produced for the management of *Grapholita molesta* and *Cydia pomonella*. In this study, mating disruption dispensers were used for the protection of *P. armandii*. Healthy *P. armandii* individuals in need of protection can be surrounded by such dispensers to allow the increased emission of anti-aggregation pheromones. Of course, slow-release pouches, bottles, and tubes and Disrupt Micro-Flake can also be used for the release of anti-aggregation pheromones (Gillette et

al., 2006). The effect of release devices on *D. armandii* still needs to be verified. Furthermore, 2, 4, 6 and 8 weeks after the aggregation of *D. armandii* and the release of verbenone, the mean attack density of the treatment group was significantly lower than that of the control group. The results of this study further show that verbenone functions as an anti-aggregation pheromone of *D. armandii*, which is consistent with the results of previous studies focusing on this species (Zhao et al., 2017b).

Verbenone was also found to exert effects on *D. ponderosae* and *D. valens* (Gillette et al., 2006, 2012). In our study, the difference in the anti-aggregation effect between the experimental and control groups was more significant in the early stage of the experiment than during the late stage of the experiment. The reason for this result may be that the attractant contained all the confirmed *D. armandii* pheromones (frontalin, *exo*-brevicomins and myrtenal) at the beginning of the experiment, and their attraction effects were too strong as the experiment proceeded. Nevertheless, the treatment group showed a significant difference from the control group for the data collected at the end of the experiment ( $P < 0.01$ ) (Fig. 6). Furthermore, it can be inferred that the protection effect may be stronger in the wild without artificially assisted aggregation than under experimental conditions.

In some bark beetle species, verbenone combined with multiple other components (ipsdienol and angiosperm or green-leaf volatiles) may provide enhanced efficacy over verbenone alone (Bertram and Paine, 1994; Huber and Borden, 2001; Borden et al., 2003; Pureswaran and Borden, 2004). In our previous study, myrtenol was found to be produced by infected *P. armandii* after *D. armandii* attack and had significant toxicity to *D. armandii*, especially females (Zhao et al., 2019). Thus, myrtenol has the potential to improve the anti-aggregation effect of verbenone. The mortality rate in the treatment group fell by 37.5% compared with that in the control (Figs. 7, 8). The final mortality rate revealed that the survival rate of healthy *P. armandii* could be effectively promoted by treatment with the anti-aggregation pheromone verbenone. Applied research regarding the use of verbenone to resist invasion by *D. ponderosae* and *D. valens* revealed that 70% of control trees were clearly dead, while none of the treated trees were dead (Gillette et al., 2006). The control efficiency of verbenone against *D. armandii* was inferior to that against *D. ponderosae* and *D. valens*. The reason for this result may be that the sensitivity of *D. armandii* to verbenone is inferior to that of *D. ponderosae* and *D. valens*. Of course, this speculation requires further verification. Another reason may be that the effect of the attractant was too strong. The third reason may be that the release time of verbenone was chosen to cover the outbreak period of *D. armandii* but not the whole flying period and that the mating disruption dispensers with verbenone were bundled around vulnerable healthy *P. armandii* at breast height but did not cover the entire ecological niches of *D. armandii*. This is the first tree protection study in regard to *D. armandii*, the color and shape of chosen release device and trap (Hakyemez and Cebeci, 2020; Polat, 2019), and the release speed of verbenone, and the optimal experimental conditions may not have been achieved. This study demonstrated that verbenone is effective in the protection of *P. armandii* trees, but how to enhance this effect requires further study. Further studies should explore the devices used to release verbenone, and more conservation research should be conducted to further improve the protection efficiency of *P. armandii*.





**Figure 8.** Experimental findings: trees with black labels were experimental trees, and trees with red label were control trees

## Conclusion

Previous research confirmed verbenone as an anti-aggregation pheromone of *D. armandii* (Zhao et al., 2017b), the current study represents the first condition survey of infected *P. armandii* and the first tree protection research. The current study provides new possibilities for the protection of vulnerable healthy *P. armandii* against attack by *D. armandii*. We measured the DBH, tree height and basal area of infected *P. armandii* and vulnerable healthy *P. armandii* based on these characteristics. The ecological niche range and attack density of infected *P. armandii* provide a theoretical basis for the identification of appropriate locations for the application of anti-aggregation pheromones among vulnerable healthy *P. armandii*. *Dendroctonus* spp. are known to use pheromones and host volatiles when attacking host trees and attracting partners (Blomquist et al., 2010). Semiochemicals might be a key factor determining successful mass colonization by *Dendroctonus* spp., which can overcome the defense system of host trees (Chen et al., 2015). In recent years, research has concentrated on the control and management of *D. armandii*, while the characteristics of infected *P. armandii* and the protection of healthy *P. armandii* have received less attention. Initially, it was thought that the role of verbenone was different in different *Dendroctonus* spp. These differences determined that research in the new species must be done step by step. The aim of this study was to determine whether verbenone has a remarkable anti-aggregation effect in the complicated field environment. Our results demonstrate that the anti-aggregation pheromone verbenone can effectively lower the attack density of

*D. armandii* and reduce the ultimate mortality of vulnerable healthy *P. armandii*. Verbenone was significantly effective in the protection of healthy *P. armandii* (Fig. 7). The functions of verbenone are similar among the majority of *Dendroctonus* spp., and the compound usually acts as an anti-aggregation pheromone (Lindgren and Miller, 2002), similar to its function in *D. valens*, *D. ponderosae* and *D. brevicomis* (Gillette et al., 2006; Fettig et al., 2009a). Notably, how to improve the impact (by adding other components, by changing the release rate of the lure, by changing the hanging position and so on) still needs further study.

**Acknowledgements.** This research was funded by the National Key Research and Development Program of China (2017YFD0600104) and the National Natural Science Foundation of China (31870636).

## REFERENCES

- [1] Bechtold, W. A. (2004): Largest-crown-width prediction models for 53 species in the Western United States. – *Western Journal of Applied Forestry* 19: 245-251.
- [2] Bertram, S. L., Paine, T. D. (1994): Influence of aggregation inhibitors (verbenone and ipsdienol) on landing and attack behavior of *Dendroctonus brevicomis* (Coleoptera: Scolytidae). – *Journal of Chemical Ecology* 20: 1617-1629.
- [3] Blazenec, M., Jakus, R. (2009): Effect of (+)-limonene and 1-methoxy-2-propanol on *Ips typographus* response to pheromone blends. – *Journal of Forest Research* 20: 37-44.
- [4] Blomquist, G. J., Figueroa-Teran, R., Aw, M., Song, M. M., Gorzalski, A., Abbott, N. L., Chang, E., Tittiger, C. (2010): Pheromone production in bark beetles. – *Insect Biochemistry and Molecular Biology* 40: 699-712.
- [5] Borden, J. H., Chong, L. J., Earle, T. J., Huber, D. P. W. (2003): Protection of lodgepole pine from attack by the mountain pine beetle, *Dendroctonus ponderosae* (Coleoptera: Scolytidae) using high doses of verbenone in combination with nonhost bark volatiles. – *Forestry Chronicle* 79: 685-691.
- [6] Borden, J. H., Birmingham, A. L., Burleigh, J. S. (2006): Evaluation of the push-pull tactic against the mountain pine beetle using verbenone and non-host volatiles in combination with pheromone baited trees. – *Forestry Chronicle* 82: 579-590.
- [7] Buttery, R. G., Light, D. M., Nam, Y. L., Merrill, G. B., Roitman, J. N. (2000): Volatile components of green walnut husks. – *Journal of Agricultural and Food Chemistry* 48: 2858-2861.
- [8] Cale, J. A., Taft, S., Najjar, A., Klutsch, J. G., Hughes, C. C., Sweeney, J. D., Erbilgin, N. (2015): Mountain pine beetle (*Dendroctonus ponderosae*) can produce its aggregation pheromone and complete brood development in naïve red pine (*Pinus resinosa*) under laboratory conditions. – *Canadian Journal of Forest Research* 45: 1873-1877.
- [9] Cale, J. A., Ding, R. S., Wang, F. A., Rajabzadeh, R., Erbilgin, N. (2019): Ophiostomatoid fungi can emit the bark beetle pheromone verbenone and other semiochemicals in media amended with various pine chemicals and beetle-released compounds. – *Fungal Ecology* 39: 285-295.
- [10] Cao, Q. J., Wickham, J. D., Chen, L., Ahmad, F., Lu, M., Sun, J. H. (2018): Effect of oxygen on verbenone conversion from *cis*-verbenol by gut facultative anaerobes of *Dendroctonus valens*. – *Frontiers in Microbiology* 9: 464.
- [11] Chen, H., Tang, M. (2007): Spatial and temporal dynamics of bark beetles in Chinese white pine in Qinling Mountains of Shaanxi Province, China. – *Environmental Entomology* 36: 1124-1130.

- [12] Chen, H., Li, Z., Tang, M. (2010): Laboratory evaluation of flight activity of *Dendroctonus armandii* (Coleoptera: Curculionidae: Scolytinae). – Canadian Entomologist 142: 378-387.
- [13] Chen, G. F., Song, Y. S., Wang, P. X., Chen, J. Y., Zhang, Z., Wang, S. M., Huang, X. B., Zhang, Q. H. (2015): Semiochemistry of *Dendroctonus armandii* Tsai and Li (Coleoptera: Curculionidae: Scolytinae): both female-produced aggregation pheromone and host tree kairomone are critically important. – Chemoecology 25: 135-145.
- [14] Faccoli, M., Stergulc, F. (2008): Damage reduction and performance of mass trapping devices for forest protection against the spruce bark beetle, *Ips typographus* (Coleoptera Curculionidae Scolytinae). – Annals of Forest Science 65: 309.
- [15] Fettig, C. J., Mckelvey, S. R., Borys, R. R., Dabney, C. P., Hamud, S. M., Nelson, L. J., Seybold, S. J. (2009a): Efficacy of verbenone for protecting Ponderosa Pine stands From Western Pine Beetle (Coleoptera: Curculionidae: Scolytinae) attack in California. – Journal of Economic Entomology 102: 1846-1858.
- [16] Fettig, C. J., Mckelvey, S. R., Dabney, C. P., Borys, R. R., Huber, D. P. W. (2009b): Response of *Dendroctonus brevicornis* to different release rates of nonhost angiosperm volatiles and verbenone in trapping and tree protection studies. – Journal of Applied Entomology 133: 143-154.
- [17] Gillette, N. E., Stein, J. D., Owen, D. R., Webster, J. N., Fiddler, G. O., Mori, S. R., Wood, D. L. (2006): Verbenone-releasing flakes protect individual *Pinus contorta* trees from attack by *Dendroctonus ponderosae* and *Dendroctonus valens* (Coleoptera: Curculionidae, Scolytinae). – Agricultural and Forest Entomology 8: 243-251.
- [18] Gillette, N. E., Erbilgin, N., Webster, J. N., Pederson, L., Mori, S. R., Stein, J. D., Owen, D. R., Bischel, K. N., Wood, D. L. (2009): Aerially applied verbenone-releasing laminated flakes protect *Pinus contorta* stands from attack by *Dendroctonus ponderosae* in California and Idaho. – Forest Ecology and Management 257: 1405-1412.
- [19] Gillette, N. E., Hansen, E. M., Mehmehl, C. J., Mori, S. R., Webster, J. N., Erbilgin, N., Wood, D. L. (2012): Area-wide application of verbenone-releasing flakes reduces mortality of white bark pine *Pinus albicaulis* caused by the mountain pine beetle *Dendroctonus ponderosae*. – Agricultural and Forest Entomology 14: 367-375.
- [20] Hakyemez, A., Cebeci, H. H. (2020): Field trial of liquid pheromone capsule (Galopro Pinowit®) against bark beetles in Istanbul (Turkey) forests. – Applied Ecology and Environmental Research 18: 1819-1827.
- [21] Hu, X., Wang, C., Chen, H., Ma, J. (2013): Differences in the structure of the gut bacteria communities in development stages of the Chinese white pine beetle (*Dendroctonus armandii*). – International Journal of Molecular Sciences 14: 21006-21020.
- [22] Hu, X., Li, M., Zhang, F. P., Chen, H. (2016): Influence of starvation on the structure of gut-associated bacterial communities in the Chinese White Pine Beetle (*Dendroctonus armandii*). – Forests 7: 126.
- [23] Huber, D. P. W., Borden, J. H. (2001): Protection of lodgepole pines from mass attack by mountain pine beetle, *Dendroctonus ponderosae*, with nonhost angiosperm volatiles and verbenone. – Entomologia Experimentalis et Applicata 99: 131-141.
- [24] Kainulainen, P., Holopainen, J. K. (2002): Concentrations of secondary compounds in Scots pine needles at different stages of decomposition. – Soil Biology & Biochemistry 34: 37-42.
- [25] Krause, A. M., Townsend, P. A., Lee, Y., Raffa, K. F. (2018): Predators and competitors of the mountain pine beetle *Dendroctonus ponderosae* (Coleoptera: Curculionidae) in stands of changing forest composition associated with elevation. – Agricultural and Forest Entomology 20: 402-413.
- [26] Lindgren, B. S., Miller, D. R. (2002): Effect of verbenone on five species of bark beetles (Coleoptera : Scolytidae) in lodgepole pine forests. – Environmental Entomology 31: 759-765.

- [27] Liu, Z. D., Xu, B. B., Miao, Z. W., Sun, J. H. (2013): The pheromone frontalin and its dual function in the invasive bark beetle *Dendroctonus valens*. – Chemical Senses 38: 485-495.
- [28] Molyneux, R. J., Stevens, K. L., James, L. F. (1980): Chemistry of toxic range plants: volatile constituents of broomweed (*Gutierrezia sarothrae*). – Journal of Agricultural and Food Chemistry 28: 1332-1333.
- [29] Payne, T. L., Billings, R. F. (1989): Evaluation of (S)-verbenone applications for suppressing southern pine beetle (Coleoptera: Scolytidae) infestations. – Journal of Economic Entomology 82: 1702-1708.
- [30] Perkins, D. L., Jorgensen, C. L., Rinella, M. J. (2015): Verbenone decreases Whitebark Pine mortality throughout a Mountain Pine Beetle outbreak. – Forest Science 61: 747-752.
- [31] Pham, T., Chen, H., Yu, J. M., Dai, L. L., Zhang, R. R., Vu, T. Q. T. (2014): The differential effects of the blue-stain fungus *Leptographium qinlingensis* on monoterpenes and sesquiterpenes in the stem of Chinese White Pine (*Pinus armandii*) saplings. – Forests 5: 2730-2749.
- [32] Polat, B. (2019): Efficacy of mass trapping of tomato leafminer (*Tuta absoluta*) with different types and colours of traps in open- field tomato. – Applied Ecology and Environmental Research 17: 15721-15730.
- [33] Progar, R. A. (2003): Verbenone reduces mountain pine beetle attack in lodgepole pine. – Western Journal of Applied Forestry 18: 229-232.
- [34] Progar, R. A. (2005): Five-year operational trial of verbenone to deter mountain pine beetle (*Dendroctonus ponderosae*; Coleoptera: Scolytidae) attack of lodgepole pine (*Pinus contorta*). – Environmental Entomology 34: 1402-1407.
- [35] Pureswaran, D. S., Borden, J. H. (2004): New repellent semiochemicals for three species of *Dendroctonus* (Coleoptera: Scolytidae). – Chemoecology 14: 67-75.
- [36] Pureswaran, D. S., Hofstetter, R. W., Sullivan, B. T. (2008): Attraction of the southern pine beetle, *Dendroctonus frontalis*, to pheromone components of the western pine beetle, *Dendroctonus brevicomis* (Coleoptera: Curculionidae: Scolytinae), in an allopatric zone. – Environmental Entomology 37: 70-78.
- [37] Randolph, K. C. (2010): Equations relating compacted and uncompact live crown ratio for common tree species in the south. – Southern Journal of Applied Forestry 34: 118-123.
- [38] Robles, C., Bousquet-Melou, A., Garzino, S., Bonin, G. (2003): Comparison of essential oil composition of two varieties of *Cistus ladanifer*. – Biochemical Systematics and Ecology 31: 339-343.
- [39] Shepherd, W. P., Sullivan, B. T. (2019): Southern Pine Beetle (Coleoptera: Curculionidae: Scolytinae) pheromone component *trans*-verbenol: enantiomeric specificity and potential as a lure adjuvant. – Environmental Entomology 48: 193-201.
- [40] Stephen, C. (2001): Review of the operational IPM program for the southern pine beetle. – Integrated Pest Management Reviews 6: 293-336.
- [41] Sun, J. H., Lu, M., Gillette, N. E., Wingfield, M. J. (2013): Red Turpentine Beetle: innocuous native becomes invasive tree killer in China. – Annual Review of Entomology 58: 293-311.
- [42] Wang, X. L., Chen, H., Ma, C., Li, Z. (2010): Chinese white pine beetle, *Dendroctonus armandii* (Coleoptera: Scolytinae), population density and dispersal estimated by mark-release-recapture in Qinling Mountains, Shaanxi, China. – Applied Entomology and Zoology 45: 557-567.
- [43] Xie, S. A., Lv, S. J. (2012): An improved lure for trapping the bark beetle *Dendroctonus armandii* (Coleoptera: Scolytinae). – European Journal of Entomology 109: 569-577.
- [44] Zhao, M. Z., Dai, L. L., Fu, D. Y., Gao, J., Chen, H. (2017a): Electrophysiological and behavioral responses of *Dendroctonus armandii* (Coleoptera: Curculionidae: Scolytinae)

to two candidate pheromone components: frontalin and *exo*-brevicomin. – Chemoecology 27: 91-99.

- [45] Zhao, M. Z., Dai, L. L., Sun, Y. Y., Fu, D. Y., Chen, H. (2017b): The pheromone verbenone and its function in *Dendroctonus armandii* (Coleoptera: Curculionidae: Scolytinae). – European Journal of Entomology 114: 53-60.
- [46] Zhao, M. Z., Liu, B., Sun, Y. Y., Wang, Y. Y., Dai, L. L., Chen, H. (2019): Presence and roles of myrtenol, myrtanol and myrtenal in *Dendroctonus armandii* (Coleoptera: Curculionidae: Scolytinae) and *Pinus armandii* (Pinales: Pinaceae: Pinoideae). – Pest Management Science 76: 188-197.

# INFLUENCE OF ACID MINE WATER ON THE DIVERSITY AND METABOLITE SHIFT OF MICROBIAL POPULATIONS OF THE RHIZOSPHERE OF COMMON REED (*PHRAGMITES AUSTRALIS*)

MANG, K. C. – NTUSHELO, K.\*

*Department of Agriculture and Animal Health, University of South Africa, South Africa  
(e-mail: kaluchimdimang@yahoo.com; phone: +27-(0)-748-366-063)*

*\*Corresponding author  
e-mail: ntushk@unisa.ac.za; phone: +27-(0)-789-027-944*

(Received 19<sup>th</sup> Jun 2019; accepted 25<sup>th</sup> Oct 2019)

**Abstract.** Common reed (*Phragmites australis* (Cav.) Trin. ex Steud.) grows widely in various acid mine water bodies and remediates these polluted sites. There exists only a paucity of studies on the effect of acid mine water on microbial diversity and secondary metabolite compositions of the rhizosphere of the common reed. The aim of this study was therefore to determine the influence of acid mine drainage on the microbial diversity of the rhizosphere of the common reed as well as on its secondary metabolite composition. Two acid mine water bodies were selected for study and were compared with a normal water body. The acid mine status of the water bodies was confirmed by assessing a set of physicochemical properties, microbial diversity was measured using BIOLOG EcoPlates and secondary metabolite compositions were determined by nuclear magnetic resonance. Results showed that acid mine drainage reduces rhizosphere microbial diversity as well as influences secondary metabolite composition.

**Keywords:** *rhizoremediation, microbes, bioremediation, Shannon index, BIOLOG EcoPlates*

## Introduction

Acid mine drainage (AMD) also known as acid rock drainage is a process that occurs as a result of the contact between oxygenated water and mineral pyrite which leads to the oxidation of the pyrite and the production of acids (Evangelou, 1995; Blowes et al., 2003). Areas affected by AMD are usually lost but there are various remediation technologies adopted by many countries to mitigate the impact of AMD, among them is the use of reeds such as *Typha* sp. and *Phragmites* sp. which can adsorb heavy metals. *Phragmites australis* (Cav.) Trin. ex Steud.) is a large perennial grass that is predominant in wetlands in the temperate and tropical regions of the world. The microbes associated with the rhizosphere of *P. australis* are believed to contribute to the remediation ability of the plant via the synthesis of metabolites which enhances the growth of plant and hyperaccumulation of the pollutants by both the plant and associated microbes (Bulgarelli et al., 2012; Kawasaki et al., 2016; Robertson-Albertyn et al., 2017; Pétriacq et al., 2017).

Rhizoremediation effectiveness is based on the complementary process between the plants and the microbes where plants pull contaminants into their rhizosphere and the microbes degrade them either in the rhizosphere or in the plant itself or both (Barac et al., 2004; Muratova et al., 2008). *Phragmites australis* employs this method of remediation (Scholes et al., 1999). However, very little is known about the rhizosphere microbial diversity and secondary metabolite profiles of *P. australis* in acid mine sites. This study is aimed at determining the influence of acid mine drainage on the diversity of rhizosphere microbes and the secondary metabolite profiles of *P. australis*. The effect of acid mine drainage on microbial diversity, in general, is understood and therefore the concern of the authors of this manuscript focused on the rhizosphere microbes due to their role in



bioremediation and the uniqueness of their habitat. The understanding of the influence of acid mine water on the diversity of microbial populations in the rhizosphere of the bioremedial *P. australis* and the metabolite shift may prove to be vital knowledge for bioremediation processes and microbes adaptations in acid mine.

## Materials and Methods

This study was undertaken to assess the effect of acid mine drainage on the microbial diversity and secondary metabolite shifts of rhizosphere soil of two acid mine sites (Wuinze 17 and Lan 3) and one non-acid mine site (Florida Lake) in the Gauteng province in South Africa which were all within a 17.7 Km radius. Rhizosphere soil sampling was done on the edge of the water body where the plant roots are constantly submerged in water. In three field study regimes undertaken, water was also sampled to determine its physicochemical parameters to assess the extent of acid mine drainage. Acid mine water and contaminated soils are characterised by high electrical conductivity (EC), high total dissolved solutes (TDS), high salinity (Sa), and low pH which is why these parameters were measured to confirm acid mine contamination of the selected sites. The temperature was also measured to evaluate the temperature variation in the acid mine drainage sites and the non-acid mine drainage site. Following the sampling of the water, and soil, microbial diversity of the rhizosphere soil was assessed as well as secondary metabolite profiles of the rhizosphere soil.

## Study Area

Lan 3 (S 26°07.820', E 027°46.680' and elevation of 1693 m), a tailing dam of Mintails Mogale Gold Mine in Randfontein and Wuinze 17 (S 26°07.171', E 027°43.305' and elevation of 1670 m), a tailing dam of Sibanye Gold Mine were the acid mine sampling sites in this study. Both sampling sites are located in Randfontein, Gauteng Province, South Africa. Florida Lake is a normal water body which serves as a control in this study. It is also found in the Gauteng Province of South Africa and has a GPS of S 26°10.625', E 027°54.220' and 1673 m elevation. Details of the sampling sites are shown in Fig. 1.

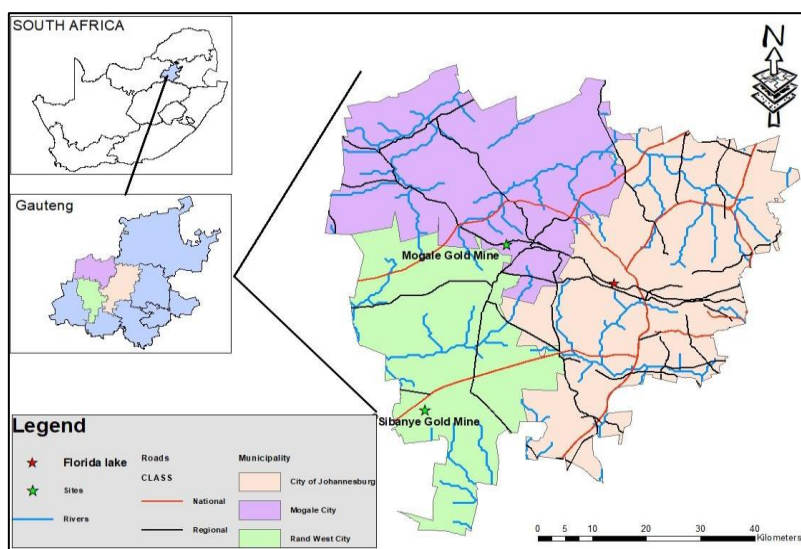


**Figure 1.** Map showing the sampling sites (Mogale Gold Mine, Sibanye Gold Mine and Florida Lake)

### Sample Collection

From each of three sampling sites, three sampling points were identified. Water was scooped with a bucket from each sampling point and physicochemical parameters, namely, pH, temperature, salinity, total dissolved solutes and electrical conductivity were measured on-site using a multi-parameter ion-specific meter (Hanna instruments, version HI9828, SN 08334776). Furthermore, three rhizosphere soil samples (one sample per each uprooted reed plant that was 1 m apart) were collected and pooled equally to form a 1 gram sample. The soil samples were transported in ice to the laboratory where a further composite sample of 3 grams was pooled from each of the 1 gram samples which represented a sampling site. Details of the sampling and analysis done are shown in *Fig. 2* and *Table 1* respectively.

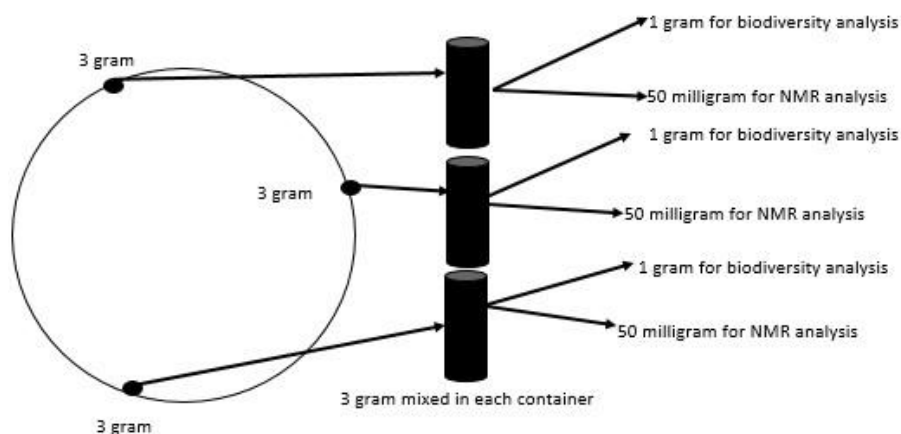


**Figure 2.** Diagrammatic representation of rhizosphere soil sample collection in a water body. Notice that the sampling was done on the edge of muddy waters. Water was scooped with a bucket from the same spots where rhizosphere soil samples were collected. This process was done on each sampling period

**Table 1.** Summary of the samples collected and analysis done. Lan and Wuinze 17 are acid mine sites and Florida Lake is a normal water body

Sampling sites	Samples collected	Analysis done
Wuinze 17	Water	Physicochemical properties
Wuinze 17	Rhizosphere soil	Biodiversity and secondary metabolite profile
Florida Lake	Water	Physicochemical properties
Florida Lake	Rhizosphere soil	Biodiversity and secondary metabolite profile
Lan 3	Water	Physicochemical properties
Lan 3	Rhizosphere soil	Biodiversity and secondary metabolite profile

### Assessment of Microbial Community Functional Diversity

Within two hours of sampling three grams of rhizosphere soil (one composite sample for each of the three sites) were mixed with 27 mL of sterile 0.85% sodium chloride solution, vortexed for five minutes and the silt was allowed to settle for an additional five minutes. 180  $\mu$ L of the water fraction was dispensed into each of the 96 wells of the BIOLOG Ecoplate. One BIOLOG Ecoplate was used for each of the sampling sites and



therefore a total of three plates were used per sampling regime resulting in a total of 9 plates used for the three regimes. The plates were sealed with parafilm and incubated in the dark at 25°C. Absorbance was measured at 590 nm with a VarioSkan Flash (Thermoscientific) absorbance scanner at 0, 24, 48, 72, 96 and 120 hours after incubation. The purple coloration of the BIOLOG Ecoplate is an indication of the substrate utilization and functional diversity. The measured absorbance is used to calculate the Shannon index of biodiversity which indicates the measure of the microbial community present in the sampling sites.

### Physicochemical Data Analysis

Measurements of physicochemical parameters were analyzed by analysis of variance (ANOVA). One way ANOVA was done using SAS version 9.4 with a significant level of  $p < 0.05$ . Post hoc testing was carried out using the Tukey test to test the differences among all possible pairs of treatments. The mean and standard deviation of all the samples were recorded for each sampling sites. Results of this analysis are presented in Table 2A-C.

**Table 2A.** Rhizosphere soil and water collected from the three sampling sites (Wuinze 17 at Sibanye Gold Mine, Florida Lake at Florida Roodepoort, and Lan 3 at Minitails Mogale Gold Mine) on September 2017

Sample ID	Temp.	EC	TDS	Sa	pH	SI
WW11	12±1.23 <sup>c</sup>	2286±128.3 <sup>b</sup>	1969.50±15.9 <sup>b</sup>	1.59±0.05 <sup>b</sup>	6.12±1.58 <sup>b</sup>	NA
WW22	12±1.23 <sup>c</sup>	2286±128.3 <sup>b</sup>	1969.50±15.9 <sup>b</sup>	1.59±0.05 <sup>b</sup>	6.12±1.58 <sup>b</sup>	NA
WW33	12±1.23 <sup>c</sup>	2286±128.3 <sup>b</sup>	1969.50±15.9 <sup>b</sup>	1.59±0.05 <sup>b</sup>	6.12±1.58 <sup>b</sup>	NA
WS14	NA	NA	NA	NA	NA	3.24±0.13 <sup>b</sup>
WS25	NA	NA	NA	NA	NA	3.24±0.13 <sup>b</sup>
WS36	NA	NA	NA	NA	NA	3.24±0.13 <sup>b</sup>
FW47	16.0±1.46 <sup>b</sup>	167.9±4.56 <sup>c</sup>	135.2±19.5 <sup>c</sup>	0.10±0.02 <sup>c</sup>	8.11±2.53 <sup>a</sup>	NA
FW58	16.0±1.46 <sup>b</sup>	167.9±4.56 <sup>c</sup>	135.2±19.5 <sup>c</sup>	0.10±0.02 <sup>c</sup>	8.11±2.53 <sup>a</sup>	NA
FW69	16.0±1.46 <sup>b</sup>	167.9±4.56 <sup>c</sup>	135.2±19.5 <sup>c</sup>	0.10±0.02 <sup>c</sup>	8.11±2.53 <sup>a</sup>	NA
FS410	NA	NA	NA	NA	NA	4.55±2.60 <sup>a</sup>
FS511	NA	NA	NA	NA	NA	4.55±2.60 <sup>a</sup>
FS612	NA	NA	NA	NA	NA	4.55±2.60 <sup>a</sup>
LW713	22.3±2.04 <sup>a</sup>	6142±267.8 <sup>a</sup>	4407±236.9 <sup>a</sup>	3.75±0.89 <sup>a</sup>	5.03±1.56 <sup>c</sup>	NA
LW814	22.3±2.04 <sup>a</sup>	6142±267.8 <sup>a</sup>	4407±236.9 <sup>a</sup>	3.75±0.89 <sup>a</sup>	5.03±1.56 <sup>c</sup>	NA
LW915	22.3±2.04 <sup>a</sup>	6142±267.8 <sup>a</sup>	4407±236.9 <sup>a</sup>	3.75±0.89 <sup>a</sup>	5.03±1.56 <sup>c</sup>	NA
LS716	NA	NA	NA	NA	NA	2.89±0.04 <sup>c</sup>
LS817	NA	NA	NA	NA	NA	2.89±0.04 <sup>c</sup>
LS918	NA	NA	NA	NA	NA	2.89±0.04 <sup>c</sup>

Mean ± standard deviation. Mean with the same superscript letters are not significant at  $p < 0.05$ . On the sample ID, the first superscript letter is for the site (W=Wuinze 17, F=Florida Lake, L=Lan 3), the second superscript letter is for sample type (W=Water, S=Soil), and the superscript number is for sampling points (1-9). Three rhizosphere soil samples were collected from each of the nine points (1-9) shown in Fig. 2. From each sampling point, water was also scooped and its temperature (Temp.), electrical conductivity (EC), total dissolved solids (TDS), salinity (Sa), and pH determined. Shannon indices (SI) of soil samples collected from two acid mine sites (W 1-3 for Wuinze 17 sampling points; and L 7-9 for Lan 3 sampling points) and the non-acid mine site (F 4-6 for Florida Lake) are represented

**Table 2B.** Rhizosphere soil and water collected from the three sampling sites (Wuinze 17 at Sibanye Gold Mine, Florida Lake at Florida Roodepoort, and Lan 3 at Minitails Mogale Gold Mine) on November 2017

Sample ID	Temp.	EC	TDS	Sa	pH	SI
WW11	10.7±1.05 <sup>c</sup>	1724±104.6 <sup>b</sup>	1546.3±12.7 <sup>b</sup>	1.22±0.03 <sup>b</sup>	6.54±1.08 <sup>b</sup>	NA
WW22	10.7±1.05 <sup>c</sup>	1724±104.6 <sup>b</sup>	1546.3±12.7 <sup>b</sup>	1.22±0.03 <sup>b</sup>	6.54±1.08 <sup>b</sup>	NA
WW33	10.7±1.05 <sup>c</sup>	1724±104.6 <sup>b</sup>	1546.3±12.7 <sup>b</sup>	1.22±0.03 <sup>b</sup>	6.54±1.08 <sup>b</sup>	NA
WS14	NA	NA	NA	NA	NA	2.81±0.08 <sup>b</sup>
WS25	NA	NA	NA	NA	NA	2.81±0.08 <sup>b</sup>
WS36	NA	NA	NA	NA	NA	2.81±0.08 <sup>b</sup>
FW47	14.2±1.11 <sup>b</sup>	111.9±2.74 <sup>c</sup>	102.4±14.3 <sup>c</sup>	0.05±0.01 <sup>c</sup>	7.05±1.12 <sup>a</sup>	NA
FW58	14.2±1.11 <sup>b</sup>	111.9±2.74 <sup>c</sup>	102.4±14.3 <sup>c</sup>	0.05±0.01 <sup>c</sup>	7.05±1.12 <sup>a</sup>	NA
FW69	14.2±1.11 <sup>b</sup>	111.9±2.74 <sup>c</sup>	102.4±14.3 <sup>c</sup>	0.05±0.01 <sup>c</sup>	7.05±1.12 <sup>a</sup>	NA
FS410	NA	NA	NA	NA	NA	3.34±0.04 <sup>a</sup>
FS511	NA	NA	NA	NA	NA	3.34±0.04 <sup>a</sup>
FS612	NA	NA	NA	NA	NA	3.34±0.04 <sup>a</sup>
LW713	19.87±1.2 <sup>a</sup>	4236±148.2 <sup>a</sup>	3682±156.2 <sup>a</sup>	3.10±0.36 <sup>a</sup>	5.87±1.15 <sup>c</sup>	NA
LW814	19.87±1.2 <sup>a</sup>	4236±148.2 <sup>a</sup>	3682±156.2 <sup>a</sup>	3.10±0.36 <sup>a</sup>	5.87±1.15 <sup>c</sup>	NA
LW915	19.87±1.2 <sup>a</sup>	4236±148.2 <sup>a</sup>	3682±156.2 <sup>a</sup>	3.10±0.36 <sup>a</sup>	5.87±1.15 <sup>c</sup>	NA
LS716	NA	NA	NA	NA	NA	2.7±0.12 <sup>c</sup>
LS817	NA	NA	NA	NA	NA	2.7±0.12 <sup>c</sup>
LS918	NA	NA	NA	NA	NA	2.7±0.12 <sup>c</sup>

Mean ± standard deviation. Mean with the same superscript letters are not significant at  $p < 0.05$ . On the sample ID, the first superscript letter is for the site (W=Wuinze 17, F=Florida Lake, L=Lan 3), the second superscript letter is for sample type (W=Water, S=Soil), and the superscript number is for sampling points (1-9). Three rhizosphere soil samples were collected from each of the nine points (1-9) shown in Fig. 2. From each sampling point, water was also scooped and its temperature (Temp.), electrical conductivity (EC), total dissolved solids (TDS), salinity (Sa), and pH determined. Shannon index (SI) of samples collected from two acid mine sites (W 1-3 for Wuinze 17 sampling points; and L 7-9 for Lan 3 sampling points) and the non-acid mine site (F 4-6 for Florida Lake) are represented

### Biodiversity Data Analysis

Absorbance values obtained from the VarioSkan Flash absorbance scanner were adjusted by subtracting the baseline absorbance value (0-hour absorbance). The 96-hour absorbance values differentiated between the three water bodies the most and were, therefore, the only ones considered for further analysis. The Shannon index of diversity ( $H$ ) was calculated following the approach of Gryta et al. (2014). One way analysis of variance (ANOVA) was done on all the biodiversity indicators using SAS version 9.4 at a significant level of  $p < 0.05$ . Shannon index was correlated with temperature, electrical conductivity, total dissolved solutes, salinity, and pH; and 0.8 and -0.8 were set as the cut-off for Pearson correlation coefficients at a significant level of  $p < 0.05$  (Table 3). Results of the microbial diversity are presented in Table 2A-C and Fig. 3.

### Secondary Metabolite Shift Assessment

Secondary metabolite profiles of rhizosphere soil from the three sites were done using a 600 MHz Varian NMR spectroscopy. NMR spectra were processed with ACD/NMR

and principal component analysis of intensity data was analysed using MetaboAnalyst. Principal component analysis plots are presented in Fig. 4.

**Table 2C.** Rhizosphere soil and water collected from the three sampling sites (Wuinze 17 at Sibanye Gold Mine, Florida Lake at Florida Roodepoort, and Lan 3 at Minitails Mogale Gold Mine) on June 2018

Sample ID	Temp.	EC	TDS	Sa	pH	SI
WW11	7.9±0.31 <sup>b</sup>	1791.3±10.9 <sup>b</sup>	1557.2±1.15 <sup>b</sup>	1.24±0.02 <sup>b</sup>	6.50±0.31 <sup>b</sup>	NA
WW22	7.9±0.31 <sup>b</sup>	1791.3±10.9 <sup>b</sup>	1557.2±1.15 <sup>b</sup>	1.24±0.02 <sup>b</sup>	6.50±0.31 <sup>b</sup>	NA
WW33	7.9±0.31 <sup>b</sup>	1791.3±10.9 <sup>b</sup>	1557.2±1.15 <sup>b</sup>	1.24±0.02 <sup>b</sup>	6.50±0.31 <sup>b</sup>	NA
WS14	NA	NA	NA	NA	NA	3.33±0.05 <sup>a</sup>
WS25	NA	NA	NA	NA	NA	3.33±0.05 <sup>a</sup>
WS36	NA	NA	NA	NA	NA	3.33±0.05 <sup>a</sup>
FW47	5.4±0.2 <sup>c</sup>	114.5±0.36 <sup>c</sup>	119.3±0.42 <sup>c</sup>	0.09±0.01 <sup>c</sup>	7.20±0.01 <sup>a</sup>	NA
FW58	5.4±0.2 <sup>c</sup>	114.5±0.36 <sup>c</sup>	119.3±0.42 <sup>c</sup>	0.09±0.01 <sup>c</sup>	7.20±0.01 <sup>a</sup>	NA
FW69	5.4±0.2 <sup>c</sup>	114.5±0.36 <sup>c</sup>	119.3±0.42 <sup>c</sup>	0.09±0.01 <sup>c</sup>	7.20±0.01 <sup>a</sup>	NA
FS410	NA	NA	NA	NA	NA	3.34±0.01 <sup>a</sup>
FS511	NA	NA	NA	NA	NA	3.34±0.01 <sup>a</sup>
FS612	NA	NA	NA	NA	NA	3.34±0.01 <sup>a</sup>
LW713	12.3±0.15 <sup>a</sup>	4424.3±1.15 <sup>a</sup>	3823±1.0 <sup>a</sup>	3.20±0.10 <sup>a</sup>	5.53±0.11 <sup>c</sup>	NA
LW814	12.3±0.15 <sup>a</sup>	4424.3±1.15 <sup>a</sup>	3823±1.0 <sup>a</sup>	3.20±0.10 <sup>a</sup>	5.53±0.11 <sup>c</sup>	NA
LW915	12.3±0.15 <sup>a</sup>	4424.3±1.15 <sup>a</sup>	3823±1.0 <sup>a</sup>	3.20±0.10 <sup>a</sup>	5.53±0.11 <sup>c</sup>	NA
LS716	NA	NA	NA	NA	NA	2.80±0.71 <sup>b</sup>
LS817	NA	NA	NA	NA	NA	2.80±0.71 <sup>b</sup>
LS918	NA	NA	NA	NA	NA	2.80±0.71 <sup>b</sup>

Mean ± standard deviation. Mean with the same superscript letters are not significant at p<0.05. On the sample ID, the first superscript letter is for the site (W=Wuinze 17, F=Florida Lake, L=Lan 3), the second superscript letter is for sample type (W=Water, S=Soil), and the superscript number is for sampling points (1-9). Three rhizosphere soil samples were collected from each of the nine points (1-9) shown in Fig. 2. From each sampling point, water was also scooped and its temperature (Temp.), electrical conductivity (EC), total dissolved solids (TDS), salinity (Sa), and pH determined. Shannon index (SI) of samples collected from two acid mine sites (W 1-3 for Wuinze 17 sampling points; and L 7-9 for Lan 3 sampling points) and the non-acid mine site (F 4-6 for Florida Lake) are represented

**Table 3.** Correlation coefficients of the Shannon index of biodiversity and the physicochemical parameters for rhizosphere soil and water samples collected from the sampling points

Parameters	Shannon index of biodiversity		
	September 2017	November 2017	June 2018
pH	0.48	0.24	0.95
Temperature	-0.20	-0.88	-0.97
Salinity	-0.47	-0.29	-0.97
TDS	-0.46	-0.27	-0.97
EC	-1.00	-0.88	-0.96

Values greater or equal to 0.80 or -0.80 are taken as the threshold cut off in this study (n=3). Correlation is significant at the level p<0.05. TDS and EC stand for total dissolved solids and electrical conductivity

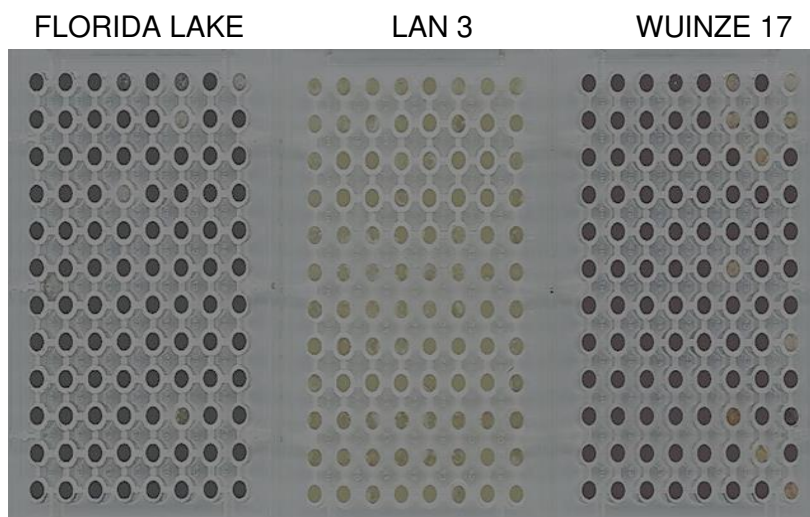


**Figure 3.** Ninety-six well BIOLOG Ecoplates showing catabolic activities of the microbial community of the rhizosphere of *Phragmites australis* after 96 hours of incubation. The ecoplates are pre-coated with 31 carbon substrates and the purple colour of the well indicates utilization of the substrate by the microbes in the water. Notice that no substrate turned purple in the middle 96 well ecoplate showing complete loss of microbial activities as a result of acid mine drainage. All the sets of BIOLOG Ecoplates looked similar and therefore only one set (sampled in September 2017) was shown

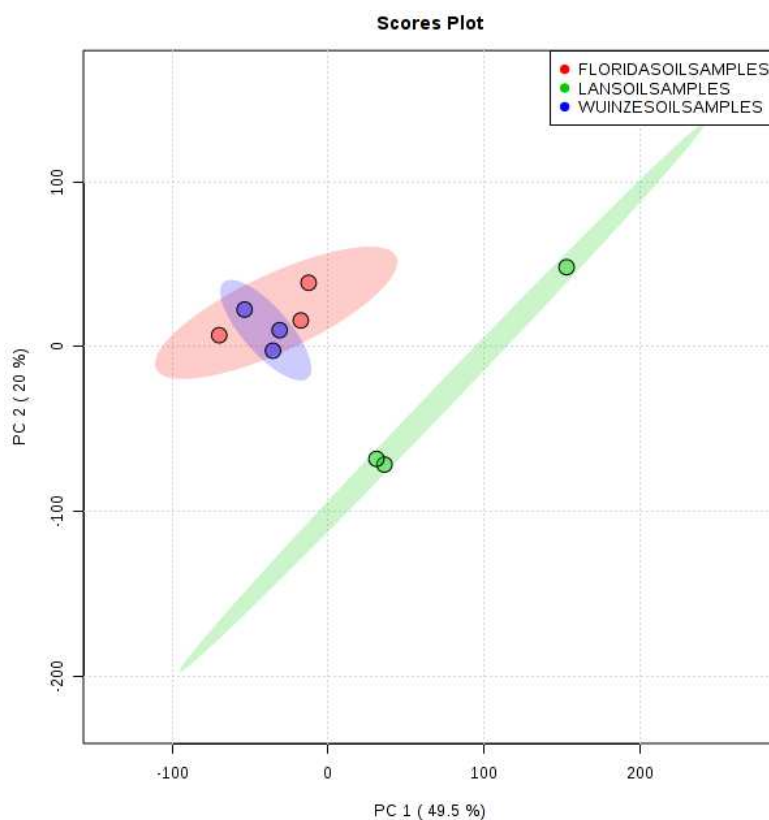


**Figure 4.** Principal component analysis showing the secondary metabolite shifts of soil samples of *Phragmites australis*. Florida Lake and Wuinze 17 clustered together indicating closeness in their metabolites. The metabolites of Lan 3 were differentiated from the other two sites

## Results

Measurements of physicochemical parameters of the water bodies confirmed that the sites selected as acid mine sites indeed showed characteristics of acid mine pollution and the normal site had characteristics of a regular water body. This was shown by the low pH, and high electrical conductivity (EC) and total dissolved solids (TDS) values in the acid mine sites and relatively normal in the water samples from Florida Lake and also the significant difference at  $p < 0.05$  across the three sampling sites for the physicochemical parameters. The applications of BIOLOG EcoPlates in the evaluation of microbial diversity by many researchers have proven to be effective in providing a good indication of microbial diversity (Wang et al., 2008; Nautiyal et al., 2010; Ling et al., 2012; Zhang et al., 2013, 2014; Deng et al., 2014; Xu et al., 2015; Liu et al., 2015; Raghawendra et al., 2019). In this study, BIOLOG EcoPlates were used to measure the microbial diversity of rhizosphere soil of *Phragmites australis*. Microbial diversity in the two acid mine sites was reduced compared to the normal water body. However, the Wuinze 17 site retained most of its microbial diversity despite having a relatively high electrical conduction and low pH characteristic of acid mine water. Although these parameters had values higher than those of Florida they were still far less than those of the very harsh Lan 3 site. Proton NMR spectroscopy has also proved effective in secondary metabolite profiling of different samples (Blow, 2008; De Meyer et al., 2008; Nicholson and Lindon, 2008; Alves et al., 2009; Pontoizeau et al., 2010; Ravanbakhsh et al., 2015; Alonso et al., 2015). The secondary metabolites profiles as observed in this study showed diversity among the sampling sites. However, one of the acid mine sites (Wuinze 17) showed close clustering of the metabolites with the normal water body (Florida Lake). This could be attributed to the ability of the rhizosphere microbes associated with *Phragmites australis* to increase the pH of Wuinze 17 that was 1.03 above the pH of Lan 3 site (an acid mine site) to meet the acceptable limits of DWAF (1996) guidelines as well as the not so high EC in Wuinze 17. This could lead to the production of metabolites similar to the ones produced by the microbes in Florida Lake.

### *Physicochemical Characteristics*

The results of the physicochemical parameters showed that there were significant differences between each of the parameters across the two acid mine sites (Wuinze 17 and Lan 3) and the non-acid mine site (Florida Lake) (Table 2A-C). The acid mine drainage samples from the two acid mine sites (Wuinze 17 and Lan 3) showed higher electrical conductivity, salinity, total dissolved solids and low pH when compared to the non-acid mine drainage (Florida Lake) (Table 2A-C). The findings of many researchers have shown acid mine drainage to be characterized by pH values that are less than five (Dagmar Kock, 2008; Denef et al., 2010; USGS, 2012; Masindi et al., 2015; Chen et al., 2016; Teng et al., 2017). The guidelines stipulated for acid mine treated water according to DWAF (1996) are 6 – 9 for pH, 0 – 1 200 mg/L for total dissolved solutes, and 0 – 450  $\mu\text{S}/\text{cm}$  for electrical conductivity. The pH values of Wuinze 17 (acid mine site) and Florida Lake (normal water body) were observed to be within the recommended guideline. This could be an indication of more remediation activities of *Phragmites australis* and the associated rhizosphere microbes in Wuinze 17 than in Lan 3. This could be attributed to the difference in the pH between the two acid mine drainage sites that ranges from 0.67 to 1.09. Furthermore, the electrical conductivity and total dissolved

solids of Florida Lake was within the required guideline confirming the lake as a regular water body.

### ***Microbial Community Functional Diversity***

In this study, the Shannon index of biodiversity was done to assess the microbial diversity of the two acid mine water and the non-acid mine water. High Shannon index indicates more diversity of microbial communities in the sampling sites. The non-acid mine water showed more diversity than the acid mine water.

### ***Shannon Index of Biodiversity***

The Shannon indices differ significantly across the three sampling sites in this study (Table 2A-C and Fig. 3). Florida Lake (non-acid mine drainage site) was observed to be more diversified in the microbial community than the two acid mine sites (Wuinze 17 and Lan 3). The Shannon diversity index of Florida Lake was higher than the two acid mine sites and this was also shown by the higher number of BIOLOG Ecoplate wells which had turned purple indicating the presence of microbes that had the potential to utilize the substrate pre-coated in the well. Wuinze 17 showed higher Shannon index values than Lan 3 presenting Lan 3 as the less diversified site.

### ***Correlation analysis of the Shannon index of Biodiversity and Physicochemical Parameters***

The acid mine drainage influenced the microbial diversity of the common reed's rhizosphere. This finding is based on the correlation between the physicochemical parameters and the Shannon index (Table 3). Pearson correlation coefficients of 0.8 and -0.8 were set as the cut-off in this study at a significant level of  $p < 0.05$ . Correlated with salinity and total dissolved solute, the SI had a negative correlation coefficient with the highest negative correlation recorded in the third sampling. The negative correlation means that as salinity and total dissolved solids increase, the rhizosphere microbial diversity decreases. Similarly, electric conductivity showed a strong negative correlation with the Shannon index of biodiversity in all the three sampling periods. However, pH showed a positive correlation with the Shannon index with the strongest correlation recorded in the third sampling period. This positive correlation implied that the increase in pH results in the corresponding increase in microbial diversity. This correlation study provided an insight into the response of the microbial diversity with changes in environmental conditions.

### ***Secondary Metabolites Assessment***

The acid mine drainage influenced the secondary metabolite compositions of the rhizosphere soil and roots of *Phragmites australis*. This is evident in the metabolite profiles observed in the principal component analysis (PCA) of secondary metabolites in the soil samples (Fig. 4). Surprisingly, the non-acid mine Florida Lake and the acid mine Wuinze17 soil samples showed similar metabolite shift that differs from Lan 3 soil samples. It was expected that the acid mine sites would cluster together instead of the grouping of Florida Lake and Wuinze 17 which resulted from the PCA of NMR data. This could be attributed to the normality of Florida Lake and the fact that Wuinze 17 is not static water and therefore receives fresh supplies of water which may sometimes be fresh. Furthermore, the compliance of the pH values of the two sites to the DWAF (1996)

guidelines could be another contributing factor to the clustering of the sites. This is reaffirmed by the closeness of Shannon index of both sites indicating the presence of similar microbes capable of producing similar metabolites.

## Discussion

Although there are dynamics in studies investigating aspects of pollution due to mining, conclusions drawn from these studies confirm the loss of biodiversity as a result of pollution. As such the production of secondary metabolites by the affected organisms is likely to change to reflect the new natural imbalances. This phenomenon was further re-established in this work. However, the focus of the authors of this manuscript was on microbes associated with the rhizosphere of *Phragmites australis* because of their role in bioremediation and the uniqueness of their habitat. Efforts in ecosystem restoration in acid mine environments need to focus on preserving rhizosphere associated microbes to maintain their mutual relationship with their associated bioremediating plant. Results of this study clearly showed that the diversity of the *P. australis* rhizosphere associated microbes of the two acid mine drainage sites (Wuize 17 and Lan 3) were reduced when compared to the non-acid mine drainage site (Florida Lake) in all the sampling periods. The correlation between the physicochemical parameters and the Shannon index of biodiversity showed that the acid mine drainage influenced microbial diversity (Table 3). The secondary metabolite analysis showed metabolite shifts among the soil samples in the three sampling sites indicating diversity and difference in their secondary metabolite composition.

The reasons for the loss of diversity in the acid mine sites in this study could have been caused by the pH gradient. A neutral pH of 7 could pose no environmental problems to the existing organisms. Brady and Weil (1996) suggested that extreme pH affects the survival of microorganisms directly or indirectly via the control of auxiliary environmental parameters relating to pH like nutrient availability and cationic metal solubility. This suggestion was supported by the work done by Amaral-Zettler et al. (2011), Li et al. (2014), Sun et al. (2014) and Sun et al. (2015) who observed that pH affects the microbial structure and composition of environments. Kuang et al. (2013) stated that the acidic nature of acid mine drainage water tends to pose a major risk factor to existing diversity of microbial community and structure when discharged directly into water bodies. Furthermore, many researchers have reported that the low pH in acid mine drainage water accelerates the solubility of many metals, and in addition with low availability of organic carbon, it creates highly challenging and extreme environmental growth conditions for the microbial community (Dopson et al., 2003; Slonczewski et al., 2009). The work of these researchers was consistent with the results obtained in this study because the acid mine sites with low pH showed less microbial diversity than the non-acid mine site based on the Shannon index.

Sun et al. (2015) observed a strong correlation between temperature and microbial community. The authors further observed a strong and significant link between temperature and microbial community variance. Volant et al. (2014), and Edwards et al. (1999) reported temperature as a crucial factor that shapes the community composition of microbes in acid mine drainage. Similarly, in this present study, the temperature was observed to correlate strongly with the Shannon index of biodiversity. This finding indicated the influence of the environmental temperature on microbial community composition. However, it should be stated that the three sampling sites in this study are

within a 17.7 km radius and therefore fall under the same climatic zone and therefore the difference in the water temperature was not large but had however a significant influence on the Shannon index an indication of the elasticity of the Shannon index. Further studies on water temperature and the Shannon index are recommended to deepen understanding of the dependence of microbial activity and water temperature.

Salinity can influence and possibly change soil environment leading to changes in the soil microbial composition, structure, and biomass. This implied that salinity brought about by the presence of dissolved solids in the acid mine plays a major role in determining the diversity and composition of microbes and the metabolites produced by the microbes in order to adapt to the changing environment. The correlation analysis of the Shannon index of biodiversity with the physicochemical parameters also showed that indeed salinity must have reduced diversity in this study. A plethora of similar studies agree with the results of this study (Batra and Manna, 1997; Pathak and Rao, 1998; Rousk et al., 2011; Setia et al., 2011; Andronov et al., 2012; Yan et al., 2015; Chen et al., 2017). The reduction of microbial biomass in the high saline environment is due to osmotic stress that leads to lysing and drying of cells (Laura, 1974; Sarig and Steinberger, 1994; Sarig et al., 1996; Batra and Manna, 1997; Pathak and Rao, 1998; Rietz and Haynes, 2003; Yuan et al., 2007a).

Yaish et al. (2016) discovered that soil salinity causes a reduction in the bicarbonate and calcium carbonate of the soil. A discovery that was consistent with the work done by Setia et al. (2013) where the effect of salinity in the reduction of the global carbon stocks was observed due to the reduction in the microbial activity. This implies that an increase in the salinity of the environment results in a corresponding decrease in the microbial structure and possibly the diversity. The extreme environmental condition of the acid mine drainage might be the cause of the change in the microbial activity and the diversity of the heterogeneous microbial community in this study. This was evidenced in the work done by Keshri et al. (2015) who discovered that the Vanadium mine water samples were less acidic and saline with higher bacterial diversity. This result concurs with the results obtained in this study where the Florida Lake, a non-acid mine drainage sites and Wuinze 17, an acid mine drainage site, which were less acidic were observed to have higher microbial diversity than Lan 3, an acid mine drainage site that was more acidic.

Previous studies showed a correlation between the physicochemical parameters and the microbial community composition (Dopson et al., 2003; Slonczewski et al., 2009). This present study supported the work done by Dopson et al. (2003) and Slonczewski et al. (2009) because correlation coefficients of the biodiversity indicator, showed both positive and negative correlation with different physicochemical parameters. For example, electrical conductivity showed a strong negative correction throughout the sampling periods in this study. Some studies indicated that increase in soil electrical conductivity leads to decrease in soil respiration and consequently affect the soil microbial community (Adviento-Borbe et al., 2006; Yuan et al., 2007b; Wong et al., 2009). These results were in agreement with the results obtained in this study where the two acid mine sites with high electrical conductivity experienced low microbial diversity in terms of the Shannon index. This reduction in Shannon index could be attributed to the reduction in the cell respiration or the osmotic stress faced by the soil microbes.

There are variations in the sensitivity of enzymatic activities to varying salinity in the soil (Frankenberger and Bingham, 1982; Garcia and Hernandez, 1996; Pan et al., 2013). This could be attributed to variation in the metabolite profiles caused by the varying salinity state in the environment. Work done by many researchers has shown that



variation in salt tolerance among microorganisms' influences the microbial community structure and metabolite profiles in saline soils more than the non-saline soils (Quesada et al., 1982; Del-Moral et al., 1987; Zahran et al., 1992; Killham, 1994; Pankhurst et al., 2001; Oren, 2001; Gros et al., 2003; Sagot et al., 2010). Furthermore, some studies have shown the relationships between enzyme activities and the metabolites produced by both plants and microbes in response to harsh environment factors (Sagot et al., 2010; Sulpice et al., 2010; Méndez-García et al., 2015; Jian et al., 2016). Similarly, in this study, the diverse metabolites produced by the microbes could be a surviving factor for those organisms and possibly be responsible for the metabolite shifts observed between the acid mine sites and non-acid mine sites in this study.

Tian et al. (2014) pointed out that for effective remediation in constructed wetlands using macrophytes like *P. australis*, microbial communities present in the rhizosphere of plant species selected for the bioremediation play major roles in promoting the growth of plants and biodegrading the contaminants. The understanding of the influence of the acid mine water on the rhizospheres' microbes in this present study unveiled the need to preserve these microbes in order to enhance the remediation processes of the macrophytes.

## Conclusion

This study evaluated the influence of the acid mine drainage on the microbial diversity and metabolite shift of the common reed's rhizosphere. The evaluation was successful and provided a clear distinction of the metabolite profiles and microbial diversities of the acid mine drainage (AMD) sites and the non-acid mine drainage site. The AMD sites showed a low microbial diversity which is evident in the biodiversity indicator. However, Wuinze 17 and the non-acid mine site showed similar metabolite profile. This could be attributed to remediating ability of the microbes associated with the rhizosphere of *Phragmites australis* leading to the compliance of pH values of Wuinze 17 to DWAF (1996) guidelines and the closeness of the Shannon index of biodiversity values of both sites (Wuinze 17 and Florida Lake). The closeness in their Shannon index could imply the presence of similar microbes capable of producing similar metabolites. The present study suggests further study on the identification of the microbial communities in the three sampling sites and the remediation ability of the identified microorganisms across environmental pollutants.

**Acknowledgements.** The authors wish to thank the Agricultural Research Council - University of South Africa Climate Change Collaboration Centre for their financial support.

**Author Contributions.** Kalu Chimdi Mang performed the sample collection, data analyses and writing of the manuscript. Khayaletu Ntushelo assisted in the sample collection, data analysis and contributed immensely to the writing and editing of the manuscript.

**Conflicts of Interests.** The authors declared no conflict of interests.

## REFERENCES

- [1] Adviento-Borbe, M. A. A., Doran, J. W., Drijber, R. A., Dobermann, A. (2006): Soil electrical conductivity and water content affect nitrous oxide and carbondioxide emissions in intensively managed soils. – *Journal of Environmental Quality* 35: 1999-2010.
- [2] Alonso, A., Marsal, S., Julià, A. (2015): Analytical methods in untargeted metabolomics: State of the Art in 2015. – *Frontiers in Bioengineering and Biotechnology* 3: 23.
- [3] Alves, A., Rantalainen, M., Holmes, E., Nicholson, J. K., Ebbels, T. M. D. (2009): Analytic properties of statistical total correlation spectroscopy based information recovery in <sup>1</sup>H NMR metabolic data sets. – *Analytical Chemistry* 81: 2075-2084.
- [4] Amaral-Zettler, L. A., Zettler, E. R., Theroux, S. M., Palacios, C., Aguilera, A., Amils, R. (2011): Microbial community structure across the tree of life in the extreme Rio Tinto. – *ISME Journal* 5: 42-50.
- [5] Andronov, E. E., Petrova, S. N., Pinaev, A. G., Pershina, E. V., Rakhimgalieva, S. Z., Akhmedenov, K. M., Sergaliev, N. K. (2012): Analysis of the structure of microbial community in soils with different degrees of salinization using T-RFLP and real-time PCR techniques. – *Eurasian Soilless Science* 45: 147-156.
- [6] Barac, T., Taghavi, S., Borremans, B., Provoost, A., Oeyen, L., Colpaert, J. V., Vangronsveld, J., van der Lelie, D. (2004): Engineered endophytic bacteria improve phytoremediation of water-soluble, volatile, organic pollutants. – *Nature Biotechnology* 22: 583-588.
- [7] Batra, L., Manna, M. C. (1997): Dehydrogenase activity and microbial biomass carbon in salt affected soils of semi-arid and arid regions. – *Arid Land Research Management* 11: 295-303.
- [8] Blow, N. (2008): Metabolomics: Biochemistry's new look. – *Nature* 455: 697-700.
- [9] Blowes, D. W., Ptacek, C. J., Jambor, J. L., Weisener, C. G. (2003): The geochemistry of acid mine drainage. – In: Holland, H. D., Turekian, K. K. (eds.) *Treatise on geochemistry*. Oxford, Elsevier, pp. 150-204.
- [10] Brady, N. C., Weil, R. R. (1996): *The nature and properties of soils*. – Prentice-Hall Inc., New Jersey.
- [11] Bulgarelli, D., Rott, M., Schlaeppi, K., Ver Loren van Themaat, E., Ahmadinejad, N., Assenza, F., Rauf, P., Huettel, B., Reinhardt, R., Schmelzer, E., Peplies, J., Gloeckner, F. O., Amann, R., Eickhorst, T., Schulze-Lefert, P. (2012): Revealing structure and assembly cues for *Arabidopsis* root-inhabiting bacterial microbiota. – *Nature* 488: 91-95.
- [12] Chen, L. X., Huang, L. N., Méndezgarcía, C., Kuang, J. L., Hua, Z. S., Liu, J., Shu, W. S. (2016): Microbial communities, processes and functions in acid mine drainage ecosystems. – *Current Opinion in Biotechnology* 38: 150-158.
- [13] Chen, L., Li, C., Feng, Q., Wei, Y., Zheng, H., Zhao, Y., Feng, Y., Li, H. (2017): Shifts in soil microbial metabolic activities and community structures along a salinity gradient of irrigation water in a typical arid region of China. – *Science of the Total Environment* 598: 64-70.
- [14] Dagmar Kock, A. S. (2008): Quantitative microbial community analysis of three different sulfidic mine tailing dumps generating acid mine drainage. – *Applied Environmental Microbiology* 74: 5211-5219.
- [15] De Meyer, T., Sinnaeve, D., Van Gasse, B., Tsiporkova, E., Rietzschel, E. R., De Buyzere, M. L., Gillebert, T. C., Bekaert, S., Martins, J. C., Van Criekinge, W. (2008): NMR-based characterization of metabolic alterations in hypertension using an adaptive, intelligent binning algorithm. – *Analytical Chemistry* 80: 3783-3790.
- [16] Del-Moral, A., Quesada, E., Ramos-Cormenzana, A. (1987): Distribution and types of bacterial isolated from an inland saltern *Annales de l'Institut Pasteur*. – *Microbiology* 138: 59-66.

- [17] Deneff, V. J., Mueller, R. S., Banfield, J. F. (2010): AMD biofilms: Using model communities to study microbial evolution and ecological complexity in nature. – ISME Journal 4: 599-610.
- [18] Deng, J., Brettar, I., Luo, C. W., Auchtung, J., Konstantinidis, K. T., RodriH., James, M.T. (2014): Stability, genotypic and phenotypic diversity of *Shewanella baltica* in the redox transition zone of the Baltic Sea. – Environmental microbiology 16: 1854-1866.
- [19] Department of Water Affairs and Forestry (DWAFF) (1996): Agricultural Use: Irrigation 4. – South African Water Quality Guidelines, Pretoria.
- [20] Dopson, M., Baker-Austin, C., Koppineedi, P. R., Bond, P. L. (2003): Growth in sulfidic mineral environments: metal resistance mechanisms in acidophilic micro-organisms. – Microbiology 149: 1959-1970.
- [21] Edwards, K. J., Gihring, T. M., Banfield, J. F. (1999): Seasonal variations in microbial populations and environmental conditions in an extreme acid mine drainage environment. – Applied Environment Microbiology 65: 3627-3632.
- [22] Evangelou, V. P. (1995): Pyrite Oxidation and its Control. – New York7 CRC Press, 275p.
- [23] Frankenberger, W. T., Bingham, F. T. (1982): Influence of salinity on soilless enzyme activities. – Soilless Science Society of American Journal 46: 1173-1177.
- [24] Garcia, C., Hernandez, T. (1996): Influence of salinity on the biological and biochemical activity of a calciorthird soil. – Plant Soilless 178: 255-263.
- [25] Gros, R., Poly, F., Monrozier, L. J., Faivre, P. (2003): Plant and soil microbial community responses to solid waste leachates diffusion on grassland. – Plant Soilless 255: 445-455.
- [26] Gryta, A., Frac, M., Oszust, K. (2014): The Application of the Biolog EcoPlate Approach in Ecotoxicological Evaluation of Dairy Sewage Sludge. – Applied Biochemistry and Biotechnology 174: 1434-1443.
- [27] Jian, S. Y., Li, J. W., Chen, J., Wang, G. S., Mayes, M. A., Dzantor, K. E., Hui, D. F., Luo, Y. Q. (2016): Soil extracellular enzyme activities, soil carbon and nitrogen storage under nitrogen fertilization: A meta-analysis. – Soil Biology and Biochemistry 101: 32-43.
- [28] Kawasaki, A., Donn, S., Ryan, P. R., Mathesius, U., Devilla, R., Jones, A., Watt, M. (2016): Microbiome and exudates of the root and rhizosphere of brachypodium distachyon, a model for wheat. – PLoS ONE 11: 1-10.
- [29] Keshri, J., Mankazana, B. B. J., Momba, M. N. B. (2015): Profile of bacterial communities in South African mine-water samples using Illumina next-generation sequencing platform. – Applied Microbiology and Biotechnology 99: 3233-3242.
- [30] Killham, K. (1994): Soil ecology. – Cambridge University Press, UK, pp. 152-154.
- [31] Kuang, J. L., Huang, L. N., Chen, L. X., Hua, Z. S., Li, S. J., Hu, M., Li, J. T., Shu, W. S. (2013): Contemporary environmental variation determines microbial diversity patterns in acid mine drainage. – ISME Journal 7: 1038-1050.
- [32] Laura, R. D. (1974): Effects of neutral salts on carbon and nitrogen mineralization of organic-matter in soil. – Plant Soilless 41: 113-127.
- [33] Li, J., Sun, W., Wang, S., Sun, Z., Lin, S., Peng, X. (2014): Bacteria diversity, distribution and insight into their role in S and Fe biogeochemical cycling during black shale weathering. – Environmental Microbiology 16: 3533-3547.
- [34] Ling, Q., Bao, J., Li, R., Tao, Y., Bao, Q. (2012): Analysis of carbon metabolism diversity characters of air microbes in Huangshan Scenic Spot Using Biolog-Eco Method. – Journal of Basic Science and Engineering 1: 008.
- [35] Liu, B., Li, Y., Zhang, X., Wang, J., Gao, M. (2015): Effects of chlortetracycline on soil microbial communities: Comparisons of enzyme activities to the functional diversity via Biolog EcoPlates. – European Journal of Soil Biology, <http://dx.doi.org/10.1016/j.ejsobi.2015.01.002>.
- [36] Masindi, V., Mugeru, W. G., Hlanganani, T., Marinda, D-B. (2015): Passive remediation of acid mine drainage using cryptocrystalline magnesite: A batch experimental and geochemical modelling approach. – Water SA 41: 1-10.

- [37] Méndez-García, C., Peláez, A. I., Mesa, V., Sánchez, J., Golyshina, O. V., Ferrer, M. (2015): Microbial diversity and metabolic networks in acid mine drainage habitats. – *Frontier in Microbiology* 6: 1-17.
- [38] Muratova, A. Y., Dmitrieva, T. V., Panchenko, L. V., Turkovskaya, O. V. (2008): Phytoremediation of oil-sludge-contaminated soil. – *International Journal of Phytoremediation* 10: 486-502.
- [39] Nautiyal, C. S., Chauhan, P. S., Bhatia, C. R. (2010): Changes in soil physicochemical properties and microbial functional diversity due to 14 years of conversion of grassland to organic agriculture in semi-arid agro ecosystem. – *Soil Tillage Research* 109: 55-60.
- [40] Nicholson, J. K., Lindon, J. C. (2008): Systems biology: Metabonomics. – *Nature* 455: 1054-1056.
- [41] Oren, A. (2001): The bioenergetics basis for the decrease in metabolic diversity at increasing salt concentrations: implications for the functioning of salt lake ecosystems. – *Hydrobiology* 466: 61-72.
- [42] Pan, C. C., Liu, C. A., Zhao, H. L., Wang, Y. (2013): Changes of soil physicochemical properties and enzyme activities in relation to grassland salinization. – *European Journal of Soilless Biology* 55: 13-19.
- [43] Pankhurst, C. E., Yu, S., Hawke, B. G., Harch, B. D. (2001): Capacity of fatty acid profiles and substrate utilization patterns to describe differences in soil microbial communities associated with increased salinity or alkalinity at three locations in South Australia. – *Biology and Fertility of Soils* 33: 204-217.
- [44] Pathak, H., Rao, D. L. N. (1998): Carbon and nitrogen mineralization from added organic matter in saline and alkali soils. – *Soilless Biology and Biochemistry* 30: 695-702.
- [45] Pétriacq, P., Williams, A., Cotton, A., McFarlane, A. E., Rolfe, S. A., Ton, J. (2017): Metabolite profiling of non-sterile rhizosphere soil. – *Plant Journal* 92(1): 147-162.
- [46] Pontoizeau, C., Herrmann, T., Toulhoat, P., Elena-Herrmann, B., Emsley, L. (2010): Targeted projection NMR spectroscopy for unambiguous metabolic profiling of complex mixtures. – *Magnetic Resonance in Chemistry* 48: 727-733.
- [47] Quesada, E., Ventosa, A., Ramoscormenzana, A., Rodriguezvalera, F. (1982): Types and properties of some bacteria isolated from hypersaline soils. – *Journal of Applied Bacteriology* 53: 155-161.
- [48] Raghawendra, K., Avinash, M., Bhavanath, J. (2019): Bacterial community structure and functional diversity in subsurface seawater from the western coastal ecosystem of the Arabian Sea, India. – *Gene* 701: 55-64.
- [49] Ravanbakhsh, S., Liu, P., Bjordahl, T. C., Mandal, R., Grant, J. R., Wilson, M., Eisner, R., Sineelnikov, I., Hu, X., Luchinat, C., Greiner, R., Wishart, D. S. (2015): Accurate, fully-automated NMR spectral profiling for metabolomics. – *PLoS ONE* 10: e0124219.
- [50] Rietz, D. N., Haynes, R. J. (2003): Effects of irrigation-induced salinity and sodicity on soil microbial activity. – *Soilless Biology and Biochemistry* 35: 845-854.
- [51] Robertson-Albertyn, S., Terrazas, R. A., Balbirnie, K., Blank, M., Janiak, A., Szarejko, I., Chmielewska, B., Karcz, J., Morris, J., Hedley, P. E., George, T. S., Bulgarelli, D. (2017): Root Hair Mutations Displace the Barley Rhizosphere Microbiota. – *Frontier in Plant Science* 8: 1-15.
- [52] Rousk, J., Elyaagubi, F. K., Jones, D. L., Godbold, D. L. (2011): Bacterial salt tolerance is unrelated to soil salinity across an arid agroecosystem salinity gradient. – *Soilless Biology and Biochemistry* 43: 1881-1887.
- [53] Sagot, B., Gaysinski, M., Mehiri, M., Guignonis, J. M., LeRudulier, D., Alloing, G. (2010): Osmotically induced synthesis of the dipeptide N-acetyl glutamyl glutamine amide is mediated by a new pathway conserved among bacteria. – *Proceedings of the National Academy of Sciences* 107: 12652-12657.
- [54] Sarig, S., Steinberger, Y. (1994): Microbial biomass response to seasonal fluctuation in soil-salinity under the canopy of desert halophytes. – *Soilless Biology and Biochemistry* 26: 1405-1408.

- [55] Sarig, S., Fliessbach, A., Steinberger, Y. (1996): Microbial biomass reflects a nitrogen and phosphorous economy of halophytes grown in salty desert soil. – *Biology and Fertility of Soils* 21: 128-130.
- [56] Scholes, L. N. L., Shutes, R. B. E., Revitt, D. M., Purchase, D., Forshaw, M. (1999): The removal of urban pollutants by constructed wetlands during wet weather. – *Water Science and Technology* 40: 333-340.
- [57] Setia, R., Marschner, P., Baldock, J., Chittleborough, D., Verma, V. (2011): Relationships between carbon dioxide emission and soil properties in salt-affected landscapes. – *Soilless Biology and Biochemistry* 43: 667-674.
- [58] Setia, R., Gottschalk, P., Smith, P., Marschner, P., Baldock, J., Setia, D., Smith, J. (2013): Soil salinity decreases global soil organic carbon stocks. – *Science of the Total Environment* 465: 267-272.
- [59] Slonczewski, J. L., Fujisawa, M., Dopson, M., Krulwich, T. A., Robert, K. P. (2009): Cytoplasmic pH measurement and homeostasis in bacteria and archaea. – *Advance in Microbiology and Physiology* 55: 1-79.
- [60] Sulpice, R., Trenkamp, S., Steinfath, M., Usadel, B., Gibon, Y., Witucka-Wall, H., Pyl, E. T., Tschoep, H., Steinhäuser, M. C., Guenther, M., Hoehne, M., Rohwer, J. M., Altmann, T., Fernie, A. R., Stitt, M. (2010): Network analysis of enzyme activities and metabolite levels and their relationship to biomass in a large panel of *Arabidopsis* accessions. – *The Plant Cell* 22: 2872-2893.
- [61] Sun, M., Xiao, T. F., Ning, Z. P., Xiao, E., Sun, W. M. (2014): Microbial community analysis in rice paddy soils irrigated by acid mine drainage contaminated water. – *Applied Microbiology and Biotechnology* 99(6): 2911-22.
- [62] Sun, W. M., Xiao, T. F., Sun, M., Dong, Y. R., Ning, Z. P., Xiao, E., Tang, S., Li, J. W. (2015): Diversity of sediment microbial community in response to acid mine drainage pollution gradients in the Aha watershed (Southwest China). – *Applied Environmental Microbiology*, doi:10.1128/AEM.00935-15.
- [63] Teng, W. K., Kuang, J. L., Luo, Z. H., Shu, W. S. (2017): Microbial diversity and community assembly across environmental gradients in acid mine drainage. – *Minerals* 7: 106.
- [64] Tian, W., Zhao, Y., Sun, H., Bai, J., Wang, Y., Wu, C. (2014): The effect of irrigation with oil-polluted water on microbial communities in estuarine reed rhizosphere soils. – *Ecology and Engineering* 70: 275-281.
- [65] USGS (2012): Coal-Mine-Drainage Projects in Pennsylvania. – Pennsylvania Water Science Center (Accessed 17 April 2012).
- [66] Volant, A., Bruneel, O., Desoeuvre, A., Héry, M., Casiot, C., Bru, N., Delpoux, S., Fahy, A., Javerliat, F., Bouchez, O. (2014): Diversity and spatiotemporal dynamics of bacterial communities: physicochemical and other drivers along an acid mine drainage. – *FEMS Microbiology and Ecology* 90: 247-263.
- [67] Wang, G. H., Liu, J. J., Qi, X. N., Jin, J., Wang, Y., Liu, X. B. (2008): Effects of fertilization on bacterial community structure and function in a black soil of Dehui region estimated by Biolog and PCR-DGGE methods. – *Acta Ecology Sinica* 28: 220-226.
- [68] Wong, V. N. L., Dalal, R. C., Greene, R. S. B. (2009): Carbon dynamics of sodic and saline soils following gypsum and organic material additions: a laboratory incubation. – *Applied Soilless Ecology* 41: 29-40.
- [69] Xu, W. H., Ge, Z. W., Poudel, D. R. (2015): Application and optimization of Biolog EcoPlates in functional diversity studies of soil microbial communities. – *MATEC Web of Conference* 22: 04015.
- [70] Yaish, M. W., Al-Lawati, A., Jana, G. A., Patankar, H. V., Glick, B. R. (2016): Impact of soil salinity on the structure of the bacterial endophytic community identified from the roots of Caliph Medic (*Medicago truncatula*). – *PLOS ONE* 11(7): e0159007.

- [71] Yan, N., Marschner, P., Cao, W. H., Zuo, C. Q. (2015): Influence of salinity and water content on soil microorganisms. – International Soil Water Conservation Research 3: 316-323.
- [72] Yuan, B. C., Li, Z. Z., Liu, H., Gao, M., Zhang, Y. Y. (2007a): Microbial biomass and activity in salt affected soils under arid conditions. – Applied Soilless Ecology 35: 319-328.
- [73] Yuan, B. C., Xu, X. G., Li, Z. Z., Gao, T. P., Gao, M., Fan, X. W., Deng, H. M. (2007b): Microbial biomass and activity in alkalized magnesian soils under arid conditions. – Soilless Biology and Biochemistry 39: 3004-3013.
- [74] Zahran, H. H., Moharram, A. M., Mohammad, H. A. (1992): Some ecological and physiological-studies on bacteria isolated from salt-affected soils of Egypt. – Journal of Basic Microbiology 32: 405-413.
- [75] Zhang, H., Li, G., Song, X., Yang, D., Li, Y., Qiao, J., Zhang, J., Zhao, S. (2013): Changes in soil microbial functional diversity under different vegetation restoration patterns for Hulunbeier Sandy Land. – Acta Ecology Sinica 33: 38-44.
- [76] Zhang, T. Y., Wu, Y-H., Zhuang, L. L., Wang, X. X., Hu, H. Y. (2014): Screening heterotrophic microalgal strains by using the Biolog method for biofuel production from organic wastewater. – Journal of Algal Research 6: 175-179.

## AN EVALUATION OF SOME ENTOMOPATHOGENIC FUNGI FOR GREEN PEACH APHID (*MYZUS PERSICAE* [SULZER]), (HOMOPTERA: APHIDIDAE) UNDER LABORATORY CONDITIONS

KILIÇ, E.

Department of Basic Pharmaceutical Science, Faculty of Pharmacy, Erzincan Binali Yıldırım University, 24100 Erzincan, Turkey  
(e-mail: ekilic@erzincan.edu.tr; phone: +90-507-587-7012)

(Received 28<sup>th</sup> Apr 2020; accepted 20<sup>th</sup> Aug 2020)

**Abstract.** This study was carried out between 2014 and 2017 in Erzincan province Turkey. Our aim was to test pathogenesis of soil isolated entomopathogenic fungi from Erzincan and the *Myzus persicae* (Sulzer), (Homoptera: Aphididae). A total of 78 entomopathogenic fungi isolates including 63 *Beauveria bassiana* and 15 *Metarhizium anisopliae* were obtained. Our study was followed by incubation for 12 days and the first cases were seen on the third day. It was recorded that *B. bassiana* isolates caused the highest mortality rate on the 3rd day (BbEMRKZ2a, 10.50%); 5th day (BbEMRKZ5b and BbEÜ3, 22.39%); 7th day (MaEM3i, 45.71); 9th day (BbEMRKZ1a and BbER4, 50.00%), and after 12 days (BbEİ5, 62.54%). Also, it was recorded that *M. anisopliae* isolates caused the highest mortality rate on the 3rd day (MaEMR1a, 5.78%), 5th day (MaET3, 23.32%), 7th day (BbER4, 37.4%), 9th day (MaEİ3 50.84%), and after 12 days (MaET3, 60.01%). In the control group, the highest mortality rate was 1.12% at the end of the incubation period.

**Keywords:** biocontrol, *Beauveria bassiana*, *Metarhizium anisopliae*, *Myzus persicae*

### Introduction

Aphids are one of the most destructive pests in agricultural production. They cause direct physical damage by extracting carbohydrates and amino acids from plant phloem and also indirectly through spreading a variety of viruses (Milner, 1997; Dedryver et al., 2010; Kim et al., 2013). Some of their species are cosmopolitan, such as; green peach aphid (*Myzus persicae* (Sulzer)), and black bean aphid (*Aphis fabae* Scopoli, 1763). they cause the large economic yield losses over the three hundred plants at the world (Aydemir, 2008; Dedryver et al., 2010; Kim et al., 2013). Most researcher reported that chemical pesticide application is the most commonly used method of aphid control, but it cannot wipe aphids out since aphids easily develop resistance to chemical insecticides and multiply very rapidly. Moreover, the over use of pesticide has resulted in environmental pollution as well as adverse effects on the health of humans and other organisms (Dedryver et al., 2010). As a principle, the increased volume of the world-wide trade of agricultural crop production also requires environmentally friendly pest control. Biocontrol is an alternative to chemical pesticides used in the management of plant pests (Ren and Chen, 2012). A group of them are microbial control agents and called entomopathogens (Clarkson and Charnley, 1996; Butt and Copping, 2000; Hajek, 2004). Entomopathogens (bacteria, fungi, virus, nematode, etc.) are living organisms used to kill insects and to create an epidemic disease that spreads rapidly but targets only the harmful pest (Clarkson and Charnley, 1996; Butt and Copping, 2000; Hajek, 2004). Entomopathogenic fungi (EPF) are the most important microbial pathogens of insect pests and they are unlike bacteria and viruses that have to be ingested to cause diseases, fungi typically infect insects by direct penetration of the cuticle followed by multiplication in

the hemocoel (McCoy et al., 1998; Lacey et al., 2001; St. Kılıç and Yıldırım, 2008; St. Leger et al., 2011). EPF are approximately, 60% of insect diseases are caused by pathogenic fungi (Faria and Wraight, 2007). The approach thirty of commercial mycoinsecticides are known to infect aphids, and several species frequently cause naturally epizootics in aphid populations (Gustafsson, 1965; Thoizon, 1970; Balazy, 1993; Keller, 1997; Goettel et al., 2005; Kim et al., 2013). Most aphid-pathogenic fungi are in the order of Entomophthorales (Zygomycota), however, several Hypocreales (Ascomycota) genera, such as *Beauveria*, *Verticillium*, and *Paecilomyces*, are also known to infect aphids (Miller, 1997). Most researcher reported that we can use *B. bassiana* and *M. anisopliae* as microbial control agents for aphids which have a wide host range and widely distributed in all regions of the world, in addition both species can be easily isolated from insects and soil (Butt, 2004; Meyling et al., 2006; Freed et al., 2011a, b). So far, a variety of strains of *B. bassiana* and *M. anisopliae* have been used for the control of aphids (Jackson et al., 1985; Steenberg and Humber, 1999; Devi et al., 2003; Kim, 2004; Shia and Feng, 2004; Quesada-Moraga et al., 2006; Kim et al., 2010). In the present study, it was aimed to determine the pathogenicity of 63 isolates of *B. bassiana*, and 15 isolates of *M. anisopliae*, an entomopathogenic fungi, taken from Erzincan province and isolated from soil and control *M. persicae* under laboratory conditions .

## Materials and methods

### *Aphid culture*

The green peach aphid (*Myzus persicae* (Sulzer)) (Homoptera: Aphididae) were collected from different fields in 2016-2017-2018 at Erzincan. The aphids were reared on common bean, *Phaseolus vulgaris* L. under laboratory conditions [(25 °C ± 2 and 70% ± 10 R.H.) (16: 8 h (L:D))] (Kim et al., 2013).

### *Collecting soil samples*

The province of Erzincan (39°02'N to 40°05'N, 38°16'E to 40°45'E) covers ca. 11,900 km<sup>2</sup> of Turkey and is located in the eastern part of Anatolia, which has a continental climate. Soil samples were collected from different geographical sites distributed through the Erzincan province (Merkez, Üzümlü, Tercan, Mercan, Kemaliye, Kemah, İliç, Çayırılı, Otlukbeli, Refahiye; *Fig. 1*).



**Figure 1.** Soil samples were collected from different geographical sites distributed through the Erzincan province



Soil samples were collected with a garden spade to a depth of 20 cm after removal of surface litter. At every site, five 500 g soil samples were collected from five randomly selected points from an area of 50 cm<sup>2</sup>, placed in clear plastic bags (30-25 cm), sealed with a rubber band and returned to the laboratory. There were 30 samples from cultivated habitats (24 samples from field crops, 1 sample from fruit and vegetable crops, 4 samples from vegetable crops, 1 sample from sugar beet crops) and 30 samples from natural habitats (26 samples from natural pastures, 3 samples from forest, 1 sample from meadow).

### ***Isolation and identification of fungi***

Insect-associated fungi were isolated from soil samples by using ‘Galleria bait method’ (Zimmermann, 1986). The wax moth larvae, *Galleria mellonella* L., were reared continuously in constant darkness at 28 °C. The third or fourth instar larvae (approximately 30 days after hatching) were used as baits. Ten larvae were placed on the soil samples in each box and covered with a lid and incubated at 25 ± 1 °C for two weeks. The larvae were examined on days 7 and 14 after inoculation. Surface of dead larvae were sterilized by 3% sodium hypochlorite for 3 min and then rinsed twice with sterile distilled water. After removing free water of the larvae surface, they were placed onto PDA plates. The fungi were identified using morphological characteristics of reproductive structures with the aid of relevant taxonomic literature (De Hoog, 1972; Samson et al., 1988; Humber, 1998; Luangsa-Ard et al., 2007). As a result, we obtained 78 fungal isolates and we gave a code for every isolates. These fungal cultures consist of the 63 isolates of *B. bassiana*, and 15 isolates of *Metarhizium anisopliae*. They were isolated from soil at Erzincan province (2014-2016) (Table 1).

### ***Preparation of conidial suspension***

*Conidia* of *B. bassiana* and *M. anisopliae* isolates were harvested by scraping the surface of 3-week-old sporulating cultures grown on Potato Dextrose Agar (PDA). The spores were harvested 0.01% Tween 80 and drained with chesse cloth into the sterilized glass Erlenmeyer flasks. Then it was rinsed on a rinsing device for 5 min. After that, the spores were counted in the suspensions using a hemocytometer to 3 × 10<sup>7</sup> spores/ml (Thakur and Sandhu, 2010).

### ***Incubation of fungal spores and the treatment of aphids***

The following leaf dipping technique was used as described by Krutmuang and Mekchay, 2005; Ghatwary, 2000. The discs of common bean leaves were prepared, dipped in the tested spore suspensions for 10 s, then left to dry at room temperature and provided to the aphid in Petri dishes. In order to keep the leaves alive for 12 days, leaf stems were covered with a sterilized cotton roll in the size of 40 × 60 mm and 2 ml sterilized and distilled water containing 1% of NPK (20-20-20) fertilizer. In addition to keep the humidity at 100%, 3 ml of sterilized and distilled water was added on the filter paper. To prevent the leaves from contacting the wet surface, a plastic circular sheet with a diameter of 5 cm was placed under them. After each treatment, sides of Petri dishes were covered with parafilm. Treatments were repeated three times for each fungus isolates (Table 1). For control treatment, the same process was followed but 3 ml of sterilized and distilled water with 0.01% of Tween 80 was used instead of fungus isolates. After application of 25 aphid nymphs, were used for each treated leaves and incubated at (25 °C ± 2 and 70% ± 10) humidity.

**Table 1.** Fungal material and their geographical origin (2014-2016) at Erzincan

<i>Fungi species</i>	No	Code	Substrate (soil)	Geographical origin of isolates
<i>Beauveria bassiana</i>	1	BbEMRKZ1a	Vegetable field	CENTER
	2	BbEMRKZ1b		
	3	BbEMRKZ2a	Fruit garden	
	4	BbEMRKZ2b		
	5	BbEMRKZ3	Field (barley-wheat)	
	6	BbEMRKZ4a	Meadow-grassland	
	7	BbEMRKZ4b		
	8	BbEMRKZ5a	Forest	
	9	BbEMRKZ5b		
	10	BbEÜ1a	Vegetable field	Üzümlü
	11	BbEÜ1b		
	12	BbEÜ2a	Fruit garden	
	13	BbEÜ2b		
	14	BbEÜ3	Field (barley-wheat)	
	15	BbEÜ4	Meadow-grassland	
	16	BbEÜ5a	Forest	
	17	BbEÜ5b		
	18	BbEK1a	Vegetable field	
	19	BbEK1b		
	20	BbEK2a	Fruit garden	
	21	BbEK2b		
	22	BbEK3a	Field (barley-wheat)	
	23	BbEK3b		
	24	BbEK4	Meadow-grassland	
	25	BbEK5a	Forest	
	26	BbEK5b		
	27	BbEİ1	Vegetable field	İliç
	28	BbEİ2	Fruit garden	
	29	BbEİ3	Field (barley-wheat)	
	30	BbEİ4	Meadow-grassland	
	31	BbEİ5	Forest	
	32	BbEKLY1	Vegetable field	Kemaliye
	33	BbEKLY2a	Fruit garden	
	34	BbEKLY2b		
	35	BbEKLY4	Meadow-grassland	
	36	BbEKLY5	Forest	
	37	BbER1	Vegetable field	Refahiye
	38	BbER2	Fruit garden	
	39	BbER3	Field (barley-wheat)	
	40	BbER4	Meadow-grassland	
	41	BbER5a	Forest	
	42	BbER5b		
	43	BbER5c		
	44	BbEM1	Vegetable field	
	45	BbEM2	Fruit garden	

	46	BbEM3	Field (barley-wheat)	Tercan		
	47	BbEM4	Meadow-grassland			
	48	BbEM5	Forest			
	49	BbET1	Vegetable field			
	50	BbET2	Fruit garden			
	51	BbET3	Field (barley-wheat)			
	52	BbET4	Meadow-grassland			
	53	BbET5	Forest			
	54	BbEÇ1	Vegetable field		Çayırli	
	55	BbEÇ2	Fruit garden			
	56	BbEÇ3	Field (barley-wheat)			
	57	BbEÇ4	Meadow-grassland			
	58	BbEÇ5	Forest			
		59	BbEO1		Vegetable field	Otlukbeli
		60	BbEO2		Fruit garden	
61		BbEO3	Field (barley-wheat)			
62		BbEO4	Meadow-grassland			
63		BbEO5	Forest			
<i>Metarhizium anisopliae</i>		64	MaEMR1a	Vegetable field	Merkez	
		65	MaEMR2b			
		66	MaEÜ1a	Vegetable field	Üzümlü	
	67	MaEÜ1b				
	68	MaEK1a	Vegetable field	Kemah		
	69	MaEk1b				
	70	MaEİ3	Field (barley-wheat)	İliç		
	71	MaEKLY1a	Fruit garden	Kemaliye		
	72	MaEKLY1b				
	73	MaER3	Field (barley-wheat)	Refahiye		
	74	MaEM1	Vegetable field	Mercan		
	75	MaEM3	Field (barley-wheat)			
	76	MaET3	Field (barley-wheat)	Tercan		
	77	MaEÇ3	Field (barley-wheat)	Çayırli		
78	MaEO3	Field (barley-wheat)	Otlukbeli			

### Statistical analysis

In order to determine the pathogenicity of *B. bassiana* and *M. anisopliae* isolates on aphids, dead and alive insects were checked every two days after the treatment. On the first 3 days there were no death cases and so the values were taken as 0 (zero). In the case when measurement number is below 50, angle transformation is applied to adjust the value of 0% to the normal distribution. In the present study, data were adjusted for arc-sin transformation to normalize the statistical distribution.

The inoculation values measured at the 1-12<sup>th</sup> days were subjected to the one way analysis of variance (ANOVA;  $\alpha = 0.05$ ) using 11.0 SPSS software for Windows (SPSS Inc., 2002). Comparison of the isolates found to be different from the controls was made using Tukey test ( $\alpha = 0.05$ ) in ANOVA.

## Results

### *Pathogenicity of B. bassiana on M. persicae*

The infection rates of the 63 *B. bassiana* isolates at  $3 \times 10^7$  conidia/ml concentration on larval stages of *M. persicae*. Were shown at Table 2. Within 12 days post inoculation the first deaths were seen on the third day. At the end of the 3<sup>rd</sup> day, BbEMRKZ2a isolate had the highest mortality rate with 10.50%. On the 5<sup>th</sup> day, BbEMRKZ5b and BbEÜ3, isolates had the highest mortality rate with 22.39%, while BbEM5 and BbEO2 isolates showed the lowest mortality rate of 9.04%. On the 7<sup>th</sup> day, BbER4 isolate had the highest mortality rate with 37.4%, while, BbEM5 and BbEO2, isolates showed the lowest mortality rate of 19.84%. On the 9<sup>th</sup> day, BbEMRKZ1a and BbER4 isolates had the highest mortality rate with 50.00%, while BbEKLY2b isolate showed the lowest mortality rate of 31.64%. On the 12<sup>th</sup> day, BbEİ5 isolate had the highest mortality rate with 62.54%, while BbEMRKZ5a, BbEÜ2b, BbEKLY4, BbEM5 and BbEO2 isolates showed the lowest mortality rate of 49.17%. In the control group, the highest mortality rate was 1.12% at the end of the incubation period.

**Table 2.** Corrected percentage mortality of *B. bassiana* isolates (at spore concentration:  $3 \times 10^7$  conidia/ml) on *M. persicae* (%Mean  $\pm$  StDev) 12 days post inoculation

Isolation of <i>B. bassiana</i>	3 <sup>rd</sup> day	5 <sup>th</sup> day	7 <sup>th</sup> day	9 <sup>th</sup> day	12 <sup>th</sup> day
	Mean $\pm$ StDev	Mean $\pm$ StDev	Mean $\pm$ StDev	Mean $\pm$ StDev	Mean $\pm$ StDev
BbEMRKZ1a	4.79 <sup>A</sup> $\pm$ 0.84	18.88 <sup>A B</sup> $\pm$ 0.67	35.75 <sup>A-C</sup> $\pm$ 0.43	50.00 <sup>A</sup> $\pm$ 0.19	61.67 <sup>A B</sup> $\pm$ 0.02
BbEMRKZ1b	4.08 <sup>A</sup> $\pm$ 0.84	21.46 <sup>A B</sup> $\pm$ 0.53	31.62 <sup>A-E</sup> $\pm$ 0.17	40.80 <sup>A-F</sup> $\pm$ 0.28	60.86 <sup>A B</sup> $\pm$ 0.15
BbEMRKZ2a	10.64 <sup>A</sup> $\pm$ 2.16	18.32 <sup>A B</sup> $\pm$ 0.03	31.59 <sup>A-E</sup> $\pm$ 0.31	40.82 <sup>A-F</sup> $\pm$ 0.15	55.02 <sup>A B</sup> $\pm$ 0.25
BbEMRKZ2b	3.24 <sup>A</sup> $\pm$ 0.84	18.12 <sup>A B</sup> $\pm$ 0.48	27.42 <sup>A-E</sup> $\pm$ 0.24	40.82 <sup>A-F</sup> $\pm$ 0.09	55.00 <sup>A B</sup> $\pm$ 0.06
BbEMRKZ3	3.24 <sup>A</sup> $\pm$ 1.69	19.63 <sup>A B</sup> $\pm$ 0.91	32.39 <sup>A-E</sup> $\pm$ 0.49	45.00 <sup>A-E</sup> $\pm$ 0.06	52.50 <sup>A B</sup> $\pm$ 0.06
BbEMRKZ4a	6.61 <sup>A</sup> $\pm$ 1.34	19.96 <sup>A B</sup> $\pm$ 0.10	31.62 <sup>A-E</sup> $\pm$ 0.17	40.82 <sup>A-F</sup> $\pm$ 0.15	55.83 <sup>A B</sup> $\pm$ 0.02
BbEMRKZ4b	3.24 <sup>A</sup> $\pm$ 1.34	16.60 <sup>A B</sup> $\pm$ 0.14	32.43 <sup>A-E</sup> $\pm$ 0.29	42.49 <sup>A-F</sup> $\pm$ 0.06	51.67 <sup>A B</sup> $\pm$ 0.02
BbEMRKZ5a	8.30 <sup>A</sup> $\pm$ 0.84	17.45 <sup>A B</sup> $\pm$ 0.11	33.31 <sup>A-E</sup> $\pm$ 0.10	40.83 <sup>A-F</sup> $\pm$ 0.02	49.17 <sup>B</sup> $\pm$ 0.02
BbEMRKZ5b	7.79 <sup>A</sup> $\pm$ 2.54	22.39 <sup>A B</sup> $\pm$ 0.28	34.99 <sup>A-D</sup> $\pm$ 0.07	44.16 <sup>A-F</sup> $\pm$ 0.02	61.68 <sup>A B</sup> $\pm$ 0.09
BbEÜ1a	6.25 <sup>A</sup> $\pm$ 1.34	16.54 <sup>A B</sup> $\pm$ 0.27	26.61 <sup>A-E</sup> $\pm$ 0.19	39.99 <sup>A-F</sup> $\pm$ 0.07	53.34 <sup>A B</sup> $\pm$ 0.08
BbEÜ1b	6.61 <sup>A</sup> $\pm$ 1.34	19.96 <sup>A B</sup> $\pm$ 0.10	31.62 <sup>A-E</sup> $\pm$ 0.17	40.82 <sup>A-F</sup> $\pm$ 0.15	55.83 <sup>A B</sup> $\pm$ 0.02
BbEÜ2a	3.24 <sup>A</sup> $\pm$ 1.34	16.60 <sup>A B</sup> $\pm$ 0.14	32.43 <sup>A-E</sup> $\pm$ 0.29	42.49 <sup>A-F</sup> $\pm$ 0.06	51.67 <sup>A B</sup> $\pm$ 0.02
BbEÜ2b	8.30 <sup>A</sup> $\pm$ 0.84	17.45 <sup>A B</sup> $\pm$ 0.11	33.31 <sup>A-E</sup> $\pm$ 0.10	40.83 <sup>A-F</sup> $\pm$ 0.02	49.17 <sup>B</sup> $\pm$ 0.02
BbEÜ3	7.79 <sup>A</sup> $\pm$ 2.54	22.39 <sup>A B</sup> $\pm$ 0.28	34.99 <sup>A-D</sup> $\pm$ 0.07	44.16 <sup>A-F</sup> $\pm$ 0.02	61.68 <sup>A B</sup> $\pm$ 0.09
BbEÜ4	4.79 <sup>A</sup> $\pm$ 1.34	19.15 <sup>A B</sup> $\pm$ 0.03	29.14 <sup>A-E</sup> $\pm$ 0.10	41.65 <sup>A-F</sup> $\pm$ 0.15	53.34 <sup>A B</sup> $\pm$ 0.08
BbEÜ5a	8.75 <sup>A</sup> $\pm$ 2.54	20.75 <sup>A B</sup> $\pm$ 0.22	34.13 <sup>A-E</sup> $\pm$ 0.16	42.49 <sup>A-F</sup> $\pm$ 0.06	60.03 <sup>A B</sup> $\pm$ 0.26
BbEÜ5b	5.44 <sup>A</sup> $\pm$ 1.34	17.31 <sup>A B</sup> $\pm$ 0.44	26.61 <sup>A-E</sup> $\pm$ 0.19	39.15 <sup>A-F</sup> $\pm$ 0.09	54.17 <sup>A B</sup> $\pm$ 0.15
BbEK1a	3.24 <sup>A</sup> $\pm$ 1.34	19.63 <sup>A B</sup> $\pm$ 0.91	33.26 <sup>A-E</sup> $\pm$ 0.37	45.00 <sup>A-E</sup> $\pm$ 0.06	53.33 <sup>A B</sup> $\pm$ 0.02
BbEK1b	4.79 <sup>A</sup> $\pm$ 1.34	19.15 <sup>A B</sup> $\pm$ 0.03	29.14 <sup>A-E</sup> $\pm$ 0.10	41.65 <sup>A-F</sup> $\pm$ 0.15	53.34 <sup>A B</sup> $\pm$ 0.08
BbEK2a	5.55 <sup>A</sup> $\pm$ 0.00	19.87 <sup>A B</sup> $\pm$ 0.31	35.83 <sup>A-C</sup> $\pm$ 0.02	40.83 <sup>A-F</sup> $\pm$ 0.02	55.84 <sup>A B</sup> $\pm$ 0.08
BbEK2b	4.79 <sup>A</sup> $\pm$ 0.15	16.60 <sup>A B</sup> $\pm$ 0.14	31.62 <sup>A-E</sup> $\pm$ 0.17	41.66 <sup>A-F</sup> $\pm$ 0.09	50.00 <sup>A B</sup> $\pm$ 0.06
BbEK3a	7.37 <sup>A</sup> $\pm$ 0.00	20.75 <sup>A B</sup> $\pm$ 0.22	32.48 <sup>A-E</sup> $\pm$ 0.07	42.49 <sup>A-F</sup> $\pm$ 0.06	53.35 <sup>A B</sup> $\pm$ 0.34
BbEK3b	6.64 <sup>A</sup> $\pm$ 2.54	20.75 <sup>A B</sup> $\pm$ 0.22	33.26 <sup>A-E</sup> $\pm$ 0.31	43.33 <sup>A-F</sup> $\pm$ 0.02	58.39 <sup>A B</sup> $\pm$ 0.60
BbEK4	4.79 <sup>A</sup> $\pm$ 0.84	19.96 <sup>A B</sup> $\pm$ 0.10	30.83 <sup>A-E</sup> $\pm$ 0.02	41.65 <sup>A-F</sup> $\pm$ 0.15	55.00 <sup>A B</sup> $\pm$ 0.06
BbEK5a	3.24 <sup>A</sup> $\pm$ 1.69	19.63 <sup>A B</sup> $\pm$ 0.91	32.39 <sup>A-E</sup> $\pm$ 0.49	45.00 <sup>A-E</sup> $\pm$ 0.06	52.50 <sup>A B</sup> $\pm$ 0.06
BbEK5b	6.61 <sup>A</sup> $\pm$ 1.34	19.96 <sup>A B</sup> $\pm$ 0.10	31.62 <sup>A-E</sup> $\pm$ 0.17	40.82 <sup>A-F</sup> $\pm$ 0.15	55.83 <sup>A B</sup> $\pm$ 0.02

BbEİ1	3.88 <sup>A</sup> ±0.84	17.37 <sup>A B</sup> ±0.31	34.99 <sup>A-D</sup> ±0.07	40.83 <sup>A-F</sup> ±0.02	53.34 <sup>A B</sup> ±0.15
BbEİ2	5.78 <sup>A</sup> ±1.34	15.71 <sup>A B</sup> ±0.27	29.94 <sup>A-E</sup> ±0.22	39.96 <sup>A-F</sup> ±0.26	50.83 <sup>A B</sup> ±0.08
BbEİ3	4.79 <sup>A</sup> ±0.84	17.45 <sup>A B</sup> ±0.11	28.89 <sup>A-E</sup> ±0.96	44.15 <sup>A-F</sup> ±0.15	55.85 <sup>A B</sup> ±0.15
BbEİ4	3.24 <sup>A</sup> ±0.84	19.15 <sup>A B</sup> ±0.03	29.98 <sup>A-E</sup> ±0.07	38.33 <sup>A-F</sup> ±0.02	60.86 <sup>A B</sup> ±0.15
BbEİ5	3.24 <sup>A</sup> ±0.84	16.21 <sup>A B</sup> ±1.04	33.30 <sup>A-E</sup> ±0.16	45.00 <sup>A-E</sup> ±0.06	62.54 <sup>A</sup> ±0.27
BbEKLY1	2.50 <sup>A</sup> ±0.84	13.01 <sup>A B</sup> ±0.67	30.72 <sup>A-E</sup> ±0.46	39.96 <sup>A-F</sup> ±0.26	53.33 <sup>A B</sup> ±0.02
BbEKLY2a	3.24 <sup>A</sup> ±0.84	16.60 <sup>A B</sup> ±0.14	25.77 <sup>A-E</sup> ±0.19	43.33 <sup>A-F</sup> ±0.02	52.50 <sup>A B</sup> ±0.06
BbEKLY2b	1.12 <sup>A</sup> ±0.00	11.09 <sup>A B</sup> ±1.15	21.35 <sup>C-E</sup> ±0.85	31.64 <sup>F</sup> ±0.10	50.00 <sup>A B</sup> ±0.06
BbEKLY4	1.12 <sup>A</sup> ±0.00	9.91 <sup>A B</sup> ±0.18	21.62 <sup>B-E</sup> ±0.12	34.99 <sup>C-F</sup> ±0.07	49.17 <sup>B</sup> ±0.02
BbEKLY5	0.56 <sup>A</sup> ±0.84	11.64 <sup>A B</sup> ±0.05	23.32 <sup>B-E</sup> ±0.03	35.83 <sup>B-F</sup> ±0.02	50.83 <sup>A B</sup> ±0.08
BbER1	2.24 <sup>A</sup> ±1.34	9.91 <sup>A B</sup> ±0.18	23.32 <sup>B-E</sup> ±0.03	31.66 <sup>F</sup> ±0.02	52.52 <sup>A B</sup> ±0.44
BbER2	2.78 <sup>A</sup> ±0.84	14.15 <sup>A B</sup> ±0.04	27.43 <sup>A-E</sup> ±0.23	38.33 <sup>A-F</sup> ±0.02	54.17 <sup>A B</sup> ±0.02
BbER3	3.24 <sup>A</sup> ±0.84	21.66 <sup>A B</sup> ±0.03	36.66 <sup>A-C</sup> ±0.02	45.83 <sup>A-D</sup> ±0.02	58.36 <sup>A B</sup> ±0.28
BbER4	3.88 <sup>A</sup> ±0.84	19.69 <sup>A B</sup> ±0.75	37.41 <sup>A B</sup> ±0.48	50.00 <sup>A</sup> ±0.19	60.01 <sup>A B</sup> ±0.07
BbER5a	4.08 <sup>A</sup> ±0.84	21.46 <sup>A B</sup> ±0.53	31.62 <sup>A-E</sup> ±0.17	40.80 <sup>A-F</sup> ±0.28	60.86 <sup>A B</sup> ±0.15
BbER5b	10.64 <sup>A</sup> ±2.16	18.32 <sup>A B</sup> ±0.03	31.59 <sup>A-E</sup> ±0.31	40.82 <sup>A-F</sup> ±0.15	55.02 <sup>A B</sup> ±0.25
BbER5c	3.24 <sup>A</sup> ±0.84	18.12 <sup>A B</sup> ±0.48	27.42 <sup>A-E</sup> ±0.24	40.82 <sup>A-F</sup> ±0.09	55.00 <sup>A B</sup> ±0.06
BbEM1	3.24 <sup>A</sup> ±1.69	19.63 <sup>A B</sup> ±0.91	32.39 <sup>A-E</sup> ±0.49	45.00 <sup>A-E</sup> ±0.06	52.50 <sup>A B</sup> ±0.06
BbEM2	3.88 <sup>A</sup> ±0.84	12.30 <sup>A B</sup> ±0.40	29.12 <sup>A-E</sup> ±0.18	39.96 <sup>A-F</sup> ±0.26	54.17 <sup>A B</sup> ±0.02
BbEM3	2.50 <sup>A</sup> ±0.84	18.27 <sup>A B</sup> ±0.14	30.72 <sup>A-E</sup> ±0.46	44.16 <sup>A-F</sup> ±0.02	53.33 <sup>A B</sup> ±0.02
BbEM4	3.24 <sup>A</sup> ±0.84	13.73 <sup>A B</sup> ±0.89	24.04 <sup>A-E</sup> ±0.36	35.75 <sup>B-F</sup> ±0.43	50.00 <sup>A B</sup> ±0.06
BbEM5	0.28 <sup>A</sup> ±0.00	9.04 <sup>B</sup> ±0.23	19.84 <sup>D</sup> ±0.40	33.30 <sup>D-F</sup> ±0.16	49.17 <sup>B</sup> ±0.02
BbET1	1.63 <sup>A</sup> ±0.84	10.81 <sup>A B</sup> ±0.05	21.66 <sup>B-E</sup> ±0.03	35.83 <sup>B-F</sup> ±0.02	50.00 <sup>A B</sup> ±0.06
BbET2	1.12 <sup>A</sup> ±0.84	14.84 <sup>A B</sup> ±0.35	28.30 <sup>A-E</sup> ±0.10	40.80 <sup>A-F</sup> ±0.28	52.50 <sup>A B</sup> ±0.00
BbET3	4.79 <sup>A</sup> ±1.34	21.52 <sup>A B</sup> ±0.39	33.24 <sup>A-E</sup> ±0.44	45.00 <sup>A-E</sup> ±0.06	53.34 <sup>A B</sup> ±0.08
BbET4	6.61 <sup>A</sup> ±1.69	21.66 <sup>A B</sup> ±0.03	32.45 <sup>A-E</sup> ±0.22	39.16 <sup>A-F</sup> ±0.02	56.67 <sup>A B</sup> ±0.02
BbET5	3.24 <sup>A</sup> ±1.34	16.60 <sup>A B</sup> ±0.14	32.43 <sup>A-E</sup> ±0.29	42.49 <sup>A-F</sup> ±0.06	51.67 <sup>A B</sup> ±0.02
BbEÇ1	4.79 <sup>A</sup> ±0.84	14.15 <sup>A B</sup> ±0.04	27.28 <sup>A-E</sup> ±0.72	38.32 <sup>A-F</sup> ±0.09	50.83 <sup>A B</sup> ±0.08
BbEÇ2	8.07 <sup>A</sup> ±0.47	20.75 <sup>A B</sup> ±0.22	35.77 <sup>A-C</sup> ±0.30	45.83 <sup>A-D</sup> ±0.02	58.34 <sup>A B</sup> ±0.09
BbEÇ3	0.28 <sup>A</sup> ±0.84	13.91 <sup>A B</sup> ±0.54	27.86 <sup>A-E</sup> ±1.79	39.10 <sup>A-F</sup> ±0.54	54.24 <sup>A B</sup> ±0.92
BbEÇ4	0.00 <sup>A</sup> ±0.00	10.81 <sup>A B</sup> ±0.05	23.32 <sup>B-E</sup> ±0.03	34.99 <sup>C-F</sup> ±0.07	51.67 <sup>A B</sup> ±0.02
BbEÇ5	0.28 <sup>A</sup> ±0.00	12.91 <sup>A B</sup> ±0.87	24.16 <sup>A-E</sup> ±0.03	35.71 <sup>B-F</sup> ±0.69	53.35 <sup>A B</sup> ±0.40
BbEO1	3.24 <sup>A</sup> ±0.84	13.73 <sup>A B</sup> ±0.89	24.04 <sup>A-E</sup> ±0.36	35.75 <sup>B-F</sup> ±0.43	50.00 <sup>A B</sup> ±0.06
BbEO2	0.28 <sup>A</sup> ±0.00	9.04 <sup>B</sup> ±0.23	19.84 <sup>D</sup> ±0.40	33.30 <sup>D-F</sup> ±0.16	49.17 <sup>B</sup> ±0.02
BbEO3	1.63 <sup>A</sup> ±0.84	10.81 <sup>A B</sup> ±0.05	21.66 <sup>B-E</sup> ±0.03	35.83 <sup>B-F</sup> ±0.02	50.00 <sup>A B</sup> ±0.06
BbEO4	1.12 <sup>A</sup> ±0.84	14.84 <sup>A B</sup> ±0.35	28.30 <sup>A-E</sup> ±0.10	40.80 <sup>A-F</sup> ±0.28	52.50 <sup>A B</sup> ±0.00
BbEO5	4.79 <sup>A</sup> ±1.34	21.52 <sup>A B</sup> ±0.39	33.24 <sup>A-E</sup> ±0.44	45.00 <sup>A-E</sup> ±0.06	53.34 <sup>A B</sup> ±0.08
control	0.28 <sup>A</sup> ±0.84	0.28 <sup>C</sup> ±0.84	0.28 <sup>F</sup> ±0.84	1.12 <sup>G</sup> ±0.84	1.12 <sup>C</sup> ±0.84

Means within columns with the same letter are not statistically different (Tukey's test at  $p \leq 0.05$ )

### ***Pathogenicity of M. anisopliae on M. persicae***

The infection rates of the 63 *B. bassiana* isolates at  $3 \times 10^7$  conidia/ml on larval stages of *M. persicae* were showed in Table 3. Within 12 days post inoculation the first deaths were observed 3<sup>rd</sup> day. At the end of the 3<sup>rd</sup> day, MaEMR1a, isolate had the highest mortality rate with 5.78%. On the 5<sup>th</sup> day, MaET3 isolate had the highest

mortality rate with 23.32%, while MaEMR2b, MaEÜ1a, MaEKLY1a MaEÇ3 MaEO3 isolates showed the lowest mortality rate of 9.91%. On the 7<sup>th</sup> day, MaEM3 isolates had the highest mortality rate with 45.71%, while MaER3 isolates showed the lowest mortality rate of 22.08%. On the 9<sup>th</sup> day, MaEİ3 isolate had the highest mortality rate with 50.84%, while MaER3 isolate showed the lowest mortality rate of 32.48%. On the 12<sup>th</sup> day, MaET3 isolates had the highest mortality rate with 60.01%, while MaEKLY1a and MaEKLY1b isolates showed the lowest mortality rate of 49.17%. In the control group, the highest mortality rate was 1.12% at the end of the incubation period.

**Table 3.** Corrected percentage mortality of *M. anisopliae* isolates (at spore concentration:  $3 \times 10^7$  conidia/ml) on *M. persicae* (%Mean  $\pm$  StDev) 12 days post inoculation

Isolates of <i>M. anisopliae</i>	3 <sup>rd</sup> day	5 <sup>th</sup> day	7 <sup>th</sup> day	9 <sup>th</sup> day	12 <sup>th</sup> day
	Means $\pm$ StDev.	Means $\pm$ StDev.	Means $\pm$ StDev.	Means $\pm$ StDev.	Means $\pm$ StDev.
MaEMR1a	5.78 <sup>A</sup> $\pm$ 1.69	18.12 <sup>A</sup> $\pm$ 0.48	27.28 <sup>A-E</sup> $\pm$ 0.72	34.89 <sup>C-F</sup> $\pm$ 0.49	50.82 <sup>A-B</sup> $\pm$ 0.90
MaEMR2b	1.63 <sup>A</sup> $\pm$ 0.84	9.91 <sup>A-B</sup> $\pm$ 0.18	19.06 <sup>E</sup> $\pm$ 0.24	34.13 <sup>C-DEF</sup> $\pm$ 0.16	51.67 <sup>A-B</sup> $\pm$ 0.08
MaEÜ1a	0.28 <sup>A</sup> $\pm$ 0.00	9.91 <sup>A-B</sup> $\pm$ 0.18	23.29 <sup>B-E</sup> $\pm$ 0.12	41.58 <sup>A-F</sup> $\pm$ 0.68	53.35 <sup>A-B</sup> $\pm$ 0.40
MaEÜ1b	0.00 <sup>A</sup> $\pm$ 0.00	11.47 <sup>AB</sup> $\pm$ 0.38	24.16 <sup>A-E</sup> $\pm$ 0.03	46.66 <sup>A-C</sup> $\pm$ 0.08	58.35 <sup>A-B</sup> $\pm$ 0.15
MaEK1a	0.00 <sup>A</sup> $\pm$ 0.00	19.06 <sup>AB</sup> $\pm$ 0.24	34.99 <sup>A-D</sup> $\pm$ 0.07	50.83 <sup>A</sup> $\pm$ 0.08	58.34 <sup>A-B</sup> $\pm$ 0.02
MaEk1b	0.00 <sup>A</sup> $\pm$ 0.00	18.91 <sup>A</sup> $\pm$ 0.59	37.49 <sup>A</sup> $\pm$ 0.07	50.83 <sup>A</sup> $\pm$ 0.02	60.00 <sup>A-B</sup> $\pm$ 0.00
MaEİ3	0.00 <sup>A</sup> $\pm$ 0.00	18.27 <sup>AB</sup> $\pm$ 0.14	33.26 <sup>A-E</sup> $\pm$ 0.31	50.84 <sup>A</sup> $\pm$ 0.15	59.17 <sup>A-B</sup> $\pm$ 0.02
MaEKLY1a	0.00 <sup>A</sup> $\pm$ 0.00	9.91 <sup>A-B</sup> $\pm$ 0.18	21.62 <sup>B-E</sup> $\pm$ 0.12	34.99 <sup>C-F</sup> $\pm$ 0.07	49.17 <sup>B</sup> $\pm$ 0.02
MaEKLY1b	0.56 <sup>A</sup> $\pm$ 0.84	11.64 <sup>A</sup> $\pm$ 0.05	22.50 <sup>B-E</sup> $\pm$ 0.00	35.83 <sup>B-F</sup> $\pm$ 0.02	49.17 <sup>B</sup> $\pm$ 0.08
MaER3	0.56 <sup>A</sup> $\pm$ 0.84	11.64 <sup>AB</sup> $\pm$ 0.05	24.16 <sup>A-E</sup> $\pm$ 0.03	32.48 <sup>E-F</sup> $\pm$ 0.07	50.00 <sup>A-B</sup> $\pm$ 0.06
MaEM1	2.24 <sup>A</sup> $\pm$ 1.34	11.47 <sup>A</sup> $\pm$ 0.38	24.16 <sup>A-E</sup> $\pm$ 0.03	35.82 <sup>B-F</sup> $\pm$ 0.09	56.67 <sup>A-B</sup> $\pm$ 0.09
MaEM3	3.88 <sup>A</sup> $\pm$ 0.84	19.06 <sup>AB</sup> $\pm$ 0.24	34.99 <sup>A-D</sup> $\pm$ 0.07	43.32 <sup>A-F</sup> $\pm$ 0.09	55.86 <sup>A-B</sup> $\pm$ 0.34
MaET3	4.79 <sup>A</sup> $\pm$ 0.00	23.32 <sup>A</sup> $\pm$ 0.03	39.99 <sup>A</sup> $\pm$ 0.07	48.33 <sup>A-B</sup> $\pm$ 0.15	60.01 <sup>A-B</sup> $\pm$ 0.07
MaEÇ3	1.63 <sup>A</sup> $\pm$ 0.84	9.91 <sup>A-B</sup> $\pm$ 0.18	19.06 <sup>E</sup> $\pm$ 0.24	34.13 <sup>C-F</sup> $\pm$ 0.16	51.67 <sup>A-B</sup> $\pm$ 0.08
MaEO3	0.28 <sup>A</sup> $\pm$ 0.00	9.91 <sup>A-B</sup> $\pm$ 0.18	23.29 <sup>B-E</sup> $\pm$ 0.12	41.58 <sup>A-F</sup> $\pm$ 0.68	53.35 <sup>A-B</sup> $\pm$ 0.40
Control	0.28 <sup>A</sup> $\pm$ 0.84	0.28 <sup>C</sup> $\pm$ 0.84	0.28 <sup>F</sup> $\pm$ 0.84	1.12 <sup>G</sup> $\pm$ 0.84	1.12 <sup>C</sup> $\pm$ 0.84

Means within columns with the same letter are not statistically different (Tukey's test at  $p \leq 0.05$ )

It is observed that the death rates have increased as time progressed for all isolates of both species. As the entomopathogenic fungi feed in the host and complete their development, secondary metabolites are secreted to kill the host therefore, the host is dying more rapidly. At the same time, the fungus develops inside the host and due to the breakdown the integument of the intestine hyphae appear on the host body surface.

## Discussion

Cosmopolitan species such as *Beauveria bassiana* and *Metarhizium anisopliae* from entomopathogenic fungi have a large spectrum of arthropod hosts. They originally are isolated from soil. Most aphid-pathogenic fungi are in the order of Entomophthorales (Zygomycota), however, several Hypocreales (Ascomycota) genera, such as *Beauveria*,

*Verticillium*, and *Paecilomyces*, are also known to infect aphids (Miller, 1997). *B. bassiana* isolates were isolated from all types of area but *M. anisopliae* were obtained only cultural area (Table 1). *B. bassiana* isolates can be used successfully as a commercial. But an analysis of the results showed that there was a significant difference in the fungal virulence against *M. persicae* (Tukey's test at  $p \leq 0.05$ ). Our *B. bassiana* isolates had the highest mortality rate with 63.35%. Also, *M. anisopliae* had the highest mortality rate with 65.84%. The results of our research overlap with previous research (Vu et al., 2007; Kim et al., 2013). Adult *M. persicae* were tested with isolates by using bait and direct contact methods. Results showed that the adult of *M. persicae* showed differences in susceptibility in the two species of *B. bassiana* and *M. anisopliae*. Our results show us that the isolate that kills as soon as possible and the isolate which has the highest mortality rate at the end of the 12- day incubation period are different from each other. Also, the virulence of the isolates of both entomopathogenic fungi are different and however, they did not show stability, different isolates were found to have different rates of mortality during this 12-day incubation period (Tables 2 and 3).

## Conclusion

Entomopathogenic fungi are used successfully in the control of pest insects and especially in the integrated pest management system (IPM) nowadays. It is important to know the virulence of the newly developed mycoinsecticides as well as their mortality rates. At the end of the study, we obtained a total of 78 isolates including 63 *Beauveria bassiana* isolates and 15 *Metarhizium anisopliae* as entomopathogenic fungi.

Based on the study; the isolates of both species were pathogenic to *M. persicae* and BbEİ5 isolates had the highest mortality rate with 62.54%. the *B. bassiana* isolates BbEKLY4 and BbEO2 were found the lowest mortality rate of 49.17%. Also in the case of *M. anisopliae*; MaEk1b and MaET3 isolates had the highest mortality rate while MaEMR1a isolates found the lowest mortality rate. Our results indicated that all of these isolates BbEİ5, MaEk1b and MaET3 have a broad host range and can be used as biocontrol agents for *M. persicae*, and as biological control agents.

**Acknowledgements.** The entomopathogenic fungus isolation of this study was supported by the Erzincan Binali Yıldırım University Research Foundation (FEN-A-300614-0104). In addition, in the identification of fungus species and other studies were supported by Özlem GÜVEN (Kahramanmaraş Sütçü İmam University, Department of Biology); Mariam CHUBINISVILI (NLE Agricultural University of Georgia) and for statistically analyzed Mustafa ALKAN (Republic of Turkey Ministry of Agriculture and Forestry, Directorate of Plant Protection Central Research Institute).

## REFERENCES

- [1] Aydemir, M. (2008): Zirai Mücadele Teknik Talimatları. Cit.1-2-3-4-5. – Başak Matbaacılık ve Tan. Hiz. Ltd. Şti. Ankara-Türkiye.
- [2] Balazy, S. (1993): Entomophthorales. Flora of Poland (Flora Polska), Fungi (Mycota). Vol. 24. – Polish Academy of Sciences, Krakow.
- [3] Burges, H. D. (ed.) (1981): Microbial Control of Pests and Plant Diseases 1970–1980. – Academic Press, London.
- [4] Butt, T. M., Copping., L. (2000): Fungal biological control agents. – Pesticide Outlook 11: 186-191.

- [5] Butt, T. M., Ibrahim, L., Ball, B. V., Clark, S. J. (1994): Pathogenicity of the entomogenous fungi *Metarhizium anisopliae* and *Beauveria bassiana* against crucifer pests and the honey bee. – *Biocontrol Sci. Technol.* 4: 207-214.
- [6] Butt, T. M., Jackson, C. W., Magan, N. (2001): Introduction—Fungal Biological Control Agents: Progress, Problems and Potential. – In: Butt, T. M., Jackson, C. W., Magan, N. (eds.) *Fungal Biological Control Agents: Progress, Problems and Potential*. CABI Publishing, Wallingford, pp. 1-8.
- [7] Clarkson, J. M., Charnley, A. K. (1996): New insights into the mechanisms of fungal pathogenesis in insects. – *Trends Microbiol.* 4(5): 197-203.
- [8] De Hoog, G. S. (1972): The genera *Beauveria*, *Isaria*, *Tritirachium* and *Acrodontium* gen. nov. – *Study Mycol.* 1: 1-41.
- [9] Dedryver, C.-A., Le Ralec, A., Fabre, F. (2010): The conflicting relationships between aphids and men: a review of aphid damage and control strategies. – *C. R. Biologies* 333: 539-553.
- [10] Devi, K. U., Murali Mohan, C. H., Padmavathi, J., Ramesh, K. (2003): Susceptibility to fungi of cotton boll worms before and after a natural epizootic of the entomopathogenic fungus *Nomuraea rileyi* (Hyphomycetes). – *Biocontrol Science and Technology* 13(3): 367-371.
- [11] Faria, M. R. and Wraight, S. P. (2007): Mycoinsecticides and mycoacaricides: a comprehensive list with worldwide coverage and international classification of formulation types. – *Biological Control* 43: 237-256.
- [12] Freed, S., Jin, F. L., Ren, S. X. (2011a): Determination of genetic variability among the isolates of *Metarhizium anisopliae* var. *anisopliae* from different geographical origins. – *World, J. Microbiol. Biotechnol.* 27: 359-370.
- [13] Freed, S., Jin, F. L., Ren, S. X. (2011b): Phylogenetics of entomopathogenic fungi isolated from the soils of different ecosystems. – *Pakistan J. Zool.* 43: 417-425.
- [14] Ghatwary, W. G. T. (2000): Integrated management of certain piercing sucking insects infesting some vegetables crops. – Ph. D. Thesis Fac. Agric Zagazig. Uni., Egypt.
- [15] Goettel, M. S., Eilenberg, J., Glare, T. R. (2005): Entomopathogenic Fungi and Their Role in Regulation of Insect Populations. – In: Gilbert, L. I., Iatrou, K., Gill, S. (eds.) *Comprehensive Molecular Insect Science*. Vol. 6. Elsevier, Oxford, pp. 361-406.
- [16] Gustafsson, M. (1965): On species of the genus *Entomophthora* in Sweden. I. Classification and distribution. – *Lantbrukshögskolans Annaler* 31: 103-212.
- [17] Hajek, A. (2004): *Natural Enemies: An Introduction to Biological Control*. – Cambridge University Press, Cambridge.
- [18] Humber, R. A. (1998): *Entomopathogenic Fungal Identification*. APS/ESA Workshop. USDA-ARS Plant Protection Research Unit, Ithaca.
- [19] Jackson, C. W., Heale, J. B., Hall, R. A. (1985): Traits associated with virulence to the aphid *Macrosiphoniella sanborni* in eighteen isolates of *Verticillium lecanii*. – *Ann. Appl. Biol.* 105: 39-48.
- [20] Keller, S. (1997): The genus *neozygites* (Zygomycetes, entomophthorales) with special reference to species found in the tropics. – *Sydowia* 49: 118-146.
- [21] Kılıç, E., Yıldırm, E. (2008): The use of entomopathogen fungi in control of whiteflies (Homoptera: Aleyrodidae). – *Atatürk Üniversitesi, Ziraat Fakültesi Dergisi* 39: 249-254.
- [22] Kim, J. J. (2004): Pathological studies of *Verticillium lecanii* on the cotton aphid control. – Ph. D. thesis. Chonnam National University, Korea.
- [23] Kim, J. J., Goettel, M. S., Gillespie, D. R. (2010): Evaluation of *Lecanicillium longisporum*, Vertalec® against the cotton aphid, *Aphis gossypii*, and cucumber powdery mildew, *Sphaerotheca fuliginea* in a greenhouse environment. – *Crop Protection* 29: 540-544.
- [24] Kim, J. J., Jeong, G., Han, J. H., Lee, S. (2013): Biological control of aphid using fungal culture and culture filtrates of *Beauveria bassiana*. – *Mycobiology* 41(4): 221-224.



- [25] Krutmuang, P., Mekchay, S. (2005): Pathogenicity of entomopathogenic fungi *Metarhizium anisopliae* against termites. – Conference on International Agricultural Research for Development, Stuttgart-Hohenheim, 11-13 October 2005.
- [26] Lacey, L. A., Frutos, R., Kaya, H. K., Vail, P. (2001): Insect pathogens as biological control agents: do they have a future? – *Biol Control* 21: 230-248.
- [27] Luangsa-Ard, J. J., Tسانathai, K., Mongkolsamrit, S., Hywel-Jones, N. L. (2007): Atlas of Invertebrate-Pathogenic Fungi of Thailand. Vol. 1. – BIOTEC, NSTDA, Pathum Thani, Thailand.
- [28] McCoy, C. W., Samson, R. A., Boucias, D. G. (1998): Entomogenous Fungi. – In: Ignoffo, C. M., Mandava, N. B. (eds.) Handbook of Natural Pesticides. Part A. Entomogenous Protozoa and Fungi, Microbial Pesticides. CRC Press, Inc., Boca Raton, FL, pp. 151-236.
- [29] Meyling, N. V., Pell, J. K., Eilenberg, J. (2006): Dispersal of *Beauveria bassiana* by the activity of nettle insects. – *Journal of Invertebrate Pathology* 93: 121-126.
- [30] Milner, R. J. (1997): Prospects for biopesticides for aphid control. – *Entomophaga* 42: 227-239.
- [31] Ouedraogo, R. M., Cusson, M., Goettel, M. S., Brodeur, J. (2003): Inhibition of fungal growth in thermoregulating locusts, *Locusta migratoria*, infected by the fungus *Metarhizium anisopliae* var *acridum*. – *J Invertebr Pathol.* 82: 103-109.
- [32] Quesada-Moraga, E., Maranhao, E. A. A., Valverde-García, P., Santiago-Álvarez, C. (2006): Selection of *Beauveria bassiana* isolates for control of the whiteflies *Bemisia tabaci* and *Trialeurodes vaporariorum* on the basis of their virulence, thermal requirements and toxicogenic activity. – *Biol. Control* 36: 274-287.
- [33] Ren, S. X., Chen, X. X. (2012): Biological Control. – China Agriculture Press, Beijing, pp. 227-262.
- [34] Samson, R. A., Evans, H. C., Latge, J. P. (1988): Atlas of Entomopathogenic Fungi. – Springer, New York.
- [35] Shia, W. B., Feng, M. G. (2004): Lethal effect of *Beauveria bassiana*, *Metarhizium anisopliae*, and *Paecilomyces fumosoroseus* on the eggs of *Tetranychus cinnabarinus* (Acari: Tetranychidae) with a description of a mite egg bioassay system. – *Biol. Cont.* 30: 165-173.
- [36] St. Leger, R. J., Wang, C., Fang, W. (2011): New perspectives on insect pathogens. – *Fungal Biology Reviews* 25: 84-88.
- [37] Steenberg, T., Humber, R. A. (1999): Entomopathogenic potential of *Verticillium* and *Acremonium* species (Deuteromycotina: Hyphomycetes). – *J. Invertebr. Pathol.* 73: 309-314.
- [38] Thakur, R., Sandhu, S. S. (2010): Distribution, occurrence and natural invertebrate hosts of indigenous entomopathogenic fungi of Central India. – *Indian J Microbiol* 50(1): 89-96.
- [39] Thoizon, G. (1970): Specificité du parasitisme des aphides par les entomophthorales. – *Ann. Soc. Ent. Fr. (N. S.)* 6(3): 517-562.
- [40] Vu, V. H., Hong, S. I., Kim, K. (2007): Selection of entomopathogenic fungi for aphid control. – *Journal of Bioscience and Bioengineering* 104(6): 498-505. <https://doi.org/10.1263/jbb.104.498>.
- [41] Zimmermann, G. (1986): The *Galleria* bait method for detection of entomopathogenic fungi in soil. – *J. Appl. Entomol.* 102: 213-215.

# RESPONSE OF MICROBIAL ACTIVITY TO BIOTURBATION OF NEREID (*PERINEREIS AIBUHITENSIS*) IN INTERTIDAL MUDFLAT SEDIMENTS

MA, Y.<sup>1#</sup> – WANG, Y. Z.<sup>1#</sup> – XIONG, C. J.<sup>2</sup> – XIONG, H. J.<sup>3\*</sup>

<sup>1</sup>*Fisheries College of Jimei University, Engineering Research Center of the Modern Technology for Eel Industry, Ministry of Education, Xiamen 361021, China*

<sup>2</sup>*College of Foreign Language, Hunan University, Changsha 410006, China*

<sup>3</sup>*College of Food and Biological Engineering, Jimei University, Xiamen 361021, China*

*#Ying Ma and Yongzhong Wang should be considered joint first authors.*

*\*Corresponding author  
e-mail: [hjxiong@jmu.edu.cn](mailto:hjxiong@jmu.edu.cn)*

(Received 21<sup>st</sup> May 2020; accepted 17<sup>th</sup> Sep 2020)

**Abstract.** Although numerous studies have reported the effects of the nereid polychaete bioturbation on sediments, its effects on soil microbial activity remain poorly understood. For this study, nereids (*Perinereis aibuhitensis*) were introduced to intertidal mudflat sediments in a laboratory experiment, and the resulting bioturbation effects on soil microbial activity dynamics were investigated via the Biolog ECO method. The results reveal high microbial utilization of carbohydrates, amino acids, and polymers, while the utilization of carboxylic acids, amines, and miscellaneous contents was low. After introducing nereids, the physicochemical characteristics and heavy metal values did not significantly change; however, the sediment microbial activity and the carbon substrate utilization diversity increased significantly. Furthermore, in a specific sowing range, higher sowing density of nereids showed a higher enhancing effect on microbial activity and carbon substrate utilization diversity. Nereid bioturbation is therefore suggested to increase the microbial utilization of carbohydrates and amino acids, while it decreases the utilization of polymers.

**Keywords:** *nereid polychaete, marine sediment, biological disturbance, bacteria, metabolic response, Biolog ECO*

## Introduction

The polychaete *Perinereis aibuhitensis* is a common invertebrate of the phylum Annelida and the family Nereidae. It is widely distributed along the coastal and estuarine regions of the Northwest Pacific (Tian et al., 2019), and plays a vitally important role in the coastal intertidal ecosystem due to its bioturbation activity. Bioturbation is the physical agitation, mixing and restructuring of sedimentary particles by benthic organisms. The bioturbation of burrowing, breathing, and feeding of nereids reworks the physical structure of the sediment, extends the contact area of bottom sediments with dissolved oxygen (Wenzhöfer et al., 2004), thus promoting the mineralization and decomposition of organic matter (Tsutsumi et al., 2005; Deng, 2006). The polychaete nereid also exhibits the ability of bioaccumulation and soluble binding of heavy metals (Berthet et al., 2003; Durou et al., 2005), and can enhance the release of buried hydrocarbons pollutants in sediments (Tian et al., 2019), thus helping to improve the benthic environment.

Macrobenthic bioremediation is largely implemented via influencing microorganisms within the sediments, and it is vital in illuminating microorganism variations during the

bioturbation process. Previous studies have shown that macrobenthic bioturbation of burrowing imposed a selective pressure and exerted a functionally-conserved altering effect on sediment microbes even under different environmental conditions (Booth et al., 2019). Microbial communities within burrows are distinct from those at the sediment surface, and different burrow types of benthic animals incubate diverse bacterial taxa (Marinelli et al., 2002; Bertics and Ziebis, 2009; Pischedda et al., 2011). With the benthic bioturbation of feeding, burrowing and other activities, sediments were loosened and large grains became small, thus contributing to microorganism degradation and soil eutrophication alleviation (Sun et al., 2019). Macrobenthic bioturbation has also been reported to facilitate the bacteria-mediated nitrification and denitrification process (Banks et al., 2013), affect the release and distribution of polycyclic aromatic hydrocarbons (PAHs), and stimulate the development of hydrocarbon degrading bacteria, which may help the bioremediation process in oil-contaminated sediments (Cuny et al., 2007). Our previous studies reported that bioturbation of introduced macrobenthos increased the diversity of archaea and favored the development of ecologically important bacteria and archaea (Ma et al., 2015; Deng et al., 2015). However, studies about the influence of bioturbation on microbial activities have rarely been reported.

Community level physiological catabolic profiles (CLPPs) has been used as an important method for studying the microbial community structure of soil for many years (Garland and Mills, 1991; Murugan et al., 2014), and has been widely used for the assessment of microbial functional diversity in agricultural and forest soils under different administration process (Grayston et al., 1998; Islam et al., 2011; Chaudhry et al., 2012). In addition, estimating the soil microbial communities through C source use patterns has been proven to be a sensitive method for detecting variations caused by management practices (Gomez et al., 2006), and the test species has expanded from prokaryote bacteria to eukaryotic algae (Kim et al., 2017). Biolog GN and ECO microplates (Biolog, Inc.) were typically used in CLPPs analyses, while ECO plates, first described by Insam (1997), have more frequently been used in microbial ecology studies. The ECO-plate is composed of 96 wells and contains 31 different carbon sources and a blank, each carbon source and blank have 3 repeats; these carbon sources are regarded to be more relevant to the ecological functions of microorganisms perform in ecosystems (Choi and Dobbs, 1999; Loranger-Merciris et al., 2006). The Biolog ECO plate assay reflects the microbial metabolic diversity within the ecosystem via testing of a reduced number of ecologically relevant carbon sources (Nautiyal et al., 2010). In this study, a laboratory experiment was designed to simulate bioturbation of mudflat sediments using nereids, and Biolog ECO was utilized to investigate the influence of nereid bioturbation on microbial activities.

## Materials and methods

### *Experiment setup and sample collection*

Intertidal mudflat sediments were collected from Xiamen, Fujian province, China (118°6' 20" E, 24°34' 49" N). After removing large particles and macrobenthos, the sediments were completely mixed and evenly divided into 12 plastic boxes (each with a dimension of about 42 × 30 × 19.2 cm), and the weight of sediment deposited in each box was about 20 kg. Polychaete nereids (*Perinereis aibuhitensis*) were bought from Fuqing, Fujian Province, and were temporally cultured in seawater at room temperature for three days. Active nereids with similar size were weighed and measured, and were selected for the ensuing experiment. Nereids were sowed in culture boxes in three different densities:

10, 20, and 30 individuals per box, named as T10, T20, and T30, respectively. Each sowing density had three replicates. Furthermore, three boxes were designed as blank controls without nereids, and this control group was named C. To simulate daily tidal cycles, seawater was injected into the boxes at 8 am to cover the soil surface, and was released at 8 pm each day of the experiment. The experiment started on October 1<sup>st</sup> and ended on November 15<sup>th</sup> 2014 with a total duration of 45 days.

Sediment samples were collected from each culturing box at 0, 3, 7, 14, 21, 28, 35, and 45 days after the sowing of nereids, and were used for Biolog ECO analysis. Detailed information for the samples is shown in *Table 1*.

**Table 1.** Samples collected in the laboratory bioremediation model

Control group without nereids	Treatment groups with nereids			Sampling date	Interval after sowing nereids (d)
	10 individuals per box	20 individuals per box	30 individuals per box		
C-0d	T10-0d	T20-0d	T30-0d	Oct. 1, 2014	0d
C-3d	T10-3d	T20-3d	T30-3d	Oct. 4, 2014	3d
C-7d	T10-7d	T20-7d	T30-7d	Oct. 8, 2014	7d
C-14d	T10-14d	T20-14d	T30-14d	Oct. 15, 2014	14d
C-21d	T10-21d	T20-21d	T30-21d	Oct. 22, 2014	21d
C-28d	T10-28d	T20-28d	T30-28d	Oct. 29, 2014	28d
C-35d	T10-35d	T20-35d	T30-35d	Nov. 5, 2014	35d
C-45d	T10-45d	T20-45d	T30-45d	Nov. 15, 2014	45d

### **Determination of microbial activity in sediments**

Biolog ECO plates were utilized to determine the metabolic diversity of soil bacterial communities. About 5 g sediment were added to a 250 ml conical flask with 45 ml of 0.85% sterilized saline water, and were shaken for 1 h at 180 rpm on a shaker; then, the mixture was left standing for 30 min. The supernatant was diluted to 10<sup>-3</sup> and 150 µL of the dilution were inoculated in the well of the preheated Biolog ECO plate and incubated at 28 °C for seven days. The optical density ( $\lambda = 590$  nm) of each well was determined immediately (0 h) as well as every 24 h.

Average well color development (AWCD) indicates the oxidizing capacity of sediment microorganisms, cultured in Biolog microplates and typically represents the overall metabolic capacity of microorganisms (Garland and Mill, 1991).  $AWCD = \sum(R-C)/31$ , where R is the optical density of every well with added carbon source, C is the absorbance value of the control well (without a carbon source), and 31 stands for 31 types of carbon sources. Data obtained at 96 h were used to calculate relative utilization ratios for different carbon sources and microbial metabolic diversity indices. The relative utilization ratio was determined via the percentage of AWCD of a certain carbon substrate in the total AWCD of all carbon substrates. The formulas used to calculate the Shannon-Wiener Diversity H', the Simpson index D, and the Pielou evenness index Jsw have been described earlier (Dobranic and Zak, 1999). Data were subjected to statistical analysis using Excel 2010 and SPSS 17.0, and were analyzed by one-way ANOVA among multiple groups or a Student's t-test between two groups. A value of  $p < 0.05$  was considered statistically significant. The principal component analysis (PCA) was performed with Canon software.

## Results

### *Nereid growth and survival*

By the end of the experiment, all nereids were dug out from each culture box. Survival rate, body weight, and body length were assessed, and the resulting data are listed in *Table 2*. Nereid survival rate were higher than 80% for each treatment group, and in the culture box of ten individuals, the survival rate reached up to 100%. Body weight and body length increased for all treatments, and the largest values were also detected in the culture box of ten individuals, indicating that a more diluted sowing density might be better for nereid growth. However, the differences among different groups were not significant ( $P > 0.05$ ).

**Table 2.** Survival rate, body weight, and body length of nereid in a laboratory experiment

	Before sowing nereids	45 days after sowing nereids		
		10 individuals /box	20 individuals /box	30 individuals /box
Survival rate		100.0%	80.0%	85.6%
Body weight± SD (g)	1.76±0.35	2.30±0.46	2.06±0.49	2.11±0.39
Body length±SD (cm)	14.21±1.67	15.58±1.01	14.56±1.98	14.91±2.38

Note: Data were obtained from three replicates. SD means standard deviation

### *Overview of sediment microbial metabolic activity*

The AWCD values of samples that were collected at different times, determined after 96 h of incubation, which corresponds to the maximum growth time of microorganisms in the Biolog ECO plates, are shown in *Fig. 1*. The AWCD values of the control group (C) without nereids gradually decreased over the course of the experiment, indicating a decreasing trend of sediment microbial activity. The AWCD value of group T10 (with nereids at a density of 10 per box) also showed a decreasing trend, except for the value of the sample collected at day seven. The variations of AWCD curves of groups T20 and T30 (with sowing densities of 20 and 30 per box, respectively) were similar: the values increased at 7 d and 3 d, respectively, followed by a decrease until 21 d, and increasing again until the end of the experiment (45 d). Most of the AWCD values of T20 and T30 were higher than those at the beginning of the experiment (0 d), indicating that the overall sediment microbial activities of groups T20 and T30 increased during experiment.

A comparison between samples collected at the same time revealed that all average AWCD values of treatment samples (except the value of T30-21d) were higher than those of control samples, and most of the differences reached significant levels ( $P < 0.05$ , *Table S1*), suggesting that nereid bioturbation stimulated the overall microbial metabolic activity. Different nereid density exerted a different influence on microbial activity. The microbial activity value order of treatment samples changed severely before 21 d: on the third day after nereid sowing, the AWCD of T30 was significantly higher than in the other two treatments ( $P < 0.05$ , *Table S1*); however, on the seventh day, T20 was maximal, and T10 became the highest on the 14<sup>th</sup> and 21<sup>st</sup> day, respectively, among all the samples collected at the same times. These results indicate that in the early stage of the experiment (before 7 d), higher nereid density influenced the microbial activity more quickly, while in the mid stage of the experiment (7 d - 21 d), the influence of a lower nereid density grew gradually. However, 21 days after nereid sowing, the influence of higher nereid

density increased again, and the AWCD values of T20 and T30 were significantly higher than those of T10 after 28 days of nereid sowing ( $P < 0.05$ , Table S1). In summary, the average AWCD value of T10 was lower than in other treatments, and the values of T20 and T30 were similar. These results indicate that in a certain sowing range, higher sowing density of nereids seemed to have a more enhancing effect on microbial activity.

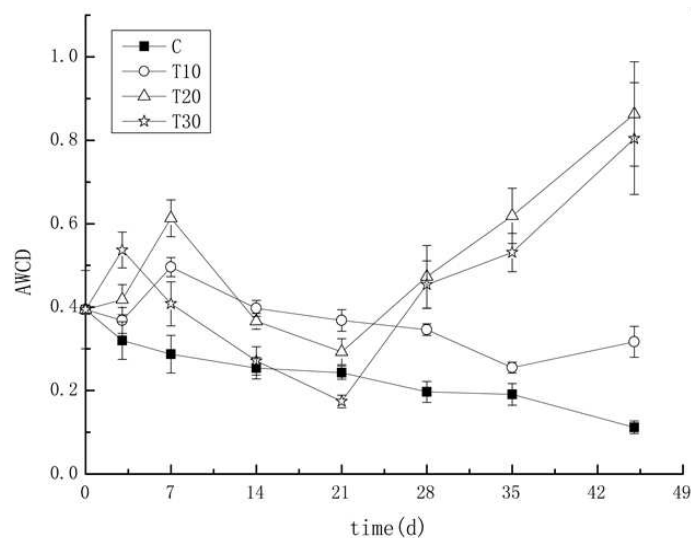


**Figure 1.** AWCD values of mudflat samples collected at different times after incubating for 96 h. C indicates the control group without nereids; T10, T20, and T30 indicate treatment samples with different densities of nereids (10, 20, and 30 individuals per box, respectively). Error bars indicate the standard deviation of the means ( $n = 3$ )

### **Carbon source utilization profile of mudflat sediment microbial communities**

There are 31 single carbon sources and one blank control with three repeats distributed on the Biolog ECO microplate. The 31 carbon substrates can be roughly divided into six substrate categories (Preston-Mafham et al., 2002), which are 9 carboxylic acids, 7 carbohydrates, 6 amino acids, 4 polymers, 2 amines, and 3 miscellaneous. The relative carbon source utilization ratios were determined via the AWCD at 96 h incubation, and the categorized substrate utilization patterns by microbial communities are shown in Fig. 2. Overall, the utilization of microbial communities for carbohydrates, amino acids, and polymers were higher, while those for carboxylic acids, amines, and miscellaneous were lower. Further analysis indicated that, except for samples collected at 28 d and 35 d, the microbial utilization for carbohydrates of all treatment samples with nereids were significantly higher than those of control samples ( $p < 0.05$ , Table S2). However, the polymer utilization of all treatment samples was significantly lower than that of control samples ( $p < 0.05$ , Table S3). Furthermore, the microbial utilization of amino acids of most of the treatment samples was significantly higher than that of control samples ( $p < 0.05$ , Table S4). These results suggest that nereid bioturbation stimulated microbial utilization of carbohydrates and amino acids, but decreased the microbial utilization of polymers. In the process of the experiment, the microbial utilization of amines in control samples increased with time, while in the treatment group, the utilization for amines was not consistent among samples with different nereid density (Fig. 2, Table S5). The microbial utilization for carboxylic acids and miscellaneous also increased slightly during

the experiment; however, the microorganisms utilizing carboxylic acids and miscellaneous were not abundant, and the nereid bioturbation effects on the microbial utilization for these substrates differed at different sampling times (Fig. 2, Table S6, Table S7).

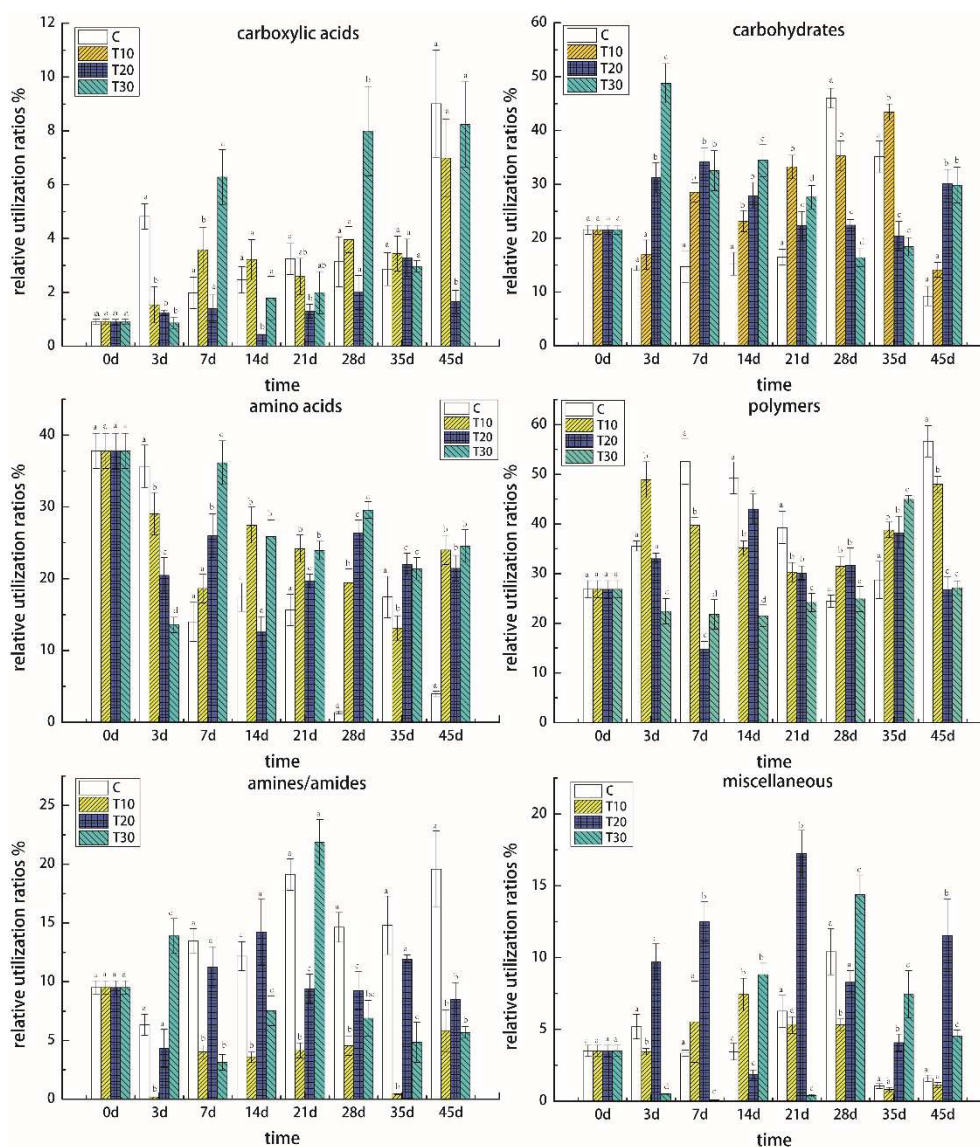


**Figure 2.** Categorized substrate utilization patterns at different sampling times by microbial communities from mudflat sediments after 96 h of incubation. Values indicated by a same letter are not significantly different ( $P > 0.05$ ). Error bars indicate the standard error of the mean ( $n=3$ ). C indicates the control group without nereids; T10, T20, and T30 indicate treatment samples with different nereid densities (10, 20, and 30 individuals per box, respectively)

### Microbial functional diversity indices analysis

Microbial functional diversity can be reflected via carbon source utilization diversity indices (Kong et al., 2013). The calculated diversity indices are shown in Fig. 3. In the control group without nereids, the Shannon index and Simpson index both decreased with time during the experiment, indicating a decreasing trend of microbial functional



diversity. However, in the treatment group with nereids, all diversity indices were at high levels, and most of them were higher than those of samples collected at the beginning. This suggested that nereid bioturbation in mudflat sediments increased the microbial functional diversity. Compared to control samples collected at the same day, all nereid bioturbated samples had higher diversity indices, except for T30 samples collected at 14 d and 21 d. Furthermore, during the later period of the experiment (after 28 d), the differences between control and treatment samples reached significant levels ( $P < 0.05$ , *Table S8*, *Table S9*). Considering the effects of different nereid density, the microbial functional diversity ranked in the following order:  $T20 > T30 > T10$ , suggesting that nereid density was not simply positively correlated with microbial functional diversity, but a higher nereid density seemed to increase microbial diversity. The above variations were similar to those of microbial activity. As for the Pielou index, no obvious change trend was present after introducing nereids to the sediments, and most of the differences of the Pielou evenness indices between control and treatment groups did not reach significant levels ( $p > 0.05$ , *Table S10*).

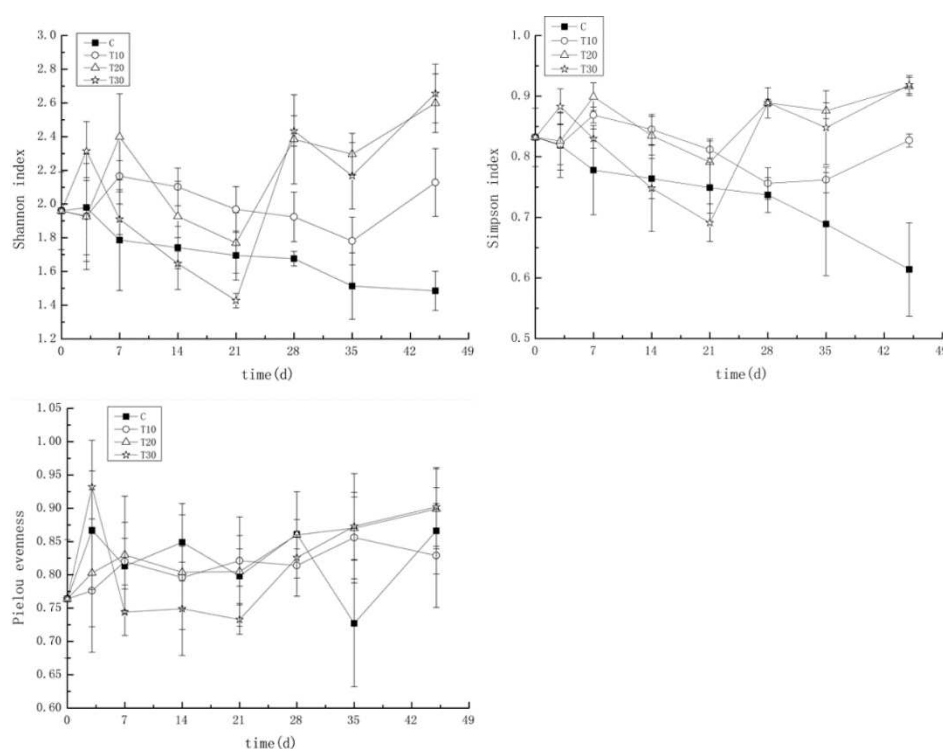


**Figure 3.** Carbon source utilization diversity indices of microbial communities in mudflat sediments. C indicates control group without nereids; T10, T20, and T30 indicate treatment samples with different nereid densities (10, 20, and 30 individuals per box, respectively)

### ***Relationship of carbon source utilization patterns of microbial communities in different samples***

Principal component analysis (PCA) was used to determine the degree of differentiation in carbon source metabolization between treatments and control, and the results are shown in *Fig. 4*. PC1 and PC2, representing the first and the second principal component, explained 46.7% and 14.8% of data variance, respectively. *Fig. 4* shows that the control samples without nereids (C-, shown by open circles) and the treatment samples



collected before nereid sowing (T0, labeled by open square) were mainly located in the lower left part of the PCA, and separated from other treatment samples with nereids (labeled with filled circle, triangle, and diamond); only one sample (C-28d) was a little removed from them. However, many T10-samples were also located in this region, suggesting that a lower nereid density had less influence than those with higher nereid density.

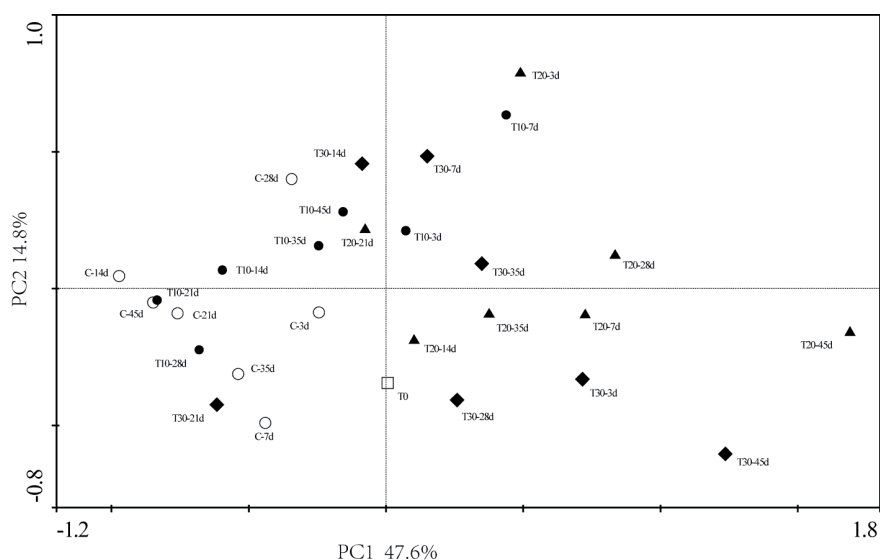


**Figure 4.** Principal component analysis (PCA) for microbial carbon source utilization profiles in mudflat sediments. C (open circles) indicates the control group without nereids; T10 (filled circles), T20 (filled triangles), and T30 (filled diamonds) indicate treatment samples with different densities of nereids (10, 20, and 30 individuals per box, respectively). -3d, 7d, 14d, etc. denote sampling times. T0 (open square) indicates treatment sample collected before sowing nereids

## Discussion

Compared to microbial community structure, microbial activities and functional diversity are more important indexes, reflecting ecological function. Biolog ECO is a fast, inexpensive, reproducible and sensitive method for detecting the activity of soil microbial communities (Islam et al., 2011; Weber and Legge, 2011; Sprocati et al., 2014; Rutgers et al., 2016). Its application has been well described on variety of research areas (Kim et al., 2017). Biolog ECO has also been used for exploring the effects of large herbivores grazing on soil microbial metabolic profiles (Qu et al., 2020), however, studies about the influence of macrobenthos bioturbation on microbial activities have never been reported.

In this study, the response of microbial activities to nereid polychaete bioturbation in intertidal mudflat sediments was investigated via the Biolog ECO method in a 45-day laboratory experiment. Results showed that the bacteria presented in the intertidal sediments prefer to utilize the easy-to-use carbon sources, such as carbohydrates, amino acids, and polymers, which were consisted with findings reported in an artificial mangrove wetland (Yin and Yan, 2020). Results also revealed that nereid bioturbation significantly improved the sediment microbial activity, and increased the carbon substrate utilization diversity. A possible reason may be that the bioturbating activities, such as migrating, feeding, excreting, and burrowing, changed sediment structure and porosity,

loosened sediment particles and enriched dissolved oxygen in sediments (Satoh and Okabe, 2013; Boeker and Geist, 2016), thus promoting microbial metabolic activity. Previous studies reported that high levels of organics in mudflat sediments might increase the bacterial abundance and improve the bacterial degradation ability for organics (Dai and Sun, 2007), and microbial metabolic activity will be stronger when organic matter content is higher in sediments (Su et al., 2018). Nereid excrements could also be used as metabolic substrate for soil bacteria and promote bacterial growth. Previous studies indicated a higher functional diversity on the basis of carbon source utilization profiles, suggesting an improvement of soil quality (Gomez et al., 2006; Islam et al., 2011; Chaudhry et al., 2012). Nereid bioturbation increased bacterial activity and metabolic functional diversity, which might be one of the important mechanisms of bioremediation using nereids.

The influence of different nereid densities on microbial activity was different. Overall, a higher nereid density had more influence, particularly in the early and late periods of the experiment, while in the mid stage of the experiment, a lower nereid density influenced more apparently. A possible reason might be that, in the culture box with higher nereid density, some nereids died due to overcrowding and closed experiment boxes, and as these dead bodies and wastes accumulated, bioturbation and bacterial activity were inhibited. In the late period of the experiment, the decreased nereid density was beneficial for the survivals growth and activity and thus, the bacterial activity increased again.

The physicochemical characteristics in the mudflat sediments did not change significantly under nereid bioturbation (data not shown), possibly due to the short bioremediation time. Nevertheless, the response of microbial activity and metabolic functional patterns changed severely, indicating that microbial variations are more sensitive and can be used as early warnings for environmental change. Future improvements will include extending the experimental period, using larger experimental boxes, and performing field experiment as a comparison. These will enable us to better understand the response of microbial activity to nereid bioturbation. In addition, the microbial utilization of carbohydrates and amino acids increased, while that of polymers decreased after nereid introduction. However, the causes and mechanisms for such variations in carbon source utilization, and what roles these variations play in the nereid bioremediation, require further investigation. Future studies should focus on variations of functional bacteria during bioturbation, which would be benefit for illuminating the bioremediation mechanism.

## Conclusion

Microbial communities in mudflat sediments are more sensitive compared to physicochemical indexes and can be used as early warnings for environmental change. After introducing nereid to mudflat sediments, the sediment microbial activity and the carbon substrate utilization diversity increased significantly. In a certain sowing range, higher sowing density of nereids showed a more enhancing influence on microbial activity. Bioturbation enhanced microbial activity for utilizing carbohydrates and amino acids, but decreased the microbial utilization of polymers. However, the results were obtained in the laboratory simulation experiment and need to be verified in the field. In addition, the relationship between the changes of sediment microbial activities and environmental factors during nereids bioturbation needs to be further studied.

**Acknowledgements.** This work was supported by the National Natural Science Foundation of China (No. 31272669) and the Key Science and Technology Program of Fujian Province of China (2016N0022).

## REFERENCES

- [1] Banks, J. L., Ross, D. J., Keough, M. J., Macleod, C. K., Keane, J., Eyre, B. D. (2013): Influence of a burrowing, metal-tolerant polychaete on benthic metabolism, denitrification and nitrogen regeneration in contaminated estuarine sediments. – *Marine Pollution Bulletin* 68: 30-37.
- [2] Berthet, B., Mouneyrac, C., Amiard, J. C., Amiard-Triquet, C., Berthelot, Y., Le Hen, A., Mastain, O., Rainbow, P. S., Smith, B. D. (2003): Accumulation and soluble binding of cadmium, copper, and zinc in the polychaete *Hediste diversicolor* from coastal sites with different trace metal bioavailabilities. – *Archives Environmental Contamination Toxicology* 45: 468-478.
- [3] Bertics, V. J., Ziebis, W. (2009): Biodiversity of benthic microbial communities in bioturbated coastal sediments is controlled by geochemical microniches. – *The ISME Journal* 3: 1269-1285.
- [4] Boeker, C., Geist, J. (2016): Lampreys as ecosystem engineers: burrows of *Eudontomyzon* sp. and their impact on physical, chemical, and microbial properties in freshwater substrates. – *Hydrobiologia* 777: 171-181.
- [5] Booth, J. M., Fusi, M., Marasco, R., Mboobo, T., Daffonchio, D. (2019): Fiddler crab bioturbation determines consistent changes in bacterial communities across contrasting environmental conditions. – *Scientific Reports* 9: 3749.
- [6] Chaudhry, V., Rehman, A., Mishra, A., Chauhan, P. S., Nautiyal, C. S. (2012): Changes in bacterial community structure of agricultural land due to long-term organic and chemical amendments. – *Microbial Ecology* 64: 450-460.
- [7] Choi, K. H., Dobbs, F. C. (1999): Comparison of two kinds of Biolog microplates (GN and ECO) in their ability to distinguish among aquatic microbial communities. – *Journal of Microbiological Methods* 36: 203-213.
- [8] Cuny, P., Miralles, G., Cornet-Barthaux, V., Acquaviva, M., Stora, G., Grossi, V., Gilbert, F. (2007): Influence of bioturbation by the polychaete *Nereis diversicolor* on the structure of bacterial communities in oil contaminated coastal sediments. – *Marine Pollution Bulletin* 54: 452-459.
- [9] Dai, J. H., Sun, M. Y. (2007): Organic matter sources and their use by bacteria in the sediments of the Altamaha estuary during high and low discharge periods. – *Organic Geochemistry* 38: 1-15.
- [10] Deng, J. S. (2006): Bioremediation effect of introducing *Perinereis aibuhitensis* Grube and *Scapharca subcrenata* Lischke on shrimp pond. – Ocean University of China, Qingdao.
- [11] Deng, F., Ma, Y., Li, J., Wang, Y. Z., Yan, Q. P., Yan, X. Z., Lin, M. (2015): Archaeal community structure and response to ark shell bioturbation in typical intertidal mudflats, Southeast coast of China. – *Continental Shelf Research* 106: 97-106.
- [12] Dobranic, J. K., Zak, J. C. (1999): A microtiter plate procedure for evaluating fungal functional diversity. – *Mycologia* 91: 756-765.
- [13] Durou, C., Mouneyrac, C., Amiard-Triquet, C. (2005): Tolerance to metals and assessment of energy reserves in the polychaete *Nereis diversicolor* in clean and contaminated estuaries. – *Environmental Toxicology* 20: 23-31.
- [14] Garland, J. L., Mills, A. L. (1991): Classification and characterization of heterotrophic microbial communities on basis of patterns community-level sole-carbon-source utilization. – *Applied and Environmental Microbiology* 57: 2351-2359.
- [15] Gomez, E., Ferreras, L., Toresani, S. (2006): Soil bacterial functional diversity as influenced by organic amendment application. – *Bioresource Technology* 97: 1484-1489.

- [16] Grayston, S. J., Wang, S., Campbell, C. D., Edwards, A. C. (1998): Selective influence of plant species on microbial diversity in the rhizosphere. – *Soil Biology and Biochemistry* 30: 369-378.
- [17] Insam, H. (1997): A new set of substrates proposed for community characterization in environmental samples. – In: Insam, H., Rangger, A. (eds.) *Microbial Communities*. Springer-Verlag, Berlin Heidelberg.
- [18] Islam, M. R., Chauhan, P. S., Kim, Y., Kim, M., Sa, T. (2011): Community level functional diversity and enzyme activities in paddy soils under different long-term fertilizer management practices. – *Biology and Fertility of Soils* 47: 599-604.
- [19] Kim, J., Rehmann, L., Ray, M. (2017): Development of microalgal bioassay based on the community level physiological profiling (CLPP). – *Algal Research* 25: 47-53.
- [20] Kong, X., Wang, C., Ji, M. (2013): Analysis of microbial metabolic characteristics in mesophilic and thermophilic bio-filters using Biolog plate technique. – *Chemical Engineering Journal* 230: 415-421.
- [21] Loranger-Merciris, G., Barthes, L., Gastine, A., Leadley, P. (2006): Rapid effects of plant species diversity and identity on soil microbial communities in experimental grassland ecosystems. – *Soil Biology and Biochemistry* 38: 2336-2343.
- [22] Ma, Y., Hu, A., Yu, C. P., Yan, Q. P., Yan, X. Z., Wang, Y. Z., Deng, F., Xiong, H. J. (2015): Response of microbial communities to bioturbation by artificially introducing macrobenthos to mudflat sediments for in situ bioremediation in a typical semi-enclosed bay, southeast China. – *Marine Pollution Bulletin* 94: 114-122.
- [23] Marinelli, R. L., Lovell, C. R., Wakeham, S. G., Ringelberg, D. B., White, D. C. (2002): Experimental investigation of the control of bacterial community composition in macrofaunal burrows. – *Marine Ecology Progress Series* 35: 1-13.
- [24] Murugan, R., Loges, R., Taube, F., Sradnick, A., Joergensen, R. G. (2014): Changes in soil microbial biomass and residual indices as ecological indicators of land use change in temperate permanent grassland. – *Microbial Ecology* 67(4): 907-918.
- [25] Nautiyal, C. S., Chauhan, P. S., Bhatia, C. R. (2010): Changes in soil physico-chemical properties and microbial functional diversity due to 14 years of conversion of grassland to organic agriculture in semi-arid agroecosystem. – *Soil and Tillage Research* 109: 55-60.
- [26] Pischedda, L., Militon, C., Gilbert, F., Cuny, P. (2011): Characterization of specificity of bacterial community structure within the burrow environment of the marine polychaete *Hediste (Nereis) diversicolor*. – *Research in Microbiology* 162(10): 1033-1042.
- [27] Preston-Mafham, J., Boddy, L., Randerson, P. F. (2002): Analysis of microbial community functional diversity using sole-carbon-source utilisation profiles -a critique. – *FEMS Microbiology Ecology* 42: 1-14.
- [28] Qu, T., Guo, W., Yang, C., Zhang, J., Yang, Y., Wang, D. (2020): Grazing by large herbivores improves soil microbial metabolic activity in a meadow steppe. – *Grassland Science*, doi: 10.1111/grs.12282.
- [29] Rutgers, M., Wouterse, M., Drost, S., Breure, A., Mulder, C., Stone, D., Creamer, R., Winding, A., Bloem, J. (2016): Monitoring soil bacteria with community-level physiological profiles using Biolog<sup>TM</sup> ECO-plates in the Netherlands and Europe. – *Applied Soil Ecology* 97: 23-35.
- [30] Satoh, H., Okabe, S. (2013): Spatial and temporal oxygen dynamics in macrofaunal burrows in sediments: a review of analytical tools and observational evidence. – *Microbes and Environments* 28: 166-179.
- [31] Sprocati, A. R., Alisi, C., Tasso, F., Fiore, A., Marconi, P., Langella, F., Kothe, E. (2014): Bioprospecting at former mining sites across Europe: microbial and functional diversity in soils. – *Environmental Science and Pollution Research* 21: 6824-6835.
- [32] Su, L., Huang, T., Li, N., Zhang, H., Wen, G., Li, Y., Chen, J., Wang, X. (2018): Characteristics of sediment oxygen demand in a drinking water reservoir. – *Environmental Science* 39: 1159-1166.

- [33] Sun, T., Liu, C., Li, X., An, D., Yu, H., Ma, Z., Liu, F. (2019): The effect of substrate grain size on burrowing ability and distribution characteristics of *Perinereis aibuhitensis*. – *Acta Oceanologica Sinica* 38(12): 52-58.
- [34] Tian, S., Tong, Y., Hou, Y. (2019): The effect of bioturbation by polychaete *Perinereis aibuhitensis* on release and distribution of buried hydrocarbon pollutants in coastal muddy sediment. – *Marine Pollution Bulletin* 149: 110487.
- [35] Tsutsumi, H., Kinoshita, K., Srithongouthai, S., Sato, A., Nagata, S., Inoue, A., Yoshioka, M., Ohwada, K., Hama, D. (2005): Treatment of the organically enriched sediment below the fish-farm with the biological activities of the artificially mass-cultured colonies of a small deposit feeding polychaete, *Capitella* sp. I. – *Benthos Research* 60: 25-38.
- [36] Weber, K. P., Legge, R. L. (2011): Dynamics in the bacterial community-level physiological profiles and hydrological characteristics of constructed wetland mesocosms during start-up. – *Ecological Engineering* 37: 666-677.
- [37] Wenzhöfer, F., Glud, R. (2004): Small-scale spatial and temporal variability in coastal benthic O<sub>2</sub> dynamics: Effects of fauna activity. – *Limnology and Oceanography* 49: 1471-1481.
- [38] Yin, Y., Yan, Z. (2020): Variations of soil bacterial diversity and metabolic function with tidal flat elevation gradient in an artificial mangrove wetland. – *Science of the Total Environment* 718: 137385.

## APPENDIX

### Supplementary Information

**Table S1.** Statistical analysis of the AWCD values of different sediment samples collected at the same times

Sampling time	C	T10	T20	T30
0d	0.394±0.094 <sup>a</sup>	0.394±0.094 <sup>a</sup>	0.394±0.094 <sup>a</sup>	0.394±0.094 <sup>a</sup>
3d	0.320±0.045 <sup>c</sup>	0.368±0.031 <sup>bc</sup>	0.418±0.036 <sup>b</sup>	0.537±0.043 <sup>a</sup>
7d	0.287±0.045 <sup>d</sup>	0.496±0.023 <sup>b</sup>	0.613±0.044 <sup>a</sup>	0.408±0.053 <sup>c</sup>
14d	0.254±0.026 <sup>b</sup>	0.397±0.019 <sup>a</sup>	0.366±0.019 <sup>a</sup>	0.271±0.034 <sup>b</sup>
21d	0.243±0.016 <sup>c</sup>	0.368±0.026 <sup>a</sup>	0.293±0.031 <sup>b</sup>	0.174±0.015 <sup>d</sup>
28d	0.197±0.025 <sup>c</sup>	0.346±0.014 <sup>b</sup>	0.473±0.075 <sup>a</sup>	0.454±0.057 <sup>a</sup>
35d	0.191±0.026 <sup>c</sup>	0.255±0.013 <sup>c</sup>	0.619±0.066 <sup>a</sup>	0.531±0.046 <sup>b</sup>
45d	0.112±0.015 <sup>c</sup>	0.317±0.037 <sup>b</sup>	0.863±0.125 <sup>a</sup>	0.804±0.134 <sup>a</sup>

Notes: C indicates the control group without nereids; T10, T20, and T30 indicate treatment samples with different nereid densities (10, 20, and 30 individuals per box, respectively). Values are means ± SD (n = 3). Different superscript letters represent a significant difference (p < 0.05) between two groups at the same sampling times. The same below

**Table S2.** Statistical analysis of the relative utilization ratios of carbohydrates by the bacteria communities in different sediment samples collected at the same times

Sampling time	C	T10	T20	T30
0d	21.57±0.82 <sup>a</sup>	21.57±0.82 <sup>a</sup>	21.57±0.82 <sup>a</sup>	21.57±0.82 <sup>a</sup>
3d	14.45±0.45 <sup>a</sup>	16.91±2.73 <sup>a</sup>	31.24±2.81 <sup>b</sup>	48.77±3.64 <sup>c</sup>
7d	14.71±2.98 <sup>a</sup>	28.51±1.78 <sup>b</sup>	34.14±2.67 <sup>b</sup>	32.52±3.73 <sup>b</sup>
14d	15.26±2.12 <sup>a</sup>	23.16±1.95 <sup>b</sup>	27.91±2.45 <sup>b</sup>	34.47±3.02 <sup>c</sup>
21d	16.49±1.45 <sup>a</sup>	33.26±2.13 <sup>b</sup>	22.28±2.65 <sup>c</sup>	27.62±2.17 <sup>d</sup>
28d	46.02±1.84 <sup>a</sup>	35.27±2.79 <sup>b</sup>	22.41±1.04 <sup>c</sup>	16.37±1.68 <sup>d</sup>
35d	35.11±2.97 <sup>a</sup>	43.41±1.55 <sup>b</sup>	20.43±2.72 <sup>c</sup>	18.42±1.67 <sup>c</sup>
45d	9.24±1.81 <sup>a</sup>	14.12±1.38 <sup>a</sup>	30.09±2.69 <sup>b</sup>	29.84±3.34 <sup>b</sup>

**Table S3.** Statistical analysis of the relative utilization ratios of polymers by the bacteria communities in different sediment samples collected at the same times

Sampling time	C	T10	T20	T30
0d	26.84±1.75 <sup>a</sup>	26.84±1.75 <sup>a</sup>	26.84±1.75 <sup>a</sup>	26.84±1.75 <sup>a</sup>
3d	35.54±0.98 <sup>a</sup>	48.87±3.61 <sup>b</sup>	33.01±1.07 <sup>a</sup>	22.40±2.57 <sup>c</sup>
7d	52.53±4.52 <sup>a</sup>	39.71±1.63 <sup>b</sup>	14.75±1.62 <sup>c</sup>	21.79±2.96 <sup>d</sup>
14d	49.25±3.21 <sup>a</sup>	35.11±1.43 <sup>b</sup>	43.01±2.98 <sup>c</sup>	21.53±2.14 <sup>d</sup>
21d	39.24±3.26 <sup>a</sup>	30.29±1.94 <sup>b</sup>	30.12±1.43 <sup>b</sup>	24.19±1.84 <sup>c</sup>
28d	24.43±1.21 <sup>a</sup>	31.47±1.87 <sup>b</sup>	31.69±3.42 <sup>b</sup>	24.89±2.55 <sup>a</sup>
35d	28.72±3.74 <sup>a</sup>	38.79±1.57 <sup>b</sup>	38.23±3.33 <sup>b</sup>	44.93±0.73 <sup>c</sup>
45d	56.62±3.12 <sup>a</sup>	47.96±1.66 <sup>b</sup>	26.74±2.58 <sup>c</sup>	27.14±1.40 <sup>c</sup>

**Table S4.** Statistical analysis of the relative utilization ratios of amino acids by the bacteria communities in different sediment samples collected at the same times

Sampling time	C	T10	T20	T30
0d	37.81±2.45 <sup>a</sup>	37.81±2.45 <sup>a</sup>	37.81±2.45 <sup>a</sup>	37.81±2.45 <sup>a</sup>
3d	35.66±2.95 <sup>a</sup>	29.04±2.96 <sup>b</sup>	20.47±2.46 <sup>c</sup>	13.56±1.06 <sup>d</sup>
7d	14.00±2.71 <sup>a</sup>	18.62±1.98 <sup>a</sup>	25.97±3.06 <sup>b</sup>	36.17±3.04 <sup>c</sup>
14d	17.42±1.96 <sup>a</sup>	27.46±2.51 <sup>b</sup>	12.56±2.16 <sup>a</sup>	25.88±2.28 <sup>b</sup>
21d	15.64±2.19 <sup>a</sup>	24.19±1.89 <sup>b</sup>	19.65±1.02 <sup>c</sup>	23.93±1.27 <sup>b</sup>
28d	1.36±0.23 <sup>a</sup>	19.45±1.93 <sup>b</sup>	26.39±1.79 <sup>c</sup>	29.56±1.14 <sup>c</sup>
35d	17.44±2.90 <sup>a</sup>	13.08±1.75 <sup>b</sup>	22.02±1.55 <sup>c</sup>	21.40±1.55 <sup>c</sup>
45d	3.95±0.39 <sup>a</sup>	24.00±2.06 <sup>b</sup>	21.44±1.79 <sup>b</sup>	24.55±2.27 <sup>b</sup>

**Table S5.** Statistical analysis of the relative utilization ratios of amines by the bacteria communities in different sediment samples collected at the same times

Sampling time	C	T10	T20	T30
0d	9.50±0.59 <sup>a</sup>	9.50±0.59 <sup>a</sup>	9.50±0.59 <sup>a</sup>	9.50±0.59 <sup>a</sup>
3d	6.33±0.88 <sup>a</sup>	0.19±0.00 <sup>b</sup>	4.32±1.64 <sup>a</sup>	13.90±1.48 <sup>c</sup>
7d	13.46±1.06 <sup>a</sup>	4.02±0.57 <sup>b</sup>	11.24±1.74 <sup>a</sup>	3.14±0.67 <sup>b</sup>
14d	12.17±1.22 <sup>a</sup>	3.56±0.45 <sup>b</sup>	14.22±2.79 <sup>a</sup>	7.51±1.26 <sup>c</sup>
21d	19.13±1.34 <sup>a</sup>	4.15±0.64 <sup>b</sup>	9.41±1.23 <sup>c</sup>	21.86±1.95 <sup>a</sup>
28d	14.63±1.27 <sup>a</sup>	4.55±0.83 <sup>b</sup>	9.23±1.66 <sup>c</sup>	6.89±1.54 <sup>bc</sup>
35d	14.80±2.48 <sup>a</sup>	0.44±0.04 <sup>b</sup>	11.94±0.35 <sup>a</sup>	4.84±1.72 <sup>c</sup>
45d	19.59±3.25 <sup>a</sup>	5.79±1.78 <sup>b</sup>	8.52±1.41 <sup>b</sup>	5.68±0.49 <sup>b</sup>

**Table S6.** Statistical analysis of the relative utilization ratios of carboxylic acids by the bacteria communities in different sediment samples collected at the same times

Sampling time	C	T10	T20	T30
0d	0.90±0.10 <sup>a</sup>	0.90±0.10 <sup>a</sup>	0.90±0.10 <sup>a</sup>	0.90±0.10 <sup>a</sup>
3d	4.82±0.47 <sup>a</sup>	1.54±0.68 <sup>b</sup>	1.25±0.09 <sup>b</sup>	0.86±0.20 <sup>b</sup>
7d	1.98±0.58 <sup>a</sup>	3.58±0.84 <sup>b</sup>	1.40±0.53 <sup>a</sup>	6.28±1.02 <sup>c</sup>
14d	2.46±0.49 <sup>a</sup>	3.22±0.74 <sup>a</sup>	0.43±0.01 <sup>b</sup>	1.79±0.81 <sup>a</sup>
21d	3.24±0.58 <sup>a</sup>	2.59±0.67 <sup>ab</sup>	1.29±0.26 <sup>b</sup>	1.99±0.78 <sup>ab</sup>
28d	3.14±0.93 <sup>a</sup>	3.96±0.49 <sup>a</sup>	2.00±0.63 <sup>a</sup>	7.99±1.66 <sup>b</sup>
35d	2.86±0.61 <sup>a</sup>	3.44±0.65 <sup>a</sup>	3.29±0.69 <sup>a</sup>	2.96±0.21 <sup>a</sup>
45d	9.01±1.99 <sup>a</sup>	6.99±1.45 <sup>a</sup>	1.66±0.42 <sup>b</sup>	8.24±1.58 <sup>a</sup>

**Table S7.** Statistical analysis of the relative utilization ratios of miscellaneous by the bacteria communities in different sediment samples collected at the same times

Sampling time	C	T10	T20	T30
0d	3.50±0.39 <sup>a</sup>	3.50±0.39 <sup>a</sup>	3.50±0.39 <sup>a</sup>	3.50±0.39 <sup>a</sup>
3d	5.19±0.86 <sup>a</sup>	3.45±0.22 <sup>b</sup>	9.71±1.25 <sup>c</sup>	0.50±0.02 <sup>d</sup>
7d	3.34±0.22 <sup>a</sup>	5.52±2.84 <sup>a</sup>	12.49±1.39 <sup>b</sup>	0.10±0.01 <sup>c</sup>
14d	3.44±0.59 <sup>a</sup>	7.44±1.12 <sup>b</sup>	1.86±0.31 <sup>c</sup>	8.82±0.79 <sup>b</sup>
21d	6.26±1.11 <sup>a</sup>	5.29±0.59 <sup>a</sup>	17.24±1.62 <sup>b</sup>	0.39±0.09 <sup>c</sup>
28d	10.41±1.61 <sup>a</sup>	5.30±0.43 <sup>b</sup>	8.28±0.80 <sup>a</sup>	14.38±1.37 <sup>c</sup>
35d	1.05±0.17 <sup>a</sup>	0.81±0.15 <sup>a</sup>	4.08±0.59 <sup>b</sup>	7.44±1.65 <sup>c</sup>
45d	1.58±0.24 <sup>a</sup>	1.11±0.19 <sup>a</sup>	11.54±2.52 <sup>b</sup>	4.54±0.41 <sup>c</sup>

**Table S8.** Statistical analysis of the Shannon indexes of carbon source utilizations of bacteria in different sediment samples collected at the same times

Sampling time	C	T10	T20	T30
0d	1.960±0.230 <sup>a</sup>	1.960±0.230 <sup>a</sup>	1.960±0.230 <sup>a</sup>	1.960±0.230 <sup>a</sup>
3d	1.979±0.319 <sup>a</sup>	1.928±0.229 <sup>a</sup>	1.926±0.315 <sup>a</sup>	2.315±0.175 <sup>a</sup>
7d	1.786±0.229 <sup>c</sup>	2.165±0.092 <sup>ab</sup>	2.399±0.255 <sup>a</sup>	1.910±0.090 <sup>bc</sup>
14d	1.742±0.126 <sup>b</sup>	2.102±0.112 <sup>a</sup>	1.927±0.208 <sup>ab</sup>	1.647±0.154 <sup>b</sup>
21d	1.695±0.145 <sup>b</sup>	1.968±0.136 <sup>a</sup>	1.769±0.180 <sup>ab</sup>	1.427±0.043 <sup>c</sup>
28d	1.676±0.043 <sup>b</sup>	1.924±0.147 <sup>b</sup>	2.384±0.264 <sup>a</sup>	2.434±0.090 <sup>a</sup>
35d	1.513±0.197 <sup>b</sup>	1.781±0.142 <sup>b</sup>	2.296±0.124 <sup>a</sup>	2.168±0.197 <sup>a</sup>
45d	1.485±0.116 <sup>c</sup>	2.128±0.201 <sup>b</sup>	2.599±0.174 <sup>a</sup>	2.556±0.174 <sup>a</sup>

**Table S9.** Statistical analysis of the Simpson indexes of carbon source utilizations of bacteria in different sediment samples collected at the same times

Sampling time	C	T10	T20	T30
0d	0.832±0.048 <sup>a</sup>	0.832±0.048 <sup>a</sup>	0.832±0.048 <sup>a</sup>	0.832±0.048 <sup>a</sup>
3d	0.819±0.053 <sup>a</sup>	0.820±0.033 <sup>a</sup>	0.826±0.048 <sup>a</sup>	0.883±0.029 <sup>a</sup>
7d	0.778±0.074 <sup>b</sup>	0.869±0.013 <sup>a</sup>	0.899±0.023 <sup>a</sup>	0.830±0.016 <sup>ab</sup>
14d	0.764±0.033 <sup>ab</sup>	0.845±0.025 <sup>a</sup>	0.835±0.032 <sup>a</sup>	0.748±0.071 <sup>b</sup>
21d	0.749±0.042 <sup>ab</sup>	0.812±0.014 <sup>a</sup>	0.791±0.038 <sup>a</sup>	0.691±0.031 <sup>b</sup>
28d	0.737±0.029 <sup>b</sup>	0.756±0.026 <sup>b</sup>	0.889±0.025 <sup>a</sup>	0.889±0.006 <sup>a</sup>
35d	0.689±0.085 <sup>c</sup>	0.762±0.021 <sup>bc</sup>	0.876±0.013 <sup>a</sup>	0.848±0.061 <sup>ab</sup>
45d	0.614±0.077 <sup>c</sup>	0.827±0.011 <sup>b</sup>	0.916±0.015 <sup>a</sup>	0.919±0.015 <sup>a</sup>

**Table S10.** Statistical analysis of the Pielou evenness indexes of carbon source utilizations of bacteria in different sediment samples collected at the same times

Sampling time	C	T10	T20	T30
0d	0.764±0.044 <sup>a</sup>	0.764±0.044 <sup>a</sup>	0.764±0.044 <sup>a</sup>	0.764±0.044 <sup>a</sup>
3d	0.867±0.049 <sup>b</sup>	0.776±0.032 <sup>c</sup>	0.803±0.031 <sup>c</sup>	0.932±0.011 <sup>a</sup>
7d	0.813±0.066 <sup>a</sup>	0.820±0.035 <sup>a</sup>	0.830±0.038 <sup>a</sup>	0.744±0.035 <sup>a</sup>
14d	0.849±0.058 <sup>a</sup>	0.796±0.047 <sup>ab</sup>	0.804±0.036 <sup>ab</sup>	0.749±0.027 <sup>b</sup>
21d	0.798±0.041 <sup>a</sup>	0.821±0.038 <sup>a</sup>	0.805±0.032 <sup>a</sup>	0.733±0.022 <sup>b</sup>
28d	0.861±0.022 <sup>a</sup>	0.814±0.046 <sup>a</sup>	0.860±0.025 <sup>a</sup>	0.826±0.031 <sup>a</sup>
35d	0.727±0.035 <sup>b</sup>	0.856±0.028 <sup>a</sup>	0.870±0.047 <sup>a</sup>	0.873±0.019 <sup>a</sup>
45d	0.866±0.065 <sup>a</sup>	0.829±0.048 <sup>a</sup>	0.899±0.010 <sup>a</sup>	0.902±0.029 <sup>a</sup>

## CARBON STORAGE IN AN INTACT REPUBLIC OF CONGO'S FOREST

EKOUNGOULOU, R.<sup>1,2\*</sup> – MIKOUENDANANDI, M. R. B. E.<sup>3</sup> – LIU, X. D.<sup>2</sup>

<sup>1</sup>*Ecole Nationale Supérieure d'Agronomie et de Foresterie, Université Marien Ngouabi, BP 69  
Brazzaville, Congo*

<sup>2</sup>*Beijing Key Laboratory of Forest Resources and Ecosystem Process, College of Forestry,  
Beijing Forestry University, 100083 Beijing, China*

<sup>3</sup>*Department of Forest Economics and Management, School of Economics and Management,  
Beijing Forestry University, 100083 Beijing, China*

*\*Corresponding author*

*e-mail: romeoekous@gmail.com; phone: +242-064-640-101*

(Received 20<sup>th</sup> Jun 2020; accepted 6<sup>th</sup> Oct 2020)

**Abstract.** Tropical forests are considered major carbon sinks and can help to militate with effectiveness against climate change. The study aimed to assess above-and below-ground biomass and tree carbon storage in Ngoyili tropical forest, and its involvement in sustainable management. The study site is located at Ngoyili forest, in Lesio-louna protected area, in south-eastern Republic of Congo. Trees inventory were performed with circular plots, each 1256 m<sup>2</sup>, i.e. 40 m of plot diameter. In five studied plots, trees with DBH  $\geq$  10 cm at 1.3 m above the ground have been measured and identified. The analyses were conducted using allometric models method. 115 trees recorded were divided into 32 species and 15 families. The results showed that in Ngoyili, the mean storage biomass has been built up for aboveground biomass (273.1 t.ha<sup>-1</sup>), as well as for belowground biomass (64.1 t.ha<sup>-1</sup>), with a significant difference between forest plots ( $P < 0.001$ ). It was obvious that aboveground biomass in plot 3 (363.8 t. ha<sup>-1</sup>) was higher than those of plot 1, plot 2, plot 4 and plot 5. Ngoyili forest faces an uncertain future under climate change but can continue to store large amounts of carbon in a warmer world, if countries limit greenhouse gas emissions.

**Keywords:** *aboveground biomass, allometric models, belowground biomass, ecosystem, Ngoyili*

### Introduction

In recent years, the estimation of forest carbon stocks has gained prominence due to the role of forests in the mitigation of global climate change through carbon storage in biomass (Lewis et al., 2013; Goussanou et al., 2016; Mensah et al., 2017). In line with this, successful implementation of climate change mitigation policies requires accurate estimation and mapping of terrestrial biomass carbon stock. But, the accuracy of estimation depends on the availability of reliable allometric equations as there is a high degree of uncertainty with commonly used pantropic allometric equations (Chave et al., 2014; Ekoungoulou et al., 2014c; Fayolle et al., 2016).

Protecting intact forests is essential to ensuring carbon storage and many other ecosystem services (Pan et al., 2011; Ekoungoulou et al., 2014a). Thus, conserving existing intact forests in combination with restoring and managing sustainably degraded forests is almost certain to be a key action to help meet the Paris accord targets. The idea of financially incentivizing local and national initiatives to spare forest land and favor reforestation has thus received further attention, as evidenced by the united nations' reducing emissions from deforestation, forest degradation, and forest conservation,



sustainable management of forest, and enhancement of forest carbon stocks (REDD+) program (Chave et al., 2019).

Protected areas in Central Africa are generally managed for biodiversity and recreation with consideration given to the preservation of other services like water or carbon storage (Ekoungoulou et al., 2014b). Their mandate for biodiversity conservation is unquestioned, although not always implemented in a very efficient way and of the 314 protected areas recorded in Central Africa, only 10 sites benefit from a management plan formally approved by the authorities and several important sites (i.e., Garamba and Virunga national parks) are under extreme pressures by armed factions and/or afflux of people displaced by war (Nasi et al., 2012).

There is high degree of uncertainty with commonly used pantropical equation (Ekoungoulou et al., 2018b) to estimate forest biomass carbon stocks (Chave et al., 2014) because, the predictive power of these equations differs among sites; for some regions, the relative error could be low, while for others, it could be high (Chave et al., 2005). For example, in Colombia forest, the type II models of Chave et al. (2005) over estimate aboveground biomass by  $54.7 \pm 135.7\%$  (Alvarez et al., 2012) whereas in Cameroon forest Chave et al. (2005), estimates total aboveground biomass across different sites with an average error of 20.3% (Djomo et al., 2010). The study of Litton (2008) also showed that the existing generalized allometry underestimate biomass across all size by a mean of 43% compared to site and species-specific models.

Due to absence of species-specific or mixed-species allometric equations, Africa's forest biomass and carbon stocks has been widely estimated by using pantropical equations (Djomo et al., 2010; Henry et al., 2011; Ekoungoulou, 2014; Ploton et al., 2016). However, tree allometry depends on environmental and genetic factors that vary from region to region (Feldpausch et al., 2012; Vieilledent et al., 2012). Consequently, these equations are unlikely to yield accurate tree biomass estimates at other sites (Vieilledent et al., 2012; Chave et al., 2014). A large number of regression equations have been already published, and the selecting of a limited subset of these, is specifically based on their mathematical simplicity and their applied relevance (Chave et al., 2014; Ekoungoulou, 2018; Sullivan et al., 2020). Typical estimation of aboveground biomass (AGB) in lowland rainforest values vary between 150-700 Mg.ha<sup>-1</sup> using the calculation based on the model developed by Chave et al. (2014) which is now a standard model (*Eqs. 1 and 2*) for tropical forests (Ekoungoulou et al., 2018b; Sullivan et al., 2020). According to the report of recent studies (Henry et al., 2011; Chave et al., 2014; Ngomanda et al., 2014; Fayolle et al., 2016), in Republic of Congo none referential allometric equation existed for the forests of the country. This shows how researchers have been given little attention on the efforts to improve forest biomass and carbon estimation.

This research focused on above-and below-ground biomass assessment, and their carbon stock. The aim of this study was to estimate the trees biomass (aboveground biomass + belowground biomass) and carbon stock in Ngoyili forest ecosystem (Southern Republic of Congo). The results of this study will be useful by the Republic of Congo's Forest Economics Ministry.

## Materials and Methods

### Study area

The study site is located in South-eastern Republic of Congo (S3°15.95'; E15°27.15'), in the Pool Administrative Department, close to Lefini wildlife reserve and Kinkala city,

around 160 km northern of Brazzaville, in Republic of Congo (*Fig. 1*). Ngoyili forest ecosystem (study area) is a part of Lesio-louna protected area located in Teke plateau (*Fig. 1*), close to Imvouba village, and managed by the Lesio-louna project (PLL). However, Teke plateau is a vast area of wooded and non-wooded grasslands interspersed with galleries forests and small dry forest patches, extending from south-east Republic of Gabon through central Republic of Congo and southern Democratic Republic of Congo to northern Republic of Angola. The Lesio-louna reserve lies within central plateau region of Congo. Including the adjacent southern portion of the Lefini wildlife reserve, it reaches an area of approximately 1,748 km<sup>2</sup>.

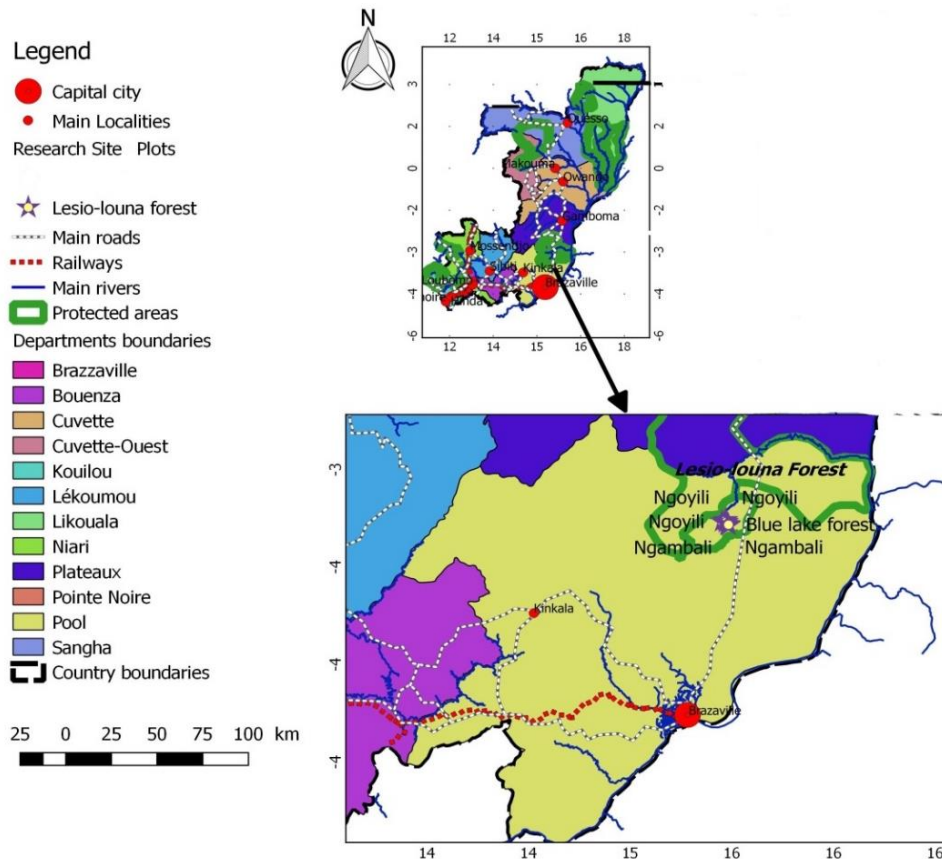


**Figure 1.** Study area location

## Climate

Climate of Lesio-louna Sanctuary is clearly the same as Teke plateau, Guineo equatorial type, as sub-humid climate Bas Congo. The dry season lasts 3-4 months (June, July, August, September), the short dry season (January-February) is relatively little marked by a slowdown of the rains. The highest annual rainfall recorded in March-April and October-November (ANAC, 2013; Ekoungoulou, 2014). The average temperature is comprised between 20 to 27 °C and atmospheric moisture is still very high (*Fig. 2*). From a global view, the Lesio-louna and Teke plateau are subject to the influence of two types of climates as mentioned by ANAC (2013): In northern of Teke plateau (Lesio-louna), there are a climate of sub-equatorial characterized by above 1600 mm.an<sup>-1</sup> rainfall, dry season from 1 to 3 months, an average annual temperature of 22 °C with seasonal

amplitudes of 35 °C; In southern of Teke plateau (Lesio-louna) it's a climate of low Congolese type, characterized by below 1600 mm.an<sup>-1</sup> rainfall, dry season of 4-5 months an average annual temperature about 25 °C, with seasonal amplitudes (4 to 6 °C) (Fig. 2). The climate of Lesio-louna is a tropical equatorial climate which is characterized by the absence of large dry seasons and low temperature differences (ANAC, 2013). Every month, there shall be at least 50 mm of water. There are two rainy seasons (March-May and September- December) and two dry seasons (June- August and January -February).

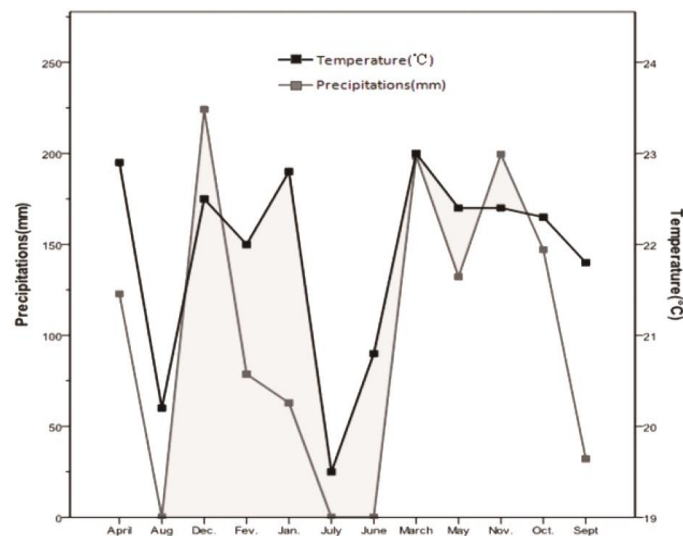


**Figure 2.** Climograph of the main meteorological station around the study area (mean from 1970 - 2012)

### Data collection

Fieldwork was based on technology using circular plots, each 1256 m<sup>2</sup> i.e. 40 m of diameter. The study had retained 5 circular plots, each separated by roughly 200 m. All data were collected during the period from October to December 2012. A total of 5 inventoried plots were centered in the site called by Ngoyili gallery forest. Also Ngoyili is an evergreen lowland tropical moist forest. Dendrometry have been performed on plots with a slope < 5° (almost flat). Measurements have been performed solely on the trees with DBH ≥ 10 cm at 1.3 m heights (Ekoungoulou et al., 2018a), and only these were marked and identified with a nail and polyvinyl chloride plastic label. Thus, equipment such as compass, forestry tape meter, double decameter, GPS has been used during data collection period (Ekoungoulou et al., 2018c). From the circular plot center to the first circle (small circle), the radius was 0-6 m i.e. 12 m of diameter and tree inventory 10-29.9 cm DBH (only trees with DBH ≥ 10 cm were measured). From the plot center to the second circle (medium circle), the radius was 0-14 m i.e. 28 m of diameter, with tree inventory 30-60 cm DBH. From plot center to the third circle (large circle), the radius was 0-20 m i.e. 40 m of diameter with tree inventory > 60 cm DBH. Data collected from each plot was then recorded (Ekoungoulou et al., 2017). Field measurements have been conducted according to AfriTRON ([www.afritron.org](http://www.afritron.org)) and forest plots ([www.forestplots.net](http://www.forestplots.net)) protocols.

## Data analysis

### Above-and below-ground biomass

Once measurement field is finished (Ekoungoulou and Mikouendanandi, 2020), the data has been digitized in spreadsheets according to standard procedures outlined in the data organization section (Lopez-Gonzalez et al., 2011). The general checklist of species composing the flora procession has been established (Ekoungoulou et al., 2018a) after digital processing of five sample plots, on the basis of The African plants database (v.3.4.0) of Conservatory and Botanical Garden of Geneva, Switzerland and South African National Biodiversity Institute, Pretoria (Accessed 17 September 2019 at <http://www.ville-ge.ch/musinfo/bd/cjb/africa/recherche.php>), and The Xycol database (The list of scientific and vernacular woods names: accessed 17 September 2019 at [http://www.xycol.net/index.php?categorie=0&sess\\_langue=430](http://www.xycol.net/index.php?categorie=0&sess_langue=430)).

Aboveground biomass (ABG) was quantified using generic allometric equations. The allometric equation proposed by Chave et al. (2014) was used for estimation of aboveground biomass (Eqs. 1 and 2). The mathematical expression of the mentioned allometric model (model 7) is as follows:

$$AGB_{est} = \exp [-1.803 - 0.976E + 0.976 \ln(\rho) + 2.673(D) - 0.0299[\ln(D)]^2] \quad (\text{Eq.1})$$

where  $E$  is defined as:

$$E = (0.178 \times TS - 0.938 \times CWD - 6.61 \times PS) \times 10^{-3} \quad (\text{Eq.2})$$

$E$  is a measure of environmental stress;  $TS$  is the temperature seasonality;  $\ln$  is the natural logarithm;  $D$  is diameter at breast height (in cm);  $AGB_{est}$  is the estimate aboveground biomass (in kg), and  $\rho$  (in  $\text{g.cm}^{-3}$ ) is the wood specific gravity (Zanne et al., 2009; Carsan et al., 2012). Indeed,  $E$  increases with temperature seasonality, which relates to the amount of time a plant is exposed to stressful temperature, and a negative quantity  $CWD$  (climatic water deficit) increases in magnitude with increasing annualized water stress. The dependence of  $E$  on  $PS$  (precipitation seasonality) is less obvious but appears to be mostly driven by monsoon dominated rainfall regime (Chave et al., 2014). Wood density ( $\rho$ ) was extracted from global wood density (Zanne et al., 2009) database (<http://datadryad.org/handle/10255/dryad.235>: Accessed August 20, 2019). Some wood densities have been provided by African Wood Density Database (Accessed August 20, 2019 at <http://apps.worldagroforestry.org/treesandmarkets/wood/>) according to Carsan et al. (2012).

However, belowground biomass (BGB) quantification has been made using allometric model (Eqs. 3 and 4) proposed by Mokany et al. (2006). The mathematical expression for this allometric model is as follows:

$$Y = 0.205 \times AGB \text{ if } AGB \leq 125 \text{ kg} \quad (\text{Eq.3})$$

$$Y = 0.235 \times AGB \text{ if } AGB > 125 \text{ kg} \quad (\text{Eq.4})$$

where  $Y$  is belowground biomass (BGB, in Kg), and  $AGB$  is aboveground biomass (in kg). The values of the plots per hectare were extrapolated using an expansion factor which

indicates the area represented by each plot, and then to finally obtain biomass (AGB and BGB) and carbon stock in  $t.ha^{-1}$ . This standardization was necessary in order to be able to easily interpret the results and also make comparisons with other studies. Expansion factor is 10,000 (in  $m^2$ ) divided by plot area (in  $m^2$ ). Biomass and carbon stock have been converted in  $t.ha^{-1}$  after calculation from Kg. Moreover, the estimation of carbon stock has been calculated by dividing biomass by two for each plot. Carbon stock is typically derived from live biomass by assuming 50% of the biomass is made up carbon (Brown, 1997; Cairns et al., 1997; Basuki et al., 2009; Ekoungoulou et al., 2018b).

### Statistical analyses

Statistical analyses were performed using the softwares called by statistical program from social sciences (SPSS) version 18.0 and SigmaPlot version 10.0. Study area's location map has been performed using the ArcGIS v.9.3 software. Data were analyzed using one-way ANOVA (Ekoungoulou and Mikouendanandi, 2020). Separations were performed by Duncan's multiple range tests. Differences at  $P < 0.05$  were considered to be significant. The means and sample variance were equal in all five studied plots during the research period according to analysis performed with statistical program from social sciences.

## Results and Discussion

The investigation revealed a total number of 115 trees with  $DBH \geq 10$  cm in the study area have been recorded. These grouped trees were belonged to 15 botanical families and 32 species. A total of 115 trees were divided into 5 plots (Table 1). Floristic richness shows the total number of species, present in Ngoyili forest. The most represented species in study site with height relative diversity index were *Eriocoelum macrocarpum* Gilg ex Radlk ( $n = 21$ , recorded in all 5 studied plots), followed by *Xylopiya rubescens* Oliv. var. *rubescens* ( $n = 10$ , present in plot 1, plot 4 and plot 5). In this Ngoyili riparian forest, the most number of trees were recorded in plot 3 ( $n = 30$ ), followed by plot 1 ( $n = 24$ ), plot 4 ( $n = 24$ ), plot 2 ( $n = 20$ ), and plot 5 ( $n = 17$ ). It was obvious that aboveground biomass (AGB) in plot 3 ( $363.8 t.ha^{-1}$ ) were higher than those of plot 1, plot 2, plot 4 and plot 5 (Fig. 3 and Table 1). The higher belowground biomass (BGB) has been recorded in plot 3 with  $85.5 t.h^{-1}$  (Fig. 3). However, Fig. 4b shows that the mean diameter at breast height (DBH) recorded in plot 1 was higher than those of others studied plots; but the mean AGB and BGB of plot 1 was less than those of plot 3 and plot 4.

**Table 1.** Distribution of tree biomass in Ngoyili tropical gallery forest and description of the study site

Plot	<i>n</i>	AGB	BGB	DBH	Area State
Plot1	24	273.9	64.3	31.7	Swampy
Plot2	20	236.6	55.6	25.9	Swampy
Plot3	30	363.8	85.5	29.8	Swampy
Plot4	24	293.6	69	26.9	Swampy
Plot5	17	197.5	46.4	28.2	AUE

DBH: average diameter at breast height of trees (in cm), AGB: Aboveground biomass ( $t.ha^{-1}$ ), BGB: Belowground biomass ( $t.ha^{-1}$ ), AUE: An undisturbed ecosystem with a terra firme area, n: number of trees

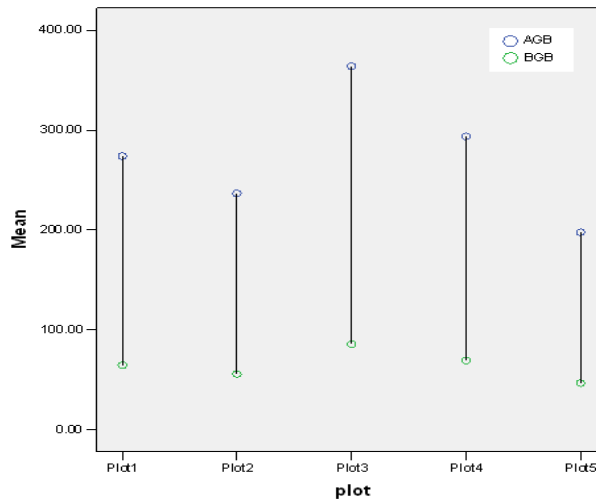


**Figure 3.** Relationship between mean aboveground biomass (AGB, in  $t.ha^{-1}$ ) and mean belowground biomass (BGB, in  $t.ha^{-1}$ ) by plot in Ngoyili forest using allometric models with the point style graph

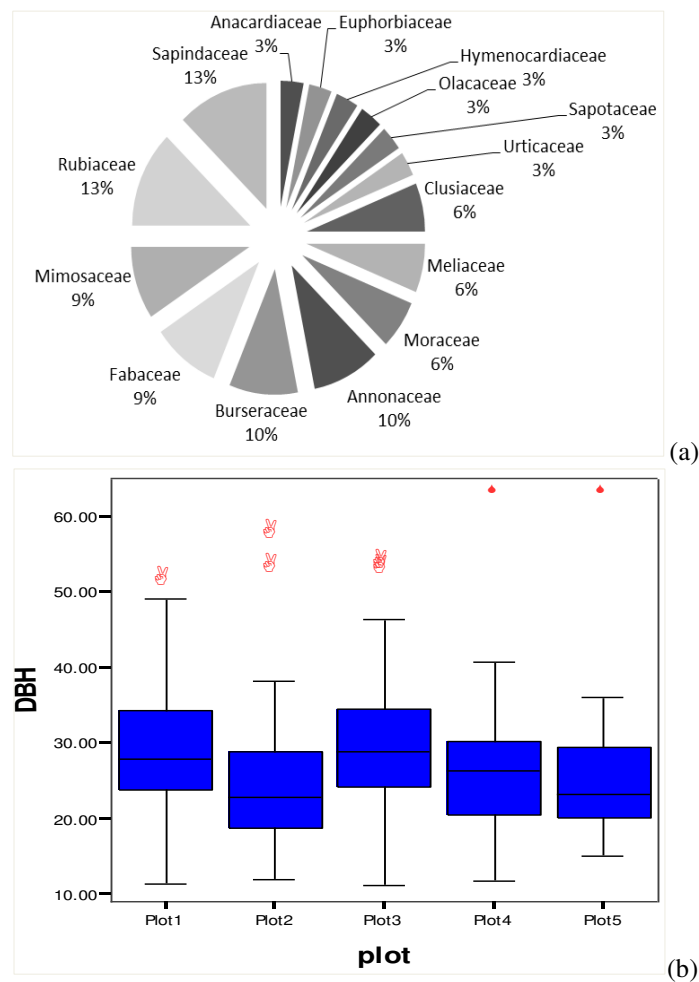


**Figure 4.** Phytodiversity overview including trees diameters distribution of Ngoyili forest ecosystem. (a) Relative frequency of specific spectra families recorded in study area. (b) Mean trunk diameters distribution of trees by plot in study site (in cm)

*Table 1* shows that plot 1 (273.9 t.ha<sup>-1</sup>) has a lower AGB than plot 3 (363.8 t.ha<sup>-1</sup>), while the DBH of plot 1 (31.7 cm) is higher than plot 3 (29.8 cm). BGB of plot 1 (64.3 t.ha<sup>-1</sup>) is low compared to plot 3 (85.5 t.ha<sup>-1</sup>), while the DBH of plot 3 (29.8 cm) is lower than that of plot 1 (31.7 cm). Since the area state is the same, both for plot 1 and plot 3, so this difference in biomass could be due to the nature and composition of plots' soil. The results showed that in Ngoyili mixed evergreen forest ecosystem, the mean biomass has been built up for AGB (273.1 t.ha<sup>-1</sup>) as well as for BGB (64.1 t.ha<sup>-1</sup>), with a significant difference between forest plots ( $P < 0.001$ ). One-way ANOVA applied on five plots data of Ngoyili statistically revealed significant difference regarding the test for equal means ( $P < 0.001$ , confidence interval at 95%). Levene's test for homogeneity of variance for means shows a significant difference ( $P = 0.012$ ).

Also, *Table 2* shows that the trees in plot 3 are neither from Fabaceae, nor from Mimosaceae. Leguminosea plants have the ability to capture nitrogen from the atmosphere. Fabaceae and Mimosaceae are taxonomically the Leguminosea, and have the capacity to enrich the soil with atmospheric nitrogen through the symbiotic phenomenon between the rhizobium bacteria and the nodules of the roots from Leguminosea plants (PROTA, 2008). In this ecosystem, the most represented botanical families are those of Sapindaceae (4 tree species), followed by Rubiaceae (4 tree species), then Mimosaceae (3 tree species), Burseraceae (3 tree species), Annonaceae (3 tree species) and Fabaceae with 3 tree species (*Fig. 4a*). In Sapotaceae (3%), Euphorbiaceae (3%), Hymenocardiaceae (3%) a very low proportion of relative frequency of botanical families were founded (*Fig. 4a*). Contrariwise, the weakliest represented botanical families each have one species. These are the following families: Urticaceae, Sapotaceae, Olacaceae, Hymenocardiaceae, Euphorbiaceae and Anacardiaceae (*Fig. 4a*).

Relatively few studies to date have quantified the measurement error or model uncertainty associated with the estimates of forest biomass. In one of the comprehensive studies, Chave et al. (2004) assessed the effects of measurement error (stem diameter), model uncertainty associated with height-diameter relationships, and sampling uncertainty on estimates of tropical carbon stock in Panama. They reported that the uncertainty (standard deviation) in the aboveground biomass for individual trees averaged 47% of the estimate, with 31% arising from uncertainty in the allometric model and 16% from measurement error. At the stand level, however, the effect of measurement error was reduced to less than 1%, and the total uncertainty reduced to 10% due to allometric uncertainty and 10% due to sampling uncertainty.

About the long-term thermal sensitivity of Earth's tropical forests, Sullivan et al. (2020) indicates a heat threshold of 32 °C in daytime temperature. Above this point tropical forest carbon declines more quickly with higher temperatures, regardless of which species are present. Sullivan et al. (2020) conclude that tropical forests have long-term capacity to adapt to some climate change, in part because of their high biodiversity, as tree species better able to tolerate new climatic conditions grow well and replace less well-adapted species, over the long-term.

In another study, Djomo et al. (2010) propagated uncertainty in carbon stock estimates in tropical forest in Cameroon using the statistical propagation techniques described in Chave et al. (2005), and reported that uncertainty in allometric equations contributed 30% of the total uncertainty in carbon stock estimates. These estimates may have overestimated the uncertainty due to allometric models (Yanai et al., 2010). Another limitation of these studies is that they have focused on tropical forests. Previous studies

have tended to focus on uncertainty in carbon stock estimates (Ekoungoulou et al., 2015), rather than uncertainty in carbon change over time.

**Table 2.** Distribution of species by family recorded in Ngoyili forest

Species	Family	n	$\rho$	DBH	Plot
<i>Allophylus africanus</i> P. Beauv.	Sapindaceae	2	0.450	12.6-13.7	P3
<i>Berlinia bracteosa</i> Benth.	Annonaceae	4	0.603	18.8-34	P3, P5
<i>Colletocema dewevrei</i> (De Wild.) E.M.A. Petit	Rubiaceae	1	0.650	23.3	P2
<i>Colletocema</i> spp.	Rubiaceae	1	0.650	57	P2
<i>Dacryodes buettneri</i> (Engl.) H.J.Lam	Burseraceae	6	0.513	11.4-30.8	P1, P2, P4
<i>Dacryodes letestui</i> (Pellegr.) H. J. Lam	Burseraceae	3	0.548	21.1-25.6	P1, P2
<i>Dacryodes</i> spp.	Burseraceae	1	0.561	23.3	P2
<i>Entandrophragma cylindricum</i> (Sprague) Sprague	Meliaceae	2	0.572	25.6-38.4	P3
<i>Entandrophragma utile</i> (Dawe & Sprague) Sprague	Meliaceae	1	0.537	24.5	P3
<i>Eriocoelum macrocarpum</i> Gilg ex Radlk.	Sapindaceae	21	0.523	15.8-53.1	P1, P2, P3, P4, P5
<i>Eriocoelum</i> spp.	Sapindaceae	3	0.523	22.8-31.9	P3, P4
<i>Ficus deltoidea</i> Jack	Moraceae	2	0.650	29-38.3	P3
<i>Ficus</i> spp.	Moraceae	1	0.410	29-33.4	P3
<i>Hymenocardia ulmoides</i> Oliv.	Hymenocardiaceae	3	0.702	22.9-33.8	P5
<i>Millettia laurentii</i> De Wild.	Fabaceae	3	0.761	11.9-52.5	P2
<i>Millettia pinnata</i> L.	Fabaceae	2	0.650	21.2-33.8	P4
<i>Mitragyna</i> spp.	Rubiaceae	2	0.528	34.6-46.3	P3
<i>Mitragyna stipulosa</i> (DC.) Kuntze	Rubiaceae	9	0.575	11.2-63	P1, P3, P4, P5
<i>Musanga cecropioides</i> R. Br.	Urticaceae	2	0.243	20.1-32.4	P5
<i>Omphalocarpum elatum</i> Miers	Sapotaceae	1	0.550	29.8	P2
<i>Ongokea gore</i> (Hua) Pierre	Olaceae	3	0.749	11.4-40.7	P1
<i>Pancovia laurentii</i> (De Wild.) Gilg ex De Wild.	Sapindaceae	1	0.650	15.6	P2
<i>Pentaclethra eetveldeana</i> De Wild. & T. Durand	Mimosaceae	8	0.663	16.4-33.2	P2, P5
<i>Pentaclethra macrophylla</i> Benth.	Fabaceae	1	0.841	50.9	P1
<i>Piptadeniastrum africanum</i> (Hook. f.) Brenan	Mimosaceae	7	0.605	18-40.8	P1, P4, P5
<i>Piptadeniastrum</i> spp.	Mimosaceae	1	0.605	15	P5
<i>Sorindeia juglandifolia</i> (A.Rich.) Planch. ex Oliv.	Anacardiaceae	4	0.650	14.3-31.5	P1, P3, P4
<i>Symphonia globulifera</i> L.f.	Clusiaceae	5	0.600	14-31.5	P3, P4
<i>Symphonia</i> spp.	Clusiaceae	1	0.600	35.7	P3
<i>Uapaca heudelotii</i> Baill.	Euphorbiaceae	3	0.614	24.6-52.3	P3
<i>Xylopia aethiopica</i> (Dunal) A. Rich.	Annonaceae	1	0.442	38.3	P2
<i>Xylopia rubescens</i> Oliv. var. <i>rubescens</i>	Annonaceae	10	0.615	11.7-49.1	P1, P4, P5

DBH is ranged diameter at breast height of trees (in cm); n is number of tree;  $\rho$  is mean of wood density (wood specific gravity, in  $\text{g.cm}^{-3}$ ) values retrieved from the global wood density database at <http://datadryad.org/handle/10255/dryad.235>: Accessed August 20, 2019, and African Wood Density Database at <http://apps.worldagroforestry.org/treesandmarkets/wood/>: Accessed August 20, 2019; P is plot which tree species has been founded in each area. Trees taxonomy was homogenized according to the African plants database (version 3.4.0) from Conservatory and Botanical Garden of Geneva, Switzerland and South African National Biodiversity Institute, Pretoria (Accessed 17 September 2019 at <http://www.ville-ge.ch/musinfo/bd/cjb/africa/recherche.php>), and The Xycol database (The list of scientific and vernacular woods names: accessed 17 September 2019 at [http://www.xycol.net/index.php?categorie=0&sess\\_langue=430](http://www.xycol.net/index.php?categorie=0&sess_langue=430))



Regarding field methods for sampling tree height for tropical forest biomass estimation, Sullivan et al. (2018) founded that allometries constructed with just 20 locally measured values could often predict tree height with lower error than regional or climate-based allometries (mean reduction in prediction error is 0.46 m). The prediction performance of locally derived allometries improved with sample size, but with diminishing returns in performance gains when more than forty trees were sampled. Estimate of stand-level biomass produced using local allometries to estimate tree height show no over- or under- estimate bias when compared with biomass estimates using field measurement, and found that sampling strategies that included measuring the heights of the ten largest diameter in a plot outperformed (in terms of resulting in local height-diameter models with low height prediction error) entirely random of diameter size-class stratified approaches.

With regard to our present study, difference in biomass storage could certainly be the type of tree species, nature of tree, composition and nature of plots' soil. There are many Fabaceae trees in this Ngoyili mixed evergreen forest ecosystem, which is characterized by growth and a spectacular development as reported by Ekoungoulou et al. (2014c). Therefore, the roots of Fabaceae's trees have swellings called nodules that contain nitrogen-fixing bacteria (PROTA, 2008; Fayolle et al., 2013; Ekoungoulou, 2014). These key factors mentioned, resulted in heterogeneity of biomass play an important role about carbon storage, carbon gains, and carbon residence time and carbon balance. Environmental variations have also an impact on carbon storage.

However, a possible alternative to use a model integrating tree height into biomass estimation based on diameter measurements in forest inventory would be better for the future studies. Carbon change is arguably the more important of two metrics as it is the basis for United Nations Framework Convention on Climate Change (UNFCCC) reporting, including programmes such as REDD+ which is designed to incentivize management of forests for increased carbon sequestration (Holdaway et al., 2014). Furthermore, the variation of carbon stocks in this protected area could be due to the fact that wet soil of this riparian forest is a peat ecosystem in several places. Peatlands play a key role in storing carbon in the soil, and also supplying trees with nutrients. The present study provided new data appropriate for next carbon cartography as part to monitor forest carbon in Republic of Congo. Based on the uncertainty of these present equations, we suggested that the uncertainty of future models may be probably less important with the carbon equation when calculating carbon stocks with double time periods.

## Conclusion

Tropical forests had a key role in mitigation of greenhouse gases in atmosphere. These forests are considered as major carbon sinks and can help to militate against climate change. The validity of pantropical equations, however, remains to be tested in particular environmental conditions, i.e. swamps or temporarily flooded forest, which may constrain the allometric relationship between height and diameter. Including height parameter in allometric equations which reflects growing conditions could improve their accuracy and applicability. This study allowed us to understand that Ngoyili riparian mixed tropical forest's plot 3 (363.8 t.ha<sup>-1</sup> and 85.5 t.ha<sup>-1</sup> for aboveground biomass and belowground biomass respectively) has recorded a higher carbon stock compared to others plots in the same site of protected area. The results of this work revealed that in Ngoyili forest tree biomass and carbon stock varied by tree species and also by sampled plot. This evergreen

intact tropical forest can participate effectively to mitigate the global climate change by photosynthesis phenomenon. The findings of this study will be used by REDD+ Congo project managed by CN-REDD+, under the supervision of Republic of Congo's Ministry of Forest Economics, and then to help country to receive carbon credit through voluntary carbon market. This study can serve as a support or a milestone for researchers working in the same field, in order to address the influence of climate and soil on the heterogeneity of carbon quantification in each forest and each carbon reservoir.

**Acknowledgements.** The authors would like to thank Chinese government under the China Scholarship Council ([www.csc.edu.cn](http://www.csc.edu.cn)) and Beijing Forestry University ([www.bjfu.edu.cn](http://www.bjfu.edu.cn)) for supporting this work. We greatly acknowledge Superior National School for Agronomy and Forestry (Ecole Nationale Supérieure d'Agronomie et de Foresterie - ENSAF) from Marien Ngouabi University (Université Marien Ngouabi – [www.umng.cg](http://www.umng.cg)) for its contribution. The National Key Research and Development Project of China (2017YFD0600106) also supported this study. Two anonymous referees have provided substantial contribution and the authors address to them their heartfelt thanks.

**Conflicts of Interests.** The authors have declared that no competing interests exist. The founding sponsors had no role in the design of the study; in the collection, analyses, or interpretation of data; in the writing of the manuscript, and in the decision to publish the results.

## REFERENCES

- [1] Alvarez, E., Duque, A., Saldarriaga, J., Cabrera, K., De las Salas, G., Del Valle, I. (2012): Tree above-ground biomass allometries for carbon stocks estimation in the natural forests of Colombia. – *Forest Ecology and Management* 267: 297-308.
- [2] ANAC, National Agency of Congo's Civil Aviation (2013): Annual Report on Congolese Meteorological National Situation. – National Agency of Congo's Civil Aviation, Brazzaville, Congo (in French).
- [3] Basuki, T. M., van Laake, P. E., Skidmore, A. K., Hussin, Y. A. (2009): Allometric equations for estimating the above-ground biomass in tropical lowland Dipterocarp forests. – *Forest Ecology and Management* 257: 1684-1694.
- [4] Brown, S. (1997): Estimating Biomass and Biomass Change of Tropical Forests: A Primer. FAO Forestry Paper 134. – Food and Agriculture Organization of the United Nations, Rome, Italy.
- [5] Cairns, A. M., Brown, S., Helmer, H. E., Baumgardner, A. G. (1997): Root biomass allocation in the world's upland forests. – *Oecologia* 111: 1-11.
- [6] Carsan, S., Orwa, C., Harwood, C., Kindt, R., Stroebel, A., Neufeldt, H., Jamnadass, R. (2012): African Wood Density Database. – World Agroforestry Centre, Nairobi, Kenya, <http://apps.worldagroforestry.org/treesandmarkets/wood/> [Accessed 08.20.2019].
- [7] Chave, J., Condit, R., Aguilar, S., Hernandez, A., Lao, S., Perez, R. (2004): Error propagation and scaling for tropical forest biomass estimates. – *Philosophical Transactions of the Royal Society: Biological Sciences* 359(1443): 409-420.
- [8] Chave, J., Andalo, C., Brown, S., Cairns, M. A., Chambers, J. Q., Eamus, D. (2005): Tree allometry and improved estimation of carbon stocks and balance in tropical forests. – *Oecologia* 145(1): 87-99.
- [9] Chave, J., Rejou-Mechain, M., Burquez, A., Chidumayo, E., Colgan, M. S., Delitti, W. B. C. (2014): Improved allometric models to estimate the aboveground biomass of tropical trees. – *Global Change Biology* 20(10): 3177-3190.
- [10] Chave, J., Davies, J. S., Phillips, L. O., Lewis, L. S., Sist, P., Schepaschenko, D. (2019): Ground Data Are Essential for Biomass Remote Sensing Missions. – *Surveys in Geophysics* 40: 863-880.

- [11] Djomo, N. A., Ibrahima, A., Saborowski, J., Gravenhorst, G. (2010): Allometric equations for biomass estimations in Cameroon and pan moist tropical equations including biomass data from Africa. – *Forest Ecology and Management* 260: 1873-1885.
- [12] Ekoungoulou, R. (2014): Carbon Stocks Evaluation in Tropical Forest, Congo. Carbon Stocks in Forest Ecosystems. – Lambert Academic Publishing, Saarbrucken, Germany.
- [13] Ekoungoulou, R., Liu, X. D., Ifo, S. A., Loumeto, J. J., Folega, F. (2014a): Carbon stock estimation in secondary forest and gallery forest of Congo using allometric equations. – *International Journal of Scientific & Technology Research* 3(3): 465-474.
- [14] Ekoungoulou, R., Liu, X. D., Loumeto, J. J., Ifo, S. A. (2014b): Tree Above-And Below-Ground Biomass Allometries for Carbon Stocks Estimation in Secondary Forest of Congo. – *Journal of Environmental Science, Toxicology and Food Technology* 8(4): 09-20.
- [15] Ekoungoulou, R., Liu, X. D., Loumeto, J. J., Ifo, S. A., Bocko, Y. E., Koula, F. E., Niu, S. (2014c): Tree allometry in tropical forest of Congo for carbon stocks estimation in above-ground biomass. – *Open Journal of Forestry* 4(5): 481-491.
- [16] Ekoungoulou, R., Niu, S. K., Loumeto, J. J., Ifo, S. A., Bocko, Y. E., Liu, X. D. (2015): Evaluating the carbon stock in above-and below-ground biomass in a moist central African forest. – *Applied Ecology and Environmental Sciences* 3(2): 51-59.
- [17] Ekoungoulou, R., Nzala, D., Liu, X. D., Niu, S. K. (2017): Ecological and structural analyses of trees in an evergreen lowland Congo basin forest. – *International Journal of Biology* 10(1): 31-43.
- [18] Ekoungoulou, R. (2018): Managing Tropical Forest Ecosystems. Tropical Trees. – Lambert Academic Publishing, Saarbrucken, Germany.
- [19] Ekoungoulou, R., Folega, F., Mukete, B., Ifo, S. A., Loumeto, J. J., Liu, X. D., Niu, S. K. (2018a): Assessing the effectiveness of Protected Areas on Floristic Diversity in Tropical Forests. – *Applied Ecology and Environmental Research* 16(1): 837-853.
- [20] Ekoungoulou, R., Nzala, D., Liu, X. D., Niu, S. K. (2018b): Tree biomass estimation in central African forests using allometric models. – *Open Journal of Ecology* 8(3): 209-237.
- [21] Ekoungoulou, R., Niu, S. K., Folega, F., Nzala, D., Liu, X. D. (2018c): Carbon stocks of coarse woody debris in central African tropical forests. – *Sustainability in Environment* 3(2): 142-160.
- [22] Ekoungoulou, R., Mikouendanandi, E. B. R. M. (2020): Lettuce (*Lactuca sativa* L.) Production in Republic of Congo Using Hydroponic System. – *Open Access Library Journal* 7(5): e6339.
- [23] Fayolle, A., Doucet, J. L., Gillet, J. F., Bourland, N., Lejeune, P. (2013): Tree allometry in Central Africa: Testing the validity of pantropical multi-species allometric equations for estimating biomass and carbon stocks. – *Forest Ecology and Management* 305: 29-37.
- [24] Fayolle, A., Panzou, G. J. L., Drouet, T., Swaine, M. D., Bauwens, S., Vleminckx, J., Doucet, J. L. (2016): Taller Trees, Denser Stands and Greater Biomass in Semi-Deciduous than in Evergreen Lowland Central African Forests. – *Forest Ecology and Management* 374: 42-50.
- [25] Feldpausch, T. R., Lloyd, J., Lewis, S. L., Brien, R. J. W., Gloor, M., Monteagudo, M. A. (2012): Tree Height Integrated into Pantropical Biomass Forest Estimates. – *Biogeosciences* 9: 3381-3403.
- [26] Goussanou, C. A., Guendehou, S., Assogdadjo, A. E., Kaire, M., Sinsin, B., Cuni-Sanchez, A. (2016): Specific and generic stem biomass and volume models of trees in a West Africa tropical semi-deciduous forest. – *Silva Fennica* 50(2): 1-22.
- [27] Henry, M., Picard, N., Trotta, C., Manlay, R. J., Valentini, R., Bernoux, M., Saint-Andre, L. (2011): Estimating tree biomass of sub-sahara African forests: a review of available allometric equations. – *Silva Fennica* 45(3): 477-569.
- [28] Holdaway, J. R., McNeill, S. J., Mason, N. W. H., Carswell, F. E. (2014): Propagating Uncertainty in Plot-Based Estimates of Forest Carbon Stock and Carbon Stock Change. – *Ecosystems* 17: 627-640.

- [29] Lewis, S. L., Sonke, B., Sunderland, T., Begne, S. K., Lopez-Gonzalez, G., van der Heijden, G. M. F., Zemagho, L. (2013): Above-ground biomass and structure of 260 African tropical forests. – *Philosophical Transactions of the Royal Society: Biological Sciences* 368: 20120295.
- [30] Litton, C. M. (2008): Allometric models for predicting aboveground biomass in two widespread wood plants in Hawaii. – *Biotropica* 40(3): 313-320.
- [31] Lopez-Gonzalez, G., Lewis, S. L., Burkitt, M., Phillips, O. L. (2011): ForestPlots.net: a web application and research tool to manage and analyse tropical forest plot data. – *Journal of Vegetation Science* 22: 610-613.
- [32] Mensah, S., Veldtman, R., Seifert, T. (2017): Allometric Models for Height and Aboveground Biomass of Dominant Tree Species in South African Mistbelt Forests. – *Southern Forests: A Journal of Forest Science* 79: 19-30.
- [33] Mokany, K., Raison, R. J., Prokushkin, A. S. (2006): Critical analysis of root: shoot ratios in terrestrial biomes. – *Global Change Biology* 12(1): 84-96.
- [34] Nasi, R., Billand, A., Vanvliet, N. (2012): Managing for timber and biodiversity in the Congo Basin. – *Forest Ecology and Management* 268: 103-111.
- [35] Ngomanda, A., Obiang, N. L. E., Lebamba, J., Mavouroulou, Q. M., Mankou, G. S., Picard, N. (2014): Site-Specific versus Pantropical Allometric Equations: Which Option to Estimate the Biomass of A Moist Central African Forest? – *Forest Ecology and Management* 312: 1-9.
- [36] Pan, Y., Birdsey, R. A., Fang, J., Houghton, R., Kauppi, P. E., Kurz, W. A. (2011): A Large and Persistent Carbon Sink in the World's Forests. – *Science* 333(6045): 988-993.
- [37] Ploton, P., Barbier, N., Takoudjou-Momo, T. S., Rejou-Mechain, M., Bosela, B. F., Chuyong, G. (2016): Closing a Gap in Tropical Forest Biomass Estimation: Taking Crown Mass Variation into Account in Pantropical Allometries. – *Biogeosciences* 13: 1571-1585.
- [38] PROTA, Plant Resources of Tropical Africa (2008): Lumber 1. Plant Resources of Tropical Africa. – Backhuys Publishers, CTA. Wageningen, Netherlands (in French).
- [39] Sullivan, J. P. M., Lewis, L. S., Hubau, W., Qie, L., Baker, R. T., Banin, F. L. (2018): Field methods for sampling tree height for tropical forest biomass estimation. – *Methods in Ecology and Evolution* 9: 1179-1189.
- [40] Sullivan, J. P. M., Lewis, L. S., Affum-Baffoe, K., Castilho, C., Ekoungoulou, R., Phillips, O. L. (2020): Long-term thermal sensitivity of Earth's tropical forests. – *Science* 368(6493): 869-874.
- [41] Vieilledent, G., Vaudry, R., Andriamanohisoa, S. F. D., Rakotonarivo, O. S., Randrianasolo, H. Z., Razafindrabe, H. N. (2012): A Universal Approach to Estimate Biomass and Carbon Stock in Tropical Forests Using Generic Allometric Models. – *Ecological Applications* 22(2): 572-583.
- [42] Yanai, D. R., Battles, J. J., Richardson, D. A., Blodgett, A. C., Wood, M. D., Rastetter, B. E. (2010): Estimating uncertainty in ecosystem budget calculations. – *Ecosystems* 13(2): 239-248.
- [43] Zanne, A. E., Lopez-Gonzalez, G., Coomes, D. A., Jansen, S., Lewis, S. L., Miller, R. B., Chave, J. (2009): Data from: Towards a Worldwide Wood Economics Spectrum. – *Global Wood Density Database*. V2, Dryad Digital Repository, Dataset: <https://datadryad.org/stash/dataset/doi:10.5061/dryad.234> [Accessed 08.20.2019].

## APPLICATION OF ALLELOPATHIC PHENOMENA TO ENHANCE GROWTH AND PRODUCTION OF CAMELINA (*CAMELINA SATIVA* (L.))

ABBAS, A.<sup>1</sup> – HUANG, P.<sup>1\*</sup> – HUSSAIN, S.<sup>2</sup> – SAQIB, M.<sup>3</sup> – HE, L.<sup>1</sup> – SHEN, F.<sup>1</sup> – DU, D.<sup>1\*</sup>

<sup>1</sup>*Institute of Environment and Ecology, School of Environment and Safety Engineering, Jiangsu University, Zhenjiang 212013, PR China*

<sup>2</sup>*College of Agronomy, Northwest A & F University, Yangling, PR China*

<sup>3</sup>*Agronomic Research Institute, Ayub Agricultural Research Institute, Faisalabad, Pakistan*

*\*Corresponding authors*

*e-mail: huangjiehp@163.com; daolindu@163.com*

(Received 10<sup>th</sup> Jul 2020; accepted 7<sup>th</sup> Oct 2020)

**Abstract.** Field grown camelina suffers from various biotic and environmental stresses, affecting its growth and productivity. Allelopathy is a biochemical interaction that occurs between plants by releasing allelochemicals. It has become a sustainable approach that can help to deal with these stresses. When allelochemicals are released and applied at low concentrations, they stimulate crop growth. The potential role of allelopathy in the control of weeds, insects, and diseases is well illustrated. The use of allelopathic crops in the mulching, intercropping, and crop rotations is very useful for weed control. When released at high concentrations, these allelochemicals can also interfere with biochemical and physiological processes, thus affecting plant performance. In this review, we discuss the potential effects of allelopathy: (a) enhancing the growth performance of camelina, (b) controlling weeds, insects, and diseases, and (c) enhancing tolerance to environmental stresses. Based on previous evidence, we also discussed the mechanism, with which allelochemicals promote crop growth and confer tolerance to environmental stimuli and concluded that these allelopathic features can enhance camelina production in the future.

**Keyword:** *allelochemicals, Camelina sativa, weed management, insect pest, abiotic stresses tolerances*

### Introduction

Allelopathy's definition was familiarized by plant physiologist Molisch (1937) to raise biochemical (both, inhibitory and stimulatory) interactions between all kinds of plants. Later, it was defined as the direct and indirect, beneficial or destructive effect of a plant on another plant through different compounds. These compounds are emitted from different plant parts through residual decomposition, root exudation, stem flow, and leaching into the environment (Birkett et al., 2001). The most important part of allelopathy depends on the presence of chemical compounds that are released from living or disintegrating plant parts (Dayan et al., 2000). The naturally occurring metabolites and chemicals of plants play a vital role in the processes of biologically, ecologically, and various ecosystem processes, and are interconnected with neighboring plants and the environment (Cheng and Cheng, 2015). Allelochemicals may play a role in different plants with different mechanisms of actions, and the negative and positive types of interactions are reported based on the target plant and concentration under-examined (De Albuquerque et al., 2011; Eichenberg et al., 2014). Approximately 300,000 plant species produce several kinds of secondary metabolites or compounds, but a limited proportion of these chemicals has been examined and their effects on agro-ecosystems and other processes in different plants have been evaluated. In allelopathy,

the source of the compound's release into the environment (*Fig. 1*) is also important, and it plays a vital role in other plant processes and different agro-ecosystems (Dayan, 2006). The use of allelopathy mechanisms is conducive to crop growth and helps to increase their dominance against different problems (Inderjit, 2005).

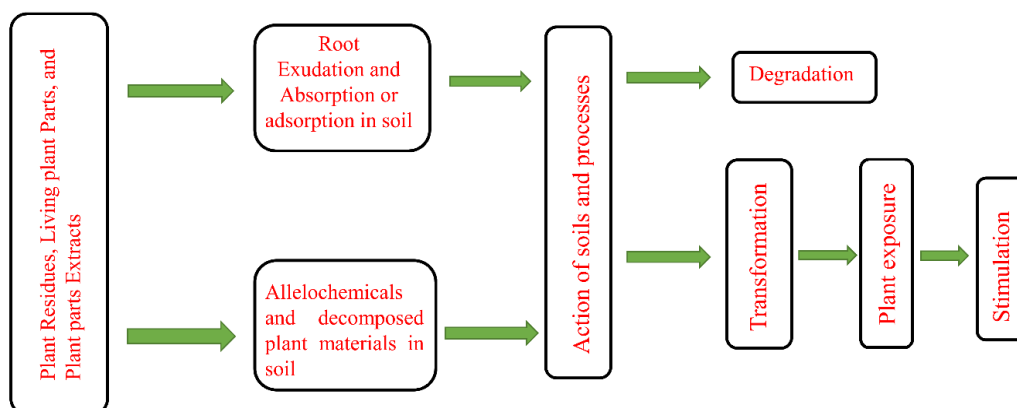


**Figure 1.** Allelopathy framework; chemical release into the atmosphere, after dilution reaches into the soil and available for plant roots. The leaching process may also help plant residues and extracts to reach into soil. Root intervention, absorption, root exudation, decomposition, degradation, transformation, and stimulation with plant process involve in allelopathy framework or mechanism in agriculture systems

Among the oil-seeded crops, camelina is one of the most important crops for bio-based and oil production purposes. Camelina is commonly known as flax and is native to the Mediterranean regions of Europe and Asia (Obour et al., 2015; Yuan and Li, 2020). The crop is also distributed in South America, New Zealand, and Australia and appears to be adopted and perform better under cold environments (Campbell et al., 2013). Compared with other oilseed crops, it has the capability to perform better under different drought stress levels, which makes it very successful in areas with arid environments and less rainfall (Obour et al., 2015). Camelina is commonly used to produce biofuels, and bio-based products (Tabatabaie and Murthy, 2017; Kalita et al., 2018), humans (Rahman et al., 2018), and animal nutrition (Ponnampalam et al., 2019). In addition, it is used in the food industry to prevent food oxidation, loss of flavor, discoloration, and the formation of toxic compounds (Abramovic and Nikolic, 2007). Due to abiotic stresses, plant germination and growth are unreasonable, and the yields of major crops (including oilseed crops) in different countries have dropped significantly (Haq et al., 2014). Compared with other oilseed crops, camelina has several agronomic benefits because of its ability to survive in dry nature and harsh environments. However, due to abiotic stresses, there have been some promising problems from germination to harvesting (Waraich et al., 2016). In the past, researchers have also tried to evaluate the response of *C. sativa* to different abiotic stresses and other factors (fertilizers, greenhouse experiments, etc.) (Wang and Frei, 2011). Today, camelina is considered to be the most important crop in oil production, and farmers all over the world are trying to grow for good economic benefits and oil production (Keske et al., 2013). Yohannes et al. (2020) studied the consequence of salt stress (treated with KCl and NaCl) on the germination performance of camelina and reported that salinity reduced the germination rate, depending on the salt level. Salinity also negatively

affects seed vigor index, germination percentages, root and seedling length, which are critical for growth and yield (Amiri-Darban et al., 2020). Drought stress also possessed negative effects on camelina growth and productivity (Adam et al., 2012). Kamkar et al. (2011) demonstrated heat stress also causes a reduction in the growth and productivity of camelina. Researchers from all over the world have also tried to study the ionic effects of different abiotic stresses on different crops (Kusvuran et al., 2015; Morales et al., 2017), and conclude that *C. sativa* seedling or germination is also reduced due to different abiotic stresses (Adam et al., 2012). Nonetheless, compared with other crops, research work on camelina with their productive features under different abiotic stresses is still limited (Pavlista et al., 2015; Hunsaker et al., 2013). Aiken et al. (2015) and Pavlista et al. (2016) reported that optimal environmental conditions and normal irrigation facilities can improve the germination, seedling growth, and productivity of *C. sativa*.

Weeds' infestations in Camelina's growing areas are the major threats to seed yield and quality, as they are competing for lights, water, and nutrients (Berti et al., 2016; Lenssen et al., 2012). Nitrogen competition between weeds and camelina crop reduces protein content, seed yield, and fatty acid quantity; these variables show a positive response to nitrogen fertilizers (Jiang et al., 2013; Jiang and Caldwell, 2016). Moreover, chemical control is not an effective method of weed management; because camelina is tolerant to broad-leaved herbicides, and it is characterized by a narrow mode of action (Berti et al., 2016). In addition, some pre-emergence herbicides may also cause injuries to the camelina plants (Jha and Stougaard, 2013). Recently, most countries are striving to reduce the use of pesticides to meet new environmental challenges (Barzman and Dachbrodt-Saaydeh, 2011). Few studies have reported the use of zero-herbicides for weed management in oilseed crops (including *C. sativa*), such as mechanical control (Heiska, 2009) and intercropping methods (Sacuke and Ackermann, 2006). When choosing a sustainable method of weed control of *C. sativa*, the use of zero herbicides seems to be a priority in many agricultural systems. The use of allelopathy for crop improvement and weed management has been discussed for major crops (Farooq et al., 2011a). However, only a few studies have reported the use of allelopathy to improve the crop performance, and as a weed control strategy for *C. sativa*. In this review, we reveal for the first time the major problems associated with camelina cultivation and study how allelopathic phenomena promote the production of camelina and respond to biotic and abiotic stresses.

### **Crop growth promotion**

Growth enhancing effects of allelopathy for the major crops are described in the literature (Kamran et al., 2019; Ming et al., 2020); however, there is a lack of information about allelopathy in promoting the growth of *C. sativa*. Several studies were discussed, and it was found that the application of low concentrations of allelochemicals stimulates the germination process (Findura et al., 2020) and growth (Kamran et al., 2019) of the major field crops. The application of aqueous crop extracts either applied exogenously (foliar spray), and seed treatment promotes the germination and growth of crops (Farooq et al., 2018). Exogenous application of allelochemicals as a foliar spray could be approved as an effective method. According to Kamran et al. (2019) aqueous extract of sorghum (3% and 5%) imposed a significant improvement of seedling growth, chlorophyll content, and carotenoid protein content in maize. A recent

study conducted by Lameirão et al. (2020), reported that low concentrations of chestnut (*Castanea henryi*) extract promoted seed germination, increased the seedling development, chlorophyll content, and antioxidant enzyme activity in maize. Phenolic compounds are among the important class of allelochemicals (Ameena et al., 2014), which can be applied exogenously to promote the growth of the crop. Allelopathic water extracts can increase the germination rate, improve crop stand, and seedling growth when used as a seed treatment, thereby improving plant growth (Maqbool et al., 2012). Farooq et al. (2018) reported that allelopathic water extracts, applied as a seed treatment, significantly promoted the growth, yield, and yield-related attributes in wheat (*Triticum aestivum* L.), moringa, sunflower (*Helianthus annuus* L.), sorghum, and brassica water extracts commonly used as seed treatments (Farooq et al., 2018).

Successful crop production depends largely on the optimal supply of nutrients. Soil is the basic medium that provides all essential nutrients for crop growth. Nutrients, in the form of a solution, are taken up by plant roots. Allelochemicals, when release by plant roots, greatly influences the absorption of nutrients. Under normal as well as stress conditions, allelochemicals promote nutrient uptake status by altering the nutrient forms and soil microbial populations. Allelochemicals played an important role in nutrient management because they have a great influence on biological nitrification and nutrient acquisition and in this way increase nutrients absorption (Jabran et al., 2012). Nitrogen (N) is an important macronutrient and plays an essential role in plant growth and development. Allelochemicals have significantly improved nitrogen use efficiency (NUE) by reducing N losses. These secondary metabolites inhibit biological nitrification by reducing the enzyme activity that plays a role in the nitrification process. Crop water extract of sorghum, sunflower, and rice (*Oryza sativa* L.) also have shown positive effects in this process (Farooq et al., 2013). Phenolics as an important secondary metabolite (Jabran and Farooq, 2013), promote the uptake and release Phosphorus, and Iron. Therefore, allelopathy considered a unique method to enhance crop NUE without causing environmental pollution, however, special attention needs to be paid to the camelina crop.

It is difficult to determine the mechanisms underlying the application of allelochemicals. The production of secondary metabolites by shikimic acid, malonic acid, melvonic acid, methylerythritol phosphate, and isoprenoid pathways are well documented (Taiz and Zeiger, 2010). When applied at low concentrations, secondary metabolites increased the germination rates by reducing seed dormancy, promote root growth by increasing the absorption and utilization of water and nutrients, and promote plant growth by increasing chlorophyll content, transpiration, and photosynthesis rate. Several studies also reported that the application of low concentrations of allelochemicals enhances enzyme activation (gibberellins and auxins), stimulates cell division, enhances ion absorption, and in this way increases plant growth and development.

## Weed management

Camelina, also known as false flax, is an important crop of Brassicaceae and can grow successfully under various environmental conditions. However, the control of weeds is currently the main challenge for the successful camelina production (Lenssen et al., 2012; Berti et al., 2016). Weed infestation can cause severe yield reductions and quality declines, mainly through competition for lights, space, and other inputs (Jiang



and Caldwell, 2016; Leclère et al., 2019). The major weeds of camelina are *Berberis vulgaris* (L.), *Capsella bursa-pastoris* (L.) *Lepidium campestre*, *Thlaspi arvense* (L.), *Raphanus raphanistrum*, *Galium aparine* (also known as catchweed) (Al-Shehbaz, 2012; Malhi et al., 2014; Sagun and Auer, 2017; Zhang and Auer, 2020), *Camelina laxa*, *Camelina hispida* (Zhang and Auer, 2019), *Lepidium latifolium* (pepper weed), *Setaria faberi* (foxtail) (Rizzitello et al., 2019), *Cirsium arvense* (field thistle), *Elymus repens* (L.), *Matricaria recutita*, *Sonchus oleraceus*, and *Trifolium pretense* (Saucke and Ackermann, 2006). Various perennial broad-leaved weeds, such as *Convolvulus Arvensis* (bindweed), and *Chondrilla juncea* (L.) (naked weed) also caused a significant reduction in camelina production. With the passage of time, the chemical control of weeds is less effective because it increases environmental pollution (Sodaizadeh and Hosseini, 2012). In addition, the use of herbicides can also cause injuries to camelina (Leclère et al., 2019). The application of herbicides mainly causes damage to plants by reducing the efficiency of photosynthesis (Kaiser et al., 2013). Several organic alternatives to chemically controlled weeds have been reported in the literature (Macías et al., 2019; Fracchiolla et al., 2020). Allelopathy is a promising tool that can be successfully used for weeds control without causing environmental pollution and the development of herbicide resistance (Razzaq et al., 2010). Allelopathy involves the release of allelochemicals, which act as natural pesticides, can reduce environmental pollution and resistance development in weed species (Farooq et al., 2011a). Allelopathy can be successfully used for weeding of field crops through mix intercropping (Iqbal and Cheema, 2007), crop rotation (Mamolos and Kalburtji, 2001; Farooq et al., 2011a), use of ground cover and soil residue embedding, and allelopathy water extracts (Ahmad et al., 1995; Cheema et al., 2000a; Matloob et al., 2010) (Table I). In addition, the use of smothering crops (such as rye (*Secale cereals* L.), buckwheat (*Fagopyrum esculentum*), and Black Mustard (*Brassica nigra*) can also be successfully used for weeds management (Jabran and Farooq, 2013). Intercropping can be an effective tool for weed management (Saudy, 2015). Various studies have shown that intercropping with allelopathic crops has been used for integrated weed management (Farooq et al., 2011a; Baumann et al., 2002). Allelopathic crops reduce the weed population by releasing allelochemicals and inhibit the weed-crop competition (Liebman and Davis, 2000; Ali et al., 2000). For example, Saucke and Ackermann (2006) reported that intercropping camelina (*C. sativa*) with pea (*Pisum sativum* L.) significantly reduce the weeds by 52-63% as compared with the sole crop. Crop rotation, temporal diversification of crops, with the inclusion of allelopathic crops can help reduce the weed population (Jabran and Farooq, 2013). In crop rotation, the allelochemicals in the rhizosphere released from the root of plants and the decomposition of previous crop residues help to suppress weeds (Voll et al., 2004; Mamolos and Kalburtji, 2001). *Setaria faberi*, a common weed of *C. sativa*, can be managed through crop rotations with maize-soybean, and soybean-wheat-maize (Schreiber, 1992). The use of allelopathic crops as mulching also useful for reducing the weed germination and seedling growth, by releasing of certain allelochemicals (Teasdale and Mohler, 2000; Bilalis et al., 2003; Rawat et al., 2017). Cover crops, by releasing allelochemicals, and alterations in soil physicochemical properties helpful in managing the weed population (Tursun et al., 2018). Various studies have reported the potential of allelopathic crops to reduce weeds in major crops (Cheema et al., 2000a, 2004). Therefore, there is an urgent need to classify allelopathic crops to reduce weeds in *C. sativa*. The use of allelopathic water extracts (aqueous extract) has caused

widespread concern in the suppression of weeds (Farooq et al., 2020). The water-soluble allelochemicals (secondary metabolites) are first extracted in water and then used to control weeds (Bonanomi et al., 2006). Sorgaab, a water extract of sorghum, is one of the most commonly used water extracts for weed control (Cheema et al., 2002a). The application of sorgaab for suppressing of weeds in major crops such as wheat, cotton (*Gossypium hirsutum* L.), rice, and maize (Iqbal et al., 2009; Cheema et al., 2004), have been well reported. The sunflower water extract is rich in chlorogenic, ferulic acid, and vanillic acids (Ghafar et al., 2001), and has the potential to inhibit the growth of grassy and broadleaf weeds (Anjum and Bajwa, 2010). The combined application of various allelopathic water extracts may have more benefits in controlling weeds, as compared with the sole application (Cheema et al., 2003; Jamil et al., 2009). Different crops have released specific types of allelochemicals, and each allelochemical has control of a specific type of weed. Gramine/Hordenine, well-known allelochemicals, can inhibit the growth of *Capsella bursa-pastoris* (the major weed of *C. sativa*) (Nawaz et al., 2014). The mechanisms underlying the control of weeds through allelopathy are not well understood. Some reports have discussed that the application of high concentrations of allelochemicals may interfere with cell division, hormonal balancing, mineral absorption and transport, plant water relations, oscillations of stomata, membrane permeability, respiration and photosynthesis, and the process of protein metabolism (Gupta et al., 2018; Nawaz et al., 2018). This phytotoxic activity of allelochemicals can inhibit the growth of weeds.

**Table 1.** The application of allelopathy for the suppression of weeds in different crops

Weed species	Allelopathic source	Weed control (%)	Reference
<i>Convolvulus arvensis</i>	Allelopathic water extracts Sunflower ( <i>Helianthus annuus</i> L.)	Reduction in total weed density and DW (17.19% and 35.92%, respectively)	Naseem et al. (2010)
	Allelopathic water extracts Sorghum ( <i>Sorghum bicolor</i> L.)	Reduction in total weed density and DW (by 31.58% and 44.11-59.62%, respectively)	Khaliq et al. (2002); Cheema et al. (2001)
	Allelopathic crop rotations (Sorghum (surface mulch)	Reduction in total weed DW (81%)	Cheema et al. (2000b)
	Combine application of allelopathic water extracts and herbicides Sorghum (10 L ha <sup>-1</sup> ) + S. metolachlor (2.3 kg a.i. ha <sup>-1</sup> Dualgold 960 EC)	Reduction in total weed DW (79.32%)	Khaliq et al. (2002)
<i>Setaria faberi</i>	Maize-soybean, and soybean-wheat-maize	Completely inhibit the weed growth	Schreiber (1992)
<i>Capsella bursa-pastoris</i>	Allelochemicals application of Gramine/Hordenine	Inhibited the weed density and biomass	Nawaz et al. (2014)
Major weeds of <i>C. sativa</i>	Allelopathic intercropping with Camelina ( <i>C. sativa</i> ) with pea ( <i>Pisum sativum</i> L.)	Reduce the weeds by 52-63%	Saucke and Ackermann (2006)

## Pest and disease management

*Camelina sativa* is an important source of biodiesel and classified as a minor crop (Sobiech et al., 2020). In the cultivation of minor crops, insects and diseases can cause serious harm to growth, yield, and yield-related aspects (Olivier et al., 2011; Meynard et al., 2018). Many types of insects, such as *Lygus hesperus* Knight (Naranjo and Stefanek, 2012), *Lygus* spp. (Naranjo et al., 2011), *Phyllotreta cruciferae*, *Ceutorhynchus obstructus*, and *Meligethes aeneus* (Scottish Rural Colleges, 2013) are regarded as pests of camelina crop. Some other types such as *Ceutorhynchus cyanipennis* and *C. americanus* also caused damaging effects for camelina crop (Malik et al., 2018). In addition, various diseases, such as *Leptosphaeria maculans*, *Sclerotinia*, *Peronospora*, *Botrytis sclerotinia*, *Ustilago*, aster yellows (Olivier et al., 2011; Soroka et al., 2015) and *Sclerotinia sclerotiorum* (Ehrensing and Guy, 2008) are among the important diseases of camelina causing a severe reduction in growth, and yield losses. *Camelina sativa* is also susceptible to other diseases such as damping-off, white rust, and downy mildew (Séguin-Swartz et al., 2009). Recently, to reduce pest populations, the most reliance is on the use of pesticides. Although chemical pest control methods have made significant contributions to improving crop performances, certain challenges are also associated with them. The increasing cost of pesticides, environmental concerns, and resistance against pesticides are among the major challenge for using pesticides for pest control (Farooq et al., 2013). A number of options are available for reducing insect populations and disease control without any environmental hazards. Reducing the pest population through the allelopathic phenomenon is included among the innovative pest control methods (Nawaz et al., 2018). Neem (*Azadirachta indica* L.) is rich in azadirachtin and is the most commonly used to reduce insect populations (Khan et al., 2014). The application of some types of allelochemicals extracted from *Chenopodium ficifolium* (Dang et al., 2010), and *Eucalyptus globulus* (Farooq et al., 2011a) are among the allelopathic measures used for controlling the insect populations. Allelochemicals also were shown their role to reduce damage to plant diseases (Nawaz et al., 2018). Aqueous extracts of many allelopathic plants are known to reveal antifungal and antibacterial possessions. According to Bajwa et al. (2004), the water extract of *Parthenium* (*Parthenium hysterophorus*) exhibited antifungal activity against fungal diseases. Momilactone A and momilactone B are important allelochemicals in rice and play a role in suppressing fungal and bacterial diseases (Kong et al., 2004). For major crops, antifungal and antibacterial activities of allelochemicals are well understood but their effectiveness against camelina-specific diseases remains to be further explored.

## Abiotic stress tolerance

As an annual crop, *C. sativa* can adopt under a wide range of environmental conditions (Hunsaker et al., 2011; Schillinger et al., 2012). However, under field conditions, the crop is also pronounced to various abiotic stresses (Schillinger et al., 2012; Gesch, 2014; Gesch and Cermak, 2011), which retard the growth, and yield losses (Berti et al., 2011). Some studies have reported complete crop failure under abiotic stress conditions. Among abiotic stress, high temperature (Gesch, 2014; Schillinger et al., 2012), drought stress (Eberle et al., 2015), salinity stress (Khalid et al., 2015; Heydarian et al., 2018), and waterlogging (Gesch and Cermak, 2011) are among major limiting factors for camelina growth and its production. Various researchers have been

documented the optimum temperature ranges for better emergence and growth of *C. sativa*. Russo et al. (2010) recorded 100% germination at 4 °C, 10 °C, 16 °C, 21 °C, and 27 °C. They also reported that the temperature above 32 °C might decline the germination rates. According to Gesch (2014), high temperature has resulted in the decrement of seed yield and oil content of *C. sativa*, even under optimal water conditions. Similar findings were also reported by (Schillinger et al., 2012), unveiled that high temperature significantly hinders the seed yield of *C. sativa*. Allelopathy has great potential to enhance crop tolerance to cope with environmental stresses (Fig. 2). Farooq et al. (2018) reported that the application of crop water extracts (through seed priming or foliar spray application) significantly promoted wheat growth and yield-related aspects under heat stress. The increase in growth and yield attributed to the decrease in MDA content and membrane leakage under heat stress.

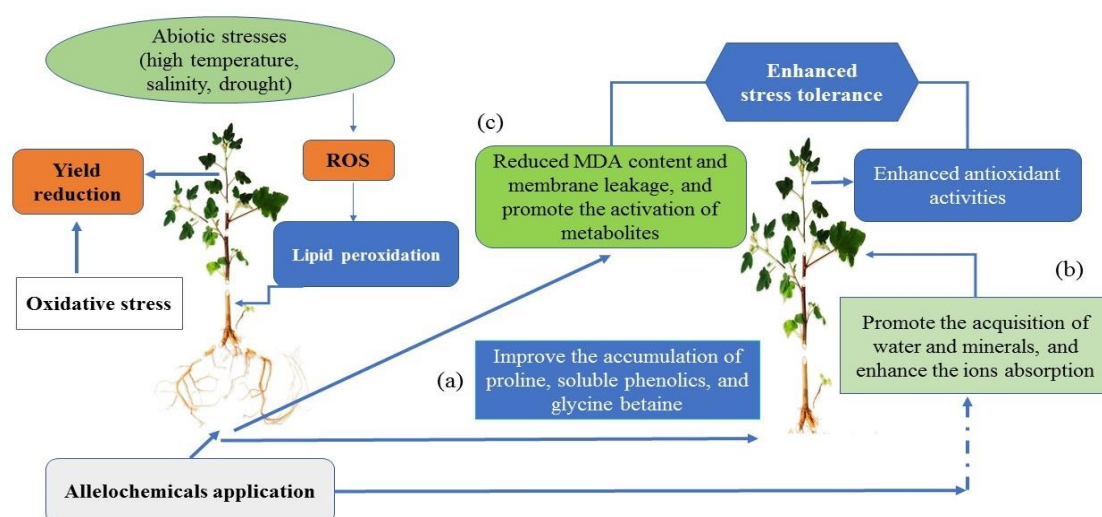


**Figure 2.** Application of allelochemicals to enhance the tolerance against abiotic stresses. Allelochemicals; applied at low concentrations, (a) improve the accumulation of proline, soluble phenolic, and glycine betaine, (b) promote the acquisition of water and minerals, and enhance the ions absorption. Under stress conditions, allelochemicals (c) reduce the malondialdehyde (MDA) content and membrane leakage and promote the activation of metabolites

Khalid et al. (2015) reported that salinity stress results in postponed germination, decrease seedling emergence, plant growth (plant height), relative water content, and chlorophyll (CHL) contents (CHL *a*, *b* and total CHL) in *C. sativa*. The higher concentration of Na<sup>+</sup> and Cl<sup>-</sup> in chloroplast are resulted in a reduction in photosynthesis. In addition, salinity also causes an increment in electric conductivity (52.8%), guaiacol peroxidase, and malondialdehyde content in stressed camelina plants as compared with untreated plants. Similarly, Morales et al. (2017) found reduced germination, plant growth, chlorophyll content, and stomatal size in camelina depending on cultivars and salinity levels. In the same study, increased proline content was also reported with increasing salinity levels. In a recent study, Yohannes et al. (2020) demonstrated that salt stress (with KCl and NaCl) can be caused a marked reduction in germination attributes (such as germination speed, germination percentage, and index), root and shoot length, root shoot ratio, and fresh weights of Camelina seedling depending on

stress level. Farooq et al. (2011b) explored the role of allelopathy in enhancing resistance to salinity. In this regard, the authors reported that seed priming with sunflower water extract could not only increase the germination rate but also increase seedling growth. Wang et al. (2019) studied the effect of goldenrod (*Solidago canadensis*) leaf extract on lettuce (*Lactuca sativa* L.) and reported that at low concentrations goldenrod extract promotes root growth and leaf width under high salt concentrations. One possible mechanism is that at low concentration, the allelochemicals released by goldenrod leaf extracts can produce the reactive oxygen molecules in plant cells, and then have a positive effect on the seed germination and seedling growth of lettuce (Prithiviraj et al., 2007).

Drought is another abiotic stress imposed negative effects on the growth and productivity of *C. sativa*. In this regard, Ahmed et al. (2017) reported that drought stress resulted in decreasing growth attributes (length, and dry and fresh weights of the root and shoot), photosynthetic and transpiration rates, leaves stomatal conductance, and soluble proteins content in treated camelina plant as compared with untreated one. In the same study, an increment in proline content, soluble sugars, and amino acid content was also reported under drought stress. Similarly, Waraich et al. (2017) demonstrated that water deficit conditions (60% field capacity (FC)) resulted in decreasing leaf area index, crop growth rates, leaf area duration, net assimilation rates, and yield-related attributes (1000-seed weight, and seed yield) in camelina as compared to normally irrigated plants (100% FC). In a recent study, Gao et al. (2018) have documented the decreased photosynthesis and transpiration rates, stomatal conductance, and root and shoot biomass of camelina under water deficit conditions. Farooq et al. (2018) reported that crop water extracts (applied through seed priming or foliar spray) promote the growth, yield, and yield-related aspects in wheat, subjected to drought stress. The improvement was attributed to the reduced MDA contents and membrane leakage under drought stress.

Under stress conditions, allelopathic substances (secondary metabolites) play a vital role in the production of reactive oxygen species (ROS) at first, and then in the activation of the antioxidant defense system (Farooq et al., 2013). In addition, these substances also promote the acquisition of water and minerals, chloroplast function, the activation of metabolites, and enhance the absorption of ions (Waśkiewicz et al., 2013), thus playing an active role in the defense system. Moreover, allelochemicals can also produce hormonal imbalance, which can lead to the overproduction of some useful hormones, which is crucial for the smooth operation of different physiological processes under stress. Allelochemicals also improve the accumulation of proline, soluble phenolic, and glycine betaine, which may lead to the stabilize of the biological membrane under stress conditions (Farooq et al., 2018). The increased allelochemicals-induced activities of antioxidant enzymes also responsible for stress tolerance (Ye et al., 2006).

The enhancement of abiotic stress tolerance using allelopathic phenomena has been reported for major crops. However, reports on the use of allelopathy to enhance stress tolerance in camelina are limited and further studies are needed.

### Limitations and implementations

Allelochemicals are mainly composed of secondary metabolites with different natural pathways (*Fig. 1*) and some allelochemicals change the process during

extraction. Therefore, researchers must carefully determine whether plants have allelopathic potential or separate and identify allelochemicals using organic solvents and aqueous extracts from plant tissues. The type and quantity of allelochemicals released into the environment depend on the combined effects of the plant itself (plant factors) and environmental factors (De Albuquerque et al., 2010). Plants from the same environment or close in taxonomy do not necessarily show similar secondary metabolites production, so they may not secrete the same quantity and quality of allelochemicals or have similar allelopathic effects (Chon and Nelson, 2010). A large number of studies have shown that allelopathy has good application potential in agricultural production. So far, many allelopathic crops have been used in agricultural production, but their application is limited to small-scale and regional areas. In nature, plant products represent a vast diversity of compounds with a variety of biological activity (Inderjit, 2005). The natural products represent a diverse class of chemical compounds. These allelochemicals will have an impact on different species of plants. There are limitations to the successful use of allelochemicals in weed management. In implementing of natural products to effective weed/pest management, some of these factors include: (i) the concentration of the compounds is very low, (ii) the half-life of allelochemicals is usually very short, (iii) the weed selectivity is narrow, and (v) high-cost production.

## Conclusion and future prospects

This review for the first time highlights the potential of allelopathy to promote the growth of camelina plants, as well as the potential to control weeds, insects, and diseases of *C. sativa*. When applied at low concentrations, allelochemicals can reduce seed dormancy, increase water and nutrient absorption; improve photosynthesis and respiration rate, thereby promoting germination, root, and plant growth. The use of allelopathic crops in the form of cover crops, mulching, and including in crop rotations can be useful in weed management. Correspondingly, studies to date have shown that allelochemicals have great potential in controlling of insects and diseases.

In the past, most research was on the use of allelopathy on major crops, but a lot of work needs to be done on camelina. Future research should be carried out: (a) to establish the feasible technique of using allelochemicals for camelina under field experimentation, (b) to study the definite mechanisms related to enhancing the growth of camelina (c) to illustrate the optimum concentrations of allelochemicals for promoting the growth and development in camelina, (d) to screen the diverse range of crops with greater pest-suppress ability, and (e) to find the advance biotechnological tools to enhance biological weed/pest control in camelina.

**Acknowledgments.** This work was supported by the National Natural Science Foundation of China (31200316, 31770446), Senior Talent Fund of Jiangsu University (11JDG150), China Postdoctoral Science Foundation (2012M520999), the State Key Research Development Program of China (2017YFC1200100).

**Conflict of interests.** Authors declare that there is not any conflict of interests.

## REFERENCES

- [1] Abramovic, H., Butinar, B., Nikolic, V. (2007): Changes occurring in phenolic content, tocopherol composition and oxidative stability of *Camelina sativa* oil during storage. – *Food Chem* 104: 903-909.
- [2] Adam, H. D., Luce, C. H., Breshears, D. D., Allen, C. D., Weiler, M., Hale, V. C., Smith, A. M. S., Huxman, T. E. (2012): Ecohydrological consequences of drought- and infestation- triggered tree die-off: insights and hypotheses. – *Ecohydrol* 5: 145-159.
- [3] Ahmad, S., Rehman, A., Cheema, Z. A., Tanveer, A., Khaliq, A. (1995): Evaluation of some crop residues for their allelopathic effects on germination and growth of cotton and Cottonweeds. – 4th Pakistan Weed Science Conference, Faisalabad, pp. 63-71.
- [4] Ahmed, Z., Waraich, E. A., Rashid, A., Shahbaz, M. (2017): Morpho-physiological and biochemical responses of camelina (*Camelina sativa* crantz) genotypes under drought stress. – *Int J Agric Biol* 19: 1-7.
- [5] Aiken, R., Baltensperger, D., Krall, J., Pavlista, A., Johnson, J. (2015): Planting methods affect emergence, flowering and yield of spring oilseed crops in the US Central High Plains. – *Industrial Crops and Products* 69: 273-277.
- [6] Ali, Z., Malik M. A., Cheema M. A. (2000): Studies on determining a suitable canola-wheat intercropping pattern. – *Int J Agric Biol* 2: 42-44.
- [7] Al-Shehbaz, I. A. (2012): A generic and tribal synopsis of the Brassicaceae (Cruciferae). – *Taxon* 61: 931-954.
- [8] Ameena, M., Geethakumari, V. L., Sansamma, G. (2014): Allelopathic influence of purple nutsedge (*Cyperus rotundus* L.) root exudates on germination and growth of important field crops. – *Int J Agric Sci* 10: 186-189.
- [9] Amiri-Darban, N., Nourmohammadi, G., Shirani Rad, A. H., Mirhadi, S. M. J., Majidi H. I. (2020): Potassium sulfate and ammonium sulfate affect quality and quantity of camelina oil grown with different irrigation regimes. – *Ind Crops Prod* 148: 112308.
- [10] Anjum. T., Bajwa, R. (2010): Sunflower phytochemicals adversely affect wheat yield. – *Natural Product Res* 24: 825-837.
- [11] Bajwa, R., Shafique, S., Anjum, T., Shafique, S. (2004): Antifungal activity of allelopathic plant extracts IV: growth response of *Drechslera hawaiiensis*, *Alternaria alternata* and *Fusarium moniliforme* to aqueous extract of *Parthenium hysterophorus*. – *Int J Agric Sci* 6: 511-516.
- [12] Barzman, M., Dachbrodt-Saaydeh, S. (2011): Comparative analysis of pesticide action plans in five European countries. – *Pest Manage Sci* 67: 1481-1485.
- [13] Baumann, D. T., Bastiaans, L., Kropff, M. J. (2002): Intercropping system optimization for yield, quality, and weed suppression combining mechanistic and descriptive models. – *Agron J* 94: 734-742.
- [14] Berti, M., Wilckens, R., Fischer, S., Solis, A., Johnson, B. (2011): Seeding date influence on camelina seed yield, yield components, and oil content in Chile. – *Ind Crops Prod* 34: 1358-1365.
- [15] Berti, M., Gesch, R., Eynck, C., Anderson, J., Cermak, S. (2016): Camelina uses, genetics, genomics, production, and management. – *Ind Crops Prod* 94: 690-710.
- [16] Bilalis, D., Sidiras, N., Economou, G., Vakali, C. (2003): Effect of different levels of wheat straw soil surface coverage on weed flora in *Vicia faba* crops. – *J Agron Crop Sci* 189: 233-241.
- [17] Birkett, M. A., Chamberlain, K., Hooper, A. M., Pickett, J. A. (2001): Does allelopathy offer real promise for practical weed management and for explaining rhizosphere interactions involving higher plants? – *Plant Soil* 232: 31-39.
- [18] Bonanomi, G., Sicurezza, M. G., Caporaso, S., Esposito, A., Mazzoleni, S. (2006): Phytotoxicity dynamics of decaying plant materials. – *New Phytol* 169: 571-578.

- [19] Campbell, M. C., Rossi, A. F., Erskine, W. (2013): Camelina (*Camelina sativa* (L.) Crantz): agronomic potential in Mediterranean environments and diversity for biofuel and food uses. – *Crop Pasture Sci* 64: 388-398.
- [20] Cheema, Z. A., Asim, M., Khaliq A (2000a): Sorghum allelopathy for weed control in cotton (*Gossypium arboreum* L.). – *Int J Agric Biol* 2: 37-40.
- [21] Cheema, Z. A., Rakha, A., Khaliq, A. (2000b): Use of sorghum water extract and sorghum mulch for weed management in mungbean. – *Pak J Agri Sci* 37: 140-144.
- [22] Cheema, Z. A., Khaliq, A., Akhtar S (2001): Use of sorghum water extract (sorghum water extract) as a natural weed inhibitor in spring mungbean. – *Int J Agric Biol* 3: 515-518.
- [23] Cheema, Z. A., Iqbal, M., Ahmad, R. (2002a): Response of wheat varieties and some rabi weeds to allelopathic effects of sorghum water extract. – *Int J Agric Biol* 4: 52-55.
- [24] Cheema, Z. A., Khaliq, A., Ali K. (2002b): Efficacy of Sorgaab for weed control in wheat grown at different fertility levels. – *Pak J Weed Sci Res* 8: 33-38.
- [25] Cheema, Z. A., Khaliq, A., Mubeen, M. (2003): Response of wheat and winter weeds to foliar application of different plant water extracts of sorghum (*S. bicolor*). – *Pak J Weed Sci Res* 9: 89-97.
- [26] Cheema, Z. A., Khaliq, A., Saeed, S. (2004): Weed control in maize (*Zea mays* L.) through sorghum allelopathy. – *J Sustain Agri* 23: 73-86.
- [27] Cheng, F., Cheng, Z. (2015): Research Progress on the use of Plant Allelopathy in Agriculture and the Physiological and Ecological Mechanisms of Allelopathy. – *Front Plant Sci* 6.
- [28] Dang, Q. L., Lee, G. Y., Choi, Y. H., Choi, G. J., Jang, K. S., Park, M. S., Soh, H. S., Han, Y. H., Lim, C. H., Kim, J. C. (2010): Insecticidal activities of crude extracts and phospholipids from *Chenopodium ficifolium* against melon and cotton aphid, *Aphis gossypii*. – *Crop Protec* 29: 1124-1129.
- [29] Dass, A., Shekhawat, K., Choudhary, A. K., Sepat, S., Rathore, S. S., Mahajan, G., Chauhan, B. S. (2017): Weed management in rice using crop competition-a review. – *Crop Protection*. 95: 45-52.
- [30] Dayan, F. E. (2006): Factors modulating the levels of the allelochemical sorgoleone in *Sorghum bicolor*. – *Planta* 224: 339-346.
- [31] Dayan, F. E., Romagni, J. G., Duke, S. O. (2000): Investigating the mode of action of natural phytotoxins. – *J Chem Ecol* 26: 2079-2094.
- [32] De Albuquerque, M. B., Santos, R. C., Lima, L. M., Melo Filho, P. A., Nogueira, R. J. M. C., Da Câmara, C. A. G., Ramos, A. R. (2011): Allelopathy, an alternative tool to improve cropping systems. A review. – *Agron Sustain Develop* 31: 379-395.
- [33] Eberle, C. A., Thom, M. D., Nemecek, K. T., Forcella, F., Lundgren, J. G., Gesch, R. W., Riedell, W. E., Papiernik, S. K., Wagner, A., Peterson, D. H. (2015): Using pennycress, camelina, and canola cash cover crops to provision pollinators. – *Ind Crops Prod* 75: 20-25.
- [34] Ehrensing, D. T., Guy, S. O. (2008): Oilseed Crops: Camelina. – Oregon State University Extension Service EM, 8953.
- [35] Eichenberg, D., Ristok, C., Kroeber, W., Bruelheide, H. (2014): Plant polyphenols - implications of different sampling, storage and sample processing in biodiversity-ecosystem functioning experiments. – *Chem Ecol* 30: 676-692.
- [36] Farooq, M., Jabran, K., Cheema, Z. A., Wahid, A., Siddique, K. H. M. (2011a): The role of allelopathy in agricultural pest management. – *Pest Manage Sci* 67: 493-506.
- [37] Farooq, M., Habib, M., Rehman, A., Wahid, A., Munir, R. (2011b): Employing aqueous allelopathic extracts of sunflower in improving salinity tolerance in rice. – *J Agric Soc Sci* 7: 75-80.
- [38] Farooq, M., Bajwa, A. A., Cheema, S. A., Cheema, Z. A. (2013): Application of allelopathy in crop production. – *Int J Agric Biol* 15: 1367-1378.



- [39] Farooq, M., Nadeem, F., Arfat, M. Y., Nabeel, M., Musadaq, S., Cheema, S. A., Nawaz, A. (2018): Exogenous application of allelopathic water extracts helps improving tolerance against terminal heat and drought stresses in bread wheat (*Triticum aestivum* L. Em. Thell.). – *J Agron Crop Sci* 204: 298-312.
- [40] Farooq, N., Abbas, T., Tanveer, A., Jabran, K. (2020): Allelopathy for Weed Management. – In: Mérillon, J.-M., Ramawat, K. G. (eds.) *Co-evolution of Secondary Metabolites*. Springer, Cham, pp. 505-519.
- [41] Findura, P., Hara, P., Szparaga, A., Kocira, S., Czerwińska, E., Bartoš, P., Nowak, J., Treder, K. (2020): Evaluation of the effects of allelopathic aqueous plant extracts, as potential preparations for seed dressing, on the modulation of cauliflower seed germination. – *Agriculture* 10(4): 122.
- [42] Fracchiolla, M., Renna, M., D'Imperio, M., Lasorella, C., Santamaria, P., Cazzato, E. (2020): Living mulch and organic fertilization to improve weed management, yield and quality of broccoli raab in organic farming. – *Plants* 9(2): p.177.
- [43] Gao, L., Caldwell, C. D., Jiang, Y. (2018): Photosynthesis and growth of Camelina and canola in response to water deficit and applied nitrogen. – *Crop Sci* 58: 393-401.
- [44] Gesch, R. W. (2014): Influence of genotype and sowing date on Camelina growth and yield in the north central US. – *Ind Crops Prod* 54: 209-215.
- [45] Gesch, R., Cermak, S. (2011): Sowing date and tillage effects on fall-seeded camelina in the northern Corn Belt. – *Agronomy Journal* 103: 980-987.
- [46] Ghafar, A., Saleem, B., Haq, A., Qureshi, M. J. (2001): Isolation and identification of allelochemicals of sunflower (*Helianthus annuus* L.). – *Int J Agri Biol* 3: 21-22.
- [47] Gupta, D. K., Palma, J. M., Corpas, F. J. eds. (2018): *Antioxidants and Antioxidant Enzymes in Higher Plants*. – Springer, Cham.
- [48] Haq, T., Ali, A., Nadeem, S. M., Maqbool, M., Ibrahim, M. (2014): Performance of canola cultivars under drought stress induced by withholding irrigation at different growth stages. – *Soil & Environ* 33: 43-50.
- [49] Heiska, S. (2009): Developing Weed Control Methods for Camelina: A Newly Introduced, High-Value Oil Seed Crop. – In: Kingely, R. V. (ed.) *Weeds: Management, Economic Impacts and Biology*. – Nova Science Publishers, New York, pp. 41-59.
- [50] Heydarian, Z., Yu, M., Gruber, M., Coutu, C., Robinson, S. J., Hegedus, D. D. (2018): Changes in gene expression in Camelina sativa roots and vegetative tissues in response to salinity stress. – *Sci Rep* 8(1): 1-22.
- [51] Hunsaker, D., French, A., Clarke, T., El-Shikha, D. (2011): Water use, crop coefficients, and irrigation management criteria for Camelina production in arid regions. – *Irrig Sci* 29: 27-43.
- [52] Hunsaker, D. J., French, A. N., Thorp, K. R. (2013): Camelina water use and seed yield response to irrigation scheduling in an arid environment. – *Irrig Sci* 31: 911-929.
- [53] Inderjit (2005): Soil microorganisms: an important determinant of allelopathic activity. – *Plant Soil* 274: 227-236.
- [54] Iqbal, J., Cheema, Z. A. (2007): Effect of allelopathic crops water extracts on glyphosate dose for weed control in Cotton (*Gossypium hirsutum* L.). – *Allelopathy J* 19: 403-410.
- [55] Iqbal, J., Cheema, Z. A., Mushtaq, M. N. (2009): Allelopathic crop water extracts reduce the herbicide dose for weed control in cotton (*Gossypium hirsutum*). – *Int J Agric Biol* 11: 360-366.
- [56] Jabran, K., Chauhan, B. S. (2018): Overview and Significance of Non-chemical Weed Control. – In: Jabran, K., Chauhan, B. S. (eds.) *Non-chemical Weed Control*. 1st Ed. Elsevier, New York, pp. 1-8.
- [57] Jabran, K., Farooq, M. (2013): Implications of Potential Allelopathic Crops in Agricultural Systems. – In: Cheema, Z. A., Farooq, M., Wahid, A. (eds.) *Allelopathy: Current Trends and Future Applications*. Springer, Berlin, pp. 349-385.

- [58] Jabran, K., Farooq, M., Aziz, T., Siddique, K. H. M. (2012): Allelopathy and Crop Nutrition. – In: Cheema, Z. A., Farooq, M., Wahid, A. (eds.). Allelopathy: Current Trends and Future Applications. Springer, Berlin, pp. 113-143.
- [59] Jabran, K., Mahajan, G., Sardana, V., Chauhan, B. S. (2015): Allelopathy for weed control in agricultural systems. – *Crop Protec* 72: 57-65.
- [60] Jamil, M., Cheema, Z. A., Mushtaq, M. N., Farooq, M., Cheema, M. A. (2009): Alternative control of wild oat and canary grass in wheat fields by allelopathic plant water extracts. – *Agron Sustain Dev* 29: 475-482.
- [61] Jha, P., Stougaard, R. N. (2013): Camelina (*Camelina sativa*) tolerance to selected pre-emergence herbicides. – *Weed Technol* 27: 712-717.
- [62] Jiang, Y., Caldwell, C. D. (2016): Effect of nitrogen fertilization on Camelina seed yield, yield components, and downy mildew infection. – *Cand J Plant Sci* 96: 17-26.
- [63] Jiang, Y., Caldwell, C. D., Falk, K. C., Lada, R. R., MacDonald, D. (2013): Camelina yield and quality response to combined nitrogen and sulfur. – *Agron J* 105: 1847-1852.
- [64] Kaiser, Y. I., Menegat, A., Gerhards, R. (2013): Chlorophyll fluorescence imaging: a new method for rapid detection of herbicide resistance in *Alopecurus myosuroides*. – *Weed Res* 53: 399-406.
- [65] Kalita, D. J., Tarnavchyk, I., Sibi, M., Moser, B. R., Webster, D. C., Chisholm, B. J. (2018): Biobased poly (vinyl ether) derived from soybean oil, linseed oil, and camelina oil: synthesis, characterization, and properties of crosslinked networks and surface coatings. – *Prog Organic Coat* 125: 453-462.
- [66] Kamkar, B., Daneshmand, A. R., Ghooshchi, F., Shiranirad, A. H., Safahani Langeroundi, A. R. (2011): The effects of irrigation regimes and nitrogen rates on some agronomic traits of canola under a semiarid environment. – *Agric Water Manage* 98: 1005-1012.
- [67] Kamran, M., Cheema, Z. A., Farooq, M., Ali, Q., Anjum, M. Z., Raza, A. (2019): Allelopathic influence of sorghum aqueous extract on growth, physiology and photosynthetic activity of maize (*Zea mays* L.) seedling. – *Philipp Agric Sci* 102: 33-41.
- [68] Keske, C. M. H., Hoag, D. L., Brandess, A., Johnson, J. J. (2013): Is it economically feasible for farmers to grow their own fuel? A study of *Camelina sativa* produced in the western United States as an on-farm biofuel. – *Biomass Bioenerg* 54: 89-99.
- [69] Khalid, H., Kumari, M., Grover, A., Nasim, M. (2015): Salinity stress tolerance of camelina investigated in vitro. – *Sci Agric Bohem* 46: 137-144.
- [70] Khaliq, A., Aslam, Z., Cheema, Z. A. (2002): Efficacy of different weed management strategies in mungbean (*Vigna radiata* L.). – *Int J Agric Biol* 4: 237-239.
- [71] Khan, A. A., Afzal, M., Qureshi, J. A., Khan, A. M., Raza A. M. (2014): Botanicals, selective insecticides, and predators to control *Diaphorina citri* (Hemiptera: Liviidae) in citrus orchards. – *Int Sci* 21: 717-726.
- [72] Kong, C., Liang, W., Xu, X., Hu, F., Wang, P., Jiang, Y. (2004): Release and activity of allelochemicals from allelopathic rice seedlings. – *J Agric Food Chem* 52: 2861-2865.
- [73] Kusvuran, A., Nazli, R. I., Kusvuran, S. (2015): The effects of salinity on seed germination in perennial ryegrass (*Lolium perenne* L.) varieties. – *J Agric Na Sci* 2: 78-84.
- [74] Lameirão, F., Pinto, D. F., Vieira, E. F., Peixoto, A., Freire, C., Sut, S., Rodrigues, F. (2020): Green-sustainable recovery of phenolic and antioxidant compounds from industrial chestnut shells using ultrasound-assisted extraction. Optimization and evaluation of biological activities in vitro. – *Antioxidants* 9(3): 267.
- [75] Leclère, M., Jeuffroy, M. H., Butier, A., Chatain, C., Loyce, C. (2019): Controlling weeds in camelina with innovative herbicide-free crop management routes across various environments. – *Ind Crops Prod* 140: p.111605.
- [76] Lenssen, A. W., Iversen, W. M., Sainju, U. M., Caesar-Tonthat, T. C., Blodgett, B. L., Allen, B. L., Evans, R. G. (2012): Yield, pests, and water use of durum and selected crucifer oilseeds in two-year rotations. – *Agronomy J* 104: 1295-1304.

- [77] Liebman, M., Davis, A. S. (2000): Integration of soil, crop, and weed management in low-external- input farming systems. – *Weed Res* 40: 27-47.
- [78] Macías, F. A., Mejías, F. J., Molinillo, J. M. (2019): Recent advances in allelopathy for weed control: from knowledge to applications. – *Pest Manage Sci* 75: 2413-2436.
- [79] Malhi, S. S., Johnson, E. N., Hall, L. M., May, W. E., Phelps, S., Nybo, B. (2014): Effect of nitrogen fertilizer application on seed yield, N uptake, and seed quality of *Camelina sativa*. – *Cand J Soil Sci* 94: 35-47.
- [80] Malik, M. R., Tang, J., Sharma, N. et al. (2018): *Camelina sativa*, an oilseed at the nexus between model system and commercial crop. – *Plant Cell Rep* 37: 1367-138.
- [81] Mamolos, A. P., Kalburtji, K. L. (2001): Significance of allelopathy in crop rotation. – *J Crop Prod* 4: 197-218.
- [82] Maqbool, N., Wahid, A., Farooq, M., Cheema, Z. A., Siddique, K. H. M. (2012): Allelopathy and abiotic stress interaction in crop plants. – *Allelopathy* 451-468.
- [83] Matloob, A., Khaliq, A., Farooq, M., Cheema, Z. A. (2010): Quantification of allelopathic potential of different crop residues for the purple nut sedge suppression. – *Pak J Weed Sci Res* 16: 1-12.
- [84] Meynard, J. M., Charrier, F., Fares, M., Le Bail, M., Magrini, M. B., Charlier, A., Messéan, A. (2018): Socio-technical lock-in hinders crop diversification in France. – *Agron Sustain Dev* 38: 54.
- [85] Ming, Y., Zhu, Z. J., Li, J., Hu, G. X., Fan, X. M. and Yuan, D. Y. (2020): Allelopathic Effects of *Castanea henryi* aqueous extracts on the growth and physiology of *Brassica pekinensis* and *Zea mays*. – *Chem Biodiv*. DOI: 10.1002/cbdv.202000135.
- [86] Molisch, H. (1937): *Der Einfluss einer Pflanze auf die andere - Allelopathie*. – Fisher, Jena.
- [87] Morales, D., Potlakayala, S., Soliman, M., Daramola, J., Weeden, H., Jones, A., Kovak, E., Lowry, E., Patel, P., Puthiyaparambil, J., Goldman, S. (2017): Effect of biochemical and physiological response to salt stress in *Camelina sativa*. – *Commun Soil Sci Plant Ana* 48: 716-729.
- [88] Naranjo, S. E., Ellsworth, P. C., Dierig, D. A. (2011): Impact of *Lygus* spp. (Hemiptera: Miridae) on damage, yield and quality of *Lesquerella* (*Physaria fendleri*), a potential new oil-seed crop. – *J Eco Ento* 104: 1575-1583.
- [89] Naranjo, S. E., Stefanek, M. A. (2012): Feeding behavior of a potential insect pest, *Lygus hesperus*, on four new industrial crops for the arid southwestern USA. – *Ind Crops Prod* 37: 358-361.
- [90] Naseem, M., Aslam, M., Ansar, M., Azhar, M. (2010): Allelopathic effects of sunflower water extract on weed control and wheat productivity. – *Pak J Weed Sci Res* 15: 107-116.
- [91] Nawaz, A., Farooq, M., Cheema, S. A., Cheema, Z. A. (2014): Role of allelopathy in weed management. – *Recent Advances in Weed Management*. DOI: 10.1007/978-1-4939-1019-9\_3.
- [92] Nawaz, A., Sarfraz, M., Sarwar, M., Farooq, M. (2018): Ecological Management of Agricultural Pests Through Allelopathy. – Mérillon, J.-M., Ramawat, K. G. (eds.) *Coevolution of Secondary Metabolites*. Springer, Cham, pp. 1-33. DOI: 10.1007/978-3-319-76887-8\_17-1.
- [93] Obour, A. K., Sintim, H. Y., Obeng, E. et al. (2015): Oilseed camelina (*Camelina sativa* L Crantz): production systems, prospects and challenges in the USA great plains. – *Adv Plants Agric Res* 2: 68-76.
- [94] Olivier, C., Séguin-Swartz, G., Galka, B., Olfert, O. (2011): Aster yellows in leafhoppers and field crops in Saskatchewan, Canada, 2001-2008. – *Am J Plant Sci Biotechnol* 141: 425-462.
- [95] Pavlista, A. D., Hergert, G. W., Margheim, J. M., Isbell, T. A. (2016): Growth of spring *Camelina* (*Camelina sativa*) under deficit irrigation in western Nebraska. – *Ind Crops Prod* 83: 118-123.

- [96] Ponnampalam, E. N., Kerr, M. G., Butler, K. L., Cottrell, J. J., Dunshea, F. R., Jacobs, J. L. (2019): Filling the out of season gaps for lamb and hogget production: diet and genetic influence on carcass yield, carcass composition and retail value of meat. – *Meat Sci* 148: 156-163.
- [97] Prithiviraj, B., Perry, L. G., Badri, D. V., Vivanco, J. M. (2007): Chemical facilitation and induced pathogen resistance mediated by a root-secreted phytotoxin. – *New Phytol* 173: 852-860.
- [98] Rahman, M. J., de Camargo, A. C., Shahidi, F. (2018): Phenolic profiles and antioxidant activity of defatted camelina and Sophia seeds. – *Food Chem* 240: 917-925.
- [99] Rawat, L. S., Maikhuri, R. K., Bahuguna, Y. M., Jha, N. K., Phondani, P. C. (2017): Sunflower allelopathy for weed control in agriculture systems. – *J Crop Sci Biotechnol* 20: 45-60.
- [100] Razaq, A., Cheema, Z. A., Jabran, K., Farooq, M., Khaliq, A., Haider, G., Basra, S. M. A. (2010): Weed management in wheat through combination of allelopathic water extract with reduced doses of herbicides. – *Paki J Weed Sci Res* 16: 247-256.
- [101] Rizzitello, R., Zhang, C. J., Auer, C. (2019): Camelina (*Camelina sativa* L. Crantz) Crop performance, insect pollinators, and pollen dispersal in the northeastern US. – bioRxiv. DOI: <https://doi.org/10.1101/756619>.
- [102] Russo, V., Bruton, B., Sams, C. (2010): Classification of temperature response in germination of Brassicas. – *Ind Crops Prod* 31: 48-51.
- [103] Sagun, V. G., Auer, C. (2017): Pollen morphology of selected Camelinaeae (Brassicaceae). – *Palynol* 41: 255-266.
- [104] Saucke, H., Ackermann, K. (2006): Weed suppression in mixed cropped grain peas and false flax (*Camelina sativa*). – *Weed Res* 46: 453-461.
- [105] Saady, H. S. (2015): Maize cowpea intercropping as an ecological approach for nitrogen use rationalization and weed suppression. – *Arch Agron Soil Sci* 61: 1-14.
- [106] Schillinger, W. F., Wysocki, D. J., Chastain, T. G., Guy, S. O., Karow, R. S. (2012): Camelina: planting date and method effects on stand establishment and seed yield. – *Field Crops Res* 130: 138-144.
- [107] Schreiber, M. M. (1992): Influence of tillage, crop rotation and weed management on grain foxtail (*Setaria faberi*) population dynamics and corn yield. – *Weed Sci* 40: 645-653.
- [108] Scottish Rural Colleges (2013): Camelina: physical requirements. – [http://www.sruc.ac.uk/info/120186/novel\\_and\\_non-food\\_crops/166/camelina/3](http://www.sruc.ac.uk/info/120186/novel_and_non-food_crops/166/camelina/3).
- [109] Séguin-Swartz, G., Eynck, C., Gugel, R., Strelkov, S., Olivier, C., Li, J., Klein-Gebbinck, H., Borhan, H., Caldwell, C., Falk, K. (2009): Diseases of *Camelina sativa* (falseflax). – *Cand J Plant Pathol* 31: 375-386.
- [110] Sobiech, Ł., Grzanka, M., Kurasiak-Popowska, D., Radzikowska, D. (2020): Phytotoxic effect of herbicides on various *Camelina* [*Camelina sativa* (L.) Crantz] genotypes and plant chlorophyll fluorescence. – *Agric* 10: 185.
- [111] Sodaiezadeh, H., Hosseini, Z. (2012): Allelopathy: an environmentally friendly method for weed control. – International Conference on Applied Life Sciences (ICALS2012), Turkey, September 10-12.
- [112] Soroka, J., Olivier, C., Grenkow, L., Séguin-Swartz, G. (2015): Interactions between *Camelina sativa* (Brassicaceae) and insect pests of canola. – *Canad Entomol* 147: 193-214.
- [113] Sun, C., Cao, H., Shao, H., Lei, X., Xiao, Y. (2011): Growth and physiological responses to water and nutrient stress in oil palm. – *Afric J Biotechnol* 10: 10465-10471.
- [114] Tabatabaie, S. M. H., Murthy, G. S. (2017): Effect of geographical location and stochastic weather variation on life cycle assessment of biodiesel production from camelina in the northwestern USA. – *Int J Life Cycl Assess* 22: 867-882.
- [115] Taiz, L. and Zeiger, E. (2010): *Plant Physiology*, 5th Ed. – Sinauer Associates, Sunderland, MA. <https://www.sinauer.com/media/wysiwyg/tocs/PlantPhysiology5.pdf>.

- [116] Teasdale, J. R., Mohler, C. L. (2000): The quantitative relationship between weed emergence and the physical properties of mulches. – *Weed Sci* 48: 385-392.
- [117] Tursun, N., Işık, D., Demir, Z., Jabran, K. (2018): Use of living, mowed, and soil-incorporated cover crops for weed control in apricot orchards. – *Agron* 8: 150.
- [118] Voll, E., Franchini, J. C., Tomazon, R., Cruz, D., Gazziero, D. L., Brighenti, A. M. (2004): Chemical interactions of *Brachiaria plantaginea* with *Commelina bengalensis* and *Acanthospermum hispidum* in soybean cropping systems. – *J Chem Ecol* 30: 1467-1475.
- [119] Wang, Y., Frei, M. (2011): Stressed food - the impact of abiotic environmental stresses on crop quality. – *Agric Eco Environ* 141: 271-286.
- [120] Wang, C., Wu, B., Jiang, K. (2019): Allelopathic effects of Canada goldenrod leaf extracts on the seed germination and seedling growth of lettuce reinforced under salt stress. – *Ecotoxicol* 28: 103-116.
- [121] Waraich, E. A., Ahmed, Z., Ahmad, R., Saifullah, Shahbaz, M., Ehsanullah. (2016): Modulation in growth, development, and yield of *Camelina sativa* by nitrogen application under water stress conditions. – *J Plant Nut* 40: 726-735.
- [122] Waraich, E. A., Ahmed, Z., Ahmad, R., Shabbir, R. N. (2017): Modulating the phenology and yield of *camelina sativa* L. by varying sowing dates under water deficit stress conditions. – *Soil Environ* 36: 84-92.
- [123] Waśkiewicz, A., Muzolf-Panek, M., Goliński, P. (2013): Phenolic Content Changes in Plants under Salt Stress. – In: Ahmad, P. et al. (eds.) *Ecophysiology and Responses of Plants under Salt Stress*. Springer, New York, pp. 283-314. DOI: 10.1007/978-1-4614-4747-4\_11.
- [124] Ye, S. F., Zhou, Y. H., Sun, Y., Zou, L. Y., Yu, J. Q. (2006): Cinnamic acid causes oxidative stress in cucumber roots, and promotes incidence of *Fusarium* wilt. – *Environ Experi Bot* 56: 255-262.
- [125] Yohannes, G., Kidane, L., Beyene, T. (2020): Effect of salt stresses on seed germination and early seedling growth of *Camelina sativa* L. – *Ethiop J Sci* 12: 1-19.
- [126] Yuan, L., Li, R. (2020): Metabolic engineering a model oilseed *Camelina sativa* for the sustainable production of high-value designed oils. – *Front Plant Sci* 11. DOI: 10.3389/fpls.2020.00011.
- [127] Zhang, C. J., Auer, C. (2019): Overwintering assessment of *Camelina* (*Camelina sativa*) cultivars and congeneric species in the northeastern US. – *Ind Crops Prod* 139: 111532.
- [128] Zhang, C. J., Auer, C. (2020): Hybridization between *Camelina sativa* (L.) Crantz and common Brassica weeds. – *Ind Crops Prod* 147: 112240.

# REGIONAL FLOOD FREQUENCY ANALYSIS, USING L-MOMENTS, ARTIFICIAL NEURAL NETWORKS AND OLS REGRESSION, OF VARIOUS SITES OF KHYBER-PAKHTUNKHWA, PAKISTAN

KHAN, M. S. R.<sup>1\*</sup> – HUSSAIN, Z.<sup>2</sup> – AHMAD, I.<sup>1</sup>

<sup>1</sup>*Department of Mathematics and Statistics, International Islamic University, H-10 Islamabad, Pakistan*

<sup>2</sup>*Research Centre for Modelling and Simulation (RCMS), National University of Sciences and Technology (NUST), H-12 campus, Islamabad, Pakistan*

*\*Corresponding author*

*e-mail: shafeeq.phdst02@iiu.edu.pk; phone: +92-3347-603-022*

(Received 10<sup>th</sup> Aug 2020; accepted 19<sup>th</sup> Nov 2020)

**Abstract.** This study provides the results of flood frequency analysis adopting a regional approach using annual maxima's of peak flows (APF) of eight catchments located on various small rivers of Khyber-Pakhtunkhwa, Pakistan. Initial screening reveals that the recorded data of APF for all catchments are independent, random, free from significant trend and identically distributed. L-moments based heterogeneity measure indicates that the study region is homogeneous. The results of  $|Z\text{-Dist}|$  statistic and L-moment ratio diagram being goodness of fit measures are in favor of Generalized Pareto (GPA) distribution among five candidates of regional distribution. For the ungauged sites, flood quantiles have been estimated through OLS regression and artificial neural networks (ANN). The estimated quantiles using ANN method are relatively accurate compared to OLS regression. The historical assessment indicates that quantile estimates obtained through ANN and index flood method are close to the highest recorded APF values for shorter as well as longer return periods for each site.

**Keywords:** *annual maximum peaks, GPA distribution, L-moments, least squares regression, machine learning methods, ungauged sites*

**Abbreviations:** APF, Annual maxima's of Peak Flows; KPK, Khyber-Pakhtunkhwa; RFA, Regional frequency analysis; GPA, Generalized Pareto; GNO, Generalized Normal; GLO, Generalized Logistic; GEV, Generalized Extreme Value; PE3, Pearson Type-3; ANN, Artificial Neural Networks; OLS, Ordinary Least Square; RA, Regression Analysis; AARF, Average Annual Rainfall; long, Longitude; lat, Latitude; ele, Elevation; ARMS, Average Rainfall in Monsoon;  $l_1$ , first sample L-moment

## Introduction

Frequency analysis of extreme events (like floods, rainfall, winds and droughts, etc.) is necessary for effective planning and management against these natural disasters. Moreover the estimates of frequency analysis are also useful in design and development of hydrological structures such as dams, barrages, culverts, bridges etc., to ensure public safety and the effective use of surface water resources. For this purpose, different approaches are available in literature like at-site or regional. At-site frequency analysis may not be a preferred choice with a shorter or limited span of recorded data set at any site or is inapplicable for the estimation at any specific site with no observed record (ungauged site). Moreover, estimates using at-site frequency analysis may suffer from sampling variability especially with the shorter span of observed data while estimation for longer return periods (Cunnane, 1988; Hosking and Wallis, 1993). In this scenario,

regional frequency analysis (RFA) (combining sites based on similar site characteristics) is an optimum choice. Advantages of using RFA are many folds like more reliable estimation of quantiles at gauged sites and estimation or improvement of the quantiles at ungauged or partially/poorly gauged sites within the homogeneous region(s) through interpolation/extrapolation of the T-years quantiles of gauged sites. RFA using L-moments is a popular method of estimation and has been used frequently in various case studies worldwide. For example; in Canada, (Requena et al., 2017); in Norway, (Hailegeorgis and Alfredsen, 2017); in Iran, (Mesbahzadeh et al., 2019); in India, (Alam et al., 2016); in Korea, (Lee and Kim, 2019); in China, (Yang et al., 2010); in Turkey, (Aydoğan et al., 2016). GREHYS (1996a, b) provided a detailed comparison of several regional flood estimation procedures. A brief of the development in RFA has been illustrated in Malekinezhad and Zare-Garizi (2014). RFA has been applied in few of the published studies related to Pakistan. These include Hussain and Pasha (2009), Hussain (2011), Ahmad et al. (2017), Shahzadi et al. (2013), Ahmad et al. (2013, 2016), Batool (2017), Khan et al. (2017), Fawad et al. (2018, 2019). Few highlighted points in the some published literature related to flood frequency analysis in Pakistan are:

The study of Hussain and Pasha (2009) is the first application (to the best of authors' knowledge) of L-moments based RFA in Pakistan. The study area consists of seven sites of three major rivers of Punjab namely Jhelum, Chenab and Ravi with annual maximum peak flows as the main variable for analysis. The results of various accuracy measures calculated through simulation experiments reveal that Generalized Normal (GNO) Distribution is the robust distribution for the study area.

In another study, Hussain (2011) used annual maximum peak flows of seven sites located on the mainstream of the biggest river of the river systems of Pakistan namely the Indus River. The study area was divided into two regions, the upper half containing four sites (Tarbela, Kalabagh, Chashma and Taunsa) and the lower half containing three sites (Guddu, Sukkur and Kotri). Pearson Type-3 (PE3) was identified as robust regional distribution for the upper half while Generalized Logistic (GLO) Distribution for the sites of the lower half of the region.

The study of Ahmad et al. (2017) performed L-moments based RFA using 10 days average of low flows of nine sites belong to the different rivers of river systems of Pakistan. The study area includes 6 sites of Indus River (Tarbela, Kalabagh, Chashma, Tausa, Guddu and Sukkur), 1 site of Kabul River (Nowshera), 1 site of Jhelum River (Mangla) and 1 site of Chenab River (Marala). The study area was divided into two homogeneous regions (Region 1 consisting of Tarbela, Nowshera, Kalabagh and Taunsa while Region 2 includes Chashma, Guddu, Mangla and Marala) using basin drainage area in square miles and mean annual minimum flow. The study concluded that the best fit distribution for Region 1 is GNO and for Region 2 is Generalized Pareto (GPA).

Hussain (2017) analysed various sites of the major rivers located in Punjab, Pakistan namely Jhelum, Chenab, Ravi and Sutlej using L-moments based RFA. The results showed that the best-fitted regional distribution, for the region consisting of two sites (Trimmu and Panjnad) at the confluence of the rivers is PE3, while for the region consisting of the rest of the nine sites (Mangla, Rasul, Marala, Khanki, Qadirabad, Balloki, Sidhnai, Suleimanki and Islam) is GNO. Similar results have been reported in Hussain and Pasha (2009). Moreover, a multiple linear regression model in log transformed form was developed to estimate the mean value of the APF for ungauged locations using average rainfall during monsoon and catchment area of the corresponding rivers as explanatory variables. Adequacy of the developed regression

model was established using statistical measures and comparison of the estimated floods with historical flood information available at the gauged sites.

The aforementioned details reveal that the catchments of major rivers located in Punjab and the Indus River have been the focus of the published studies so far. Therefore, there is a need to adopt standard procedures for analyzing APF of small rivers and streams of other parts of the country, especially Khyber Pakhtunkhwa (the north-western area of Pakistan). An important feature of these rivers or streams is that most of them originate in Pakistan with natural flows and are not or less affected by man-made changes like construction of barrages and dams, etc. Furthermore, floods are increasing in frequency and intensity in Pakistan by the year 2000 and their trends are alarming from 2010 onwards (Government of Pakistan, 2016). The area of KPK is known as more vulnerable to flash flooding due to its steep geography and mountainous land. This region is badly affected from flash floods in 1992 and 2010 (Pakistan Meteorological Department, 2012). Therefore, estimation of magnitude and frequency associated to these floods is a desperate need for the area of KPK to generate flood risk maps, management of stream water and feasibilities/designing of new hydraulic structures for the rivers and streams located in the province using a standard methodology available in details in Hosking and Wallis (1997).

In RFA, various methods are used to develop and estimate the forecast equation for ungauged sites. These methods include regression with linear/non-linear approaches (Griffis and Stedinger, 2007; Sivakumar and Singh, 2012; Hailegeorgis and Alfredsen, 2017; Ouali et al., 2017), artificial neural networks (Aziz et al., 2014; Anilan et al., 2016), satellite precipitation products (Gado et al., 2017), remotely sensed precipitation information (Faridzad et al., 2018), etc. None of the adopted method(s) so far received universal acceptability; however, success depends on the availability and suitability of gauged site characteristics. Anilan et al. (2016) illustrated details of commonly used site characteristics as independent variables in different studies around the world for estimation at ungauged sites adopting regression and ANN methods. These site characteristics are drainage area, slope of stream, and mean annual rainfall. Availability and identification of the most influential site characteristics that can be used for the estimation at ungauged site within the region is an ongoing area of research. Development of an adequate model depends on the site characteristics having significant relationship with the recorded data sets at gauged sites. This study has used available or significant site characteristic(s) using ANN and regression methods, emphasizing the justification of critical assumptions associated with the estimation procedures. In addition, a comparison has been made with the historical flood data to evaluate the reliability of the given estimates using different methods.

Main objectives of the study are:

- i. Estimation of flood quantiles at gauged sites of important rivers/streams of the area of KPK using L-moments based RFA.
- ii. Development of a suitable relationship for the estimation of quantiles at ungauged sites.
- iii. Historical comparison of the provided estimates for validity and reliability of the provided estimates.



## Materials and Methods

### Study area and data descriptions

APF in cusecs, of eight sites of important rivers of KPK, Pakistan namely Naranji, Bagiari, Dallus, Shahi Bala, Garandi, Chprial, Shah Alam, and Kalpani Raisalpur, have been used to perform RFA. The observed flow record and the site characteristics are provided by Provincial Irrigation Department of KPK. Details of the site characteristics including average annual rainfall (AARF), longitude (long), latitude (lat), elevation (ele), and average rainfall during monsoon season (ARMS) are given in *Table 1*. There are few missing observations in the data at sites Naranji, Bagiari, Shahi Bala, Chprial, Jani Khwar, and Kalpani Raisalpur. *Table 1* also illustrates the percentage of these missing observations. These missing values are estimated by the averages of APF at the respective sites. Geographical locations of the eight sites are given in *Fig. 1*.

**Table 1.** Site characteristics and details of missing observations of eight sites of Khyber-Pakhtunkhwa, Pakistan

S. No.	Site Name	Latitude (North)	Longitude (East)	Elevation (meters)	AARF (mm)	ARMS (mm)	Percentage of MO
1	Naranji	34.2480	72.3427	356	639	272	6
2	Bagiari	34.2254	72.1543	313	559	227	10
3	Dallus	34.1650	71.5931	310	460	151	0
4	Shah Alam	34.1669	71.3689	397	422	204	0
5	Shahi Bala	34.1702	71.7466	300	460	151	12
6	Chprial	34.9866	72.3520	1243	478	212	6
7	Garandi	34.0869	71.4719	328	384	105	0
8	Kalpani Raisalpur	34.3303	71.9085	345	556	222	6

Note: average annual rainfall (AARF); average rainfall during monsoon (ARMS); missing observations (MO), *mm* denotes millimeter

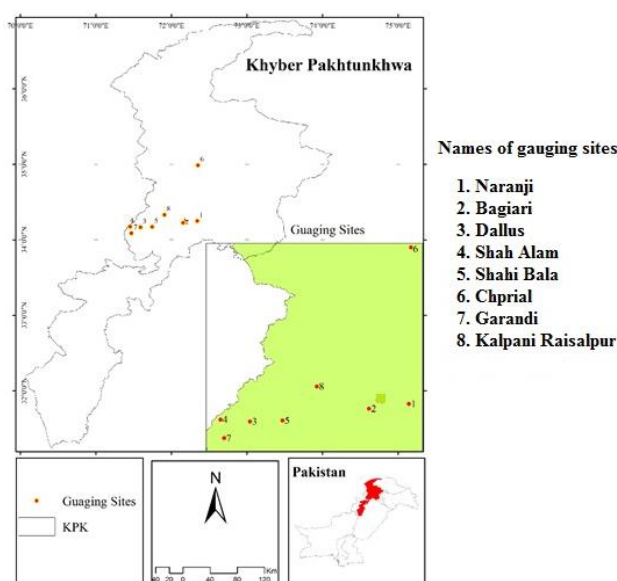


**Figure 1.** Study area and geographical locations of the sites of Khyber-Pakhtunkhwa, Pakistan

### Data preprocessing

This section provides details of measures related to data preprocessing for RFA.

#### Run test

Run test of randomness given in (Bradley, 1968; Hirsch et al., 1992) has been used to check the randomness of APF at each site. The test statistics of Run test for large sample is:

$$Z = \frac{R - E(R)}{S.E.(R)} \quad (\text{Eq.1})$$

Here,  $R$  is the total number of runs,  $E(R)$  is the expected value of  $R$ ,  $S.E.(R)$  is the standard error of  $R$ .

#### Rank Sum test

To validate the assumption of the identical distribution of the data of each site, Rank-Sum test has been used. The details of this test are available in Hirsch et al., 1992.

For small samples, i.e. if  $n_1$  and  $n_2$  are less than ten, following test statistics is used

$$W = \text{mini}(W_1 - W_2)$$

where,  $W_1$  is the sum of the rank of first group and  $W_2$  is the sum of the rank of the second group.

In case of large sample, i.e. greater than ten, the test statistic is

$$Z_w = \frac{W - \mu_w}{\sigma_w} \quad (\text{Eq.2})$$

Here

$$\mu_w = \frac{n_1(n_1+n_2+1)}{2} \text{ and } \sigma_w = \sqrt{\frac{n_1n_2(n_1+n_2+1)}{12}}$$

#### Wald-Wolfowitz test

An important assumption with respect to the data that it is independent and free from significant trends is tested through the Wald-Wolfowitz test (Wald and Wolfowitz, 1943). For a sample size of less than ten, the test statistics is given as:

$$K = \sum_{i=1}^{n-1} x_i x_{i+1} + x_1 x_n$$

With expected mean and variance

$$\mu_k = \frac{s_1^2 - s_2}{n-1}, \text{ and } \sigma_k^2 = \frac{s_2^2 - s_4}{n-1} - E(K)^2 + \frac{s_1^4 - 4s_1^2s_2 + 4s_1s_3 + s_2^2 - 2s_4}{(n-1)(n-2)},$$

with  $s_t = \sum_{i=1}^n x_i^t, t = 1,2,3,4$

For large sample, i.e. greater than ten, the test statistics is:

$$Z_{ww} = \frac{K - \mu_k}{\sigma_k} \quad (\text{Eq.3})$$

### Measures of RFA

Discordancy measure ( $D_i$ ) has been calculated for each site within the initial group of sites to check whether any site is discordant or not. Formula to calculate  $D_i$  is:

$$D_i = \frac{1}{3} N(t_i - \bar{t})^T S^{-1} (t_i - \bar{t}), \quad i = 1,2,3, \dots, N$$

$$S = \sum_{i=1}^N (t_i - \bar{t}) (t_i - \bar{t})^T \quad (\text{Eq.4})$$

where  $t_i$  and  $\bar{t}$  are the  $i$ th site sample L-moments ratios and their means respectively.  $N$  is the total number of sites in the region.

Heterogeneity measures have been calculated to check the homogeneity of the region. The statistic to compute heterogeneity measure ( $H$ ) is:

$$H = \frac{V - \mu_v}{\sigma_v} \quad (\text{Eq.5})$$

where  $V = \left[ \frac{\sum_{i=1}^N n_i (\tau^i - \tau^R)^2}{\sum_{i=1}^N n_i} \right]^{\frac{1}{2}}$  and  $\mu_v$  is average value and  $\sigma_v$  is the simulation-based standard deviation obtained by fitting four-parameters Kappa distribution.

|Z-Dist| statistic has been used as a goodness-of-fit criterion. The formula for |Z-Dist| is:

$$|\text{Z-Dist}| = \frac{\tau_4^{\text{Dist}} - \tau_4^R + \beta_4}{\sigma_4} \quad (\text{Eq.6})$$

where  $\tau_4^{\text{Dist}}$  is L-kurtosis of candidate probability distribution, regional L-kurtosis is  $\tau_4^R$ , its bias is  $\beta_4$  and the standard deviation is  $\sigma_4$  calculated through simulations.

The regional quantiles using quantile function of the best-fitted regional distribution are used to estimate at-site flood quantiles using the following equation:

$$\hat{Q}_i(F) = l_1^{(i)} \hat{q}(F) \quad (\text{Eq.7})$$

For site  $i$ ,  $\hat{Q}_i(F)$  is flood quantile at given return period,  $l_1^{(i)}$  is mean of APF and  $\hat{q}(F)$  is regional quantile

### Artificial neural networks

ANN is receiving increasing popularity in statistical hydrology. This study uses back propagation neural network (BPNN) because of its suitability for prediction of river flows (Maier and Dandy, 2000; Abrahart et al., 2004). The model comprises an input, hidden and output layers. Neuron layers interact via a network of feed forward weighted connection. For computations, every input of the neurons multiplied by weight which is known as connection parameter and combined output with some bias is produced. This value is managed with an activation function. Logistic activation function is used because it provides accurate results for river flow prediction (Shamseldin et al., 2002). A typical logistic activation function is given below.

$$f(x) = \frac{1}{1+e^{-x}} \quad (\text{Eq.8})$$

The relationship between the mean of the APF of each site ( $l_i$ ) and site characteristics of the region is estimated using ANN model.  $l_i$  is the estimated or dependent variable and the site characteristics are used as an input or independent variables of the model.

## Results and Discussion

### Data preprocessing

The results for the validation of critical assumptions for the data at each site of the region are provided in *Table 2* including test statistics and their respective p-values.

**Table 2.** Test statistics calculated and corresponding p-values of the Run Test, Rank Sum Test and Wald-Wolfowitz Test of eight sites of KPK, Pakistan

S. No.	Site name		Run Test	Rank Sum	Wald-Wolfowitz
1	Naranji	Test statistic	-0.4460	-1.6560	0.9353
		P-value	0.6556	0.0977	0.3496
2	Bagiari	Test statistic	0.2930	1.3400	1.6385
		P-value	0.7695	0.1802	0.1013
3	Dallus	Test statistic	-1.0590	-0.6900	1.2807
		P-value	0.2892	0.4902	0.2003
4	Shah Alam	Test statistic	0.3716	-0.6640	-0.2300
		P-value	0.7102	0.5067	0.8181
5	Shahi Bala	Test statistic	-0.7675	-0.4080	1.9036
		P-value	0.4427	0.6833	0.0570
6	Chprial	Test statistic	-1.0890	1.6010	1.5120
		P-value	0.2762	0.1094	0.1305
7	Garandi	Test statistic	0.7188	1.1350	-1.0420
		P-value	0.4723	0.2564	0.2973
8	Kalpani Raisalpur	Test statistic	-0.3483	1.4670	1.0960
		P-value	0.7276	0.1424	0.2729

The results of *Table 2* illustrate that the data of all sites fulfill important assumptions of RFA procedure at 5% significance level. Therefore, it is suitable to perform RFA.

The descriptive statistics in term of L-moments and values of  $D_i$  for each site using *Equation 4* are given in *Table 3*. The critical value of  $D_i$  for eight sites is 2.14 (Hosking and Wallis, 1997). The results of *Table 3* show that the value of  $D_i$  for the site “Garandi” is slightly greater than the critical value of 2.14. Therefore, there is a need for close examination of the observed data series at this site. A time series plot of APF of the site Garandi is illustrated in *Fig. 2*. The plot shows high variations (like observation number 25 in the year 2003) and a gradual decreasing pattern from observations number 16 to 20 (from the year 1994 to 1999). Importantly, these changes did not affect the statistical randomness of the observed APF but increased the values of L-skewness and L-kurtosis at this site, resultantly a slightly higher value of  $D_i$ .

**Table 3.** Descriptive statistics and discordancy measures of eight sites of KPK, Pakistan

S. No.	Site Names	n	$l_1$	t	$t_3$	$t_4$	$t_5$	$D_i$
1	Naranji	52	5447.02	0.445	0.333	0.235	0.151	1.57
2	Bagiari	31	5767.03	0.488	0.218	-0.037	0.013	1.06
3	Dallus	25	8196.84	0.474	0.252	0.066	-0.030	0.22
4	Shah Alam	30	7343.07	0.400	0.265	0.048	-0.011	0.84
5	Shahi Bala	25	2792.40	0.514	0.242	0.067	0.043	0.88
6	Chpriar	34	10479.75	0.442	0.263	0.065	0.026	0.12
7	Garandi	33	1004.63	0.449	0.374	0.172	0.108	2.21
8	Kalpani Raisalpur	34	34773.34	0.368	0.336	0.159	0.075	1.10

Note: n is the number of observations at each site,  $l_1$  is the first sample L-moment, t is the sample L-CV,  $t_3$  is the sample L-skewness,  $t_4$  is the sample L-kurtosis,  $t_5$  is the sample L-moment ratio based on 5<sup>th</sup> sample L-moment and  $D_i$  is the discordancy measure

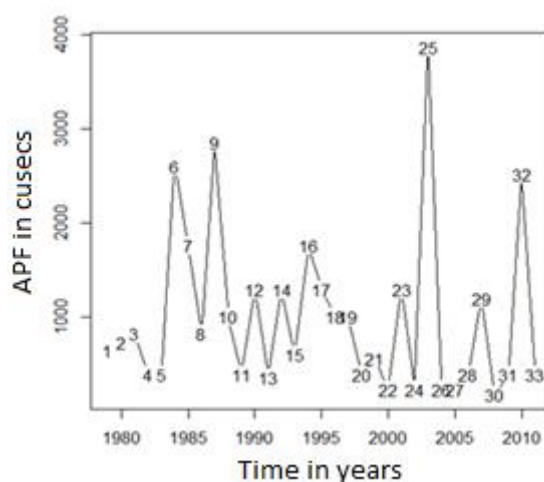


**Figure 2.** Time series plot of the site Garandi

Keeping in view that few abrupt changes are typical in extreme value analysis, the observed APF at this site have passed other preprocessing steps and less number of sites in the region, this site has been retained for further analysis. The study of Hussain and

Pasha, 2009 had also suggested retaining a site with a  $D_i$  value less than 3 and no serious irregularities or inconsistencies in the observed data series.

### Heterogeneity measures

The study area consists of eight geographically contiguous sites. Therefore, it is reasonable to assume that the factors influencing the site's flow behavior are homogenous in nature. Keeping this in view, the group of eight sites is treated as a region and heterogeneity measures are calculated using Equation 5. The values of  $H$  based on first three sample L-moment ratios are 0.52, -0.41 and 0.48, respectively; suggesting that the region is definitely homogeneous and suitable to perform RFA.

### Goodness of fit measures

To find the best fit regional distribution for the study area, estimated values of  $|Z\text{-Dist}|$  statistic obtained through Equation 6 for five standard three-parameter distributions in the family of extreme value distributions, i.e. Generalized Extreme Value (GEV), Generalized Pareto (GPA), GNO, GLO and PE3 are available in Table 4. These findings indicate that only one distribution, i.e. GPA distribution fulfils the criteria of best fit regional distribution (having value of  $|Z\text{-Dist}| \leq 1.64$ ).

**Table 4.** Values of  $|Z\text{-Dist}|$  statistic for each candidate distributions

Distributions	GLO	GNO	GEV	GPA	PE3
$ Z\text{-dist} $	5.23	3.29	4.12	1.09	1.85

L-moment ratio diagram (a graphical goodness of fit procedure), provided in Fig. 3, shows that average point of sample L-skewness and L-kurtosis lies closest to the theoretical curve of GPA distribution so as the tendency of the points, i.e. sample L-kurtosis and L-skewness for eight sites. Therefore, L-moment ration diagram (like  $|Z\text{-Dist}|$  statistic) favors GPA distribution as best-fit regional distribution. The results of both goodness-of-fit measures are in agreement to each other.

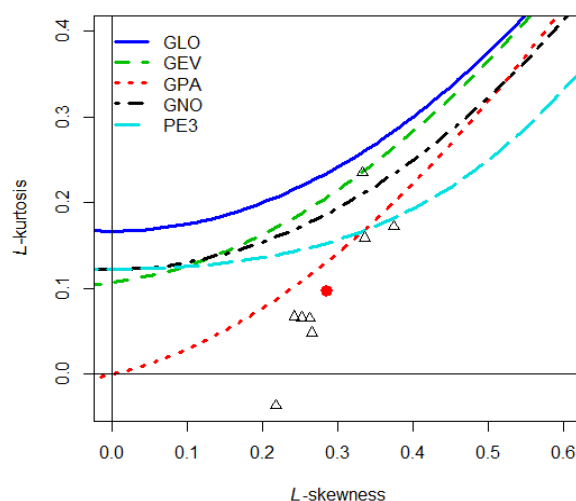


**Figure 3.** L-moment ratio diagram of the region

### Estimates of parameters of regional distribution and quantiles

After the selection of GPA as best-fit regional distribution, its parameters have been estimated by the method of L-moments. The quantile function of GPA distribution has been used to estimate the regional flood quantiles for 5, 10, 20, 50 and 100 years return periods and results are provided in *Table 5*.

**Table 5.** Estimated parameters of GPA distribution and regional quantiles for various return periods in years

Distribution	Estimated Parameters			Quantiles				
	$\varepsilon$	$\alpha$	k	5	10	20	50	100
GPA	0.0685	1.0209	0.0960	1.5910	2.1775	2.7264	3.3980	3.8682

Estimated quantiles at each site using *Equation 7* are given in *Table 6* for 5, 10, 20, 50 and 100 years return periods.

**Table 6.** Estimated quantiles at each site using *Equation 4* for various return periods

S. No.	Site names	At-site quantiles				
		5	10	20	50	100
1	Naranji	8666	11861	14851	18509	21070
2	Bagiari	9175	12558	15723	19596	22308
3	Dallus	13041	17849	22348	27853	31707
4	Shah Alam	11683	15990	20020	24952	28404
5	Shahi Bala	4443	6080	7613	9489	10802
6	Chpriar	16673	228120	28572	35610	40538
7	Garandi	1598	2188	2739	3414	3886
8	Kalpani Raisalpur	55324	75719	94806	118160	134510

### Estimation for ungauged sites using OLS regression and ANN

As mentioned earlier that this study has used OLS regression and ANN to develop a model with dependent variable  $l_1$  (at-site mean of APF) and site characteristics as independent variables. The estimates of the model will be used to predict the mean of APF for an ungauged site within the homogeneous region. This estimated mean can be used to predict the quantiles of ungauged site using index flood procedure.

#### Development of OLS regression model

For the development of a log-transformed simple linear regression model, the most relevant site characteristic is used as an independent variable. The development of multiple linear regression model has not been considered due to the presence of strong significant correlations between the explanatory variables (i.e. the problem of multicollinearity). The details of the procedure are:

To identify the most important site characteristic among available, i.e. having the highest degree of linear relationship with  $l_1$ , correlations between  $l_1$  and site characteristic have been calculated. This correlation matrix is provided in *Table 7*.

**Table 7.** Correlations between  $l_1$  and site characteristics. Parenthesis include P-values for testing the significance of correlation coefficient

	$l_1$	Latitude	Longitude	Elevation	AARF	ARMS
$l_1$	1.0000	0.2366 (0.5727)	0.1434 (0.7348)	0.0564 (0.8945)	0.3343 (0.4143)	0.3426 (0.4061)
Latitude	0.2366	1.0000	0.6333 (0.0919)	0.9677 (0.0001)	0.1221 (0.7733)	0.3318 (0.4220)
Longitude	0.1434	0.6333	1.0000	0.4913 (0.2163)	0.7767 (0.0234)	0.7188 (0.0445)
Elevation	0.0564	0.9677	0.4913	1.0000	-0.0776 (0.8551)	0.1847 (0.6615)
AARF	0.3343	0.1221	0.7767	-0.0776	1.0000	0.8601 (0.0061)
ARMS	0.3426	0.3318	0.7188	0.1847	0.8601	1.0000

Results of *Table 7* show that the correlation between  $l_1$  and ARMS is highest and statistically significant. Therefore, ARMS can be chosen as the most relevant variable for the development of simple linear regression model. However, for further investigation of the choice of ARMS as the most suitable independent variable, the frequencies of recorded APF at eight sites during four seasons of a year namely summer (monsoon), autumn, winter and spring have been calculated to observe the trends of occurrence of APF in a season, if any. The percentages of these frequencies of occurrence are illustrated in *Table 8*. These values show that the highest percentage of frequencies of occurrence of APF at all sites is in the monsoon season. Therefore, ARMS is the most suitable variable for the development of a simple linear regression model.

**Table 8.** Percentage (%) of frequencies of occurrence of APF in four seasons of a year.

S. No.	Site names	$n_i$	Monsoon (%)	Autumn (%)	Winter (%)	Spring (%)
1	Naranji	52	84	12	2	2
2	Bagiari	31	80	4	10	6
3	Dallus	25	60	8	8	24
4	Shah Alam	30	80	0	0	20
5	Shahi Bala	25	74	12	0	14
6	Chpriar	34	59	0	3	38
7	Garandi	33	67	9	9	15
8	Kalpani Raisalpur	34	82	3	6	9

Note: The time period for Monsoon is from June to September, autumn is from October to November, winter is from December to February and spring is from March to May

Based on the above discussion, the model using OLS estimation method in log-transformed form is:

$$\ln(\hat{l}_1) = 1.6702 \ln(ARMS) \quad (\text{Eq.9})$$

The intercept term is not included in the model as being statistically insignificant (at 5% level of significance), high standard error and practically insignificant, i.e. there is supposed to be no flood in the region with the value of ARMS as zero (the floods in



Pakistan are usually dependent on the monsoon rainfall (Hussain and Pasha, 2009)). For the estimated model in Equation 9, the value of  $R^2$  (coefficient of determination) is 0.9931 and adjusted- $R^2$  is 0.9921. This show that the linear regression line fits the data of 8 sites adequately. The estimated regression coefficient, standard error of the estimate, t-calculated and its corresponding p-value are given in Table 9. Results of Table 9 show that the estimated regression coefficient is statistically significant with low standard error.

**Table 9.** Results of fitted regression model. Here ARMS is average rainfall in monsoon season and S.E. is standard error of the regression coefficient

	<b>Coefficient</b>	<b>S.E.</b>	<b>t-value</b>	<b>P-value</b>
<b>ln (ARMS)</b>	1.6702	0.0525	31.81	0.0000

These details show that the model is adequate, still, assumptions related to the error term (normality, zero mean and homoscedasticity) are requisite (for details, see Gujarati, 2003). To check these assumptions, normal probability plot of residuals (illustrated in Fig. 4) and Anderson-Darling normality test with the null hypothesis that “the residuals follow normal distribution” have been applied. The calculated value of Anderson-Darling test statistic is 0.268 with its corresponding p-value as 0.58. As the p-value exceeds 5% level of significance; therefore, we are unable to reject the null hypothesis that the error term follows normal distribution. Moreover, the probability plot of residuals in Fig. 4 indicate that the normality assumption with respect to residuals seems appropriate as the points follow the straight line, with a standard deviation of 0.78 and mean as zero. To check for the homoscedasticity of the error term, White's Test for heteroscedasticity has been applied under the null hypothesis that the variances for the errors are equal. The corresponding test statistic for White's test is  $W = 0.0260$  with the corresponding p-value as 0.88. This shows that we are unable to reject that the residuals are homoscedastic. All these details show that the estimated regression model in Equation 9 is an adequate fit. Therefore, can be used to predict  $l_1$  for each ungauged site within the homogeneous region.

#### Artificial neural networks

For the application of machine learning methods, the complete data set is usually divided into training, validation and test datasets with the ratio of 60 percent, 20 percent and 20 percent, respectively. This division is useful for large data. In the present study, leave one out cross-validation (LOOCV) approach is used for the training and validation of the sample data set as it is usually considered more useful for smaller data sets. In LOOCV approach, the data set is divided into two parts; if the data set contains  $n$  observations, then one observation is used for the validation, i.e.  $(x_1, y_1)$  and remaining " $n - 1$ " observations  $\{(x_2, y_2), (x_3, y_3), \dots, (x_n, y_n)\}$  are in training dataset to predict the average value of the dependent variable (which is  $\hat{l}_1$  in this case). This process is repeated  $n$  times (equals to the total number of observations in the sample) and generate  $n$  times mean square error. The estimate of test mean squared error can be obtained from  $n$  test errors as:

$$CV_{(n)} = \frac{1}{n} \sum_{i=1}^n MSE_i \quad (\text{Eq.10})$$

where MSE denotes mean squared error. For more details of this method see James et al. (2013) and Kuhn and Johnson (2013). The primary objective of training of ANN is to reduce the error among the target output and ANN output through adjusting weights.

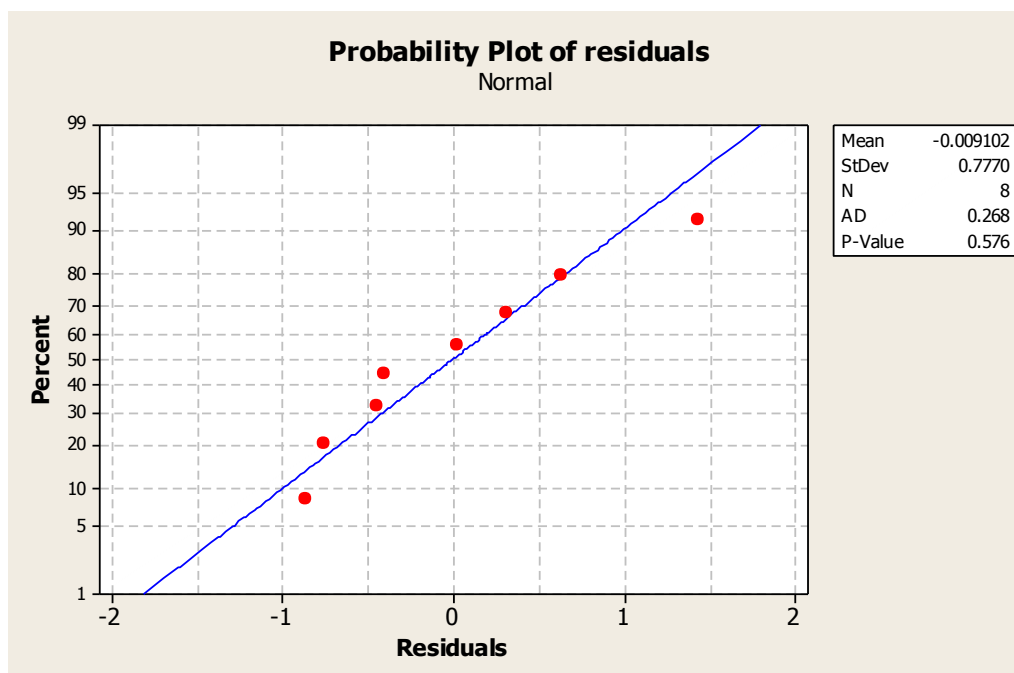


**Figure 4.** Probability plot of estimated residuals, number of observations ( $N$ ), arithmetic mean (mean), standard deviation ( $StDev$ ) and Anderson-Darling test statistic ( $AD$ ) with the corresponding  $p$ -value

The “caret” package of R-language has been used for the training of ANN. To select the best ANN model, different combinations of hidden layers and neurons have been observed against the MSE of observed and fitted mean values ( $\hat{l}_1$ ) of the entire region. The model with minimum MSE relative to other models has been selected. ANN algorithm with two hidden layers, four neurons in the first layer and two in the second layer, have been used. To avoid overfitting of the model so as ensuring the quality of the developed ANN model, testing MSE and training MSE have been compared. Training of ANN has been terminated for an observed increase in the test MSE or even decrease in the training MSE. The function of input and output variables is:

$$f(l_1) = g(lat, long, ele, AARF, ARMS) \quad (Eq.11)$$

Few of the published studies have also developed such ANN model with only two input variables and three hidden layers for the estimation of floods, for instance, Aziz et al. (2014). The graphical representation of the fitted model is shown in Fig. 5.

Predicted values of  $l_1$  by using ANN and OLS regression methods are provided in Table 10. The results show that predicted values of  $l_1$  through ANN are close to their true values relative to regression estimates.

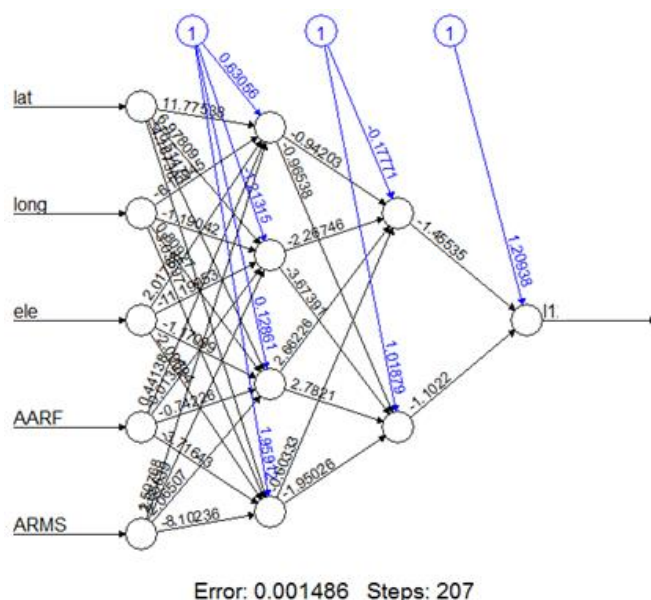


**Figure 5.** Graphical representation of ANN procedure to show the convergence of the model. Average annual rainfall (AARF), longitude (long), latitude (lat), elevation (ele), average rainfall during monsoon season (ARMS) and  $l_1$  is the mean of APF of each site

**Table 10.** Estimated values of  $l_1$  of gauged sites through ANN and regression analysis (RA)

S. No.	Site name	$l_1$ (observed)	$l_1$ (fitted) using ANN	$l_1$ (fitted) using RA
1	Naranji	5447	5306	11648
2	Bagiari	5767	6516	8611
3	Dallus	8197	8705	4359
4	Shah Alam	7343	7311	7204
5	Shahi Bala	2792	2236	4359
6	Chpriar	10480	11034	7682
7	Garandi	1005	979	2376
8	Kalpani Raisalpur	34773	33383	8297

### Practical validation of the estimates

The estimates of flood quantiles obtained through RFA are accurate and reliable but their practical validation is still crucial. For this assessment, a comparison is given in *Table 11* where the estimated quantiles are compared with the first and second highest values of APF for each respective site. Results of *Table 11* show that the predicted quantiles through OLS regression analysis for smaller return period (10 years) are comparable with the highest values of observed APF for Naranji, Bagiari, Shah Alam, Shahi Bala, Chpriar and Garandi sites. A notable point is that the OLS regression analysis provides reasonably close estimates of flood quantiles within the span of the observed data. The estimated quantiles using OLS regression analysis for longer return periods (100 years) or outside the available span of the data, show large deviations from highest values of observed APF for all the sites. This is a usual and major disadvantage of using OLS regression analysis for estimating flood quantiles for longer return periods or beyond the span of the observed data series.

The comparison further reveals that the estimated flood quantiles obtained using RFA are nearly close to the highest values of observed APF of all the sites for shorter and longer return periods. This shows the strength of the adopted procedure for the estimation of quantiles. Moreover, the comparison of the estimated quantiles using ANN reveals that the estimates are accurate and close to the highest values of APF for all the sites. Therefore, ANN would be a preferred method relative to OLS regression for estimation at ungauged sites within the region.

**Table 11.** Comparison of estimated flood quantiles using RFA, artificial neural networks (ANN) and regression analysis (RA) with highest observed APF at various sites

S. no.	Site name	Highest observed values of APF (year)		Estimates using RFA			Estimates using ANN			Estimates using RA		
		Highest	2 <sup>nd</sup> Highest	10	20	100	10	20	100	10	20	100
1	Naranji	30000 (2010)	15704 (1997)	11861	14851	21070	11554	14466	20524	25364	31757	45057
2	Bagiari	16688 (2006)	16023 (2010)	12558	15723	22308	14188	17764	25204	18751	23478	33310
3	Dallus	21700 (2010)	19984 (2006)	17849	22348	31707	18954	23732	33671	9491	11884	16860
4	Shah Alam	20000 (2010)	18513 (2005)	15990	20020	28404	15919	19931	28278	15687	19641	27867
5	Shahi Bala	8911 (1995)	7427 (1996)	6080	7613	10802	4870	6097	8651	9491	11884	16860
6	Chpriar	33836 (1993)	24639 (2003)	22820	28572	40538	24025	30082	42680	16728	20945	29716
7	Garandi	3869 (2003)	2860 (1987)	2188	2739	3886	2133	2670	3789	5173	6478	9190
8	Kalpani Raisalpur	118604 (2010)	80615 (2008)	75719	94806	134510	72691	91015	129131	18066	22621	32094

## Summary and Conclusion

The results of this study contributes in terms of unique area of study for the application of L-moments based RFA, emphasizes on the justification of basic assumptions associated to RFA, application of ANN to estimate floods and so on. Few key findings are summarized below:

For preprocessing of the APF at various sites, necessary assumptions have been tested using nonparametric tests. The findings show that the recorded data sets at all sites are random, independent, identically distributed, and free from significant trends. The values of discordancy statistic  $D_i$  show that the site “Garandi” is discordant in the group of eight sites. One possible reason for the slightly higher value of  $D_i$  may be high skewness of the data due to the presence of high outliers. In flood estimation, high outliers should not be discarded from the data. Moreover, considering the fewer number of sites for the analysis and the observed APF have passed the other preprocessing steps related to RFA; the site “Garandi” is retained in the analysis.

The estimates of L-moment ratios showed that there exists deviations in the recorded data series at various sites. However, the L-kurtosis values are comparatively small then the L-skewness values. One possible reason for these fluctuations is the erratic cycles of monsoon rainfall because floods in Pakistan usually rely on the extreme spells of

monsoon rainfall. Hussain (2017) found similar results for the sites of river basins in Punjab, Pakistan.

The set of eight sites is homogenous as confirmed by the heterogeneity measure based on L-moments. After the confirmation of homogeneity in the region, L-moment ration diagram and  $|Z\text{-Dist}|$  statistic showed that GPA distribution is the best-fit regional distribution. Estimates of regional quantiles show the rising trend for smaller to longer return periods and larger than the mean values of recorded APF of each site. The results of this study reveal that the shape/distribution associated to the frequency of observed APF for the sites of north-western streams and rivers of the country is different relative to the sites of the Indus River and its major eastern tributaries. For the region of KPK, the identified regional distribution is GPA while for the sites of the Indus River and its eastern tributaries these are GNO, GLO or PE3, etc. as suggested in Hussain and Pasha (2009), Hussain (2011, 2017), and Ahmad et al. (2017). This shows that the observed APF of various sites of the current study area has low L-kurtosis values against high values of L-skewness.

OLS regression and ANN methods have been used to predict the average of APF for ungauged sites. Comparison of the estimates reveals that predictions based on ANN are more accurate relative to the OLS regression.

For applied validation of the estimates, a comparison has been demonstrated using the first and second highest of observed APF of each respective site. RFA estimates have similar tendencies like the highest recorded APF for various return periods at all sites. In addition, the estimates using ANN (although the given comparison is only for gauged locations) are very similar to the highest observed APF of each respective site for various return period quantiles. Hence, ANN is a preferred method for estimating flood quantiles at ungauged sites within the homogeneous regions (particularly for larger return periods).

Findings of this research will not only useful for officials concerned with the management of flood risk but it will be beneficial for agriculture water management and to improve design capacity of the current and proposed hydrological schemes within the study region. These results can also be useful to improve the quality of quantiles of poorly gauged sites within the homogeneous region. For future studies, the focus would be to include maximum available sites of the province to perform RFA. Secondly, the inclusion of few other site characteristics for the development of models to estimate quantiles at ungauged sites. Another important area is to perform RFA using variables other than annual maxima's like 3 days, 5 days or 7 days maxima's to add more data for the application of L-moments based RFA. Supposedly, it will further improve the quality and usefulness of the estimates for the officials dealing with disasters management.

**Acknowledgements.** Authors are very grateful to the Higher Education Commission, Pakistan for financial support under the project number: 5790/Federal/NRPU/R&D/HEC/2016. We are also thankful to the Irrigation Department of Khyber Pakhtunkhwa for providing flood data for the study.

## REFERENCES

- [1] Abrahart, R., Kneale, P. E., See, L. M. (eds.) (2004): Neural networks for hydrological modeling. – CRC Press.
- [2] Ahmad, I., Shah, S. F., Mahmood, I., Ahmad, Z. (2013): Modeling of monsoon rainfall in Pakistan based on Kappa distribution. – *Sci. Int. (Lahore)* 25(2): 333-336.
- [3] Ahmad, I., Fawad, M., Akbar, M., Abbas, A., Zafar, H. (2016): Regional Frequency Analysis of Annual Peak Flows in Pakistan Using Linear Combination of Order Statistics. – *Polish Journal of Environmental Studies* 25(6): 2255-2264.
- [4] Ahmad, I., Yasin, M., Fawad, M., Saghir, A. (2017): Regional frequency analysis of low flows using L-moments for Indus Basin, in Pakistan. – *Pakistan Journal of Science* 69(1): 75-84.
- [5] Alam, J., Muzzammil, M., Khan, M. K. (2016): Regional flood frequency analysis: comparison of L-moment and conventional approaches for an Indian catchment. – *ISH Journal of Hydraulic Engineering* 22(3): 247-253.
- [6] Anilan, T., Satilmis, U., Kankal, M., Yuksek, O. (2016): Application of Artificial Neural Networks and regression analysis to L-moments based regional frequency analysis in the Eastern Black Sea Basin, Turkey. – *KSCE Journal of Civil Engineering* 20(5): 2082-2092.
- [7] Aydoğan, D., Kankal, M., Önsoy, H. (2016): Regional flood frequency analysis for Çoruh Basin of Turkey with L-moments approach. – *Journal of Flood Risk Management* 9(1): 69-86.
- [8] Aziz, K., Rahman, A., Fang, G., Shrestha, S. (2014): Application of artificial neural networks in regional flood frequency analysis: a case study for Australia. – *Stochastic environmental research and risk assessment* 28(3): 541-554.
- [9] Batool, Z. (2017): Flood Frequency Analysis of Stream Flow in Pakistan Using L-Moments and TL-Moments. – *International Journal of Advance Research, Ideas and Innovations in Technology* 3(4): 136-142.
- [10] Bradley, J. V. (1968): Distribution-free statistical tests. – No. 04; QA278. 8, B7.
- [11] Cunnane, C. (1988): Methods and merits of regional flood frequency analysis. – *Journal of Hydrology* 100(1-3): 269-290.
- [12] Faridzad, M., Yang, T., Hsu, K., Sorooshian, S., Xiao, C. (2018): Rainfall frequency analysis for ungauged regions using remotely sensed precipitation information. – *Journal of hydrology* 563: 123-142.
- [13] Fawad, M., Ahmad, I., Nadeem, F. A., Yan, T., Abbas, A. (2018): Estimation of wind speed using regional frequency analysis based on linear-moments. – *International Journal of Climatology* 38(12): 4431-4444.
- [14] Fawad, M., Yan, T., Chen, L., Huang, K., Singh, V. P. (2019): Multiparameter probability distributions for at-site frequency analysis of annual maximum wind speed with L-Moments for parameter estimation. – *Energy* 153: 724-737.  
<https://doi.org/10.1016/j.energy.2019.05.153>.
- [15] Gado, T. A., Hsu, K., Sorooshian, S. (2017): Rainfall frequency analysis for ungauged sites using satellite precipitation products. – *Journal of Hydrology* 554: 646-655.
- [16] Government of Pakistan (2016): Annual flood report 2016. – Ministry of Water and Power, Office of the Chief Engineer Advisor and Chairman, Federal Flood Commission, Islamabad. Available at:  
<http://www.ffc.gov.pk/download/AFR/Annual%20Flood%20Report%202016.pdf>.
- [17] GREHYS (1996a): Inter-comparison of regional flood frequency procedures for Canadian rivers. – *Journal of hydrology (Amsterdam)* 186: 85-103.
- [18] GREHYS (1996b): Presentation and review of some methods for regional flood frequency analysis. – *Journal of hydrology (Amsterdam)* 186: 63-84.
- [19] Griffis, V. W., Stedinger, J. R. (2007): The use of GLS regression in regional hydrologic analyses. – *Journal of Hydrology* 344(1-2): 82-95.

- [20] Gujarati, D. N. (2003): Basic Econometrics. – McGraw-Hill, New York.
- [21] Hailegeorgis, T. T., Alfredsen, K. (2017): Regional flood frequency analysis and prediction in ungauged basins including estimation of major uncertainties for mid-Norway. – *Journal of Hydrology: Regional Studies* 9: 104-126.
- [22] Hirsch, R. M., Helsel, D. R., Cohn, T. A., Gilroy, E. J. (1992): Statistical analysis of hydrologic data. – In: Maidment, D. R. (ed.) *Handbook of Hydrology*, Chapter 17. McGraw-Hill, New York.
- [23] Hosking, J. R. M., Wallis, J. R. (1993): Some statistics useful in regional frequency analysis. – *Water resources research* 29(2): 271-281.
- [24] Hosking, J. R. M., Wallis, J. R. (1997): *Regional frequency analysis: an approach based on L-moments*. – Cambridge University Press.
- [25] Hussain, Z., Pasha, G. R. (2009): Regional flood frequency analysis of the seven sites of Punjab, Pakistan, using L-moments. – *Water resources management* 23(10): 1917-1933.
- [26] Hussain, Z. (2011): Application of the regional flood frequency analysis to the upper and lower basins of the Indus River, Pakistan. – *Water resources management* 25(11): 2797-2822.
- [27] Hussain, Z. (2017): Estimation of flood quantiles at gauged and ungauged sites of the four major rivers of Punjab, Pakistan. – *Natural hazards* 86(1): 107-123.
- [28] James, G., Witten, D., Hastie, T., Tibshirani, R. (2013): *An introduction to statistical learning with Applications in R*. – New York: Springer.
- [29] Khan, S. A., Hussain, I., Hussain, T., Faisal, M., Muhammad, Y. S., Mohamd Shoukry, A. (2017): Regional Frequency Analysis of Extremes Precipitation Using L-Moments and Partial L-Moments. – *Advances in Meteorology*, article ID: 6954902.
- [30] Kuhn, M., Johnson, K. (2013): *Applied predictive modeling*. – Springer, New York.
- [31] Lee, D. H., Kim, N. W. (2019): Regional Flood Frequency Analysis for a Poorly Gauged Basin Using the Simulated Flood Data and L-Moment Method. – *Water* 11(8): 1717.
- [32] Maier, H. R., Dandy, G. C. (2000): Neural networks for the prediction and forecasting of water resources variables: a review of modelling issues and applications. – *Environmental modelling & software* 15(1): 101-124.
- [33] Malekinezhad, H., Zare-Garizi, A. (2014): Regional frequency analysis of daily rainfall extremes using L-moments approach. – *Atmosfera* 27(4): 411-427.
- [34] Mesbahzadeh, T., Soleimani Sardoo, F., Kouhestani, S. (2019): Flood frequency analysis for the Iranian interior deserts using the method of L-moments: A case study in the Loot River Basin. – *Natural Resource Modeling* 32(2): e12208.
- [35] Ouali, D., Chebana, F., Ouarda, T. B. (2017): Fully nonlinear statistical and machine-learning approaches for hydrological frequency estimation at ungauged sites. – *Journal of Advances in Modeling Earth Systems* 9(2): 1292-1306.
- [36] Pakistan Meteorological Department (2012): The implementation of diagnostic study for 2010 flood and extreme moon soon rains 2011 in Pakistan under sustainable development through peace building, governance and economic recovery in KP and support landslide IDPs in Hunza Nagar and Gilgit district when UNDP surves as implementing partner. – Available at [http://www.pmd.gov.pk/reports/flood\\_diagnostic\\_2010\\_2011.pdf](http://www.pmd.gov.pk/reports/flood_diagnostic_2010_2011.pdf).
- [37] Requena, A. I., Ouarda, T. B., Chebana, F. (2017): Flood Frequency Analysis at Ungauged Sites Based on Regionally Estimated Stream flows. – *Journal of Hydrometeorology* 18(9): 2521-2539.
- [38] Shahzadi, A., Akhter, A. S., Saf, B. (2013): Regional frequency analysis of annual maximum rainfall in monsoon region of Pakistan using L-moments. – *Pakistan Journal of Statistics and Operation Research* 9(1): 111-136.
- [39] Shamseldin, A. Y., Nasr, A. E., O'Connor, K. M. (2002): Comparison of different forms of the multi-layer feed-forward neural network method used for river flow forecast combination. – *Hydrology and earth system sciences* 6(4): 671-684.

- [40] Sivakumar, B., Singh, V. P. (2012): Hydrologic system complexity and nonlinear dynamic concepts for a catchment classification framework. – *Hydrology and Earth System Sciences* 16(11): 4119.
- [41] Wald, A., Wolfowitz, J. (1943): An exact test for randomness in the non-parametric case based on serial correlation. – *The Annals of Mathematical Statistics* 14(4): 378-388.
- [42] Yang, T., Xu, C. Y., Shao, Q. X., Chen, X. (2010): Regional flood frequency and spatial patterns analysis in the Pearl River Delta region using L-moments approach. – *Stochastic Environmental Research and Risk Assessment* 24(2): 165-182.



# EFFICACY OF VARIOUS NPK APPLICATION METHODS ON THE YIELD OF DIFFERENT SUNFLOWER (*HELIANTHUS ANNUUS* L.) GENOTYPES GROWN DURING SPRING SEASONS

MAHMOOD, H. N.

*Biotechnology and Crop Science Department, College of Agricultural Engineering Sciences,  
University of Sulaimani, Sulaimani, Kurdistan Region, Iraq  
(e-mail: hekmat.mahmood@univsul.edu.iq; phone: +964-7501-269-838)*

(Received 23<sup>rd</sup> Aug 2020; accepted 30<sup>th</sup> Nov 2020)

**Abstract.** Sunflower (*Helianthus annuus* L.) is a member of the Compositae family. It is one of the world's leading oilseed crops, mainly cultivated for its oil content. A field study was conducted at two different locations to determine the effect of various applications of NPK fertilizer on the yields of different genotypes. The experimental design was a complete block design, replicated three times. Fertilizer application methods (fertigation, foliar, and control) formed the main plots and three different sunflower genotypes (Sevar, Dea, Local) formed the sub-plots. The data was subjected to analysis of variance, and correlation coefficient and path analysis were used. Dea genotype had the highest achene yield of 8,384.721 kg ha<sup>-1</sup> under foliar applications at both locations. Correlation studies between achene yield and all its components were highly significant at both locations. However, 1000 achene weight at a second location, was not significant. The results showed that the maximum positive direct effect of 1.00 on achene yield was exerted by achene weight at both locations. This study indicated that achene weight is an important characteristic concerning the achene yield of sunflower.

**Keywords:** *fertigation, foliar, correlation, path analysis, yield improvement*

## Introduction

Sunflower (*Helianthus annuus* L.) is a widely distributed and adaptable oilseed crop of the world. It is the fourth most commonly grown oil crop worldwide after oil-palm, soybean, and rapeseed which constitute over 87% of global vegetable oil productions, and it accounts for about 12% of edible vegetable oil (Demir et al., 2006; Murphy, 2010; Siddiqi et al., 2012; Shafi et al., 2013; Taran et al., 2013; Hakim et al., 2013; Nasreen et al., 2015; Rauf et al., 2017). The crop is an essential oilseed crop consumed worldwide due to its high content of unsaturated fatty acids and zero cholesterol level, which are necessary for the human diet (Onemli and Gucer, 2010; Alberio et al., 2015). For optimal plant growth, nutrients must be present in sufficient and balanced quantities. Soil contains natural reserves of plant nutrients, but these reserves are mainly not available in the forms of plants. They have released only a small part through biological or chemical processes activity. Production of these nutrients naturally is not sufficient to meet the plant requirements. To compensate for these low nutrients, fertilizers must be used (Chen, 2006; Ahmad et al., 2010; Akbari et al., 2011). The ability to reach sunflower achenes maximum productivity is related, in part, with suitable mineral nutrition of the plant (Aquino et al., 2013). Fertilizer containing major nutrients is usually applied to meet the nutrient deficiencies of the soil; however, uptake of N is often low (50%), which may have some environmental consequences (Scheiner et al., 2002). Hussain et al. (2000) reported that higher yields could be obtained by applying chemical fertilizers. Ultimately, the required fertilizers in the soil will increase the production of crops (Adediran et al., 2005). Nutrient management is one of the main factors that influence sunflower achene yield, achene oil, and fatty acid contents. Farmers have traditionally applied organic

manure plus nitrogen (N) and phosphate (P) fertilizers, resulting in overuse of N and P but insufficient potassium (K) input in sunflower production (Tuo et al., 2010). Nitrogen, phosphorus, and potash are the main nutrients, which are likely to become deficient in most soils, and their application usually results in increased production. Nitrogen (N) is the most nutrient required by sunflowers and has an impact on seed size, leaf numbers and sizes, seed weight, and seed yields. However, increasing the N rate increases seed protein, but decreases oil concentration (Darby et al., 2013). Phosphorus (P) and Potassium (K) are coming in second because these nutrients are naturally available in the soil and consider low soluble compounds.

Fertigation application methods is a technique, which can reduce the cost of fertilizer use by eliminating operating and improving the efficiency of nutrient. Also, it could conceivably reduce leaching or denitrification (gaseous) losses of nitrogen and lower the luxury uptake of nutrients by plants. Combined application of irrigation and nitrogen through fertigation is now becoming a common practice in modern agriculture because of its advantages over broadcast N application. The N-fertigation was found efficient for growth and yield of sunflower (Popoola et al., 2016). Hebbar et al. (2004), reported that reduced loss of nutrients could be through fertigation compared to soil application of fertilizer. Fertigation allows users to put the fertilizers in the plant root zone or on the canopy at the desired frequency, amount, and concentration at the appropriate time (Kumar et al., 2000).

Foliar application of nitrogen was beneficial to sunflower growth, development, and yield (Haseeb and Maqbool, 2015). The time and duration of foliar application determine the fate of plant yield (Varga and Svecnjak, 2006). It is since foliar-applied nitrogen is absorbed by plants more rapidly than other methods. Nitrogen is considered to be an essential part of different structural and metabolic compounds in plants (Hassan et al., 2010).

Many researchers use correlation coefficient and path analysis. Path analysis provides information about the direct and indirect effect character on seed yield, and it helps in examining the relative contribution of individual variables towards sunflower seed yield (Janamma et al., 2008). Correlation coefficient and path coefficient analysis assists in identifying the traits that are useful and helps in the selection of superior criteria to improve achene yield.

The objective of this study was to investigate the effect of both (fertigation and foliar NPK application) on achene yield and yield components of three sunflower genotypes.

## Material and Methods

### *Plant material and location of the experiment*

This study was conducted in two different locations in the government of Sulaimani, Kurdistan Region of Iraq. The first location, Agricultural Research Station at Kanipanka (Longitude of 045° 43' 22" E, the altitude of 548 masL, and latitude of 35° 22' 22" N), in Sharazoor intermountain 35 km east of Sulaymaniyah. The second location, Qlyasan, the experimental station of the College of Agricultural Engineering Sciences, the University of Sulaimani, (latitude: 35° 34' 17" N, Longitude: 045° 22' 00" E, altitude: 757 masL) from April to July 2017. The climate is a semi-arid environment; hot and dry in summer, cold and wet in winter, and rainy season autumn to winter. During that period, the temperature ranged from 18°C to 39°C, and the average relative humidity was 31% in the region (Kurdistan Regional Government, 2018; see *Table 1*).

**Table 1.** Agrometeorological parameters at Kanipanka and Qlyasan locations 2017

Locations	Month	Air Temperature °C		Relative humidity (%)
		Minimum	Maximum	
Kanipanka	April	11.24	23.62	42
	May	15.75	33.54	30.3
	June	21.01	39.73	21.4
	July	26.7	44.57	19
Qlyasan	April	11.00	34.00	55
	May	13.00	40.00	35
	June	21.00	47.00	28
	July	28.00	48.00	20

### Soil sampling and analysis

The soil samples were collected at a depth of 0-60 cm for laboratory analysis at each location. It was air-dried gently, crushed, and tested for physical and chemical properties. Details of soil properties are shown in *Table 2*.

**Table 2.** Physicochemical properties of the soil samples for locations of the experimental field

Physicochemical properties		Locations	
		Kanipanka	Qlyasan
Particle size distribution (g kg <sup>-1</sup> )	Sand	36	107
	Silt	529	435
	Clay	435	458
	Texture class	Silty Clay	Silty Clay
Total Nitrogen (mg kg <sup>-1</sup> )		1.03	1.07
Available Phosphate (mg kg <sup>-1</sup> )		7.2	6.28
Soluble Potassium (mmol L <sup>-1</sup> )		0.06	0.06
PH		7.70	7.59
EC (dS m <sup>-1</sup> )		0.22	0.49
Organic matter (g kg <sup>-1</sup> )		14.8	22.4
CaCO <sub>3</sub> (g kg <sup>-1</sup> )		208.3	304.3

### Fertilizer placement methodology

Liquid NPK fertilizer (20-20-20), EC Fertilizer: Guaranteed Content (W/W) %. Nitrogen (N) 20% Urea (CH<sub>4</sub>N<sub>2</sub>O), Phosphorus (P) 20% Phosphoric acid (H<sub>3</sub>PO<sub>4</sub>), and Potassium (K) 20% Potassium Chloride (KCl). Three methods of application used during this study: Fertigation (application of fertilizers with irrigation water): as recommended for fertigation, 30 liters of NPK covering one hectare. The appropriate NPK rate was mixed with water, then applied with irrigation to the appropriate plot. Foliar application: To spraying sunflower leaves, 3 liters of NPK was mixed with 1000 liters of water, which is adequate to cover one hectare as recommended for foliar application. Spraying leaves with the appropriate rate were carried out where wind speed at minimal. Zero NPK application (control): This treatment is a no fertilizer added to the plot, NPK (0, 0, 0).

### ***Sunflower genotype***

The sunflower genotypes were a single cross hybrid Sevar, single cross hybrid Dea, were obtained from the Crop Improvement Department, University of Arizona, USA, and a Local genotype.

### ***Experimental design and treatments***

The treatments were carried out in a completely randomized design (RCBD) as a split-plot factorial experiment, with three methods of NPK fertilizer application (fertigation, foliar, and zeroes NPK fertilizer, as the main plot. At the same time, the sub-plot factors encompassed three sunflower genotypes (Sevar, Dea, and Local) with three repetitions, comprised of 27 experimental units. The sub-plot was 2 m by 1.2 m in size, and each consisted of two rows spaced at 0.60 m with a plant distance of 0.25 m. The seeds were planted in line during April 6<sup>th</sup>, and 10<sup>th</sup> of 2017 at the first and second locations respectively, after completion of germination, the seedlings were thinned out to one plant hole<sup>-1</sup>. All the NPK application methods presented on the same day, then irrigated. The NPK application was applied in two equal doses. The first dose for both (fertigation and foliar) application were applied 25 days after sowing (DAS). The second dose was applied at 50 DAS.

### ***Data recorded***

At each location, five fully mature plants were harvested in each plot. Achene yield components and average achene yields per plot were recorded at a seed moisture content of about 10%. The plant was harvested at 106 DAS at the first location (Kanipanka), while at 105 DAS, plants were harvested at the second location (Qlyasan), respectively.

Biological yield (kg ha<sup>-1</sup>) was measured as the above-ground biomass per plant by weighting the whole plants, including seeds and stalks from the plant samples collected during full maturity, expressed in metric grams, then converted to (kg ha<sup>-1</sup>).

Seed yield (kg ha<sup>-1</sup>): The seed weight of the five representative plants was added to net plot seed weight, and later the average of seed yield was converted to (kg ha<sup>-1</sup>).

Harvest index, was expressed as the ratio of seed yield to biological yield (Singh and Stoskopf, 1971).

### ***Statistical analysis***

All data were subjected to statistical analysis by the technique of variance of the split-plot design using XLSTAT (2016). For a direct comparison of treatments, the least significant difference tests (LSD) at levels of 0.05 was used. For testing the main effects of NPK fertilizer application on sunflower genotypes, the data were subjected to analysis of variance (ANOVA).

## **Results**

Data present in *Table 3* explain the effect of methods of NPK application on achene yield and its components at both locations and their average. The results obtained from the variance analysis of data indicated that the NPK application methods influenced all studied characters highly significantly, except for the harvest index, which responded only significantly at the first location. In contrast, at the second location, the head diameter, a number of achenes plant<sup>-1</sup>, 1000 achene weight, and biological yield

responded highly significantly to the effect of NPK application methods, while the significant effect was recorded for the head weight, achene weight, and achene yield. Still, no significant response was recorded for the harvest index. Regarding the average of both locations, all studied characters exhibited a highly significant response to the NPK application methods. At both locations and their average, the methods of fertigation and foliar NPK application exceeded the control treatment significantly (see *Appendix*).

**Table 3.** Effect of NPK application methods on achene yield and its components at both locations and their average

NPK application methods	Head diameter (cm)	Head weight (g)	Achene weight (g)	No. of achenes plant <sup>-1</sup>	1000 Achene weight (g)	Harvest index	Biological yield (kg ha <sup>-1</sup> )	Achene yield (kg ha <sup>-1</sup> )
First location								
<b>Fertigation</b>	19.931 a	191.204 a	124.780 a	1870.139 a	66.659 a	0.390 a	21210.269 a	8318.716 a
<b>Foliar</b>	19.466 a	180.691 a	116.513 a	1850.454 a	62.842 a	0.377 a	20525.547 a	7767.564 a
<b>Control</b>	14.121 b	95.278 b	64.160 b	1312.216 b	48.673 b	0.299 b	14602.814 b	4277.381 b
LSD (P≤ 0.05)	0.883	25.430	16.326	233.802	4.995	0.053	2182.515	1088.414
Second location								
<b>Fertigation</b>	16.960 a	134.050 a	83.903 a	1271.464 a	49.252 a	0.303 a	18223.180 a	5593.558 a
<b>Foliar</b>	16.556 a	134.162 a	83.247 a	1350.677 a	51.032 a	0.300 a	18308.092 a	5549.831 a
<b>Control</b>	13.528 b	78.627 b	47.989 b	976.828 b	41.569 b	0.254 a	12358.803 b	3199.268 b
LSD (P≤ 0.05)	0.672	27.591	26.812	160.693	3.907	N. S	2554.827	1787.459
Average of both locations								
<b>Fertigation</b>	18.446 a	162.627 a	104.342 a	1570.802 a	57.955 a	0.347 a	19716.725 a	6956.137 a
<b>Foliar</b>	18.011 a	157.426 a	99.880 a	1600.565 a	56.937 a	0.338 a	19416.819 a	6658.698 a
<b>Control</b>	13.824 b	86.952 b	56.075 b	1144.522 b	45.121 b	0.277 b	13480.808 b	3738.324 b
LSD (P≤ 0.05)	0.461	15.585	13.038	117.833	2.634	0.036	1395.618	869.220

LSD value for NPK at P≤ 0.01 = Highly significant \*\*, LSD value at P≤ 0.05 = Significant \*, N. S. = Statistically non-significant

*Table 4* shows the averages of achene yield and its components at both locations and their average for sunflower genotypes. The differences among genotypes were highly significant for all studied characters at both locations and their average except the harvest index and 1000 achene weight at the first and second locations, respectively, which was only significant. About the head diameter and the number of achenes plant<sup>-1</sup>, the highest value recorded by Sevar genotype, while the lowest value recorded by Local genotype at both locations and their average. The same trade was shown for the harvest index except for the second location, in which the Dea exhibited Sevar genotypes. No significant differences were found between Sevar and Dea genotypes for the number of achene plant<sup>-1</sup> at the first location and their average at both locations. However, and harvest index at the second location and their average at both locations. The head weight, achene weight, 1000 achenes weight, biological yield, and achene yield, and their average, Dea genotype produced the highest value at both locations. In the case of local genotype, 1000 achene weight at the second location, showed the highest value while Sevar genotype showed the lowest value. No significant differences were recorded between Sevar and Dea genotype for the head weight, 1000 achene weight at the second location.

**Table 4.** Effect of sunflower genotypes on achene yield and its components at both locations and their average

Sunflower genotypes	Head diameter (cm)	Head weight (g)	Achene weight (g)	No. of achenes plant <sup>-1</sup>	1000 Achene weight (g)	Harvest index	Biological yield (kg ha <sup>-1</sup> )	Achene yield (kg ha <sup>-1</sup> )
First location								
<b>Sevar</b>	20.071 a	149.824 b	104.170 b	1879.371 a	54.122 b	0.387 a	17495.754 b	6944.716 b
<b>Dea</b>	18.104 b	187.248 a	126.895 a	1851.685 a	67.370 a	0.349 b	23834.082 a	8459.687 a
<b>Local</b>	15.342 c	130.100 c	74.388 c	1301.753 b	56.681 b	0.330 b	15008.794 c	4959.257 c
LSD (P≤0.05)	0.779	13.306	11.134	159.797	3.460	0.035	1249.812	742.249
Second location								
<b>Sevar</b>	18.056 a	126.516 a	77.977 b	1418.955 a	44.594 b	0.308 a	16496.97 b	5198.522 b
<b>Dea</b>	15.793 b	131.353 a	86.220 a	1285.796 b	47.073 ab	0.310 a	18506.315 a	5748.051 a
<b>Local</b>	13.194 c	88.970 b	50.941 c	894.218 c	50.187 a	0.239 b	13886.788 c	3396.084 c
LSD (P≤0.05)	0.686	9.236	5.720	106.969	3.573	0.026	988.116	381.335
Average of both locations								
<b>Sevar</b>	19.063 a	138.170 b	91.074 b	1649.163 a	49.358 c	0.347 a	16996.363 b	6071.619 b
<b>Dea</b>	16.949 b	159.301 a	106.558 a	1568.740 a	57.222 a	0.329 a	21170.198 a	7103.869 a
<b>Local</b>	14.268 c	109.535 c	62.665 c	1097.986 b	53.434 b	0.284 b	14447.791 c	4177.671 c
LSD (P≤0.05)	0.491	7.668	5.925	91.029	2.355	0.021	754.21	395.026

LSD value for Sunflower genotype at P≤0.01 = Highly significant \*\*, LSD value at P≤0.05 = Significant \*, N. S. = Statistically non-significant

As seen in *Table 5* in which illustrate the interaction effect between NPK application methods and sunflower genotypes on achene yield and its components at both locations and their average. At the first location, all characters responded to this effect significant except biological yield. At the second location, all characters showed a significant response to the interaction effect, except 1000 achene weight and biological yield. While at the average of both locations, the head diameter, head weight, achene weight, number of achenes plant<sup>-1</sup>, and achene yield showed a highly significant response to this effect. Still, the 1000 achene weight and harvest index showed a significant response and not significant response produced by biological yield. The maximum value for head diameter recorded by the interaction between fertigation application and Sevar genotype with 22.543, 20.167 and 21.355 cm for both locations and their average respectively, but the lowest values were 12.527, 11.583 and 12.055 cm, respectively, recorded by the interaction between the treatment of control and Local genotype. The highest value for the head weight, achene weight, and achene yield were recorded by the interaction between the foliar application associated with Dea genotype 225.450 g, 149.981 g, and 9998.808 kg ha<sup>-1</sup>, respectively at the first location. However, the values were 157.282 g, 101.559 g, and 6770.634 kg ha<sup>-1</sup>, respectively, at the second location. While for the average of both locations, the values were 191.366 g, 125.770 g, and 8384.721 kg ha<sup>-1</sup>, respectively.

However, the lowest value for these characters was 85.380 g, 52.640 g and 3509.346 kg ha<sup>-1</sup>, respectively at the first location and 59.343 g, 31.884 g, and 2125.611 kg ha<sup>-1</sup> at the second location, while as the average of both locations were 72.362 g, 42.262 g and 2817.479 kg ha<sup>-1</sup>, respectively.

**Table 5.** Effect of the interaction between NPK application methods and sunflower genotypes on yield and its components at both locations and their average

NPK Application methods and sunflower genotypes		Head diameter (cm)	Head weight (g)	Achene weight (g)	No. of achenes plant <sup>-1</sup>	1000 Achene weight (g)	Harvest index	Biological yield (kg ha <sup>-1</sup> )	Achene yield (kg ha <sup>-1</sup> )
First location									
Fertigation	Sevar	22.543 a	188.262 b	137.089 a	2181.161 a	62.834 b	0.449 a	20352.213 a	9139.301 a
	Dea	20.250 b	224.040 a	149.006 a	2055.619 a	72.754 a	0.386 bc	25733.018 a	9933.750 a
	Local	17.000 c	161.309 cd	88.246 c	1373.638 bc	64.388 b	0.334 cde	17545.577 a	5883.096 c
Foliar	Sevar	22.377 a	173.012 bc	117.278 b	2164.527 a	54.191 c	0.406 ab	19384.875 a	7818.557 b
	Dea	19.520 b	225.450 a	149.981 a	1973.474 a	75.804 a	0.387 bc	25790.796 a	9998.808 a
	Local	16.500 cd	143.610 d	82.280 c	1413.359 b	58.531 bc	0.337 cd	16400.971 a	5485.327 c
Control	Sevar	15.293 de	88.198 f	58.144 d	1292.425 bc	45.342 d	0.305 de	12750.175 a	3876.290 d
	Dea	14.543 e	112.255 e	81.697 c	1525.961 b	53.553 c	0.273 e	19978.433 a	5446.505 c
	Local	12.527 f	85.380 f	52.640 d	1118.263 c	47.125 d	0.319 de	11079.833 a	3509.346 d
LSD (P≤ 0.05)		1.350	23.047	19.284	276.776	5.994	0.061	N. S	1285.613
Second location									
Fertigation	Sevar	20.167 a	150.247 ab	94.461 a	1507.304 b	48.328 a	0.333 a	18757.205 a	6297.443 a
	Dea	16.797 c	140.963 b	92.292 a	1301.099 c	50.827 a	0.296 abc	20582.992 a	6152.842 a
	Local	13.917 d	110.939 c	64.956 b	1005.991 d	48.602 a	0.281 bcd	15329.343 a	4330.391 b
Foliar	Sevar	18.917 b	148.578 ab	92.199 a	1701.722 a	46.895 a	0.338 a	18245.313 a	6146.609 a
	Dea	16.667 c	157.282 a	101.559 a	1363.327 bc	50.647 a	0.322 ab	21025.550 a	6770.634 a
	Local	14.083 d	96.627 cd	55.984 bc	986.982 d	55.555 a	0.239 de	15653.412 a	3732.252 bc
Control	Sevar	15.083 d	80.722 d	47.273 c	1047.838 d	38.559 a	0.253 cd	12488.396 a	3151.516 c
	Dea	13.917 d	95.815 cd	64.810 b	1192.963 cd	39.744 a	0.312 ab	13910.403 a	4320.677 b
	Local	11.583 e	59.343 e	31.884 d	689.682 e	46.404 a	0.198 e	10677.609 a	2125.611 d
LSD (P≤ 0.05)		1.188	15.998	9.907	185.275	N. S	0.046	N. S	660.491
Average of both location									
Fertigation	Sevar	21.355 a	169.254 bc	115.775 a	1844.232 a	55.581 b	0.391 a	19554.709 a	7718.372 a
	Dea	18.523 b	182.502 ab	120.649 a	1678.359 b	61.790 a	0.341 bc	23158.005 a	8043.296 a
	Local	15.458 c	136.124 d	76.601 c	1189.815 d	56.495 b	0.307 cd	16437.460 a	5106.743 c
Foliar	Sevar	20.647 a	160.795 c	104.738 b	1933.125 a	50.543 c	0.372 ab	18815.094 a	6982.583 b
	Dea	18.093 b	191.366 a	125.770 a	1668.401 b	63.226 a	0.355 ab	23408.173 a	8384.721 a
	Local	15.292 c	120.118 e	69.132 c	1200.171 d	57.043 b	0.288 de	16027.191 a	4608.790 c
Control	Sevar	15.188 c	84.460 g	52.708 d	1170.132 d	41.951 d	0.279 de	12619.285 a	3513.903 d
	Dea	14.230 d	104.035 f	73.254 c	1359.462 c	46.649 c	0.292 de	16944.418 a	4883.591 c
	Local	12.055 e	72.362 g	42.262 e	903.972 e	46.764 c	0.258 e	10878.721 a	2817.479 e
LSD (P≤ 0.05)		0.851	13.281	10.263	157.667	4.078	0.036	N. S	684.205

LSD value for interaction at P≤ 0.01 = Highly significant \*\*, LSD value for at P≤ 0.05 = Significant \*, N. S.= Statistically non-significant

Respect to the number of achene plant<sup>-1</sup>, the values restricted between 1118.263 achenes for the interaction between control and local genotype to 2181.161 achenes for the interaction between fertigation application coupled with Sevar genotype at the first location, while at the second location and the average of both locations the values ranged between 689.682 and 903.972 achenes for the interaction between control and local genotype to 1701.722 and 1933.125 achenes for the interaction of foliar application associated with Sevar genotype.

Concerning 1000 achene weight, the values of this character restricted between 45.342 g for the interaction between control and Sevar genotype to 75.804 g for the interaction between foliar and Dea genotype at the first location. However, the average values of both locations were between 41.951 to 63.226 g.

Regarding the harvest index at the first location and the average of both locations, the highest values were 0.449, and 0.391 recorded by the interaction of the fertigation application with Sevar genotype. However, for the interaction between foliar application with Sevar genotype, the highest value of 0.338 was recorded, at the second location. Interaction between control and Dea genotype, the lowest value was 0.273 at the first location. The lowest value of 0.198, and 0.258 at the second location and the average of both locations exhibited by the interaction between control and Local genotype, respectively.

In this study, the effect of location on achene yield and its components, as shown in *Table 6*. The effect was highly significant for all characters, and the exceeding of the first location was significant. The first location predominated the second location by 13.76; 34.69; 41.98; 39.84; 25.60; 24.12; 15.24 and 41.97 % for the head diameter, head weight, achene weight, number of achenes plant<sup>-1</sup>, 1000 achene weight, harvest index, biological yield, and achene yield, respectively.

**Table 6.** Effect of locations on sunflower yield and its components

Locations	Head diameter (cm)	Head weight (g)	Achene weight (g)	No. of Achenes plant <sup>-1</sup>	1000 Achene Weight (g)	Harvest index	Biological yield (kg ha <sup>-1</sup> )	Achene yield (kg ha <sup>-1</sup> )
First	17.839 a	155.724 a	101.818 a	1677.603 a	59.391 a	0.355 a	18779.544a	6787.885a
Second	15.681 b	115.613 b	71.713 b	1199.656 b	47.285 b	0.286 b	16296.693b	4780.885b
LSD (P≤0.05)	1.022	26.228	10.088	244.430	2.812	0.017	1915.131	672.505

LSD value for locations at P≤ 0.01 = Highly significant \*\*, LSD value at P≤ 0.05 = Significant \*

The correlation coefficient was obtained among all pairs of study characters for achene yield and its components at the first location presented in *Table 7*. The head diameter exhibited a highly significant and positive correlation with head weight, achene weight, number of achenes plant<sup>-1</sup>, harvest index, and achene yield (r = 0.812, 0.855, 0.947, 0.915, and 0.855) respectively. In contrast, this character produced a significant and positive correlation with biological yield (r = 0.668). A highly significant and positive correlation was showed between head weight with achene weight, the number of achenes plant<sup>-1</sup>, 1000 achene weight, biological yield, and achene yield (r = 0.968, 0.826, 0.933, 0.907, and 0.968) respectively, but the correlation was significant and positive with harvest index (r = 0.759). Achene weight was highly significant and positively associated with the number of achenes plant<sup>-1</sup>, 1000 achene weight, harvest index, biological yield, and achene yield (r = 0.916, 0.863, 0.799, 0.927, and 0.999) respectively. A highly significant and positive correlation is recorded between the number of achenes plant<sup>-1</sup> with harvest index and achene yield (r = 0.852, and 0.916) respectively. Moreover, the number of achenes plant<sup>-1</sup> produced a significant and positive correlation with biological yield (r = 0.792). 1000 achene weight showed a highly significant and positive correlation between biological yield and achene yield (r = 0.884, and 0.863). Harvest index exhibited a highly significant and positive correlation with achene yield (r = 0.799). The biological yield recorded a highly significant and positive correlation with achene yield (r = 0.927).



**Table 7.** Simple correlation among all pairs of characters at first location

Characters	Head diameter (cm)	Head weight (g)	Achene Weight (g)	No. of Achenes plant <sup>-1</sup>	1000 Achene weight (g)	Harvest index	Biological yield (kg ha <sup>-1</sup> )	Achene yield (kg ha <sup>-1</sup> )
Head diameter (cm)	1							
Head weight (g)	0.812**	1						
Achene weight (g)	0.855**	0.968**	1					
No. of Achenes plant <sup>-1</sup>	0.947**	0.826**	0.916**	1				
1000 Achene weight (g)	0.569	0.933**	0.863**	0.600	1			
Harvest index	0.915**	0.759*	0.799**	0.852**	0.539	1		
Biological yield (kg ha <sup>-1</sup> )	0.668*	0.907**	0.927**	0.792*	0.884**	0.521	1	
Achene yield (kg ha <sup>-1</sup> )	0.855**	0.968**	0.999**	0.916**	0.863**	0.799**	0.927**	1

\*\* Correlation is significant at 0.01 probability level, \* Correlation is significant at 0.05 probability level

The correlation coefficient between all pairs of study characters for achene yield and its components obtained at the second location present in *Table 8*. The head diameter showed a highly significant and positive correlation with head weight, achene weight, number of achenes plant<sup>-1</sup>, harvest index, and achene yield ( $r = 0.864, 0.845, 0.927, 0.821,$  and  $0.845$ ) respectively. However, this character produced a significant and positive correlation with biological yield ( $r = 0.756$ ). A high correlation was recorded between head weight with achene weight, a number of achenes plant<sup>-1</sup>, harvest index, biological yield, and achene yield ( $r = 0.991, 0.882, 0.873, 0.959,$  and  $0.991$ ) respectively. The character achene weight exhibited a highly significant and positive correlation with the number of achenes plant<sup>-1</sup>, harvest index, biological yield, and achene yield ( $r = 0.885, 0.897, 0.959,$  and  $0.999$ ), respectively. A highly significant and positive correlation was associated with the number of achenes plant<sup>-1</sup> with harvest index and achene yield ( $r = 0.931,$  and  $0.885$ ), respectively.

**Table 8.** Simple Correlation among all pairs of characters at the second location

Characters	Head diameter (cm)	Head weight (g)	Achene Weight (g)	No. of Achenes plant <sup>-1</sup>	1000 Achene weight (g)	Harvest index	Biological yield (kg ha <sup>-1</sup> )	Achene yield (kg ha <sup>-1</sup> )
Head diameter (cm)	1							
Head weight (g)	0.864**	1						
Achene weight (g)	0.845**	0.991**	1					
No. of Achenes plant <sup>-1</sup>	0.927**	0.882**	0.885**	1				
1000 Achene weight (g)	0.149	0.396	0.335	0.065	1			
Harvest index	0.821**	0.873**	0.897**	0.931**	-0.019	1		
Biological yield (kg ha <sup>-1</sup> )	0.756*	0.959**	0.959**	0.763*	0.535	0.750*	1	
Achene yield (kg ha <sup>-1</sup> )	0.845**	0.991**	0.999**	0.885**	0.335	0.897**	0.959**	1

\*\* Correlation is significant at 0.01 probability level, \* Correlation is significant at 0.05 probability level

Moreover, the same trait produced a significant and positive correlation with biological yield ( $r = 0.763$ ). Harvest index showed a highly significant and Correlation values with achene yield ( $r = 0.897$ ), while the Correlation was significant and positive with biological yield ( $r = 0.750$ ). The biological yield showed a highly significant and positive correlation with the achene yield ( $r = 0.959$ ).

The data were subjected to path analysis to determine the relative importance of the characters. *Figures 1 and 2*, explain the path coefficient analysis direct (Diagonal) and indirect (Sub diagonal) effect of various characters on sunflower achene yield at both locations. The path coefficient analysis at both locations revealed that achene weight had a higher positive direct effect on achene yield reached (1.00). In contrast, all other characters showed a low positive and negative direct effect on the achene yield. Thus, the maximum positive indirect effect was (0.968, and 0.991) recorded by achene weight via head weight, and followed by (0.927, and 0.959) for achene weight via biological yield at both locations respectively.

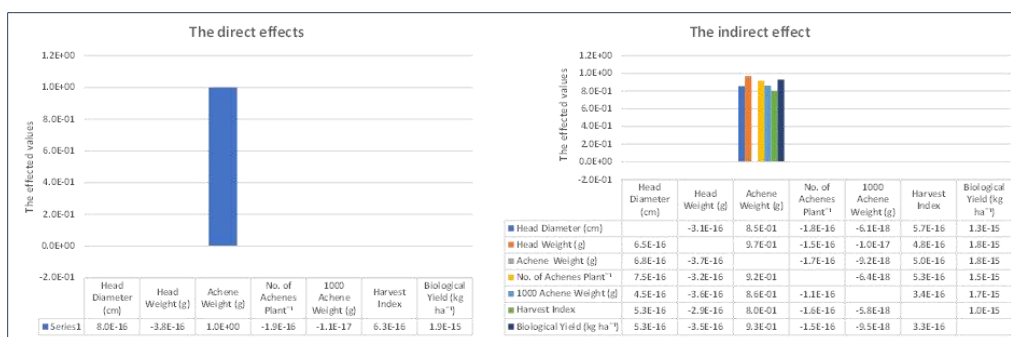


Figure 1. Direct and indirect effects on achene yield and its components at the first location

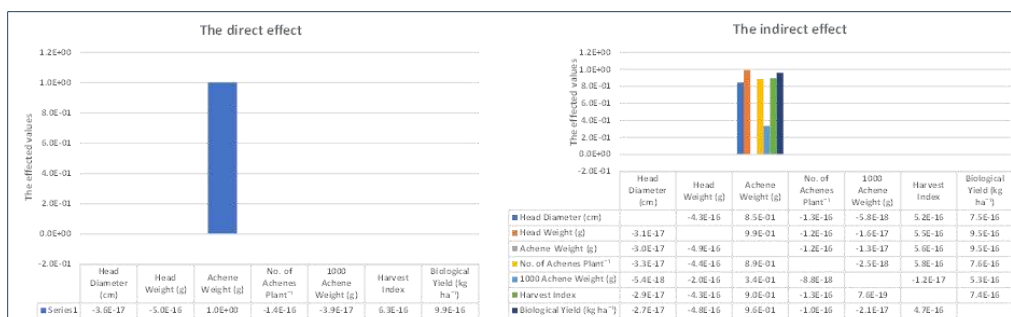


Figure 2. Direct and indirect effects on achene yield and its components at the second location

## Discussion

The NPK application under field conditions was examined on three sunflower genotypes for some agronomic parameters as well as for achene yield. The treatments were comprised of fertigation and foliar NPK (20, 20, 20) application, with control NPK (0, 0, 0), combined with three sunflowers (Sevar, Dea, and Local) genotypes.

The study results indicated that sunflower yield and its components were significantly different due to the NPK application, the treated plot (fertigation and foliar application) and control plot showed different values for achene yield and its components. Fertigation

application produced a plant with a higher head diameter, leading to an increase in the achene weight and finally leading to maximum achene yield compared to control application. These results collaborate with Malik et al. (2004) that increasing levels of N, P, and K increased yield, and it is components of sunflower (head diameter, number of achenes head<sup>-1</sup>, 1000-achene weight). However, the statistical variation showed no significant differences between fertigation and foliar application at both locations and their average for all studied characters. These results collaborated with the work of Kaka (2008), who examined the effect of foliar application on sunflower yield and concluded that Urea (N) as foliar spray significantly increase sunflower yield and yield components. It is a well-established fact that foliar application of N in the form of Urea enhances vegetable growth and yield components compare to control treatment. This enhancement may be due to cell division and expansion, which increase the rate of photosynthesis, which ultimately, increase the chlorophyll content by increasing the rubisco activity (Brady and Weil, 2005; Kaka, 2008; Hassanlouee and Baghbani, 2013). Also, Iqbal et al. (2008) reported a progressive increase in achene yield, and it is components with increasing levels of N, P, and K.

The study witnessed a significant effect of sunflower genotypes; therefore, the increase of achene yield depends on genotypes and NPK application. Notably, the Dea genotype exceeded Sevar and Local genotype in achene yield, and most of it is components. Our results collaborate Ozer et al. (2004) and Zheljzakov et al. (2008), who reported significant differences in yield potential among various sunflower hybrids.

The effect of interaction between foliar NPK application on achene yield of Dea sunflower genotype at both locations and their average was significantly notable, as assessed from the higher head weight and achene weight over the other combinations between fertilizer application and genotypes. The same results were reported by Abbasi et al. (2005). Foliar feeding of nutrients may promote the root absorption of the same nutrient or other nutrients through improving root growth and increasing nutrients uptake (Saqib et al., 2006).

The exceeding of achene yield and its components in the first location may be due to the favorable environmental conditions prevailing in this location to grow this crop. Higher seed yields may be due to different environmental conditions at each location.

Head weight was affected by environmental factors, and also final seed yield was significantly affected by environmental factors. Also, Sidlauskas and Bernotas (2003) and Denčić et al. (2012) concluded that productivity and quality are highly influenced by genotype, environment, and interaction.

The correlation coefficient between achene yield and most of the studied characters were positively and highly significant at both locations. Selection of head diameter, head weight, achene weight, number of achenes plant<sup>-1</sup>, harvest index, and biological yield recorded a highly significant and positive correlation with achene yield. The results align with the earlier findings of Hladni et al. (2006), Khokhar et al. (2006), Srimuenwai (2006), Kaya et al. (2007), Machikowa and Saetang (2008), Sowmya et al. (2010), Patil (2011), Pivetta et al. (2012), and Singh et al. (2018).

Path coefficient analysis showed that achene weight has the highest direct and indirect positive effect on achene yield. Thus, the achene weight had a more substantial influence on the achene yield of sunflower. Shankar et al. (2006); Arshad et al. (2007); and Hidayatullah et al. (2008) applied the path coefficient by partitioning the genotypic correlations into direct and indirect effects of the traits. However, Habib et al. (2006) reported positive direct effects of the number of seed per head on seed yield. However,

Ashoke et al. (2000); and Tahir et al. (2002) also studied the positive direct effect of head diameter and 100-achene weight on achene weight per head. Therefore, it can be concluded that direct and indirect selection of achene weight can improve sunflower achene yield.

## Conclusion and Recommendation

The results obtained from this study concluded that fertigation and foliar application of NPK increase the diameter of the sunflower head. Therefore, a larger head size produced a higher number of achenes. This increase in the number of achenes per head ultimately increases seed yield. Thus, it is recommended to conduct further study to investigate the effect of fertigation and foliar applications of NPK on sunflower seed oil content. More studies are also needed to determine the influence of this type of NPK application on the number of achenes per head at different growing seasons.

## REFERENCES

- [1] Abassi, M. K., Kazmi, M., Hussan, F. U. (2005): Nitrogen use efficiency and herbage production of an established grass sward in relation to moisture and nitrogen fertilization. – *Journal of plant nutrition* 28(10): 1693-1708.
- [2] Adediran, J. A., Taiwo, L. B., Akande, M. O., Sobulo, R. A., Idowu, O. J. (2005): Application of organic and inorganic fertilizer for sustainable maize and cowpea yields in Nigeria. – *Journal of plant nutrition* 27(7): 1163-1181.
- [3] Ahmed, A. G., Orabi, S. A., Gaballah, M. S. (2010): Effect of bio-NP fertilizer on the growth, yield and some biochemical components of two sunflower cultivars. – *International Journal of Academic Research* 2(4).
- [4] Akbari, P., Ghalavand, A., Sanavy, A. M., Alikhani, M. A. (2011): The effect of biofertilizers, nitrogen fertilizer and farmyard manure on grain yield and seed quality of sunflower (*Helianthus annuus* L.). – *Journal of Agricultural Technology* 7(1): 173-184.
- [5] Alberio, C., Izquierdo, N. G., Aguirrezábal, L. A. N. (2015): Sunflower crop physiology and agronomy. – *AOCS, Elsevier*, pp. 53-91.
- [6] Aquino, L. A. D., da Silva, F. D., Berger, P. G. (2013): Agronomic characteristics and nutritional status of irrigated sunflower cultivars. – *Revista Brasileira De Engenharia Agrícola E Ambiental* 17(5): 551-557.
- [7] Arshad, M., Ilyas, M. K., Khan, M. A. (2007): Genetic divergence and path coefficient analysis for seed yield traits in sunflower (*Helianthus annuus* L.) hybrids. – *Pak. J. Bot* 39(6): 2009-2015.
- [8] Ashoke, S., Mohamed Sheriff, N., Narayanan, S. L. (2000): Character association and path coefficient analysis in sunflower. – *Crop Res* 20(3): 453-456.
- [9] Brady, C. N., Weil, R. R. (2005): *The nature and properties of soils*. – Pearson Education, Inc.
- [10] Chen, J. H. (2006): The combined use of chemical and organic fertilizers and/or biofertilizer for crop growth and soil fertility. – *International workshop on sustained management of the soil-rhizosphere system for efficient crop production and fertilizer use* 16(20): 1-11.
- [11] Darby, H., Harwood, H., Cummings, E., Madden, R., Monahan, S. (2013): 2012 Sunflower population and nitrogen rate trial. – *Northwest Crops & Soils program* 253.
- [12] Demir, A. O., Göksoy, A. T., Büyükcangaz, H., Turan, Z. M., Köksal, E. S. (2006): Deficit irrigation of sunflower (*Helianthus annuus* L.) in a sub-humid climate. – *Irrigation Science* 24(4): 279-289.

- [13] Denčić, S., Mladenov, N., Kobiljski, B. (2012): Effects of genotype and environment on breadmaking quality in wheat. – International Journal of plant production 5(1): 71-82.
- [14] Habib, H., Mehdi, S. S., Rashid, A., Anjum, M. A. (2006): Genetic association and path analysis for seed yield in sunflower (*Helianthus annuus* L.). – Pak. j. Agri. Sci 43(3-4): 136-139.
- [15] Hakim, K., Hidayat, R., Bakht, J., Sher, A. K., Ayub, K. K. (2013): Genotype X Environment interactions and heritability estimates for home agronomic characters in sunflower. – The J. Anim. and Plant Sci. 23: 1177-1184.
- [16] Haseeb, M., Maqbool, N. (2015): Influence of foliar applied nitrogen on reproductive growth of sunflower (*Helianthus annuus* L.) under water stress. – Agricultural Sciences 6(12): 1413.
- [17] Hassan, S. W. U. L., Oad, F. C., Shamasuddin, T., Gandahi, A. W., Siddiqui, M. H., Oad, S. M., Jagirani, A. W. (2010): Effect of N application and N splitting strategy on maize N uptake, biomass production and physio-agronomic characteristics. – Sarhad Journal of Agriculture 26(4): 551-558.
- [18] Hassanlouee, M., Baghbani, F. (2013): Effects of stages and amount of nitrogen foliar application on yield and yield components in hybrid Alestar sunflower. – ARPN Journal of Agricultural and Biological Science 8(3): 224-226.
- [19] Hebbar, S. S., Ramachandrappa, B. K., Nanjappa, H. V., Prabhakar, M. (2004): Studies on NPK drip fertigation in field grown tomato (*Lycopersicon esculentum* Mill.). – European Journal of Agronomy 21(1): 117-127.
- [20] Hidayatullah, M., Jatoi, S. A., Ghafoor, A., Mahmood, T. (2008): Path coefficient analysis of yield component in tomato (*Lycopersicon esculentum*). – Pak. J. Bot. 40(2): 627-635.
- [21] Hladni, N., Škorić, D., Kraljević-Balalić, M., Sakač, Z., Jovanović, D. (2006): Combining ability for oil content and its correlations with other yield components in sunflower (*Helianthus annuus* L.). – Helia 29(44): 101-110.
- [22] Hussain, T. I., Ahmed, M. A., Haq, M. A., Jamil, M., Zia, M. H. (2000): EM Technology- A new look for IPNM. – Proc. Symp., Integrated Plant Nutrient Management, NFDC, Islamabad, Pakistan.
- [23] Iqbal, J., Hussain, B., Saleem, M. F., Munir, M. A., Aslam, M. (2008): Bioeconomics of autumn planted sunflower (*Helianthus annuus* L.) hybrids under different NPK application. – Pak. J. Agri. Sci. 45(3): 19-24.
- [24] Janamma, P., Jabeen, F., Ranganatha, A. (2008): Association analysis in sunflower (*Helianthus annuus* L.). – J. Res. ANGRAU 36(2-3): 55-59.
- [25] Kaka, A. H. (2008): To study the effect of integrated nutrient management on quantitative and qualitative characters of sunflower. – agris.fao.org. 1-76.
- [26] Kaya, Y., Evci, G., Durak, S., Pekcan, V., Gücer, T. (2007): Determining the relationships between yield and yield attributes in sunflower. – Turkish Journal of Agriculture and Forestry 31(4): 237-244.
- [27] Khokhar, M. I., Sadaqat, H. A., Tahir, M. N. (2006): Association and effect of yield related traits on achene yield in sunflower. – Int. J. Agric. Biol. 8(4): 450-451.
- [28] Kumar, S., Asrey, R., Singh, R. (2000): Fertigation: need of modern agriculture. – Yojana-Delhi 44(7): 31-33.
- [29] Kurdistan Regional Government. (2018): Kurdistan's geography and climate. – Available at: <http://cabinet.gov.krd/a/d.aspx?s=010000&l=12&a=18656>.
- [30] Machikowa, T., Saetang, C. (2008): Correlation and path coefficient analysis on seed yield in sunflower. – Suranaree J. Sci. Technol 15(3): 243-248.
- [31] Malik, M. A., Saleem, M. F., Sana, M., Rehman, A. (2004): Suitable level of N, P and K for harvesting the maximum economic returns of sunflower (*Helianthus annuus* L.). – International Journal of Agriculture and Biology (Pakistan) 6(2): 240-242.
- [32] Murphy, D. J. (2010): Improvement of industrial oil crops. – In: Singh, B. P. (ed.) Industrial crops and uses. CABI International, Cambridge, pp. 183-206.

- [33] Nasreen, S., Khan, M. A., Zia, M., Ishaque, M., Uddin, S., Arshad, M., Zarrin, F. (2015): Response of sunflower to various pre-germination techniques for breaking seed dormancy. – Pakistan Journal of Botany 47(2): 413-416.
- [34] Onemli, F., Gucer, T. (2010): Response to drought of some wild species of *Helianthus* at seedling growth stage. – Helia 33(53): 45-54.
- [35] Ozer, H., Polat, T., Ozturk, E. (2004): Response of irrigated sunflower (*Helianthus annuus* L.) hybrids to nitrogen fertilization: growth, yield and yield components. – Plant Soil and Environment 50(5): 205-211.
- [36] Patil, L. C. (2011): Research note correlation and path analysis in sunflower populations. – Electronic Journal of Plant Breeding 2(3): 442-447.
- [37] Pivetta, L. G., Guimarães, V. F., Fioreze, S. L., Pivetta, L. A., Castoldi, G. (2012): Evaluation of sunflower hybrids and the relationship between productive and qualitative parameters. – Revista Ciência Agronômica 43(3): 561-568.
- [38] Popoola, O., Adesanya, K., Olawale, O., Ayanrinde, A. (2016): Factorial analysis on the effect of NPK fertilizer, micronutrients and N-placement on the growth and yield of sunflower. – IJESR 4(1): 22-37.
- [39] Rauf, S., Jamil, N., Tariq, S. A., Khan, M., Kausar, M., Kaya, Y. (2017): Progress in modification of sunflower oil to expand its industrial value. – Journal of the Science of Food and Agriculture 97(7): 1997-2006.
- [40] Saqib, M., Zörb, C., Schubert, S. (2006): Salt-resistant and salt-sensitive wheat genotypes show similar biochemical reaction at protein level in the first phase of salt stress. – Journal of Plant Nutrition and Soil Science 169(4): 542-548.
- [41] Scheiner, J. D., Gutiérrez-Boem, F. H., Lavado, R. S. (2002): Sunflower nitrogen requirement and 15N fertilizer recovery in Western Pampas, Argentina. – European Journal of Agronomy 17(1): 73-79.
- [42] Shafi, M., Bakht, J., Yousaf, M., Khan, M. A. (2013): Effects of irrigation regime on growth and seed yield of sunflower (*Helianthus annuus* L.). – Pak. J. Bot 45(6): 1995-2000.
- [43] Shankar, V. G., Ganesh, M., Ranganatha, A. R. G., Bhave, M. H. V. (2006): A study on correlation and path analysis of seed yield and yield components in sunflower (*Helianthus annuus* L.). – Agricultural Science Digest 26(2): 87-90.
- [44] Siddiqi, M. H., Ali, S., Bakht, J., Khan, P., Aslam, S., Khan, N. (2012): Evaluation of sunflower lines and their crossing combinations for morphological characters. yield and oil contents. – Pak. J. Bot. 44(2): 687-690.
- [45] Sidlauskas, G., Bernotas, S. (2003): Some factors affecting seed yield of spring oilseed rape (*Brassica napus* L.). – Agronomy Research 1(2): 229-243.
- [46] Singh, I., Stoskopf, N. (1971): Harvest index in cereal 1. – Agronomy Journal 63(2): 224-226.
- [47] Singh, V. K., Chander, S. (2018): Correlation analysis for seed yield and its component traits in sunflower. – Journal of Pharmacognosy and Phytochemistry 7(3): 2299-2301.
- [48] Sowmya, H. C., Shadakshari, Y. G., Pranesh, K. J., Srivastava, A., Nandini, B. (2010): Character association and path analysis in sunflower (*Helianthus annuus* L.). – Electronic Journal of Plant Breeding 1(4): 828-831.
- [49] Srimuenwai, P. (2006): Improvement of agronomic characters, oil content and yield of synthetic varieties of sunflower. – M. Sc. thesis, School of Crop Production Technology, Institute of Agriculture, Suranaree University of Thechnology, Thailand, 80p.
- [50] Tahir, M. H. N., Sadaqat, H. A., Bashir, S. (2002): Correlation and path coefficient analysis of morphological traits in sunflower (*Helianthus annuus* L.) populations. – Int. J. Agri. Biol 4(3): 341-343.
- [51] Taran, S. A., Baloch, D. M., Khan, N. U., Bakht, J., Ghaloo, S. H., Shahwani, M. N., Kakar, M. S. (2013): Earliness and yield performance of sunflower hybrids in uplands of Balochistan, Pakistan. – Pak. J. Bot 45(4): 1397-1402.

- [52] Tuo, D., An, H., Zhang, J., Li, Z. H. (2010): The current situation of sunflower fertilizer technology at home and abroad and its development trend. – Inner Mongolia Agricultural Science and Technology 6: 1-2.
- [53] Varga, B., Svečnjak, Z. (2006): The effect of late-season urea spraying on grain yield and quality of winter wheat cultivars under low and high basal nitrogen fertilization. – Field Crops Research 96(1): 125-132.
- [54] XLSTAT version (2016): XLSTAT 2016. – Data analysis and statistics with Microsoft Excel, Paris, France, MacOS ed.
- [55] Zheljzkov, V. D., Vick, B. A., Ebelhar, M. W., Buehring, N., Baldwin, B. S., Astatkie, T., Miller, J. F. (2008): Yield, oil content, and composition of sunflower grown at multiple locations in Mississippi. – Agronomy Journal 100(3): 635-642.

## APPENDIX

*Mean squares of variance analysis for achene yield and its components at both locations and their average*

S. O. V	d. f	Head diameter (cm)	Head Weight (g)	Achene weight (g)	No. of achenes plant <sup>-1</sup>	1000 Achene weight (g)	Harvest index	Biological yield (kg ha <sup>-1</sup> )	Achene yield (kg ha <sup>-1</sup> )
First location									
Block	2	1.241	545.962	7.424	98144.94	10.573	0.0006	1618367	32996.8
NPK application	2	93.804**	24911.43**	9725.821**	902047.4**	808.189**	0.0216*	1.19E+08**	43226305**
E(a)	4	0.456	377.642	155.647	31920.54	14.568	0.0017	2781557	691770.1
Genotype	2	50.790**	7583.406**	6240.381**	955249.8**	444.477*	0.0076*	1.86E+08**	27735305**
NPK *	4	2.268*	598.964*	511.474*	97006.05*	44.524*	0.0040*	865083.1 <sup>N.S</sup>	2273242*
Genotype E(b)	12	0.576	167.796	117.483	24201.02	11.349	0.0012	1480429	522152.3
Second location									
Block	2	2.424	1864.317	349.104	111185.3	17.14	0.0004	11232187	1551588
NPK application	2	31.667**	9233.879*	3800.107*	349273.7**	227.631**	0.0067 <sup>N.S</sup>	1.05E+08**	16889532*
E(a)	4	0.264	444.530	419.782	15078.72	8.913	0.0027	3811504	1865718
Genotype	2	53.253**	4844.21**	3065.317**	669619.5**	70.682*	0.0146*	48285819**	13623766**
NPK *	4	1.590*	328.273*	149.175*	52828.7*	22.589 <sup>N.S</sup>	0.0029*	1293115 <sup>N.S</sup>	663006.4*
Genotype E(b)	12	0.446	80.851	31.009	10844.51	12.100	0.0007	925366.1	137819.5
Average of both locations									
Location	1	15168.81**	993919.5**	406524.3**	1.12E+08**	153626.8**	5.545**	1.66E+10**	1.81E+09**
Block/L	4	1.832	1205.14	178.264	104665.1	13.856	0.0005	6425277	792292.4
E(a)	2	117.202**	32160.79**	12805.55**	1171728**	916.119**	0.0263**	2.23E+08**	56914111**
NPK application	2	8.268	1984.519	720.381	79592.83	119.701	0.0021	858904.1	3201727
NPK *	4	0.360	411.086	287.715	23499.63	11.741	0.0022	3296531	1278744
Location E(b)/L	8	103.945**	11229.48**	8920.185**	1595622**	278.361**	0.0189**	2.07E+08**	39645662**
Genotype	2	0.099	1198.131	385.513	29247.4	236.798	0.0033	27332793	1713410
Genotype *	4	3.375**	696.316**	494.126**	119764**	37.82*	0.0027*	1211356 <sup>N.S</sup>	2196136**
Location NPK *	4	0.482	230.921	166.524	30070.77	29.293	0.0042	946842.4	740112.5
Genotype NPK *	4	0.511	124.324	74.246	17522.77	11.725	0.0009	1202898	329985.9
Genotype L E(c)/L	24								

LSD value at  $P \leq 0.01$  = Highly significant \*\*, LSD value at  $P \leq 0.05$  = Significant \*, N. S. = Statistically non-significant

# GRAIN YIELD AND ENVIRONMENTAL IMPACTS OF ALTERNATIVE RICE (*ORYZA SATIVA* L.) ESTABLISHMENT METHODS IN MYANMAR

HTWE, T.<sup>1</sup> – TECHATO, K.<sup>1,2</sup> – CHOTIKARN, P.<sup>1,3,4</sup> – SINUTOK, S.<sup>1,4\*</sup>

<sup>1</sup>*Faculty of Environmental Management, Prince of Songkla University, 90110 Songkhla, Thailand*

<sup>2</sup>*Environmental Assessment and Technology for Hazardous Waste Management Research Center, Prince of Songkla University, 90110 Songkhla, Thailand*

<sup>3</sup>*Marine and Coastal Resources Institute, Faculty of Environmental Management, Prince of Songkla University, 90110 Songkhla, Thailand*

<sup>4</sup>*Coastal Oceanography and Climate Change Research Center, Prince of Songkla University, 90110 Songkhla, Thailand*

*\*Corresponding author*

*e-mail: ssutinee@gmail.com; phone +66-74-286-847; fax: +66-74-429-758*

(Received 26<sup>th</sup> Aug 2020; accepted 18<sup>th</sup> Dec 2020)

**Abstract.** Field experiments were conducted in the summer rice growing season of 2019 in Myanmar, to examine the grain yield and environmental impacts of rice under two alternative crop establishment methods: system of rice intensification (SRI) and modified SRI (MSRI), and two conventional methods: farmers' practices (FP) and direct seeded rice (DSR). A randomized complete block design with five replications was used. In the present study, the leaf area index (LAI) with all tested methods was not significantly different at flowering and harvesting stages. Grain yield and the soil and plant analysis development (SPAD) reading at flowering stage did not significantly differ among the three transplanted methods. However, DSR showed significantly lower yield than FP and MSRI. This reduction might be due to shorter panicle length and fewer spikelets per panicle in DSR. The global warming potentials were 4066.94, 4067.08, 4475.75 and 4136.74 kg CO<sub>2</sub> eq ha<sup>-1</sup> for SRI, MSRI, FP and DSR, respectively. MSRI emitted less greenhouse gas (GHG) than FP with statistically similar grain yield, indicating that it could be a better alternative to other methods. In addition, somewhat closer spacing with two seedlings per hill (MSRI) can further enhance rice yield with higher resource use efficiency in Myanmar or similar agroclimatic regions.

**Keywords:** *MSRI, GHGs emission, sustainable, LAI, plant spacing*

## Introduction

To feed the growing population, germplasm development and crop production management are important in improving resource use efficiency (Guo et al., 2017; Roberts et al., 2018). Rice cultivation consumes more water than other crops. Water resources are becoming scarce as a result of climate change, with a short rainy period and urban consumption patterns. Today's intensive agriculture relies heavily on chemical fertilizers and affects the environment adversely (Iqbal et al., 2019). Combination of organic and inorganic fertilizers can increase grain yield (Hasanuzzaman et al., 2010) and support sustainable crop productivity (Myint et al., 2011). Along with this, farmers need to modify their management practices to adapt to current and further changing demands (GRiSP, 2013).



Different rice cultivation methods have been adopted depending on the available resources and geographic conditions. Transplanting rice is the predominant practice in Myanmar, as this provides a chance to suppress weed growth before transplanting rice seedlings and favours easy management. However, some farmers in Myanmar are interested in direct seeding of rice, since the labour for transplanting and seedbed preparation can be saved. Weed infestation, however, is a common problem in directly seeded rice (DSR), as rice and weeds germinate at the same time, and land levelling is necessary for effective weed control. The yield of direct seeded rice was lower than that of transplanted rice in Dera Ismail Khan, Pakistan (Javaid et al., 2012). Similarly, early transplanted rice had higher grain yield than directly seeded rice (Kumhar et al., 2016). However, grain yields of direct seeded and transplanted method were not significantly different (Rana et al., 2014). The SRI method resulted higher leaf area index (LAI), grain yield and harvest index (HI) in comparison with a non-SRI method or direct seeded rice in India (Tomar et al., 2018). In Bangladesh, the grain yield under SRI and the recommended transplanting method were statistically similar (Nahar et al., 2018). Different rice varieties respond differently to the SRI method (Kesh et al., 2017). Thus, Stoop et al. (2002) encouraged testing the SRI method for specific environments and considering some changes, for example, in spacing or age of seedling to be transplanted, for successful application.

Harvest index of rice varies by genotype, season, location, nutrient condition and plant density (Amanullah and Inamullah, 2016; Bozorgi et al., 2011; Mohamad, 1994). Leaf area index (LAI) is a well-known growth indicator influenced by variety, plant density, soil nutrient status, CO<sub>2</sub>, temperature, crop establishment method and season (Fagade and De Datta, 1971; Geethalakshmi et al., 2017). Hirooka et al. (2017) stated that LAI at the heading stage of rice in farmers' field in Loa PDR, correlated with the grain yield. The soil and plant analysis development (SPAD) chlorophyll meter is widely used nowadays to estimate nitrogen (N) status in leaves. Light intensity in low N conditions affects the reading, and different points of rice leaves give different measured values (Yuan et al., 2016).

Three main gases: methane (CH<sub>4</sub>), carbon dioxide (CO<sub>2</sub>) and nitrous oxide (N<sub>2</sub>O) are responsible for increasing global warming potential in agriculture. Rice fields are considered the major source of methane emission which can lead to global warming potential (Arunrat et al., 2016). However, rice is a staple food crop for most people in Southeast Asian countries. Therefore, increasing rice production to accommodate the growing population is crucial while it need to perform better management of rice cultivation method to mitigate greenhouse gas emission (Islam et al., 2018a; Wang et al., 2016). It is demonstrated that decomposition of organic matter in flood rice field is ideal for methanogenesis. Nitrogen fertilizer application method, rate, time and fertilizer type, and water status of field have a significant effect on nitrous oxide emission (Islam et al., 2018b; Millar et al., 2014). Methane production in rice field is affected by number of factors. Application of sulphate containing fertilizer, gypsum, and intermittent irrigation could reduce its emission (Aulakh et al., 2001; Oo et al., 2016). Yi-hu et al. (2014) investigated the effect of different kinds of organic fertilizer on GHGs emission. The results revealed that all organic fertilizer emitted more than non-fertilized treatment. In addition, green manure had greater effect on CH<sub>4</sub> emission than animal and biogas residues (Traore et al., 2017).

Myanmar is an agricultural country where agriculture contributes 20% of the GDP. The actual total sown area of paddy rice was about 7.21 million hectares in 2015-2016,

comprising monsoon and summer paddy (MOALI, 2016). System of rice intensification method (SRI) was introduced in northern Myanmar and spread to other parts of Myanmar. This is a strategy contributing to climate resilient cultural practices in Myanmar and it is aiming for higher productivity and profitability by using effective natural resources management practices (Hom et al., 2015; MRDS, 2015). The number of seedlings per hill affected the number of panicles per hill and final grain yield (Promsomboon et al., 2019). Therefore, the number of effective tillers for a unit area is one of the most important yield components for increasing the grain yield. One issue with the SRI method is the cost and drudgery for refilling places of the dead seedlings during the recovery period. Based on above mentioned, we modified the SRI method here to have two seedlings per hill, instead of one seedling per hill, to reduce those costs and increase the number of the effective tillers per unit area. This study was conducted to investigate how the alternative crop establishment methods: SRI, MSRI perform and contribute to grain yield, and global warming potential in comparison with FP and DSR.

## Materials and methods

### *Experimental procedure*

Field experiments were conducted in the summer rice growing season in 2019, at Pwint Phyu Seed Farm (20°21'41.3"N, 94°40'24.3"E), in central Myanmar (*Fig. 1*). A randomized complete block design with five replications was used. The treatments were system of rice intensification (SRI), modified SRI (MSRI), farmer's usual transplanting method (FP) and directly seeded rice (DSR). The SRI and MSRI were considered as alternative rice cultivation methods for the protection and conservation of the limited resources without compromising grain yield. Yadanartoe rice variety was planted in this study since most of the farmers in that region use this variety. The minimum and maximum temperature and rainfall during the experiment were recorded in the experimental farm, and given in *Table 1*. The rainy weather was observed only in the later growth stage of rice. The soil is silty clay loam with a pH of 6.59, total N of 0.27%, available phosphorus (P) of 0.02 ppm, exchangeable potassium (K) of 0.468 cmol<sub>c</sub> kg<sup>-1</sup>, and cation exchange capacity (CEC) of 18.03 cmol<sub>c</sub> kg<sup>-1</sup>. The seeds were soaked for 24 h and incubated for another 24 h before seeding. Then, the germinated seeds were sown on well prepared raised beds and seedlings were transplanted to the main field as per treatments (SRI, MSRI, FP). For DSR, the sprouted seeds were planted manually to the line with the seed rate of 80 kg per acre to compensate the damage from rodents, poor seedlings establishment in low lying spot area, and suppress the growth of weed. Simplifications of some differences among the treatments are shown in *Table 2*.

**Table 1.** Weather condition during the experiment

Months	Rainfall (mm)	Minimum temperature (°C)	Maximum temperature (°C)
01 March – 31 March	-	18	41
01 April – 30 April	-	20	43
01 May – 31 May	8.13	26	43
01 June – 30 June	72.13	21	43
01 July – 05 July	5.08	25	36

**Table 2.** Simplification of some components in different rice cultivation methods

Components	System of rice intensification (SRI)	Modified system of rice intensification (MSRI)	Farmers' practices (FP)	Direct seeded rice (DSR)
Farmyard manure at final land preparation (t ha <sup>-1</sup> )	15	15	-	-
Chemical fertilizer (N-P <sub>2</sub> O <sub>5</sub> -K <sub>2</sub> O kg ha <sup>-1</sup> )	5-5-5	5-5-5	53-29-37	53-29-37
Application time				
- At final land preparation	-	-	Full dose of P <sub>2</sub> O <sub>5</sub> , 1/3 dosage of nitrogenous fertilizer and half dose of K <sub>2</sub> O	Full dose of P <sub>2</sub> O <sub>5</sub> , 1/3 dosage of nitrogenous fertilizer and half dose of K <sub>2</sub> O
- 2 weeks after transplanting	Half dose of N, P <sub>2</sub> O <sub>5</sub> , K <sub>2</sub> O	Half dose of N, P <sub>2</sub> O <sub>5</sub> , K <sub>2</sub> O	1/3 dosage of nitrogenous fertilizer	
- 4 weeks after seeding				1/3 dose of nitrogenous fertilizer
- Panicle initiation (PI)	Half dose of N, P <sub>2</sub> O <sub>5</sub> , K <sub>2</sub> O	Half dose of N, P <sub>2</sub> O <sub>5</sub> , K <sub>2</sub> O	1/3 dose of nitrogenous fertilizer and half dose of K <sub>2</sub> O	1/3 dose of nitrogenous fertilizer and half dose of K <sub>2</sub> O
Transplanting (seedling(s)/hill)	1	2	3 to 4	Directly seeded
Seedling age (days)	15	15	30	-
Spacing (cm <sup>2</sup> )	25×25	25×25	20×20	25 cm between row
Water level	Moist condition at vegetative growth stage and 2-5 cm from PI to 2 weeks before harvest was maintained	Moist condition at vegetative growth stage and 2-5 cm from PI to 2 weeks before harvest was maintained	2-8 cm of water level was kept throughout growing season up to 2 weeks before harvest	2-8 cm of water level was kept throughout growing season up to 2 weeks before harvest



**Figure 1.** Overview of the experiment

A multipseQ device (PhotosynQ, United States) was used for photosynthetic efficiency measurement (maximum and effective quantum yield, and chlorophyll (SPAD) reading) (Kuhlgert et al., 2016; Ndikuryayo et al., 2020). The fully developed uppermost leaf was measured at the 1/3 from the leaf tip position for four random hills per plot, and the averages were used to get the mean value by treatment. Measurements were taken from 10:00 to 11:00. The maximum quantum yield was measured at predawn (Shanker et al., 2019).

Each plot occupied 7.5 m × 21 m and the plots were surrounded by bunds (0.3 m height × 0.3 m width), and the bunds were separated by 1 m wide alleys (Pimratch et al., 2015). At the harvesting time, 5 m × 5 m at the center of the plot was harvested for grain yield determination, which was converted to kg ha<sup>-1</sup>. The moisture content of rice was 14% (dry weight basis). Straw was over dried at 70 °C until constant weight and the dry weight of straw was recorded. Twelve randomly hills from each plot were selected, and the average value per plot was used for the yield components and plant height data (Chen et al., 2019). The plant height was measured from the base of the plant to the longest leaf tip at early tillering stage, panicle initiation (PI; BBCH 34) and flowering stages (BBCH 61) while it was measured from the base of the plants to the tip of panicle at harvesting stage (BBCH 89; Lancashire et al., 1991). ImageJ software was applied for the leaf area measurement (Savvides and Fotopoulos, 2018). The leaf area index and harvest index were calculated with *Equations 1* and *2* (Yoshida, 1981).

$$\text{Leaf area index (LAI)} = \frac{\text{Total leaves area (cm}^2\text{)}}{\text{Ground area where the leaves have been taken (cm}^2\text{)}} \quad (\text{Eq.1})$$

$$\text{Harvest index (HI)\%} = \frac{\text{Dry weight of grain yield (kg ha}^{-1}\text{)}}{\text{Dry weight of the total aboveground biomass (kg ha}^{-1}\text{)}} \quad (\text{Eq.2})$$

### **Greenhouse gas emissions**

The greenhouse gas emission was calculated with the following formulas (Arunrat and Pumijumnong, 2017; IPCC, 2006; Tubiello et al., 2015; Yodkhum et al., 2018) and calculation was considered within the farm gate. The global warming potential (GWP) conversion parameters of CO<sub>2</sub>, CH<sub>4</sub> and N<sub>2</sub>O (over 100 years) were 1, 25 and 298 kg ha<sup>-1</sup> CO<sub>2</sub> equivalent (IPCC, 2007). Imidacloprid (70% WP) insecticide was used in this experiment and emission factors were presented in *Table 3*. Annual methane emission for 1 ha was estimated by the multiplication of adjusted daily emissions factor (EF<sub>i</sub>) with the duration of rice (days) (*Eqs. 3* and *4*). The fields under FP and DSR were continuously flooded, and weeding was done by manually.

$$EF_i = EF_c \times SF_w \times SF_p \times SF_0 \quad (\text{Eq.3})$$

where: EF<sub>c</sub> = baseline emissions factor for continuously flooded field without organic amendments, SF<sub>w</sub> = a scaling factor for varying water status in rice cultivation, SF<sub>p</sub> = a scaling factor for water status of field before cultivation, SF<sub>0</sub> = a scaling factor for farmyard manure (FYM) application.

$$SF_0 = (1 + \sum_i ROA_i \times CFOA_i)^{0.59} \quad (\text{Eq.4})$$

where:  $ROA_i$  = amount of farmyard manure applied ( $t\ ha^{-1}$ ),  $CFOA_i$  = conversion factor for farmyard manure  $i$ .

Direct and indirect emissions by synthetic fertilizer were calculated by *Equations 5 and 6* (IPCC, 2006).

$$\text{Direct } N_2O \text{ emissions (kg } N_2O \text{ yr}^{-1}) = (F_{SN} \times 0.01 \times 44/28) \quad (\text{Eq.5})$$

$$\text{Indirect } N_2O \text{ emissions (kg } N_2O \text{ yr}^{-1}) = [(F_{SN} \times \text{Frac}_{GASF} \times 0.01) + (F_{SN} \times \text{Frac}_{Leach} \times 0.0075)] \times 44/28 \quad (\text{Eq.6})$$

where:  $\text{Frac}_{GASF}$  = fraction of synthetic fertilizer that volatilizes as  $NH_3$  and  $NO_x$ ,  $\text{Frac}_{Leach}$  = fraction of synthetic fertilizer that leaches as  $NH_3$  and  $NO_x$ .

**Table 3.** Emission factors for the calculation of greenhouse gas

Activity	Emission factor	Unit	References
Diesel	2.76	kgCO <sub>2</sub> eq L <sup>-1</sup>	Ilahi et al., 2019
Insecticide	5.1	kgCO <sub>2</sub> eq kg <sup>-1</sup>	Arunrat and Pumijumnong, 2017; Lal et al., 2004
EF <sub>c</sub>	1.3	kgCH <sub>4</sub> ha <sup>-1</sup> day <sup>-1</sup>	IPCC, 2006
SF <sub>w</sub>	0.52 = SRI and MSRI, 1 = FP and DSR		IPCC, 2006
SF <sub>p</sub>	1 in all methods		IPCC, 2006
CFOAi	0.14		IPCC, 2006
Frac <sub>Leach</sub>	0.3	Kg.N kg <sup>-1</sup> N applied	Tubiello et al., 2015
Frac <sub>GASF</sub>	0.1	Kg.NH <sub>3</sub> -N. + NO <sub>x</sub> -N.kg <sup>-1</sup> N applied	Tubiello et al., 2015

### Statistical analysis

One-way ANOVA was performed to test the differences among the treatments means. Comparison of means were made by Tukey's test at 5% level of confidence. Before conducting ANOVA, a homogeneity test (Levene's test) and a normality test (Kolmogorov-Smirnov) were carried out.

## Results

### Plant height (cm)

The plant height of rice under the different rice cultivation methods at tillering, PI, flowering and harvesting stages is shown in *Figure 2*. At the tillering stage, the heights with SRI, MSRI and DSR did not significantly differ. The FP method showed the shortest plant height among the treatments ( $P < 0.001$ ). At PI stage, there was no significantly different ( $P > 0.05$ ). As for flowering stage, the tallest plants were observed with the SRI method, which was on par with the MSRI. The shortest plant height occurred under FP, without significantly difference from DSR ( $P < 0.001$ ). The plants grown under SRI and MSRI were significantly higher than those under FP and DSR at harvesting stage ( $P < 0.001$ ).

### Leaf area index (LAI)

Rice cultivation methods affected LAI at different growth stages (*Fig. 3*). The highest LAI with MSRI and DSR methods achieved at PI stage, while the FP method



showed the highest LAI at flowering stage. At PI stage, LAI of MSRI and DSR was significantly higher than those of the other three methods ( $P < 0.001$ ). Regarding LAI at flowering stage, the higher LAI values were observed under MSRI, FP and DSR although there were no significantly different among the treatments ( $P > 0.05$ ). All methods showed statistically similar LAI at harvesting stage ( $P > 0.05$ ).

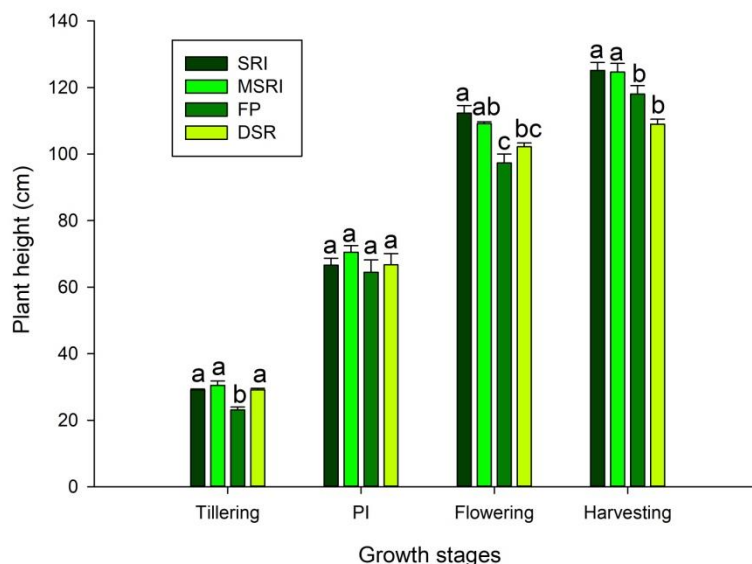


**Figure 2.** Plant heights by four rice cultivation methods at different growth stages. SRI = System of Rice Intensification, MSRI = Modified System of Rice Intensification, FP = Farmer's practices, DSR = Direct Seeded Rice, PI = Panicle initiation. Bars indicate mean  $\pm$  SE ( $n = 5$ ). Significant differences are shown by different lowercase letters ( $P < 0.05$ )

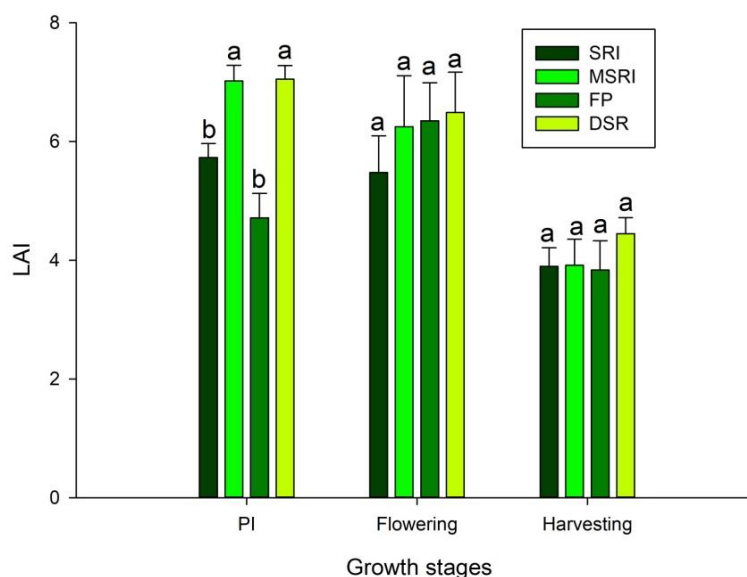


**Figure 3.** Leaf area index (LAI) by rice cultivation method at different growth stages. SRI = System of rice intensification, MSRI = Modified system of rice intensification, FP = Farmers' practices, DSR = Direct seeded rice, PI = Panicle initiation. Bars indicate mean  $\pm$  SE ( $n = 5$ ). Significant differences are shown by different lowercase letters ( $P < 0.05$ )

### Number of tillers $m^{-2}$

Number of tillers  $m^{-2}$  was significantly affected by planting method. At tillering stage, the most number of tillers  $m^{-2}$  was observed with DSR, followed by MSRI, FP and SRI ( $P < 0.001$ ). At PI stage, similar trend was observed, in that, the SRI method had significantly lower number of tillers than the other methods ( $P < 0.001$ ). At flowering stage, the number of tillers with three transplanted methods were not significantly different while DSR produced the most number of tillers  $m^{-2}$  among the treatments (Fig. 4;  $P < 0.001$ ).

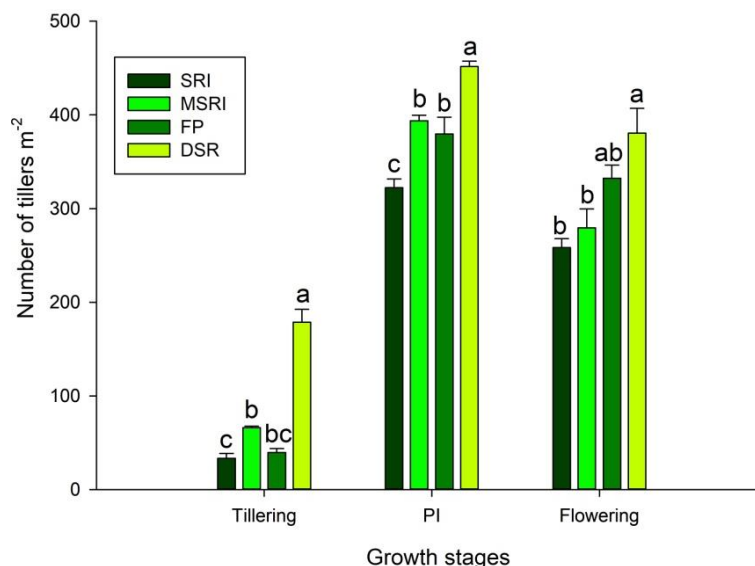


**Figure 4.** Number of tillers by rice cultivation method at different growth stages. SRI = System of rice intensification, MSRI = Modified system of rice intensification, FP = Farmers' Practices, DSR = Direct seeded rice, PI = Panicle initiation. Bars indicate mean  $\pm$  SE ( $n = 5$ ). Significant differences are shown by different lowercase letters ( $P < 0.05$ )

### Chlorophyll SPAD value and Phi2 in light and in the dark conditions

Chlorophyll content (SPAD) is an indirect indicator of nitrogen status of the leaf. The chlorophyll content, in this study, was measured with the multispeQ device. SPAD values of all the treatments were statistically similar at PI stage ( $P > 0.05$ ). SRI and MSRI methods showed significantly higher chlorophyll content than DSR ( $P = 0.012$ ) at flowering stage, while there were no significantly different among three transplanted treatments. Chlorophyll contents under DSR and FP were not statistically different (Fig. 5). Phi2 (fraction of light utilized for photochemistry) in daytime and in the dark condition was not affected by the planting method (Fig. 6;  $P > 0.05$ ).

### Grain yield and its attributes

Effects of rice cultivation methods on yield components are shown in Table 4. Among the yield components, there were no significantly differences in 1000-grain weight, number of panicles  $m^{-2}$  and filled grain percentages. The SRI and MSRI methods showed significantly longer panicles than FP and DSR ( $P < 0.001$ ). Panicle lengths of SRI and MSRI were statistically similar. Furthermore, the SRI and MSRI

produced more spikelets per panicle than FP and DSR ( $P < 0.001$ ). The least number of spikelets per panicle was observed with DSR.

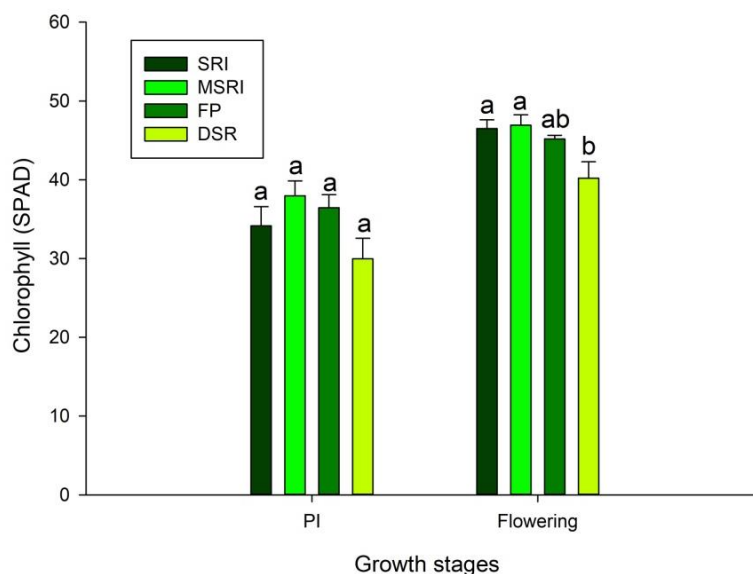


**Figure 5.** Chlorophyll content (SPAD) by rice cultivation method at PI and flowering stages. SRI = System of rice intensification, MSRI = Modified system of rice intensification, FP = Farmers' Practices, DSR = Direct seeded rice, PI = Panicle initiation. Bars indicate mean  $\pm$  SE ( $n = 5$ ). Significant differences are shown by different lowercase letters ( $P < 0.05$ )

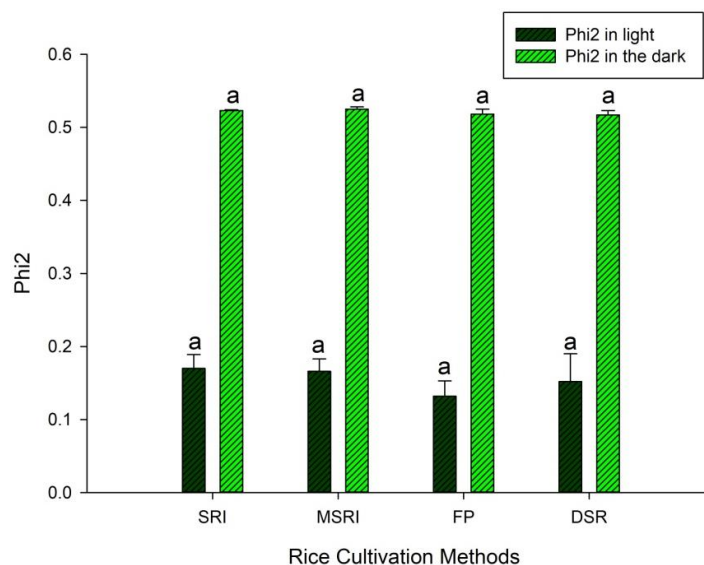


**Figure 6.** Phi2 by rice cultivation method in light and in the dark conditions at flowering stage. SRI = System of rice intensification, MSRI = Modified system of rice intensification, FP = Farmers' practices, DSR = Direct seeded rice. Bars indicate mean  $\pm$  SE ( $n = 5$ )

Grain yield of SRI, MSRI and FP methods were not significantly different, while DSR produced a significantly lower grain yield than other tested methods (Table 5;



P = 0.013). The yield of SRI and DSR were statistically similar. Harvest index of rice was not affected by cultivation methods in this study (P > 0.05).

**Table 4.** Yield components and panicle lengths of different rice cultivation methods (mean ± SE)

Treatment	1000-grain weight (g)	Spikelets panicle <sup>-1</sup>	Number of panicles m <sup>-2</sup>	Filled grain (%)	Panicle length (cm)
SRI	25.38 ± 0.23	135.48 ± 8.05 a	254.82 ± 16.96	91.20 ± 0.76	28.17 ± 0.23 a
MSRI	25.00 ± 0.13	131.18 ± 4.13 a	268.99 ± 27.44	89.50 ± 0.64	26.78 ± 0.46 a
FP	25.50 ± 0.80	94.23 ± 7.47 b	283.11 ± 20.35	86.94 ± 1.78	23.96 ± 0.52 b
DSR	25.46 ± 0.55	61.98 ± 2.74 c	328.66 ± 23.25	89.40 ± 1.43	23.78 ± 1.01 b
Significance	ns	***	ns	ns	***

SRI = System of rice intensification, MSRI = Modified system of rice intensification, FP = Farmers' practices, DSR = Direct seeded rice. Significant differences are shown by different lowercase letters (P < 0.05). \*\*\* = significantly different at P < 0.001, ns = non-significant

**Table 5.** Grain yield and harvest index by rice cultivation method (mean ± SE)

Treatment	Grain Yield (kg ha <sup>-1</sup> )	Harvest Index (%)
SRI	6587.79 ± 267.98 ab	52.78 ± 1.14
MSRI	6662.95 ± 182.63 a	52.59 ± 2.67
FP	6819.65 ± 178.37 a	56.33 ± 1.72
DSR	5816.29 ± 158.01 b	49.37 ± 1.70
Significance	*	ns

SRI = System of rice intensification, MSRI = Modified system of rice intensification, FP = Farmers' practices, DSR = Direct seeded rice. Significant differences are shown by different lowercase letters (P < 0.05). \* = significantly different at P < 0.05, ns = non-significant

### Greenhouse gas emissions

The calculated greenhouse gas emission of different rice cultivation methods is depicted in Figure 7. The global warming potentials were 4066.94, 4067.08, 4475.75 and 4136.74 kg CO<sub>2</sub> eq ha<sup>-1</sup> for SRI, MSRI, FP and DSR, respectively. Higher N<sub>2</sub>O emission was occurred under FP and DSR, which was contributed from higher amount of chemical fertilizer application than those under SRI and MSRI (alternative methods). In the case of methane emission, the application of FYM (15 t ha<sup>-1</sup>) accounted for increasing emission of CH<sub>4</sub> under SRI and MSRI methods.

### Discussion

Potentially facing water scarcity, climate change and soil degradation, agricultural practices that will sustain productivity for future generations are crucial. Performances of different rice establishment methods were evaluated experimentally in this study. The plant heights of SRI and MSRI were generally taller than those of FP and DSR, indicating better crop growth of the former. However, number of tillers m<sup>-2</sup> was affected by cultivation method at all growth stages, with the lowest value generally provided by the SRI method. This in turn was mainly affected by the number of hill m<sup>-2</sup>. At harvesting stage, the FP method produced 10 and 5% more effective tillers m<sup>-2</sup> than SRI and MSRI, respectively, in the present study (Table 4). In a previous study, grain yield

reduction due to lower plant density could not be offset by increased application of N fertilizer (Huang et al., 2013). Therefore, optimum plant population per unit area is important for increasing grain yield.

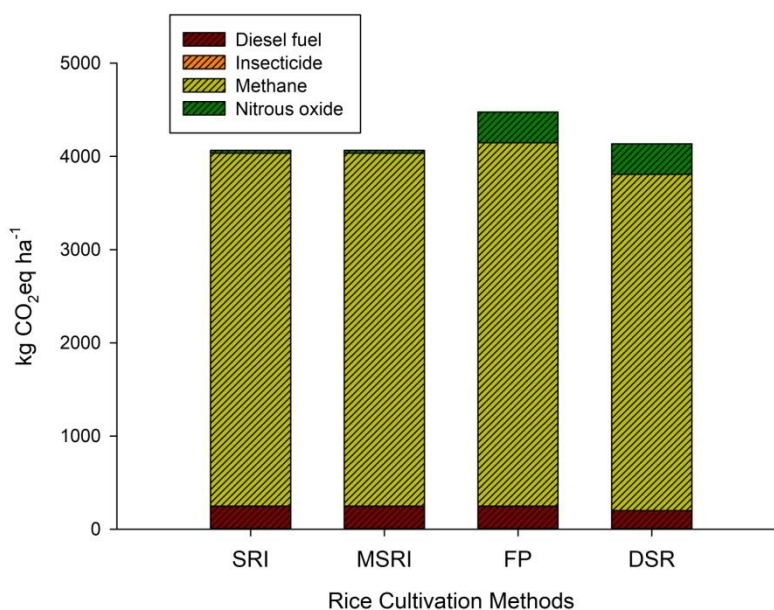


**Figure 7.** Greenhouse gas emission from different rice cultivation methods. SRI = System of rice intensification, MSRI = Modified system of rice intensification, FP = Farmers' practices, DSR = Direct seeded rice

Leaf area index is an important parameter affecting grain yield of rice. Leaf area index of rice is influenced by leaf size and number of leaves per unit area (Tanaka and Kawano, 1965). In the present study, rice cultivation methods affected leaf area index significantly at PI stage. The MSRI and DSR attained the higher LAI than the others, which was mainly attributed by number of leaves per field area. Our results are in line with the report of Gautam et al. (2019), which revealed SRI with some modification gave higher LAI than conventional transplanted rice at PI stage in India. In addition, dry direct seeded rice achieved higher LAI than traditional transplanted rice (Ishfaq et al., 2020). The earlier studies of Sen et al. (2014) and Singh et al. (2014) reported that a wider spacing gave greater LAI value for transplanted rice than a closer one. At flowering and harvesting stages, all rice establishment methods had statistically similar LAI. The MSRI method gave the highest LAI at PI stage, which then decreased gradually towards the harvesting stage. This might be due to the drying of some tillers in the later growth stages.

Chlorophyll content (SPAD) is an indirect indicator of nitrogen status of the leaf. Chlorophyll content at PI stage was influential on grain yield of rice (Ramesh et al., 2002; Gholizadeh et al., 2017). In addition, leaf N content at flowering stage is also important for grain filling and it was positively and significantly correlated with grain yield (Ghosh et al., 2020). In the present study, SPAD value under DSR was low although there was not significantly different from others at PI stage. The SPAD values of SRI, MSRI and FP were statistically similar at flowering stage. However, SRI and MSRI had more leaf nitrogen than DSR. This might be due to higher plant populations per unit

area in DSR, competing for the resources. Phi2 is the fraction of light that is used for photochemistry (Kramer et al., 2004). Phi2 in both light and dark conditions were not affected by planting method in this study. Similarly, different N levels did not significantly affect Phi2 of rice in a hydroponic experiment (Shrestha, 2012). However, SRI with 20 cm × 20 cm, resulted in higher chlorophyll content, maximum and effective quantum of PSII than the recommended rice transplanted method in India. Effective quantum yield of PSII (Phi2) was affected by crop management practices under unstressed conditions (Thakur et al., 2010a).

There was no significant difference in grain yield among SRI, MSRI and FP. In fact, production with SRI was statistically similar to DSR. In other words, MSRI and FP yielded significantly more than DSR. That higher yield was mainly contributed by a greater number of spikelets per panicle, and longer panicle length of the former. Although, DSR had more panicles per unit area, it could not compensate for a smaller number of spikelets per panicle. Our results are supported by Huang et al. (2011). They reported shorter panicles length and a smaller number of spikelets per panicle was observed under DSR and this was related to the poorer nutritional status with DSR in comparison with transplanted rice. Birhane (2013) reported that panicle length of transplanted rice was significantly longer than that of direct seeded rice. In a previous study, transplanted rice gave higher grain yield than DSR (Dileep et al., 2018; Hossain et al., 2002). However, the productions of direct seeded and transplanted rice were statistically similar in the reports of Liu et al. (2015) and Kar et al. (2018). The effectiveness of weed control in DSR might be one of the reasons for differences in grain yield. Harvest index (HI) is the ratio of paddy rice to total plant biomass, excluding the root. In the present study, HI of rice was affected by cultivation method. Similarly, HI with SRI and recommended management practices (RMP) were statistically similar (Thakur et al., 2010b). However, Chandankute et al. (2015) reported grain and HI under SRI method were higher than that under FP. This might be due to differences in agroclimatic conditions. A 20 cm × 20 cm spacing with 3 seedlings per hill achieved the highest HI in Iran (Bozorgi et al., 2011).

Rice cultivation emits greenhouse gases: carbon dioxide, methane and nitrous oxide which contribute global warming potential (GWP). Methane emission from the rice field is affected by water regime, crop duration and manure application in the present study. Methane emission under DSR was a little bit lower than those under SRI and MSRI methods in this study. However, in a previous report, SRI and wet seeded rice emitted 26.8 and 16.6% lesser CH<sub>4</sub> over transplanted method, respectively (Ramesh and Rathika, 2020). It might be due to differences in fertilizer application. In addition, Fazli and Man (2014) reported that modifications of current rice cultivation method in Malaysia can suppress CH<sub>4</sub> emission. In the present study, the GWP were 4066.94, 4067.08, 4475.75 and 4136.74 kg CO<sub>2</sub> eq ha<sup>-1</sup> for SRI, MSRI, FP and DSR, respectively. These were within the range of the report by Arunrat and Pumijumnong (2017). FYM was responsible for elevating GHGs emission in alternative rice cultivation methods while nitrogenous fertilizer compounded to anoxia effect for increasing it in FP and DSR. Application of organic manure increased GHGs emission compared with nonfertilized treatment. The effect is more obvious in conventional method than that in SRI (Ly et al., 2013). Some other reports revealed the effect of farmyard manure on GHGs emission although it depends on many factors, for instance, time of FYM application (Linguist et al., 2012; Pokhrel and Soni, 2019; Ren et al., 2017). The lower value of GHGs emission was observed in DSR method than that in FP

in the present study, which could be explained by different in lower fuel consumption for tillage operation and crop duration. However, weed infestation was serious in DSR, hence, the field was continuously flooded. That anoxia condition attributed to comparatively high CH<sub>4</sub> emission under direct seeded rice in the present study.

## Conclusions

Farming practices that preserve the natural resources and ensure economic returns are crucial for sustainable agriculture. Effective quantum yield of PSII and maximum quantum yield of PSII were not affected by cultivation method. This study concluded that SPAD value at flowering stage and grain yield of system of rice intensification (SRI), modified system of rice intensification (MSRI) and farmers' practices (FP) were not significantly different. Direct seeded rice (DSR) produced the lowest grain yield among the tested methods. Global warming potentials of SRI and MSRI were approximately 10% lower than that of FP. Of the two superior cultivation methods in term of grain yield, the MSRI method utilized fewer resources (inputs) of chemical fertilizer, seeds and water, in comparison with the FP method. Further adjustment of plant spacing with optimum combination of organic and chemical fertilizers was recommended to make agriculture more productive and sustainable.

**Acknowledgements.** This research was funded by the Interdisciplinary Graduate School of Energy System Scholarship (IGS-Energy 2017/2-004), Faculty of Environmental Management, Prince of Songkla University (PSU) (SD-ENV 01/2019) and Graduate School of PSU. The authors thank Assoc. Prof. Dr. Seppo Karrila and the Research and Development Office, PSU for assistance with proofing the English. First author is grateful to Department of Agriculture, Ministry of Agriculture, Livestock and Irrigation of Myanmar for offering the resources in conducting the experiment.

## REFERENCES

- [1] Amanullah, Inamullah (2016): Dry matter partitioning and harvest index differ in rice genotypes with variable rates of phosphorus and zinc nutrition. – *Rice Science* 23(2): 78-87.
- [2] Arunrat, N., Pumijumnong, N. (2017): Practices for reducing greenhouse gas emissions from rice production in Northeast Thailand. – *Agriculture* 7.
- [3] Arunrat, N., Wang, C., Pumijumnong, N. (2016): Alternative cropping systems for greenhouse gases mitigation in rice field: a case study in Phichit province of Thailand. – *Journal of Cleaner Production* 133: 657-671.
- [4] Aulakh, M. S., Wassmann, R., Rennenberg, H. (2001): Methane emissions from rice fields-quantification, role of management, and mitigation options. – *Advances in Agronomy* 70: 193-260.
- [5] Birhane, A. (2013): Effect of planting methods on yield and yield components of rice (*Oryza sativa* L.) varieties in Tahtay Koraro Wereda, Northern Ethiopia. – *International Journal of Technology Enhancements and Emerging Engineering Research* 1(5).
- [6] Bozorgi, H. R., Faraji, A., Danesh, R. K. (2011): Effect of plant density on yield and yield components of rice. – *World Applied Sciences Journal* 12(11): 2053-2057.
- [7] Chandankute, R. K., Verma, V. K., Meena, R. N., Meena, K. C., Singh, R. K. (2015): Effect of various crop establishment method and integrated nutrient management on

- growth, yield and economics of rice (*Oryza sativa* L.). – Journal of Pure and Applied Microbiology 9(4): 2997-3003.
- [8] Chen, S., Yin, M., Zheng, X., Liu, S., Chu, G., Xu, C., Wang, D., Zhang, X. (2019): Effect of dense planting of hybrid rice on grain yield and solar radiation use in Southeastern China. – Agronomy Journal 111: 1229-1238.
- [9] Dileep, K., Pasupalak, S., Baliarsingh, A. (2018): Effect of establishment methods and sowing time on growth and yield of rice varieties (*Oryza sativa* L.). – The Pharma Innovation Journal 7(4): 904-907.
- [10] Fagade, S. O., De Datta, S. K. (1971): Leaf area index, tillering capacity, and grain yield of tropical rice as affected by plant density and nitrogen level. – Agronomy Journal 63: 503-506.
- [11] Fazli, P., Man, H. C. (2014): Comparison of methane emission from conventional and modified paddy cultivation in Malaysia. – Agriculture and Agricultural Science Procedia 2: 272-279.
- [12] Gautam, P., Lal, B., Nayak, A. K., Raja, R., Panda, B. B., Tripathi, R., Shahid, M., Kumar, U., Baig, M. J., Chatterjee, D., Swain, C. K. (2019): Inter-relationship between intercepted radiation and rice yield influence by transplanting time, method, and variety. – International Journal of Biometeorology 63: 337-349.
- [13] Geethalakshmi, V., Bhuvanewari, K., Lakshmanan, A., Sekhar, N. U. (2017): Assessment of climate change impact on rice using controlled environment chamber in Tamil Nadu, India. – Current Science 112(10).
- [14] Gholizadeh, A., Saberioon, M., Boruvka, L., Wayayok, A., Soom, M. A. M. (2017): Leaf chlorophyll and nitrogen dynamics and their relationship to lowland rice yield for site-specific paddy management. – Information Processing in Agriculture 4: 259-268.
- [15] Ghosh, M., Swain, D. K., Jha, M. K., Tewari, V. K., Bohra, A. (2020): Optimizing chlorophyll meter (SPAD) reading to allow efficient nitrogen use in rice and wheat under rice-wheat cropping system in eastern India. – Plant Production Science 23(3): 270-285.
- [16] GRiSP (2013): The Global Rice Science Partnership. Rice Almanac. 4<sup>th</sup> Ed. – International Rice Research Institute, Los Banos (Philippines).
- [17] Guo, J., Hu, X., Gao, L., Xie, K., Ling, N., Shen, Q., Hu, S., Guo, S. (2017): The rice production practices of high yield and high nitrogen use efficiency in Jiangsu, China. – Scientific Reports. 7: 2101.
- [18] Hasanuzzaman, M., Ahamed, K. U., Rahmatullah, N. M., Akhter, N., Nahar, K., Rahman, M. L. (2010): Plant growth characters and productivity of wetland rice (*Oryza sativa* L.) as affected by application of different manures. – Emirates Journal of Food and Agriculture 22(1): 46-58.
- [19] Hirooka, Y., Homma, K., Maki, M., Sekiguchi, K., Shiraiwa, T., Yoshida, K. (2017): Evaluation of the dynamics of the leaf area index (LAI) of rice in farmer's fields in Vientiane Province, Lao PDR. – Journal of Agricultural Meteorology 73(1): 16-21.
- [20] Hom, N. H., Htwe, N. M., Hein, Y., Than, S. M., Kywe, M., Htut, T. (2015): Myanmar Climate-Smart Agriculture Strategy. – CGIAR Research Program on Climate Change, Agriculture and Food Security (CCAFS), International Rice Research Institute (IRRI). Ministry of Agriculture and Irrigation (MOAI), Naypyitaw, Myanmar. <https://ccafs.cgiar.org/resources/publications/myanmar-climate-smart-agriculture-strategy>.
- [21] Hossain, M. F., Salam, M. A., Uddin, M. R., Pervez, Z., Sarkar, M. A. R. (2002): A comparative study of direct seeding versus transplanting method on the yield of Aus rice. – Pakistan Journal of Agronomy 1(2-3): 86-88.
- [22] Huang, M., Zou, Y., Jiang, P., Xia, B., Feng, Y., Cheng, Z., Mo, Y. (2011): Yield component differences between direct-seeded and transplanted super hybrid rice. – Plant Production Science 14(4): 331-338.

- [23] Huang, M., Yang, C., Ji, Q., Jiang, L., Tan, J., Li, Y. (2013): Tillering responses of rice to plant density and nitrogen rate in a subtropical environment of southern China. – *Field Crops Research* 149: 187-192.
- [24] Ilahi, S., Wu, Y., Raza, M. A. A., Wei, W., Imran, M., Bayasgalankhuu, L. (2019): Optimization approach for improving energy efficiency and evaluation of greenhouse gas emission of wheat crop using data envelopment analysis. – *Sustainability* 11: 3409.
- [25] IPCC (2006): Guidelines for National Greenhouse Gas Inventories. – Intergovernmental Panel on Climate Change, Geneva.
- [26] IPCC (2007): Climate Change 2007: The Physical Science Basis. IPCC Fourth Assessment Report (AR4). Contribution of Working Group 1 to the Fourth Assessment Report of the Intergovernmental Panel on Climate Change. – Intergovernmental Panel on Climate Change, Geneva.
- [27] Iqbal, A., He, L., Khan, A., Wei, S., Akhtar, K., Ali, I., Ullah, S., Munsif, F., Zhao, Q., Jiang, L. (2019): Organic manure coupled with inorganic fertilizer: an approach for the sustainable production of rice by improving soil properties and nitrogen use efficiency. – *Agronomy* 9: 651.
- [28] Ishfaq, M., Akbar, N., Anjum, S. A., Anwar-Ul-Haq, M. (2020): Growth, yield and water productivity of dry direct seeded rice and transplanted aromatic rice under different irrigation management regimes. – *Journal of Integrative Agriculture* 19(11): 2656-2673.
- [29] Islam, S. F-U., Groenigen, J. W. V., Jensen, L. S., Sander, B. O., Neergaard, A. D. (2018a): The effective mitigation of greenhouse gas emissions from rice paddies without compromising yield by early-season drainage. – *Science of The Total Environment* 612: 1329-1339.
- [30] Islam, S. M. M., Gaihre, Y. K., Biswas, J. C., Singh, U., Ahmed, M. N., Sanabria, J., Saleque, M. A. (2018b): Nitrous oxide and nitric oxide emissions from lowland rice cultivation with urea deep placement and alternate wetting and drying irrigation. – *Scientific Reports* 8: 17623.
- [31] Javaid, T., Awan, I. U., Baloch, M. S., Shah, I. H., Nadim, M. A., Khan, E. A., Khakwani, A. A., Abuzar, M. R. (2012): Effect of planting methods on the growth and yield of coarse rice. – *Journal of Animal and Plant Sciences* 22(2): 358-362.
- [32] Kar, I., Yadav, S., Mishra, A., Behera, B., Khanda, C., Kumar, V., Kumar, A. (2018): Productivity trade-off with different water regimes and genotypes of rice under non-puddled conditions in Eastern India. – *Field Crops Research* 222: 218-229.
- [33] Kesh, H., Ram, K., Jangid, K. (2017): System of rice intensification: a review on resource conserving method of rice crop establishment. – *International Journal of Current Microbiology and Applied Sciences* 6(11): 2315-2328.
- [34] Kramer, D. M., Jhonson, G., Kiirats, O., Edwards, G. E. (2004): New fluorescence parameters for the determination of  $Q_A$  redox state and excitation energy fluxes. – *Photosynthesis Research* 79: 209-218.
- [35] Kuhlert, S., Austic, G., Zegarac, R., Osei-Bonsu, I., Hoh, D., Chilvers, M. I., Roth, M. G., Bi, K., TerAvest, D., Weebadde, P., Kramer, D. M. (2016): MultispeQ Beta: a tool for large-scale plant phenotyping connected to the open PhotosynQ network. – *Royal Society Open Science* 3: 160592.
- [36] Kumhar, B. L., Chavan, V. G., Rajemahadik, V. A., Kanade, V. M., Dhopavkar, R. V., Ameta, H. K., Tilekar, R. N. (2016): Effect of different rice establishment methods on growth, yield and different varieties during *Kharif* season. – *International Journal of Plant, Animal and Environmental Sciences* 6(2): 127-131.
- [37] Lal, R. (2004): Carbon emission from farm operations. – *Environment International* 30: 981-990.

- [38] Lancashire, P. D., Bleiholder, H., Boom, T. V. D., Langeluddeke, P., Stauss, R., Weber, E., Witzemberger, A. (1991): A uniform decimal code for growth stages of crops and weeds. – *Annals of Applied Biology* 119: 561-601.
- [39] Linqvist, B. A., Adviento-Borbe, M. A., Pittelkow, C. M., Kessel, C. V., Groenigen, K. J. V. (2012): Fertilizer management practices and greenhouse gas emissions from rice systems: a quantitative review and analysis. – *Field Crops Research* 135: 10-21.
- [40] Liu, H., Hussain, S., Zheng, M., Peng, S., Huang, J., Cui, K., Nie, L. (2015): Dry direct-seeded rice as an alternative to transplanted-flooded rice in Central China. – *Agronomy for Sustainable Development* 35(1): 285-294.
- [41] Ly, P., Jensen, L. S., Bruun, T. B., Neergaard, A. D. (2013): Methane (CH<sub>4</sub>) and nitrous oxide (N<sub>2</sub>O) emissions from the system of rice intensification (SRI) under a rain-fed lowland rice ecosystem in Cambodia. – *Nutrient Cycling in Agroecosystems* 97: 13-27.
- [42] Millar, N., Doll, J. E., Robertson, G. P. (2014): Management of Nitrogen Fertilizer to Reduce Nitrous Oxide (N<sub>2</sub>O) Emissions from Field Crops. – *Climate Change and Agriculture Fact Sheet Series - MSU Extension Bulletin E3152*. Michigan State University, Michigan.
- [43] MOALI (2016): Ministry of Agriculture, Livestock and Irrigation. – Myanmar Agriculture Sector in Brief, Myanmar.
- [44] Mohamad, O., Suhaimi, O., Abdullah, M. Z. (1994): The relationships between harvest index, grain yield and biomass in rice. – *MARDI Res. J* 22(1): 29-34.
- [45] MRDS (2015): Myanmar Rice Sector Development Strategy. – Naypyitaw, Myanmar.
- [46] Myint, A. K., Yamakawa, T., Zenmyo, T., Thao, H. T. B., Sarr, P. S. (2011): Effects of organic-manure application on growth, grain yield, and nitrogen, phosphorus, and potassium recoveries of rice variety Manawthukha in paddy soils of differing fertility. – *Communications in Soil Science and Plant Nutrition* 42(4): 457-474.
- [47] Nahar, L., Sarker, A. B. S., Mahbub, M. M., Akter, R. (2018): Effect of crop establishment method and nutrient management on yield and yield attributes of short duration T. *Aman* rice. – *Bangladesh Agronomy Journal* 21(1): 117-123.
- [48] Ndikuryayo, C., Ochwo-Ssemakula, M., Gibson, P., Lamo, J. (2020): Resistance to *rice yellow mottle virus* and performance of selected improved rice genotypes in central Uganda. – *Crop Protection* 129: 105041.
- [49] Oo, A. Z., Win, K. T., Motobayashi, T., Bellingrath-Kimura, S. D. (2016): Effect of cattle manure amendment and rice cultivars on methane emission from paddy rice soil under continuously flooded conditions. – *Journal of Environmental Biology* 37: 1029-1036.
- [50] Pimratch, S., Butsat, S., Kesmala, T. (2015): Application of blue-green and mineral fertilizers to direct seeding lowland rice. – *ScienceAsia* 41: 305-314.
- [51] Pokhrel, A., Soni, P. (2019): Energy balance and environmental impacts of rice and wheat production: a case study in Nepal. – *International Journal of Agricultural and Biological Engineering* 12(1): 201-207.
- [52] Promsomboon, P., Sennoi, R., Puthmee, T., Marubodee, R., Ruanpan, W., Promsomboon, S. (2019): Effect of seedlings numbers per hill on the growth and yield of Kum Bangpra rice variety (*Oryza sativa* L.). – *International Journal of Agricultural Technology* 15(1): 103-112.
- [53] Ramesh, T., Rathika, S. (2020): Evaluation of rice cultivation systems for greenhouse gases emission and productivity. – *International Journal of Ecology and Environmental Sciences* 2(2): 49-54.
- [54] Ramesh, K., Chandrasekaran, B., Balasubramanian, T. N., Bangarusamy, U., Sivasamy, R., Sankaran, N. (2002): Chlorophyll dynamics in rice (*Oryza sativa*) before and after

- flowering based on SPAD (chlorophyll) meter monitoring and its relation with grain yield. – *Journal of Agronomy and Crop Science* 188: 102-105.
- [55] Rana, M. M., Mamun, M. A. A., Zahan, A., Ahmed, M. N., Mridha, M. A. J. (2014): Effect of planting methods on yield and yield attributes of short duration *Aman* Rice. – *American Journal Plant Sciences* 5: 251-255.
- [56] Ren, F., Zhang, X., Liu, J., Sun, N., Wu, L., Li, Z., Xu, M. (2017): A synthetic analysis of greenhouse gas emissions from manure amended agricultural soils in China. – *Scientific Reports* 7: 8123.
- [57] Roberts, D. P., Mattoo, A. K. (2018): Sustainable agriculture- enhancing environmental benefits, food nutritional quality and building crop resilience to abiotic and biotic stresses. – *Agriculture* 8(8).
- [58] Savvides, A. M., Fotopoulos, V. (2018): Two inexpensive and non-destructive techniques to correct for smaller-than-gasket leaf area in gas exchange measurements. – *Frontiers in Plant Science* 9: 548.
- [59] Sen, A., Sarkar, M. A. R., Begum, M., Zaman, F., Ray, S. (2014): Effect of spacing and weed management on the growth of BRR1 dhan56. – *International Journal of Experimental Agriculture* 4(3): 20-29.
- [60] Shanker, A. K., Coe, R., Sirault, X. (2019): Integrated high-resolution phenotyping, chlorophyll fluorescence induction kinetics and photosystem II dynamics under water stress and heat in wheat (*Triticum aestivum*). – bioRxiv. <http://dx.doi.org/10.1101/510701>.
- [61] Shrestha, S. P. (2012): Genotypic responses of upland rice to an altitudinal gradient. – PhD Thesis, University of Hohenheim, Hohenheim.
- [62] Singh, K. L., Devi, K. N., Athokpam, H. S., Singh, N. B., Sagolshem, K. S., Meetei, W. H., Mangang, C. A. (2014): Effect of cultivars and planting geometry on weed infestation, growth and yield in transplanted rice. – *An International Quarterly Journal of Environmental Sciences* 8(1-2): 1-5.
- [63] Stoop, W. A., Uphoff, N., Kassam, A. (2002): A review of agricultural research issues raised by the system of rice intensification (SRI) from Madagascar: opportunities for improving farming systems for resource-poor farmers. – *Agricultural Systems* 71: 249-274.
- [64] Tanaka, A., Kawano, K. (1995): Leaf characters relating to nitrogen response in the rice plant. – *Soil Science and Plant Nutrition* 11(6): 31-38.
- [65] Thakur, A. K., Uphoff, N., Antony, E. (2010a): An assessment of physiological effects of system of rice intensification (SRI) practices compared with recommended rice cultivation practices in India. – *Experimental Agriculture* 46(1): 77-98.
- [66] Thakur, A. K., Rath, S., Roychowdhury, S., Uphoff, N. (2010b): Comparative performance of rice with system of rice intensification (SRI) and conventional management using different plant spacings. – *Journal of Agronomy and Crop Science* 196: 146-159.
- [67] Tomar, R., Singh, N. B., Singh, V., Kumar, D. (2018): Effect of planting methods and integrated nutrient management on growth parameters, yield and economics of rice. – *Journal of Pharmacognosy and Phytochemistry* 7(2): 520-527.
- [68] Traore, B., Samake, F., Babana, A., Hang, M. (2017): Effects of different fertilizers on methane emission from paddy field of Zhejiang, China. – *African Journal of Environmental Science and Technology* 11(1): 89-93.
- [69] Tubiello, F. N., Condor-Golec, R. D., Salvatore, M., Piersante, A., Federici, S., Ferrara, A., Rossi, S., Flammini, A., Cardenas, P., Biancalani, R., Jacobs, H., Prasula, P., Prospero, P. (2015): Estimating Greenhouse Gas Emissions in Agriculture. A Manual to



- Address Data Requirements for Developing Countries. – Food and Agriculture Organization of the United Nations, Rome.
- [70] Wang, W., Lai, D. Y. F., Wang, C., Tong, C., Zeng, C. (2016): Effects of inorganic amendments, rice cultivars and cultivation methods on greenhouse gas emissions and rice productivity in a subtropical paddy field. – *Ecological Engineering* 95: 770-778.
- [71] Yi-hu, M., Dao-jian, G., Li-jun, L., Zhi-qin, W., Hao, Z., Jian-chang, Y. (2014): Changes in grain yield of rice and emission of greenhouse gases from paddy fields after application of organic fertilizer made from maize straw. – *Rice Science* 21(4): 224-232.
- [72] Yodkhum, S., Sampattagul, S., Gheewala, S. H. (2018): Energy and environmental impact analysis of rice cultivation and straw management in northern Thailand. – *Environmental Science and Pollution Research* 25: 17654-17664.
- [73] Yoshida, S. (1981): *Fundamentals of Rice Crop Science*. – The International Rice Research Institute (IRRI). Philippines.
- [74] Yuan, Z., Cao, Q., Zhang, K., Ata-Ul-Karim, S. T., Tian, Y., Zhu, Y., Cao, W., Liu, X. (2016): Optimal leaf positions for SPAD meter measurement in rice. – *Frontiers in Plant Science* 7: 719.

## SIMULATION STUDY ON THE ARTIFICIAL ECOSYSTEM OF MARINE RANCHING AT DALIAN ZHANGZI ISLAND

WANG, G. <sup>1,2\*</sup> – GUAN, X. X. <sup>1</sup> – SHI, Y. H. <sup>1</sup>

<sup>1</sup>*School of Geography, Liaoning Normal University, Dalian 116029, China*

<sup>2</sup>*Southern Marine Science and Engineering Guangdong Laboratory (Guangzhou), Guangzhou 511458, China*

*\*Corresponding author  
e-mail: wanggeng@lnnu.edu.cn*

(Received 26<sup>th</sup> Aug 2020; accepted 30<sup>th</sup> Nov 2020)

**Abstract.** This study is based on the Vensim model with the Yesso scallop food chain as the core, combined with the multiple feedback effects of functional groups and environmental changes, to build an ecological-environment-economy system dynamics simulation model of marine ranching, which is both human and natural. Multi-factor feedback scenarios are simulated and predicted. The research results show that under natural conditions, the yield of Yesso scallop is mainly affected by natural disasters, with a stable period of about 10 billion grains, and the output value fluctuates around 10,236,922 EUR. The four controllable variables, fishing policy, development environment of Yesso scallop, sudden major natural disaster coefficient, and long-thorn starfish outbreak coefficient, have the most significant impact on Yesso scallop production. The large-scale outbreak and sudden large-scale outbreak of the long thorn starfish natural disasters can cause destructive production reductions in the Yesso scallop, but the local economic losses can be minimized through human control. The simulation model provides a scientific and feasible method for exploring the ecological elasticity of marine ranches and the maximum output of economic species.

**Keywords:** *ecosystem, system dynamics, ecological restoration, multi-scenario simulation*

### Introduction

China is the world's largest fishery country, and marine fisheries are an important part of Chinese agricultural economy. However, because Chinese mariculture and marine ecological protection have not been carried out simultaneously, the negative interaction between fishery productivity and environmental carrying capacity has become prominent, and phenomena such as extensive aquaculture, sea eutrophication, overfishing and habitat destruction have become increasingly serious (Lin, 2012; Wang and Hu, 2013; Liu, 2014). Marine ranches are meant to be harmonious with the environment and ecology, and integrate environmental protection, resource conservation, efficient production and recreational fisheries into a new marine economy (Yang et al., 2016), which provides practical possibilities for countries around the world to delay environmental degradation and increase economic output. This effective method has received wide attention from international scholars.

Throughout the development of marine ranching in various countries in the world, international scholars have conducted large-scale exploration and research on the development of marine ranching ecosystems, with fruitful results but large differences. Foreign scholars are mainly devoted to the study of in-depth fish life habits and the physical and ecological properties of fish reefs (Felley et al., 2008; Kim et al., 2013), while Chinese scholars are mainly devoted to the research of marine ranch site selection, artificial reef selection and biological control and domestication technology. Scholars have been exploring marine ranches more and more deeply. The research of marine ranch ecosystems has made great progress and major breakthroughs in many aspects. Through summary and discovery:

In terms of release methods, the transition from single multiplication and release to high-quality seed selection and timely stocking has been realized (Hong et al., 2009; Pan et al., 2010; Cheng and Jiang, 2010); in seed breeding, it has successfully moved from cage culture research to seawater stocking research (Wood and Peschken, 1990; Holby and Hall, 1994; Ottera et al., 1998; Rørvik et al., 2000; Luo and Fang, 2019); in research sites from indoor experimental exploration to practical simulation research on the sea area (Rubio et al., 2014; Taylor et al., 2016; Yu et al., 2016; Chen et al., 2018); in environmental restoration from passive damage restoration to active adjustment and maintenance. However, despite the abundant research results of marine ranch breeding, release and ecological engineering technology, there is still a lack of research on marine ranch ecosystem theory and management models. Currently, short-term single-disciplinary theoretical and technical experimental investigations are the main focus, and less analyze the operating mechanism of marine ranching ecosystems from the perspective of ecosystem integrity, especially the lack of long-term, continuous, and dynamic system studies, resulting in serious conflicts between economic output, ecosystems, and marine environments in the construction of existing marine ranches.

This paper takes Dalian Zhangzi Island Marine Ranching as an example. By constructing a marine ranching ecosystem dynamic model, this article explores the evolution mechanism and elastic process of the marine ranching ecosystem from the perspective of an artificial ecosystem. Based on the adaptive cycle principle, multi-scenario simulation simulates the optimal marine ranching the maximum economic output provides a feasible theoretical basis and operational specifications for the sustainable development of marine ranches.

## Materials and Methods

### Study area

Zhangzi Island in Changhai County is located at 124°47' east longitude and 39° north latitude. It covers an area of approximately 14.3595 km<sup>2</sup>. It is surrounded by islands such as Zhangzi Island, Dalian Island, Big Mouse Island, and Small Mouse Island. Zhangzi Island is close to the two major fishing grounds in Liaoning (Haiyang Island Fishing Ground and Bohai Bay Fishing Ground), about 56 nautical miles away from Dalian. Zhangzi Island is located in the mid-latitude zone between the Eurasian continent and the Pacific Ocean (*Figure 1*). It has a sub-humid monsoon climate in the northern temperate zone with significant monsoons and plenty of sunshine. The sea area of Zhangzi Island is affected by the ocean monsoon climate, the air is mild and humid, the temperature difference between day and night is small, and the frost-free period is relatively long up to about 220 days. The annual average temperature in the sea area of Zhangzi Island is about 10°C, the coldest month is January, the average temperature is minus 7.1°C; the hottest month is August, the average temperature is 25.3°C. The average annual rainfall in the sea area of Zhangzi Island is 633mm, and the rainfall is concentrated in July, August and September each year (Zhang et al., 2020).

The economy of Zhangzi Island has gradually developed from a collective economy formed by marine fishery and its affiliated industries to a collective enterprise focusing on marine economic product breeding, marine transportation, and product processing. The sea area of Zhangzi Island is located at 39 degrees north latitude and belongs to the Yellow Sea waters. It is the largest sub-planting and multiplication area of Yesso scallop (*Mizuhopecten yessoensis*) in China. Over the years, adhering to the ecological concept of "cultivating the sea for thousands of hectares and raising the sea for thousands of years", it has now developed into a large-scale, standardized, world-class modern marine ranch covering an area of 1,600

square kilometers. Its ecological value and practical results have won worldwide attention and recognition (Sun et al., 2018). Zhangzi Island Marine Ranch has a national Yesso scallop seed field and 5 improved breeding bases. It mainly produces scallops, abalones, sea cucumbers, Zhangzi Island oysters, real sea squirts and other sea treasures. There are more than 6 billion second-level seed of scallops, contributing more than 70% of the total profit. In 2015, the Yesso scallop fishery on Zhangzi Island passed the MSC sustainable fishery standard certification, becoming the first fishery in China to obtain the international sustainable fishery standard certification. The Yesso scallop germplasm was created and the improved species expanded, making it the first batch of pollution-free water in the country. The output of products ranks the leading level in the country. As the core product of Zoneco Group Company Limited (Co., Ltd.), Yesso scallop is an important profit growth point for the company. *Table 1* shows the income of the Yesso scallop project of Zhangzi Island Marine Ranch. It can be seen from the table that Zoneco Group Co., Ltd. saw a significant increase in the annual income of the "Yesso scallop project" from 2006 to 2017, and the income was good. After 2011, the annual income of the Yesso scallop has declined significantly. In recent years, due to the "lost" event of the Yesso scallop, the income of the Yesso scallop project has dropped sharply. Zoneco Group Co., Ltd. issued a performance bulletin, and the announcement showed that the company lost 399 million yuan in 2019 and made a profit of 32.11 million yuan in the same period last year, a decrease of 1341.79%. The "lost" incident of the Zhangzi Island Yesso scallop has brought huge losses to the local economic construction and residents' lives. It is urgent to restore the balanced development of the ecological and economic construction of the Zhangzi Island marine ranches.



**Figure 1.** Geographical location map of Zhangzi Island research area

**Table 1.** Income of Yesso scallop project of Zoneco Group Company Limited

Year	Income (EUR)	Year	Income (EUR)
2006	54444761.6634	2011	152088884.5049
2007	47266839.3439	2012	135976920.8247
2008	54702576.0626	2013	123328608.7526
2009	71253161.9311	2017	98857521.5235
2010	116469204.9177		

## ***Research methods and data sources***

### ***Research methods***

Marine ranching is a complex dynamic system coupled by the three of natural society and artificial society. Conventional experiments cannot accurately simulate and predict the endogenous changes and stress mechanisms of complex giant systems. System Dynamics originates from cybernetics, which was created by Wienes. In 1956, Professor J. W. Forrester of Massachusetts Institute of Technology (MIT) based on system theory, absorbed the essence of cybernetics and information theory, and formally established the discipline of system dynamics. System dynamics model (SD) is established by the Massachusetts institute of technology in system theory, information theory, cybernetics and computer technology as the foundation, according to the state of the system, control and information feedback to reflect the dynamic mechanism of the actual system, and through the establishment of simulation model, using a scientific method of computer simulation experiment was carried out. As a non-phenomenological "affair" method, SD can use the system structure, the causal relationship of each link and the feedback loop to establish a comprehensive conceptual model, and solve the system performance through simulation, combining qualitative and quantitative methods. System Dynamics has two distinct characteristics: endogenous and feedback, which is very effective for solving high-order, multi-loop and nonlinear complex feedback system problems (Xiong et al., 2013, 2016; Zhang et al., 2015). The dynamic changes of marine ranching ecosystems are highly consistent with the evolutionary laws of complex feedback systems, so it is a good choice to study the integrity of marine ranching ecosystems from the perspective of system theory. This paper uses the system dynamics method to simulate the marine ranching ecosystem to fill the gap in the marine ranching field to grasp the evolution process and mechanism of the system through simulation, and to provide ideas for long-term, dynamic and strategic simulation research.

### ***Data sources***

This article adopts an objective attitude and corresponding methods to conduct on-site visits, and uses relevant data collected from field investigations as the main data source for marine ranching ecosystem simulation research. The rest of the data comes from the "China Fishery Statistical Yearbook" (2010-2016), "Statistical Yearbook of Fishery Production in Dalian, Liaoning Province" (2010-2016); "Annual Report of Zonoco Group Co., Ltd."; partly derived from existing literature estimates and project survey data; partly derived from table function determination, and other parameters Based on the model multiple simulation runs.

### ***Construction of a marine ranching artificial ecosystem model***

As one of the main economic fish and shellfish exported by Dalian Zhangzi Island Marine Ranching, Yesso scallop are not only the key to ensuring a stable and balanced marine ecological environment, but also an important guarantee for promoting local social and economic development. However, in recent years, the annual yield of Yesso scallop from the Zhangzi Island Marine Ranching in Dalian has severely restricted the local economic development and affected the biological and ecological balance of the sea area of Zhangzi Island. Based on this, this article mainly builds a Yesso scallop growth and development model with predictive function around the Yesso scallop food chain. Searching for the elasticity of marine ranches through model operation and exploring the

maximum output of Yesso scallop has certain guiding significance for realizing the friendly and sustainable development of the social economy and marine ecology of Dalian Zhangzi Island.

### *System boundary and structure*

There is frequent material exchange, energy conversion and information transmission activities between the internal components of the marine ranch ecosystem, and between the interior and the surrounding environment. Therefore, the marine ranch ecosystem is not a closed and isolated space, but an open complex giant system. The goal of this research is to explore the optimal and maximum output of the Yesso scallop. Therefore, the boundary of the system is delineated according to the research needs, and the factors closely related to the Yesso scallop are included in the system as endogenous variables. The external environmental factors affecting the growth and development of the Yesso scallop were regarded as exogenous variables. *Figure 2* is a block diagram of the marine ranch system model structure, which mainly reflects the predation relationship between the internal components of the Yesso scallop ecosystem, the regulation effect of benthic saprophytes on water quality, the stress of water temperature changes on aquatic organisms, the influence of human and natural factors on the nutrient content and the influence of artificial fishing on the yield of Yesso scallop. Due to the mobility of seawater in the ocean and the connectivity of the marine ranch system, the model boundaries are not strictly divided by region. Only endogenous and exogenous variables are included in the marine ranch ecosystem model, so that the system constitutes one closed circuit, for system dynamics simulation study.

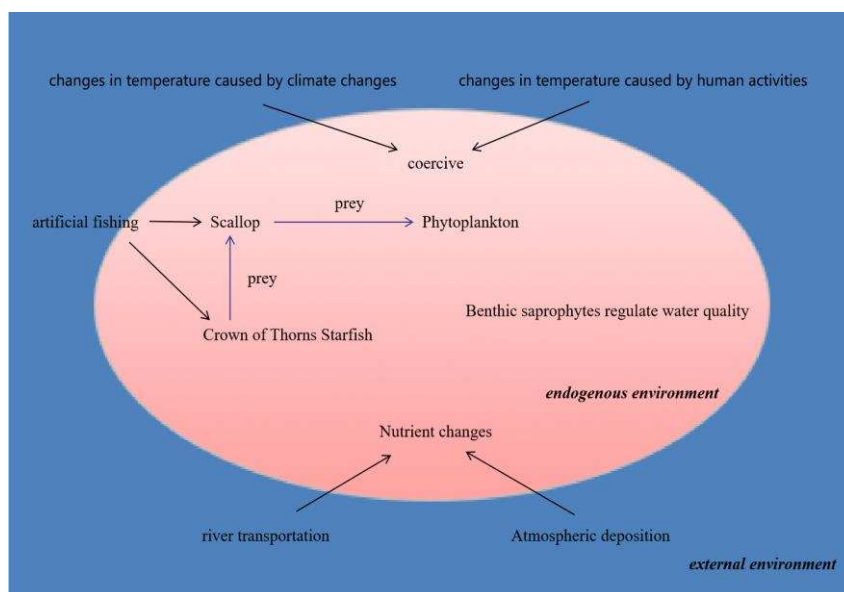


**Figure 2.** Block diagram of marine ranch system model

As phytoplankton is the main food source of Yesso scallop, it directly limits the population of Yesso scallop. Long thorn starfish (*Acanthaster planci*) is the main natural enemy of Yesso scallop. Real-time monitoring of Yesso scallop is a prerequisite for controlling the production of Yesso scallop. Therefore, the endogenous variables of the system model are composed of the Yesso scallop food web, which can be divided into

plankton groups and benthic organisms. The number of plankton, the number of Yesso scallop, the number of long thorn starfish, and the number of benthic saprophytes are mainly (Table 2). As the most important factor in the marine ecosystem model, Yesso scallop not only provide support for social and economic development, but also a key influencing factor to ensure the stability of the marine ecological environment. Therefore, based on the integrity of the ecosystem, this paper divides the marine ecosystem into three parts: the Yesso scallop ecological subsystem, the socioeconomic subsystem, and the environmental subsystem. The simulation work of the marine ranching artificial ecosystem of the Yesso scallop is carried out.

**Table 2.** A brief table of internal and external growth variables of marine ranching Yesso scallop system model

Endogenous variables	Exogenous variables (factors)
Number of plankton	Regional climate change influencing factors (storm surge, water temperature, etc.)
Yesso scallop production	Human activities impact factors (fishing policy, stocking, etc.)
Number of Long thorn Starfish	Value of economic investment funds (economic investment, output value, etc.)
Number of benthic saprophytes	Factors affecting the development of the Yesso scallop environment construction (base construction coefficient)

Sudden changes in regional climate, resulting in over-cold or over-heated seawater temperature, will affect the spawning rate of Yesso scallop and slow the development of Yesso scallop. Affected by global climate change, the occurrence of natural disasters such as typhoons will also have a certain impact on the stability of the marine ranching ecosystem. Therefore, the exogenous variables of the system model are determined by the environmental factors of Yesso scallop, human intervention, and economic development. The composition mainly includes regional climate change, human activities, economic investment, etc. (Table 2). Taking into account the complexity of the marine ranching ecosystem, through preliminary research and literature review, comprehensive consideration of the internal elements and external factors of the system, and appropriately simplified the Yesso scallop ecological subsystem and its interaction with the environment, social and economic subsystems relationship.

System dynamics believes that the behavior mode and characteristics of the system mainly depend on the internal dynamic structure and feedback mechanism. On the basis of the above-mentioned system model boundary and structure analysis, according to the specific physical and economic geography of the study area, a qualitative analysis of the internal structure of the marine ecosystem is carried out to further study the cause and effect between the various components of the marine ranching ecosystem model positive and negative feedback relationship. The causal circuit diagram of the marine ranching system model is shown in Figure 3.

- (1) Implementation of marine ranching technology → + artificial reef construction → + phytoplankton → + scallops
- (2) Implementation of marine ranching technology → + artificial reef construction → + benthic detrital organisms → + inorganic salt content → + phytoplankton → + scallops
- (3) The implementation of marine ranching technology → - long thorn starfish → + scallops

- (4) The implementation of marine ranching technology → + marine ranching investment → + scallops → +GDP → + marine ranching innovation research → + marine ranching technology implementation

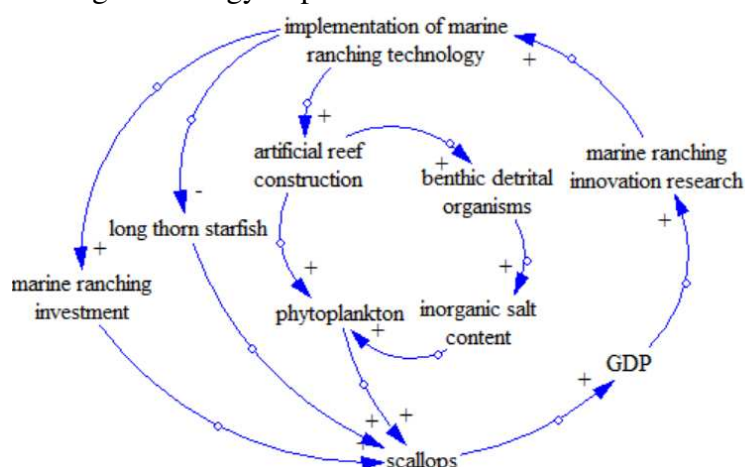


**Figure 3.** Causal circuit diagram of marine ranching system model

The causal chain 1 is a positive feedback causal chain that characterizes the ecological process of marine ranches, which means that artificial reefs in marine ranches can provide a living environment for phytoplankton and Yesso scallop, and promote their growth and development. The causal chain 2 is a positive feedback causal chain that characterizes the water quality environment of marine ranches, which means that benthic detrital organisms in the marine ranching artificial ecosystem can not only regulate the water quality environment, but also ensure sufficient food to ensure the normal growth and development of the Yesso scallop. The causal chain 3 is a negative feedback causal chain of the ecosystem. The increase in the number of long thorn starfish leads to a decrease in the number of Yesso scallop. Therefore, a monitoring system is set up to control the number of long thorn starfish in real time to ensure the survival rate of the Yesso scallop. The causal chain 4 is a positive feedback causal chain that represents the socio-economic characteristics of marine ranches. The initial investment in marine ranching technology can increase the production of Yesso scallop, thereby driving local GDP to attract the government to increase construction efforts and speed up innovative research on marine ranches. Form an ecological-economic virtuous circle.

### Structural analysis

Dalian Zhangzi Island Marine Ranch relies on the natural ecological proliferation of the sea to cultivate Yesso scallop to increase the output of fishery resources, thereby driving local economic development. Comprehensively considering the internal elements of the system and the main external factors, the model is divided into marine ecological subsystems, social economic subsystems and environmental subsystems. The social economic subsystem and the environmental subsystem jointly restrict the ecological subsystem, and the ecological subsystem has different degrees of feedback to the social economic subsystem and the environmental subsystem. The marine ecology-socio-economic-environmental coupling study is the basis for the overall study of the Zhangzi Island marine ranching and a prerequisite for a more comprehensive study of the marine ranching, which can make the model output more realistic and closer to reality.



### *Marine ecological subsystem*

Zhangzi Island marine ranching ecosystem mainly describes the growth process of plankton, Yesso scallop, long thorn starfish, and benthic detrital organisms: the model sets that the supplement of Yesso scallop larvae comes from mature Yesso scallop spawning and artificial breeding release. The number of Yesso scallop is limited by food sources, natural enemies long thorn starfish and living space. Lack of food, excessive number of long thorn starfish, and exceeding the ecological capacity of living space may cause the migration or death of Yesso scallop, causing serious economic losses. If the long thorn starfish multiplies too fast, it will pose a great threat to the survival and development of the Yesso scallop. Therefore, a long thorn starfish monitoring mechanism is set up in the marine ranching to monitor the number of long thorn starfish in real time to prevent more long thorn starfish from invading. The model sets that the long thorn starfish has two death methods: natural death and man-made fishing. Benthic detrital organisms can decompose marine animal and plant debris into inorganic matter, so that the residual energy can be reused by phytoplankton, etc. and can maintain the material circulation and energy flow of the ecosystem. The model sets that the number of benthic detrital organisms mainly depends on the birth rate, mortality, and control of predation factors by natural enemies.

### *Socioeconomic subsystem*

The social and economic benefits of marine ranches are mainly based on the maximum output of the shellfish. By optimizing marine fishery resources, the social and economic growth will be promoted, and the recreational projects of marine ranches will also promote the development of social economy. The social and economic investment has increased the scale of marine ranches, and the monitoring system is more advanced and complete. Artificial seedlings and seedling selection are developed under the guidance of excellent scientific research to develop more cost-effective and labor-saving methods, so that the social economy and marine ranching operations can feed back and make progress together.

### *Environmental subsystem*

Environmental stress factors mainly include non-optimum temperature, lack of the nutrients and natural disasters. Yesso scallop seedlings are extremely sensitive to temperature. Seawater temperature below 5°C or higher than 25°C will affect the Yesso scallop seedlings and even cause death. The nutrient content of seawater has a certain impact on the growth process of the oyster shellfish. The bloom phenomenon caused by the excessive nutrient salt concentration will pose a great threat to the life of marine organisms, which can cause suffocation or poisoning. Natural disasters such as storm surges, tsunamis, and sudden climate changes have a great impact on the growth and development of marine ranches including the Yesso scallop. The artificial habitat construction of the Yesso scallop and the prevention of natural disasters can directly affect the economic benefits of the Yesso scallop.

### *Flow graph construction and model verification*

Vensim is owned by Ventana Systems, Inc. A graphical interface software for visualized, documented, simulated, analyzed, and optimized dynamic system model was

developed. Based on the Vensim system dynamics software, the dynamic flow diagram of the marine ranch ecosystem is drawn, as shown in *Figure 4*.

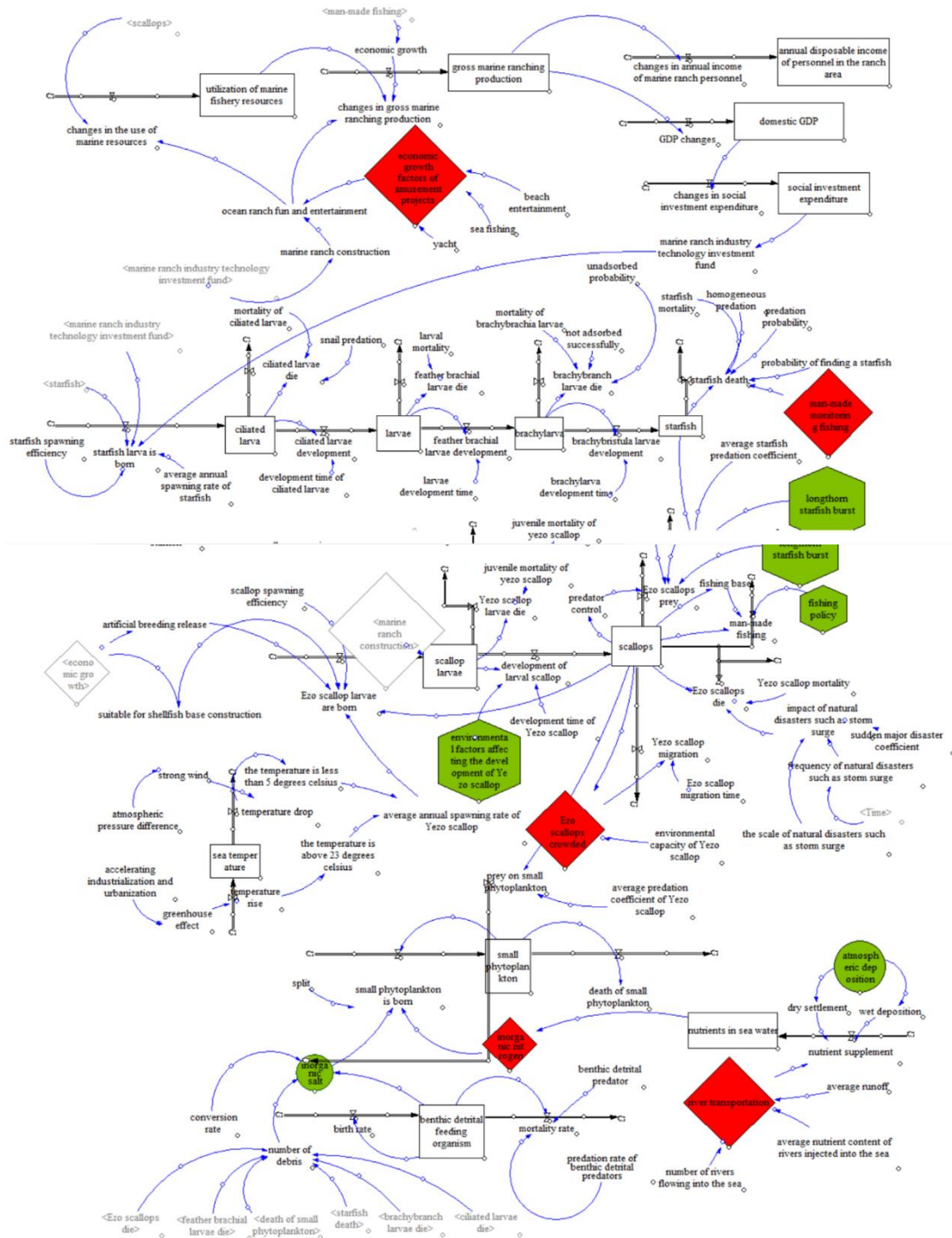


**Figure 4.** Systematic flow diagram of Zhangzi Island marine ranching system

After the model is established, it is particularly important to verify the authenticity of the model according to the purpose-related validity test (Wang and Zhang, 2020). After the repeated debugging process of "simulation operation-verification-correction-

simulation operation" and the process of consulting experts, this research passed the following inspection contents:

1. Structural test. Through the rationality inspection of the system model boundary, variable parameters and logical relationship, it is found that the system model boundary and variable simplification degree is relatively appropriate, and the feedback relationship is basically consistent with the natural development law of things; 2. Behavioral test. Through testing of different modes such as direct operation of the model, testing of extreme conditions, sensitivity analysis, etc., the marine ranching ecosystem model basically restores the behavior patterns observed in the actual marine ranching, and found that human interference under environmental changes and other scenarios, the system expectation is similar to the actual situation; 3. Authenticity check. Since the model construction involves part of the historical data of the study area, part of the historical data of the study area is used to verify the authenticity. After the operation simulation of the model, combined with the annual report data of the Zhangzi Island marine ranching and relevant literature analysis, the simulated data and the real data are combined the dynamic development trend is analyzed to verify that the fit between the two is relatively good (*Table 3, Figure 5*).

**Table 3.** Comparison data of simulated annual output and actual annual output of *Yesso scallop*

Year	Simulation value	Actual value	Year	Simulation value	Actual value
2006	233.21	244.8	2010	1713	2580
2007	377.01	750.2	2011	3452	3500
2008	630.5	1203	2012	6099	5894
2009	1040	1729	2013	8172	7486

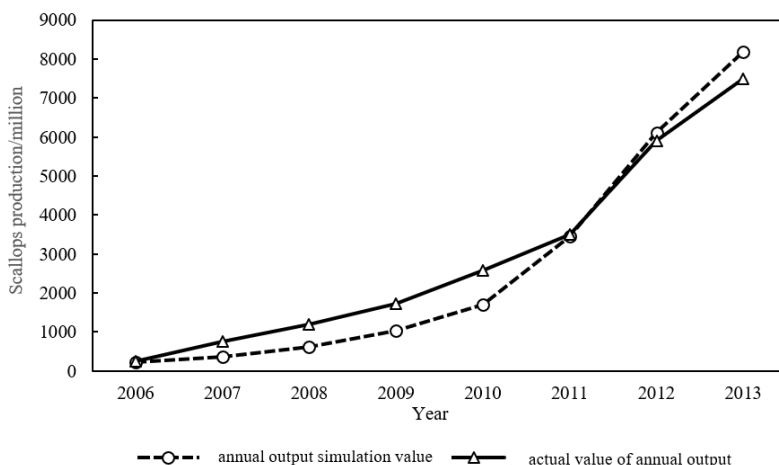


**Figure 5.** Comparison diagram of annual output fitting of *Yesso scallop*

## Results

### *Basic simulation and the results of marine ranching ecosystem model*

The object of the analogue simulation research is Zhangzi Island marine ranching. The period simulated in the model is from 1996 to 2040, with a time step of 0.5 year. According to the reversed data resources mentioned before, several main initial value settings of the

model is that there are initially 4,000,000 Yesso scallop larvae, and 500 crown-of-thorns starfish. The initial amount of phytoplankton is 2,000/L.

Based on the causality and parameter values of the model and for the time being ignored the other external factors, the SD model of the marine ranching is simulated dynamically (Figure 6). The basic simulation results show that the changing increasing speed of the Yesso scallop's quantity is from stable to exponential and stable again. Before 2004, while the initial constructed marine ranching, the output amount of Yesso scallop is stably 4,000,000 per year, which cannot meet the markets' needing. The state of imbalance between supply and demand restricts development. As the developing of marine ranching and the increase of artificial intervention, setting good artificial reefs to providing better growing environment, the Yesso scallop's increasing rate becoming exponential before reaching environment capacity, the output can be 8.9 billion, 2225 times to the initial amount. After 2014, the amount of Yesso scallop reached environment capacity, the quantity become stable, the output remains at around 10 billion. With the continuous improvement of scientific and technological means and innovative research in marine ranches, marine ranches are equipped with corresponding monitoring systems to monitor the invasion of long thorn starfish. If the main enemy of Yesso scallop, long thorn starfish migrate into the marine ranch breeding area, the marine ranch The management staff will take measures such as timely fishing to achieve the purpose of timely stop loss and ensure that the Yesso scallop are in an ideal living condition. After increasing the environmental capacity of the Yesso scallop in the marine ranch ecosystem through manual intervention, the number of Yesso scallop will again show a substantial increase. This shows that putting artificial reefs to build marine ranches can effectively increase the yield of Yesso scallop and bring significant economic benefits.

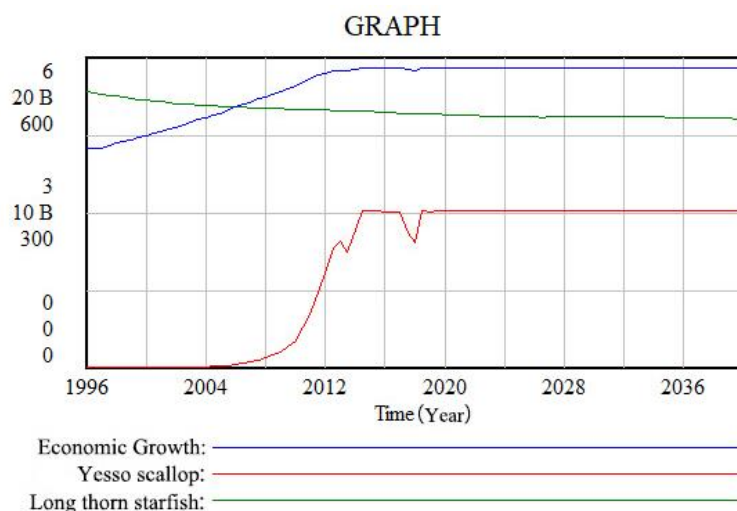


**Figure 6.** Simulation output of Zhangzi Island marine ranching economic growth Yesso scallop starfish

### ***The sensitivity analysis of marine ranching ecosystem model***

The sensitivity analysis can directly simulate the observed variables' sensitivity to the controlled variables and the function trace by marine ranching ecosystem model. The most important factor can be known through model's sensitivity tests and influence analysis to ground the amorous scenario diagnosis restore and adaptive management. There are 5 main control variables (uncertain variables) in this research to perform

sensitivity test and the influence degree of Yesso scallop: fishing policy, environmental factors of Yesso scallop's growth, sudden weighty natural disaster probability, and outbreak probability of crown-of-thorns starfish, atmospheric deposition. All those became the theoretical base of continuing amorous scenario simulation; specific regulatory parameters are *Table 4* and *Table 5*.

**Table 4.** Sensitivity test setup profile

Control variables	Initial value	Regulation sector	Times	Distribution	Observed variables
Fishing policy	0.5	0.25-0.7	200	Mean random distribution	Yesso scallop
Environmental factors of Yesso scallop's growth	1	0.5-1	200	Mean random distribution	Yesso scallop
Sudden weighty natural disaster probability	0	0-1	200	Mean random distribution	Yesso scallop
Outbreak probability of crown-of-thorns starfish	0	0-1	200	Mean random distribution	Yesso scallop
Atmospheric deposition	0.2	0.1-0.4	200	Mean random distribution	Yesso scallop

**Table 5.** Formulations involved in control variables in sensitivity test

Control variables	Formulation
Fishing policy	Artificial fishery= fishing policy * fishing fundament*Yesso scallop
Environmental factors of Yesso scallop's growth	Yesso scallop larva growth= Yesso scallop larva /time of grow* relevant environment factors
sudden weighty natural disaster probability	natural disaster coercion = natural disaster probability *Storm surges and other disasters' scale* Storm surge and other disasters' frequency
outbreak probability of crown-of-thorns starfish	Starfish predation amount on Yesso scallop = Starfish * Starfish mean predatory coefficient+ Starfish * crown-of-thorns starfish outbreak *500* Starfish mean predatory coefficient)* predatory control
atmospheric deposition	dry deposition= atmospheric deposition *0.23 wet deposition= atmospheric deposition *0.2

The sensitivity analysis of the model can choose the scenario factor resources, prepare for the marine ranching system scenario simulation, ensure scenario factors and the combination, and ensure the range of the parameters. As *Figure 7* shows, a,b,c,d are atmospheric deposition, fishing policy, environmental impact, coefficient of sudden major natural disasters, Yesso scallop sensitivity test results. The sensitivity analysis of the marine ranching system model shows that atmospheric factors nearly not influent the Yesso scallop's growth, fishing policy, environmental factors of Yesso scallop's growth, sudden weighty natural disaster probability, outbreak probability of crown-of-thorns starfish are sensitive factors. The annual amount of Yesso scallop and the trend of amount are big by those factors.

### ***The amorous scenario simulation of marine ranching ecosystem model***

Different scenarios can be settled to simulate different evolutionary mechanism by changing relevant parameters in the amorous scenario simulation to get the main factors of Yesso scallop's amount. According to sensitivity analysis, fishing policy, there are 4 main control variables which affect the amount: environmental impact, sudden weighty natural disaster probability and outbreak probability of crown-of-thorns starfish. Different scenario

disturbance model can be artificial adjusted to base for diagnose and reserve policy. There are artificial disturbance and ecosystem's positive and negative feedback adjustments affect the marine ranching Yesso scallop culture. Based on sensitivity analysis, through artificial and environmental disturbance, control 4 control variables to precede amorous scenario simulation experiment. The threshold of the Yesso scallop's death can be found and used for amorous scenario simulation of marine ranching ecosystem through many model running and adjust variables.

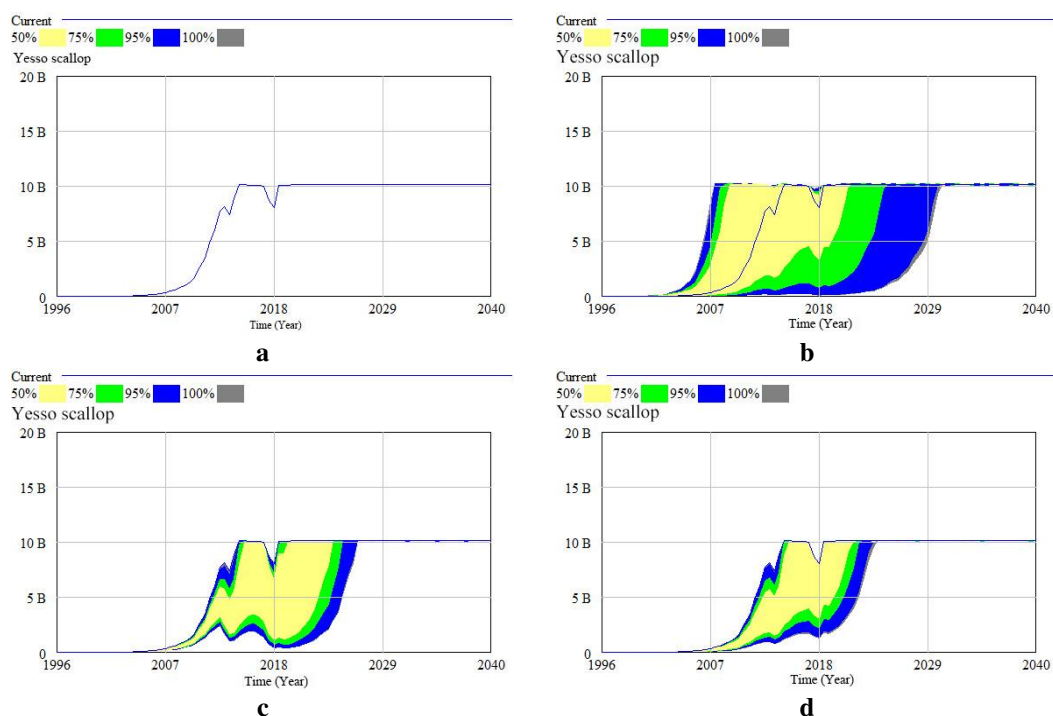


**Figure 7.** Atmospheric deposition, fishing policy, environmental impact, sudden weighty natural disaster probability and Yesso scallop sensitivity test results

### Scenario simulation of artificial activity

Marine ranching as an artificial ecosystem, artificial activities effect the fishes' growth and breed. Further experiments carried on 2 variables which are fishing policy and environmental factors of Yesso scallop in order to fully understand how the artificial disturbance effect marine ranching ecosystem. Set the threshold of fishing policy is 0.9, the threshold of environmental factors of Yesso scallop's growth is 0.07. Adding experts' views and local experiments within each threshold of fishing policy and environmental factors of Yesso scallop choose a changing interval to get the maximum and minimum value to visual simulation. Specific control variable parameters are in *Table 6*.

**Table 6.** Human activity disturbance scenario control variable parameter table

Number	Control variables	Present value	Control value	
			A	B
1	Fishing policy	0.5	0.8	1.2
2	Environmental factors of Yesso scallop's growth	1	0.1	0.5



(1) disturbance by a single factor

From fishing policy scenario A1 and B1 in the *Figure 8*, the change of fishing policy greatly affects the output of Yesso scallop. Long thorn starfishes are still monitored by the marine ranching monitoring system, and they are caught when they are found. The number of starfish in the marine ranching waters is decreasing year by year. The local economic growth rate become slowly because of the slow rate of Yesso scallop's grow amount which is effected by slightly adjust fishing policy (A1). The slow economic growth trend has led to a decrease in the investment in the construction and research of marine ranching. The research and practice of the seedling, release, and subsistence environment of the Yesso scallop has been slow. It will not be until 2026 that the production of Yesso scallop has increased in a wide range. The economy grew steadily. When sharp rise the fishing policy (B1), long thorn starfishes are still monitored by the marine ranching monitoring system, and they are caught when they are found. The number of starfish in the marine ranching waters is decreasing year by year. The economic growth and Yesso scallop's amount both decrease fast, the amount in 2006 is merely 2719. To guarantee the sustainable production of Yesso scallop, stop over fishing it can stop the decrease of production. After resuming normal production and development, the amount can be 340,000 in 2040, which is a quarter of the initial amount. The local economy is also showing a downward trend due to the reduction in the production of Yesso scallop. However, because the local economic benefits are also related to the recreational projects of the marine ranching, the basic business status of the marine ranch is guaranteed to a certain extent, and the local economic loss is reduced. The additional economic benefits of marine ranches can continue to be used in the construction of the Yesso scallop culture area, providing a suitable growth and development environment for the Yesso scallop, so that it can still grow slowly under the large-scale fishing policy. Slightly increase fishing amount can extend the time of fast growing Yesso scallop amount, greatly increase fishing amount can decrease the Yesso scallop's total amount.

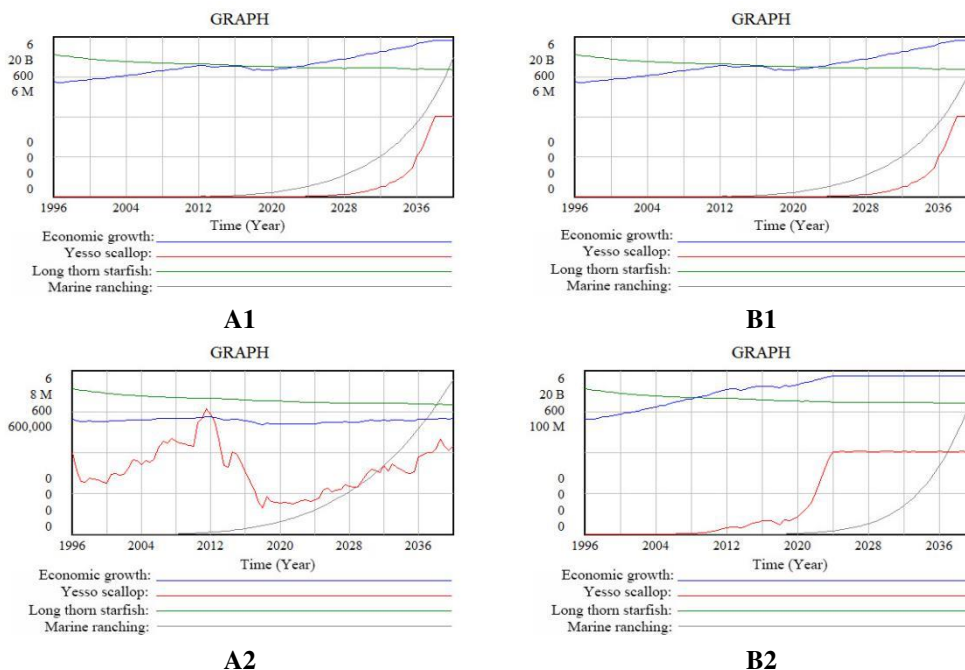


**Figure 8.** Simulation results of single factor disturbance in the scenario of human activity interference

From the scenario of environmental factors of Yesso scallop's growth A2 and B2 in the *Figure 8*, the change of environment can directly affect the growing process and total amount. Greatly changing the environmental factors of Yesso scallop's growth (A2), can make the amount change from increase to decrease, the economic curve also decreases. After the Yesso scallop reached the environmental capacity in 2011, due to insufficient food and space resources, the Yesso scallop began to migrate or even die. By 2018, the output of the Yesso scallop was only 1 million. Long thorn starfishes are still monitored by the marine ranching monitoring system, and they are caught when they are found. The number of starfish in the marine ranching waters is decreasing year by year. With the accumulation of capital, the construction curve of marine ranches has grown rapidly. Marine ranches have gradually implemented measures to improve the bottom quality of the sea Yesso scallop culture, expand the breeding space, and ensure adequate food. The current situation of substantial reduction in production due to insufficient resources and growth space, the production of Yesso scallop has gradually recovered from 2019 and entered a state of steady growth. It is expected that the production will reach 6 million in 2050. Slightly regulating the development of environmental factors in the early stage will limit the growth and development of the Yesso scallop (B2), which greatly restricts the growth of the Yesso scallop, and the yield growth trend is slow. Long thorn starfishes are still monitored by the marine ranching monitoring system, and they are caught when they are found. The number of starfish in the marine ranching waters is decreasing year by year. The production of Yesso scallop in 2003 was 35 million pieces, and the yield curve gradually showed an increasing trend since then. Around 2020, the construction of marine ranching has been vigorously developed. After breaking the original environmental factors, the production of Yesso scallop has increased sharply. After about four years, it will reach a new dynamic balance, at which time the output will reach about 10 billion. It can be seen that the slight adjustment of the developmental environmental factors has delayed the development of marine ranches to a certain extent, and has a lagging effect on the production of Yesso scallop and local economic growth. Substantial adjustments to the developmental environmental impact factors will break the original ecological balance, cause severe fluctuations in the production of the Yesso scallop, and severely restrict local economic growth.

(2) disturbance by double factor

Combining fishing policy and environmental factors of Yesso scallop's growth to make a two-factor disturbance scenario simulation fatherly analyze the Yesso scallop's influence by changing of fishing policy and environmental factors of Yesso scallop's growth. The scenarios are in *Table 7*.

**Table 7.** Parameter table of two-factor control variables for artificial disturbance scenarios

A1A2	0.8	0.1
A1B2	0.8	0.5
B1A2	1.2	0.1
B1B2	1.2	0.5

The scenario A1A2 in the *Figure 9* shows that while slightly change the fishing policy and greatly change the environmental factors, the Yesso scallop grows slowly, and cannot meet the lost after fishing. Long thorn starfishes are still monitored by the marine ranching



monitoring system, and they are caught when they are found. The number of starfish in the marine ranching waters is decreasing year by year. The amount of Yesso scallop constantly decreases, the population is merely 55096 in 2018, the economic growth decrease, too. Artificial intervals improve the marine environment to make sure the Yesso scallop can grow and breed normally, and avoid the extinction of Yesso scallop, which fully shows the advantage of marine ranching. The scenario A1B2 in the *Figure 9* shows that, while slightly change the fishing policy and the environmental factors, there is little effect on Yesso scallop's growing and the economic grow with it. In the former stage the Yesso scallop is affected by fishing policy, but thanks to the good environment, the output steadily grows and can be 21,940,000 in 2014. After the population reach the environmental capacity and continue the fishing, the output obviously decreases, but the good marine ranching environment makes sure the exponential output growth of Yesso scallop, thus the local economic can grow whit it. The scenario B1A2 in the *Figure 9* shows that, while greatly change the fishing policy and the environmental factors, the effect of Yesso scallop and local economic is severe. Long thorn starfishes are still monitored by the marine ranching monitoring system, and they are caught when they are found. The number of starfish in the marine ranching waters is decreasing year by year. The output and population of Yesso scallop decrease largely, the local economic decrease severely, too. When the large scale of fishing and sever environment happen, the output decrease and population is merely 50 in 2023. Though there is huge development of marine ranching, the environment and fishery still restrict the growth of Yesso scallop. The scenario B1B2 in the *Figure 9* shows that, while greatly change the fishing policy and slightly change the environmental factors, the output and local economic also decrease. Comparing to B1A2, though the output decrease, the speed is low because of the good environment. The development of marine ranching improves the environment, and after 2016, the output grows slowly.

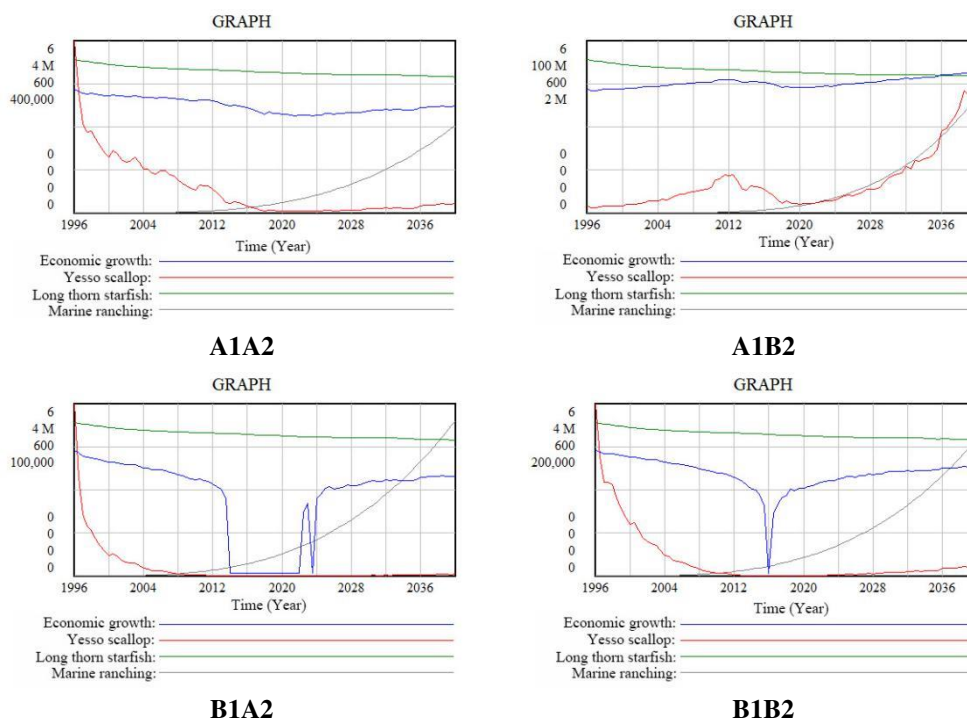


**Figure 9.** Simulation results of two-factor disturbance under the condition of human activity disturbance

*Ecological environment disturbance scenario simulation*

The cultivation of Yesso scallop under the disturbance of ecological environment is an important research direction for the management of marine ranches and ensuring the yield of Yesso scallop. The sudden outbreak of natural enemies of Yesso scallop and the arrival of large-scale natural disasters seriously endanger the life and safety of Yesso scallop. Therefore, the single factor disturbance of sudden major natural disaster coefficient and crown-of-thorns starfish burst coefficient is simulated, and the threshold method is still used to select the regulation interval, and the threshold value of sudden major natural disaster coefficient is 3.2. The threshold value of crown-of-thorns starfish burst coefficient is 1.95. The regulation range of sudden major natural disaster coefficient is 1-4, and that of crown-of-thorns starfish burst coefficient is 0.1-0.26. See *Table 8* for details.

**Table 8.** Parameter table of regulating variables of ecological environment disturbance scenario simulation

Serial Number	Regulatory Variable	Present Value	Regulatory Value	
			A	B
1	Coefficient of sudden major natural disasters	0	1	4
2	Burst coefficient of crown-of-thorns starfish	0	1.5	1.95

From the scenarios A3 and B3 of sudden major natural disasters (*Fig. 10*), it can be seen that different coefficients of sudden major natural disasters will reduce the total yield of Yesso scallop to varying degrees. A slight adjustment of the sudden major natural disaster coefficient A3 can make the production of Yesso scallop fall slightly and fluctuate obviously, reaching the lowest yield of 438270000 Yesso scallop in 2019. Long thorn starfishes are still monitored by the marine ranching monitoring system, and they are caught when they are found. The number of starfish in the marine ranching waters is decreasing year by year. With the addition of marine ranch construction, the resistance of Yesso scallop to sudden major natural disasters increased, and the variable index increased to a stable state to ensure the stable development of economy. When the sudden major natural disaster coefficient (B3) is greatly adjusted, there is a great threat to the growth and development of Yesso scallop. Sudden major natural disasters can destroy the living space of Yesso scallop, resulting in a sharp decrease in the yield of Yesso scallop, with a minimum value of 275277. Although the construction and restoration of marine ranches can improve the living environment of Yesso scallop, the yield increase rate of Yesso scallop is slow due to the large damage intensity of sudden major natural disasters. It can be seen that the slight regulation of sudden major natural disasters has little impact on Yesso scallop, and it can enter the state of value-added and maintain steady development as soon as possible after marine ranches are repaired and the environment is improved. However, greatly regulating the coefficient of sudden major natural disasters will greatly destroy the living space of Yesso scallop, even if it is added to the restoration of marine ranch, it will seriously lag behind the local economic development.

It can be seen from the scenarios A4 and B4 of the crown-of-thorns starfish outbreak in 2012 that the crown-of-thorns starfish will significantly reduce the production and local economy of Yesso scallop, but the yield can still be restored and maintained stable in the

later stage. Small-scale explosions of crown-of-thorns starfish will cause fluctuations and decline in the production of Yesso scallop, which will lead to small fluctuations in the local economy (A4). Small-scale outbreaks of crown-of-thorns starfish can be eliminated as soon as possible, after the complete elimination of crown-of-thorns starfish, Yesso scallop resume to grow to the environment and remain stable. The large-scale outbreak of crown-of-thorns starfish will lead to a sharp increase in the number of crown-of-thorns starfish when food is abundant and no natural predators are caught (B4). Due to the large number of crown-of-thorns starfish and a wide range of predation, the yield of Yesso scallop has dropped sharply to 125509, and the local economy has dropped below the initial value, which is only half of that in the bumper harvest year. Due to the excessive number of crown-of-thorns starfish, the yield of Yesso scallop continued to grow slowly even during the construction of marine ranches, and the yield did not increase significantly until the initial results of the new construction of marine ranches in 2026, and reached a new environmental capacity in 2033. It can be seen that the crown-of-thorns starfish, as the survival natural enemy of the Yesso scallop, has little impact on the yield and the local economy when the quantity can be controlled, but the growth and development of the Yesso scallop is greatly affected after the large-scale outbreak, which restricts the local economic development to a great extent.

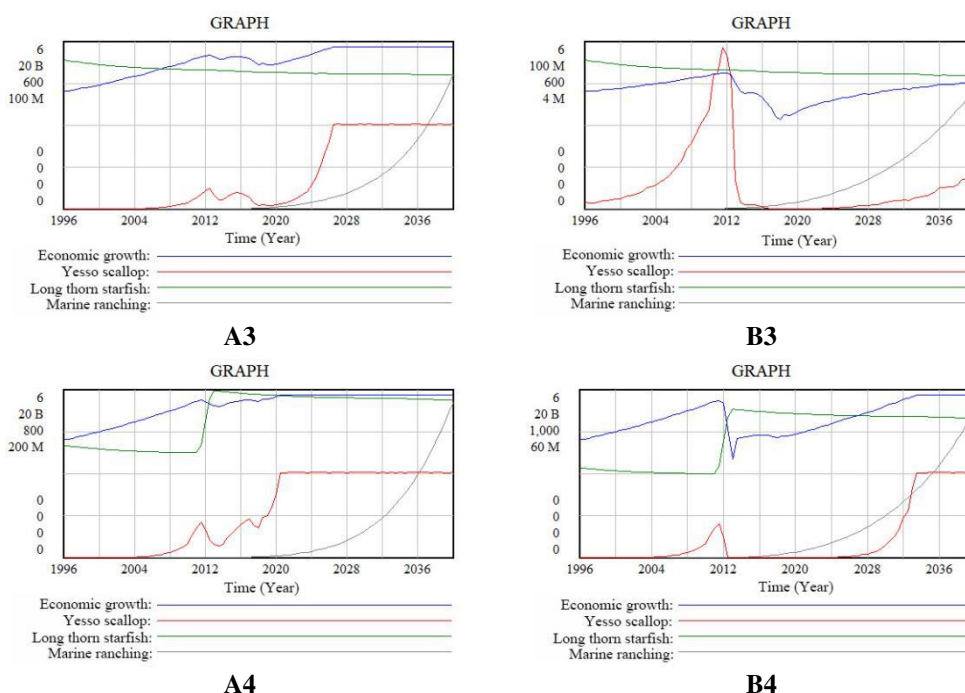


**Figure 10.** Simulation results of single factor disturbance in ecological environment disturbance scenario

## Conclusion

This paper takes the overall marine ranches artificial ecosystem of Zhangzi Island as the background, from the point of view of ecosystem integrity, combined with the multiple feedback effects of food chain, human intervention and environmental change at the core of Yesso scallop. The system dynamics model is used to simulate the marine ranch artificial ecosystem of Zhangzi Island and the following conclusion are drawn:

The simulation and diagnosis of the feedback mechanism of Zhangzi Island marine ranches artificial ecosystem by system dynamics provides a feasible method for analyzing the overall evolution process of marine ranch ecosystem.

The basic scenario simulation shows that the implementation of marine ranch construction has a significant effect on the proliferation of Yesso scallop, and the total yield of Yesso scallop can be increased to 2500 times of the initial value.

Fishing policy, environmental factors affecting the development of Yesso scallop, sudden major natural disaster coefficient and crown-of-thorns starfish are the sensitive factors that have great influence on the yield of Yesso scallop in the model, which lays a theoretical foundation for follow-up multi-scenario simulation.

The simulation results of human disturbance scenarios show that overfishing can lead to the depletion of Yesso scallop, and a good living environment is conducive to the restoration of normal growth of Yesso scallop.

The simulation results of ecological environment disturbance show that sudden major natural disasters and large-scale outbreaks of crown-of-thorns starfish can cause destructive destruction to Yesso scallop, but the number of crown-of-thorns starfish and the degree of protection from disasters can be controlled artificially by constructing marine ranches, which can help the Yesso scallop recover its yield slowly.

Through the basic simulation and multi-scenario simulation of the model, the temporary environmental capacity of Yesso scallop shrimp was judged and the main factors affecting the yield of Yesso scallop shrimp were simulated. This research believes that: A. Marine ranching is a dynamic artificial ecosystem, and follow-up research should pay more attention to the complexity and integrity of the system to deeply study the internal operating mechanism and dynamic changes of the system. B. A good growth environment, including adequate food source, is conducive to promoting shrimp reduced Yesso scallop to ocean waters to ranch accommodation environment, but also break the existing ecological system of dynamic balance, the higher the powerful guarantee of ecosystem balance, so should pay attention to repair and improve the growth environment of the shrimp, reduced Yesso scallop, to ensure the shrimp Yesso scallop production steadily improving. C. In order to ensure that Yesso scallop shrimp can survive large-scale in severe natural disasters, it is suggested to strengthen the follow-up construction of marine ranch to consolidate the base of Yesso scallop shrimp and further research on disaster prevention, so as to make the yield of Yesso scallop shrimp increased significantly. D. In order to avoid the severe loss of production caused by the outbreak of natural enemies, it is suggested to continue to strengthen the research on the monitoring system of Marine ranches, timely protect the Yesso scallop from invasion by foreign enemies, and maintain the yield safety of the Yesso scallop. E. A good Marine ranching management system is the cornerstone for the construction of Marine ranching. The management department should formulate reasonable fishing policies, strengthen fishery resource management system, ensure the healthy growth of Yesso scallop and promote the sustainable development of fishery resources.

## Discussion

In this paper, the food chain of Yesso scallop in the marine ecosystem is taken as the core structure flow chart. Due to the problem of too wide coverage, other economic fish and shellfish in the marine ranch are not included. At the same time, the crown-of-thorns starfish is the top predator in the sea area, and the natural enemy of the crown-of-thorns

starfish, the giant triton, is not added. In order to improve the model, other fishery organisms will be added to the follow-up study and the domestication system will be added for simulation. In addition, there are few environmental factors in this paper, and most of them are replaced by one factor of natural disaster. Therefore, it is impossible to judge the impact of various other environment factors on Yesso scallop and the response mechanism of Yesso scallop. In the follow-up study, we can refer to the Chinese and foreign literature more, through the study of the impact of marine natural disaster on other organisms transition to marine ranches and through countless running simulations to get the optimal parameters to improve and optimize the model.

**Acknowledgements.** This article is supported by the study on Engineering Technology of Planning, Construction and Management for Marine Ranching in Guangdong Province(GML2019ZD0402). We gratefully thank for helping and supporting.

## REFERENCES

- [1] Chen, Z. M., Mao, P. S., Yan, J., Wu, Y. Y., Wu, S. J. (2018): The technology process and design method of modern marine cage and ranching. – Guangdong Shipbuilding 37(2): 46-49, 77.
- [2] Cheng, J. H., Jiang, Y. Z. (2010): A Review and prospect of Marine living resources proliferation and release. – Chinese Fisheries Science 17(3): 610-617.
- [3] Felley, J. D., Vecchione, M., Wilson, R. R. (2008): Small-scale distribution of deep-sea demersal nekton and other megafauna in the Charlie-Gibbs Fracture Zone of the Mid-Atlantic Ridge. – Deep Sea Research Part II Topical Studies in Oceanography 55(1-2): 153-160.
- [4] Holby, O., Hall, P. O. J. (1994): Chemical fluxes and mass balances in a marine fish cage farm. III. Silicon. – Aquaculture 120(3-4): 305-318.
- [5] Hong, B., Sun, Z. Z., Zhang, Y. P., Zeng, Z. C., Tian, Z. Q. (2009): Evaluation on the effect of multiplication and release of fishery resources in the upper reaches of Huangpu river. – Aquatic science and technology information 36(4): 178-181.
- [6] Kim, S. K., Yoon, S. C., Youn, S. H., Park, S. U., Corpus, L. S., Jang, I. K. (2013): Morphometric changes in the cultured starry flounder, *Platichthys stellatus*, in open marine ranching areas. – Journal of Environmental Biology 34(2): 197.
- [7] Lin, G. J. (2012): "Big country effects" of Chinese fisheries concerning with their characteristics, strategy and policy making. – Fishery Information & Strategy 27(4): 264-271.
- [8] Liu, H. (2014): Research on marine fisheries' contribution to marine economy in China. – Ocean University of China.
- [9] Luo, Y., Fang, Q. W. (2019): Transformation of traditional aquatic enterprises to marine ranches. – Ocean and Fishery 2: 45-46.
- [10] Ottera, H., Kristiansen, T. S., Svasand, T. (1998): Evaluation of anchor tags used in sea-ranching experiments with atlantic cod (*Gadus morhua* L.). – Fisheries Research (Netherlands) 35(3): 237-246.
- [11] Pan, X. W., Yang, L. L., Ji, W. W., Liu, Z. L. (2010): Research progress of multiplication and release technology. – Jiangsu Agricultural Sciences 4: 246-250.
- [12] Rørvik, K-A., Steien, S. H., Saltkjelsvik, B., Thomassen, M. S. (2000): Urea and trimethylamine oxide in diets for seawater farmed rainbow trout: effect on fat belching, skin vesicle, winter ulcer and quality grading. – Aquaculture Nutrition 6(4): 247-254.

- [13] Rubio, F., Kamp, L., Carpino, J., Faltin, E., Loftin, K., Molgó, J., Aráoz, R. (2014): Colorimetric microtiter plate receptor-binding assay for the detection of freshwater and marine neurotoxins targeting the nicotinic acetylcholine receptor. – *Toxicon* 91: 45-56.
- [14] Sun, Q. C., Tan, Y. H., Li, J. B. (2018): Ecological protection and exploration of island in China in new era. – *Ocean Development and Management* 35(8): 22-27.
- [15] Taylor, A. L., Nowland, S. J., Hearnden, M. N., Hair, C. A., Fleming, A. E. (2016): Sea ranching release techniques for cultured sea cucumber *Holothuria scabra* (Echinodermata: Holothuroidea) juveniles within the high-energy marine environments of northern Australia. – *Aquaculture* 465: 109-116.
- [16] Wang, X. J., Hu, Q. G. (2013): Analysis on the coordination degree between mariculture and marine ecological environment in China. – *China's Rural Economy* 11: 86-96.
- [17] Wang, G., Zhang, H. H. (2020): Research hotspots and trends of marine ecosystem services based on bibliometrics. – *Acta Ecologica Sinica* 40(7): 2496-2505.
- [18] Wood, L., Peschken, A. A. (1990): *Aquaculture: Marine Farming of Atlantic Salmon*. – *Geography* 75(3): 211-221.
- [19] Xiong, J. X., Chen, D. L., Peng, B. F., You, X. J. (2016): Temporal and spatial difference of dynamic simulation of ecological carrying capacity in Dongting lake region. – *Economic Geography* 36(4): 164-172.
- [20] Xiong, Y., Li, J. Z., Jiang, D. L. (2018): Optimized decision-making of water resources supply and demand system in Changsha-Zhuzhou-Xiangtan urban agglomeration based on the analog simulation. – *Acta Geographica Sinica* 68(9): 1225-1239.
- [21] Yang, H. S., Huo, D., Xu, Q. (2016): My view on the construction of modern Marine ranching. – *Ocean and lakes* 47(6): 1069-1074.
- [22] Yu, J., Chen, P. M., Feng, X. (2016): Food habits and trophic levels for 4 species of economical shrimps in the pearl river estuary shallow waters. – *Journal of Southern Agriculture* 47(5): 736-741.
- [23] Zhang, M. J., Guan, D. J., Su, W. C. (2015): Scenarios simulation and indices threshold determination of ecological security in three gorges reservoir based on system dynamics. – *Acta Ecologica Sinica* 35(14): 4880-4890.
- [24] Zhang, J. F., Cai, H. J., Zhao, Y. N., Chen, W. H., Hu, S. Q., Liu, Y., Liu, C. F. (2020): Seasonal variation in the total organic carbon contents and the  $\delta^{13}\text{C}$  values of macroalgae in the rocky intertidal zone of the Zhangzi island. – *Marine Sciences* 44(2): 56-65.

## APPENDIX

Average predation coefficient of scallop = 0.061325

Small phytoplankton predation = scallop shrimp \* scallop average predation coefficient

Small phytoplankton = small phytoplankton are born - small phytoplankton die - small phytoplankton are eaten

Split = 1.02

Small phytoplankton birth = Small phytoplankton \* inorganic nitrogen \* inorganic salt \* 2.08222 \* fission

Inorganic nitrogen = nutrient salt in seawater \* 0.2 + 0.1

Integ = initial value of seawater nutrient supplement = 0.13

Dry settlement = atmospheric settlement \* 0.23

Atmospheric deposition = 0.1

Wet settlement = atmospheric settlement \* 0.2

Inorganic salt = 0.01 \* LN(1 + ABS(benthic Detritus feeding organisms \* quantity of detritus \* conversion rate))

Conversion rate = 0.24

Detritus quantity = (death of small phytoplankton + death of starfish + death of short carpal larvae + death of feathered carpal larvae + death of shrimp scallop) \* 12

Birth rate =  $0.42 * \text{LN}(\text{benthic detritus eater}) + 14$   
Integ = birth rate - initial death rate of benthic detrital feeding organism = 7  
Benthic detritus feeding on natural enemies = 0.8  
Mortality rate = (benthic detritus feeding organism + benthic detritus feeding organism natural enemies) \* rate of benthic detritus feeding organism natural enemies  
Predator predation rate of benthic detritus = 0.2  
Number of rivers flowing into seawater = 0.078  
River transport = average nutrient content of rivers into the sea \* number of rivers into the sea \* average runoff  
Nutrient supplement = (dry settlement + wet settlement) \* river transport  
Average runoff = 0.75  
Average nutrient content in rivers into the sea = 0.2  
Atmospheric pressure difference = 0.3  
High wind = atmospheric pressure difference \* 0.1 + 0.23  
Temperature less than 5 ° C = temperature drop \* 0.13  
Average annual spawning rate of scallop shrimp = IF THEN ELSE(temperature above 23 ° c >= temperature below 5 ° c, 1, 0)  
Temperature above 23 degrees Celsius = IF THEN ELSE(increase in temperature >= 23, 1, 0)  
Temperature rise = greenhouse effect \* 0.15  
Integ = temperature rise - temperature fall Initial value = -0.4  
Temperature reduction = 0.2 \* DELAY1(high wind generated, 2)  
Greenhouse effect = accelerated industrialization and urbanization \* 0.1  
Industrialization, urbanization process plus = 1  
Economic growth =  $0.2 * \text{LN}(1 + \text{ABS}(\text{fished} * 423)) + 0.1$   
Artificial breeding flow =  $0.5 * \text{LN}(\text{economic growth})$   
Construction of suitable shellfish basement = economic growth \* 0.64  
Scallop oviposition efficiency = 0.4  
Larvae birth = artificial breeding release + scallop \*(spawning efficiency + average annual spawning rate of scallop) \* suitable for shellfish basement construction  
Marine ranching construction = Investment in Marine ranching industry and technology \* 0.00052  
Integ = larvae birth - larvae development - larvae death + initial value of marine ranch construction = 12  
Larva death = larva mortality \* larva death  
Larvae mortality rate = 0.23  
Development environment impact factor = 0.5  
Time of scallop development = RANDOM UNIFORM(0.13, 0.32, 0.14)  
Larva development = larva/developmental time \* environmental impact factors of scallop  
Scallop crowding = MAX(0, Scallop - scallop environmental capacity)  
Predation control = IF THEN ELSE(>=50, 1, 0)  
Integ = young development of Scallop - artificial fishing - death of scallop - predation of scallop - initial migration value of scallop =  $4e+006$   
Scallop predation = (starfish \* average predation coefficient + starfish \* Long spiny Starfish outbreak \* 500 \* average predation coefficient) \* Predation control  
Fishing base = IF THEN ELSE(scallop >= 60, 1, 0)  
Manmade fishing = fishing policy \* fishing base \* Prawn scallop  
Fishing policy = 1.2  
Spiny starfish outbreak = 0  
Death of Scallop = death rate of scallop \* death rate of scallop \* impact of natural disasters such as storm surge  
Scallop mortality rate = 0.01  
Impact of natural disasters such as storm surge = scale of natural disasters such as storm surge \* frequency of natural disasters such as storm surge + coefficient of sudden major disasters \* scale of natural disasters such as storm surge \* frequency of natural disasters such as storm surge

Scallop migration = Scallop crowding/migration time  
Scallop migration time =0.02  
Environmental capacity of shrimp scallop =1e+010  
Coefficient of sudden major disaster =0  
Natural calamities such as storm surge frequency = with look up = timelookup ([ (1996, 0) - (2056,0.2)], (2010,0.06),0.11 (2011), (2012,0.09),0.88 (2013), (2014,0.09),0.06 (2015), (2017,0.98),0.094 (2020), (2030,0.094),0.094 (2040), (2050,0.094))  
Scale of natural disasters such as storm surge =RANDOM UNIFORM(0.5, 1.5, 2)  
Starfish spawning efficiency =0.24  
Starfish larvae birth = starfish \* starfish spawning efficiency \* Starfish spawning efficiency +10+LN(ABS(Investment in Marine Ranching Industry technology \*0.0053))  
Average annual spawning rate of starfish =0.5  
Integ = Starfish larva birth - ciliary larva development - initial value of ciliary larva death 34  
Ciliary larva death = snail predation + ciliary larva \* ciliary larva death  
Mortality rate of cilia larvae =0.23  
Snail predation =0.5  
Development time of ciliated larvae =5  
Development of cilia larvae = development time of cilia larvae/cilia larvae  
Integ = development of ciliary larva - development of carpal larva - initial value of death of carpal larva 32  
Larvae mortality rate =0.13  
Carpal larvae death = carpal larvae \* Carpal larvae death  
Development of carpal larvae = development time of carpal larvae/carpal larvae  
Development time of carpal larvae =5  
Larvae with short wrists had a mortality rate of 0.3  
Integ = development of brachial larva - development of brachial larva - initial value of death of brachial larva 12  
The unadsorbed probability is -0.24  
Failed to adsorb 0.3  
Death of brachiophora larva = brachiophora larva \*(unsuccessful adsorption + probability of failure + mortality of brachiophora larva)  
Development of short carpal larvae = short carpal larvae/short carpal larvae development time  
Development time of short carpal larvae =4  
Starfish mortality rate: 0.01  
Starfish death = (starfish \* starfish death rate + catch by human monitoring \* probability of starfish discovery + probability of cannibalism by one species \* probability of cannibalism by another species)  
Starfish INTEG = Development of short carpal larvae - initial value of starfish death 534  
Homogeneous predation  
Species predation probability 0.01  
Probability of finding starfish =RANDOM UNIFORM(0.01, 0.8, 0.01)  
Artificial surveillance fishing =RANDOM UNIFORM(0.4, 5, 4)  
Average predation coefficient of starfish =20  
Investment in Marine ranching industry technology = social investment expenditure \*0.12  
Integ = larva development of Scallop - artificial fishing - death of scallop - predation of scallop - initial migration value of scallop 4e+006  
Change in Marine resource utilization = (scallop with shrimp)\*1000  
Integ = initial value of change of Marine fishery resources utilization 0.5  
Manmade fishing = fishing policy \* fishing base \* Prawn scallop  
Economic growth =0.2\*LN(1+ABS(fished \*423))+0.1  
Gross domestic product of Marine ranching = INTEG Initial value of gross domestic product change of Marine ranching 4234  
Beach entertainment =RANDOM UNIFORM(0.1, 1, 0.3)



Sea fishing =RANDOM UNIFORM(0.1, 1, 0.2)

Yacht =RANDOM UNIFORM(0.1,1, 0.3)

Economic growth factor = beach recreation + sea fishing + yacht

Marine ranching construction = Investment in Marine ranching industry and technology \*0.00052

Marine Ranching recreation = Marine ranching construction + economic growth factor of recreational activities

Annual income changes of Marine ranchers = gross product of Marine ranches \* 3.4E-005

Integ = Initial value of annual income variation of Marine ranchers

GDP change = Marine ranching GDP \*0.000108+354

Domestic GDPinteg= initial value of GDP change =745654

Change in social investment expenditure = DOMESTIC GDP\*0.3

Integ = Initial change value of social investment expenditure =32134

# GENOTYPE × ENVIRONMENT INTERACTION AND STABILITY ANALYSES CONCERNING THE YIELD AND QUALITY CHARACTERISTICS OF PROMISING POTATO (*SOLANUM TUBerosum*) GENOTYPES

KARAN, Y. B.\* – YILMAZ, G.

*Department of Field Crop Science, Faculty of Agriculture, Tokat Gaziosmanpasa University, 60250 Tokat, Turkey*

*\*Corresponding author  
e-mail: ybkaran@gmail.com*

(Received 27<sup>th</sup> Aug 2020; accepted 18<sup>th</sup> Dec 2020)

**Abstract.** This experiment was carried out in three different locations with different environmental characteristics such as altitude, soil structure and precipitation in the Central Black Sea Region in Turkey between 2017-2018. The aim of this study was to investigate performance, dry matter ratio and total tuber yield of 15 different promising potato clones and five different potato commercial cultivars in various environments. The average tuber yields across the environments was 32.44 ton/ha while the average of standard cultivars was 35.13 ton/ha and average of advanced clones was 31.54 ton/ha. The mean dry matter ratio was 19.64%, which was 20.22% for commercial varieties and 20.03% for advanced clones. In terms of the stability and genotype × environment interaction for tuber yield, regression coefficients varied from  $\beta_i = 0.10$  to 3.39. PAI-8-857, PAI-8-3-15, PAI-8-6-35 and PAI-8-5-34 were closest to  $\beta_i = 1$  in all environments in respect of the general average and regression coefficient. PAI-8-857 and GOU 6/28 were better suited to grow in all environments. The dry matter values were also subjected to stability and genotype × interaction analyses. The regression coefficients varied from  $\beta_i = 0.06$  to 2.76. PAI-8-8-57 clone had higher dry matter content than other genotypes under suitable conditions.

**Keywords:** *adaptation, altitude, clones, dry matter content, regression coefficient, tuber yield*

## Introduction

Potato, *Solanum tuberosum*, is estimated to have been cultured by selection from wild species found in the Andes in South America about 10,000 years ago. It is the third most important food crop (FAO, 2018). Potato is cultivated in more than 125 countries. Almost 52% of the total cultivation area lies in the temperate region in Europe, 34% of Asia, and 14% of Africa. The total world potato production was at 368.2 million tons in 2018 (FAO, 2018). Turkey is one of the lowland tropics, and the nineteenth largest producer of potato in the World. Turkey is Middle East's largest producer after Iran, with a production of almost 4.6 million tons in 2018 (FAO, 2018).

Potatoes are cultivated in various environments (Haverkort, 1990). Potatoes are grown in a wide area from the sea level up to elevations of 4000 m. The maximum capacity and genuine tuber dry matter contents and tuber yield are acquired in areas with mild climates (Van der Zaag, 1984; Stol et al., 1991). The dry matter content of potato tubers ranges from 18 and 28% depending on the genotype and environment (Er and Uranbey, 1998).

Genotype and environment interactions are correlated with the performance of genotypes that indicate stability when planted in various environments. Ruswandi et al. (2008) reported selection of high-efficiency and quality genotypes based on multi environment testing.

According to Roostaei et al. (2014), the Genotype and environment interactions factor is a major issue faced by plant breeders in plant breeding programs. GEI is essential for the acquirement of new and superior breeding lines as reported by many research results (Niringiye et al., 2014; Hongyu et al., 2014). Important features of an optimal variety include high yield stability under adverse environmental conditions. Furthermore, advanced crop cultivars need to have higher yield levels as well as in other features and this superiority should be expressed in the primary areas where the crop is cultivated (Martin et al., 1988).

The aim of this study was to evaluate the dry matter content and total tubers yields of fifteen promising potato clones and five commercial varieties under at three different locations in the Middle Black Sea Region in Turkey in 2017-2018 for genotype environmental interactions and stability analyses.

## Materials and methods

This investigation was conducted in Erbaa (276 m – 294 m), Kazova (571 m) and Artova (1191 m), Middle Black Sea Region in Turkey, during growing seasons of 2017-2018 years. The multi locational trials were carried out at three locations and two years that differed with respect to soil type, vegetation, annual precipitation and temperatures and elevations (*Table 1*). Accordingly, the trial in the geographical field position in the first year Tokat-Erbaa; there are 40.58° north latitude and 36.89° eastern longitude. The altitude is 276 m. In the second year, 40.53° north latitude and 36.93° eastern longitude, altitude is 291 m. The field trial area in Tokat-Kazova is between 40.33° north latitude and 36.36° eastern longitude geographically location, altitude is 571 m. The Tokat-Artova between 40.13° and 36.33° east longitude and north latitude and altitude is 1191 m.

**Table 1.** Description of the experimental locations. (Source: Turkish State Meteorological Service)

Location	Altitude (m)		Soil type		Average precipitation (mm)			Min. temperature/mean annual max. (°C)		
	2017	2018	2017	2018	2017	2018	Long term (1964-2017)	2017	2018	Long term (1964-2017)
Tokat-Erbaa	276	294	Silty clay loam	Silty clay loam	408.5	406.6	488.4	2.7 °C /25.9 °C	6.2 °C /25.3 °C	4.0 °C /23.9 °C
Tokat-Kazova	571	571	Clay loam	Clay loam	391.9	329.9	433.4	0.4 °C /24.5 °C	4.4 °C /23.8 °C	1.7 °C /22.2 °C
Tokat-Artova	1191	1191	Sandy clay loam	Sandy clay loam	372.4	464.1	464.1	-3.9 °C /20.6 °C	0.7 °C /19.5 °C	-3.2 °C /18.0 °C

Weather conditions such as soil, temperature and rainfall data were recorded during the experimental years and long-term period are presented in *Table 1*. In all locations, average temperatures were higher than the long-term averages in both years. On the other hand, total precipitations were lower compared to the long-term values in both years. The total precipitation was 408.5 mm in Erbaa location in 2017. In 2018, total precipitation was 406.6 mm in Erbaa location. In Tokat-Erbaa temperature range was 2.7 °C and 25.9 °C in 2017, and 6.2 °C and 25.3 °C in 2018. Tokat Kazova had average annual rainfall of 329.9 mm in 2017 and 433.4 mm in 2018. Also, in Tokat

Kazova in the first year of experiment minimum and maximum temperature 0.4 °C and 24.5 °C, respectively. As for the second year of experiment minimum and maximum temperature in Tokat Kazova location was 4.4 °C and 23.8 °C respectively. Total annual precipitation in Tokat-Artova location was 464.1 mm in the first year and 464.1 mm in the second year. The minimum and maximum temperature values in Tokat Artova were -3.9 °C and 20.6 °C in 2017, and 0.7 °C and 19.5 °C in 2018, respectively.

### ***Plant material used in experiment***

In the experiment, 15 different promising potato breeding lines and 5 different commercially available cultivars were used as plant material (*Table 2*).

**Table 2.** *Plant material used in the experiment*

Number	Genotype name	Pedigree	Maturity	Breeding institution	Tuber flesh color
1	PAI-8-1-6	Provento × Marfona	Early to intermediate	PAI	Light yellow
2	PAI-8-3-15	Agria × Van Gogh	Intermediate to late	PAI	Yellow
3	PAI-8-5-34	Atlantic × Hermes	Early	PAI	Yellow
4	PAI-8-6-35	Agria × Granola	Very early to early	PAI	Yellow
5	PAI-8-7-49	Atlantic × R. Russet	Early to intermediate	PAI	Cream
6	PAI-8-8-57	Provento × Granola	Early to intermediate	PAI	Yellow
7	PAI-8-9-63	L. Rosetta × Granola	Very early to early	PAI	Light yellow
8	PAI-8-11-79	Atlantic × Laura	Early to intermediate	PAI	Light yellow
9	PAI-8-12-86	Atlantic × Granola	Early to intermediate	PAI	Cream
10	PAI-8-15-138	Atlantic × Konsul	Early	PAI	Light yellow
11	GOÜ-3/110	Serrana × TS-9	Late	GOU	Yellow
12	GOÜ-4/4	Granola × TS-2	Intermediate to late	GOU	Light yellow
13	GOÜ-6/28	Serrana × LT-7	Intermediate to late	GOU	Light yellow
14	GOÜ-7/12	Serrana × TS-4	Intermediate to late	GOU	Cream
15	GOÜ-10/15	MF-1 × LT-7	Intermediate to late	GOU	Cream
16	Agata	BM5272 × Sirco	Very early to early	Agrico	Light yellow
17	Alegria	Flava × _@	Very early		Yellow
18	Agria	Quarta × Semlo	Intermediate to late	Agrico	Yellow
19	Lady Claire	Agria × KW 78-34-470	Early	Meijer Seed Potatoes Ltd	Light yellow
20	Lady Olympia	Agria × KW 78-34-470	Early	Meijer Seed Potatoes Ltd	Yellow

PAI: Potato Research Institute, Nigde-Turkey; GOU: Gaziosmanpasa University Faculty of Agriculture

### ***Methods***

At all locations, the study was arranged in a completely randomized block design. The trial consisted of three replications. Potato genotypes of tubers were planted in Erbaa in early March, in Kazova in the second decade of April, and in Artova in May in the first decade of May in both years. For both years and both sites, the plot size for each genotype consists of 4 rows of 6 m. length. Planting of potato tubers was performed at spacing of 70 cm between rows and 30 cm between plants. At each site and year, plots were fertilized with 120 kg nitrogen, phosphorus, potassium ha<sup>-1</sup> in the form of 15:15:15. The entire rate of phosphorus and potassium were applied at the time of planting. Nitrogen fertilizer was applied at 80 kg/ha at the beginning of tuber formation. (Tugay et al., 1995). The potato varieties and promising clones were watered to maintain adequate moisture levels with drip irrigation. According to FAO, for high yields, the crop water requirements for a 120 to 150 day crop are 500 to 700 mm,

depending on climate. The water needs of potato plants are generally lower during the first stages of the plant development and they gradually increase towards maturation and the later stages of tuber growth (FAO, 2020). In both years, irrigation was started in Erbaa in mid-May, in Kazova in early June, and in Artova in mid-June. Irrigation intervals were approximately 10 days in all environments. The amount of water applied varied between 50 and 100 mm per event to bring the soil moisture level to field capacity. Cultural and chemical practices such as weeding and pest-control were used in all locations and years. The fields were harvested when the plants reached harvest maturity. Tubers were harvested in early September in Erbaa, at end of September in Kazova and in the mid of October in Artova in both years. After harvest, the tubers were stored for 8 weeks. Dry matter content was measured as weight in water, which can be turned into specific gravity by the formula: Specific Gravity ( $\text{gcm}^{-3}$ ) = Weight in air / (Weight in air – Under water weight). 5 kg tubers were randomly taken from each location with water then weighed first in air and then in water. (Meijers and Van Veldhuisen, 1972). Total tuber yield per hectare was calculated using tuber weight of center rows.

### ***Evaluation of the data***

#### *Statistical analyses*

The experimental design used was a randomized complete block design with three replications at each location and year. An analysis of variance (ANOVA) was done for each potato genotype and cultivar separately as randomized complete block design. Combined ANOVA result of each location and years showed significant ( $P < 0.01$ ) genotypic differences for dry matter content and total tuber yield. Potato genotypes and cultivars were compared using Duncan statistical test with SPSS software (Duzgunes et al., 1987).

#### *Stability analysis or parametric approach*

Genotype  $\times$  environment interaction variances should be statistically significant before performing stability analysis. Because of this, combining multiple experiments and repeated experiments in a year, the genotype  $\times$  location, genotype  $\times$  year and genotype  $\times$  location  $\times$  year interaction in the variance analysis chart should be identified by checking the F test by means of the F test (Arshad, 1990). Yield stability and adaptation terms are often used in different senses (Lin et al., 1986; Becker and Leon, 1988). The process to be performed after the interactions are important is to create a bilateral genotype  $\times$  environment interaction chart by using the mean values of the genotypes in the environment (İkiz, 1972;1976; Yıldırım et al., 1979 and Arshad, 1990). From this chart, the stability criteria such as the regression coefficients on the environmental mean of the genotypes and the squared deviations of this regression can be calculated (Finlay and Wilkinson 1963). From this table, stability criteria such as regression coefficients of genotypes (Y) on environment (X) can be calculated later (Arshad, 1990), where:  $X_{ij}$  = The mean of  $i^{\text{th}}$  genotype at the  $j^{\text{th}}$  environment;  $\bar{X}..$  = Genotypes general average in all environment;  $g_i$  = Effect of  $i^{\text{th}}$  genotype;  $e_j$  = Effect of  $j^{\text{th}}$  environment;  $(ge)_{ij}$  =  $i$ . genotype  $j$ . interacts with the environment and is estimated by  $(ij - i. - .j + ..)$ .

The main parameters of genotype  $\times$  environment analyses are summarized in *Table 3* (Lin et al., 1986).

**Table 3.** Detailed bilateral chart for genotype environment interaction

Genotypes	E <sub>1</sub>	E <sub>j</sub>	E <sub>q</sub>	Genotype average	Effect of genotype (g <sub>ii</sub> )
G <sub>1</sub>	x <sub>11</sub>	x <sub>1j</sub>	x <sub>1e</sub>	$\bar{X}_{.1}$	$\bar{X}_{.1} - \bar{X}_{..}$
G <sub>i</sub>	x <sub>i1</sub>	x <sub>ij</sub>	x <sub>ie</sub>	$\bar{X}_{.i}$	$\bar{X}_{.i} - \bar{X}_{..}$
G <sub>g</sub>	x <sub>g1</sub>	x <sub>gj</sub>	x <sub>ge</sub>	$\bar{X}_{.g}$	$\bar{X}_{.g} - \bar{X}_{..}$
Environment average	$\bar{X}_{.1}$	$\bar{X}_{.j}$	$\bar{X}_{.e}$	$\bar{X}_{..}$ general average	
Effect of environment (E <sub>j</sub> )	$\bar{X}_{.1} - \bar{X}_{..}$	$\bar{X}_{.j} - \bar{X}_{..}$	$\bar{X}_{.e} - \bar{X}_{..}$		

According to Finlay and Wilkinson (1963), the regression of the genotype values that each genotype received in different environments was calculated on environmental averages.

$$\beta_i = \frac{\sum_j (x_{ij} - \bar{X}_{.i})(\bar{X}_{.j} - \bar{X}_{..})}{\sum_j (\bar{X}_{.j} - \bar{X}_{..})^2} \quad (\text{Eq.1})$$

where: i = genotypes; j = environments;  $x_{ij} - \bar{X}_{.i}$  = It is the difference between the phenotype value of the I; genotype and the mean of the genotype on all environmental;  $\bar{X}_{.j} - \bar{X}_{..}$  = effect of j<sup>th</sup> environment;  $\beta_i$ : regression coefficient for the response of the i<sup>th</sup> genotype to varying environments; q: number of environments.

The regression coefficient ( $\beta_i$ ) were used as measures of stability, with respect to Finlay and Wilkinson (1963). Regression coefficients approaching 1.0 show mean stability, but to determine adaptability, the genotype should always be associated and interpreted with the average total tuber yield and dry matter content.

Genotypes with regression coefficients close to 1.0 and high total tuber yields and dry matter contents are adapted to all environments. Genotypes with low average total tuber yields and dry matter content with regression coefficients close to 1.0 are poorly adapted to all environments regression coefficients over 1.0 means that genotypes have higher sensitivity to environmental variation with below average stability and great specific adaptability to high yielding environments.

Regression coefficients below 1.0 represents a measure of stability against environmental change and more specific adaptation to low efficiency environments. Confidence limits are calculated by multiplying the standard error of the mean with the appropriate t-value. The t-value is determined by the probability and the degrees of freedom (n-1). *Figure 1* illustrates genotypic patterns when regression is plotted against genotypic performance.

## Results and discussion

### Total tuber yield (ton/ha)

The results in *Table 4* showed that total tuber yield per hectare. Since each year and location were regarded as an environment in respect of stability, the study was conducted with 15 advanced generation clones and 5 commercial varieties in six environments. Total tuber yields were notably influenced by genotypes and different environments (*Table 4*). Accordingly, the overall mean of the test in regards of tuber

yield 32.44 ton/ha., average of standard commercial cultivars 35.13 ton/ha., average of advanced clones was 31.54 ton/ha.

$\beta_i > 1$ poorly adapted $X_i < X$ to favourable environments	$\beta_i > 1$ $X_i = X$	medium adapted to favourable environments	$\beta_i > 1$ well adapted to $X_i > X$ favourable environments
$\beta_i = 1$ poorly adapted $X_i < X$ to all environments	$\beta_i = 1$ $X_i = X$	medium adapted to all environments	$\beta_i = 1$ well adapted to $X_i > X$ all environments
$\beta_i < 1$ bad adapted to $X_i < X$ unfavourable environments	$\beta_i < 1$ $X_i = X$	medium adapted to unfavourable environments	$\beta_i < 1$ well adapted to $X_i > X$ unfavourable environments

**Figure 1.** Mathematical and verbal correction of genotypic adaptation

In 2017, the tuber yield of genotypes ranged from 5.46 ton/ha (PAI-8-9-63) to 42.67 ton/ha (Agria) in Erbaa, from 9.30 ton/ha (GOU 4/4) to 39.28 ton/ha (Agata) in Kazova, and from 7.44 ton/ha (PAI-8-9-63) to 49.31 ton/ha (PAI-8-1-6) in Artova. In 2018, the total tuber yield of genotypes ranged from 18.00 ton/ha (PAI-8-9-63) to 48.56 ton/ha (GOU 7/12) in Erbaa, from 17.44 ton/ha (PAI-8-9-63) to 46.96 ton/ha (PAI-8-8-57) in Kazova, and from 13.81 ton/ha (PAI-8-9-63) to 50.98 ton/ha (PAI-8-8-57) in Artova. PAI-8-8-57 and GOU 6/28 clones had high yields in all locations and years (Table 4).

The highest total tuber yield occurred in Erbaa in Agria variety in both years. The highest tuber yield produced in Kazova from GOU 6/28 (39.28 ton/ha) in 2017. Second year of this study, the results showed that the highest total tuber yield were belonged to the PAI-8-8-57 (46.96 ton/ha). However, PAI-8-857 and GOU 6/28 (46.62 ton/ha) were statistically in the same group. In Artova, first year of study, the tuber yields were highest with PAI-8-1-6, PAI-8-8-57, GOU 6/28, PAI -8-5-34, Alegria, Lady Olympia, PAI-8-7-49, PAI-8-12-86 and GOU 10/15. Also, these genotypes were statistically in the same group. The highest tuber yield produced in Artova from PAI-8-8-57 (50.98 ton/ha) in 2018. In terms of locations, the highest average tuber yields in decreasing order were in Artova, Kazova and Erbaa locations in both years (Table 4).

In parallel with this study, yields of 13 potato clones were investigated by Hajianfar et al. (2017). These potato clones had yield levels in the range of 35.19-41.22 t/ha. These clones were significantly superior to the check cultivar, Agria whose yield was 28.58 ton/ha, and other potato clones.

In a potato breeding program, three promising clones with good quality and quantity features were defined among 18 superior potato genotypes in Iran (Hassanpanah and Hassanabadi, 2012). In another study, stability of 13 promising potato clones for high total tuber yield in different environmental condition was studied. Among the potato clones, three with high stability performance and good characteristics compared to the check cultivars were selected (Hassanpanah and Hassanabadi, 2014).

When all environments were considered separately, PAI-8-8-57 and GOU 6/28 clones produced highest tuber yields compare to other clones. In all environments, genotypic differences were statistically significant ( $P < 0.01$ ) for tuber yields.

According to Finlay and Wilkinson (1963) a regression coefficient closest at  $\beta_i = 1$  shows average sensitiveness. When this is correlated with high average total tuber yield the genotype has general adaptively and when correlated with low average total tuber yield, the genotype has poor adaptability. High and stable yield levels in potato tubers are always desirable. It is also reported that tuber yield is one of the most important components for the person trying to define an ideal variety (Hoopes and Plaisted, 1987).

When the findings of total tuber yield were investigated in regards of stability and GEI, and the regression coefficients varied from  $\beta_i = 0.10$  to 3.39. Accordingly, PAI-8-857, PAI-8-3-15, PAI-8-6-35 and PAI-8-5-34 were closest to  $\beta_i = 1$  in the all environmental in respect to the general average and regression coefficient. PAI-8-8-57 and GOU 6/28 were better suited to grow than other clones in all environmental (Table 4 and Fig. 2).

**Table 4.** Total tuber yield (ton/ha) and regression coefficients ( $\beta_i$ ) of clones and cultivars in all environments

Genotype	Erbaa				Kazova				Artova				Genotype average	Effect of genotype ( $\beta_i$ )	$\beta_i$
	2017		2018		2017		2018		2017		2018				
Agata	25.73	d-h**	27.65	bcd**	39.28	a**	39.62	abc**	25.16	bc**	29.71	de**	31.19	-1.24	0.50
Alegria	33.61	a-e	38.60	ab	37.72	ab	39.81	abc	44.35	a	40.38	a-d	39.08	6.64	0.57
Agria	42.67	a	47.85	a	26.20	cd	42.25	ab	36.55	ab	44.72	abc	40.04	7.61	0.64
Lady Claire	30.21	b-g	35.85	abc	25.80	c	30.85	bcd	21.91	cd	35.95	b-e	30.09	-2.34	0.55
Lady Olympia	21.21	f-h	28.50	bcd	36.60	ab	38.51	abc	43.16	a	43.51	a-d	35.25	2.81	1.75
<b>Cultivar average</b>	<b>30.68</b>		<b>35.69</b>		<b>33.12</b>		<b>38.20</b>		<b>34.23</b>		<b>38.85</b>		<b>35.13</b>		
GOÜ 3/110	20.75	f-h	26.50	bcd	29.57	cde	27.27	cde	17.27	cde	22.23	ef	23.93	-8.51	0.10
GOÜ 4/4	22.89	e-h	37.42	ab	9.30	f	19.49	de	9.49	de	24.14	ef	20.45	-11.98	0.31
GOÜ 6/28	33.61	a-e	38.50	ab	39.28	a	46.62	a	46.62	a	49.65	ab	42.38	9.94	1.88
GOÜ 7/12	40.40	ab	48.56	a	27.18	c	35.82	abc	10.83	de	39.95	a-d	33.79	1.35	0.20
GOÜ 10/15	9.24	ij	18.50	d	17.77	d	40.71	ab	40.71	a	42.52	a-d	28.24	-4.19	3.39
PAI-8-1-6	19.11	g-i	22.01	cd	33.37	abc	30.80	bcd	49.31	a	43.93	a-d	33.09	0.65	1.69
PAI-8-3-15	30.28	b-g	35.88	abc	31.26	abc	38.55	abc	26.31	bc	39.28	a-d	33.59	1.16	0.96
PAI-8-5-34	30.95	b-f	37.42	ab	34.08	abc	30.52	bcd	44.32	a	46.45	abc	37.29	4.85	0.85
PAI-8-6-35	33.90	a-e	31.09	bcd	30.61	abc	37.34	abc	37.34	ab	43.90	a-d	35.70	3.26	0.96
PAI-8-7-49	15.51	h-j	24.83	bcd	33.83	abc	42.45	ab	42.45	a	40.79	a-d	33.31	0.87	2.31
PAI-8-8-57	38.50	abc	35.01	abc	37.49	ab	46.96	a	46.96	a	50.98	a	42.65	10.21	1.29
PAI-8-9-63	5.46	j	18.00	d	13.07	ef	17.44	e	7.44	e	13.81	f	12.54	-19.90	0.82
PAI-8-11-79	27.92	c-g	32.49	bc	36.49	ab	37.70	abc	37.70	ab	34.04	cde	34.39	1.96	0.56
PAI-8-12-86	34.50	a-d	25.00	bcd	27.52	c	41.15	ab	41.15	a	34.39	cde	33.95	1.52	0.59
PAI-8-15-138	23.16	d-h	30.05	bcd	34.55	abc	36.18	abc	16.18	cde	26.43	ef	27.76	-4.68	0.46
<b>Clone average</b>	<b>25.75</b>		<b>30.75</b>		<b>29.02</b>		<b>35.27</b>		<b>31.60</b>		<b>36.83</b>		<b>31.54</b>		
<b>Environmental average</b>	26.98		31.99		30.05		36.00		32.26		37.34		<b>32.44</b>		<b>1.00</b>
<b>Effect of environment</b>	-5.46		-0.45		-2.39		3.57		-0.18		4.90		<b>Confidence interval</b>		
													± 4.67		± 0.52

\*\*Significant at 1% level of probability



In environments with different characteristics such as altitude, temperature, precipitation and soil types, the findings of the advanced generation clones and varieties with different properties have been examined. According to this GOU 6/28 clone showed well adapted in the favorable environmental. PAI-8-1-6, PAI-8-7-49, GOU 10/15 clones and Lady Olympia cultivar showed medium adapted in the favorable environments. PAI-8-8-57, PAI-8-5-34 clones and Alegria and Agria cultivars showed well adapted in the all environments. PAI-8-6-35, PAI-8-12-86, PAI-8-3-15, PAI-8-11-79 and Agata, Lady Claire cultivars showed medium adapted in the all environments. PAI-8-9-63 clone cultivar showed poorly adapted in the all environments.

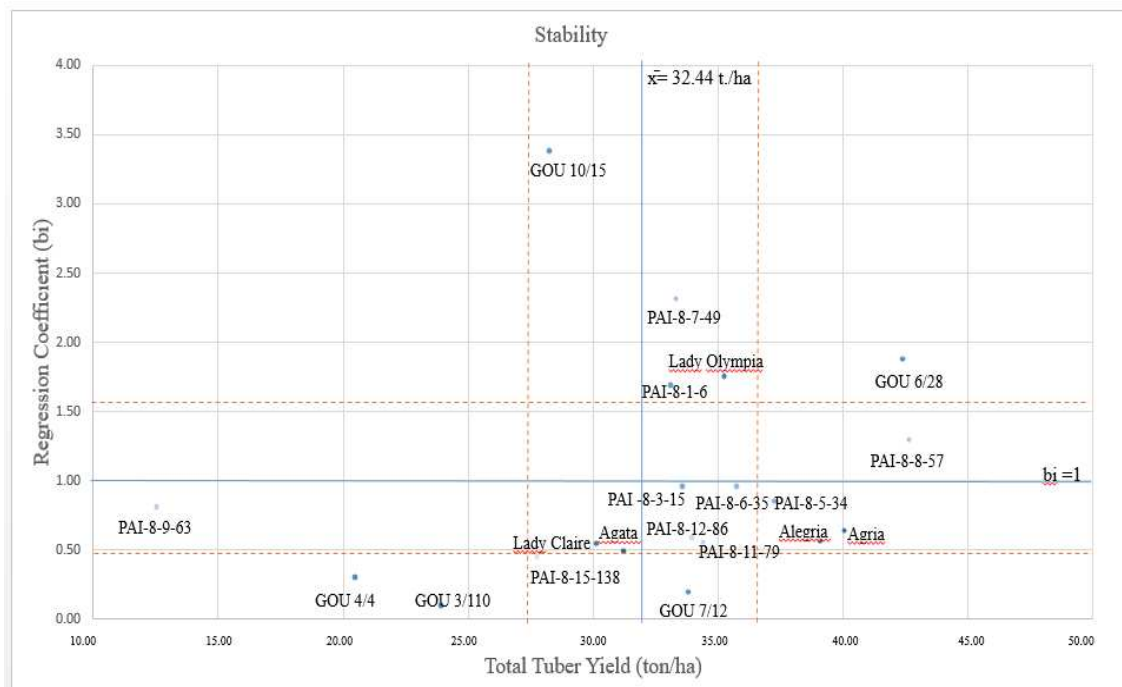


**Figure 2.** Adaptation classes of clone and varieties of total tuber yield (ton/ha)

While GOU 7/12 and PAI-8-15-138 clones showed medium adapted in the unfavorable environment, GOU 4/4 and GOU 3/110 clones showed poorly adapted in the unfavorable environment (Fig. 2).

### Dry matter content (%)

In this research, the dry matter percent of the potato clones and cultivars were given in Table 5. Accordingly, first year of this study the overall average of the promising clones and cultivars in regards of the dry matter ratio 20.70% in Erbaa, 19.07% in Kazova, 18.21% in Artova. In the second year of this study, the overall mean of the tubers in regards of the dry matter ratio was 19.92% in Erbaa, 19.73% in Kazova, 20.22% in Artova. The overall mean of the study in regards of dry matter was 19.64%, average of standard commercial varieties 19.47%, mean of promising clones was 19.70%. Dry matter ratios of the 15 promising clones and 5 commercial varieties were different. In this research, the dry matter ratio of the genotypes varied from 17.35 to 21.96%.

According to *Table 5*, the maximum dry matter ratio was observed from PAI-8-7-49 clone (% 21.96) in all genotypes, in all locations and years. Similarly, the highest dry matter was obtained from Lady Olympia (% 20.62) in all commercial cultivars.

In 2017, the dry matter content of genotypes ranged between 16.93% (Agata) and 23.37% (PAI-8-8-57) in Erbaa, between 15.57% (PAI-8-1-6) and 22.87% (PAI-8-7-49) in Kazova, and between 17.50% (PAI-8-12-86) and 21.07% (PAI-8-7-49) in Artova. In 2018, the dry matter content of genotypes ranged between 17.20% (Agata) and 22.87% (PAI-8-7-49) in Erbaa, between 16.40% (PAI -8-5-34) and 21.90% (PAI-8-7-49) in Kazova, and between 17.50% (PAI-8-12-86) and 22.40% (PAI-8-7-49) in Artova (*Table 5*).

**Table 5.** Total dry matter (%) and regression coefficients ( $\beta_i$ ) of clones and cultivars in all environments

Genotype	Erbaa				Kazova				Artova				Genotype average	Effect of genotype ( $\mu_i$ )	$\beta_i$
	2017		2018		2017		2018		2017		2018				
Agata	16.93	f**	17.20	d**	19.03	cde**	17.90	cde**	14.87	f**	18.30	bc**	17.37	-2.27	0.69
Alegria	18.35	ef	18.30	bcd	20.10	bcd	20.50	abc	18.63	bc	20.50	abc	19.83	0.19	0.19
Agria	19.80	a-f	19.20	a-d	19.00	cde	20.00	abc	17.43	cde	19.70	abc	19.19	-0.45	0.93
Lady Claire	20.67	a-e	19.20	a-d	21.47	ab	20.70	abc	18.97	abc	20.90	abc	20.32	0.68	0.43
Lady Olympia	20.93	a-e	21.10	ab	19.53	b-e	21.50	a	18.97	abc	21.70	ab	20.62	0.98	1.06
<b>Cultivar average</b>	<b>19.34</b>		<b>19.00</b>		<b>19.83</b>		<b>20.12</b>		<b>17.77</b>		<b>20.22</b>		<b>19.47</b>		
GOU 3/110	20.13	a-f	19.00	a-d	17.43	efg	18.00	b-e	17.93	cd	18.30	bc	18.47	-1.18	0.80
GOU 4/4	21.53	a-e	20.70	abc	18.37	def	19.00	a-e	19.50	abc	21.70	ab	20.13	0.49	1.11
GOU 6/28	22.30	a-d	20.50	abc	18.20	def	20.70	abc	17.47	cde	20.10	abc	19.88	0.24	1.74
GOU 7/12	22.50	abc	19.80	a-d	19.13	cde	20.40	abc	15.23	ef	21.70	ab	19.79	0.15	2.79
GOU 10/15	19.47	b-f	20.70	abc	16.53	fg	21.10	abc	19.40	abc	19.70	abc	19.48	-0.16	0.61
PAI-8-1-6	19.13	c-f	19.50	a-d	15.57	g	15.80	e	16.10	def	18.00	bc	17.35	-2.29	1.41
PAI-8-3-15	22.97	ab	20.70	abc	18.03	def	19.70	a-d	19.40	abc	20.40	abc	20.20	0.56	1.41
PAI-8-5-34	19.90	a-f	19.90	a-d	16.63	fg	16.40	e	17.83	cd	18.80	abc	18.24	-1.40	0.99
PAI-8-6-35	22.40	a-d	18.00	cd	20.73	bc	21.40	ab	19.10	abc	20.90	abc	20.42	0.78	0.90
PAI-8-7-49	22.43	a-d	21.10	ab	22.87	a	21.90	a	21.07	a	22.40	a	21.96	2.32	0.32
PAI-8-8-57	23.37	a	21.10	ab	19.03	cde	20.20	abc	18.33	bcd	21.00	abc	20.51	0.86	1.89
PAI-8-9-63	20.60	a-e	20.70	abc	20.73	bc	19.80	a-d	20.47	ab	20.90	abc	20.53	0.89	0.06
PAI-8-11-79	18.80	def	19.40	a-d	20.53	bc	19.90	abc	19.00	abc	20.00	abc	20.06	0.41	0.22
PAI-8-12-86	20.50	a-e	21.30	a	17.83	ef	16.60	de	15.33	ef	17.50	c	18.18	-1.46	1.80
PAI-8-15-138	21.30	a-e	20.50	abc	20.57	bc	21.00	abc	19.17	abc	19.10	abc	20.27	0.63	0.50
<b>Clone average</b>	<b>21.16</b>		<b>20.19</b>		<b>18.81</b>		<b>19.46</b>		<b>18.36</b>		<b>20.03</b>		<b>19.70</b>		
<b>Environmental average</b>	<b>20.70</b>		<b>19.92</b>		<b>19.07</b>		<b>19.73</b>		<b>18.21</b>		<b>20.22</b>		<b>19.64</b>		<b>1.00</b>
<b>Effect of environment</b>	1.06		0.27		-0.57		0.09		-1.43		0.58		<b>Confidence Interval</b>		
													<b>±0.75</b>		<b>±0.44</b>

\*\*Significant at 1% level of probability

Dry matter contents of the 15 promising potato breeding lines and commercial cultivars varied from each other. When all the environments were analyzed separately,

it was identified that some of the advanced clones could have a dry matter ratio of over 20%. These clones have the capacity to be utilized as clones with supreme dry matter content. These are PAI-8-7-49 (% 21.96), PAI-8-9-63(% 20.53), PAI-8-8-57 (% 21.51), PAI-8-6-35 (%20.42), PAI-8-15-138 (% 20.27), PAI -8-3-15 (% 20.20), GOU4/4 (% 20.13), PAI-8-11-79 (% 20.06). Results of dry matter content indicated that differences among different cultivars and promising clones were significant statistically ( $P < 0.01$ ) in all locations and years. It has been reported that late maturing cultivars accumulate higher dry matter content in cool climatic conditions and high-altitude locations. In addition, differences in quality of seed tubers affect the content of dry matter (Yılmaz and Karan, 2011).

When the research findings are examined in regards of GEI interaction and stability of the dry matter contents, the regression coefficients varied from  $\beta_i = 0.06$  to 2.76. When the suitability in regards of dry matter ratio was examined, PAI-8-8-57 had maximum dry matter content in the suitable condition. GOU 6/28 and GOU 7/12 indicated medium adaptation in the suitable condition, PAI8-12-86 was bad adapted to favorable environments. Lady Olympia and PAI-8-6-35 had high dry matter content in the all environments. Agria, GOU 4/4 and PAI-8-3-15 were medium adapted in the all environments. GOU 6/28, PAI-8-5-34, PAI-8-1-6 and Agata produced lowest dry matter content in the all environments. PAI-8-7-49 and PAI-8-9-63 clones were superior in that they had high dry matter contents even in unfavorable conditions.

GOU4/4, PAI 8-6-35 and PAI-8-3-15 clones were superior to other clones in regards of dry matter ratio. The mean dry matter ratio of these clones in all locations and years was upward the overall mean and the regression coefficient was closest to  $\beta_i = 1$  (Table 5 and Fig. 3). Dry matter content of genotypes was affected by environment. When stability of a genotype for dry matter is high, efficient selection for specific dry matter percentages is possible (Wang et al., 2017).

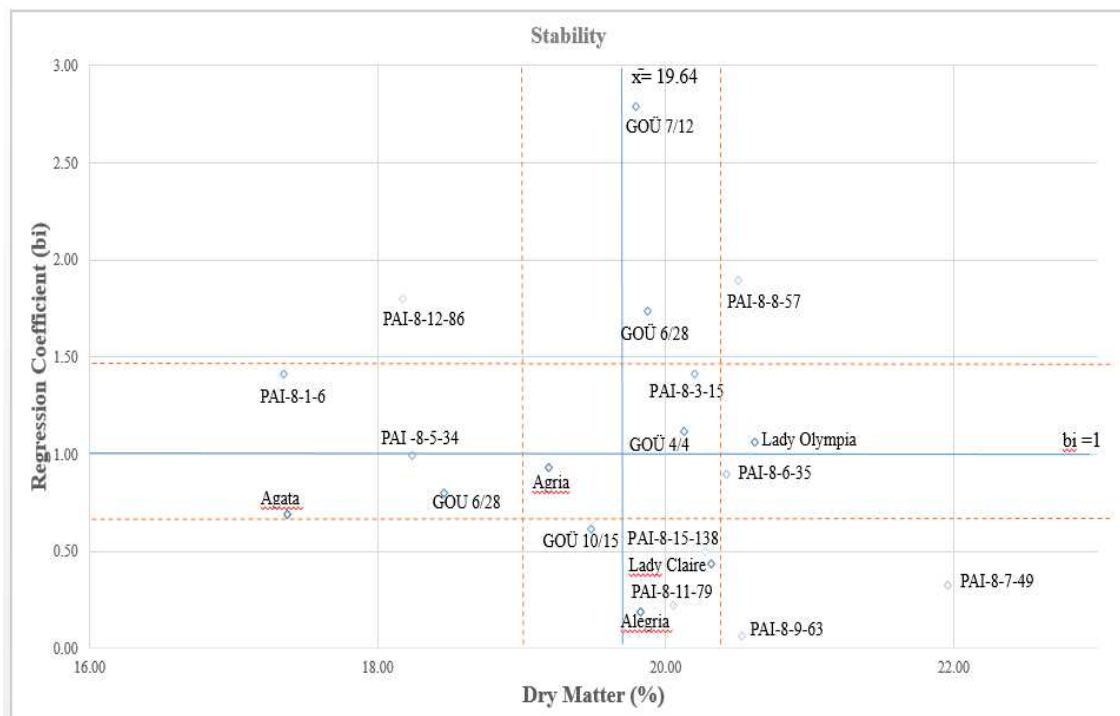


Figure 3. Adaptation classes of clone and varieties of dry matter ratio (%)

## Conclusion

Stability of some potato cultivars was investigated by Jankowska et al. (2015). However, contrary to Jankowska et al. (2015), the genotypes in the present study were evaluated in six locations, not just in one. Generally, stability evaluation is based on the data from multi-environment experiments. To acquire reliable stability assessments, an adequate number of environments is required (Lenartowicz et al., 2020).

GEI for yield and quality is a common reality that has been showed in multiple environment experiments with a large number of species of crop plants including potato (Mallory and Porter, 2007; Mulema et al., 2008).

Field trials in this experimental were carried out in various locations in terms of different climate, weather and soil types. Based on the GEI analysis, genotypes from different programs was found to be stable for dry matter and tuber yield.

The research confirmed the presence of remarkable variation among the genotypes as dry matter ratio and for tuber yield. The genotypes were observed to have different reactions to dry matter ratio and tuber yield in the various environments. The observed significant GEI for dry matter ratio and total tuber yield indicated that potato breeders should take into account the GEI while advancing stable genotypes defined by maximum total tuber yield and dry mater content. The observed significant genotype × environment interactions for dry matter ratio and total tuber yield are of major importance to plant breeders.

In all years and locations, the tuber yield average of standard varieties was 35.13 t/ha. PAI-8-8-57 (42.65 t/ha), GOU 6/28 (42.38 t/ha), PAI-8-5-34 (37.29 t/ha) and PAI-8-6-35 (35.70 t/ha) clones yielded more than the average of commercially registered varieties.

As the average of all years and locations, average dry matter of standard varieties was 19.47%. The clones which were found to be superior for total tuber yield (PAI-8-8-57, GOU 6/28, PAI-8-5-34 and PAI-8-6-35) generally had higher dry matter contents. In addition to these clones, GOU 4/4, GOU7/12, GOU10/15, PAI-8-3-15, PAI-8-7-49, PAI-8-9-63 and PAI-8-11-79 clones had higher dry matter contents than the standard varieties.

The locations investigated were highly different from each other. While the highest total tuber yield was obtained from Artova location, the lowest total tuber yield was obtained from Erbaa location.

As a result of this research, GOU 6/28 clone have been applied to The Republic of Turkey Ministry of Agriculture and Forestry Variety Registration and Seed Certification Center for National variety of registration by Tokat Gaziosmanpasa University Faculty of Agriculture.

**Acknowledgements.** The authors gratefully thank The Scientific and Technological Research Council of Turkey for financial support of the Project.

## REFERENCES

- [1] Arshad, Y. (1990): Research on some stability parameters used to determine genotypes' adaptability. (Genotiplerin uyum yeteneklerini belirlemede kullanılan bazı stabilite parametreleri üzerine araştırmalar). – Master Thesis. Ege University, İzmir (in Turkish).

- [2] Becker, H. C., Leon, J. (1988): Stability analysis in plant breeding. – Plant Breeding 101: 1-23.
- [3] Duzgunes, O., Kesici, T., Kavuncu, O., Gürbüz, F. (1987): Research and Trial Methods. Statistical Methods-II. (Araştırma ve deneme metotları istatistik metotları-II). – Publication Number: 1021, Textbook. Ankara University, Faculty of Agriculture, Ankara (in Turkish).
- [4] Er, C., Uranbey, S. (1998): Starch and Sugar Plants (Nişasta ve seker bitkileri). – Publication number: 1504, Textbook: 458. Ankara University, Faculty of Agriculture, Ankara (in Turkish).
- [5] FAO (2018): Food and Agriculture Organization of the United Nations. – <http://www.fao.org/faostat/en/#data/QC> (accessed 13.07.2020).
- [6] FAO (2020): Food and Agriculture Organization of the United Nations. Land & Water. – <http://www.fao.org/land-water/databases-and-software/crop-information/potato/en/>.
- [7] Finlay, K. W., Wilkinson, G. N. (1963): The analysis of adaption in a plant breeding program. – Aust. Jour. Agric. Res. 14: 742-754.
- [8] Hajianfar, R., Hassanpanah, D., Nosrati, A. E. (2017): Evaluation of advanced potato clones derived from breeding program in spring cultivated areas of Iran. – Horticultural Communication Biosci. Biotech. Res. Comm. 10(1): 127-133.
- [9] Hassanabadi, H., Hassanpanah, D. (2012): Evaluation of quantitative and qualitative characters of promising potato clones in Ardabil (article in Persian with an abstract in English). – Iranian Journal of Agricultural Science. 22: 219-233.
- [10] Hassanabadi, H., Hassanpanah, D. (2014): Evaluating quantitative and qualitative traits of promising potato clones and commercial cultivars using the GGE BI- plot and AMMI models. – Iranian Journal of Agricultural Science. 30: 149-164.
- [11] Haverkort, A. J. (1990): Ecology of potato cropping systems in relation to latitude and altitude. Agricultural Systems 32(3): 251-72.
- [12] Hongyu, K., Garcia-Pena, M., Borges, de Araújo L., do Santos, Dias, C. T. (2014): Statistical analysis of yield trials by AMMI analysis of genotype × environment interaction. – Biometrical Letters 51(2): 89-102.
- [13] Hoopes, R. W., Plaisted, R. L. (1987): Potato. Chap. 11. – In: W. R. Fehr (ed.) Principles of Cultivar Development. Vol. 2. Macmillan, New York.
- [14] Ikiz, F. (1972): Genotype-environment interactions (Genotip-cevre interaksyonları). – Plant breeding seminar. – Turkey Association of Agricultural Researchers Publications, Bornova-Izmir, pp. 207-226 (in Turkish).
- [15] Ikiz, F. (1976): Genotype x environment interaction statistics in wheat breeding (Bugday islahinda genotip x cevre interaksyonu istatistik analizleri). – PhD Thesis. Ege University, Faculty of Agriculture, Agronomy Genetics Course, İzmir (in Turkish).
- [16] Jankowska, J., Pietraszko, M., Lutomirska, B. (2015): The analysis of yielding stability of some potato (*Solanum tuberosum* L.) cultivars on light soils. – Fragn Agron 32: 32-43 (in Polish).
- [17] Lenartowicz, T., Piepho, H. P., Przystalki, M. (2020): Stability analysis of tuber yield and starch yield in mid-late and late maturing starch cultivars of potato (*Solanum tuberosum*). – Potato Research 63(2): 179-197.
- [18] Lin, C. S., Binns, M. R., Lefkovich, L. P. (1986): Stability analysis: where do we stand? – Crop Science 26: 894-899.
- [19] Mallory, E. L., Porter, G. A. (2007): Potato yield stability under contrasting soil management strategies. – Agronomy Journal 99: 501-510.
- [20] Martin, F. W., Flores, N. A., Carmer, S. G. (1988): Identification of the key environment for determination of yield stability in sweet potato. – Trap. Agric. (Trinidad) 65: 313-316.
- [21] Meijers, C. P., van Veldhuisen, G. (1972): De spreiding van de soortelijke gewichten van aardappelen. – Bedrijfsontwikkeling 3: 813-818 (in Dutch).

- [22] Mulema, J. M. K., Adipala, E., Olanya, O. M., Wagoire, W. (2008): Yield stability analysis of late blight resistant potato selections. – *Journal of Experimental Agriculture* 44(2): 145-155.
- [23] Niringiye, C. S., Ssemakula, G. N., Namakula, J., Kigozi, C. B., Alajo, A., Mpembe, I., Mwanga, R. O. M. (2014): Evaluation of promising sweet potato clones in selected agro ecological zones of Uganda. – *Time Journals of Agriculture and Veterinary Sciences* 2(3): 81-88.
- [24] Roostaei, M., Mohammadi, R., Amri, A. (2014): Rank correlation among different statistical models in ranking of winter wheat genotypes. – *The Crop Journal* 2: 154-163. <http://dx.doi.org/10.1016/j.cj.2014.02.002>.
- [25] Ruswandi, D., Anggia, E., Hastini, T., Suhada, A., Istifadah, N., Ismail, A., Suryadi, E., Ruswandi, S., Rostini, D. N. (2008): Selection of DR Unpad field corn hybrids based on their yield stabilities and adaptabilities in eight location in Indonesia. – *Zuriat* 19(1): 71-85.
- [26] Stol, W., de Koning, G. H. J., Kooman, P. L., Haverkort, A. J., van Keulen, H., Penning de Vries FWT (1991): *Agro-Ecological Characterization for Potato Production*. – Centre for Agrobiological Research (CABO-DLO) Wageningen.
- [27] Tugay, M. E., Citir, A., Yilmaz, G., Çagatay, K., Kara, K. (1995): Research on seed potato production. (Tohumluk Patates Uretim Uzerine Arastirmalar). – The Scientific and Technological Research Council of Turkey (TUBITAK). Final Report of the Project no 950. Gaziosmanpasa University, Faculty of Agriculture (in Turkish).
- [28] Turkish State Meteorological Service (TSMS) (2018): Meteorological District Office of Record of Climate Data, Tokat (in Turkish).
- [29] Vander Zaag, D. E. (1984): Reliability and significance of a simple method of estimating the potential yield of the potato crop. – *Potato Research* 27: 51-73.
- [30] Wang, Y., Snodgrass, L. B., Bethke, P. C., Bussan, A. J., Holm, D., Novy, R. G., Pavek, M. J., Porter, G. A., Rosen, C. J., Sathuvalli, V., Thompson, A. L., Thornton, M. T., Endelman, J. B. (2017): Reliability of measurement and genotype×environment interaction for potato specific gravity. – *Crop Science* 57: 1-7.
- [31] Yildirim, M. B., Ozturk, A., Ikiz, F., Puskulcu, H. (1979): *Statistical-Genetic Methods in Plant Breeding*. (Bitki Islahinda Istatistik-Genetik Yontemler). – Publication No: 20. Aegean Regional Agricultural Research Institute, Menemen, İzmir (in Turkish).
- [32] Yilmaz, G., Karan, Y. B. (2011): The performance of seed potato (*Solanum tuberosum*) produced in different production areas in Turkey- Tokat- Artova conditions. – International I. Ali Numan Kirac Agriculture Congress, Eskisehir, 27-30 April (in Turkish).

## SEED BIOPRIMING WITH OSMO-TOLERANT RHIZOBACTERIA ENHANCES THE TOLERANCE OF ALFALFA (*MEDICAGO SATIVA* L.)-RHIZOBIA SYMBIOSIS TO WATER DEFICIT

LAHRIZI, Y.<sup>1,2</sup> – OUKALTOUMA, K.<sup>1,3</sup> – MOURADI, M.<sup>4</sup> – FARISSI, M.<sup>4</sup> – QADDOURY, A.<sup>1</sup> – BOUIZGAREN, A.<sup>2</sup> – GHOULAM, C.<sup>1,3\*</sup>

<sup>1</sup>*Team of Plant Biotechnology and Symbiosis Agro-physiology, Faculty of Sciences and Techniques, PO. Box 549, Gueliz 40000, Marrakesh, Morocco*

<sup>2</sup>*Unit of Plant Breeding, National Institute for Agronomic Research (INRA), PO. Box 533, Marrakesh, Morocco*

<sup>3</sup>*Agrobiosciences Program, Mohamed VI Polytechnic University, Benguerir, Morocco*

<sup>4</sup>*Laboratory of Biotechnology and Sustainable Development of Natural Resources (LB2DRN), Polydisciplinary Faculty, PO. Box 592, Beni Mellal 23000, Morocco*

\*Corresponding author  
e-mail: c.ghoulam@uca.ma

(Received 2<sup>nd</sup> Sep 2020; accepted 30<sup>th</sup> Nov 2020)

**Abstract.** The present study aims to assess the beneficial effect of seed biopriming with osmo-tolerant rhizobacteria on alfalfa (*Medicago sativa* L.)-rhizobia symbiosis submitted to water deficit. The experiment was carried out under greenhouse conditions on six symbiotic combinations involving two Moroccan alfalfa populations *Adis-Tata* and *Demnate2* and an American *Moapa* variety inoculated with *RcRh09* and *Ensifer meliloti* (*Rm1021*) strains. Half of the plants of each symbiotic combination were submitted to water deficit consisting of 40% field capacity (FC) of substrate, while the other half were kept under optimal irrigation conditions (80% FC). After five weeks of water deficit, some agro-physiological and biochemical properties associated with water deficit tolerance in alfalfa were selected for further focus. Results showed that seed biopriming significantly increased plant growth and nodulation in all of the tested symbiotic combinations under water deficit in comparison to unprimed seeds. Physiologically, the biopriming significantly improved photosynthetic-related traits such as chlorophyll contents, the maximum quantum yield of PS II ( $F_v/F_m$ ) and stomatal conductance. Also, the macronutrient concentrations (P and K), the relative water content and membrane integrity, reflected by low malonyldialdehyde and electrolyte leakage values, were found improved by the pre-germination treatment. Our findings confirmed that the biopriming was an effective treatment for improving alfalfa growth and nodulation under water deficit.

**Keywords:** lucerne, drought stress, growth, photosynthesis, pre-germination treatment

### Introduction

Alfalfa (*Medicago sativa* L.), is the most cultivated perennial forage legume in the world thanks to its high biomass yields and good adaptation to wide variations of pedoclimatic conditions. It can produce about 11 to 18 t ha<sup>-1</sup> of dry matter (Liatukienė et al., 2008; Shen et al., 2009; Teixeira et al., 2011). The shoot part of alfalfa is rich in proteins for animal feed. Besides, its nutritional importance, alfalfa cropping improves soil fertility and structure by nitrogen and organic matter input in the soil and decrease leaching and erosion (Egamberdieva et al., 2011). Indeed, as leguminous species, alfalfa can establish a N<sub>2</sub>-fixing symbiotic association with the soil rhizobia. Therefore, it can

adapt to low mineral nitrogen levels in the soil and thus, it allows farmers to save at least a part of chemical N fertilizer costs and avoid them polluting to the groundwater.

Local populations of alfalfa are widely used in the traditional agrosystems of Moroccan mainly Oases and Atlas Mountains. They present high variability in their tolerance to biotic stresses and their adaptation to different soil and climatic conditions. However, the richness of this genetic heritage is threatened by several factors, such as prolonged periods of drought, soil and irrigation water salinity and diseases (Bouizgaren et al., 2013; Farissi et al., 2013; Mouradi et al., 2016a).

Water deficit is the main limiting factor of plant growth and productivity, particularly in the Mediterranean regions where climate changes caused a decrease of water availability and an increase of temperature. Indeed, the production season of alfalfa in Morocco coincided with the summer period characterized by high temperature and evapotranspiration that impose more irrigation. Currently, irrigation water resources are increasingly scarce, and alfalfa is submitted to moderate to severe water deficit reducing its performance in terms of forage production and persistence (Bouizgaren et al., 2013). To keep forage production under these water shortage conditions, many strategies are implemented such as the selection of the most drought-tolerant genotypes, adapted irrigation practices and plants and seeds treatments (Annicchiarico et al., 2011; Mouradi et al., 2016b). As treatment, seeds osmopriming and halopriming, based on immersion of the seeds into osmotic solutions as Polyethylene glycol and in salt as NaCl solutions respectively, improved seed germination performance and the seedling growth of Moroccan alfalfa populations under water deficit (Mouradi et al., 2016b) and salinity (Farissi et al., 2018). In the other hand, the pre-germination treatment of seeds with beneficial microorganisms (biopriming) is becoming increasingly important. It consists in the immersion of seeds in a microbial suspension for a pre-determined period followed by drying of seeds to prevent onset of germination (O'Callaghan, 2016). The biopriming has been used for the first time to improve plant tolerance to biotic stress, such as pathogen attack. The application of beneficial microorganisms to seeds is an efficient mechanism for placement of microbial inocula into soil where they will be well positioned to colonize seedling roots. Several studies have documented the beneficial effects of seed priming on growth of legumes. Moreover, Seed priming enhances the production and accumulation of osmolytes under stressed environments by altering metabolic processes (Tabassum et al., 2017). As reported by Sharifi and Khavazi (2011), the biopriming of maize seeds with different *Azotobacter* and *Azospirillum* strains significantly increased grain yield, crop growth rate and dry matter accumulation. However, Kasim et al. (2013) found that biopriming of wheat seeds with *Azospirillum brasilense* and *Bacillus amyloliquefaciens* strains increased drought tolerance in wheat plants through upregulation of genes related to stress.

In this context, the present study aims at highlighting the beneficial effect of seed biopriming with indigenous osmo-tolerant rhizobacteria on the performance of some Moroccan alfalfa (*Medicago sativa* L.) populations and their symbiosis under water deficit. We hypothesize that the presence of osmotic stress tolerant indigenous rhizobacteria around the alfalfa seeds could enhance their post-germination performances by improving symbiosis tolerance to drought stress. Our study focused on the agro-physiological and biochemical aspects associated with the tolerance of alfalfa to this environmental constraint. This could ensure adequate plant nutrition and contribute to forage yield improvement and stability in marginal soils.



## Material and methods

### *Plant material*

Two Moroccan alfalfa (*M. sativa* L.) populations, *Adis-Tata* (*Ad*), and *Demnate2* (*Dm2*) contrasting for their responses to drought stress, and an American *Moapa* variety (*Mo*) were used in the present study. The seeds were provided by the National Institute for Agronomical Research (INRA), Marrakech, Morocco. The two Moroccan populations *Ad* and *Dm2* are originated from the South-Western oasis (Tafilalet) and the High Atlas Mountain of Morocco, where they cultivated by local farmers for many centuries (Bouizgaren et al., 2013; Mouradi et al., 2018). Continuous natural and human selection has led, by this time, to their adaptation to the local habitats with distinction in the agro-morphological characteristics of the landraces, which have reached Hardy-Weinberg equilibrium (Farissi et al., 2013). The *Mo* variety was used as a reference variety recommended for arid and semi-arid areas.

### *Seed biopriming and culture*

Alfalfa seeds of uniform size were surface-disinfected by ethanol 95% for 30 s and 5% sodium hypochlorite for 5 min then rinsed several times with sterilized deionized water. Rhizobacteria suspensions were prepared with yeast extract mannitol (YEM) in Petri dishes for 48 h at 28°C. The resulting colonies in each dish were suspended in 20 mL of 1% methyl cellulose (Sigma-Aldrich, Milwaukee, WI, USA) in sterile deionized water and scraped gently with a spatula to obtain bacterial slurries (Moeinzadeh et al., 2010). Half of the seeds of the three alfalfa genotypes were soaked for 20 min in the slurries, spread on paper towel to absorb the excess slurry, and air-dried overnight under a fume hood. This lot is considered as the bioprimed seeds. However, the other half of the seeds is considered as the unprimed seeds, it was rinsed several times with the same solution of 1% of methylcellulose without rhizobacteria and air-dried under a fume hood.

Seeds were firstly germinated for 48 h in Petri dishes contained two layers of filter paper soaked with sterile deionized water. Young seedlings were then transferred in 06 cm and 11 cm height pots filled with 380 g of sterile substrate (sand and peat with the proportion 4:1, respectively). One week after, the number of seedlings was adjusted to six per pot and the seedlings were inoculated separately with suspensions ( $10^8$  to  $10^9$  CFU mL<sup>-1</sup>) of indigenous rhizobial strain *RcRh09* isolated from *Rich* region (Latrach et al., 2017) and *Ensifer meliloti Rm1021* as the reference strain. The inoculated plants were grown under greenhouse conditions at the Faculty of Sciences and Techniques - Marrakesh with an approximate temperature of 30/20°C (day/night), 50–80% of relative humidity, 16 h photoperiod (twenty-two Klux) and 900 to 1200 PAR  $\mu\text{mol m}^{-2} \text{s}^{-1}$ . One week after inoculation, half of the plants (randomly selected) of each symbiotic combination were subjected to water deficit conditions (40% of substrate field capacity), while the other half were kept under optimal irrigation conditions (80% of field capacity). To adjust the substrate field capacity, the pots were weighed at 8:00 am before every irrigation and the amount needed were added. Pots without plants were considered as evaporation controls. During the trial period, the plants were watered alternately two times a week with sterile distilled water and nitrogen free nutrient Hoagland solution. After five weeks of water deficit, the plants were harvested and some agro-physiological and biochemical parameters related to

water deficit tolerance were assessed. Three pots containing six plants each were used per symbiotic combination, per treatment and each pot was considered as replicate.

### ***Dry biomass***

Dry weights were assessed at the end of experiment by separating the plants parts, shoots, roots and nodules. Then, they oven-dried at 75°C for 48 h and weighed for the determination of shoot dry weight (SDW), root dry weight (RDW) and nodule dry weight (NDW). Nodules number and total biomass (TDW) were also determined. Six plants for each genotype and treatment were randomly selected and grouped as three replicates.

### ***Plant height and leaf area***

The plant height (PH) was measured at the end of the stress period for plants stemmed from bioprimed and unprimed seeds of each symbiotic combination subjected to the drought stress in comparison to their respective controls. The leaf area (LA) was determined by image analysis using Image J Software available from the National Institutes of Health (<http://rsb.info.nih.gov/ij/index.html>). Six plants per treatment were used and grouped as three replicates.

### ***Relative water content (RWC)***

RWC was determined in plant leaves by according to Ghoulam et al. (2002). Firstly, the fresh weights (FW) were determined and the leaflets were kept in distilled water for 4 h to determine their turgid weight (TW). Then, their dry weights (DW) were determined by drying them in a hot air for 48 h. The RWC was calculated according to Equation 1:

$$RWC(\%) = (FW - DW) / (TW - DW) \times 100 \quad (\text{Eq.1})$$

Three replicates per treatment per symbiotic combination were considered for this parameter.

### ***Stomatal conductance ( $g_s$ )***

The leaf stomatal conductance ( $g_s$ ) was determined by using a leaf porometer (Leaf porometer; model SC1, Decagon Devices, version 2012). This device was calibrated before measurement at 10:30 am. Six plants per treatment per symbiotic combination were considered and grouped as three replicates.

### ***The maximum quantum efficiency of Photosystem II ( $F_v/F_m$ )***

The maximum quantum efficiency of Photosystem II ( $F_v/F_m$ ) was determined using a portable fluorescence meter (Chlorophyll Fluorometer OS-30p, Opti-Sciences, Hudson, New Hampshire, USA) after 10–15 min of dark adaptation. It is based on determining the  $F_v/F_m$  ratio according to Equation 2:

$$F_v/F_m = (F_m - F_0) / F_m \quad (\text{Eq.2})$$

Where  $F_m$  is maximal fluorescence and  $F_0$  is minimal fluorescence of dark-adapted leaves respectively, and  $F_v$  is the variable fluorescence. Six plants per treatment per symbiotic combination were considered and grouped as three replicates.

### **Total chlorophyll (Chl) content**

Chlorophyll (Chl a+b) was extracted with acetone in a mortar, using a proportion of 0.5 g of fresh leaf tissue and 5 mL of acetone (80%, v/v). Chlorophyll concentration was measured by the method described by Arnon (1949). The homogenate was centrifuged for 10 min at  $5000 \times g$ , the absorbance (OD) of the supernatant was measured at 663 and 645 nm. Chl (a+b) were determined according to *Equation 3*:

$$Chl(a + b) = (8.02 \times OD_{663}) + (20.20 \times OD_{645}) \quad (\text{Eq.3})$$

### **Potassium and phosphorus contents**

Total P and  $K^+$  contents were determined as described by Ghoulam et al. (2002). A sample of 0.5 g dry mass of alfalfa shoots was ashed at  $600^\circ\text{C}$  for 4 h. The ash was then dissolved in 10N hydrochloric acid. The resulting suspensions were then filtered using filter papers and diluted with deionized water. The plant P content was determined using Olsen method (Olsen, 1954) and the content of  $K^+$  was determined using flame spectrophotometer (model AFP100, Biotech Engineering Management Co. Ltd., UK). Six plants per treatments per symbiotic association were grouped as three replicates.

### **Electrolyte leakage (EL)**

The electrolyte leakage was determined by method described by Ghoulam et al. (2002). Leaf discs (50 mg) were rinsed several times with distilled water and placed in flasks containing 10 mL of double-distilled water. Then, the initial electrical conductivity ( $EC_1$ ) of the solution was determined using a conductivity meter (HI8820N, Hanna Instruments, Woonsocket, Rhode Island, USA) after incubation for 24 h at  $25^\circ\text{C}$  in a rotary shaker (100 rpm). A second electrical conductivity ( $EC_2$ ) of the samples was determined after autoclaving at  $121^\circ\text{C}$  for 20 min, followed by stirring for 30 min at  $25^\circ\text{C}$ . The electrolyte leakage (EL) was expressed by the ratio of  $C_1$  and  $C_2$  using the *Equation 4*:

$$EL(\%) = (EC_1/EC_2) \times 100 \quad (\text{Eq.4})$$

Six seedlings per treatment per genotypes were considered.

### **Malonyldialdehyde (MDA) content**

The level of lipid peroxidation in the leaves was determined by estimating malondialdehyde (MDA) contents according to the method described by Heath and Packer (1968). Leaves samples (100 mg) were ground in 0.5 mL of 10% (w/v) trichloroacetic acid (TCA). The homogenate was then added with 0.5 mL of acetone and then centrifuged for 15 min at  $8000 \times g$ . To 500  $\mu\text{L}$  of the MDA extract, 1 mL of phosphoric acid ( $\text{H}_3\text{PO}_4$ , 0.1%) and 1 mL of thiobarbituric acid (TBA, 0.6%) were added. Afterwards, Samples were stirred and then heated at  $95^\circ\text{C}$  for 30 min. Then, the reaction was stopped by an ice bath and then added 1.5 mL of 1-butanol followed by

centrifugation at  $8000 \times g$  for 15 min. The butanol layer obtained was recovered to read its absorbance at 532 nm. The MDA contents were expressed as  $\mu\text{mol g}^{-1}$  FM by referring to the molecular extinction coefficient of the complex MDA-TBA:  $155 \text{ mM}^{-1} \text{ cm}^{-1}$ .

### Statistical analysis

Significant changes ( $P < 0.05$ ) were determined by the three-way analysis of variance (ANOVA III) and Tukey's test was applied for the comparison of the considered means. All the statistical analysis was performed by SPSS (21.0) software (SPSS, Chicago, Illinois, USA, 2012) using three replicates per combination per treatment for the considered parameters. The means values and standard errors were also calculated.

## Results

### Growth parameters

Water deficit significantly ( $p < 0.001$ ) decreased the total plant biomass in all of the tested symbiotic combinations compared to their corresponding controls (80% FC). There was a significant ( $p < 0.05$ ) variation between the studied symbiotic combinations for almost all of the considered growth parameters. In addition, the plants from the treated seeds presented the lowest reductions compared to those from untreated seeds. In contrast, the biopriming improved total dry weight (TDW) of drought sensitive plants. The shoot dry weight (SDW) was significantly ( $p < 0.001$ ) reduced by water deficit (40% FC) in all of the studied symbiotic combinations as compared to control plants (Table 1). However, decrease in SDW was relatively lower in primed plants than the unprimed ones. The plants of *AD-RcRh09* symbiotic combination from the bioprimed seeds showed lower decrease of SDW under drought stress by 10.18% than those of *Mo-Rm1021* presenting a decrease of 50.16%. Under drought stress, the roots dry weight (RDW) was significantly ( $p < 0.001$ ) decreased in all of the studied combinations. Besides, this reduction was less pronounced in *Ad-RcRh09* and *Ad-Rm1021* obtained from the bioprimed seeds with 11.70, 13.40% respectively, in comparison with the unprimed ones. For the nodules dry weight (NDW), water deficit significantly ( $p < 0.001$ ) reduced this parameter in all combinations. However, the seed biopriming significantly ( $p < 0.01$ ) improved the nodulation under water deficit particularly for the combination *Ad-RcRh09* presenting a reduction not exceeding 10.50% for the plants obtained from bioprimed seeds versus 20.49% for those from the unprimed ones.

For the plant height (PH), water deficit caused lowest reductions in *Ad-RcRh09*, *Ad-Rm1021* and *Dm2-Rm1021* of primed seeds with the respective values of 25.42, 33.98 and 35.35% (Table 2). Under water deficit condition (40% FC), the nodules number was lower in all of the symbiotic combinations comparatively to their corresponding controls. In addition, the biopriming improved this parameter in symbiotic combinations involving *Ad* population. Furthermore, *Ad-RcRh09* combination of primed seeds showed the lowest reduction values of 6.35% versus 33.62% for plants from unprimed seeds and *Dm2-Rm1021* presented the highest reduction values of 56.83% for unprimed seeds versus 45.73% for the primed seeds (Table 2).

**Table 1.** Effect of seeds biopriming on: Total Dry Weight (TDW), shoot dry weight (SDW), root dry weight (RDW) and nodules dry weight (NDW) in the six alfalfa-rhizobia symbioses involving (*Adis-Tata*, *Demnate2* and *Moapa* and *RcRh09* and *Rm1021* strains) grown under drought stress. Values are means of three replicates  $\pm$  standard errors

Symbiotic associations		TDW (g/6plant)			SDW (g/6plant)			RDW (g/6plant)			NDW (mg/6plant)		
		Water deficit		Reduction %	Water deficit		Reduction %	Water deficit		Reduction %	Water deficit		Reduction %
		80%FC	40%FC		80%FC	40%FC		80%FC	40%FC		80%FC	40%FC	
Ad-RcRh09	Unp	2.04 $\pm$ 0.02 <sup>c-e</sup>	1.71 $\pm$ 0.03 <sup>fg</sup>	16.31	0.84 $\pm$ 0.03 <sup>cd</sup>	0.74 $\pm$ 0.01 <sup>k</sup>	12.65	0.93 $\pm$ 0.03 <sup>gh</sup>	0.70 $\pm$ 0.01 <sup>lmn</sup>	25.09	23.05 $\pm$ 0.03 <sup>i</sup>	18.33 $\pm$ 0.02 <sup>j</sup>	20.49
	Biop	2.30 $\pm$ 0.03 <sup>b</sup>	2.03 $\pm$ 0.06 <sup>c-e</sup>	11.74	0.92 $\pm$ 0.03 <sup>bc</sup>	0.82 $\pm$ 0.01 <sup>ij</sup>	10.18	1.20 $\pm$ 0.02 <sup>b</sup>	1.06 $\pm$ 0.01 <sup>ijk</sup>	11.70	26.15 $\pm$ 0.03 <sup>h</sup>	23.40 $\pm$ 0.86 <sup>kl</sup>	10.50
Ad-Rm1021	Unp	1.82 $\pm$ 0.02 <sup>f</sup>	1.43 $\pm$ 0.04 <sup>hi</sup>	21.28	1.04 $\pm$ 0.02 <sup>efgh</sup>	0.76 $\pm$ 0.03 <sup>ghi</sup>	27.48	1.05 $\pm$ 0.02 <sup>ij</sup>	0.79 $\pm$ 0.05 <sup>mn</sup>	25.08	21.43 $\pm$ 0.01 <sup>g</sup>	17.02 $\pm$ 0.01 <sup>i</sup>	20.58
	Biop	1.93 $\pm$ 0.04 <sup>e</sup>	1.67 $\pm$ 0.02 <sup>fg</sup>	13.49	1.09 $\pm$ 0.02 <sup>efg</sup>	0.88 $\pm$ 0.01 <sup>f-i</sup>	19.51	1.24 $\pm$ 0.01 <sup>efg</sup>	1.08 $\pm$ 0.01 <sup>k-m</sup>	13.40	28.40 $\pm$ 0.03 <sup>j</sup>	23.33 $\pm$ 0.02 <sup>m</sup>	17.83
Dm2-RcRh09	Unp	2.04 $\pm$ 0.03 <sup>c-e</sup>	1.30 $\pm$ 0.02 <sup>i</sup>	36.38	0.97 $\pm$ 0.01 <sup>ef</sup>	0.68 $\pm$ 0.02 <sup>k</sup>	30.48	1.23 $\pm$ 0.01 <sup>efg</sup>	0.80 $\pm$ 0.01 <sup>n</sup>	34.51	14.13 $\pm$ 0.03 <sup>n</sup>	8.06 $\pm$ 0.03 <sup>p</sup>	42.94
	Biop	2.55 $\pm$ 0.03 <sup>a</sup>	1.92 $\pm$ 0.02 <sup>e</sup>	24.84	1.12 $\pm$ 0.02 <sup>a</sup>	0.85 $\pm$ 0.09 <sup>f-i</sup>	24.18	1.27 $\pm$ 0.01 <sup>bcd</sup>	0.90 $\pm$ 0.03 <sup>fgh</sup>	28.95	30.09 $\pm$ 0.05 <sup>f</sup>	23.68 $\pm$ 0.26 <sup>o</sup>	21.29
Dm2-Rm1021	Unp	2.23 $\pm$ 0.05 <sup>cd</sup>	1.30 $\pm$ 0.03 <sup>i</sup>	41.77	0.87 $\pm$ 0.02 <sup>de</sup>	0.63 $\pm$ 0.04 <sup>hi</sup>	27.69	1.11 $\pm$ 0.02 <sup>bc</sup>	0.72 $\pm$ 0.04 <sup>jk</sup>	34.83	38.48 $\pm$ 0.24 <sup>b</sup>	21.35 $\pm$ 0.03 <sup>j</sup>	44.51
	Biop	2.29 $\pm$ 0.03 <sup>b</sup>	1.55 $\pm$ 0.02 <sup>gh</sup>	32.07	1.19 $\pm$ 0.01 <sup>bc</sup>	0.87 $\pm$ 0.03 <sup>fgh</sup>	26.82	1.07 $\pm$ 0.01 <sup>b</sup>	0.82 $\pm$ 0.01 <sup>kl</sup>	23.60	44.35 $\pm$ 0.17 <sup>a</sup>	33.34 $\pm$ 0.02 <sup>d</sup>	24.83
Mo-RcRh09	Unp	2.30 $\pm$ 0.02 <sup>b</sup>	0.95 $\pm$ 0.03 <sup>i</sup>	58.64	0.92 $\pm$ 0.02 <sup>efg</sup>	0.59 $\pm$ 0.02 <sup>jk</sup>	35.51	1.15 $\pm$ 0.01 <sup>def</sup>	0.80 $\pm$ 0.03 <sup>n</sup>	30.35	17.35 $\pm$ 0.01 <sup>m</sup>	8.00 $\pm$ 0.05 <sup>p</sup>	53.87
	Biop	2.53 $\pm$ 0.03 <sup>a</sup>	1.43 $\pm$ 0.03 <sup>de</sup>	43.68	1.43 $\pm$ 0.01 <sup>b</sup>	0.99 $\pm$ 0.01 <sup>efg</sup>	30.54	1.21 $\pm$ 0.01 <sup>a</sup>	0.82 $\pm$ 0.02 <sup>c-e</sup>	32.14	28.62 $\pm$ 0.02 <sup>g</sup>	18.85 $\pm$ 0.03 <sup>k</sup>	34.14
Mo-Rm1021	Unp	2.05 $\pm$ 0.03 <sup>c-e</sup>	0.84 $\pm$ 0.03 <sup>de</sup>	58.93	1.06 $\pm$ 0.03 <sup>cd</sup>	0.53 $\pm$ 0.03 <sup>f-i</sup>	50.16	1.12 $\pm$ 0.01 <sup>c-e</sup>	0.64 $\pm$ 0.01 <sup>hi</sup>	42.56	30.85 $\pm$ 0.03 <sup>e</sup>	17.08 $\pm$ 0.04 <sup>m</sup>	44.62
	Biop	2.16 $\pm$ 0.03 <sup>bc</sup>	1.23 $\pm$ 0.04 <sup>c-e</sup>	42.90	1.14 $\pm$ 0.05 <sup>bc</sup>	0.73 $\pm$ 0.01 <sup>efg</sup>	36.44	1.67 $\pm$ 0.01 <sup>bc</sup>	1.16 $\pm$ 0.01 <sup>gh</sup>	30.74	34.50 $\pm$ 0.29 <sup>c</sup>	25.91 $\pm$ 0.02 <sup>m</sup>	24.91
Symbiosis Biopriming Water deficit Interactions	df				df			df			df		
	5		F		5			5			5		
	1	2.23 <sup>NS</sup>			1	0.584 <sup>NS</sup>		1	2.538 <sup>*</sup>		1	9.430 <sup>***</sup>	
	1	15.650 <sup>***</sup>			1	14.831 <sup>***</sup>		1	12.935 <sup>**</sup>		1	11.867 <sup>**</sup>	
1	59.498 <sup>***</sup>			1	75.659 <sup>***</sup>		1	64.351 <sup>***</sup>		1	33.505 <sup>***</sup>		
23	136.916 <sup>***</sup>			23	92.983 <sup>***</sup>		23	196.957 <sup>***</sup>		23	9621.469 <sup>***</sup>		

\*: Significance at 0.05 probability level; \*\*: significance at 0.01 probability level; \*\*\*: significance at 0.001 probability level; NS: not significant at 0.05. Unp: unprimed seeds; Biop: biopriming seeds; FC: field capacity

**Table 2.** Effect of seeds biopriming on: Plant height (PH), Nodules number (NN) and Leaf area (LA) in the six alfalfa-rhizobia symbioses involving (*Adis-Tata*, *Demnate2* and *Moapa* and *RcRh09* and *Rm1021*) grown under water deficit. Values are means of three replicates  $\pm$  standard errors

Symbiotic associations		PH (cm)			NN (/6plants)			LA (cm <sup>2</sup> )		
		Water deficit		Reduction%	Water deficit		Reduction %	Water deficit		Reduction %
		80% FC	40% FC		80% FC	40% FC		80% FC	40% FC	
Ad-RcRh09	Unp	13.17 $\pm$ 0.16 <sup>c-j</sup>	9.67 $\pm$ 0.33 <sup>g-k</sup>	26.58	57.67 $\pm$ 1.19 <sup>fg</sup>	48.00 $\pm$ 1.51 <sup>hi</sup>	16.76	0.84 $\pm$ 0.02 <sup>fgh</sup>	0.73 $\pm$ 0.03 <sup>ghi</sup>	13.44
	Biop	19.67 $\pm$ 1.15 <sup>e-d</sup>	14.67 $\pm$ 0.59 <sup>d-i</sup>	25.42	105.67 $\pm$ 2.30 <sup>b</sup>	87.33 $\pm$ 1.51 <sup>fg</sup>	17.35	0.92 $\pm$ 0.02 <sup>efg</sup>	0.82 $\pm$ 0.01 <sup>f-i</sup>	10.18
Ad- Rm1021	Unp	16.50 $\pm$ 1.31 <sup>b-j</sup>	10.67 $\pm$ 0.44 <sup>h-k</sup>	35.35	76.33 $\pm$ 1.83 <sup>d</sup>	50.67 $\pm$ 1.19 <sup>ghi</sup>	33.62	1.04 $\pm$ 0.03 <sup>cd</sup>	0.84 $\pm$ 0.02 <sup>f-i</sup>	19.49
	Biop	17.17 $\pm$ 0.75 <sup>b-f</sup>	11.33 $\pm$ 0.59 <sup>h-k</sup>	33.98	99.67 $\pm$ 2.00 <sup>bc</sup>	93.33 $\pm$ 1.74 <sup>c</sup>	6.35	1.09 $\pm$ 0.05 <sup>bc</sup>	0.88 $\pm$ 0.01 <sup>efg</sup>	19.51
Dm2-RcRh09	Unp	18.33 $\pm$ 0.44 <sup>a-d</sup>	9.17 $\pm$ 0.59 <sup>jk</sup>	50.00	91.00 $\pm$ 2.06 <sup>c</sup>	50.67 $\pm$ 1.74 <sup>ghi</sup>	44.32	0.87 $\pm$ 0.02 <sup>efg</sup>	0.63 $\pm$ 0.02 <sup>jk</sup>	27.69
	Biop	19.00 $\pm$ 0.29 <sup>a-d</sup>	11.17 $\pm$ 0.44 <sup>a-d</sup>	41.23	123.33 $\pm$ 1.65 <sup>a</sup>	91.33 $\pm$ 1.43 <sup>c</sup>	25.95	1.19 $\pm$ 0.01 <sup>b</sup>	0.87 $\pm$ 0.02 <sup>efg</sup>	26.82
Dm2-Rm1021	Unp	15.67 $\pm$ 1.32 <sup>c-h</sup>	7.75 $\pm$ 1.67 <sup>k</sup>	50.53	69.67 $\pm$ 1.43 <sup>de</sup>	34.00 $\pm$ 1.14 <sup>jk</sup>	51.20	0.97 $\pm$ 0.02 <sup>de</sup>	0.74 $\pm$ 0.02 <sup>hi</sup>	23.63
	Biop	16.50 $\pm$ 0.16 <sup>b-g</sup>	10.67 $\pm$ 0.72 <sup>h-k</sup>	35.35	75.67 $\pm$ 2.57 <sup>d</sup>	64.00 $\pm$ 0.99 <sup>ef</sup>	15.42	1.12 $\pm$ 0.01 <sup>bc</sup>	0.85 $\pm$ 0.03 <sup>fgh</sup>	24.18
Mo-RcRh09	Unp	21.33 $\pm$ 1.00 <sup>ab</sup>	10.00 $\pm$ 1.71 <sup>f-k</sup>	53.13	75.67 $\pm$ 1.43 <sup>d</sup>	32.67 $\pm$ 1.43 <sup>k</sup>	56.83	0.92 $\pm$ 0.01 <sup>ef</sup>	0.59 $\pm$ 0.01 <sup>k</sup>	35.51
	Biop	22.33 $\pm$ 1.90 <sup>a</sup>	12.83 $\pm$ 1.15 <sup>ijk</sup>	42.54	78.00 $\pm$ 1.14 <sup>d</sup>	42.33 $\pm$ 1.43 <sup>ij</sup>	45.73	1.43 $\pm$ 0.02 <sup>a</sup>	0.99 $\pm$ 0.01 <sup>f-i</sup>	30.54
Mo- Rm1021	Unp	18.17 $\pm$ 0.72 <sup>a-e</sup>	8.33 $\pm$ 0.87 <sup>h-k</sup>	54.13	62.00 $\pm$ 1.14 <sup>ef</sup>	29.67 $\pm$ 0.87 <sup>k</sup>	52.15	1.06 $\pm$ 0.03 <sup>cd</sup>	0.53 $\pm$ 0.01 <sup>k</sup>	50.16
	Biop	19.83 $\pm$ 2.32 <sup>abc</sup>	11.17 $\pm$ 0.44 <sup>h-k</sup>	43.70	106.33 $\pm$ 2.00 <sup>b</sup>	53.00 $\pm$ 1.71 <sup>gh</sup>	50.16	1.14 $\pm$ 0.03 <sup>bc</sup>	0.73 $\pm$ 0.01 <sup>ij</sup>	36.44
Symbiosis Biopriming Water deficit Interactions		df	F		df	F		df	F	
		5	0.999 <sup>NS</sup>		5	3.403 <sup>**</sup>		5	0.584 <sup>NS</sup>	
		1	4.245 <sup>*</sup>		1	25.791 <sup>***</sup>		1	14.831 <sup>***</sup>	
		1	148.968 <sup>***</sup>		1	44.170 <sup>***</sup>		1	75.659 <sup>***</sup>	
	23	21.374 <sup>***</sup>		23	240.168 <sup>***</sup>		23	92.938 <sup>***</sup>		

\*: Significance at 0.05 probability level; \*\*: significance at 0.01 probability level; \*\*\*: significance at 0.001 probability level; NS: not significant at 0.05. Unp: Unprimed seeds; Biop: Bioprimed seeds; FC: field capacity

For the LA, the water deficit significantly ( $p < 0.001$ ) reduced this parameter in all studied symbiotic combinations. However, the plants from bioprimed seeds showed the lowest LA reductions under this constraint as compared to the unprimed ones. In this regard, under water deficit, the lowest reduction values were presented by *Ad-RcRh09* for primed seeds with 10.18%, and the highest reduction was recorded in *Mo-Rm1021* from unprimed seeds by 50.16% (Table 2).

### Relative water content

Water deficit substantially reduced the relative water content in leaves of alfalfa but the seed biopriming significantly improved this parameter under this constraint for all of the tested symbiotic combinations. Indeed, *Mo-Rm1021* and *Mo-RcRh09* from bioprimed seeds presented the lowest RWC with 46.49 and 47.44% respectively under water deficit among all of the tested genotypes. For the well-watered control plants (80% FC), the biopriming treatment had no significant effect on RWC in all of the tested symbiotic combinations. The most pronounced positive effects of biopriming on RWC were noted in *Ad-Rm1021* and *Ad-RcRh09* stressed plants with an increase of 66.57 and 65.01% respectively as compared with plants from unprimed seeds (Fig. 1).

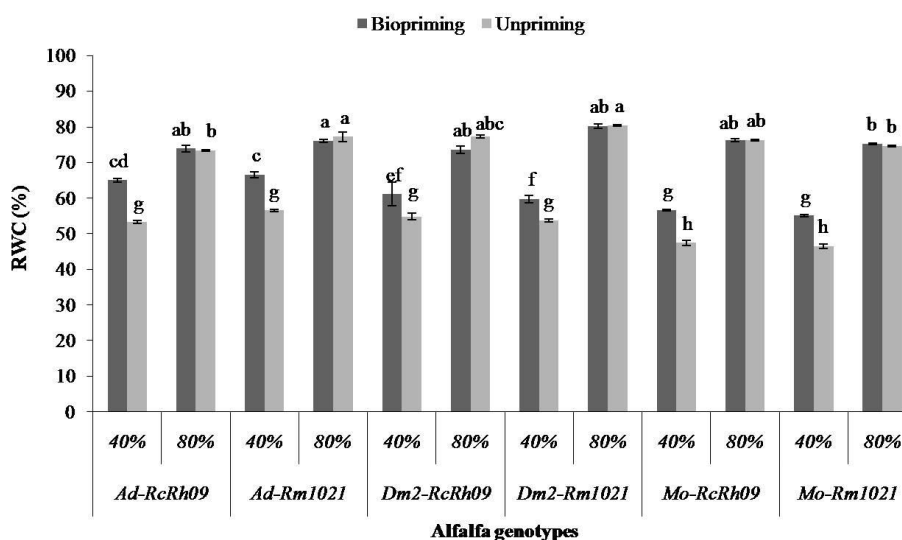


**Figure 1.** Effect of seeds biopriming on plants relative water content (RWC) in six symbiotic combinations involving (*Ad*, *Dm2*, *Mo* and *RcRh09* and *Rm1021*) under water deficit (40% FC). Values are means of three replicates  $\pm$  standard errors

### Stomatal conductance ( $g_s$ )

Water deficit significantly ( $p < 0.001$ ) decreased the  $g_s$  in all of the studied symbiotic combinations (Table 3). The decreases were more pronounced in symbioses involving *Dm2* and *Mo* populations, showing reductions exceeding 24.05% for plants grown from primed seeds in both watering conditions. The biopriming had a significant effect ( $p < 0.001$ ) on  $g_s$  and caused decrease of this parameter in plants grown under water deficit condition. Under these latter conditions, the lowest values of  $g_s$  were observed in all symbiotic combinations from primed seeds and involving *RcRh09* strain (Fig. 2). Indeed, the combination *Ad-RcRh09* from primed seeds showed the lowest  $g_s$  of

54.53 mmol H<sub>2</sub>O m<sup>-2</sup> s<sup>-1</sup>. Moreover, under this water constraint, the  $g_s$  varied from 54.53 to 98.25 mmol H<sub>2</sub>O m<sup>-2</sup> s<sup>-1</sup> registered respectively for primed treatment of *Ad-RcRh09* and *Dm2-Rm1021*.

**Table 3.** Results of three-way analysis of variance (ANOVA III) of biopriming, water deficit and symbiotic combination effects and their interactions for the considered parameters

Dependent variables	Independent variables							
	Symbiosis		Biopriming		Water deficit		Interactions	
	df	F	df	F	df	F	df	F
RWC	5	0.692 <sup>NS</sup>	1	4.245*	1	235.681***	23	105.627***
$g_s$	5	1.503 <sup>NS</sup>	1	7.936**	1	130.077***	23	30.182***
$F_v/F_m$	5	2.863*	1	7.285**	1	40.593***	23	35.843***
Total Chl content	5	1.135 <sup>NS</sup>	1	4.182*	1	285.361***	23	50,857***
P content	5	8.374***	1	18.564***	1	8.171**	23	33.233***
K <sup>+</sup>	5	1.726 <sup>NS</sup>	1	11.985**	1	108.961***	23	84.019***
EL	5	2.921*	1	23.634***	1	21.937***	23	19.678***
MDA content	5	0.460 <sup>NS</sup>	1	49.647***	1	6.140*	23	4.743***

\*: Significance at 0.05 probability level; \*\*: significance at 0.01 probability level; \*\*\*: significance at 0.001 probability level; NS: not significant at 0.05

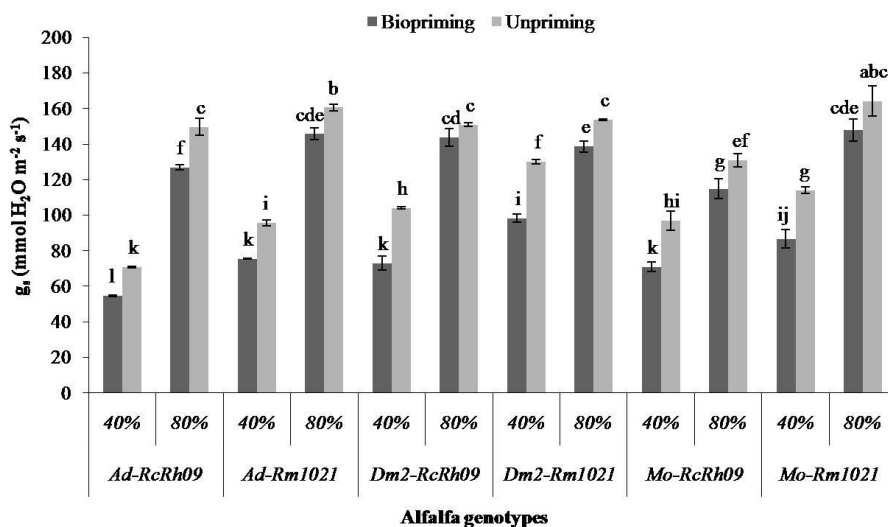


**Figure 2.** Effect of seeds biopriming on stomatal conductance ( $g_s$ ) in the six symbiotic combinations involving (*Ad*, *Dm2*, *Mo* and *RcRh09* and *Rm1021*) under water deficit (40% FC). Values are means of three replicates  $\pm$  standard errors

### Maximum quantum yield of photosystem II (PS II) ( $F_v/F_m$ )

The results showed that under water deficit, the  $F_v/F_m$  ratio was significantly ( $p < 0.001$ ) decreased in the majority of the studied symbiotic associations. This decrease was more obvious in symbiotic combinations from unprimed seeds (Table 3). Indeed, the decrease was more pronounced in combinations involving *Mo* variety under water-stressed conditions. In addition, water deficit increased  $F_v/F_m$  ratios for all plants from bioprimed seeds as compared to the ones from unprimed seeds (Fig. 3, Table 3).



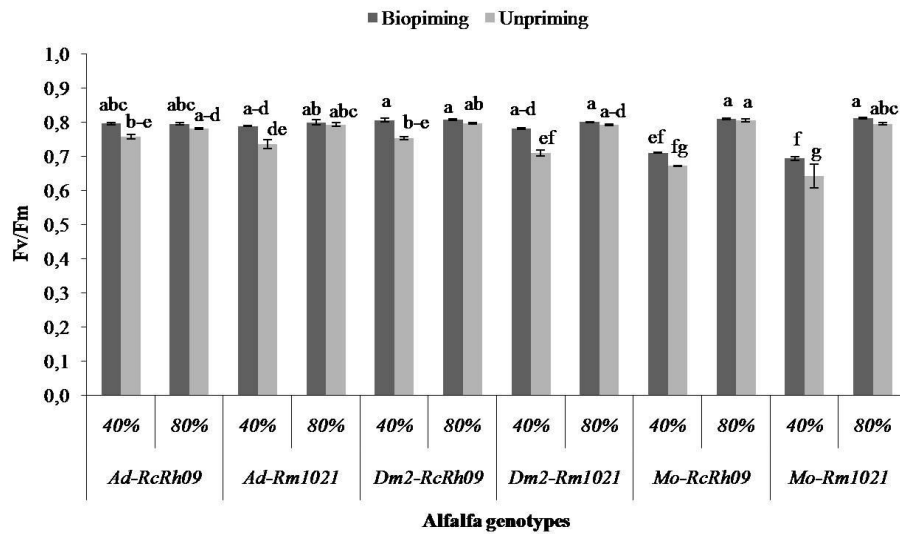


**Figure 3.** Effect of seeds biopriming on chlorophyll fluorescence ratio ( $F_v/F_m$ ) in the six symbiotic combinations involving (*Ad*, *Dm2*, *Mo* and *RcRh09* and *Rm1021*) under water deficit (40% FC). Values are means of three replicates  $\pm$  standard errors

#### Total chlorophyll content (*T. Chl* content)

The results showed that the total chlorophyll content in all of studied symbiotic combinations was significantly ( $p < 0.001$ , Table 3) reduced under water deficit condition. However, the biopriming treatment improved this parameter in all of the studied associations (Fig. 4). In fact, under water deficit, the highest value of chlorophyll content was noted in *Ad-RcRh09* from the bioprimered seeds with  $9.68 \text{ mg g}^{-1} \text{ FM}$  versus  $5.09 \text{ mg g}^{-1} \text{ FM}$  as the lowest content recorded in *Mo-RcRh09* combination from the unprimed seeds (Fig. 4).

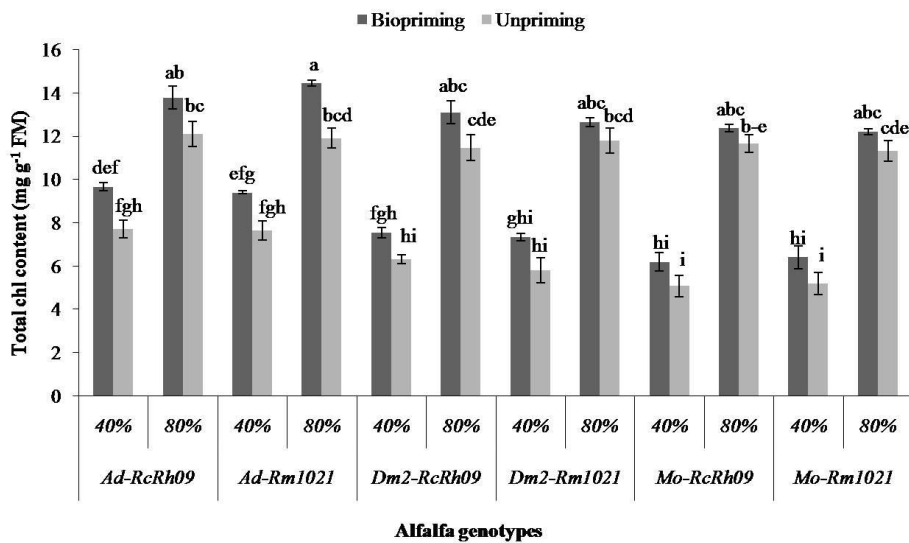


**Figure 4.** Effect of seeds biopriming on Total chlorophyll content in the six symbiotic combinations involving (*Ad*, *Dm2*, *Mo* and *RcRh09* and *Rm1021*) under water deficit (40% FC). Values are means of three replicates  $\pm$  standard errors

### P and K<sup>+</sup> contents

Water deficit decreased plant P content in the majority of considered associations except *Ad-RcRh09* and *Dm2-Rm1021*. For plants from bioprimed seeds, the P content has been significantly ( $p < 0.001$ ) improved in the leaves of almost all of the studied symbiotic associations. The increases of P contents varied from 5.18% to 29.19% under water deficit (40% FC) in bioprimed seeds of *Dm2-RcRh09* and *Mo-RcRh09* respectively. The highest value of this parameter was observed in *Ad-RcRh09* for bioprimed seeds under water constraint with the content of 9.27 mg g<sup>-1</sup> DM (Fig. 5).

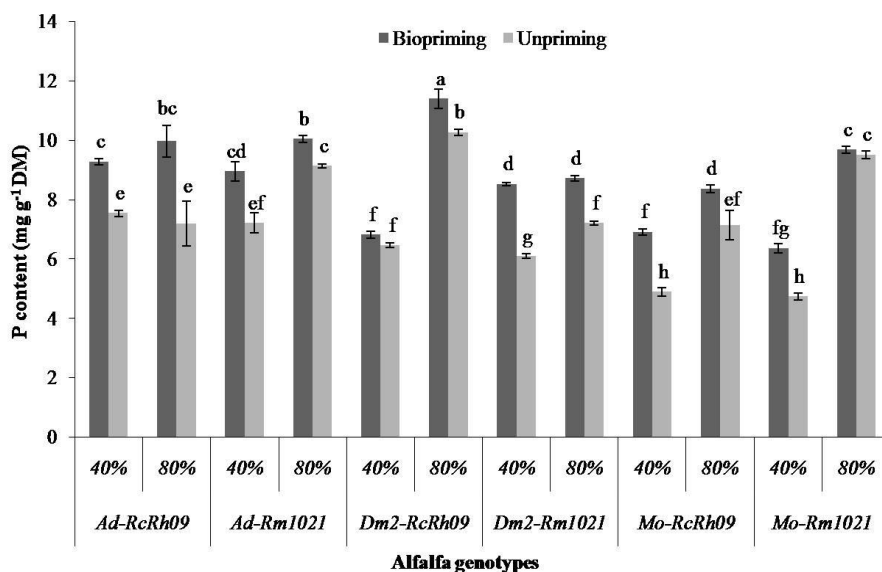


**Figure 5.** Effect of seeds biopriming on plant P content in the six symbiotic combinations involving (*Ad*, *Dm2*, *Mo* and *RcRh09* and *Rm1021*) under water deficit (40% FC). Values are means of three replicates  $\pm$  standard errors

For K<sup>+</sup> content, our results indicated that seed biopriming improved K<sup>+</sup> accumulation in alfalfa leaves. However, its content was significantly increased in plants from primed seeds and under both watering conditions. The most important values of K<sup>+</sup> contents were noticed in *Ad-RcRh09*, *Mo-Rm1021*, *Dm2-RcRh09* and *Dm2-Rm1021* plants from bioprimed seeds and under water stress with 36.67, 35.07, 34.27 and 33.13 mg g<sup>-1</sup> DM respectively (Fig. 6).

### Electrolyte leakage (EL) and Malonyldialdehyde (MDA) contents

The results showed that the EL increased significantly under water deficit ( $p < 0.001$ ) (Table 3). Biopriming treatment reduced significantly ( $p < 0.001$ ) this membrane disturbing effect compared to the plants from unprimed seeds under both water regimes. Higher EL has been noted under water deficit condition in all of the studied symbiotic combinations with significant variation between them (Table 3, Fig. 7). Water deficit induced the highest EL values in *Mo-RcRh09* and *Mo-Rm1021* plants from unprimed seeds with the percentages of 82.8 and 73.96%, respectively.

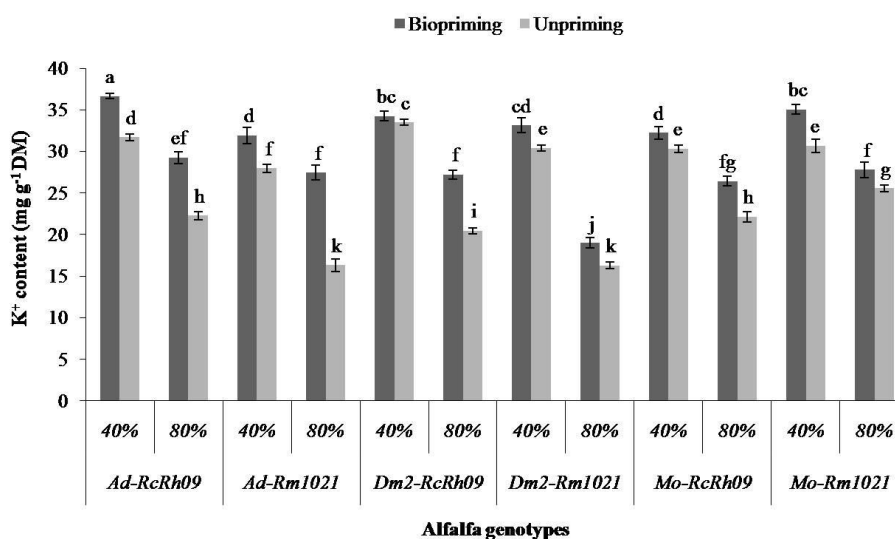


**Figure 6.** Effect of seeds biopriming on K<sup>+</sup> content in the six symbiotic combinations involving (Ad, Dm2, Mo and RcRh09 and Rm1021) under water deficit (40% FC). Values are means of three replicates ± standard errors

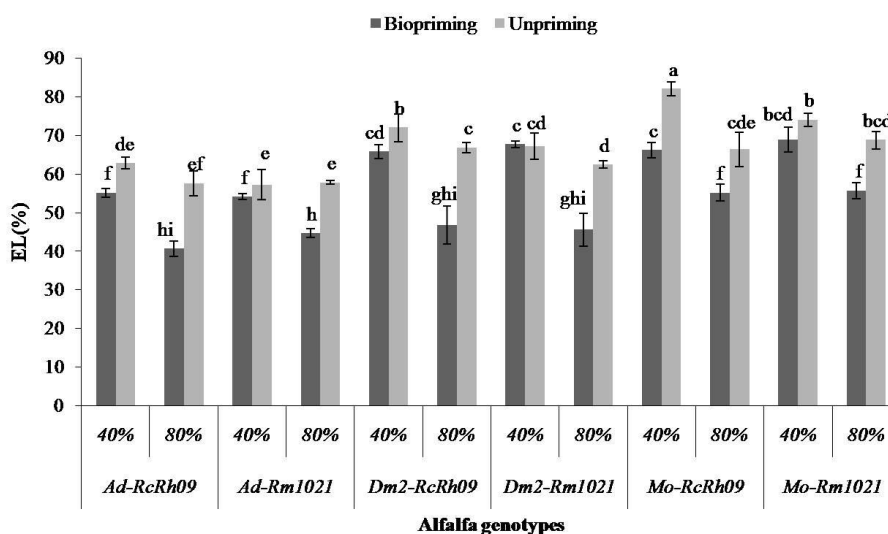


**Figure 7.** Effect of seeds biopriming on electrolytes leakage in the six symbiotic combinations involving (Ad, Dm2, Mo and RcRh09 and Rm1021) under water deficit (40% FC). Values are means of three replicates ± standard errors

Water deficit caused an increase of MDA contents in all of the tested combinations as compared to their corresponding controls (Fig. 8). Pretreatment of the alfalfa seeds with rhizobacteria increased the MDA content of the leaves in all symbiotic associations under drought stress (40% FC). Interestingly, we noticed that MDA content was lower in the plants from bioprimered seeds compared to those from unprimed seeds under both water regimes of 80% FC and 40% FC. The highest value of MDA was registered in *Mo-Rm1021* combination from unprimed seeds when submitted to water deficit and reached 0.65 μmol g<sup>-1</sup> FM.

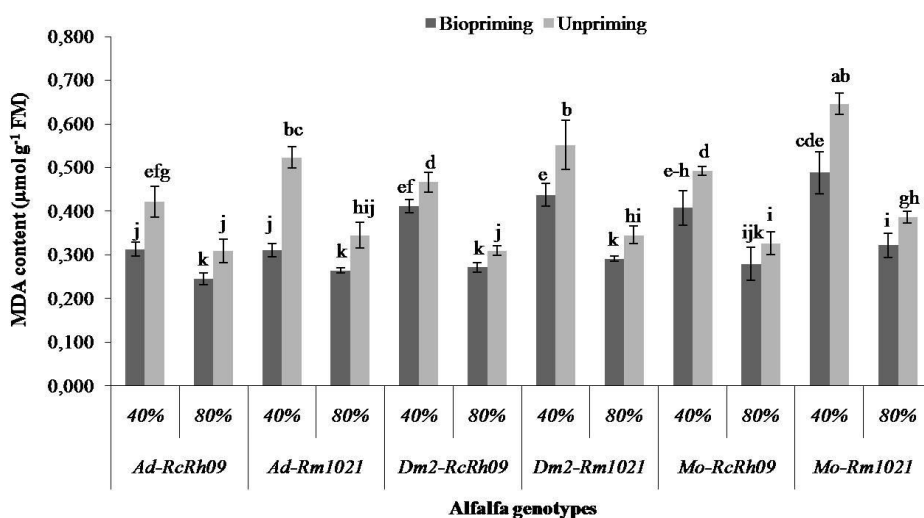


**Figure 8.** Effect of seeds biopriming on MDA content in the six symbiotic combinations involving (*Ad*, *Dm2*, *Mo* and *RcRh09* and *Rm1021*) under water deficit (40% FC). Values are means of three replicates  $\pm$  standard errors

## Discussion

Water deficit is the main limiting factor of plant productivity in the majority of agricultural regions in the world, particularly in the Mediterranean regions (Lipiec et al., 2013), it may reduce the plant growth, mineral uptake, legume nodulation and the water content in plants. The aim of this present study was to assess the effect of seed biopriming with indigenous rhizobacteria on the performance of N<sub>2</sub>-fixing alfalfa symbiosis under water deficit. Our results showed that water deficit (40% FC) significantly ( $p < 0.001$ ) reduced growth and nodulation in all of the studied symbiotic combinations. These results are similar to that of Farissi et al. (2013) and Mouradi et al. (2016) on some Moroccan populations of *M. sativa*, such as *Adis Tata* and *Demnate 2*. However, the seed biopriming with rhizobacteria strain significantly improved the tolerance to water deficit in most of the tested symbiotic combinations by improving plant growth, nodulation,  $g_s$ , RWC and membrane integrity. The achievements related to the positive effect of seed biopriming on total plant biomass and nodulation under drought stress agrees with those documented by Moeinzadeh et al. (2010) for sunflower, (Shukla et al., 2015) for wheat and (Singh et al., 2016) for pea. Thus, the increase of growth could be explained by the premobilization of the seed reserves and the activation of metabolic and physiological processes related to stress tolerance during the priming period (Farooq et al., 2006). Furthermore, the biopriming has greatly improved TDW in the water deficit sensitive plants. The highest nodules biomass was noted under drought stress in *Dm2-RcRh09*, *Ad-RcRh09*, *Dm2-Rm1021* and *Ad-Rm1021* from bioprimed seeds. Thus, this parameter could be regulated by hormones (Liu et al., 2018) or controlled by availability of assimilates (Voisin et al., 2010). Nodules growth maybe directly linked to the total plant growth (Mengel, 1994) and depend upon environmental factors in this case drought stress. The alfalfa plants obtained from primed seeds presented high RWC, compared to those obtained from unprimed seeds, for all of the studied combinations under water deficit. Besides, the combinations *Mo-RcRh09*,

*Dm2-RcRh09* and *Dm2-Rm1021* from primed seeds showed also the most significant increases of RWC under stress in comparison with those from unprimed seeds. Moreover, drought not only affects plant water relations through the reduction of RWC, but also stomatal conductance, limiting thus gas exchange, transpiration, and carbon assimilation (photosynthesis) rates. Therefore, the biopriming could correct these negative effects by limiting water loss in all of the studied combinations under water deficit. The results showed that the exposure to water deficit caused a decrease of the activity of the PS II, evaluated by the ratio  $F_v/F_m$  in sensitive genotypes (*Mo* and *Dm2*) but the biopriming treatment alleviated this negative impact. This parameter is generally known as the maximum quantum yield of primary photochemistry or the maximum electron transport rate of PS II (Waldhoff et al., 2002), which is an indicator of the functional integrity of photosystem II (PSII) in dark-adapted leaves. In this study, we found a close relationship between the leaf water status and the efficiency of PS II. In fact, the symbiotic combinations that maintained a high level of RWC under water deficit presented a high  $F_v/F_m$  ratio, which could be due to the low damage level caused to PS II. Based on the obtained results, the reduction in total Chl content under water deficit has been associated with a decrease in PS II performance and this may be related to the degradation of Chl that could cause photosynthetic inactivation (Blackburn, 2007). Total Chl content has generally been reduced under water deficit due to its slow synthesis or its rapid degradation (Mouradi et al., 2016b). The plants developed from bioprimed seeds showed better response to drought by the protection of membrane integrity, the maintenance of high values of osmotica as  $K^+$ . Likewise, the P contents were more critically decreased in plants from unprimed seeds than in those from primed ones under water deficit. However, the most important values of the  $K^+$  content were presented in *Mo-Rm1021*, *Dm-RcRh09*, *Ad-RcRh09* and *Ad-Rm1021* plants from bioprimed seeds and under water stress. Several reports suggested that  $K^+$  enhances plants resistance to drought through its function in osmotic adjustment, stomata opening control and energy balance (Wang et al., 2013). P is important for cells structure and functioning. Because of the biopriming seeds, the P accumulation has been significantly ( $p < 0.001$ ) improved in the leaves of almost all the studied symbiotic associations. This could be due to the enhancement of acid phosphatase enzymes activity and synthesis under stress (Nasri et al., 2011). However, adequate nutrient uptake depends on proper seed germination, seedling vigor, root growth and the activation of tolerance mechanisms such as osmoregulators and ROS detoxification. Briefly, seeds biopriming enhanced the plant nutritional status under water deficit of the studied combinations with significant variation between them. In addition, some research works also postulated that requirement of phosphorus was decreased in bioprimed plants as compared to unprimed ones (Gholami et al., 2009). The MDA could be indicator for oxidative damage on cell membrane under stress. Indeed, to investigate the effect of biopriming on membrane stability under drought, we measured MDA content and the degree of membrane permeability, reflected by electrolytes leakage, in alfalfa leaves. The results showed that the MDA content was significantly ( $p < 0.05$ ) increased under drought, signaling high peroxidation of membrane phospholipids, in all the studied symbiotic combinations with significant ( $p < 0.001$ ) variation between them. Nevertheless, seeds biopriming treatment reduced electrolytes leakage and MDA production and hence improved membrane stability in most of the alfalfa seedlings under severe drought stress (40% FC).

## Conclusion

Based on our achieved results in this study we noticed that the use of beneficial bacteria is a promising approach to control drought stress in alfalfa. This may be due to the combined improvement of morphological, physiological, and metabolic parameters induced by the “biopriming” treatment in the host plant. Our results confirmed that this biopriming technique enhanced plants vigor and then their drought tolerance in all the studied symbiotic combinations. Biopriming with osmo-tolerant rhizobacteria alleviated the adverse effect caused by water deficit (40% FC) on alfalfa plants growth, nodulation, water balance, photosynthesis performance and membrane integrity then improved their tolerance to these constraints. Finally, we confirmed that biopriming, which consists in soaking seeds in slurry of osmo-tolerant rhizobacteria, could be an effective method for seed priming and enhancing of alfalfa tolerance to drought stress. Furthermore, the study of biopriming relatively to the chemical seed treatment will be of great interest.

## REFERENCES

- [1] Annicchiarico, P., Pecetti, L., Abdelguerfi, A., Bouizgaren, A., Carroni, A. M., Hayek, T., M<sup>o</sup>Hammadi Bouzina, M., Mezni, M. (2011): Adaptation of landrace and variety germplasm and selection strategies for lucerne in the Mediterranean basin. – *Field Crop Research* 120(2): 283-291.
- [2] Arnon, D. I. (1949): Copper Enzymes in Isolated Chloroplasts. Polyphenoloxidase in *Beta Vulgaris*. – *Plant Physiology* 24(1): 1-15.
- [3] Blackburn, G. A. (2007): Hyperspectral remote sensing of plant pigments. – *Journal of Experimental Botany* 58(4): 855-867.
- [4] Bouizgaren, A., Farissi, M., Ghoulam, C., Kallida, R., Faghire, M., Barakate, M., Al Feddy, M. N. (2013): Assessment of summer drought tolerance variability in Mediterranean alfalfa (*Medicago sativa* L.) cultivars under Moroccan fields conditions. – *Archives of Agronomy and Soil Science* 59(1): 147-160.
- [5] Egamberdieva, D., Kucharova, Z., Davranov, K., Berg, G., Makarova, N., Azarova, T., Chebotar, V., Tikhonovitch, I., Kamilova, F., Validoy, S. H., Lugtenberg, B. (2011): Bacteria able to control foot and root rot and to promote growth of cucumber in salinated soils. – *Biology and Fertility of Soils* 47(2): 197-205.
- [6] Farissi, M., Bouizgaren, A., Faghire, M., Bargaz, A., Ghoulam, C. (2013): Agrophysiological and biochemical properties associated with adaptation of *Medicago sativa* populations to water deficit. – *Turkish Journal of Botany* 37(6): 1166-1175.
- [7] Farissi, M., Mouradi, M., Farssi, O., Bouizgaren, A., Ghoulam, C. (2018): Variations in leaf gas exchange, chlorophyll fluorescence and membrane potential of *Medicago sativa* root cortex cells exposed to increased salinity: The role of the antioxidant potential in salt tolerance. – *Archives of Biological Sciences* 70(3): 413-423.
- [8] Farooq, M., Basra, S. M. A., Tabassum, R., Afzal, I. (2006): Enhancing the performance of direct seeded fine rice by seed priming. – *Plant Production Science* 9(4): 446-456.
- [9] Gholami, A., Shahsavani, S., Nezarat, S. (2009): The effect of plant growth promoting rhizobacteria (PGPR) on germination, seedling growth and yield of maize. – *World Academy of Science, Engineering and Technology* 37: 19-24.
- [10] Ghoulam, C., Foursy, A., Fares, K. (2002): Effects of salt stress on growth, inorganic ions and proline accumulation in relation to osmotic adjustment in five sugar beet cultivars. – *Environmental and Experimental Botany* 47(1): 39-50.
- [11] Heath, R. L., Packer, L. (1968): Photoperoxidation in isolated chloroplasts. – *Archives of Biochemistry and Biophysics* 125(1): 189-198.

- [12] Kasim, W. A., Osman, M. E., Omar, M. N., Abd El-Daim, I. A., Bejai, S., Meijer, J. (2013): Control of Drought Stress in Wheat Using Plant-Growth-Promoting Bacteria. – *Journal of Plant Growth Regulation* 32(1): 122-30.
- [13] Latrach, L., Mouradi, M., Farissi, M., Bouizgaren, A. (2017): Physiological characterization of rhizobial strains nodulating alfalfa (*Medicago sativa* L.) isolated from soils of Southeastern Morocco. – *Applied Journal of Environmental Engineering Science* 4: 353-364.
- [14] Liatukienė, A., Liatukas, Z., Ruzgas, V. (2008): Winterhardiness as the key factor for selecting accessions of *Medicago sativa* L. high-yielding germplasm. – *Biologija* 54(2): 129-133.
- [15] Lipiec, J., Doussan, C., Nosalewicz, A., Kondracka, K. (2013): Effect of drought and heat stresses on plant growth and yield: a review. – *International Agrophysics* 27(4): 463-477.
- [16] Liu, H., Zhang, C., Yang, J., Yu, N., Wang, E. (2018): Hormone modulation of legume-rhizobial symbiosis. – *Journal of integrative plant biology* 60(8): 632-648.
- [17] Mengel, K. (1994): Symbiotic dinitrogen fixation - its dependence on plant nutrition and its ecophysiological impact. – *Journal of Plant Nutrition and Soil Science* 157(3): 233-241.
- [18] Moeinzadeh, A., Sharif-Zadeh, F., Ahmadzadeh, M., Tajabadi, F. H. (2010): Biopriming of sunflower (*Helianthus annuus* L.) seed with *Pseudomonas fluorescens* for improvement of seed invigoration and seedling growth. – *Australian Journal of Crop Science* 4(7): 564-570.
- [19] Mouradi, M., Bouizgaren, A., Farissi, M., Makoudi, B., Kabbadj, A., Very, A. A., Sentenac, H., Qaddoury, A., Ghoulam, C. (2016a): Osmopriming improves seeds germination, growth, antioxidant responses and membrane stability during early stage of moroccan alfalfa populations under water deficit. – *Chilean Journal of Agricultural Research* 76(3): 265-72.
- [20] Mouradi, M., Farissi, M., Bouizgaren, A., Makoudi, B., Kabbadj, A., Very, A. A., Sentenac, H., Qaddourya, A., Ghoulam, C. (2016b): Effects of water deficit on growth, nodulation and physiological and biochemical processes in *Medicago sativa*-rhizobia symbiotic association. – *Arid Land Research and Management* 30(2): 193-208.
- [21] Mouradi, M., Farissi, M., Bouizgaren, A., Qaddoury, A., Ghoulam, C. (2018): *Medicago sativa*-rhizobia symbiosis under water deficit: Physiological, antioxidant and nutritional responses in nodules and leaves. – *Journal of Plant Nutrition* 41(3): 384-95.
- [22] Nasri, N., Kaddour, R., Rabhi, M., Plassard, C., Lachaal, M. (2011): Effect of salinity on germination, phytase activity and phytate content in lettuce seedling. – *Acta Physiologiae Plantarum* 33(3): 935-942.
- [23] O'Callaghan, M. (2016): Microbial inoculation of seed for improved crop performance: issues and opportunities. – *Applied Microbiology and Biotechnology* 100(13): 5729-46.
- [24] Olsen, S. R. (1954): Estimation of Available Phosphorus in Soils by Extraction with Sodium Bicarbonate. – D.C. US Dept. of Agriculture, Washington, US. pp: 60.
- [25] Sharifi, R. S., Khavazi, K. (2011): Effects of seed priming with Plant Growth Promoting Rhizobacteria (PGPR) on yield and yield attribute of maize (*Zea mays* L.) hybrids. – *Journal of Food, Agriculture and Environment* 9(3-4): 496-500.
- [26] Shen, Y., Li, L., Chen, W., Robertson, M., Unkovich, M., Bellotti, W., Probert, M. (2009): Soil water, soil nitrogen and productivity of lucerne-wheat sequences on deep silt loams in a summer dominant rainfall environment. – *Field Crops Research* 111(1-2): 97-108.
- [27] Shukla, N., Awasthi, R., Rawat, L., Kumar, J. (2015): Seed biopriming with drought tolerant isolates of *Trichoderma harzianum* promote growth and drought tolerance in *Triticum aestivum*. – *Annals of Applied Biology* 166(2): 171-182.
- [28] Singh, V., Upadhyay, R. S., Sarma, B. K., Singh, H. B. (2016): Seed bio-priming with *Trichoderma asperellum* effectively modulate plant growth promotion in pea. – *International Journal of Agriculture, Environment and Biotechnology* 9(3): 361-365.

- [29] Tabassum, T., Farooq, M., Ahmad, R., Zohaib, A., Wahid, A. (2017): Seed priming and transgenerational drought memory improves tolerance against salt stress in bread wheat. – *Plant Physiology and Biochemistry* 118: 362-369.
- [30] Teixeira, E. I., Brown, H. E., Meenken, E. D., Moot, D. J. (2011): Growth and phenological development patterns differ between seedling and regrowth lucerne crops (*Medicago sativa* L.). – *European Journal of Agronomy* 35(1): 47-55.
- [31] Voisin, A. S., Munier-Jolain, N. G., Salon, C. (2010): The nodulation process is tightly adjusted to plant growth. An analysis using environmentally and genetically induced variation of nodule number and biomass in pea. – *Plant and Soil* 337(1-2): 399-412.
- [32] Waldhoff, D., Furch, B., Junk, W. J. (2002): Fluorescence parameters, chlorophyll concentration, and anatomical features as indicators for flood adaptation of an abundant tree species in Central Amazonia: *Symmeria paniculata*. – *Environmental and Experimental Botany* 48(3): 225-235.
- [33] Wang, M., Zheng, Q., Shen, Q., Guo, S. (2013): The critical role of potassium in plant stress response. – *International journal of molecular sciences* 14(4): 7370-7390.



## ANTHOCYANIN-RICH PHENOLIC EXTRACTS OF BLACK CHOKEBERRY (*ARONIA MELANOCARPA*) ATTENUATE INFLAMMATION INDUCED BY LIPOPOLYSACCHARIDE IN RAW 264.7 CELLS

MA, Y.<sup>1#</sup> – WEI, L.<sup>2#</sup> – XU, Q.<sup>1</sup> – WANG, Y.<sup>2</sup> – LI, Z.<sup>1</sup> – ZHOU, W.<sup>3</sup> – MENG, X.<sup>4\*</sup>

<sup>1</sup>Center of Experiment Teaching, Shenyang Normal University, Shenyang 110034, China  
(e-mail/phone: ma1976@126.com/+86-138-0401-0160 – Y. Ma; 1183759107@qq.com – Q. Xu; Lizheholle@163.com – Z. Li)

<sup>2</sup>College of Food Science, Shenyang Agriculture University, Shenyang 110866, China  
(e-mail/phone: weilulusy@126.com/+86-158-2745-6126 – L. Wei; 308579439@qq.com – Y. Wang)

<sup>3</sup>Food Inspect Monitoring, Experiment Center, Ctr Chaoyang, Chaoyang 122000, China  
(e-mail: 3518299636@qq.com)

<sup>4</sup>Shenyang Agricultural University, Shenyang, Liaoning 110866, China

\*Corresponding author

e-mail: mengxjsy@126.com, phone: +86-133-9011-7107

#These authors have contributed equally to this work

(Received 5<sup>th</sup> Sep 2020; accepted 21<sup>st</sup> Dec 2020)

**Abstract.** *Aronia melanocarpa* berries and their extracts, have become well known for their notable health benefits. The present study investigated the anti-inflammatory effect of anthocyanin-rich phenolic extracts of Ame (*Aronia melanocarpa*) in LPS (lipopolysaccharide)-stimulated RAW 264.7 murine macrophage cells. The results showed that Ame pre-treatment significantly ameliorated oxidative stress and inflammatory biomarker activities, as evidenced by reductions in the production of ROS (reactive oxygen specie), MDA (malondialdehyde), and NO (nitric oxide), as well as suppression of iNOS (inducible nitric oxide synthase), COX-2 (cyclooxygenase) and PGE2 (prostaglandin E2) mRNA levels; remarkably elevated the level of anti-inflammatory cytokine IL (interleukin)-10; and reduced the levels of the pro-inflammatory cytokines IL-1p, IL-6, and TNF-a (tumour necrosis factor). Additionally, we observed an attenuation of the cell apoptosis levels and the mRNA expression of apoptosis factors such as caspase-3 and caspase-9. In summary, the results highlight the health benefit of Ame against inflammation in LPS-stimulated RAW 264.7 cells.

**Keywords:** *Aronia melanocarpa* anthocyanins, anti-inflammatory activity, cell apoptosis, apoptosis factors

### Introduction

Our inclusion of berries in the diet is gaining popularity due to their richness in health-beneficial nutrients, such as phenolic compounds, flavonoids, anthocyanidins and antioxidant vitamins (Hwang et al., 2014b). For the past several years, a growing amount of evidence has indicated that the consumption of plant foods rich in polyphenolic compounds is correlated with a lower risk of the development for oxidative stress-related diseases and has a beneficial effect beyond the actions of vitamins (Denev et al., 2012).

Recent studies have shown an increasing interest in *Aronia melanocarpa* (black chokeberry), which belongs to the Rosaceae family and originates from North America (Jakobek et al., 2012). It is a rich source of phenolic compounds, particularly

proanthocyanidins and anthocyanins. Many earlier studies have shown that the concentrations phenolic compounds is many times higher than those in apples, red raspberries, blackberries, sweet rowanberries, blackthorn, sweet cherry, sour cherry, blueberries, raspberries, etc. (Castañeda-Ovando et al., 2009; Pellati et al., 2004; Polat et al., 2017). *Aronia* berries are extensively used for the production of juices, preserves, jams, wines and food colorants (Simić et al., 2016), and a number of health benefits have been ascribed to their intake (Mcdougall et al., 2016). In vitro and in vivo studies have demonstrated that black chokeberry has a wide range of positive effects, such as inhibition of cancer cell proliferation (Tao et al., 2017), antimutagenic effects, neuroprotective effects (Lee et al., 2017) and antidiabetic capabilities (Ciocoiu et al., 2017). It also displays several health-promoting properties in relation to chronic diseases, especially gastroprotective, hepatoprotective, and cardioprotective effects, which are related to its anti-inflammatory properties (Jurikova et al., 2017). Thus, *aronia* berries have potential as functional food ingredients. Inflammation is a complex physiopathological phenomenon that is mediated by activated inflammatory cells of the immune system, including macrophages (Yoon et al., 2012). It may induce various chronic diseases including cancer, cardiovascular diseases, Alzheimer's disease, type II diabetes, arthritis, metabolic syndrome, neurological diseases, and infectious diseases (Ahn et al., 2015; Hwang et al., 2014a). Lipopolysaccharide (LPS) is an endotoxin that is a potent inducer of inflammation and triggers the activation of macrophages that later release biomarkers of oxidative stress and inflammatory mediators, which then induce apoptosis (Khan et al., 2016).

Oxidative stress is considered a harmful disequilibrium between the generation and removal of radicals including lipid peroxidation products and ROS (reactive oxygen species) (Sivasinprasasn et al., 2016). Furthermore, ROS may damage biological molecules such as lipids, proteins and DNA and are crucial promoters of inflammation and cardiovascular disease (Rop et al., 2010). Inflammatory mediators include cell cytokines. Stimulated macrophages will release large amounts of cell cytokines such as IL (interleukin)-1 $\beta$ , IL-6, IL-10, TNF- $\alpha$  (tumour necrosis factor) and other inflammatory mediators such as PGE2 (prostaglandin E2), iNOS (inducible nitric oxide synthase) and COX-2 (cyclooxygenase) during the inflammation process (Zdařilová et al., 2010). Thus, inhibition of the production of these inflammatory mediators is an important target in the treatment of inflammatory diseases. It has been reported that oxidative stress can impair function and trigger apoptosis (Isaak et al., 2017). Caspase-3 and Caspase-9 are directly involved in the process of apoptosis and are important pro-apoptotic molecules.

Compared with the synthetic anti-inflammation constituents, natural bioactive ingredients have higher efficiency and are economical. Besides, synthetic anti-inflammation constituents may exhibit toxicity and side-effects. Thus, it is necessary to search for more natural bioactive resources. Natural plant extracts including *Aronia melanocarpa* extract have shown beneficial effects on inflammation via the reduction of damage due to oxidative stress, apoptosis and modulation of inflammation cytokine expression.

Recently, works by Ah Ra Goh have indicated that *Aronia melanocarpa* extract exerts anti-inflammatory activities by inhibiting expression of pro-inflammatory mediators and ROS generation in HaCaT cells (Goh et al., 2016). Similar results were also obtained showing that intake of anthocyanin-rich black chokeberry juice can inhibit both the release of TNF- $\alpha$ , IL-6 and IL-8 in human peripheral monocytes and the activation of the NF- $\kappa$ B pathway in RAW 264.7 macrophage cells (Appel et al., 2015).

Herein, we investigated the anti-inflammatory effects and action mechanisms of *Aronia melanocarpa* extract and how it exerts an anti-inflammatory effect in LPS

(lipopolysaccharide)-inflamed murine RAW264.7 macrophage cells in the present study. To the best of our knowledge, this is the first study that evaluated the anti-inflammatory properties of *Aronia melanocarpa* extract from three aspects: oxidative stress, inflammatory mediators, and apoptosis. The study further investigated whether *Aronia melanocarpa* extract could be used as a potential novel ingredient in anti-inflammatory health products or as a candidate drug for the prevention of inflammation.

## Materials and methods

### Materials and reagents

Ripe fruits of *Aronia melanocarpa* cultivars (“Fukangyuan Number 1”) were harvested in Haicheng City (41°47’41”N, 122°40’42”E), Anshan Province, China. The *Aronia melanocarpa* were submitted to 60% alcoholic extraction, and the extracts were preserved at -20 °C for use. All the chemicals and reagents were purchased from Wanlei and Dingguo Biological Technology Co., Ltd. (Shenyang, Liaoning, China).

### Phytochemical analysis

#### Anthocyanin phenolic acids

Anthocyanins were quantified by HPLC (High Performance Liquid Chromatography) experiments according to a previously described method (Wang et al., 2016). The column was a Dikma Platisil C18 column (4.6 mm × 250 mm inner diameter, 5 µm), and the solvent system used was 0.5% water solution in formic acid (A) and 100% HPLC grade acetonitrile (B) (elution conditions: 0-40 min from 0 to 40% B; 40-45 min, 40-45% B, 45-52 min, 0% B; flow rate 0.7 mL min<sup>-1</sup>, injection volumes were 20 µL). Data were recorded at 520 nm. Anthocyanin components were quantified based on the calibration curves of structurally related external standards (cyanidin-3-glucoside). The standard concentration ranged from 0.5 × 10<sup>-3</sup> to 1.5 × 10<sup>-3</sup> mg/mL.

The phenolic acids were quantified using an HPLC system (Agilent 1100, Palo Alto, CA, USA) at 210 nm. They were separated using a 0.1% water solution of formic acid as solvent A and HPLC grade acetonitrile in 0.1% formic acid as solvent B (elution conditions: 0-45 min from 0 to 45% B; 45-52 min 0% B; flowrate = 0.7 ml min<sup>-1</sup>; injection volumes 10 µl). Each component was quantified based on the calibration curves of the structurally related external standards (gallic acid, protocatechuic acid, p-hydroxybenzoic acid, chlorogenic acid, caffeic acid, benzoic acid, p-coumaric acid, ferulic acid, cinnamic acid). The standard concentration ranged from 2.5 × 10<sup>-5</sup> to 50 × 10<sup>-5</sup> mg/mL (Polat et al., 2017).

#### Total polyphenol content, anthocyanins, flavonoids and proanthocyanidin

The slightly modified method of Wang et al. (2016a) was applied to evaluate the total polyphenol content in the *Aronia melanocarpa* extracts. In short, 0.5 mL of the sample and 3 mL of Folin-Ciocalteu’s reagent were incubated in the dark for 5 min at room temperature. Then, 2.4 mL of 7.5% sodium carbonate was injected and incubated for 2 h at room temperature in the dark. The absorbance values of the reaction mixture were then measured at 765 nm. Gallic acid (0-100 µg/mL) was used as the standard (mg GAE/g).

The total anthocyanin content in the samples was determined by the pH-differential method. Briefly, 0.025 M potassium chloride and 0.4 M sodium acetate were separately

adjusted to pH 1.0 and pH 4.5 with hydrochloric acid. Next, 1 mL of the sample and 24 mL of buffer were incubated in the dark at room temperature for 15 min, and the absorbance was measured at 510 nm and 700 nm with distilled water as the blank control. Finally, the total anthocyanin content was calculated according to the formula given by Wang et al. (2016a).

The total flavonoid content of chokeberry cultivars was evaluated by the NaNO<sub>2</sub>-AlNOs-NaOH method. The sample solution (0.1 ml) was mixed with 4 ml of ethanol (30%), followed by 0.5 mL of NaNO<sub>2</sub> (10%), 0.5 mL of Al(NO<sub>3</sub>)<sub>3</sub> (10%) and 4 ml of NaOH (4%). After incubation at room temperature for 30 min, the absorbance was measured at 510 nm and the total flavonoids content was calculated as rutin equivalents (mg RE/g).

The proanthocyanidin content of black chokeberries was evaluated by the method of Pedro et al. (2015) with modifications. Briefly, the sample solutions (1 mL) were mixed with 5 ml of 1% vanillin (1.0 g vanillin in 100 mL of methanol) and 10% conc-H<sub>2</sub>SO<sub>4</sub> (10 mL conc-H<sub>2</sub>SO<sub>4</sub> in 100 mL of methanol) at a proportion of 1:1 (v/v). After incubation for 30 min at 25 °C, the absorbance was measured at 500 nm and the proanthocyanidin content was calculated as catechin (mg CE/g).

### **Measurement of anti-inflammatory capacity**

#### *Cell culture and treatment*

The mouse macrophage cell line Raw 264.7 (obtained from the cell bank of the Chinese Academy of Sciences, Shanghai, China) was cultured in complete DMEM (Dulbecco's Modified Eagle's Medium) with 10% heat-inactivated fetal bovine serum. Briefly, Raw 264.7 cells were seeded in 96-well and 6-well plates at a density of 10<sup>3</sup> cells/well and incubated at 37 °C, 5% CO<sub>2</sub> in a humidified incubator and allowed to attach overnight before the experiments. The Ame (*Aronia melanocarpa*) was filtered through a microfiltration membrane (0.22 µm) prior to addition to the culture media and was resuspended in DMEM to achieve a final concentration of 50 µg/mL. Cells were treated with the following:

- i. DMEM only (control group)
- ii. Ame added for 4 h daily for two consecutive days (Ame group)
- iii. LPS at 1 µg/mL for 24 h (LPS group)
- iv. Ame for 4 h daily for two consecutive days and then LPS at 1 µg/mL for another 24 h (LPS/Ame group)

The combination of dose/time for the Ame and LPS treatments was established based on preliminary MTT viability assays (data not shown). The cells and cell supernatants were collected and immediately frozen (-20 °C or -80 °C) until analysis.

#### *Determination of ROS level*

The measurement of ROS was performed according to the instructions given by the manufacturer of the kit (Shenyang Wanlei Bioengineering Institute, Shenyang, China). Briefly, DCFH-DA (2',7'-Dichlorodihydrofluorescein diacetate) was added to the serum-free culture medium to a final concentration of 10 µM. After incubation for 20 min at 37 °C, the cells were then collected and centrifuged at 1000 g for 10 min. Supernatants were removed carefully, after which the cells were resuspended in 200 µL of PBS and the fluorescence easily measured at  $\lambda_{\text{excitation}}$  490 nm and  $\lambda_{\text{emission}}$  530 nm. ROS production levels for each treatment were normalized to the non-stimulated control and expressed as % control.

### *Determination of lipid peroxidation*

Lipid peroxidation was determined by measuring the MDA (malondialdehyde) in cells using a commercial MDA Kit (Shenyang Wanlei Bioengineering Institute, Shenyang, China). The absorbance was read on a microplate reader at 532 nm. MDA production levels for each treatment were normalized to the non-stimulated control and expressed as % control.

### *Nitric oxide (NO) inhibitory activity*

The measurement of NO (nitric oxide) in Raw 264.7 cells was performed using a commercial NO kit (Nanjing Jiancheng Bioengineering Institute, Nanjing, China) according to the manufacturer's instructions. The optical density was measured using a microplate reader at 550 nm. NO production levels for each treatment were normalized to the non-stimulated control and expressed as percent control.

### *RNA isolation and reverse transcription-polymerase chain reaction (RT-PCR)*

Total RNA was isolated using a total RNA extraction kit, and 1 µg of RNA was used for cDNA synthesis using a Super M-MLV reverse transcriptase kit (BioTeke Corporation, Beijing, China) according to the manufacturer's protocol. After amplifying cDNA using real-time quantitative PCR with a SYBR green PCR Master Mix (Solarbio Life Sciences Institute, Beijing, China) according to our protocol, the levels of mRNA expression were quantified using an RT-PCR (RNA isolation and reverse transcription-polymerase chain reaction) system (Exicycler™ 96, Bioneer, Daejeon, Korea). The primers' details used in this study are presented in *Table 1*. The thermal cycling parameters were as follows: 1 cycle at 94 °C for 5 min, 94 °C for 10 s, 60 °C for 20 s and 72 °C for 30 s, followed by 40 cycles of 2.5 min at 7 °C, 1.5 min at 40 °C, melting for 34 s at 60 °C to 94 °C and 2 min at 25 °C. The nucleotide sequence of each primer and the size of the PCR products are shown in *Table 1*. mRNA expression was analyzed using the  $2^{-\Delta\Delta C_t}$  method and normalized with respect to the expression of the p-actin housekeeping gene.

### *Apoptosis assay by flow cytometry*

Annexin V-FITC/PI staining was performed to measure apoptosis by using an Apoptosis Detection Kit (Kaiji Bioengineering Institute, Nanjing, China) according to the manufacturer's protocol. Briefly, cells from different treatment groups were collected and washed twice with cold PBS (phosphate buffered saline). The cell supernatant was carefully removed by centrifugation at 300×g for 5 min, and the cells were resuspended in 500 µL binding buffer, followed by the addition of 5 µL of Annexin V-FITC and 5 µL of PI (propidium iodide). After 15 min of incubation at room temperature in darkness, each sample was analyzed with flow cytometry (C 6, Becton Dickinson and Company, New Jersey, USA).

### *Statistical analysis*

All experimental results are expressed as means and were performed in triplicate; the data in the tables and figures represent mean values ± standard deviation. One-way ANOVA (Analysis of variance) with Duncan's multiple range test was used to examine the differences between groups. Significant differences were considered to be  $p < 0.05$  or  $p < 0.01$ .

**Table 1.** The oligonucleotide primer sets for the real-time PCR analysis

Name	Sequence (5'—3')	Length	Tm	size
PGE2 F	GCCATTATGACCATCACCTTCG	22	61.8	250
PGE2 R	GCCATTATGACCATCACCTTCG	23	60.1	
iNOS F	GCAGGGAATCTTGGAGCGAGTTG	23	67.1	139
iNOS R	GTAGGTGAGGGCTTGGCTGAGTG	23	65	
COX-2 F	TTCCTCCCGTAGCAGATGACT	21	58.9	205
COX-2 R	AACCCAGGTCCTCGCTTA	18	55.1	
IL-βF	TGGTACATCAGCACCTCACA	20	54.7	132
IL-βR	GAAGGCATTAGAAACAGTCC	20	51.5	
IL-6 F	TGTATGAACAACGATGATGCAC	22	56.7	194
IL-6 R	CTGGCTTTGTCTTTCTTGTT	20	52.2	
IL-10 F	GAAGACAATAACTGCACCCACT	22	56.2	162
IL-10 R	ACCCAAGTAACCCTTAAAGTCC	22	56.5	
caspase-3 F	TGACTGGAAAGCCGAAAC	18	53.7	203
caspase-3 R	GGACTGGATGAACCACGAC	19	55	
caspase-9 F	CACTGCCTCATCATCAACAA	20	54.5	168
caspase-9 R	CATCAAAGCCGTGACCAT	18	54.1	
TNF-α F	AGAAAGCATGATCCGCGAC	19	58.3	236
TNF-α R	TTGTGAGTGTGAGGGTCTGG	20	55.8	
P-actin F	CTGTGCCCATCTACGAGGGCTAT	23	64.5	155
P-actin R	TTTGATGTCACGCACGATTTC	22	63.2	

## Results and discussion

### Chemical composition

The detailed composition and contents of the *Aronia melanocarpa* extract are shown in Table 2. In the present study, 4 individual anthocyanins and 9 phenolic acids were identified in Ame. Ame possessed a high content of phenolic contents ( $655.11 \pm 21.6$  mg gallic acid equivalent/g), anthocyanins ( $195.76 \pm 19.43$  mg/g) and flavonoids ( $75.28 \pm 6.82$  mg rutin equivalent/g). HPLC-MS/MS (Liquid chromatography-mass spectrometry/mass spectrometry) analysis detected 4 anthocyanin pigments, with cyanidin 3-galactoside ( $92.44 \pm 8.96$  mg/g) and cyanidin 3-arabinoside ( $27.7 \pm 4.51$  mg/g) being the most representative anthocyanins in Ame. The present results indicated that anthocyanins predominated in the phenolic fractions of Ame, which are responsible for several beneficial actions in human health. That consistent with previous reports (Parzonko et al., 2015). The 9 main phenolic acids identified using HPLC methodology allowed the identification of Ame polyphenols based on standards. The most common and abundant phenolic acid compounds identified in Ame are benzoic acid and chlorogenic acid. These results are consistent with those previously reports (Polat et al., 2017).

### The effects of Ame on biomarkers of oxidative stress: ROS and MDA

A sustained pro-inflammatory state, characterized by excessive ROS production, is the common denominator in the development, progression, and complication of many diseases (Gasparri et al., 2017). For this reason, the measurement of ROS intracellular production could represent a very useful parameter to quantify oxidative stress induced by LPS. To investigate whether treatment with Ame influences LPS-induced ROS production, ROS was measured. According to our results, Ame itself caused no increase

in basal ROS generation in RAW 264.7 macrophages ( $p > 0.05$ ), while Ame significantly ( $0.01 < p < 0.05$ ) suppressed the intracellular ROS production of LPS-stimulated RAW 264.7 macrophages based on 36% or higher changes relative to the LPS-stimulated controls (Fig. 1A). It suggesting that Ame phytochemicals may play a role in health maintenance by reducing oxidative stress (Goh et al., 2016).

**Table 2.** Quantification and determination of total and individual phenolic compounds in Ame

Compound <sup>a</sup>	Ame (mg/g)	Phenolic acid <sup>c</sup>	Ame (mg/g)
Total phenolic content	655.11 ± 21.6	Protocatechuic acid	0.102 ± 0.07
Flavonoid content	75.28 ± 6.82	P-hydroxybenzoic acid	0.055 ± 0.02
Proanthocyanidin content	0.06 ± 0.02	Chlorogenic acid	1.643 ± 0.31
<b>Anthocyanins<sup>b</sup></b>		Caffeic acid	0.686 ± 0.17
Cyanidin 3-galactoside	92.44 ± 8.96	Benzoic acid	10.206 ± 1.22
Cyanidin 3-glucoside	4.04 ± 0.37	P-coumaric acid	0.295 ± 0.08
Cyanidin 3-arabinoside	27.7 ± 4.51	Ferulic acid	0.267 ± 0.10
Cyanidin 3-xyloside	6.21 ± 0.54	Cinnamic acid	0.253 ± 0.15
Total anthocyanins	195.76 ± 19.43	Gallic acid	0.045 ± 0.02

Values are means ± SD (n = 3)

<sup>a</sup>Individual phenolic compounds were compared with standard reference compounds

<sup>b</sup>Identified using HPLC-ESI-MS<sub>2</sub>

<sup>c</sup>Identified using HPLC

Lipid peroxidation is a free-radical-mediated chain reaction involving several types of free radicals, which could be arrested through enzymatic means or by free radical scavenging by antioxidants and is considered one of the major manifestations of oxidative stress (Divya et al., 2015). Therefore, we used a lipid peroxidation assay to strengthen our findings in the above-mentioned regions. In the present study, we assessed the effect of topical administration of Ame during mouse macrophage cell LPS exposure by measuring the concentration of the short-chain aldehyde, MDA, which is the by-product of lipid peroxidation. As shown in Figure 1B, LPS application obviously enhanced MAD (machine analysis display). Pre-treatment with Ame significantly ( $0.01 < p < 0.05$ ) reduced the MDA level, suggesting that Ame might be involved in the prevention of inflammation dysfunction via reducing the oxidative stress level in macrophages. These results obtained for the first time with *Aronia melanocarpa*, which are consistent with those previously reported by several authors, who tested the efficacy of different bioactive compounds against LPS-induced damage in macrophage cell models (Bak et al., 2013; Gasparini et al., 2017; Lee et al., 2013).

### The effects of Ame on inflammatory mediators

#### Inflammatory mediators: NO, PGE2, iNOS and COX-2

NO, PGE2, iNOS and COX-2 are the most important indicators for assessing inflammation injury. iNOS expression can increase the production of NO (Lee et al., 2013), which is also reported to affect the activity of COX-2 (Li and Wang, 2011). Similar to iNOS, COX-2 is also an inducible pro-inflammatory enzyme. COX-2 can convert arachidonic acid into PGE2, which can contribute to the pain and swelling associated with inflammation (Lee et al., 2013).

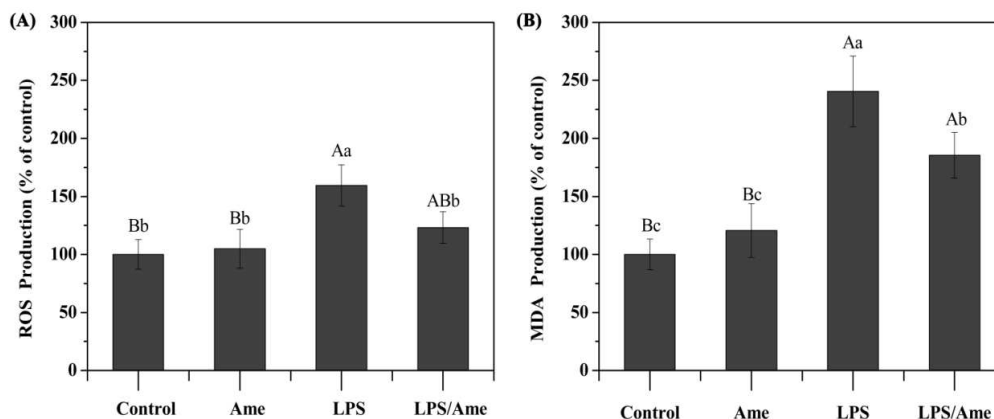


**Figure 1.** The effects of Ame on biomarkers of oxidative stress (A and B): ROS and MDA. Ame, treatment with Ame alone; LPS, treatment with LPS alone; LPS/Ame, Ame pre-treatment followed by LPS treatment. The results are presented as the mean  $\pm$  SD ( $n = 3$ ). One-way (ANOVA) followed by Duncan's multiple range tests was performed to analyze the statistical differences among means. The different superscript lowercase letters denote significant differences between groups, and  $p < 0.05$  or  $p < 0.01$  was considered statistically significant

The effects of Ame on the level of NO and PGE2 in the culture media of RAW 264.7 cells were determined after 24 h treatment with 1  $\mu$ g/mL LPS. As shown in *Figure 2A*, there was no basal NO production during the incubation with only Ame without LPS ( $p > 0.05$ ). After treatment with LPS, the NO concentration in the medium increased by approximately 2.45-fold (245.29%) compared to the control (100%). However, Ame at 50  $\mu$ g/mL significantly inhibited the production of NO ( $p < 0.01$ ).

The inhibitory effects of Ame on LPS-induced PGE2 secretion in RAW 264.7 cells were determined using RT-PCR (real-time polymerase chain reaction). As shown in *Figure 2B*, when the macrophages were not stimulated with LPS, PGE2 was almost undetectable in the medium with or without Ame ( $p > 0.05$ ), while treatment with LPS caused an elevated production of PGE2 ( $p < 0.01$ ), which was greatly reduced by Ame ( $p < 0.01$ ). In this study, Ame effectively decreased NO production and PGE2 mRNA expression, indicating that Ame might be useful for suppressing the inflammatory process.

To investigate whether the Ame fractions had inhibitory activities against NO and PGE2 production via inhibition of iNOS and COX-2, RT-PCR analysis was used. As shown in *Figure 2C* and *D*, the expression of iNOS and COX-2 mRNA only showed an almost undetectable change between the unstimulated group and the Ame pre-treatment group. After LPS treatment, iNOS and COX-2 mRNA expression were markedly increased, whereas cotreatment with Ame significantly suppressed the expression of iNOS and COX-2 mRNA. These results are consistent with the inhibitory effect of Ame on NO and PGE2 release. The inhibitory profiles of Ame for iNOS and COX-2 overlapped with the profiles for NO and PGE2 production. On the basis of these results, it was concluded that Ame inhibited iNOS-mediated NO and COX-2-mediated PGE2 production. A similar finding was reported by a previous study, where blueberry extract was found to alleviate NO, PGE2 and COX-2 (Xu et al., 2016).

#### *Inflammatory cytokines: IL-1 $\beta$ , IL-6, TNF- $\alpha$ and IL-10*

Cytokines are a critical component of immune defense, but, on the other hand, inappropriate or excessive production of IL-1 $\beta$ , IL-6, TNF- $\alpha$  and IL-10 has been linked



with the pathogenesis of a number of chronic inflammatory diseases (Yaqoob et al., 2010). IL-1 $\beta$  is known to induce fever and inflammation, finally leading to apoptosis. Moreover, it has been shown that IL-6 can be secreted by macrophages in response to specific microbial molecules to initiate the innate immune system (Yoon et al., 2009) and is a crucial checkpoint regulator of neutrophil trafficking by orchestrating chemokine production and leukocyte apoptosis (Fang et al., 2015). TNF- $\alpha$  is involved in many different cellular processes, including the production of numerous cytokines and acute phase proteins, and thus contributes to many pathophysiologic processes (Liu, 2005). On the other hand, IL-10 is a type of anti-inflammatory factor that down-regulates inflammatory responses and plays a role in inflammatory mediators of antagonism.

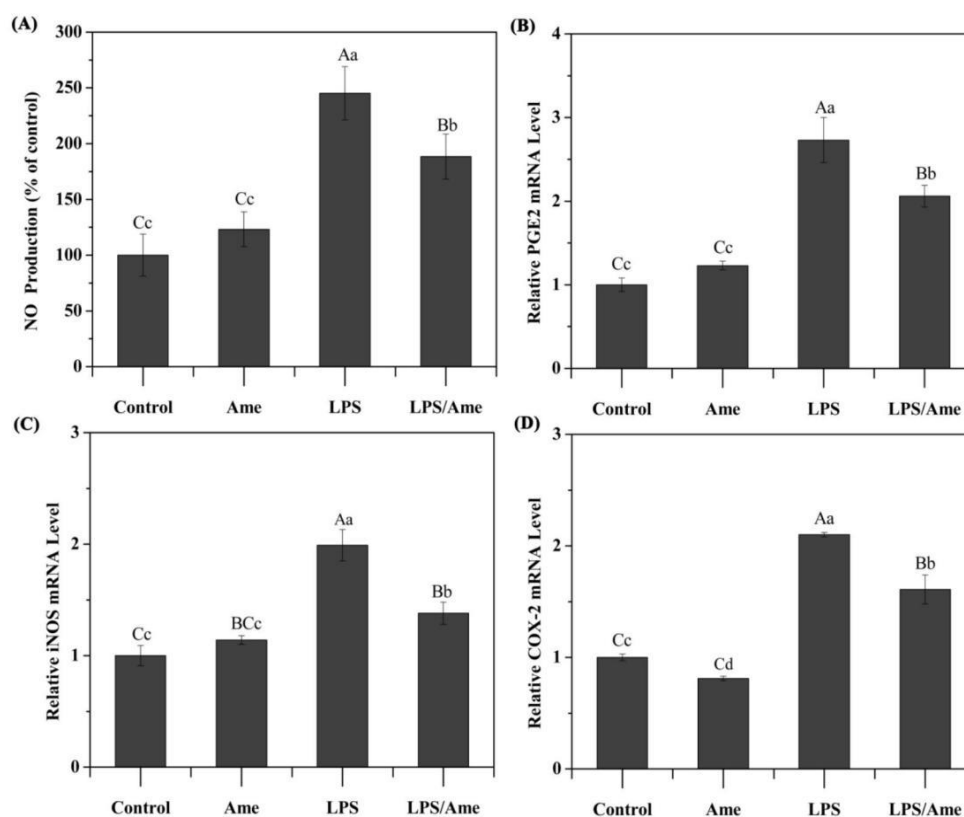


**Figure 2.** The effects of Ame on inflammatory mediators (A, B, C and D): NO, PGE2, iNOS and COX-2. Ame, treatment with Ame alone; LPS, treatment with LPS alone; LPS/Ame, Ame pre-treatment followed by LPS treatment. The results are presented as the mean  $\pm$  SD ( $n = 3$ ). One-way (ANOVA) followed by Duncan's multiple range test was performed to analyze the statistical differences among means. The different superscript lowercase letters denote significant differences between groups, and  $p < 0.05$  or  $p < 0.01$  was considered statistically significant

As shown in Figure 3A, B and C, Ame itself caused no increase in the aforementioned cytokine mRNA expression in RAW 264.7 macrophages ( $p > 0.05$ ). When compared with cells treated with LPS alone, Ame resulted in an approximately 66%, 16% and 21% reduction in the mRNA expression of IL-1 $\beta$ , IL-6 and TNF- $\alpha$ , respectively. All of these reductions were significant ( $p < 0.05$ ), especially IL-1 $\beta$  ( $p < 0.01$ ). A different trend was found for IL-10: in unstimulated cells, IL-10 secretion increased to 104% ( $p > 0.05$ ) of the control with 50  $\mu\text{g/mL}$  Ame; in this case, an

increase in IL-10 mRNA expression was observed with Ame + LPS treatments, with a significant increase ( $p < 0.01$ ) compared to LPS-treated cells. The present results demonstrated that bioactive compounds in response to Ame exhibited a significant adjustment of inflammatory cytokines in RAW264.7 macrophages after exposure to LPS that helps decrease inflammatory damage.

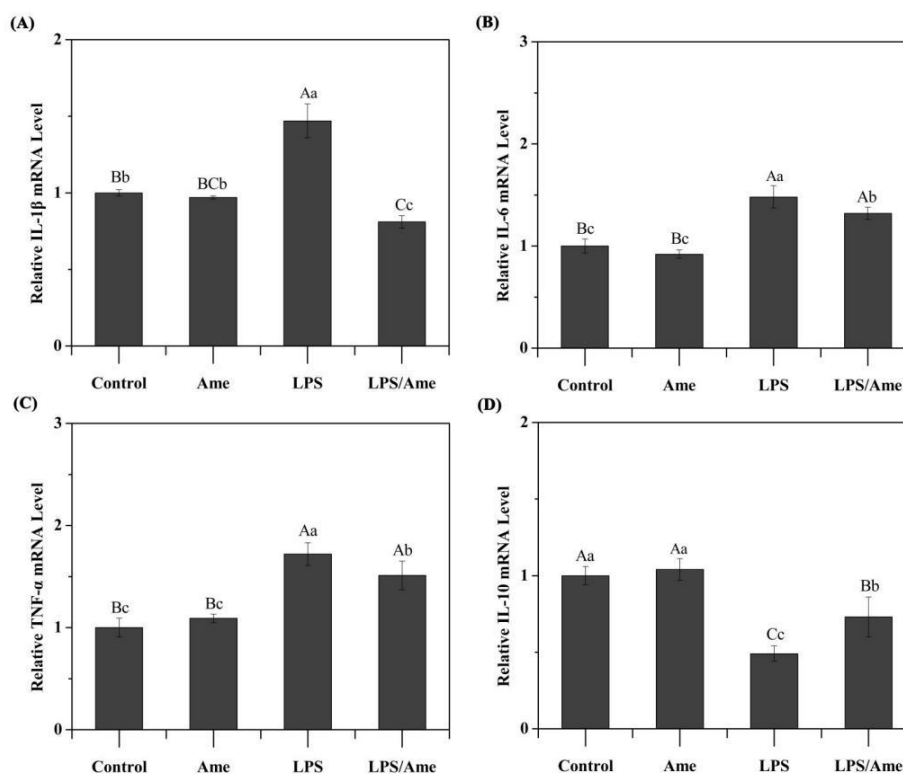


**Figure 3.** The effects of Ame on inflammatory cytokines (A, B, C and D): IL-1 $\beta$ , IL-6, TNF- $\alpha$  and IL-10. Ame, treatment with Ame alone; LPS, treatment with LPS alone; LPS/Ame, Ame pre-treatment followed by LPS treatment. The results are presented as the mean  $\pm$  SD ( $n = 3$ ). One-way (ANOVA) followed by Duncan's multiple range tests was performed to analyze the statistical differences among means. The different superscript lowercase letters denote significant differences between groups, and  $p < 0.05$  or  $p < 0.01$  was considered statistically significant

Previous reports (Appel et al., 2015) have suggested that the phenolics from chokeberry concentrate inhibit the release of TNF- $\alpha$ , IL-6 and IL-8 in LPS-induced RAW264.7 macrophages. These results are in line with the data obtained in other studies performed on RAW264.7 macrophages in which the expression of pro- and anti-inflammatory cytokines induced by LPS was improved by Ame (Appel et al., 2015) and other different bioactive compounds from strawberries (Gasparri et al., 2017), blueberries (Wang et al., 2017), and *Lonicera caerulea* L (Wang et al., 2016b).

### The effects of Ame on apoptosis

#### Biomarkers of apoptosis: caspase-3 and caspase-9

Caspases are known as important mediators of apoptosis and contribute to leading cells undergoing apoptosis to irreversible cell death. Caspase-3 and caspase-9 play major roles

in the pathway of extrinsic apoptosis and endogenous apoptosis (Meng et al., 2017). Studies have shown that upregulation of caspase and TNF- $\alpha$  is an important factor in apoptosis (Chu et al., 2016). Therefore, we measured the activation of caspase-3 and caspase-9 with RT-PCR. As shown in *Figure 4A* and *B*, Ame itself caused no increase in caspase-3 and caspase-9 mRNA expression in RAW 264.7 macrophages ( $p > 0.05$ ), while treatment with LPS for 24 h resulted in the activation of caspase-3 and caspase-9 as is apparent in comparison to the control groups ( $p < 0.01$ ), but Ame treatment at 50  $\mu\text{g/mL}$  significantly protected against caspase-3 and caspase-9 activation ( $p < 0.01$ ). Interestingly, the mRNA expression of caspase-3 and caspase-9 after Ame + LPS treatment was similar to the control group ( $p > 0.05$ ). These observations indicate that Ame can down-regulate mRNA expression of caspase-3 and caspase-9, thereby reducing macrophage cell death, which is an important step in preserving the immune system following inflammatory damage. In contrast to previous studies, we first evaluated the anti-inflammatory activity of Ame by exploring one aspect of apoptosis.

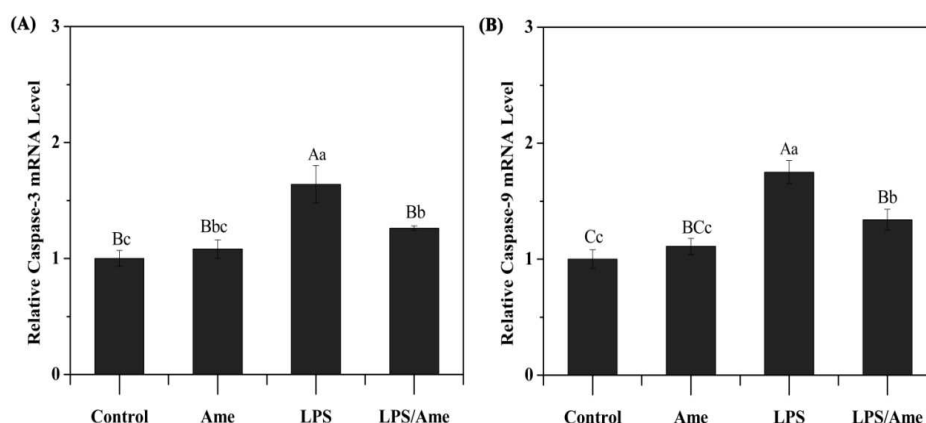


**Figure 4.** The effects of Ame on biomarkers of apoptosis (A and B): caspase-3 and caspase-9. Ame, treatment with Ame alone; LPS, treatment with LPS alone; LPS/Ame, Ame pre-treatment followed by LPS treatment. The results are presented as the mean  $\pm$  SD ( $n = 3$ ). One-way (ANOVA) followed by Duncan's multiple range test was performed to analyze the statistical differences among means. The different superscript lowercase letters denote significant differences between groups, and  $p < 0.05$  or  $p < 0.01$  was considered statistically significant

#### Apoptosis detected by flow cytometry

Flow cytometry was used to determine in which phase of the cell cycle the RAW 264.7 macrophages had accumulated and whether apoptotic events occurred in response to LPS exposure. As shown in *Figure 5*, in RAW 264.7 macrophages cells, LPS exposure groups resulted in typical apoptotic changes in the cells compared with cells from the untreated groups. When treated with 50  $\mu\text{g/mL}$  Ame, the apoptotic rate remarkably reduced the severity of apoptosis compared with the LPS groups (early apoptosis: 12.23% vs. 11.05%, late apoptosis: 21.65% vs. 11.01%, total apoptosis: 33.88% vs. 23.06%, respectively,  $p < 0.05$ ). Treatment with Ame could therefore block RAW 264.7 cell apoptosis. Furthermore, Ame itself caused no increase in the apoptosis rate in RAW 264.7 macrophages ( $p > 0.05$ ). The results showed that the early stages of apoptosis were lower than the late apoptosis. This also suggests that the reduction in cell inflammatory damage from the *Aronia melanocarpa* extracts was at least partially due to apoptosis of the RAW 264.7 cells.

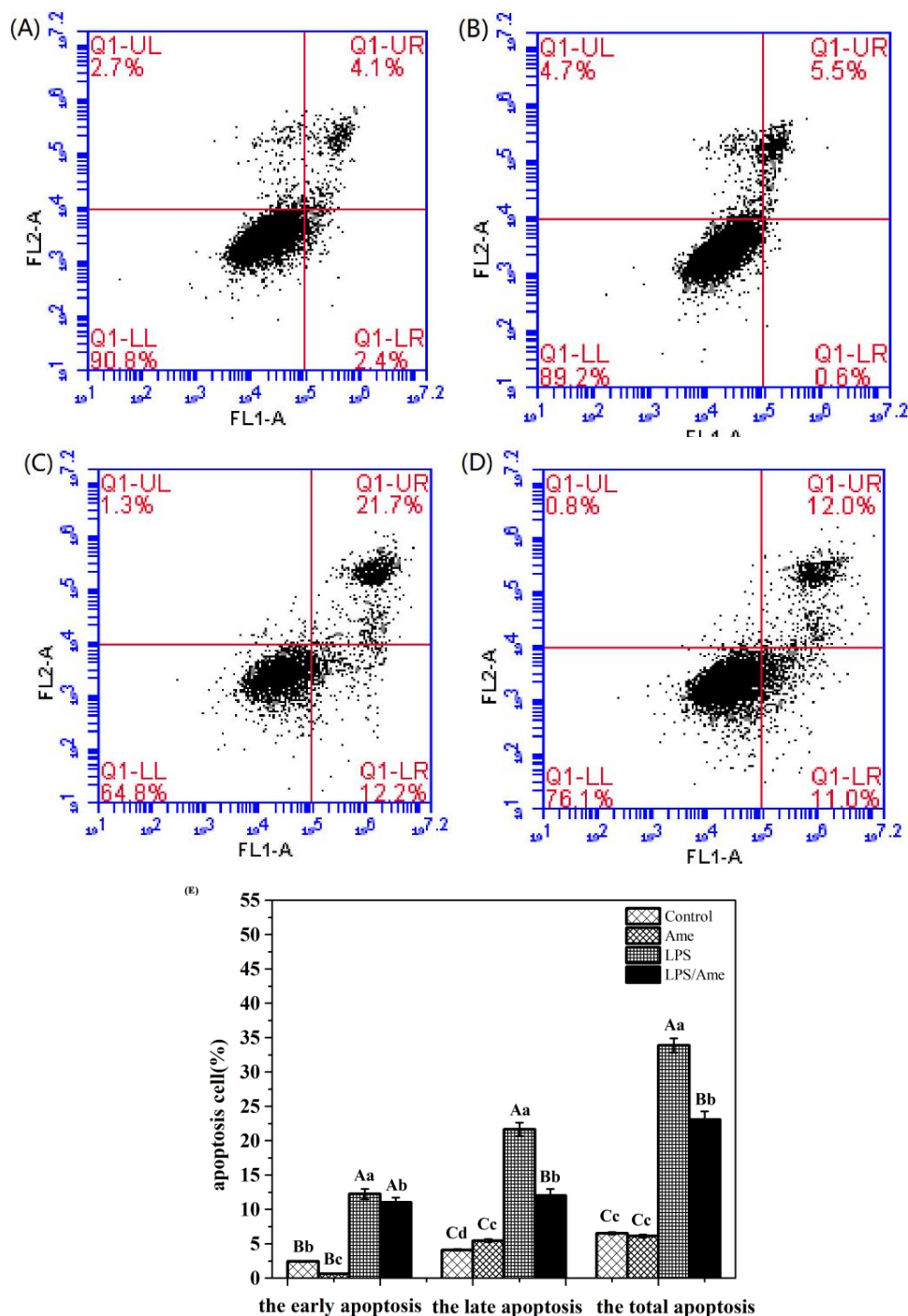


**Figure 5.** The effects of Ame on apoptosis detected by flow cytometry. Images of flow cytometry detection of RAW 264.7 macrophage apoptosis (A, B, C and D). (A) Control; (B) Ame, treatment with Ame alone; (C) LPS, treatment with LPS alone; (D) LPS/Ame, Ame pre-treatment followed by LPS treatment. UL, necrotic cells. UR, late stage apoptotic cells. LR, early stage apoptotic cells. LL, live cells. (E) The results of flow cytometry detection of RAW 264.7 macrophage apoptosis in the early stage and late stage of apoptosis. The results are presented as the mean  $\pm$  SD ( $n = 3$ ). One-way (ANOVA) followed by Duncan's multiple range test was performed to analyze the statistical differences among means. The different superscript lowercase letters denote significant differences between groups, and  $p < 0.05$  or  $p < 0.01$  was considered statistically significant

## Conclusions

In summary, we found that the *Aronia melanocarpa* extract, containing anthocyanins as its main phenolic components, could reduce LPS-induced inflammation by inhibiting the development of oxidative stress (via evaluation of ROS and MDA), regulating the activity of inflammatory mediators (NO, PGE2, iNOS and COX-2), attenuating the production of pro-inflammatory cytokines (IL-1 $\beta$ , IL-6 and TNF- $\alpha$ ), and increasing the expression of anti-inflammatory cytokines (IL-10). *Aronia melanocarpa* extract also attenuated the LPS-induced biomarkers of apoptosis: caspase-3 and caspase-9 prevented apoptosis of RAW 264.7 macrophages. Our results demonstrate that polyphenolic substances in *Aronia melanocarpa* extracts, especially anthocyanins, possess anti-inflammatory activities, *Aronia melanocarpa* extract has the potential to be developed as a novel ingredient in anti-inflammatory health products or as a candidate drug for the prevention of inflammation.

In this paper, *Aronia melanocarpa* were extracted and enriched to obtain freeze-dried powder with high anthocyanin content. The components in freeze-dried powder were identified by various methods, and its antioxidant ability was measured in vitro. Then its anti-inflammatory properties were explored from oxidative stress, inflammatory factors and apoptosis. On the basis of this paper, we can further supplement the paper and study the anthocyanin extract of *Liriodendron nigrum* in more details and more perfectly.

The mechanism of anthocyanin prevention and protection of anti-inflammatory inhibition in *Aronia melanocarpa* needs further study. It can be deeply studied from the perspective of proteomics and combined with gene knockout technology to accurately find the gene or protein site regulated by anthocyanin.

The digestion, absorption and metabolism of anthocyanins in mice or human body need to be studied. Its metabolic transformation is studied by measuring metabolites in blood and urine.

This paper studies the inhibitory effect of anthocyanin extract of *nigrum* on inflammation by RT-PCR method  $\beta$ , tumor necrosis factor- $\alpha$ , iNOS, COX2, and reports that the above inflammatory mediators are regulated by NF- $\kappa$ B. We need to continue to study the next step.

**Funding.** This project was the key planned project of year 2020 of Department of Science & Technology of Liaoning province (Serial number 2020JH2/10200039).

**Conflict of interests.** The authors declare that there is no conflict of interests.

## REFERENCES

- [1] Ahn, S., Siddiqi, M. H., Noh, H. Y., Kim, Y. J., Kim, Y. J., Jin, C. G., Yang, D. C. (2015): Anti-inflammatory activity of ginsenosides in LPS-stimulated RAW 264.7 cells. – *Science Bulletin* 60(8): 773-784.
- [2] Appel, K., Meiser, P., Millán, E., Collado, J. A., Rose, T., Gras, C. C., Muñoz, E. (2015): Chokeberry (*Aronia melanocarpa* (Michx.) Elliot) concentrate inhibits NF- $\kappa$ B and synergizes with selenium to inhibit the release of pro-inflammatory mediators in macrophages. – *Fitoterapia* 105: 73-82.
- [3] Bak, M. J., Truong, V. L., Kang, H. S., Jun, M., Jeong, W. S. (2013): Anti-inflammatory effect of procyanidins from wild grape (*Vitis amurensis*) seeds in LPS-induced RAW 264.7 cells. – *Oxidative Medicine & Cellular Longevity* 2013(20): 409321.

- [4] Castañeda-Ovando, A., Pacheco-Hernández, M. D. L., Páez-Hernández, M. E., et al. (2009): Chemical studies of anthocyanins: a review. – *Food Chemistry* 113(4): 859-871.
- [5] Chu, B. F., Lin, H. C., Huang, X. W., Huang, H. Y., Wu, C. P., Kao, M. C. (2016): An ethanol extract of *Poria cocos* inhibits the proliferation of non-small cell lung cancer A549 cells via the mitochondria-mediated caspase activation pathway. – *Journal of Functional Foods* 23: 614-627.
- [6] Ciocoiu, M., Badescu, L., Badescu, M. (2017): Health Status Improved by *Aronia Melanocarpa* Polyphenolic Extract. – Soto-Hernández, M. et al (eds.) *Phenolic Compounds*. IntechOpen, London.
- [7] Denev, P. N., Kratchanov, C. G., Ciz, M., Lojek, A., Kratchanova, M. G. (2012): Bioavailability and antioxidant activity of black chokeberry (*Aronia melanocarpa*) polyphenols: in vitro and in vivo evidences and possible mechanisms of action: a review. – *Comprehensive Reviews in Food Science & Food Safety* 11(5): 471-489.
- [8] Divya, S. P., Wang, X., Pratheeshkumar, P., Son, Y. O., Roy, R. V., Kim, D., Asha, P. (2015): Blackberry extract inhibits UVB-induced oxidative damage and inflammation through MAP kinases and NF- $\kappa$ B signalling pathways in SKH-1 mice skin. – *Toxicology & Applied Pharmacology* 284(1): 92-99.
- [9] Fang, Y., Li, X., Li, L., et al. (2015): The role of Nrf2 in protection against Pb-induced oxidative stress and apoptosis in SH-SY5Y cells. – *Food & Chemical Toxicology* 86: 191-201.
- [10] Gasparrini, M., Forbes-Hernandez, T. Y., Giampieri, F., Afrin, S., Alvarez-Suarez, J. M., Mazzoni, L., Battino, M. (2017): Anti-inflammatory effect of strawberry extract against LPS-induced stress in RAW 264.7 macrophages. – *Food & Chemical Toxicology* 102: 1-10.
- [11] Goh, A. R., Youn, G. S., Yoo, K. Y., Won, M. H., Han, S. Z., Lim, S. S., Park, J. (2016): *Aronia melanocarpa* concentrate ameliorates pro-inflammatory responses in HaCaT keratinocytes and 12-O-tetradecanoylphorbol-13-acetate-induced ear edema in mice. – *Journal of Medicinal Food* 19(7): 654.
- [12] Hwang, S. J., Kim, Y. W., Park, Y., Lee, H. J., Kim, K. W. (2014a): Anti-inflammatory effects of chlorogenic acid in lipopolysaccharide-stimulated RAW 264.7 cells. – *Inflammation Research* 63(1): 81-90.
- [13] Hwang, S. J., Yoon, W. B., Lee, O. H., Cha, S. J., Kim, J. D. (2014b): Radical-scavenging-linked antioxidant activities of extracts from black chokeberry and blueberry cultivated in Korea. – *Food Chemistry* 146(1): 71.
- [14] Isaak, C. K., Petkau, J. C., Blewett, H., K, O., Siow, Y. L. (2017): Lingonberry anthocyanins protect cardiac cells from oxidative-stress-induced apoptosis. – *Can J Physiol Pharmacol* 95(8): 904-910.
- [15] Jakobek, L., Drenjančević, M., Jukić, V., Šeruga, M. (2012): Phenolic acids, flavonols, anthocyanins and antiradical activity of “Nero”, “Viking”, “Galicianka” and wild chokeberries. – *Scientia Horticulturae* 147: 56-63.
- [16] Jurikova, T., Mlcek, J., Skrovankova, S., Sumczynski, D., Sochor, J., Hlavacova, I., Orsavova, J. (2017): Fruits of black chokeberry *Aronia melanocarpa* in the prevention of chronic diseases. – *Molecules* 22(6): 944.
- [17] Khan, M. S., Ali, T., Kim, M. W., Jo, M. H., Jo, M. G., Badshah, H., Kim, M. O. (2016): Anthocyanins protect against LPS-induced oxidative stress-mediated neuroinflammation and neurodegeneration in the adult mouse cortex. – *Neurochemistry International* 100: 1-10.
- [18] Lee, S. Y., Kim, H. J., Han, J. S. (2013): Anti-inflammatory effect of oyster shell extract in LPS-stimulated raw 264.7 cells. – *Preventive Nutrition & Food Science* 18(1): 23.
- [19] Lee, H. Y., Jin, B. W., Ryu, G., Yang, W. S., Kim, N. Y., Kim, M. K., Ma, C. J. (2017): Neuroprotective effect of *Aronia melanocarpa* extract against glutamate-induced oxidative stress in HT22 cells. – *Bmc Complementary & Alternative Medicine* 17(1): 207.

- [20] Li, C., Wang, M. H. (2011): Anti-inflammatory effect of the water fraction from hawthorn fruit on LPS-stimulated RAW 264.7 cells. – *Nutrition Research & Practice* 5(2): 101.
- [21] Liu, Z. G. (2005): Molecular mechanism of TNF signaling and beyond. – *Cell Research* (English edition) 15(1): 24.
- [22] Mcdougall, G. J., Austin, C., Van, S. E., Martin, P. (2016): Salal (*Gaultheria shallon*) and aronia (*Aronia melanocarpa*) fruits from Orkney: phenolic content, composition and effect of wine-making. – *Food Chemistry* 205: 239.
- [23] Meng, L. S., Li, B., Li, D. N., et al. (2017): Cyanidin-3-O-glucoside attenuates amyloid-beta (1-40)-induced oxidative stress and apoptosis in SH-SY5Y cells through a Nrf2 mechanism. – *Journal of Functional Foods* 38: 474-485.
- [24] Parzonko, A., Oświt, A., Bazyłko, A., Naruszczyk, M. (2015): Anthocyanins-rich *Aronia melanocarpa* extract possesses ability to protect endothelial progenitor cells against angiotensin II induced dysfunction. – *Phytomedicine International Journal of Phytotherapy & Phytomedicine* 22(14): 1238-1246.
- [25] Pedro, A. C., Granato, D., Rosso, N. D. (2015): Extraction of anthocyanins and polyphenols from black rice (*Oryza sativa* L.) by modeling and assessing their reversibility and stability. – *Food Chemistry* 191: 12-20.
- [26] Pellati, F., Benvenuti, S., Magro, L., Melegari, M., Soragni, F. (2004): Analysis of phenolic compounds and radical scavenging activity of *Echinacea* spp. – *Journal of Pharmaceutical & Biomedical Analysis* 35(2): 289-301.
- [27] Polat, M., Guclu, S. F., Okatan, V., Ercisli, S., Ozaydin, A. G., Colak, A. M., Askin, M. A. (2017): Determination of phenolic compounds in *Aronia melanocarpa* genotypes grown in Turkey. – *Oxidation Communications* 40(1): 131-137.
- [28] Rop, O., Mlcek, J., Jurikova, T., Valsikova, M., Sochor, J., Reznicek, V., Kramarova, D. (2010): Phenolic content, antioxidant capacity, radical oxygen species scavenging and lipid peroxidation inhibiting activities of extracts of five black chokeberry (*Aronia melanocarpa* (Michx.) Elliot). – *Cultivars* 4(22): 2431-2437.
- [29] Simić, V. M., Rajković, K. M., Stojičević, S. S., et al. (2016): Optimization of microwave-assisted extraction of total polyphenolic compounds from chokeberries by response surface methodology and artificial neural network. – *Separation & Purification Technology* 160: 89-97.
- [30] Sivasinprasasn, S., Pantan, R., Thummayot, S., et al. (2016): Cyanidin-3-glucoside attenuates angiotensin II-induced oxidative stress and inflammation in vascular endothelial cells. – *Chemico-Biological Interactions* 260: 67-74.
- [31] Tao, Y., Wang, Y., Pan, M., et al. (2017): Combined ANFIS and numerical methods to simulate ultrasound-assisted extraction of phenolics from chokeberry cultivated in China and analysis of phenolic composition. – *Separation & Purification Technology* 178: 178-188.
- [32] Wang, Y., Li, B., Ma, Y., Wang, X., Zhang, X., Zhang, Q., Meng, X. (2016a): *Lonicera caerulea* berry extract attenuates lipopolysaccharide induced inflammation in BRL-3A cells: oxidative stress, energy metabolism, hepatic function. – *Journal of Functional Foods* 24: 1-10.
- [33] Wang, Y., Zhu, J., Meng, X., Liu, S., Mu, J., Ning, C. (2016b): Comparison of polyphenol, anthocyanin and antioxidant capacity in four varieties of *Lonicera caerulea* berry extracts. – *Food Chemistry* 197(Pt A): 522-529.
- [34] Wang, H., Guo, X., Liu, J., Li, T., Fu, X., Liu, R. H. (2017): Comparative suppression of NLRP3 inflammasome activation with LPS-induced inflammation by blueberry extracts (*Vaccinium* spp.). – *Rsc Advances* 7(46): 28931-28939.
- [35] Xu, W., Zhou, Q., Yao, Y., Li, X., Zhang, J., Su, G., Deng, A. (2016): Inhibitory effect of Gardenblue blueberry (*Vaccinium ashei* Reade) anthocyanin extracts on lipopolysaccharide-stimulated inflammatory response in RAW 264.7 cells. – *J Zhejiang Univ Sci B* 17(6): 425-436.

- [36] Yaqoob, P., Calder, P. C., Gibney, M. J., Macdonald, I. A., Roche, H. M. (2010): The immune and inflammatory systems. – *Nutrition & Metabolism*: 312-338.
- [37] Yoon, W. J., Ham, Y. M., Kim, K. N., Park, S. Y., Lee, W. J. (2009): Anti-inflammatory activity of brown alga *Dictyota dichotoma* in murine macrophage raw 264.7 cells. – *Journal of Medicinal Plant Research* 3(1): 1-8.
- [38] Yoon, W. J., Heo, S. J., Han, S. C., Lee, H. J., Kang, G. J., Kang, H. K., Yoo, E. S. (2012): Anti-inflammatory effect of sargachromanol G isolated from *Sargassum siliquastrum* in RAW 264.7 cells. – *Archives of Pharmacal Research* 35(8): 1421-1430.
- [39] Zdařilová, A., Svobodová, A. R., Chytilová, K., Šimánek, V., Ulrichová, J. (2010): Polyphenolic fraction of *Lonicera caerulea* L. fruits reduces oxidative stress and inflammatory markers induced by lipopolysaccharide in gingival fibroblasts. – *Food & Chemical Toxicology an International Journal Published for the British Industrial Biological Research Association* 48(6): 1555-1561.



# COMPREHENSIVE ASSESSMENT OF REGIONAL SUSTAINABILITY VIA EMERGY, GREEN GDP AND DEA: A CASE STUDY IN GUIZHOU PROVINCE, CHINA

YI, Q. G.<sup>1,2</sup> – CHEN, H. T.<sup>1</sup> – LI, X.<sup>3\*</sup> – MA, C.<sup>4</sup>

<sup>1</sup>*School of economics, Guizhou university of finance and economics, Guiyang 550025, China*

<sup>2</sup>*Western institute of green development strategy of China, Guiyang 550025, China*

<sup>3</sup>*School of Management Science and Engineering, Guizhou university of finance and economics, Guiyang 550025, China*

<sup>4</sup>*School of Big Data Application and Economics, Guizhou university of finance and economics, Guiyang 550025, China*

*\*Corresponding author*

*e-mail: 361740439@qq.com; phone: +86-181-8515-3106; fax: +86-851-8851-0571*

(Received 5<sup>th</sup> Sep 2020; accepted 30<sup>th</sup> Nov 2020)

**Abstract.** We propose a comprehensive eco-efficiency framework based on emergy theory, green gross domestic product (GGDP) and data envelopment analysis (DEA) to get a thorough assessment of regional sustainability. The paper evaluates the sustainable development of Guizhou Province from 2000 to 2017 based on emergy analysis, GGDP and DEA. Moreover, the GGDP, which has deducted the undesirable output, is selected as the output index to calculate the eco-efficiency of Guizhou Province and further evaluate its sustainable development level by the super-SBM model. The results showed that the growth rate of the GGDP in Guizhou Province was far lower than that of the GDP. The proportion of the GGDP in GDP showed a trend of continuous decline from 78.32% to 60.60% mainly due to the high consumption of non-renewable resource products. Moreover, there were seven effective years during 2000-2017. There was redundancy in capital input and labor input, and the input and output were not optimal in the ineffective years. Therefore, we suggest that Guizhou Province should achieve technological progress by introducing talents, perfect industrial layout, optimize the industrial structure, and gradually realize the transformation industry from high energy consumption, high emission and high pollution to low energy consumption, low emission and low pollution.

**Keywords:** *eco-efficiency, green gross domestic product (GGDP), emergy analysis, super-SBM, undesirable output*

## Introduction

It is necessary to measure and evaluate the regional sustainable development status comprehensively to realize sustainable development. At present, the evaluation methods widely accepted and applied include ecological footprint, emergy analysis, emergy ecological footprint (Zhao et al., 2005), green GDP (He et al., 2016), comprehensive evaluation method (Cabello et al., 2014), etc. Eco-efficiency has been put forward as an index to analyze sustainable development (Schaltegger and Burritt, 2000), that is, the ratio of the value of services and products to the environmental impact. Its core idea is to exchange the maximum economic value with the minimum resource consumption and environmental pollution degree (Scholz and Wiek, 2005). The accounting methods of eco-efficiency can be summarized into three types: single ratio method, index system method and model method (Mandal, 2010; Victor et al., 2017; Yue et al., 2020). The three accounting methods have their advantages and disadvantages. The model method

mainly includes the ecological footprint method, data envelopment analysis (DEA) and some extension models of DEA (Hua et al., 2007; Yin et al., 2014; Li et al., 2019; Ren et al., 2020), while DEA has been widely used in recent years due to its unique advantages. Firstly, DEA requires relatively little information. Secondly, it does not need dimensional processing of original input-output data. Finally, it directly assigns weights to the indexes without the need to determine the weights artificially, which overcomes the influence of subjective factors on the results. At present, the theory of eco-efficiency has been constantly developed and improved and has been applied in many research fields (Kim et al., 2018; Xiang et al., 2020) with the integration of other methods, such as emergy analysis (EMA) (Wu et al., 2018; Cao et al., 2019), ecological footprint (He et al., 2016), life cycle assessment (LCA) (Park et al., 2016; Masuda, 2019), etc.

DEA model for accounting eco-efficiency needs to determine the inputs and outputs. Heretofore, gross domestic product (GDP) is the key indicator of output (Yin et al., 2014; Robaina-Alves et al., 2015). GDP did not consider the resources and environment loss cost, there are differences in the selection of undesirable outputs, and some pollutants in the discharge of "three wastes" are usually selected as the undesirable output (Li et al., 2019; Wang et al., 2020). The processing methods of undesirable output are different, such as undesirable output as an input method, reciprocal conversion method, directional distance function method and modified DEA model. The results of the different studies could not be compared. When evaluating regional eco-efficiency based on DEA model, most studies take GDP as the desirable output (Jin et al., 2014). But GDP ignores the depletion of resources and damage to the environment in the process of economic growth. As a supplement and improvement to GDP, GGDP refers to the GDP after deducting the value of resource consumption and environmental pollution loss, which overcomes the disadvantage of GDP not considering resource and environmental factors (Talberth and Bohara, 2006; Boyd, 2007). "Although some studies stated that the GGDP should be used in future regional-scale eco-efficiency measurements, these kinds of studies are few, especially in China" (He et al., 2016). He et al. (2016) used DEA model to evaluate the eco-efficiency of Jiangsu Province and took GGDP as the output. However, unreasonably, they still took pollutant emission which has been deducted from GGDP as undesirable output. In addition, for ease of calculation, they changed the nature of undesirable output by taking it as an input.

In order to make up for the above deficiencies and accurately evaluate the regional sustainability, the holistic eco-efficiency method has been built by aggregating emergy analysis (EMA), DEA and GGDP into an improved framework. By taking GGDP as the output after deducting undesirable output, the paper provides a theoretical basis for sustainable development decision making in Guizhou Province and a new way of thinking for a comprehensive evaluation of regional sustainable development level. This study aimed to comprehensively evaluate the sustainable development level of Guizhou Province by the new ecological efficiency framework and put forward suggestions for improvement.

## Methodology and methods

### *Study area*

Guizhou Province, with its fragile ecological environment and large mountainous area, is an important ecological barrier in the upper reaches of the Yangtze River and the Pearl River (*Figure 1*). At present, it faces major ecological problems such as soil

erosion, forest degradation, biodiversity reduction and water resources shortage. Under the background that the country attaches importance to the development of the west and further deepens the development of the west, the actual situation of the underdeveloped areas in China requires the region to develop its economy according to its own resource advantages in the future, so as to realize the regional sustainable development. Therefore, as an inland open economic pilot zone, it is particularly important to ensure the sustainable development of Guizhou. This paper made a preliminary evaluation of the sustainable development level of Guizhou Province with combined emergy and GGDP accounting, then used DEA to calculate the eco-efficiency. The research results can be used for reference in other areas.

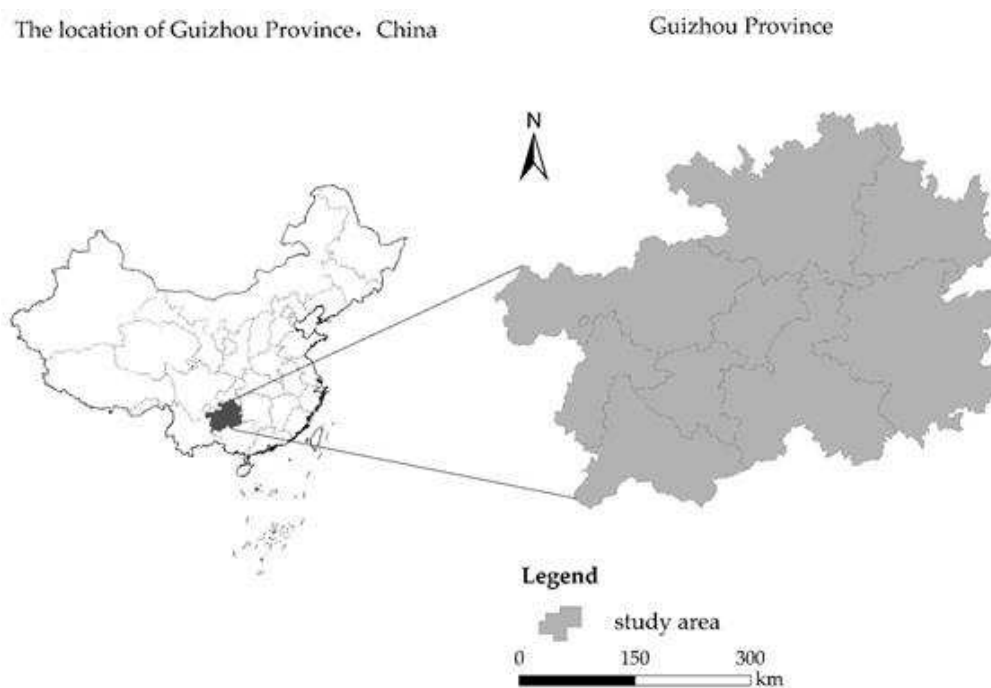


**Figure 1.** The location of Guizhou Province, China

### ***Emergy analysis***

The concept of emergy was proposed in the 1980s by Odum (1988), a famous American ecologist. It has been widely used by scholars to study and evaluate an urban ecological economic system, agricultural ecosystem and marine ecosystem (Odum, 1996, 2000; He et al., 2016; Wu et al., 2018; Cao et al., 2019). The solar emergy of each product and resource is calculated as follows:

$$E = M \times T \quad (\text{Eq.1})$$

where  $E$  is the emergy (sej);  $M$  is the available energy (J);  $T$  is the transformity of a product or a resource.

Emergy indicators can be used to comprehensively evaluate the sustainable development ability of the system based on emergy theory. Emergy evaluation indicators are shown in *Table 1*.

**Table 1.** Emergy evaluation indicators for Guizhou

Indicators	Expression
Renewable Resources	R
Nonrenewable Resources	N
Imports	IMP
Exports	EXP
Total Emergy Used	U=R+N+IMP-EXP
Emergy Yield Ratio (EYR)	EYR=(R+N+IMP)/IMP
Environmental loading ratio(ELR)	ELR=(U-R)/R
Emergy-based sustainability index (ESI)	ESI =EYR/ELR

### GGDP accounting based on emergy analysis

Gross domestic product (GDP) is an important indicator to measure and reflect the economic development level of a country or region. However, there are limitations in the accounting of GDP, which ignores the impact of human economic activities on resources and the environment. Green GDP (GGDP) makes up for the deficiency of GDP and includes the cost of resource consumption and environmental damage into the accounting, which can reflect the real wealth of the society and the idea of sustainable development. GGDP is calculated based on emergy analysis in the paper.

#### Total emergy

The core idea of emergy theory is to convert different kinds of resources or products into uniform units of emergy and then measure through solar transformity. The calculation formula of the total emergy of the system is as follows:

$$E = \sum_{i=1} E_i = \sum_{i=1} (M_i \times T) \tag{Eq.2}$$

where  $E$  is the total emergy of the system (sej);  $E_i$  is the total emergy (sej) of the  $i$ th resource or product;  $M_i$  is the raw data (sej) for the  $i$ th resource or product;  $T$  is the transformity of a product or a resource.

#### Emdollar value

Emdollar value refers to the amount of money equivalent to the emergy of an economic system when it is converted into money. Its calculation formula is the ratio of the emergy of resources or products to emergy/dollar ratio, namely

$$V_i = E_i / R \tag{Eq.3}$$

$$R = \sum_{j=1} E_j / GDP \tag{Eq.4}$$

where  $V_i$  is the emdollar value of the  $i$ th resource or product (\$);  $E_i$  is the total emergy of the  $i$ th resource or product (sej);  $R$  is emergy/dollar ratio (sej/\$);  $\sum_{j=1} E_j$  is the sum of the total emergy utilized by the system (including renewable environmental resources, nonrenewable environment resources, nonrenewable resources products, money flows).  $GDP$  is the gross domestic product (\$).

**GGDP**

The calculation formula of GGDP is as follows:

$$GGDP = GDP - \sum A - \sum B - \sum C \quad (\text{Eq.5})$$

where  $\sum A$  is the total emdollar value of nonrenewable natural resources;  $\sum B$  is the total emdollar value of nonrenewable resource products;  $\sum C$  is the total emdollar value of waste materials. The specific indicator system is shown in *Table 2*.

**Table 2.** Emergy analysis in Guizhou Province

Category	Item	Transformity <sup>a</sup> (sej/J)
Renewable natural resources	Solar radiation energy	1
	Rain chemical energy	623
	Rain geo-potential energy	15444
	Wind kinetic energy	8888
	Earth cycle energy	29000
Nonrenewable natural resources	Topsoil loss	74000
Renewable resource products	Hydropower	80000
	Cereal	148000
	Beans	690000
	Potato	83000
	Oil plants	690000
	Bast fiber plants	83000
	Sugarcane	84000
	Tobacco	84900
	Vegetables	83000
	Tea	200000
	Fruits	530000
	Meat	4000000
	Milk	2000000
	Eggs	2000000
	Honey	84000
	Aquatic products	2000000
	Forest products	44000
Nonrenewable resource products	Raw coal	40000
	Gasoline	66000
	Kerosene	66000
	Diesel	66000
	Fuel oil	54000
	Natural gas	53000
	Steels	1.40E+15
	Cement	2.07E+15
	Nitrogenous fertilizers	3.80E+15
	Phosphatic fertilizer	3.90E+15
	Potash fertilizers	1.10E+15
	Compound fertilizers	2.80E+15
	Pesticides	1.60E+15
	Plastic membranes	3.80E+14
	Currency flow	Import commodities
Foreign capital utilized		1.66E+12
Foreign exchange earnings from tourism		1.73E+12
Labor services		3.80E+05
Export commodities		1.66E+12
Waste material	Waste gas	4.80E+04
	Wastewater	8.60E+05
	Solid waste	1.80E+06

<sup>a</sup>Transformities are taken from Odum (1996, 2000)

### DEA model

Charnes et al. (1978) put forward the concept of Data Envelopment Analysis (DEA). The traditional CCR model and VRS model do not consider the slack of input and output. Tone (2001) proposed a non-radial and non-angular SBM model based on slack variables. However, the traditional SBM model cannot sort effective decision-making units. Based on this, Tone (2002) proposed the super- SBM model, which can effectively distinguish the conditions of effective decision units. Super efficiency SBM model is as follows:

$$\begin{aligned}
 \min \delta &= \frac{\frac{1}{m} \sum_{i=1}^m \bar{x}_i / x_{i0}}{\frac{1}{s} \sum_{r=1}^s \bar{y}_r / y_{r0}} \\
 \bar{x} &\geq \sum_{j=1, \neq 0}^n \lambda_j x_j \\
 \text{s.t.} \quad \bar{y} &\leq \sum_{j=1, \neq 0}^n \lambda_j y_j \\
 \bar{x} &\geq x_0, \bar{y} \leq y_0 \\
 \sum_{j=1, \neq 0}^n \lambda_j &= 1 \\
 \bar{y} &\geq 0, \lambda \geq 0
 \end{aligned} \tag{Eq.6}$$

where  $n$  is the number of decision-making units (DMU);  $m$  and  $s$  are the numbers of input indicators and output indicators;  $\bar{x}$  and  $\bar{y}$  are the slack variables of input and output;  $\lambda$  is a constant vector; If  $\delta \geq 1$ , DMU is said to be effective. If  $\delta \leq 1$ , DMU is said to be ineffective. The higher the  $\delta$ , the higher the ecological efficiency.

Technically and empirically, DEA has the following requirements on DMU: Firstly, DMU in the reference set should have the characteristics of the same type; Secondly, it is generally considered that the number of elements in reference set is not less than three times of the total number of input and output indicators (He et al., 2016). This paper will take Guizhou Province as the research object and carry out empirical analysis based on relevant data of Guizhou Province from 2000 to 2017, which meets the basic requirements of DEA. In the DEA efficiency evaluation process, capital stock and labor input are taken as inputs, and GGDP is taken as output. The efficiency is called green efficiency to distinguish it from traditional eco-efficiency. Among them, the capital stock is invested using the perpetual inventory method. The data calculation is based on the year 2000 and the estimation formula is:

$$K_t = (1 - \delta_t)K_{t-1} + I_t \tag{Eq.7}$$

where  $K_t$  is the capital stock at the end of the year;  $\delta_t$  is the depreciation rate;  $I_t$  is the actual investment. The investment indicator of the year is the total fixed capital formation.

Labor input is the total number of people employed at the end of each year. The desirable output is calculated by GGDP. In the calculation process, GDP is calculated based on the price of the year 2000. The GGDP has deducted the undesirable output

such as resource loss and environmental pollution, which directly solves the problem of the undesirable output. The ecological efficiency was calculated using DEA-SLVER Pro5.0 software developed by Tone (2002).

### Data source

Here we used data from 2000 to 2017 to evaluate the eco-efficiency of Guizhou Province. The basic data of renewable environmental resources, non-renewable environmental resources, renewable resource products, non-renewable resource products, monetary flow and the total number of employees employed at the end of each year were collected from the Guizhou Statistical Yearbooks 2001–2018 (which presents data from 2000 to 2017). And the basic data of waste gas, waste water and solid waste were obtained from the China Statistical Yearbooks 2001–2018. The total fixed capital formation data were collected from the National Bureau of Statistics website. The emergy calculation formula, emergy conversion coefficient and transformity used in this paper refer to the research results of Odum (1996, 2000) and Brown and Ulgiati (2016).

## Results and Discussions

### Emergy analysis

The sustainable development index of Guizhou from 2000 to 2017 was calculated to analyze the sustainability of the economic development of Guizhou Province based on emergy analysis. Emergy yield ratio (EYR) is defined as the ratio of the emergy used to the emergy input. This index is a standard to measure the production efficiency of a system. The higher the EYR is, the higher the production efficiency of the system will be. Although EYR had fluctuations in Guizhou Province, the overall declined during the past 18 years, with the maximum in 2002 and the minimum in 2017 (*Figure 2*). The main reason for the decrease of EYR was that the feedback input into Guizhou's economic system increased sharply, including the utilization of foreign capital and the import of resources.

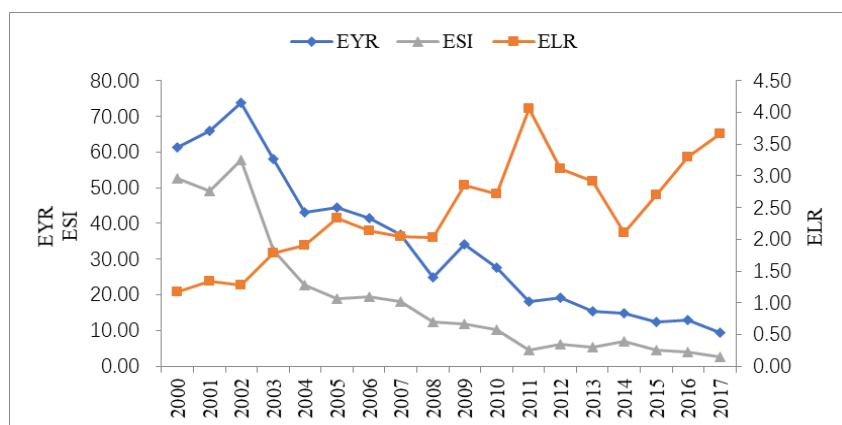


**Figure 2.** Trend of emergy-based indices in Guizhou Province from 2000 to 2017

Environmental loading ratio (ELR) is defined as the ratio of the total emergy of non-renewable resources to the total emergy of renewable resources. The indicator represents the environmental pressure of the system. The higher the ELR is, the greater

the environmental pressure of the system is. ELR increased volatility from 2000 to 2017 (Figure 2), among which ELR showed a significant decline from 2011 to 2014. However, the trend did not last long. An obvious upward trend from 2014 to 2017 indicated that the economic development of Guizhou Province put increasing pressure on the environment in recent years.

The overall change trends of EYR and ELR of Guizhou were similar to that of Changsha (Wu et al., 2018). Emergy-based sustainability index (ESI) is defined as the ratio of EYR to ELR. When ESI is between 1 and 10, it means that the economic system is dynamic and has development potential. When ESI is larger than 10, it is a sign of economic underdevelopment. When ESI is less than 1, it means that the economic system is consumption-oriented (Lei et al., 2020). The ESI and EYR was roughly the same trend (Figure 2). ESI was more than 10 before 2011 and that Guizhou Province was economically underdeveloped. After 2011, ESI was between 1 and 10. The economic system of Guizhou Province had the potential for development and there was room for improvement.

### Analysis of GGDP

Guizhou Province saw a marked increase in both GDP and GGDP from 2000 to 2017 (Figure 3). The growth rate of GDP was much faster than that of GGDP in recent ten years. He et al. (2016) reported similar results that traditional GDP grew faster, while green GDP grew slower and the gap between the two was growing. The ratio of GGDP to GDP was 78.32% in 2000, dropping to 60.60% in 2017. The declining ratio of GGDP to GDP in Guizhou Province is mainly due to the rising emdollar value of non-renewable resource products and wastes in recent years, especially non-renewable resource products (Figure 4). The emdollar value of non-renewable resource products surged by 16.68 times, and the emdollar value of wastes increased by 7.64 times. Raw coal was the non-renewable resource product with the largest consumption, accounting for more than half of non-renewable resource products during the study period. At the same time, solid waste accounted for more than 50% of the waste. This indicates that Guizhou Province consumed a large amount of non-renewable resource products and discharged a large amount of waste in the economic development process from 2000 to 2017. The rapid economic development came at the cost of resource consumption and environmental damage.

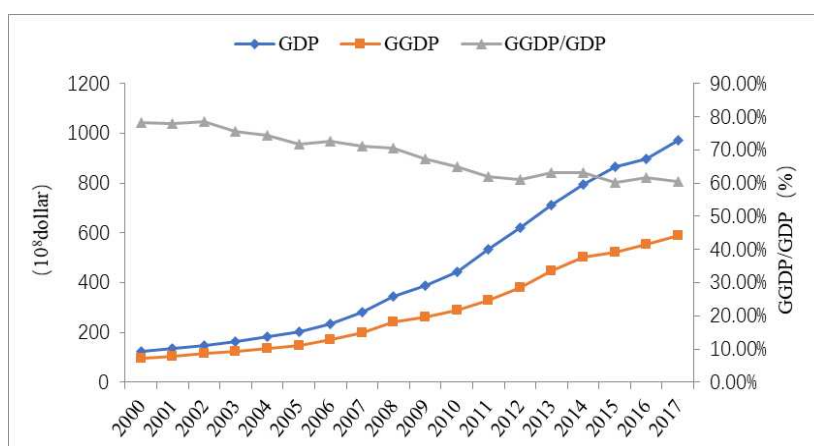
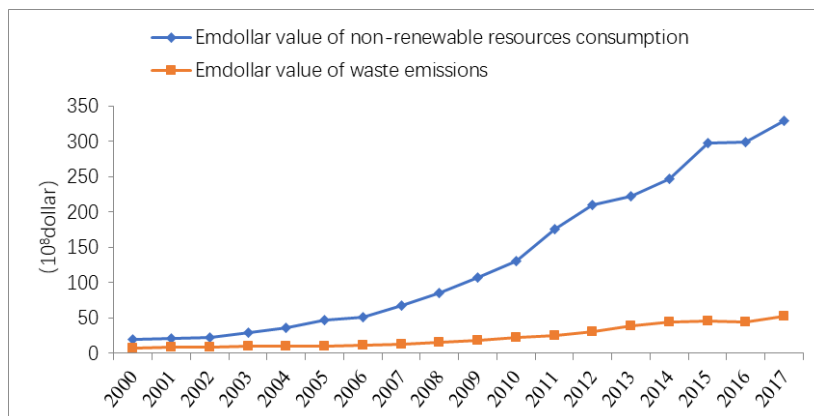


Figure 3. The trends of GDP and GGDP of Guizhou Province from 2000 to 2017





**Figure 4.** Emdollar value of non-renewable resources consumption and waste emissions of Guizhou Province from 2000 to 2017

## DEA

We used DEA-SOLVER Pro5.0 software to calculate the eco-efficiency (green efficiency) of Guizhou Province from 2000 to 2017. The results are shown in *Table 3*. The average green efficiency of Guizhou Province during 2000 - 2017 was 0.986, less than 1. Both capital input and labor input were redundant, and labor redundancy was more serious than capital redundancy. There was a shortfall in economic output. During the study period, the effective years of DEA were 2000, 2008, 2010, 2011, 2013, 2014 and 2017, and their green efficiency were all greater than 1, while the remaining years were ineffective. The effective years of Guizhou Province accounted for 39%, higher than Jiangsu Province with 20% (He et al., 2016). The highest green efficiency was 1.132 in 2000 and the lowest was 0.887 in 2004. It can be seen that the green efficiency of Guizhou Province was lower and its performance was poor in 2000-2006. Capital input was not redundant, but labor input was relatively redundant and GGDP output was insufficient during these six years. Excessive input of labor still showed the phenomenon of insufficient output, which indicates that the economic development input of Guizhou Province in this period was mainly low-quality labor force, and the high-quality labor force was relatively scarce, which failed to realize the optimal efficiency of labor input. The redundancy of labor input had been alleviated, and the green efficiency was higher than the previous stage since 2007. In the last five years, the green efficiency in 2013 and 2014 was more than 1 and ranked high. However, in 2015 and 2016, the green efficiency declined significantly, and capital and labor input utilization were insufficient, leading to the failure of optimal allocation of input factors and output factors. Green efficiency in 2017 ranked second, efficient utilization of capital and labor force and insufficient output indicate that there was still much room for improvement in the economic development of Guizhou Province. In the future, investment in scientific and technological innovation should be increased to achieve efficient and high-quality development.

To sum up, on the one hand, Guizhou Province needs to make full use of renewable energy, such as abundant hydropower, sunlight and wind, and strictly controls the discharge of waste. On the other hand, Guizhou should improve the quality of the labor force and formulate the policy of attracting talents. Since the 2015 "Guiyang International Big Data Industry Expo" was held in Guiyang, the capital of Guizhou

Province, the province has focused on the development of big data industry, which has brought vitality and opportunities to the economic development. Guizhou should seize this opportunity and follow a characteristic path of sustainable development based on big data. Besides, Guizhou should fully exploit rich tourism resources, focus on creating a "colorful Guizhou", and develop characteristic ecological tourism as a new economic growth point of Guizhou.

**Table 3.** The results of the super-SBM model of Guizhou Province from 2000 to 2017

DMU	Score	Rank	Capital excess	Labor excess	GGDP shortage
2000	1.132	1	42.876	201.709	0.000
2001	0.943	14	0.000	201.690	0.919
2002	0.935	15	0.000	239.753	0.952
2003	0.891	17	0.000	278.539	6.038
2004	0.887	18	0.000	319.461	6.090
2005	0.921	16	0.000	77.656	9.374
2006	0.948	13	0.000	86.481	5.369
2007	0.992	8	0.000	5.714	1.343
2008	1.025	4	48.470	0.000	0.000
2009	0.990	9	0.000	19.032	1.214
2010	1.014	6	0.000	49.670	0.000
2011	1.001	7	0.028	3.116	0.000
2012	0.989	11	0.000	1.682	3.974
2013	1.019	5	79.583	9.382	0.000
2014	1.032	3	0.000	0.000	15.667
2015	0.971	12	178.557	11.144	0.000
2016	0.990	10	58.760	7.963	0.000
2017	1.067	2	0.000	0.000	37.169
Mean	0.986	-	22.682	84.055	4.895

The comprehensive application of multiple sustainable development evaluation methods can complement each other's advantages and make up for the weak persuasive effect of single evaluation method, which can evaluate the status of the research area more comprehensively and point out the improvement direction for enhancing the regional sustainable development ability. The green GDP accounting based on emergy theory not only measures the consumption of non-renewable resource products, but also measures the pollution loss caused by waste discharge, indicating that the economic development of Guizhou Province is based on resource consumption and environmental pollution. DEA efficiency evaluation model further points out that DEA invalid years have insufficient utilization rate of capital input and labor input.

The green GDP excluding the undesirable output is selected as the output index, which provides a new idea for DEA efficiency evaluation to solve the undesirable output problem. The following aspects can be further studied in the later stage. Firstly, only the negative effects of non-renewable resource consumption and environmental pollution loss are considered in the process of calculating green GDP based on emergy theory. Since the positive effects of resource and environment improvement in Guizhou need to be highlighted, the later stage can try to explore the accounting in this aspect. Secondly, in DEA efficiency evaluation, further research will consider technological innovation input from the perspective of R&D intelligence input and capital input.

## Conclusions

This study applied the emergy analysis theory, GGDP and super-SBM model to comprehensively calculate the sustainable development level of the study region, and analyzed the deficiencies and improvement directions in the economic development from 2000 to 2017. The GGDP with undesirable output deducted is selected as the output, which provides a new idea for DEA efficiency evaluation to solve the problem of undesirable output.

First, based on the emergy evaluation indicators of Guizhou Province, it can be concluded that the environmental loading ratio of Guizhou presented an overall trend of increase mainly due to the increasing use of non-renewable resources from 2000 to 2017, while the emergy yield ratio and emergy-based sustainability index generally presented a trend of decline. The main reasons for the decline of productivity were the large increase in the utilization of foreign capital and the import of resources.

Second, GGDP and GDP from 2000 to 2017 in Guizhou Province simultaneously rose, but the growth rate of GGDP was less than that of GDP. The proportion of GGDP in GDP had been decreasing from 78.32% to 60.60%, mainly due to the dramatic increase in consumption of nonrenewable resource products and waste emissions, which had widened the gap between the GGDP and GDP.

Third, 2000-2017 was divided into two stages with 2008 as the cut-off point. The green efficiency of the second stage was higher on the whole than that of the first stage, and the ineffective years of DEA mostly fell in the first stage. There were seven years in which the green efficiency was greater than 1, that is, DEA was effective in Guizhou Province from 2000 to 2017. In the remaining eleven years, DEA was ineffective. In the ineffective years, there were redundant capital investment and redundant labor input, and the factor combination of input and output did not reach the optimal state.

**Acknowledgements.** This research was supported by the Natural Science Research project of Department of Education of Guizhou Province (Qian Jiao He KY Zi (2015)365), and University-level Research Fund of Guizhou University of Finance and Economics (2019XYB07). The authors are grateful to the colleague Jun-hong Zhao for helping me improve the text of this article.

## REFERENCES

- [1] Boyd, J. (2007): Nonmarket benefits of nature: what should be counted in green GDP? – *Ecological Economics* 61(4): 716-723.
- [2] Brown, M. T., Ugiati, S. (2016): Emergy assessment of global renewable sources. – *Ecological Modelling* 39: 148-156.
- [3] Cabello, J. M., Navarro, E., Prieto, F., Rodríguez, B., Ruiz, F. (2014): Multicriteria development of synthetic indicators of the environmental profile of the Spanish regions. – *Ecological Indicators* 39: 10-23.
- [4] Cao, L., Zhou, Z., Yi, Y., Huang, Y., Cao, G. (2019): Is metabolism in all regions of China performing well? - Evidence from a new DEA-Malmquist productivity approach. – *Ecological Indicators* 106: 105487.
- [5] Charnes, A., Cooper, W. W., Rhodes, E. (1978): Measuring the efficiency of decision making units. – *European Journal of Operational Research* 2(78): 429-444.
- [6] He, J., Wan, Y., Feng, L., Ai, J., Wang, Y. (2016): An integrated data envelopment analysis and emergy-based ecological footprint methodology in evaluating sustainable development, a case study of Jiangsu Province, China. – *Ecological Indicators* 70: 23-34.

- [7] Hua, Z., Bian, Y., Liang, L. (2007): Eco-efficiency analysis of paper mills along the Huai River: an extended DEA approach. – *Omega* 35(5): 578-587.
- [8] Jin, J., Zhou, D., Zhou, P. (2014): Measuring environmental performance with stochastic environmental DEA: The case of APEC economies. – *Ecological Modelling* 38: 80-86.
- [9] Kim, J., Jeon, E., Cho, S., Kim, H. (2018): The promotion of environmental management in the South Korean health sector—Case study. – *Sustainability* 10(6): 2081.
- [10] Lei, K., Wang, Z., Ton, S. (2008): Holistic emergy analysis of Macao. – *Ecological Engineering* 32: 30-43.
- [11] Li, X., Cai, Q., Yang, X. Y. (2019): Environmental efficiency assessment and difference analysis of industrial cluster districts in China. – *Applied Ecology and Environmental Research* 17(4): 9035-9049.
- [12] Mandal, S. K. (2010): Do undesirable output and environmental regulation matter in energy efficiency analysis? evidence from Indian cement industry. – *Energy Policy* 10: 6076-6083.
- [13] Masuda, K. (2019): Eco-Efficiency assessment of intensive rice production in Japan: joint application of life cycle assessment and data envelopment analysis. – *Sustainability* 11(19): 5368.
- [14] Odum, H. T. (1988): Self-organization, transformity, and information. – *Science* 242(4882): 1132.
- [15] Odum, H. T. (1996): *Environmental Accounting: Emery and Environmental Decision Making*. – John Wiley & Sons, New York.
- [16] Odum, H. T. (2000): Emery evaluation of an OTEC electrical power system. – *Energy* 25: 389-393.
- [17] Park, Y. S., Egilmez, G., Kucukvar, M. (2016): Emery and end-point impact assessment of agricultural and food production in the United States: A supply chain-linked Ecologically-based Life Cycle Assessment. – *Ecological Indicators* 62: 117-137.
- [18] Ren, W., Zhang, Z., Wang, Y., Xue, B., Chen, X. (2020): Measuring regional eco-efficiency in China (2003-2016): A “Full World” perspective and network data envelopment analysis. – *International Journal of Environmental Research and Public Health* 17(10): 3456.
- [19] Robaina-Alves, M., Moutinho, V., Macedo, P. (2015): A new frontier approach to model the eco-efficiency in European countries. – *Journal of Cleaner Production* 103: 562-573.
- [20] Schaltegger, S., Burritt, R. (2000): *Contemporary environmental accounting: issues, concepts and practice*. – Greenleaf Publishing, Sheffield, UK.
- [21] Scholz, R. W., Wiek, A. (2005): Operational eco-efficiency: comparing firms’ environmental investments in different domains of operation. – *Journal of Industrial Ecology* 4: 155-170.
- [22] Talberth, J., Bohara, A. K. (2006): Economic openness and green GDP. – *Ecological Economics* 58(4): 743-758.
- [23] Tone, K. (2001): A slacks-based measure of efficiency in data envelopment analysis. – *European Journal of Operational Research* 130(3): 498-509.
- [24] Tone, K. (2002): A slacks-based measure of super-efficiency in data envelopment analysis. – *European Journal of Operational Research* 143(1): 32-41.
- [25] Victor, M., Mara, M., Margarita, R. (2017): The economic and environmental efficiency assessment in EU cross-country: evidence from DEA and quantile regression approach. – *Ecological Indicators* 78: 85-97.
- [26] Wang, C., Hsu, H., Wang, Y., Nguyen, T. (2020): Eco-Efficiency assessment for some European countries using slacks-based measure data envelopment analysis. – *Applied Sciences* 10(5): 1760.
- [27] Wu, Y., Que, W., Liu, Y., Li, J., Cao, L., Liu, S., Zeng, G., Zhang, J. (2018): Efficiency estimation of urban metabolism via emergy, DEA of time-series. – *Ecological Indicators* 85: 276-284.

- [28] Xiang, H., Wang, Y., Huang, Q., Yang, Q. (2020): How much is the eco-efficiency of agricultural production in west China? Evidence from the village level data. – *International Journal of Environmental Research and Public Health* 17(11): 4049.
- [29] Yin, K., Wang, R., An, Q., Yao, L., Liang, J. (2014): Using eco-efficiency as an indicator for sustainable urban development: a case study of Chinese provincial capital cities. – *Ecological Indicators* 36: 665-671.
- [30] Yue, L., Xue, D., Draz, M. U., Ahmad, F., Li, J., Shahzad, F., Ali, S. (2020): The double-edged sword of urbanization and its nexus with eco-efficiency in China. – *International Journal of Environmental Research and Public Health* 17: 446.
- [31] Zhao, S., Li, Z. Z., Li, W. L. (2005): A modified method of ecological footprint calculation and its application. – *Ecological Modelling* 185: 65-75.

# THE EFFECT OF INCREASED NITROGEN LEVELS ON SOIL CO<sub>2</sub> EMISSION CAUSED BY MICROBIAL RESPIRATION IN THE RIPARIAN ZONE OF THE THREE GORGES RESERVOIR

HE, L. P. \* – LIN, J. J. – LAN, B. – DUAN, L. Y. – XU, Z. J. – LIAO, Y. H.

*Key Laboratory of Water Environment Evolution and Pollution Control in the Three Gorges Reservoir, Chongqing Three Gorges University, Chongqing 404100, China*

*\*Corresponding author  
e-mail: hlp\_weird@163.com*

(Received 9<sup>th</sup> Sep 2020; accepted 30<sup>th</sup> Nov 2020)

**Abstract.** The increase of atmospheric nitrogen deposition has greatly affected soil CO<sub>2</sub> emission caused by microbial respiration, probably resulting in the acceleration of global warming. However, the effect of atmospheric nitrogen deposition on soil CO<sub>2</sub> emission is not still entirely clear, especially in riparian zone ecosystems. In this study, we studied the riparian zone of the Three Gorges Reservoir after a 36-d soil incubation with four nitrogen species, including NH<sub>4</sub>Cl, NaNO<sub>3</sub>, CO(NH<sub>2</sub>)<sub>2</sub> and CO(NH<sub>2</sub>)<sub>2</sub> (28%), as well as NH<sub>4</sub>NO<sub>3</sub> (72%) with three nitrogen addition levels to the soil at 44.39, 88.77 and 133.16 μg N g<sup>-1</sup>. Soil cumulative carbon respiration was promoted by 13.37%, 21.55% and 27.59% with the nitrogen addition of 44.39, 88.77 and 133.16 μg N g<sup>-1</sup> soil, respectively, increasing linearly with the increase of nitrogen addition levels. However, it was not changed with the nitrogen species. In conclusion, soil cumulative carbon respiration increased with the nitrogen addition levels regardless of the nitrogen species. Thus, induced by atmospheric nitrogen deposition, soil CO<sub>2</sub> emission from riparian zone should not be ignored in the twenty-first century.

**Keywords:** *atmospheric nitrogen deposition, soil cumulative carbon respiration, the Yangtze River, nitrogen species*

## Introduction

Atmospheric nitrogen (N) deposition has increased more than 10-fold since the industrial revolution (Holland et al., 1999) and it will continuously do so in the coming decades (Galloway et al., 2008). The increase of atmospheric N deposition has greatly affected soil CO<sub>2</sub> emission caused by microbial respiration (He et al., 2018; Meyer et al., 2018), probably resulting in the acceleration of global warming. Therefore, assessing the effect of atmospheric N deposition increase on soil microbial respiration is an urgent issue.

A large number of studies have examined this scientific problem and found that atmospheric N deposition inhibits (Riggs and Hobbie, 2016; Li et al., 2017; Peng et al., 2020), promotes (Tu et al., 2013; Fang et al., 2017; Liang et al., 2018), or does not change (Peng et al., 2010; He et al., 2018; Zhao et al., 2020) soil microbial respiration in forest, grassland, pasture, cropland and wetland ecosystems. This dispute may be due to the difference of N addition species, N addition levels and soil properties. Firstly, inconsistent results were also discovered between the addition of ammonium and nitrate (Puri and Ashman, 1999; Min et al., 2011) and between that of inorganic and organic N (Ramirez et al., 2010; Du et al., 2014). Secondly, high level of ammonium addition relatively inhibits soil microbial respiration compared to that of nitrate (Min et al., 2011; Li et al., 2017) because the decline of soil acidity caused by ammonium addition is larger than that caused by nitrate addition. Finally, changed by N increase, soil properties such as pH

(Rousk et al., 2009; Chen et al., 2016; Li et al., 2017), dissolved organic carbon (DOC) (Wang et al., 2003; Chen et al., 2014; Eberwein et al., 2015) and Carbon (C):N ratio (Gong et al., 2019) are closely related to soil microbial respiration. Therefore, treated with different N species and levels, more soil ecosystems with different soil properties should be investigated for the accurate assessment of the effect of N increase on soil C loss by microbial respiration from the terrestrial ecosystem.

The riparian zone of the Three Gorges Reservoir (TGR) is the largest one in the world (Bao et al., 2015), locating in the third-largest N deposition area of the world. The atmospheric N flux in this area is even as high as 50 kg N ha<sup>-1</sup> a<sup>-1</sup> with the composition of 72% inorganic N and 28% organic N (Yuan et al., 2009; Zhang et al., 2020). The soil of the riparian zone is exposed to air when it comes out of water, which is conducive to the rapid propagation of aerobic microorganisms. Meanwhile, atmospheric N deposition will alleviate the N limitation of soil microbial metabolism, which may lead to a large amount of soil C respiration loss from the riparian zone (Chen et al., 2014; Kamble and Baath, 2016). Thus, the influence of N deposition on soil C loss by microbial respiration should be concerned in the riparian zone of the TGR.

In this study, we aimed to discuss the effect of atmospheric N deposition on soil CO<sub>2</sub> emission caused by microbial respiration based on a 36-d soil incubation executed by four N species with three N addition levels. We hypothesized that: (i) soil microbial respiration would be promoted by the increased N addition levels and the decreased soil C:N ratio; (ii) the N species had no significant effect on soil microbial respiration.

## Materials and methods

### *Site description and soil sampling*

The riparian zone of the TGR is located in the transection area of Chongqing and Hubei province, China. It is a north subtropical humid monsoonal climatic with an average annual temperature of 18.2°C and an average annual precipitation of 1053.15 mm (1981-2018, <https://power.larc.nasa.gov>). It has experienced continuous artificial drying-rewetting cycles since 2003. The area of its mainstream and tributaries is about 349 km<sup>2</sup> (He, 2011). A year is divided into the dry period and the flooding period, according to the fluctuation of the water level caused by the operation of the TGR and the dry period is about six months (Chen et al., 2019b). During the dry period, the soil of the riparian zone exposes to air, whereas during the flooding period, it is inundated by the water of the TGR.

Intact soil was randomly collected from the riparian zone of the TGR within the Wanzhou section (N30°47.28'~30°50.10', E108°21.35'~108°23.41', *Fig. 1*) by polypropylene containers (13.5 cm×10.02 cm×6.8 cm) in June 2017. After the sampling, the containers were sealed tightly, stored at 4°C and immediately transported to a laboratory within 24 h. Soil physicochemical properties are listed in *Table 1*.

### *Experimental design and soil incubation*

Nitrogen treatments consisted of four N species (NH<sub>4</sub>Cl, NaNO<sub>3</sub>, CO(NH<sub>2</sub>)<sub>2</sub>, CO(NH<sub>2</sub>)<sub>2</sub> (28%) plus NH<sub>4</sub>NO<sub>3</sub> (72%)) with three N levels (44.39, 88.77 and 133.16 µg N g<sup>-1</sup> soil). Meanwhile, a control without N treatment was set up. Three replicates were set up for both the control and the N treatments. In total, we incubated 39 jars ((4 × 3 + 1) × 3).



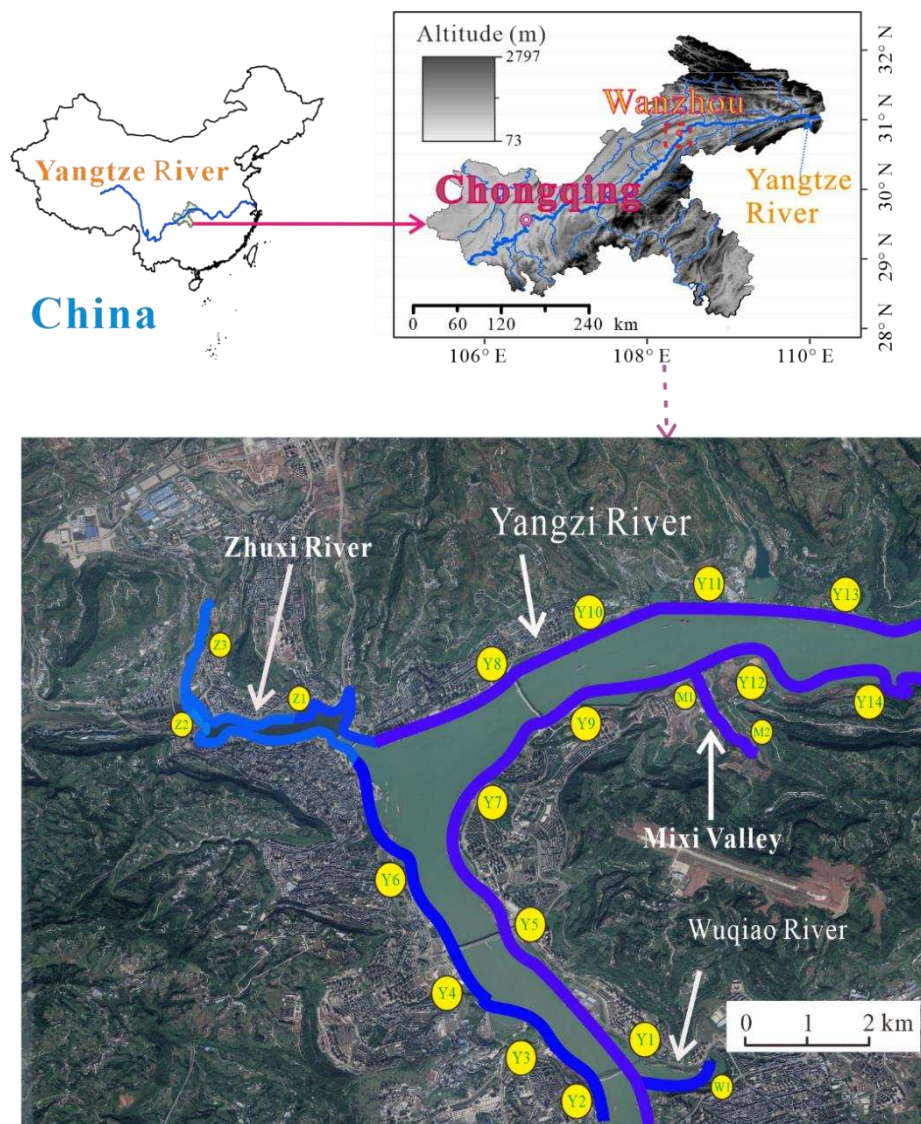


**Figure 1.** Soil sample sites

**Table 1.** Soil physicochemical properties in the riparian zone

Physicochemical properties	Values
pH	8.55 (0.03)
total C (mg g <sup>-1</sup> )	14.83 (0.24)
total N (mg g <sup>-1</sup> )	0.27 (0.01)
C/N ratio	54.36 (1.43)
DOC (mg kg <sup>-1</sup> )	61.38 (1.35)
Gravimetric water content (%)	40.00 (0.91)
Clay (%)	10.55 (5.25)
Silt (%)	23.40 (7.87)
Sand (%)	66.05 (15.23)

Note: values represent means of three replicates with standard deviation in parenthesis

First, 200 g soil was placed in 470 mL jars as quickly as possible and stabilized at ambient temperature for three days to avoid soil disturbance. After the stabilization, the



jars were added with 50 mL N solution (corresponding to the above N treatments) every 10 days and incubated in a growth chamber (SW-96P, Sang woo scientific, Korea) at 20°C in the dark for 36 days. After four times of N solution addition, the N addition levels were 44.39, 88.77 and 133.16 µg N g<sup>-1</sup> soil corresponding to the atmospheric N deposition fluxes of 50, 100 and 150 kg N ha<sup>-1</sup> a<sup>-1</sup>, respectively. The controls were added with four times of 50 mL deionized water. All samples were destructed for chemical analysis at the end of the incubation.

### ***Soil respiration rate and cumulative C respiration***

Soil respiration rate ( $R_s$ ) was measured on the day of 1, 2, 4, 6, 8, 15, 22, 29 and 36. Before gas sampling, each jar was sealed airtight to accumulate CO<sub>2</sub> for 1 h. The headspace gas was extracted by a 10 mL syringe equipped with a three-way stopcock (Discofix<sup>o</sup>, R C, B. Braun, Germany) through a septum in the middle of a lid at the start and the end of the CO<sub>2</sub> accumulative period. The collected gas was stored in a 5 ml syringe (GASTIGHT<sup>o</sup>, R #1005 Hamilton, Shimadzu, Japan), and then was injected into a gas chromatography (GC7890, Agilent Technologies, USA) for analysing the CO<sub>2</sub> concentration.  $R_s$  was calculated according to the method of Robertson et al. (1999).

Soil cumulative C respiration ( $C_{um}$ ) was calculated as Eq.1 (Lin et al., 2015):

$$C_{um(i+1)} = \frac{(R_{i+1} + R_i) \times (t_{i+1} - t_i) \times 24}{2} + C_{um(i)} \quad (\text{Eq.1})$$

where  $C_{um(i+1)}$  is  $C_{um}$  on the  $i+1$  sampling time (µg CO<sub>2</sub>-C g<sup>-1</sup> soil,  $i = 1$ ,  $C_{um(i)} = 0$ );  $R_{i+1}$  is  $R_s$  on the  $i+1$  sampling time (µg CO<sub>2</sub>-C g<sup>-1</sup> soil hr<sup>-1</sup>),  $t$  is the sample time (d).

### ***Soil physicochemical properties***

Soil pH was determined in a soil: water (1:2.5 w/w) slurry (Orion 3 Star, Thermo Electron, USA). Total C and N content were detected by an element analyser (EA5000, Elementar, Germany). DOC was extracted with 10 ml deionized water (soil: water=1:10 w/w), then filtered through a 0.45µm filter (ALBET). Finally, it was determined by a total organic carbon analyser (TOC-LCPH/CPN, Shimadzu, Japan). Soil gravimetric water content was measured by drying 1 g soil in a furnace at 105°C for 24 h, and then was weighted. The distribution of soil particle size was analysed by hydrometer method (Ashworth et al., 2001).

### ***Data analysis***

The differences of  $R_s$  among the soil treatments were assessed by a repeated measure ANOVA after normality test (Shapiro-Wilk test). An exponential decay function was applied to explore the relationship between  $R_s$  and the incubation time, and a linear function was used to detect the relationship between  $C_{um}$  and the varieties of soil chemical properties. A two-way ANOVA was used to determine the statistical differences of  $C_{um}$  and the soil chemical properties after the incubation among the N addition species and levels at  $P < 0.05$ . The influence factors of soil respiration in terms of soil chemical properties were analysed by a principal component analysis (PCA) based on the standardization datum of soil pH, C: N ratio, DOC, total C and total N after the incubation. All statistical analyses were performed by IBM SPSS 17.0 for windows.

## Results

### Soil CO<sub>2</sub> emission

Soil respiration rate decreased rapidly during the initial 6 d and then tended to be stable, which was accorded with the trend of exponential decay for all the N treatments (Fig. 2). N addition significantly promoted  $R_s$ , especially during 1-4 days ( $P < 0.05$ ). Compared to the control,  $C_{um}$  was promoted by 13.37% (i.e. 50 kg N ha<sup>-1</sup> a<sup>-1</sup>), 21.55% (i.e. 100 kg N ha<sup>-1</sup> a<sup>-1</sup>) and 27.59% (i.e. 150 kg N ha<sup>-1</sup> a<sup>-1</sup>) (Fig. 3,  $P < 0.05$ ), increasing linearly with the N addition levels for all the N species (Fig. 4,  $P < 0.05$ ).  $C_{um}$  was significantly influenced by the increase of N levels ( $P < 0.001$ ), but not changed with the N species (Table 2,  $P = 0.129$ ).

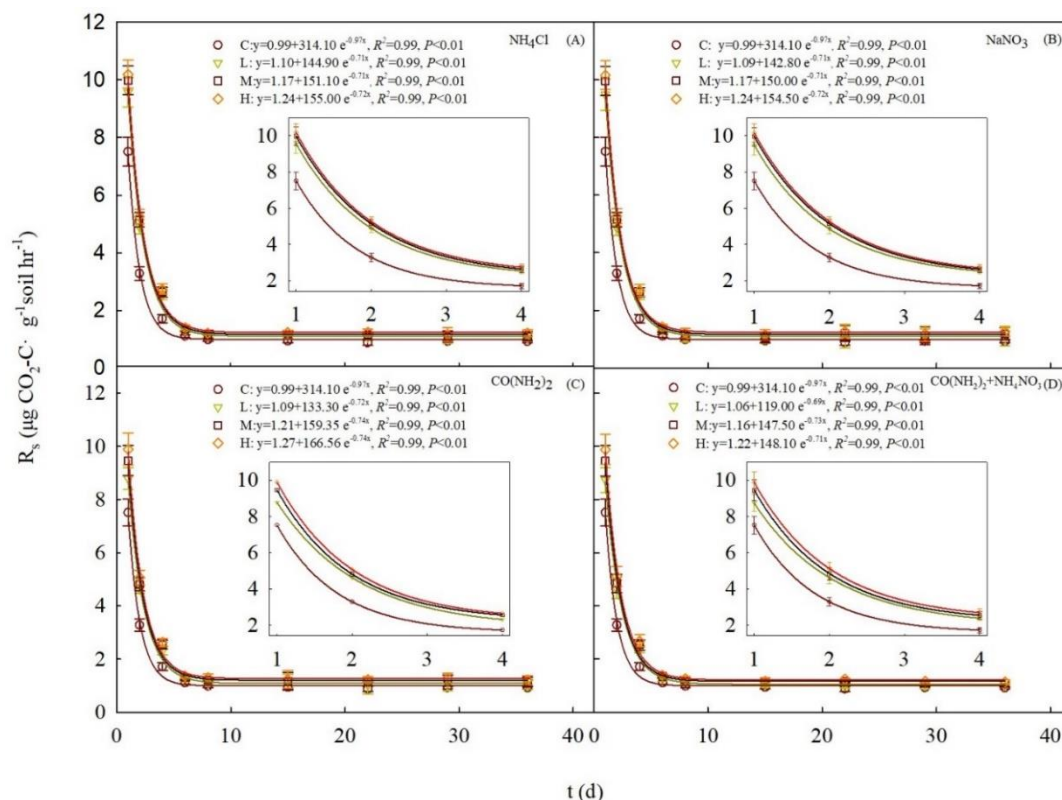


**Figure 2.** Soil respiration rate ( $R_s$ ) during the 36-d incubation. C, L, M and H represent the N addition of 0, 44.39, 88.77 and 133.16  $\mu\text{g N g}^{-1}$  soil, respectively. “y” and “x” represent  $R_s$  and the incubation time, respectively. Bars represent the standard deviations of the mean ( $n=3$ )

### The varieties of soil chemical properties

Compared to the control, soil pH significantly decreased under  $\text{NH}_4\text{Cl}$  (Table 3,  $P < 0.05$ ), but was not significantly changed under  $\text{NaNO}_3$ ,  $\text{CO}(\text{NH}_2)_2$  and  $\text{CO}(\text{NH}_2)_2$  plus  $\text{NH}_4\text{NO}_3$  ( $P > 0.05$ ) at the end of the incubation. Soil DOC increased by 3.85%, while total C decreased by 0.59% across the N treatments, not changed by the N addition species and levels (Table 2,  $P > 0.05$ ). Soil C: N ratio decreased and total N increased, with the N addition levels for all the N species (Tables 2 and 3,  $P < 0.001$ ).

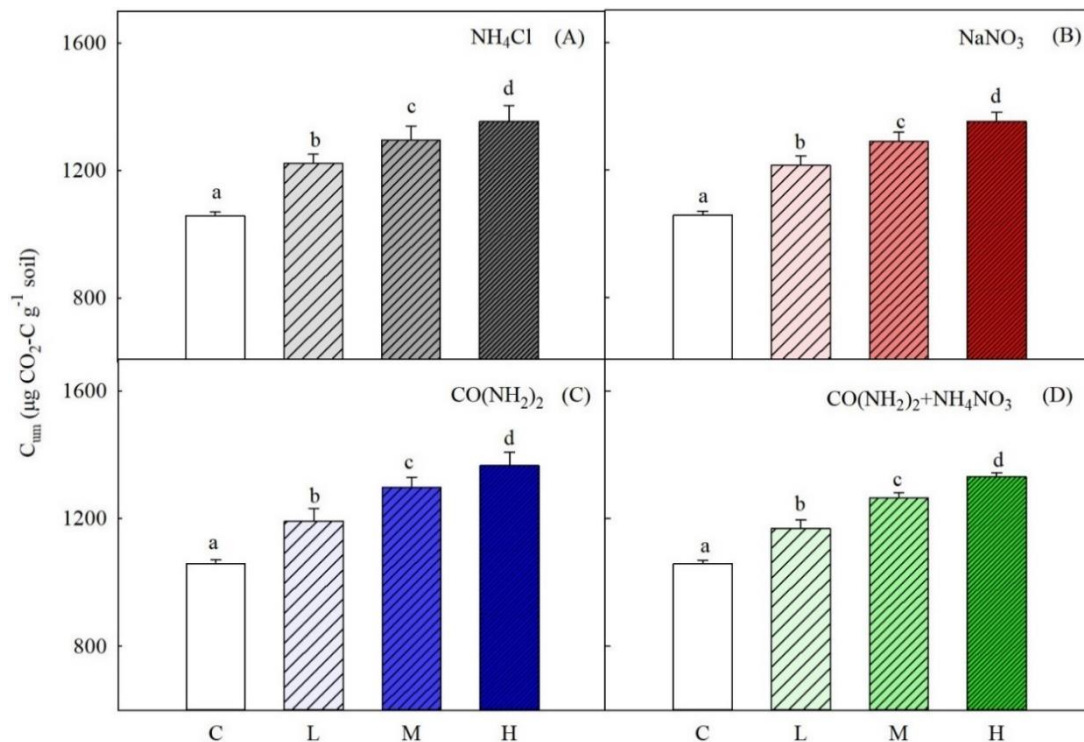


**Figure 3.** Cumulative soil C respiration ( $C_{um}$ ) under the N treatments after the 36-d incubation. C, L, M and H represent the N addition of 0, 44.39, 88.77 and 133.16  $\mu\text{g N g}^{-1}$  soil, respectively. Different lowercases represent the significant differences among the N addition levels ( $P < 0.05$ ); Bars represent the standard deviations of the mean ( $n=3$ )

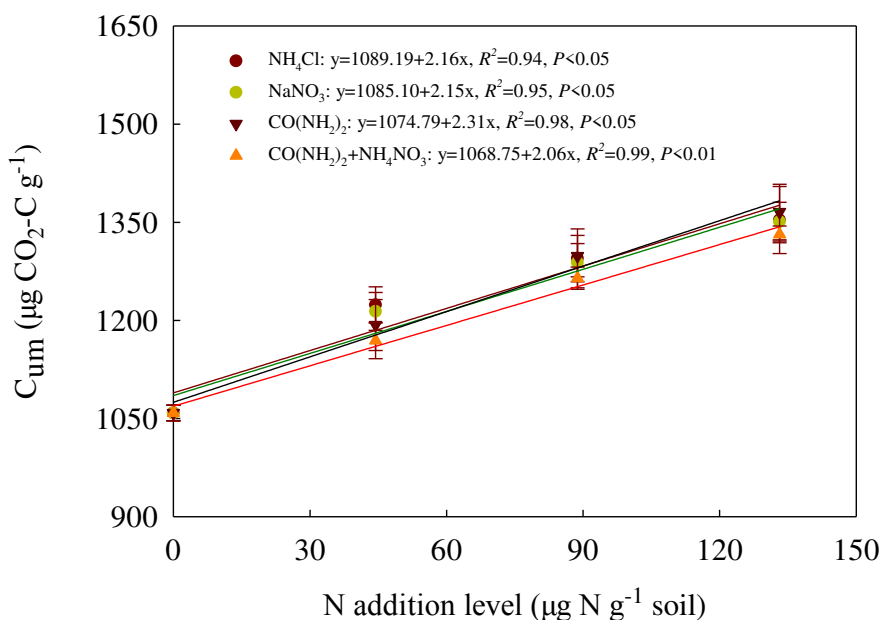


**Figure 4.** The relationship between Cumulative soil C respiration ( $C_{um}$ ) and the N addition levels. “y” and “x” represent  $C_{um}$  and the N addition level, respectively. Bars represent the standard deviations of the mean ( $n=3$ )

**Table 2.** Results from two-way ANOVA (*P* values) to test the effects of N addition species and levels on Cumulative soil C respiration (*C<sub>um</sub>*) and soil chemical properties

Response variable	Main effects		Interaction effects
	N species	N levels	N species*N levels
pH	0.001	0.523	0.245
Total C	0.300	0.990	1.000
Total N	<0.001	<0.001	0.003
C/N	1.000	<0.001	1.000
DOC	0.883	0.545	0.145
<i>C<sub>um</sub></i>	0.129	<0.001	0.925

Note: n=36

**Table 3.** Soil chemical properties at the end of the incubation

N species	Chemical properties	N levels (µg N g <sup>-1</sup> soil)			
		C	L	M	H
NH <sub>4</sub> Cl	pH	7.95 (0.08) a	7.75 (0.07) b	7.82 (0.01) b	7.78 (0.04) b
	Total C (mg g <sup>-1</sup> )	13.74 (0.29)	13.67 (0.19)	13.65 (0.24)	13.64 (0.22)
	Total N (mg kg <sup>-1</sup> )	270.33 (9.50) a	299.92 (9.10) b	329.51 (9.50) c	359.10 (9.50) d
	C/N	50.86 (1.07) a	45.61 (0.80) b	41.44 (0.60) c	37.99 (0.46) d
	DOC (mg kg <sup>-1</sup> )	57.19 (1.71)	59.91 (1.78)	60.03 (1.50)	57.46 (0.67)
NaNO <sub>3</sub>	pH	7.95 (0.08)	7.94 (0.04)	7.92 (0.06)	7.91 (0.08)
	Total C (mg g <sup>-1</sup> )	13.74 (0.29)	13.68 (0.19)	13.65 (0.20)	13.64 (0.25)
	Total N (mg kg <sup>-1</sup> )	270.33 (9.50) a	298.34 (10.02) b	331.28 (10.77) c	360.76 (10.21) d
	C/N	50.86 (1.07) a	45.60 (0.81) b	41.44 (0.58) c	38.00 (0.45) d
	DOC (mg kg <sup>-1</sup> )	57.19 (1.71)	58.85 (2.25)	60.54 (1.84)	58.76 (0.73)
CO(NH <sub>2</sub> ) <sub>2</sub>	pH	7.95 (0.08)	7.91 (0.13)	7.88 (0.05)	7.86 (0.04)
	Total C (mg g <sup>-1</sup> )	13.74 (0.29)	13.68 (0.28)	13.66 (0.19)	13.66 (0.28)
	Total N (mg kg <sup>-1</sup> )	270.33 (9.50) a	300.42 (8.90) b	331.67 (9.48) c	361.44 (10.27) d
	C/N	50.86 (1.07) a	45.63 (0.76) b	41.46 (0.62) c	38.04 (0.49) d
	DOC (mg kg <sup>-1</sup> )	57.19 (1.71)	60.13 (1.68)	60.52 (2.15)	58.56 (0.73)
CO(NH <sub>2</sub> ) <sub>2</sub> plus NH <sub>4</sub> NO <sub>3</sub>	pH	7.95 (0.08)	7.90 (0.12)	7.89 (0.07)	7.84 (0.08)
	Total C (mg g <sup>-1</sup> )	13.74 (0.29)	13.68 (0.20)	13.66 (0.21)	13.65 (0.20)
	Total N (mg kg <sup>-1</sup> )	270.33 (9.50) a	299.67 (9.17) b	328.77 (8.99) c	361.29 (9.13) d
	C/N	50.86 (1.07) a	45.62 (0.77) b	41.45 (0.57) c	38.41 (0.45) d
	DOC (mg kg <sup>-1</sup> )	57.19 (1.71)	60.39 (1.94)	58.23 (0.73)	59.27 (2.28)

Note: values represent means of three replicates with standard deviation in parenthesis. Means within each row followed by different lowercases represent a significant difference among the N levels (*P*<0.05)

### The relationship between *C<sub>um</sub>* and the varieties of soil chemical properties

Soil cumulative C respiration was negatively and linearly related to the varieties of soil C: N ratio and total C (Fig. 5A and E, *P*<0.01), while positively and linearly related to the varieties of soil total N (Fig. 5B, *P*<0.01). No significant correlations were observed between *C<sub>um</sub>* and the varieties of soil pH and DOC (Fig. 5C-D, *P*>0.05).

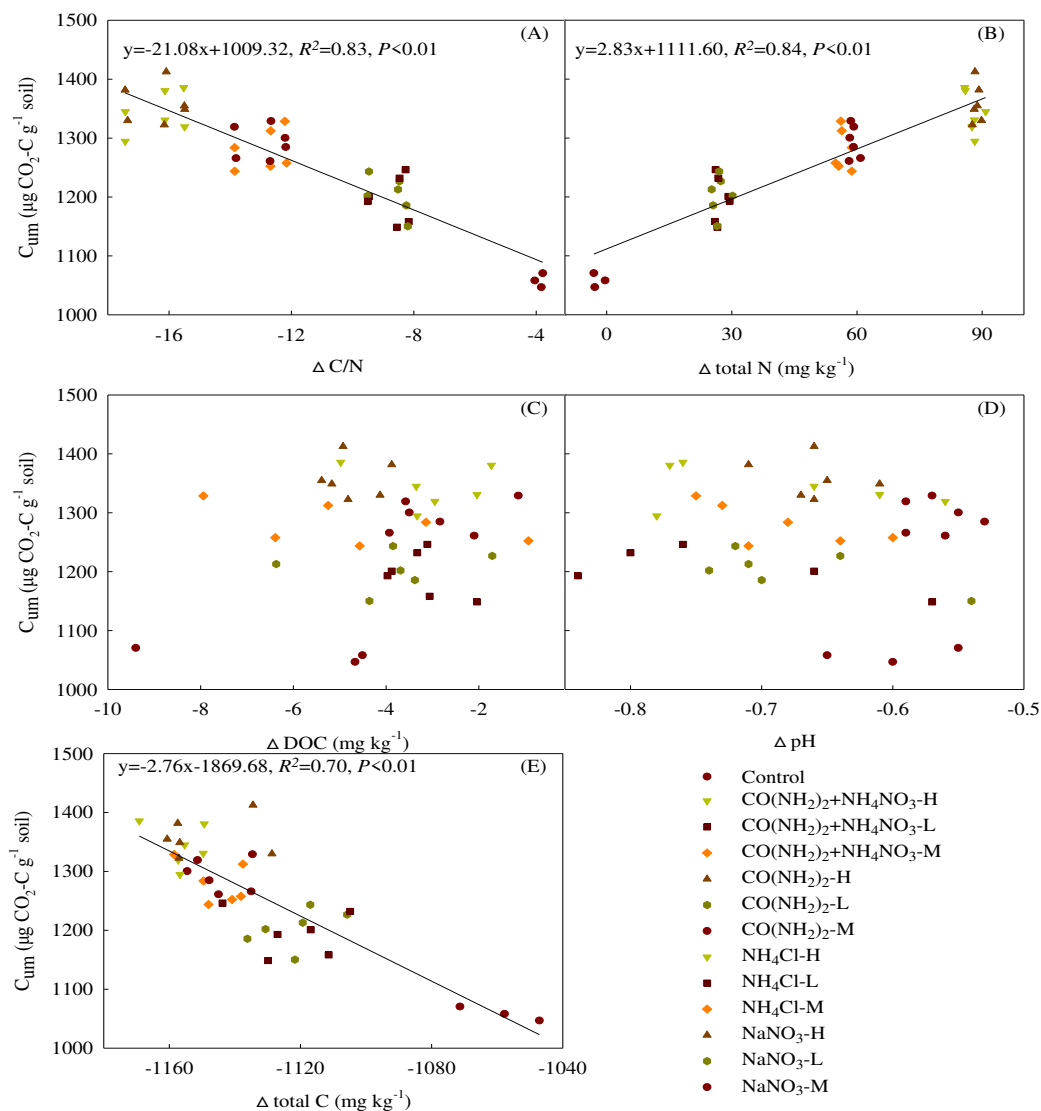


**Figure 5.** The relationships between Cumulative soil C respiration ( $C_{um}$ ) and the varieties of the chemical properties. L, M and H represent the N addition of 44.39, 88.77 and 133.16  $\mu\text{g N g}^{-1}$  soil, respectively. “ $\Delta$ ” represents the varieties of the soil chemical properties before and after the incubation. “y” and “x” represent the variables in horizontal and vertical coordinates

## Discussion

Our results indicated that  $C_{um}$  increased with the N addition levels by alleviating soil microbial N limitation regardless of the N species (Fig. 6), which would result in a large amount of soil CO<sub>2</sub> emission from riparian zone in the future. Thus, induced by atmospheric N deposition, soil CO<sub>2</sub> emission should be concerned in riparian zone.

### The effect of N addition levels on soil C/N ratio and CO<sub>2</sub> emission

Soil C: N ratio decreased with the N addition levels for all the N species (Table 2 and Table 3,  $P < 0.001$ ). Soil total N increased with the N addition levels ( $P < 0.001$ ), which is the reason for the results. Gong et al. (2019) discovered the same trend in a field study of temperate grassland.

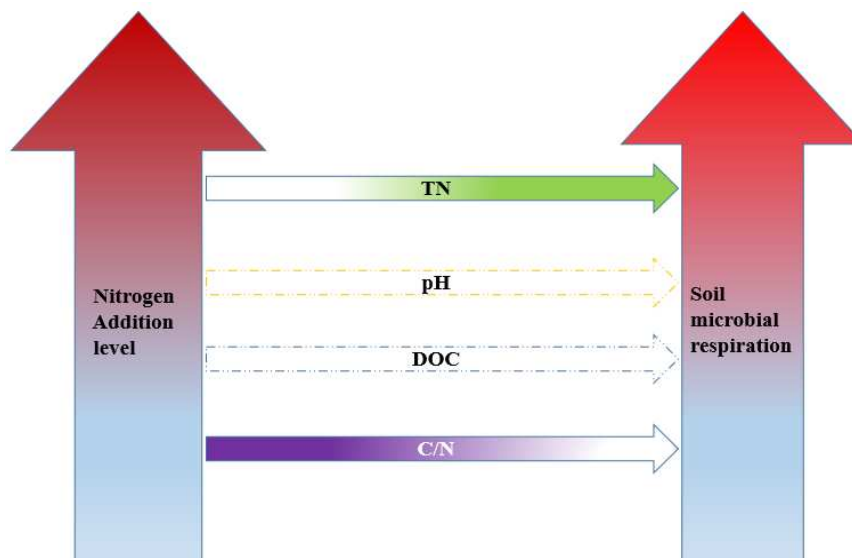


**Figure 6.** The response of soil microbial respiration to the N addition levels in terms of the varieties of soil chemical properties. The colours of the arrows changing from light to dark and from dark to light represent the increase and decrease of soil chemical properties, respectively. Dash and solid lines represent insignificant and significant relationships, respectively

As we hypothesized,  $C_{um}$  increased with the N addition levels for all the N species (Fig. 3,  $P < 0.05$ ). The alleviation of soil microbial nutrition limitation is the reason for the results, supported by the results of PCA (PC1 represented by soil C: N ratio and total N, Fig. 7) and the negatively linear relationship between  $C_{um}$  and the variety of soil C: N ratio (Fig. 5A,  $P < 0.01$ ). N addition increases soil microbial respiration in forest, pasture, grassland, wetland, cropland and bamboo ecosystems, which is consistent with our results; Meanwhile, inconsistent results of inhibiting and no effect were also observed (Table 4). The differences of soil pH and C and N availability (Leifeld et al., 2008; Eberwein et al., 2015) might be the reasons for the inconformity.

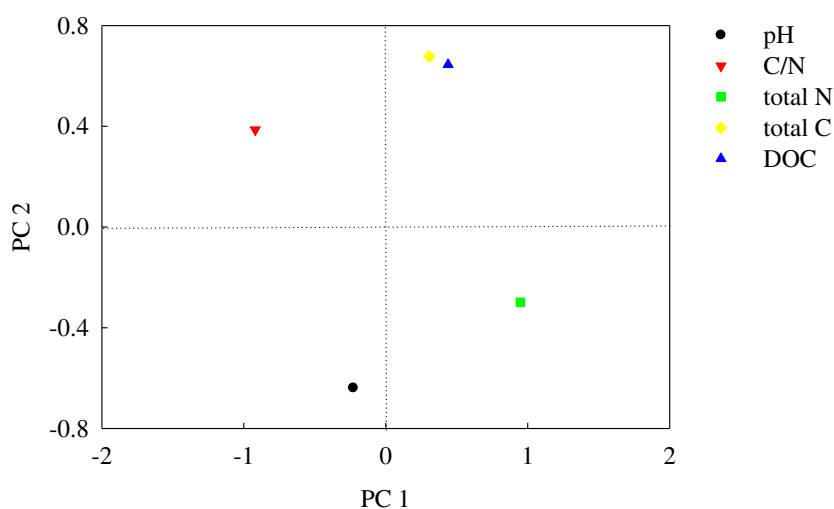


**Figure 7.** The principal component analysis (PCA) of the soil chemical properties after the incubation. The first two principal components (PCs) account for 41 and 30% of the variances in the soil chemical properties

**Table 4.** The response of soil respiration to N addition in different soil ecosystems

Ecosystems	N species	N levels (kg N ha <sup>-1</sup> yr <sup>-1</sup> )	Response of soil respiration to N addition	References
Forest	NH <sub>4</sub> NO <sub>3</sub>	100	-	(Zheng et al., 2018)
	NH <sub>4</sub> NO <sub>3</sub>	100	-	(Li et al., 2017)
	NH <sub>4</sub> NO <sub>3</sub>	50,150	-	(Peng et al., 2020)
	NH <sub>4</sub> NO <sub>3</sub>	50	+	(Sun et al., 2019)
	NH <sub>4</sub> NO <sub>3</sub>	50	+	(Chen et al., 2019a)
	CO(NH <sub>2</sub> ) <sub>2</sub>	50, 100	ns	(Zhao et al., 2018)
	NH <sub>4</sub> NO <sub>3</sub>	50,150,300	-	(Yan et al., 2020)
Pasture	NH <sub>4</sub> NO <sub>3</sub>	44.20	+	(Fang et al., 2017)
	CO(NH <sub>2</sub> ) <sub>2</sub>	100	+	(Wang et al., 2020)
	NH <sub>4</sub> NO <sub>3</sub>	<8, > 8	ns, -	(Wang et al., 2019b)
Grassland	CO(NH <sub>2</sub> ) <sub>2</sub>	100	-	(Riggs and Hobbie, 2016)
	CO(NH <sub>2</sub> ) <sub>2</sub>	100, 200, 300, 400, 500	-	(Zeng et al., 2018)
	CO(NH <sub>2</sub> ) <sub>2</sub>	100	-	(Riggs et al., 2015)
	CO(NH <sub>2</sub> ) <sub>2</sub>	23, 92	+	(Zhang et al., 2014)
	CO(NH <sub>2</sub> ) <sub>2</sub>	100	ns	(Zhao et al., 2020)
	NH <sub>4</sub> NO <sub>3</sub>	50, 100	ns	(He et al., 2018)
	NH <sub>4</sub> NO <sub>3</sub>	44.2	ns	(Fang et al., 2018)
Wetland	CO(NH <sub>2</sub> ) <sub>2</sub>	100, 200	-	(Wei et al., 2018)
	NH <sub>4</sub> NO <sub>3</sub>	0.10, 0.20, 0.50 mg N g <sup>-1</sup> soil	-	(Tao et al., 2013)
	NH <sub>4</sub> NO <sub>3</sub>	30, 60	-	(Min et al., 2011)
Bamboo	NH <sub>4</sub> NO <sub>3</sub>	40, 80	+	(Wang et al., 2019a)
	NH <sub>4</sub> NO <sub>3</sub>	50,100	+	(Tu et al., 2013)
Cropland	CO(NH <sub>2</sub> ) <sub>2</sub>	120, 180, 240	+	(Liang et al., 2018)
Riparian zone	NH <sub>4</sub> Cl, NaNO <sub>3</sub> , CO(NH <sub>2</sub> ) <sub>2</sub> , CO(NH <sub>2</sub> ) <sub>2</sub> (28%) plus NH <sub>4</sub> NO <sub>3</sub> (72%)	50, 100, 150	+	This study

Note: “+”, “-” and “ns” represent promoting, inhibiting and no significant impact of N addition on soil microbial respiration

### **The effect of N species on soil CO<sub>2</sub> emission**

Again, as we hypothesized, the N species had no effect on C<sub>um</sub> (Fig. 3 and Table 2, P>0.05), which is supported by the results of Ramirez et al. (2010). However, Du et al. (2014) discovered that inorganic and organic N addition inhibits and promotes soil microbial respiration, respectively, and Wang et al. (2018) found that the mixture addition of inorganic and organic N has higher inhibition on soil microbial respiration than single organic or inorganic N addition, which are inconsistent with our results. This inconformity should be due to the difference of soil microbial activity caused by different N addition species and soil properties (Geisseler and Scow, 2014), and needs a further study.

The results suggested that soil CO<sub>2</sub> emission from riparian zone caused by atmospheric N deposition should be considered when we establish an estimation model of soil CO<sub>2</sub> emission from the terrestrial ecosystem. In addition, for improving the ecological effect of the TGR, land management measures should be taking to reduce exogenous N input to the riparian zone during the dry period.

## Conclusion

This study discussed the effect of nitrogen increase on soil carbon dioxide emission caused by microbial respiration in the riparian zone of the Three Gorges Reservoir based on a 36-d soil incubation. The increase of the nitrogen addition levels decreased soil carbon: nitrogen ratio and promoted soil microbial respiration regardless of the nitrogen species. The findings suggest that, induced by atmospheric nitrogen deposition, soil carbon dioxide emission should be concerned in riparian zone. However, a long-term soil incubation should be launched for the better understanding of the effect of exogenous nitrogen input on soil microbial carbon dioxide emission. Meanwhile, this study only discussed the effect of nitrogen increase on soil microbial respiration in terms of soil chemical properties; the deep microbial mechanism should be discussed in the future.

**Acknowledgments.** This work was supported by the National Natural Science Foundation of China (31770529); Program of Chongqing Science and Technology Commission (cstc2018jcyjAX0813); the Science and Technology Research Program of Chongqing Municipal Education Commission (KJ1710260, KJQN201801233, KJZD-K201801201); the Chongqing Municipal Key Laboratory of Institutions of Higher Education (WEPKL2016LL-03).

## REFERENCES

- [1] Ashworth, J., Keyes, D., Kirk, R., Lessard, R. (2001): Standard procedure in the hydrometer method for particle size analysis. – *Communications in Soil Science and Plant Analysis* 32(56): 633-642.
- [2] Bao, Y., Gao, P., He, X. (2015): The water-level fluctuation zone of Three Gorges Reservoir - a unique geomorphological unit. – *Earth-science Reviews* 150: 14-24.
- [3] Chen, R., Senbayram, M., Blagodatsky, S., Myachina, O., Dittert, K., Lin, X., Blagodatskaya, E., Kuzyakov, Y. (2014): Soil C and N availability determine the priming effect: microbial N mining and stoichiometric decomposition theories. – *Global Change Biology* 20(7): 2356-2367.
- [4] Chen, D., Li, J., Lan, Z., Hu, S., Bai, Y., Niu, S. (2016): Soil acidification exerts a greater control on soil respiration than soil nitrogen availability in grasslands subjected to long-term nitrogen enrichment. – *Functional Ecology* 30(4): 658-669.
- [5] Chen, F., Yan, G., Xing, Y., Zhang, J., Wang, Q., Wang, H., Huang, B., Hong, Z., Dai, G., Zheng, X. (2019a): Effects of N addition and precipitation reduction on soil respiration and its components in a temperate forest. – *Agricultural and Forest Meteorology* 271: 336-345.
- [6] Chen, X., Zhang, S., Liu, D., Yu, Z., Zhou, S., Li, R., Liu, Z., Lin, J. (2019b): Nutrient inputs from the leaf decay of *Cynodon dactylon* (L.) Pers in the water level fluctuation zone of a Three Gorges tributary. – *Science of The Total Environment* 688: 718-723.
- [7] Du, Y., Guo, P., Liu, J., Wang, C., Yang, N., Jiao, Z. (2014): Different types of nitrogen deposition show variable effects on the soil carbon cycle process of temperate forests. – *Global Change Biology* 20(10): 3222-3228.



- [8] Eberwein, J. R., Oikawa, P. Y., Allsman, L. A., Jenerette, G. D. (2015): Carbon availability regulates soil respiration response to nitrogen and temperature. – *Soil Biology and Biochemistry* 88: 158-164.
- [9] Fang, C., Ye, J. S., Gong, Y., Pei, J., Yuan, Z., Xie, C., Zhu, Y., Yu, Y. (2017): Seasonal responses of soil respiration to warming and nitrogen addition in a semi-arid alfalfa-pasture of the Loess Plateau, China. – *Science of The Total Environment* 590-591: 729-738.
- [10] Fang, C., Li, F., Pei, J., Ren, J., Gong, Y., Yuan, Z., Ke, W., Zheng, Y., Bai, X., Ye, J. (2018): Impacts of warming and nitrogen addition on soil autotrophic and heterotrophic respiration in a semi-arid environment. – *Agricultural and Forest Meteorology* 248: 449-457.
- [11] Galloway, J. N., Townsend, A. R., Erisman, J. W., Bekunda, M., Cai, Z., Freney, J. R., Martinelli, L. A., Seitzinger, S. P., Sutton, M. A. (2008): Transformation of the nitrogen cycle: recent trends, questions, and potential solutions. – *Science* 320(5878): 889-892.
- [12] Geisseler, D., Scow, K. M. (2014): Long-term effects of mineral fertilizers on soil microorganisms - A review. – *Soil Biology and Biochemistry* 75: 54-63.
- [13] Gong, S., Zhang, T., Guo, J. (2019): Warming and nitrogen addition change the soil and soil microbial biomass C:N:P stoichiometry of a meadow steppe. – *International Journal of Environmental Research and Public Health* 16(15): 2705.
- [14] He, X. B. (2011): Preliminary study on soil erosion at the water-level-fluctuating zone of the Three Gorges Reservoir. – *Research of Soil and Water Conservation* 18(06): 190-195.
- [15] He, Y., Qi, Y., Dong, Y., Peng, Q., Guo, S., Yan, Z., Li, Z., Wang, L. (2018): Effects of changing C and N availability on soil respiration dynamics in a temperate grassland in northern China. – *Geoderma* 329: 20-26.
- [16] Holland, E. A., Dentener, F. J., Braswell, B. H., Sulzman, J. M. (1999): Contemporary and pre-industrial global reactive nitrogen budgets. – *Biogeochemistry* 46(3): 7-43.
- [17] Kamble, P. N., Baath, E. (2016): Comparison of fungal and bacterial growth after alleviating induced N-limitation in soil. – *Soil Biology and Biochemistry* 103: 97-105.
- [18] Leifeld, J., Zimmermann, M., Fuhrer, J. (2008): Simulating decomposition of labile soil organic carbon: effects of pH. – *Soil Biology and Biochemistry* 40(12): 2948-2951.
- [19] Li, Y., Sun, J., Tian, D., Wang, J., Ha, D., Qu, Y., Jing, G., Niu, S. (2017): Soil acid cations induced reduction in soil respiration under nitrogen enrichment and soil acidification. – *Science of The Total Environment* 615: 1535-1546.
- [20] Liang, G., Cai, A., Wu, H., Wu, X., Cai, D. (2018): Soil biochemical parameters in the rhizosphere contribute more to changes in soil respiration and its components than those in the bulk soil under nitrogen application in croplands. – *Plant and Soil* 449(8): 681-687.
- [21] Lin, J., Zhu, B., Cheng, W. (2015): Decadally cycling soil carbon is more sensitive to warming than faster-cycling soil carbon. – *Global Change Biology* 21(12): 4602-4612.
- [22] Meyer, N., Welp, G., Rodionov, A., Borchard, N., Martius, C., Amelung, W. (2018): Nitrogen and phosphorus supply controls soil organic carbon mineralization in tropical topsoil and subsoil. – *Soil Biology and Biochemistry* 119: 152-161.
- [23] Min, K., Kang, H., Lee, D. (2011): Effects of ammonium and nitrate additions on carbon mineralization in wetland soils. – *Soil Biology and Biochemistry* 43(12): 2461-2469.
- [24] Peng, Q., Dong, Y., Qi, Y., Xiao, S., He, Y., Ma, T. (2010): Effects of nitrogen fertilization on soil respiration in temperate grassland in Inner Mongolia, China. – *Environmental Earth Sciences* 62(6): 1163-1171.
- [25] Peng, Y., Song, S., Li, Z., Li, S., Chen, G., Hu, H., Xie, J., Chen, G., Xiao, Y., Liu, L. (2020): Influences of nitrogen addition and aboveground litter-input manipulations on soil respiration and biochemical properties in a subtropical forest. – *Soil Biology and Biochemistry* 142: 107694.
- [26] Puri, G., Ashman, M. R. (1999): Microbial immobilization of <sup>15</sup>N-labelled ammonium and nitrate in a temperate woodland soil. – *Soil Biology and Biochemistry* 31(6): 929-931.

- [27] Ramirez, K. S., Craine, J. M., Fierer, N. (2010): Nitrogen fertilization inhibits soil microbial respiration regardless of the form of nitrogen applied. – *Soil Biology and Biochemistry* 42(12): 2336-2338.
- [28] Riggs, C. E., Hobbie, S. E. (2016): Mechanisms driving the soil organic matter decomposition response to nitrogen enrichment in grassland soils. – *Soil Biology and Biochemistry* 99: 54-65.
- [29] Robertson, G. P., Coleman, D. C., Bledsoe, C. S., Sollins, P. (1999): Standard soil methods for long-term ecological research. – Oxford University Press, New York.
- [30] Rousk, J., Brookes, P. C., Baath, E. (2009): Contrasting soil pH effects on fungal and bacterial growth suggest functional redundancy in carbon mineralization. – *Applied and Environmental Microbiology* 75(6): 1589-1596.
- [31] Sun, S., Wu, Y., Zhang, J., Wang, G., Deluca, T. H., Zhu, W., Li, A., Duan, M., He, L. (2019): Soil warming and nitrogen deposition alter soil respiration, microbial community structure and organic carbon composition in a coniferous forest on eastern Tibetan Plateau. – *Geoderma* 353: 283-292.
- [32] Tao, B., Song, C., Guo, Y. (2013): Short-term effects of nitrogen additions and increased temperature on wetland soil respiration, Sanjiang Plain, China. – *Wetlands* 33(4): 727-736.
- [33] Tu, L. H., Hu, T. X., Zhang, J., Li, X. W., Hu, H. L., Liu, L., Xiao, Y. L. (2013): Nitrogen addition stimulates different components of soil respiration in a subtropical bamboo ecosystem. – *Soil Biology and Biochemistry* 58: 255-264.
- [34] Wang, W., Dalal, R. C., Moody, P. W., Smith, C. J. (2003): Relationships of soil respiration to microbial biomass, substrate availability and clay content. – *Soil Biology and Biochemistry* 35(2): 273-284.
- [35] Wang, Q., Liu, S., Wang, Y., Tian, P., Sun, T. (2018): Influences of N deposition on soil microbial respiration and its temperature sensitivity depend on N type in a temperate forest. – *Agricultural and Forest Meteorology* 260-261: 240-246.
- [36] Wang, J., Fu, X., Zhang, Z., Li, M., Cao, H., Zhou, X., Ni, H., Wang, X. (2019a): Responses of soil respiration to nitrogen addition in the Sanjiang Plain wetland, northeastern China. – *Plos One* 14(1): e0211456.
- [37] Wang, J., Song, B., Ma, F., Tian, D., Li, Y., Yan, T., Quan, Q., Zhang, F., Li, Z., Wang, B. (2019b): Nitrogen addition reduces soil respiration but increases the relative contribution of heterotrophic component in an alpine meadow. – *Functional Ecology* 33(11): 2239-2253.
- [38] Wang, Y., Wang, D., Shi, B., Sun, W. (2020): Differential effects of grazing, water, and nitrogen addition on soil respiration and its components in a meadow steppe. – *Plant and Soil* 447(1): 581-598.
- [39] Wei, L., Su, J., Jing, G., Zhao, J., Liu, J., Cheng, J., Jin, J. (2018): Nitrogen addition decreased soil respiration and its components in a long-term fenced grassland on the Loess Plateau. – *Journal of Arid Environments* 152: 37-44.
- [40] Xu, W., Zhao, Y., Liu, X., Dore, A. J., Zhang, L., Liu, L., Cheng, M. (2018): Atmospheric nitrogen deposition in the Yangtze River basin: spatial pattern and source attribution. – *Environmental Pollution* 232: 546-555.
- [41] Yan, W., Chen, X., Peng, Y., Zhu, F., Zhen, W., Zhang, X. (2020): Response of soil respiration to nitrogen addition in two subtropical forest types. – *Pedosphere* 30: 478-486.
- [42] Yuan, L., Zhou, X. B., Gu, X. Y. (2009): Temporal and spatial variation of atmospheric wet nitrogen deposition in typical areas of Chongqing. – *Acta Ecologica Sinica* 29(11): 6095-6101.
- [43] Zeng, W., Chen, J., Liu, H., Wang, W. (2018): Soil respiration and its autotrophic and heterotrophic components in response to nitrogen addition among different degraded temperate grasslands. – *Soil Biology and Biochemistry* 124: 255-265.
- [44] Zhang, C., Niu, D., Hall, S. J., Wen, H., Li, X., Fu, H., Wan, C., Elser, J. J. (2014): Effects of simulated nitrogen deposition on soil respiration components and their temperature sensitivities in a semiarid grassland. – *Soil Biology and Biochemistry* 75: 113-123.

- [45] Zhang, L., Tian, M., Peng, C., Fu, C., Yang, F. (2020): Nitrogen wet deposition in the Three Gorges Reservoir area: Characteristics, fluxes, and contributions to the aquatic environment. – *Science of The Total Environment* 738: 140309.
- [46] Zhao, B., Wang, J. S., Cao, J., Xiu, H., Gadow, K. V. (2018): Inconsistent autotrophic respiration but consistent heterotrophic respiration responses to 5-years nitrogen addition under natural and planted *pinus tabulaeformis* forests in northern China. – *Plant and Soil* 429(1): 375-389.
- [47] Zhao, X., Li, Y., Xie, Z., Li, P. (2020): Effects of nitrogen deposition and plant litter alteration on soil respiration in a semiarid grassland. – *Science of The Total Environment* 740: 139634.
- [48] Zheng, S., Bian, H., Quan, Q., Xu, L., Chen, Z., He, N. (2018): Effect of nitrogen and acid deposition on soil respiration in a temperate forest in China. – *Geoderma* 329: 82-90.

## EFFECT OF STRAW SUBSTITUTING PARTIAL MINERAL N FERTILIZER ON N DISTRIBUTION OF MAIZE PLANTS AND SOIL IN NORTHEAST CHINA

LIU, J. H.<sup>1,2</sup> – GENG, Y. H.<sup>1</sup> – LI, J.<sup>1</sup> – CAO, G. J.<sup>1\*</sup> – ZHANG, Z. Q.<sup>1</sup>

<sup>1</sup>*College of Resources and Environment, Jilin Agricultural University, Changchun, Jilin 130118, P. R. China*

<sup>2</sup>*National experimental teaching demonstration center for agricultural resources and environment, Jilin Agricultural University, Changchun, Jilin 130118, P. R. China  
(phone: +86-0431-8453-2955)*

*\*Corresponding author  
e-mail: cgj72@126.com*

(Received 11<sup>th</sup> Sep 2020; accepted 30<sup>th</sup> Nov 2020)

**Abstract.** Reducing mineral N fertilizer application rate and improving N use efficiency is important for sustainable agriculture. Whether straw return could substitute partial mineral N fertilizer in the applying year is still not conclusive in the case of spring corn planting in Northeast China. This work was conducted to investigate the optimal substitution rate through a field experiment with no fertilization (CK), 100% mineral N (IF), 25%/50%/75%/100% straw application combined with reduced mineral N fertilizer (S25/ S50/ S75/ S100) at a total of 240 kg N/hm<sup>2</sup> application rate in Jilin Province, Northeast China. The results showed that there was no significant difference in corn yield between straw application treatments and IF except for S100, which was 11.1% lower. Compared to IF, corn straw application did not affect N uptake amount and nitrogen harvest index ( $p > 0.05$ ), while S75 obviously increased N use efficiency by 29.6%. Straw application decreased NO<sub>3</sub><sup>-</sup>-N content and resisted downward migration in the soil profile. In conclusion, integrated application of 75% corn straw with reduced mineral N fertilizer at a total of 240 kg N/hm<sup>2</sup> was a reasonable fertilization practice as it reduced NO<sub>3</sub><sup>-</sup>-N content and prevented leaching in soil profile as well as increased N use efficiency without negative effect on corn yield.

**Keywords:** *yield, equal N application rate, NH<sub>4</sub><sup>+</sup>-N, NO<sub>3</sub><sup>-</sup>-N, nitrogen use efficiency*

### Introduction

Nitrogen, as one of the three essential nutrient elements for crop production, plays an important role in the growth of stems, leaves and grains as it is the main component of protein. In order to obtain high crop yield, enough nitrogen should be supplied to plants during their growth. Mineral nitrogen is extensively used for crop production worldwide and urea is the most commonly used in China (Zhu et al., 2002). While sufficient application of mineral nitrogen fertilizer increases crop yield and quality, its negative impacts on the environment have been documented, such as soil acidification and compaction (Guo et al., 2010; Cai et al., 2015), eutrophication of surface water (Zhang et al., 2011), contamination of groundwater (Hillin et al., 2003; De Paz et al., 2004), accelerating global warming by greenhouse gases emission (Galloway et al., 2003; Battye et al., 2017).

Spring corn is one of the dominant crops in Northeast China, where one third of corn grains in China is produced. The most common fertilization practice in this area is to use 100% mineral N fertilizer. During 1980 to 2010, the application rate of nitrogen for corn in this area has been steadily growing from 100 kg N/hm<sup>2</sup> to more than 300 kg N/hm<sup>2</sup> (Gao et al., 2010), while the nitrogen use efficiency dropped from 52.6% to 20% (Zhang

et al., 2008; Cui et al., 2008; Zhi et al., 2020) and its adverse effect has been observed. However, what concurrently happening is less applying organic fertilizer such as animal manure and straw in farmland mainly due to the inconvenient application of such materials.

As planting area and grain yield of corn is growing steadily in Northeast China, corn straw is also rising in recent years. In 2015, the total corn straw yield in Northeast China was 159 million tons, accounting for 19.2% of the national straw output (Li et al., 2017a). How to dispose such large amount of straw in a short-term is still a challenge to local farmer since the low temperature and humidity of soil makes decomposition process slow. In the past several decades, most of corn straw was burnt after harvest or before sowing, which resulted in the loss of organic matter reduced to soil as well as serious air pollution. In order to solve these problems and improve the fertility of black soil, conservation tillage which includes less or no tillage combined with straw application has been recommended. Numerous studies have proved that straw application could improve soil fertility, water holding capacity and carbon sequestration (Liu et al., 2014; Li et al., 2016).

Compared with mineral fertilizer, corn straw has lower N concentration and slower releasing rate, which greatly increases N use efficiency and reduces N loss via farmland runoff. Furthermore, the application of crop straw in farmland soil also alleviates the issue of wastes disposal in corn production. Thus, straw application combined with mineral fertilizer has been recommended by many scientists in recent years (Rasool et al., 2008; Lu et al., 2009; Demelash et al., 2014; Zhang et al., 2015).

As discussed above, corn straw application is beneficial for soil and crop growth. While one remarkable thing is that the results were obtained on the base of the constant amount of mineral N fertilizer combined with more corn straw (Wang et al., 2018a; Afreh et al., 2018). Few researches were carried out on equally total nitrogen application amount (organic N + mineral N) on spring corn in Northeast China. So, there is little knowledge about whether corn straw application could substitute partial mineral N fertilizer. In addition, many long-term experiments have been taken to evaluate the effect of corn straw on soil properties and crop growth after several years of application (Wang et al., 2018b; Xu et al., 2019). However, its temporal influence was seldom estimated in the fertilization year, which might bring some undesirable negative impacts on yield and soil environment.

In this paper, integrated various ratio of corn straw to mineral N fertilizer at an equally total N application rate of 240 kg N/hm<sup>2</sup> was studied in the fertilization year to evaluate its effect on (1) corn yield, (2) nitrogen uptake characteristics of corn plants in different growth stage, (3) nitrate, ammonium distribution in the soil profile (0-100 cm). We assumed that an appropriate ratio of straw application could substitute partial mineral N fertilizer characterized by higher N use efficiency, less NO<sub>3</sub><sup>-</sup>-N content and leaching in soil profile without negative effect on corn yield.

## Material and Methods

### *Field experimental site and design*

Field work was conducted at the experimental station of Jilin Agricultural University (43°49'6.6"N, 125°23'56.4"E), which lies in Changchun City, Jilin province in Northeast China. It is a continental monsoon climate with an average annual rainfall of 582 mm (more than 60% of the rainfall occurs during June to August) and average annual temperature of 5.5°C. The sunshine time is 2688 hours per year and the annual average

effective accumulated temperature is 2900°C. The frost free period is 132 days per year. The soil is classified as phaeozems according to FAO soil taxonomy, and maize has been planted at least 20 years without straw return. Analyses indicated pH, organic matter, total N, available N, P and K of the top 0-20 cm soil was 6.89, 27.4 g/kg, 1.26 g/kg, 150.7 mg/kg, 31.2 mg/kg, 136.1 mg/kg, respectively.

The field work was done in 2015 with six treatments (*Table 1*) and three replicates in a randomized complete block design. Each plot was 58.5 m<sup>2</sup> (6.5 m×9 m) with 2 m wide of buffering strip around it. 25%, 50%, 75%, 100% straw application was set and the rest N, P, K was supplied by mineral fertilizer after nutrients in straw was subtracted in order to maintain the totally same rates of 240 kg N /hm<sup>2</sup>, 154 kg P<sub>2</sub>O<sub>5</sub>/hm<sup>2</sup> and 197 kg K<sub>2</sub>O /hm<sup>2</sup>. Corn straw was taken from other field with Nitrogen (N), phosphorus (P), potassium (K) and moisture contents of 0.72%, 0.25%, 1.50%, 30%, respectively, and crushed into 2-5 cm length before applying. 100% straw application amount was determined by grain yield of 12000 kg/hm<sup>2</sup> and the ratio of grain to straw was 1: 1.2, which was a relatively higher output in local area. The fertilizers were urea (N 46%), diammonium (N 18%, P<sub>2</sub>O<sub>5</sub> 46%) and superphosphate (P<sub>2</sub>O<sub>5</sub> 46%), potassium chloride (K<sub>2</sub>O 60%), which were products of DQL chemical fertilizer Co., Ltd, China and Yuntianhua Co., Ltd, China. The fertilization detail of each treatment was listed in *Table 1*.

**Table 1.** Details of fertilization in each treatment (kg/hm<sup>2</sup>)

Treatment code	Treatment	Organic material				Mineral fertilizer		
		Rate	N	P <sub>2</sub> O <sub>5</sub>	K <sub>2</sub> O	N	P <sub>2</sub> O <sub>5</sub>	K <sub>2</sub> O
CK	-	0	0	0	0	0	0	0
IF	100 % mineral N	0	0	0	0.0	240.0	154	197
S25	25% maize straw+ mineral N	3600	18.1	6.3	37.8	221.9	147.7	159.2
S50	50% maize straw+ mineral N	7200	36.2	12.6	75.6	203.8	141.4	121.4
S75	75% maize straw+ mineral N	10800	54.3	18.9	113.4	185.7	135.1	83.6
S100	100% maize straw	14400	72.4	25.2	151.2	167.6	128.8	45.8

Note: CK represented no fertilization treatment, IF represented merely mineral N fertilization treatment, S25/ S50/ S75/ S100 delegated 25%/ 50%/ 75%/ 100% corn straw return + remaining N supplemented by mineral N

Corn (*Zea mays* L.) hybrid variety XY335 was sowed at one seed per hole with the planting density of 6.5×10<sup>4</sup> plants/hm<sup>2</sup> on 3 May 2015. All mineral P and K fertilizers, 40% mineral N fertilizer and all straw were mixed with top 20 cm soil before sowing as basal fertilizer. A half of the rested mineral N fertilizer was applied at the beginning of stem elongation and the other half was applied at inflorescence emergence as top dressing after sample collection. The seeds were sowed after plough, and there was no other tillage during maize growth. It was rain-fed agriculture and no irrigation was given. Weeds were controlled by applying herbicides (atrazine and acetochlor). Corns were harvested on September 29, 2015.

### Field investigation and sample collection

One week after seed germination, number of plants in the whole plot was counted to calculate the germination rate. The plant was sampled in leaf development, early stem elongation, 9 or more nodes detectable, tassel emergency, early grain development, early milk, early ripening and fully ripening stage, which corresponded to 18, 47, 64, 76, 96,

111, 121 and 131 days after germination, respectively. Soil samples were simultaneously taken in tassel emergency and fully ripening stage.

Representative 3-5 plants were sampled in each plot at each sampling time, washed in deionized water, separated into leaf, stem, ear and grain, oven-dried at 105°C for 20 min, followed by drying at 65°C until the weight was constant. Then, the plants were crushed and sieved for further analysis. For the last sampling stage, plants in 10 m<sup>2</sup> in the middle of each plot were harvested manually to calculate the grain yield on the basis of 14% moisture content and to determine grain yield components of 1000-grain weight, rows per ear, grain number per row, grain number per ear. No-ear plants were counted in the whole plot.

The soil of 0-100 cm depth was taken from each plot using a soil probe, and divided into 5 subsamples at each 20 cm depth. The surface litter was removed before sampling and 3 sites in each plot were randomly taken and then mixed. The soil samples were put into self-sealing plastic bags and brought to lab, stored at -20°C for nitrate and ammonium analysis.

### **Sample analysis**

The total N concentration of plants was analyzed by a micro- Kjeldahl procedure after digested by H<sub>2</sub>SO<sub>4</sub>-H<sub>2</sub>O<sub>2</sub> (Nelson et al., 1973). The concentration of ammonium and nitrate was measured by continuous flow analyzer (SEAL AutoAnalyzer 3-AA3, Bran and Luebbe, Germany) after being extracted by 2 mol/L KCl (López Pasquali et al., 2007).

### **Data processing**

$$\text{NUE} = \frac{N_f - N_{ck}}{F} \times 100\% \quad (\text{Zhang et al., 2008}) \quad (\text{Eq.1})$$

$$\text{NHI} = \frac{G_N}{TP_N} \quad (\text{Afreh et al., 2018}) \quad (\text{Eq.2})$$

$$\text{NAE} = \frac{Y - Y_0}{F} \quad (\text{Afreh et al., 2018}) \quad (\text{Eq.3})$$

NUE (%) is nitrogen use efficiency, N<sub>f</sub> is the nitrogen uptake by plant in fertilization treatment, N<sub>ck</sub> is the nitrogen uptake by plant in control, F is the application amount of mineral N fertilizer, NHI is nitrogen harvest index, G<sub>N</sub> is the grains nitrogen uptake, TP<sub>N</sub> is the total nitrogen uptake by plant, NAE (kg/kg) is nitrogen agronomic efficiency, Y is the grain yield in fertilization treatment, Y<sub>0</sub> is the grain yield in control.

The data were analyzed using SPSS Statistics 17.0 (SPSS, Inc., Chicago, IL, USA), and differences between treatments were compared by the method of least significant difference (LSD) test at the 0.05 level. Microsoft Excel 2016 was adopted for calculating and drawing.

## **Results**

### **Grain yield and its components**

Corn grain yield and its components are indicated in *Table 2*. The results showed that treatments significantly affected germination rate, 1000-grain weight, grains per ear and grain yield ( $p < 0.05$ ).

**Table 2.** Germination rate and grain yield components of corn in different fertilization treatments

Treatment	Germination rate (%)	No-ear Ratio (%)	1000-grain weight (g)	Rows per ear	Grains per ear	Grain yield (kg/hm <sup>2</sup> , DW)
CK	94.9 ± 1.3 a	9.8 ± 1.3 a	228.3 ± 23.6 e	16.1 ± 0.6 ab	505.4 ± 97.8 c	5654 ± 666 c
IF	92.5 ± 1.0 b	5.9 ± 3.5 b	339.7 ± 12.7 ab	16.3 ± 0.3 a	662.5 ± 25.8 ab	8357 ± 189 a
S25	93.2 ± 1.3 b	0.7 ± 1.3 c	315.3 ± 2.7 abc	16.3 ± 0.1 a	574.4 ± 49.3 bc	8175 ± 123 ab
S50	93.7 ± 3.1 b	1.5 ± 1.3 c	303.1 ± 37.5 cd	16.4 ± 0.2 a	644.8 ± 36.6 ab	8235 ± 534 a
S75	89.9 ± 2.5 c	3.4 ± 4.2 c	304.6 ± 14.3 bc	16.5 ± 0.6 a	673.7 ± 35.1 a	8402 ± 735 a
S100	80.0 ± 0.8 c	8.0 ± 0.0 ab	349.2 ± 8.7 a	14.1 ± 1.5 b	565.5 ± 58.9 ab	7432 ± 232 b

Note: Different letters in the same column signified significant difference at  $p < 0.05$ . CK represented no fertilization treatment, IF represented merely mineral N fertilization treatment, S25/ S50/ S75/ S100 delegated 25%/ 50%/ 75%/ 100% corn straw return + remaining N supplemented by mineral N

Germination rate in all fertilization treatments was 1.2-14.9% lower than CK and decreased as straw application was increasing with S75, S100 significantly lower than S25, S50 by an average of 8.5% ( $p < 0.05$ ). Appropriate straw application (S25, S50, S75) decreased no-ear ratio by an average of 4.0% compared to IF and 7.9% compared to CK. S100 had an opposite effect on it. Meanwhile, S100 decreased rows per ear by 2.2 and grain yield by 925 kg/hm<sup>2</sup> compared to IF. No significant difference was found for the grain per ear values of different treatments ( $p > 0.05$ ). Grain yield of the 100% mineral treatment was significantly lower than the others ( $p < 0.05$ ).

### Nitrogen accumulation in corn plant

The N assimilation of whole corn plant in different growth stage was showed in *Figure 1*. The tassel emergency stage (represented vegetative stage) as well as fully ripening stage (represented reproductive stage) was selected to analyze N distribution in different plant organ and the results were listed in *Figure 2*.

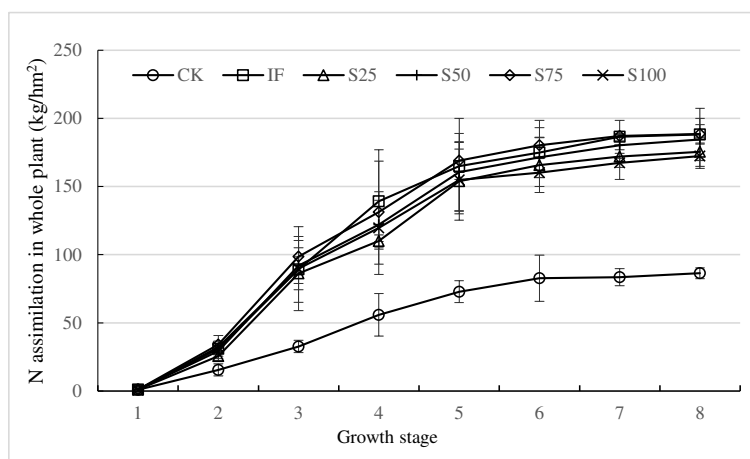


**Figure 1.** N assimilation amount in whole corn plant during different growth period in different fertilization treatments. Growth stages: 1- leaf development, 2-early stem elongation, 3-9 or more nodes detectable, 4- tassel emergency, 5- early grain development, 6- early milk stage, 7- early ripening and 8- fully ripening. CK represented no fertilization treatment, IF represented merely mineral N fertilization treatment, S25/S50/S75/S100 delegated 25%/50%/75%/100% corn straw return + remaining N supplemented by mineral N



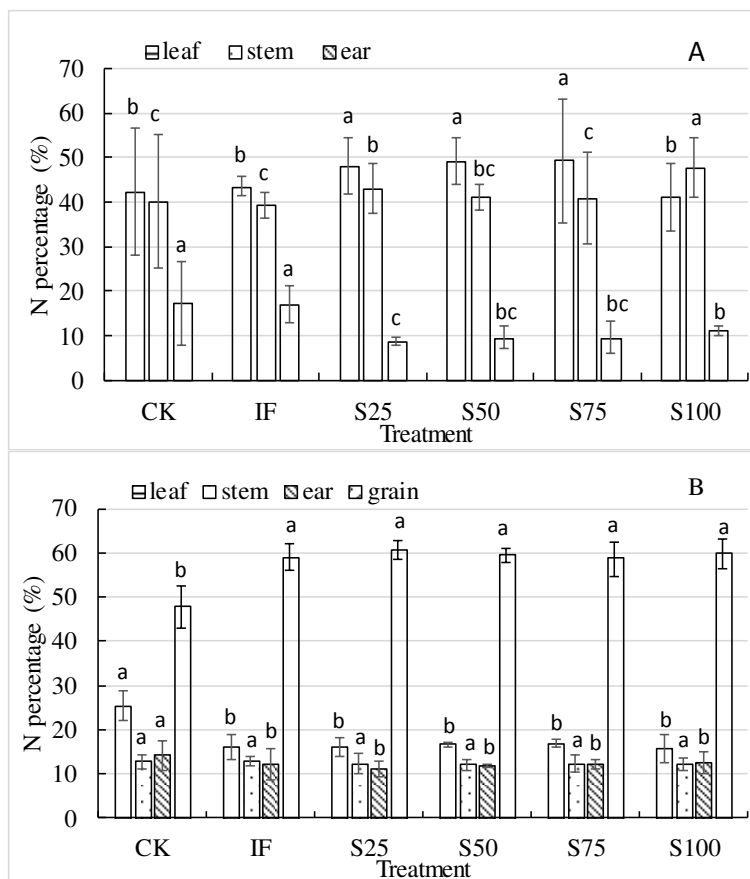


**Figure 2.** N uptake in different plant organ to the total of plant in tassle emergency (A) and fully ripening stage (B). CK represented no fertilization treatment, IF represented merely mineral N fertilization treatment, S25/S50/S75/S100 delegated 25%/50%/75%/100% corn straw return + remaining N supplemented by mineral N

Compared with CK, fertilization significantly increased N assimilation amount by 86.0-102.3 kg/hm<sup>2</sup>, or 99.7%-118.5% in the fully ripening stage. But there was no obvious difference between straw application treatments and IF except for S100 in leaf development stage and early ripening stage, which was significantly lower than IF ( $p < 0.05$ ).

Straw application promoted N accumulating in leaves and stems during vegetative growth as N proportion in leaves for S25, S50 and S75 was obviously higher than other organs during tassle emergency stage. And N proportion in ears increased significantly from 8.8% in S25 to 11.1% in S100. In fully ripening stage, N proportion in leaves decreased from an average of 47.0% in tassle emergency stage to an average of 16.3%, and stems declined from 43.3% to 12.2%. While for ears, it increased from 9.8% to 11.9%. For IF, N in leaves and stems decreased by 27.5% and 26.6%, respectively, which were lower than those of straw application treatments.

### Nitrogen use efficiency

N uptake by plant and relevant indicators are list in Table 3. Compared with CK, N uptake and N harvest index was significantly higher for fertilization treatments. While no significant difference was found for N uptake by plant between IF and the straw

application treatments ( $p > 0.05$ ). The N use efficiency of the S75 was 12.6% significantly higher than IF ( $p < 0.05$ ). No significant difference was observed for nitrogen harvest index and apparent nitrogen recovery ( $p > 0.05$ ) (Table 3), while the N agronomic efficiency of the S100 was significantly lower than the rest four straw application treatment and IF ( $p < 0.05$ ).

**Table 3.** Nitrogen use efficiency of corn in different fertilizer treatments

Treatment	N uptake by plant (kg/hm <sup>2</sup> )	N use efficiency (%)	N harvest index	N agronomic efficiency (kg/kg)
CK	86.3 ± 4.1 b	-	0.45 ± 0.02 b	-
IF	188.2 ± 8.4 a	42.5 ± 3.5 bc	0.51 ± 0.03 a	11.3 ± 0.8 a
S25	175.5 ± 5.0 a	40.2 ± 2.2 c	0.53 ± 0.02 a	11.4 ± 0.6 a
S50	184.6 ± 8.6 a	48.2 ± 4.2 abc	0.52 ± 0.03 a	12.7 ± 2.6 a
S75	188.6 ± 11.6 a	55.1 ± 6.2 a	0.51 ± 0.01 a	14.8 ± 4.0 a
S100	172.3 ± 19.5 a	51.3 ± 11.6 ab	0.52 ± 0.04 a	10.6 ± 1.4 b

Note: Different letters in the same column signify significant difference at  $p < 0.05$ . CK represented no fertilization treatment, IF represented merely mineral N fertilization treatment, S25/ S50/ S75/ S100 delegated 25%/ 50%/ 75%/ 100% corn straw return + remaining N supplemented by mineral N

### Nitrate distribution in soil profile

Nitrate distribution in soil profile is indicated in Table 4. NO<sub>3</sub><sup>-</sup>-N in all straw application treatments were lower than IF in both growth stages, and decreased with soil depth and straw application increasing.

**Table 4.** NO<sub>3</sub><sup>-</sup>-N content in soil profile in different fertilization treatments in tasseling and fully ripening stage (mg/kg)

	Profile	CK	IF	S25	S50	S75	S100
Tassel emergency stage	0-20 cm	3.4 ± 0.9 d	22.6 ± 2.9 a	19.8 ± 1.0 ab	17.5 ± 1.0 bc	16.4 ± 1.1 c	14.5 ± 2.7 c
	20-40 cm	4.0 ± 1.6 d	22.1 ± 5.5 a	19.5 ± 1.6 b	13.1 ± 2.5 c	9.2 ± 0.9 c	10.3 ± 3.0 c
	40-60 cm	3.3 ± 1.1 d	18.1 ± 1.9 a	15.7 ± 3.0 b	10.6 ± 1.8 c	8.9 ± 1.5 c	5.2 ± 1.3 d
	60-80 cm	3.0 ± 0.9 c	12.6 ± 6.6 ab	13.8 ± 1.6 a	11.4 ± 1.7 b	4.5 ± 1.0 c	3.1 ± 0.8 c
	80-100 cm	2.5 ± 0.2 d	13.5 ± 1.0 a	11.5 ± 0.9 b	5.6 ± 1.2 c	3.2 ± 0.3 d	2.7 ± 0.5 d
Fully ripening stage	0-20 cm	2.9 ± 0.3 c	19.3 ± 1.9 a	17.3 ± 5.6 ab	15.0 ± 2.1 ab	14.5 ± 2.1 ab	13.0 ± 1.0 b
	20-40 cm	2.5 ± 0.7 d	18.2 ± 3.5 b	23.3 ± 2.1 a	21.7 ± 4.4 ab	11.9 ± 1.7 c	11.4 ± 2.4 c
	40-60 cm	2.0 ± 0.6 d	24.6 ± 2.7 a	16.3 ± 3.2 b	14.6 ± 1.6 b	10.0 ± 0.7 c	10.5 ± 1.5 c
	60-80 cm	1.2 ± 0.4 d	23.2 ± 2.8 a	14.1 ± 2.2 b	15.5 ± 2.4 b	9.1 ± 0.4 c	9.2 ± 1.0 c
	80-100 cm	1.5 ± 0.3 d	20.3 ± 2.1 a	15.1 ± 2.2 b	14.5 ± 1.5 b	8.1 ± 1.8 c	7.3 ± 1.7 c

Note: Different letters in the same column signify significant difference at  $p < 0.05$ . CK represented no fertilization treatment, IF represented merely mineral N fertilization treatment, S25/ S50/ S75/ S100 delegated 25%/ 50%/ 75%/ 100% corn straw return + remaining N supplemented by mineral N

In the tassel emergency stage, NO<sub>3</sub><sup>-</sup>-N of the 0-20 cm for all straw application treatments were 12.4%, 22.6%, 27.4% and 35.8% lower than IF, respectively. The differences of the latter three treatments were significant at 0.05 levels, indicating an obvious decreasing trend with increasing straw application rate. Compared to IF, the mean reduction of the four straw application treatments was 5.6 mg/kg in 0-20 cm,

9.0 mg/kg in 20-40 cm, 8.0 mg/kg in 40-60 cm, 4.4 mg/kg in 60-80 cm and 7.8 mg/kg in 80-100 cm. The average NO<sub>3</sub><sup>-</sup>-N contents in 0-20 cm and 80-100 cm soil layer of all straw application treatments were 17.1 mg/kg and 5.8 mg/kg, respectively. It decreased by 11.3 mg/kg from the top layer to the lowest layer, which was larger than that of 9.1 mg/kg in IF. More straw application was added, lower NO<sub>3</sub><sup>-</sup>-N was obtained. For S100, it decreased by 8.1- 12.9 mg/kg in different soil layers, or 35.8%-80.0% compared with corresponding layers of IF, which decreased more than other straw application treatments.

In the fully ripening stage, NO<sub>3</sub><sup>-</sup>-N in all straw application treatments was still lower than IF. For IF, NO<sub>3</sub><sup>-</sup>-N distribution in soil profile showed a completely opposite characteristic to tassel emergency stage as 40-100 cm soil layers was 3.9 mg/kg higher than that in 0-40 cm, which indicated that more NO<sub>3</sub><sup>-</sup>-N migrated to deeper soil layers. But for all straw application treatments, it was still higher in the two top layers than that in 40-100 cm with an average content of 14.8 mg/kg to 12.0 mg/kg, which decreased by 4.0 mg/kg in 0-40 cm and 10.7 mg/kg in 40-100 mg/kg compared with the corresponding layers of IF. A larger decreasing occurred in deeper layers of straw application treatments indicated that straw combined with reduced mineral N fertilizer prevented nitrate nitrogen leaching in soil profile. As straw application increasing accompanied by mineral N fertilizer application decreasing, less NO<sub>3</sub><sup>-</sup>-N was left in soil profile. S100 had the lowest level with a decrease of 6.3-14.1 mg/kg, or 32.6%- 64.0% in different soil layers compared with IF.

#### ***Ammonium distribution in soil profile***

Ammonium distribution in soil profile is indicated in *Table 5*. NH<sub>4</sub><sup>+</sup>-N in all fertilization treatments was significantly higher than CK ( $p < 0.05$ ) and high level of straw application was significantly higher than IF.

**Table 5.** NH<sub>4</sub><sup>+</sup>-N content in soil profile in different fertilization treatments in tasseling and fully ripening stage (mg/kg)

	Profile	CK	IF	S25	S50	S75	S100
Tassel emergency stage	0-20 cm	3.2 ± 1.0 b	11.8 ± 1.6 a	11.3 ± 1.6 a	12.3 ± 1.2 a	12.5 ± 3.3 a	10.6 ± 2.7 a
	20-40 cm	3.8 ± 0.7 c	12.0 ± 1.3 a	12.8 ± 1.9 a	10.5 ± 2.4 ab	11.3 ± 1.8 ab	8.9 ± 0.2 b
	40-60 cm	3.6 ± 0.5 d	5.6 ± 0.6 c	5.8 ± 0.3 c	10 ± 1.7 ab	10.6 ± 1.2 a	8.8 ± 0.3 b
	60-80 cm	2.5 ± 0.7 c	5.8 ± 0.9 b	5.3 ± 0.6 b	9.7 ± 1.4 a	10.6 ± 1.2 a	6.8 ± 0.8 b
	80-100 cm	1.1 ± 0.5 c	3.2 ± 0.6 b	3.1 ± 0.5 b	4.5 ± 0.9 ab	5.3 ± 1.2 a	5.2 ± 0.8 a
Fully ripening stage	0-20 cm	2.3 ± 0.5 c	9.2 ± 1.0 b	12.6 ± 1.1 a	11.5 ± 2.6 ab	12.9 ± 1.4 a	13.4 ± 2.5 a
	20-40 cm	2.5 ± 0.5 c	8.5 ± 0.9 b	11.7 ± 0.9 a	11.3 ± 0.3 a	11.8 ± 0.3 a	10.8 ± 0.8 a
	40-60 cm	2.3 ± 0.4 d	3.4 ± 0.3 d	6.1 ± 0.7 c	8.8 ± 0.9 ab	8.6 ± 0.9 b	10.1 ± 0.9 a
	60-80 cm	1.5 ± 0.2 e	4.0 ± 0.4 d	4.5 ± 0.5 d	10.7 ± 1.0 b	14.0 ± 0.8 a	8.7 ± 0.6 c
	80-100 cm	0.9 ± 0.1 c	5.7 ± 0.7 b	5.6 ± 0.2 b	5.3 ± 0.7 b	7.4 ± 0.3 a	7.3 ± 0.8 a

Note: Different letters signified significant difference at  $p < 0.05$  among different treatments. CK represented no fertilization treatment, IF represented merely mineral N fertilization treatment, S25/S50/S75/S100 delegated 25%/50%/75%/100% corn straw return + remaining N supplemented by mineral N

In the tassel emergency stage, no significant difference was found between NH<sub>4</sub><sup>+</sup>-N content of IF and straw application treatments in the 0-20 cm and 20-40 cm soil layers ( $p > 0.05$ ). While it was obviously increased by 3.2 mg/kg in 40-60 cm, 2.3 mg/kg in

60-80 cm and 1.3 mg/kg in 80-100 cm. S75 had the highest  $\text{NH}_4^+\text{-N}$  content, which was 5.9% - 89.3% more than IF in different soil layers.

In the fully ripening stage,  $\text{NH}_4^+\text{-N}$  in each soil layer increased with straw application increasing and it was significantly higher ( $p < 0.05$ ) than IF and CK by an average of 3.5 mg/kg and 7.8 mg/kg, respectively. The same as tasseling stage,  $\text{NH}_4^+\text{-N}$  declined with soil depth, while straw application treatments could slow down this trend in 40-80 cm with an average of 8.9 mg/kg compared with 3.7 mg/kg of IF. Compared to tassel emergency stage,  $\text{NH}_4^+\text{-N}$  in CK and IF declined by 0.9 mg/kg and 1.5 mg/kg, respectively. Whereas straw application treatments enhanced  $\text{NH}_4^+\text{-N}$  content by an average of 0.9 mg/kg, which meant that straw combined with mineral N fertilizer relatively kept N in the form of  $\text{NH}_4^+\text{-N}$  long time and it may be related to the inhibition of nitrification.

## Discussion

### *Effect of straw application combined with reduced mineral N on corn grain yield*

In the present work, the corn yield of straw application treatments was significantly higher ( $p < 0.05$ ) than CK, which was consistent with other results (Uzoma et al., 2011; Liang et al., 2013). However, it did not show significantly higher than merely mineral fertilizer (IF) treatment in our research. There were two kinds of completely different view on the effect of applying organic matter on grain yield. Some results showed organic combined with mineral fertilizer improved crop yield greatly, such as Subehia et al. (2013), who confirmed that 50% N replaced by farmyard manure greatly increased rice and wheat yield than 100% chemical fertilizer treatment. While a number of previous studies had opposite results, which indicated that nitrogen application amount was the key factor affecting crop yield compared to fertilizer types. For example, Basso et al. (2005) and Biau et al. (2012) thought there was no significant difference in corn yield between treatments of manure, compost and mineral fertilizer in multi-year field experiment. Luo (2015) found that nitrogen improved corn yield by 53.5%- 130.7%, while organic fertilizer only increased by 8.8%- 22.1%. Zhou et al. (2013) deemed that low and high organic and mineral nitrogen ratio was adverse to yield and recommended the best ratio of 2:3 for improvement of Soda Alkali soil.

In our result, straw combined with mineral N fertilizer didn't significantly increase corn yield compared with IF. It partly was relative to the higher background of SOM in testing soil. New added straw in our study mineralized slowly in the fertilizing year and its contribution to increase SOM was relatively small on the high background. Oldfield (2019) found that crop yield increased significantly with the increase of SOM as it was below 2%. Zhang et al. (2016) carried out one field experiment on a typically low SOM soil, and also believed that the increase of SOC determined the increase of crop yield. Li et al. (2017b) suggested that replacing partial NPK fertilizers by manure could sustain high corn yield when SOC reached 41.96 Mg C/ha in the Northeast China Plain. If SOC was higher than this threshold, the effect would not be realized. Additionally, it would take at least decade to unfold this effect because it was a long time for microorganism to mineralize manure to release nutrients for crops to take up. Biau et al. (2012) found that the mineral N fertilizer had higher average grain yield and plant N uptake than pig slurry and attributed the result to agronomic management practices and the climate. Therefore, the effect of straw application on grain yield and plant N uptake was determined by multiple factors and it was a comprehensive result. In order to evaluate it correctly, the

response of corn crops to different forms of N fertilizer should be considered in the same farming practices and climate.

Furthermore, corn yield didn't keep in the increasing trend, but decreased when straw application increased to 100%. We attributed this phenomenon to its lower germination rate and rows per ear. Although some studies showed that organic matter enhanced the soil water content and was benefit of germination and crop growth (Li et al., 2020), the straw application amount and mode was extremely important factors determined its effect on plant growth (Wang et al., 2018b; Zhen et al., 2020). For example, Fan et al. (2005) found that 3.75 t/ha straw combined with mineral N and P increased soil water-holding capacity and improved water availability to plants to increase grain yield, in which the application straw amount was much lower than our experiment and did not influence corn germination rate. Liu et al. (2020) discovered that subsoiling with straw application was a promising strategy to improve wheat yield and water use efficiency for retaining soil water availability, in which subsoiling was done by a rotary cultivator in 40-45 cm soil depth. It was deeper than our study and kept the surface soil unchanged so that it had little effect on the surface evaporation of soil moisture, and however increased the water holding capacity of subsoil. Zhao et al. (2011) also pointed out that high quantities of decomposed cow dung and mineral fertilizers increased field moisture capacity by 11.25% and increased grain yield by 0.8%-9.4% than the single chemical fertilizers. The difference between our results was the types of organic matter, which affected soil structure and consequent water availability differently. Moreover, there was no artificial irrigation in our testing area which made the soil germinating condition even worse in a windy and less rainfall climate.

### ***Effect of straw application combined with reduced mineral N on N accumulation in corn plant***

In the present work, as long as the total nitrogen application rates was identical, no matter it was in inorganic/organic form, or combining, their nitrogen harvest index changed little, and was significantly higher than no fertilization treatment. However, this result was not consistent with some others which believed that different nitrogen forms and combining ratio influenced harvest index obviously (Tan et al., 2011). We attributed it to the high background level of SOM which decreased the effect of added straw, and it was also partly related to incomplete decomposition of straw in a short time.

In the whole growth period, fertilization treatments (both organic and inorganic) promoted nitrogen accumulation in plant, and they were significantly higher than CK because more N was supplied, which is in-line with previous reports (Berenguer et al., 2008). Abbasi and Almas (2012) reported that integrated use of organic and inorganic N sources increased corn growth and N uptake by plants compared to sole application of organic or chemical N fertilizer. Rees and Castle (2002) deemed that total uptake of N by plants in poultry manure was higher than those in ammonium sulphate.

In addition, S75 had the highest nitrogen use efficiency in our study which indicated that appropriately combined with straw and mineral N fertilizer could increase nitrogen use efficiency significantly. Dordas et al. (2008) and Martínez et al. (2017) pointed out that nitrogen use efficiency decreased with increased mineral fertilizer supply. However, our result was consistent with their conclusion except for S100, which was a little lower than other straw application treatments. We attributed it to the lower germination rate which affected grain yield, as well as to the higher straw application amount which consumed more mineral N for microbial growth so as to decrease the source of N for corn

absorbing. Zhi et al. (2020) conducted a  $^{15}\text{N}$  tracer experiments and deemed that nitrogen use efficiency was different regionally which caused more by soil properties than by climatic factors. In his study, nitrogen use efficiency in Northeast China was 47%, which was much higher than in North Central region of China (28%). In our study, the average nitrogen use efficiency of straw application treatments was 48.7% and the mineral N fertilizer treatment was 42.5%, which was greatly higher than the average of 38% in Chinese corn system (Zhi et al., 2020).

### ***Effect of straw application combined with reduced mineral N on $\text{NO}_3^-$ -N distribution in soil profile***

In all, S75 and S100 greatly declined  $\text{NO}_3^-$ -N in 0-100 cm soil profile compared with IF and S25, S50. More  $\text{NO}_3^-$ -N was kept in 0-40 cm in all straw application treatments, while a migrating to deeper soil was discovered in IF, which indicated that straw application combined with reduced mineral N fertilizer affected  $\text{NO}_3^-$ -N distribution in soil profile by two ways, one was to decrease its content and the other was to resist its downward migration to deeper soil layers.

Nevertheless, the results of studies about the effects of organic matter application on nitrate leaching found in literature were discording. Martínez et al. (2017) found that N remained in organic form when manure was applied and was less prone to losses than mineral N fertilizer. Berenguer et al. (2008) reported that pig slurry treatment had relatively lower level of residual  $\text{NO}_3^-$ -N than equivalent dose of mineral fertilizers and suggested that more N was immobilized as form of  $\text{NH}_4^+$ -N in the soil. Bai et al. (2015) also supported the view that beneficial reduction of nitrate leaching was elicited by organic fertilizers. However, some research indicated that manure increased the risk of nitrate leaching if it was applied in autumn-winter application or in soils with high soil organic matter (Chambers et al., 2000; Chalmers, 2001; Wang et al., 2002). We attributed these different opinions to drainage amounts, which was supported by Jabloun et al. (2015) who revealed that N leaching had a positive relationship with precipitation. In the area of abundant rainfall or artificial irrigation, especially in spring and autumn when the absorption capacity of plants to nitrogen was low, high drainage amount took more nitrogen to migrate down. But in the place with less rain, such as our testing position, more nitrogen fixed by microorganism or absorbed by soil aggregates and stayed in the upper soil which decreased the risk of N leaching with a positive impact on the environment.

### ***Effect of straw application combined with reduced mineral N on $\text{NH}_4^+$ -N distribution in soil profile***

Consistent with most of previous research, the application of N (both organic and mineral) in this work enhanced the soil ammonium content in 0-40 cm, which was higher than CK (Martínez et al., 2017). In tassel emergency stage, there was no significant difference about  $\text{NH}_4^+$ -N between IF treatment and other straw application treatments in the two top layers. But when corn was in mature period, all straw application treatments had higher  $\text{NH}_4^+$ -N than IF treatment, which could be relative to its sustained release during the whole growth period and the high adsorption capacity caused by straw return. Additionally, temperature at this time was enough high to activate mineralization of microorganisms. And in the later stage of growth, the ability of absorbing nitrogen by plants was weaken and biodegradable organic N was still decomposed by microorganism which resulted in a higher ammonium content than IF during fully ripening stage.  $\text{NH}_4^+$ -N

fixed in the interlayers of the clay minerals or absorbed by the surface of soil particles was not uptake by crop, and was not lost through volatilization, but was immobilized in soil and played an important role in the N budget.

## Conclusions

Straw return, as an important component of conservation tillage, has been widely adopted across the Northeast plain of China. Straw contains many nutrients which can slowly release for plant growth by microbial mineralization. Whether the released nutrients can replace partial chemical-fertilizers on the purpose of reducing fertilizer application in the fertilization year is still unclear in the intensive and continuous corn planting system in Northeast China.

Our results showed that although straw application did not lead to significantly increase in corn yield compared with merely mineral N fertilizer, 50% -75% straw application combined with reduced mineral N fertilizer on a total N application rate of 240 kg N/hm<sup>2</sup> was a relatively better fertilizing strategies from the perspective of both nitrogen use efficiency and residual nitrogen in soil in the fertilization year. This fertilization practice not only improved nitrogen use efficiency by 5.7-12.6% compared with merely mineral N fertilizer, but also reduced NO<sub>3</sub><sup>-</sup>-N amount and its migration to the lower soil layers to avoid contaminating groundwater. Ammonium content in straw return treatments was higher than merely inorganic fertilizer treatment in the fully ripening stage, which should be further researched to evaluate its role to the next planting in the future study.

**Acknowledgements.** Authors gratefully acknowledge Lichun Wang of the Jilin Agricultural Science Research Institute for field trial setup and maintenance, and Jingmin Yang of Jilin Agricultural University for the support of chemical analysis. This study was partially funded by the national key research and development program of China (2017YFD0201505).

## REFERENCES

- [1] Abbasi, M. K., Almas, K. (2012): Microbial biomass carbon and nitrogen transformations in a loam soil amended with organic-inorganic N sources and their effect on growth and N-uptake in maize. – *Ecological Engineering* 39: 123-132.
- [2] Afreh, D., Zhang, J., Guan, D. H., Liu, K. L., Song, Z. W., Zheng, C. Y., Deng, A. X., Feng, X. M., Zhang, X., Wu, Y., Huang, Q. R., Zhang, W. J. (2018): Long-term fertilization on nitrogen use efficiency and greenhouse gas emissions in a double maize cropping system in subtropical China. – *Soil & Tillage Research* 180: 259-267.
- [3] Bai, J. S., Cao, W. D., Xiong, J., Zeng, N. H., Gao, S. J., Shimizu, K. (2015): Integrated application of February Orchid (*Orychophragmus violaceus*) as green manure with chemical fertilizer for improving grain yield and reducing nitrogen losses in spring maize system in northern China. – *Journal of Integrative Agriculture* 14: 2490-2499.
- [4] Basso, B., Ritchie, J. T. (2005): Impact of compost, manure and inorganic fertilizer on nitrate leaching and yield for a 6-year maize-alfalfa rotation in Michigan. – *Agriculture, Ecosystems and Environment* 108: 329-341.
- [5] Battye, W., Aneja, V. P., Schlesinger, W. H. (2017): Is nitrogen the next carbon? – *Earths Future* 5: 894-904.
- [6] Berenguer, P., Santiveri, F., Boixadera, J., Lloveras, J. (2008): Fertilization of irrigated maize with pig slurry combined with inorganic nitrogen. – *Eur. J. Agron.* 28: 635-645.

- [7] Biau, A., Santiveri, F., Mijangos, I., Lloveras, J. (2012): The impact of organic and inorganic fertilizers on soil quality parameters and the productivity of irrigated maize crops in semiarid regions. – *European Journal of Soil Biology* 53: 556-61.
- [8] Cai, Z. J., Wang, B. R., Xu, M. G., Zhang, H. M., He, X. H., Zhang, L., Gao, S. D. (2015): Intensified soil acidification from chemical N fertilization and prevention by manure in an 18-year field experiment in the red soil of southern china. – *J. Soils Sediments* 15: 260-270.
- [9] Chalmers, A. G. (2001): A review of fertilizer, lime and organic manure use on farm crops in Great Britain from 1983 to 1987. – *Soil Use Manage* 17: 254-262.
- [10] Chambers, B. J., Smith, K. A., Pain, B. F. (2000): Strategies to encourage better use of nitrogen in animal manures. – *Soil Use Manage* 16: 157-161.
- [11] Cui, Z. L., Zhang, F. S., Chen, X. P., Miao, Y. X., Li, J. L., Shi, L. W., Xu, J. F., Ye, Y. L., Liu, C. S., Yang, Z. P., Zhang, Q., Huang, S. M., Bao, D. (2008): On-farm evaluation of an in-season nitrogen management strategy based on soil  $N_{min}$  test. – *Field Crops Research* 105: 48-55.
- [12] De Paz, J. M., Ramos, C. (2004): Simulation of nitrate leaching for different nitrogen fertilization rates in a region of Valencia (Spain) using a GIS–GLEAMS system. – *Agric., Ecosyst & Environ.* 103: 59-73.
- [13] Demelash, N., Bayu, W., Tesfaye, S., Ziadat, F., Sommer, R. (2014): Current and residual effects of compost and inorganic fertilizer on wheat and soil chemical properties. – *Nutr. Cycl. Agroecosyst* 100: 357-367.
- [14] Dordas, C. A., Lithourgidis, A. S., Matsi, T., Barbayiannis, N. (2008): Application of liquid cattle manure and inorganic fertilizers affect dry matter nitrogen accumulation, and partitioning in maize. – *Nutr. Cycl. Agroecosyst* 80: 283-296.
- [15] Fan, T., Stewart, B. A., Yong, W., Luo, J. J., Zhou, G. Y. (2005): Long-term fertilization effects on grain yield, water-use efficiency and soil fertility in the dryland of Loess Plateau in China. – *Agriculture, Ecosystems & Environment* 106: 313-329.
- [16] Galloway, J. N., Aber, J. D., Erisman, J. W., Seitzinger, S. P., Howarth, R. W., Cowling, E. B., Cosby, B. J. (2003): The nitrogen cascade. – *Bioscience* 53: 341-356.
- [17] Gao, Q., Feng, G. Z., Wang, Z. G. (2010): Present situation of fertilizer application on spring maize in Northeast China. – *Chinese Agricultural Science Bulletin* 26: 229-231. (in Chinese).
- [18] Guo, J. H., Liu, X. J., Zhang, Y., Shen, J. L., Han, W. X., Zhang, W. F., Christie, P., Goulding, K. W. T., Vitousek, P. M., Zhang, F. S. (2010): Significant acidification in major Chinese croplands. – *Science* 327: 1008-1010.
- [19] Hillin, C. K., Hudak, P. F. (2003): Nitrate contamination in the Seymour aquifer, north central Texas, USA. – *Bull. Environ. Contam. Toxicol.* 70: 674-679.
- [20] Jabloun, M., Schelde, K., Tao, F. L., Olesen, J. E. (2015): Effect of temperature and precipitation on nitrate leaching from organic cereal cropping systems in Denmark. – *European Journal of Agronomy* 62: 55-64.
- [21] Li, X. H., Guo, H. H., Zhu, Z. L., Dong, H. Y., Yang, L. P., Zhang, X. J. (2016): Effects of different straw return modes on contents of soil organic carbon and fractions of soil active carbon. – *Trans. Chin. Soc. Agric. Eng.* 32: 130-135.
- [22] Li, H. L., Wang, C., Sun, H. T., Yan, X. L., Liang, Q. (2017a): Comprehensive utilization and sustainable development of agriculture straw. – *Journal of Agricultural Mechanization Research* 39: 256-262. (in Chinese).
- [23] Li, H., Feng, W. T., He, X. H., Zhu, P., Gao, H. J., Sun, N., Xu, M. G. (2017b): Chemical fertilizers could be completely replaced by manure to maintain high maize yield and soil organic carbon (SOC) when SOC reaches a threshold in the Northeast China Plain. – *Journal of Integrative Agriculture* 16: 937-946.
- [24] Li, Y. Z., Song, D. P., Dang, P. F., Wei, L. N., Qin, X. L., Siddique, K. H. M. (2020): Combined ditch buried straw return technology in a ridge-furrow plastic film mulch system: Implications for crop yield and soil organic matter dynamics. – *Soil & Tillage Research*



- 199: 1-9.
- [25] Liang, B., Zhao, W., Yang, X. Y., Zhou, J. B. (2013): Fate of nitrogen-15 as influenced by soil and nutrient management history in a 19-year wheat–maize experiment. – *Field Crops Res.* 144: 126-134.
- [26] Liu, C., Lu, M., Cui, J., Li, B., Fang, C. M. (2014): Effects of straw carbon input on carbon dynamics in agricultural soils: a meta-analysis. – *Glob. Change Biol.* 20: 1366-1381.
- [27] Liu, Z., Ma, F. Y., Hu, T. X., Zhao, K. G., Gao, T. P., Zhao, H. X., Ning, T. Y. (2020): Using stable isotopes to quantify water uptake from different soil layers and water use efficiency of wheat under long-term tillage and straw return practices. – *Agricultural Water Management* 229: 1-9.
- [28] López Pasquali, C. E., Fernández Hernando, P., Durand Alegría, J. S. (2007): Spectrophotometric simultaneous determination of nitrite, nitrate and ammonium in soils by flow injection analysis. – *Analytica Chimica Acta* 600(1-2): 177-182.
- [29] Lu, F., Wang, X. K., Han, B., Ouyang, Z. Y., Duan, X. N., Zheng, H., Miao, H. (2009): Soil carbon sequestrations by nitrogen fertilizer application, straw return and no-tillage in China's cropland. – *Global Change Biol.* 15: 281-305.
- [30] Luo, L., Wang, C. B., Pang, H. C., Yang, S. C., Li, Y. Y., Jiang, W. L. (2015): Effects of combined application of organic and inorganic fertilizers on physical and chemical properties and crop yields in alkali-saline soil. – *Agricultural Research in the Arid Areas* 33(4): 105-111. (in Chinese).
- [31] Martínez, E., Domingo, F., Roselló, A., Serra, J., Boixadera, J., Lloveras, J. (2017): The effects of dairy cattle manure and mineral N fertilizer on irrigated maize and soil N and organic C. – *European Journal of Agronomy* 83: 78-85.
- [32] Nelson, D. W., Sommers, L. E. (1973): Determination of total nitrogen in plant material. – *Agronomy Journal* 65: 109-112.
- [33] Oldfield, E. E., Bradford, M. A., Wood, S. A. (2019): Global meta-analysis of the relationship between soil organic matter and crop yields. – *Soil* 5: 15-32.
- [34] Rasool, R., Kukal, S. S., Hira, G. S. (2008): Soil organic carbon and physical properties as affected by long-term application of FYM and inorganic fertilizers in maize–wheat system. – *Soil Till. Res.* 101: 31-36.
- [35] Rees, B., Castle, K. (2002): Nitrogen recovery in soils amended with organic manures combined with inorganic fertilizers. – *Agronomie* 22: 739-746.
- [36] Subehia, S., Sepehya, S., Rana, S. S., Negi, S. C., Sharma, S. K. (2013): Long-term effect of organic and inorganic fertilizers on rice (*Oryza sativa* L.)-wheat (*Triticum aestivum* L.) yield, and chemical properties of an acidic soil in the western Himalayas. – *Exp. Agric.* 49: 382-394.
- [37] Tan, D. S., Liu, Z. H., Jiang, L. H., Zhang, Q., Zheng, F. L., Lin, H. T., Gao, X. H., Xu, Y. (2011): Effect of different fertilization patterns on maize yield, economic benefit and  $\text{NO}_3^-$ -N of soil in Nansi lake basin. – *Chinese Journal of Soil Science* 42: 887-890. (in Chinese).
- [38] Uzoma, K. C., Inoue, M., Andry, H., Fujimaki, H., Zahoor, A., Nishihara, E. (2011): Effect of cow manure biochar on maize productivity under sandy soil condition. – *Soil Use Manag* 27: 205-212.
- [39] Wang, Y., Yamamoto, K., Yakushido, K. (2002): Changes in nitrate N content in different soil layers after the application of livestock waste compost pellets in a sweet corn field. – *Soil Sci. Plant Nutr.* 48: 165-170.
- [40] Wang, S. C., Zhao, Y. W., Wang, J. Z., Zhu, P., Cui, X., Han, X. Z., Xu, M. G., Lu, C. A. (2018a): The efficiency of long-term straw return to sequester organic carbon in Northeast China's cropland. – *Journal of Integrative Agriculture* 17: 436-448.
- [41] Wang, X. J., Jia, Z. K., Liang, L. Y., Zhao, Y. F., Yang, B. P., Ding, R. X., Wang, J. P., Nie, J. F. (2018b): Changes in soil characteristics and maize yield under straw return system in dryland farming. – *Field Crops Research* 218: 11-17.
- [42] Xu, J., Han, H. F., Ning, T. Y., Li, Z. J., Lal, R. (2019): Long-term effects of tillage and straw management on soil organic carbon, crop yield, and yield stability in a wheat-maize

- system. – *Field Crops Research* 233: 33-40.
- [43] Zhang, F. S., Wang, J. Q., Zhang, W. F., Cui, Z. L., Ma, W. Q., Chen, X. P., Jiang, R. F. (2008): Nutrient use efficiencies of major cereal crops in China and measures for improvement. – *Acta Pedologica Sinica* 45: 915-924. (in Chinese).
- [44] Zhang, F. S., Cui, Z. L., Fan, M. S., Zhang, W. F., Chen, X. P., Jiang, R. F. (2011): Integrated soil-crop system management: reducing environmental risk while increasing crop productivity and improving nutrient use efficiency in China. – *J. Environ. Qual.* 40: 1051-1057.
- [45] Zhang, X., Davidson, E. A., Mauzerall, D. L., Searchinger, T. D., Dumas, P., Shen, Y. (2015): Managing nitrogen for sustainable development. – *Nature* 528: 51-59.
- [46] Zhang, Y. L., Li, C. H., Wang, Y. W., Hu, Y. M., Christie, P., Zhang, J. L., Li, X. L. (2016): Maize yield and soil fertility with combined use of compost and inorganic fertilizers on a calcareous soil on the North China Plain. – *Soil & Tillage Research* 155: 85-94.
- [47] Zhao, J. W., Zhou, L. R. (2011): Combined application of organic and inorganic fertilizers on black soil fertility and maize yield. – *Journal of Northeast Agricultural University (English Edition)* 18(2): 24-29.
- [48] Zhen, W., Song, X. D., Wang, C. R., Hu, Y. J., Si, Z. S. (2020): The effect of the change of corn straw treatment mode on the occurrence of corn disease, insect pests and weeds in Heilongjiang Province. – *Heilongjiang Science* 11: 43-47.
- [49] Zhi, Q., Li, S. L., Zhang, X., Zhu, F. F., Li, P. P., Sheng, R., Chen, X., Zhang, L. M., He, J. Z., Wei, W. X., Fang, Y. T. (2020): Fertilizer nitrogen use efficiency and fates in maize cropping systems across China: Field <sup>15</sup>N tracer studies. – *Soil & Tillage Research* 197: 1-9.
- [50] Zhou, L. R., Yang, D. C. (2013): Screening of salinization of farmland organic manure and inorganic fertilizer ratio. – *Journal of Northeast Agricultural University* 44(11): 25-28. (in Chinese).
- [51] Zhu, Z. L., Chen, D. L. (2002): Nitrogen fertilizer use in China- contributions to food production impacts on the environment and best management strategies. – *Nutrient Cycling in Agroecosystems* 63: 117-127.

## EFFICACY OF SNEB183 (*SINORHIZOBIUM FREDII*) AGAINST SOYBEAN CYST NEMATODE (*HETERODERA GLYCINES*) UNDER FIELD AND GROWTH CHAMBER CONDITIONS

WANG, Y. Y.<sup>1\*</sup> – YUAN, R. H.<sup>1</sup> – LIAN, X. L.<sup>1</sup> – SIKANDAR, A.<sup>2</sup> – ZHU, X. F.<sup>2</sup> – LIU, X. Y.<sup>3</sup> – FAN, H. Y.<sup>2</sup> – CHEN, L. J.<sup>2</sup> – DUAN, Y. X.<sup>2</sup>

<sup>1</sup>*College of Bioscience s and Biotechnology, Shenyang Agricultural University, Shenyang 110866, Liaoning, China*

<sup>2</sup>*Nematology Institute of Northern China, Shenyang Agricultural University, Shenyang 110866, Liaoning, China*

<sup>3</sup>*College of Sciences, Shenyang Agricultural University, Shenyang, China*

\*Corresponding author

e-mail: wyuanyuan1225@syau.edu.cn; phone: +86-1389-8182-096

(Received 24<sup>th</sup> Sep 2020; accepted 21<sup>st</sup> Dec 2020)

**Abstract.** Soybean cyst nematode (*Heterodera glycines*) has become a serious risk for soybean production globally. Chemical nematicides pose a severe threat to human health and also pollute the environment whereas, biological control is a safe and eco-friendly method used to control pathogens. The aim of this study was to discover novel biocontrol agents against *H. glycines* by coating soybean seeds with biocontrol agent Sneb183 (*Sinorhizobium fredii*) and to assess its potential to control this pest. The stability and efficiency of Sneb183 (*S. fredii*) to control *H. glycines* in field and growth chamber experiments were investigated. Seed coating with Sneb183 significantly decreased the presence of *H. glycines* by 35.58%, 64.09% and 50.43% in experiments J2 (second-stage juveniles), J3 (third-stage juveniles) and J4 (fourth-stage juveniles), respectively as compared to control. A progressive increase in the concentrations of the Sneb183 resulted in a significant reduction of *H. glycines*. Additionally, Sneb183 boosted seed germination and seed vigor index. Moreover, seed coating with Sneb183 increased plant biomass. These results demonstrate that Sneb183 (*S. fredii*) is a promising biocontrol agent against *H. glycine* and biomass promoter of soybean.

**Keywords:** *pathogen, biocontrol, seed germination, vigorous index, biomass*

### Introduction

Soybean (*Glycine max* L.) is a chief source of food and oil products throughout the world. Plant-parasitic nematodes (PPN) can simply destroy oil crops by feeding and also facilitates the spread other pathogenic organisms such as bacteria, viruses and fungi (Palomares-Rius et al., 2017; Sikandar et al., 2020a). Some of them are obligate parasites in nature whereas, others are sedentary such as root-knot nematodes of the genus *Meloidogyne* and cyst nematodes of the genera *Heterodera* and *Globodera* (Kihika et al., 2017; Palomares-Rius et al., 2017).

Soybean cyst nematode (*Heterodera glycines*) has adversely affected growth and seed yield of soybean globally (Rincker et al., 2017). It causes an enormous threat to soybean production, manifested in up to 1.5 billion USD global losses and 120 million USD worth of damage in China annually (Moens et al., 2008; Hosseini and Matthews, 2014). Synthetic chemical nematicides have been applied to manage nematodes but their haphazard uses cause serious consequences on human's health and environment (Sikandar et al., 2020b). That's why several chemical nematicides have been banned in

different countries (Nicol et al., 2011). With increasing demands of safe and eco-friendly strategies for management and prevention of *H. glycines* are needed urgently.

Recently, the applications of biocontrol agents are capable of controlling *H. glycines*. Biological control is generally safe as compared to synthetic chemical control. There is the richness of soil-borne microbes in rhizosphere soil like *Sinorhizobium* (Tian et al., 2014), *Pseudomonas* spp. (Prabhukarthikeyan et al., 2018; Meena et al., 2019) *Bacillus* spp. (Zhao et al., 2018; Beeman and Tylka, 2018) and *Burkholderia* spp. (Ji et al., 2010; Kurepin et al., 2015) these are valuable for plant growth.

Several microbial strains have antagonistic potential toward plant-parasitic nematodes (Gao et al., 2016; Zhai et al., 2018; Xiang et al., 2018). Soybean seed treated by *B. simplex* effectively reduced *H. glycines* by triggering induced systemic resistance (Xiang et al., 2013; Xiang et al., 2016). Zhao et al. (2019) also reported that soybean seeds treated with Sneb159 (*Microbacterium maritopicum*) reduced the *H. glycines* in field and growth chamber experiments. Sneb183 (*Sinorhizobium fredii*) was isolated from nodules of soybean and efficiently decreased *H. glycines* by reducing oxygen consumption of J2s (Tian et al., 2014; Wang et al., 2020). Seed coating with plant growth-promoting bacteria is an effective and simple technique against pathogens (Pathak et al., 2016).

Therefore, keeping in view the biocontrol ability of Sneb183 (*Sinorhizobium fredii*) toward *H. glycine*, the study was aimed to explore the evaluation of Sneb183 (*Sinorhizobium fredii*) on growth of soybean and control of *H. glycine* by seed coating in field and growth chamber. The outcomes of the current study should help in the progression of valuable and marketable biocontrol agents.

## Materials and Methods

### *Isolation of cysts and J2 of SCN*

Soil samples from 2 cm depth were obtained from the rhizosphere of soybean (*Glycine max* cv Liaodou 15, a SCN-susceptible cultivar) grown in greenhouse of Nematology Institute of Northern China (NINC), Shenyang Agricultural University, China. Cysts were collected through hand-picking under a stereomicroscope (Nikon SMZ800, Nikon, Tokyo, Japan) and were surface-sterilized by 0.1% HgCl<sub>2</sub> solution for 1 minute and then rinsed three times with distilled water for the complete elimination of HgCl<sub>2</sub>. The cysts were shifted in Baermann funnel at 25°C and J2s were collected every two or three days (Liu, 1995).

### *Effect of Sneb183 on the seedling growth of soybean*

*Sinorhizobium fredii* Sneb183 preserved at -80°C was suspended in sterilized water and adjusted to 1.0×10<sup>8</sup> cfu/ml with a hemocytometer under a microscope. The medium was sterilized in steam autoclave machine (Zealway (Xiamen) Instrument Co., Ltd. Model no.GI54DS) for 30 min at 121°C. The 1.0 mL of suspension was poured to 50 mL sterilized TY liquid medium (Duelli and Noel, 1997). Cultures were maintained at 28°C and 150 rpm for 168 h in a shaker (ZWY-1102C incubator shaker), the fermentation broth was labelled as Sneb183F.

Soybean seeds Liaodou15 were used in all the experiments. Seeds were surface-sterilized with 0.5% NaOCl for 10 min and then washed several times with sterile distilled water and air-dried (Hosseini and Matthews, 2014). Seeds were equally coated with Sneb183F with a ratio of 70:1 (g/ml) and distilled water was used as a control treatment

(Zhou et al., 2017). The coated seeds were transferred into the petri dish contained wet filter paper and incubated at  $28 \pm 1^\circ\text{C}$  for one week (Fan et al., 2017; Sikandar et al., 2019). Germination of seeds was counted on a daily basis. After 7 days of incubation, the radicles were cut off, and the fresh weight of radicles per 10 seeds was calculated. The average germination percentage  $\pm$  SE (standard error) of triplicate experiments was calculated. Seedling vigour index (VI) was determined by using the *Eq.1* described by Abdul-Baki and Anderson (1973).

$$\text{Vigor index (VI)} = (\text{M.S.L} + \text{M.R.L}) \times \text{G\%} \quad (\text{Eq.1})$$

whereas; M.S.L (Mean shoot length); M.R.L (Mean root length); G% (Germination percentage).

### ***Biocontrol efficiency of Sneb183 against H. glycines in growth chamber experiments***

Coated seeds with 1x, 5x and 10x diluted Sneb183 fermentation filtrate were planted in pots (25 cm in diameter) with sterilized soil and sand (2:1) and irrigated on alternate days with N-free Hoagland's solution, in which  $\text{KNO}_3$  and  $\text{Ca}(\text{NO}_3)_2$  were substituted with  $\text{KH}_2\text{PO}_4$  and  $\text{CaCl}_2$  (Hoagland and Arnon, 1950). Plants were placed in the illuminated chamber (16-h photoperiod and  $23^\circ\text{C}$ – $26^\circ\text{C}$  temperature). At the second true leaf stage, 2 ml freshly hatched J2s (approximately 1,500) were inoculated into two 1-cm-deep holes around the stem base by pipetting. The number of juveniles was observed after 7 days post-inoculation (dpi) by acid fuchsin staining and mature females were calculated at 35 dpi. The experiment was conducted in a completely randomized block design, and all growth chamber treatments were replicated eight times.

### ***Biocontrol efficiency of Sneb183 against H. glycines in field experiments***

Field experiments were conducted at Kangping County (Liaoning Province, China) during 2018. Each experiment comprised of two treatments: Sterilized seeds coated with Sneb183 as treated and with distilled water as the control. All treatments were arranged in a randomized complete block design with five replications. Experimental plots were 7-m long, 3.5-m wide and contained 6 rows (70 seeds per row). After 35 days, 12 seedlings were randomly selected by using the Z-shaped sampling method. Seedlings were carefully removed and the number of females was counted immediately on the roots. 100 ml of rhizosphere soil samples were randomly collected for experimental plots. The females in the soil were isolated and counted as described above. The length of shoots and roots, the root weight and fresh weight of whole plants were recorded for all sixty seedlings per treatment. Then, the number of juveniles inside the roots was determined in twenty-five seedlings and the dry weight of the plants seedlings were measured from thirty-five other seedlings. Randomly selected plants were evaluated for plant height, number of pods and seeds per plant. Seeds were threshed, and 100-seed weight was measured four times per plot.

### ***Effect of Sneb183 on the development of soybean cyst nematode (SCN) in soybean roots***

Plants were inoculated with J2s of SCN as described above. Two days after inoculation, plants were transferred to new pots and effect of Sneb183 on the development of SCN in soybean root was determined. Roots samples were collected at 3, 6, 9, 12, 15, 18, 21, 24, 27, and 30 days after the nematode inoculation. For each time interval, six

plants were randomly selected. Roots were carefully removed from pots, washed gently and weighed. The clean roots were stained with 0.1% acid fuchsin solution. The distribution of the different developmental stages, namely J2, J3, J4 and adults were calculated under a stereomicroscope. The entire experiment was repeated twice.

### ***Effect of Sneb183 on J2s Infiltration of Soybean Root Position***

After 3 days of inoculation of J2, the root system of soybean was carefully removed and stained. Then, the number of J2s was observed under stereomicroscope. According to the distance of 0.5 cm from the root tumor as a distance unit, the number of invasion of J2s at different distance units was calculated.

### ***Statistical analysis***

In order to assess the significant effects, data was analyzed by using one-way analysis of variance (ANOVA). Means difference for each trial was calculated by the Duncan multiple range test. All statistical procedures were directed by IBM-SPSS statistics 25.0 version software and graphs were built on Sigma Plot 10.0 software.

## **Results**

### ***Effect of Sneb183 on the seedling growth of soybean***

The effect of fermentation on the seedling growth of soybean is shown in *Fig. 1* and *Fig. 2*. The significant difference ( $P < 0.05$ ) was observed in coated seeds with fermentation broth of Sneb183 which boosted the germination up to 92%. Fresh and dry weight of radicles demonstrated the potential of Sneb183 which increased to 9.63% and 19.23%, respectively as compared to control. The mean root length, mean shoot length and vigor index were significantly boosted up to 29.33%, 21.55% and 39.33%, respectively by seed coating with *Sinorhizobium fredii* (Sneb183).

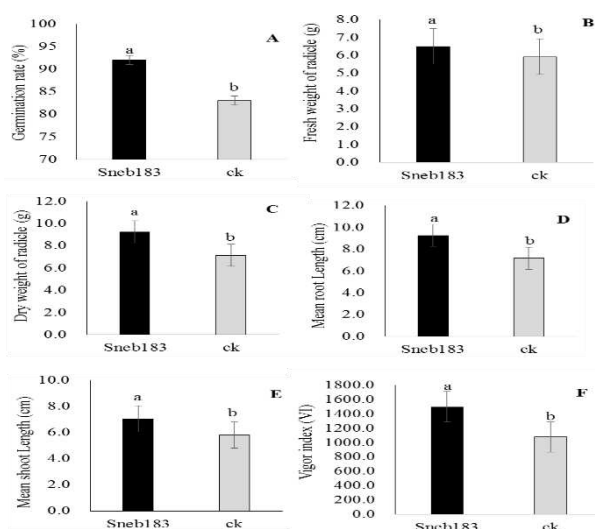


**Figure 1.** Effect of Sneb183 on the seedling growth of soybean. (A) Germination percentage of soybean seeds. (B) Fresh weight of radical. (C) Dry weight of radicals. (D) Mean root length. (E) Mean shoot length. (F) Vigour index of treated and untreated seeds. Different letters on bar indicates that values are significantly different according to Duncan's multiple range test at  $P > 0.05$



**Figure 2.** Efficiency of coating with Sneb183 on the germination of soybean seeds

### ***Biocontrol efficiency of Sneb183 against *H. glycines* in growth chamber experiments***

The *Sinorhizobium fredii* Sneb183 was tested for its potential against *H. glycines* in growth chamber experiments. The plants were monitored regularly to examine the number of juveniles at 7 dpi and mature females at 35 dpi.

Table 1 demonstrated that all the treated seed with different dilution of fermentation Sneb183 efficiently reduced the invasion of J2s and development of matured females. However, nematicidal potential was directly related to the concentration of fermentation of Sneb183. The maximum potential of Sneb183 was observed in 1x dilution because less number of juveniles and females recorded in this dilution as compared to 5x and 10x dilution. A progressive increase in the concentrations of the Sneb183 resulted were significantly reduced *H. glycines*.

**Table 1.** Effects of Sneb183 at different dilution on *H. glycines* in growth chamber experiments

Treatments	1x	5x diluted	10x diluted	CK
Juveniles	91.1±13.09	98.9±20.49	107.4±15.85	151.8±25.27
Females	62.4±9.67	70.4±11.33	78.4±17.21	119.4±26.37
ANOVA Test				
S.S	4118.45	4061.25	4205.0	5248.80
df	1	1	1	1
M.S	4118.45	4061.25	4205.0	5248.80
F	31.08	14.82	15.36	7.87
P	0.000	0.001	0.001	0.012

Data represent the Mean±Standard deviation. Whereas; S.S (Sum of square); M.S (Mean square); df (Degree of freedom); F (F-value); P (significant value)

### ***Biocontrol efficiency of Sneb183 against *H. glycines* in field experiments***

To determine the biological control effect of Sneb183 on *H. glycines* and growth parameters were evaluated under field conditions. The plant height and shoot length were increased by Sneb183 (Table 2). Sneb183 significantly reduced the number of cyst on the roots up to 27.14% as compared with the control. The number of seeds and number of pods were increased in Sneb183-treated plants (Table 3). It is clear from outcomes of field experiment that the Sneb183 displayed a drastic decrease in no. of cysts (Table 2 and Table 3).

**Table 2.** The growth condition of soybean and cyst number on soybean roots in field

Treat.	Shoot length (cm)	Plant height (cm)	Root length (cm)	Fresh weight (g)	Root weight (g)	Cyst
Sneb183	24.7± 5.6	100.1±12.4	21.8±4.3	7.8±0.93	1.5±0.25	63.8±8.2
Control	21.7 ±2.8	96.6±11.20	17.7±2.8	5.3±0.85	1.2±0.29	116±13
ANOVA Test						
S.S	45.36	61.25	87.65	31.53	0.61	13833.80
df	1	1	1	1	1	1
M.S	45.36	61.25	87.65	31.53	0.61	13833.80
F	2.35	0.44	6.48	40.14	8.4	111.36
P	0.14	0.517	0.020	0.000	0.009	0.000

Data represent the Mean±Standard deviation. Whereas; S.S (Sum of square); M.S (Mean square); df (Degree of freedom); F (F-value); P (significant value)

**Table 3.** Effects of rhizobium Sneb183 on soybean yield

Treat.	Pot number per plant	Seed number per plant	100-seed weight (g)
Sneb183	46.30±5.03	133.20±7.67	26.42±2.98
Control	36.70±3.06	97.40±7.32	24.74±2.25
ANOVA Test			
S.S	344.45	6408.20	14.03
df	1	1	1
M.S	344.45	6408.20	14.03
F	26.04	113.98	2.01
P	0.000	0.000	0.173

Data represent the Mean±Standard deviation. Whereas; S.S (Sum of square); M.S (Mean square); df (Degree of freedom); F (F-value); P (significant value)

### **Effect of Sneb183 on the development of SCN in soybean roots**

The Sneb183 was verified for its ability to control on the development of SCN in soybean roots. Plants were examined frequently to observe the development of soybean cyst nematode at 3, 6, 9, 12, 15, 18, 21, 24, 27, and 30 days after inoculation. Data in *Fig. 3* and *Fig. 4* presented that Sneb183-treated plant efficiently inhibited the invasion of J2s into soybean roots and reduced the invasion up to 35.58%. It also exhibited the development of nematodes J3 and J4 and reduced the development up to 64.09% and 50.43%, respectively. In comparison, at all dpi-s control seedling had maximum population of SCN but, Sneb183-treated plants displayed significantly less nematodes.

### **Effect of Sneb183 on J2s Infiltration of Soybean Root Position**

The effect of *S. fredii* Sneb183 on the infiltration of J2 in soybean root was calculated. The invasion of J2 infiltration at different distance units from the root tumor was represented in *Figure 5*. The maximum J2 were attracted at 2 cm whereas their minimum attraction was observed at 0.5 cm and 4 cm distance units from the soybean root tumor.



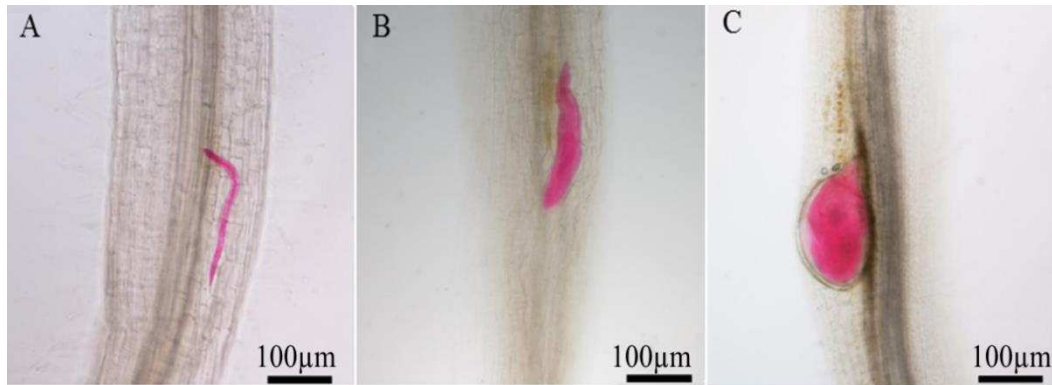


**Figure 3.** Development of SCN in soybean roots. (A) J2 in the root system. (B) J3 in the root system. (C) J4 in the root system. These pictures were taken in compound microscope (Olympus bx53 compound microscope, Olympus Co., Tokyo, Japan) and Each scale bar = 100 μm

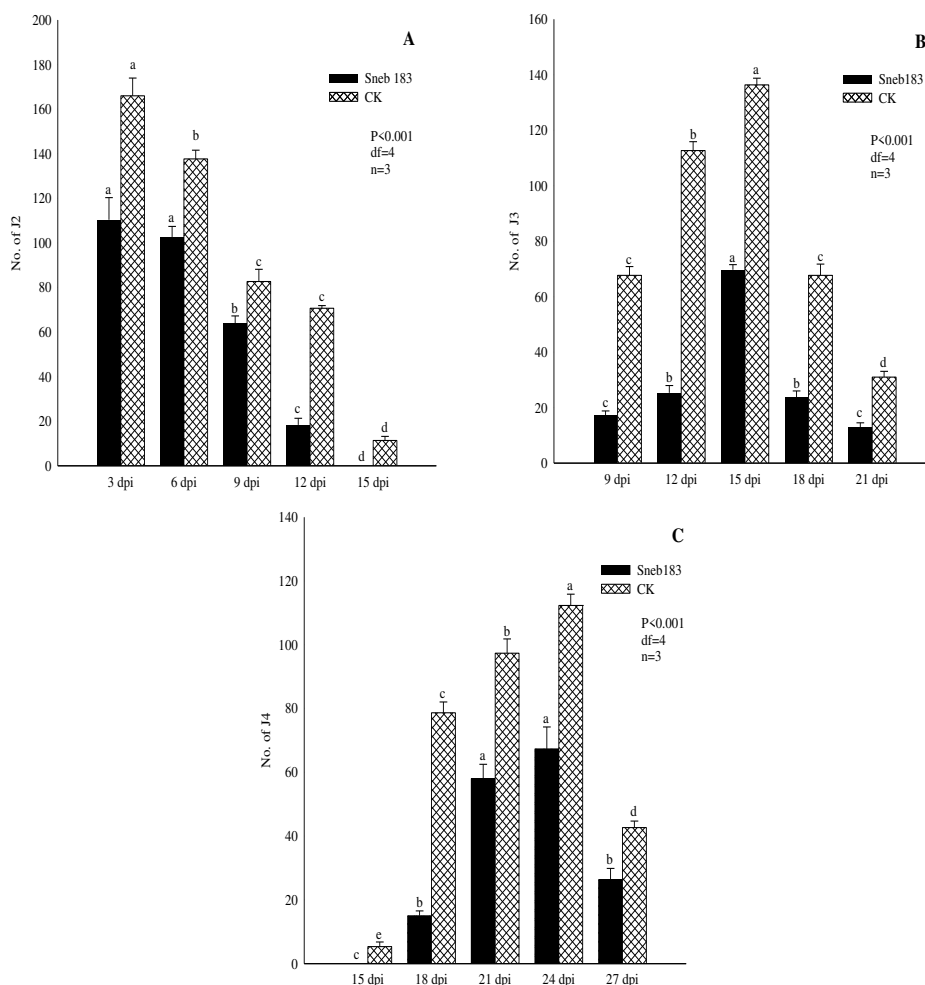


**Figure 4.** Effect of Sneb183 on the development of SCN in soybean roots. (A) Number of J2 in the root system. (B) Number of J3 in the root system. (C) Number of J4 in the root system. Different letters on bar indicates that values are significantly different according to Duncan's multiple range test at  $P > 0.05$

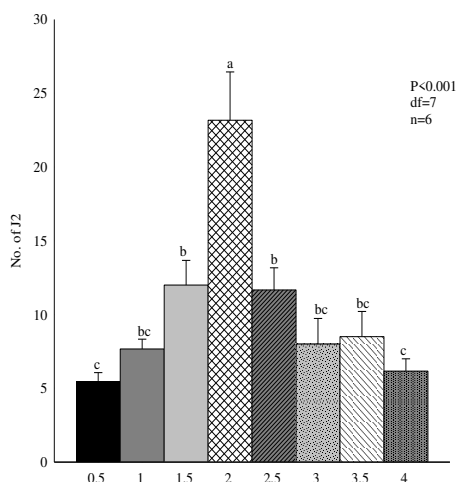


**Figure 5.** Efficacy of Sneb 183 (*Sinorhizobium fredii*) on J2 Infiltration of Soybean Root Position. Different letters on bar indicates that values are significantly different according to Duncan's multiple range test at  $P > 0.05$

## Discussion

Soybean is an essential legume but it is threatened by soybean cyst nematode (*H. glycines*). Plant growth promoting bacteria are very effective biocontrol agents in current agriculture (Kumari and Sivakumar, 2005; Séry et al., 2016). In present study, soybean seeds coating with Sneb183 effectively delay the development of juvenile and also suppressed the number of adult females of *H. glycines* as compared to control in growth chamber experiment. Liu et al. (2018) also supported our finding by explaining that seed coating with SnebYK (*Klebsiella pneumoniae*) had capability to control development of juvenile and adults of *H. glycines*. Zhou et al. (2017) described that the *Sinorhizobium fredii* Sneb183 significantly promoted plant growth and reduced soybean cyst nematode. The outcomes showed that seed coating improved biomass and also reduced nematodes infection. Thus, our results are agree with Kang et al. (2018) who reported that the seeds coating with Sneb545 *B. simplex* promoted resistance in soybean toward *H. glycines*. The findings of Zhao et al. (2019) are in agreement with our findings that seeds treated with Sneb159 *M. maritropicum* has the potential toward *H. glycines* in field and growth chamber experiments.

Seed coating with plant growth-promoting bacteria enhanced germination of seeds. Seed dressing with fungus and bacteria displayed enhanced germination, seedling vigor and reduced nematodes infection (Zhao et al., 2018; Sikandar et al., 2019). Seed coating with Sneb183 is a reasonable and effective way to boosted the germination of seeds and reduce invasion of nematodes in soybean roots.

*Rhizobium*-legume interaction is a mutual relationship which is important symbionts that provide nitrogen to soybean (Coba de la Peña et al., 2018). Sneb183 significantly enhanced seedling growth, particularly that of the root of soybean. Non-symbiotic nitrogen fixing bacteria provide nitrogen and increasing growth of plant (Hayat et al., 2010). They particularly increase weight (Singh et al., 2017) and root surface area of plant (Wang et al., 2015).

Soybean is an excellent and susceptible host of *H. glycine* however, seeds coating with Sneb183 expressively enhanced biomass and reduced the nematode infection in soybean.

Although, many methods have been used in modern agriculture to control *H. glycine*, but implication of seed coating with Sneb183 is limited to a fewer study. The results of present study demonstrated that Sneb183 is beneficial for seed coating, in order to promote plant growth and reduced nematode invasion and development. These consequences presented that seed coating is an effective and reasonable alternative approach to control *H. glycine*.

## Conclusion

It is concluded that Sneb183 have nematicidal potential toward soybean cyst nematode and also presented remarkable growth-promoting characters in both field and growth chamber experiments in view of our findings. Current outcomes could provide a foundation for *S. fredii* (Sneb183) as a biocontrol agent for soybean cyst nematode (*H. glycine*). It can be considered as a commercial biocontrol agent, however, before commercial recommendation further studies are desired to evaluate its active component screening and mechanisms of action.

**Acknowledgements.** This work was supported by the Special Fund for China Agriculture Research System (CARS-04-PS13) and National Parasitic Resources Center (NPRC-2019-194-30).

**Conflict of interests.** All authors have no conflict of interests.

## REFERENCES

- [1] Abdul-Baki, A. A., Anderson, J. D. (1973): Vigor determination in soybean seed by multiple criteria 1. – Crop science 13: 630-633.
- [2] Beeman, A. Q., Tylka, G. L. (2018): Assessing the effects of Ilevo and Votivo seed treatments on reproduction, hatching, motility, and root penetration of the soybean cyst nematode, *Heterodera glycines*. – Plant disease 102: 107-113.
- [3] Coba de la Peña, T., Fedorova, E., Pueyo, J. J., Lucas, M. M. (2018): The symbiosome: legume and rhizobia co-evolution toward a nitrogen-fixing organelle? – Frontiers in plant science 8: 2229.
- [4] Duelli, D. M., Noel, K. D. (1997): Compounds exuded by *Phaseolus vulgaris* that induce a modification of *Rhizobium etli* lipopolysaccharide. – Molecular plant-microbe interactions 10: 903-910.
- [5] Fan, S., Dong, L., Han, D., Zhang, F., Wu, J., Jiang, L., Cheng, Q., Li, R., Lu, W., Meng, F. (2017): GmWRKY31 and GmHDL56 enhances resistance to *Phytophthora sojae* by regulating defense-related gene expression in soybean. – Frontiers in Plant Science 8: 781.
- [6] Gao, H., Qi, G., Yin, R., Zhang, H., Li, C., Zhao, X. (2016): *Bacillus cereus* strain S2 shows high nematicidal activity against *Meloidogyne incognita* by producing sphingosine. – Scientific reports 6: 28756.
- [7] Hayat, R., Ali, S., Amara, U., Khalid, R., Ahmed, I. (2010): Soil beneficial bacteria and their role in plant growth promotion: a review. – Annals of Microbiology 60: 579-598.
- [8] Hoagland, D. R., Arnon, D. I. (1950): The water-culture method for growing plants without soil. – Circular. California agricultural experiment station 347: 257.
- [9] Hosseini, P., Matthews, B. F. (2014): Regulatory interplay between soybean root and soybean cyst nematode during a resistant and susceptible reaction. – BMC plant biology 14: 300.

- [10] Ji, X., Lu, G., Gai, Y., Gao, H., Lu, B., Kong, L., Mu, Z. (2010): Colonization of *Morus alba* L. by the plant-growth-promoting and antagonistic bacterium *Burkholderia cepacia* strain Lu10-1. – *BMC microbiology* 10: 243.
- [11] Kang, W., Zhu, X., Wang, Y., Chen, L., Duan, Y. (2018): Transcriptomic and metabolomic analyses reveal that bacteria promote plant defense during infection of soybean cyst nematode in soybean. – *BMC plant biology* 18: 86.
- [12] Kihika, R., Murungi, L. K., Coyne, D., Hassanali, A., Teal, P. E. A., Torto, B. (2017): Parasitic nematode *Meloidogyne incognita* interactions with different *Capsicum annum* cultivars reveal the chemical constituents modulating root herbivory. – *Scientific Reports* 7: 2903.
- [13] Kumari, N. S., Sivakumar, C. V. (2005): Integrated management of root-knot nematode, *Meloidogyne incognita* infestation in tomato and grapevine. – *Communications in Agricultural and Applied Biological Sciences* 70: 909-914.
- [14] Kurepin, L. V., Park, J. M., Lazarovits, G., Bernards, M. A. (2015): *Burkholderia phytofirmans*-induced shoot and root growth promotion is associated with endogenous changes in plant growth hormone levels. – *Plant growth regulation* 75: 199-207.
- [15] Liu, W. (1995): *The Research Technique of Plant Pathogenic Nematodes*. – *Screen Method of Nematodes in Soil and Plants*, Liaoning Science and Technology Press, Shenyang, China 47-49.
- [16] Liu, D., Chen, L., Zhu, X. F., Wang, Y. Y., Xuan, Y. H., Liu, X. Y., Chen, L. J., Duan, Y. X. (2018): *Klebsiella pneumoniae* SnebYK Mediates Resistance Against *Heterodera glycines* and Promotes Soybean Growth. – *Frontiers in Microbiology* 9: 1134.
- [17] Meena, K. S., Annamalai, M., Prabhukarthikeyan, S., Keerthana, U., Yadav, M., Rath, P., Jena, M., Prajna, P. (2019): Agriculture Application of *Pseudomonas*: A View on the Relative Antagonistic Potential Against Pests and Diseases. – In: Kumar, A., Meena, V. (eds.) *Plant Growth Promoting Rhizobacteria for Agricultural Sustainability*. Springer, Singapore.
- [18] Moens, M., Li, Y., Ou, S., Liu, X., Peng, D. (2008): Identification of *Heterodera glycines* using PCR with sequence characterised amplified region (SCAR) primers. – *Nematology* 10: 397-403.
- [19] Nicol, J. M., Turner, S. J., Coyne, D. L., Nijs, L. D., Hockland, S., Maafi, Z. T. (2011): Current Nematode Threats to World Agriculture. – In: Jones, J., Gheysen, G., Fenoll, C. (eds.) *Genomics and Molecular Genetics of Plant-Nematode Interactions*. Springer Netherlands, Dordrecht.
- [20] Palomares-Rius, J. E., Escobar, C., Cabrera, J., Vovlas, A., Castillo, P. (2017): Anatomical Alterations in Plant Tissues Induced by Plant-Parasitic Nematodes. – *Frontiers in Plant Science* 8: 1987.
- [21] Pathak, R., Gehlot, P., Singh, S. K. (2016): Seed Priming-Mediated Induced Disease Resistance in Arid Zone Plants. – In: Choudhary, D., Varma, A. (eds.) *Microbial-mediated Induced Systemic Resistance in Plants*. Springer, Singapore.
- [22] Prabhukarthikeyan, S., Keerthana, U., Raguchander, T. (2018): Antibiotic-producing *Pseudomonas fluorescens* mediates rhizome rot disease resistance and promotes plant growth in turmeric plants. – *Microbiological research* 210: 65-73.
- [23] Rincker, K., Cary, T., Diers, B. W. (2017): Impact of soybean cyst nematode resistance on soybean yield. – *Crop Science* 57: 1373-1382.
- [24] Séry, D. J-M., Kouadjo, Z. G. C., Voko, B. R., Zézé, A. (2016): Selecting Native Arbuscular Mycorrhizal Fungi to Promote Cassava Growth and Increase Yield under Field Conditions. – *Frontiers in Microbiology* 7: 2063.
- [25] Sikandar, A., Zhang, M. Y., Zhu, X. F., Wang, Y. Y., Ahmed, M., Iqbal, M. F., Javeed, A., Xuan, Y. H., Fan, H. Y., Liu, X. Y., Chen, L. J., Duan, Y. X. (2019): Effects of *Penicillium chrysogenum* strain Sneb1216 against root-knot nematodes (*Meloidogyne incognita*) in cucumber (*Cucumis sativus* L.) under greenhouse conditions. – *Applied Ecology and Environmental Research* 17: 12451-12464.

- [26] Sikandar, A., Zhang, M., Wang, Y., Zhu, X., Liu, X., Fan, H., Xuan, Y., Chen, L., Duan, Y. (2020a): In vitro evaluation of *Penicillium chrysogenum* Snef1216 against *Meloidogyne incognita* (root-knot nematode). – Scientific Reports 10: 8342.
- [27] Sikandar, A., Zhang, M., Wang, Y., Zhu, X., Liu, X., Fan, H., Xuan, Y., Chen, L., Duan, Y. (2020b): Review article: *Meloidogyne incognita* (Root-knot nematode) a risk to agriculture. – Applied Ecology and Environmental Research 18: 1679-1690.
- [28] Singh, R. P., Jha, P., Jha, P. N. (2017): Bio-inoculation of Plant Growth-promoting Rhizobacterium *Enterobacter cloacae* ZNP-3 Increased Resistance Against Salt and Temperature Stresses in Wheat Plant (*Triticum aestivum* L.). – Journal of Plant Growth Regulation 36: 783-798.
- [29] Tian, F., Chen, L., Wang, Y., Zhu, X., Duan, Y. (2014): Action mode of *Sinorhizobium fredii* Sneb183 on the activity of soybean cyst nematode. – Chinese Journal of Biological Control 30: 540-545.
- [30] Wang, B., Mei, C., Seiler, J. R. (2015): Early growth promotion and leaf level physiology changes in *Burkholderia phytofirmans* strain PsJN inoculated switchgrass. – Plant Physiology and Biochemistry 86: 16-23.
- [31] Wang, Y., Sikandar, A., Zhao, Y., Zhao, J., Liu, D., Zhu, X., Liu, X., Fan, H., Chen, L., Duan, Y. (2020): Effect of Culture Filtrate of *Sinorhizobium Fredii* Sneb183 on the Activity and Behavior of Soybean Cyst Nematode (*Heterodera glycine* Ichino, 1952). – Applied Ecology and Environmental Research 18: 1129-1140.
- [32] Xiang, P., Chen, L., Zhu, X., Wang, Y., Duan, Y. (2013): Screening and identification of bacterium to induce resistance of soybean against *Heterodera glycines*. – Chinese Journal of Biological Control 29: 661-666.
- [33] Xiang, P., Zhu, F., Chen, J., Li, H., Lu, W., Li, B., Chen, L., Duan, Y. (2016): Analysis of the APX Gene Expressed in Soybean Infected by *Heterodera glycines* and Coated with Bio-control Bacteria Sneb545. – Philippine Agricultural Scientist 99(4): 365-369.
- [34] Xiang, N., Lawrence, K. S., Donald, P. A. (2018): Biological control potential of plant growth-promoting rhizobacteria suppression of *Meloidogyne incognita* on cotton and *Heterodera glycines* on soybean: A review. – Journal of Phytopathology 166: 449-458.
- [35] Zhai, Y., Shao, Z., Cai, M., Zheng, L., Li, G., Huang, D., Cheng, W., Thomashow, L. S., Weller, D. M., Yu, Z. (2018): Multiple modes of nematode control by volatiles of *Pseudomonas putida* 1A00316 from Antarctic soil against *Meloidogyne incognita*. – Frontiers in microbiology 9: 253.
- [36] Zhao, D., Zhao, H., Zhao, D., Zhu, X., Wang, Y., Duan, Y., Xuan, Y., Chen, L. (2018): Isolation and identification of bacteria from rhizosphere soil and their effect on plant growth promotion and root-knot nematode disease. – Biological control 119: 12-19.
- [37] Zhao, J., Liu, D., Wang, Y., Zhu, X., Xuan, Y., Liu, X., Fan, H., Chen, L., Duan, Y. (2019): Biocontrol potential of *Microbacterium maritypicum* Sneb159 against *Heterodera glycines*. – Pest Management Science 75(12): 3381-3391.
- [38] Zhou, Y., Wang, Y., Zhu, X., Liu, R., Xiang, P., Chen, J., Liu, X., Duan, Y., Chen, L. (2017): Management of the soybean cyst nematode *Heterodera glycines* with combinations of different rhizobacterial strains on soybean. – PloS one 12: e0182654.

# A STATISTICAL APPROACH ON SEASONAL POPULATION CHANGES AND HABITAT PREFERENCES ON COASTAL AND WATERFOWL SPECIES AROUND EKŞISU REEDS (ERZINCAN-TURKEY): USING NEGATIVE BINOMIAL REGRESSION

AZIZOĞLU, E.<sup>1\*</sup> – ADIZEL, O.<sup>2</sup> – KARA, R.<sup>3</sup>

<sup>1</sup>*Hakkari University, Çölemerik Vocational School, Department of Plant and Animal Production, 30100-Hakkari, Turkey*

<sup>2</sup>*Department of Biology, Faculty of Science, Van Yüzüncü Yil University, 65080-Van, Turkey*

<sup>3</sup>*Hakkari University, Yüksekova Vocational School, Department of Plant and Animal Production, 30100-Hakkari, Turkey*

\*Corresponding author  
e-mail: [erkanazizoglu@hakkari.edu.tr](mailto:erkanazizoglu@hakkari.edu.tr)

(Received 25<sup>th</sup> Sep 2020; accepted 21<sup>st</sup> Dec 2020)

**Abstract.** The present study was performed in order to analyze the population density of 55 coastal and waterfowl species belonging to 15 families in Ekşisu Reeds using negative binomial regression models according to their habitat preferences. For this study, *Anas crecca* was chosen as a reference species. Population changes of 55 different species were interpreted in relation to it. Accordingly, increases by 4.48 fold ( $p < 0.001$ ) in *Anas platyrhynchos* population, 3.45 fold ( $p < 0.001$ ) in *Fulica atra* population, 2.45 fold ( $p < 0.05$ ) in *Larus armenicus* population ( $p < 0.05$ ), and 1.77 fold ( $p < 0.05$ ) in *Tadorna ferruginea* population were noted. In addition, the population of 19 species decreased. Of the seasons, autumn was taken as a reference, thus a 1.50 fold-increase ( $p < 0.01$ ) was recorded in the winter season. Changes in other seasons were not statistically significant. When the reed habitat was taken as reference, it was determined that there was a 1.33 times increase ( $p < 0.05$ ) in the water surface habitat and 36% decrease in agricultural areas ( $p < 0.05$ ). Meadows and marshland habitats were not found statistically significant.

**Keywords:** *bird population, count data, habitat, negative binomial regression, overdispersion*

## Introduction

Wetlands comprise aquatic and terrestrial areas (Keddy, 2010), exhibiting the high levels of biodiversity and biological efficiency of the ecosystems (Whittaker and Likens, 1973; Gibbs, 1993; Cassado and Montes, 1995; Sala et al., 2000; Butchart et al., 2010; Barnosky et al., 2011). Water, soil and wildlife, which are wetland components, have contributed to human society as a source of livelihood (Millennium Ecosystem Assessment, 2005; Clarkson et al., 2013). However, factors such as excessive population growth, industrialization, urbanization and unconscious agriculture negatively affected wetlands (Kiziroğlu, 2001). Due to its geographical location, Turkey possesses a favorable position for wetlands, offering habitats for many species (Kiziroğlu, 2009; Keddy, 2010). Bird species in particular are known as bio indicators of wetlands and globally endangered bird species are dependent on them (Green, 2014). Population densities and distribution of these species are determined by vegetation, which is directly related to the main sources of life (Waterhouse et al., 2002). Thus, habitats associated with vegetation ideal for these are in a constant change, as a result of many natural and anthropogenic causes. Especially, it is well-known that seasonal changes of temperature and precipitation are effective directly or indirectly on the

habitats of birds, resulting in changes regarding distribution and population of bird species (Newton, 2008; Mengesha and Bekele, 2008). In that context, many studies have been carried out on the association of habitat preferences of coastal and waterfowl species with population sizes and distributions (Muriuki et al., 1997; Clark and Shutler, 1999; Webb, 2010; Gomes et al., 2017; Azizoğlu et al., 2019). The different processes occurring in the breeding and wintering areas of birds determine the habitats, distributions and effects on population dynamics of birds. Estimating the density of species throughout their distribution is a valuable tool for biodiversity and ecological studies (Gaston and Rodrigues, 2003). Distribution of birds depending on population densities is determined by various counting techniques. Associating ecological census data such as individual number, population density with habitat types is very important in terms of bird distribution and habitat preferences (Bibby et al., 2000; Pearce and Ferrier, 2001; Kaminski et al., 2006; O'Hara and Kotze, 2010; Erdinç et al., 2017; Azizoğlu and Adizel, 2017).

Counting is the most common method used to classify bird populations (Bibby et al., 2000). A substantial assumption is needed to use unadjusted point counts to assess populations of coastal and waterfowl species. The variations in the numbers (e.g. between seasons or types of habitat) represent a variation in the actual bird population being sampled (Farnsworth et al., 2005). The correlation between these censuses and the population size (Okosodo et al., 2016; Durmuş et al., 2018) and distribution (Joseph et al., 2009; Çelik and Durmuş, 2020) of the species with their habitats is usually done by nonlinear statistical calculations (White and Bennetts, 1996; Yeşilova et al., 2016). One approach for overcoming the effect of over-dispersion is negative binomial regression (Agresti, 1997; Hilbe, 2007; Yeşilova et al., 2010). In several study, in the identification of species richness and intensities of bird population a negative binomial regression model has been used (White and Bennetts, 1996; Rékási et al., 1997; Frost et al., 1999; Small et al., 2003; O'Hara, 2005; Durmuş et al., 2018; Çelik and Durmuş, 2020). Data from this study were fitted with negative binomial regression.

It is known that the population densities of bird species are largely influenced by spatial ground (McCain, 2009). Site-based conservation is considered important in combating global biodiversity loss (Joppa et al., 2008; Nagendra, 2008).

Wetland identification and protection activities in the western part of Turkey are more common than the eastern regions. For this reason, the information on wetlands in eastern Anatolia very limited. Ekşisu reed is an important area with different habitats preferred by birds in the east. Therefore, the high concentration of environmental pressures on the Ekşisu reeds and habitat losses in the area, determination of seasonal population changes and habitat preferences of Ekşisu reed as a research subject has a particular importance.

To develop a sustainable conservation strategy for birds and habitats, it is important to define bird habitats and estimate how birds are distributed and how they use them. Compared to biodiversity studies, habitat uses and seasonal distribution of birds are little known. For this reason, seasonal distributions of bird species living in the Ekşisu reed and area uses were investigated.

## Materials and Methods

The study area, Ekşisu reed (37 S 553321, 4397154 UTM) is located in province of Erzincan in the Eastern Anatolia Region of Turkey (*Fig. 1*). Ekşisu reed constitutes one

of the most important wetlands of Turkey is supplied with hot and cold water springs. It is an important wetland with its healing waters, floating islands and surrounding historical settlements (Sunkar and Taşkıran, 2011).

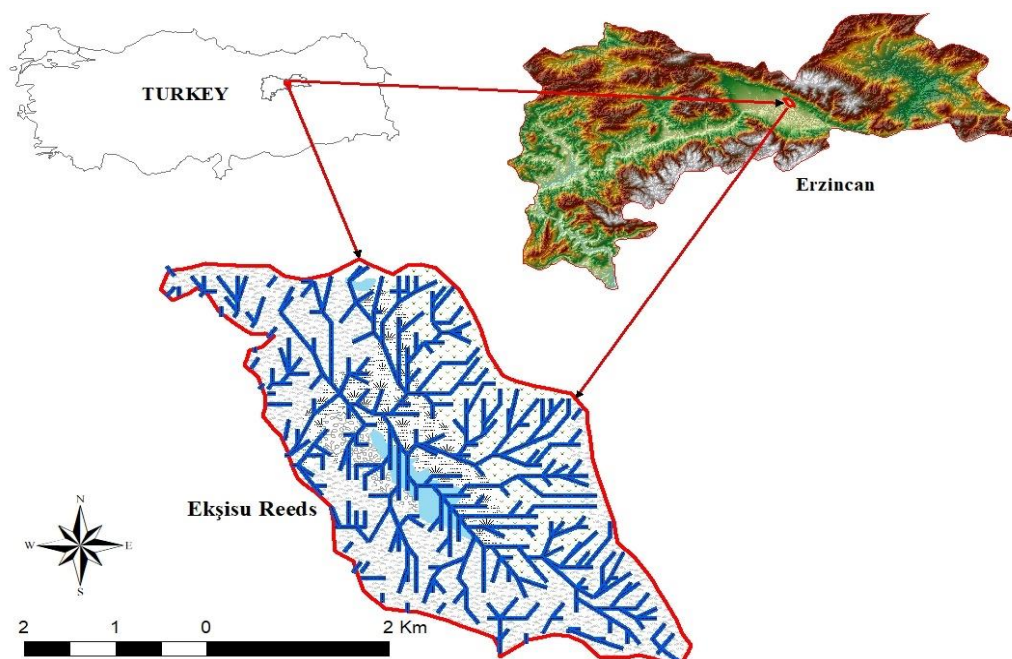


**Figure 1.** Ekşisu Reeds Location Map

For this study, the coastal and waterfowl species that use the borders of Ekşisu Reeds were investigated. In the study, this species in the area, population sizes, arrival / departure times from/to the area, seasonal distributions and statuses were determined.

A monitoring methodology has been established to determine habitat preferences, population densities, ecological and biological status of these species. A 35-day field study was conducted between 2016 and 2018 for the identified species (*Table 1*). In order to determine the population densities and habitat use conditions and distribution of the determined species, observations were performed at least 15-day periods. During the migration and reproduction periods, these observations were intensified, usually starting with the sunrise, when individuals were active, and continued until sunset.

**Table 1.** Observation work schedule for coastal and waterfowl species

Seasons	Spring	Summer	Autumn	Winter	Total
Number of Days	10	9	7	7	35

### **Species data**

The coordinates of the Ekşisu reeds and the track record were taken by GPS, and the boundary of the area, the boundaries of the habitat and the observation points were determined. The GPS records of the research area were transferred to the Geographic Information Systems (GIS) based digital environment. After determining the limits, each layer was converted to 0.25 km<sup>2</sup> square format using ArcMap 10.2 program. At



least 3 coordinates were taken in each frame and the species distributions were recorded according to the determined coordinates.

The borders transferred to the digital environment were then placed on the Corine 2012 habitat boundaries from the Esri online system using the Arcmap 10.2 program. Subsequently, five habitat types such as reed area, marshland, meadow area, water surface, and agricultural land were determined and assessed for the area they cover (Table 2, Fig. 2).

**Table 2.** Area covered by habitat types (ha)

Habitat	Swamp area	Meadows area	Agricultural land	Water surface	Reeds area	Total
Area (ha)	119	215	405	28	27	<b>794</b>

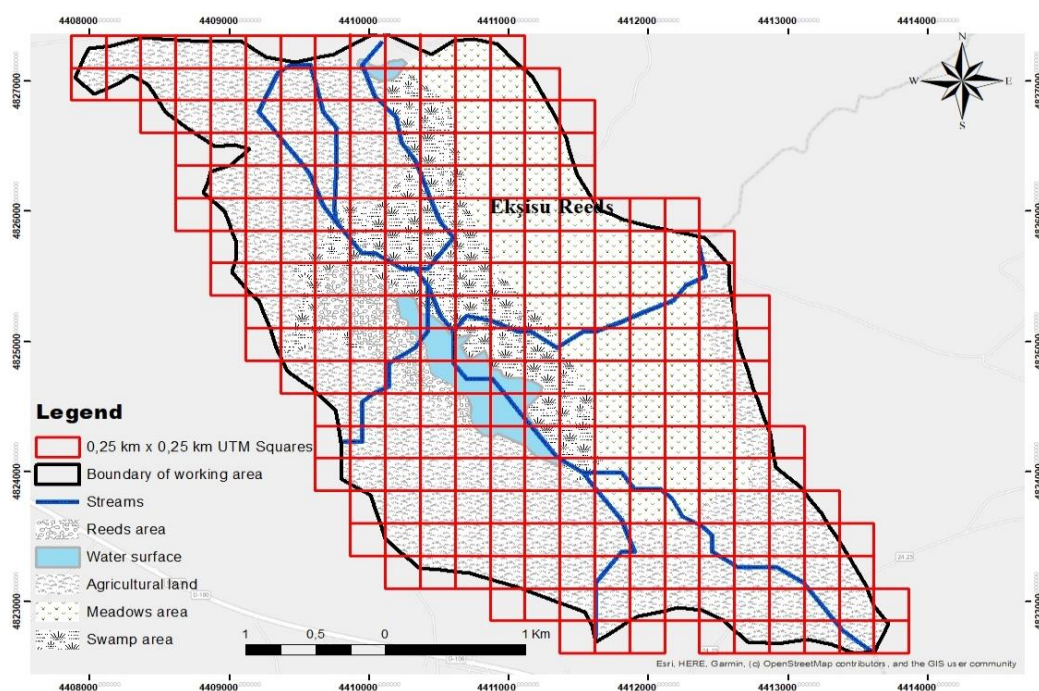


**Figure 2.** Map of the study area divided into 0.25 x 0.25 km UTM squares and habitat structure (Corine, 2012)

## Species distribution modelling

### Statistical analysis

Five environmental variables were selected for the Ekşisu reed, the seasonal population changes of the coastal and waterfowl around the reed, and the modeling of habitat preferences. Changes in species populations were compared using R 3.5.3 statistics program. Foreign, ggplot2 and MASS packages were used in statistical analysis.

For the analysis of the bird population in Ekşisu Reeds, the population variable is dependent whereas season, habitat and species were independent variables. Consequently, population~ season + habitat + species model has been composed. Since

dependent variable (population) was obtained by counting (Count data), the variable is Poisson distribution (Fig. 3).

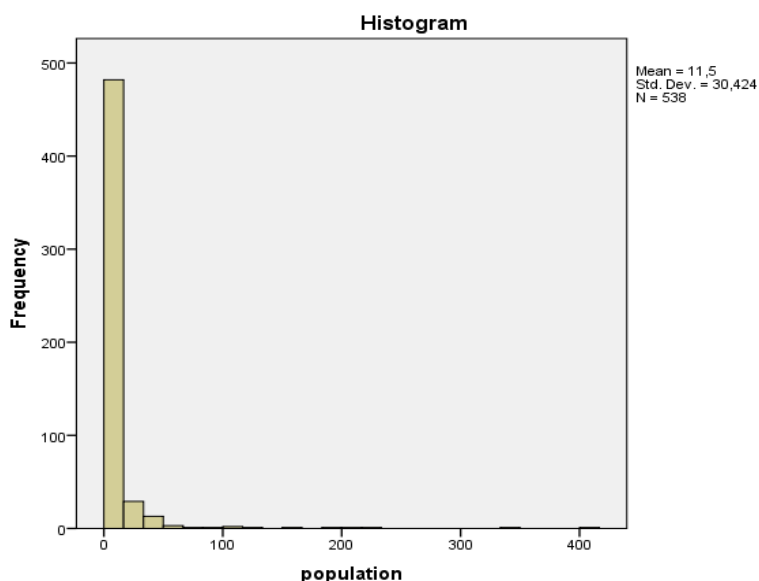


**Figure 3.** Distribution of bird population in Ekşisu Reeds

As the dependent variable, the population obtained by counting (Count data), is Poisson distribution (Fig. 3). Log-likelihood function for Poisson regression (PR) model (Eq.1) can be written as in the previous reports (Khoshgoftaar et al., 2005; Achim et al., 2007).

$$L(\beta | y_i, x_i) = \sum_{i=1}^n y_i x_i' \beta - \exp(x_i' \beta) - \ln y_i! \quad (\text{Eq.1})$$

The graph of the population was obtained as skewed to the right. Variance and average were recorded as 925.602 and 11.5, respectively (Table 3). Variance > mean status is called over dispersion (Agresti, 1997). Excessive spill test result was obtained as 12.681, indicating excessive distribution in the dependent variable.

**Table 3.** Descriptive statistics of “population”

	N	Minimum	Maximum	Mean	Std. Deviation	Variance
Population	538	1	415	11.50	30.424	925.602

Therefore, Poisson and negative binomial regressions were applied to the model. The AIC value of the Poisson regression was 7489.5 and the BIC value was 7755.38. In Poisson and negative binomial regressions, a method with smaller AIC and BIC values is preferred (Liu and Cela, 2008). For this reason, negative binomial regression parameter estimates, which also model over-spread, are used. Negative binomial regression (NB) model log likelihood function (Eq.2) is computed (Lawles, 1987).

$$L(\beta, \alpha, y) = \sum_{i=1}^n \left[ \frac{1}{\alpha} \log(1 + \alpha \mu_i) - y_i \log\left(1 + \frac{1}{\alpha \mu_i}\right) + \log \Gamma\left(y_i + \frac{1}{\alpha}\right) - \log \Gamma\left(\frac{1}{\alpha}\right) - \log y_i! \right] \quad (\text{Eq.2})$$

## Results and Discussion

The present study revealed that 55 coastal and waterfowl species belonging to 15 families have been identified. According to IUCN conservation status, 50 (90.9%) of these species are LC (Least Concern), 4 (7.3%) (Ferruginous duck-*Aythya nyroca*, Northern Lapwing-*Vanellus vanellus*, Armenian Gull-*Larus armenicus*, Eurasian Oystercatcher-*Haematopus ostralegus* NT (Near Threatened) was noted as 1 (1.8%) (Common Pochard-*Aythya farina*, VU (Vulnerable) status. In addition, according to the area uses and periods, the bird species were classified as local visitor (LV), (N=14; 25.5%), Summer Visitor (SV) (N= 25; 45.5%), Transit Migratory (T) (N=11; 20.0%), and Winter Visitor (WV) (N=5; 9.0%) (Table 4).

It is important to relate data based on ecological censuses to habitat types (Beerens et al., 2011; Gomes et al., 2017) to determine their density and distribution, to reveal the species-field relationship (Bibby et al., 2000; Pearce and Ferrier, 2001; Kaminski et al., 2006; O'Hara and Kotze, 2010; Girma et al., 2017). These counts are generally performed using various parameters with nonlinear statistical calculations (White and Bennetts, 1996; Joseph et al., 2009; Luo and Qu, 2015; Okosodo et al., 2016; Yeşilova et al., 2016; Erdiñç et al., 2017; Durmuş et al., 2018; Çelik and Durmuş, 2020).

In our study, according to parameter estimates, habitat ( $p < 0.05$ ), season ( $p < 0.01$ ) and species ( $p < 0.001$ ) were found statistically significant. In addition, since the number of individuals observed in every season in the area constantly varies, *Anas crecca* was considered as the reference species. Population changes of 55 different species were interpreted according to this species.

According to the species of *Anas crecca*, 53% decrease in the population of *Actitis hypoleucost* ( $p < 0.001$ ), 89% decrease in the population of *Anas acuta* ( $p < 0.001$ ), 4.48 fold- increase in the population of *Anas platyrhynchos* ( $p < 0.001$ ), 72% decrease in the population of *Ardea alba* ( $p < 0.001$ ), 29% decrease in the population of *Ardea cinerea* ( $p < 0.001$ ), 90% decrease in the population of *Ardea purpuea* ( $p < 0.001$ ), 29% decrease in the population of *Ardea ralloides* ( $p < 0.01$ ), 81% decrease in the population of *Aythya ferina* ( $p < 0.001$ ), 88% decrease in the population of *Botaurus stellaris* ( $p < 0.001$ ), 80% decrease in the population of *Calidris minuta* ( $p < 0.001$ ), 62% decrease in the population of *Charadrius dubius* ( $p < 0.01$ ), 53% decrease in the population of *Ciconia ciconia* ( $p < 0.05$ ), 75% decrease in the population of *Ciconia nigra* ( $p < 0.001$ ), 89% decrease in the population of *Cinclus cinclus* ( $p < 0.001$ ), 63% decrease in the population of *Egretta garzetta* ( $p < 0.001$ ), 3.45 fold-increase in the population of *Fulica atra* ( $p < 0.001$ ), 86% reduction in the population of *Haematopus ostralegus* ( $p < 0.001$ ), 81% decrease in the population of *Ixobrychus minutus* ( $p < 0.001$ ), 2.45 fold-increase in the population of *Larus armenicus* ( $p < 0.05$ ), 68% reduction in the population of *Netta rufina* ( $p < 0.001$ ), 76% decrease in the population of *Spatula querquedula* ( $p < 0.05$ ), 1.77 fold-increase in the population of *Tadorna ferruginea* ( $p < 0.05$ ), and 76% decrease in the population of *Tringa ochropus* ( $p < 0.05$ ) were recorded. The changes in the populations of other species were not statistically significant (Table 4).

As the changes in the number of species and their distribution between seasons are mostly observed in autumn, autumn was taken as reference among season. According to

this season, 1.50 fold- increase was noted in the winter season ( $p < 0.01$ ). Changes in other seasons were not statistically significant (Table 5). Of the habitats, the reed habitat was taken as reference, it was determined that there were 1.33 fold- increase in the water surface habitat ( $p < 0.05$ ) and 36% decrease in agricultural areas ( $p < 0.05$ ). Meadowland and marshland habitats were not statistically significant (Table 6).

**Table 4.** Parameter estimates of negative binomial regression and  $\text{Exp}(\text{estimate} - e^{\hat{\beta}})$  values, IUCN and Region statuses of species

Parameters Species	English name of species	Estimate	Std. Error	z value	Pr(> z )	Exp (estimate)	IUCN	Region Status
(Intercept)		<b>2.144831</b>	<b>0.239373</b>	<b>8.960</b>	<b>&lt; 2e-16</b>	<b>8.533 ***</b>		
1. <i>Actitis hypoleucos</i>	Common Sandpiper	-0.835050	0.238699	-3.498	0.000468	0.436 ***	LC	SV
2. <i>Anas acuta</i>	Northern Pintail	-2.146227	0.521270	-4.117	3.83e-05	0.117 ***	LC	SV
4. <i>Anas platyrhynchos</i>	Mallard	1.504085	0.233522	6.441	1.19e-10	4.480 ***	LC	L
5. <i>Anser anser</i>	Greylag Goose	-1.124608	0.858197	-1.310	0.190050	0.320	LC	TM
6. <i>Ardea alba</i>	Great Egret	-1.263021	0.299121	-4.222	2.42e-05	0.283 ***	LC	SV
7. <i>Ardea cinerea</i>	Grey Heron	-1.166908	0.241113	-4.840	1.30e-06	0.313 ***	LC	SV
8. <i>Ardea purpurea</i>	Purple Heron	-2.280732	0.635432	-3.589	0.000332	0.102 ***	LC	TM
9. <i>Ardeola ralloides</i>	Squacco Heron	-1.151349	0.382971	-3.006	0.002644	0.316 **	LC	TM
10. <i>Aythya ferina</i>	Common Pochard	-1.634037	0.301301	-5.423	5.85e-08	0.190 ***	VU	SV
11. <i>Aythya fuligula</i>	Tufted Duck	-1.450031	0.856617	-1.693	0.090505	0.234	LC	WV
12. <i>Aythya nyroca</i>	Ferruginous Duck	0.107587	0.339193	0.317	0.751103	1.112	NT	TM
13. <i>Botaurus stellaris</i>	Great Bittern	-2.065417	0.594480	-3.474	0.000512	0.127 ***	LC	SV
14. <i>Bubulcus ibis</i>	Cattle Egret	0.055279	0.351524	0.157	0.875044	1.05	LC	SV
15. <i>Calidris minuta</i>	Little Stint	-1.605148	0.385357	-4.165	3.11e-05	0.201 ***	LC	SV
16. <i>Charadrius dubius</i>	Little Ringed Plover	-0.972232	0.317229	-3.065	0.002178	0.379 **	LC	SV
17. <i>Ciconia ciconia</i>	White Stork	-0.752995	0.316584	-2.379	0.017383	0.472 *	LC	SV
18. <i>Ciconia nigra</i>	Black Stork	-1.384599	0.342754	-4.040	5.35e-05	0.251 ***	LC	SV
19. <i>Cinclus cinclus</i>	White-throated Dipper	-2.143179	0.991863	-2.161	0.030714	0.117 *	LC	L
20. <i>Coturnix coturnix</i>	Common Quail	-0.025996	0.754874	-0.034	0.972529	0.980	LC	SV
21. <i>Egretta garzetta</i>	Little Egret	-0.995373	0.239918	-4.149	3.34e-05	0.371 ***	LC	SV
22. <i>Fulica atra</i>	Common Coot	1.240324	0.243449	5.095	3.49e-07	3.45 ***	LC	L
23. <i>Gallinago gallinago</i>	Common Snipe	-0.696260	0.567199	-1.228	0.219619	0.501	LC	WV
24. <i>Gallinula chloropus</i>	Common Moorhen	-0.418034	0.295555	-1.414	0.157243	0.663	LC	L
25. <i>Gelochelidon nilotica</i>	Gull-billed Tern	-1.097766	0.625142	-1.756	0.079084	0.336	LC	TM
26. <i>Grus grus</i>	Common Crane	-0.062657	0.307483	-0.204	0.838531	0.641	LC	L
27. <i>Haematopus ostralegus</i>	Eurasian Oystercatcher	-1.924204	0.774970	-2.483	0.013030	0.146 *	NT	SV
28. <i>Himantopus himantopus</i>	Black-winged Stilt	-0.038286	0.417713	-0.092	0.926971	0.962	LC	SV
29. <i>Ixobrychus minutus</i>	Little Bittern	-1.646111	0.446147	-3.690	0.000225	0.193 ***	LC	TM
30. <i>Larus armenicus</i>	Armenian Gull	0.901105	0.449180	2.006	0.044844	2.459 *	NT	L
31. <i>Larus genei</i>	Slender-billed Gull	-0.640851	0.605780	-1.058	0.290103	0.527	LC	TM
32. <i>Larus michahellis</i>	Yellow-legged Gull	0.190526	0.239315	0.796	0.425955	1.209	LC	L
33. <i>Larus ridibundus</i>	Black-headed Gull	-0.458530	0.809035	-0.567	0.570876	0.631	LC	WV
34. <i>Mareca penelope</i>	Eurasian Wigeon	-2.250289	1.219783	-1.845	0.065063	0.105	LC	TM
35. <i>Netta rufina</i>	Red-crested Pochard	-1.148147	0.518620	-2.214	0.026839	0.319 *	LC	SV
36. <i>Nycticorax nycticorax</i>	Black-crowned Night-heron	0.164509	0.344229	0.478	0.632716	1.178	LC	SV
37. <i>Phalacrocorax carbo</i>	Great Cormorant	-0.717197	0.791077	-0.907	0.364614	2.04	LC	TM
38. <i>Philomachus pugnax</i>	Ruff	-0.031402	0.464392	-0.068	0.946089	0.969	LC	SV
39. <i>Platalea leucorodia</i>	Eurasian Spoonbill	-0.863995	0.858994	-1.006	0.314501	2.370	LC	TM

Paramaters Species	English name of species	Estimate	Std. Error	z value	Pr(> z )	Exp (estimate)	IUCN	Region Status
40. <i>Plegadis falcinellus</i>	Glossy Ibis	-0.113007	0.759875	-0.149	0.881776	0.895	LC	SV
41. <i>Podiceps cristatus</i>	Great Crested Grebe	-0.513334	0.312978	-1.640	0.100972	0.600	LC	L
42. <i>Porphyrio porphyrio</i>	Purple Swamphen	-0.507203	0.378870	-1.339	0.180660	0.602	LC	L
43. <i>Scolopax rusticola</i>	Eurasian Woodcock	-0.931936	0.834295	-1.117	0.263980	0.394	LC	WV
44. <i>Spatula clypeata</i>	Northern Shoveler	-0.466308	0.330623	-1.410	0.158423	0.631	LC	L
45. <i>Spatula querquedula</i>	Garganey	-1.410002	0.281190	-5.014	5.32e-07	0.244 ***	LC	L
46. <i>Sternaula hirundo</i>	Common Tern	-0.338820	0.347773	-0.974	0.329929	0.718	LC	SV
47. <i>Sternula albifrons</i>	Little Tern	-0.346917	0.576518	-0.602	0.547344	0.707	LC	SV
48. <i>Tachybaptus ruficollis</i>	Little Grebe	0.299071	0.278810	1.073	0.283420	1.34	LC	L
49. <i>Tadorna ferruginea</i>	Ruddy Shelduck	0.574302	0.249532	2.302	0.021363	1.775 *	LC	SV
50. <i>Tadorna tadorna</i>	Common Shelduck	-0.244156	0.547760	-0.446	0.655788	0.783	LC	WV
51. <i>Tringa glareola</i>	Wood Sandpiper	-0.997045	0.609558	-1.636	0.101905	0.368	LC	TM
52. <i>Tringa nebularia</i>	Common Greenshank	-0.289097	0.476692	-0.606	0.544207	0.749	LC	SV
53. <i>Tringa ochropus</i>	Green Sandpiper	-1.402836	0.553126	-2.536	0.011206	0.246*	LC	L
54. <i>Tringa totanus</i>	Common Redshank	-0.141490	0.239035	-0.592	0.553904	0.868	LC	SV
55. <i>Vanellus vanellus</i>	Northern Lapwing	-0.362271	0.246952	-1.467	0.142385	0.696	NT	SV

Signif. codes: 0 '\*\*\*' 0.001 '\*\*' 0.01 '\*' 0.05 '.' 0.1 ' ' 1, LC- Least Concern, NT-Near Threatened, VU-Vulnerable /L-Local, TM-Transit Migrant, SV-Summer Visitor, WV-Winter Visitor; Species reference: "*Anas crecca* -Common Tea

**Table 5.** Parameter estimates of negative binomial regression and  $Exp(estimate-e^{\hat{\beta}})$  values (Seasons)

Paramaters (Seasons)	Estimate	Std. Error	z value	Pr(> z )	Exp (estimate)
1.Spring	0.231974	0.100789	2.302	0.021358	1.259*
2.Summer	-0.180844	0.120778	-1.497	0.134307	0.835
3.Winter	0.405192	0.132748	3.052	0.002271	1.50**

Signif. codes: 0 '\*\*\*' 0.001 '\*\*' 0.01 '\*' 0.05 '.' 0.1 ' ' 1, -Season Reference: Autumn

**Table 6.** Parameter estimates of negative binomial regression and  $Exp(estimate-e^{\hat{\beta}})$  values (Habitat)

Paramaters (Habitat)	Estimate	Std. Error	z value	Pr(> z )	Exp (estimate)
1. Swamp area	-0.008649	0.139583	-0.062	0.950590	0.992
2. Meadows area	0.134097	0.131472	1.020	0.307742	1.143
4. Water Surface	0.286303	0.118213	2.422	0.015439	1.331 *
5. Agricultural land	-0.447072	0.218313	-2.048	0.040575	0.639 *

Signif. codes: 0 '\*\*\*' 0.001 '\*\*' 0.01 '\*' 0.05 '.' 0.1 ' ' 1, -Habitat Reference: Reeds Area

Many studies have been performed in order to ascertain the population dynamics and habitat preferences of bird species (Webb, 2010; Fraixedas, 2017; Gomes et al., 2017; Azizoğlu et al., 2019; Çelik and Durmuş, 2020). In particular, the effects of seasonal changes in population densities of coastal and waterfowl, different environmental changes in wintering and breeding areas on species distribution and habitat preferences are well-documented (Muriuki et al., 1997; Clark and Shutler, 1999; Gómez and Bayly,



2010; Webb, 2010; Beerens et al., 2011; Austini et al., 2014; Azizoğlu and Adizel, 2017; Çelik and Durmuş, 2020). Along with this study, five habitat types, which were the reed area, meadow area, water surface, swamp area and agricultural lands preferred by the coastal and waterfowl species, were determined. Also, the population size of the species and their distribution according to the habitats and their differences according to the seasons were evaluated (Fig. 4). Accordingly, a total of 6187 individuals belonging to 55 species were counted (Tables 7-8). The species were mostly seen in the water surface (N=3079) habitat. The habitat with the lowest population density was determined as agricultural land (N=104) (Table 7). The season with the highest number of species was determined as the spring period (N= 3236), and the summer with the lowest number (N= 728) (Table 8). The findings of this study were largely consistent with the previous reports.

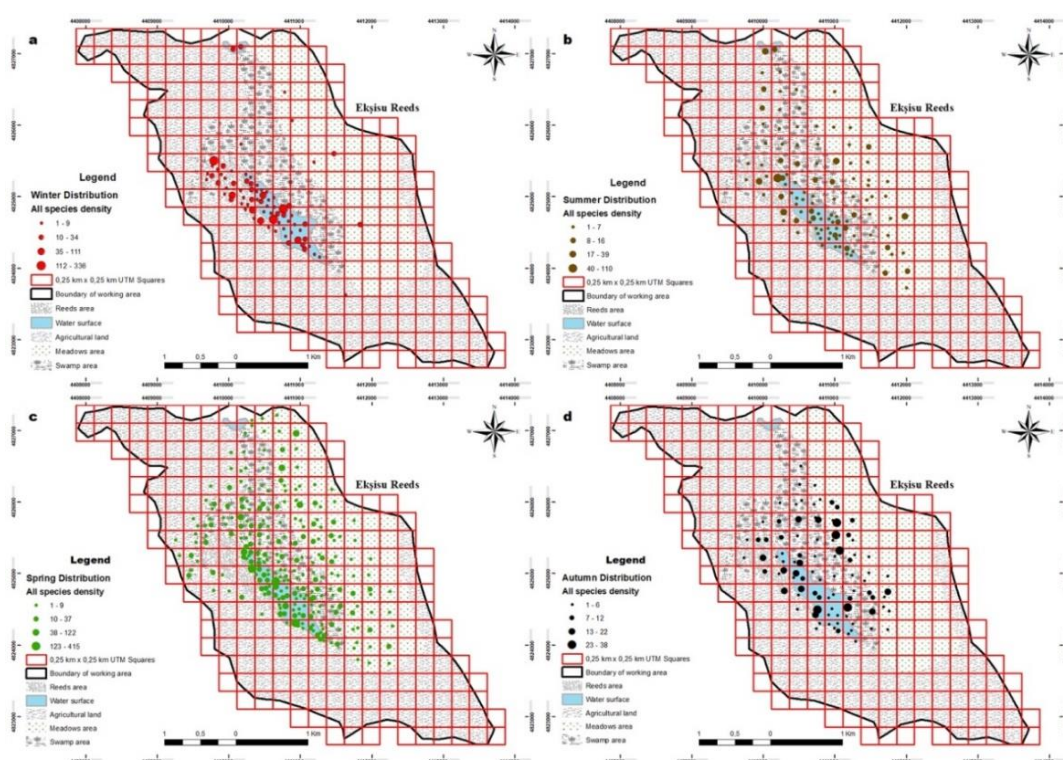


**Figure 4.** Seasonal population distribution maps of the species identified in Ekşisu Reeds (a: Winter Distribution, b: Summer Distribution, c: Spring Distribution, d: Autumn Distribution)

**Table 7.** Distribution of species populations according to the habitats

Habitat	Mean	N	Std. Deviation	Sum
Swamp area	7.46	108	8.205	806
Meadows area	8.05	146	12.761	1175
Reeds area	14.41	71	40.796	1023
Water surface	16.12	191	42.318	3079
Agricultural land	4.73	22	3.693	104
Total	11,5	538	30.424	6187

**Table 8.** Distribution of species populations according to the seasons

Season	Mean	N	Std. Deviation	Sum
Spring	11.85	273	32.798	3236
Summer	7.51	97	12.574	728
Autumn	7.56	91	7.512	688
Winter	19.94	77	48.086	1535
Total	11.5	538	30.424	6187

## Conclusion

Bird populations vary according to species, seasons and habitats and it was noted that the areas were used reproduction, feeding and accommodation. The spring season has gained ornithological importance as the migratory birds migrated to the region for breeding periods. This season was mostly preferred by coastal and waterfowl species. Of the habitat types, water surface was the most preferred habitat, which was preferred by waterfowl species for feeding purposes. Although the limited coverage of the area, reeds, meadows and marshland habitats, which are important for breeding and feeding opportunities, have been determined to be effective in using the area.

Herewith the study, changes in species populations were compared statistically. The variance of the population variable, which was taken as a dependent variable, was higher than the mean, which indicated excessive distribution. For this reason, negative binomial regression parameter estimates, which also model over-spread, are used.

As a conclusion, Ekşisu Reeds were found to be an important habitat for many bird species and other living things like all wetlands but it was noted that the area has been exposed to many anthropogenic pressures such as unconscious agricultural activities, hunting, drainage works, overgrazing. Therefore, conservation of the area is important for the continuation of the generation of bird species and other living things.

**Acknowledgements.** This study was summarized from a part of the "Erzincan Province Terrestrial and Inland Water Ecosystems Biological Diversity and Inventory Monitoring Project" conducted by the Ministry of Agriculture and Forestry, General Directorate of Nature Conservation and National Parks (Turkey). We would like to thank for their valuable contributions.

## REFERENCES

- [1] Achim, Z. K., Christian, S. J. (2007): Regression Models for Count Data in R. – <http://CRAN.R-project.org>. Date of access: 15.11.2019.
- [2] Agresti, A. (1997): Categorical Data Analysis. – John and Wiley & Sons, Incorporation, New Jersey, Canada.
- [3] Austin, J., Slattery, S., Clarke, R. G. (2014): Waterfowl populations of conservation concern: learning from diverse challenges, models and conservation strategies. – *Wildfowl* 4: 470-497.
- [4] Azizoğlu, E., Adızel, Ö. (2017): Determination of Seasonal Habitat Usage and Population Distributions of Bird Species Detected in and Around of Yüksekova Nehil Reed (Hakkari -Turkey). – *ADYÜTAYAM* Cilt 5, Sayı 1: 10-19.
- [5] Azizoğlu, E., Çelik, E., Adızel, Ö. (2019): Bayburt İli (Türkiye) Kuşları ve Sulak AlanPotansiyeli, *Doğu Fen Bilimleri Dergisi*. – *Journal of Natural & Applied Sciences of East* 2(1): 16-28.

- [6] Barnosky, A. D., Matzke, N., Tomiya, S., Wogan, G. O. U., Swartz, B., Quental, T. B., Marshall, C., McGuire, J. L., Lindsey, E. L., Maguire, K. C., Mersey, B., Ferrer, E. A. (2011): Has the Earth's sixth mass extinction already arrived? – *Nature* 471: 51-57.
- [7] Beerens, J. M., Gawlik, D. E., Herring, G., Cook, M. I. (2011): Dynamic habitat selection by two wading bird species with divergent foraging strategies in a seasonally fluctuating wetland. – *The Auk* 128(4): 651-662.
- [8] Bibby, C. J., Burgess, D. N., Hill, A. D., Mustoe, S. (2000): *Bird Census Techniques*. – Second Edition, Academic Press, ISBN 0-12-095831-7, London, United Kingdom, 86p.
- [9] Butchart, S. H. M., Walpole, M., Collen, B., Van Strien, A., Scharlemann, J. P., Almond, R. E., Baillie, J. E., Bomhard, B., Brown, C., Bruno, J., Carpenter, K. E., Carr, G. M., Chanson, J., Chenery, A. M., Csirke, J. (2010): Global biodiversity: indicators of recent declines. – *Science* 328(5982): 1164-1168.
- [10] Cassado, S., Montes, C. (1995): *Guia de los Lagos y Humedales de Espania*. – J.M. Reyero Editor, Madrid, 255p.
- [11] Clark, R. G., Shutler, D. (1999): Avian Habitat selection: Pattern from process in nest-site use by ducks? – *Ecology* 80(1): 272-287.
- [12] Clarkson, B. R., Ausseil, A. E., Gerbeaux, P. (2013): *Wetland Ecosystem Services*. – In: Dymond J. R. (ed.) *Ecosystem services in New Zealand - conditions and trends*. Manaaki Whenua Press, Lincoln, New Zealand.
- [13] Çelik, E., Durmuş, A. (2020): Nonlinear Regression Applications in Modeling Over-Dispersion of Bird Populations. – *The J. Anim. Plant Sci.* 30(2): 345-354.
- [14] Durmuş, A., Yeşilova, A., Çelik, E., Kara, R. (2018): Using Poisson and Negative Binomial Regression Models on Birds Population in Dönemeç Delta. – *Yuzuncu Yil University Journal of Agricultural Sciences* 28(1): 78-85.
- [15] Erdinç, S., Yeşilova, A., Ser, G. (2017): Using The Poisson and Negative Binomial Regression Modeling of Zooplankton Aquatic Insect Count Data. – *Yyü Tar Bil Derg (YYU J Agr Sci)* 27(1): 58-64.
- [16] Farnsworth, G. L., Nichols, J. D., Sauer, J. R., Fancy, S. G., Pollock, K. H., Shriner, S. A., Simons, T. R. (2005): *Statistical Approaches to the Analysis of Point Count Data: A Little Extra Information Can Go a Long Way*1. – USDA Forest Service Gen. Tech. Rep. PSW-GTR-191.
- [17] Fraixedas, S. (2017): *Bird populations in a changing world: implications for Nort European conservation*. – Doctoral School in Environmental, Food and Biological Sciences (YEB) University of Helsinki Finland, 61p.
- [18] Frost, K. J., Lowry, L. F., Ver Hoef, J. M. (1999): Monitoring the trend of harbor seals in Prince William Sound, Alaska, after the Exxon Valdez oil spill. – *Mar. Mam. Sci.* 15(2): 494-506.
- [19] Gaston, K. J., Rodrigues, A. S. L. (2003): Reserve selection in regions with poor biological data. – *Conservation Biology* 17: 188-195.
- [20] Gibbs, J. P. (1993): The importance of small wetlands for the persistence of local populations of wetland associated animals. – *Wetlands* 13: 25-31.
- [21] Girma, Z., Mamo, Y., Mengesha, G., Verma, A., Asfaw, T. (2017): Seasonal abundance and habitat use of bird species in and around Wondo Genet Forest, south central Ethiopia. – *Ecol. Evol.* 7(10): 3397-3405.
- [22] Gomes, M., Rabaça, J. E., Godinho, C., Ramos, J. A. (2017): Seasonal variation in bird species richness and abundance in riparian galleries in Southern Portugal. – *Acta Ornithol.* 52(1): 69-80.
- [23] Gómez, M. C., Bayly, N. J. (2010): Habitat use, abundance, and persistence of Neotropical migrant birds in a habitat matrix in northeast Belize. – *Journal Field Ornithol.* 81(3): 237-251.
- [24] Green, A. J., Elmberg, J. (2014): Ecosystem services provided by waterbirds. – *Biological Reviews* 89: 105-122. doi: 10.1111/brv.12045.
- [25] Hilbe, J. M. (2007): *Negative Binomial Regression*. – Cambridge, U.K.



- [26] Joppa, L. N., Loarie, S. R., Pimm, S. L. (2008): On the protection of “protected areas”. – *Proc. Natl. Acad. Sci. USA* 105: 6673-6678.
- [27] Joseph, L. N., Elkin, C., Martin, T. G., Possingham, H. P. (2009): Modeling Abundance Using N-Mixture Models: The Importance of Considering Ecological Mechanisms. – *Ecological Applications* 19(3): 631-642.
- [28] Kaminski, M. R., Baldassarre, G. A., Pearse, A. T. (2006): Waterbird responses to hydrological management of wetlands reserve program habitats in New York. – *Wildlife Society Bulletin* 34(4): 921-926.
- [29] Keddy, P. A. (2010): *Wetland ecology: principles and conservation*. – Cambridge University Press, Cambridge, 497p.
- [30] Khoshgoftaar, T. M., Gao, K., Szabo, R. M. (2005): Comparing software fault predictions of pure and zero-inflated Poisson regression models. – *International Journal of Systems Science* 36(11): 707-715.
- [31] Kızıroğlu, İ. (2001): *Birds, Our Flying Friends, Chapter 6: Ecological Potpourri (Ekolojik Potpori)*. – Takav Printing house. Pub. Inc. Ankara, 391.
- [32] Kızıroğlu, İ. (2009): *Birds of Turkey. Species List, and Red List of Birds of Turkey*. – Hacettepe University, Environmental Education, Bird Investigations and Public Relations Center, Ankara, 86.
- [33] Lawles, J. F. (1987): Negative binomial and mixed Poisson regression. – *The Canadian Journal of Statistics* 15(3): 209-225.
- [34] Liu, W., Cella, J. (2008): Count data models in SAS. – *SAS Global Forum*, 371.
- [35] Luo, J., Qu, Y. (2015): Estimation of group means when adjusting for covariates in generalized linear models. – *Pharm Stat.* 14(1): 56-62.
- [36] McCain, C. M. (2009): Global analysis of bird elevation diversity. – *Global Ecology and Biogeography* 18: 346-360.
- [37] Mengesha, G., Bekele, A. (2008): Diversity and relative abundance of birds of Alatish National Park. – *International Journal of Ecology and Environmental Sciences* 34: 215-222.
- [38] Millennium Ecosystem Assessment (2005): *Ecosystems and human well-being: Wetland and water Synthesis*. – Available online: [http://www.millenniumassessment.org/proxy/Document 358](http://www.millenniumassessment.org/proxy/Document%20358).
- [39] Muriuki, J. N., De Klerk, H. M., Williams, H. P., Bennun, A. L., Crowe, T. M., Berge, E. B. (1997): Using patterns of distribution and diversity of Kenyan birds to select and prioritize areas for Conservation. – *Biodiversity and Conservation* 6: 191-210.
- [40] Nagendra, H. (2008): Do parks work? Impact of protected areas on land cover clearing. – *Ambio* 37: 330-337.
- [41] Newton, I. (2008): *The ecology of bird migration*. – London, UK, Academic Press.
- [42] O'Hara, R. B. (2005): Species richness estimators: How many species can dance on the head of a pin? – *J. Anim. Ecol.* 74: 375-386.
- [43] O'Hara, R. B., Kotze, D. J. (2010): Do not log-transform count data. – *Methods in Ecology and Evolution* 1: 118-122.
- [44] Okosodo, E. F., Orimaye, J. O., Ogunyemi, O. O. (2016): Habitat Effects on Avian Species Abundance and Diversity in Idanre Forest Reserve South Western Nigeria. – *International Journal of Plant, Animal and Environmental Sciences* 6(3).
- [45] Pearce, J., Ferrier, S. (2001): The practical value of modelling relative abundance of species for regional conservation planning: a case study. – *Biological Conservation* 98: 33-43.
- [46] Rékási, J., Rozsa, L., Kiss, B. J. (1997): Patterns in the distribution of avian lice (Phthiraptera: Amblycera, Ischnocera). – *J. Avian Biol.* 28(2): 150-156.
- [47] Sala, O. E., Chapin III, F. S., Armesto, J., Berlow, E., Bloomfield, J., Dirzo, R., Huber-Sanwald, E., Huenneke, L. F., Jackson, R. B., Kinzig, A., Leeman, S. R., Lodge, D. M., Mooney, H. A., Oesterheld, M., Poff, N. L., Sykes, M. T., Walker, B. H., Walker, M., Wall, D. H. (2000): Global biodiversity scenarios for the year 2100. – *Science* 287: 1770.

- [48] Small, R. J., Pendleton, G. W., Pitcher, K. W. (2003): Trends in abundance of Alaska harbor seals, 1983-2002. – *Mar. Mam. Sci.* 19(2): 344-362.
- [49] Sunkar, M., Taşkiran, P. (2011): Ekşisu Sazlığı (Erzincan) Oluşumu, Sorunlar ve Çözüm Önerileri. – II. Türkiye Sulak Alanlar Kongresi, 22-24 Haziran 2011 S.1-10.
- [50] Waterhouse, F. L., Mather, M. H., Seip, D. (2002): Distribution and abundance of birds relative to elevation and biogeoclimatic zones. – *B.C. Journal of Ecosystems and Management* 2(2).
- [51] Webb, E. (2010): Effect of management strategy on waterfowl food availability and selection at wetland reserve program sites in the Mississippi Alluvial Valley. – Arkansas Center for Energy, Natural Resources and Environmental Studies Grant Final Report, 1-10.
- [52] White, G. C., Bennetts, R. E. (1996): Analysis of frequency count data using the negative binomial distribution. – *Ecology* 77(8): 2549-2557.
- [53] Wittaker, R. H., Likens, G. E. (1973): Primary production: the biosphere and man. – *Human Ecology* 1: 257-369.
- [54] Yeşilova, A., Kaydan, B., Kaya, Y. (2010): Modeling insect-egg data with excess zeros using zero inflated regression models. – *Hacet. J. Math. Stat.* 39(2): 273-282.
- [55] Yeşilova, A., Özgökçe, M. S., Atlihan, R., Polat Yıldız, Ş., Karaca, İ., Ser, G. (2016): Modeling of the arthropod population densities in the coastal band of Lake Van using mixture poisson regression. – *Fresenius Environmental Bulletin* 25: 1768-1778.

# THE EFFECTS OF DIFFERENT NITROGEN APPLICATION AND SEEDING RATES ON THE YIELD AND GROWTH TRAITS OF DIRECT SEEDED RICE (*ORYZA SATIVA* L.) USING CORRELATION ANALYSIS

TANG, J. C.<sup>1#</sup> – CHEN, Q. H.<sup>1#</sup> – HAO, R. Q.<sup>1#</sup> – LI, Z. X.<sup>1</sup> – LU, B. L.<sup>1,2,3\*</sup>

<sup>1</sup>Hubei Collaborative Innovation Center for Grain Industry, Agricultural college, Yangtze University, Jingzhou Hubei 434025, China

e-mail: 201872415@yangtzeu.edu.cn (Tang, J. C.); kawhichen@yeah.net (Chen, Q. H.); rachel15337179705@163.com (Hao, R. Q.); 201872409@ yangtzeu.edu.cn (Li, Z. X.)

<sup>2</sup>Engineering Research Center of Ecology and Agricultural Use of Wetland, Ministry of Education, Jingzhou Hubei 434025, China

<sup>3</sup>Hubei Provincial Key Laboratory of Waterlogged Disasters and Agricultural Use of Wetland, Jingzhou Hubei 434025, China

<sup>#</sup>These authors contributed equally to this work.

\*Corresponding author  
e-mail: blin9921@sina.com

(Received 26<sup>th</sup> Sep 2020; accepted 21<sup>st</sup> Dec 2020)

**Abstract.** Optimization of nitrogen (N) application rate and seeding rates to coordinate the balanced development of crop growth and yield is important for the efficient use of resources and the cultivation of high-quality and high-yield crops. In this study, four levels of N application rates (N0 0 kg ha<sup>-1</sup>, N1 150 kg ha<sup>-1</sup>, N2 190 kg ha<sup>-1</sup>, and N3 240 kg ha<sup>-1</sup>) and three direct seeding rates (D1 22.22 kg ha<sup>-1</sup>, D2 25.00 kg ha<sup>-1</sup>, and D3 28.57 kg ha<sup>-1</sup>) were used to explore their effects on the yield and growth characteristics of direct seeded rice (*Oryza sativa* L.) in China. Canonical correlation analysis showed that the soil–plant analyses development (SPAD) value, leaf area index (LAI), and plant height were closely related to grain yield, spikelet number per panicle, and seed setting rate, and the increase in the SPAD value may have caused the increase in the number of effective panicles and the decrease in 1000-grain weight. Gray correlation analysis showed that plant height and leaf area index were essential indices that affected grain yield. For increased grain yield, medium N and medium density (N2D2) were suitable for hybrid rice, whereas high N and high density (N3D3) were suitable for conventional rice. Plant height and leaf area index may be used as important growth indices to control yield.

**Keywords:** nitrogen fertilizer, sowing rate, mechanical seeding, canonical correlation analysis, Gray correlation analysis, grain yield, growth parameter

## Introduction

Rice feeds more than half of the world's population, and the main areas for its cultivation and consumption are in Asia (Kumar and Ladha, 2011; Abid et al., 2015). In China, direct seeding is a method of rice cultivation that solves the problems of labor shortage and low profits (Chen et al., 2009; Liu et al., 2015). Reasonable nitrogen application rates and seeding rates promote the growth and grain yield of direct-seeded rice, reducing resource waste and environmental pollution (Aslam et al., 2002; Liang et al., 2013).

Nitrogen (N), one of the basic nutrient elements required for plant growth, is a key limiting factor for crop growth and production (Tang et al., 2019). In developing countries,

soil fertility is the most important factor that limits crop yields, half of the increase for which is due to the use of inorganic fertilizers (Rodríguez et al., 2014; Alemineu et al., 2020). The amount of N fertilizer applied should be determined based on local soil conditions and the characteristics of specific rice varieties, rather than simply increasing the amount of N fertilizer to achieve the goal of higher yields (Rezaei et al., 2009). Excessive application of N fertilizer can lead to a decline in N use efficiency and yield (Peng et al., 2007). It has been reported that the yield components and yield of rice under medium N levels (210 kg ha<sup>-1</sup>, 260 kg ha<sup>-1</sup>, and 315 kg ha<sup>-1</sup>) are significantly higher than under low (160 kg ha<sup>-1</sup>) and high (420 kg ha<sup>-1</sup>) N levels (Li et al., 2020). Studies have also shown that the best N application rate in paddy fields is 60 kg ha<sup>-1</sup>, and the yield of rice will not increase if the N application rate exceeds it (Rezaei et al., 2009). In addition to the N application rate, the seeding rate of rice also strongly affects grain yield. Plant population density is the primary factor that affects the occurrence of tillering (Schnier et al., 1990). The lower the seeding density, the taller the plant, the greater the tillering efficiency, the lower the sterility, and the higher the grain yield (Thapa et al., 2019). However, excessive plant population density can lead to greater plant height and weaker stalks, increasing the potential for losses due to lodging and disease (Dofing and Knight, 1994). When previous studies are summarized, it becomes clear that suitable N application rates and seeding rates differ markedly among regions, and further systematic study is needed. It is also clear that crop growth traits are closely related to yield. However, most research on the correlation between crop growth indices and yield or yield components has considered the relationships between individual indices in isolation, ignoring the relationships between variable groups. The results of such analyses may be incomplete or superficial (Liu et al., 2014; Li et al., 2019a).

In this study, hybrid rice and conventional rice were used as experimental crops. We tested multiple N application rates and seeding rates and used canonical correlation analysis and grey correlation analysis to assess the effects of growth characteristics on rice yield. We identified the optimal N application and sowing rates for hybrid and conventional rice, and identified growth characteristics that were most closely related to yield. The findings of this research provide a scientific basis and theoretical guidance for efficient crop planting.

## Materials and Methods

### *Experimental materials*

The rice varieties C Liangyouhuazhan (hybrid) and Huanghuazhan (conventional) were provided by Golden Nonghua Seed Industry Co., Ltd. (Beijing, China) and Hubei Seed Group Co., Ltd. (Wuhan, China), respectively.

### *Field site and experimental design*

The experiments were conducted from 2018 to 2019 in the Agricultural Science and Technology Industrial Park of Yangtze University, Huazhong Agricultural High-Tech Industrial Development Zone, Jingzhou City, Hubei Province, China (30°22' N, 112°40' E). The test area was located in the Jiangnan Plain in the middle reaches of the Yangtze River. It has a subtropical monsoon climate with an average annual sunshine duration of approximately 2000 hours and a total annual solar radiation value of approximately 460–480 kilojoule cm<sup>-2</sup>. The average annual precipitation is

1100–1300 mm, and the precipitation from April to September accounts for 70% of the total annual precipitation. The soil type was a light loam (Kakingski soil texture classification system), and the basic physical and chemical properties of the soil in the 0-20 cm depth were as follows: a pH of 7.74, an organic matter content of 22.18 g kg<sup>-1</sup>, an alkaline N content of 73.63 mg kg<sup>-1</sup>, an available phosphorus content of 28.55 mg kg<sup>-1</sup>, and a fast-acting potassium content of 186.40 mg kg<sup>-1</sup>.

Seeds were sown on June 1<sup>st</sup>, and the harvest date was October 2<sup>nd</sup>. The experiment used a split-plot design. There were four N fertilizer application rates (N3 240 kg ha<sup>-1</sup>, N2 195 kg ha<sup>-1</sup>, N1 150 kg ha<sup>-1</sup> and N0 0 kg ha<sup>-1</sup>) and three sowing rates (D3 28.57 kg ha<sup>-1</sup>, D2 25.00 kg ha<sup>-1</sup>, and D1 22.22 kg ha<sup>-1</sup>). The N application rate was the main plot factor and sowing rate was the subplot factor. Each treatment was replicated three times for each rice variety, the area of each plot was 30 m<sup>2</sup>, and the total number of plots was 72. Details of N fertilizer and seeding management are shown in *Table 1*. The ratio of N, P<sub>2</sub>O<sub>5</sub>, and K<sub>2</sub>O in the compound fertilizer was 15:15:15, and 46% of the applied N was in the form of urea. Compound fertilizer was applied as a base fertilizer at sowing, urea was applied at the tillering stage, and compound fertilizer was applied at the panicle initiation stage. The ratio of N applied for the three periods was 5:3:2. The content of P<sub>2</sub>O<sub>5</sub> and K<sub>2</sub>O in each treatment was adjusted to 168 kg ha<sup>-1</sup> using calcium superphosphate (16% P<sub>2</sub>O<sub>5</sub>) and potassium chloride (60% K<sub>2</sub>O). Sowing was performed using mechanical direct seeding at three direct seeding densities (seeding rates) of 25 cm × 14 cm (28.57 kg ha<sup>-1</sup>), 25 cm × 16 cm (25.00 kg ha<sup>-1</sup>), and 25 cm × 18 cm (22.22 kg ha<sup>-1</sup>). Other management practices, such as disease and pest control, were performed according to local routine management. For example, the pretilachlor was applied 24 hours after rice seeding; the validamycin was used to control rice sheath blight from June to July; the flubendiamide was used to control rice borer (*Cnaphalocrocis medinalis*) in August.

**Table 1.** N fertilizer and seeding management used in this study

Treatment	During sowing (N application, kg ha <sup>-1</sup> )	At the tillering stage (N application, kg ha <sup>-1</sup> )	During panicle initiation stage (N application, kg ha <sup>-1</sup> )	Total N application (kg ha <sup>-1</sup> )	Seeding rate (kg ha <sup>-1</sup> )
N3D3	120.00	72.00	48.00	240.00	28.57
N3D2	120.00	72.00	48.00	240.00	25.00
N3D1	120.00	72.00	48.00	240.00	22.22
N2D3	97.50	58.50	39.00	195.00	28.57
N2D2	97.50	58.50	39.00	195.00	25.00
N2D1	97.50	58.50	39.00	195.00	22.22
N1D3	75.00	45.00	30.00	150.00	28.57
N1D2	75.00	45.00	30.00	150.00	25.00
N1D1	75.00	45.00	30.00	150.00	22.22
N0D3	0.00	0.00	0.00	0.00	28.57
N0D2	0.00	0.00	0.00	0.00	25.00
N0D1	0.00	0.00	0.00	0.00	22.22

### Measurement indices

SPAD value, leaf area index (LAI), dry matter accumulation, and plant height were assessed at the heading stage (80% of panicle emerged), and the largest tiller number of

rice plants at the tillering stage was recorded. An area of 0.5 m<sup>2</sup> was selected from each plot for the measurement of these growth characteristics. A SPAD-502 Plus chlorophyll analyzer (Konica Minolta, Japan) was used to measure the first complete leaf on the main stem, and the average of the upper third, middle third, and lower third of the leaf was taken as the SPAD value for the plant. Leaf area was measured using Image J 1.51j8 (National Institutes of Health, USA). Plants were selected for measurement of plant height, killed at a temperature of 105°C, dried to constant weight at 80°C, and weighed.

Yield and yield components were assessed after the maturation (95% of rice husk were yellow) of the rice plants. An area of 5 m<sup>2</sup> was selected from the central part of each plot for yield measurement. Ten rice plants were selected to investigate the average effective panicle number. Simultaneously, five plants were randomly selected for measurement of the number of grains per ear, the seed setting rate, and the 1000-grain weight.

### Correlation analyses

Canonical correlation analysis is a multivariate mathematical statistical analysis method for studying the relationship between two groups of variables (Hardoon et al., 2004). Its purpose is to seek linear combinations of two separate sets of variables, such that the correlation between the two sets of variables is maximized. In this study, SPAD ( $x_1$ ), LAI ( $x_2$ ), dry matter accumulation ( $x_3$ ), number of tillers ( $x_4$ ), and plant height ( $x_5$ ) were regarded as one set of variables. Grain yield ( $y_1$ ), effective panicle number ( $y_2$ ), spikelet number per panicle ( $y_3$ ), seed setting rate ( $y_4$ ), and 1000-grain weight ( $y_5$ ) were regarded as another set of variables, and canonical correlation analysis was performed between the two variable sets.

Gray correlation analysis (Peng and Zhang, 2010) was used to assess the correlation between individual growth characteristics (SPAD, LAI, dry matter accumulation, number of tillers, and plant height) and the reference series (yield). The greater the degree of correlation, the closer the changes between the growth characteristics and yield, and the closer their relationship. Yield ( $Y_j$ ) was set as the reference series, and the growth characteristic parameters were set as the comparison series ( $X_i$ ). The correlation coefficient between growth parameters ( $X_i$ ) and yield ( $Y_j$ ) and the degree of correlation of each factor were:

Correlation coefficient:

$$\xi_i(k) = \frac{\min_i \min_k |Y_j(k) - X_i(k)| + \zeta \max_i \max_k |Y_j(k) - X_i(k)|}{|Y_j(k) - X_i(k)| + \zeta \max_i \max_k |Y_j(k) - X_i(k)|} \quad (\text{Eq.1})$$

Degree of correlation:

$$r_i = \frac{1}{n} \sum_{k=1}^n \xi_i(k) \quad (\text{Eq.2})$$

In this formula (Eq.1),  $\xi_i(k)$  is the correlation coefficient between  $X_i$  and  $Y_j$  at the point  $K$ ,  $\zeta$  is the resolution coefficient of gray correlation ( $\zeta = 0.5$ );  $\min_i \min_k |Y_j(k) - X_i(k)|$  is the absolute value of the second-level minimum difference, and  $\max_i \max_k |Y_j(k) - X_i(k)|$  is the absolute value of the second-level maximum difference. The correlation degree between the comparison series and the reference series

is determined according to the degree of correlation  $r_i$  (Eq.2) to determine the importance of the comparison sequence to the reference sequence.

### **Statistical analysis**

The data were analyzed and plotted using Data Processing System 7.05 (Qiyi Tang, China) and ORIGIN 2019 (OriginLab Corp., Northampton, MA, USA), respectively. Following a two-way ANOVA, treatment means were compared using the least significant difference (LSD) test at a  $p \leq 0.05$  level of significance.

## **Results**

### ***Effect of N fertilizer application rate and seeding rates on hybrid rice yield and its components***

Hybrid rice yield and yield components under different N fertilizer rates and seeding rates are summarized in *Table 2*. Grain yield of each treatment increased initially and then decreased as N fertilizer and seeding rates were increased in 2018 and 2019. Grain yield was significantly higher in the N2 treatment than in the N1, N3, and N0 treatments by 6.58–67.15% in 2018 and 8.70–60.00% in 2019. There were no significant yield differences between the N1 and N3 treatments in either year. Grain yield of the D2 treatment was significantly higher than that of the D3 and D1 treatments by 4.90% and 11.01%, respectively, in 2018 and by 3.48% and 6.15%, respectively, in 2019. Yield was significantly higher in the D3 treatment than in the D1 treatment by 5.82% in 2018 and by 2.58% in 2019. Grain yield of the N1D2 and N2D2 treatments was higher than that of other N application and seeding rate combinations in 2018, and grain yield of the N2D2 treatment was higher than that of other combinations in 2019.

The effective panicle number and spikelet number per panicle of hybrid rice increased in response to N fertilization, but seed setting rate and 1000-grain weight decreased. The effective panicle number in the N2 treatment was significantly higher than in the N3, N1, and N0 treatments by 7.07%, 19.84%, and 43.09%, respectively. The spikelet number per panicle in the N2 treatment was significantly higher than in the N1 and N0 treatments by 3.60% and 2.92%, respectively, and lower than in the N3 treatment by 16.51%. The higher the seeding rate, the higher the effective panicle number but the lower the number of spikelets per panicle and the seed setting rate. The 1000-grain weight of the D2 treatment was higher than that of the D1 and D3 treatments by 0.12% and 1.37%, respectively. Other yield components of the D2 treatment were in the middle of the three seeding rates. Compared with other N application and seeding rate combinations, the best yield performance of the N2D2 treatment may have been due to its high effective panicle number and the consistent responses of the other yield components.

### ***Effect of N fertilizer application rate and seeding rates on conventional rice yield and its components***

The yield and yield components of conventional rice under different N fertilizer and seeding rates are summarized in *Table 3*. Grain yield of each treatment increased as N fertilizer and seeding rates were increased in 2018 and 2019. Grain yield was significantly higher in the N3 treatment than in the N2, N1, and N0 treatments by 9.88–81.04% (2018) and 5.03–51.31% (2019). There were no significant differences between the N1 and N2 treatments in either year. Grain yield was significantly higher in the D3 treatment than in

the D2 and D1 treatments by 4.49% and 7.27% in 2018 and by 4.17% and 4.66% in 2019. There were no significant differences between the D1 and D2 treatments in either year. Grain yield of the N3D2 treatment was higher than that of other N application and seeding rate combinations in 2018, and grain yield of the N3D3 treatment was higher than that of other combinations in 2019.

**Table 2.** Hybrid rice yield and yield components under different N fertilizer application rates and seeding rates

Treatment	Number of effective panicles (10 <sup>4</sup> ha <sup>-1</sup> )	Number of spikelets per panicle	Seed setting rate (%)	1000-grain weight (g)	Grain yield (kg ha <sup>-1</sup> )	
					2018	2019
Treatment of N application rate						
N3	347.45±7.76b	182.41±2.98a	75.10±0.27d	23.99±0.11c	10.76±0.22b	11.04±0.19b
N2	372.03±8.90a	175.84±2.74b	78.67±0.26c	24.20±0.15b	11.50±0.38a	12.00±0.06a
N1	310.43±10.51c	170.85±2.05c	81.53±0.15b	24.52±0.04a	10.79±0.20b	10.95±0.19b
N0	260.00±1.07d	150.92±1.65d	84.66±0.05a	24.61±0.08a	6.88±0.39c	7.50±0.04c
Treatment of density						
D3	335.40±7.20a	166.48±1.08c	78.60±0.16c	24.12±0.05b	10.00±0.18b	10.34±0.14b
D2	331.24±7.39a	170.36±2.38b	79.59±0.20b	24.45±0.08a	10.49±0.09a	10.70±0.10a
D1	300.79±2.26b	173.18±2.83a	81.78±0.14a	24.42±0.11a	9.45±0.30c	10.08±0.10c
Treatment of interaction						
N3D3	358.43±13.05a	179.85±2.52b	74.22±0.20c	23.63±0.09c	10.73±0.17a	10.43±0.36c
N3D2	360.19±12.43a	181.42±5.79b	75.19±0.80b	24.34±0.16a	11.03±0.42a	11.62±0.17a
N3D1	323.71±9.95b	185.98±2.92a	75.88±0.18a	24.35±0.38b	10.52±0.22a	11.07±0.20b
N2D3	367.95±26.13ab	172.82±4.35b	77.19±0.78c	24.23±0.14a	11.10±0.88b	12.00±0.08ab
N2D2	390.14±17.00a	178.17±3.00a	78.08±0.26b	24.32±0.23a	12.01±0.37a	12.26±0.15a
N2D1	358.00±26.38b	176.55±2.11a	80.73±0.29a	24.27±0.10a	11.37±0.43ab	11.76±0.11b
N1D3	323.86±10.29a	167.93±1.99b	79.92±0.14c	24.28±0.05b	10.70±0.52b	10.66±0.37b
N1D2	316.50±6.50ab	168.31±0.49b	81.05±0.22b	24.62±0.23a	12.23±0.51a	11.50±0.35a
N1D1	290.93±19.27b	176.32±5.01a	83.63±0.36a	24.55±0.07a	9.45±0.39c	10.68±0.07b
N0D3	291.36±16.46a	145.34±0.93b	83.06±0.33c	24.59±0.19b	7.48±0.75a	8.27±0.20a
N0D2	258.14±15.03b	153.56±1.94a	84.03±0.39b	24.47±0.06b	6.69±0.35ab	7.42±0.08b
N0D1	230.51±1.75b	153.86±3.06a	86.89±0.11a	25.03±0.09a	6.46±0.46b	6.80±0.05c

Different letters (a, b, c) indicate significant differences among different seeding rates under a given N application rate (LSD's multiple range tests,  $p < 0.05$ ). Four nitrogen application rates (N0, 0 kg ha<sup>-1</sup>; N1, 150 kg ha<sup>-1</sup>; N2, 190 kg ha<sup>-1</sup>; N3, 240 kg ha<sup>-1</sup>) and three seeding rates (D1, 22.22 kg ha<sup>-1</sup>; D2, 25.00 kg ha<sup>-1</sup>; D3, 28.57 kg ha<sup>-1</sup>) were tested. The yield components are shown as the mean values of two years' data

As the rate of N application increased, the effective panicle number, spikelet number per panicle, and 1000-grain weight of conventional rice increased, whereas the seed setting rate decreased. The effective panicle number, spikelet number per panicle, and 1000-grain weight were significantly higher in the N3 treatment than in the N2, N1, and N0 treatments by 5.31–33.63%, 3.83–18.88%, and 0.31–1.59%, respectively. However, the seed setting rate was significantly lower in the N3 treatment than in the N0–2 treatments by 1.59–6.02%. As the rate of seeding increased, the effective panicle number and 1000-grain weight of conventional rice increased, whereas the seed setting rate and spikelet number per panicle decreased. Compared with other N application and seeding rate combinations, the better yield performance of the N3D3 treatment may have been due to its high 1000-grain weight and the consistent responses of the other yield components.



**Table 3.** Conventional rice yield and yield components under different N fertilizer application rates and seeding rates

Treatment	Number of effective panicles ( $10^4 \text{ ha}^{-1}$ )	Number of spikelets per panicle	Seed setting rate (%)	1000-grain weight (g)	Grain yield ( $\text{kg ha}^{-1}$ )	
					2018	2019
Treatment of N application rate						
N3	388.94±10.94a	167.59±2.50a	81.75±0.10d	22.33±0.07a	10.12±0.26a	9.82±0.06a
N2	369.34±18.61b	161.41±0.95b	85.18±0.27c	22.26±0.18ab	9.21±0.34b	9.35±0.07b
N1	334.66±3.03c	155.12±0.82c	86.51±0.19b	22.15±0.09ab	9.17±0.25b	9.29±0.02b
N0	291.06±7.63d	140.98±0.86d	87.77±0.48a	21.98±0.25b	5.59±0.27c	6.49±0.07c
Treatment of density						
D3	349.83±2.67a	153.26±0.43c	83.83±0.47c	22.40±0.23a	8.85±0.34a	8.99±0.06a
D2	344.26±8.97a	156.78±0.89b	85.50±0.30b	22.23±0.08a	8.47±0.10ab	8.63±0.14b
D1	343.91±15.44a	158.78±1.61a	86.58±0.21a	21.91±0.08b	8.25±0.54b	8.59±0.12b
Treatment of interaction						
N3D3	365.52±13.36b	163.62±4.23c	80.58±0.86b	23.09±0.18a	9.86±0.54b	10.02±0.09a
N3D2	391.84±19.45a	167.40±2.37b	80.96±0.92b	21.98±0.06b	10.81±0.53a	9.66±0.13a
N3D1	409.47±14.98a	171.74±0.98a	83.71±0.12a	22.16±0.10b	9.71±0.66b	9.77±0.07a
N2D3	393.47±16.38a	158.27±1.01b	83.53±0.65b	21.56±0.33b	9.68±0.59a	9.64±0.22a
N2D2	359.39±27.17b	161.81±1.69a	85.82±0.80a	22.55±0.19a	9.13±0.70ab	9.22±0.46ab
N2D1	355.15±12.49b	164.15±3.56a	86.18±1.01a	22.27±0.07ab	8.83±0.36b	9.19±0.56b
N1D3	345.18±11.09a	152.63±1.00b	85.28±0.53b	22.13±0.10a	9.72±0.13a	9.56±0.12a
N1D2	340.78±2.76ab	154.63±1.73ab	86.87±0.17ab	22.49±0.30a	8.58±0.51b	9.23±0.15a
N1D1	318.00±21.36b	158.09±0.49a	87.39±0.54a	21.99±0.09a	9.21±0.62ab	9.07±0.06a
N0D3	295.16±15.39a	138.53±2.24b	85.95±2.34b	22.07±0.75a	6.15±0.36a	6.73±0.27a
N0D2	285.03±12.45a	143.26±2.07a	88.34±0.69a	21.53±0.53b	5.35±0.44a	6.41±0.15a
N0D1	293.00±14.07a	141.15±3.16ab	89.02±0.54a	21.55±0.08b	5.27±0.69a	6.33±0.21a

Different letters (a, b, c) indicate significant differences among different seeding rates under a given N application rate (LSD's multiple range tests,  $p < 0.05$ ). Four nitrogen application rates (N0, 0  $\text{kg ha}^{-1}$ ; N1, 150  $\text{kg ha}^{-1}$ ; N2, 190  $\text{kg ha}^{-1}$ ; N3, 240  $\text{kg ha}^{-1}$ ) and three seeding rates (D1, 22.22  $\text{kg ha}^{-1}$ ; D2, 25.00  $\text{kg ha}^{-1}$ ; D3, 28.57  $\text{kg ha}^{-1}$ ) were tested. The yield components are shown as the mean values of two years' data

### ***Effect of N fertilizer application rate and seeding rates on growth characteristics of hybrid rice***

Growth characteristics of hybrid rice under each treatment are shown in Table 4. As the N application rate increased, the SPAD value, LAI, and dry matter accumulation of hybrid rice initially increased and then decreased, whereas the plant height continued to increase. There were no significant differences in the number of tillers under the N1, N2, and N3 treatments. The SPAD value, LAI, and dry matter accumulation were significantly higher in the N2 treatment than in the N3, N1, and N0 treatments by 2.64-10.96%, 2.61-165.82%, and 17.67-64.48%, respectively. Plant height was significantly higher in the N3 treatment than in the N2, N1, and N0 treatments by 1.30-26.89%. All the growth indices of the D1 treatment were lower than those of the D2 and D3 treatments, and the plant height and LAI of D1 differed significantly from those of D2 and D3. The dry matter accumulation, SPAD value, number of tillers, and plant height were higher in the D2 treatment than in the D3 treatment, and the SPAD value of D2 was significantly higher than that of D3 by 0.85%. The SPAD value, LAI, dry matter accumulation, and the number of tillers were higher in the N2D2 treatment than in other N application and seeding rate combinations.

**Table 4.** Growth characteristics of hybrid rice under different N fertilizer application rates and seeding rates

Treatment	SPAD	LAI	Dry matter accumulation (10 <sup>3</sup> kg ha <sup>-1</sup> )	Number of tillers (10 <sup>4</sup> ha <sup>-1</sup> )	Plant height (cm)
Treatment of N application rate					
N3	43.19±0.19b	6.14±0.12b	11.09±0.40b	530.89±12.90a	127.55±0.69a
N2	44.33±0.55a	6.30±0.12a	13.52±0.75a	552.00±28.76a	125.91±0.32b
N1	42.21±0.42c	4.30±0.13c	11.49±0.38b	550.44±14.38a	119.60±0.35c
N0	39.95±0.30d	2.37±0.11d	8.22±0.52c	469.56±29.10b	100.52±0.40d
Treatment of density					
D3	42.35±0.30b	4.88±0.09a	11.01±0.31a	523.17±25.72ab	117.52±0.34b
D2	42.71±0.31a	4.82±0.09a	11.34±0.33a	545.50±16.73a	118.24±0.81b
D1	42.21±0.23b	4.63±0.17b	10.89±0.23a	508.50±23.30b	119.43±0.37a
Treatment of interaction					
N3D3	43.06±0.56a	6.01±0.10b	12.04±0.55a	522.67±28.02a	126.78±1.27b
N3D2	43.06±0.51a	6.18±0.15a	10.87±0.71b	537.33±17.47a	126.32±2.18b
N3D1	43.46±0.78a	6.24±0.11a	10.37±0.54b	532.67±23.18a	129.56±1.62a
N2D3	43.99±0.56b	6.31±0.06b	13.42±0.78ab	545.33±40.86ab	125.24±1.31b
N2D2	45.15±0.72a	6.56±0.10a	14.16±0.99a	597.33±45.00a	126.96±0.73a
N2D1	43.86±0.75b	6.02±0.25c	12.99±0.60b	513.33±12.22b	125.52±0.99ab
N1D3	42.52±0.62a	4.75±0.16a	10.83±1.84a	580.67±27.30a	118.28±0.76b
N1D2	42.69±0.50a	4.06±0.13b	11.79±0.23a	586.00±42.00a	121.28±0.64a
N1D1	41.43±0.23b	4.07±0.13b	11.85±1.04a	484.67±28.59b	119.24±0.52b
N0D3	39.83±0.36a	2.43±0.08a	7.77±0.75a	444.00±38.16a	99.76±0.46b
N0D2	39.95±0.36a	2.48±0.06a	8.52±0.72a	461.33±27.59a	98.40±1.36b
N0D1	40.09±0.52a	2.19±0.21b	8.36±0.25a	503.33±75.80a	103.40±1.12a

Different letters (a, b, c) indicate significant differences among different seeding rates under a given N application rate (LSD's multiple range tests,  $p < 0.05$ ). Four nitrogen application rates (N0, 0 kg ha<sup>-1</sup>; N1, 150 kg ha<sup>-1</sup>; N2, 190 kg ha<sup>-1</sup>; N3, 240 kg ha<sup>-1</sup>) and three seeding rates (D1, 22.22 kg ha<sup>-1</sup>; D2, 25.00 kg ha<sup>-1</sup>; D3, 28.57 kg ha<sup>-1</sup>) were tested. The indicators in the table are the average of two years

### **Effect of N fertilizer application rate and seeding rates on growth characteristics of conventional rice**

Growth characteristics of conventional rice under each treatment are shown in *Table 5*. The SPAD value, LAI, and plant height increased as the rate of N application increased. There were no significant differences in the number of tillers or dry matter accumulation among the N1, N2, and N3 treatments. The SPAD value, LAI, and plant height were significantly higher in the N3 treatment than in the N2, N1, and N0 treatments by 2.87–11.63%, 22.13–162.33%, and 5.12–19.61%, respectively. The dry matter accumulation was significantly higher in the D3 treatment than in the D2 and D1 treatments by 7.87% and 10.51%; the LAI was significantly higher in D3 than in D2 and D1 by 4.61% and 7.58%; and the number of tillers was significantly lower in D3 than in D2 by 5.46%. There were no significant differences in the SPAD value among D1, D2, and D3. The plant height of D1 was higher than that of D2 and D3 by 1.43 and 1.15%, respectively. The LAI of the N3D3 treatment was higher than other N application and seeding rate combinations, and the various growth traits of the N3D3 treatment were consistent with this result.

**Table 5.** Growth characteristics of conventional rice under different N fertilizer application rates and seeding rates

Treatment	SPAD	LAI	Dry matter accumulation (10 <sup>3</sup> kg ha <sup>-1</sup> )	Number of tillers (10 <sup>4</sup> ha <sup>-1</sup> )	Plant height (cm)
Treatment of N application rate					
N3	44.06±0.28a	5.85±0.06a	11.33±0.34a	532.89±32.53a	113.43±1.13a
N2	42.83±0.26b	4.79±0.18b	10.75±0.54a	500.22±23.48ab	107.91±0.69b
N1	42.70±0.30b	4.59±0.12c	10.15±1.05a	524.00±26.26a	107.22±0.97b
N0	39.47±0.23c	2.23±0.09d	8.67±0.18b	466.44±28.71b	94.83±1.04c
Treatment of density					
D3	42.20±0.25a	4.54±0.10a	10.83±0.32a	496.17±17.56b	105.54±1.39ab
D2	42.27±0.36a	4.34±0.08b	10.04±0.23b	524.83±24.32a	105.25±1.24b
D1	42.32±0.13a	4.22±0.16c	9.80±0.36b	496.67±25.32b	106.75±0.56a
Treatment of interaction					
N3D3	44.04±0.80a	6.06±0.05a	11.92±0.92a	500.67±26.63b	111.98±1.64b
N3D2	43.98±0.42a	6.03±0.10a	11.47±0.85a	575.33±56.72a	113.10±2.75ab
N3D1	44.17±0.52a	5.46±0.03b	10.59±0.81b	522.67±30.02b	115.20±2.32a
N2D3	42.65±0.33a	5.28±0.21a	12.16±0.69a	478.67±23.18b	105.30±0.65b
N2D2	43.07±0.83a	4.54±0.02b	8.90±0.51b	540.67±26.03a	106.60±1.31b
N2D1	42.75±0.57a	4.54±0.34b	9.39±1.21b	481.33±24.19b	111.84±1.87a
N1D3	42.60±0.62a	4.56±0.04a	10.63±0.78a	533.33±31.64a	106.28±2.33a
N1D2	42.60±0.49a	4.55±0.12a	11.13±0.99a	522.67±37.17a	107.44±1.07a
N1D1	42.90±0.63a	4.66±0.24a	10.48±1.43a	516.00±37.47a	107.94±1.16a
N0D3	39.51±0.21a	2.25±0.11a	8.60±0.35a	472.00±41.62a	98.60±2.87a
N0D2	39.43±0.67a	2.22±0.10a	8.68±0.28a	460.67±37.17a	93.86±3.12b
N0D1	39.47±0.59a	2.22±0.07a	8.72±0.27a	466.67±60.58a	92.02±0.83b

Different letters (a, b, c) indicate significant differences among different seeding rates under a given N application rate (LSD's multiple range tests,  $p < 0.05$ ). Four nitrogen application rates (N0, 0 kg ha<sup>-1</sup>; N1, 150 kg ha<sup>-1</sup>; N2, 190 kg ha<sup>-1</sup>; N3, 240 kg ha<sup>-1</sup>) and three seeding rates (D1, 22.22 kg ha<sup>-1</sup>; D2, 25.00 kg ha<sup>-1</sup>; D3, 28.57 kg ha<sup>-1</sup>) were tested. The indicators in the table are the average of two years

### Response of rice yield to different N application rates and seeding rates

We used regression simulation analysis to analyze the relationships between N application rate, sowing rate, and rice yield. The following binary quadratic equations were obtained:

Hybrid rice:

$$y_1 = -40.3579 + 0.0691n + 3.5676d - 1.1367 \times 10^{-4}n^2 - 0.0661d^2 - 1.0122 \times 10^{-3}nd \quad (\text{Eq.3})$$

Conventional rice:

$$y_1 = 9.1697 + 0.0325n - 0.3599d - 4.5817 \times 10^{-5}n^2 + 9.2691 \times 10^{-3}d^2 - 2.2258 \times 10^{-4}nd \quad (\text{Eq.4})$$

In these equations,  $y_1$  represents grain yield (10<sup>3</sup> kg ha<sup>-1</sup>),  $n$  represents the N application rate (kg ha<sup>-1</sup>), and  $d$  represents the seeding rate (kg ha<sup>-1</sup>). The  $F$ -tests of (Eq.3) and (Eq.4) were highly significant ( $P < 0.01$ ), indicating that the equations accurately

expressed the relationships between N rate, seeding rate, and yield of hybrid rice or conventional rice.

Figure 1 shows plots of (Eq.3) and (Eq.4); both are convex parabolic surfaces. According to (Eq.3), the yield of hybrid rice was predicted to reach a maximum when the N application rate and seeding rates were 190.32 kg ha<sup>-1</sup> and 25.54 kg ha<sup>-1</sup>, respectively. According to (Eq.4), the yield of conventional rice was predicted to reach a maximum when the N application rate and seeding rates were 238.74 kg ha<sup>-1</sup> and 28.57 kg ha<sup>-1</sup>, respectively. As shown in Figure 1, the grain yield of hybrid and conventional rice increased initially, then decreased as N fertilizer and seeding rates were increased. This result demonstrates that only the appropriate amounts of N application and seeding promote high yields; it also provides a theoretical basis for the optimization of N fertilizer and seeding rates.

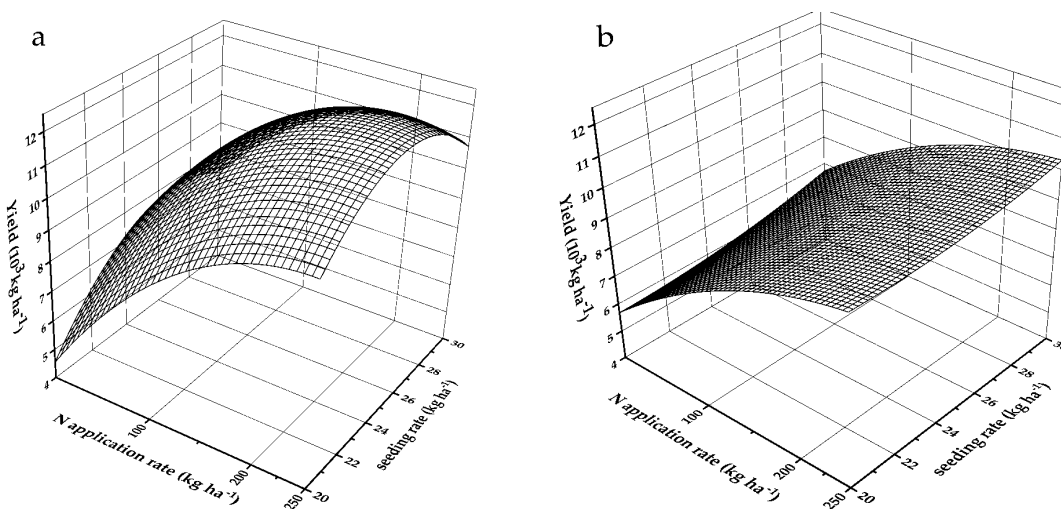


Figure 1. Relationship between rice yield, N application rate, and seeding rate in (a) hybrid rice and (b) conventional rice. Yields are the average of two years

### The canonical correlation between growth traits and rice yield and its components

The growth of rice plants affects yield formation. We therefore used canonical correlation analysis to explore the relationship between growth traits and yield and its components. As shown in Table 6, the correlation coefficients of canonical variables I, II, and III were relatively large (0.9883, 0.8803, and 0.8201, respectively) and highly significant ( $P < 0.01$ ). However, the eigenvalues of canonical variables I and II accounted for 94.80% of the total, and canonical correlation analysis was therefore carried out for canonical variables I and II.

Table 6. Canonical correlation analysis of growth traits, yield and yield components

No.	Canonical correlation coefficient	Eigenvalues	Wilk's	Chi-square value	df	Sig.
1	0.9883	42.1413	0.0012	118.023	25	0.0001
2	0.8803	3.4441	0.0508	52.1445	16	0.0001
3	0.8201	2.0547	0.2258	26.042	9	0.002
4	0.5512	0.4365	0.6897	6.5004	4	0.1648
5	0.096	0.0093	0.9908	0.1621	1	0.6873

Because the units of the original variables were inconsistent, we used standardized canonical coefficients in the analysis to give canonical correlation models  $u$  and  $v$ . The correlation coefficient (canonical load factor) between the original variable and the canonical variable was also calculated. The calculation results are shown in *Table 7*, and the compositions of canonical variables I and II (Eq.5–8) are:

$$u_1 = 0.2199x_1 - 0.6085x_2 + 0.0493x_3 - 0.0604x_4 - 0.6354x_5 \quad (\text{Eq.5})$$

$$v_1 = -0.4005y_1 + 0.0505y_2 - 0.4867y_3 + 0.2885y_4 + 0.1809y_5 \quad (\text{Eq.6})$$

$$u_2 = 2.1927x_1 - 0.9744x_2 + 0.3605x_3 - 0.2252x_4 - 1.1354x_5 \quad (\text{Eq.7})$$

$$v_2 = 0.3592y_1 + 1.0819y_2 - 0.2952y_3 + 0.9618y_4 + 0.2311y_5 \quad (\text{Eq.8})$$

**Table 7.** Canonical variables and canonical load factors

Character(U)	Canonical variable ( I )		Canonical variable ( II )	
	$u_1$	$r$	$u_2$	$r$
SPAD ( $x_1$ )	0.2199	-0.8596	2.1927	0.5025
LAI ( $x_2$ )	-0.6085	-0.9294	-0.9744	0.3144
Dry matter accumulation ( $x_3$ )	0.0493	-0.7931	0.3605	0.3073
Number of tillers ( $x_4$ )	-0.0604	-0.6913	-0.2252	0.2003
Plant height ( $x_5$ )	-0.6354	-0.9770	-1.1354	-0.1224
Character (V)	Canonical variable ( I )		Canonical variable ( II )	
	$v_1$	$r$	$v_2$	$r$
Grain yield ( $y_1$ )	-0.4005	-0.9433	0.3592	0.1672
Effective panicle number ( $y_2$ )	0.0505	-0.6481	1.0819	0.6786
Spikelet number per panicle ( $y_3$ )	-0.4867	-0.9616	-0.2952	-0.1044
Seed setting rate ( $y_4$ )	0.2885	0.8721	0.9618	0.3338
1000-grain weight ( $y_5$ )	0.1809	-0.3574	0.2311	-0.6327

For canonical variables I ( $u_1, v_1$ ), the correlation coefficients between  $u_1$  and the SPAD value ( $x_1$ ), LAI ( $x_2$ ), and plant height ( $x_5$ ) were relatively high ( $-0.8596, -0.9294, \text{ and } -0.9770$ , respectively). Therefore,  $u_1$  mainly described the comprehensive characteristics of the SPAD value, LAI, and plant height. As the SPAD value, LAI, and plant height decreased,  $u_1$  tended to increase. In the same way,  $v_1$  was negatively correlated with grain yield ( $y_1$ ) and spikelet number per panicle ( $y_3$ ) and positively correlated with seed setting rate ( $y_4$ ). The associated correlation coefficients were  $-0.9433, -0.9616, \text{ and } -0.8721$ , respectively. Therefore,  $v_1$  mainly described the comprehensive characteristics of grain yield, spikelet number per panicle, and seed setting rate. As grain yield and spikelet number per panicle decreased and seed setting rate increased,  $v_1$  tended to increase. This linear combination showed that the SPAD value, LAI, and plant height were closely related to grain yield, spikelet number per panicle, and seed setting rate. The increase in the SPAD value, LAI, and plant height may have caused the increase in grain yield and spikelet number per panicle and the decrease in seed setting rate.

For canonical variables II ( $u_2, v_2$ ), the correlation coefficient between  $u_2$  and the SPAD value ( $x_1$ ) was the highest (0.5025). Therefore,  $u_2$  mainly described the characteristic of

the SPAD value, and as the SPAD value increased,  $u_2$  also increased. In the same way,  $v_2$  had a positive correlation with effective panicle number ( $y_2$ ) and a negative correlation with 1000-grain weight ( $y_5$ ) with correlation coefficients of 0.6786 and  $-0.6327$ , respectively. Therefore,  $v_2$  mainly described the comprehensive traits of effective panicle number and 1000-grain weight. As effective panicle number increased and 1000-grain weight decreased,  $v_2$  tended to increase. This linear combination showed that the SPAD value was closely related to effective panicle number and 1000-grain weight. The increase in the SPAD value may have caused the increase in the number of effective panicles and the decrease in 1000-grain weight.

### ***The Gray correlation analysis between growth traits and grain yield***

We used the gray correlation analysis method to analyze the degree of influence of growth traits on the yield of direct seeded rice across different N application rates and sowing rates. As shown in *Figure 2*, the relative strength of the relationship between individual growth traits and yield was: plant height ( $x_5$ ) > LAI ( $x_2$ ) > SPAD ( $x_1$ ) > dry matter accumulation ( $x_3$ ) > the number of tillers ( $x_4$ ). The correlations of yield with plant height and LAI were relatively high, indicating that these two traits had a greater impact on yield across different N application rates and sowing rates.

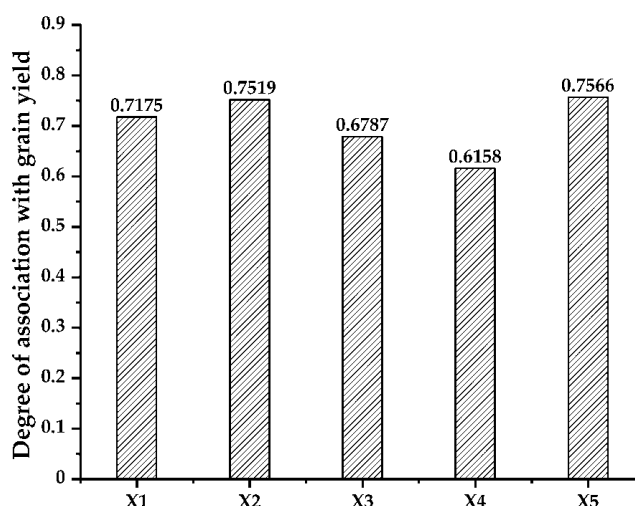


**Figure 2.** Degree of association between growth traits and grain yield.  $x_1$  represents SPAD,  $x_2$  represents LAI,  $x_3$  represents dry matter accumulation,  $x_4$  represents the number of tillers, and  $x_5$  represents plant height

## **Discussion**

Rice yield is regulated by genomic regions called quantitative trait loci and influenced by the external environment. Yield is one of the most important and complex agronomic traits (Wang et al., 2012; Zeng et al., 2017; Zhang et al., 2017). Chuma et al. (2020) showed that in high and middle altitude areas, when the N application rate exceeds  $120 \text{ kg ha}^{-1}$ , yield is reduced due to excessive tillers. Wang et al. (2014) suggested that a medium seeding density ( $25 \text{ cm} \times 17 \text{ cm}$ ) of direct seeded rice is suitable for high-yield hybrid rice. In this study, the effective panicle number of hybrid rice was highest in the medium N and medium density (N2D2) treatment, which was conducive to the

production of grain yield. Too high or too low N application rates and sowing rates caused the yield to decrease. A regression analysis predicted that an N application rate of 190.32 kg ha<sup>-1</sup> and a seeding rate of 25.54 kg ha<sup>-1</sup> would produce the highest yield of hybrid rice. The SPAD value, LAI, dry matter accumulation, and the number of tillers were higher in the N2D2 treatment than in any other rate combination. Conventional rice had the largest thousand-grain weight under high N application rate and high density (N3D3), which was conducive to the production of grain yield. A regression analysis predicted that an N application rate of 238.74 kg ha<sup>-1</sup> and a seeding rate of 28.57 kg ha<sup>-1</sup> would produce the highest grain yield of conventional rice. Grain yield of each treatment increased as N fertilizer rate and seeding rates were increased. There was no significant difference in grain yield between the N1 and N2 treatments in 2018 and 2019, but the grain yield of conventional rice increased significantly when the N application rate was increased to 240 kg ha<sup>-1</sup>. The yield of conventional rice increased with an increase in seeding rate. LAI of the N3D3 treatment was highest compared with other N application and seeding rate combinations, and the various growth traits of the N3D3 treatment were more consistent. These results suggest that suitable N application rates and sowing rates of hybrid rice and conventional rice are quite different. Specifically, the optimal N application rate and sowing rate of conventional rice are higher than those of hybrid rice.

In rice, yield depends on indirect traits such as plant height, growth period, tillering ability, ear length, seed length, seed setting rate, and the number of grains per panicle, as well as direct traits such as unit area and/or the number of panicles per plant, filled grains per ear, and 1000-grain weight (Sakamoto and Matsuoka, 2008; Huang et al., 2013). Previous studies have shown that rice yield has a significant positive correlation with leaf area and dry weight (Li et al., 2019b). Some scholars believe that increasing plant height is an effective way to increase yield without lodging (Li et al., 2019a). The SPAD value is related to the N content of the plant, and the SPAD value of crop leaves can be used as a reference trait for adjusting grain yield (Swain and Sandip, 2010). In this study, a canonical correlation analysis of crop growth traits and yield traits showed that the SPAD value, LAI, and plant height were closely related to grain yield, spikelet number per panicle, and seed setting rate. The increase in the SPAD value, LAI, and plant height may have caused the increase in grain yield and spikelet number per panicle and the decrease in seed setting rate. Another linear combination showed that the SPAD value had a close relationship with effective panicle number and 1000-grain weight. The increase in the SPAD value may have caused the increase in the number of effective panicles and the decrease in 1000-grain weight. A Gray correlation analysis showed that plant height and leaf area index had the largest correlations with grain yield, indicating that they are essential indices that affect grain yield. In the follow-up research, if more hybrid and conventional rice varieties are used as materials, it will be more conducive to perfecting the research conclusions and guiding practical production.

## Conclusion

The yield of direct seeded rice showed a downward parabolic trend as N application rate and sowing rate increased. Excessive N application and sowing rate were not conducive to the production of higher yield, but the optimal N application rate and sowing rate of conventional rice were higher than those of hybrid rice.

**Author Contributions.** Lu, B. L. conceived and designed the research framework; Chen, Q. H. and Hao, R. Q. performed the experiments and analyzed the data; Tang, J. C. wrote the manuscript; Li, Z. X. revised the manuscript; Lu, B. L. supervised the work and finalized the manuscript. All authors read and approved the manuscript.

**Funding.** This work was supported by the National Key Research and Development Program of China (No. 2017YFD030140404).

## REFERENCES

- [1] Abid, M., Khan, I., Mahmood, F., Ashraf, U., Anjum, S. A. (2015): Response of Hybrid Rice to Various Transplanting Dates and Nitrogen Application Rates. – *Philippine Agricultural Scientist* 98(1): 98-104.
- [2] Aleminew, A., Alemayehu, G., Adgo, E., Tadesse, T. (2020): Influence of nitrogen on the growth and use efficiency of rainfed lowland rice in northwest Ethiopia. – *Journal of Plant Nutrition* 43(15): 2243-2258.
- [3] Aslam, M., Hussain, S., Nazir, M. S. (2002): Biological response of direct-seeded coarse rice to seeding density and planting time. – *Pakistan Journal of Agricultural Sciences* 39(1): 28-31.
- [4] Chen, S., Cai, S., Chen, X., Zhang, G. (2009): Genotypic Differences in Growth and Physiological Responses to Transplanting and Direct Seeding Cultivation in Rice. – *Rice Science* 16(2): 143-150.
- [5] Chuma, B. A., Cotter, M., Kalisa, A., Rajaona, A., Senthilkumar, K., Stuerz, S., Vincent, I., Asch, F. (2020): Altitude, temperature, and N Management effects on yield and yield components of contrasting lowland rice cultivars. – *Journal of Agronomy and Crop Science* 206(4): 456-465.
- [6] Dofing, S. M., Knight, C. W. (1994): Yield Component Compensation in Uniculm Barley Lines. – *Agronomy Journal* 86(2): 273-276.
- [7] Hardoon, D. R., Szedmak, S., Shawe-Taylor, J. (2004): Canonical Correlation Analysis: An Overview with Application to Learning Methods. – *Neural computation* 16(12): 2639-2664.
- [8] Huang, R., Jiang, L., Zheng, J., Wang, T., Wang, H., Huang, Y., Hong, Z. (2013): Genetic bases of rice grain shape: so many genes, so little known. – *Trends in plant science* 18(4): 218-226.
- [9] Kumar, V., Ladha, J. K. (2011): Direct Seeding of Rice. Recent Developments and Future Research Needs. – *Advances in Agronomy* 111: 297-413.
- [10] Li, R., Li, M., Ashraf, U., Liu, S., Zhang, J. (2019a): Exploring the Relationships Between Yield and Yield-Related Traits for Rice Varieties Released in China from 1978 to 2017. – *Frontiers Plant Science* 10: 543.
- [11] Li, Y., Lai, R., Li, W., Liu, J., Huang, M., Tang, Y., Tang, X., Pan, S., Duan, M., Tian, H., Wu, L., Wang, S., Mo, Z. (2019b):  $\gamma$ -Aminobutyric Acid Regulates Grain Yield Formation in Different Fragrant Rice Genotypes Under Different Nitrogen Levels. – *Journal of Plant Growth Regulation* 39(2): 738-750.
- [12] Li, B., Gong, L., Qu, H., Jin, D., Sun, W. (2020): Effects of Nitrogen Application Rate on Rice Growth and Yield in Liaohe Delta. – *Crops* 1: 173-178. (in Chinese with English abstract).
- [13] Liang, X. Q., Li, H., Wang, S. X., Ye, Y. S., Ji, Y. J., Tian, G. M., van Kessel, C., Linquist, B. A. (2013): Nitrogen management to reduce yield-scaled global warming potential in rice. – *Field Crops Research* 146: 66-74.
- [14] Liu, H., Hussain, S., Zheng, M., Peng, S., Huang, J., Cui, K., Nie, L. (2015): Dry direct-seeded rice as an alternative to transplanted-flooded rice in Central China. – *Agronomy for Sustainable Development* 35(1): 285-294.



- [15] Lui, S., Cao, H., Yang, H., Liu, S. (2014): The Correlation Analysis Between Tomato Yield, Growth Characters and Water and Nitrogen Supply. – *Scientia Agricultura Sinica* 47(22): 4445-4452. (in Chinese with English abstract).
- [16] Peng, X., Liu, Y., Luo, S., Fan, L., Song, T., Guo, Y. (2007): Effects of Site-Specific Nitrogen Management on Yield and Dry Matter Accumulation of Rice from Cold Areas of Northeastern China. – *Agricultural Sciences in China* 6(6): 715-723.
- [17] Peng, J., Zhang, K. (2010): Notice of Retraction: Research on linkage development between manufacturing and logistics industry of Yangtze Delta region - Based on gray correlation analysis. – *International Conference on Computer and Communication Technologies in Agriculture Engineering*, Chengdu.
- [18] Rezaei, M., Vahed, H. S., Amiri, E., Motamed, M. K., Azarpour, E. (2009): The Effects of Irrigation and Nitrogen Management on Yield and Water Productivity of Rice. – *World Applied Sciences Journal* 7(2): 203-210.
- [19] Rodríguez, M. C., Zientara-Rytter, K., Sirko, A. (2014): *Nutrient Use Efficiency in Plants*. – Springer International Publishing, Cham, Switzerland.
- [20] Sakamoto, T., Matsuoka, M. (2008): Identifying and exploiting grain yield genes in rice. – *Current Opinion in Plant Biology* 11(2): 209-214.
- [21] Schnier, H. F., Dingkuhn, M., Datta, S. K. D., Mengel, K., Faronilo, J. E. (1990): Nitrogen Fertilization of Direct-Seeded Flooded vs. Transplanted Rice: I. Nitrogen Uptake, Photosynthesis, Growth, and Yield. – *Crop Science* 30(6): 1276.
- [22] Swain, D. K., Sandip, S. J. (2010): Development of SPAD Values of Medium- and Long-duration Rice Variety for Site-specific Nitrogen Management. – *Journal of Agronomy* 9(2): 38-44.
- [23] Tang, J., Sun, Z., Chen, Q., Damaris, R. N., Lu, B., Hu, Z. (2019): Nitrogen Fertilizer Induced Alterations in the Root Proteome of Two Rice Cultivars. – *International journal of molecular sciences* 20(15): 3674.
- [24] Thapa, S., Thapa, K., Shrestha, J., Chaudhary, A. (2019): Effect of seedling age, seeding density and nitrogen fertilizer on growth and grain yield of rice (*Oryza sativa* L.). – *International Journal of Applied Biology* 3(1): 81-87.
- [25] Wang, S., Wu, K., Yuan, Q., Liu, X., Liu, Z., Lin, X., Zeng, R., Zhu, H., Dong, G., Qian, Q., Zhang, G., Fu, X. (2012): Control of grain size, shape and quality by OsSPL16 in rice. – *Nature Genetics* 44(8): 950-954.
- [26] Wang, D. Y., Chen, S., Wang, Z., Ji, C. L., Xu, C. M., Zhang, X. F., Singh Chauhan, B. (2014): Optimizing Hill Seeding Density for High-Yielding Hybrid Rice in a Single Rice Cropping System in South China. – *Plos One* 9(10): e109417.
- [27] Zeng, D., Tian, Z., Rao, Y., Dong, G., Yang, Y., Huang, L., Leng, Y., Xu, J., Sun, C., Zhang, G., Hu, J., Zhu, L., Gao, Z., Hu, X., Guo, L., Xiong, G., Wang, Y., Li, J., Qian, Q. (2017): Rational design of high-yield and superior-quality rice. – *Nature Plants* 3: 17031.
- [28] Zhang, L., Yu, H., Ma, B., Liu, G., Wang, J., Wang, J., Gao, R., Li, J., Liu, J., Xu, J., Zhang, Y., Li, Q., Huang, X., Xu, J., Li, J., Qian, Q., Han, B., He, Z., Li, J. (2017): A natural tandem array alleviates epigenetic repression of IPA1 and leads to superior yielding rice. – *Nature Communications* 8: 14789.

# EFFECTS OF MAGNETIZED BRACKISH WATER ON SEED GERMINATION, SEEDLING GROWTH, PHOTOSYNTHESIS AND DRY MATTER DISTRIBUTION OF COTTON (*GOSSYPIUM HIRSUTUM* L.)

ZHANG, J. H. – WANG, Q. J.\* – WEI, K. – SUN, Y. – MU, W. Y.

*State Key Laboratory of Eco-hydraulics in Northwest Arid Region of China, Xi'an University of Technology, Xi'an 710048, China*

*\*Corresponding author  
e-mail: wquanjiu@163.com*

(Received 27<sup>th</sup> Sep 2020; accepted 18<sup>th</sup> Dec 2020)

**Abstract.** Magnetized water is widely used in agricultural irrigation as a new type of biomagnetic technology in China. In order to understand the biological effects of different strength magnetized brackish water, seed germination and potted experiments were carried out to study its effects of magnetized brackish water with different magnetic intensities (0, 100 mT, 300 mT, 500 mT) on seed germination and seedling growth. The germination vigor indexes of cotton cultivated with magnetized brackish water significantly increased, and the germination potential and vigor index increased by 39.4-60.6% and 129.1-246.3%, respectively. The emergence rate of cotton under magnetized brackish water irrigation was faster and higher, with an increase range of 7.5-41.9%. The net photosynthetic rate ( $P_n$ ) and instantaneous water use efficiency ( $iWUE$ ) of cotton under magnetized brackish water irrigation increased significantly, whereas the stomatal limit value ( $L_s$ ) decreased. The total biomasses of cotton under magnetized brackish water irrigation were significantly increased, but the stem weight ratio and leaf weight ratio had no significant changes. Hence, magnetized brackish water can promote the utilization of water and light, and cotton irrigated with 300 mT magnetic field intensity is most conducive to the growth of cotton seedlings.

**Keywords:** *magnetic water treatment, biological effect, early growth of cotton, water use efficiency, efficiency of utilization of light*

## Introduction

Fresh water resources are an important material basis for human survival and development, as well as a basic condition for agricultural production (Shrestha et al., 2017). With the rapid development of social economy and the continuous increase of population, the lack of fresh water resources has become a worldwide problem, posing a serious threat to agricultural production and the ecological environment (Wang et al., 2020). Therefore, how to solve the problem of fresh water resource crisis has become a very urgent task (Murshed and Kaluarachchi, 2018).

In order to alleviate the contradiction between the supply and demand of fresh water resources, in recent years, countries in the world have taken the development and utilization of low-quality water as an important means (Zhou et al., 2019), and brackish water is widely distributed and has large reserves, so it has become the main water source for development and utilization (Faulkner et al., 2019). The scientific and reasonable development and utilization of brackish water resources play an extremely important role in alleviating the shortage of fresh water resources, expanding agricultural water sources, fighting drought, and increasing production (Honarparvar et al., 2019). However, brackish water irrigation can easily cause secondary salinization of the soil, causing the soil salinity of the plough layer or the concentration of the soil solution to exceed the salinity tolerance of the crop,

thereby affecting crop growth and yield (Huang et al., 2019). Therefore, the treatment and scientific use of brackish water, the prevention and control of soil secondary salinization, and the maintenance of sustainable development of land resources have become the core issues in the development and utilization of brackish water (Zhong et al., 2018; Mollahosseini and Abdelrasoul, 2019).

With the development of magnetized water research, this technology has also achieved good results in agricultural irrigation (Aliverdi et al., 2015; Al-Ogaidi et al., 2017). Some researchers conducted irrigation experiments with magnetized saline water (brackish water), and the results showed that magnetization treatment can reduce the harm of brackish water (brackish water), promote crop growth, and increase crop yield (Alavi et al., 2020; Liu et al., 2020). Surendran et al. (2016) indicated that under field conditions, the yield of eggplant under magnetized water irrigation increased by 17.0%. Hozayn et al. (2019) showed that the grain yield, straw yield, and biological yield of magnetized brackish water increased by 19.24%, 33.97%, and 26.99%, respectively. Moreover, studies on the early growth of crops with magnetized water irrigation found that magnetized water irrigation significantly improved the germination rate, germination index, activity index, salt tolerance index, and other physiological factors of corn (*Zea mays* L.) seeds, and promoted the growth of seedlings under saline conditions (Aghamir et al., 2015). Sayed and Sayed (2014) indicated that magnetized water irrigation had a significant positive effect on the growth parameters (plant height, leaf area, leaf, stem, root brackish weight, and dry weight) of broad bean (*Vicia Faba* L.) seedlings. Studies on the utilization of light energy of crops by magnetized water irrigation showed that the net photosynthetic rate, stomatal conductance, intercellular CO<sub>2</sub> concentration, and water use efficiency of *Populus×euramericana* 'Neva' in magnetized brackish water irrigation were all increased, while transpiration rate and stomatal limit value were all decreased compared with that of unmagnetized water (Liu et al., 2019a). Alfaidi et al. (2017) found that the contents of chlorophyll a, b, carotenoids, total pigment, soluble protein, and total protein in guinea grass (*panicum maximum*) leaves were significantly increased after irrigating with magnetized water. More importantly, the growth promoting effect of magnetized water is related to the magnetic field strength and irrigation water quality. Massah et al. (2019) indicated that the intensity of magnetic field and the type of treated water had a significant effect on the germination and growth characteristics of wheat seeds. The germination rate of seeds treated with 400 mT of distilled water was the highest (53.3%), the brackish weight of seedlings treated with 600 mT of distilled water was the highest, and the root length of wheat seeds treated with 400 mT of groundwater was the largest (155.3 mm).

To sum up, remarkable achievements have been made in irrigating wheat, corn, broad bean, and eggplant with magnetized water, but the research on irrigating cotton with magnetized water is insufficient. At the same time, there are few studies on the magnetization of brackish water. Therefore, it is necessary to explore the effects of magnetized brackish water with different magnetic fields on the growth of crops, especially on the fragile and sensitive seedling stage of crop growth. Therefore, in this paper, cotton was used as experimental material, through the analysis of cotton seed germination, seedling emergence, seedling growth, photosynthetic characteristics parameters and biomass distribution pattern, the effects of magnetized brackish water with different magnetization intensities (0, 100 mT, 300 mT, 500 mT) on cotton seedling growth and photosynthetic characteristics were discussed, and the suitable cotton seed germination and seedling were determined. The results can provide a theoretical basis and technical support for the efficient utilization of brackish water resources in arid and semiarid areas.

## Materials and methods

### Experimental site description

The experimental site is located in Bazhou Irrigation Experimental Station of Xinjiang Tarim River Basin Authority, which is located in the Bayingoleng Mongolian Autonomous Prefecture of Xinjiang in the middle of Eurasia continent (Liang et al., 2020). It is a typical continental arid climate type and an important cotton (*Gossypium hirsutum* L.) planting area in Northwest China (Chen et al., 2020). The experimental station is 41°35'N and 86°10'E, with an elevation of 901 m (Yang et al., 2016). The annual average precipitation is only 58 mm, and the maximum potential evaporation is 2788.2 mm (Tian et al., 2017). The annual sunshine in this region is 3036.2 h, the frost-free period is 144-241 d, the average wind speed is 2.4 m·s<sup>-1</sup>, the highest wind speed is 22 m·s<sup>-1</sup> (Li et al., 2019). The annual average maximum, minimum and average temperatures are 11.5, 42.2, and 30.9 °C, respectively (Tan et al., 2017). The brackish water used for irrigation in the test station is groundwater with an average salinity of 5.49 g·L<sup>-1</sup> and a pH of 7.84.

### Magnetizer and magnetized water device

Three external CHQ permanent magnet magnetizers (Shanghai Juncai Magnetic Materials Co., LTD., China) with magnetic field strength of 100 mT, 300 mT, and 500 mT were used in the test, and they were made of sintered Rufe-B. The effective magnetic field area was 8 cm×10 cm and the magnetic field intensities are calibrated with the 5180-Gaussian Meter (F.W. BELL Co., USA). The magnetized water device is composed of a water box, peristaltic pump, magnetizer, water pipeline, and valves. The water pipeline is a PVC pipe with a 2.5 cm diameter (cross-sectional area of 4.91 cm<sup>2</sup>), and the length of the pipeline passing through the magnetic field (effective magnetic distance) is 10 cm. As shown in *Fig. 1*, 100 L of irrigation water was placed in the water box, and a pipeline was opened one at a time through a valve control. The peristaltic pump was used to circulate the water in a closed pipeline. A section of the circulating pipeline was placed between the two poles of the magnetizer, and the magnetic induction line was cut perpendicular to the magnetic field. The flow rate was adjusted to 0.5 m·s<sup>-1</sup> by the peristaltic pump, and the flow was cyclically magnetized by the magnetic field. The magnetization time was 30 min.

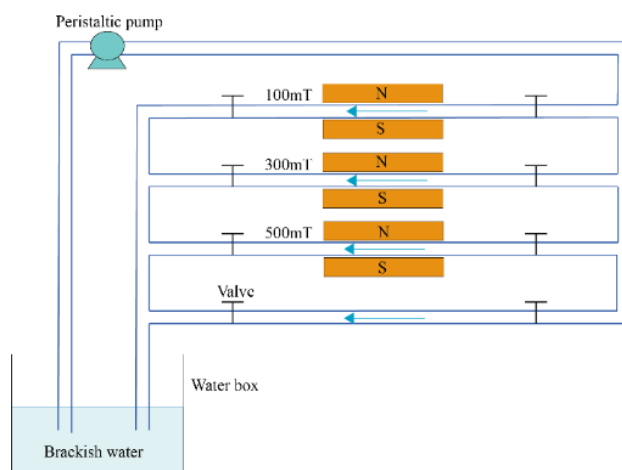


**Figure 1.** Schematic diagram of magnetized brackish water device

### **Experimental design and process**

The above magnetized water device was used to magnetize brackish water with different magnetic field intensities. Unmagnetized brackish water was used as a control, and a total of 4 treatments were formed: unmagnetized brackish water (BM0), 100 mT magnetized brackish water (BM1), 300 mT magnetized brackish water (BM3) and 500 mT magnetized brackish water (FM5). A series of experiments including cotton seed germination and potted experiments in a cotton field were carried out with the four kinds of treated water to analyze the influence of magnetized brackish water with different magnetic field intensities on cotton seed germination and seedling growth, in 2018.

#### **Experiment 1—seed germination test**

Seed germination tests were performed as described in a previous study with three repetitions (Fu et al., 2010). 50 cotton seeds of the same size and full grain were selected and arranged evenly in a petri dish with tweezers. The petri dish was then marked and covered with a layer of filter paper. 20 mL of treated water was added to the corresponding culture dish and the seeds were covered with a layer of fine paper. After the seeds had reached the constant weight, the excess water was drained, and then the seeds were placed in the culture dish in the incubator at  $28 \pm 1$  °C, with a light intensity of 800 Lx. The number of germinations was recorded every day, and the corresponding treatment water was added in time to maintain the moisture content of the filter paper. The radicle length of cotton seeds was measured on the eighth day. The germination condition was evaluated by calculating germination potential (*GP*), germination rate (*GR*), germination index (*GI*), and vigor index (*VI*). The Calculation methods for each index are as Eq.1-Eq.4 (Mosse et al., 2013).

$$GP = \frac{N_4}{N_T} \times 100\% \quad (\text{Eq.1})$$

$$GR = \frac{N_8}{N_T} \times 100\% \quad (\text{Eq.2})$$

$$GI = \sum \frac{G_t}{Dt} \quad (\text{Eq.3})$$

$$VI = GI \times L \quad (\text{Eq.4})$$

where,  $N_4$  and  $N_8$  are the number of seeds germinated in 4 days and 8 days, respectively.  $N_T$  is the total number of seeds,  $G_t$  is the number of seeds germinated at day  $t$  ( $Dt$ ), and  $L$  is the average radicle length of seed on the eighth day.

#### **Experiment 2—potted experiments in a cotton field**

To simulate the growth environment of field cotton, all the potted plants were buried in the cotton field, randomly divided, and repeated three times. Saline alkali soil from 0-20 cm depth from the surface of the cotton field was used in the experiment. According

to the soil texture classification of the U.S. Department of Agriculture, the soil was sandy loam (64.27% sand, 32.83% silt, 2.9% clay), and soil bulk density was  $1.63 \text{ g}\cdot\text{cm}^{-3}$ , saturated water content was  $0.395 \text{ cm}^3\cdot\text{cm}^{-3}$ , the wilting coefficient was  $0.050 \text{ cm}^3\cdot\text{cm}^{-3}$ , field capacity was  $0.196 \text{ cm}^3\cdot\text{cm}^{-3}$ , and soil extract conductivity (ECe) was  $5.47 \text{ ds}\cdot\text{m}^{-1}$ . The inner diameter and height of the plastic basin used in the test were 30 cm and 20 cm respectively, and 8 air holes with a diameter of 10 mm were set at the bottom of the basin. After the fertilizer and soil were mixed evenly, each barrel was uniformly loaded with 20 kg of soil sample. The fertilizer added per barrel was as follows: carbamide (N 45.4%) 6.8 g, compound fertilizer (N 12%, P 18%, K 15%) 6.4 g, organic fertilizer (organic matter > 35%) 24 g. The amount of water applied before sowing was calculated according to the amount of spring irrigation in the field (100 mm). After sowing, the cotton at the seedling stage was no longer irrigated as in the field. Each pot was seeded with 20 cotton seeds, with a sowing depth of 2-3 cm. As in the field, the soil surface was covered with plastic film mulch after sowing.

Fourteen days after sowing, the rate of emergence was measured and only 4 cotton plants were kept in each pot, with the remaining seedlings being removed. The length of cotton seedlings was then measured, the dust on the surface was removed, and the brackish weight of the seedling was measured after washing and drying. Then, the seedlings were placed in an oven at  $105 \text{ }^\circ\text{C}$  for 1 h and dried at  $75 \text{ }^\circ\text{C}$ , and the dry weight of the seedling was measured after they had cooled down. Plant height, stem diameter at cotyledon node, number of leaves per plant, and area of single leaf of potted cotton were measured. The stem diameter was measured with an electronic Vernier caliper with an accuracy of 0.01 mm. The number of leaves was counted manually. Plant height, leaf width, and vein length were measured with measuring tape with an accuracy of 1 mm. The area of a single leaf was calculated with the formula  $\text{length} \times \text{width} \times 0.84$  (Tan et al., 2017). The growth indexes of potted cotton seedlings were measured every 10 days after final singling. Thirty days after final singling, the net photosynthetic rate ( $P_n$ ), stomatal conductance ( $G_s$ ), intercellular  $\text{CO}_2$  concentration ( $C_i$ ), and transpiration rate ( $T_r$ ) of the main functional leaves (from the top to the bottom of the fourth leaf) of cotton seedlings were measured using LC Pro SD full-automatic portable photosynthetic instrument (UK ADC) equipped with an LED artificial light source. Then, the stomatal limit  $L_s=1-C_i/C_a$  ( $C_a$  is atmospheric  $\text{CO}_2$  concentration) and instantaneous water use efficiency  $iWUE=P_n/T_r$  were calculated (Liu et al., 2017). When determining the photosynthesis parameters of cotton seedlings, according to the meteorological environment conditions during 10:00-12:00 am in the cotton field, the light intensity was set as  $1100 \mu\text{mol}\cdot\text{m}^{-2}\cdot\text{s}^{-1}$ , the concentration of  $\text{CO}_2$  was  $360 \mu\text{mol}\cdot\text{mol}^{-1}$ , and the temperature was  $30 \text{ }^\circ\text{C}$ . Forty days after final singling, the cotton seedlings were removed slowly. The cotton branches were then cut with fruit scissors, the dust was removed from the surface, the cotton branches were washed and dried, and the dry weight of each part was weighed.

### **Data processing and analysis**

The data were recorded in Excel 2016 and analyzed using SPSS 22.0 software (IBM Corp. USA). The least significant difference (LSD) method ( $P < 0.05$ ) was used for comparison of multiple values.

## Results and Discussion

### *Analysis of germination characteristics of cotton seeds*

Seed germination refers to the process of resuming material synthesis and metabolism after the vigorous seed swells, prompting the radicle to expose the seed coat (Hadi et al., 2018; Yue et al., 2019). Seed germination is extremely susceptible to external environmental factors such as light, temperature, moisture, and salinity (Castillo et al., 2017; Luo et al., 2019), and magnetized water treatment also has an important impact on seed germination (Sappington and Rifai, 2018). Germination characteristics of cotton cultivated with different magnetized brackish water were analyzed by comparing Germination potential (*GP*), germination rate (*GR*), germination index (*GI*), and vigor index (*VI*) (Table 1). Compared with unmagnetized brackish water, the *GP*, *GR*, *GI*, and *VI* of magnetized brackish water were significantly increased ( $P < 0.05$ ), with the ranges of 39.4-60.6%, 23.5-49.0%, 30.0-58.5%, and 129.1-246.3%, respectively, and the *VI* was the most sensitive to magnetized brackish water treatment. The results were consistent with the research results of Massah et al. (2019), who applied magnetized brackish water to promote the germination of wheat seeds. The increase range of germination potential was greater than that of germination rate, while the increase range of vigor index was greater than that of germination index, indicating that brackish water magnetization could significantly improve the seed vigor of cotton and enhance the germination potential of cotton. This may be due to magnetized brackish water has a function similar to plant growth hormone, which can stimulate the activity of the seed enzyme system or accelerate the synthesis of related enzymes, enhance the enzymatic reactions in seeds, and thus improve the seed activity (Boe and Salunkhe, 1963). Compared with the germination indexes of cotton seeds cultivated by brackish water with different magnetized intensities, it could be found that the germination indexes of cotton seeds cultivated by BM3 improved the most, the *VI* of cotton seeds treated with BM5 was significantly higher than that of BM1, while the *GP*, *GR*, *GI* had no significant difference ( $P > 0.05$ ).

**Table 1.** Germination indexes of cotton seeds under different strength of magnetized brackish water ( $n=3$ )

Treatment	Germination potential ( <i>GP</i> ) (%)	Germination rate ( <i>GR</i> ) (%)	Germination index ( <i>GI</i> )	Vigor index ( <i>VI</i> )
BM0	22.0±2.0c	34.0±2.0c	8.0±0.3c	7.0±1.4d
BM1	30.7±2.3b	42.0±2.0b	10.5±0.4b	16.0±1.2c
BM3	35.3±1.2a	50.7±4.2a	12.8±0.5a	24.2±1.7a
BM5	32.0±2.0ab	45.3±1.2b	11.2±0.2b	19.0±0.8b

Different letters within a column indicate significant differences among all treatments at  $P < 0.05$

### *Effect of magnetized brackish water irrigation on the emergence rate of cotton*

High seedling emergence rate and seedling uniformity are the guarantees for high and stable yield (Wang et al., 2016; Liang et al., 2018). The emergence of cotton seeds started 3 days after sowing (Fig. 2). With the increase of emergence time, the emergence rate of cotton gradually increased and tended to be stable. The emergence rate of cotton under magnetized brackish water irrigation was faster and higher. The emergence rate and full seedling formation of cotton irrigated with BM0 was 58.9% and 9 d, respectively, while the emergence rates of cotton irrigated with BM1, BM3 and BM5 were 63.3%, 83.6%, and 70.0% respectively, and the full seedling formations were 9 d, 8 d, and 9 d,

respectively. Compared with BM0, the emergence rate of cotton irrigated with magnetized brackish water increased by 7.5-41.9%, and the full seedling formation of cotton irrigated with BM3 was advanced by 1 d. Similarly, Moussa (2011) applied magnetized brackish water irrigation to improve the emergence rate of snow peas and chickpeas. The effect of BM3 on cotton seedling emergence was the best, while the effect of BM5 on cotton seedling emergence was better than that of BM1.

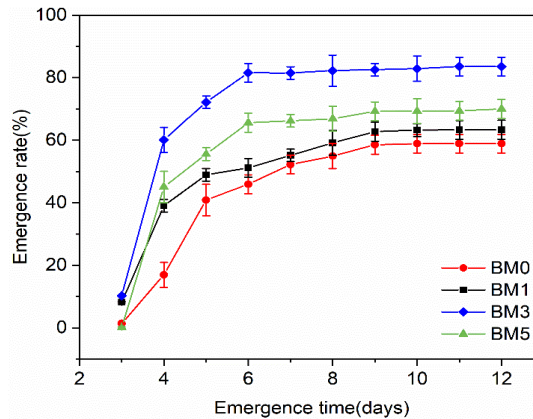


**Figure 2.** The effect of different strength of magnetized brackish water irrigation on the emergence rate of cotton ( $n=3$ ). The error bars represent standard deviations

The vitality of cotton seedlings was analyzed by seedling height, root length, fresh weight, dry weight, and seedling water content (Velmalala et al., 2018). The cotton seeds were removed 14 days after sowing and seedling activity indexes were measured and analyzed (Table 2). Compared to unmagnetized brackish water, the activity of cotton seedling under magnetized brackish water irrigation was significantly increased ( $P < 0.05$ ), and the seedling height, root length, fresh weight, dry weight, and water content increased by 41.6-55.2%, 29.5-54.5%, 55.1-76.4%, 23.1-35.8%, and 5.8-6.3%, respectively. Among them, seedling root length and seedling fresh weight increased significantly, while seedling water content increased less than 8%, indicating that magnetized brackish water mainly improves seedling vitality and ensures the seedling healthy by promoting seedling root growth and increasing seedling fresh weight (Surendran et al., 2016). The effects of magnetized brackish water irrigation with different magnetic field strengths on the activity of cotton seedlings were significantly different ( $P < 0.05$ ). FM3 had the best promoting effect on seedling vigor, while the seedling water content had no significant difference ( $P > 0.05$ ). The seedling height, fresh weight, and dry weight of cotton irrigated with FM5 were 1.7-5.6% higher than those with FM1, but the difference was not significant.

**Table 2.** Characteristics of seedling activity of cotton under magnetized and unmagnetized brackish water ( $n=3$ )

Treatment	Seedling height (cm)	Seedling root length (cm)	Fresh weight (g)	Dry weight (g)	Seedling water content (%)
BM0	4.2±0.1c	2.9±0.2c	2.64±0.07c	0.58±0.02c	78.13±0.09c
BM1	5.9±0.3b	4.0±0.3b	4.09±0.12b	0.71±0.01b	82.63±0.59a
BM3	6.5±0.1a	4.5±0.4a	4.65±0.42a	0.78±0.03a	83.03±2.09a
BM5	6.0±0.2b	3.8±0.1b	4.32±0.27ab	0.73±0.01b	82.97±1.3a

Different letters within a column indicate significant differences among all treatments at  $P < 0.05$



### Effect of magnetized brackish water irrigation on growth characteristics of cotton

Crops adapt to environmental stress by changing their growth rate and morphology (Ramírez-Pérez et al., 2018; Dzedzic et al., 2019). The growth indexes of cotton all increased with the increase of growth time, and there was a small difference between the growth indexes of cotton irrigated with magnetized and unmagnetized brackish water 10 d after final singling. With the increase of growth time, the difference between the growth indexes of cotton irrigated with magnetized and unmagnetized brackish water gradually increased (Fig. 3). In the same growth period, the plant height, stem diameter, leaf number, and single leaf area of magnetized brackish water irrigation were larger than those of unmagnetized brackish water. After 10-40 d of final singling, the average growth rate of BM0 irrigated cotton plant height was  $0.31 \text{ cm}\cdot\text{d}^{-1}$ , and the peak growth rate of plant height was 30-40 d after final singling. While the average growth rates of cotton plant height under BM1, BM3 and BM5 were 0.44, 0.60, and  $0.53 \text{ cm}\cdot\text{d}^{-1}$ , respectively, and all the peaks of plant height growth rate were 30-40 d after final singling. Compared to FM0, the plant height of cotton irrigated with BM1, BM3, and BM5 increased by 52.0%, 100.7%, and 79.1%, respectively, 40 d after final singling (Fig. 3A), which was consistent with the research results of (Yusuf and Ogunlela, 2015). After 10-40 d of final singling, the average growth rate of BM0 irrigated cotton stem diameter was  $0.07 \text{ mm}\cdot\text{d}^{-1}$ , and the peaks growth rate of stem diameter were 10-20 d after final singling. While the average growth rates of cotton stem diameter under BM1, BM3, and BM5 were 0.11, 0.14, and  $0.12 \text{ mm}\cdot\text{d}^{-1}$ , respectively, and all the peaks of stem diameter growth rate were 30-40 d after final singling. Compared to BM0, the stem diameter of cotton irrigated with BM1, BM3, and BM5 increased by 57.9%, 108.1% and 76.6%, respectively, 40 d after final singling (Fig. 3B). Compared to BM0, the number of cotton leaves irrigated with BM1, BM3 and BM5 increased by 55.6%, 100.0%, and 77.8% (Fig. 3C), respectively, while the single leaf area increased by 38.0%, 83.2%, and 59.4% (Fig. 3D), respectively, 40 d after final singling. Compared with different intensities of magnetized brackish water, BM3 had the greatest promoting effect on cotton growth, while BM5 had a better promoting effect on cotton growth than BM1.

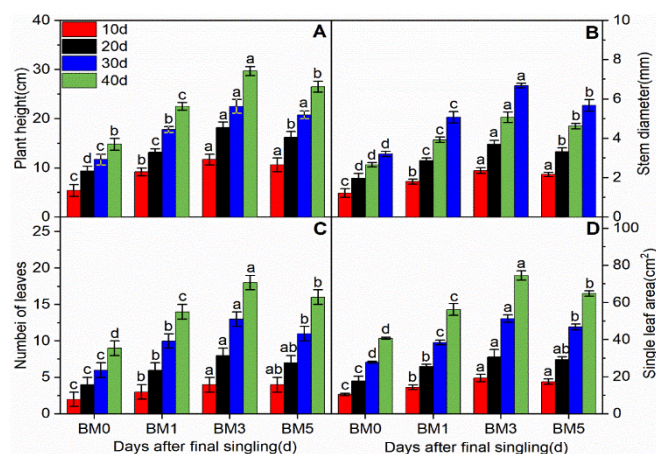


**Figure 3.** Effect of magnetized and unmagnetized brackish water irrigation on cotton morphological indexes. 10d, 20d, 30d and 40d represent 10d, 20d, 30d and 40d after final singling, respectively. BM0 represents unmagnetized brackish water, while BM1, BM3 and BM5 represent brackish water treated with magnetic field intensities of 100mT, 300mT and 500mT, respectively (n=3). The error bars represent standard deviations. Different letters within a column indicate significant differences among all treatments at  $P < 0.05$

### ***Effect of magnetized brackish water irrigation on photosynthetic characteristic parameters of cotton***

Photosynthesis is a key process that promotes the growth and development of crops (Kulmala et al., 2019), and magnetized brackish water irrigation plays a role in crop growth by affecting the photosynthesis process (Liu et al., 2020). The characteristic photosynthetic parameters of magnetized and unmagnetized brackish water irrigated cotton are shown in Fig. 4. The net photosynthetic rate ( $P_n$ ) of cotton irrigated with BM0 was  $12.60 \mu\text{mol}\cdot\text{m}^{-2}\cdot\text{s}^{-1}$ , and the  $P_n$  of cotton irrigated with BM3 and BM5 increased by 45.2% and 26.4%, respectively, while there was no significant difference between BM1 and BM0 (Fig. 4A). The transpiration rate ( $T_r$ ) of cotton irrigated with BM0 was  $4.86 \text{mmol}\cdot\text{m}^{-2}\cdot\text{s}^{-1}$ , and the  $T_r$  of cotton irrigated with BM1 was 2.9% bigger than that of BM0, while the  $T_r$  of cotton irrigated with BM3 and BM5 was increased by 2.1-14.1%, but all the difference was not significant (Fig. 4B). The stomatal conductance ( $G_s$ ) of cotton irrigated with BM0 was  $0.180 \text{mmol}\cdot\text{m}^{-2}\cdot\text{s}^{-1}$ , and the  $G_s$  of cotton irrigated with BM3 and BM5 increased by 46.7% and 42.2%, respectively, while there was no significant difference between BM1 and BM0 (Fig. 4C). The intercellular  $\text{CO}_2$  concentration ( $C_i$ ) of cotton irrigated with BM0 was  $126.8 \mu\text{mol}\cdot\text{mol}^{-1}$ , and the  $C_i$  of cotton irrigated with BM1, BM3 and BM5 increased by 22.4%, 54.9%, and 41.0%, respectively (Fig. 4D). Compared with BM0, the instantaneous water use efficiency ( $iWUE$ ) of cotton irrigated with BM3 and BM5 increased by 25.1% and 23.8% (Fig. 4E), while the stomatal limit ( $L_s$ ) decreased by 25.0% and 21.9% (Fig. 4F). The  $L_s$  of cotton irrigated with BM1 decreased by 18.8%, while  $iWUE$  did not change significantly. This indicated that magnetized water treatment could effectively improve the stomatal conductance of cotton seedlings, reduce stomatal limitation and improve the supply of  $\text{CO}_2$ , thus improving the photosynthetic carbon assimilation capacity and enhancing the utilization efficiency of light energy and water. This is consistent with the research results of Hasan et al. (2017) and Qiu et al. (2011). Comparing the effects of magnetized brackish water with different intensities on the photosynthetic characteristic parameters of cotton, it could be found that the  $L_s$  of cotton irrigated with BM3 was the lowest, while the  $P_n$  and  $iWUE$  were the largest, and BM5 was better than BM1. In this study, magnetized water irrigation maintained relatively high  $P_n$ ,  $G_s$ ,  $C_i$ ,  $T_r$ ,  $iWUE$ , and chlorophyll SPAD values and low  $L_s$  values (Fig. 4A-F). Some studies have shown that magnetization treatment can improve the activity of related enzymes in the plant and increase the metabolism rate of crops (ul Haq et al., 2016). Free water increased in magnetized crop cells, the photochemical activity of chlorophyll increased, the rate of photophosphorylation accelerated, and the net photosynthetic rate increased (Huuskonen et al., 1998).

The relationship between photosynthetic parameters of cotton irrigated with magnetized brackish water was fitted and analyzed (Fig. 5). There was a positive linear relationship between net photosynthetic rate and stomatal conductance (Fig. 5A,  $R^2 = 0.496$ ), indicating that the increase of photosynthesis under magnetized brackish water irrigation was caused by the increase of stomatal conductance of leaves (Liu et al., 2009). There was also a positive linear correlation between the transpiration rate and stomatal conductance (Fig. 5B,  $R^2 = 0.544$ ). The reason was that magnetization promoted the stomatal opening of cotton leaves, and high stomata led to high transpiration (Yang et al., 2013). The slope of net photosynthetic rate and stomatal conductance (35.11) was greater than that of transpiration rate and stomatal conductance (11.49), which was due to the increase of stomatal conductance, and the rise of transpiration rate was lagging

behind that of stomatal conductance. Therefore, the slope of the net photosynthetic rate and stomatal conductance was greater than that of transpiration rate and stomatal conductance. The net photosynthetic rate of cotton irrigated with magnetized brackish water was negatively correlated with stomatal limitation value (Fig. 5C,  $R^2 = 0.429$ ), which indicated that stomatal limitation was the dominant type of photosynthesis restriction. The results showed that the amount of carbon dioxide entering the leaves provided sufficient raw materials for photosynthetic reaction. Instantaneous water use efficiency was negatively correlated with the stomatal limitation value (Fig. 5D,  $R^2 = 0.151$ ), and the correlation coefficients were low. Magnetized brackish water irrigation could improve the water use efficiency of cotton by reducing stomatal limitation and enhancing photosynthesis use efficiency (Zlotopolski, 2017).

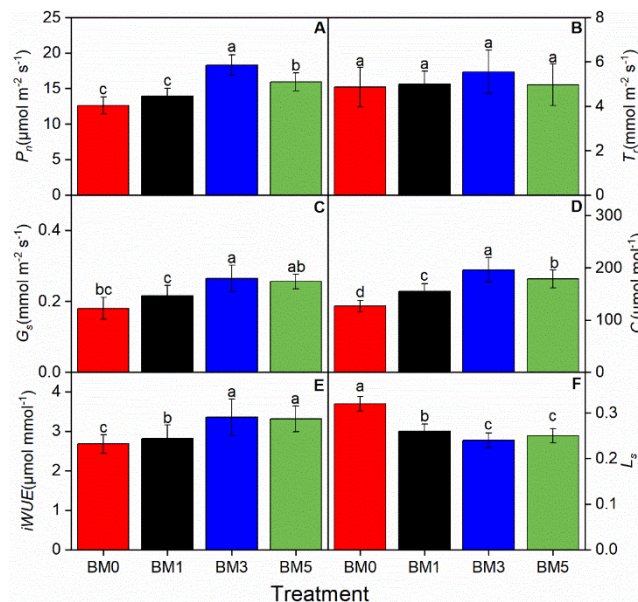


**Figure 4.** Characteristic photosynthetic parameters of cotton irrigated with magnetized and unmagnetized brackish water. FM0 represents unmagnetized brackish water, while BM1, BM3 and BM5 represent brackish water treated with magnetic field intensities of 100mT, 300mT and 500mT, respectively.  $P_n$ ,  $G_s$ ,  $C_i$ ,  $T_r$ ,  $iWUE$  and  $L_s$  represent the net photosynthetic rate, stomatal conductance, intercellular  $\text{CO}_2$  concentration, transpiration rate, instantaneous water use efficiency and stomatal limit, respectively ( $n=3$ ). The error bars represent standard deviations. Different letters within a column indicate significant differences among all treatments at  $P < 0.05$

### Effect of magnetized brackish water irrigation on cotton biomass and its distribution

Biomass is the basis of crop yield (Richards et al., 2019), and magnetized brackish water affects the final yield of crops through the dry matter accumulation process of magnetized water (Ghanati et al., 2015). According to the cotton biomass analysis, there was a significant difference between magnetized and unmagnetized brackish water treated cotton, but there was no significant difference between different magnetization intensities (Table 3). Compared with unmagnetized brackish water, magnetized brackish water irrigated stem, leaf, root dry weight and total dry matter increased by 2.7-18.4%, 1.9-20.0%, 52.2-69.3%, and 5.5-20.7%, respectively, among which the root dry weight increased the most. In terms of stem weight ratio, BM5 reduced by 7.9% compared with

BM0, while BM1 and BM3 had no significant difference from BM0. For leaf weight ratio, there was no significantly difference between magnetized and unmagnetized brackish water. For root shoot ratio, BM1, BM3 and BM5 increased by 22.4%, 54.9%, and 41.0%, respectively, compared to BM0, while the difference between different magnetic field strengths was not significant. The root system is an important organ that is in direct contact with the soil and is responsible for absorbing soil water and nutrients. The health of the root system directly affects crop growth and yield (Hefner et al., 2019). Seedling root weight of cotton irrigated with magnetized water was significantly higher than that of unmagnetized water, which indicated that magnetization could promote root growth and development in cotton seedlings, improve the selective absorption capacity for nutrient ions, and avoid excessive absorption of  $\text{Na}^+$  in cells and the resulting damage, thus reducing the inhibitory effect of salt stress on the growth of cotton seedlings (Liu et al., 2019b). Magnetized brackish water can increase the frequency of mitosis of plant cells, increase RNA content in root tip growth area, accelerate root tissue differentiation, promote cell volume increase in the root elongation area, promote radicle elongation, and enhance absorption of nutrients by roots (Boe and Salunkhe, 1963). Therefore, magnetized brackish water can enhance the absorption of water and nutrients by increasing the dry matter ratio of roots, thus promoting the accumulation of total biomass of cotton as a whole (Liu et al., 2017).

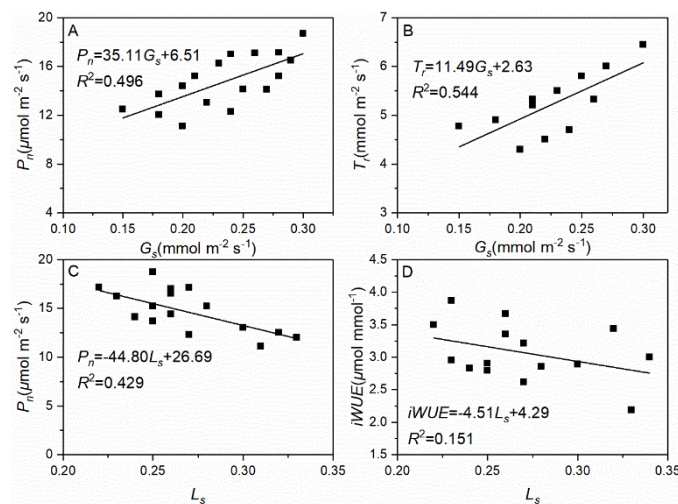


**Figure 5.** Linear regression between indicators related photosynthesis.  $P_n$ ,  $G_s$ ,  $T_r$ ,  $iWUE$  and  $L_s$  represent the net photosynthetic rate, stomatal conductance, transpiration rate, instantaneous water use efficiency and stomatal limit, respectively ( $n=3$ ). The error bars represent standard deviations. Different letters within a column indicate significant differences among all treatments at  $P < 0.05$

**Table 3.** Biomass and its distribution of cotton irrigated with magnetized and unmagnetized brackish water ( $n=3$ )

Treatment	Stem (g)	Leaf (g)	Root (g)	Total dry weight (g)	Stem weight ratio (%)	Leaf weight ratio (%)	Root shoot ratio (%)
BM0	5.01±0.07b	9.87±0.19b	1.05±0.09b	15.94±0.22b	31.47±0.85a	61.93±0.35a	7.07±0.58b
BM1	5.15±0.43b	10.05±1.13b	1.60±0.18a	16.81±1.22b	30.73±3.25a	59.74±3.39a	10.53±0.56a
BM3	5.93±0.17a	11.62±0.22ab	1.68±0.13a	19.24±0.25a	30.84±0.51a	60.41±0.36a	9.60±0.92a
BM5	5.56±0.48ab	11.85±1.27a	1.78±0.12a	19.19±1.68a	28.97±0.62b	61.67±1.19a	10.34±1.54a

Different letters within a column indicate significant differences among all treatments at  $P < 0.05$



## Conclusions

The germination potential, germination rate, germination index, and vigor index of magnetized brackish water cotton were all significantly increased, and the increase range of germination potential was greater than that of germination rate, while that of vigor index was greater than that of germination index. The emergence rate of cotton irrigated with magnetized brackish water was 7.5–41.9%, and full seedling formation of cotton irrigated with 300 mT magnetized brackish water was advanced by 1 d. Under magnetized brackish water irrigation, the seedling vigor indexes such as seedling length, seedling root length, seedling brackish weight, seedling dry weight, and seedling water content were significantly increased ( $P < 0.05$ ). The increase range of seedling root length and seedling brackish weight was larger, while the increase range of seedling water content was slight. Magnetized brackish water with different intensities could improve cotton photosynthesis and water use efficiency, promote cotton morphological development, and increase cotton biomass. Under the magnetic field strength of 300 mT, the magnetized brackish water irrigation is most beneficial to the growth of cotton seedlings. In agricultural irrigation, 300 mT magnetic field strength should be used to magnetize brackish water to improve the effectiveness of brackish water resources. The results can provide guidance for the efficient utilization of magnetized brackish water in arid and semiarid areas. However, this study only focused on the magnetization of brackish water quality and its effect on the growth of early cotton seedlings, while the effects of magnetized water with different water quality on the physiological growth characteristics, yield, and quality of cotton at the later growth stage need to be further studied.

**Acknowledgements.** This study was funded by the National Natural Science Foundation of China (41830754, 51239009 and 41907010), Basic Research Plan of Natural Science of Shaanxi Province (2020JQ-616).

## REFERENCES

- [1] Aghamir, F., Bahrami, H. A., Malakouti, M. J., Eshghi, S. (2015): Magnetized water effects on seed germination and seedling growth of corn (*Zea mays*) under saline conditions. – American Journal of Life Sciences 3(2): 184-195.
- [2] Al-Ogaidi, A. A. M., Wayayok, A., Rowshon, M. K., Abdullah, A. F. (2017): The influence of magnetized water on soil water dynamics under drip irrigation systems. – Agricultural Water Management 180: 70-77.
- [3] Alavi, S. A., Ghehsareh, A. M., Soleymani, A., Panahpour, E., Mozafari, M. (2020): Peppermint (*Mentha piperita* L.) growth and biochemical properties affected by magnetized saline water. – Ecotoxicology and Environmental Safety 201: 110775.
- [4] Alfaidi, M. A., Al-Toukhy, A. A., Al-Zahrani, H. S., Howladar, M. M. (2017): Effect of irrigation by magnetized sea water on guinea grass (*Panicum maximum*) leaf content of chlorophyll a, b, carotenoids, Pigments, protein & proline. – Advances in Environmental Biology 11(1): 73-84.
- [5] Aliverdi, A., Parsa, M., Hammami, H. (2015): Increased soybean-rhizobium symbiosis by magnetically treated water. – Biological Agriculture & Horticulture 31(3): 167-176.
- [6] Boe, A. A., Salunkhe, D. K. (1963): Effects of magnetic fields on tomato ripening. – Nature 199(4888): 91-92.
- [7] Castillo, G., Flores-Enríquez, V., Márquez-Guzmán, J., Núñez-Farfán, J., Oyama, K., Collazo-Ortega, M. (2017): Coping with stressful environments: An experimental study of seed germination and seedling survival of Mexican riverweeds under natural conditions. –

- Aquatic Botany 138: 24-28.
- [8] Chen, W. L., Jin, M. G., Ferré, T. P. A., Liu, Y. F., Huang, J. O., Xian, Y. (2020): Soil conditions affect cotton root distribution and cotton yield under mulched drip irrigation. – Field Crops Research 249: 107743.
- [9] Dziedzic, E., Bieniasz, M., Kowalczyk, B. (2019): Morphological and physiological features of sweet cherry floral organ affecting the potential fruit crop in relation to the rootstock. – Scientia Horticulturae 251: 127-135.
- [10] Faulkner, P. C., Hala, D., Rahman, M. S., Petersen, L. H. (2019): Short-term exposure to 12‰ brackish water has significant effects on the endocrine physiology of juvenile American alligator (*Alligator mississippiensis*). – Comparative Biochemistry and Physiology Part A: Molecular & Integrative Physiology 236: 110531.
- [11] Fu, Q. L., Liu, C., Ding, N. F., Lin, Y. C., Guo, B. (2010): Ameliorative effects of inoculation with the plant growth-promoting rhizobacterium *Pseudomonas* sp. DW1 on growth of eggplant (*Solanum melongena* L.) seedlings under salt stress. – Agricultural Water Management 97(12): 1994-2000.
- [12] Ghanati, F., Mohamadalkhani, S., Soleimani, M., Afzalzadeh, R., Hajnorouzi, A. (2015): Change of growth pattern, metabolism, and quality and quantity of maize plants after irrigation with magnetically treated water. – Electromagnetic Biology and Medicine 34(3): 211-215.
- [13] Hadi, S. M. S., Ahmed, M. Z., Hameed, A., Khan, M. A., Gul, B. (2018): Seed germination and seedling growth responses of toothbrush tree (*Salvadora persica* Linn.) to different interacting abiotic stresses. – Flora 243: 45-52.
- [14] Hasan, M. M., Alharby, H. F., Hajar, A. S., Hakeem, K. R. (2017): Leaf gas exchange, Fv/Fm ratio, ion content and growth conditions of the two Moringa species under magnetic water treatment. – Pakistan Journal of Botany 49(3): 921-928.
- [15] Hefner, M., Labouriau, R., Nørremark, M., Kristensen, H. L. (2019): Controlled traffic farming increased crop yield, root growth, and nitrogen supply at two organic vegetable farms. – Soil and Tillage Research 191: 117-130.
- [16] Honarparvar, S., Zhang, X., Chen, T., Na, C., Reible, D. (2019): Modeling technologies for desalination of brackish water-toward a sustainable water supply. – Current Opinion in Chemical Engineering 26: 104-111.
- [17] Hozayn, M. M., Salim, M. A., El-Monem, A., Amany, A., El-Mahdy, A. A. (2019): Effect of magnetic brackish-water treatments on morphology, anatomy and yield productivity of wheat (*Triticum Aestivum*). – Alexandria Science Exchange Journal 40: 604-617.
- [18] Huang, M. Y., Zhang, Z. Y., Zhu, C. L., Zhai, Y. M., Lu, P. R. (2019): Effect of biochar on sweet corn and soil salinity under conjunctive irrigation with brackish water in coastal saline soil. – Scientia Horticulturae 250: 405-413.
- [19] Huuskonen, H., Lindbohm, M. L., Juutilainen, J. (1998): Teratogenic and reproductive effects of low-frequency magnetic fields. – Mutation Research/Reviews in Mutation Research 410(2): 167-183.
- [20] Kulmala, L., Pumpanen, J., Kolari, P., Dengel, S., Berninger, F., Köster, K., Matkala, L., Vanhatalo, A., Vesala, T., Bäck, J. (2019): Inter- and intra-annual dynamics of photosynthesis differ between forest floor vegetation and tree canopy in a subarctic Scots pine stand. – Agricultural and Forest Meteorology 271: 1-11.
- [21] Li, M., Du, Y. J., Zhang, F. C., Bai, Y. G., Fan, J. Q., Zhang, J. H., Chen, S. M. (2019): Simulation of cotton growth and soil water content under film-mulched drip irrigation using modified CSM-CROPGRO-cotton model. – Agricultural Water Management 218: 124-138.
- [22] Liang, S. M., Ren, C., Wang, P. J., Wang, X. T., Li, Y. S., Xu, F. H., Wang, Y., Dai, Y. Q., Zhang, L., Li, X. P., Zhan, K., Yang, Q. F., Sui, Q. J. (2018): Improvements of emergence and tuber yield of potato in a seasonal spring arid region using plastic film mulching only on the ridge. – Field Crops Research 223: 57-65.
- [23] Liang, J. P., He, Z. J., Shi, W. J. (2020): Cotton/mung bean intercropping improves crop

- productivity, water use efficiency, nitrogen uptake, and economic benefits in the arid area of Northwest China. – *Agricultural Water Management* 240: 106277.
- [24] Liu, F. L., Andersen, M. N., Jensen, C. R. (2009): Capability of the ‘Ball-Berry’ model for predicting stomatal conductance and water use efficiency of potato leaves under different irrigation regimes. – *Scientia Horticulturae* 122(3): 346-354.
- [25] Liu, X. M., Ma, F. Y., Zhu, H., Ma, X. S., Guo, J. Y., Wan, X., Wang, L., Wang, H. T., Wang, Y. P. (2017): Effects of magnetized water treatment on growth characteristics and ion absorption, transportation, and distribution in *Populus × euramericana* ‘Neva’ under NaCl stress. – *Canadian Journal of Forest Research* 47(6): 828-838.
- [26] Liu, X. M., Wang, L., Cui, H. R., Zhu, H., Bi, S. S., Zhang, Z. H., Meng, S. Y., Song, C. D., Wang, H. T., Ma, F. Y. (2019a): Effects of magnetic treatment on the ascorbate–glutathione cycle and endogenous hormone levels in *Populus × euramericana* ‘Neva’ under cadmium stress. – *Canadian Journal of Forest Research* 49(9): 1147-1158.
- [27] Liu, X. M., Zhu, H., Meng, S. Y., Bi, S. S., Zhang, Y., Wang, H. T., Song, C. D., Ma, F. Y. (2019b): The effects of magnetic treatment of irrigation water on seedling growth, photosynthetic capacity and nutrient contents of *Populus × euramericana* ‘Neva’ under NaCl stress. – *Acta Physiol Plant* 41(11): 1-13.
- [28] Liu, X. M., Wang, L., Wei, Y., Zhang, Z. H., Zhu, H., Kong, L. G., Meng, S. Y., Song, C. D., Wang, H. T., Ma, F. Y. (2020): Irrigation with magnetically treated saline water influences the growth and photosynthetic capability of *Vitis vinifera* L. seedlings. – *Scientia Horticulturae* 262: 109056.
- [29] Luo, Y., Liang, J., Zeng, G. M., Li, X. D., Chen, M., Jiang, L. B., Xing, W. L., Tang, N., Fang, Y. L., Chen, X. W. (2019): Evaluation of tetracycline phytotoxicity by seed germination stage and radicle elongation stage tests: A comparison of two typical methods for analysis. – *Environmental Pollution* 251: 257-263.
- [30] Massah, J., Dousti, A., Khazaei, J., Vaezzadeh, M. (2019): Effects of water magnetic treatment on seed germination and seedling growth of wheat. – *Journal of Plant Nutrition* 42(11-12): 1283-1289.
- [31] Mollahosseini, A., Abdelrasoul, A. (2019): Recent advances in thin film composites membranes for brackish groundwater treatment with critical focus on Saskatchewan water sources. – *Journal of Environmental Sciences* 81: 181-194.
- [32] Mosse, K. P., Verheyen, T. V., Cruickshank, A. J., Patti, A. F., Cavagnaro, T. R. (2013): Soluble organic components of winery wastewater and implications for reuse. – *Agricultural water management* 120: 5-10.
- [33] Moussa, H. R. (2011): The impact of magnetic water application for improving common bean (*Phaseolus vulgaris* L.) production. – *New York Science Journal* 4(6): 15-20.
- [34] Murshed, S. B., Kaluarachchi, J. J. (2018): Scarcity of fresh water resources in the Ganges Delta of Bangladesh. – *Water Security* 4: 8-18.
- [35] Qiu, N. W., Tan, Y. H., Shen, X., Han, R., Lin, Y., Ma, Z. Q. (2011): Biological effects of magnetized water on seed germination, seedling growth and physiological characteristics of wheat. – *Plant Physiology Communications* 47(8): 803-810.
- [36] Ramírez-Pérez, L. J., Morales-Díaz, A. B., Benavides-Mendoza, A., de-Alba-Romenus, K., González-Morales, S., Juárez-Maldonado, A. (2018): Dynamic modeling of cucumber crop growth and uptake of N, P and K under greenhouse conditions. – *Scientia Horticulturae* 234: 250-260.
- [37] Richards, R. A., Cavanagh, C. R., Riffkin, P. (2019): Selection for erect canopy architecture can increase yield and biomass of spring wheat. – *Field Crops Research* 244: 107649.
- [38] Sappington, E. N., Rifai, H. S. (2018): Low-frequency electromagnetic treatment of oilfield produced water for reuse in agriculture: effect on water quality, germination, and plant growth. – *Environmental Science and Pollution Research* 25: 34380-34391.
- [39] Sayed, H. E., Sayed, A. E. (2014): Impact of magnetic water irrigation for improve the growth, chemical composition and yield production of broad bean (*Vicia faba* L.) plant. – *Journal of Experimental Agriculture International* 4: 476-496.

- [40] Shrestha, N. K., Du, X., Wang, J. (2017): Assessing climate change impacts on fresh water resources of the Athabasca River Basin, Canada. – *Science of the Total Environment* 601: 425-440.
- [41] Surendran, U., Sandeep, O., Joseph, E. J. (2016): The impacts of magnetic treatment of irrigation water on plant, water and soil characteristics. – *Agricultural Water Management* 178: 21-29.
- [42] Tan, S., Wang, Q. J., Xu, D., Zhang, J. H., Shan, Y. Y. (2017): Evaluating effects of four controlling methods in bare strips on soil temperature, water, and salt accumulation under film-mulched drip irrigation. – *Field Crops Research* 214: 350-358.
- [43] Tian, F. Q., Yang, P. J., Hu, H. C., Liu, H. (2017): Energy balance and canopy conductance for a cotton field under film mulched drip irrigation in an arid region of northwestern China. – *Agricultural Water Management* 179: 110-121.
- [44] ul Haq, Z., Iqbal, M., Jamil, Y., Anwar, H., Younis, A., Arif, M., Fareed, M. Z., Hussain, F. (2016): Magnetically treated water irrigation effect on turnip seed germination, seedling growth and enzymatic activities. – *Information Processing in Agriculture* 3: 99-106.
- [45] Velmala, S. M., Vuorinen, I., Uimari, A., Piri, T., Pennanen, T. (2018): Ectomycorrhizal fungi increase the vitality of Norway spruce seedlings under the pressure of *Heterobasidion* root rot in vitro but may increase susceptibility to foliar necrotrophs. – *Fungal biology* 122(2-3): 101-109.
- [46] Wang, P. C., Mo, B. T., Long, Z. F., Fan, S. Q., Wang, H. H., Wang, L. B. (2016): Factors affecting seed germination and emergence of *Sophora davidii*. – *Industrial Crops and Products* 87: 261-265.
- [47] Wang, X. X., Xu, Z. S., Gou, X. J. (2020): Allocation of fresh water recourses in China with nested probabilistic-numerical linguistic information in multi-objective optimization. – *Knowledge-Based Systems* 188: 105014.
- [48] Yang, Z. S., Quna, Q. M., Wu, T. D. (2013): Difference studies for the stomatal conductance and the leaf Chlorophyll concentration in different positions of *Lilium regale* leaves. – *IERI Procedia* 5: 284-290.
- [49] Yang, P. J., Hu, H. C., Tian, F. Q., Zhang, Z., Dai, C. (2016): Crop coefficient for cotton under plastic mulch and drip irrigation based on eddy covariance observation in an arid area of northwestern China. – *Agricultural Water Management* 171: 21-30.
- [50] Yue, S. D., Zhou, Y., Zhang, Y., Xu, S. C., Gu, R. T., Xu, S., Zhang, X. M., Zhao, P. (2019): Effects of salinity and temperature on seed germination and seedling establishment in the endangered seagrass *Zostera japonica* Asch. & Graebn. in northern China. – *Marine pollution bulletin* 146: 848-856.
- [51] Yusuf, K. O., Ogunlela, A. O. (2015): Impact of magnetic treatment of irrigation water on the growth and yield of tomato. – *Notulae Scientia Biologicae* 7: 345-348.
- [52] Zhong, W. W., Ji, C., Li, H. Y., Hou, J. W., Chen, V. (2018): Fouling mitigation in submerged VMD for the treatment of brackish groundwater concentrates with transverse vibration and crystallizer. – *Desalination* 426: 32-41.
- [53] Zhou, B., Zhou, H. X., Puig-Bargués, J., Li, Y. K. (2019): Using an anti-clogging relative index (CRI) to assess emitters rapidly for drip irrigation systems with multiple low-quality water sources. – *Agricultural Water Management* 221: 270-278.
- [54] Zlotopolski, V. (2017): Magnetic treatment reduces water usage in irrigation without negatively impacting yield, photosynthesis and nutrient uptake in lettuce. – *International Journal of Applied Agricultural Sciences* 3(5): 117-122.



## ARBUSCULAR MYCORRHIZAL FUNGI ALLEVIATE THE TOXICITY OF CADMIUM INTERACTION AFFECTING THE GROWTH OF RYEGRASS (*LOLIUM PERENNE* L.)

SUN, M. L.<sup>1</sup> – LI, T.<sup>1</sup> – LI, D. M.<sup>1</sup> – ZHAO, Y. L.<sup>1</sup> – GAO, F. M.<sup>1</sup> – SUN, L. F.<sup>1\*</sup> – SUN, G. Y.<sup>2,3</sup>

<sup>1</sup>*Crop Resources Institute of Heilongjiang Academy of Agricultural Sciences s, Harbin 150040, China*

<sup>2</sup>*College of Life Science, Northeast Forest University, Harbin 150040, China*

<sup>3</sup>*Key Laboratory of Saline-alkali Vegetation Ecology Restoration, Ministry of Education, Northeast Forestry University, Harbin 150040, China*

\*Corresponding author

e-mail: [sunlianfa@aliyun.com](mailto:sunlianfa@aliyun.com); phone: 0451 8665 1186  
address: No.368 Xuefu Road, Harbin, Heilongjiang 150040, China

(Received 6<sup>th</sup> Oct 2020; accepted 21<sup>st</sup> Dec 2020)

**Abstract.** A pot experiment was conducted to examine the effects of *Glomus mosseae* on some growth and physiological parameters, and cadmium (Cd) amounts in ryegrass (*Lolium perenne* L.) plants under the toxic levels of Cd. The experiment was carried out with two treatments (*G. mosseae* inoculation and non-inoculation), each having four Cd concentrations (0, 30, 90 and 180 mg Cd kg<sup>-1</sup> soil). The results showed that mycorrhizal infection rate of *G. mosseae* was still as high as 43% under 180 mg kg<sup>-1</sup> Cd concentration, indicating that *G. mosseae* colonized plants were tolerant to Cd stress. In non-inoculated and inoculated plants, by increasing Cd concentration in the soil, growth parameters, root activity, growth index, biomass, N and P content in plant and photosynthetic characteristic were reduced. Root activity, growth index, biomass, N and P content, photosynthetic physiology, superoxide dismutase (SOD) and catalase (CAT) contents of *G. mosseae* inoculated plants were increased compared to non-inoculated plants, whereas malondialdehyde (MDA) content decreased to a certain extent. In conclusion, inoculation of *G. mosseae* enhanced the resistance and tolerance of ryegrass to Cd stress, reduced the damage of harmful substances to cells, and promoted its growth.

**Keywords:** *Glomus mosseae*, cadmium stress, plant growth, nutrition accumulation, photosynthetic characteristics

### Introduction

In the natural ecosystem, 80% of all terrestrial plant species form symbiotic associations between arbuscular mycorrhiza fungi (AMF) and their roots (Smith and Read, 1997). The AMF obtain carbohydrates from the host plants. In return, the fungi benefit their host plants principally by enriching nutrition uptake, enhancing resistance to pathogens (Poza et al., 2002), improving tolerance to drought stress (Augé et al., 1994) and improving soil structure (Rillig and Steinberg, 2002). In addition, AM symbiosis has been shown to take an active part in plant resistance to heavy metal contamination including Zn, Pb, Cu, Cr and Cd (Shetty et al., 1995; Díaz et al., 1996; Davies et al., 2001; Chen et al., 2007; Shahabivand et al., 2012). For example, Vodnik (2008) demonstrated that AM symbiosis can prevent plant from absorbing heavy metal by secreting some organic compounds in soils to chelate metal ions. Gonzalez-Chavez (2002) have investigated that AM fungi colonized in *H. lanatus* carried out their role by aiding the host to fix toxic metals within the rhizospheric zone, thereby preventing the uptake of toxic metals into the plant (Gonzalez-Chavez et al., 2010).

In recent years, heavy metals released to soils bring about irreversible soil degradation and hence severely limit vegetation establishment, which mainly resulted from human activities (Shukurov et al., 2005; Rajkumar et al., 2012). Cadmium (Cd) is non-essential heavy metal element for plant growth with phytotoxicity even at very low concentration- $0.5 \text{ mg kg}^{-1}$  (Yong et al., 2009). Cd enters the aquatic environment from natural (weathering of rocks) as well as anthropogenic sources (industrial effluents, agricultural run offs) (Schützendübel et al., 2002). The presence of an excessive amount of Cd causes an inhibition of enzyme activities, water imbalance and alterations of membrane permeability in plants (Yılmaz and Parlak, 2011). It exerts an adverse effect on seed germination (Peralta et al., 2001), morphology, growth and the photosynthetic processes in plants, even leading to plant death (Zorrig et al., 2013; Hassan and Mansoor, 2014; Asgher et al., 2015). Improper discharge of Cd into environment has resulted in severe contaminations, and subsequently threatened the environmental quality and human health over the long-term (Kirkham, 2006; Ali et al., 2013).

Mycorrhizal fungi have been found to influence Cd uptake and accumulation in plants with changes in its immobilization and mobilization in Cd-polluted soils (Chen et al., 2004b). Investigations indicated that many plant species, such as *Fragaria vesca*, *Viola calaminaria*, *Veronica rechingeri*, *Thymus polytrichus* and *Lolium perenne*, growing well at natural heavy metal polluted sites and all of them were colonized by AMF (Turnau et al., 2001; Whitfield et al., 2004; Zarei et al., 2008a; Alguacil et al., 2011). Ryegrass (*Lolium perenne* L.) was used as a model plant because of its rapid growth, tolerance to various environments, soil types and its common use in phytoremediation studies (Arienzo et al., 2004; Meng et al., 2011). The objectives of our experiment were to investigate the efficiency of AMF application into different Cd-added soils (0, 30, 90 and  $180 \text{ mg Cd kg}^{-1}$  soil) for alleviating the toxicity of Cd to *L. perenne*. Mainly focused on the effects of AMF on plant growth, nutrition accumulation, photosynthetic characteristics, and antioxidant activities of *L. perenne* grown in different Cd-added soils. The results of this study will provide new insights into the mechanism of Cd phytotoxicity alleviation in associate with AM inoculation.

## Methods and materials

### *Experimental design*

The experiment was designed as a  $4 \times 2$  factorial treatments of Cd level and AMF inoculation organized in a completely randomized design with three replications. Treatments consisted of full factorial combinations of four Cd levels (0, 30, 90 and  $180 \text{ mg kg}^{-1}$ ) applied as  $3\text{CdSO}_4 \cdot 8\text{H}_2\text{O}$ , two AMF treatments (inoculated and non-inoculated) in soils planted with ryegrass under greenhouse conditions. The average day and night temperatures were maintained at  $25^\circ\text{C}$  and  $23^\circ\text{C}$ , respectively, and a 12 h photoperiod with a light intensity  $400 \mu\text{mol m}^{-2} \text{ s}^{-1}$ . The relative humidity was 75%.

### *Soil preparation*

A sandy loam soil from the 20-30 cm layer was collected from in forestry station, Northeast Forestry University of Heilongjiang province (latitude,  $126^\circ 63' \text{N}$ ; longitude,  $45^\circ 72' \text{E}$ , northeast China). It was air-dried, sieved (2 mm mesh) and stored at  $25^\circ\text{C}$  before use. The soil was steam-sterilized ( $121^\circ\text{C}$  for 2 h) by autoclaving to eliminate indigenous mycorrhizal propagules and pathogens, and more specifically to eliminate the influence of

the AM fungal species used. The soils were artificially contaminated with  $3\text{CdSO}_4 \cdot 8\text{H}_2\text{O}$  at the following rates: 0 (control), 30, 90 and  $180 \text{ mg Cd kg}^{-1}$ . Deionized water was added to the soils to achieve moisture content of 60-70% of field capacity. To ensure even distribution of Cd, soils were thoroughly mixed while adding  $3\text{CdSO}_4 \cdot 8\text{H}_2\text{O}$  and water. The soils were incubated at room temperature (about  $20 \pm 5^\circ\text{C}$ ) for one month to achieve an equilibrium condition, and to lower the effects of soil preparation and disturbance.

### ***Mycorrhiza inoculum and host plants***

The AM fungal inoculum (*G. mosseae*) was propagated using *Trifolium pretense* L. as host plants, and the inoculum was the mixture of spores, hyphae, colonized root fragments and substrates. Approximately 50 g of each AM fungal inoculum was added to 1 kg sterilized soils. Seeds of ryegrass (*Lolium perenne* L.) were surface sterilized in a 10% v/v solution of  $\text{H}_2\text{O}_2$  for 10 min, washed in sterilized distilled water and were germinated on wet filter paper in Petri dishes. Two days later, the ryegrass seedlings were selected for uniformity and transplanted into plastic pots. 20 seedlings were transplanted into each pot (12 cm $\times$ 15 cm). Seedlings in pots were irrigated every second day until water drained from the bottom of the pot. After 2 weeks, the cultivated seedlings reached a height of 10 cm, they were thinned a density of 10 plants pot $^{-1}$  and supplied with 1/2 Hoagland's solution every week.

### ***Estimation of mycorrhizal infection rate***

The mycorrhizal infection rate was determined by trypanblue staining (McGonigle et al., 1999). After dyeing, the mycorrhizal infection rate was determined by the modified cross method under the microscope.

$$\text{Mycorrhizal infection rate (\%)} = \frac{\text{the number of root segments forming clumps}}{\text{the number of measured root segments}} \times 100 \quad (\text{Eq.1})$$

### ***Estimation of root vigor***

Roots were sampled from each treatment (three replicates) were taken. The mixture of roots and soil was placed in a polythene bag and washed with tap water. The roots were carefully refrigerated for further testing. The root vigor was determined using the TTC method (Zhang, 1990).

### ***Estimation of gas exchange***

Net photosynthesis ( $P_n$ ), stomatal conductance ( $G_s$ ), transpiration rate ( $T_r$ ) and intercellular  $\text{CO}_2$  concentration ( $C_i$ ) were measured on expanded leaves. Photosynthetic rate measured at  $400 \mu\text{mol m}^{-2} \text{s}^{-1} \text{CO}_2$  under  $800 \mu\text{mol m}^{-2} \text{s}^{-1} \text{PFDF}$  was used to calculate photorespiration with a portable photosynthetic system (CIRAS-1, PP systems, UK).

### ***Antioxidant enzymes assays***

SOD activity was measured according to the method of Wang et al. (1990). Fresh tissues (0.2 g) were ground to a fine powder in liquid  $\text{N}_2$  then homogenized in 2 mL of phosphate buffer (pH 7.8). The reaction mixture was comprised of 50 mM phosphate buffer (pH 7.8), 130 mM methionine, 750  $\mu\text{M}$  nitro-bluetetrazolium, 100  $\mu\text{M}$  EDTA-

Na<sub>2</sub>, 100 μM EDTA, 100 μM riboflavin, and 0.1 ml of enzyme extract in a final volume of 4 ml. The reaction mixture was incubated for 30 min under 4000 Lx, and absorbance was determined at 560 nm. Catalase (CAT) activity was measured at 25°C previously according to the method of Paglia and Valentine (1987) that used hydrogen peroxide as substrate and one unit of catalase was defined as the rate constant of the first order reaction (k).

### ***Measurements of lipid peroxidation***

MDA content was measured following the method of Zhang et al. (1990). Fresh tissues (0.2 g) were ground to a fine powder in liquid N<sub>2</sub> then homogenized in 2 mL of 10% trichloroacetic acid (TCA). The mixture was centrifuged at 10,000 r/min for 10 min. For every 2 mL of the supernatant, 2 mL of 0.6% 2-thiobarbituric acid (TBA) was mixed. The mixture was incubated at 100°C for 15 min and then transferred into an ice bath to stop the reaction. The tubes were centrifuged at 10,000 r/min for 10 min and the absorbance of the resulting supernatant was measured at 450, 532 and 600 nm. The concentration of MDA (IM) in the solution was estimated according to the following formula:

$$MDA \text{ concentration} = 6.45(A_{532} - A_{600}) - 0.56A_{450} \quad (\text{Eq.2})$$

where A<sub>450</sub>, A<sub>532</sub> and A<sub>600</sub> were represent wavelength measured at 450, 532 and 600 nm.

### ***Measurements of plant growth and biomass***

The middle growth stage was 45 days after sowing. Fresh plants were collected from each pot after plant establishment at the middle growth stage. The 10 plants were collected and rinsed twice with distilled water, and subsequently, the growth parameters (plant height, root length, root/shoot ratio, aboveground, underground, and total biomass per plant) were measured. Plant height was determined with meter rule (cm) from the base of the plant (above the ground level) to the apical region of the leaf. The root length (the longest root) was also obtained using meter rule (cm). Aboveground, underground, and total biomass were weighted after drying the plant samples in a hot air oven at 60°C using a constant weight. Root/shoot ratio = Underground biomass/aboveground biomass.

### ***Statistical analysis***

Statistical analysis was performed using the SPSS 17.0 program. The data were analyzed by analysis of variance (ANOVA), where means and standard derivations were calculated for the three replicates. To detect the statistical significance of differences ( $P < 0.05$ ) among Cd levels, the Tukey test was performed. T-test was performed to detect the statistical significance of differences between non-inoculated and inoculated with AM fungi treatments.

## Results

### *Mycorrhizal infection rates*

Mycorrhizal infection rate of *G. mosseae* to the root of ryegrass was observed in different Cd-contaminated soils (Fig. 1). The rates of mycorrhiza infection were generally reduced (from 69% to 43%) in the presence of Cd ( $P < 0.05$ ). The rates of mycorrhiza infection in 30, 90 and 180 mg Cd kg<sup>-1</sup> soils were significantly decreased by 16.14%, 24.93% and 58.45%, respectively, compared with Cd-uncontaminated soil.

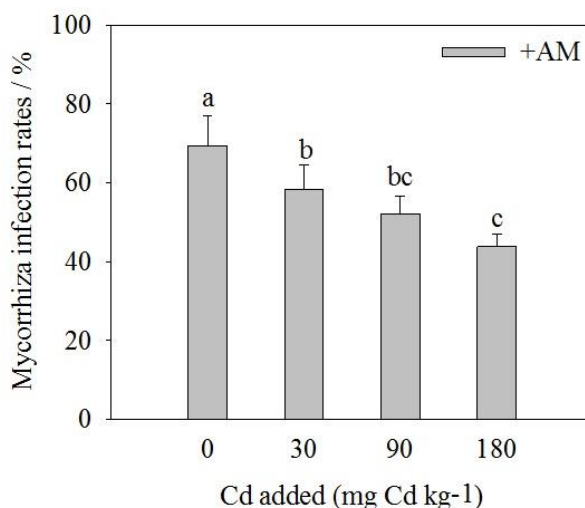


**Figure 1.** Mycorrhiza infection rates of *L. perenne* inoculated with *G. mosseae* with increasing Cd level. Abbreviations: +AM, inoculated with AMF. Values shown are averages, calculated using 3 replicates for each treatment ( $\pm$  s.d. of the mean). Different letters indicate significant differences at  $P < 0.05$

### *Root vigor*

The two-way interaction between Cd and AMF factors was significant for root vigor ( $P < 0.05$ ) (Fig. 2). There were significant decreases in root vigor for the plants exposed to Cd compared with Cd-uncontaminated plants. Root vigor was negatively affected by Cd, decreasing with rising the Cd level in both *G. mosseae*-inoculated and without inoculated plants, but without significant when added at 30 and 90 mg Cd kg<sup>-1</sup> in *G. mosseae*-inoculated soils and at 90 and 180 mg Cd kg<sup>-1</sup> in without inoculated soils, respectively. *G. mosseae* inoculation significantly increased root vigor compared with non-inoculated soil at 0, 90 and 180 Cd kg<sup>-1</sup> levels. Compared to non-inoculated plants, root vigor increased by 43.27%, 70.56% and 55.33% for *G. mosseae*-inoculated plants added with 0, 90 and 180 mg Cd kg<sup>-1</sup>, respectively.

### *Photosynthetic characteristic*

Net photosynthetic rate ( $P_n$ ), stomatal conductance ( $G_s$ ), transpiration rate ( $T_r$ ) and intercellular CO<sub>2</sub> concentration ( $C_i$ ) were presented in Table 1. The *G. mosseae* inoculation had higher  $T_r$  and  $P_n$  than non-inoculated treatments, indicating AMF alleviated Cd-induced photosynthetic inhibition of ryegrass leaves. At the highest Cd level,  $P_n$ ,  $G_s$ , and  $T_r$  of *G. mosseae* inoculated plants were increased by 54.91% ( $P < 0.05$ ), 37.79% ( $P < 0.05$ ) and 10.06% ( $P > 0.05$ ), respectively, in comparison to non-inoculated

plants. Photosynthetic characteristics of ryegrass were sensitive to Cd addition in non-inoculated plants. In general,  $P_n$  decreased with increasing Cd levels in non-inoculated plants. The decrease of  $G_s$  in Cd-contaminated plants was accompanied with those of  $T_r$ , but at different extents among treatments. On the contrary, the increase of  $C_i$  in 180 mg Cd kg<sup>-1</sup> treatment was of 8.98% ( $P>0.05$ ) if compared to the 90 mg Cd kg<sup>-1</sup> treatment.

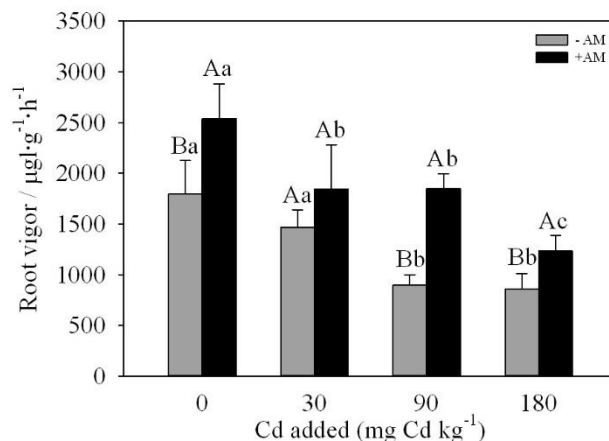


**Figure 2.** Root vigor of *L. perenne* inoculated with *G. mosseae* with increasing Cd level. Abbreviations: -AM, non-inoculated with arbuscular mycorrhizal fungi (AMF); +AM, inoculated with AMF. Values shown are averages, calculated using 3 replicates for each treatment ( $\pm$ s.d. of the mean). Different lowercase letters are significantly difference ( $P<0.05$ ) among Cd levels by the Tukey test. Different uppercase letters are significantly difference ( $P<0.05$ ) between non-inoculated and inoculated with AM fungi treatments by the t-test

**Table 1.** Gas exchange parameters of ryegrass leaves inoculated with *G. mosseae* with increasing Cd level

Treatment Cd added (mg kg <sup>-1</sup> )	AM fungi		Mean (Cd)	AM fungi		Mean (Cd)
	-AM	+AM		-AM	+AM	
	<b>Net photosynthetic rate (<math>\mu\text{mol m}^{-2} \text{s}^{-1}</math>)</b>			<b>Transpiration rate (<math>\mu\text{mol m}^{-2} \text{s}^{-1}</math>)</b>		
0	3.01A	3.44A	3.13 A	0.88A	1.17A	1.05 A
30	2.62AB	2.91A	2.67 A	0.87A	1.04AB	0.95 A
90	2.21AB	2.83A	2.42 A	0.80A	0.87B	0.82 A
180	1.73 bB	2.68 aA	2.11 A	0.74A	0.89B	0.76 A
Mean (AM fungi)	2.39 b	2.97 a		0.82 b	0.99 a	
	<b>Stomatal conductance (<math>\mu\text{mol m}^{-2} \text{s}^{-1}</math>)</b>			<b>Intercellular CO<sub>2</sub> concentration (<math>\mu\text{mol m}^{-2} \text{s}^{-1}</math>)</b>		
0	49.81 A	56.90A	55.35 A	280.7A	301.3A	291.00 A
30	40.12A	47.5AB	45.80 AB	262.8A	291.9A	277.35 A
90	36.39AB	38.12BC	39.26 AB	247.8A	281.8A	264.80 A
180	23.10 B	36.21C	30.15 B	265.9A	249.3A	257.60 A
Mean (AM fungi)	37.35 a	44.68 a		264.30 a	281.08 a	

Which each row, mean values (n=3) with the different lowercase letter are significantly difference ( $P<0.05$ ) among AM fungi treatments by the Tukey test. Within each column, mean values (n=3) with the different uppercase letter are significantly difference ( $P<0.05$ ) among Cd levels by the Tukey test

### Antioxidant activity

The enhanced SOD and CAT activities were observed for the plants exposed to Cd compared with the control (Fig. 3). SOD activity increased linearly with Cd addition levels, and no significant difference was found between Cd addition levels of 90 and 180 mg kg<sup>-1</sup> ( $P>0.05$ ). The maximum SOD activity was recorded at 180 mg Cd kg<sup>-1</sup> in both *G. mosseae*-inoculated and without inoculated plants (0.69 and 0.67 U mg<sup>-1</sup> FW<sup>-1</sup>, respectively). There was no significant difference in SOD activity between *G. mosseae*-inoculated and without inoculated plants under the same Cd concentration ( $P>0.05$ ). CAT activity also increased linearly with increasing Cd levels, whereas, a decline in CAT activity with an increase in 180 mg Cd kg<sup>-1</sup> level was observed.

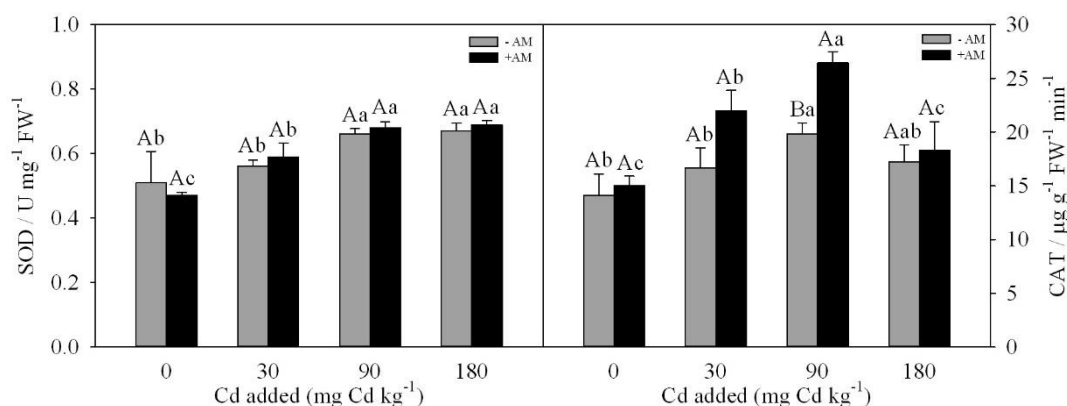


**Figure 3.** Antioxidative enzyme activities of *L. perenne* L. inoculated with *G. mosseae* with increasing Cd level. Abbreviations: -AM, non-inoculated with arbuscular mycorrhizal fungi (AMF); +AM, inoculated with AMF. Values shown are averages, calculated using 3 replicates for each treatment ( $\pm$ s.d. of the mean). Different lowercase letters are significantly difference ( $P<0.05$ ) among Cd levels by the Tukey test. Different uppercase letters are significantly difference ( $P<0.05$ ) between non-inoculated and inoculated with AM fungi treatments by the t-test

CAT activity of *G. mosseae*-inoculated and non-inoculated plants showed the same change trend, first increased and then decreased. But the increase range of inoculated was higher than that of non-inoculated plants. The CAT activity was different among different Cd pollution concentrations in both *G. mosseae*-inoculated and non-inoculated plants. There was no significant difference in CAT activity between inoculated and non-inoculated plants under 0 and 30 Cd kg<sup>-1</sup> concentration. CAT activity was the highest in both inoculated and non-inoculated plants under 90 Cd kg<sup>-1</sup> concentration, and the CAT activity of inoculated plants increased by 29.6% compared with that of non-inoculated plants at this concentration ( $P<0.05$ ). While the CAT activity of the inoculated and non-inoculated plants decreased under 120 Cd kg<sup>-1</sup> concentrations, but it was slightly higher than that of the control. There was no significant difference in CAT activity between *G. mosseae*-inoculated and without inoculated plants under 120 Cd kg<sup>-1</sup> concentration ( $P>0.05$ ).

### Lipid peroxidation

The effect of Cd and AMF on MDA content is shown in Fig. 4. There were significant increases in MDA content for the plants exposed to Cd compared with Cd-

uncontaminated plants ( $P < 0.05$ ). Whether inoculated or not, MDA content increased linearly with increasing Cd levels. No-inoculated plants had significantly higher MDA content than plants inoculated with *G. mosseae* at all Cd levels ( $P < 0.05$ ). Thus, decreased MDA indicated that AMF relieved the damage of Cd to cell membrane.

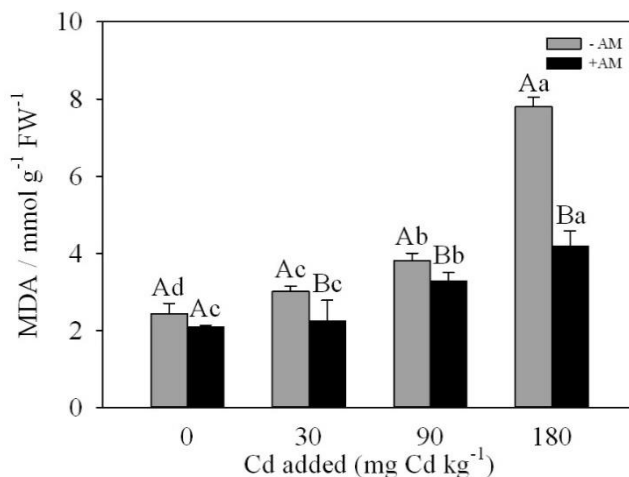


**Figure 4.** MDA content of *L. perenne* L. inoculated with *G. mosseae* with increasing Cd level. Abbreviations: -AM, non-inoculated with arbuscular mycorrhizal fungi (AMF); +AM, inoculated with AMF. Values shown are averages, calculated using 3 replicates for each treatment ( $\pm$ s.d. of the mean). Different lowercase letters are significantly difference ( $P < 0.05$ ) among Cd levels by the Tukey test. Different uppercase letters are significantly difference ( $P < 0.05$ ) between non-inoculated and inoculated with AM fungi treatments by the t-test

### Plant growth and biomass

Results describing plant height, root length, root/shoot ratio, aboveground biomass, underground biomass and total biomass for different treatments are presented in *Table 2*. Plant growth was influenced by Cd level. Whether *G. mosseae* inoculated or not, decreasing plant height, root length, and biomass (underground and aboveground) were observed with in high Cd levels (*Table 2*). Obviously, high Cd levels inhibited ryegrass growth. When compared to Cd-uncontaminated plants, Cd addition decreased plant height, root length, aboveground biomass and underground biomass by 30.67%, 36.51%, 19.31% and 30.46% for *G. mosseae* inoculated treatments and 18.72%, 45.58%, 18.23% and 29.98% for non-inoculated treatments at Cd addition levels of 180 mg kg<sup>-1</sup>, respectively. At the low Cd level (30 mg kg<sup>-1</sup>), Cd stress had no significant effect on aboveground traits (plant height and aboveground biomass), but significant decrease underground traits (root length and underground biomass). Therefore, low soil Cd level increased the root/shoot ratio of ryegrass. The application of AMF alleviated the inhibitory effect of Cd on ryegrass growth traits (*Table 2*). At the highest Cd level, plant height, root length, aboveground, underground and total biomasses of *G. mosseae* inoculated plants were increased by 16.46% ( $P > 0.05$ ), 18.60% ( $P < 0.05$ ), 23.33% ( $P < 0.05$ ), 22.86% ( $P < 0.05$ ) and 24% ( $P < 0.05$ ), respectively as compared to the control plants. In generally, inoculation with *G. mosseae* had no effect on root/shoot ratio in different Cd levels.



**Table 2.** Growth characteristics of *L. perenne* inoculated with *G. mosseae* with increasing Cd level

Treatment Cd added (mg kg <sup>-1</sup> )	AM fungi		Mean (Cd)	AM fungi		Mean (Cd)
	-AM	+AM		-AM	+AM	
	<b>Plant height (cm)</b>			<b>Root length (cm)</b>		
0	20.89 AB	25.76 A	23.33	14.67 A	16.87 A	15.77
30	21.67 A	27.11 A	24.39	12.37 B	13.89 B	13.13
90	20.03 AB	24.23 A	22.13	12.02 B	12.55 C	12.29
180	16.98 B	17.86 B	17.42	7.69 C	10.71 D	9.2
Mean (AM fungi)	19.89b	23.74a		11.69	13.51	
	<b>Root /shoot ratio</b>			<b>Aboveground biomass (g)</b>		
0	0.817 B	0.832 B	0.825	0.0417 A	0.0523 A	0.0470
30	0.868 A	0.908 A	0.888	0.0382 AB	0.0522 A	0.0452
90	0.820 B	0.841 B	0.831	0.0376 AB	0.0461 B	0.0419
180	0.720 C	0.725 C	0.723	0.0341 B	0.0422 B	0.0382
Mean (AM fungi)	0.806	0.827		0.0379	0.0482	
	<b>Underground biomass (g)</b>			<b>Total biomass (g)</b>		
0	0.0348 A	0.0447 B	0.0398	0.0740 A	0.0970 AB	0.0855
30	0.0342 A	0.0510 A	0.0426	0.0724 A	0.1032 A	0.0878
90	0.031 A	0.0388 C	0.0349	0.0686 AB	0.0849 BC	0.0768
180	0.0242 B	0.0313 D	0.0278	0.0600 B	0.0735 C	0.0668
Mean (AM fungi)	0.0311	0.0414		0.0688	0.0897	

Which each row, mean values (n=10) with the different lowercase letter are significantly difference (P<0.05) among AM fungi treatments by the Tukey test. Within each column, mean values (n=3) with the different uppercase letter are significantly difference (P<0.05) among Cd levels by the Tukey test

### Plant N and P uptake

Plant N and P uptake in ryegrass plants decreased with Cd addition, especially in non-inoculated plants (Table 3). In soil added with 30 mg Cd kg<sup>-1</sup>, non-inoculated controls had the highest P content in leaves. However, Cd stress had no significant influence on P content in leaves colonized by *G. mosseae*. In all Cd treatments, the *G. mosseae* inoculation had profound effects on N and P accumulation in leaf and root. Overall, *G. mosseae* inoculation increased N and P contents in leaves and roots. In soil added with 30 and 180 mg Cd kg<sup>-1</sup>, N content of roots colonized by *G. mosseae* was significantly higher than that of without inoculation (P<0.05). However, N content of leaves colonized by *G. mosseae* were significantly higher than that of without inoculation in low Cd level (30 and 90 mg Cd kg<sup>-1</sup>) (P<0.05). P content in leaves and roots of *G. mosseae*-inoculated plants was significantly higher than the non-inoculated plants at the same Cd addition level except 90 mg Cd kg<sup>-1</sup> level treatment (P<0.05). Therefore, not all the N and P accumulation in both leaf and root of *G. mosseae* inoculated plants were significantly higher than those of non-inoculated controls in Cd-contaminated soil.

**Table 3.** N and P concentrations of ryegrass leave and root inoculated with *G. mosseae* with increasing Cd level

Treatment Cd added (mg kg <sup>-1</sup> )	AM fungi		Mean (Cd)	AM fungi		Mean (Cd)
	-AM	+AM		-AM	+AM	
	<b>Root N content (g kg<sup>-1</sup>)</b>			<b>Leave N content (g kg<sup>-1</sup>)</b>		
0	0.60 aA	0.63 aA	0.62 A	1.15 aA	1.26 aA	1.21 A
30	0.57 bA	0.69 aA	0.63 A	0.96 bAB	1.22 aA	1.09 A
90	0.51 aB	0.52 aB	0.52 B	0.81 bB	0.88 aC	0.85 B
180	0.32 bC	0.49 aB	0.41 C	0.80 aB	0.76 aD	0.78 C
Mean (AM fungi)	0.50 b	0.58 a		0.93 b	1.03 a	
	<b>Root P content (g kg<sup>-1</sup>)</b>			<b>Leave P content (g kg<sup>-1</sup>)</b>		
0	3.29 bA	4.11 aA	3.70 A	3.22 bB	4.31 aA	3.77 B
30	2.48 aB	2.45 aB	2.47 B	4.25 aA	4.20 aA	4.23 A
90	1.80 bC	2.31 aB	2.06 C	3.11 bBC	4.22 aA	3.67 B
180	1.75 bC	2.12 aBC	1.94 C	3.26 bB	4.26 aA	3.76 B
Mean (AM fungi)	2.33 b	2.75 a		3.46 b	4.25 a	

Which each row, mean values (n=3) with the different lowercase letter are significantly difference (P<0.05) among AM fungi treatments by the Tukey test. Within each column, mean values (n=3) with the different uppercase letter are significantly difference (P<0.05) among Cd levels by the Tukey test. – AM=non-mycorrhizal, +AM= with mycorrhizal

## Discussion

The AM fungal specie (*G. mosseae*) used in our research successfully colonized ryegrass plants grown in Cd-contaminated soils, indicating that *G. mosseae* is Cd tolerant and able to maintain an efficient symbiosis with ryegrass root systems even under high Cd stress. However, Cd contamination decreased ryegrass colonization by *G. mosseae*. Similar findings were found for maize (Chen et al., 2004a), sunflower (Hassan et al., 2013) and other plants (Li et al., 2009). The reduction in root colonization rate with Cd addition indicates the toxicity of Cd for AM fungal species.

In our study, we found that the rate of mycorrhizal infection inoculated with *G. mosseae* decreased with the increase of Cd concentration, but the rate was still as high as 43% under high concentration of Cd (180 mg Cd kg<sup>-1</sup>). Secondly, compared with the plants of non-inoculated with *G. mosseae*, the inoculated plants improved the root activity at the same Cd concentration level, indicating that AM fungal has strong tolerance and resistance to Cd contamination. Gao (2017) showed that low concentration Cd could promote plant growth, whereas high concentration can inhibit plant growth, which are consistent with our results.

By Cd stress, net photosynthetic rate (*P<sub>n</sub>*), stomatal conductance (*G<sub>s</sub>*) and transpiration rate (*T<sub>r</sub>*) and intercellular CO<sub>2</sub> concentration (*C<sub>i</sub>*) of ryegrass leaf are lower, which indicated photosynthetic capacity under Cd stress were more obvious inhibitory effect. This is related to the effect of Cd stress on photosynthesis by affecting the absorption, reduction and assimilation of N, P, Fe and Mg related to photosynthesis, reducing pigment content, inhibiting stomatal opening, destroying photosynthetic apparatus, affecting water balance and electron transport (Bishnoi et al., 1993).

However, the increase in  $C_i$  index of non-inoculated *G. mosseae* at high Cd concentration ( $180 \text{ mg Cd kg}^{-1}$ ) may be due to the decrease in net photosynthetic rate, which reduces the consumption of intercellular  $\text{CO}_2$  and increases the concentration of intercellular  $\text{CO}_2$  (Anjum et al., 2016).  $P_n$ ,  $G_s$ ,  $T_r$  and  $C_i$  of ryegrass inoculated with *G. mosseae* alleviated the negative effects of photosynthesis to some extent. Chen (2017) found that under the stress of Cd, AM fungi inoculation restored the photosynthesis of female poplar to a certain extent. This is related to the promotion of host plant nutrient balance and antioxidant capacity by inoculation of AM fungi as well as the increase of host photosynthetic capacity and photochemical efficiency (Li et al., 2016).

MDA has been widely used as an indicator of membrane lipid peroxidation damage. Under the stress of Cd, the balance between the production and clearance of reactive oxygen species is broken, which is likely to cause oxidative damage to cells and excessive accumulation of ROS and inhibit plant growth (Maiti et al., 2012). In this experiment, with the increase of Cd pollution concentration, MDA content in both inoculated and non-inoculated with *G. mosseae* plants showed an increased trend, indicating that Cd stress caused the increase of reactive oxygen species in leaves and promoted the degree of membrane lipid peroxidation in leaves. Under the same concentration of Cd, MDA content in the leaves of the inoculated with *G. mosseae* was lower than that of the non-inoculation leaves, which alleviated the Cd toxicity to a certain extent, cleared the excess reactive oxygen species, and reduced the damage to the cell membrane. SOD and CAT can effectively remove harmful substances produced under the stress of Cd, such as superoxide anions, and help to keep ROS at controlled level and reduce stress state (Ning and Yan, 2019). In this study, the SOD concentration of plants in the inoculated and non-inoculated with *G. mosseae* increased with the increase of Cd concentration, while the content of CAT first increased and then decreased. The results showed that with the increase of Cd concentration, the accumulation of reactive oxygen radicals led to the increase of CAT activity. The CAT activity of inoculated plants increased more, and the ability of scavenging active oxygen free radical was stronger, which improved the resistance of ryegrass to Cd pollution. The increase in SOD and CAT activity could possibly be the result of both a direct effect of heavy metal ions and an indirect effect mediated via an increase in levels of superoxide radicals (Chongpraditnun et al., 1992), which could alleviate cell membrane damage. However, the stress of high concentration of Cd ( $180 \text{ mg kg}^{-1}$ ) may cause the inactivation of CAT protein, indicating that antioxidant enzymes of plants have certain limits on the clearance of reactive oxygen species. Compared with non-inoculated with *G. mosseae*, inoculated plants reduced the damage of harmful substances to cells, which could be confirmed by increasing the biomass, plant height, root length and MDA content of ryegrass by inoculated *G. mosseae*.

The plant height and root/shoot ratio of the inoculated and non-inoculated AM fungal plants, and the aboveground, underground and total biomass of the inoculated AM fungal plants first increased and then decreased under low Cd concentration. Compared with non-inoculated with *G. mosseae*, inoculated plants alleviated Cd pollution and promoted the growth of ryegrass. On the one hand, after mycorrhizal fungi infect the host, the mycorrhizal fungi secrete mucus, polyphosphoric acid, organic acid and the metal chelating peptide formed by plants can adsorb heavy metals in the root, inhibit the Cd transport to the aboveground part of ryegrass, and reduce the toxicity of Cd stress to ryegrass (Wang et al., 2010). On the other hand, inoculation of AM fungi can expand the absorption area of roots, improve the absorption ability of ryegrass to nutrients and

mineral elements, and promote the growth of plants. Meanwhile, AM fungi can produce various growth hormones to promote the growth and development of plant roots. However, with the increase of Cd concentration, the inoculated AM fungi plants were all poisoned by Cd. Zarei (2008b) proved that AM fungi diversity decreased in the soil contaminated by high concentration of zinc. Inoculation of AM fungi improved the tolerance of ryegrass to Cd stress to some extent, but it was still affected by high concentration of Cd.

Heavy metal pollution tends to adversely affect the nutritional status of plants, mainly due to the inhibition of nutrient uptake. Tanaka and Yano (2010) found that increase in the N uptake in plants of AM fungi inoculated. Our research showed that plants of inoculated with *G. mosseae* increased the N and P contents in roots and leaves compared with the non-inoculated plants under the stress of Cd, which indicated that AM fungi promoted the nutrient uptake of ryegrass. This may be related to the fact that the plants infected by AM fungi changes the composition of soil microbial community, leading to the increase of saprophytes, the acquisition of nitrogen in organic matter, and the promotion of nitrogen uptake by plants (Cuéllar et al., 2015). Cruz (2017) found that plant roots of AM fungi infected changed the configuration of roots and increased the absorption capacity of active root areas, which promoting the absorption of N, P and mineral elements. Moreover, in the same Cd level, the content of N and P in leaves of inoculated with *G. mosseae* was higher than that of root. Cui (2019) found that Cd tolerance genotypes reduced Cd transport to leaves and reduced the toxicity of Cd to plant leaves by reducing GmHMA18 expression.

## Conclusion

In summary, compared with uncontaminated ryegrass, the growth of inoculated and non-inoculated AM fungi ryegrass was inhibited with the increase of Cd pollution concentration. Compared with non-inoculation of AM fungi ryegrass, inoculation of AM fungi could improve the resistance and tolerance of ryegrass to Cd stress, and to a certain extent, restored mycorrhizal activity, plant growth and biomass, photosynthetic physiology, and N and P content in roots and leaves. Moreover, the content of SOD and CAT was increased, MDA was decreased, which could alleviate the damage of harmful substances on cells and promote the growth of ryegrass. We propose that AM fungi might potentially be important not only in protecting plants against Cd toxicity, but also in its bioaccumulation and phytoremediation techniques in these polluted soils.

**Acknowledgements.** The study was supported by the National Natural Science Foundation of China (41701289), China Postdoctoral Science Foundation (2018M640287).

## REFERENCES

- [1] Alguacil, M. M., Torrecillas, E., Caravaca, F., Fernández, D. A., Azcón, R., Roldán, A. (2011): The application of an organic amendment modifies the arbuscular mycorrhizal fungal communities colonizing native seedlings grown in a heavy-metal-polluted soil. – *Soil Biology & Biochemistry* 43: 1498-1508.
- [2] Ali, H., Khan, E., Sajad, M. A. (2013): Phytoremediation of heavy metals-Concepts and applications. – *Chemosphere* 91: 869-81.

- [3] Anjum, S. A., Ashraf, U., Khan, I., Tanveer, M., Saleem, M. F., Wang, L. (2016): Aluminum and Chromium Toxicity in Maize: Implications for Agronomic Attributes, Net Photosynthesis, Physio-Biochemical Oscillations, and Metal Accumulation in Different Plant Parts. – *Water Air & Soil Pollution* 227: 326.
- [4] Arienzo, M., Adamo, P., Cozzolino, V. (2004): The potential of *Lolium perenne* for revegetation of contaminated soil from a metallurgical site. – *Science of the Total Environment* 319: 13-25.
- [5] Asgher, M., Khan, M. I., Anjum, N. A., Khan, N. A. (2015): Minimising toxicity of cadmium in plants--role of plant growth regulators. – *Protoplasma* 252: 399-413.
- [6] Augé, R. M., Duan, X., Ebel, R. C., Stodola, A. J. W. (1994): Nonhydraulic signalling of soil drying in mycorrhizal maize. – *Planta* 193: 74-82.
- [7] Bishnoi, N. R., Chugh, L. K., Sawhney, S. K. (1993): Effect of Chromium on Photosynthesis, Respiration and Nitrogen Fixation in Pea (*Pisum sativum* L.) Seedlings. – *Journal of Plant Physiology* 142: 25-30.
- [8] Chen, B. D., Liu, Y., Shen, H., Li, X. L., Christie, P. (2004a): Uptake of cadmium from an experimentally contaminated calcareous soil by arbuscular mycorrhizal maize (*Zea mays* L.). – *Mycorrhiza* 14: 347-354.
- [9] Chen, B. D., Liu, Y., Shen, H., Li, X. L., Christie, P. (2004b): Uptake of cadmium from an experimentally contaminated calcareous soil by arbuscular mycorrhizal maize (*Zea mays* L.). – *Mycorrhiza* 14: 347-54.
- [10] Chen, B. D., Zhu, Y. G., Duan, J., Xiao, X. Y., Smith, S. E. (2007): Effects of the arbuscular mycorrhizal fungus *Glomus mosseae* on growth and metal uptake by four plant species in copper mine tailings. – *Environmental Pollution* 147: 374-380.
- [11] Chen, L. H., Hu, X. W., Yang, W. Q., Wang, X. J., Tan, L. J., Zhang, J. (2017): Effects of arbuscular mycorrhizae fungi inoculation on absorption of Pb and Cd in females and males of *Populus deltoides* when exposed to Pb and Cd pollution. – *Acta Scientiae Circumstantiae* 37: 308-317.
- [12] Chongpraditnun, P., Mori, S., Chino, M. (1992): Excess Copper Induces A Cytosolic Cu, Zn-Superoxide Dismutase in Soybean Root. – *Plant & Cell Physiology* 33: 239-244.
- [13] Cruz, A. F., Oliveira, B. F. D., Pires, M. D. C. (2017): Optimum Level of Nitrogen and Phosphorus to Achieve Better Papaya (*Carica papaya* var. *Solo*) Seedlings Growth and Mycorrhizal Colonization. – *International Journal of Fruit Science*: 1-10.
- [14] Cuéllar, A. E., Martínez, L. R., Espinosa, R. R., Cuéllar, E. E. (2015): Nitrogen and arbuscular mycorrhizal fungi (AMF) effect on two commercial sweet potato clones on an insectisol soil. – *Centro Agrícola* 42: 39-46.
- [15] Cui, G., Ai, S., Chen, K., Wang, X. (2019): Arbuscular mycorrhiza augments cadmium tolerance in soybean by altering accumulation and partitioning of nutrient elements, and related gene expression. – *Ecotoxicology and environmental safety* 171: 231-239.
- [16] Davies, F. T., Puryear, J. D., Newton, R. J., Egilla, J. N., Grossi, J. A. S. (2001): Mycorrhizal fungi enhance accumulation and tolerance of chromium in sunflower (*Helianthus annuus*). – *Journal of Plant Physiology* 158: 777-786.
- [17] Díaz, G., Azcón-Aguilar, C., Honrubia, M. (1996): Influence of arbuscular mycorrhizae on heavy metal (Zn and Pb) uptake and growth of *Lygeum spartum* and *Anthyllis cytisoides*. – *Plant and Soil* 180: 241-249.
- [18] Duan, N., Yan, M. (2019): Effects of AM fungi on growth and physiological characteristics of *Medicago sativa* in different composite substrates in coal mining subsidence areas. – *Guihaia* 39(5): 650-660.
- [19] Gao, Y., Liu, B., Song, W. J., Jiang, Y. Y., Lu, M., Wang, K. Y., Yang, X. H. (2017): The effect of *Gigaspora rosea* on growth and physiological resistance of *Nicotiana tabacum* under Cd stress. – *Journal of Fungal Research* 15(1): 27-32.
- [20] Gonzalez-Chavez, C., D'Haen, J., Vangronsveld, J., Dodd, J. C. (2002): Copper sorption and accumulation by the extraradical mycelium of different *Glomus* spp. (arbuscular mycorrhizal fungi) isolated from the same polluted soil. – *Plant & Soil* 240(2): 287-297.

- [21] Gonzalez-Chavez, C., Harris, P. J., Dodd, J., Meharg, A. A. (2010): Arbuscular mycorrhizal fungi confer enhanced arsenate resistance on *Holcus lanatus*. – *New Phytologist* 155: 163-171.
- [22] Hassan, S. E., Hijri, S. A. (2013): Effect of arbuscular mycorrhizal fungi on trace metal uptake by sunflower plants grown on cadmium contaminated soil. – *New Biotechnol* 30: 780-787.
- [23] Hassan, M., Mansoor, S. (2014): Oxidative stress and antioxidant defense mechanism in mung bean seedlings after lead and cadmium treatments. – *Turkish Journal of Agriculture & Forestry* 38: 55-61.
- [24] Kirkham, M. B. (2006): Cadmium in plants on polluted soils: Effects of soil factors, hyperaccumulation, and amendments. – *Geoderma* 137: 19-32.
- [25] Li, Y., Peng, J., Shi, P., Zhao, B. (2009): The effect of Cd on mycorrhizal development and enzyme activity of *Glomus mosseae* and *Glomus intraradices* in *Astragalus sinicus* L. – *Chemosphere* 75: 894-899.
- [26] Li, M. L., Li, H., Wang, K. R., Shi, L., Liu, J., Zhang, L. (2016): Effect of arbuscular mycorrhizae on the growth, photosynthetic characteristics and cadmium uptake of peanut plant under cadmium stress. – *Environmental Chemistry* 35: 2344-2352.
- [27] Maiti, S., Ghosh, N., Mandal, C., Das, K., Adak, M. K. (2012): Responses of the maize plant to chromium stress with reference to antioxidation activity. – *Brazilian Journal of Plant Physiology* 24: 203-212.
- [28] McGonigle, T. P., Miller, M. H., Evans, D. G. (1990): A new method which gives an objective measure of colonization of roots by vesicular-arbuscular mycorrhizal fungi. – *New Phytologist* 115: 495-501.
- [29] Meng, L., Qiao, M., Arp, H. P. H. (2011): Phytoremediation efficiency of a PAH-contaminated industrial soil using ryegrass, white clover, and celery as mono- and mixed cultures. – *Journal of Soils & Sediments* 11: 482-490.
- [30] Paglia, D. E., Valentine, W. N. (1987): Studies on the quantitative and qualitative characterization of glutathione peroxidase. – *J. Lab. Med.* 70: 158-165.
- [31] Peralta, J. R., Gardeatorresdey, J. L., Tiemann, K. J., Gomez, E., Arteaga, S., Rascon, E., Parsons, J. G. (2001): Uptake and effects of five heavy metals on seed germination and plant growth in alfalfa (*Medicago sativa* L.). – *Bulletin of Environmental Contamination and Toxicology* 66: 727-734.
- [32] Pozo, M. J., Cordier, C., Dumas-Gaudot, E., Gianinazzi, S., Barea, J. M., Azcón-Aguilar, C. (2002): Localized versus systemic effect of arbuscular mycorrhizal fungi on defence responses to *Phytophthora* infection in tomato plants. – *J Exp Bot* 53: 525-534.
- [33] Rajkumar, M., Sandhya, S., Prasad, M. N., Freitas, H. (2012): Perspectives of plant-associated microbes in heavy metal phytoremediation. – *Biotechnology Advances* 30(15): 62-74.
- [34] Rillig, M. C., Steinberg, P. D. (2002): Glomalin production by an arbuscular mycorrhizal fungus: a mechanism of habitat modification? – *Soil Biology & Biochemistry* 34: 1371-1374.
- [35] Schützendübel, A., Nikolova, P., Rudolf, C., Polle, A. (2002): Cadmium and H<sub>2</sub>O<sub>2</sub>-induced oxidative stress in *Populus × canescens* roots. – *Plant Physiology & Biochemistry* 40: 577-584.
- [36] Shahabivand, S., Maivan, H. Z., Goltapeh, E. M., Sharifi, M., Aliloo, A. A. (2012): The effects of root endophyte and arbuscular mycorrhizal fungi on growth and cadmium accumulation in wheat under cadmium toxicity. – *Plant Physiology & Biochemistry* 60: 53-8.
- [37] Shetty, K. G., Hetrick, B. A., Schwab, A. P. (1995): Effects of mycorrhizae and fertilizer amendments on zinc tolerance of plants. – *Environmental Pollution* 88: 307-314.
- [38] Shukurov, N., Pen-Mouratov, S., Steinberger, Y. (2005): The impact of the Almalyk Industrial Complex on soil chemical and biological properties. – *Environmental Pollution* 136(3): 31-40.

- [39] Smith, S. E., Read, D. J. (1997): Mycorrhizal symbioses. – Second edition, Academic Press, London, U.K.
- [40] Tanaka, Y., Yano, K. (2010): Nitrogen delivery to maize via mycorrhizal hyphae depends on the form of N supplied. – *Plant Cell and Environment* 28: 1247-1254.
- [41] Turnau, K., Ryszka, P., Gianinazzi-Pearson, V., Tuinen, D. V. (2001): Identification of arbuscular mycorrhizal fungi in soils and roots of plants colonizing zinc wastes in southern Poland. – *Mycorrhiza* 10: 169-174.
- [42] Vodnik, D., Grcman, H., Macek, I., Elteren, J. T., Kovacevic, M. (2008): The contribution of glomalin-related soil protein to Pb and Zn sequestration in polluted soil. – *Science of the Total Environment* 392: 130-136.
- [43] Wang, M. Y., Xia, R. X., Wang, P. (2010): Effects of arbuscular mycorrhizal fungi on available iron and metals sequestered by glomalin in different rhizospheric soil of *Poncirus trifoliata*. – *Journal of Fujian Agriculture and Forestry University* 39: 42-46.
- [44] Whitfield, L., Richards, A. J., Rimmer, D. L. (2004): Relationships between soil heavy metal concentration and mycorrhizal colonisation in *Thymus polytrichus* in northern England. – *Mycorrhiza* 14: 55-62.
- [45] Yılmaz, D. D., Parlak, K. U. (2011): Changes in proline accumulation and antioxidative enzyme activities in *Groenlandia densa* under cadmium stress. – *Ecological Indicators* 11: 417-423.
- [46] Yong, Y., Zhang, F. S., Li, H. F., Jiang, R. F. (2009): Accumulation of cadmium in the edible parts of six vegetable species grown in Cd-contaminated soils. – *Journal of Environmental Management* 90: 1117-1122.
- [47] Zarei, M., Koenig, S., Hempel, S., Nekouei, M. K., Savaghebi, G., Buscot, F. (2008a): Community structure of arbuscular mycorrhizal fungi associated to *Veronica rechingeri* at the Anguran zinc and lead mining region. – *Environmental Pollution* 156: 1277-1283.
- [48] Zarei, M., Saleh-Rastin, N., Jouzani, G. S., Savaghebi, G., Buscot, F. (2008b): Arbuscular mycorrhizal abundance in contaminated soils around a zinc and lead deposit. – *European Journal of Soil Biology* 44: 381-391.
- [49] Zhang, Z. L. (1990): Experimental guidance of plant physiology. – Second edition, Beijing: Higher Education Press 39-160.
- [50] Zorrig, W., Khouni, A. E., Ghnaya, T., Davidian, J. C., Abdelly, C., Berthomieu, P. (2013): Lettuce—a species with a high capacity for cadmium (Cd) accumulation and growth stimulation in the presence of low Cd concentrations. – *Journal of Horticultural Science & Biotechnology* 88: 72-72.

## LAND USE/LAND COVER CHANGES ANALYSIS IN SUDANO GUINEAN REGION OF BENIN

AYENIKAFO, O. M.<sup>1</sup> – WANG, Y. F.<sup>1,2\*</sup>

<sup>1</sup>*College of economics and management, Northeast Forestry University, Harbin 150040, China*

<sup>2</sup>*Business School of Shanghai Dianji University, Shanghai, China*

*\*Corresponding author*

*e-mail: wyfbhs@sina.com; phone: +86-133-9115-0016*

(Received 10<sup>th</sup> Oct 2020; accepted 21<sup>st</sup> Dec 2020)

**Abstract.** Deforestation processes driven by anthropogenic activities lead to the loss of biodiversity and the alteration of ecological systems. In this paper, we examined the land use / land cover change trends from 2000 to 2020 in the Sudano-Guinean region of Benin, and analysed the driving factors of those changes. The adopted method is based on the diachronic analysis of the land cover through the use of remote sensing data specifically, Landsat satellite images of 2000 and 2020. The results showed that natural forest vegetation and Savannah strongly decreased, whereas farmland and the built-up area increased. Indeed, forest land lost 3.22%, 2.01%, and 1.57%, in Bante, Glazoué, and Ouèssè, respectively. The intensification of human activities was identified as the proximate driver while population growth, a growing demand for agricultural and forest products coupled with improved infrastructure were identified as the underlying drivers of deforestation. To achieve sustainable management goal for forest resources in Benin, the introduction of alternative sources of energy, sustainable farming practices, diversification of income sources, the promotion of community participation, should be implemented.

**Keywords:** *Benin, Sudano-Guinean zone, land use/land cover change, forest change, remote sensing*

### Introduction

Land use / land cover change (LULC) is one of the main causes of terrestrial surface alteration, therefore discussions on sustainable development should take this into account. LULC change is regarded as all change observed in the natural landscape of Earth (Lambin and Meyfroidt, 2010), leading not only to loss of biodiversity, but also to climate change (Verburg et al., 2009; Hibbard et al., 2010; Lambin and Meyfroidt, 2011; Meyfroidt et al., 2013; Van Asselen and Verburg, 2013). According to Turner and Billie (2001), numerous human activities constitute the main causes that have recently been influencing the biosphere in several ways. Indeed, it was highlighted that LULC change is regarded as the major indicator of Earth's terrestrial surface alteration inducted by human populations. Therefore, land use is considered to be a major driver (Foley et al., 2005) due to anthropogenic activities such as agriculture, pasture, and urbanization for their negative impact on the environment. Schaldach et al. (2006) has stated that these change will in the future cause an increase demand of food and energy for the world population. Recently, numerous studies have widely integrated remote sensing (RS) and geographic information system (GIS) in the field of land use land cover change for the purpose of management of land and other natural resources. Thus, studies on monitoring and assessing LULC changes are crucial to agriculturalists, urban planners, policy maker, environmentalists and scientists (Babalola and Akinsanola, 2016). In addition, Remote sensing technologies provide the acquisition of LULC information over large areas at no cost from local to global scales (Mishra and Rai, 2016). Therefore, the integration of remote sensing and GIS approaches is regarded as the best method for extracting and



assessing the change trends of LULC changes (Kumar and Shaikh, 2013; Mishra and Rai, 2016; Mishra et al., 2018). Thapa and Murayama (2010) have stated that transition from rural to urban landscape is possible due to the population migration from village to town and city. According to Moghadam and Helbich (2013) and Li et al. (2013), the projection by 2050 indicates that around 72% of the world's population will reside in cities. This large concentration of human population in cities is not without consequences. Thapa and Murayama (2010) confirmed that the urban growth consequence on land use changes is a complex interaction between behaviour and structural factors with the demand, the technological capacity which at the end strains the environment. Socioeconomic pressures (forest patterns, agricultural, migration and urban sprawl) strongly contribute to urban growth (Thapa and Murayama, 2009). Thus, the land is used for goods and services production and as residential land for those migrating from the village to the city (Lu and Sasaki, 2008). The key for better understanding the interactions between anthropogenic activities and the environment is in performing studies on land use land cover change (Dewan et al., 2012). Lambin et al. (2001) have stated that human activities all round modification in land use/cover recently has become as the one extremely influencing our ecological systems. Thus, the change of land use and cover caused by the intensive socio-economic development lead to environmental degradation (Grimm et al., 2008). Additionally, change in forest landscape due to human activities lead to greenhouse gas increasing in the atmosphere which resulting in climate change (Dewan et al., 2012). In the last two decades, Benin Republic faced rapid population growth and urban expansion. Whereof, acquiring accurate information in the past land cover are very important for the purpose of land use planning and sustainable management. From 2000 to 2015, the population of Benin increased by around 54% from 6.7 million to 10.6 million (United Nations, 2017). From 2000 to 2015, the population density increased from around 61 inhabitants/km<sup>2</sup> to 94 inhabitants/km<sup>2</sup> (INSAE\_Benin, 2014). This has led to great loss of forest cover in the country, with an average annual deforestation rate of 1.95%. From 1990 to 2005, Benin has lost 29.2% (971000 ha) of its forest cover (Thomson, 2007). Most of populations, especially rural populations, mainly depend on forest products to survive (Schumann et al., 2012). Recently, numerous research has been performed in the field of land use land cover change by integrating remote sensing and GIS technologies (Srivastava et al., 2013; Houessou et al., 2013; Oladoye et al., 2014; Mishra and Rai, 2016; Babalola and Akinsanola, 2016; Issiaka et al., 2016; Mishra et al., 2018). Nonetheless, studies on LULC change in Benin Republic was very limited in some regions. The present study aimed to assess the forest cover change in the Sudano-Guinean region of Benin, one of the region with high population density and pressure on forest resources, for the purpose of providing accurate information for sustainable development and management of forest land.

## Materials and Methods

### *Study Area*

The study area is located in Benin, between 8° and 9° north latitude and between 2° 10 and 2° 49 east longitude. It covers an area of approximately 7,445 square kilometers (*Figure 1*). Governed by a tropical transition climate (Afouda, 1990), this area is characterized by annual average rainfall and temperature of 1,300 mm and 27 °C, respectively. The relief is a crystalline peneplain marked by the presence of inselbergs with an altitude ranging from 200 to 400 m (Adam and Boko, 1993). The soils belong to

the sizeable ferruginous ensemble of the tropical environment (Igue, 2000). Agriculture is extensive, characterized by low crop yields. Logging and climate instability have increased in recent years (Oloukoi et al., 2006).

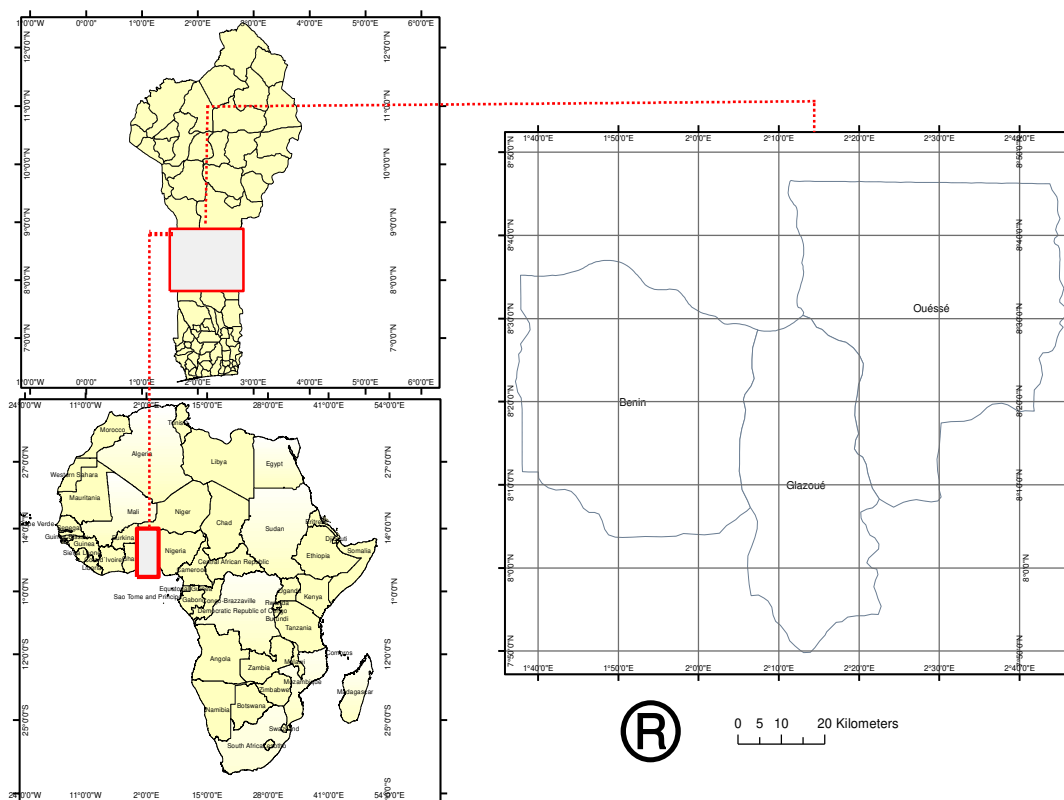


**Figure 1.** Location of the study area

### **Data collection**

According to the Landsat Worldwide Reference System (WRS), our study area is located at the Path and Row position of 174 and 59, respectively. Thus, Landsat images of the year 2000 and 2020, were freely downloaded from the website of the US Geological Survey National Center for Earth Resources Observation and Science (<http://glovis.usgs.gov/>), in order to extract crucial information on land use/ land cover change in the study area. Also, as it requires to better know the region before performing supervised classification, field observations were carried out during March 2020 to understand the characteristics of each land use/ land cover category. Thus, for each land use/ land cover class, 150 training reference points were collected using the GPS receiver. The three Landsat images were acquired in March and February because of cloud-free images or clear sky during that period (*Table 1*). Indeed, using satellite images acquired almost in the same period remains an essential advantage of land use/land cover change study. This removes the effects of change in season when investigating year-to-year change and also minimizes the discrepancies in reflectance caused by seasonal vegetation fluxes, climatic differences, and sun angle differences (Singh, 1989).

**Table 1.** Characteristics of remotely sensed data used for the study

Sensors	Acquisition date	Spatial resolution	Path/row	Band combination	Source
LT05	March 2000	30 m	174/59	5, 4,3	<a href="http://glovis.usgs.gov/">http://glovis.usgs.gov/</a> .
LE07	February 2020	30 m	174/59	5, 4,3	<a href="http://glovis.usgs.gov/">http://glovis.usgs.gov/</a> .
LC08	March 2020	30 m	174/59	6, 5,4	<a href="http://glovis.usgs.gov/">http://glovis.usgs.gov/</a> .

**Land use/land cover classification**

As shown in Figure 2, after performing the image preprocessing (radiometric calibration and atmospheric correction using the FLAASH method), we then carried out a supervised classification of the 2000 and 2020 satellite images. Firstly, field data were collected for each land category in order to identify the spectral signature of each one. Also, using the maximum likelihood algorithm, satellite images were classified into four categories, namely forest, farmland, Savannah, and built-up area. The maximum likelihood algorithm is a parametric decision whose rule is based on the probability that has a specific pixel belonging to a specific category. It has been reported that this algorithm provides a higher classification accuracy in land use/land cover study (Vadrevu, 2013). For the calculation of the observed rates of change, the global rates of change (Tg) express the proportion of an occupancy unit that changes during a given period or between two dates. It was evaluated according to the formula used by Oloukoi (2006):

$$T_g = [(S_2 - S_1 / S_1)] * 100 \tag{Eq.1}$$

where S1 and S2 are the area at t1 and t +1, respectively.

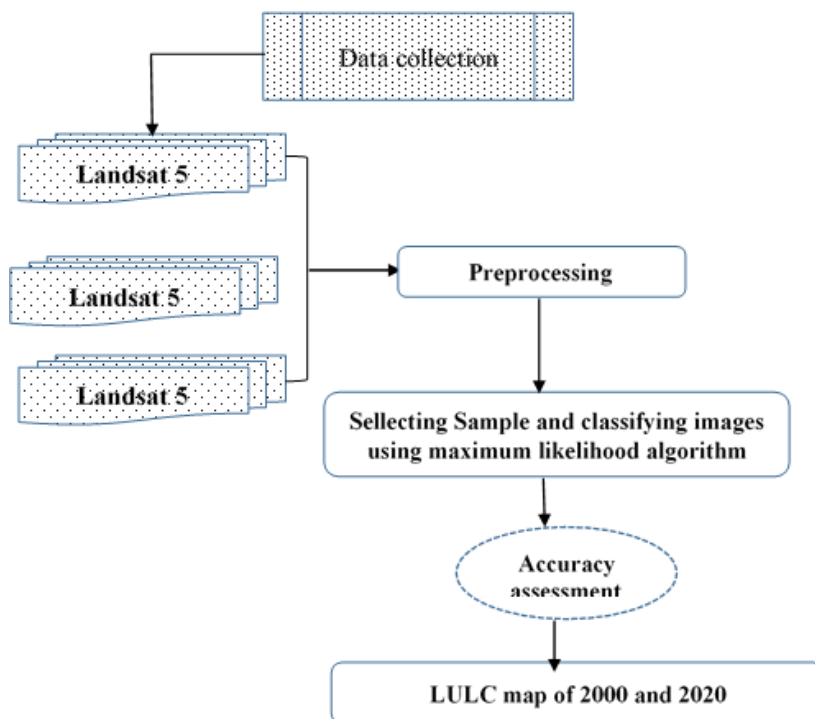


**Figure 2.** Schematic diagram of the research approach

Analysis of the rate of change values shows that positive values indicate progression, and negative values indicate regression. Values close to zero indicate that the class is relatively stable (Kpédénou et al., 2017).

### ***Socioeconomic survey***

Socio-economic surveys were carried out among the main actors whose activities affect in one way or another, the forest land. These are mainly farmers, ranchers, loggers and charcoal makers. Since statistical data on the number of these different actors is not available, the size of the sample to be surveyed at the level of each category of actor was determined using the formula of Dagnelie (1998). In total, 100 actors were interviewed. Its formula is as follows:

$$n = \frac{p(1 - p)UU^2_{\frac{\alpha}{2}}}{d^2} \quad (\text{Eq.2})$$

where p being the proportion of each category of actors, obtained from an exploratory survey, d = 10% (margin of error varying from 0 to 20%).

## **Results**

### ***Evolution in a forest area during the last two decades***

During our survey, the landscape of our study area was classified into four categories, including forest, farmland, wooded land, and bare land, in Bante, Glazoué, and Ouèssè. The total area for each year in the area under study reveals that the greater part of the change has been occurred in forest conversion to other land categories. Based on analysis performed from 2000 to 2020 in Bante (*Table 2*), it was noted that one category experienced negative change while three others experienced positive change. Indeed, Builtup land had the highest positive change rate (12.54%), followed by Farm and Savannah with 12.36% and 6.64%, respectively. On the other hand, Forest land experienced the highest negative change rate (-3.22%). During the period from 2000 to 2020, Forest land lost 6,563.65 ha each year, in favor of Farmland, Builtup land, and Savannah. In Glazoué, the landscape has been changed in different ways compared to Bante (*Table 3*). It was noted that two categories of the landscape experienced a negative change, and two others experienced a positive change. Farmland had the highest positive change rate (7.83%), followed by Builtup land with 5.79%, while Savannah and forest land lost 0.97% and 2.01 %, respectively. From 2000 to 2020, 1091.2 ha of forests and 930.65 ha of Savannah disappeared in favor of farmland and Builtup area, each year. In Ouèssè, the landscape dynamics has been occurred in the same way as in Glazoué (*Table 4*). However, the statistics of change were different, it was noted that two categories of the landscape experienced a negative change, and two others experienced a positive change. Indeed, farmland had the highest positive change rate (6.69%) followed by the Builtup area with 5.49%. In comparison, forest and Savannah lost 1.57% and 0.46%, respectively. On the other hand, forests experienced the highest negative change rate and lost each year 2,882.55 ha, while wooded land lost 344.65 ha.

**Table 2.** Evolution of land use/cover in Bantè, from 2000 to 2020

Land use/cover classes	Spatial area coverage				The annual rate of change	
	2000		2020		2000-2020	
	Area(ha)	%	Area(ha)	%	ha/year	%/year
Forest	203936	77.25	72663	27.53	-6563,65	-3.22
Farmland	44407	16.82	154150	58.39	5487,15	12,36
Savannah	15005	5.68	34937	13.23	996,60	6.64
Bare land	637	0.24	2235	0.85	79,90	12.54
Total	263985	100	263985	100		

**Table 3.** Evolution of land use/cover in Glazoué from 2000 to 2020

Land use/cover classes	Spatial area coverage				The annual rate of change	
	2000		2020		2000-2020	
	Area(ha)	%	Area(ha)	%	ha/year	%/year
Forest	54282	30.89	32458	18.47	-1091,20	-2.01
Farmland	25500	14.51	65412	37.23	1995,60	7.83
Savannah	95476	54.34	76863	43.74	-930,65	-0.97
Bare land	453	0.26	978	0.56	26,25	5.79
Total	175711	100	175711	100		

**Table 4.** Evolution of land use/cover in Ouèssè from 2000 to 2020

Land use/cover classes	Spatial area coverage				The annual rate of change	
	2000		2020		2000-2020	
	Area(ha)	%	Area(ha)	%	ha/year	%/year
Forest	183025	59.60	125374	40.83	-2882,55	-1.57
Farmland	47523	15.47	111084	36.17	3178,05	6.69
Savannah	75652	24.63	68759	22.39	-344,65	-0.46
Bare land	896	0.29	1879	0.61	49,15	5.49
Total	307096	100	307096	100		

### **Proximate drivers of deforestation**

Analysis of *Table 5* reveals that agriculture, fuelwood collection, pasture and Forest fire are the main drivers of deforestation in the study area. For pastoralists and charcoal makers, the most important drivers of deforestation are agriculture and fuelwood collection. For farmers and loggers, it is above all agriculture and fuelwood collection that lead to significant deforestation too. On the other hand, hunters point out agriculture and fuel wood collection as the main drivers of deforestation.

**Table 5.** Variation in the score of the direct factors of deforestation according to the categories of actors

Drivers	Actors				
	Farmers (n=35)	Breeders (n=15)	Loggers (n=20)	Charcoal makers (n=15)	Hunters (n=15)
Agriculture	85	80	83	89	90
Fuel Wood collection	10	15	8	8	5
Pasture	12	3	5	2	3
Forest fire	3	2	4	1	2

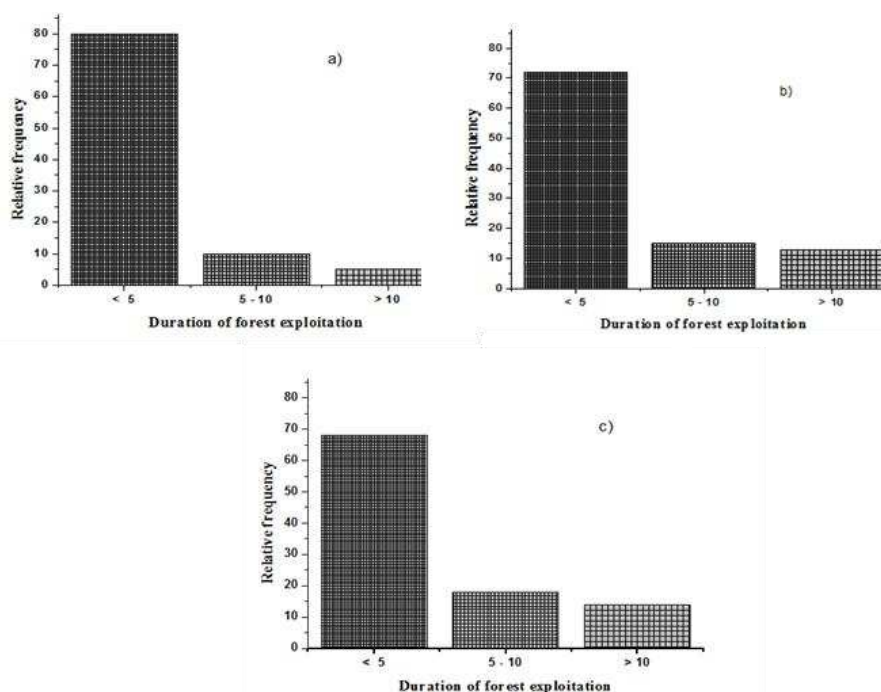


**Figure 3.** Duration of exploitation of forest lands in the city of a) Banté, b) Glazoué and c) Ouèssè

## Discussion

During the last two decades, the rapid population increase has been led to major change in the landscape of the Sudano-Guinean region of Benin. Thus, we conducted the present research for the purpose to analyse the land use / land cover change and its drivers. The results reveal a regression of forest lands in favor of farm lands and Builtup area, from 2000 to 2020. This suggests an increasing demand for cultivation lands by the local population and also lands for implementing new agglomerations. Indeed, from 2000 to 2020, forest lands have lost 3.22%, 2.01% and 1.57% in Banté, Glazoué and Ouèssè, respectively. However, Farmland and Builtup area experienced positive change during the same period. Our results are consistent with those found by Mama et al. (2013) in the northern part of Benin, Avakoudjo et al. (2014) and Ousséni et al. (2016), during the period from 1986 to 2016. These studies have shown a continuous regression of forests in favor of farm lands and Builtup area. Indeed, deforestation results from the interaction of a set of socio-economic, political and institutional factors. According to the literature, these factors are categorized into proximate and underlying causes, and they have been

extensively described by several authors, notably Lambin et al. (1999), Ojima, Galvin and Turner (1994), and Meyer and Turner (1992). Geist and Lambin (2002) define proximate causes as human actions that directly affect the environment, and can be illustrated by agricultural expansion, infrastructure expansion and timber extraction (Lambin, 1994; Kaimowitz and Angelsen, 1998; Arima et al., 2005; Caldas et al., 2007; Pacheco and Pocard-Chapuis, 2012). However, the underlying causes are the indirect causes that can be considered as the socio-economic, political, technological and demographic forces that underlie the immediate causes (Kaimowitz and Angelsen, 1998; Geist and Lambin, 2002). Therefore, according to Geist and Lambin (2002), deforestation can be explained as a result of the interaction of several factors rather than a single cause. Indeed, it results from a combination of factors working together. For example, economic factors can influence land use decision making by changing input prices. These price changes can lead to land conversion. For example, deforestation can result in a decrease in input prices. Similarly, policies and demographic factors influence deforestation. In fact, policies that favor farmers' access to credit or the market can accelerate the conversion of forests to cropland. In addition, the increase or decrease in population impacts land use. Carr (2009) has reported that migration is one of the most important demographic factors that affect land cover change. Thus, taking into account the availability of data in the study area, four causes of deforestation were analysed. Three of which are underlying causes and one is immediate cause. The underlying causes analysed are demographic changes, infrastructure development and market factors. The immediate cause is related to the expansion of agriculture. Generally, numerous studies in Benin have reported that agriculture is the main driver of deforestation (Mama et al., 2013; Avakoudjo et al., 2014; Ousséni et al., 2016; Ngo Makak et al., 2018). Indeed, in our study area, rapid expansion of perennial and annual crop in the 2000s seems to have happened simultaneously with the region's landscape change. The Landsat data classification reveals that forest lands decreased from 2000 to 2020 at the same time that introduced intensification of crop started as a result of market factors. Indeed, the results revealed that market-related factors (e.g., demand for maize, manioc, yam, rice, cotton) should be one of the driving forces influencing forest land decrease. Generally, all perennial and annual crops increased in cultivated areas from 2000 to 2020 (*Table 6*). In conclusion, the most important annual crops are increasing in surface area at an increasing rate, resulting in decreasing in forest areas.

**Table 6.** Annual and perennial cultivated area by region

Year	Annual crop		Perennial crop	
	2000	2020	2000	2020
Banté	31867	89305	32540	98845
Ouèssè	38125	89657	45658	87124
Glazoué	23758	58235	21428	45712
Total	93750	237197	99626	231681

Although agriculture and cotton cultivation are reputedly main proximate causes of landscape change, it is crucial to point out here that several research on landscape change have also revealed strong correlation between population and road network in leading to these changes (Allen and Barnes, 1985; Kaimowitz and Angelsen, 1998; Mather and Needle, 2000; Carr, 2004; Pfaff et al., 2007). Although, correlation analysis between

population, roads, and deforestation in the study area has not been done in this study, it is essential to make some comments. From 2002 to 2018, the population in the study area increased from 269454 to 431340 people – an increase of 60.1% (Table 7). For Hountondji (2008), the increasing rate of population growth in the study area still contributing to the forest land losses due to the increase in the demand of natural resources. Thus, population growth reputedly should also be one of the driving forces of deforestation in the region. Also, the renovation of the main roads linking Banté, Ouèssé and Glazoué to the capital city Cotonou, and the appearance of secondary routes seem to be contributing to the deforestation in the region. However, the most challenging aspect for landholders in the Chaco region is the lack of infrastructure, such as paved roads.

**Table 7.** Total population in the study area

Year	Years			% change (2002-2018)
	2002	2013	2018	
Banté	82129	107181	123739	50.7
Ouèssé	96850	142017	163956	69.3
Glazoué	90475	124431	143645	58.8
Total	269454	373629	431340	60.1

## Conclusion

This study highlights the relevance of the cartographic approach from satellite images. It thus contributes to the interpretation of landscape dynamics in the Sudano-Guinean zone of Benin. It reveals that the current human pressures on the forest resources are in rupture with the capacities of regeneration of the natural plant formations, which are thus seriously threatened. Also, a rapid extension of areas with agricultural influence is observed to the detriment of densely wooded formations. This global movement, starting from urban centers and rural hamlets, associated with an intensification of human activities, questions the sustainability of ecological, economic, and social processes in an area strongly dependent on climatic conditions. It, therefore, seems urgent to develop an integrated and participative management strategy both at the local and regional levels in order to conserve natural resources sustainably. The principles of this management must be based on the concerted development, between local decision-makers and populations, of development plans taking into account the clear definition of agricultural areas, the protection of natural areas as well as the control of ecological flows and processes whose areas are the subject. Therefore, it would be better for further studies, to examine the effects of climate change on land use/land cover change, and the effects of land use/land cover change on biodiversity composition.

## REFERENCES

- [1] Adam, S. K., Boko, M. (1993): Benin. – New edition. Cotonou, Benin, Editions of Flamboyant Edicéf, 93p.
- [2] Afouda, F. (1990): Water and crops in central and northern Benin: study of the variability of water budgets in their relations with the rural environment of the African savannah. – Thesis, University of Paris IV (Sorbonne), France, 448p.



- [3] Allen, J. C., Barnes, D. F. (1985): The causes of deforestation in developing countries. – *Annals of the Association of American Geographers* 75: 163-184.
- [4] Arima, E. Y., Walker, R. T., Perz, S. G., Caldas, M. (2005): Loggers and forest fragmentation: Behavioral models of road building in the Amazon basin. – *Annals of the Association of American Geographers* 95: 525-541.
- [5] Avakoudjo, J., Mama, A., Toko, I., Kindomihou, V., Sinsin, B. (2014): Dynamique de l'occupation du sol dans le Parc National du W et sa périphérie au nord-ouest du Bénin. – *International Journal of Biological and Chemical Sciences* 8(6): 2608-2625.
- [6] Babalola, O., Akinsanola, A. (2016): Change detection in land surface temperature and land use land cover over Lagos Metropolis, Nigeria. – *J. Remote. Sens. GIS* 5(3): 1-7.
- [7] Caldas, M., Walker, R., Arima, E., Perz, S., Wood, C., Aldrich, S., Simmons, C. (2007): Theorizing land cover and land use change: The peasant economy of Amazonian deforestation. – *Annals of the Association of American Geographers* 97(1): 86-110.
- [8] Carr, D. L. (2004): Proximate population factors and deforestation in tropical agricultural frontiers. – *Population and Environment* 25(6): 585-612.
- [9] Carr, D. L. (2009): Population and deforestation: Why rural migration matters. – *Progress in Human Geography* 33(3): 355-378.
- [10] Dagnelie, P. (1998): *Statistique théorique et appliquée (Tome 2)*. – De Boeck & Larquier, Paris-Bruxelles, 659p.
- [11] Dewan, A. M., Yamaguchi, Y., Rahman, M. Z. (2012): Dynamics of land use/cover changes and the analysis of landscape fragmentation in Dhaka Metropolitan, Bangladesh. – *Geo Journal* 77(3): 315-330.
- [12] EU (2017): Decree No. 331/2017 of 06 July 2017 defining the categorization of Protected Areas of the Republic of Benin according to the nomenclature of the World Union for the Conservation of Nature (IUCN). – *Official Journal of the European Union*.
- [13] Foley, J. A., DeFries, R., Asner, G. P., Barford, C., Bonan, G., Carpenter, S. R., Snyder, P. K. (2005): Global consequences of land use. – *Science* 309(5734): 570-574.
- [14] Geist, H. J., Lambin, E. F. (2002): Proximate causes and underlying driving forces of tropical deforestation. – *Bioscience* 52(2): 143-150.
- [15] Grimm, N. B., Faeth, S. H., Golubiewski, N. E., Redman, C. L., Wu, J., Bai, X., Briggs, J. M. (2008): Global change and the ecology of cities. – *Science* 319(5864): 756-760.
- [16] Guy, C., Jacques, L. B., Martin, T. (2005): The plural forest: a new way of managing and using the forest, the case of the Forêt de l'Aigle. – *Vertigo*: 4298.
- [17] Hibbard, K., Janetos, A., Van Vuuren, D. P., Pongratz, J., Rose, S. K., Betts, R., Feddema, J. J. (2010): Research priorities in land use and land-cover change for the Earth system and integrated assessment modelling. – *Int J Climatol* 30(13): 2118-2128.
- [18] Houessou, L. G., Teka, O., Toko, I., Lykke, A. M., Sinsin, B. (2013): Land use and land-cover change at "W" biosphere reserve and its surroundings areas in Benin Republic (West Africa). – *Environ Nat Resour Res.* 3(2).
- [19] Hountondji, Y. H. (2008): *Dynamique environnementale en zones sahélienne et soudanienne de l'Afrique de l'Ouest: Analyse des modifications et évaluation de la dégradation du couvert végétal*. – Thèse de doctorat; Université de Liège, 153p.
- [20] Igue, A. M. (2000): *The use of a soil and terrain database for land evaluation procedures: Case study of Central Benin*. – Thèse, Université de Hohenheim, Allemagne, 235p.
- [21] INSAE\_Benin (2014): *Densité de la population*. – National Institute of Statistics and Economic Analysis.
- [22] Issiaka, N. T., Arouna, O., Imorou, I. T. (2016): *Cartographie De La Dynamique Spatio-Temporelle Des Parcours Naturels des Troupeaux Transhumants Dans Les Communes De Banikoara Et De Karimama Au Bénin (Afrique De L'ouest)*. – *European Scientific Journal* 12(32): 251-268.
- [23] Kaimowitz, D., Angelsen, A. (1998): *Economic, models of tropical deforestation: A review*. – Bogor: Center for International Forestry Research.

- [24] Kpédénou, K. D., Boukprès, T., Tanzidani, T., Tchamie, K. (2016): Quantification of land use changes in Yoto Prefecture (Southeast Togo) using Landsat satellite imagery. – *Biogeographical Research and Environmental Studies Laboratory (University of Lomé), Environmental Science Journal*, pp. 137-156.
- [25] Kumar, M., Shaikh, V. R. (2013): Site suitability analysis for urban development using GIS based multicriteria evaluation technique. – *J Indian Soc Remote Sens* 41(2): 417-424.
- [26] Lambin, E. F., Baulies, X., Bockstael, N., Fischer, G., Krug, T., Leemans, R., Vogel, C. (1999): Land-use and land-cover change (LUCC) - Implementation strategy (IGBP Report 48/IHDP Report 10). – A core project of the International Geosphere-Biosphere Programme and the International Human Dimensions Programme on Global Environmental Change. Stockholm: IGBP Secretariat & Bonn, Switzerland: IHDP Secretariat.
- [27] Lambin, E. F., Turner, B. L., Geist, H. J., Agbola, S. B., Angelsen, A., Bruce, J. W., Coomes, O. (2001): The causes of land-use and land-cover change: moving beyond the myths. *Global environmental change-human and policy dimensions*. – *Glob Environ Change* 11(4): 261-269.
- [28] Lambin, E. F., Meyfroidt, P. (2010): Land use transitions: socio-ecological feedback versus socio-economic change. – *Land Use Policy* 27(2): 108-118.
- [29] Lambin, E. F., Meyfroidt, P. (2011): Global land use change, economic globalization, and the looming land scarcity. – *Proc Natl Acad Sci USA* 108(9): 3465-3472.
- [30] Li, X., Zhou, W., Ouyang, Z. (2013): Forty years of urban expansion in Beijing: what is the relative importance of physical, socioeconomic, and neighborhood factors? – *Appl Geogr* 38(1): 1-10.
- [31] Lu, X., Sasaki, K. (2008): Urbanization process and land use policy. – *Ann Reg Sci* 42: 769-786.
- [32] Mama, A., Sinsin, B., De Cannière, C., Bogaert, J. (2013): Anthropisation et dynamique des paysages en zone soudanienne au nord du Bénin. – *Tropicultura* 31(1): 78-88.
- [33] Mather, A. S., Needle, C. L. (2000): The relationships of population and forest trends. – *The Geographical Journal* 166(1): 2-13.
- [34] Meyer, W. B., Turner II, B. L. (1992): Human population growth and global land-use/land-cover change. – *Annual Review of Ecology and Systematics* 23: 39-61.
- [35] Meyfroidt, P., Lambin, E. F., Erb, K. H., Hertel, T. W. (2013): Globalization of land use: distant drivers of land change and geographic displacement of land use. – *Curr Opin Environ Sustain* 14: 78.
- [36] Mishra, V. N., Rai, P. K. (2016): A remote sensing aided multi-layer perceptron- Markov chain analysis for land use and land cover change prediction in Patna district (Bihar), India. – *Arabian J Geosci* 9(4): 249.
- [37] Mishra, V. N., Rai, P. K., Prasad, R., Punia, M., Nistor, M. M. (2018): Prediction of spatio-temporal land use/land cover dynamics in rapidly developing Varanasi district of Uttar Pradesh, India using Geospatial approach: a comparison of hybrid models. – *Appl Geomat* 10(3): 257-276.
- [38] Moghadam, H. S., Helbich, M. (2013): Spatiotemporal urbanization processes in the megacity of Mumbai, India: Markov chains-cellular automata urban growth model. – *Appl Geogr* 40: 140-149.
- [39] Ngo Makak, R., Sanou, P., Toure, I., Tchindjang, M., Makak, J. S. (2018): Analyse diachronique de l'occupation des terres pour la conception d'une base de données géo-référencées de suivi des dynamiques territoriales dans la commune rurale de Koumbia au Burkina Faso. – *Revue Scientifique et Technique Forêt et Environnement Du Bassin Du Congo* 10: 23-35.
- [40] Ojima, D. S., Galvin, K. A., Turner II, B. L. (1994): The global impact of land-use change. – *Bioscience* 44(5): 300-304.

- [41] Oladoye, A. O., Aduradola, A. M., Adedire, M. O., Agboola, D. A. (2014): Composition and stand structure of a regenerating tropical rainforest ecosystem in South-western Nigeria. – *International Journal of Biodiversity and Conservation* 6(11): 764-776.
- [42] Oloukoi, J., Mama, V. J., Agbo, F. B. (2006): Modeling the dynamics of land use in the Hills department in Benin. – *Remote sensing* 6(4): 305-323.
- [43] Oloukoi, J. (2012): Usefulness of remote sensing and geographic information systems in the study of the spatial dynamics of land use in central Benin. – Doctoral thesis in Geography, UAC, Benin, 304p.
- [44] Ousséni, A., Gervais, E. C., Dramane, I. (2016): Dynamique de l'occupation des terres et état de la flore et de la végétation dans le bassin supérieur de l'Alibori au Bénin. – *Journal of Applied Biosciences* 108: 10543-10552.
- [45] Pacheco, P., Pocard-Chapuis, R. (2012): The complex evolution of cattle ranching development amid market integration and policy shifts in the Brazilian Amazon. – *Annals of the Association of American Geographers* 102(6): 1366-1390.
- [46] Pfaff, A., Robalino, J., Walker, R., Reis, E., Aldrich, S., Caldas, M., Kirby, K. (2007): Road investments, spatial spillovers & deforestation in the Brazilian Amazon. – *Journal of Regional Science* 47(1): 109-123.
- [47] Schaldach, R., Alcamo, J., Heistermann, M. (2006): The multi-scale land use change model landshift: a scenario analysis of land use change and environmental consequences in Africa. – In: 3<sup>rd</sup> International Congress on Environmental Modelling and Software, Burlington, Vermont, USA.
- [48] Schumann, K., Wittig, R., Thiombiano, A., Becker, U., Hahn, K. (2012): Uses, management, and population status of the baobab in eastern Burkina Faso. – *Agrofor Syst* 85(2): 263-278.
- [49] Singh, A. (1989): Review article: Digital change detection techniques using remotely-sensed data. – *International Journal of Remote Sensing* 10(6): 989-1003.
- [50] Srivastava, P. K., Singh, S. K., Gupta, M., Thakur, J. K., Mukherjee, S. (2013): Modeling Impact of Land Use Change Trajectories on Groundwater Quality Using Remote Sensing and GIS. – *Environ Eng Manag J.* 12(12): 2343-55.
- [51] Thapa, R. B., Murayama, Y. (2009): Examining spatiotemporal urbanization patterns in Kathmandu valley, Nepal: remote sensing and spatial metrics approaches. – *Remote Sens* 1: 534-556.
- [52] Thapa, R. B., Murayama, Y. (2010): Drivers of urban growth in the Kathmandu valley, Nepal: examining the efficacy of the analytic hierarchy process. – *Appl Geogr* 30(1): 70-83.
- [53] Thomson, G. (2007): Benin political geography. – <http://www.encyclopediaindia.com/place/africa/benin-political-geography/benin>. Accessed 8 Feb 2018.
- [54] Turner II., B. L. (2001): Land-use and land-cover change: advances in 1.5 decades of sustained international research. – *Am J Agr Econ* 10(4): 269-272.
- [55] United Nations (2017): Benin population (2017-12-21). – <http://worldpopulationreview.com/countries/benin-population>. Accessed 05 Feb 2018.
- [56] Vadrevu, K. P. (2013): Introduction to Remote Sensing. – In: Campbell, J. B., Wynne, R. H. (eds.) *The Photogrammetric Record*. Fifth ed., Guilford Press, New York.
- [57] Van Asselen, S., Verburg, P. H. (2013): Land cover change or land-use intensification: simulating land system change with a global scale land change model. – *Glob Change Biol* 19(12): 3648-3667.
- [58] Verburg, P. H., van de Steeg, J., Veldkamp, A., Willemsen, L. (2009): From land cover change to land function dynamics: a major challenge to improve land characterization. – *J Environ Manag* 90(3): 1327-35.

## CHANGES IN PHYSIOLOGICAL CHARACTERISTICS AND TRANSCRIPT EXPRESSION PROFILES IN THE LATENT BUD SPROUTING OF *PINUS MASSONIANA* (MASSON'S PINE)

ZHU, Y. Y.<sup>1#</sup> – QI, D. P.<sup>2#</sup> – ZHAO, Y.<sup>3,4</sup> – XIAO, F.<sup>3</sup> – YANG, B.<sup>1</sup> – XU, J. J.<sup>1</sup> – ZHOU, J. W.<sup>1</sup> – WANG, G.<sup>1\*</sup>

<sup>1</sup>Guizhou Academy of Forestry, Guiyang, Guizhou, China

<sup>2</sup>Guizhou Meteorological Center, Guiyang, Guizhou, China

<sup>3</sup>Guizhou University, Guiyang, Guizhou, China

<sup>4</sup>Guizhou Provincial Forest Resources and Environment Research Center, Guiyang, Guizhou, China

\*Corresponding author

e-mail: zynjfu@163.com; phone: +86-182-7537-4373

#These authors have contributed equally to this work and should be considered as co-first authors

(Received 15<sup>th</sup> Oct 2020; accepted 21<sup>st</sup> Dec 2020)

**Abstract.** The latent bud regeneration ability at the center of *Pinus massoniana* needle bundles is strong, and can provide a large amount of material for asexual reproduction. Topping *P. massoniana* can induce latent bud sprouting, but the mechanisms underlying the sprouting process are unclear. In this study, physiological indexes were examined during the sprouting of coniferous buds. Additionally, the transcript expression profile of the sprouting process was obtained by high-throughput sequencing. The results showed that increases in N and the endogenous hormone indole-3-acetic acid (IAA) could promote dormancy release and lateral branching of *P. massoniana*. Abscisic acid had a protective effect on the dormancy of *P. massoniana* buds. The expression of phenylpropanoid biosynthesis- and flavonoid biosynthesis-related genes may be induced by differences in test material synthesis and transport caused by changes in the nutrient composition of *P. massoniana* needles after apical topping. The observed upregulated expression of IAA transport- and response-related genes may be pertinent to the dormancy release of axillary buds. The observed activation of transcription factors within the TCP and MADS-box families may be associated with lateral meristem formation. The results of this study provide fundamental data for studying the dormancy and development of latent buds in *P. massoniana*.

**Keywords:** *Pinus massoniana*, latent bud, dormancy release, endogenous hormone, topping

**Abbreviations:** IAA: indole-3-acetic acid; GA<sub>3</sub>: gibberellic acid; ABA: abscisic acid; ZR: zeatin riboside; POD: peroxidase; 6-BA: 6-benzylaminopurine; SOD: superoxide dismutase; TCP: TCP family transcription factor; MADS-box: MADS-box gene family; NBT: nitroblue tetrazolium; CTAB: cetyl trimethylammonium bromide; TPM: transcripts per million; TMM: trimmed mean of M-values; GO: gene ontology; DEGs: differentially expressed genes; KEGG: The Kyoto Encyclopedia of Genes and Genomes

### Introduction

The needles of *Pinus massoniana* are extremely shortened shoots. The latent buds at the center of the base of the needle bundles can develop, grow and form new shoots under certain conditions. This regenerative ability is very strong and can provide a large amount of material for the asexual reproduction of *P. massoniana*, which can accelerate the breeding process. Previous study of the growth process of the latent buds of *P. massoniana* has shown that the effect of temperature on the sprouting of latent buds is the most direct. It has also been found that the time required between pruning and sprouting is the longest in winter, and the shortest in summer (only about 23 d). The

sprouting rate was negatively correlated with the age of the tree. The average number, length and diameter of latent buds grown with different concentrations of the exogenous hormones indole-3-acetic acid (IAA), gibberellic acid (GA<sub>3</sub>) and 6-benzylaminopurine (6-BA) were higher than those of the untreated control buds (Zhu et al., 2018).

There have been many reports on the application of coniferous latent bud sprouting in pines used for production. Chen et al. (1989) used coniferous bundles of young shoots of *P. elliottii*, *P. taeda* and *P. massoniana* as scions, and successfully curated a set of grafting techniques that use the coniferous latent buds to sprout into branches. A regeneration system for *P. massoniana* using the axillary buds at the base of the coniferous leaves of robust seedlings was by established (Zhang et al., 2006; Zhu et al., 2010). At present, the cause and mechanism of latent bud sprouting are not clear. Transcriptome (RNA sequencing) studies are essential for identifying functional elements of the genome, revealing the molecular components of cells and tissues, and determining development. In this study, changes in endogenous hormone content, peroxidase (POD) and superoxide dismutase (SOD) activities and differential expression of endogenous substances involved in the N, P, K, soluble sugar, starch and IAA pathways were investigated during the sprouting of coniferous latent buds. The results provided fundamental theoretical data for the relaxation and development of latent bud dormancy in *P. massoniana*.

## Materials and methods

### Materials

The test materials were taken from the *P. massoniana* seed orchard of the Guizhou Academy of Forestry, China. Twelve healthy 6-year-old *P. massoniana* plants of similar growth and with no pests or diseases were selected. The apical tips were trimmed to disrupt the apical dominance. The sampling technique was as described by Xu et al. (1992), who used the technique for researching larch needle nutrition. The sampling was carried out at approximately 10 am in the morning and the nutrient content of the needles was stable. Physiological indicators were sampled every 5 days until the latent buds germinated. Four sample groups, including the control (labeled P1) were used in this study. The needle sheaths were removed from the plants in all groups. In the control group (P1), the pine plant was not trimmed. In the group labeled P2, the needle bundle bases of the main branch and the side branch, and the phloem joint were trimmed 10 d after trimming the apical tips. In the group labeled P3, these tissues were trimmed after 20 d. In the group labeled P4, these tissues were trimmed after 30 d, by which point the axillary buds had sprouted. The transcriptomic samples were obtained for each of these groups after mixing and registering.

### Methods

#### *Determination of physiological indicators*

The content of hormones such as IAA and ABA were determined using enzyme-linked immunosorbent assays. The soluble sugar and starch contents were determined using the anthrone colorimetric method as described by Wang (2006). The activity of SOD was determined using nitroblue tetrazolium (NBT) reduction. The activity of POD was determined using guaiacol. The N content was determined using the Kjeldahl method and the P content was determined using the vanadium molybdate yellow

colorimetric method. The K content was determined using atomic absorption spectrophotometry. Visualization and inter-group difference analysis was performed using the R package ggstatsplot (Patil, 2018).

#### *RNA extraction and library preparation*

The RNA was extracted and purified using the CTAB, and the RNA quality and concentration were tested ( $A_{260}/A_{280} = 2.0\text{--}2.2$ ;  $A_{260}/A_{230} = 1.8\text{--}2.2$ ;  $28S/18S = 1.4\text{--}2.7$ ; RNA integrity number [RIN]  $\geq 8.0$ ). The quality of the constructed library was determined using an Agilent 2100 Bioanalyzer. The library was sequenced using an Illumina HiSeq X Ten sequencer to generate 150 bp double-ended data.

#### *Evaluation, assembly and annotation of raw data quality*

Trimmomatic was used to filter raw reads and remove the low-quality sequences with linkers (Bolger et al., 2014). Using Trinity (Haas et al., 2013), de novo assembly of transcripts was performed based on the clean data, and then redundant contigs were removed. The longest transcript in each transcript cluster was taken as a unigene, and unigenes were compared with multiple databases such as eggNOG, NR, NT, GO, Pfam, Swiss-Pro.

#### *Gene expression quantification, differential expression analysis and functional enrichment*

The spliced transcript was used as a reference sequence, and the quality-controlled assembled sequences were aligned with the reference sequence using Bowtie 2 (Langmead et al., 2012). The results were statistically compared using RSeQC. The TPM (Transcripts Per Million) calculation was performed in conjunction with Salmon software (Patro et al., 2017). Correlation heat maps were constructed using the different gene expression levels between samples. The number of shared and uniquely expressed genes (TPM > 0) in the samples were counted by Venn diagram. The read count data was normalized using TMM, and DEGseq was used to identify differentially expressed genes from the data without biological replicates. The conditions used for screening for differential gene expression were  $q\text{Value} < 0.05$  and  $|\text{FoldChange}| > 2$ . Gene expression clustering was performed on genes that displayed significant differences in expression between the experimental groups, using the R package gplots. Functional enrichment analysis of GO and KEGG enrichment were performed using Cluster Profiler (Yu et al., 2012). Visualization of gene annotation and expression was performed using MapMan (<http://mapman.gabipd.org/>). Real-time quantitative PCR (RT-qPCR) was performed on a real-time CFX96 Touch PCR instrument. The first strand of the cDNA fragment was synthesized from total RNA. The PCR reaction conditions were as follows: preheating at 95 °C for 30 s, 40 cycles of heat denaturation at 95 °C for 5 s, and annealing at 60 °C for 34 s.

## **Results**

### ***External morphological changes during the development of coniferous latent buds***

The seeds of pine species sprout long leaves. First, the cotyledons grow, then the primary leaves grow at the top of the main stem, and finally the needles (secondary

leaves) grow from the axil of the scale leaves. The first leaves of the strips are more original than secondary leaves. The primary leaves of the seedlings and the secondary leaves of the trees are very different, which leads to morphological variation between trees during their development. The seedling morphology is a reenactment of the original form of its ancestors, which is also known as the phenomenon of returning to the ancestors (Qin et al., 2012). Before the sprouting of the coniferous latent buds, the needles became thicker, with an average diameter of 0.52 mm (0.46 mm in the control group). As shown in *Figure 1*, the latent buds erupted from the base of the needle bundle and were flat (*Fig. 1a*). The strip-shaped leaves differentiated and separated (*Fig. 1b-f*). The shoots were then ejected and normal needles erupted from the base (*Fig. 1g*). This phenomenon indicates that the latent buds of *P. massoniana* have the potential to develop juvenile characteristics.

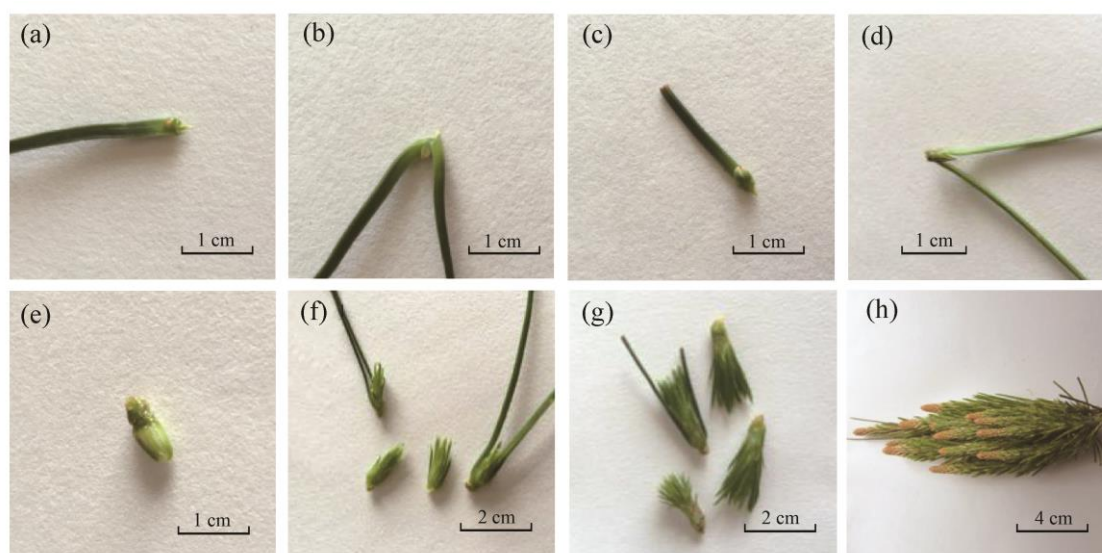


**Figure 1.** External morphological changes during the development of latent buds of *P. massoniana*

### **Analysis of physiological indicators**

There were several physiological indicators that displayed significant differences between the experimental groups (0 d; 5 d; 10 d; 15 d; 20 d; 25 d; 30 d). These included N content, GA<sub>3</sub> content, zeatin riboside (ZR) content, soluble sugar content and SOD activity ( $p < 0.05$ ; *Fig. 2*). The N content showed an increasing pattern from 0 d to 30 d. The correlation between N and K content was 0.6. When the apex dominance was broken (from 0 d to 5 d), the ABA content decreased sharply, from 83.60 ng/g to 63.16 ng/g, and then decreased steadily. The IAA content increased continuously from 50.90 ng/g to 82.16 ng/g at the peak, and after 20 d, the content decreased slightly. IAA and ABA showed negative correlation, with a correlation coefficient of -0.48. The GA<sub>3</sub> content gradually increased, but decreased after 15 d, and finally returned to its new balance. The ratio of (IAA + GA<sub>3</sub> + ZR)/ABA gradually increased from 0.796 to 1.746 at the time of bud sprouting, and the endogenous hormones reached a new equilibrium after sprouting. There was a



significant positive correlation between the soluble sugar and total starch contents; the correlation coefficient was 0.68 ( $r > 0.5$ ).

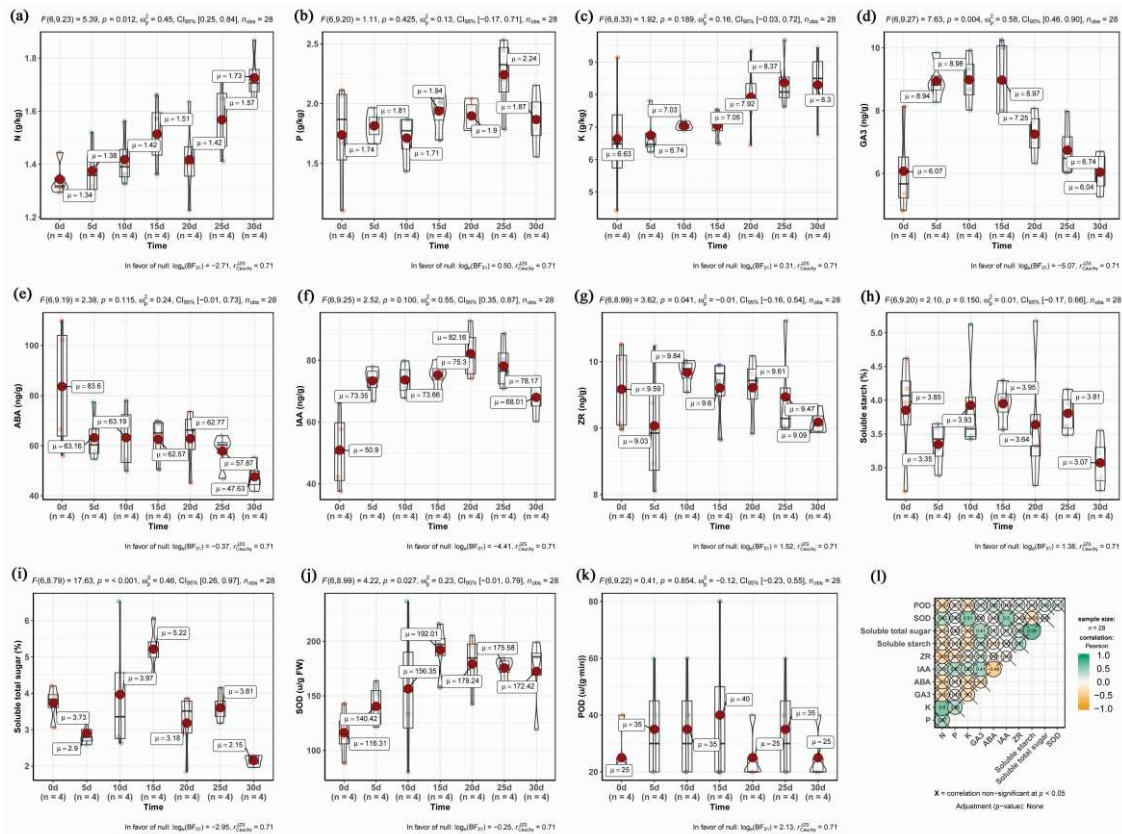


**Figure 2.** (a) N content changes; (b) P element content changes; (c) K element content changes; (d) GA<sub>3</sub> hormone content changes; (e) ABA hormone content changes; (f) IAA hormone content changes; (g) ZR hormone content changes; (h) Changes of soluble starch content; (i) change of soluble sugar content; (j) change of SOD content; (k) change of POD content; (l) correlation between indicators

## Analysis of transcriptomic expression differences

### Data quality control, splicing, annotation and comparison

In terms of the statistics on raw data quality values, the needle bundle base mass values were well distributed and the distribution of the four sample (P1-P4) bases was uniform. The number of unigenes spliced was 169751, the N50 was 393 bp, the N90 was 221 bp, and the average length was 392.82 bp. The proportion of genes that were successfully annotated in at least one database accounted for 61.59% of the total number of genes. The highest rate of annotation in a single database was 48.55%, which was observed in the Gene Ontology (GO) database. As a species that does not have a whole-genome sequence, the annotation ratio for *P. massoniana* was relatively high. The distribution frequency of redundant sequences from the samples showed that the overall trend was linear and smoothly extended; the content of redundant sequences was normal. Testing for the uniformity of distribution showed that the sequences were evenly distributed within the genes.



### Correlation between samples and determination of differentially expressed genes

The correlation coefficient between each sample was high (Fig. 3a). The Venn diagram (Fig. 3b) showed that the number of expressed genes (TPM > 0) in the samples were highly similar. Inter-group differentially expressed genes (DEGs) were identified based on expression levels and statistical findings (Fig. 3c). There were 7349 DEGs between P2 and P1, of which 5798 were upregulated and 1551 were downregulated. There were 5407 DEGs between P3 and P1, of which 2345 were upregulated, and 3062 were downregulated. There were 12,519 DEGs between P4 and P1, of which 9489 were upregulated and 3030 were downregulated. There were 2284 DEGs that were shared among the three comparisons (Fig. 3d).

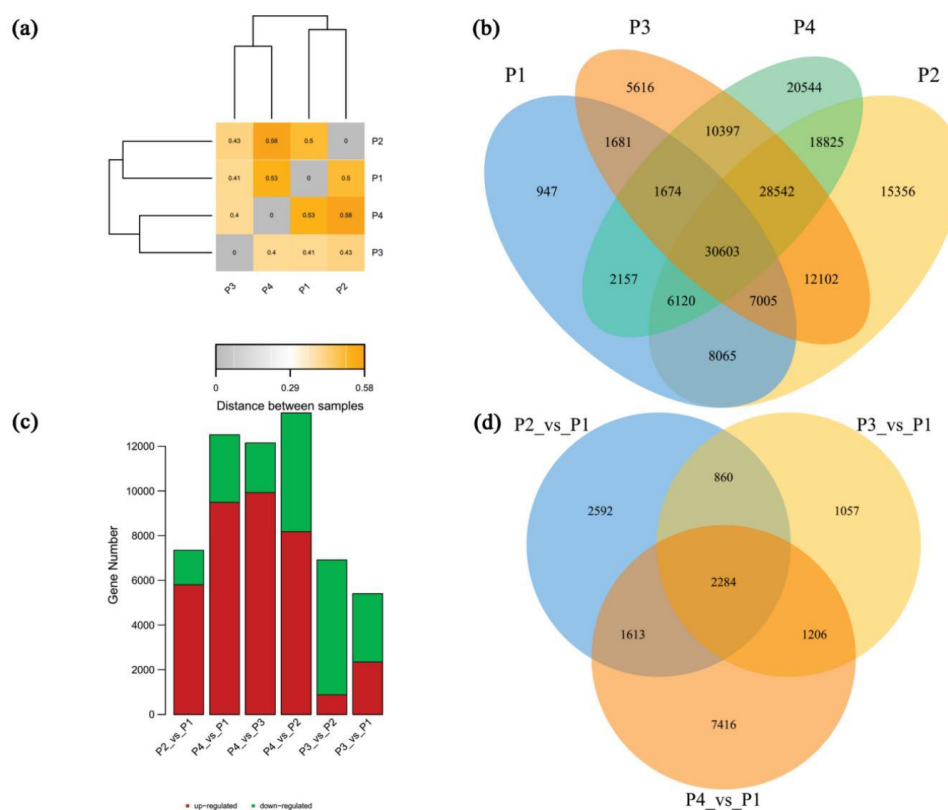


**Figure 3.** (a) Heat map of correlation analysis between samples; (b) Co-expression of Venen map; (c) Bar graph of differential gene numbers of two pairs; (d) Venen plot of differential gene between different combinations

### Differential gene trend clustering and functional enrichment

The Kyoto Encyclopedia of Genes and Genomes (KEGG) enrichment analysis was performed on the significantly differentially expressed genes obtained from the three comparisons (P2 vs P1, P3 vs P1 and P4 vs P1). The 10 pathways with the smallest p-values were selected for multi-channel enrichment visualization. The phenylpropanoid biosynthesis (ko00940) and flavonoid biosynthesis (ko00941) pathways were enriched in the three different comparisons (Fig. 4a). In the category of biological processes, GO enrichment analysis of the DEGs in the P4 vs P1 group (Fig. 4b) found that responses to oxygen-containing compounds and responses to abiotic stimulus were enriched. Expression pattern cluster analysis of the DEGs of the four comparison groups revealed

that most DEGs (4499; subcluster 2) displayed increasing expression with time (Fig. 4c). GO enrichment analysis of subcluster 2 genes (Fig. 4d) found that in the biological processes category, the response to abiotic stimulus, and hormone and cellulose biosynthetic processes were enriched. KEGG enrichment analysis of subcluster 2 genes (Fig. 4e) found that among other pathways, protein processing in endoplasmic reticulum (ko04141), starch and sucrose metabolism (ko00500), and plant hormone signal transduction (ko04075) were enriched.

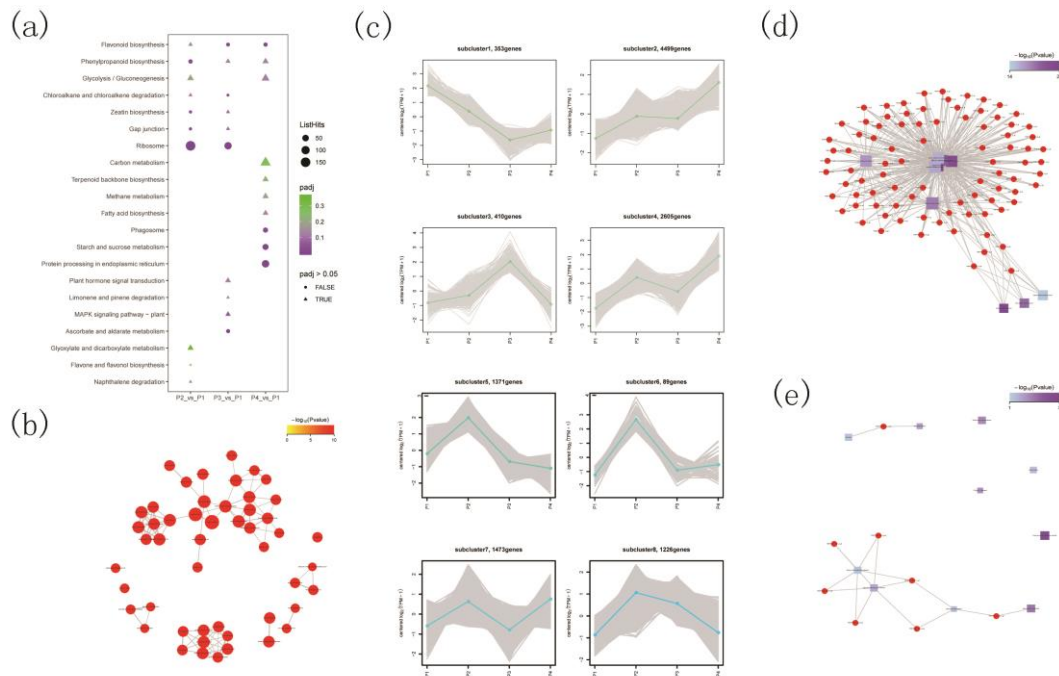


**Figure 4.** (a) multiple sets of KEGG pathway enrichment maps; (b) P4 vs P1 GO enrichment network maps (BP levels); (c) Trend line graph of differential gene expression; (d) GO enrichment analysis of subcluster2; (e) KEGG enrichment analysis of subcluster2

Among the plant hormone signaling pathways of subcluster 2, there were 18 pathway-related genes. These included many genes involved in the auxin response, such as auxin response factor 2 (TRINITY\_DN56024\_c0\_g15), auxin-responsive protein IAA27 (TRINITY\_DN55735\_c1\_g8), auxin transporter-like protein 4 (TRINITY\_DN53899\_c1\_g9) and auxin-responsive protein SAUR32 (TRINITY\_DN52413\_c0\_g2). MapMan was used for transcription factor (TF) expression visualization (Fig. 5). Some TFs showed significant upregulation; for example the expression of the TCP (Teosinte branched1/Cycloidea/Proliferating cell factors) family member TCP8 (TRINITY\_DN55474\_c0\_g2) was 4.32 times higher during the P4 period than during the P1 period (P4/P1), and the MADS-box related gene, AGAMOUS-like 42 (TRINITY\_DN55218\_c1\_g4) was 5.29 times higher during the P4 period (P4/P1).

In order to verify the reliability of transcriptomic sequencing results, 10 differentially expressed genes, including TRINITY\_DN56024\_c0\_g15, were selected for qRT-PCR. The results showed that the expression trend of all qRT-PCR results was consistent with the transcriptomic sequencing results, indicating that transcriptomic sequencing results were reliable.

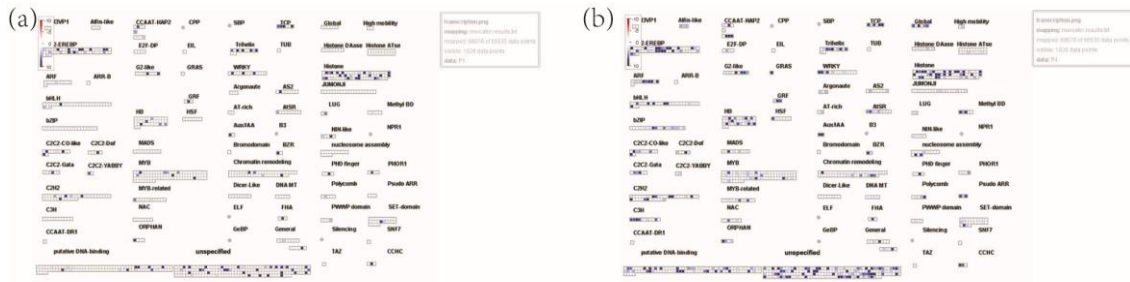


**Figure 5.** (a) Gene expression of the transcription factor P1 during mapman analysis; (b) Gene expression of the transcription factor P4 during mapman analysis

## Discussion

Apical dominance is the process by which the shoot tip inhibits the growth of the stem bud; the dormancy of the axillary bud is not definitive (Chabikwa et al., 2019). The development of leaf buds into new branches and the growth of leaf buds is precisely controlled according to internal and external factors. These factors include plant age, bud location, available nutrients, light and temperature (Luo et al., 2019). Studies have shown that temperature has the most direct effect on the sprouting of the latent buds of *P. massoniana* (Zhu et al., 2018). Axillary bud development consists of two stages: the development of meristems in the leaf axils and subsequent growth or dormancy. The branching pattern depends on a key developmental decision: whether the axillary buds grow branches or remain dormant in the leaf axils. The outcome is controlled by environmental and endogenous hormone signaling-mediated stimuli (Domagalska et al.2011; Aguilar-Martinez et al.2007).

The growth of axillary buds can be divided into four stages: initiation and formation of axillary buds, associated inhibition (apical dominance), induction (bud activation) and sustained growth of twin branches (Tan et al., 2019). Zhu et al. (2019a) observed the anatomy of the short-branched buds of *P. massoniana*, they found that the developmental pattern of the short-branched buds was similar to that of the reported long-leaved buds of *Pinus*. In this study, high-throughput sequencing technology and conventional physiological techniques were used to obtain the transcript expression profiles and the physiological trait data of the four periods: before decapitation, and 10 d, 20 d and 30 d after the topping (the axillary buds had sprouted after 30 d). The physiological data showed that the N was positively correlated with K and the correlation index reached 0.6; IAA increased continuously first and then slightly decreased, but ABA decreased continuously, the correlation coefficient of IAA with ABA was -0.48. GA<sub>3</sub> rises first and then falls, and finally stabilizes. During the axillary bud sprouting process, the (IAA + GA<sub>3</sub> + ZR)/ABA ratio increased gradually from 0.796 before pruning, to 1.746 at the time of bud sprouting (2.19-fold increase).

It has been shown that mechanical damage to the top and axillary bud growth of tobacco (*Nicotiana tabacum*) may affect ABA transduction, and most ABA-responsive transcripts negatively regulate the sprouting of the axillary buds of tobacco (Wang et al., 2018). This indicates that the increase in N and IAA contents observed in this study, promoted dormancy release and lateral branching of *P. massoniana* buds. ABA may have a detrimental effect on the dormancy release of the latent buds of *P. massoniana*. In addition, exogenous hormone of 6-BA could promote the dormant bud germination

earlier and different concentrations of IAA, GA<sub>3</sub> and 6-BA could improve the quantity and quality of scions, especially the best treatment is 100ppm GA<sub>3</sub> (Zhu et al., 2019b).

TCP proteins directly affect growth through tKEGG multi-group enrichment visualization analysis found that phenylpropanoid biosynthesis (ko00940) and flavonoid biosynthesis (ko00941) were enriched in all three group comparisons. The phenylpropanoid pathway produces a large array of structurally diverse molecules, including hydroxycinnamic acids and flavonoids such as flavonols, anthocyanins, dihydrochalcones and their glycoside derivatives (Dare et al., 2017). Several studies have shown that auxin, cytokinin, strigolactones and other hormones participate in the development of lateral tissues. Auxin maintains apical dominance primarily through polar transport, directly inhibiting cytokinin biosynthesis and inhibiting tissue growth through AXR1-dependent auxin signaling pathways (Tanaka et al., 2006; Tarkowska et al., 2004). Removal of the apical dominance can open the auxin polar transport channels between the axillary bud and the main stem. This allows polar transport of auxin within the main stem to promote the growth of the axillary bud (Balla et al., 2011). The expression of *MdPIN15*, *MdSMXL1*, *MdSMXL3*, *MdSMXL4* and *MdSMXL11* has been shown to increase with the sprouting and growth of axillary buds. These genes are candidates for the regulation of the sprouting of axillary buds (Liu, 2018). During the sprouting of the latent buds of *P. massoniana*, the IAA content increased continuously and then decreased slightly. Clustering analysis of the significantly differentially expressed genes between the three comparison groups found that most of the metabolic pathways showed a trend of upregulation. The observed IAA transport and response-related gene activation may be related to axillary bud dormancy release.

The cell cycle, and indirectly affect growth by influencing plant hormone signaling and the circadian clock (Danisman, 2016). Class I TCP genes (TCP6-9, 11, 14-16 and 19-23) are mainly positive regulators of cell division in seed sprouting, leaf and floral organ development, gametophyte development and senescence (Dhaka et al., 2017). Dormancy-associated MADS-box genes are members of the short vegetative phase (SVP)-like MADS-box group and play a key role in the dormancy of perennial plants (Zhao et al., 2018). In this study, the expression of TCP8 (TRINITY\_DN55474\_c0\_g2) was 4.32 times higher during the P4 period than during P1 (P4/P1), and that of MADS-box related AGAMOUS-like 42 (TRINITY\_DN55218\_c1\_g4) was 5.29 times higher during the P4 period (P4/P1). The activation of TCP and MADS-box TFs may be associated with the formation of lateral meristems.

## Conclusion

High-throughput sequencing technology and routine physiological experiments were used to obtain the transcript expression profiles and the physiological trait data of four different groups of *P. massoniana*: no-topping, and 10 d, 20 d and 30 d after topping. There played the crucial roles in the latent bud sprouting of *P. massoniana* of endogenous hormones. Increases in N and IAA content promoted dormancy release and lateral branching of *P. massoniana* buds. ABA had a detrimental effect on the dormancy release of *P. massoniana*. The activation of IAA transport and response-related genes may be associated with the dormancy release of axillary buds. The activation of TCP and MDAS-box transcription factors may be associated with lateral meristem formation.

In this study, the physiological changes and transcript expression of *P. massoniana* during latent bud sprouting were preliminarily revealed, and it was helpful to

understand the mechanism of latent bud sprouting. In the future study, the change of metabolites during sprouting will be studied, and the clonal utilization of latent bud of *P. massoniana* will be also carried out.

**Acknowledgements.** The study was financially supported by the Science and Technology Talent Platform Project of Guizhou Province (grant number [2018]5261), National Key Research and Development Project (grant number 2017YFD0600301) and Guizhou Science and Technology Plan Project (grant number [2017]1098).

## REFERENCES

- [1] Aguilar-Martínez, J. A., Poza-Carrión, C., Cubas, P. (2007): Arabidopsis branched acts as an integrator of branching signals within axillary buds. – *Plant Cell* 19(2): 458-472.
- [2] Balla, J., Kalousek, P. (2011): Competitive canalization of pin-dependent auxin flow from axillary buds controls pea bud outgrowth. – *The Plant Journal: for Cell and Molecular Biology* 65(4): 571-7.
- [3] Bolger, A. M., Lohse, M., Usadel, B. (2014): Trimmomatic: a flexible trimmer for Illumina sequence data. – *Bioinformatics* 30(15): 2114-2120.
- [4] Chabikwa, T. G., Brewer, P. B., Beveridge, C. A. (2019): Initial bud outgrowth occurs independent of auxin flow from out of buds. – *Plant Physiol* 179(1): 55-65.
- [5] Chen, X. Y., He, L. H. (1989): A latest way for reproduction of pine - the technique of needle bundle grafting. – *Forestry Research* 2(2).
- [6] Danisman, S. (2016): TCP transcription factors at the interface between environmental challenges and the plant's growth responses. – *Front Plant Sci* 7: 1930.
- [7] Dare, A. P., Yauk, Y. K., Tomes, S., McGhie, T. K., Rebstock, R. S., Cooney, J. M., Atkinson, R. G. (2017): Silencing a phloretin-specific glycosyltransferase perturbs both general phenylpropanoid biosynthesis and plant development. – *Plant J* 91(2): 237-250.
- [8] Dhaka, N., Bhardwaj, V., Sharma, M. K., Sharma, R. (2017): Evolving tale of TCPs: new paradigms and old lacunae. – *Front Plant Sci* 8: 479.
- [9] Domagalska, M. A., Leyser, O. (2011): Signal integration in the control of shoot branching. – *Nat Rev Mol Cell Biol* 12(4): 211.
- [10] Haas, B. J., Papanicolaou, A., Yassour, M., Grabherr, M., Blood, P. D., Bowden, J. (2013): Denovo transcript sequence reconstruction from RNA-seq using the trinity platform for reference generation and analysis. – *Nat Protoc* 8(8): 1494.
- [11] Langmead, B., Salzberg, S. L. (2012): Fast gapped-read alignment with Bowtie 2. – *Nat Methods* 9(4): 357.
- [12] Liu, X. J. (2018): Genome-Wide Identification, Phylogeny and Expression Analysis of PIN and SMXL Family During Axillary Bud Outgrowth in Apple. – MFA Thesis, Northwest A and F University, Xian.
- [13] Luo, L., Takahashi, M., Kameoka, H., Qin, R., Shiga, T., Kanno, Y., Kyojuka, J. (2019): Developmental analysis of the early steps in strigolactone-mediated axillary bud dormancy in rice. – *Plant J* 97(6): 1006-1021.
- [14] Patil, I. (2018): ggstatsplot: "ggplot2" Based Plots with Statistical Details. – CRAN. <https://github.com/IndrajeetPatil/ggstatsplot>.
- [15] Patro, R., Duggal, G., Love, M. I., Irizarry, R. A., Kingsford, C. (2017): Salmon provides fast and bias-aware quantification of transcript expression. – *Nat Methods* 14(4): 417.
- [16] Qin, G., Zhou, Z. et al. (2012): Excellent Germplasm Resources of *Pinus Massoniana* in China. – China Forestry Publishing Press, Beijing, pp. 38-39.
- [17] Tan, M., Li, G., Chen, X., Xing, L., Ma, J., Zhang, D., An, N. (2019): Role of cytokinin, strigolactone and auxin export on outgrowth of axillary buds in apple. – *Front Recent Dev Plant Sci* 10: 616.

- [18] Tanaka, H., Dhonukshe, P., Brewer, P. B., Friml, J. (2006): Spatiotemporal asymmetric auxin distribution: a means to coordinate plant development. – *Cell Mol Life Sci* 63(23): 2738-2754.
- [19] Tarkowska, D., Tarkowski, P., Göran, S., Astot, C., Anders, N., Norbaek, R. (2004): Auxin regulation of cytokinin biosynthesis in *Arabidopsis thaliana*: a factor of potential importance for auxin-cytokinin-regulated development. – *Proc Natl Acad Sci* 101(21): 8039-8044.
- [20] Wang, X. K. (2006): *Plant Physiology and Biochemistry Experiment Principle and Technology*. – Higher Education Press, Beijing.
- [21] Wang, W. F., Chen, P., Lv, J., Chen, L., Sun, Y. H. (2018): Transcriptomic analysis of topping-induced axillary shoot outgrowth in *Nicotiana tabacum*. – *Gene* 646: 169-180.
- [22] Xu, C., Chen, X., Chen, Z. (1992): Sampling techniques for larch needle nutrition diagnosis. – *Forestry Science and Technology* 3: 5-7.
- [23] Yu, G., Wang, L. G., Han, Y., He, Q. Y. (2012): Cluster Profiler: an R package for comparing biological themes among gene clusters. – *OMICS: J Integr Biol* 16(5): 284-287.
- [24] Zhang, Y., Wei, Z. M., Xi, M., Shi, J. S. (2006): Efficient plant regeneration in vitro in *Pinus massoniana*. – *Journal of Molecular Cell Biology* 39(3): 271-276.
- [25] Zhao, K., Zhou, Y., Ahmad, S., Xu, Z., Li, Y., Yang, W., Zhang, Q. (2018): Comprehensive cloning of *Prunus mume* dormancy associated MADS-Box genes and their response in flower bud development and dormancy. – *Front Plant Sci* 9: 17.
- [26] Zhu, L. H., Wu, X. Q., Qu, H. Y., Ji, J., Ye, J. R. (2010): Micropropagation of *Pinus massoniana* and mycorrhiza formation in vitro. – *PCTOC* 102(1): 121-128.
- [27] Zhu, Y. Y., Yang, B., Xu, J. J., Zhou, J. W., Wang, G. (2018): Effect of different factors on sprouting of *Pinus massoniana* dormant buds. – *Guizhou Agric Sci* 46(8): 32-34.
- [28] Zhu, X. K., Wu, F., Shi, Ch., Wang, H., Zhu, Y. (2019a): Morphologic and anatomic observations of *Pinus massoniana* after axillary bud dormancy release. – *Journal of Northeast Forestry University* 47(5): 14-18.
- [29] Zhu, Y. Y., Xu, J. J., Yang, B., Zhou, J. W., Wang, G. (2019b): Study on the changes of endogenous hormones during the germination of coniferous latent buds of *Pinus massoniana*. – *Guizhou Forestry Sciences and Technology* 2: 1-5.

## THE EFFECTS OF Cd<sup>2+</sup> STRESS ON PHOTOSYSTEM II FUNCTIONING OF RICE (*ORYZA SATIVA* L.) LEAVES UNDER ELEVATED CO<sub>2</sub> LEVEL

LI, M. – QI, X. F. – WANG, X. H. – LI, Y. Y. – MA, L. J. – LI, X. M. – WANG, L. L.\*

College of Life Science, Shenyang Normal University, No. 253 Huanghe North Street,  
Shenyang, Liaoning 110034, China

\*Corresponding author

e-mail: email\_lena@163.com, wangqi5387402006@163.com

(Received 18<sup>th</sup> Oct 2020; accepted 21<sup>st</sup> Dec 2020)

**Abstract.** The effects of elevated levels of CO<sub>2</sub> (EC) and cadmium (Cd<sup>2+</sup>) on the photosystem II of rice leaves were studied using fast chlorophyll fluorescence technique. Rice seedlings (two-leaves-stage) were treated under atmospheric CO<sub>2</sub> (AC, 400 μmol/mol) and elevated CO<sub>2</sub> (EC, 800 μmol/mol), while applied 0, 50, 150, 250 and 500 μmol/L Cd<sup>2+</sup> concentrations respectively. Chlorophyll fluorescence parameters were measured after six days treatments. The results showed that: (1) Under Cd<sup>2+</sup>, F<sub>v</sub>/F<sub>0</sub>, φP<sub>0</sub>, Ψ<sub>0</sub>, φE<sub>0</sub> and PI<sub>ABS</sub> decreased significantly, while V<sub>K</sub>, V<sub>J</sub>, W<sub>K</sub>, M<sub>0</sub>, φD<sub>0</sub>, ABS/RC, TR<sub>0</sub>/RC, DI<sub>0</sub>/RC increased significantly compared to AC. Additional effects were found on the donor side, reaction centers and acceptor side under Cd<sup>2+</sup>, which caused a lower energy connectivity, reduction of PS II activity and electron transfer efficiency as well as an increase of heat dissipation. (2) EC significantly increased F<sub>v</sub>/F<sub>0</sub>, φP<sub>0</sub>, Ψ<sub>0</sub>, φE<sub>0</sub> and PI<sub>ABS</sub>, while significantly decreased V<sub>J</sub> and φD<sub>0</sub> compared to AC. EC increased the photo-energy conversion efficiency of PS II. (3) Under EC and Cd<sup>2+</sup> treatments, the adverse effects of Cd<sup>2+</sup> were slightly alleviated by EC in EC 50 (EC + 50 μmol/L Cd<sup>2+</sup>, the following abbreviations are consistent with this), but the negative influence on photosystem II was still the most significant.

**Keywords:** JIP-Test, OJIP curve, quantum efficiency, specific energy fluxes, performance index

### Introduction

Most of the heavy metal pollutions in soil are from the industrial wastewater discharge, agricultural phosphate fertilizer and sewage sludge, and have seriously affected much farmland and crops (Zou et al., 2020). Cadmium and mercury pollutions are especially severer than other elements (Xiao et al., 2019; Hang et al., 2009). The plants under Cd<sup>2+</sup> stress will affect in cell damages, production of toxic metabolites, inhibition of photosynthesis and respiration (Hassan et al., 2014; Meng et al., 2009; Liu et al., 2012; Singh et al., 2016). Recently, the NOAA (national oceanic and atmospheric administration, USA) detected CO<sub>2</sub> concentrations in the atmosphere as high as 414.7 μmol/mol peak, and it will continue to grow in the coming years (Kalva et al., 2014; Killi et al., 2018; Frew and Prince, 2019). Photosynthesis, as a very important metabolic reaction in green plants, responds to heavy metal stresses very quickly (Belatik et al., 2013). Fast chlorophyll fluorescence can reflect the state of photosystem II (PSII), the main part of light reaction in photosynthesis, and it has been widely used because of its convenience and non-destructiveness (Strasser et al., 2004; Chen et al., 2016). In this study, the rapid chlorophyll fluorescence induction curves and parameters of rice (*Oryza sativa* L.) seedling leaves under Cd<sup>2+</sup> and/or EC treatments were tested, so as to explore the photosynthetic effects of plants under the environmental changes.



## Materials and methods

Rice seedlings (Beijing 2, which has been widely planted in Liaoning province, China) were cultured under Hoagland nutrient solution with the control of 26 °C/22 °C day/night, 16 h/8 h light/dark period, 3000 lux illumination intensities using carbon dioxide artificial climate box. When the seedlings grew to the two-leaves-stage, applied ten treatments, each treatment had 6 pots (*Table 1*).

**Table 1.** Name of treatments

Cd <sup>2+</sup> ( $\mu\text{mol/L}$ )	0	50	150	250	500
AC (400 $\mu\text{mol/mol CO}_2$ )	AC	AC 50	AC 150	AC 250	AC 500
EC (800 $\mu\text{mol/mol CO}_2$ )	EC	EC 50	EC 150	EC 250	EC 500

After 6 days treatments, leaves of rice seedlings were measured by Pocket PEA (Hanshatech, UK) during 11:00-12:00 which had 20 min dark adaption before measurements. The positions of measurements were located in the middle and front of the second complete leaves. Three repeats were selected randomly in each pot (6 pots/treatment, a total of 18 repeats/treatment).

According to the Kautsky effect, the fluorescence change process from O step to P step is the fast chlorophyll fluorescence induction kinetic curve, and the data analysis and processing for this curve is summarized as JIP-test (Strasser et al., 2004; Guisse et al., 1995). The parameters of JIP-test are presented in *Table 2*. According to the JIP-test, the fluorescence OJIP transients were analyzed. Variable fluorescence  $V_{OP} = (F_t - F_0)/(F_P - F_0)$  (Eq. 1) were normalized on a logarithmic time scale while  $V_{OK} = (F_t - F_0)/(F_K - F_0)$  (Eq. 2) and  $V_{OJ} = (F_t - F_0)/(F_J - F_0)$  (Eq. 3) were normalized on a linear time scale. And the different kinetics,  $\Delta V_{OK}$  and  $\Delta V_{OJ}$  of treatments versus AC, can show normalized transients between the O, J, I, P steps (Li et al., 2014), which were called L-band and K-band respectively.

The significant differences of parameters were using the method of two-way ANOVA followed by LSD's multiple-range test for multiple comparisons. The data analysis was done with the SPSS statistical software (v20.0, SPSS, USA) and the figures were drawn by Origin (v9.0, Origin, USA) software.

## Results

### *OJIP curve*

The typical OJIP curve suggested that all leaves were photosynthetically active, but all curves showed inhibition tendency except under EC compared with AC. Fluorescence intensity under EC were the highest at phases I and P steps, and fluorescence intensity under AC 500 was the lowest at J, I and P steps. Fluorescence intensity of Cd<sup>2+</sup> treatments was lower than AC at I and P steps (*Fig. 1*).

Fluorescence data between O step and P step ( $V_{OP}$ ) were deviation normalized under different treatments.  $V_{OP}$  under Cd<sup>2+</sup> treatments were higher than AC. However, there was no significant difference between different Cd<sup>2+</sup> treatments.  $V_{OP}$  under EC was lower than AC (*Fig. 2*).



**Table 2.** Summary of parameters, formulae and their description using JIP-test for the analysis of the fluorescence transient O-J-I-P

Fluorescence parameters	Description
<i>Fluorescence parameters derived from the extracted data</i>	
$F_t$	Fluorescence intensity at time t after onset of actinic illumination
$F_0$	Minimal reliable recorded fluorescence, at 50 $\mu$ s
$F_P$	Maximum fluorescence, when all PS II RCs are closed
$F_K$	Fluorescence intensity at 300 $\mu$ s
$F_V/F_0$	Potential photochemical efficiency
$V_K = (F_K - F_0)/(F_M - F_0)$	Relative variable fluorescence intensity at the K-step
$V_J = (F_J - F_0)/(F_M - F_0)$	Relative variable fluorescence intensity at the J-step
$W_K = (F_K - F_0)/(F_J - F_0)$	The ratio of K step relative variable fluorescence to J step
$M_0 = 4(F_K - F_0)/(F_M - F_0)$	Approximated initial slope of the fluorescence transient
$S_m = (\text{Area})/(F_M - F_0)$	Normalized total complementary area above the O-J-I-P transient
<i>Yields or flux ratios</i>	
$\phi P_0 = TR_0/ABS = [1 - (F_0/F_M)]$	Maximum quantum yield of primary photochemistry (at t = 0)
$\Psi_0 = ET_0/TR_0 = (1 - V_J)$	Probability (at t = 0) that a trapped exciton moves an Electron into the electron transport chain beyond $Q_A^-$
$\phi E_0 = ET_0/ABS = [1 - (F_0/F_M)] \Psi_0$	Quantum yield of electron transport (at t = 0)
$\phi D_0 = 1 - \phi P_0$	Quantum yield (at t = 0) of energy dissipation
<i>Specific energy fluxes (per <math>Q_A^-</math> reducing PS II reaction center)</i>	
$ABS/RC = M_0(1/V_J)(1/\phi P_0)$	Absorption flux per RC
$TR_0/RC = M_0(1/V_J)$	Trapped energy flux per RC (at t = 0)
$ET_0/RC = M_0(1/V_J) \Psi_0$	Electron transport flux per RC (at t = 0)
$DI_0/RC = (ABS/RC) - (TR_0/RC)$	Dissipated energy flux per RC (at t = 0)
<i>Performance index</i>	
$PI_{ABS} = (RC/ABS)[\phi P_0/(1 - \phi P_0)][\Psi_0/(1 - \Psi_0)]$	Performance index on absorption basis

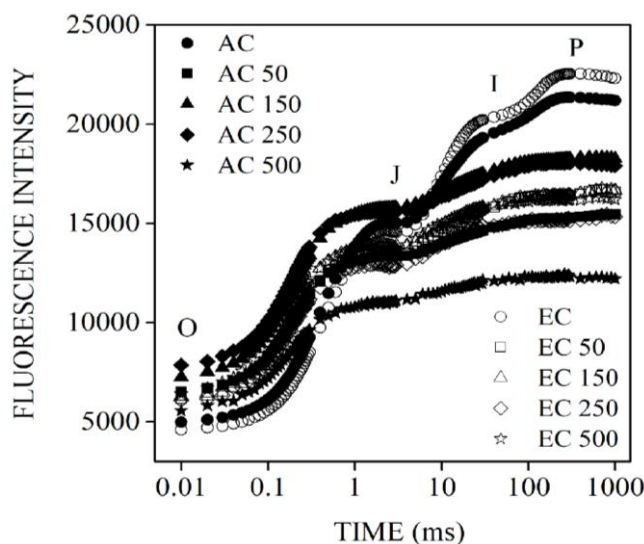


**Figure 1.** Chl a fluorescence intensity of different treatments (n = 18)

### L-band and K-band

The L-band reflects the energy connection of PS II units, and the negative L-band indicates a high system connection degree or high excitation energy utilization rate. In

our study,  $V_{OK}$  and  $\Delta V_{OK}$  showed the energy connection of PS II was higher under EC. Cd<sup>2+</sup> treatments result in a destruction of PS II energy connectivity, and the destruction became severer with the increases of Cd<sup>2+</sup> concentration (Fig. 3A).

The K-band reflects the activity of the oxygen evolving complex (OEC). A negative K-band indicates the intactness of the functional antenna. Similar to the L-band, only EC presented a negative band, while seedlings under Cd<sup>2+</sup> stress all showed OEC damage in different degrees (Fig. 3B).

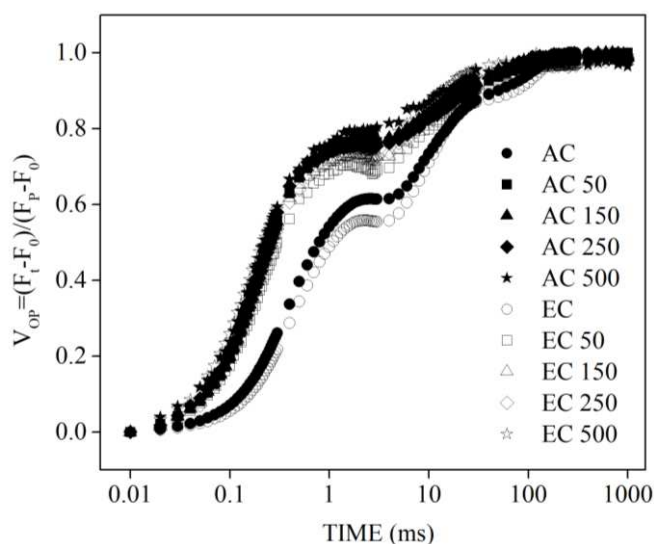


Figure 2.  $V_{OP}$  on the logarithmic scale ( $n = 18$ )

### ***Kinetic parameters changes of rapid chlorophyll fluorescence induction***

Under Cd<sup>2+</sup> treatments,  $F_v/F_0$  were significantly lower, while  $V_K$ ,  $V_J$ ,  $W_K$ ,  $M_0$  were significantly higher compared with AC ( $P < 0.01$ ). Under EC,  $F_v/F_0$  was significantly higher, while  $V_J$  was significantly lower than AC ( $p < 0.05$ ). Under combined treatments,  $V_K$ ,  $V_J$  and  $M_0$  under EC 50 treatment were significantly lower than AC 50 ( $p < 0.05$ ).  $S_m$  was significantly higher under EC 150 and EC 250 compared with the same concentrations under AC ( $p < 0.05$ ). Under EC 500,  $F_v/F_0$  and  $S_m$  were significantly higher than AC 500 ( $p < 0.05$ ) (Fig. 4).

$\phi P_o$ ,  $\Psi_o$  and  $\phi E_o$  were significantly lower, but  $\phi D_o$  was significantly higher under Cd<sup>2+</sup> treatments compared with AC ( $p < 0.01$ ). Under EC,  $\phi P_o$ ,  $\Psi_o$ , and  $\phi E_o$  were significantly higher, but  $\phi D_o$  were significantly lower compared with AC ( $p < 0.05$ ). Under EC 50,  $\phi E_o$  and  $\Psi_o$  were significantly higher than AC 50 ( $p < 0.01$ ). Under EC 500,  $\phi P_o$  and  $\phi E_o$  were significantly higher but  $\phi D_o$  was significantly lower compared with AC 500 ( $p < 0.05$ ) (Fig. 5).

Under Cd<sup>2+</sup> treatments,  $ABS/RC$ ,  $TR_o/RC$  and  $DI_o/RC$  were all significantly higher compared with AC ( $P < 0.01$ ). Under combined treatments,  $ET_o/RC$  was significantly higher in EC 50 compared with AC 50 ( $p < 0.05$ ). Under EC 500,  $ET_o/RC$  was significantly higher, but  $DI_o/RC$  was significantly lower than AC 500 ( $p < 0.05$ ) (Fig. 6).

$PI_{ABS}$  was significantly decreased compared with AC ( $p < 0.05$ ). Under EC,  $PI_{ABS}$  was significantly higher than AC ( $p < 0.05$ ). Under the combined treatments,  $PI_{ABS}$  of EC 50 was significantly higher than AC 50 ( $p < 0.05$ ) (Fig. 7).

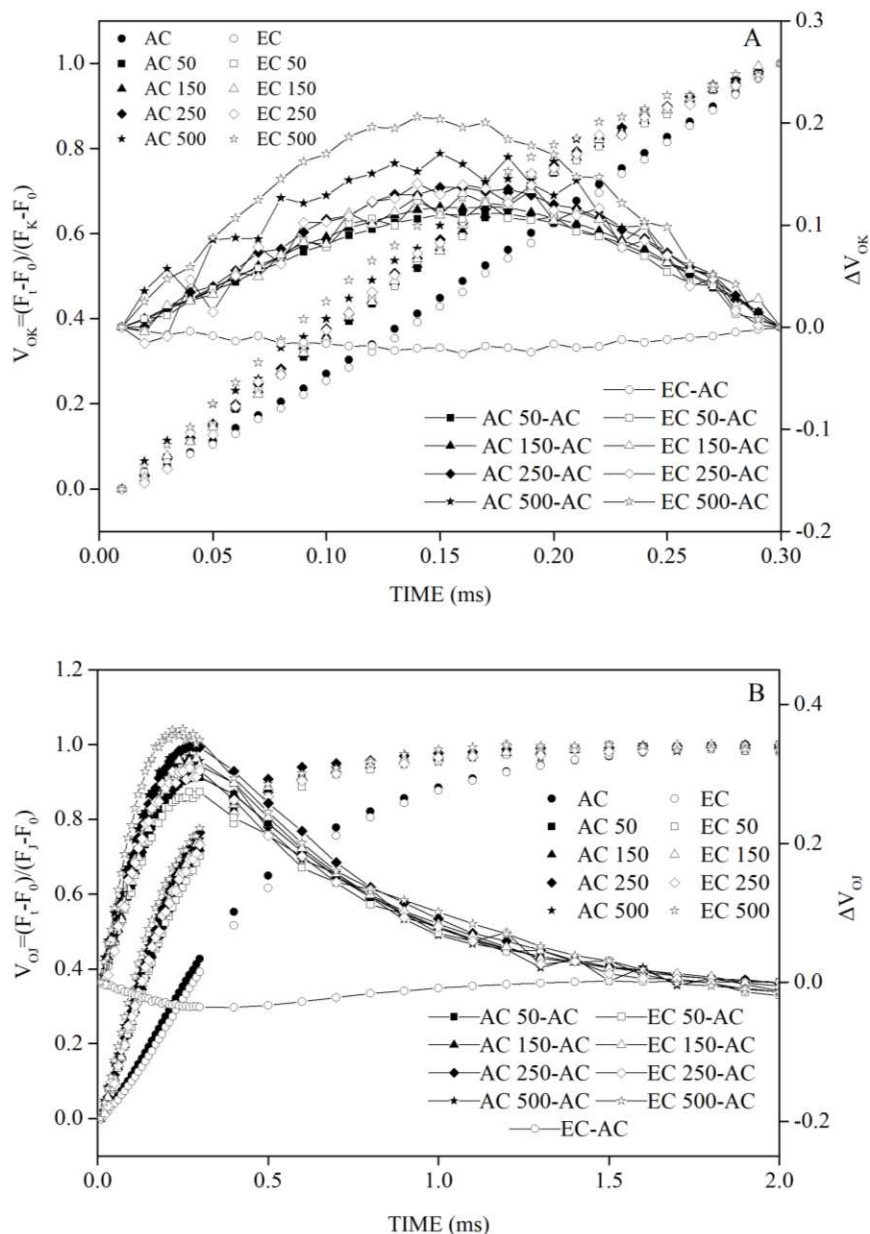


**Figure 3.** (A)  $V_{OK}$  and  $\Delta V_{OK}$ ; (B)  $V_{OJ}$  and  $\Delta V_{OJ}$ . In (A) and (B), open symbol curves represent left y-axis and closed symbol curves represent right y-axis. Left axis shows the  $V_{OK}$  and  $V_{OJ}$ . Right axis shows the  $\Delta V_{OK}$  and  $\Delta V_{OJ}$  stand for stress treatments versus control (AC).  $\Delta V_{OK}$  and  $\Delta V_{OJ}$  revealing the L-band and K-band respectively ( $n = 18$ )

## Discussion

### The effects of Cd<sup>2+</sup> stress

Our study showed that Cd<sup>2+</sup> stress improved the K step of the OJIP curve, and also caused positive K-band and L-band.  $W_K$  is the ratio of variable fluorescence  $F_K$  to the amplitude  $F_J - F_0$ , and  $V_K$  is the relative variable fluorescence intensity at the K step. Both these two parameters reflect the damage of OEC. In our results, Cd<sup>2+</sup> treatment caused lower energy connectivity and destruction of OEC intactness. The electron transfer on the PS II donor side was also affected.

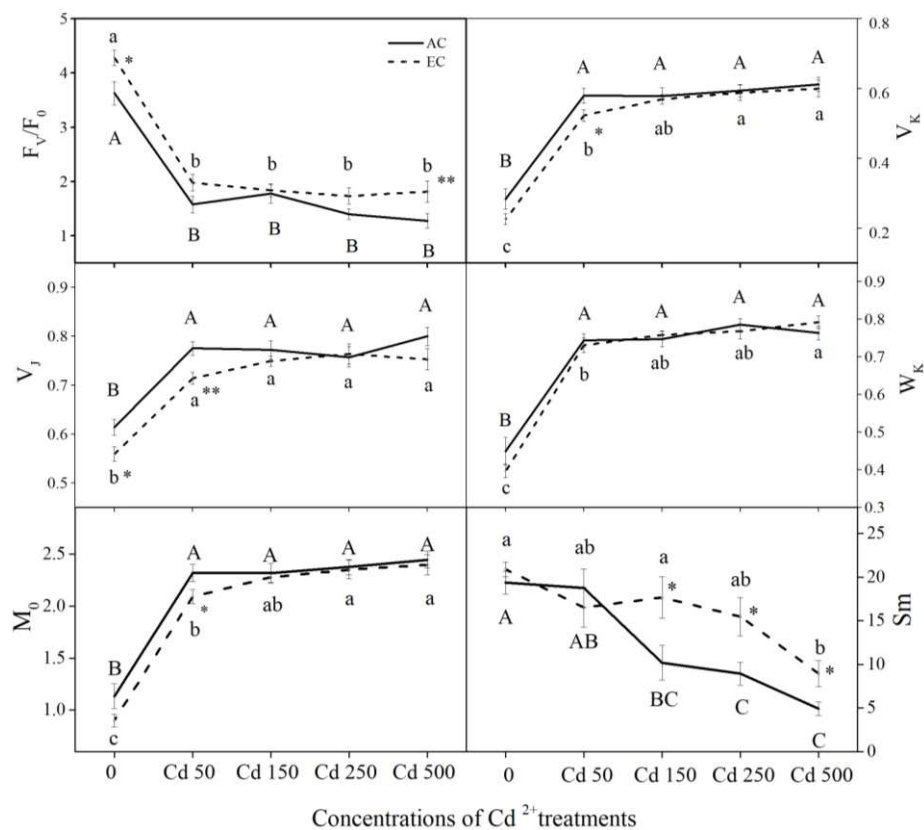


**Figure 4.** The variation trend and significant difference of fluorescence parameters under different treatments. The bars indicated standard error. For the same CO<sub>2</sub> treatments, significance differences were marked as ABC (for AC) and abc (for EC) at P < 0.05 (LSD test). For the same Cd<sup>2+</sup> concentration, an asterisk was marked to indicates significant difference in comparison with AC (\*P < 0.05; \*\*P < 0.01). The following figures are consistent with this figure (n = 18)

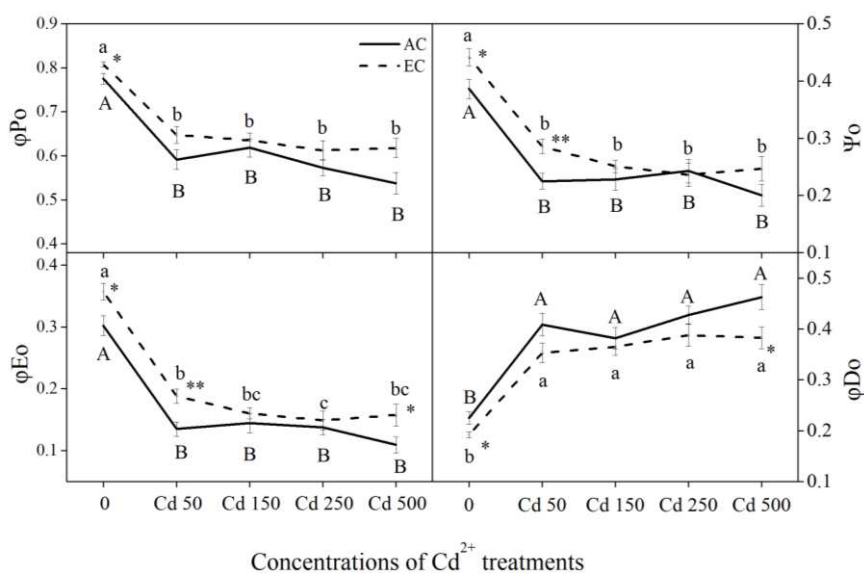


**Figure 5.** The variation trend and significant difference of quantum efficiency under different treatments (n = 18)

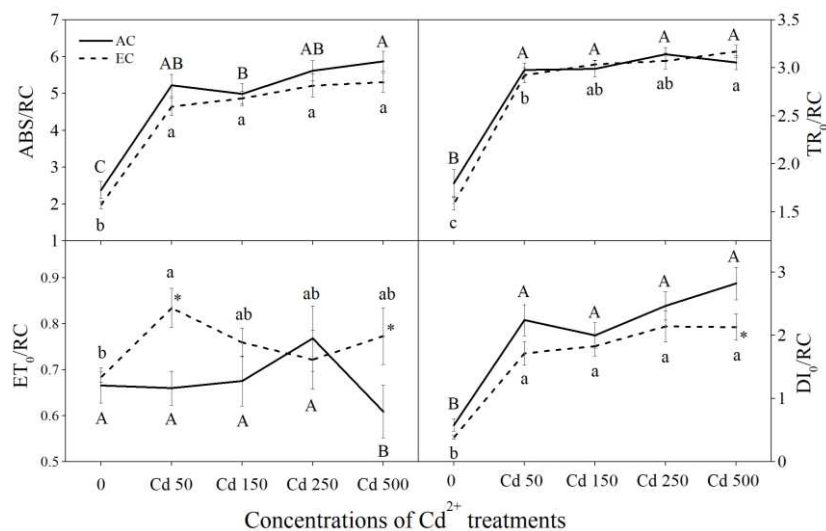


**Figure 6.** The variation trend and significant difference of specific energy fluxes under different treatments ( $n = 18$ )

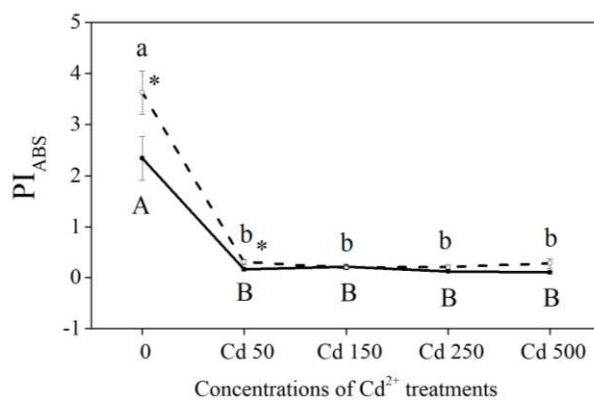


**Figure 7.** The variation trend and significant difference of comprehensive performance index under different treatments ( $n = 18$ )

$M_0$  is the initial slope of the OJIP curve, reflecting the rate at which  $Q_A$ 's reduction during O-J.  $Sm$  is the integral area of normalized OJIP curve, reflecting the energy required when  $Q_A$  is completely reduced, that is, reflecting the capacity of plastoquinone (PQ) (Strasser et al., 1995) on the acceptor side of PS II reaction center.  $\Psi_0$  reflects the ability of PS II to transfer electrons to the downstream electron transport chain. Our study showed that in PS II acceptor side, decreases in  $Sm$  and  $\Psi_0$  and the increase in  $M_0$  compared with AC showed that the activity of the electron transport beyond  $Q_A$  was inhibited under Cd<sup>2+</sup> stress. This is the same as Chu's results (Chu et al., 2018).  $\phi E_0$  reflects the quantum yield for electron transport in the reaction center.  $\phi D_0$  represents the maximum quantum yield of non-photochemical de-excitation (Li and Zhang, 2015). In this study, the capacity of PQ pool on the acceptor side decreased with the increase of Cd<sup>2+</sup> concentrations, which led to the increase of  $\phi E_0$  and  $\phi D_0$ , that is, the quantum ratio of PS II reaction center for heat dissipation increased under Cd<sup>2+</sup> stress, and the quantum ratio for electron transfer decreased. The  $Q_A$  reduction

accumulates, and more surplus energy was used to reduce Q<sub>A</sub>, which hinders the electron transfer. The ability of PS II to transfer electrons to the downstream electron transport chain was destroyed by Cd<sup>2+</sup>. The electron transfer on the acceptor side was inhibited.

F<sub>v</sub>/F<sub>0</sub> reflects the potential activity of PS II, which is proportional to the amount of PS II RCs (Luo et al., 2016) and is often used to judge whether the leaves of plants are photo-inhibition. In our study, Cd<sup>2+</sup> treatment significantly reduced F<sub>v</sub>/F<sub>0</sub> compared with AC. This is similar to the result of Essemine et al. (2020). φPo reflects the maximum photochemical quantum efficiency of the PS II reaction center which is generally stable and rarely affected by growth conditions (Kramer et al., 2004), but decreases under the stress condition (Baker, 2008). It can be seen from our results that F<sub>v</sub>/F<sub>0</sub> and φPo had the same downward trends under Cd<sup>2+</sup> stress, which might be the PS II reaction center had photo-inhibition and PS II electron transfer was blocked. V<sub>J</sub> represents the degree of closure of the reactive center of PS II. Under the treatments of Cd<sup>2+</sup>, the number of RCs decreased, and a large number of RCs closed.

Specific energy flux includes ABS/RC, TR<sub>0</sub>/RC, ET<sub>0</sub>/RC, DI<sub>0</sub>/RC etc. (Strasser et al., 2004), which reflecting the activity of PS II reaction center when Q<sub>A</sub> is in reducible state. Our results showed that under Cd<sup>2+</sup> treatments, the absorption flux per RC (ABS/RC), the energy flux trapped per RC (TR<sub>0</sub>/RC) and the dissipated energy fluxes per RC (DI<sub>0</sub>/RC) all significantly higher than AC, while the electron transport flux per RC (ET<sub>0</sub>/RC) was significantly lower under AC 500. Increase in trapping per RC (TR<sub>0</sub>/RC) can indicate impairment of the oxygen evolving complex (Kalaji et al., 2014; Franić et al., 2018). After absorbed by PS II reaction center, the light was trapped by reaction center (TR<sub>0</sub>/RC), the ABS/RC was mainly used for electron transport flux ET<sub>0</sub>/RC and dissipated flux DI<sub>0</sub>/RC (Strasser et al., 2010; Tsimilli-Michael and Strasser, 2008). It can be found from our results that, although the light energy absorbed and trapped by unit RC increased under the stress of Cd<sup>2+</sup>, the light energy used for electron transfer increased limited, so more light energy consumption occurred in dissipation flux, while photosynthesis did not increase much. This is the same as Xue's results (Xue et al., 2018). A study suggested that plants dissipate excess light energy which was not available for photosynthesis in order to reduce damage to PS II reactive centers (Appenroth et al., 2001). In our study, rice leaves may also had such a protective mechanism.

PI<sub>ABS</sub>, a comprehensive performance index based on light absorption (Brestic et al., 2012; Heerden et al., 2004) which reflects the overall function of PS II system, is the most sensitive parameter to the stressed environment. It was significantly reduced by Cd<sup>2+</sup> and inversely proportional to Cd<sup>2+</sup> concentration in our study. The result showed that Cd<sup>2+</sup> had obvious damage to photosynthetic performance of rice seedlings.

### ***The effects of EC***

Elevated CO<sub>2</sub> has been proved to be able to enhanced photosynthesis of C<sub>3</sub> plants (Lahijani et al., 2018). The OJIP curve under EC was higher at I and P steps than AC, which means the promotion of electron transport at the donor side of PS II. The change in fluorescence is the result of variation in the redox state of the PS II RCs complex (Haldimann and Strasser, 1999). Strasser et al. (1995) reported that the decrease of electron transport beyond Q<sub>A</sub><sup>-</sup> results the high fluorescence. In our study, the difference



kinetics  $\Delta V_{OP}$  revealed that seedlings under EC produced lower fluorescence, which showed less biochemical inhibition. EC produced a negative K-band and L-band, suggesting better energetic connectivity of PS II and photosynthetic performance compared with AC.

Under EC,  $M_0$  and  $S_m$  significantly decreased compared with AC, that is, the degree of openness of the RCs increased and the proportion of the inactivated RCs decreased, which was conducive to the electron transfer down from  $Q_A^-$ . The increases in  $\Psi_0$  and  $\phi E_0$  under EC indicated that EC promoted the primary light reaction and the redox reactions after  $Q_A$ .

Both  $F_v/F_0$  and  $\phi P_0$  under EC showed an increasing trend in different degrees, indicating that the increase of CO<sub>2</sub> concentration enhanced the electron transfer efficiency and the PS II light energy conversion. Compared with AC,  $\phi D_0$  and  $V_J$  were significantly reduced by EC, indicating that EC reduced the heat dissipation and increases the opening degree of RCs. In conclusion, photo-energy conversion efficiency of PS II active center can be alleviated under elevated CO<sub>2</sub>.

In the composite index of  $PI_{ABS}$ , EC significantly improved it compared with AC. The result showed that EC could improve the photosynthetic performance of rice seedlings.

### ***The effects of Cd<sup>2+</sup> stress and EC***

In our study, the K-band and L-band showed that the alleviated effect of EC on PS II donor side was not obvious under Cd<sup>2+</sup> stress. Under EC 50, the significant decrease of  $V_K$  compared with AC 50 indicated that EC could alleviate the damage of OEC caused by lower Cd<sup>2+</sup> stress.

Compared with AC 50, EC 50 had a significant decrease in  $M_0$  and a significant increase in  $\Psi_0$  and  $\phi E_0$ . These suggested that reduction of  $Q_A$  to  $Q_A^-$  was higher in EC 50 than AC 50. There were no significant differences in  $\Psi_0$  and  $\phi E_0$  under EC 150, EC 250 and EC 500 compared with the same Cd<sup>2+</sup> concentrations under AC. To sum up, elevated CO<sub>2</sub> alleviates lower concentration Cd<sup>2+</sup> stress to a certain extent in terms of PS II energy distribution.

In the specific fluxes,  $ET_0/RC$  was significantly higher under EC 50 compared with AC 50. There were no significant differences in  $ABS/RC$  and  $TR_0/RC$  under EC 50, EC 150, EC 250 and EC 500 compared with the same Cd<sup>2+</sup> concentrations under AC.  $V_J$  was significantly decreased under EC 50 compared with AC 50. It can be seen that the degree of closure of PS II active RCs was alleviated, and the electron transport was significantly increased in lower Cd<sup>2+</sup> treatment under EC. Under some stresses, PS II RCs were reversibly inactivated and became an energy trap, which could absorb light energy but could not promote electron transfer (Lee et al., 2001). In our study, EC can alleviate the energy trap, but the effect of cadmium stress cannot be completely eliminated.

$PI_{ABS}$  of EC 50 was significantly higher than AC 50. In terms of the comprehensive performance index, the effect of EC had some mitigation on 50  $\mu\text{mol/L}$  Cd<sup>2+</sup>, but was not particularly obvious in other concentrations.

Compared with the same Cd<sup>2+</sup> concentrations under AC treatments, EC 150, EC 250 and EC 500 showed little alleviated effects on specific energy flux, quantum efficiency and comprehensive performance index.

## Conclusions

In this study, the effects of elevated CO<sub>2</sub> and/or Cd<sup>2+</sup> stress in leaves of rice were studied using the rapid chlorophyll fluorescence technique. The main results were as follows: (1) Cd<sup>2+</sup> stress damaged the integrity of OEC in rice seedling leaves, which result in lower energy connectivity at the PS II donor side. Also, the effects on receptor side and the reaction centers were the decrease of RCs' number and the inhibition of the electron transfer. RCs absorbed more energy but most of the energy was used for heat dissipation; (2) Short-term elevated CO<sub>2</sub> can promote electron transfer in PS II donor side of rice seedling leaves. The photo-energy conversion efficiency of PS II increased with the increase of the openness of the RC; (3) Short-term elevated CO<sub>2</sub> can relieve the adverse effects of lower concentration Cd<sup>2+</sup> treatment, but it cannot significantly eliminate the damage of higher Cd<sup>2+</sup> stress. (4) In the future study, the intrinsic molecular mechanism changes of chlorophyll fluorescence should be concerned.

**Acknowledgements.** This work was funded by the National Natural Science Foundation of China (31600314), the Department of Education of Liaoning province Foundation (LZD201901, LZD202004).

## REFERENCES

- [1] Appenroth, K. J., Stöckel, J., Srivastava, A., Strasser, R. J. (2001): Multiple effects of chromate on the photosynthetic apparatus of *Spirodela polyrhiza* as probed by OJIP chlorophyll a fluorescence measurements. – *Environmental Pollution* 115: 49-64.
- [2] Baker, N. R. (2008): Chlorophyll fluorescence: a probe of photosynthesis in vivo. – *Annual Review of Plant Biology* 59: 89-113.
- [3] Belatik, A., Hotchandani, S., Tajmir-Riahi, H. A., Carpentier, R. (2013): Alteration of the structure and function of photosystem I by Pb<sup>2+</sup>. – *Journal of Photochemistry and Photobiology B Biology* 123: 41-47.
- [4] Brestic, M., Zivcak, M., Kalaji, H. M., Carpentier, R., Allakhverdiev, S. I. (2012): Photosystem II thermostability in situ: environmentally induced acclimation and genotype-specific reactions in *Triticum aestivum* L. – *Plant Physiology and Biochemistry* 57: 93-105.
- [5] Chen, S. G., Yang, J., Zhang, M. S., Strasser, R. J., Qiang, S. (2016): Classification and characteristics of heat tolerance in *Ageratina adenophora* populations using fast chlorophyll a fluorescence rise O-J-I-P. – *Environmental and Experimental Botany* 122: 126-140.
- [6] Chu, J. J., Zhu, F., Chen, X. Y., Liang, H. Z., Wang, R. J. (2018): Effects of cadmium on photosynthesis of *Schima superba* young plant detected by chlorophyll fluorescence. – *Environmental Science and Pollution Research* 25: 10679-10687.
- [7] Essemine, J., Qu, M. N., Lyu, M. J. A., Song, Q. F., Khan, N., Chen, G. Y., Wang, P., Zhu, X. G. (2020): Photosynthetic and transcriptomic responses of two C<sub>4</sub> grass species with different NaCl tolerance. – *Journal of Plant Physiology* 253: 153244.
- [8] Franić, M., Galić, V., Mazur, M., Šimić, D. (2018): Effects of excess cadmium in soil on JIP-test parameters, hydrogen peroxide content and antioxidant activity in two maize inbreds and their hybrid. – *Photosynthetica* 55: 660-669.
- [9] Frew, A., Price, J. N. (2019): Mycorrhizal-mediated plant-herbivore interactions in a high CO<sub>2</sub> world. – *Functional Ecology* 33: 1376-1385.
- [10] Guisse, B., Srivastava, A., Strasser, R. J. (1995): The polyphasic rise of the chlorophyll a fluorescence (O-K-J-I-P) in heat stressed leaves. – *Archives Des Sciences* 48: 147-160.



- [11] Haldimann, P., Strasser, R. J. (1999): Effects of anaerobiosis as probed by the polyphasic chlorophyll a fluorescence rise kinetic in pea (*Pisum sativum* L.) – *Photosynthesis Research* 62: 67-83.
- [12] Hang, X. S., Wang, H. Y., Zhou, J. M., Ma, C. L., Du, C. W., Chen, X. Q. (2009): Risk assessment of potentially toxic element pollution in soils and rice (*Oryza sativa*) in a typical area of the Yangtze River Delta. – *Environmental Pollution* 157: 2542-2549.
- [13] Hassan, M. J., Shao, G. S., Zhang, G. P. (2014): Influence of cadmium toxicity on growth and antioxidant enzyme activity in rice cultivars with different grain cadmium accumulation. – *Journal of Plant Nutrition* 28: 1259-1270.
- [14] Heerden, P. D. R., Strasser, R. J., Krüger, G. H. J. (2004): Reduction of dark chilling stress in N<sub>2</sub>-fixing soybean by nitrate as indicated by chlorophyll a fluorescence kinetics. – *Physiologia Plantarum* 121: 239-249.
- [15] Kalaji, H., Oukarroum, A., Alexandrov, V., Kouzmanova, M., Brestic, M., Zivcak, M., Samborska, I. A., Cetner, M. D., Allakhverdiev, S. I., Goltsev, V. (2014): Identification of nutrient deficiency in maize and tomato plants by in vivo chlorophyll a fluorescence measurements. – *Plant Physiology Biochemistry* 81: 16-25.
- [16] Kalva, M. S., Sreeharsha, R. V., Shalini, Mudalkar, S., Reddy, A. R. (2014): Persistent stimulation of photosynthesis in short rotation coppice mulberry under elevated CO<sub>2</sub> atmosphere. – *Journal of Photochemistry and Photobiology B: Biology* 137: 21-30.
- [17] Killi, D., Bussotti, F., Gottardini, E., Pollastrini, M., Mori, J., Tani, C., Papini, A., Ferrini, F., Fini, A. (2018): Photosynthetic and morphological responses of oak species to temperature and [CO<sub>2</sub>] increased to levels predicted for 2050. – *Urban Forestry and Urban Greening* 31: 26-37.
- [18] Kramer, D. M., Johnson, G., Kierats, O., Edwards, G. E. (2004): New fluorescence parameters for the determination of QA redox state and excitation energy fluxes. – *Photosynthesis Research* 79: 209-218.
- [19] Lahijani, M. J. A., Kafi, M., Nezami, A., Nabati, J., Mehrjerdi, M. Z., Shahkoomahally, S., Erwin, J. (2018): Variations in assimilation rate, photoassimilate translocation, and cellular fine structure of potato cultivars (*Solanum tuberosum* L.) exposed to elevated CO<sub>2</sub>. – *Plant Physiology and Biochemistry* 130: 303-313.
- [20] Lee, H. Y., Hong, Y. N., Chow, W. S. (2001): Photoinactivation of photosystem II complexes and photoprotection by non-functional neighbours in *Capsicum annuum* L. leaves. – *Planta* 212: 332-342.
- [21] Li, X. M., Zhang, L. H. (2015): Endophytic infection alleviates Pb<sup>2+</sup> stress effects on photosystem II functioning of *Oryza sativa* leaves. – *Journal of Hazardous Materials* 295: 79-85.
- [22] Li, X. M., Chen, M. J., Li, J., Ma, L. J., Bu, N., Li, Y. Y., Zhang, L. H. (2014): Effect of endophyte infection on chlorophyll a fluorescence in salinity stressed rice. – *Biologia Plantarum* 58: 589-594.
- [23] Liu, C. H., Huang, W. D., Kao, C. H. (2012): The decline in potassium concentration is associated with cadmium toxicity of rice seedlings. – *Acta Physiologiae Plantarum* 34: 495-502.
- [24] Luo, H. H., Tsimilli-Michael, M., Zhang, Y. L., Zhang, W. F. (2016): Combining gas exchange and chlorophyll a fluorescence measurements to analyze the photosynthetic activity of drip-irrigated cotton under different soil water deficits – *Journal of Integrative Agriculture* 15(6): 1256-1266.
- [25] Meng, H. B., Hua, S. J., Shamsi, I. H., Jilani, G., Li, Y. L., Jiang, L. X. (2009): Cadmium-induced stress on the seed germination and seedling growth of *Brassica napus* L., and its alleviation through exogenous plant growth regulators. – *Plant Growth Regulation* 58: 47-59.
- [26] National Oceanic and Atmospheric Administration (NOAA) (2019): Carbon Dioxide Levels in Atmosphere Hit Record High in May. California. – <https://www.noaa.gov/news/carbon-dioxide-levels-in-atmosphere-hit-record-high-in-may>.

- [27] Singh, S., Singh, A., Bashri, G., Prasad, S. M. (2016): Impact of Cd stress on cellular functioning and its amelioration by phytohormones: an overview on regulatory network. – *Plant Growth Regulation* 80: 253-263.
- [28] Strasser, R. J., Srivastava, A., Govindjee (1995): Polyphasic chlorophyll a fluorescence transient in plants and cyanobacteria. – *Photochemistry and Photobiology* 61: 32-42.
- [29] Strasser, R. J., Tsimilli-Michael, M., Srivastava, A. (2004): Analysis of the Chlorophyll A Fluorescence Transient. – In: Papageorgiou, G. C., Govindjee (eds.) *Chlorophyll A Fluorescence. Advances in Photosynthesis and Respiration*. Springer, Dordrecht.
- [30] Strasser, R. J., Tsimilli-Michael, M., Qiang, S., Goltsev, V. (2010): Simultaneous in vivo recording of prompt and delayed fluorescence and 820-nm reflection changes during drying and after rehydration of the resurrection plant *Haberlea rhodopensis*. – *Biochimica et Biophysica Acta* 1797: 1313-1326.
- [31] Tsimilli-Michael, M., Strasser, R. J. (2008): In Vivo Assessment of Stress Impact on Plant's Vitality: Applications in Detecting and Evaluating the Beneficial Role of Mycorrhization on Host Plants. – In: Varma, A. (ed.) *Mycorrhiza*. Springer, Berlin.
- [32] Xiao, X., Zhang, J. X., Wang, H., Han, X. X., Ma, J., Ma, Y., Luan, H. J. (2019): Distribution and health risk assessment of potentially toxic elements in soils around coal industrial areas: a global meta-analysis. – *Science of The Total Environment* 713: 135292.
- [33] Xue, Z. C., Li, J. H., Li, D. S., Li, S. Z., Jiang, C. D., Liu, L. A., Wang, S. Y., Kang, W. J. (2018): Bioaccumulation and photosynthetic activity response of sweet sorghum seedling (*Sorghum bicolor* L. Moench) to cadmium stress. – *Photosynthetica* 56(4): 1422-1428.
- [34] Zou, Z. K., Wang, Y. Q., Huang, J. L., Lei, Z., Wan, F. T., Dai, Z. Y., Yi, L. C., Li, J. L. (2020): A study on the mixture repairing effect of biochar and nano iron oxide on toxicity of Cd toward muskmelon. – *Environmental Pollution* 266: 115371.

# THE AGROECOLOGICAL IMPACT OF DIFFERENT SOWING DATES AND ROW SPACING APPLICATIONS IN QUINOA (*CHENOPODIUM QUINOA* WILLD.)

ZULKADIR, G.

*Mersin University, Applied Technology and Management School of Silifke, Organic Farming Management Department, Silifke, Mersin, Turkey  
(e-mail: gulayzulkadir@gmail.com)*

(Received 21<sup>st</sup> Oct 2020; accepted 18<sup>th</sup> Dec 2020)

**Abstract.** Similar to all plants, the region of cultivation and sowing date of the quinoa (*Chenopodium quinoa* Willd.) plant leads to variations in phenological periods, affecting grain yield (GY) and quality. The present study aimed to determine the adequate sowing date and row spacing for Q-52 quinoa variety, which is known to be suitable for Mediterranean climate conditions, in Kahramanmaraş province. For this purpose, three different row spacing distances (Namely, 20, 40 and 60 cm) were adopted with four sowing dates at 15-day intervals between March 15 and May. The study findings demonstrated that the plant emergence period was 5.0-21.0 DAS, the budding period was 19.0-38.0 DAS, the 50% of flowering period was found as 44.7-67.3 DAS, the grain-filling period (GF) was fixed as 3.2-31.0 DAS, the growth period was realized as 88.0-131.7 DAS, the GY was calculated as 9.8-323.9 kg da<sup>-1</sup>, and biological yield (BY) was determined as 70.8-528.5 kg da<sup>-1</sup>. Considering the effects of the temperatures on the growth and development of plants, it was concluded that it would be adequate to sow the crops during early or late April. The analysis of the ideal row spacing demonstrated that the highest grain and plant yield was obtained at 20 cm spacing.

**Keywords:** *biological yield, climatic stress, grain yield, phenology, plant density*

## Introduction

Quinoa (*Chenopodium quinoa* Willd.) is a plant belonging to the Amaranthaceae / Chenopodiaceae family. Although it is known that quinoa has been cultured for 5000 years and is indigenous to South America, the cultivation of the plant is common globally (Mujica and Jacobsen, 2006). Quinoa is highly resistant to adverse environmental and climatic factors (Jacobsen, 2003) such as drought, salinity, poor soil, and frost and could be grown from the sea level up to an altitude of 4000 m (Jacobsen, 2003), between -8 °C and 38 °C ambient temperatures (Zurita-Silva et al., 2014).

The cultivation ecology of the plant directly affects the plant growth and development and determines the volume and quality of the harvest. In other words, although genotypes exhibit differences under different environmental conditions, the differences in total growth period also lead to differences in product quality. To harvest high yield and quality products in quinoa cultivation, it is very important to determine the most adequate cultivation period where the plant could reach technical and physiological maturity by selecting the most adequate variety for the vegetation period (Geren et al., 2014). Although generally low temperature, high relative humidity, and short-term sunlight exposure have negative effects on plants, this is a little different for quinoa. Quinoa is a facultative short-day plant (Tan and Temel, 2017) that should be sowed at the end of winter when the soil temperature is 8 °C and when it would not experience frost after sowing (Geren et al., 2014). Although the optimum growth temperature is generally 8-35 °C, higher than 28 °C temperatures during the 50% of flowering period significantly affect the grain yield (Etchevers and Avila, 1979). Especially during transition to

generative period and 50% of flowering periods, the plant is significantly affected during the photoperiod that lasts more than 12 hours (Christiansen et al., 2010).

To maximize yield and quality in quinoa cultivation, ensuring plant requirements that are consistent with environmental conditions during the development period could be achieved by the identification of the most adequate sowing period.

The present study aimed to determine the differences between phenological and yield properties of the quinoa plant by identifying the differences that could be observed in the total growth period with different sowing dates and different row spacing in Mediterranean climate conditions.

## Material and methods

### *The location and varieties*

The trials were conducted for 2 years in 2017 at Kahramanmaraş Eastern Mediterranean Transitional Zone of Agricultural Research Station (37° 32' 17.05" and 36° 55' 05.58") and in 2018 at Kahramanmaraş Sütçü İmam University Faculty of Agriculture, Department of Field Crops' Experimental Fields (37° 35' 8.3436" and 36° 49' 26.7600). The area where the study was conducted is a region where the typical Mediterranean climate is experienced, summers are hot and dry, winters are warm and rainy. In the study, the quinoa (*Chenopodium quinoa* Willd.) variety "Q-52", which is well adapted to Mediterranean climate conditions, was used as the plant material.

### *Applications and experimental design*

The study area was deep-plowed in early winter, and was prepared for sowing in March with plowing second-class tillage equipment. The study was designed with a random blocks trial pattern with 3 replications. Four sowing dates (Namely, 23 March, 6 April, 20 April, 11 May in 2017 and 26 March, 2 April, 13 April, 26 April in 2018) were determined for the trial. The plants were sowed with 20 cm, 40 cm and 60 cm (4 rows per lot) row spacing on the lines marked with a hand marker and at 1-2 cm depth. The size of the plots was 4 m<sup>2</sup>, 8 m<sup>2</sup> and 12 m<sup>2</sup>. The amount of seed used on the test plots was 1.8 kg da<sup>-1</sup> for 20 cm row space, 1.2 kg da<sup>-1</sup> for 40 cm row space and 0.6 kg da<sup>-1</sup> for 60 cm row space.

Based on the soil nutrient content (*Table 1*), the soil was fertilized with 6 kg da<sup>-1</sup> N, 6 kg da<sup>-1</sup> P and 6 kg da<sup>-1</sup> K as basic fertilizer before sowing. Then, when the plants were about 20 cm, net 7 kg<sup>-1</sup> N was applied as the second fertilization. Based on the climate conditions, the soil was irrigated based on the water requirement of the quinoa plant (*Table 2*).

**Table 1.** Some physical and chemical soil characteristics of experimental areas in the 2017-2018

Soil properties	2017		2018	
	Values	Comments	Values	Comments
Saturation (Saturation with Water) (%)	58.00	Clay-Loamy	79.00	Clay
pH	7.76	Light Alkaline	7.40	Neutral
EC dS m <sup>-1</sup>	0.32	Light Saline	0.11	Saltless
Lime (%)	24.48	More Lime	23.00	Limy
Organic Matter (%)	2.28	Middle	2.09	Middle
Useful Phosphorus (P <sub>2</sub> O <sub>5</sub> ) kg da <sup>-1</sup>	3.20	Low	5.62	Poor
Useful Potassium (K <sub>2</sub> O) kg da <sup>-1</sup>	98.64	High	61.2	High

**Table 2.** Some meteorological parameters of experimental areas at Kahramanmaraş in 2017 and 2018

Months	Max. Temperature (° C)		Min. Temperature (° C)		Average temperature (° C)		Total rainfall (mm)		Average moisture(%)	
	2017	2018	2017	2018	2017	2018	2017	2018	2017	2018
<b>March</b>	17.9	19.7	7.2	9.6	12.2	14.2	74.2	47.4	55.1	60.8
<b>April</b>	21.8	25.5	10.1	12	15.7	18.4	68.1	71.6	49.7	45.3
<b>May</b>	26.2	28.8	14.2	15.7	19.6	21.7	105.0	28.1	54.9	52.6
<b>June</b>	33.3	32.5	19.9	19.9	26.2	25.4	3.1	39.4	43.3	49.1
<b>July</b>	39.1	35.6	23.9	23.2	30.9	28.6	0.0	0.3	34.9	46.2
<b>August</b>	37.9	36.8	23.7	23.3	29.8	29.1	0.0	0.0	46.2	43.8
<b>September</b>	36.4	34.7	21.1	21.0	27.7	27.2	0.0	0.6	38.3	38.4
<b>Total (Season)</b>	212.6	213.6	120.1	124.7	162.1	164.6	176.2	140.0	322.4	336.2
<b>Average (Season)</b>	30.4	30.5	17.2	17.8	23.2	23.5	29.4	23.3	46.1	48.0

The analysis of the soil properties at the study areas where the two-year research was conducted revealed that the soil content at the test sites was low in phosphorus, adequate in potassium and moderate in organic matter. However, based on the year and location, soil saturation was determined as clayey-loamy and clayey, respectively, and the soil was slightly alkaline-neutral, slightly saline/non-saline, highly calcareous-calcareous (Table 1).

Certain climate data for the 2017-2018 cultivation year on the study area are presented in Table 2 (Anonim, 2019). As seen in Table 2, during the trial period, total and average precipitation amount was 176.2 and 29.4 mm for the first year, 140.0 and 23.3 mm for the second year. The average temperature was 23.2 °C during the 2017 cultivation period, the average temperature was 23.5 °C in the 2018 cultivation period. The mean relative humidity in Kahramanmaraş was 46.1% and 48.0% during the cultivation periods in 2017 and 2018, respectively.

### **Application**

In the study, plant emergence period (PE, DAS), transition to generative period (TG, DAS), 50% of flowering period (FP, DAS), grain filling period (GF, DAS), growing period (GP, DAS), grain yield (GY, kg da<sup>-1</sup>) by harvested the whole plots and biological yield (aboveground biomass) by harvested the whole plots (BY, kg da<sup>-1</sup>) parameters were analyzed.

### **Statistical analyses**

After obtaining data on the parameters studied, missing data values for the second year were statistically calculated. Analysis of variance was conducted with PROC GLM in SAS v.9.3 with randomized block trial data pattern. Averages were grouped with Duncan's multiple.

## Results and discussion

In the study, the effects of various sowing date and row spacing applications on the phenological stages, GY and plant yield properties of the quinoa plant were investigated. The year, sowing date, row spacing application and interactions between these parameters are presented in *Table 3a,b,c*.

**Table 3a.** Effect of different sowing dates and different row spacings on the phenological characteristics of quinoa in 2017 and 2018

	PE (DAS)	TG (DAS)	FP (DAS)	GF (DAS)	G (DAS)	GY (kg da <sup>-1</sup> )	BY (kg da <sup>-1</sup> )
<b>Years</b>	**	**	**	**	**	**	**
2017	12.316 A	32.506 A	61.000 A	26.250 A	113.501 A	207.128 A	351.430 A
2018	8.760 B	26.993 B	54.583 B	16.699 B	92.276 B	79.487 B	331.484 B
<b>Sowing Date</b>	**	**	**	**	**	**	**
23/26 March (I)	13.020 A	35.537 A	56.667 C	22.667 B	97.103 C	164.092 C	379.758 A
06/02 April (II)	8.532 B	29.509 C	51.722 D	26.722 A	96.594 C	178.486 B	343.036 B
20/13 April (III)	7.536 C	30.452 B	58.833 B	20.111 C	103.162 B	184.901 A	371.394 A
04 May/26 April (IV)	13.065 A	23.501 D	63.944 A	16.399 D	114.694 A	45.751 D	271.640 C
<b>Row Spacing (cm)</b>	NS	NS	NS	**	**	**	**
20 cm	10.534	29.768	57.625	21.667 A	102.477 B	221.655 A	401.596 A
40 cm	10.543	29.766	57.750	20.982 B	103.474 A	138.491 B	369.886 B
60 cm	10.538	29.715	58.000	21.775 A	102.715 B	69.776 C	252.888 C

\*\* : p>0.001; NS: Not significant; PE: Plant emergence period; TG: Transition to generative period; FP: 50% of flowering period; GF: Grain filling period; GP: Growth period; GY: Grain yield; BY: Biological yield

### Plant emergence period (DAS)

It was determined that the difference between the annual time periods between the sowing and emergence of the quinoa plants on the soil was statistically significant (p<0.001). It was determined that the emergence period in the second year (8.760 DAS) was shorter when compared to the first year (12.316 DAS). The analysis of the sowing dates demonstrated that there were significant differences between PEs (p<0.001) and the emergence period for the 3<sup>rd</sup> sowing date (7.536 DAS) was shorter when compared to the other sowing dates, and it was quite long for the 1<sup>st</sup> (13.020 DAS) and 4<sup>th</sup> sowing dates (13.065 DAS). It was determined that the differences in row distances did not affect the emergence period.

It was determined that there were statistically significant differences (p<0.01) between relative year x sowing date interactions. The in detail analysis of the year x sowing date interaction demonstrated that the earliest emergence was in the 3<sup>rd</sup> sowing in 2017 with 6.053 DAS and in the 1<sup>st</sup> sowing in 2018 with 5.010 DAS. On the other hand, the latest emergence was observed in 1<sup>st</sup> sowing in the first year (21.030 DAS), and in the 4<sup>th</sup> sowing (13.021 DAS) in the second year.

The analysis of the sowing dates demonstrated that the longer emergence period observed in March was due to the later germination of the plants induced by maximum and minimum temperatures although the average temperature was over 10 °C. On the other hand, although the temperatures were not low in May, problems were experienced with the emergence period and seedling development. This could be explained by both decreasing rainfall and increasing weed growth in this period (Hirich et al., 2014).

**Table 3b.** Effect of different sowing dates and different row spacings on the phenological characteristics of quinoa in 2017 and 2018

INTERACTIONS		PE (DAS)	TG (DAS)	FP (DAS)	GF (DAS)	G (DAS)	GY (kg da <sup>-1</sup> )	BY (kg da <sup>-1</sup> )
<b>Year X Sowing Date</b>		**	**	**	**	**	**	**
2017	I	21.030	38.004	64.000	20.000	99.189	235.911	450.847
	II	9.072	32.010	58.000	26.000	105.111	269.194	394.799
	III	6.053	32.010	60.000	31.000	118.323	283.616	467.593
	IV	13.109	28.000	62.000	28.000	131.381	39.790	92.480
2018	I	5.010	33.069	49.333	25.333	95.018	92.272	308.668
	II	7.992	27.008	45.444	27.444	88.078	87.778	291.273
	III	9.018	28.893	57.667	9.222	88.000	86.187	275.194
	IV	13.021	19.002	65.889	4.796	98.008	51.711	450.800
<b>Year X Row Spacing</b>		NS	NS	NS	**	**	**	**
2017	20 cm	12.319	32.506	61.000	26.250	112.677	323.880	327.838
	40 cm	12.302	32.507	61.000	26.250	114.681	204.559	443.033
	60 cm	12.328	32.506	61.000	26.250	113.146	92.944	283.418
2018	20 cm	8.748	27.031	54.250	17.083	92.277	119.431	475.354
	40 cm	8.783	27.025	54.500	15.713	92.268	72.423	296.739
	60 cm	8.749	26.923	55.000	17.300	92.283	46.608	222.359
<b>Sowing Date X Row Spacing</b>		NS	NS	NS	**	NS	**	**
I	20 cm	13.013	35.552	56.500	21.333	96.598	195.027	323.681
	40 cm	13.032	35.553	56.833	22.500	97.880	187.902	508.506
	60 cm	13.015	35.505	56.667	24.167	96.832	109.347	307.087
II	20 cm	8.553	29.510	52.000	27.000	95.853	322.190	434.760
	40 cm	8.520	29.505	51.333	26.333	97.100	151.840	374.299
	60 cm	8.523	29.512	51.833	26.833	96.830	61.428	220.049
III	20 cm	7.535	30.527	58.667	21.000	102.788	285.487	394.999
	40 cm	7.525	30.488	59.000	19.500	104.062	170.690	377.272
	60 cm	7.547	30.340	58.833	19.833	102.635	98.527	341.910
IV	20 cm	13.033	23.485	63.333	17.333	114.667	83.918	452.946
	40 cm	13.093	23.517	63.833	15.593	114.855	43.532	219.467
	60 cm	13.068	23.502	64.667	16.267	114.562	9.802	142.508

\*\* : p>0.001; NS: Not significant; PE: Plant emergence period; TG: Transition to generative period; FP: 50% of flowering period; GF: Grain filling period; GP: Growth period; GY: Grain yield; BY: Biological yield

### **Transition to generative period (DAS)**

The analysis of the period between the plant emergence and TG revealed that the differences based on the year and sowing date were significant (p<0.001), and row spacing did not significantly affect the TG. The annual analysis of the study findings demonstrated that the second year TG (26.993 DAS) was shorter when compared to the first year TG (32.506 DAS). The analysis of the reasons for these differences demonstrated that the average temperature was higher in 2018, and the plants received the required temperatures faster and hence, the transition to the generative period was faster in 2018 than 2017. It was suggested that the facts that the average precipitation was lower in 2017 as well as the average temperatures when compared to 2018 and the vegetative period was longer in 2017 were the other factors.

Sowing date analysis demonstrated that the fastest TG was observed in 4<sup>th</sup> sowing date with 23.501 DAS and the slowest TG was observed in the 1<sup>st</sup> sowing date with 35.537 DAS. It was suggested that that increasing temperatures and decreasing precipitation lead to the reduction in the vegetative development period in plants and early TG. In April sowing, it was observed that the plants were transformed to the generative period earlier. This was due to lower temperatures after April 15 and relatively higher precipitation after mid-April when compared to early April.

**Table 3c.** Effect of different sowing dates and different row spacings on the phenological characteristics of quinoa in 2017 and 2018

INTERACTIONS Year X Sowing Date X Row Spacing		PE (DAS)	TG (DAS)	FP (DAS)	GF (DAS)	G (DAS)	GY (kg da <sup>-1</sup> )	BY (kg da <sup>-1</sup> )	
		NS	NS	NS	**	NS	**	**	
2017	I	20 cm	21.037	38.003	64.000	20.000	98.060	284.627	287.960
		40 cm	21.027	38.007	64.000	20.000	100.893	271.410	676.150
		60 cm	21.027	38.003	64.000	20.000	98.613	151.697	388.430
	II	20 cm	9.133	32.010	58.000	26.000	103.647	524.087	507.420
		40 cm	9.037	32.010	58.000	26.000	105.973	216.840	450.343
		60 cm	9.047	32.010	58.000	26.000	105.713	66.657	226.633
	III	20 cm	6.037	32.010	60.000	31.000	117.597	426.517	426.517
		40 cm	6.023	32.010	60.000	31.000	120.150	276.733	528.467
		60 cm	6.100	32.010	60.000	31.000	117.223	147.597	447.797
	IV	20 cm	13.070	28.000	62.000	28.000	131.403	60.290	89.457
		40 cm	13.120	28.000	62.000	28.000	131.707	53.253	117.173
		60 cm	13.137	28.000	62.000	28.000	131.033	58.270	70.810
2018	I	20 cm	4.990	33.100	49.000	22.667	95.137	105.427	359.401
		40 cm	5.037	33.100	49.667	25.000	94.867	104.393	340.861
		60 cm	5.003	33.007	49.333	28.333	95.050	66.997	225.743
	II	20 cm	7.973	27.010	46.000	28.000	88.060	120.293	362.100
		40 cm	8.003	27.000	44.667	26.667	88.227	86.840	298.255
		60 cm	8.000	27.013	45.667	27.667	87.947	56.200	213.465
	III	20 cm	9.033	29.043	57.333	11.000	87.980	144.457	363.481
		40 cm	9.027	28.967	58.000	8.000	87.973	64.647	226.077
		60 cm	8.993	28.670	57.667	8.667	88.047	49.457	236.023
	IV	20 cm	12.997	18.970	64.667	6.667	97.930	107.547	816.435
		40 cm	13.067	19.033	65.667	3.187	98.003	33.810	321.761
		60 cm	13.000	19.003	67.333	4.533	98.090	13.777	214.205
<b>Average</b>		10.538	29.75	57.792	21.474	102.889	143.307	341.457	
<b>CV %</b>		1.177	0.332	1.908	2.671	0.775	3.691	5.499	

\*\* : p>0.001; NS: Not significant; PE: Plant emergence period; TG: Transition to generative period; FP: 50% of flowering period; GF: Grain filling period; GP: Growth period; GY: Grain yield; BY: Biological yield

It was determined that the impact of the interaction between years' x sowing date on TG was statistically significant, while the differences between other interactions were not statistically significant. The analysis of the data on year x sowing date interaction demonstrated that the shortest TG was observed with the 4<sup>th</sup> sowing date in both years (28.000 and 19.002 DAS). It was observed that the longest TG was obtained with the 1<sup>st</sup> sowing date (38.004 and 33.069 DAS) in both years. The fact that the temperatures were



above the optimum temperature required for plant development shortened the transition to the generative period. Accordingly, Bertero et al. (2004) reported that the plant growth and development stages could differ based on the time that the plant could receive the total heat it requires.

### ***Days to 50% of flowering period (DAS)***

The analysis of the data on FP, which is one of the important stages in plant development, demonstrated that differences between FP were significant ( $p < 0.001$ ) based on the year and sowing date parameters; however, the effect of row spacing on FP was not significant. The annual analysis demonstrated that the earliest 50% of flowering (54.583 DAS) was observed in 2018, while it was observed a little later (61.000 DAS) in 2017.

The analysis of the effect of sowing date on FP demonstrated that FP varied between 51.722 (2<sup>nd</sup> sowing) and 63.944 (4<sup>th</sup> sowing) DAS. The analysis of the FP based on the sowing date demonstrated that 50% of flowering took longer in May sowing due to the transition of the plant to the generative period coincided with long DAS, since quinoa is a short-day plant. Considering that the temperatures were relatively high in the first half of April when compared to March, and precipitation decreased gradually after the second half of April, and the DAS were extended from March to May at the study site.

The analysis of the interactions between the year and the applications demonstrated that the interaction between the year x sowing date was significant while, the other interactions were statistically insignificant. FP varied between 45.444 and 65.889 DAS for the year x sowing date interaction. Based on the study years, the earliest 50% of flowering was observed in the 2<sup>nd</sup> sowing in 2017, while the latest 50% of flowering was observed in the 1<sup>st</sup> sowing with 64 DAS. The earliest 50% of flowering was observed in the 2<sup>nd</sup> sowing in the second year with 45.444 DAS and the latest 50% of flowering was observed in the 4<sup>th</sup> sowing date with 65.889 DAS.

Belmonte et al. (2018) reported that FP varied between 53.8 and 57.7 DAS in quinoa genotypes grown in Parana, Brazil ecosystem. In that study, the findings of which were generally consistent with the present study results, Belmonte et al. (2018) utilized 16 genotypes, while a single variety was used in the current study. However, the range of the findings obtained with a single variety (54.6-61.0 DAS) was wider. The high difference in the findings was due to the differences in the annual climate data during the experiments.

### ***Grain filling period (DAS)***

The period between the 50% of flowering and completion of grain filling in at least 50% of the plants in the lot is an important period that affects the crop yield and quality. Thus, the analysis of the differences in this period is a significant issue. It was observed that the analyzed factors of the year, sowing date and row spacing significantly affected the GF in the study ( $p < 0.001$ ). Comparison of the grain filling time based on the study years demonstrated that the period was longer in the first year (26.250 DAS) when compared to the second year (16.699 DAS). The analysis of average annual temperatures during the experiment generally demonstrated that the average temperature was 2 °C higher in 2018 when compared to the previous year; however, the analysis of annual temperatures demonstrated that the lowest and highest temperatures fluctuated significantly, affecting the GF.

Comparison of the grain filling time based on the sowing date, the process varied between 16.399 and 26.722 DAS and the longest GF was observed in the 2<sup>nd</sup> sowing date and the shortest was observed in the 4<sup>th</sup> sowing date. The analysis of GF based on the sowing date in the present study demonstrated that the longest GF was due to the fact that the generative period coincided with longer days in the first half of April. It was observed that this period was longer when compared to March sowing. Consistent with the findings reported by Christiansen et al. (2010), this suggested that GF gets longer as the days get longer, and in later sowing dates, the period gradually shortens due to the longer daylight, and increasing temperatures counteract the impact of the longer days, maturing the plants faster.

The analysis of this factor based on row spacing demonstrated that 20 cm row spacing (21.667 DAS) and 60 cm row spacing (21.775 DAS) exhibited similar periods and there was no statistically difference; however, a shorter period was observed with the 40 cm row spacing when compared to the other two row spacing distances (20.982 DAS) and there was a significant difference between this and the others row spacing distances. While the impact of row spacing on the plant grain filling process was also significant, it was determined that shoots did not develop in dense sowing (20 cm spacing), the plant completed development on the main stem and was not exposed to the sun sufficiently, while in sparse sowing (60 cm spacing), higher number of shoots developed and maturation of the shoot clusters extended the period, and the fact that the periods were shorter in 40 cm row spacing demonstrated that the ideal row spacing was 40 cm for GF with the applied row spacing distances.

It was determined that the effects of the interactions between year x sowing date, year x row spacing, sowing date x row spacing, and year x sowing date x row spacing on quinoa plant GF were statistically significant in the study ( $p < 0.001$ ). It was found that the GF varied between 4.796 (2018; 4<sup>th</sup> sowing) and 31.000 (2017; 3<sup>rd</sup> sowing) DAS based on the year x sowing date interaction, the same period varied between 15.713 (2018; 40 cm) and 26.250 (2017; 20, 40 and 60 cm) DAS based on the year x row spacing interaction, it varied between 15.593 (4<sup>th</sup>; 40 cm) and 27.000 (2<sup>nd</sup>; 20 cm) DAS based on sowing date x row spacing interaction, and the GF varied between 3.187 (2018; 4<sup>th</sup>; 40 cm) and 31.000 (2017; 3<sup>rd</sup>; 20, 40 and 60 cm) DAS based on the year x sowing date x row spacing interaction.

### ***Growing period (DAS)***

The analysis of the effects of year, sowing date and row spacing on the quinoa plant GP demonstrated that all three factors led to differences in GP and the differences were statistically significant ( $p < 0.001$ ). GP differed based on the year, and it was observed that it was longer in the first year (113.501 DAS) when compared to the second year (92.276 DAS). It was observed that the difference was due to higher temperature fluctuations in 2018 when compared to 2017, although the average temperature was higher in 2018. The fact that the average temperature was higher in 2018 when compared to 2017 led to shorter plant GP. Also, the fact that the precipitation was lower in 2018, unlike the temperatures, allowed the plants to mature earlier. The decrease in relative humidity with precipitation shortened the maturation period.

The differences based on sowing date were between 97.103 (1<sup>st</sup>) and 114.694 (2<sup>nd</sup>) DAS and it was observed that the GP increased as the sowing date was delayed. This could be associated with the facts that the growth of quinoa, a short-day plant, coincided with shorter days in early April sowing dates when compared to later sowing dates, the

temperatures were at favorable degrees for the germination and development of quinoa and this season was rainier, leading to the minimum GP. Although the increase in temperatures in the following periods had a positive effect on the GP, prolongation of days, resulting higher radiation levels and low relative moisture due to lower precipitation extended the GP. It was observed that differences based on row spacing varied between 102.477 (20 cm) and 103.474 (40 cm) DAS; however, the differences in GP based on 20 cm row spacing and 60 cm row spacing were not statistically significant.

The analysis of the interactions between the factors that affected the quinoa plant GP demonstrated that the differences between year x sowing date and year x row spacing interactions were statistically significant ( $p < 0.001$ ). The individual analysis of the differences demonstrated that the growth time varied between 88.000 (2018; 3<sup>rd</sup>) and 131.381 (2017; 4<sup>th</sup>) DAS based on the year x sowing date interaction and between 92.268 (2018; 40 cm) and 114.681 (2017; 40 cm) DAS based on the interaction between years' x row spacing.

In the present study, it was observed that the GP varied between 87.68 and 133.06 DAS and these figures were significantly consistent with previous study findings. In other studies, it was reported that the total GP varied between 108 and 181 DAS (Jacobsen, 2003) in Denmark and 130 and 140 DAS (Szilagyi and Jørnsgård, 2014) in Romania. The finding that these variations were due to the variety (Jacobsen, 2003; Szilagyi and Jørnsgård, 2014), photoperiod and temperatures, sowing date, soil structure and climate conditions (Hirich et al., 2012) confirmed the present study findings.

### ***Grain yield (kg da<sup>-1</sup>)***

The analysis of the GY data demonstrated that the year, sowing date and row spacing factors led to significant ( $p < 0.001$ ) differences in GY. While the GY was 207.128 kg da<sup>-1</sup> in 2017, the same yield was only 79.487 kg da<sup>-1</sup> in 2018. The analysis of the caused for this decline suggested that the soil properties were better in the first year experiment and contained more salt and organic matter when compared to the soil where the second year trial was conducted, promoting plant development and grain formation, and the low precipitation regime and higher temperatures experienced in the second year reduced the grain formation and prevented the grains to reach maturity. On the other hand, the sudden and heavy rainfall in June produced floods, destroying several plants. The decrease in the plant count and heavy down pours led to the falling of the grains and hence low GY.

The analysis based on the sowing date demonstrated that the GY varied between 45.751 (4<sup>th</sup>) and 184.901 (3<sup>rd</sup>) kg da<sup>-1</sup>. It was suggested that ideal air and soil temperatures following the sowing and precipitation sufficient for grain formation and maturing led to the highest GY. On the other hand, the coincidence of the generative period with longer days in May sowing and the negative impact of high temperatures and low relative humidity on pollen viability led to low GY (Martinez et al., 2009; Hirich et al., 2014). Furthermore, the sudden increase in temperatures accelerated weed growth and negatively affected quinoa plants that have low competitiveness during first emergence and seedling periods and led to serious decreases in plant count. This indirectly led to low GY.

It was determined that row spacing led to a change in yield between 69.776 (60 cm) and 221.655 (20 cm) kg da<sup>-1</sup>. This suggested that the decrease in the number of plants per square meter led to a decrease in GY (Geren et al., 2015).

In addition to factors such as year, sowing date and row spacing, the interactions between these factors; year x sowing date, year x row spacing, sowing date x row spacing

and year x sowing date x row spacing interactions also led to differences in GY. It was found that the differences due to all interactions were statistically significant ( $p < 0.001$ ). GY values varied between 39.790 (2017; 4<sup>th</sup>) and 283.616 (2017; III) kg da<sup>-1</sup> based on year x sowing date, between 46.608 (2018; 60 cm) and 323.880 (2017; 20 cm) kg da<sup>-1</sup> based on year x row spacing interaction, between 9.802 (4<sup>th</sup>; 60 cm) and 322.190 (2<sup>nd</sup>; 20 cm) kg da<sup>-1</sup> based on sowing date x row spacing interaction, and between 13.777 (2018; 4<sup>th</sup>; 60 cm) and 524.087 (2017; 2<sup>nd</sup>; 20 cm) kg da<sup>-1</sup> based on year x sowing date x row spacing interaction.

It was determined that the GY values obtained in the study were generally consistent with the findings obtained in previous studies on quinoa. Gesisnski (2008) reported that GY varied between 25 and 500 kg da<sup>-1</sup> in various genotypes, Bhargava et al. (2007) reported that different genotypes led to GY between 32 and 983 kg da<sup>-1</sup> with different row spacing applications and Szilagyí and Jørnsgård (2014), on the other hand, reported GY values between 170 and 296 kg da<sup>-1</sup> in Romania using various genotypes.

### **Biological yield (kg da<sup>-1</sup>)**

The analyses conducted in the study demonstrated that the plant yield varied based on the differences between years, sowing dates and row spacing and these differences were statistically significant ( $p < 0.001$ ). Annual plant yield varied between 331.484 and 351.430 kg da<sup>-1</sup> and plant yield was higher in the first year when compared to the second year. It was suggested that the difference was due to soil and climate properties during the 2018 trial. Because, a flood that could only be seen twice in a century occurred in June 2018 and broke the small plant branches. While regular rains have a positive contribution to the yield (Kır and Temel, 2016), unexpected rains have negative effects.

The analysis of the plant yield based on sowing date revealed that the yield varied between 271.640 (4<sup>th</sup>) – 379.758 (1<sup>st</sup>) kg da<sup>-1</sup>. During the first sowing, the air and soil temperatures were lower when compared to the other sowing dates. However, the precipitation was quite high, and the plants met their water requirements during the vegetation period. While the decrease in precipitation during the May sowing led to a decrease in relative humidity, the increase in the temperatures also led to the receipt of required heat by the plants at an earlier date and transition of the plants to the generative period quickly. This results in a decrease in green plant sections and consequently reduces BY (Kaya et al., 2000). On the other hand, Geren et al. (2015) as they stated in their work, higher temperatures during the 4<sup>th</sup> sowing led to an increase in weed population in the cultivation fields and preventing shoot production by the quinoa seedlings and decreasing weight per unit area. Following the first sowing, the highest BY was obtained in 3<sup>rd</sup> sowing. In this period, although precipitation decreased when compared to the first sowing, the higher air temperatures increased BY by promoting the vegetative development of the plant (Sajjad et al., 2014).

In various row spacing applications, it was observed that the plant yield varied between 252.888 (60 cm) and 401.596 (20 cm) kg da<sup>-1</sup>. The higher plant count per decare in sowing parties with low row spacing led to higher BY in these lots.

In the experiments, it was determined that interactions between the year, sowing date and row spacing parameters that affected plant yield led to significant variations in plant yield as well ( $p < 0.001$ ). It was determined that plant yield varied between 92.480 (2017; 4<sup>th</sup>) and 467.593 (2017; 3<sup>rd</sup>) kg da<sup>-1</sup> based on year x sowing date interaction, and between 222.359 (2018; 60 cm) - 475.354 (2018; 20 cm) kg da<sup>-1</sup>; based on year x row spacing interaction, between 142.508 (4<sup>th</sup>; 60 cm) and 508.506 (1<sup>st</sup>; 40 cm) kg da<sup>-1</sup> based on the

sowing date x row spacing interaction, and between 70.810 (2017; 4<sup>th</sup>; 60 cm) and 816.435 (2018; 4<sup>th</sup>; 20 cm) kg da<sup>-1</sup> based on the year x sowing date x row spacing interaction.

It was observed that the present study BY findings were consistent with previous study findings. Shams (2012) reported BY figures between 232.2 and 278.7 kg da<sup>-1</sup>, Sajjad et al. (2014) reported BY figures between 619.0 and 763.4 kg da<sup>-1</sup>, and Kir and Temel (2016) reported BY figures between 550.8 and 780.6 kg da<sup>-1</sup>.

## Conclusion

In the study, where different sowing date and plant spacing applications were investigated in Q-52 quinoa variety cultivation in Kahramanmaraş province, where Mediterranean climate prevails, it was determined that it was important to ensure the first emergence of the plant, the temperatures above the seasonal norms during the emergence led to damages in seedlings, and weed competition was weak during the seedling period. It was observed that weed competition was good after the shooting period. It was determined that quinoa plant could be sown in March and April in the Mediterranean coast, and the desired yield could not be obtained in the following months. Considering GY and BY at various row spacing applications, it was concluded that 20 cm row spacing was adequate.

## REFERENCES

- [1] Anonim (2019): T.C. Ministry of forestry and water affairs, general directorate of meteorology, Kahramanmaraş.
- [2] Belmonte, C., de Vasconcelos, E. S., Tsutsumi, C. Y., Lorenzetti, E., Hendges, C., Coppo, J. C., Martinez, A. S., Pan, R., Brito, T. S., Inagaki, A. M. (2018): Agronomic and productivity performance for quinoa genotypes in an agroecological and conventional production system. – American Journal of Plant Sciences 9(04): 880. <https://doi.org/10.4236/ajps.2018.94067>.
- [3] Bertero, H. D., de la Vega, A. J., Correa, G., Jacobsen, S. E., Mujica, A. (2004): Genotype and genotype-by-environment interaction effects for grain yield and grain size of quinoa (*Chenopodium quinoa* Willd.) as revealed by pattern analysis of international multienvironment trials. – Field Crops Research 89: 299-318. <https://doi.org/10.1016/j.fcr.2004.02.006>.
- [4] Bhargava, A., Shukla, S., Rajan, S., Ohri, D. (2007): Genetic diversity for morphological and quality traits in quinoa (*Chenopodium quinoa* Willd.) germplasm. – Genetic Resources and Crop Evolution 54(1): 167-173. <https://doi.org/10.1007/s10722-005-3011-0>.
- [5] Christiansen, J., Jacobsen, S. E., Jørgensen, S. E. (2010): Photoperiodic effect on flowering and seed development in quinoa (*Chenopodium quinoa* Willd.). – Acta Agriculturae Scandinavica Section B Soil and Plant Science 60: 539-544. <https://doi.org/10.1080/09064710903295184>.
- [6] Etchevers, J., Avila, P. (1979): Agronomic behavior of quinoa cultivation (*Chenopodium quinoa* wild) in Chile. – Simiente 36(2).
- [7] Geren, H., Kavut, Y. T., Demiroğlu Topçu, G., Ekren, S., İştıpliler, D. (2014): Effects of different sowing dates on the grain yield and some yield components of quinoa (*Chenopodium quinoa* Willd.) grown under mediterranean climatic conditions. – Journal of Agriculture Faculty of Ege University 51(3): 297-305. <https://doi.org/10.20289/euzfd.46525>.

- [8] Geren, H., Kavut, Y. T., Altınbaş, M. (2015): Effect of different row spacings on the grain yield and some yield characteristics of quinoa (*Chenopodium quinoa* Willd.) under Bornova ecological conditions. – Journal of Agriculture Faculty of Ege University 52(1): 69-78. <https://doi.org/10.20289/euzfd.64719>.
- [9] Gesinski, K. (2008): Evaluation of the development and yielding potential of *Chenopodium quinoa* Willd. under the climatic conditions of Europe, Part One: accommodation of *Chenopodium quinoa* (Willd.) to different conditions. – Acta Agrobotanica 61(1): 179-184.
- [10] Hirich, A., Allah, R. C., Jacobsen, S. E., El Youssfi, L., El Homaria, H. (2012): Using deficit irrigation with treated wastewater in the production of quinoa (*Chenopodium quinoa* Willd.) in Morocco. – Revista Científica UDO Agrícola 12(3): 570-583.
- [11] Hirich, A., Choukr-Allah, R., Jacobsen, S. E. (2014): Quinoa in Morocco—effect of sowing dates on development and yield. – Journal of Agronomy and Crop Science 200(5): 371-377. <https://doi.org/10.1111/jac.12071>.
- [12] Jacobsen, S. E. (2003): The worldwide potential for quinoa (*Chenopodium quinoa* Willd.). – Food Rev. Int. 19(1-2): 167-177. <https://doi.org/10.1081/FRI-120018883>.
- [13] Kaya, N., Yılmaz, G., Telci, İ. (2000): Agronomic and technological properties of coriander (*Coriandrum sativum* L.) populations planted on different dates. – Turk J Agric For 24: 355-364.
- [14] Kır, A. E., Temel, S. (2016): Determination of seed yield and some agronomical characteristics of different quinoa (*Chenopodium quinoa* Willd.) variety and populations under dry conditions of Iğdir plain. – Iğdir Univ. J. Inst. Sci. & Tech. 6(4): 145-154. <https://doi.org/10.21597/jist.2016624166>.
- [15] Martínez, E. A., Veas, E., Jorquera, C., San Martín, R., Jara, P. (2009): Re-introduction of quinoa into arid Chile: cultivation of two lowland races under extremely low irrigation. – J. Agron. Crop Sci. 195: 1-10. <https://doi.org/10.1111/j.1439-037X.2008.00332.x>.
- [16] Mujica, Á., Jacobsen, S. (2006): La quinua (*Chenopodium quinoa* Willd.) y sus parientes silvestres. – Botánica Económica de los Andes Centrales, pp. 449-457.
- [17] Sajjad, A., Ehsanullah, H. M., Anjum, S. A., Tanveer, M., Rehman, A. (2014): Growth and development of *Chenopodium quinoa* genotypes at different sowing dates. – J. Agricultural Research 52(4): 535-546.
- [18] Shams, A. S. (2012): Response of quinoa to nitrogen fertilizer rates under sandy soil conditions. – Proc. 13<sup>th</sup> international Conf. Agron., Fac. of Agric., Benha Univ., Egypt, 9-10 September 2012, pp. 195-205.
- [19] Szilagyi, L., Jørnsgård, B. (2014): Preliminary agronomic evaluation of *Chenopodium quinoa* Willd. under climatic conditions of Romania. – Scientific Papers, Series A. Agronomy, Vol. LVII.
- [20] Tan, M., Temel, S. (2017): Studies on the adaptation of quinoa (*Chenopodium quinoa* Willd.) to eastern anatolia region of Turkey. – AGROFOR International Journal 2(2): 33-39.
- [21] Zurita-Silva, A., Fuentes, F., Zamora, P., Jacobsen, S. E., Schwember, A. R. (2014): Breeding quinoa (*Chenopodium quinoa* Willd.): potential and perspectives. – Mol. Breed. 34: 13-30. <https://doi.org/10.1007/s11032-014-0023-5>.

# EFFECT OF ENDOPHYTE INOCULATION ON THE ACCUMULATION OF MINERAL ELEMENTS AND ORGANIC ACIDS IN RICE (*ORYZA SATIVA* L.) UNDER OSMOTIC STRESS

LI, X. M.\* – LI, Y. Y. – MA, L. J. – WANG, L. L.\*

College of Life Science, Shenyang Normal University, No. 253 Huanghe North Street,  
Shenyang, Liaoning 110034, China

\*Corresponding authors

e-mail: lxmls132@163.com, wangqi5387402006@163.com

(Received 27<sup>th</sup> Oct 2020; accepted 21<sup>st</sup> Dec 2020)

**Abstract.** This study was conducted to investigate the effects of endophyte inoculation on the growth, mineral element and organic acid content of non-endophyte inoculated seedlings (E-) and endophyte inoculated seedlings (E+) of rice (*Oryza sativa* L.) under 0, 5, 10, 15 and 20% PEG for 7 days. Osmotic stress significantly decreased plant height, shoot dry weight and chlorophyll content of the E- and E+, but root length and dry weight were first increased and then decreased. Endophyte inoculation significantly increased plant height, shoot dry weight and chlorophyll content, but decreased root length and had no effects on root dry weight. Endophyte inoculation significantly increased the K, Ca, Mg, and P contents, but reduced the Ni content of the leaves and roots under osmotic stress, while it increased the Mn content of the leaves and the Na content of the roots. Under osmotic stress the E+ accumulated more fumarate in the leaves in comparison with the E-, as well as more malate, acetate, fumarate and oxalate in the roots. These results suggest that endophyte inoculation improved osmotic stress tolerance of rice seedlings by enhancing mineral uptake and organic acid accumulation. The application of endophytes has a beneficial effect on plant tolerance to osmotic stress.

**Keywords:** *plant-endophyte interaction, essential element, organic acid, tolerance*

## Introduction

Osmotic stresses include drought and salinity. Drought is the primary factor limiting global agricultural production (Sheshbahreh et al., 2019). Drought stress affects many physiological processes, including photosynthesis, assimilate transmission, cell expansion and mineral nutrient accumulation and transfer (Devnarain et al., 2016).

Essential elements have clear physiological roles, and plants cannot complete their life cycles without them. Generally, drought inhibits the uptake and transport of most mineral ions, resulting in nutrient deficiency (Salehi et al., 2016). Maintaining the uptake and homeostasis of mineral nutrients can enhance the resistance of plants to drought stress (Waraich et al., 2011). Water deficit conditions significantly diminish the P and K content of the shoots of *Matricaria chamomilla* (Salehi et al., 2016). In stressed apple plants, uptake of N, P, K, Ca, Mg, Fe, Mn, Cu, Zn, and B was decreased in comparison with that of well-watered plants (Liang et al., 2018).

In general, metal stress significantly increases the organic acid (OA) contents of various plant organs (Mahdavian et al., 2016), but the effects of drought stress on OAs vary. In response to water stress, the abundance of the majority of OAs decreased in wheat (Bowne et al., 2012), maize (Sicher and Barnaby, 2012) and creeping bentgrass (Jespersen et al., 2017). However, Timpa et al. (1986) reported that water-stressed cotton plants showed greater total amounts of organic acids (malate, citrate and oxalate) in comparison with irrigated plants. Under drought stress, citrate, fumarate and malate

accumulation was enhanced in the leaves of drought-tolerant wheat plants, but decreased in the roots (Kang et al., 2019). Moreover, drought stress increased the citrate content of potato leaflets (Barnaby et al., 2015) as well as the succinate content of maize leaves in a greenhouse study (Witt et al., 2012) and the malate content of thyme leaves (Ashrafi et al., 2018). Kim et al. (2017) found that acetate content is positively correlated with the survivability of crop plants such as wheat, rice, maize and canola. Moreover, OAs are intermediates involved in the assimilation of carbon and nitrogen, as well as osmotic regulation (Ashrafi et al., 2018).

The interaction between plants and endophytes is helpful for plants to deal with stress environment (Jung et al., 2012; Chinnaswamy et al., 2018). Plant growth promoting bacteria can improve the seed germination and enhance seedling growth of tomato under osmotic stress (Bhatt et al., 2015). Plant growth promoting rhizobacteria (PGPR) can alter the ion content of the leaves of tomato plants under salt stress (Van Oosten et al., 2018). Plant OAs such as oxalate and butyrate are by various stress (Ashraf and Harris, 2004). Endophytic fungus *Piriformospora indica* increased the amounts of malate, citrate and oxalate in the rhizosphere soil of *Brassica napus* seedlings (Wu et al., 2018). Soil, foliar, and soil + foliar applications of PGPR to promote strawberry yield also increased OA content under field conditions (Kitir et al., 2019).

Rice is very sensitive to osmotic stress at different growth stages (Swapna and Shylaraj, 2017; Nahar et al., 2018). In a previous study, we found that endophyte inoculation improves rice growth by enhancing the uptake of nutrient and altering the accumulation of OA under  $\text{Na}_2\text{CO}_3$  or Pb stress (Li et al., 2017, 2019). There is little information on the use of endophytes to improve the accumulation of OAs and uptake of minerals in plants under osmotic stress. Therefore, this study was to investigate the potential beneficial effects of endophyte application on rice seedling under osmotic stress.

## Materials and methods

### *Endophytic fungus and plant material*

Endophytic strain EF0801 was isolated from the leaves of *Suaeda salsa* grown under saline zones across China and screened for  $\text{Na}_2\text{CO}_3$  tolerance. Molecular identification of fungus EF0801 was based on internal transcribed spacer regions, which showed that it is congeneric to *Sordariomycetes* sp. (99% similarity). EF0801 was cultured on potato dextrose agar (PDA) plates at 4°C. To produce a 5% fungus culture, plates containing 75 mL of PDA solution were inoculated at the 3-day instar stage and cultured for 12 days at  $24 \pm 1^\circ\text{C}$  with shaking at 180 rpm. The resulting fungal cultures were used for the infection treatments. The experimental materials, rice (*Oryza sativa* L.) seeds (Liaoxing1') were provided by Shenyang Agriculture University, China. Seeds were sterilized with NaOCl for 10 min, rinsed, germinated and grown on Hoagland's solution in an illumination chamber.

### *Experimental treatments*

Three-day-old rice seedlings were divided into: non endophyte inoculated seedlings (E-) and endophyte inoculated seedlings (E+). E- were grown on Hoagland's solution, whereas E+ were grown on Hoagland's solution containing 5% fermentation broth, and endophyte EF0801 colonization was achieved via the rice roots. Each group (100 seedlings/pot) was exposed to 0 (control), 5, 10, 15 or 20% PEG-6000 (w/v in Hoagland



solution). Endophyte inoculation and PEG exposure were carried out simultaneously. According the method of Liu and Chen (2007) to determine the degree of endophyte inoculation. Roots were cleared in 20% KOH, acidified by 5% acetic acid and then stained. More than 90% of the E+ were colonized, whereas the E- were not colonized. The rice seedlings were cultured in an illumination chamber (28°C/22°C day/night, 14/10 h light/dark, 800  $\mu\text{mol m}^{-2}\text{s}^{-1}$  PPFD, and 80% air humidity). Fresh Hoagland's solution was added every day. After one week, the seedlings were collected and prepared for the analyses.

### ***Estimation of growth parameters***

Shoot height and root length of ten seedlings were recorded and then they were oven-dried at 80 °C for 48 h, after which the dry weight was measured.

### ***Estimation of chlorophyll (Chl) content***

Chlorophyll were extracted from fresh leaf with 80% acetone in the dark. Chl content was measured using the method reported by Lichtenthaler (1987).

### ***Estimation of mineral elements***

The leaves and roots of seedlings were oven-dried, ground and then pass through a 100-mesh sieve. Each sample (100 mg) was digested with HNO<sub>3</sub>/HClO<sub>4</sub> (5:1 [v/v]) at 2600 kPa for 30 min in a microwave oven and brought to 50 mL with ultrapure water. The contents of macroelements (K, Ca, Mg and P) and microelements (Fe, Zn, Mn and Ni) were estimated using an inductively coupled plasma atomic emission spectrometer (ICP model Liberty 200, Varian Australia Pty. Ltd., Mulgrave Victoria, Australia) as reported by Filek et al. (2012).

$$\begin{aligned} &\text{The percentage changes in measured elemental content per seedling} \\ &(\%) = [(\text{measured elemental content in E+}) - (\text{measured elemental} \quad (\text{Eq.1}) \\ &\quad \text{content in E-})]/(\text{measured elemental content in E-}) \times 100 \end{aligned}$$

### ***Estimation of OAs***

Fresh sample was ground in deionized water, incubated at 70 °C for 15 min, and centrifuged at 10,000  $\times g$  at 4 °C for 15 min. The supernatant was filtered, evaporated to dryness under reduced pressure at 40 °C, and then dissolved in ultrapure water to allow estimation of OAs by high performance liquid chromatography (Agilent 1200 HPLC System) according to the methods reported by Li et al. (2017).

### ***Data analysis***

The normality and homoscedasticity of the data were tested prior to statistical analysis. The effects of endophyte and osmotic stress were analyzed using two-way ANOVA. The threshold of significance for differences among the treatments was used LSD multiple comparisons ( $p < 0.05$ ).

## Results

### *Growth parameter and chlorophyll (Chl) content*

Osmotic stress significantly decreased the plant height and Chl content of the E- and E+ (Fig. 1), but first increased and then decreased root length (Table 1). Endophyte inoculation significantly increased plant height and Chl content, but significantly decreased root length under osmotic stress.

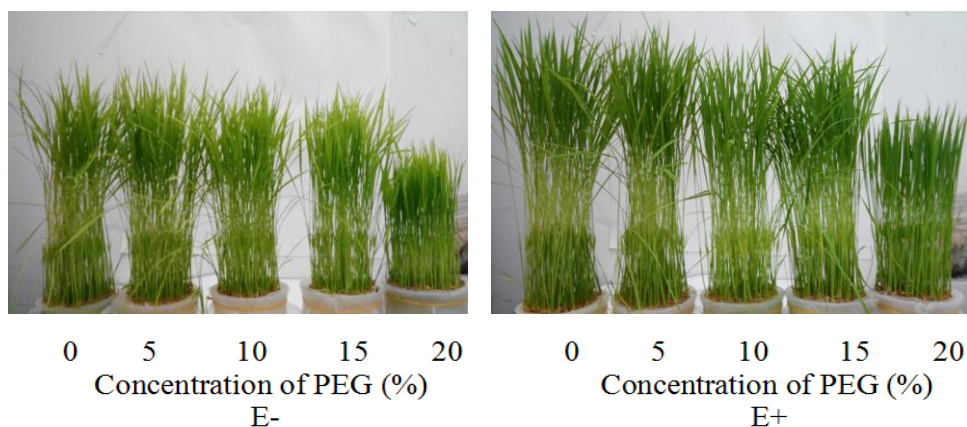


**Figure 1.** Effects of endophyte inoculation on the growth of rice seedlings subjected to osmotic stress

**Table 1.** Effects of endophyte inoculation on the growth, dry weight and Chl content of rice seedlings subjected to osmotic stress

Treatments	Plant height (cm)	Root length (cm)	Dry weight of shoots (mg/10 plant)	Dry weight of roots (mg/10 plant)	Chla+b content (mg/g·FW)
E-					
0	18.89±0.71cd	9.12±0.58b	70.68±4.29a	22.18±0.39bc	2.60±0.06c
5	17.75±0.95e	9.67±0.46a	54.76±3.09cd	24.77±0.36a	2.44±0.18cd
10	16.59±0.87f	7.94±0.56c	49.15±2.33de	22.31±0.23bc	2.30±0.15cd
15	14.94±0.90g	7.40±0.72cd	44.50±2.75ef	21.98±0.69c	2.13±0.18de
20	12.43±0.69i	6.90±0.73ed	39.37±2.67f	21.74±1.11c	1.82±0.13e
E+					
0	22.99±0.84a	8.03±0.73c	72.47±4.92a	22.34±0.65bc	3.74±0.22a
5	21.25±1.17b	8.80±0.66b	63.40±4.86b	25.09±0.66a	3.52±0.34ab
10	19.38±0.78c	7.22±0.41de	57.12±3.02bc	23.10±0.35b	3.36±0.26b
15	18.29±1.04de	7.06±0.86de	53.12±3.82cd	22.06±0.49c	2.58±0.18c
20	13.70±1.01h	6.36±0.56f	43.12±4.06ef	21.87±0.21c	2.23±0.20d

Values are the mean ± standard deviation of three replicates. Different letters indicate a significant difference at  $P < 0.05$  (LSD test)

Osmotic stress significantly decreased the shoot dry weight of the E- and E+, but first increased and then decreased the root dry weight (Table 1). Endophyte inoculation significantly increased the shoot dry weight under 5–15% PEG, but showed no effects on the root dry weight.

Osmotic stress significantly decreased the shoot dry weight of the E- and E+, but first increased and then decreased the root dry weight (*Table 1*). Endophyte inoculation significantly increased the shoot dry weight under 5–15% PEG, but showed no effects on the root dry weight.

### The elemental content of leaves

Osmotic stress significantly decreased the K and Fe contents of the E- (*Fig. 2A,D*). Endophyte inoculation significantly increased the K content of the leaves of plants subjected to 20% PEG, but it had no influence on Fe content.

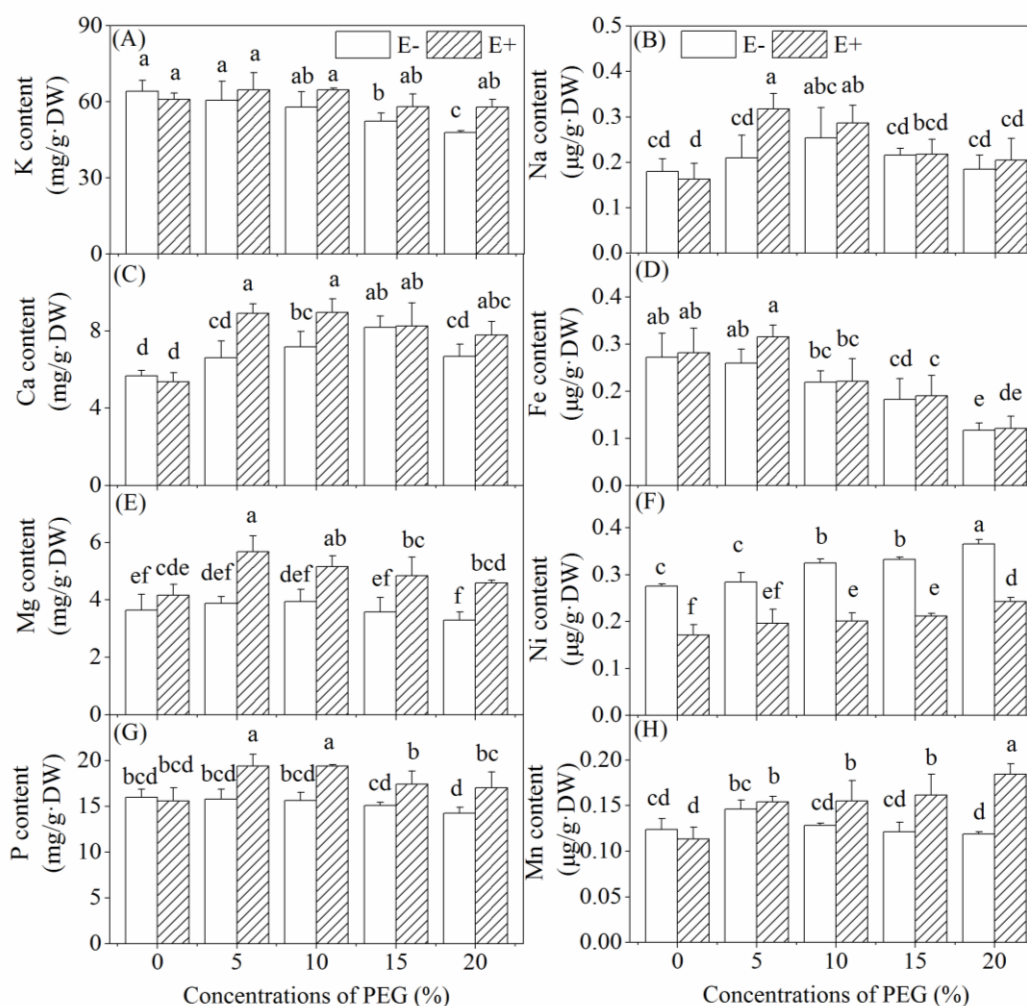


**Figure 2.** Effects of endophyte inoculation on the contents of macroelements (K, Ca, Mg and P) and microelements (Na, Fe, Ni and Mn) in the leaves of rice seedlings subjected to osmotic stress. The bars indicate the standard deviation ( $n=3$ ). Different letters indicate a significant difference at  $P < 0.05$  (LSD test)

Osmotic stress had no influence on the Na, Mg, P, or Mn contents in the leaves of the E- (*Fig. 2B,E,G,H*). In the E+ seedlings, osmotic stress increased Mn content, while it first increased and then decreased the Na, Mg and P contents. Endophyte inoculation significantly increased the Mg, P and Mn contents in plants subjected to osmotic stress

(except Mn in plants subjected to 5% PEG), while it only increased the Na content in plants subjected to 5% PEG.

Osmotic stress first increased and then decreased Ca content, while it increased Ni content in the leaves of E- and E+ (Fig. 2C,F). Endophyte inoculation significantly increased the Ca content of plants subjected to 5% and 10% PEG, but it significantly decreased Ni content under osmotic stress.

### The elemental content of roots

Osmotic stress had no influence on the K and Fe contents in the roots of the E- (Fig. 3A,D). Endophyte inoculation significantly increased the K content under 10–20% PEG, but increased the Fe content under no PEG.

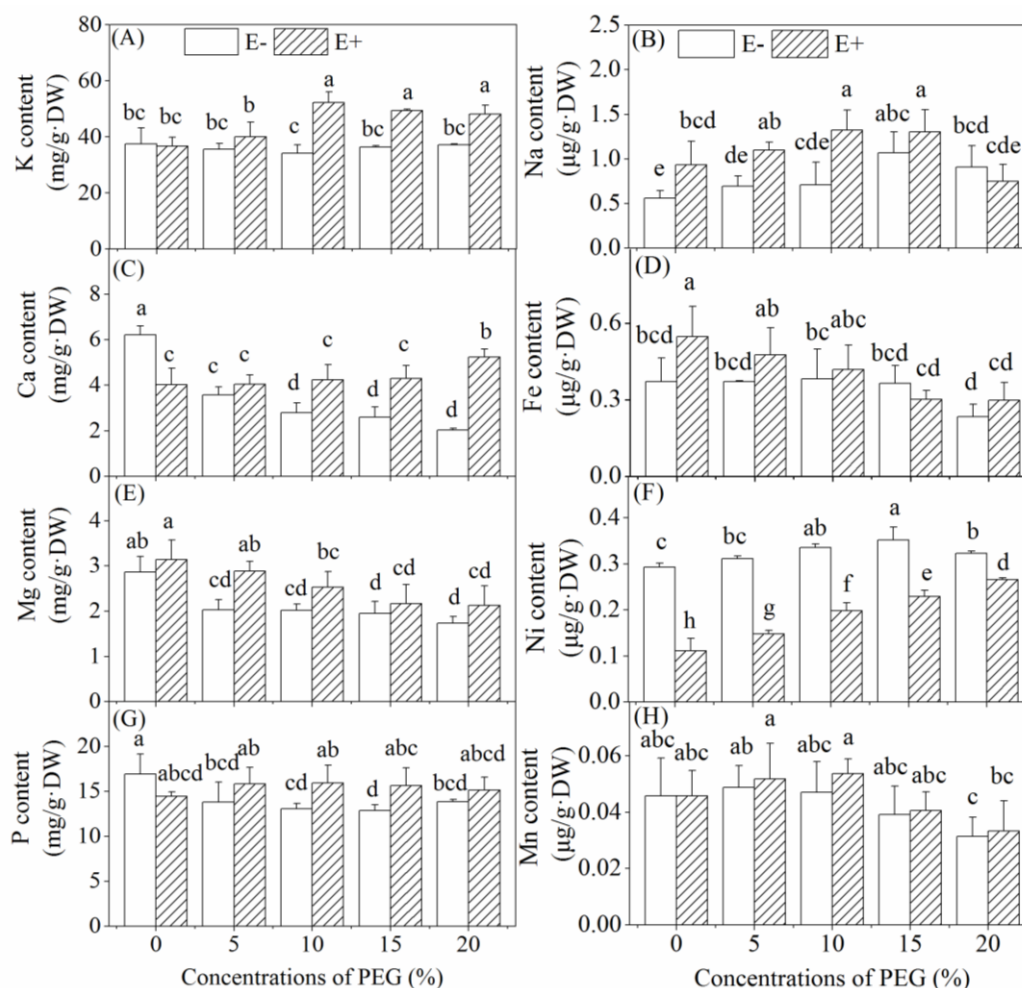


**Figure 3.** Effects of endophyte inoculation on the contents of macroelements (K, Ca, Mg and P) and microelements (Na, Fe, Ni and Mn) in the roots of rice seedlings subjected to osmotic stress. The bars indicate the standard deviation (n=3). Different letters indicate a significant difference at  $P < 0.05$  (LSD test)

Osmotic stress first increased and then decreased the Na and Ni contents in the roots of the E- (Fig. 3B,F). Endophyte inoculation significantly increased the Na content of

plants subjected to 0–10% PEG, but it significantly decreased Ni content under osmotic stress.

Osmotic stress significantly decreased the Ca, Mg, P, Mn contents in the roots of the E- (Fig. 3C,E,G,H). Endophyte inoculation significantly decreased the Ca content of plants under no PEG, but it significantly increased that of plants subjected to 10–20% PEG. Endophyte inoculation significantly increased the P content of plants subjected to 10% and 15% PEG, while it had no influence on the Mg or Mn contents of plants subjected to PEG, with the exception of increased Mg content in plants subjected to 5% PEG.

### *The percentage changes of elemental content*

For the percentage changes in the measured elemental content of the E+ relative to the E-, positive values show an increase, whereas negative values show a decrease according to Eq.1 (Table 2). Under osmotic stress, the percentage changes of most measured elements were positive values, which showed that the endophyte enhanced the total elemental content per seedling. However, the percentage change of Ni content was negative, which showed that the endophyte reduced the total Ni content per seedling.

**Table 2.** Effects of endophyte inoculation on the percentage changes in element contents per seedling subjected to osmotic stress

PEG (%)	K	Ca	Mg	P	Na	Fe	Ni	Mn
0	-2.28±0.51	-11.21±2.18	15.53±1.24	-3.64±0.61	29.98±3.47	18.92±3.14	-42.57±5.38	-5.33±1.13
5	21.62±6.14	48.08±4.44	64.73±7.15	34.78±2.63	66.42±5.89	36.33±4.55	-30.47±5.61	20.37±1.87
10	35.80±2.55	47.14±5.10	47.92±3.58	39.32±2.12	65.49±6.47	15.70±1.89	-31.61±3.16	37.42±3.61
15	33.28±3.74	26.60±1.74	51.11±6.02	32.99±3.41	21.83±2.28	3.69±1.37	-27.57±2.28	51.41±5.17
20	31.81±3.65	46.68±6.01	45.80±5.14	23.68±3.11	-6.92±3.16	20.87±4.47	-23.92±4.25	61.74±6.25

### *The OA content of leaves*

Osmotic stress significantly decreased the tartrate, citrate and fumarate contents (Fig. 4A,E,G). Endophyte inoculation showed no significant effects on the tartrate or citrate contents of the leaves in plants under osmotic stress, with the exception of the tartrate content in plants under 20% PEG and the citrate content in plants under no PEG. However, endophyte inoculation significantly increased the fumarate content of the leaves in the E+ under osmotic stress.

In contrast, osmotic stress significantly increased the acetate and lactate contents of the E- (Fig. 4C,D). The lactate content of the E- and E+ did not differ significantly except in those subjected to 20% PEG, while the acetate content of the E+ was significantly greater than that of the E- subjected to 0 and 20% PEG.

Osmotic stress first increased and then decreased the malate and succinate contents of the E- (Fig. 4B,F). The malate content of the E+ was significantly greater than that of E- subjected to no PEG, and the succinate content of the E+ was significantly greater than that of E- subjected to 0 and 10% PEG.

Osmotic stress and endophyte inoculation had no significant effects on the oxalate content in leaves (Fig. 4H).



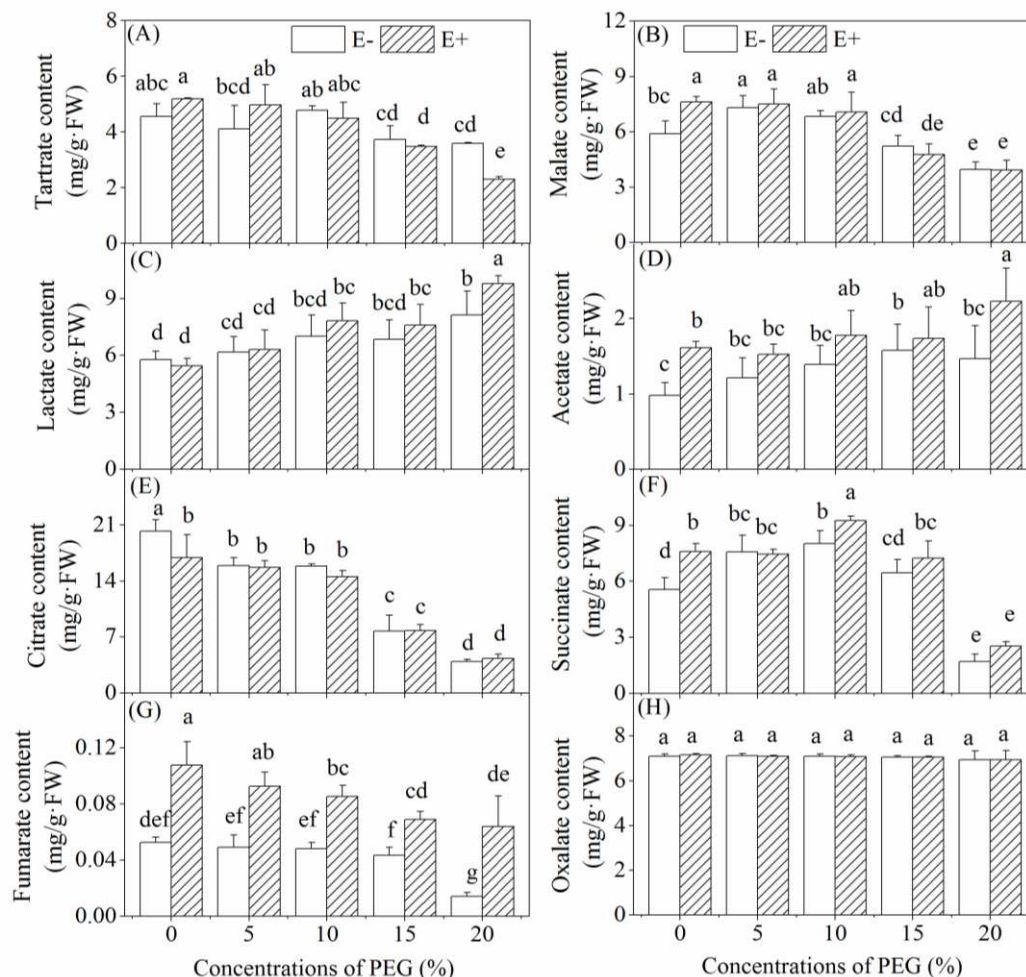


**Figure 4.** Effects of endophyte inoculation on the accumulation of eight OAs in the leaves of rice seedlings subjected to osmotic stress. The bars indicate the standard deviation ( $n=3$ ). Different letters indicate a significant difference at  $P < 0.05$  (LSD test)

### The OA content of roots

Osmotic stress significantly decreased the tartrate, malate, citrate and oxalate contents of the E- (Fig. 5A,B,E,H). Compared to the E-, the tartrate content in the roots of the E+ subjected to 5% PEG was significantly reduced, but it was significantly increased in those subjected to 20% PEG. The malate content of the E+ was significantly greater than that of the E- subjected to 10% and 20% PEG, while the oxalate content of the E+ was significantly greater than that of the E- seedlings subjected to 15% and 20% PEG. Endophyte inoculation had no significant effect on the citrate content in roots.

Osmotic stress significantly increased the lactate and succinate contents of the E- (Fig. 5C,F), but endophyte inoculation had no significant effect on either of these OAs.

Osmotic stress first decreased and then increased the acetate content (Fig. 5D), whereas first increased and then decreased the fumarate content of the E- (Fig. 5G). The acetate content of the E+ was significantly greater than that of E- subjected to 5% and 10% PEG. The fumarate content of the E+ was significantly lower than that of E- subjected to 5% PEG, but it was significantly greater than that of E- subjected to 15% and 20% PEG.

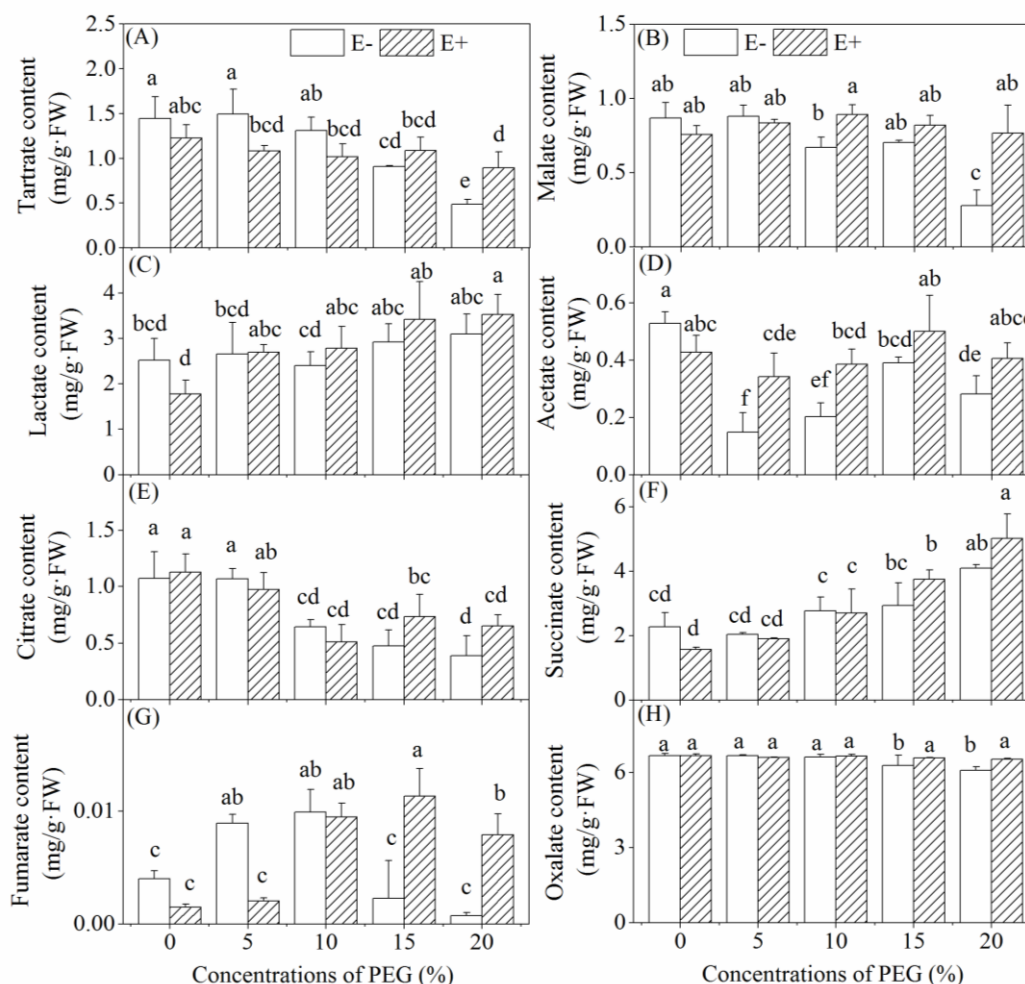


**Figure 5.** Effects of endophyte inoculation on the accumulation of eight OAs in the roots of rice seedlings subjected to osmotic stress. The bars indicate the standard deviation ( $n=3$ ). Different letters indicate a significant difference at  $P < 0.05$  (LSD test)

## Discussion

It is well established that osmotic stress significantly inhibits growth by plants (Swapna and Shylaraj, 2017; Nahar et al., 2018). We found that osmotic stress produced significant depressive effect on the rice growth (Table 1). PGPR has been shown to increase plant resistance to osmotic stress (Ghosh et al., 2019). Our results suggest that endophyte inoculation alleviated decreases in plant height, the shoot dry weight and Chl content caused by osmotic stress.

Ion-mediated up-regulation of xylem hydraulics plays an important role in optimizing the translocation of water and nutrients, as well as in regulating plant tolerance (Oddo et al., 2011). The water potential in soil significantly affected the uptake of mineral nutrients (Salehi et al., 2016). Drought stress prevents the absorption of mineral nutrients by tomato (Sánchez-Rodríguez et al., 2010). Salt stress decreased Ca, Mg, Fe, and Zn concentrations in lucerne and white melilot (Yasar et al., 2014). In this research, we found that osmotic stress significantly decreased the uptake of K and Fe by the leaves, as well as the uptake of Ca, Mg, and P by the roots. Sucre and Suárez (2011) suggest that plants increase

absorption of Na<sup>+</sup> when they are subjected to water stress. Similar to their results, we noted that the Na content of rice seedlings was significantly increased under low-concentration PEG. The content of microelement Ni in rice seedlings was significantly increased by osmotic stress, which could lead to toxicity.

Endophytes can improve the uptake of many mineral nutrients in plants (Song et al., 2014). Reestablishing the ionic homeostasis of plants under osmotic stress can increase plant resistance, which can decrease the severity of injuries caused by water deficits and alleviate growth inhibition (Waraich et al., 2011). We observed that endophyte inoculation enhanced accumulation of most mineral nutrients which alleviated the detrimental effect of osmotic stress on rice seedlings (Table 2). Increased abundance of mineral nutrients, particularly K, Ca, Mg and P, can improve the cell water potential, stomatal conductance, Chl content and photosynthetic rate of plants (Ruiz-Sánchez et al., 2010). Furthermore, endophyte inoculation inhibited accumulation of Ni under osmotic stress, which may have alleviated the toxic effect of excessive Ni on the E+.

OAs play a vital role in protecting plants from stress by regulating osmotic potential, ionic balance, and other cellular processes (Ma et al., 2011). Accumulation of OAs is an important process involved in the development of increased drought tolerance (Jespersen et al., 2017; Kang et al., 2019). In *Phyllanthus*, drought stress increased the abundance of OAs such as malic, succinic, and citric acids (Filho et al., 2018). Moreover, the increased abundance of OA, such as malate, citrate and oxalate, can improve drought tolerance of *ipt* transgenic creeping bentgrass (Merewitz et al., 2012). In this study, the lactate and succinate contents of rice increased as osmotic stress increased. However, Dickinson et al. (2018) found that legumes suffering from abiotic stress showed decreased abundance of many OAs, including malate and citrate. We also found that the tartrate, malate and citrate contents of rice decreased as osmotic stress increased. Griesser et al. (2015) reported increased abundance of citrate, succinate and tartarate in rapevine leaves under drought stress, while that of malate was decreased. These results suggest that different OAs change in different manners in response to stress.

Endophytes can modulate OA metabolism in plants (Singh et al., 2018). Wu et al. (2018) showed that the accumulation of OAs (oxalate, malate and citrate) in the rhizosphere of *Brassica napus* was improved by endophytic fungus *Piriformospora indica*. The tolerance of *Nicotiana benthamiana* to water stress was enhanced due to increased accumulation of some OAs as a result of the presence of fungal endophytes (Dastogeer et al., 2017). In this study, endophyte inoculation significantly enhanced the accumulation of fumarate in the leaves of rice seedlings, and the accumulation of malate, oxalate, fumarate in the roots, which indicated that the leaves and roots trigger different changes in OA metabolism to increase tolerance to water stress.

## Conclusions

Osmotic stress altered the accumulation of OAs and inhibited the uptake of nutrient element by rice seedlings, which alter plant growth and stress tolerance. The endophyte used in the present study is capable of enhancing accumulation of some OAs and improving nutrient absorption. The increased content of OAs and nutrient elements in E+ promoted rice growth, facilitated osmotic adjustment, and induced osmotic stress tolerance. These findings suggest that endophytes could be used to improve plant resistance to abiotic stress in an eco-friendly way. There are intricate interactions between



plant metabolism changes and each stress, so future study will investigate the signaling pathways involved in the activation of these metabolism changes.

**Acknowledgements.** This study was financially supported by grants from the National Natural Science Foundation of China (31470398, 31600314, and 31270369) and the Department of Education of Liaoning Province (LZD202004, LZD201901 and LJC201912). We thank SCINET for linguistic assistance during the preparation of this manuscript.

## REFERENCES

- [1] Ashraf, M., Harris, P. J. C. (2004): Potential biochemical indicators of salinity tolerance in plants. – *Plant Science* 166: 3-16.
- [2] Ashrafi, M., Azimi-Moqadam, M. R., Moradi, P., MohseniFard, E., Shekari, F., Kompany-Zareh, M. (2018): Effect of drought stress on metabolite adjustments in drought tolerant and sensitive thyme. – *Plant Physiology and Biochemistry* 132: 391-399.
- [3] Barnaby, J. Y., Fleisher, D., Reddy, V., Sicher, R. (2015): Combined effects of CO<sub>2</sub> enrichment, diurnal light levels and water stress on foliar metabolites of potato plants grown in naturally sunlit controlled environment chambers. – *Physiologia Plantarum* 153: 243-252.
- [4] Bhatt, R. M., Selvakumar, G., Upreti, K. K., Boregowda, P. C. (2015): Effect of biopriming with enterobacter strains on seed germination and seedling growth of tomato (*Solanum lycopersicum* L.) under osmotic stress. – *Proceedings of the National Academy of Sciences, India Section B: Biological Sciences* 85: 63-69.
- [5] Bowne, J. B., Erwin, T. A., Juttner, J., Schnurbusch, T., Langridge, P., Bacic, A., Roessner, U. (2012): Drought responses of leaf tissues from wheat cultivars of differing drought tolerance at the metabolite level. – *Molecular Plant* 5: 418-429.
- [6] Chinnaswamy, A., Coba de la Peña, T., Stoll, A., de la Peña Rojo, D., Bravo, J., Rincón, A., Lucas, M. M., Pueyo, J. J. (2018): A nodule endophytic *Bacillus megaterium* strain isolated from *Medicago polymorpha* enhances growth, promotes nodulation by *Ensifer medicae* and alleviates salt stress in alfalfa plants. – *Annals of Applied Biology* 172: 295-308.
- [7] Dastogeer, K. M. G., Li, H., Sivasithamparam, K., Jones, M. G. K., Du, X., Ren, Y. L., Wylie, S. J. (2017): Metabolic responses of endophytic *Nicotiana benthamiana* plants experiencing water stress. – *Environmental and Experimental Botany* 143: 59-71.
- [8] Devnarain, N., Crampton, B. G., Chikwamba, R., Becker, J. V. W., O'Kennedy, M. M. (2016): Physiological responses of selected African sorghum landraces to progressive water stress and re-watering. – *South African Journal of Botany* 103: 61-9.
- [9] Dickinson, E., Rusilowicz, M. J., Dickinson, M., Charlton, A. J., Bechtold, U., Mullineaux, P. M., Wilson, J. (2018): Integrating transcriptomic techniques and k-means clustering in metabolomics to identify markers of abiotic and biotic stress in *Medicago truncatula*. – *Metabolomics* 14: 126.
- [10] Filek, M., Walas, S., Mrowiec, H., Rudolphy-Skorska, E., Sieprawska, A., Biesaga-Koscielniak, J. (2012): Membrane permeability and micro- and macroelement accumulation in spring wheat cultivars during the short-term effect of salinity and PEG-induced water stress. – *Acta Physiologiae Plantarum* 34: 985-995.
- [11] Filho, E. G. A., Braga, L. N., Silva, L. M. A., Miranda, F. R., Silva, E. O., Canuto, K. M., Miranda, M. R., de Brito, E. S., Zocolo, G. J. (2018): Physiological changes for drought resistance in different species of *Phyllanthus*. – *Scientific Reports* 8: 15141.
- [12] Ghosh, D., Gupta, A., Mohapatra, S. (2019): Comparative analysis of exopolysaccharide and phytohormone secretions by four drought-tolerant rhizobacterial strains and their

- impact on osmotic-stress mitigation in *Arabidopsis thaliana*. – World Journal of Microbiology and Biotechnology 35: 90.
- [13] Griesser, M., Weingart, G., Schoedl-Hummel, K., Neumann, N., Becker, M., Varmuza, K., Liebner, F., Schuhmacher, R., Forneck, A. (2015): Severe drought stress is affecting selected primary metabolites, polyphenols, and volatile metabolites in grapevine leaves (*Vitis vinifera* cv. Pinot noir). – Plant Physiology and Biochemistry 88: 17-26.
- [14] Jespersen, D., Yu, J., Huang, B. (2017): Metabolic effects of acibenzolar-s-methyl for improving heat or drought stress in creeping bentgrass. – Frontiers in Plant Science 8: 1224.
- [15] Jung, S. C., Martinez-Medina, A., Lopez-Raez, J. A., Pozo, M. J. (2012): Mycorrhiza-induced resistance and priming of plant defenses. – Journal of Chemical Ecology 38: 651-664.
- [16] Kang, Z., Babar, M. A., Khan, N., Guo, J., Khan, J., Islam, S., Shrestha, S., Shahi, D. (2019): Comparative metabolomic profiling in the roots and leaves in contrasting genotypes reveals complex mechanisms involved in post-anthesis drought tolerance in wheat. – Plos One 14: e0213502.
- [17] Kim, J. M., To, T. K., Matsui, A., Tanoi, K., Kobayashi, N. I., Matsuda, F., Habu, Y., Ogawa, D., Sakamoto, T., Matsunaga, S., Bashir, K., Rasheed, S., Ando, M., Takeda, H., Kawaura, K., Kusano, M., Fukushima, A., Endo, T. A., Kuromori, T., Ishida, J., Morosawa, T., Tanaka, M., Torii, C., Takebayashi, Y., Sakakibara, H., Ogihara, Y., Saito, K., Shinozaki, K., Devoto, A., Seki, M. (2017): Acetate-mediated novel survival strategy against drought in plants. – Nature Plants 3: 17097.
- [18] Kitir, N., Gunes, A., Turan, M., Yildirim, E., Topcuoglu, B., Turker, M., Ozlu, E., Karaman, M. R., Fırlıdak, G. (2019): Bio-boron fertilizer applications affect amino acid and organic acid content and physiological properties of strawberry plant. – Erwerbs-Obstbau 61: 129-137.
- [19] Li, X., Ma, L., Bu, N., Li, Y., Zhang, L. (2017): Endophytic infection modifies organic acid and mineral element accumulation by rice under Na<sub>2</sub>CO<sub>3</sub> stress. – Plant and Soil 420: 1-11.
- [20] Li, X., Ma, L., Wang, L., Li, Y., Zhang, L. (2019): Endophyte infection enhances accumulation of organic acids and minerals in rice under Pb<sup>2+</sup> stress conditions. – Ecotoxicology and Environmental Safety 174: 255-262.
- [21] Liang, B., Ma, C., Zhang, Z., Wei, Z., Gao, T., Zhao, Q., Ma, F., Li, C. (2018): Long-term exogenous application of melatonin improves nutrient uptake fluxes in apple plants under moderate drought stress. – Environmental and Experimental Botany 155: 650-661.
- [22] Lichtenthaler, H. K. (1987): Chlorophylls and carotenoids: pigments of photosynthetic biomembranes. – Methods in Enzymology 148: 350-382.
- [23] Liu, R. J., Chen, Y. L. (2007): Mycorrhizology. – Science Press, 447p.
- [24] Ma, Y., Guo, L., Wang, H., Bai, B., Shi, D. (2011): Accumulation, distribution, and physiological contribution of oxalic acid and other solutes in an alkali-resistant forage plant, *Kochia sieversiana*, during adaptation to saline and alkaline conditions. – Journal of Plant Nutrition and Soil Science 174: 655-663.
- [25] Mahdavian, K., Ghaderian, S. M., Schat, H. (2016): Pb accumulation, Pb tolerance, antioxidants, thiols, and organic acids in metalcolous and non-metallicolous *Peganum harmala* L. under Pb exposure. – Environmental and Experimental Botany 126: 21-31.
- [26] Merewitz, E. B., Du, H. M., Yu, W. J., Liu, Y. M., Gianfagna, T., Huang, B. R. (2012): Elevated cytokinin content in ipt transgenic creeping bentgrass promotes drought tolerance through regulating metabolite accumulation. – Journal of Experimental Botany 63: 1315-1328.
- [27] Nahar, S., Sahoo, L., Tanti, B. (2018): Screening of drought tolerant rice through morpho-physiological and biochemical approaches. – Biocatalysis and Agricultural Biotechnology 15: 150-159.

- [28] Oddo, E., Inzerillo, S., La Bella, F., Grisafifi, F., Salleo, S., Nardini, A. (2011): Short-term effects of potassium fertilization on the hydraulic conductance of *Laurus nobilis* L. – *Tree Physiology* 31: 131-138.
- [29] Ruiz-Sánchez, M., Aroca, R., Muñoz, Y., Polón, R., Ruiz-Lozano, J. M. (2010): The arbuscular mycorrhizal symbiosis enhances the photosynthetic efficiency and the antioxidative response of rice plants subjected to drought stress. – *Journal of Plant Physiology* 167: 862-869.
- [30] Salehi, A., Tasdighi, H., Gholamhoseini, M. (2016): Evaluation of proline, chlorophyll, soluble sugar content and uptake of nutrients in the German chamomile (*Matricaria chamomilla* L.) under drought stress and organic fertilizer treatments. – *Asian Pacific Journal of Tropical Biomedicine* 6: 886-891.
- [31] Sánchez-Rodríguez, E., Rubio-Wilhelmi, M. M., Cervilla, L. M., Blasco, B., Rios, J. J., Leyva, R., Romero, L., Ruiz, J. M. (2010): Study of the ionome and uptake fluxes in cherry tomato plants under moderate water stress conditions. – *Plant and Soil* 335: 339-347.
- [32] Sheshbahreh, M. J., Dehnavi, M. M., Salehi, A., Bahreininejad, B. (2019): Effect of irrigation regimes and nitrogen sources on biomass production, water and nitrogen use efficiency and nutrients uptake in coneflower (*Echinacea purpurea* L.). – *Agricultural Water Management* 213: 358-367.
- [33] Sicher, R. C., Barnaby, J. Y. (2012): Impact of carbon dioxide enrichment on the responses of maize leaf transcripts and metabolites to water stress. – *Physiologia Plantarum* 144: 238-253.
- [34] Singh, D., Geat, N., Rajawat, M. V. S., Mahajan, M. M., Prasanna, R., Singh, S., Kaushik, R., Singh, R. N., Kumar, K., Saxena, A. K. (2018): Deciphering the mechanisms of endophyte-mediated biofortification of Fe and Zn in wheat. – *Journal of Plant Growth Regulation* 37: 174-182.
- [35] Song, M. L., Chai, Q., Li, X. Z., Yao, X., Li, C. J., Christensen, M. J., Nan, Z. B. (2014): An asexual *Epichloë* endophyte modifies the nutrient stoichiometry of wild barley (*Hordeum brevisubulatum*) under salt stress. – *Plant and Soil* 387: 153-165.
- [36] Sucre, B., Suárez, N. (2011): Effect of salinity and PEG-induced water stress on water status, gas exchange, solute accumulation, and leaf growth in *Ipomoea pes-caprae*. – *Environmental and Experimental Botany* 70: 192-203.
- [37] Swapna, S., Shylaraj, K. S. (2017): Screening for osmotic stress responses in rice varieties under drought condition. – *Rice Science* 24: 253-263.
- [38] Timpa, J. D., Burke, J. J., Quisenberry, J. E., Wendt, C. W. (1986): Effects of water stress on the organic acid and carbohydrate compositions of cotton plants. – *Plant Physiology* 82: 724-728.
- [39] Van Oosten, M. J., Stasio, E. D., Cirillo, V., Silletti, S., Ventorino, V., Pepe, O., Raimondi, G., Maggio, A. (2018): Root inoculation with *Azotobacter chroococcum* 76A enhances tomato plants adaptation to salt stress under low N conditions. – *BMC Plant Biology* 18: 205.
- [40] Waraich, E. A., Saifullah, A. R., Ehsanullah, M. Y. (2011): Role of mineral nutrition in alleviation of drought stress in plants. – *Australian Journal of Crop Science* 5: 764-777.
- [41] Witt, S., Galicia, L., Lisek, J., Cairns, J., Tiessen, A., Araus, J. L., Palacios-Rojas, N., Fernie, A. R. (2012): Metabolic and phenotypic responses of greenhouse-grown maize hybrids to experimentally controlled drought stress. – *Molecular Plant* 5: 401-417.
- [42] Wu, M., Wei, Q., Xu, L., Li, H., Oelmüller, R., Zhang, W. (2018): *Piriformospora indica* enhances phosphorus absorption by stimulating acid phosphatase activities and organic acid accumulation in *Brassica napus*. – *Plant and Soil* 432: 333-344.
- [43] Yasar, F., Uzal, Ö., Yasar, Ö., Ellialtioglu, Ş. (2014): Root, stem, and leaf ion accumulation in drought stressed green bean (*Phaseolus vulgaris* L.) genotypes treated with PEG-6000. – *Fresenius Environmental Bulletin* 23: 2656-2662.

## EFFECTS OF TRANSPLANTING CONDITIONS AND WATER MANAGEMENT ON THE YIELD, QUALITY AND AROMA OF FRAGRANT RICE

TONG, T. Y.<sup>1,2#</sup> – ZHANG, J. S.<sup>1,2#</sup> – LI, L.<sup>1,2#</sup> – LUO, H. W.<sup>1,2#</sup> – HE, R. J.<sup>3#</sup> – CAI, J. X.<sup>1</sup> – MA, L.<sup>1,2</sup> – MO, Z. W.<sup>1,2</sup> – TANG, X. R.<sup>1,2\*</sup>

<sup>1</sup>*Department of Crop Science and Technology, College of Agriculture, South China Agricultural University, 510642 Guangzhou, PR China*

<sup>2</sup>*Scientific Observing and Experimental Station of Crop Cultivation in South China, Ministry of Agriculture, 510642 Guangzhou, PR China*

<sup>3</sup>*College Of Agriculture, Forestry, Medicine and Technology, Hainan Radio and Tv University, 570208 Hainan, PR China*

*#These authors have contributed equally to this work*

*\*Corresponding author*

*e-mail: tangxr@scau.edu.cn; phone/fax: +20-8528-0204-618*

(Received 29<sup>th</sup> Jun 2020; accepted 6<sup>th</sup> Oct 2020)

**Abstract.** To explore the effects of transplanting conditions and water treatments on the yield, quality and aroma of fragrant rice, a field experiment was conducted with conventional fragrant rice cultivars, “Meixiangzhan 2” and “Xiangyaxiangzhan”, as plant materials. Four treatments were designed: (DR) dry transplanted + rainfed, (DC) dry transplanted + conventional irrigation treatments, (WR) water transplanted + rainfed, (WC) water transplanted + conventional irrigation treatments. The highest 1000-grain weight were recorded under the WR treatment, and this treatment was more beneficial to the export and accumulation of assimilates during rice growth. The average yield of the two fragrant rice cultivars in both seasons were WC > WR > DR > DC. The milled rice rate and head rice rate were maximized in WR treatment, also minimized in chalkiness and chalky grain rate in the case of all except WC treatments in the early season. Compared with WC and DC treatments, average content of 2-acetyl-1-pyrroline (2-AP) under WR and DR treatments increased by 24.11%. In conclusion, we considered WR treatment as the optimum water saving treatment for yield increase and quality improvement, as well as for increasing the aroma of fragrant rice grains.

**Keywords:** *rice, rainfed, aroma-related enzymes, 2-acetyl-1-pyrroline, yield*

### Introduction

Rice (*Oryza sativa* L.), as an important food crop, is consumed by more than half of the world’s population, and the main rice cultivars are only grown in Asia (Abid et al., 2015).

Due to its unique flavor and superior grain qualities, the fragrant rice fetches premium prices in international markets and demands are grown dramatically in recent years (Deng et al., 2018). Among the more than 100 volatile components, the aromatic compound 2-acetyl-1-pyrroline (2-AP) is the main reason for the aroma of fragrant rice (Hashemi et al., 2013). Relevant studies have confirmed that the aroma of fragrant rice is not only affected by the genetics of fragrant rice itself, but also has an important relationship with its growth and cultivation environment. The yield formation and 2-AP biosynthesis of fragrant rice were affected by many environmental factors and agronomic measures (Kong et al., 2020). In various cultivation measures, water management as an important cultivation and management measure has been concerned

by predecessors, in which dry-wet alternative irrigation, as a new irrigation technique, has been adopted by many countries (Marchesi et al., 2019; Graham Acquah et al., 2019). Dry-wet alternative irrigation regulated the precursors' accumulation, enzymes activities and genes expression of the enzymes that regulate the production of 2AP in both rice cultivars (Bao et al., 2018a).

Related studies have shown that light water-controlled irrigation can increase the aroma content of fragrant rice grains and decrease the chalky grain rate, and it is the best cultivation measure for high yield and high quality of fragrant rice (Tian et al., 2018). Strong water stress affected the physiological activity of rice in the later stage and reduced the synthesis and accumulation of 2-AP in fragrant rice, so water had a great influence on the aroma of fragrant rice (Wang et al., 2013).

Predecessors had a detailed description of intermittent irrigation and water-saving irrigation, but there were few reports on the effects of water treatment before sowing and the whole cultivation process of fragrant rice on the yield, quality and aroma of fragrant rice. To explore the differences in yield, quality and aroma of fragrant rice, two fragrant rice cultivars, "Meixiangzhan-2" and "Xiangyaxiangzhan", which were widely planted in South China, were used as experimental materials. The purpose of this study is to provide a theoretical basis for high yield, quality and more aroma of fragrant rice.

## Materials and methods

### *Experimental details*

A two-season field experiment was conducted in the Experimental Research Farm, College of Agriculture, South China Agricultural University, Guangzhou (23°09' N, 113°22' E and 11 m from mean sea level), in China in 2019. The physical and chemical properties of soil in the early season were as follows: pH 6.5, organic matter content 22.63 g/kg, total nitrogen 1.56 g/kg, total phosphorus 1.43 g/kg, total potassium 23.97 g/kg, available potassium 90.32 mg/kg, available phosphorus 75.70 mg/kg; Physical and chemical properties of soil in late season: pH 6.2, organic matter content 25.63 g/kg, total nitrogen 1.66 g/kg, total phosphorus 1.57 g/kg, total potassium 22.83 g/kg, available potassium 92.32 mg/kg, available phosphorus 45.63 mg/kg.

Two fragrant rice cultivars, "Meixiangzhan 2" (Lemont × Fengaozhan) and "Xiangyaxiangzhan" (Xiangsimiao 126 × Xiangyaruanzhan), were used as materials in the experiment. Those cultivars are well-known and widely grown in South China. The split zone test design is adopted in the experiment.

The soil conditions at transplanting were set as: dry transplanted treatment (D): the former cropping was not soaked after harvest. 5 days after harvest, rotary tillage machine was used for dry rotary tillage once and the second dry rotary tillage was carried out 3 days before transplanting rice seedlings. Water transplanted treatment (W): irrigation was carried out 3-4 cm in the field 10 days before transplanting. After keeping water for 3 days, the rotary tillage was used to rotate once. The water treatments were set as: rainfed (R), if there is no wilting of the seedlings after transplanting, no artificial irrigation was carried out. If wilting occurred, irrigation was carried out to ensure that the rice would not die. In conventional irrigation treatments (C) shallow water was maintained at the early stage, then drained and exposed the field after enough seedlings, 3-4 cm irrigation was carried out at the beginning of young panicle differentiation, then kept dry and wet alternately from booting stage to breaking stage, then kept in shallow water layer after heading to facilitate filling and fruiting, and water was cut off 5-6 days before harvest. The plot sizes of the four

treatments were  $10.5 \times 7 \text{ m}^2$ . Each treatment special fertilizer was applied for fragrant rice ( $\text{N} + \text{P}_2\text{O}_5 + \text{K}_2\text{O} \geq 6\%$ , organic matter  $\geq 25\%$ )  $750 \text{ kg/hm}^2$  at the tillering stage, and ridges were built between plots (40 cm wide and wrapped in plastic) to keep water and fertilizer. The seeds of both rice cultivars were surface sterilized with a 5% sodium hypochlorite solution and then immersed in water for 12 h and allowed to germinate in a dark thermostatic incubator at  $38 \text{ }^\circ\text{C}$  for 12 h. The germinated seeds were sown in PVC trays for nursery raising, then, PVC trays were placed in puddled field and covered with a plastic sheet. 15-day-old seedlings were transplanted to the field. Geminated seeds of both cultivars were sown on the 9th March, 2019 (early season) and the 15th July 2019 (late season) for nursery rising. Seedlings were transplanted in puddled field on the 26th March and the 2nd August, 2019 for early and late season, respectively, and harvested on 14th July (early season) and 7th November (late season) (Fig. 1).

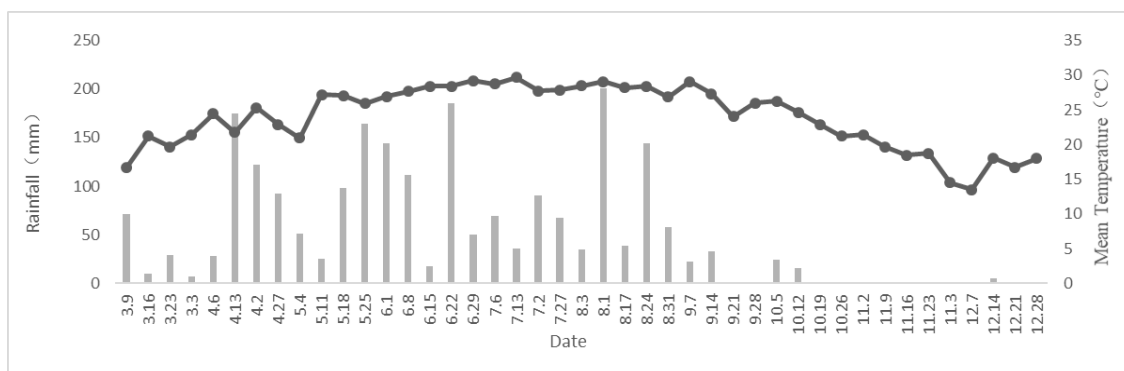


**Figure 1.** Mean weekly temperature and rainfall during the experiment

### **Treatments and plant sampling**

Experimental treatments were carried out as described:

- DR: dry transplanted + rainfed,
- DC: dry transplanted + conventional irrigation treatments,
- WR: water transplanted + rainfed,
- WC: water transplanted + conventional irrigation treatments.

Nine random rice plants from each plot were collected for estimation of accumulation and assimilation of photosynthetic matter, aroma-related enzymes and 2-acetyl-1-pyrroline (2-AP) in grains in the tillering stage (early season April on 26th, late season on September 5th), booting stage (early season on the 19th May, late season on the 24th September), full heading stage (early season on the 11th June, late season on the 10th October), 15 days after heading (early season on the 26th June, late season on the 25<sup>th</sup> October), and mature stage (early season on the 4<sup>th</sup> July, late season on the 13<sup>th</sup> November).

### **Accumulation and assimilation of photosynthetic matter**

The leaf area was measured according to the methods of Tao et al. (2006). According to the average tiller number of the community, 6 hills of rice plants with the same growth pattern were taken. The leaf area of rice samples was measured by the product of length and width of 15 flag leaves. Then the tissues of different parts of rice were cut and dried at  $105 \text{ }^\circ\text{C}$  for 30 min and dried in oven at  $80 \text{ }^\circ\text{C}$  for 30 min. The dry matter

mass was measured to determine the community growth rate (CGR) and net assimilation rate (NAR).

$$\text{CGR}(\text{g}/(\text{m}^2 \cdot \text{d})) = (W2 - W1)/(t2 - t1)$$

$$\text{NAR}(\text{g}/(\text{m}^2 \cdot \text{d})) = [(\ln \text{LAI}_2 - \ln \text{LAI}_1)/(\text{LAI}_2 - \text{LAI}_1)] \times [(W2 - W1)/(t2 - t1)]$$

where LAI1 and LAI2 are the leaf area index measured before and after, t1 and t2 are the time of the two measurements, and W1 and W2 are the dry matter mass measured before and after the two measurements.

### ***Aroma-related enzymes and 2-acetyl-1-pyrroline (2-AP) in grains***

According to the average number of tillers of the population, 3 hills of rice samples with the same growth were taken back to the laboratory, the tissues of different parts (including the leaves, stems and grains) of rice were quickly separated and placed in liquid nitrogen. The leaves, stems and grains were placed in the refrigerator at -80 °C.

The determination method of proline refers to the method of Huang et al. (2012). The contents of pyrroline-5-carboxylic acid (P5C) were measured according to the method of Luo et al. (2019). Ornithine aminotransferase (OAT) activity was assayed according to the method devised by Bao et al. (2018b), the measurement of methylglyoxal refers to the method of Hasanuzzaman et al. (2019), and the determination method of aroma (2-AP) in grains refers to the method of Du et al. (2019). The measurements were repeated in triplicate and averaged.

### ***Measurement of yield and yield-related traits***

One community sample area (1 m<sup>2</sup>) from each experimental plot was harvested at maturity, then threshed manually and sun-dried. 30 random hills of rice plants in each plot were sampled for calculating the average effective panicle number per hill. The above measures have been repeated thrice. According to the average number of effective panicles, 5 representative plants were randomly selected to determine the number of grain count per panicle, seed setting rate and 1000-grain weight.

### ***Measurement of grain quality***

After sun-dried, grains were stored at room temperature for at least three months to determine grain quality attributes. Rice grains from each treatment was taken from storage and brown rice rate was estimated using a rice huller (Jiangsu, China) while milled rice and head rice recovery rates were calculated by using a Jingmi testing rice grader (Zhejiang, China). Grains with chalkiness and chalky grain rate were estimated by using an SDE-A light box (Guangzhou, China) while an Infratec-1241 grain analyzer (FOSS-TECATOR) was used to determine the grain amylose and protein contents.

### ***Statistical analyses***

All statistical analyses were performed by using Statistix 8 (Analytical software, Tallahassee, Florida, USA). Two factors (transplanting conditions and water management) and their interactions had been tested. The data were analyzed by one-

way analysis of variance and the differences amongst means were separated by using least significant difference (LSD) test at 5% significance level.

## Results

### Community growth rate and net assimilation rate

As shown in *Table 1*, for Meixiangzhan 2, the highest community growth rate (CGR) was recorded under the WR treatment, in all except for WC treatment from booting stage to 15 days after heading in the early season, and the trend of net assimilation rate (NAR) from booting stage and 15 days after heading in early season were the same: WR > WC = DC > DR. In late season, the CGR under WR treatment was the highest at tillering stage, and the NAR had the same trend. For Xiangyaxiangzhan, there was no significant regular change in the treatments in the early season, and the CGR was the highest under WR treatment at tillering stage, and the NAR under WR treatment was also significantly higher than that of DC and WC treatment at tillering stage.

**Table 1.** Effects of transplanting conditions and water management on CGR and NAR of fragrant rice

Season	Cultivar	Treatment	CGR(g·m <sup>-2</sup> ·d <sup>-1</sup> )			NAR(g·m <sup>-2</sup> ·d <sup>-1</sup> )		
			T-B	B—H	H-HA	T-B	B—H	H-HA
Early	Meixiangzhan 2	DR	14.23±2.59b	10.53±2.51b	8.89±2.99b	4.74±1.36b	1.98±0.47b	2.21±0.74b
		DC	15.43±1.89b	8.36±3.39b	10.76±2.91ab	4.83±1.13b	2.38±1.51ab	2.83±0.76ab
		WR	14.27±3.45b	17.98±0.31a	14.09±3.29a	3.69±1.46c	3.72±0.06a	3.08±0.72a
		WC	21.55±2.52a	23.41±3.19a	10.76±2.15ab	5.28±1.31a	2.44±0.6ab	2.42±0.48ab
	Xiangyaxiangzhan	DR	14.17±3.45ab	8.24±4.85c	9.43±4.44b	5.32±1.32a	1.98±0.98b	2.74±1.05a
		DC	11.61±2.58b	25.87±3.28a	3.49±0.89c	4.53±1.41a	4.87±1.29a	1.35±0.77b
		WR	17.32±1.18a	9.82±0.14c	9.09±4.32b	5.75±0.39a	3.85±1.47ab	2.17±0.36a
		WC	12.29±1.59b	17.11±2.26b	18.26±4.65a	4.55±1.01a	4.62±1.47a	2.23±1.32a
Late	Meixiangzhan 2	DR	12.61±1.17ab	21.59±0.26a	13.48±1.97b	5.21±0.68a	5.08±0.08b	3.69±0.65a
		DC	13.16±2.59ab	22.21±0.56a	16.21±4.41a	3.74±0.74b	6.82±1.04a	3.05±0.51a
		WR	16.56±1.44a	15.26±4.92b	13.57±4.55b	5.01±0.44a	2.62±0.51c	3.31±0.94a
		WC	10.56±4.54b	20.42±1.62a	17.58±2.81a	2.31±0.71c	3.92±1.05b	3.37±0.71a
	Xiangyaxiangzhan	DR	19.13±4.79a	9.98±2.24c	16.03±4.36b	4.27±0.73a	2.19±0.55c	3.28±1.23b
		DC	18.56±4.96ab	8.28±4.74c	20.01±2.62b	4.01±1.07a	3.41±1.11bc	3.24±1.33b
		WR	12.86±1.98bc	26.23±0.55a	30.78±0.93a	4.13±0.41a	5.23±0.94a	4.18±1.67a
		WC	9.48±3.39c	14.6±2.06b	19.59±3.85b	2.52±0.14b	3.77±0.74ab	3.22±0.27b

(DR) dry transplanted + rained irrigation, (DC) dry transplanted + conventional irrigation treatments, (WR) water transplanted + rained irrigation, (WC) water transplanted + conventional irrigation treatments. T-B: Tillering stage to booting stage, B-H: Booting stage to heading stage, H-HA: Heading stage to Heading after 15 days. Small alphabetical letters above means indicate the differences ( $P < 0.05$ ) among different management treatments

### Yield and yield-related traits

As shown in *Table 2*, for Meixiangzhan 2, The trend of fertile panicle was: WR = WC > DR = DC in both early and late season. Also the highest 1000-grain weight was recorded with WR treatment in the early season. For Xiangyaxiangzhan, in the early season, the trend of fertile panicle was the same as Meixiangzhan 2. Compared with C treatments, R



treatments could also increase the 1000-grain weight of these cultivars, and the highest yield was recorded under the WR treatment in the early season. The varieties and the experiments did not influence the yield significantly, so the average yield of the two fragrant rice cultivars in both seasons were WC > WR > DR > DC.

**Table 2.** Effects of transplanting conditions and water management yield and yield-related traits

Season	Cultivar	Treatment	Fertile panicle (m <sup>-1</sup> )	Grain count per panicle	Seed setting rate (%)	1000-grain weight (g)	Actual yield (t ha <sup>-1</sup> )
Early	Meixiangzhan 2	DR	257.11 ± 0.43b	131.39 ± 6.89b	82.63 ± 3.92b	18.80 ± 0.60ab	3.25 ± 0.28b
		DC	252.33 ± 1.22b	151.90 ± 5.72a	82.57 ± 8.33b	17.55 ± 1.25b	3.33 ± 0.11b
		WR	261.42 ± 0.45a	148.32 ± 8.29a	87.91 ± 3.46a	19.36 ± 1.52a	3.48 ± 0.21a
		WC	260.22 ± 0.22a	153.04 ± 2.59a	86.91 ± 5.51a	18.82 ± 0.72ab	3.23 ± 0.43b
	Xiangyaxiangzhan	DR	252.22 ± 0.11b	124.94 ± 3.63b	82.81 ± 5.17ab	20.44 ± 0.62a	2.72 ± 0.49b
		DC	252.12 ± 1.22b	129.83 ± 8.73b	79.95 ± 1.36b	20.50 ± 0.40a	2.97 ± 0.11ab
		WR	275.94 ± 0.23a	142.16 ± 6.16a	85.31 ± 2.42a	19.66 ± 0.36ab	3.55 ± 0.43a
		WC	272.77 ± 0.32a	133.30 ± 3.02b	86.42 ± 2.44a	19.01 ± 1.40b	3.35 ± 0.28ab
Late	Meixiangzhan 2	DR	246.13 ± 1.22b	140.27 ± 19.13ab	89.12 ± 1.03a	19.11 ± 1.22b	5.68 ± 0.49a
		DC	242.22 ± 0.32b	152.75 ± 23.16a	86.89 ± 0.03a	20.79 ± 1.23a	4.64 ± 0.23b
		WR	276.58 ± 1.01a	122.45 ± 15.35b	90.13 ± 2.02a	19.21 ± 0.21b	4.80 ± 0.52b
		WC	270.13 ± 0.31a	137.95 ± 20.83ab	88.32 ± 0.05a	20.21 ± 0.93ab	5.52 ± 0.68a
	Xiangyaxiangzhan	DR	255.12 ± 1.21b	138.86 ± 11.29a	84.24 ± 1.06b	18.88 ± 0.57b	5.52 ± 0.39b
		DC	268.21 ± 0.22ab	130.70 ± 5.74b	83.33 ± 0.36b	20.28 ± 0.44a	5.62 ± 0.30a
		WR	285.54 ± 1.11a	143.27 ± 6.20a	88.29 ± 1.24ab	20.04 ± 0.66a	5.68 ± 1.19a
		WC	281.12 ± 1.65a	125.63 ± 14.95b	91.25 ± 0.33a	18.96 ± 1.55b	5.42 ± 0.85c
Early	C		1.43	1.43	13.36*	1.25	3.94
	T		0.03	0.03	12.18*	2.47	1.05
	C×T		1.66	1.66	11.17*	0.34	3.64
Late	C		16.03*	5.28*	1.46	0.81	3.19
	T		15.03*	12.22*	2.62	2.42	0.81
	C×T		5.01*	20.86*	2.01	1.65	1.74

(DR) dry transplanted + rained irrigation, (DC) dry transplanted + conventional irrigation treatments, (WR) water transplanted + rained irrigation, (WC) water transplanted + conventional irrigation treatments. Small alphabetical letters above means indicate the differences (P < 0.05) among different management treatments. \*, \*\* Significantly different at 0.05 and 0.01 probability levels, respectively. C: Cultivar; T: Treatment; C×T: Cultivar- Treatment interaction. The same as below

### Quality of fragrant rice

As shown in Table 3, for Meixiangzhan 2, there was no significant difference among the four treatments in the early season on the rate of brown rice and milled rice of this cultivar. The head rice rate maximized in WR treatment. And maximized in DR treatment in the early and late season. For Xiangyaxiangzhan, WR treatment had the highest milled rice rate and head rice rate and the lowest chalkiness and chalky grain rate in all except WC treatments in the early season, while the four treatments had no significant effect on the brown rice rate and milled rice rate of this cultivar in the late season. Each of the treatments had little effect on the length-width ratio of the two fragrant rice cultivars.

### Proline content

The effects of different transplanting conditions and water management on the proline content in the leaves of fragrant rice was shown in Table 4. For Meixiangzhan,

the trend of proline contents was: DR = DC > WR = WC at tillering stage and booting stage. And the proline content in leaves had the same trend in late season. For Xiangyaxiangzhan, DR and DC treatments maximized the leaf proline content of this cultivar at four stages (except heading after 15 days) in the early season, and the trend in the late season was similar.

**Table 3.** Effects of transplanting conditions and water management on quality of fragrant rice

Season	Cultivar	Treatment	Brown rice rate (%)	Milled rice rate (%)	Head rice rate (%)	Protein	Amylose	Akali	Chalkiness (%)	Chalky grain rate (%)	The ratio of length to width (%)
Early	<i>Meixiangzhan 2</i>	DR	74.19 ± 1.69a	61.09 ± 1.57a	55.76 ± 1.35ab	7.43 ± 0.05a	19.97 ± 0.69a	5.61 ± 0.08b	1.45 ± 0.11b	5.05 ± 1.13b	2.92 ± 0.19a
		DC	74.01 ± 0.49a	64.22 ± 0.87a	52.26 ± 1.14b	6.17 ± 0.09d	19.67 ± 0.12ab	5.53 ± 0.05bc	1.46 ± 0.03b	5.12 ± 2.29b	2.77 ± 0.05ab
		WR	76.16 ± 0.21a	63.52 ± 0.43a	57.98 ± 1.06a	6.87 ± 0.05b	18.60 ± 0.51b	5.90 ± 0.10a	2.39 ± 0.65a	5.63 ± 3.35a	2.66 ± 0.12b
		WC	75.71 ± 0.08a	66.05 ± 1.14a	57.23 ± 1.66a	6.37 ± 0.05c	19.80 ± 0.71a	5.37 ± 0.12c	1.58 ± 0.18b	5.17 ± 3.26ab	2.81 ± 0.11ab
	<i>Xiangyaxiangzhan</i>	DR	73.13 ± 0.09a	58.52 ± 1.85b	55.93 ± 1.19ab	7.33 ± 0.05a	17.30 ± 0.67a	5.73 ± 0.05a	1.06 ± 0.63ab	4.35 ± 3.22b	3.14 ± 0.21a
		DC	72.58 ± 0.42a	62.46 ± 0.24ab	54.63 ± 0.21ab	7.07 ± 0.05c	18.50 ± 1.28a	5.63 ± 0.05ab	2.08 ± 0.89a	5.66 ± 3.84a	3.03 ± 0.22a
		WR	72.49 ± 3.35a	63.25 ± 0.86a	56.52 ± 0.72a	7.17 ± 0.05bc	18.93 ± 0.05a	5.63 ± 0.05ab	0.75 ± 0.09b	3.69 ± 2.26c	2.84 ± 0.14a
		WC	72.94 ± 0.48a	61.88 ± 0.37ab	53.51 ± 0.46b	7.23 ± 0.05ab	17.10 ± 0.90a	5.60 ± 0.08b	1.49 ± 0.77ab	4.41 ± 3.13b	3.14 ± 0.15a
Late	<i>Meixiangzhan 2</i>	DR	76.76 ± 0.21a	67.48 ± 0.91a	65.22 ± 0.85a	8.27 ± 0.12a	19.13 ± 0.54a	6.67 ± 0.12a	0.61 ± 0.69c	3.12 ± 2.66b	2.67 ± 0.12a
		DC	76.66 ± 0.35a	65.62 ± 0.88a	62.19 ± 0.57b	7.97 ± 0.12b	19.07 ± 0.41a	6.72 ± 0.08a	0.78 ± 0.24b	3.37 ± 5.36b	2.74 ± 0.11a
		WR	76.58 ± 0.69a	65.56 ± 1.05a	63.24 ± 1.34ab	7.81 ± 0.08b	19.51 ± 0.43a	6.63 ± 0.12a	1.06 ± 0.68a	4.54 ± 5.21a	2.72 ± 0.09a
		WC	76.86 ± 0.11a	66.66 ± 0.48a	63.66 ± 0.48ab	8.41 ± 0.08a	18.77 ± 0.12a	6.73 ± 0.17a	0.79 ± 0.23b	3.41 ± 5.71b	2.71 ± 0.13a
	<i>Xiangyaxiangzhan</i>	DR	75.36 ± 0.37a	62.03 ± 0.54a	56.32 ± 0.21b	8.21 ± 0.08a	18.70 ± 0.08b	6.83 ± 0.12a	0.58 ± 0.48ab	4.13 ± 2.82a	2.67 ± 0.12a
		DC	74.91 ± 0.49a	62.65 ± 1.64a	55.06 ± 1.62b	7.97 ± 0.12ab	19.63 ± 0.05a	6.67 ± 0.12a	1.23 ± 0.66a	3.76 ± 2.87ab	2.77 ± 0.09a
		WR	75.05 ± 0.81a	63.76 ± 1.16a	59.57 ± 0.88a	7.92 ± 0.08b	18.92 ± 0.22b	6.67 ± 0.12a	0.16 ± 0.06b	3.59 ± 2.68b	2.81 ± 0.11a
		WC	75.55 ± 0.69a	64.51 ± 1.47a	59.84 ± 1.13a	7.97 ± 0.12ab	18.21 ± 0.36c	6.63 ± 0.12a	0.55 ± 0.11ab	3.45 ± 1.49b	2.92 ± 0.21a
Early	C		8.44**	9.75**	2.51	16.45**	20.61**	2.12	3.01	23.788**	15.98**
	T		2.04	1.79	14.68**	12.15**	4.53*	12.31**	0.92	6.99**	3.67*
	C*T		0.72	2.589	8.52**	15.73**	16.95**	10.12**	4.738*	19.58**	0.28
Late	C		11.18**	12.43**	35.46**	3.6	2.52	0.07	0.85	0.11	2.25
	T		0.74	1.22	7.27**	11.77**	5.47**	0.44	1.51	0.36	1.41
	C*T		0.17	2.29	9.38**	4.87*	2.91	0.81	1.69	1.38	0.63

**Table 4.** Effects of transplanting conditions and water management on proline content in leaves of fragrant rice ( $\mu\text{g/g}$ )

Season	Cultivar	Treatment	Tillering stage	Booting stage	Heading stage	Heading after 15 d
Early	<i>Meixiangzhan 2</i>	DR	38.11 $\pm$ 1.29a	41.81 $\pm$ 0.84a	31.77 $\pm$ 1.91b	20.49 $\pm$ 2.49a
		DC	40.33 $\pm$ 1.86a	52.43 $\pm$ 3.72a	28.71 $\pm$ 1.14b	12.76 $\pm$ 2.62bc
		WR	29.79 $\pm$ 1.63b	37.52 $\pm$ 7.22b	24.65 $\pm$ 1.26c	17.21 $\pm$ 1.62ab
		WC	30.79 $\pm$ 1.22b	34.07 $\pm$ 7.55b	40.35 $\pm$ 1.41a	11.83 $\pm$ 0.84c
	<i>Xiangyaxiangzhan</i>	DR	30.68 $\pm$ 2.88a	35.39 $\pm$ 3.54a	26.27 $\pm$ 1.38a	9.51 $\pm$ 1.06b
		DC	32.11 $\pm$ 4.66a	38.41 $\pm$ 4.18a	26.31 $\pm$ 1.72a	5.29 $\pm$ 0.51c
		WR	17.13 $\pm$ 5.21c	19.12 $\pm$ 7.48b	21.73 $\pm$ 2.07ab	14.71 $\pm$ 1.64a
		WC	21.22 $\pm$ 6.33b	24.01 $\pm$ 0.81b	19.43 $\pm$ 3.37b	3.01 $\pm$ 1.11c
Late	<i>Meixiangzhan 2</i>	DR	50.73 $\pm$ 4.66a	58.51 $\pm$ 3.66a	36.92 $\pm$ 0.61a	79.13 $\pm$ 2.68a
		DC	50.66 $\pm$ 2.54a	52.51 $\pm$ 1.33a	31.69 $\pm$ 1.33b	51.36 $\pm$ 3.49b
		WR	42.49 $\pm$ 1.33c	34.98 $\pm$ 1.92c	26.13 $\pm$ 2.57c	42.52 $\pm$ 1.43c
		WC	44.51 $\pm$ 3.05b	46.62 $\pm$ 4.39b	25.06 $\pm$ 4.13c	31.73 $\pm$ 0.82d
	<i>Xiangyaxiangzhan</i>	DR	53.54 $\pm$ 0.91a	38.84 $\pm$ 2.33a	20.48 $\pm$ 0.85a	33.48 $\pm$ 3.45a
		DC	40.97 $\pm$ 4.48b	22.67 $\pm$ 2.23b	14.35 $\pm$ 2.07b	20.98 $\pm$ 4.15bc
		WR	30.44 $\pm$ 1.02c	22.03 $\pm$ 0.77b	15.48 $\pm$ 2.41b	26.93 $\pm$ 4.54ab
		WC	36.09 $\pm$ 4.31b	18.52 $\pm$ 3.13b	12.76 $\pm$ 0.39b	20.43 $\pm$ 0.74c

As shown in Table 5, for *Meixiangzhan 2*, the trend of proline content in stem was similar to that in leaves in the early season. There was no remarkable difference among the four stages. But tillering stage, the content of proline in DR and DC treatments were significantly higher than in WR and WC treatments. For *Xiangyaxiangzhan*, the content of proline in DR and DC treatments were significantly higher than in WR and WC treatments among the four stages in the early season and the trend in the late season was similar.

**Table 5.** Effects of transplanting conditions and water management on proline content in the stem of fragrant rice ( $\mu\text{g/g}$ )

Season	Cultivar	Treatment	Tillering stage	Booting stage	Heading stage	Heading after 15d
Early	<i>Meixiangzhan 2</i>	DR	24.13 $\pm$ 4.02a	16.12 $\pm$ 2.09b	9.45 $\pm$ 0.42a	11.26 $\pm$ 0.99ab
		DC	15.99 $\pm$ 1.14b	21.36 $\pm$ 0.66a	8.45 $\pm$ 0.89bc	14.17 $\pm$ 3.70a
		WR	12.42 $\pm$ 1.37c	9.98 $\pm$ 0.71c	9.71 $\pm$ 1.22b	9.48 $\pm$ 1.02bc
		WC	12.65 $\pm$ 1.17c	13.12 $\pm$ 1.75bc	4.47 $\pm$ 0.40c	5.24 $\pm$ 0.70c
	<i>Xiangyaxiangzhan</i>	DR	15.09 $\pm$ 1.21a	11.83 $\pm$ 1.25a	3.68 $\pm$ 0.75a	5.59 $\pm$ 3.04a
		DC	16.28 $\pm$ 3.77a	11.25 $\pm$ 1.02a	2.98 $\pm$ 1.09a	4.03 $\pm$ 1.77ab
		WR	7.66 $\pm$ 1.66b	6.71 $\pm$ 1.97b	3.34 $\pm$ 1.14a	0.98 $\pm$ 0.34c
		WC	11.82 $\pm$ 2.3ab	3.44 $\pm$ 0.61c	3.31 $\pm$ 0.36a	2.53 $\pm$ 0.14b
Late	<i>Meixiangzhan 2</i>	DR	38.53 $\pm$ 4.44a	23.38 $\pm$ 1.46b	13.62 $\pm$ 1.05a	19.86 $\pm$ 3.82b
		DC	33.23 $\pm$ 3.57a	24.71 $\pm$ 3.6ab	14.58 $\pm$ 2.16a	26.91 $\pm$ 2.20a
		WR	23.31 $\pm$ 1.63b	23.62 $\pm$ 4.15b	16.30 $\pm$ 1.20a	13.40 $\pm$ 2.77c
		WC	27.59 $\pm$ 2.98b	29.94 $\pm$ 2.67a	16.82 $\pm$ 3.45a	24.31 $\pm$ 2.49ab
	<i>Xiangyaxiangzhan</i>	DR	25.49 $\pm$ 3.91a	18.91 $\pm$ 3.11a	11.14 $\pm$ 2.42a	15.84 $\pm$ 1.44a
		DC	19.39 $\pm$ 2.37b	6.57 $\pm$ 2.66bc	7.08 $\pm$ 3.27ab	10.36 $\pm$ 1.32b
		WR	14.83 $\pm$ 2.11c	7.18 $\pm$ 1.33b	5.52 $\pm$ 1.27b	5.02 $\pm$ 1.79c
		WC	18.55 $\pm$ 2.05b	3.05 $\pm$ 0.56c	4.11 $\pm$ 0.85b	3.30 $\pm$ 2.38c

### *Ornithine aminotransferase activities*

As shown in *Table 6*, for Meixiangzhan 2, the highest Ornithine aminotransferase (OAT) activity was recorded in DC treatment from heading stage to 15 days after heading (except WC treatment at heading stage) in the early season. OAT activity in the leaves of this cultivar under WR treatment was the highest at four stages (except heading stage) in the late season. For Xiangyaxiangzhan, compared with C treatments, R treatments enhanced OAT activity in leaves from tillering stage to booting stage.

**Table 6.** Effects of transplanting conditions and water management on OAT activity in the leaves of fragrant rice (*U-g-l-min-1-FW*)

Season	Cultivar	Treatments	Tillering stage	Booting stage	Heading stage	Heading after 15d
Early	Meixiangzhan 2	DR	115.77 ± 3.66a	114.58 ± 4.75a	71.72 ± 1.43b	81.23 ± 8.83ab
		DC	113.87 ± 3.44a	110.96 ± 1.12a	76.05 ± 1.63a	89.07 ± 7.66a
		WR	111.29 ± 1.04a	114.87 ± 3.77a	71.78 ± 1.15b	74.70 ± 1.76b
		WC	110.69 ± 4.64a	110.63 ± 1.53a	74.88 ± 0.87a	73.41 ± 1.40b
	Xiangyaxiangzhan	DR	113.31 ± 4.12a	110.72 ± 2.04a	73.16 ± 0.69b	75.82 ± 2.83a
		DC	112.23 ± 3.13ab	107.47 ± 7.87b	74.66 ± 0.97b	73.52 ± 2.64a
		WR	111.59 ± 2.00ab	112.08 ± 1.73a	74.35 ± 2.18b	74.26 ± 2.64a
		WC	105.34 ± 3.82b	113.27 ± 1.71a	85.62 ± 12.20a	73.57 ± 0.70a
Late	Meixiangzhan 2	DR	97.97 ± 0.99b	94.39 ± 1.30a	87.90 ± 1.70a	82.99 ± 1.39a
		DC	94.47 ± 0.58c	88.98 ± 3.10b	86.25 ± 0.98a	82.56 ± 1.60a
		WR	101.20 ± 1.28a	94.47 ± 2.91a	85.64 ± 2.35a	83.33 ± 2.85a
		WC	94.51 ± 0.92c	86.21 ± 2.79b	84.25 ± 4.73a	82.33 ± 0.84a
	Xiangyaxiangzhan	DR	96.53 ± 2.22a	89.12 ± 1.01ab	82.72 ± 2.12a	81.90 ± 2.21ab
		DC	102.07 ± 4.53a	87.83 ± 1.46b	83.65 ± 4.94a	86.33 ± 1.30a
		WR	99.25 ± 2.51a	87.86 ± 3.03b	85.35 ± 1.82a	84.02 ± 2.6ab
		WC	97.03 ± 1.78a	92.71 ± 2.51a	83.32 ± 4.52a	81.04 ± 3.32b

As shown in *Table 7*, for Meixiangzhan 2, the highest OAT activity in stems was recorded under the WC treatment at tillering stage and full heading stage in the early season, and the stems of OAT activity under DC treatment was the highest in the late season except for booting stage and 15 days after heading. For Xiangyaxiangzhan, the trend of OAT activity in the early season was the same as that of Meixiangzhan 2, and the OAT activity was highest under WC treatment at 15 days after heading in the late season.

### *Pyrroline-5-carboxylic acid content*

As shown in *Table 8*, for Meixiangzhan 2, the highest content of Pyrroline-5-carboxylic acid (P5C) in leaves was recorded under the WR treatment at four stages of the early season (except heading after 15 days). Compared with WC and DC treatments, DR and WR treatments could significantly increase the content of P5C in leaves of this cultivar in the late season. For Xiangyaxiangzhan, in the early season, compared with WC and DC treatments, WR and DR treatments could increase P5C content at tillering stage and booting stage, and P5C content under WR treatment was significantly higher than that of other treatments (except WC treatment) at tillering stage in the late season. There was no significant difference among the treatments in the other three periods.

**Table 7.** Effects of transplanting conditions and water management on OAT activity in the stem of fragrant rice ( $U \cdot g^{-1} \cdot min^{-1} \cdot FW$ )

Season	Cultivar	Treatment	Tillering stage	Booting stage	Heading stage	Heading after 15d
Early	Meixiangzhan 2	DR	110.21 ± 0.73b	113.11 ± 3.75a	72.69 ± 2.95a	74.29 ± 2.01a
		DC	109.94 ± 2.83b	114.05 ± 3.36a	71.63 ± 1.54ab	73.51 ± 0.41a
		WR	112.20 ± 4.58ab	108.65 ± 0.76b	70.61 ± 0.67b	72.66 ± 1.03a
		WC	115.59 ± 0.71a	112.80 ± 1.25a	74.38 ± 1.41a	73.13 ± 2.70a
	Xiangyaxiangzhan	DR	111.18 ± 0.68a	113.62 ± 3.37a	71.47 ± 0.72b	73.53 ± 2.06b
		DC	109.81 ± 1.40a	110.13 ± 4.57b	71.27 ± 2.81b	76.05 ± 1.55a
		WR	110.02 ± 3.26a	114.86 ± 1.41a	70.23 ± 0.72b	73.51 ± 2.53b
		WC	112.61 ± 5.26a	113.46 ± 4.20a	74.03 ± 1.69a	73.93 ± 2.54ab
Late	Meixiangzhan 2	DR	80.74 ± 3.11b	87.19 ± 2.25a	90.44 ± 4.38a	93.27 ± 4.02a
		DC	83.65 ± 2.36a	83.01 ± 2.68b	91.07 ± 4.02a	88.59 ± 0.81b
		WR	82.31 ± 4.19a	84.96 ± 3.00b	89.79 ± 3.02a	91.47 ± 2.88a
		WC	82.38 ± 3.18a	84.30 ± 3.20b	88.63 ± 3.82a	92.87 ± 4.17a
	Xiangyaxiangzhan	DR	80.98 ± 3.64a	80.53 ± 3.43b	88.67 ± 0.70a	89.47 ± 4.68ab
		DC	79.52 ± 4.62a	85.17 ± 3.35a	87.47 ± 2.26a	88.26 ± 3.66ab
		WR	82.86 ± 2.95a	86.43 ± 2.52a	86.42 ± 2.45a	87.77 ± 4.90b
		WC	83.31 ± 2.50a	81.31 ± 3.57b	88.30 ± 1.36a	93.16 ± 1.84a

**Table 8.** Effects of transplanting conditions and water management on the content of P5C in the leaves of fragrant rice ( $u \text{ mol/g-FW}$ )

Season	Cultivar	Treatment	Tillering stage	Booting stage	Heading stage	Heading after 15d
Early	Meixiangzhan 2	DR	1.48 ± 0.02b	1.70 ± 0.06a	1.96 ± 0.01ab	2.09 ± 0.10ab
		DC	1.44 ± 0.15b	1.55 ± 0.08b	2.04 ± 0.04ab	2.23 ± 0.11a
		WR	1.52 ± 0.02a	1.71 ± 0.10a	2.07 ± 0.08a	2.20 ± 0.05a
		WC	1.58 ± 0.04a	1.58 ± 0.05b	1.95 ± 0.01b	1.97 ± 0.01b
	Xiangyaxiangzhan	DR	1.65 ± 0.02ab	1.56 ± 0.02a	1.68 ± 0.02b	2.21 ± 0.06a
		DC	1.42 ± 0.07b	1.42 ± 0.04b	1.63 ± 0.01b	2.12 ± 0.09a
		WR	1.72 ± 0.05a	1.54 ± 0.02a	1.69 ± 0.01b	1.72 ± 0.02c
		WC	1.47 ± 0.19b	1.48 ± 0.03b	1.75 ± 0.04a	1.92 ± 0.09b
Late	Meixiangzhan 2	DR	1.80 ± 0.02a	2.24 ± 0.04a	2.12 ± 0.06b	2.84 ± 0.12a
		DC	1.66 ± 0.08a	2.15 ± 0.06a	2.30 ± 0.1ab	2.86 ± 0.17a
		WR	1.72 ± 0.04a	2.23 ± 0.14a	2.38 ± 0.13a	2.57 ± 0.17b
		WC	1.63 ± 0.26a	2.20 ± 0.15a	2.15 ± 0.11b	2.38 ± 0.05b
	Xiangyaxiangzhan	DR	1.71 ± 0.06b	2.07 ± 0.06a	2.08 ± 0.08a	2.68 ± 0.23a
		DC	1.67 ± 0.04b	1.99 ± 0.06a	2.11 ± 0.05a	2.43 ± 0.37a
		WR	1.84 ± 0.06b	2.07 ± 0.07a	2.22 ± 0.09a	2.55 ± 0.19a
		WC	1.87 ± 0.09a	2.07 ± 0.11a	2.16 ± 0.08a	2.55 ± 0.06a

As shown in Table 9, for Meixiangzhan 2, the content of P5C in the stem of Meixiangzhan 2 was the highest under WC treatment at four stages in the early season, and the highest content of P5C in the stem of this cultivar was recorded in WR treatment at tillering stage and 15 days after heading in the late season. For Xiangyaxiangzhan, there is no significant difference among the four treatments in the early season, but the content of P5C in WC treatment is the highest at tillering stage and heading stage.

**Table 9.** Effects of transplanting conditions and water management on the content of P5C in the stem of fragrant rice (umol/g-FW)

Season	Cultivar	Treatment	Tillering stage	Booting stage	Heading stage	Heading after 15d
Early	Meixiangzhan 2	DR	1.01 ± 0.09a	1.15 ± 0.01b	1.19 ± 0.01b	1.21 ± 0.02b
		DC	1.01 ± 0.02a	1.14 ± 0.01bc	1.27 ± 0.02a	1.29 ± 0.02a
		WR	1.03 ± 0.03a	1.12 ± 0.01c	1.21 ± 0.02b	1.32 ± 0.05a
		WC	1.08 ± 0.05a	1.18 ± 0.01a	1.32 ± 0.03a	1.28 ± 0.02a
	Xiangyaxiangzhan	DR	1.01 ± 0.02a	1.13 ± 0.02a	1.26 ± 0.09a	1.20 ± 0.03a
		DC	1.01 ± 0.07a	1.14 ± 0.01a	1.21 ± 0.06a	1.17 ± 0.03a
		WR	0.98 ± 0.01a	1.17 ± 0.01a	1.18 ± 0.03b	1.17 ± 0.02a
		WC	1.08 ± 0.03a	1.14 ± 0.04a	1.20 ± 0.03a	1.15 ± 0.01a
Late	Meixiangzhan 2	DR	1.42 ± 0.05b	1.19 ± 0.03a	1.44 ± 0.05a	1.46 ± 0.06b
		DC	1.18 ± 0.03c	1.26 ± 0.06a	1.36 ± 0.08a	1.58 ± 0.04a
		WR	1.73 ± 0.04a	1.27 ± 0.08a	1.39 ± 0.04a	1.65 ± 0.05a
		WC	1.39 ± 0.05b	1.18 ± 0.01a	1.42 ± 0.08a	1.59 ± 0.08a
	Xiangyaxiangzhan	DR	1.39 ± 0.19b	1.16 ± 0.05b	1.27 ± 0.02b	1.48 ± 0.01b
		DC	1.57 ± 0.06b	1.24 ± 0.02a	1.30 ± 0.01b	1.70 ± 0.08a
		WR	1.41 ± 0.06b	1.20 ± 0.04ab	1.23 ± 0.01c	1.56 ± 0.10b
		WC	1.89 ± 0.14a	1.22 ± 0.04ab	1.36 ± 0.02a	1.43 ± 0.07b

### Methylglyoxal content

As shown in Table 10, for Meixiangzhan 2, the methylglyoxal content in the leaves of this cultivar under DC treatment was the highest at booting stage in the early season, and there was no significant difference in methylglyoxal content among the treatments except for DR treatment at full heading stage. From tillering stage to heading stage in the late season, WR treatment maximized content of methylglyoxal in leaves of this cultivar. For Xiangyaxiangzhan, in the tillering stage of the early season, the content of methylglyoxal was the highest recorded under the WR treatment.

**Table 10.** Effects of transplanting conditions and water management on methylglyoxal in the leaves of fragrant rice (μmol/g-FW)

Season	Cultivar	Treatment	Tillering stage	Booting stage	Heading stage	Heading after 15d
Early	Meixiangzhan 2	DR	21.24 ± 0.37c	21.15 ± 0.73b	23.54 ± 0.45b	24.17 ± 1.54a
		DC	25.09 ± 0.43a	21.95 ± 0.75b	28.12 ± 1.74a	22.25 ± 0.89a
		WR	23.76 ± 0.40b	20.60 ± 0.34b	26.27 ± 0.37a	22.26 ± 2.33a
		WC	21.74 ± 0.39c	24.53 ± 0.72a	26.13 ± 0.71a	21.43 ± 0.27a
	Xiangyaxiangzhan	DR	24.50 ± 2.23b	22.42 ± 0.20a	22.08 ± 0.93a	21.53 ± 1.04a
		DC	27.64 ± 2.21ab	19.90 ± 0.56b	22.05 ± 1.51a	22.21 ± 1.10a
		WR	30.76 ± 1.42a	21.44 ± 1.05a	22.10 ± 1.09a	17.64 ± 1.17b
		WC	26.15 ± 0.56b	21.66 ± 0.56a	22.79 ± 1.75a	20.13 ± 0.76a
Late	Meixiangzhan 2	DR	23.39 ± 0.44bc	21.66 ± 0.60b	24.63 ± 0.90a	31.02 ± 1.92a
		DC	22.40 ± 2.19c	19.92 ± 1.30b	24.81 ± 0.39a	28.23 ± 1.78a
		WR	26.01 ± 0.93a	23.85 ± 1.40a	26.01 ± 1.02a	28.24 ± 0.17a
		WC	25.59 ± 1.02ab	21.22 ± 1.11b	22.26 ± 1.22b	28.38 ± 1.48a
	Xiangyaxiangzhan	DR	24.98 ± 0.37ab	24.34 ± 0.79a	25.94 ± 0.74b	26.95 ± 0.66a
		DC	23.83 ± 0.32b	21.22 ± 1.40b	26.48 ± 0.33ab	26.87 ± 1.87a
		WR	25.55 ± 0.77a	21.62 ± 1.29b	25.57 ± 1.17b	27.65 ± 2.08a
		WC	25.83 ± 1.13a	24.45 ± 2.98a	27.43 ± 0.55a	26.93 ± 0.64a

As shown in *Table 11*, for *Meixiangzhan 2*, the highest content of methylglyoxal in the stem was recorded under the DR treatment at 15 days after heading in the early season. For *Xiangyaxiangzhan*, there were no remarkable trends in the early season. And in the late season, the content of methylglyoxal trend was: DR = WR > WC > DC.

**Table 11.** Effects of transplanting conditions and water management on methylglyoxal in the stem of fragrant rice (mol/g-FW)

Season	Cultivar	Treatment	Tillering stage	Booting stage	Heading stage	Heading after 15d
Early	<i>Meixiangzhan 2</i>	DR	14.40 ± 0.61a	14.46 ± 0.24a	12.64 ± 0.52ab	16.77 ± 0.33a
		DC	14.37 ± 0.34a	14.96 ± 0.50a	12.13 ± 0.23b	15.67 ± 0.08ab
		WR	14.45 ± 0.34a	14.74 ± 0.69a	11.93 ± 0.01b	14.81 ± 0.35b
		WC	14.60 ± 0.50a	15.23 ± 0.28a	13.08 ± 0.51a	14.73 ± 1.20b
	<i>Xiangyaxiangzhan</i>	DR	13.14 ± 0.52a	12.44 ± 0.04a	11.81 ± 0.28ab	14.39 ± 0.53b
		DC	13.38 ± 0.88a	13.23 ± 1.27a	12.28 ± 0.55a	15.74 ± 0.10a
		WR	13.11 ± 0.24a	13.94 ± 0.60a	11.75 ± 0.49ab	14.95 ± 0.8ab
		WC	13.06 ± 0.64a	13.73 ± 1.29a	10.33 ± 1.49b	15.85 ± 0.42a
Late	<i>Meixiangzhan 2</i>	DR	13.95 ± 0.65ab	11.29 ± 1.16b	13.18 ± 0.58ab	14.63 ± 0.18a
		DC	13.17 ± 0.60b	12.75 ± 0.41a	12.03 ± 0.73b	15.27 ± 0.33a
		WR	13.51 ± 0.33ab	13.63 ± 0.8a	13.91 ± 0.51a	14.86 ± 0.71a
		WC	14.28 ± 0.44a	12.97 ± 0.36a	12.41 ± 1.36ab	15.31 ± 0.88a
	<i>Xiangyaxiangzhan</i>	DR	13.25 ± 0.44a	13.01 ± 0.22a	12.54 ± 1.54a	15.79 ± 0.73b
		DC	12.66 ± 0.54ab	13.03 ± 0.30a	12.78 ± 0.22a	16.78 ± 0.35a
		WR	13.13 ± 0.30a	13.55 ± 0.89a	12.45 ± 0.51a	16.21 ± 0.60ab
		WC	11.95 ± 0.13b	13.81 ± 0.07a	12.57 ± 0.17a	16.15 ± 0.08ab

### 2-acetyl-1-pyrroline content in grains

As shown in *Table 12*, for *Meixiangzhan 2*, at the mature stage of the early season, the trend of 2-Acetyl-1-Pyrroline (2-AP) content was: WR = DR > WC > DC. But at the mature stage of late season the trend of 2-AP was: WC > WR = DC > DR. For *Xiangyaxiangzhan*, the trend of grain aroma content in mature stage was consistent with that of *Meixiangzhan 2*, and compared with C treatments, the average aroma content of R treatments was increased by 5.24% in the early season, and the highest aroma at mature stage was recorded under the WR treatment in the late season.

### Discussion

Various yield components act comprehensively and coordinate with each other to form the yield of rice. Water management, as an important measure to increase yield, has been concerned by predecessors. With the decrease of irrigation water, the number of effective panicles of direct seeding rice increased at first and then decreased (Wu et al., 2019). Water-saving irrigation could increase the number of tillers in the middle and early stage, also it increased the number of effective tillers in the later stage as well as the panicle rate of tillers (Zhao et al., 2018). Light dry-wet alternative irrigation can effectively control ineffective tillers, and significantly increased panicle rate (Zhao et al., 2015). The results showed that the fertile panicle number of the two fragrant rice had no significant difference between WR and WC treatment, but were higher than DR and DC treatments which prove that water-saving irrigation maybe not only saving the resource but also can enhance or keep the fertile panicle number. Under the condition of



alternating dry and wet irrigation, it was helpful to the construction of high yield population, the coordination of nitrogen accumulation and distribution of rice plant (Peng, 2014). The results showed that the highest grain count per panicle, seed setting rate and 1000-grain weight of two fragrant rice cultivars were recorded in WR treatment (except WC treatment) which means that WR treatment was more beneficial to the export and accumulation of assimilates during rice growth, and made the yield composition more reasonable. On the other hand, compared to conventional irrigation treatment in WC treatment no extra water was applied in the rice production, thus WR treatment is beneficial to water conservation. We observed that there was no significant difference between WR and WC treatment of average yield in both seasons. Thus, WR treatment could be a water-saving cultivation.

**Table 12.** Effects of transplanting conditions and water management on the aroma (2-AP) content of fragrant rice seeds

Season	Cultivar	Treatment	HA 15d	Maturity stage
Early	<i>Meixiangzhan 2</i>	DR	258.44 ± 5.77bc	252.02 ± 5.4a
		DC	251.39 ± 8.02c	169.60 ± 5.00c
		WR	298.40 ± 5.79a	252.10 ± 8.88a
		WC	280.62 ± 8.24ab	230.56 ± 5.85b
	<i>Xiangyaxiangzhan</i>	DR	152.77 ± 4.19d	307.08 ± 16.72a
		DC	175.20 ± 15.13c	245.19 ± 4.49b
		WR	246.21 ± 7.50b	301.06 ± 15.65a
		WC	276.11 ± 3.65a	286.36 ± 12.95ab
Late	<i>Meixiangzhan 2</i>	DR	264.83 ± 11.09b	140.65 ± 6.85c
		DC	141.07 ± 8.46c	174.52 ± 10.54b
		WR	300.29 ± 14.30ab	181.79 ± 9.61b
		WC	349.02 ± 25.49a	235.11 ± 11.17a
	<i>Xiangyaxiangzhan</i>	DR	252.17 ± 4.39c	135.59 ± 5.43c
		DC	254.88 ± 5.13c	232.88 ± 14.71b
		WR	313.17 ± 10.93b	265.59 ± 8.48a
		WC	363.78 ± 22.33a	232.03 ± 3.27b

Water stress at different stages had significant effects on the quality of rice, such as chalky grain rate, protein content and fat content. Water stress treatment from flowering to 15 days after anthesis significantly reduced the head rice rate of rice, but had relatively little effect on other quality factors (Zheng et al., 2017). The results showed that there was no significant difference in brown rice rate and milled rice rate between the two fragrant rice cultivars under different treatments, while the highest head rice rate was recorded in R treatments which proved that the processing quality of rice could be improved under this treatment. The milled rice rate and head rice rate were maximized in WR treatment, also minimized in chalkiness and chalky grain rate in all except WC treatments in the early season of *Xiangyaxiangzhan*, and the four treatments had little effect on the length-width ratio of the two fragrant rice cultivars.

As the aroma characteristic substance, 2-acetyl-1-pyrroline (2-AP) of fragrant rice can form pyrroline-5-carboxylic acid by proline as nitrogen source and catalyzed by proline oxidase. Ornithine aminotransferase can also catalyze ornithine to form

pyrroline 5-carboxylic acid, decarboxylate to form 1-pyrroline, and finally combine with acetyl CoA. Under the action of pyrroline acetyltransferase to form the aroma of 2-acetyl-1-pyrroline (Yoshihashi et al., 2002). This study showed that compared with other treatments, WR treatment increased P5C content in both early and late seasons, and the content of 2-AP in grains of two fragrant rice cultivars treated with WR was enhanced, indicating that WR treatment had the effect of increasing aroma.

## Conclusions

The average yield of WR treatment was similar to WC treatment, since the varieties and the treatments did not influence the yield significantly. Furthermore, WR treatment had the highest milled rice rate and head rice rate and the lowest chalkiness and chalky grain rate all except WC treatments in the early season. WR treatment increased P5C content of two fragrant rice cultivars in both early and late seasons, and the content of 2-AP in grains of two fragrant rice cultivars under WR treatment was enhanced. Hence, WR treatment had the effect of increasing aroma. In conclusion, WR treatment could be a water-saving cultivation, and the optimum treatment for increasing yield and improving quality, also it increases the aroma of fragrant rice grains. Although, further research is required at molecular and physiological level.

**Acknowledgements.** This study was supported by the Natural Science Foundation of China (31971843). The authors declare no conflicts of interests.

## REFERENCES

- [1] Abid, M., Khan, I., Mahmood, F., Ashraf, U., Imran, M., Anjum, S. A. (2015): Response of hybrid rice to various transplanting dates and nitrogen application rates. – *Philippine Agricultural Scientist* 98: 98-104.
- [2] Bao, G., Ashraf, U., Wang, C., He, L., Wei, X., Zheng, A., Mo, Z., Tang, X. (2018): Molecular basis for increased 2-acetyl-1-pyrroline contents under alternate wetting and drying (AWD) conditions in fragrant rice. – *Plant Physiology and Biochemistry* 133: 149-157.
- [3] Deng, Q. Q., Ashraf, U., Cheng, S. R., Sabir, S. R., Mo, Z. W., Pan, S. G., Tian, H., Duan, M. Y., Tang, X. R. (2018): Mild drought in interaction with additional nitrogen dose at grain filling stage modulates 2acetyl-1-pyrroline biosynthesis and grain yield in fragrant rice. – *Applied Ecology and Environmental Research* 16: 7741-7758.
- [4] Du, P., Luo, H., He, J., Mao, T., Du, B., Hu, L. (2019): Different tillage induces regulation in 2-acetyl-1-pyrroline biosynthesis in direct-seeded fragrant rice. – *BMC Plant Biology* 19.
- [5] Graham Acquaah, S., Siebenmorgen, T. J., Reba, M. L., Massey, J. H., Mauromoustakos, A., Adviento Borbe, A., January, R., Burgos, R., Baltz Gray, J. (2019): Impact of alternative irrigation practices on rice quality. – *Cereal Chemistry* 96: 815-823.
- [6] Hasanuzzaman, M., Alam, M. M., Nahar, K., Mohsin, S. M., Bhuyan, M. H. M. B., Parvin, K., Hawrylak-Nowak, B., Fujita, M. (2019): Silicon-induced antioxidant defense and methylglyoxal detoxification works coordinately in alleviating nickel toxicity in *Oryza sativa* L. – *Ecotoxicology* 28: 261-276.
- [7] Malek, M. A., Latif, M. A. (2013): Biochemical, genetic and molecular advances of fragrance characteristics in rice. – *Critical Reviews in Plant Sciences* 32: 445-457.

- [8] Huang, Z. L., Tang, X. R., Wang, Y. L., Chen, M. J., Zhao, Z. K., Duan, M. Y., Pan, S. G. (2012): Effects of fragrant cultivation on aroma and yield of scented rice and its related physiological mechanism. – *Chinese Agricultural Science* 45: 1054-1065
- [9] Kong, L., Luo, H., Mo, Z., Pan, S., Liu, Z., Zhang, Q., Bai, S., Tang, X. (2020): Grain yield, quality and 2-Acetyl-1-Pyrroline of fragrant rice in response to Different planting seasons in south china. – *Phyton* 89: 705-714.
- [10] Luo, H., Du, B., He, L., He, J., Hu, L., Pan, S., Tang, X. (2019): Exogenous application of zinc (Zn) at the heading stage regulates 2-acetyl-1-pyrroline (2-AP) biosynthesis in different fragrant rice genotypes. – *Scientific Reports* 9: 19513.
- [11] Marchesi, C., Chauhan, B. S. (2019): The efficacy of chemical options to control *Echinochloa crus-galli* in dry-seeded rice under alternative irrigation management and field layout. – *Crop Protection* 118: 72-78.
- [12] Peng, Y. (2014): Effects of seedling age, water management and slow/controlled release fertilizer on nitrogen use characteristics and yield formation of rice. – Master Thesis, Sichuan Agricultural University, Ya'an.
- [13] Tao, H. B., Lin, S. (2006): Comparison of hole weighing method with copy weighing method and length-width correction method for determining leaf area of rice. – *Plant Physiology Newsletter* 2006: 496-498.
- [14] Tian, H., Pan, S. G., Mo, Z. W., Duan, M. Y., Tang, X. R. (2018): Effects of different water and grain fertilizer treatments on aroma, quality and yield of scented rice. – *Journal of Irrigation and Drainage* 37: 36-41.
- [15] Wang, P., Tang, X. R., Tian, H., Pan, S. G., Duan, M. Y., Nie, J., Luo, Y. M., Xiao, L. Z. (2013): Effects of water irrigation treatments at booting stage on aroma and physiological characteristics of scented rice. – *Guangdong Agricultural Sciences* 40: 1-3.
- [16] Wu, Y. X., Liu, F. Y., Sun, Y. J., Guo, C. C., Jerry Young, Yan, T. R., Sun, Z. B., Ding, F., Ma, L. (2019): Effects of interaction of water and nitrogen on yield and quality of direct seeding rice. – *Journal of Sichuan Agricultural University* 37: 604-610, 622.
- [17] Huang, N. T. T., Inatomi, H. (2002): Precursors of 2-acetyl-1-pyrroline, a potent flavor compound of an aromatic rice variety. – *Journal of Agricultural and Food Chemistry* 50: 2001-2004.
- [18] Zhao, L. M., Li, M., Zheng, D. F., Gu, C. M., Na, Y. G., Xie, B. S. (2015): Effects of irrigation method and planting density on rice yield and photosynthetic matter production characteristics in cold region. – *Journal of Agricultural Engineering* 2015: 159-169.
- [19] Zhao, H. J., Wang, Q., Sun, Y., Zeng, X. N., Zhang, X. M., Wang, P., Wang, M. L., Feng, Y. J. (2018): Effects of straw returning irrigation on rice yield and water use efficiency. – *Journal of Nuclear Agriculture* 32: 959-969.
- [20] Zheng, C. J., Li, S. (2017): Effects of water stress on rice growth and rice quality during anthesis. – *China Rice* 23: 43-45.

## APPENDIX



Instruments used to measure the content of aroma in fragrant rice

# SPATIAL HETEROGENEITY OF TOPSOIL MOISTURE AND IMPACT OF VEGETATION FACTORS ON ITS DISTRIBUTION UNDER PURE AND MIXED BLACK LOCUST (*ROBINIA PSEUDOACACIA* L.) AND CHINESE RED PINE (*PINUS TABULAEFORMIS* CARR.) FORESTS ON THE LOESS PLATEAU IN CHINA

LIANG, W. J.<sup>1</sup> – WEI, X.<sup>1,2\*</sup>

<sup>1</sup>College of Forestry, Shanxi Agricultural University, Taigu 030801, P.R. China

<sup>2</sup>Ji County Station, Chinese National Ecosystem Research Network (CNERN), Beijing 100083, P.R. China

\*Corresponding author  
e-mail: weixi@sxau.edu.cn

(Received 21<sup>st</sup> Oct 2020; accepted 21<sup>st</sup> Dec 2020)

**Abstract.** To determine the contribution of overstory and understory flora on soil water content in typical forest plantations on the Loess Plateau, standard sampling plots were established in five pure *Robinia pseudoacacia* L. and five pure *Pinus tabulaeformis* Carr. plantations, together with five more plots in mixed forests of both species. The relationships between the overstory structure, herbaceous diversity, soil water, and nutrients were analyzed using statistical methods including feature, geostatistical, and Pearson's correlation analyses. The results indicated that the topsoil moisture content of the pure forests (12.80% and 11.97%, respectively) was greater than that of the mixed forest (6.75%), but significantly lower than that of a grassland (26.97%). The canopy leaf area index (LAI), herbaceous Shannon-Wiener index, Simpson's index, and total nitrogen (TN) were important factors controlling the distribution of soil moisture (the absolute values of their correlation coefficients were more than 0.5). The spatial heterogeneity of topsoil moisture was greatest in the pure *Robinia pseudoacacia* L. forests. It was found that appropriately increasing and decreasing the significant controlling factors, including LAI, herb diversity, and soil TN, could improve the soil moisture content and mitigate its spatial heterogeneity to improve the growth of vegetation on the Loess Plateau.

**Keywords:** *overstory and understory flora, stand structure, herbaceous diversity, topsoil water distribution, soil properties*

## Introduction

Soil water in the ecosystem is the basis of plant survival, and is also an important factor restricting the growth of trees (Pueyo et al., 2014; Ma et al., 2020). On the Loess Plateau, afforestation and vegetation restoration have improved the provision of ecosystem services and the functioning of the region in recent decades (Shen et al., 2018). However, the large-scale planting of artificial forests has resulted in the consumption of excessive water and increasingly dry soil layers.

To examine the causes of these problems, most studies have focused on the structure and function of the Loess Plateau ecosystem and other ecologically sensitive areas. For example, chronic water stress can reduce forest growth (Brzostek et al., 2014), and soil water content is also affected by terrain, climate, and plant survival (Liu et al., 2018). Previous studies have reached similar conclusions regarding forest structure, soil moisture (Li et al., 2016; Martínez-Murillo et al., 2017), and soil physical and chemical properties (Shi et al., 2017). Environmental heterogeneity (including the temporal and

spatial heterogeneity of terrain, climate, soil, or water) is a well-recognized influence on plant communities because species differ both in their responses to and their effects on soil characteristics (Smith and Knapp, 2006; Li et al., 2018). The environmental indicators of different tree species are significantly varied, such as the overstory leaf area index (LAI) and transpiration rate, and the Shannon-Wiener ( $H'$ ), Simpson's ( $D$ ), and Pielou ( $J$ ) indexes of the herbs in the understory. The LAI incorporates many eco-physiological processes and can be used to scale-up leaf and water processes to ecosystem and even regional levels (Liu et al., 2018). In contrast, the diversity indexes reflect the growth of understory herbs (Sánchez-González and López-Mata, 2005).

Plant species differ in their responses to the spatial heterogeneity of resources (Grime, 1994; Endara and Jaramillo, 2011), and at the same time they create spatial heterogeneity in the process of adapting to different environments (Eldridge et al., 2019; Yu et al., 2019; Ahmad et al., 2020). Previous studies found no significant effect of plants on the spatial heterogeneity of soil moisture content (Farley and Fitter, 1999; Ronda et al., 2002). We investigated the effects of both trees and herbs on the spatial heterogeneity of soil moisture content within a semiarid region, the Western Shanxi Province, in China. Generally, the between-year variability in rainfall on a slope scale is significantly greater for grasslands than forests (Smith and Knapp, 2006), indicating that grasses face a selection pressure in overcoming the spatial heterogeneity in soil moisture content (Western et al., 1998; Sreelash et al., 2018). Grasses have the ability to amplify the spatial heterogeneity of soil moisture, and through their water uptake might reduce soil moisture to a much greater extent than woody plants, which could eventually remove trees from grasslands (Qi et al., 2004; Wubs and Bezemer, 2018). The large potential water absorption of grasses may change the spatial variability of soil moisture content in grasslands and forest-grass mixed areas. To evaluate this, two representative species, black locust (*Robinia pseudoacacia* L.) and Chinese red pine (*Pinus tabulaeformis* Carr.), growing together with understory herbs were selected to conduct a field investigation in the region.

There is much uncertainty about the significance and direction of how differences between tree species and their understory flora are impacted by differences in terms of the spatial heterogeneity of soil moisture content, and the causes of the differences are also not clear. We considered the environmental heterogeneity, including climate characteristics, forest cover, water, soil type, topography, geomorphology, and development of the area, comprehensively in this study. It was hypothesized that there were significant differences in the soil moisture content between areas covered by trees and herbs, and the canopy interception and plant uptake made different contributions to soil moisture under the different plant covers. The mechanism and process of the competition for water use between forests and grassland were quantitatively analyzed, and the impact factors of the spatial heterogeneity in soil moisture were identified. The results provide a reference for the comprehensive utilization of soil water and the optimization of the overstory and understory vegetation on the Loess Plateau.

## Materials and methods

### *Site description*

The experimental field site was located in the nested Caijiachuan watershed, which is a typical gully area of the Loess Plateau in Ji County, Shanxi Province, China. The longitude and latitude were 35°53'–36°21' N and 110°27'–111°7' E, respectively, and

the elevation ranged from 904 to 1592 m a.s.l. The annual mean temperature of the area is 10.2°C, the annual mean precipitation is 571 mm, and the annual mean potential evapotranspiration (PET) is 1724 mm. The region therefore has the typical features of a continental climate, with the PET being more than three times the annual rainfall. The soil is a Haplic Luvisol, according to the soil classification of the Food and Agriculture Organization of the United Nations (FAO). The vegetation is characterized by artificial shelterbelts of black locust (*Robinia pseudoacacia* L.) and Chinese red pine (*Pinus tabulaeformis* Carr.), with a forest cover of up to 72% over an area of 38 km<sup>2</sup>. Additional details of the shrubs present in the area have been published elsewhere (Wei et al., 2018), with the dominant herbaceous species being *Artemisia sacrorum* Ledeb., *Patrinia scabiosifolia*, *Carex rigescens*, *Rubia cordifolia* L., *Metaplexis japonica* (Thunb.) Makino.

### Field observations and soil sampling

We examined the spatial variability of the shallow soil moisture content in 15 standard plots (20 × 20 m), including five in pure *Robinia pseudoacacia* L. and five in pure *Pinus tabulaeformis* Carr. Plots, together with five in mixed forests composed of both species. The plots were scattered along different ravines in the same watershed, to ensure that precipitation and soils were as similar as possible (Fig. 1). Additionally, we selected five grassland monocultures as control groups to ensure the reliability of the experimental design (Fig. 2). The details of the standard sampling plots in the watershed was shown in Table 1 by surveyed.

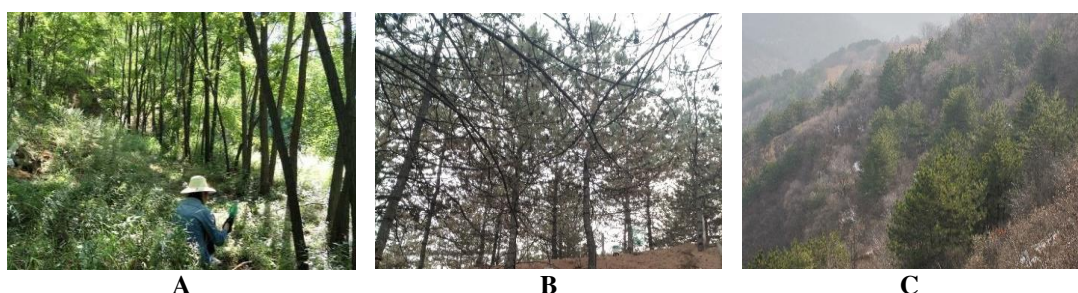


**Figure 1.** Images of selected sampling plots. (A) *Robinia pseudoacacia* L.; (B) *Pinus tabulaeformis* Carr.; (C) Mixed forest

Field surveys and measurements were conducted for all woody plants with diameters at breast height (DBHs)  $\geq 5$  cm per plot (DBH measured to the nearest 0.1 cm) during the summer growing season of 2017. The LAI of these plots was collected using a plant canopy analyzer (LAI-2000, LI-COR Company, Lincoln, NE, USA) in the morning, with no direct sunlight. Three LAI measurements were taken randomly in each plot, and their mean values were the representations of the stands. Herb layers under the forests were investigated by randomly arranging three quadrats of 1 × 1 m for calculating the indicators of richness (number of species), biodiversity, including the Shannon-Wiener index ( $H' = -\sum_{i=1}^S p_i \ln p_i$ ) and Simpson's index ( $D = 1 - \sum_{i=1}^S p_i^2$ ), and evenness (Pielou index:  $J = H' / \ln S$ ) (Shannon and Wiener, 1949; Simpson, 1949; Pielou, 1966; Daniel et al., 2019). The transpiration rate was measured by the weighing method (Takagi et al., 2006). The shallow soil volumetric moisture content at 0–20 cm depth was measured every 2 m by a soil probe (TDR 300, Spectrum Technologies, Inc.,



Plainfield, IL, USA), in a rectangular shaped alternating ridge and slope collection scheme (Fig. 3). All the sampling positions were measured unless there were large rocks or stout roots belowground, and the number of measurements per plot was >80. To avoid the influence of rainfall, soil moisture was measured at least three days after rain. Three replicated samples were established per plot, and soil samples (0–20 cm) were collected using a soil auger to represent the topsoil of the whole plot. After the air-dried soil samples were sieved (0.15 mm mesh sieve), the soil organic matter (SOM), total nitrogen (TN), total phosphorus (TP), ammonia-nitrogen (NH<sub>3</sub>-N), nitrate-nitrogen (NO<sub>3</sub>-N), and available phosphorus (AP) contents were measured in the laboratory (Wei et al., 2018), using a SmartChem-200 Discrete Wet Chemistry Analyzer (AMS/Alliance Instruments, Paris, France).

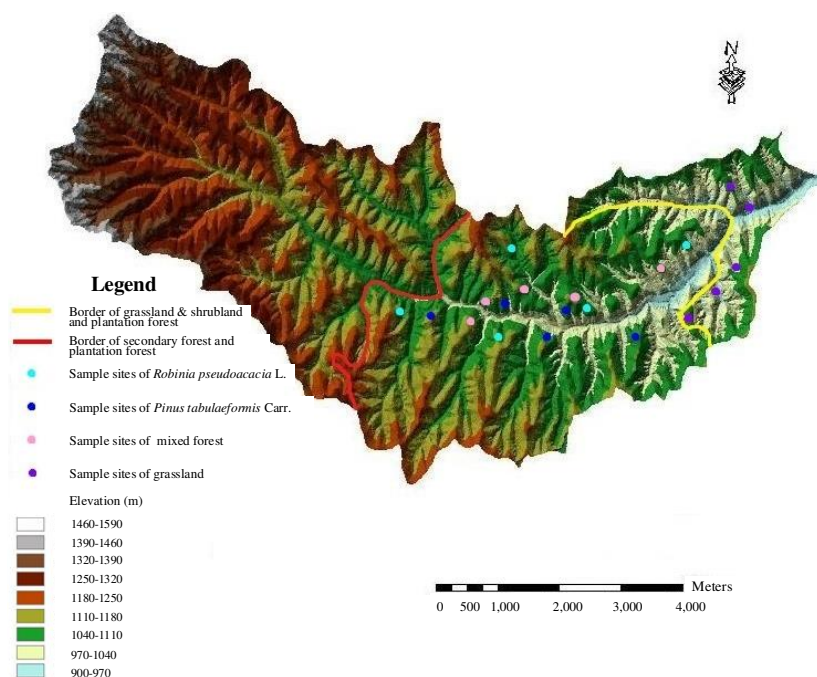


**Figure 2.** The distribution of the thirteen sampling plots in the watershed

### Data collection

Forest characteristics were calculated, including DBH, tree height, crown area, stand density, canopy density, overstory LAI, the number of species (N), Shannon-Wiener index ( $H'$ ), Simpson's index ( $D$ ), and Pielou index ( $J$ ) for both overstory and understory flora. Soil moisture and nutrients were measured and calculated (Daniel et al., 2019). Based on these indicators, a geostatistical analysis of soil moisture was conducted, using the kriging interpolation approach (Krige, 1966). The relationships between the spatial heterogeneity of the soil moisture, the overstory woody plants, and the understory herbaceous plants should be explored to determine the influence of the recommended soil moisture distribution on the vegetation. Correlations between trees, herbs, and soils were analyzed using SPSS 19.0 (IBM/International Business Machines Corporation, Armonk, NY, USA), and a geostatistical analysis of soil moisture was performed using the software Suffer 11.0 (Golden Software, Inc., Golden CO, USA).



**Table 1.** Details of the standard sampling plots in the watershed

Sample number	Abbreviation	Elevation(m)	Slope (°)	Aspect	Stand density (trees·hectare <sup>-1</sup> )	Average DBH <sup>a</sup> (cm)	Average tree height (m)	Average crown area (m <sup>2</sup> )
No.1 of black locust	BL1	1160	39	semi-shady	900	14.64	9.7	8.38
No.2 of black locust	BL2	1140	26	shady	1200	9.93	8.7	5.75
No.3 of black locust	BL3	1190	22	semi-shady	1675	8.01	4.5	5.81
No.4 of black locust	BL4	1120	22	semi-sunny	2075	12.29	9.9	11.82
No.5 of black locust	BL5	1120	15	semi-shady	2525	10.11	8.8	6.10
No.1 of Chinese red pine	CP1	1150	30	semi-sunny	700	13.47	6.9	9.27
No.2 of Chinese red pine	CP2	1130	35	shady	1200	12.82	6.4	12.27
No.3 of Chinese red pine	CP3	1150	26	semi-shady	1250	14.11	8.4	8.99
No.4 of Chinese red pine	CP4	1140	28	semi-sunny	1275	12.65	6.6	9.17
No.5 of Chinese red pine	CP5	1120	23	semi-sunny	1425	8.72	7.9	6.67
No.1 of mixed forest <sup>b</sup>	MF1	1060	35	shady	1150	11.98	9.4	7.75
No.2 of mixed forest	MF2	1110	18	semi-sunny	1600	10.80	7.4	6.55
No.3 of mixed forest	MF3	1150	33	semi-shady	1625	9.40	8.0	5.37
No.4 of mixed forest	MF4	1060	32	shady	2125	9.63	7.8	4
No.5 of mixed forest	MF5	1130	27	shady	3075	10.31	8.3	5.89
No.1 of Grassland	GL1	950	21	shady	-	-	-	-
No.2 of Grassland	GL2	960	24	semi-shady	-	-	-	-
No.3 of Grassland	GL3	1010	40	sunny	-	-	-	-
No.4 of Grassland	GL4	990	22	semi-shady	-	-	-	-
No.5 of Grassland	GL5	970	24	semi-sunny	-	-	-	-

<sup>a</sup>DBH, diameter at breast height. <sup>b</sup> Mixed forest included a mixture of black locust (*Robinia pseudoacacia* L.) and Chinese red pine (*Pinus tabulaeformis* Carr.). The data of the stand density, average DBH, average tree height, average crown height, and average crown area came from the field surveys and measurements

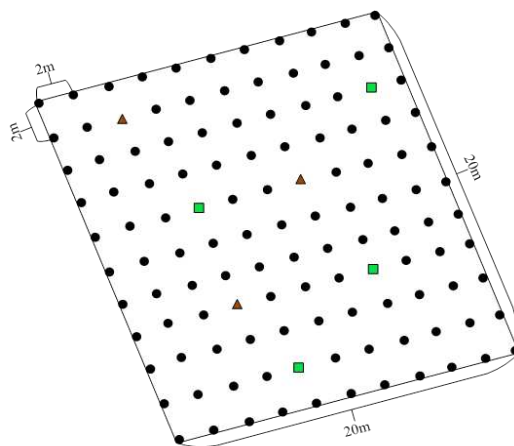


**Figure 3.** Schematic diagram of soil moisture sampling positions. In the diagram, the dots indicate the sampling points, the triangles indicate large rocks, and the squares indicate stout roots. Because the TDR probe could not be inserted into the soil at the correct angle, no soil moisture samples were collected in the positions with obstacles

## Results

### Comparison of vegetation characteristics

The major biological and soil physicochemical characteristics of the investigated plots are summarized in *Table 2*. The leaf area and transpiration of trees in the upper layer, and herbaceous plant diversity in the understory had different relationships with soil moisture and nutrients in the four types of stand. The LAI and transpiration rate trends of monoculture *Robinia pseudoacacia* L. and *Pinus tabulaeformis* Carr. followed the opposite pattern (*Fig. 4A*). The maximum LAI of pure *Robinia pseudoacacia* L. was larger than that of both pure *Pinus tabulaeformis* Carr. and mixed forests. The transpiration rate of the mixed forest was generally greater than that of the two pure species.

**Table 2.** The average value of each indicator

Stand and soil characteristics	Black locust	Chinese red pine	Mixed forest	Grassland
Canopy density	0.59±0.15 <sup>k</sup>	0.68±0.09	0.71±0.10	-
LAI <sup>a</sup>	2.32±1.23	1.95±0.22	2.04±0.49	-
Transpiration rate (g·m <sup>-2</sup> ·h <sup>-1</sup> )	26.02±7.46	27.91±9.88	33.80±17.52	-
Herb- <i>H'</i> <sup>b</sup>	1.80±0.21	1.84±0.22	1.57±0.49	2.06±0.25
Herb- <i>D</i> <sup>c</sup>	0.79±0.05	0.79±0.04	0.70±0.11	0.85±0.04
Herb- <i>J</i> <sup>d</sup>	0.86±0.03	0.84±0.02	0.83±0.08	0.89±0.03
Soil volumetric moisture content (%)	12.80±4.58	11.97±1.48	6.75±1.38	26.97±2.59
SOM <sup>e</sup> (g·kg <sup>-1</sup> )	11.23±2.68	9.10±1.97	10.22±1.43	14.30±5.07
TN <sup>f</sup> (g·kg <sup>-1</sup> )	0.67±0.20	0.65±0.25	0.38±0.08	0.43±0.13
TP <sup>g</sup> (g·kg <sup>-1</sup> )	0.64±0.14	0.64±0.13	0.53±0.06	0.62±0.07
NH <sub>3</sub> -N <sup>h</sup> (mg·kg <sup>-1</sup> )	19.87±6.53	22.68±5.92	25.93±3.35	17.43±5.38
NO <sub>3</sub> -N <sup>i</sup> (mg·kg <sup>-1</sup> )	10.65±4.97	6.79±1.48	9.13±2.87	12.49±7.20
AP <sup>j</sup> (mg·kg <sup>-1</sup> )	35.52±7.96	38.07±3.71	45.96±7.88	40.43±12.75

<sup>a</sup> LAI, leaf area index. <sup>b</sup> Herb-*H'*, Shannon-Wiener index value for the herb. <sup>c</sup> Herb-*D*, Simpson's diversity index value for the herb. <sup>d</sup> Herb-*J*, Pielou index value for the herb. <sup>e</sup> SOM, soil organic matter. <sup>f</sup> TN, total nitrogen. <sup>g</sup> TP, total phosphorus. <sup>h</sup> NH<sub>3</sub>-N, ammonia-nitrogen. <sup>i</sup> NO<sub>3</sub>-N, nitrate-nitrogen. <sup>j</sup> AP, available phosphorus. <sup>k</sup> The data in the table was presented in the forms of 'mean ± variance'

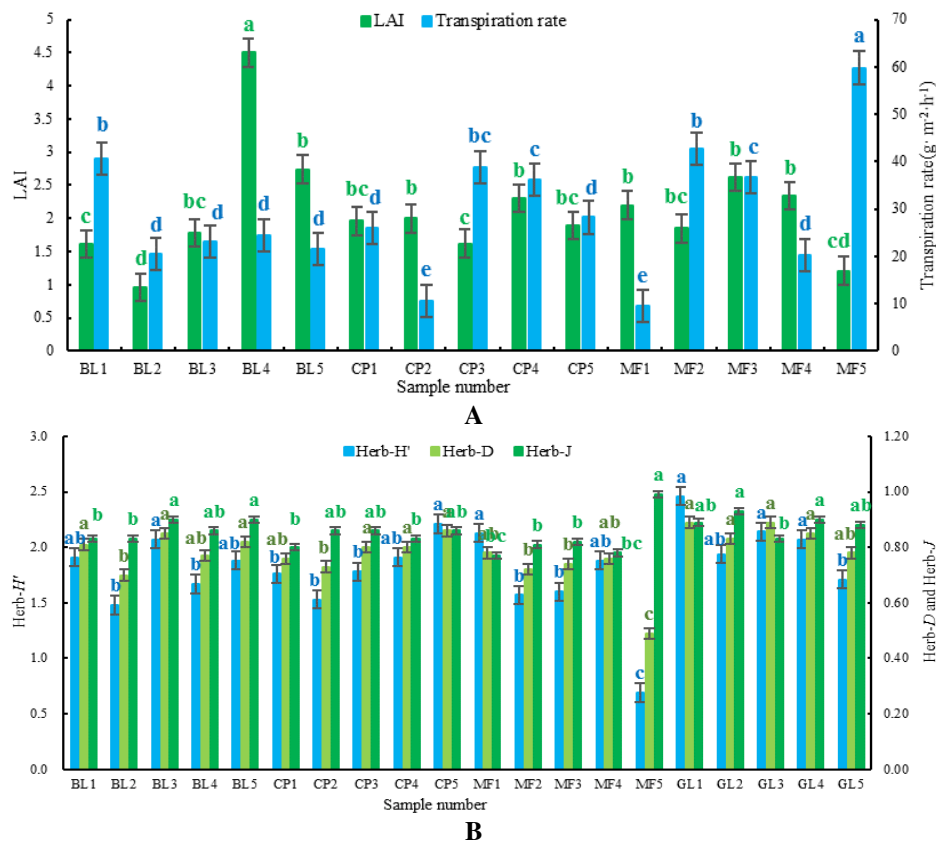


**Figure 4.** The vegetation characteristics of the different stands. (A) LAI and transpiration rate. (B) The herbaceous diversity indexes. Note: LAI, leaf area index; Herb-H', Shannon-Wiener index of the herb; Herb-D, Simpson's index of the herb; Herb-J, Pielou index of the herb. Note: BL1, 2, 3, 4, and 5 was abbreviation of No.1, 2, 3, 4, and 5 of black locust sample plots; CP 1, 2, 3, 4, and 5 was abbreviation of No.1, 2, 3, 4, and 5 of Chinese red pine sample plots; MF 1, 2, 3, 4, and 5 was abbreviation of No.1, 2, 3, 4, and 5 of mixed forest sample plots; and GL 1, 2, 3, 4, and 5 was abbreviation of No.1, 2, 3, 4, and 5 of Grassland sample plots in the figure and similarly hereinafter. The error bars are representing for standard error plus or minus. Different lowercase letters, such as a, b, c, d, and e, indicated  $P < 0.05$  in the same series of variables, through significance testing

In the understory of the different vegetation plots (Fig. 4B), the herbaceous Shannon-Wiener index values under *Robinia pseudoacacia* L. were higher than those under *Pinus tabulaeformis* Carr. and mixed forests, but lower than the pure grassland. The herbaceous Shannon-Wiener index and Simpson's index of all vegetation types displayed a similar trend, and were positively related to each other. In terms of the magnitude of the diversity indexes, the sample plots with trees were significantly lower than the monoculture grassland. The mixed forest had the lowest range of index values.

### Topsoil moisture heterogeneity

The correlations between average topsoil moisture and slope were not very strong, with the curves of their variation in the sample plots being irregular (Fig. 5). The results showed large differences in soil moisture, with the average soil moisture in the sample plots for the three types of overstory trees being lower than that of pure grassland.

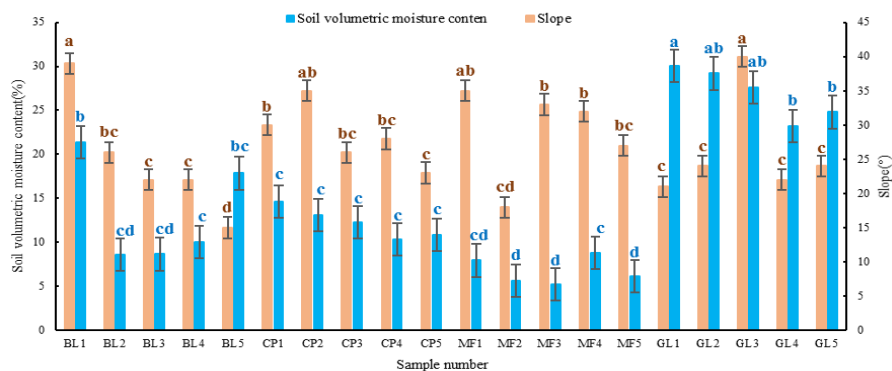


**Figure 5.** The topsoil volumetric moisture content in relation to the slope for all samples. Note: The error bars were representing for standard error plus or minus. Different lowercase letters, such as a, b, and c indicated  $P < 0.05$  in the same series of variables, through significance testing

The moisture data basically followed a normal distribution, and the spatial heterogeneity of the topsoil moisture was demonstrated through a kriging interpolation (Krige, 1966). The nugget effects were residual in all the ordinary kriging cases, the values of which showed moderate variations, with coefficients of variation (CVs) of 11.78%, 10.36%, 9.82%, and 5.44% for the data in Figures 6 to 9, respectively. The random variances ( $C_0$ ) accounted for nearly 8% of the total variances ( $C_0 + C$ ) in the topsoil moisture values of the different vegetation types, indicating that there were strong spatial autocorrelations of soil moisture values within 15 m, and the values of  $R^2$  ranged from 0.752 to 0.793. The values of these parameters demonstrated that the variances were minimal, and the number of samples was sufficient to assess the spatial variability of topsoil moisture. Additionally, the y coordinate values were small, which meant that the topsoil moisture content of the soil samples was small below the slope and large on the slope.

The range of the topsoil moisture values for all species was from 0 to 47.9%. In the figures (Figs. from 6 to 9), a bluish color indicates a high moisture content and a greenish color indicates a low moisture content. The topsoil moisture distributions of pure *Robinia pseudoacacia* L. are shown in Fig. 6, with a value ranging from 5.1% to 26.6%. In addition to terrain and vegetation factors, the distribution of soil moisture was dependent on the canopy LAI and understory diversity. In the plots with high LAI values and strong herbaceous diversity, the soil volumetric moisture content in the surface layer was large. The soil moisture content in the pure *Pinus tabulaeformis* Carr. plots ranged from 6.2% to 20.3% (Fig. 7). According to the topographical and forest plantation characteristics in the sample plots, some of the coniferous forest plots (e.g., CP1) were located in semi-sunny areas, in which the LAI values and herbaceous diversity were higher than in the shady region. The distribution of topsoil moisture was positively correlated with plant factors. A high LAI value indicated that there was a large amount of soil water in the corresponding plot. The topsoil moisture distribution of the mixed forests was slightly unusual (Fig. 8). It had smallest range of the four vegetation types, with values between 2.6% and 12.7%. The aspects of the three plots were semi-sunny, semi-shady, and shady, respectively, and were not significantly correlated with the soil water content. The soil moisture content had negative relationships with the slope, LAI, Shannon-Wiener index, and Simpson's index.

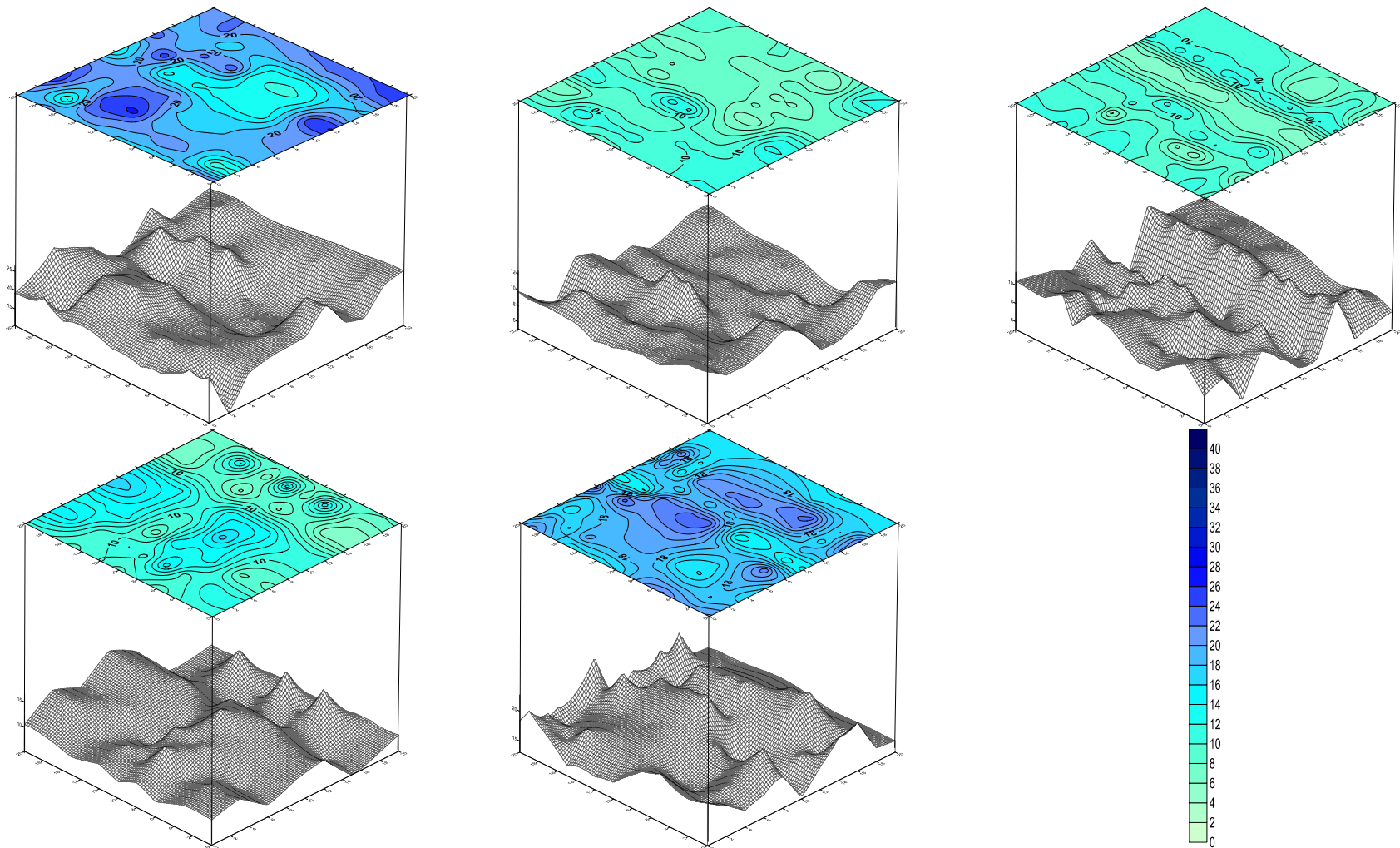


**Figure 6.** The topsoil volumetric moisture content distribution in *Robinia pseudoacacia* L. plots. (A) BL1; (B) BL2; (C) BL3; (D) BL4; (E) BL5



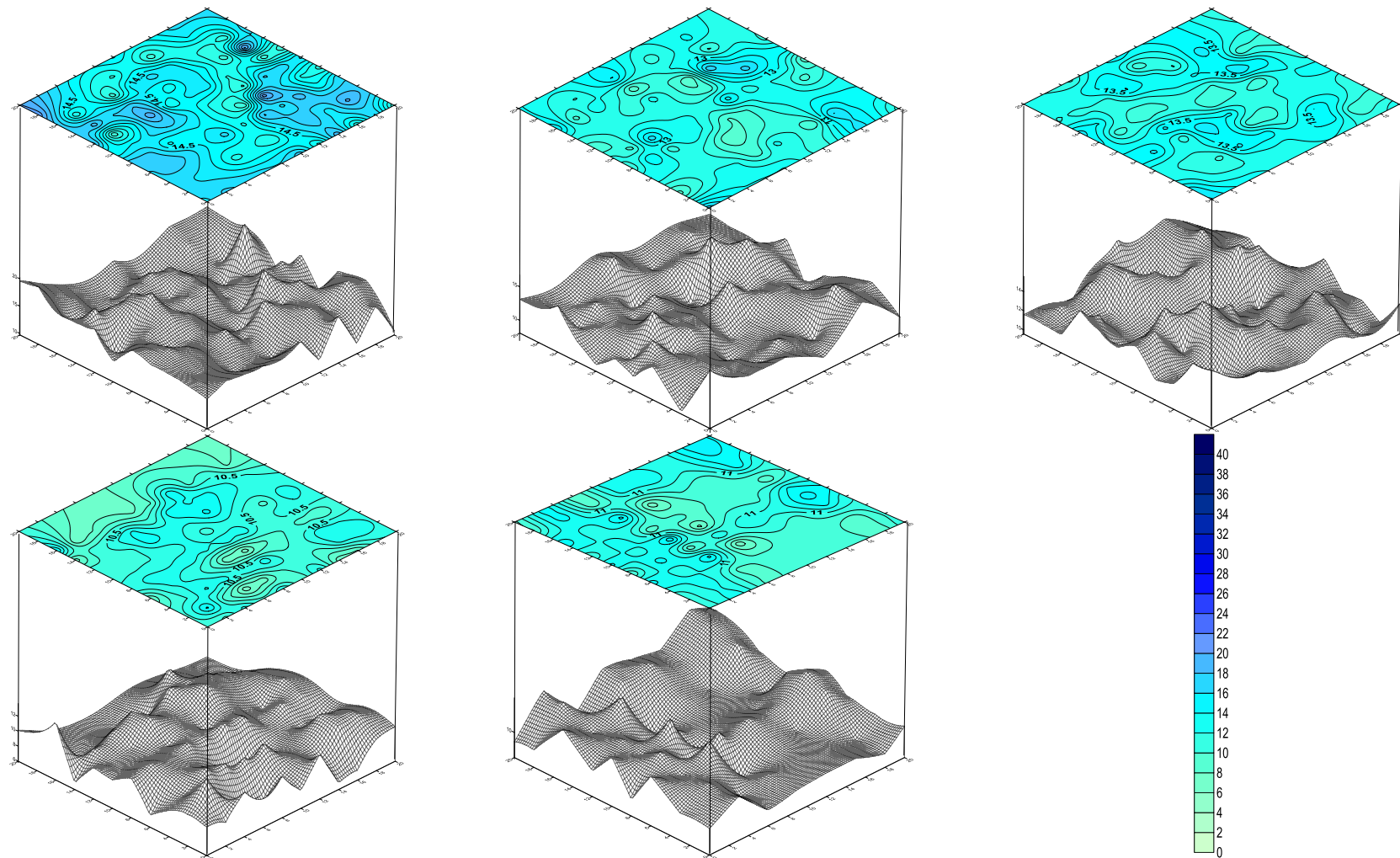


**Figure 7.** The topsoil volumetric moisture content distribution in *Pinus tabulaeformis* Carr. plots. (A) CP1; (B) CP2; (C) CP3; (D) CP4; (E) CP5

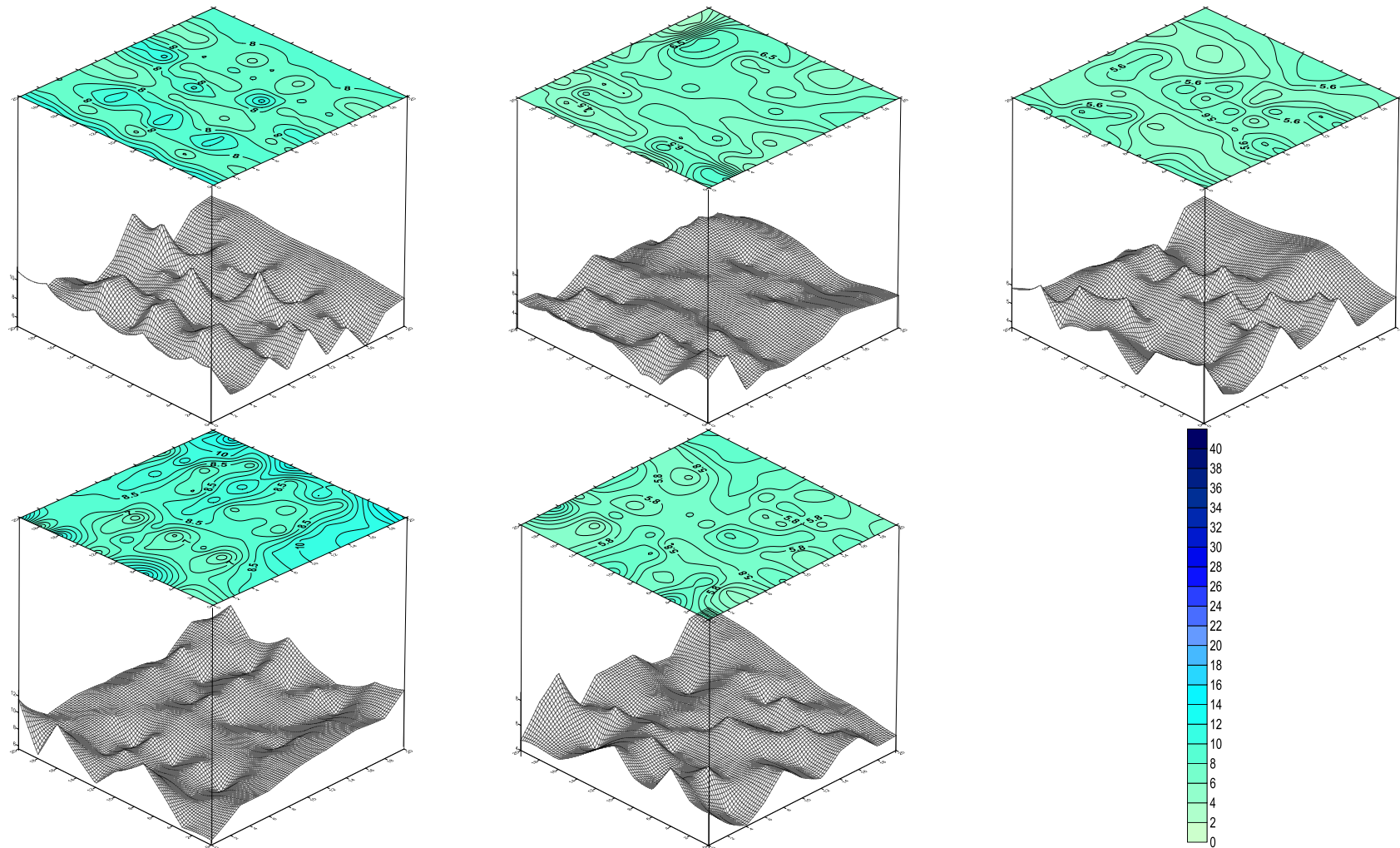


**Figure 8.** The topsoil volumetric moisture content distribution in mixed forest plots. (A) MF1; (B) MF2; (C) MF3; (D) MF4; (E) MF5

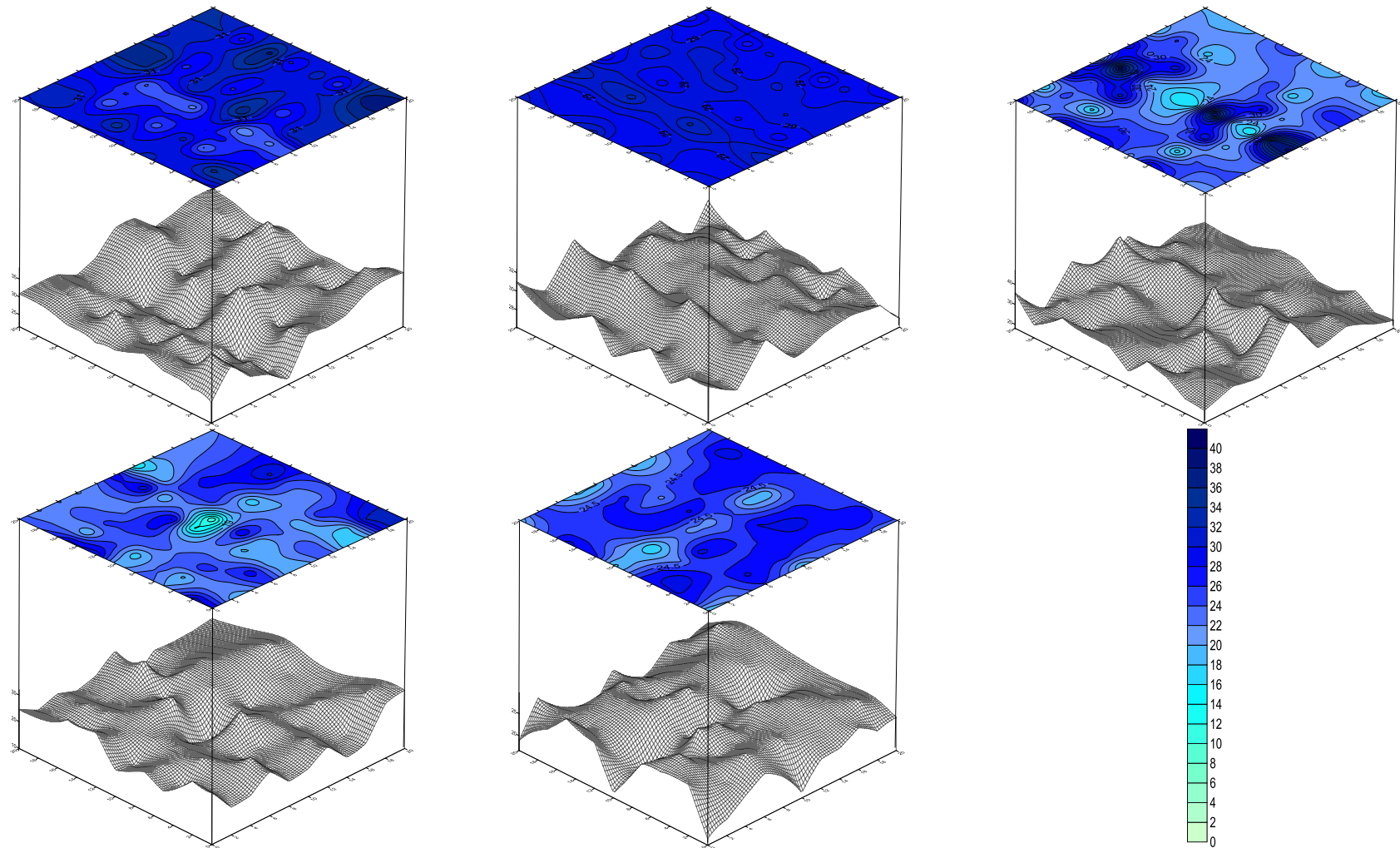


**Figure 9.** The topsoil volumetric moisture content distribution of grassland plots for reference. (A) GL1; (B) GL2; (C) GL3; (D) GL4; (E) GL5



Compared to the grassland (Fig. 9), the topsoil moisture content of both pure and mixed forests were significantly smaller under the canopies than in those areas with only a low herb coverage, most values of which were more than 15%, with a maximum of 47.9%. The values for the mixed forests had the smallest range of all the stands. From the three-dimensional models of the top soil water distribution (Figs. from 6 to 9), there was a large spatial heterogeneity of surface soil moisture in all four types of stand and the amplitude of the variations was different.

### Changes of soil properties

The soil properties are presented in Fig. 10, including soil SOM, TN, TP, NH<sub>3</sub>-N, NO<sub>3</sub>-N, and AP. The soil properties from the field sites were in correspondence with the plant and water conditions. The grassland plots had more SOM and less NH<sub>3</sub>-N than the other stands, and the pure *Robinia pseudoacacia* L. stands had more TN.

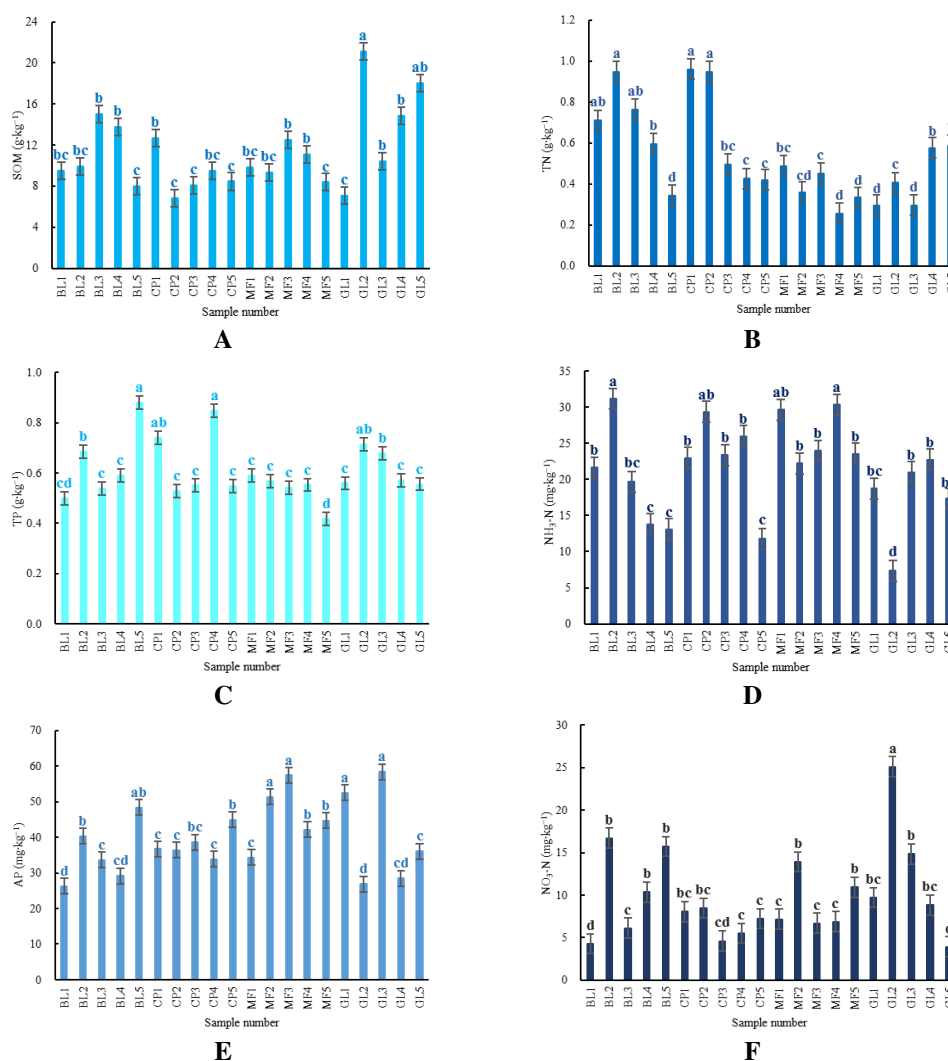


**Figure 10.** The topsoil properties of the different sampling plots. (A) Soil organic matter (SOM). (B) Total nitrogen (TN). (C) Total phosphorus (TP). (D) Ammonia-nitrogen (NH<sub>3</sub>-N). (E) Available phosphorus (AP). (F) Nitrate-nitrogen (NO<sub>3</sub>-N). Note: The error bars were representing for standard error plus or minus. Different lowercase letters, such as a, b, c, and d indicated  $P < 0.05$  in the same series of variables, through significance testing

### Relationships of topsoil moisture spatial heterogeneity with plant and soil properties

After feature and geostatistical analyses, some of the important factors that impacted on the spatial heterogeneity of topsoil moisture were determined, including canopy density, LAI, three herbaceous diversity indexes, transpiration rate, and TN. Correlation coefficients were calculated to identify the associations among all the variables through a Pearson's correlation analysis, and the results for the three plantations are shown in Table 3.

Table 3. The results of a Pearson's correlation analysis for the three plantations

Stand type	Index name	Canopy density	LAI	Herb-H'	Herb-D	Herb-J	Transpiration rate	VCM	TN
<i>Robinia pseudoacacia</i> L.	Canopy density	1.000	0.411	-0.385	-0.275	-0.167	0.047	0.689	-0.576
	LAI <sup>c</sup>		1.000	0.581	0.687	0.765	-0.105	0.584	-0.980 <sup>a</sup>
	Herb-H' <sup>d</sup>			1.000	0.991 <sup>**b</sup>	0.644	0.308	0.287	-0.465
	Herb-D <sup>e</sup>				1.000	0.704	0.257	0.354	-0.58
	Herb-J <sup>f</sup>					1.000	-0.496	-0.050	-0.629
	Transpiration rate						1.000	0.626	0.028
	VCM <sup>g</sup>							1.000	-0.703
	TN <sup>h</sup>								1.000
<i>Pinus tabulaeformis</i> Carr.	Canopy density	1.000	0.667	-0.395	-0.465	0.324	-0.602	0.893	0.127
	LAI		1.000	0.270	-0.060	-0.388	-0.147	0.504	-0.062
	Herb-H'			1.000	0.896	-0.430	0.898	-0.690	-0.751
	Herb-D				1.000	-0.026	0.986 <sup>*</sup>	-0.812	-0.922
	Herb-J					1.000	-0.122	0.179	-0.271
	Transpiration rate						1.000	-0.893	-0.845
	VCM							1.000	0.560
	TN								1.000
Mixed <i>Robinia pseudoacacia</i> L. and <i>Pinus tabulaeformis</i> Carr. forests	Canopy density	1.000	-0.869	-0.999 <sup>*</sup>	-0.998 <sup>**</sup>	0.994	0.982	0.936	-0.709
	LAI		1.000	0.854	0.875	-0.810	-0.947	-0.987	0.965
	Herb-H'			1.000	0.999 <sup>*</sup>	-0.997 <sup>*</sup>	-0.975	-0.925	0.687
	Herb-D				1.000	-0.993	-0.984	-0.941	0.717
	Herb-J					1.000	0.955	0.893	-0.628
	Transpiration rate						1.000	0.986	-0.830
	VCM							1.000	-0.911
	TN								1.000

<sup>a</sup> \*, the correlation was significant at the 0.05 level (bilateral). <sup>b</sup> \*\*, the correlation was significant at the 0.01 level (bilateral). <sup>c</sup> LAI, leaf area index. <sup>d</sup> Herb-H', Shannon-Wiener index value for the herb. <sup>e</sup> Herb-D, Simpson's index value for the herb. <sup>f</sup> Herb-J, Pielou index value for the herb. <sup>g</sup> VCM, Soil volumetric moisture content. <sup>h</sup> TN, total nitrogen

The LAI of *Robinia pseudoacacia* L. was negatively correlated with TN at the 0.05 level and the Shannon-Wiener index was positively correlated with the Simpson's index at the 0.01 level, with correlation coefficients of -0.980 and 0.991, respectively. The

Simpson's index of *Pinus tabulaeformis* Carr. was positively correlated with the transpiration rate at the 0.05 level, with a correlation coefficient of 0.986. In the mixed forests, the canopy density had significantly negative correlations with the Shannon-Wiener index and Simpson's index, with correlation coefficients of  $-0.999$  (significant at the 0.05 level) and  $-0.998$  (significant at the 0.01 level), respectively. The Shannon-Wiener index was negatively correlated with the Pielou index, which had a correlation coefficient of  $-0.997$  (significant at the 0.05 level). The relationships between the above indicators demonstrated that the influences of the overstory and understory flora on soil moisture were significant.

The connections among plantations, topsoil water, and soil properties were calculated quantitatively using their correlation coefficients. Most coefficients were greater than 0.5, indicating that the overstory and understory properties were closely correlated to the topsoil moisture and then influenced its spatial heterogeneity. In particular, canopy density, LAI, transpiration rate, and TN affected the soil water significantly in all three kinds of forest stand. When the different tree species were compared, the impacts of these factors in the mixed forests presented stronger correlations, with all correlation coefficients greater than 0.89. Although the significance of the correlation analysis results was not very strong, which reduced their credibility, the quantitative relationships between plant factors, topsoil moisture, and nutrients were still of interest and provided some evidence for the complex relationships between the upper forest canopy, herbs under the forests, topsoil moisture, and soil nutrients.

## Discussion

### *Biotic factors*

Although the spatial heterogeneity of topsoil moisture is sensitive to biotic factors, such as the canopy density, LAI, herbaceous diversity, or transpiration rate (Paluch and Gruba, 2012; Von Arx et al., 2013; Gebrekiros and Tessema, 2018), no clear conclusions have emerged from studies of different vegetation stands in the Loess Plateau (Hu et al., 2019). This is most likely because the factors controlling the spatial heterogeneity of soil water change with species composition or forest structure (Barksdale and Anderson, 2015). In the present study, the LAI, Shannon-Wiener index, and transpiration rate significantly affected the values and distributions of topsoil moisture. Similar results have been reported elsewhere. For example, transpiration can become limited by the available soil moisture in the surface and middle-layer soils (Meerveld and McDonnell, 2006), and canopy characteristics and plant diversity have been shown to be significantly and positively correlated with moisture in the topsoil (Deng et al., 2016). These findings suggest that the LAI and herbaceous diversity were likely related to the spatial heterogeneity of topsoil water more closely than the other factors (Manea and Leishman, 2014; Singh et al., 2017).

The results suggested a positive correlation between the LAI and transpiration in *Robinia pseudoacacia* L., as a representative broad-leaved tree species, and an insignificant negative correlation in *Pinus tabulaeformis* Carr., which is a typical coniferous species in the region. When the two species formed mixed forests, the negative correlations of the LAI and transpiration were significantly enhanced and the gradient of the plotted relationship between these variables also increased slightly. The stands with lower LAI values and herbaceous diversity had a lower topsoil moisture

content and less spatial heterogeneity. In the *Pinus tabulaeformis* Carr. and mixed forest plots there was a low moisture content in uphill locations and a high moisture content in downhill locations. The LAI was therefore an important variable that significantly affected the spatial heterogeneity of topsoil water. In addition, the topsoil volumetric moisture content had a close relationship with the understory vegetation (Nijland et al., 2010; Özkan and Gökbulak, 2017). The larger the LAI, the smaller the variation of the soil water distribution, except in the pure *Pinus tabulaeformis* Carr. forest. Topsoil moisture was not only affected by the herbs or lower growing vegetation but also significantly affected by the tall trees.

There are three processes that could potentially explain this. First, canopy interception and plant water uptake made different contributions to soil water conservation. In our study, trees with understory herbs absorbed more topsoil water than the monoculture grassland, indicating that canopy interception was less than the water consumption of trees. In the tree plots, a larger canopy LAI in the pure plantations often indicated a high soil moisture content, while in contrast, in the mixed forests it indicated that soil moisture was low. Different tree species and their configurations in the same stand determined the LAI and plant growth, which could then increase or decrease the topsoil moisture content and its distribution. Second, the overstory and understory vegetation competed for water use. The understory diversity significantly influenced the soil water content in the surface layer. A large diversity led to significantly less topsoil water and a very even distribution in the pure coniferous and mixed forests, while in the pure broad-leaved *Robinia pseudoacacia* L. forests it led to enhanced topsoil moisture that was less evenly distributed. Third, LAI and herbaceous diversity impacted differently on the soil moisture, with positive benefits in the broad-leaved forests and a negative impact in the other forest types. Hence, these two dominant biotic factors promoted each other synergistically in the typical broad-leaved forests, but their effects were limited in the coniferous and mixed forests in the area. Mixed forests had the lowest soil moisture content among the four types of plots, possibly because the higher stand densities had negative effects on the undergrowth herbs.

### ***Abiotic factors***

Many previous studies have reported that abiotic factors affect the soil water content and its spatial distribution (Gebrekiros and Tessema, 2018), and some have focused on the spatial heterogeneity of soil moisture (Ronda et al., 2002; Liu et al., 2018). Soil moisture is also closely related to slope and some other topographic variables (Frindte et al., 2019), but few studies have investigated the relative and interactional contributions of biotic and abiotic factors in the overstory and understory flora to the spatial variation of soil moisture. Here, topography and topsoil moisture were among the abiotic factors considered, together with the corresponding soil properties (e.g., SOM, TN, and TP), which were commonly used indicators in previous studies (Jose and Romero Diaz, 2010). Topographic and plant factors jointly determined the distribution of soil water and nutrients. Topography typically affects the distribution of many soil properties (Endara and Jaramillo, 2011). In this study, we used a feature and correlational analysis method to screen out the classes of abiotic factors.

Topographic variables including slope, aspect, and elevation were not significantly related to the spatial distribution of soil water in the different stands (Fig. 5). Among the six variables related to soil properties, only TN significantly and negatively impacted on the spatial distribution of topsoil moisture, especially in the pure *Robinia*

*pseudoacacia* L. and mixed forest plots, with a similar result reported by (Wang et al., 2015). According to the three-dimensional models of the topsoil water distribution, a smaller TN resulted in a larger variation of the water content. Based on this, we inferred that some abiotic factors represented by a TN enrichment in the topsoil might reduce the retention of topsoil water. At the same time, the correlations with biotic factors, such as the canopy LAI and Shannon-Wiener index for example, could be considered to improve the topsoil moisture content. Thus, the distribution of topsoil moisture was likely to be correlated to TN, which influenced the soil moisture content and the growth of overstory and understory flora. The variations of the spatial heterogeneity in the stands with an overstory canopy were significantly greater than those with only low growing herbs. The soil properties and water content of the vegetation displayed significant variations, so that the effect of topsoil moisture on spatial heterogeneity was limited.

### ***Implications of the topsoil moisture spatial heterogeneity***

Spatial heterogeneity in topsoil moisture is very helpful for determining the optimal sample-plot size to accurately estimate the soil moisture content (Martínez-Murillo et al., 2017). Compared with a single point sampling method, an understanding of the soil water distribution and its spatial heterogeneity in a standard sampling plot of 20 ×20 m would enhance the reliability of the relationships between soil moisture and other factors (Evans and Love, 1957). The observed autocorrelation in topsoil moisture content values over a short range (15 m) suggested that the scale of a standard sample was appropriate to avoid the influence of autocorrelation. On the other hand, the spatial heterogeneity was correlated with not only the scale but also the direction (Rossi et al., 1992), including slope position (*Figs. 6, 7, and 8*), which probably had an influence on the soil water. Generally, there was a low moisture content in uphill locations and a high moisture content in downhill locations. Because the different biotic and abiotic factors had a combined impact on the moisture content, both scale and direction should be studied when exploring the spatial distributions of these or other factors in the future.

The spatial heterogeneity of topsoil moisture is helpful for understanding underlying ecological processes, such as the competition for water between trees and herbs, mechanisms of species coexistence and the response of plants to environmental heterogeneity (Keitt et al., 2002). For example, the stands containing trees and understory herbs consumed more soil water than the grassland monoculture, and therefore canopy interception was less than the water consumption of trees. The overstory and understory vegetation competed for water, and the soil properties and water content of the vegetation displayed significant variations, which affected the spatial heterogeneity of topsoil moisture. Significantly, the spatial patterns of soil moisture in different plantations were mainly determined by the stand structure in the overstory and understory flora. Therefore, understanding the principles that control the spatial distribution of topsoil moisture and the effects of site conditions on the distribution of water might provide a valuable reference for forest management (Montes et al., 2008; Liu et al., 2018).

### **Conclusions**

The main factors controlling the spatial patterns of soil moisture were the canopy LAI, the herbaceous Shannon-Wiener and Simpson's indexes for plants growing under

the forest canopy, and TN. Additionally, the dependency of the soil water content on the tree species and the forest composition cannot be ignored. The lowest moisture content was found in uphill locations and the highest moisture content was found in downhill locations. The larger canopy LAI of the pure plantations often indicated a high soil moisture content, with the opposite situation apparent in the mixed forest. Combined with the herbaceous diversity, the overstory and understory factors impacted on the soil moisture positively in the pure *Robinia pseudoacacia* L. plots and negatively in the pure *Pinus tabulaeformis* Carr. and mixed forest plots. This study revealed the spatial heterogeneity and interactions between the overstory and understory factors of various typical vegetation types in the semiarid Loess Plateau. Moreover, the next experimental design should take more sample plots and a long-term observation to verify the results in the future. Exploring these relationships and understanding the factors controlling the spatial variation of topsoil moisture will promote the comprehensive utilization of soil water, the optimization of overstory and understory vegetation, and improve the growth of vegetation in the Loess Plateau.

**Acknowledgements.** The study was supported by the National Natural Science Foundation of China (31971644 and 31901365), Scientific and Technological Innovation Programs of Higher Education Institutions in Shanxi (2019L0394), the Shanxi Provincial Outstanding Doctoral Program for Incentive Funds for Scientific Research Projects (SXYBKY2018032), and the Fund for Introduced Talents for Shanxi Agricultural University (2018YJ09). We would like to thank our colleagues for their comments on this paper.

## REFERENCES

- [1] Ahmad, S., Liu, H., Beyer, F., Klöve, B., Lennartz, B. (2020): Spatial heterogeneity of soil properties in relation to microtopography in a non-tidal rewetted coastal mire. – *Mires & Peat* 26(4): 1-18.
- [2] Barksdale, W. F., Anderson, C. J. (2015): The influence of land use on forest structure, species composition, and soil conditions in headwater-slope wetlands of coastal Alabama, USA. – *International Journal of Biodiversity Science Ecosystem Services & Management* 11: 61-70.
- [3] Brzostek, E. R., Dragoni, D., Schmid, H. P., Rahman, A. F., Sims, D., Wayson, C. A., Johnson, D. J., Phillips, R. P. (2014): Chronic water stress reduces tree growth and the carbon sink of deciduous hardwood forests. – *Global Change Biology* 20: 2531-2539.
- [4] Daniel, J. A., Ramaraju, K., Rameshkumar, A. (2019): Comparative studies of mymarid diversity from three different zones of paddy ecosystem in Tamil Nadu, India. – *Entomon* 44(3): 173-182.
- [5] Deng, L., Wang, K. B., Li, J. P., Zhao, G. W., Shangguan, Z. P. (2016): Effect of soil moisture and atmospheric humidity on both plant productivity and diversity of native grasslands across the Loess Plateau, China. – *Ecological Engineering* 94: 525-531.
- [6] Eldridge, D. J., Travers, S. K., Val, J., Wang, J. T., Liu, H., Singh, B. K., Delgado-Baquerizo, M. (2019): Grazing regulates the spatial heterogeneity of soil microbial communities within ecological networks. – *Ecosystems* 23: 932-942.
- [7] Endara, M. J., Jaramillo, J. L. (2011): The influence of microtopography and soil properties on the distribution of the speciose genus of trees, *Inga* (Fabaceae: Mimosoidea), in Ecuadorian Amazonia. – *Biotropica* 43(2): 157-164.
- [8] Evans, R. A., Love, R. M. (1957): The step-point method of sampling—a practical tool in range research. – *Journal of Range Management Archives* 10: 208-212.

- [9] Farley, R. A., Fitter, A. H. (1999): Temporal and spatial variation in soil resources in a deciduous woodland. – *Journal of Ecology* 87: 688-696.
- [10] Frindte, K., Pape, R., Werner, K., Löffler, J., Knief, C. (2019): Temperature and soil moisture control microbial community composition in an arctic–alpine ecosystem along elevational and micro-topographic gradients. – *The ISME Journal* 13: 2031-2043.
- [11] Gebrekiros, M. G., Tessema, Z. K. (2018): Effect of *Senna obtusifolia* (L.) invasion on herbaceous vegetation and soil properties of rangelands in the western Tigray, northern Ethiopia. – *Ecological Processes* 7(1): 9.
- [12] Grime, J. P. (1994): The role of plasticity in exploiting environmental heterogeneity. – In: Caldwell, M. M., Pearcy, R. W. (eds.) *Exploitation of environmental heterogeneity by plants*, pp. 1-19.
- [13] Hu, Y. F., Dao, R. N., Hu, Y. (2019): Vegetation change and driving factors: contribution analysis in the Loess Plateau of China during 2000-2015. – *Sustainability* 11(5): 1320.
- [14] Jose, D. R. S., Romero Diaz, A. (2010): The relationships among biotic and abiotic factors as control soil degradation processes along a Mediterranean pluviometric gradient. – *Geomorphology* 12: 1399D.
- [15] Keitt, T. H., Bjørnstad, O. N., Dixon, P. M., Citron-Pousty, S. (2002): Accounting for spatial pattern when modeling organism-environment interactions. – *Ecography* 25: 616-625.
- [16] Krige, D. (1966): Two-dimensional weighted moving average trend surfaces for ore-evaluation. – *Journal of the South African Institute of Mining and Metallurgy* 66: 13-38.
- [17] Li, S., Liang, W., Fu, B. J., Lu, Y. H., Fu, S. Y., Wang, S., Su, H. M. (2016): Vegetation changes in recent large-scale ecological restoration projects and subsequent impact on water resources in China's Loess Plateau. – *Science of the Total Environment* 569-570: 1032-1039.
- [18] Li, T. Z., Tian, S., Xiang, Y. L., Fang, Y., Yan, E. R. (2018): Species, functional, structural diversity of typical plant communities and their responses to environmental factors in Miao Archipelago, China. – *The Journal of Applied Ecology* 29: 343-351.
- [19] Liu, Z. L., Jiang, F., Zhu, Y., Li, F., Jin, G. Z. (2018): Spatial heterogeneity of leaf area index in a temperate old-growth forest: Spatial autocorrelation dominates over biotic and abiotic factors. – *Science of the Total Environment* 634: 287-295.
- [20] Ma, H., Zhu, Q. K., Zhao, W. J. (2020): Soil water response to precipitation in different micro-topographies on the semi-arid Loess Plateau, China. – *Journal of Forestry Research* 31(1): 245-256.
- [21] Manea, A., Leishman, M. R. (2014): Leaf area index drives soil water availability and extreme drought-related mortality under elevated CO<sub>2</sub> in a temperate grassland model system. – *PloS One* 9: e91046.
- [22] Martínez-Murillo, J. F., Hueso-González, P., Ruiz-Sinoga, J. D. (2017): Topsoil moisture mapping using geostatistical techniques under different Mediterranean climatic conditions. – *Science of the Total Environment* 595: 400-412.
- [23] Meerveld, T. V., McDonnell, J. J. (2006): On the interrelations between topography, soil depth, soil moisture, transpiration rates and species distribution at the hillslope scale. – *Advances in Water Resources* 29: 293-310.
- [24] Montes, F., Rubio, A., Barbeito, I., Cañellasb, I. (2008): Characterization of the spatial structure of the canopy in *Pinus silvestris* L. stands in Central Spain from hemispherical photographs. – *Forest Ecology & Management* 255: 580-590.
- [25] Nijland, W., Van der Meijde, M., Addink, E. A., De Jong, S. M. (2010): Detection of soil moisture and vegetation water abstraction in a Mediterranean natural area using electrical resistivity tomography. – *Catena* 81: 209-216.
- [26] Özkan, U., Gökbulak, F. (2017): Effect of vegetation change from forest to herbaceous vegetation cover on soil moisture and temperature regimes and soil water chemistry. – *Catena* 149: 158-166.

- [27] Paluch, J. G., Gruba, P. (2012): Inter-crown versus under-crown area: contribution of local configuration of trees to variation in topsoil morphology, pH and moisture in *Abies alba* Mill. forests. – *European Journal of Forest Research* 131: 857-870.
- [28] Pielou, E. C. (1966): The measurement of diversity in different types of biological collections. – *Journal of Theoretical Biology* 13: 131-144.
- [29] Pueyo, Y., Moretfernández, D., Arroyo, A. I., Frutos Tena, Á. D., Saiz, H., López Alados, C. (2014): Spatio-temporal dynamics of soil water in a semi-arid Mediterranean ecosystem: implications for plant dynamics and spatial pattern. – *EGU General Assembly Conference Abstracts* 16: 1667P.
- [30] Qi, F., Liu, Y. S., Mikami, M. (2004): Geostatistical analysis of soil moisture variability in grassland. – *Journal of Arid Environments* 58(3): 357-372.
- [31] Ronda, R. J., Den Hurk, V., Holtslag, A. A. M. (2002): Spatial heterogeneity of the soil moisture content and its impact on the surface flux densities and near-surface meteorology. – *Journal of Hydrometeorology* 3(5): 556-570.
- [32] Rossi, R. E., Mulla, D. J., Journel, A. G., Franz, E. H. (1992): Geostatistical Tools for Modeling and Interpreting Ecological Spatial Dependence. – *Ecological Monographs* 62: 277-314.
- [33] Sánchez-González, A., López-Mata, L. (2005): Plant species richness and diversity along an altitudinal gradient in the Sierra Nevada, Mexico. – *Diversity and Distributions* 11: 567-575.
- [34] Shannon, C., Wiener, W. (1949): *The mathematical theory of communication*. – University of Illinois Press, Urbana, USA.
- [35] Shen, Y. Y., Ji, Y., Li, C. R., Luo, P. P., Wang, W. K., Zhang, Y., Nover, D. (2018): Effects of phytoremediation treatment on bacterial community structure and diversity in different petroleum-contaminated soils. – *International Journal of Environmental Research and Public Health* 15(10): 2168.
- [36] Shi, W. Y., Du, S., Morina, J. C., Guan, J. H., Wang, K. B., Ma, M. G., Yamanaka, N., Tateno, R. (2017): Physical and biogeochemical controls on soil respiration along a topographical gradient in a semiarid forest. – *Agricultural & Forest Meteorology* 247: 1-11.
- [37] Simpson, E. H. (1949): Measurement of diversity. – *Nature* 163: 688-688.
- [38] Singh, R., Sagar, R., Srivastava, P., Singh, P., Singh, J. S. (2017): Herbaceous species diversity and soil attributes along a forest-savanna-grassland continuum in a dry tropical region. – *Ecological Engineering* 103: 226-235.
- [39] Smith, M. D., Knapp, A. K. (2006): Physiological and Morphological Traits of Exotic, Invasive Exotic, and Native Plant Species in Tallgrass Prairie. – *International Journal of Plant Sciences* 162: 785-792.
- [40] Sreelash, K., Sharma, R. K., Gayathri, J. A., Upendra, B., Padmalal, D. (2018): Impact of rainfall variability on river hydrology: a case study of southern western Ghats, India. – *Journal of the Geological Society of India* 92: 548-554.
- [41] Takagi, K., Harazono, Y., Noguchi, S. I., Miyata, A., Mano, M., Komine, M. (2006): Evaluation of the transpiration rate of lotus using the stem heat-balance method. – *Aquatic Botany* 85(2): 129-136.
- [42] Von Arx, G., Graf Pannatier, E., Thimonier, A., Rebetez, M. (2013): Microclimate in forests with varying leaf area index and soil moisture: potential implications for seedling establishment in a changing climate. – *Journal of Ecology* 101: 1201-1213.
- [43] Wang, X. B., Zhou, B. Y., Sun, X. F., Yang, Y., Wei, M., Ming, Z. (2015): Soil tillage management affects maize grain yield by regulating spatial distribution coordination of roots, soil moisture and nitrogen status. – *PloS One* 10(6): e0129231.
- [44] Wei, X., Bi, H. X., Liang, W. J., Hou, G. R., Kong, L. X., Zhou, Q. Z. (2018): Relationship between soil characteristics and stand structure of *Robinia pseudoacacia* L. and *Pinus tabulaeformis* Carr. mixed plantations in the Caijiachuan Watershed: An application of structural equation modeling. – *Forests* 9: 124.



- [45] Western, A. W., Blöschl, G., Grayson, R. B. (1998): Geostatistical characterisation of soil moisture patterns in the Tarrawarra catchment. – *Journal of Hydrology* 205: 20-37.
- [46] Wubs, E. R. J., Bezemer, T. M. (2018): Plant community evenness responds to spatial plant–soil feedback heterogeneity primarily through the diversity of soil conditioning. – *Functional Ecology* 32(2): 509-521.
- [47] Yu, H. W., Shen, N., Yu, D., Liu, C. H. (2019): Effects of temporal heterogeneity of water supply and spatial heterogeneity of soil nutrients on the growth and intraspecific competition of *bolboschoenus yagara* depend on plant density. – *Frontiers in Plant Science* 9: 1987.